Chemical Enrichment of the Early Universe

Santa Fe, August 8-13

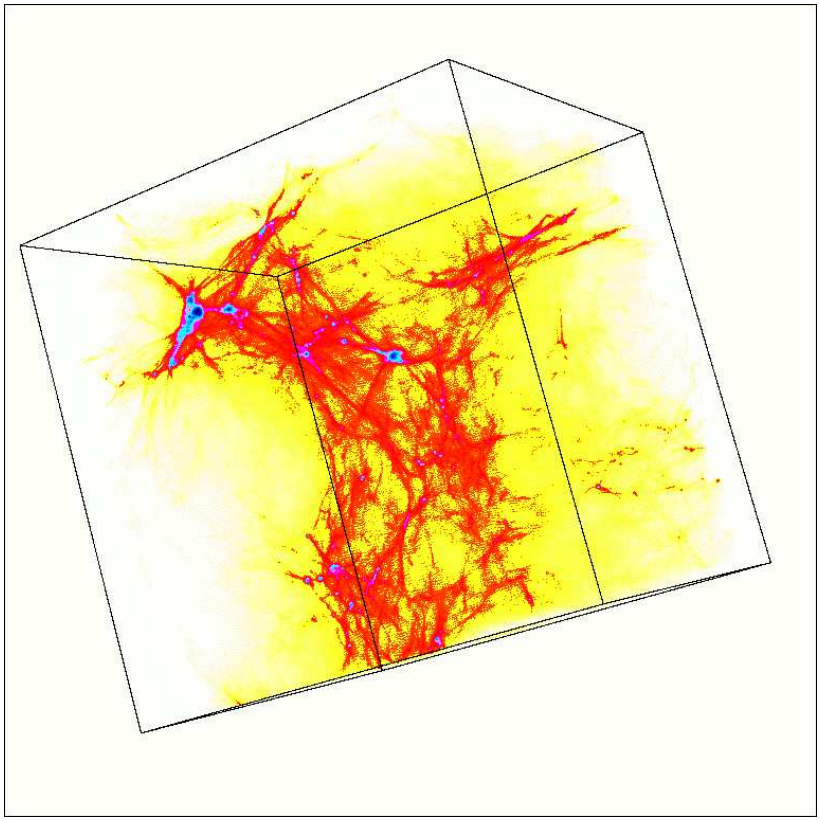

Image from simulation by Michael S. Warren

Sponsored by Los Alamos National Laboratory through funds from the Center for Space Science and Exploration, IGPP, T-6 and SciDAC SSC, and by the Joint Institute for Nuclear Astrophysics (JINA)

Scientific Organizers:
Chris Fryer, Alexander Heger, Frank Timmes, Jim Truran, Jon Weisheit

Conference Secretary: *Mary Dugan*

Edited by Alexander Heger

Alphabetical List of Speakers

Tom Abel:
Formation of the First Stars — Abstract ‖ Talk

Kevork Abazajian:
Chemical Enrichment at $z = 10^9$: An Update on Standard and Non-Standard Big Bang Nucleosynthesis — Abstract ‖ Talk

Anthony Aguire:
The Observed Enrichment of the High-z Intergalactic Medium — Abstract ‖ Talk

Tim Ashenfelter:
The Role of Early Intermediate Mass Stars on the Cosmological Evolution of the Fine Structure Constant — Abstract ‖ Talk

Tim Beers:
Frequency and Metallicity of Low-Z Stars — Abstract ‖ Talk

Edward Brown:
Diversity in Type Ia Supernovae — Abstract ‖ Talk

Judith Cohen:
Abundances in Very Metal Poor Stars — Abstract ‖ Talk

John Cowan:
Probing the Nucleosynthesis Products of the First Stars — Abstract ‖ Talk

Katia Cunha:
Galactic Metallicity Gradients Derived from OB Stars — Abstract ‖ Talk

Sara Ellison:
The CORALS Survey: Dust and Metals at $0.5 < z < 3.0$ — Abstract ‖ Talk

Roberto Gallino (presented by Oscar Straniero):
The s-Process Signature in Low-Metallicity Stars — Abstract ‖ Talk

Oleg Gnedin:
Formation of Globular Clusters in Hierarchical Cosmology — Abstract ‖ Talk

Joyce Guzik:
The Role of Pulsations in Mass Loss from Massive Stars — Abstract ‖ Talk

Alexander Heger:
Evolution of Massive Population III Stars — Abstract ‖ Talk

Falk Herwig:
The Second Stars — Abstract || Talk

Fabio Iocco:
Neutrino Backrgound from Population III stars — Abstract || Talk

Karl-Ludwig Kratz:
R-Process Data — Abstract || Talk

Don Lamb:
Gamma-Ray Bursts as a Probe of the Metallicity History of the Universe — Abstract || Talk

Jennifer Lotz:
The Colors and Metallicities of Dwarf Elliptical Galaxy Globular Cluster Systems, Nuclei, and Stellar Halos — Abstract || Talk

Peter Möller:
Global Nuclear Structure Calculations for Astrophysics, Recent Developments — Abstract || Talk

Ken Nomoto:
Nucleosynthesis in Hypernovae — Abstract || Talk

Mike Norman:
Early Enrichment of the Lyman Alpha Forest — Abstract || Talk

Katsuya Okoshi:
Evolution of Damped Lyman-alpha Systems from Hierarchical Structure Formation Models — Abstract || Talk

Ben Oppenheimer:
Cosmological Simulations of IGM Metalicity Enrichment — Abstract || Talk

Brian O'Shea:
Chemical Feedback from Massive Primordial Stars — Abstract || Talk

Michael Paul:
s-Process Laboratory Studies: New Methods and Implications — Abstract || Talk

Jason Prochaska:
Nucleosynthesis in Young Galaxies — Abstract || Talk

Yong-Zhong Qian:
r-Process Nucleosynthesis in the Early Universe and Cosmological Implications — Abstract || Talk

Ernst Rehm:
Bypassing the Triple-Alpha Process - Recent Measurements and Future Plans. Abstract || Talk

Jaehyon Rhee:
The HK-II Survey: A New Search for Very Metal-Poor Red Giant Stars Abstract || Talk

Wal Sargent:
Abundance Gradients in the Milky Way disk Abstract || Talk

Evan Scannapieco:
High-Redshift Formation of Star Clusters By Galaxy Outflows Abstract || Talk

Joe Silk:
The IMF of the First Stars Abstract || Talk

Robert Simcoe:
The Metallicity Distribution Function of the IGM at $z = 2.5$: New Constraints on the Chemical Yield of Early Galaxies Abstract || Talk

Verne Smith:
Lithium Isotopic Abundance Patterns at Low-Metallicity: Diffusion, Rotational Depletion, and Cosmic Rays Abstract || Talk

Oscar Straniero:
s-Process in Low and Very Low Metallicity AGB Stars Abstract || Talk

Xiaodong Tang:
Indirect Measurements in Charged p-Particle Induced Radiative Capture Reaction Abstract || Talk

Aparna Venkatesan:
Connecting Reionization and Metal Production by the First Stars Abstract || Talk

Daniel Whalen:
Strong Mass Outflows from the First H II Regions in the Universe Abstract || Talk

Stan Woosley:
GRBs as Probe of the First Stars and their Nucleosynthesis Abstract || Talk

Abstracts

Formation of the First Stars

Tom Abel

This talk highlights recent progress in computing the formation of the very first stars as well as the many challenges ahead to turn this into reliable predictions for observables. Some recent insights in our theoretical understanding of the chemo-thermal instabilities during the initial proto-stellar collapse are also discussed.

Chemical Enrichment at $z = 10^9$: An Update on Standard and Non-Standard Big Bang Nucleosynthesis

Kevork Abazajian

I will review recent developments in observational inferences of the primordial element abundances, their consistency with standard big bang nucleosynthesis, and non-standard models with primordial neutrino lepton number and sterile neutrinos. (LA-UR 04-2260)

The Observed Enrichment of the High-z Intergalactic Medium

Anthony Aguire

While it is known that the IGM at z $\sim$ 2-4 is enriched with metals at overdensities > 5 (with hints of enrichment at lower densities), studies to date have left open many questions concerning these metals: are there in fact metals at overdensity < 5? How does the metallicity vary with density and redshift? What is the scatter in metallicity at a given density? What are the relative elemental abundances? How do these inferences depend upon the assumed ionizing background? I will present recent and ongoing work addressing (and to a significant degree answering) all of these questions observationally, in which we apply the "pixel optical depth" technique to a set of 19 high-resolution Keck and VLT spectra.

The Role of Early Intermediate Mass Stars on the Cosmological Evolution of the Fine Structure Constant

Tim Ashenfelter

Recent analyses of Damped Lyman alpha systems (DLAs), using the many-multiplet method (MM), have indicated a possible variation in the fine structure constant. While the MM method provides statistically significant evidence of variation, it is sensistive to isotopic abundances. We show how the fine structure constant can be kept constant if a non-solar isotopic ratio of ^{24,25,26}Mg occurs at redshifts of ($0.5 < z < 1.8$). In order to obtain this non-solar isotopic ratio for Mg, we need to have a chemical evolution model that has an early IMF that is enriched in intermediate mass stars. We implement recent stellar models of low metallicity AGB stars that follow abundances beyond the CNO cycle and produce neutron-rich Mg isotopes. The resulting abundances from an AGB enhanced IMF is consistent with recent observations of DLA and metal-poor stellar abundances. We conclude that the isotopic abundance explanation for the variation of the fine structure constant adds to the existing evidence for an early enhancement of AGB stars in the early Universe. Furthermore, the MM method applied to DLAs may be an extremely useful tool for determining the nucleosynthetic history of the early Universe.

Frequency and Metallicity of Low-Z Stars

Tim Beers

I discuss the current versions of the metallicity distribution functions of stars in the halo and thick disk of the Galaxy, as determined from the HK survey of Beers and colleagues and the Hamburg/ESO survey (HES) of Christlieb and collaborators. Although the HK survey follow-up medium-resolution spectroscopic observations have been largely completed, HES observations will be continuing for the next several years. In addition, a new effort, based on recently completed automated scans of the HK survey plates has yielded a new sample of candidate metal-poor giants, being explored by Rhee and collaborators. I will comment on the time-scale for completion of these surveys. I will also describe plans for a new effort, SEGUE: The Sloan Extension for Galactic Understanding and Evolution. SEGUE will make use of the SDSS telescope to obtain medium-resoution spectroscopy of 250,000 stars in the halo and thick disk of the Milky Way, as well as an additional 3000 square degrees of *ugriz* imaging at lower latitudes than the current SDSS survey. Preliminary results based on publicly available data for some 50,000 stars in the current SDSS data releases will be described.

Diversity in Type Ia Supernovae

Edward Brown

The white dwarf progenitors of Type Ia supernovae inherit an abundance of ^{22}Ne formed from CNO during core He burning. Timmes, Brown, & Truran showed that the mass of ^{56}Ni produced in a burn to NSE depends *linearly* on the abundance of ^{22}Ne and hence linearly on the metallicity of the white dwarf progenitor. The observed scatter in the metallicity of the solar neighborhood is enough to induce a 25% variation in the mass of ^{56}Ni ejected by Type Ia supernova and is sufficient to vary the peak V-band brightness by $|\Delta M_V| \approx 0.2$. This scatter in metallicity is present out to the limiting redshifts of current observations ($z < 1$) and may help explain the correlations between peak brightness and host galaxy type. An unresolved question is to what extent the electron captures in the densest regions can increase the neutron fraction in the presence of large-scale fluid circulation. Answering this question requires incorporating realistic reaction schemes into multidimensional simulations and accurately tracking the nucleosynthetic yields. In this talk I also highlight recent efforts to incorporate Lagrangian tracer particles into Eulerian hydrodynamic simulations. Travaglio et al. have successfully used Lagrangian tracer particles to track the nucleosynthesis of type Ia supernovae, and here I report on post-processing calculations of a simulation performed with FLASH, an adaptive-mesh Eulerian code that uses the "thick flame" scheme of Khokhlov. For this initial study 10,000 tracer particles were embedded in a cylindrically symmetric two-dimensional simulation with a centered ignition.

Abundances in Very Metal Poor Stars

Judith Cohen

We discuss the detailed composition of about 50 extremely metal poor stars, including 28 extremely metal-poor (EMP) dwarfs, based on Keck/HIRES spectra. For the best observed elements between Mg and Ni, we find that the abundance ratios appear to have reached a plateau, i.e. [X/Fe] is approximately constant as a function of [Fe/H], except for Cr, Mn and Co, which show trends of abundance ratios varying with [Fe/H]. These abundance ratios at low metallicity correspond approximately to the yield expected from Type II SN with a narrow range in mass and explosion parameters; high mass Type II SN progenitors are required. The dispersion of [X/Fe] about this plateau level is surprisingly small, and is still dominated by measurement errors rather than intrinsic scatter. These results place strong constraints on the characteristics of the contributing SN.

Probing the Nucleosynthesis Products of the First Stars

John Cowan

We are using both space-based (Hubble Space Telescope, HST) and ground-based telescopes to make extensive studies of Galactic halo stars. These stars contain the nucleosynthesis products (from the rapid neutron capture process, *r*-process) from the earliest generations of stars – the progenitors of the halo stars. The observed stellar abundance distributions – from the lightest neutron-capture elements, such as Ge, along with some of the heaviest, including Pt – are providing new clues about the earliest Galactic r-process nucleosynthesis. These in turn will help to identify the characteristics and nature of the first stars in the Galaxy.

Galactic Metallicity Gradients Derived from OB Stars

Katia Cunha

The distribution of stellar abundances along the the Galactic disk is an important constraint for models of chemical evolution and galaxy formation. In this talk I will discuss the radial gradients of C, N, O, Mg, Al, Si, as well as S, from abundance determinations in young OB stars spanning a range in Galactocentric distances between 4.7 and 13.2 kpc.

The CORALS Survey: Dust and Metals at $0.5 < z < 3.0$

Sara Ellison

Since most surveys for damped Lyman alpha (DLA) systems rely on samples of optically bright QSOs, there has been a widespread concern that these surveys may be biased against metal rich, dusty intervening galaxies. Here I present new results from the CORALS survey which aims to overcome this potential observational bias by using a radio-selected sample of quasars with complete optical identifications. I will present determinations of the number density of absorbers detected in CORALS and their metallicities. A comparison with DLAs identified in previous surveys reveals the extent to which these samples have been biased due to dust extinction.

The *s*-Process Signature in Low-Metallicity Stars

Roberto Gallino (presented by Oscar Straniero)

I will discuss the overall *s*-process predictions in low-metallicity stars, both in massive stars (weak *s*-component) and in AGB stars (main *s*-component) and compare them with existent spectroscopic data of unevolved, s-enhanced and *r*-enhanced stars in the Halo. I will further address to the origin of the low-metallicity 'lead stars'. Next I will consider the problem of the *s*-appearance in field unevolved metal-poor stars with respect to the *r*-process signature.

Formation of Globular Clusters in Hierarchical Cosmology

Oleg Gnedin

The discoveries of young massive star clusters in starforming galaxies, brought by the refurbished HST, have led to a paradigm shift in our understanding of star clusters. The origin of globular clusters is associated with the regions of active star formation and is therefore directly linked to the process of galaxy formation. We use numerical simulations of a Milky Way-sized galaxy to demonstrate that realistic globular clusters can form naturally at $z > 3$ in the concordance LCDM cosmology. The clusters in our model form in the strongly baryon-dominated cores of supergiant molecular clouds. The first clusters form at $z = 12$, while the peak formation appears to be at $z = 3$-5. The zero-age mass function of globular clusters can be approximated by a power-law with the slope -2, in agreement with observations of young massive star clusters. The total mass of the cluster population is strongly correlated with the mass of its host galaxy, as well as with the local average star formation rate. The first clusters serve as important sources of ionizing radiation within their host galaxies and may lead to gamma-ray bursts and intermediate-mass black holes.

The Role of Pulsations in Mass Loss from Massive Stars

Joyce Guzik

Hydrodynamic simulations show that pulsations can grow to large amplitudes, cause the outer envelopes of stars to exceed the Eddington limit for a portion of each pulsation period, and can enhance mass loss. Nonradial pulsations can also be present in massive stars, and may be responsible for mixing in the interior which will alter stellar evolution and possibly cause episodic outbursts such as seen in giant eruptions of Eta Car and P Cyg. We will present nonlinear hydrodynamic simulations including time-dependent convection, as well as results of linear nonradial nonadiabatic pulsation studies for massive stars. We will in particular highlight differences in structure and pulsation behavior for very low-metallicity vs. solar metallicity stars. Contains only material covered by LA-UR-97-4189, LA-UR-98-5112, LA-UR 98-5480, LA-UR-04-5059.

Evolution of Massive Population III Stars

Alexander Heger

The first stars to form in the universe were different from present-day stars in several ways: Firstly, due to lack of initial metals, the initial mass function could have been different, likely preferring more massive stars. Secondly, the absence of metal does affect the mass loss rates so that massive stars may be able to retain most of their mass till their explosive deaths and pair instability supernovae may occur. Lastly, also the nucleosynthesis of the stars is altered due to the differences in initial composition and evolutionary paths. After giving a general overview of massive star evolution and their nucleosynthesis I will discuss the evolution of Pop III stars and pair instability supernovae. I will give an overview of the expected final fates of massive stars and their remnants with particular focus on Pop III stars. (LA-UR-04-5139)

The Second Stars

Falk Herwig

The ejecta of the first probably very massive stars polluted the Big Bang primordial abundance distribution with the first heavier elements. The resulting ultra metal-poor abundance distribution provided the initial conditions for the second stars of a wide range of initial masses reaching down to intermediate and low masses. The importance of these second stars for understanding the origin of the elements in the early Universe are manifold. While the massive first stars have long vanished the second stars are still around and currently observed. They are the carriers of the information about the first stars, but they are also capable of nuclear production themselves. For example, in order to use ultra or extremely metal-poor stars as a probe for the r-process in the early Universe a reliable model of the s-process in the second stars is needed. Eventually, the second stars may provide us with important clues on questions ranging from structure formation to how the stars actually make the elements, not only in the early but also in the present Universe. I will describe recent models of the AGB evolution phase of the second stars, including implications for the s-process. Comparison of these models with observations reveal problems that need to be addressed. The s-process is also a particularly useful diagnostic tool for probing the physical processes that are responsible for the creation of elements in stars, like for example rotation. I will describe a related program at LANL which includes both new experimental and theoretical work. Contains only material covered by LA-UR 04-4557, 04-4530, 04-2259, 04-0724, 03-9209, 03-8187, 04-1158.

Neutrino Backrgound from Population III stars

Fabio Iocco

We consider the contribution to the diffuse cosmic neutrino background from the first generation of stars; under simple assumptions for the star formation models we present a first order-of-magnitude estimate of the corresponding flux, showing that it could be dominant over other cosmic sources in the the energy ranges $E < 100keV$ and $1MeV < E < 4MeV$.

R-Process Data

Karl-Ludwig Kratz

Modeling the r-process represents a fascinating challenge in the interdisciplinary field of nuclear astrophysics. Basic studies of this nucleosynthesis process can already be accomplished with a knowledge of just a few nuclear properties, namely nuclear masses, beta-decay half-lives $T_{1/2}$, and beta-delayed neutron emission probabilities P_{n}. This nuclear data input comes from (still limited) experiments and global theories. Experiments at radioactive facilities have played a pioneering role in exploring the characteristics of nuclear structure in terms of the above quantities. Initial examinations paid attention to easily measurable beta-decay properties of highly unstable nuclei with magic neutron numbers (*i.e.*, so-called "waiting-point" isotopes at the r-process peaks) and/or in the phase-transition regions (*e.g.*, around $N \geq 60$, where the first "abundance trough" occurs in many r-calculations). More recent activities focus on detailed spectroscopic studies of the evolution of nuclear structure with increasing isospin, in particular the effects of "shell-quenching" far from stability. Implications of the new nuclear data input on the formation of the r-process abundance peaks and the r-matter flow beyond the third peak to the region of the Th-U cosmochronometers will be presented.

Gamma-Ray Bursts as a Probe of the Metallicity History of the Universe

Don Lamb

HETE-2 has confirmed the connection between long gamma-ray bursts (GRBs) and the collapse of massive stars. Therefore one expects GRBs to occur out to redshifts $z \sim 20$. We show that both GRBs and their afterglows are very bright, and are therefore easily detectable out to such redshifts. Consequently, high-dispersion spectroscopic observations of metal absorption line systems (ALS) in the infrared and near infrared spectra of GRB afterglows can provide important information about the metallicity history of (1) the star-forming regions of galaxies; (2) damped Lyman alpha clouds; and (3) the Lyman alpha forest (*i.e.*, low- to moderate-column depth clouds in the intergalactic medium). We discuss spectroscopic observations of the optical afterglows of GRBs at lower redshifts that illustrate the potential power of GRBs to probe the metallicity history of the universe at higher redshifts.

The Colors and Metallicities of Dwarf Elliptical Galaxy Globular Cluster Systems, Nuclei, and Stellar Halos

Jennifer Lotz

Dwarf elliptical galaxies have masses comparable to the first proto-galactic fragments and are therefore an obvious place to look for ancient stars and to track early star-formation. We present the results of a HST survey of 69 dwarf elliptical galaxies (dEs) in the Virgo and Fornax Clusters. The V-I colors of the dE globular clusters (GCs), nuclei, and underlying field star populations are used to trace the dE star-formation histories. We find that the dE GCs are as blue as the metal-poor Milky Way GC population. The observed correlation of the dE globular cluster systems' V-I color with the luminosity of the host dE is strong evidence that the globular clusters were formed within the the halos of dEs and do not have a pre-galactic origin. Assuming the majority of dE clusters are old, the mean globular cluster color-host galaxy luminosity correlation implies a cluster metallicity - galaxy luminosity relation of $Z_{GC} \propto L_B^{0.20\pm0.05}$, which is significantly shallower than the field star metallicity - host galaxy luminosity relationship observed in Local Group dwarfs ($Z_{FS} \propto L^{0.4}$). The dE stellar envelopes are 0.1-0.2 magnitudes redder in V-I than their globular clusters and nuclei, suggesting separate star-formation episodes within the dEs for the clusters and field stars. We will also present preliminary results of a program to obtain spectra for the GCs in four Virgo and Fornax Cluster dEs using GMOS-N and GMOS-S in order to derive GC ages and metallicities via line indices.

Global Nuclear Structure Calculations for Astrophysics, Recent Developments

Peter Möller

Five years ago a major development in fission barrier calculations took place. Earlier fission barriers were determined based on calculated energies for a few hundred different nuclear shapes between the ground state and separated fragments. We now determine fission barriers from potential energy surfaces based on about 4 million different shapes. Over past several years we have studied the implications of this development which allows us to determine the fission barrier structure in previously unimaginable detail. Our studies also lead us to conclude this approach allows us to calculated fission barriers in the r-process regions more reliably than earlier. I will discuss first results of this effort, which is ongoing. We have also extented our macroscopic-microscopic method to axially asymmetric shapes and have obtained global results on many ground-state properties such as the occurence of axial asymmetry of the ground state, regions of oblate-prolate shape isomerism. We also have results on the axial asymmetry of the first barrier peak. I will review these results. (LA-UR-04-3849)

Nucleosynthesis in Hypernovae

Ken Nomoto

Recent observations of abundance patterns in extremely metal-poor (EMP) stars are providing us with critical information on nucleosynthesis in Population (Pop) III supernovae (SNe) and thus on the nature of the first stars in the Universe. We have calculated nucleosynthesis in various types of Pop III SNe. We find that the yields of hyper-energetic core-collapse SNe (Hypernovae) can explain the observed trends in the abundance ratios among iron-peak elements (Mn, Co, Ni, Zn)/Fe as well as the large C/Fe ratio observed in certain C-rich EMP stars. Asphericity in the explosions strengthens the nucleosynthesis properties of hypernovae. Abundance patters in star-burst galaxies are also discussed. Our results suggest that black-hole-forming hypernovae make important contribution to the chemical enrichment at high z and low Z.

Early Enrichment of the Lyman Alpha Forest

Mike Norman

We examine the dynamical evolution and statistical properties of the supernova ejecta of massive primordial stars in a cosmological framework to determine whether this first population of stars could have enriched the universe to the levels and dispersions seen by the most recent observations of the Lyman-Alpha forest. We evolve a lambda CDM model in a 1 Mpc^3 volume to a redshift of $z = 15$ and add "bubbles" of metal corresponding to the supernova ejecta of the first generation of massive stars in all dark matter halos with masses greater than 5 times 105 solar masses. These initial conditions are then evolved to z = 3 and the distribution and levels of metals are compared to observations. In the absence of further star formation the primordial metal is initially contained in halos and filaments. Photoevaporation of metal-enriched gas due to the metagalactic ultraviolet background radiation at the epoch of reionization ($z \sim 6$) causes a sharp increase of the metal volume filling factor. At $z = 3$, $\sim 2.5\,\%$ of the simulation volume (approx. $20\,\%$ of the total gas mass) is filled with gas enriched above a metallicity of $10^{-}4\ Z_{solar}$, and less than $0.6\,\%$ of the volume is enriched above a metallicity of $10^{-3}\ Z_{solar}$. This suggests that, even with the most optimistic prescription for placement of primordial supernova and the amount of metals produced by each supernova, this population of stars cannot entirely be responsible for the enrichment of the Lyman-α forest to the levels and dispersions seen by current observations unless we have severely underestimated the duration of the Pop III epoch. However, comparison to observations show that Pop III supernovae can be significant contributors to the very low overdensity Lyman-Alpha forest.

Evolution of Damped Lyman-alpha Systems from Hierarchical Structure Formation Models

Katsuya Okoshi

I investigate Damped Lyman-alpha (DLA) systems from hierarchical structure formation models to explore the chemical enrichment in DLAs and to clarify the connection between DLAs and galaxies. I find that (1)my model reproduces distributions of properties in fundamental observables (e.g., metallicities, HI column densities, luminoisities of host galaxies) from optical and near-infrared recent observations, (2) DLA host-galaxies primarily consist of LSB dwarf galaxies (typical radius 3 kpc, surface brightness 22-27 mag arcsec^{-2}, star formation rate 10^{-2} $M_\odot$/yr, HI mass 10^9 $M_\odot$). I also discuss selection effects on DLA host-galaxies observations causing by the size and the faintness and some possibilities of exploring DLAs by radio observations.

Cosmological Simulations of IGM Metalicity Enrichment

Ben Oppenheimer

We explore the metallicity enrichment in the IGM using Springel & Hernquist's (2003) cosmological hydrodynamical simulations. Model quasar absorption line spectra are generated for different metallicity models including the Springel & Hernquist wind model which includes the ejection of metals into the IGM by star-forming galaxies. Preliminary comparisons with data suggests that this wind model is better able to account for the existence of metals into regions of low density.

Chemical Feedback from Massive Primordial Stars

Brian O'Shea

We use Enzo, an adaptive mesh cosmological code, to simulate the death of a massive primordial star in a pair-instability supernova, all in a cosmological context. We follow the evolution of the supernovae remnant to study the final distribution of metals and the variance in metallicity of sites of the second generation of stars in the universe.

s-Process Laboratory Studies: New Methods and Implications

Michael Paul

New facilities, instruments and methods become available for the experimental study of neutron capture reactions by stable and unstable nuclides and at energies relevant to the important s-process nucleosynthesis. Among those, the activation technique, is used in conjunction with accelerator mass spectrometry to access long-lived products which are not amenable to conventional decay counting. A proposed new neutron source, possibly usable for such activation measurements and based on the SARAF accelerator project in Israel, will be described.

Nucleosynthesis in Young Galaxies

Jason Prochaska

I will briefly review the role of damped Lya systems (DLA) in tracing the chemical enrichment and nucleosynthetic history of galaxies during the first few Gyr. I will (1) highlight the dust/nucleosynthesis degeneracy inherent to the observations, (2) emphasize specific abundance ratios which depart from the standard picture of Galactic stars; and (3) describe an ongoing program to discover 'metal-strong' DLAs where one can study over 25 elements (including B, Sn, Ge, Cu, Zn, Kr) in a single galaxy with an age of $< 2\,\mathrm{Gyr}$.

r-Process Nucleosynthesis in the Early Universe and Cosmological Implications

Yong-Zhong Qian

Two scenarios for r-process nucleosynthesis will be presented in connection with observations of abundances in metal-poor Galactic halo stars. The implications of each scenario for understanding observations of abundances in the intergalactic medium and damped Ly alpha systems will be discussed.

Bypassing the Triple-Alpha Process - Recent Measurements and Future Plans.

Ernst Rehm

The presence of the mass 5 and mass 8 gaps introduces a strong impedance to stellar nucleosynthesis which can only be overcome by ^{3}He and α-induced reactions. In most network calculations it is usually assumed that the mass-8 gap is bridged by the triple-alpha capture reaction which, as a three-body process, requires higher stellar temperatures and densities. It has been argued for some time, however, that other reaction paths could lead to a bypass of the triple-alpha process, leading to the formation of 'metals' in first generation stars. Making use of hydrogen, deuterium, ^{3}He and ^{4}He, produced during the Big Bang, there are three possible sequences leading to the formation of nuclei of mass 12 and beyond. With ^{7}Be formed via the ^{4}He(^{3}He,gamma)^{7}Be reaction as a starting point, these three reaction paths are:
^{7}Be(α,γ)^{11}C(p,γ)^{12}N(β^+)^{12}C
^{7}Be(p,γ)^{8}B(p,γ)^{9}C(α,p)^{12}N(β^+)^{12}C
^{7}Be(p,γ)^{8}B(α,p)^{11}C(p,γ)^{12}N(β^+)^{12}C.
In the past years experiments with radioactive beams have for the first time provided experimental values for reactions rates which were previously based only on theoretical estimates. I will summarize the measurements performed in this mass region and give a status of future experiments at a next-generation facility.

The HK-II Survey: A New Search for Very Metal-Poor Red Giant Stars

Jaehyon Rhee

The HK-II survey (Rhee, Beers, & Irwin, in preparation) originated as an extension of the original HK objective-prism survey of Beers, Preston, & Shectman (1985, 1992). HK-II was designed to discover a large sample of Very Metal-Poor (VMP) *red giant* stars with [Fe/H] ≤ -2.0 by using *digitized* objective-prism spectra and 2MASS JHK colors; many of these stars were likely to have been missed in the original (visual) selection of metal-poor candidates due to an unavoidable temperature bias. Thus far, ongoing medium-resolution spectroscopic follow-up has newly confirmed some 110/130 red giants/sub-giants with [Fe/H] ≤ -2.0 (Rhee & Beers, in preparation). Also, Rhee, Ivans, & McWilliam have recently initiated a program to obtain high-resolution spectroscopy for the HK-II VMP stars, and performed pilot observations with the KPNO 4m/Echelle & Magellan 6.5m/MIKE in May 2004. A preliminary analysis for six spectra indicates that one highly ([Eu/Fe] $> +1.0$) and two moderately ($0.5 \leq [Eu/Fe] \leq 1.0$) r-process-enhanced metal-poor stars may have been found. Here I give a comprehensive discussion of the HK-II survey; motivation, status report, and future plans.
J.R. acknowledges partial support for this work by NASA through the AAS Small Research Grant Program.

Abundance Gradients in the Milky Way disk

Wal Sargent

We give a brief acount of the physical properties and structure of the "Lyman-alpha Forest." We review recent work using QSO absorption lines on the abundances of C, O, and Si in the Intergalactic Medium (IGM) at high redshifts both as a function of redshift and as a function of overdensity. We summarize the results obtained by "stacking" spectra, by the "pixel method" and by the direct detection of weak heavy element absorption lines in high resolution echelle spectra with very high S/N. Details of some of these methods will be given by other speakers. We also discuss the variation with redshift of the contribution of C and Si to the cosmological density parameter. Various lines of evidence lead to the conclusion that the gas in the IGM had attained a mean metallicity of about 0.05 percent of the solar value by redshift $z = 6$. Finally we discuss the mounting evidence that heavy element absorption lines are produced by galactic outflows from star forming galaxies such as the "Lyman break" galaxies.

High-Redshift Formation of Star Clusters By Galaxy Outflows

Evan Scannapieco

We study the interactions of high-redshift galaxy outflows with low-mass virialized clouds of primordial composition. While atomic cooling allows star-formation in objects with virial temperatures above 10^4 K, "minihalos" with virial temperatures below this threshold are largely unable to form stars by themselves. Thus the large observed population of high-redshift starbursts may have induced widespread star-formation in neighboring $T_{\rm vir} < 10^4$ K clouds, as shocks would have resulted in intense cooling both through nonequilibrium H_2 formation and metal-line emission. Using a simple analytic model, we show that the resulting star-clusters naturally reproduce three key features of the observed population of halo globular clusters (GCs). First, the 10^4 K maximum virial temperature directly corresponds to the $\sim 10^6$ solar mass upper limit on the stellar mass of such clusters, a feature that can not be explained by any GC destruction mechanism. Secondly, the momentum imparted in such interactions is sufficient to strip the gas from its associated dark matter halo, explaining why GCs do not exhibit the dark matter potential wells that are ubiquitous in galaxies. Finally, the mixing of ejected metals into the primordial gas provides a straightforward mechanism to explain the $\sim$ -0.1 dex homogeneity of stellar metallicities within a given GC, while at the same time allowing for a large spread in metallicity between different clusters. To study the possibility of such "fine grained" mixing in detail, we use a simple, one-dimensional turbulence model to simulate shear-layer mixing in shock-outflow interactions

The IMF of the First Stars

Joe Silk

I will review the arguments that constrain the masses of the first stars. Constraints include cloud fragmentation theory, chemical enrichment and reionisation of the universe.

The Metallicity Distribution Function of the IGM at $z = 2.5$: New Constraints on the Chemical Yield of Early Galaxies

Robert Simcoe

We have measured the metallicity distribution function of the IGM zt $z = 2.5$, from observations of OVI and CIV lines in high-quality QSO spectra. Our results suggest that cosmic pollution (at least within filaments) was dominated by fairly recent galactic winds, rather than early Population III stars. Combining our observations with a slight modification of standard chemical enrichment models, we calculate the heavy-element yield of the galaxy population prior to $z = 2.5$. Comparison with local galaxies shows that these early systems must have been quite efficient at manufacturing metals and expelling them ino the IGM.

Lithium Isotopic Abundance Patterns at Low-Metallicity: Diffusion, Rotational Depletion, and Cosmic Rays

Verne Smith

Isotopic lithium abundances will be presented for 41 halo stars, all near the main-sequence turn-off. These abundances are derived from spectra with very high signal-to-noise (S/N=400-600) and spectral resolution (R=100,000-120,000), thus uncertainties in defining the Li I 6707 $\AA$ line-profiles or equivalent widths are negligible. Results are derived from two sets of spectra, with 17 stars observed on the McDonald 2.7 meter telescope and coude spectrographs, and 24 stars observed with the VLT and UVES. While no trend in the lithium abundance with effective temperature is found, a significant increase in lithium with increasing iron (or oxygen) abundance is found. Whether such a trend might result from diffusion, rotationally induced mixing, or cosmic-ray lithium production will be discussed.

s-Process in Low and Very Low Metallicity AGB Stars

Oscar Straniero

In spite of the lack of iron seeds, n-capture nucleosynthesis may survive in stars that form in a metal depleted environment. It occurs when during the thermally pulsing AGB phase, owing to the third dredge up, the envelope is enriched with primary C. Then, this C is mostly converted into N, by the H-burning shell (through the CN cycle), and later on, during the thermal pulse, this N is transformed into Ne (through the ^{14}N(α,γ)^{18}F(β^+)^{18}O(α,γ)^{22}Ne chain). Even if its initial abundance is taken 0, after few TPs the amount of ^{22}Ne within the He-rich intershell is comparable to the one found in solar composition models. This primary ^{22}Ne have two important functions: i) it may act as a neutron source (^{22}Ne(α,n)^{25}Mg, when the temperature exceeds 300 MK), ii) it provides an alternative seed for the s-process nucleosynthesis. A new generation of stellar models of low and very low metallicity AGB stars have been obtained. In this calculations, the evolution of the physical structure and the nucleosynthesis are fully coupled. The resulting nucleosynthesis (for about 500 isotopes) is presented. The main result of these calculations concerns the production of heavy isotopes (up to Pb) in iron deprived AGB stars.

Indirect Measurements in Charged p-Particle Induced Radiative Capture Reaction

Xiaodong Tang

Charged particle induced radiative capture reaction is one of the most important reaction types for nuclear astrophysics. In determining these capture reaction rates, indirect measurements play an important and sometime irreplaceable role. I will review the current status of these indirect methods.

Connecting Reionization and Metal Production by the First Stars

Aparna Venkatesan

I will review the role played by the first stars in the reionization and metal enrichment of the early universe. Primordial stellar objects have unique characteristics that can be identified through their ionizing properties and the elements created by their supernovae. By combining these two signatures with current data on reionization and the detection of metals in a variety of high-redshift and local environments, we can obtain relatively strong constraints on the mass function and ionizing efficiencies of the first stars. I will also discuss how these objects can be detected by future telescopes.

Strong Mass Outflows from the First H II Regions in the Universe

Daniel Whalen

Recent 1D radiation hydrodynamical simulations of ionization fronts from very massive Pop III stars residing in primordial halos indicate that these stars are very effective at ionizing their local environments. Shocks form in the ionized envelope that can drive half of the baryonic matter out of the halo virial radius ~ 100 pc over the main sequence lifetime of the central star even in the complete absence of any mass loss from the star itself. Such outflows can facilitate the dispersal of metals if the star is subsequently destroyed in a supernova or retard the growth of the resultant black hole if the star instead collapses. The dynamics and developmental timescales of primordial H II regions will be reviewed along with their consequences for chemical enrichment.

GRBs as Probe of the First Stars and their Nucleosynthesis

Stan Woosley

During the last six years, overwhelming evidence has accumulated that a large fraction of gamma-ray bursts (GRBs) are accompanied by nearly simultaneous supernovae. To date three supernovae have been spectroscopically identified in coincidence with GRBs: GRB 980425(SN 1998bw), GRB 030329 (2003dh), and GRB 031203, and many other GRBs display supernova-like "bumps" in their optical afterglows. All are Type Ic. However, the converse is not true. Not all Type Ic or Ib supernovae are involved in GRB production and, even with beaming, the total fraction of supernovae that make GRBs is still probably, at most, a few percent. In terms of models, GRBs seem to be associated with the deaths of particularly massive stars with unusually rapidly rotating cores. A paradigm, though still uncertain, is emerging that common supernovae, and most nucleosynthesis, come from neutron star formation and neutrino-powered explosions, but that the more massive stars produce black holes with accretion disks (collapsars). If so, novel channels for nucleosynthesis are opened up that may eventually be tested by observation. The collapsar and millisecond magnetar models for GRBs will be reviewed and its broader implications for stellar evolution and nucleosynthesis, discussed. A key isotope may be 45Sc.

Talks

The first stars

Forming the "large scale structure", a galaxy, a primordial molecular cloud, a cloud core, an accreting primordial star, and its influence on its surrounding in ab initio cosmological hydrodynamical simulations

Tom Abel
Penn State

Collaborators

- Greg Bryan (Oxford)
- Emanuele Ripamonti (Kapteyn Institute Groenningen)
- Miroslav Micic, John Wise, Steinn Sigurdsson (PSU)
- Mike Norman, Dan Whalen, Brian O'Shea (LCA, UCSD)

3D visualizations from a collaboration with Ralf Kähler at the ZIB and AEI

Outline

- Ab initio simulations
- Results & Predictions
- Challenges
  - first stars
- Some observational constraints

Heger & Woosley 2001

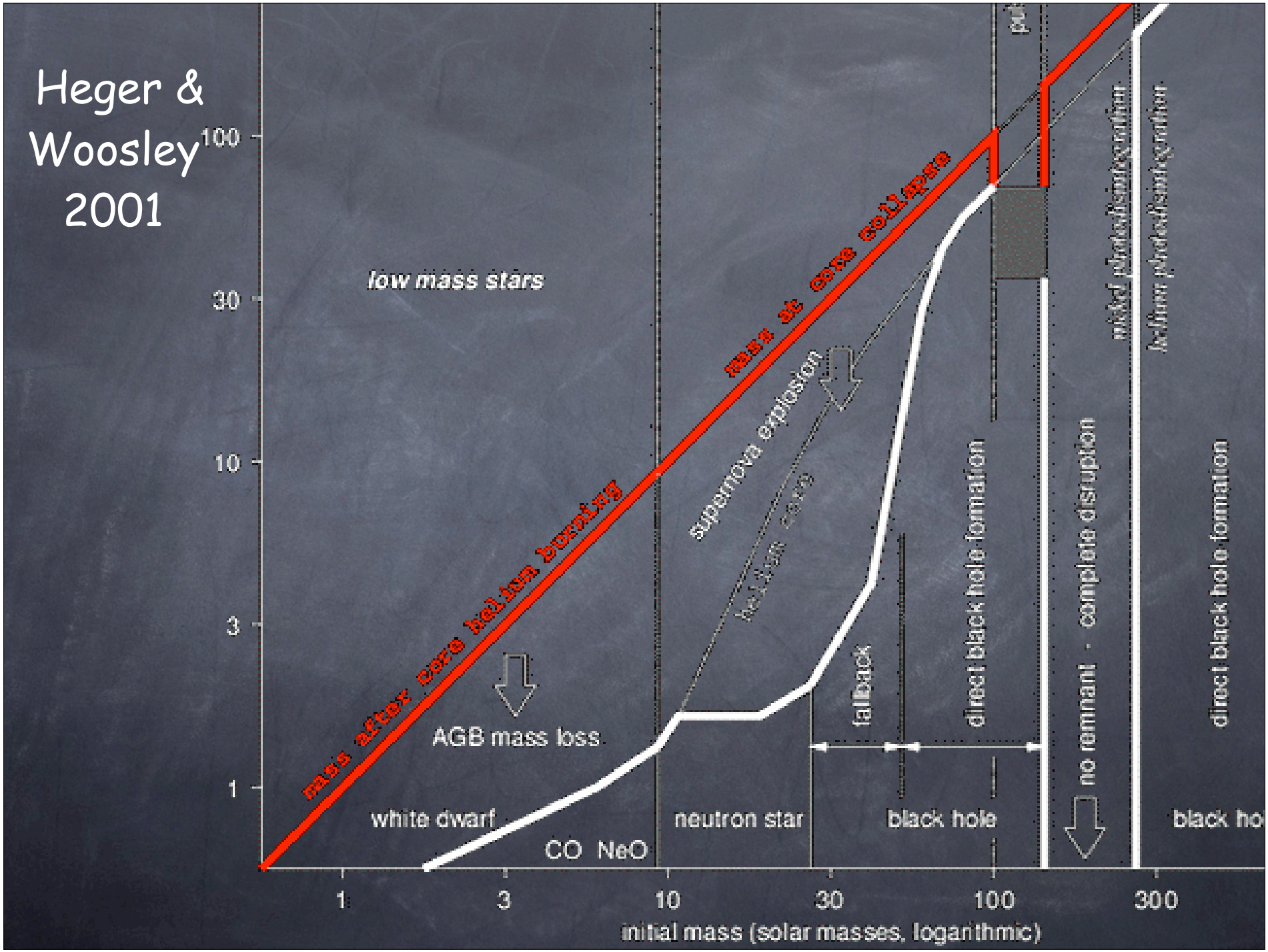

Initial Conditions

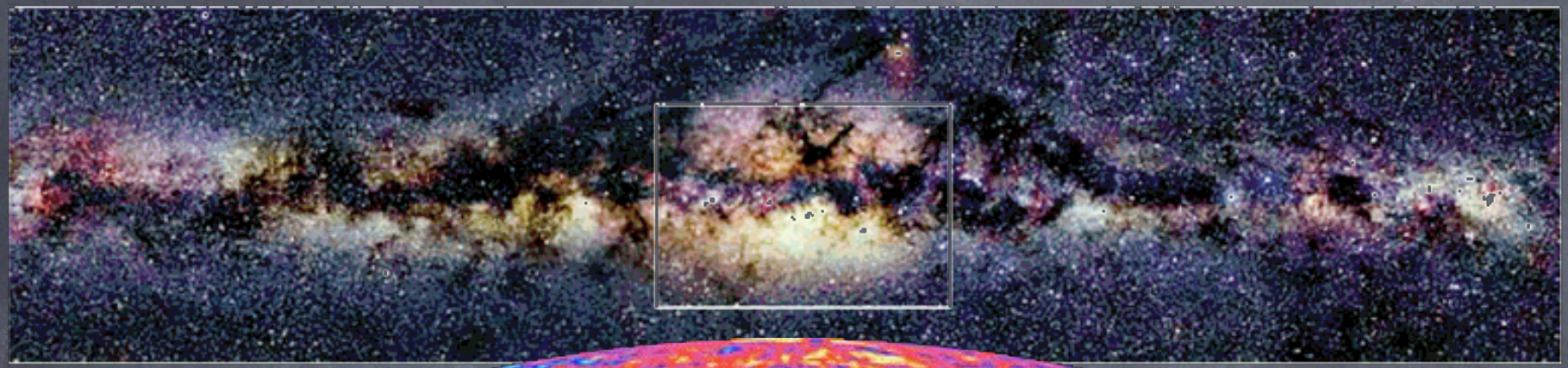

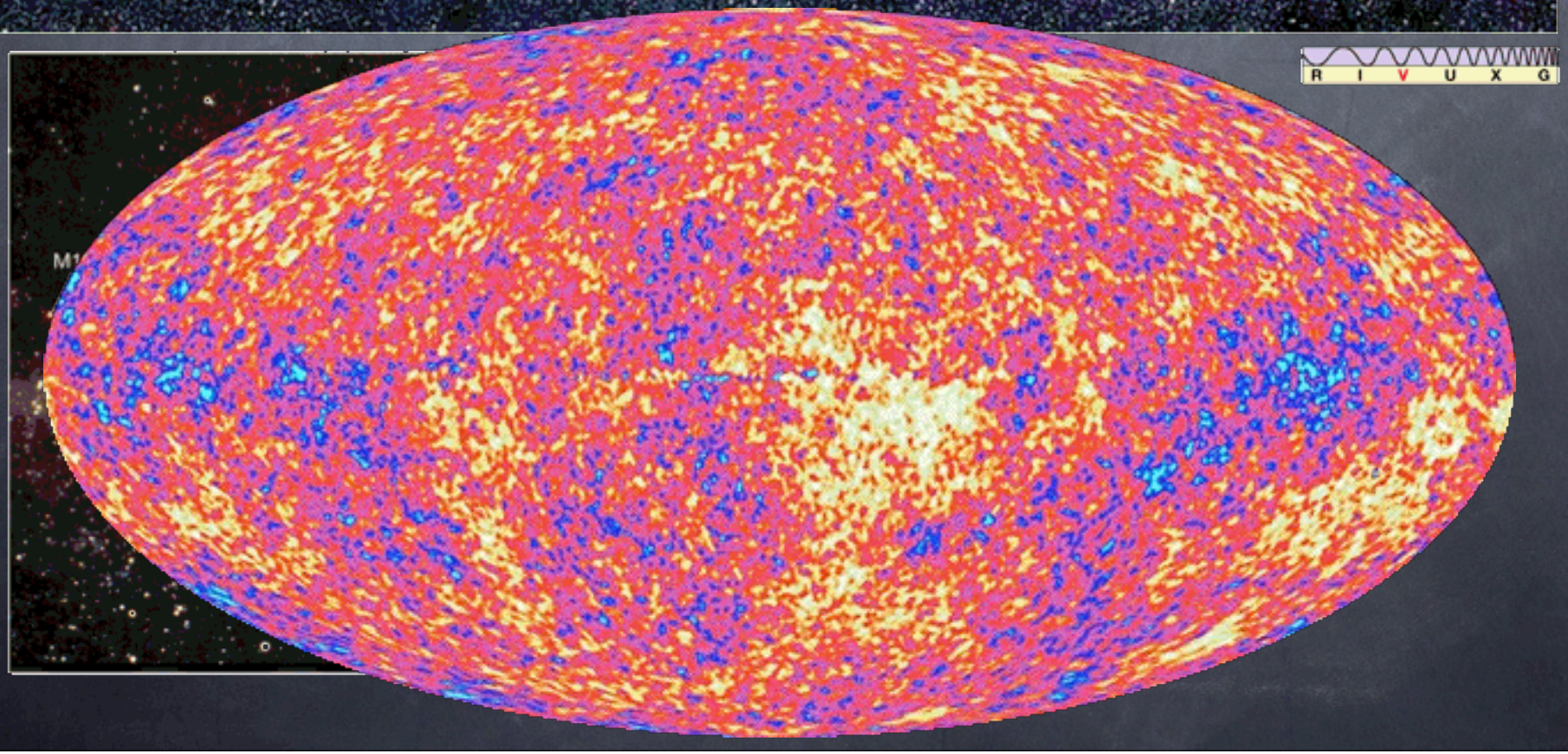

Given LCDM, First Structure Formation is a straightforward physics problem:

Ralf Kähler & Tom Abel for PBS

- Initial conditions statistically specified
- Simple but non-linear physics
  - Gravity, hydrodynamics, non-equilibirum chemistry, optically thin radiative processes
- Complex because of large range of scales required

$$\frac{\mathbf{R_{\odot}}}{\mathbf{R_{MilkyWay}}} \approx \mathbf{10^{-12}} \qquad \frac{\mathbf{P_{\odot,Kepler}}}{\mathbf{t_{Hubble}(z=30)}} \approx \mathbf{10^{-12}}$$

Time Evolution

Z=100 Z=24 Z=20.4

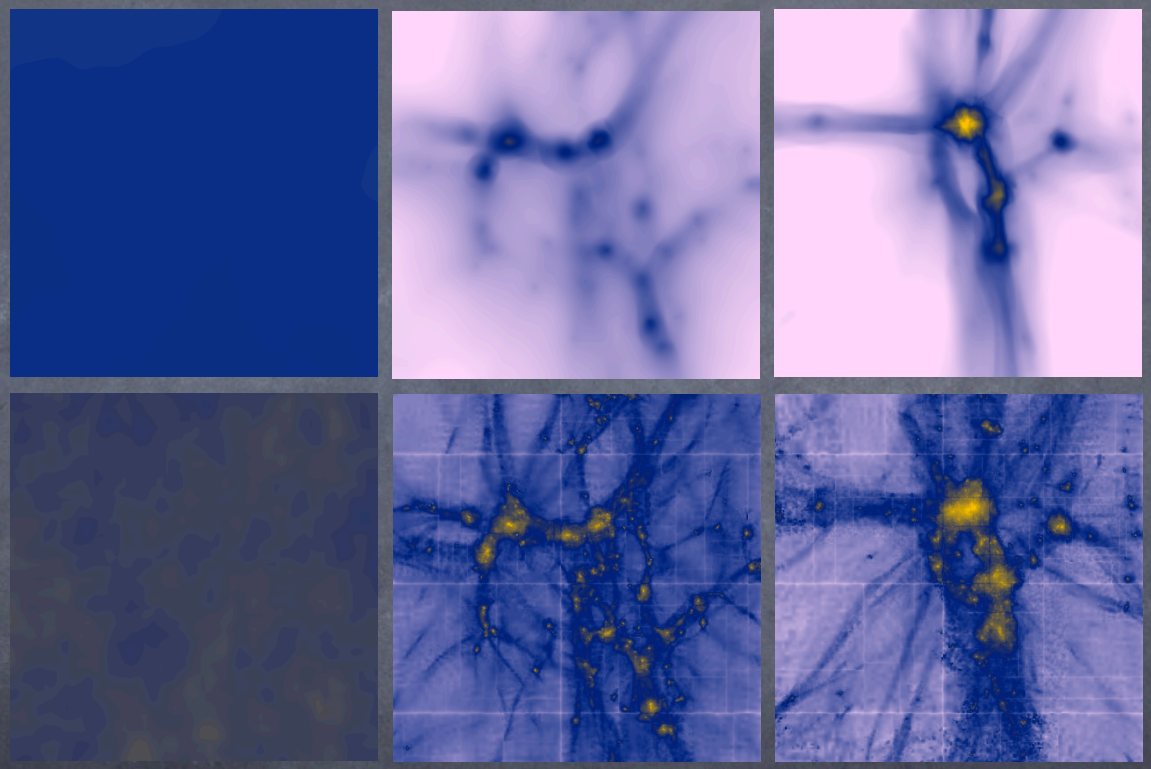

10 comoving kpc

Cosmological Jeans mass ~ 1e4 M

12 comoving kpc on a side, projection of 0.001 of the simulation volume

Primordial Gas Chemistry

-Cold Intergalactic Gas falls into DM potential wells

-associated adiabatic heating allows for chemistry

(1)	H	$+$	e^-	$\rightarrow H^+$	$+$	$2e^-$	(10)	H_2^+	$+$	H	$\rightarrow H_2$	$+$	H^+
(2)	H^+	$+$	e^-	$\rightarrow H$	$+$	$h\nu$	(11)	H_2	$+$	H^+	$\rightarrow H_2^+$	$+$	H
(3)	He	$+$	e^-	$\rightarrow He^+$	$+$	$2e^-$	(12)	H_2	$+$	e^-	$\rightarrow 2\ H$	$+$	e^-
(4)	He^+	$+$	e^-	$\rightarrow He$	$+$	$h\nu$	(13)	H_2	$+$	H	$\rightarrow 3\ H$		
(5)	He^+	$+$	e^-	$\rightarrow He^{++}$	$+$	$2e^-$	(14)	H^-	$+$	e^-	$\rightarrow H$	$+$	$2e^-$
(6)	He^{++}	$+$	e^-	$\rightarrow He^+$	$+$	$h\nu$	(15)	H^-	$+$	H	$\rightarrow 2\ H$	$+$	e^-
(7)	H	$+$	e^-	$\rightarrow H^-$	$+$	$h\nu$	(16)	H^-	$+$	H^+	$\rightarrow 2\ H$		
(8)	H	$+$	H^-	$\rightarrow H_2$	$+$	e^-	(17)	H^-	$+$	H^+	$\rightarrow H_2^+$	$+$	e^-
(9)	H	$+$	H^+	$\rightarrow H_2^+$	$+$	$h\nu$	(18)	H_2^+	$+$	e^-	$\rightarrow 2\ H$		
(10)	H_2^+	$+$	H	$\rightarrow H_2$	$+$	H^+	(19)	H_2^+	$+$	H^-	$\rightarrow H_2$	$+$	H

$3H \rightarrow H_2 + H$

Abel, Anninos, Zhang, & Norman 1997, NewA

Under the Assumption of Cold Dark Matter dominated Structure Formation Models there are no Free Parameters in our Calculation

No knobs! That's rare ...

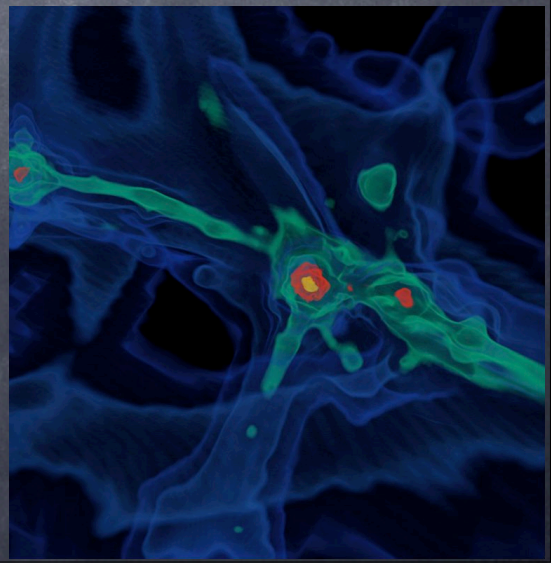

the first stars

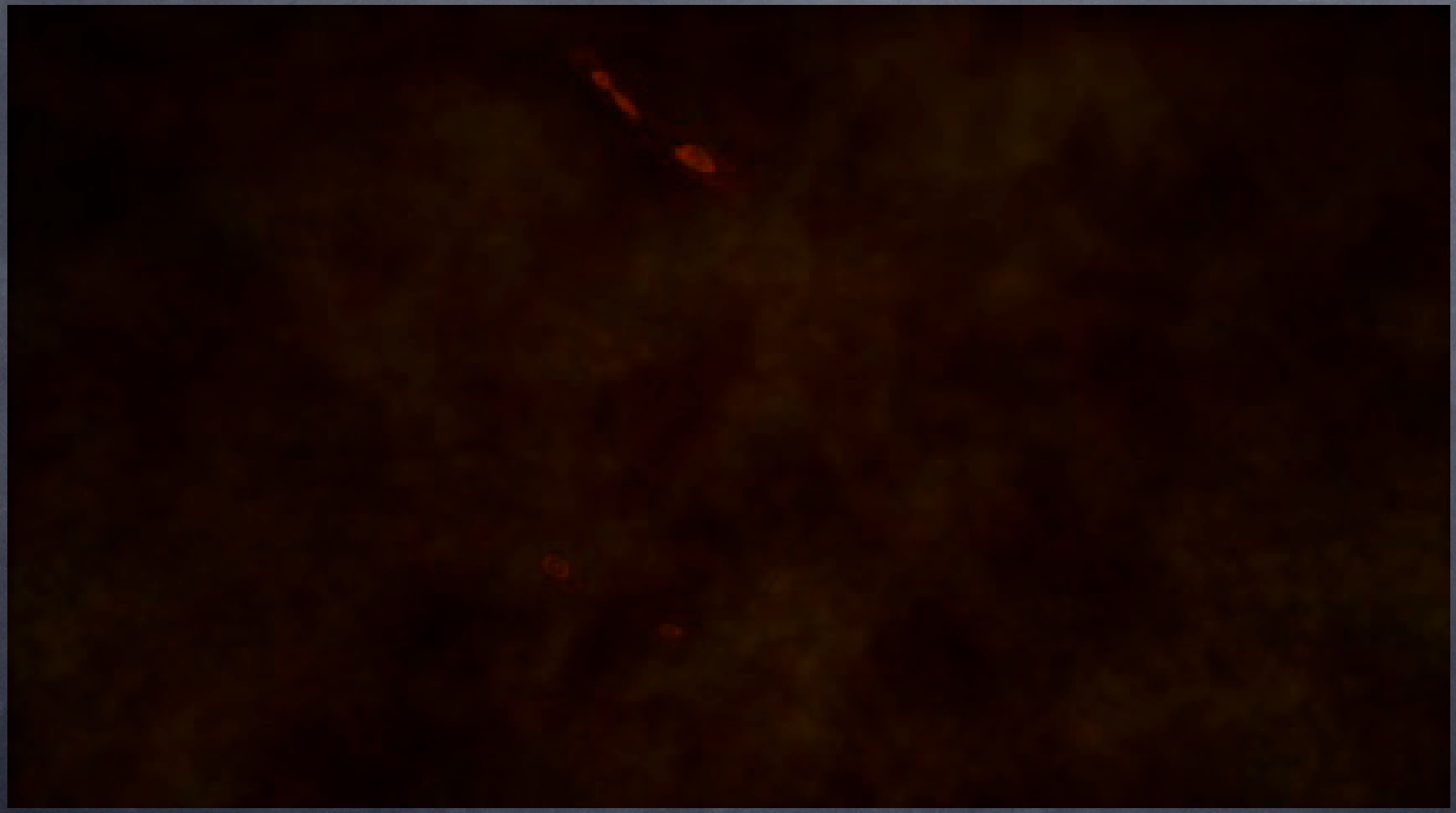

Simulation: Tom Abel (PSU), Greg Bryan (Oxford), Mike Norman (UCSD)
Viz: Ralf Kähler (AEI, ZIB), Bob Patterson, Stuart Levy, Donna Cox (NCSA), Tom Abel (PSU)
© "The Unfolding Universe" Discovery Channel 2002

Accretion Time

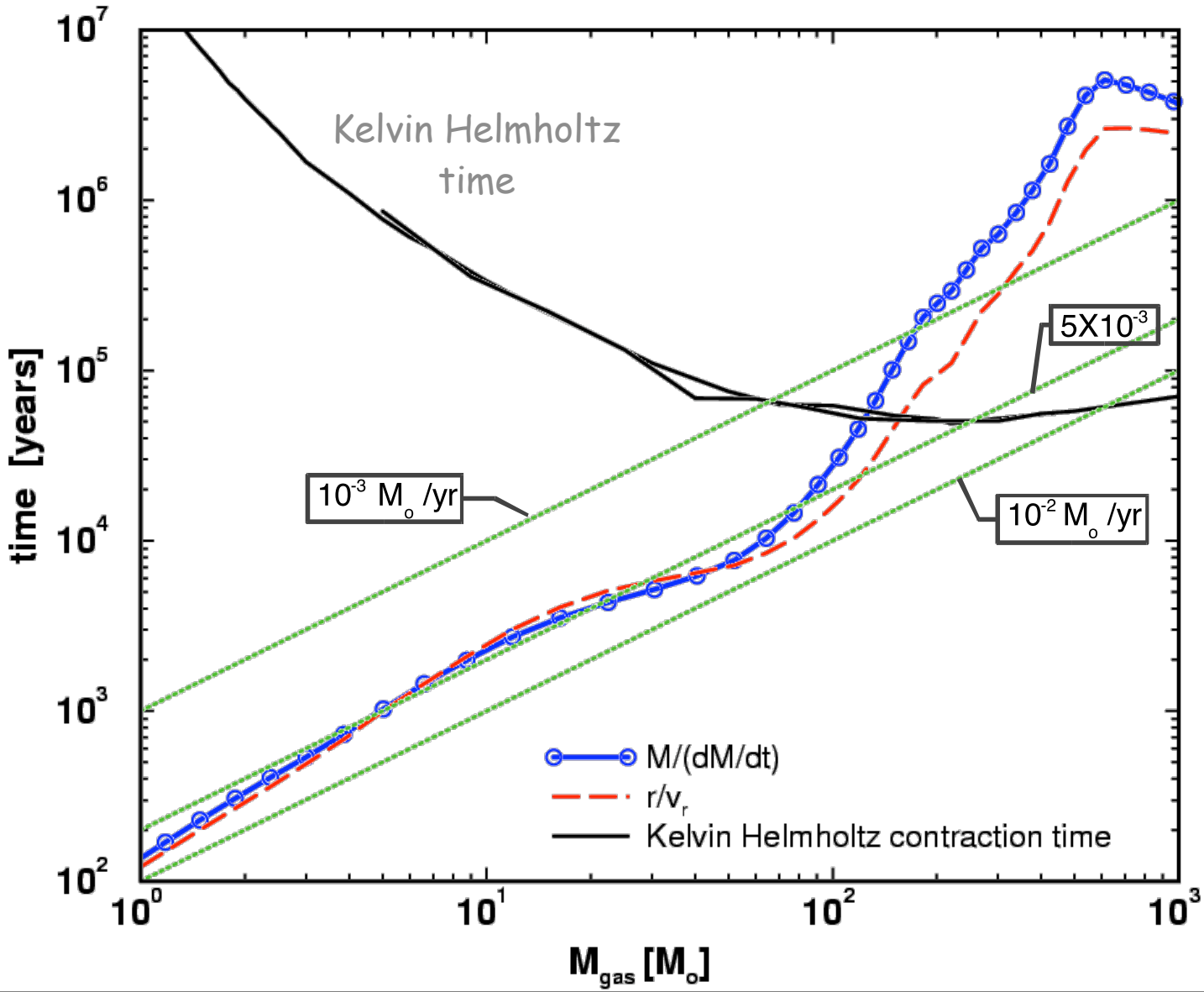

Collision Induced Emission
Stark Effect

New (thermal) instability at n>1e15 cm^-3

H2-H2 collision create temporary dipole moment that can absorb (CIA) or emit photons (CIE)

Emergence of a Planck spectrum.

Optically thin "between" the lines.

Typical mass scale five Jupiter masses

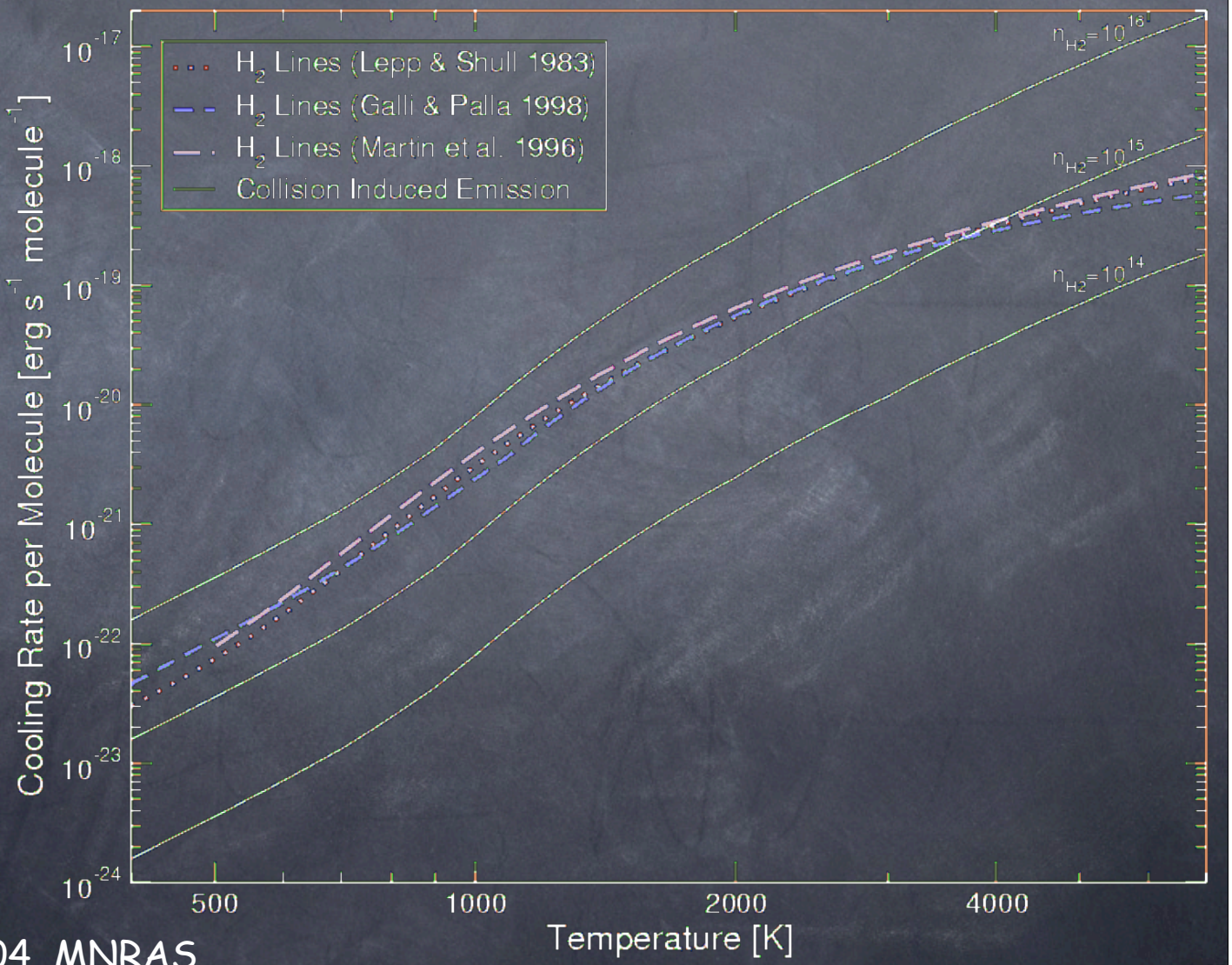

Ripamonti & Abel 2004, MNRAS

Predictable effects of radiative transfer!

Given local density and temperature one can estimate the size of the core one is in. This gives an optical depth which agrees remarkably well with numerical full radiation hydro calculations.

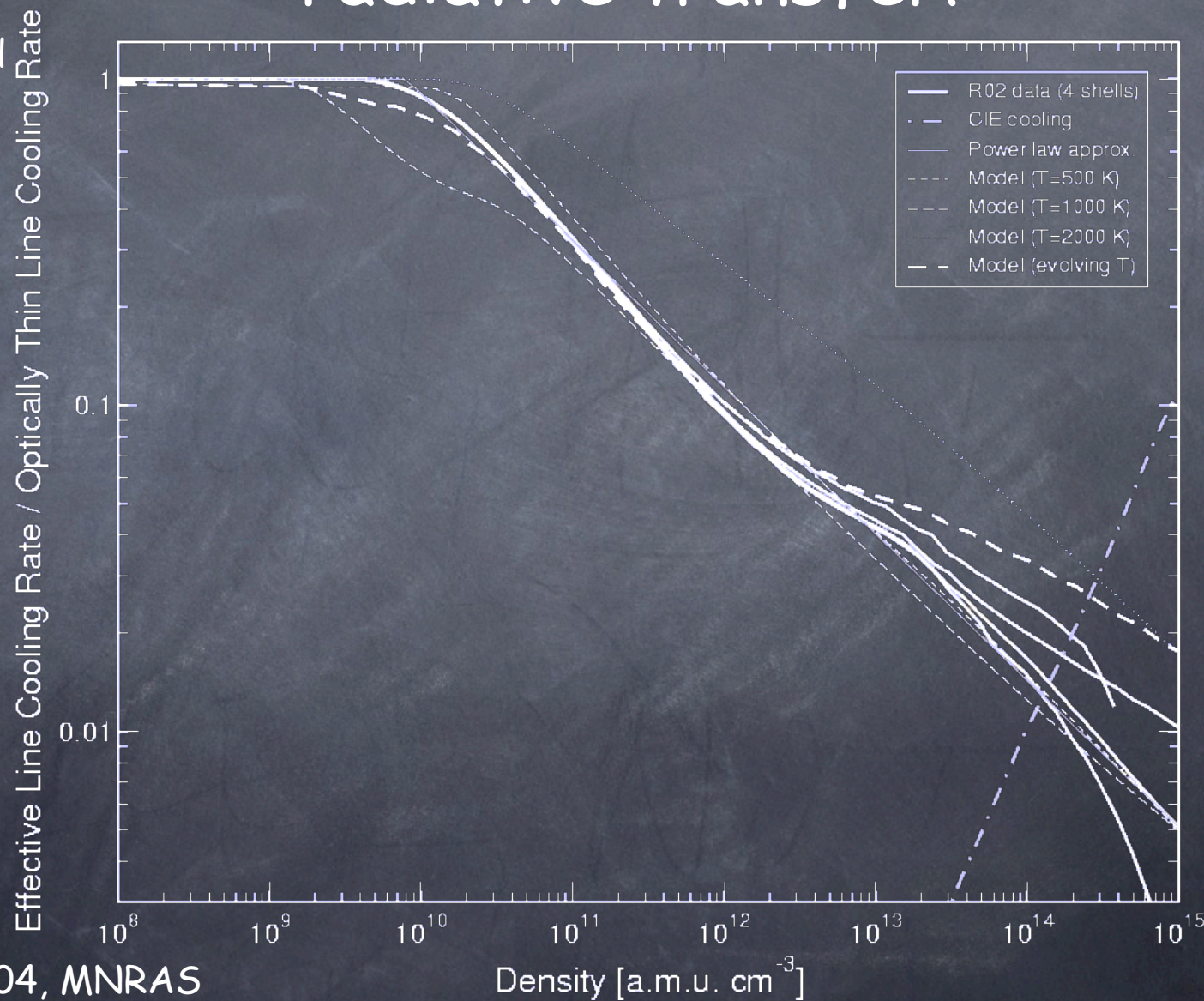

Ripamonti & Abel 2004, MNRAS

Works great in 1D!

- Evolution of 4 different shells.
- One time with full radiative transfer of hundreds molecular lines one time with, a one line cooling function modification
- Factor 100 in execution speed

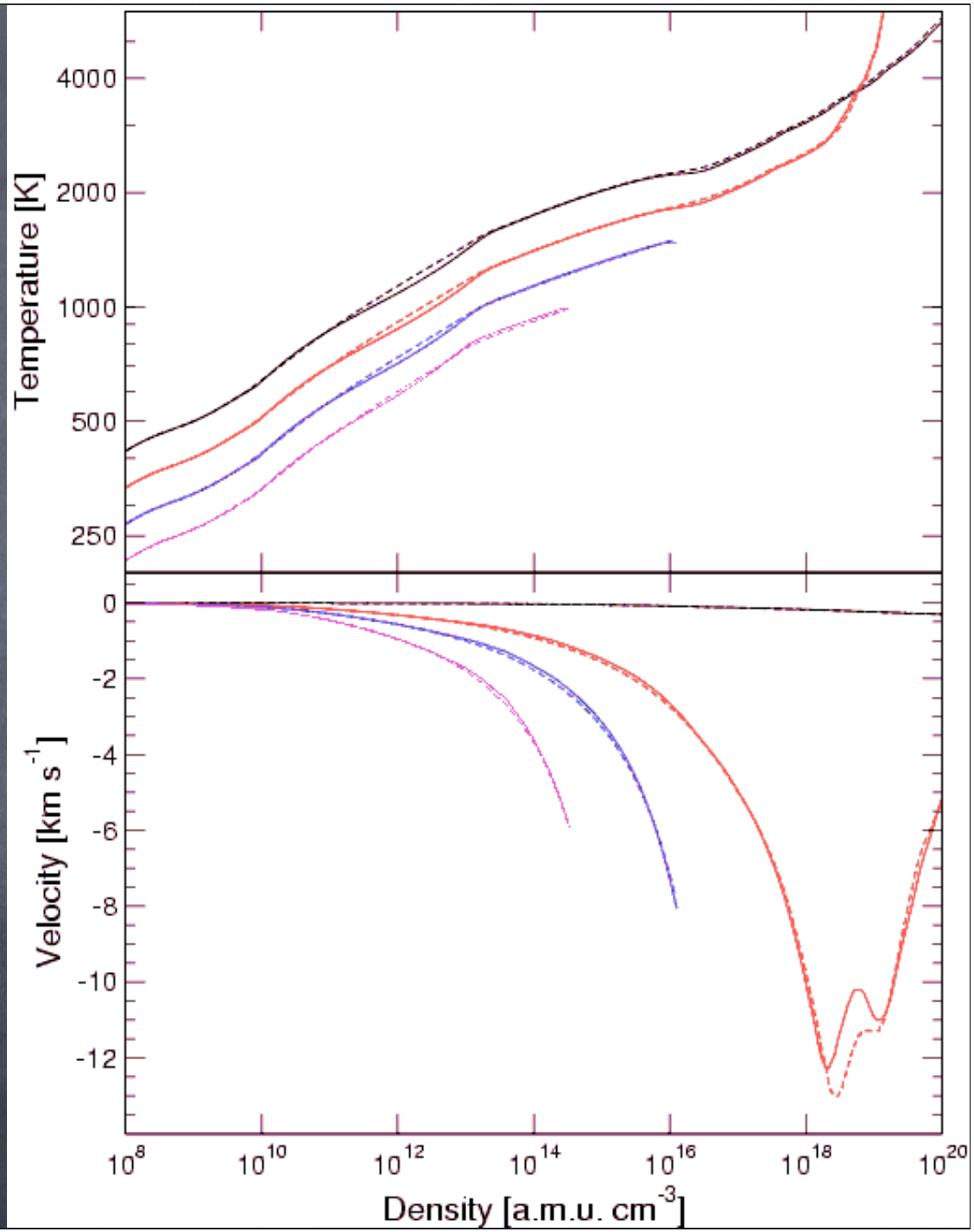

Chemo-thermal instability analysis

- Hoyle 1950, Sabano & Yoshi 1977, Silk 1983, Omukai & Yoshi 2004, Ripamonti & Abel 2004
- Linearize hydro equations -> dispersion relation
- fluctuation growth time scale always 10 times larger than their free fall time

$$C < 0$$

$$A\omega^2 + B\omega + C = 0$$

$$\begin{aligned} C = & -\frac{\mu m_{\rm H}}{k_{\rm B}T}(T\mathcal{L}_T - \rho\mathcal{L}_\rho - \mathcal{L})(\mathcal{F}_f + \frac{\mu}{2}\rho\mathcal{F}_\rho + \frac{\mathcal{F}}{2-f_{\rm H_2}}) \\ & + \frac{\mu m_{\rm H}}{k_{\rm B}T}(\mathcal{L}_f + \frac{\mu}{2}\rho\mathcal{L}_\rho + \frac{1}{6-f_{\rm H_2}}\mathcal{L})(T\mathcal{F}_T - \rho\mathcal{F}_\rho) \\ & + \frac{\mu}{2}\mathcal{F}\left[\frac{\mu}{3-f_{\rm H_2}/2}(\frac{1}{2} + \frac{\chi}{k_{\rm B}T})(T\mathcal{F}_T - \rho\mathcal{F}_\rho) - \frac{\chi}{k_{\rm B}T}(\mathcal{F}_f + \frac{\mu}{2}\rho\mathcal{F}_\rho + \frac{\mathcal{F}}{2-f_{\rm H_2}})\right] \\ & + \frac{\mu}{(3-f_{\rm H_2}/2)t_{\rm ff}}(T\mathcal{F}_T - \rho\mathcal{F}_\rho), \end{aligned}$$

Why there can be only one

- Small DM potential drives cold gas to center, cooling flow rather than molecular cloud formation
- Cooling time longer than dynamical time
- Inefficient H2 cooling allows pressure to smooth out density perturbations
- 3 H → H2 does not lead to fragmentation, initial isobaric contraction is weak because of the same cut off temperature, no independent Jeans unstable fragments form.
- Feedback from first star gives others no chance

Can be understood analytically:

Ripamonti & Abel 2004 MNRAS

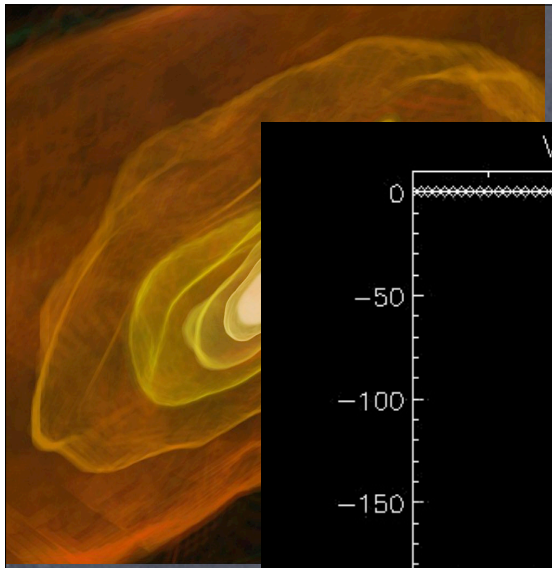

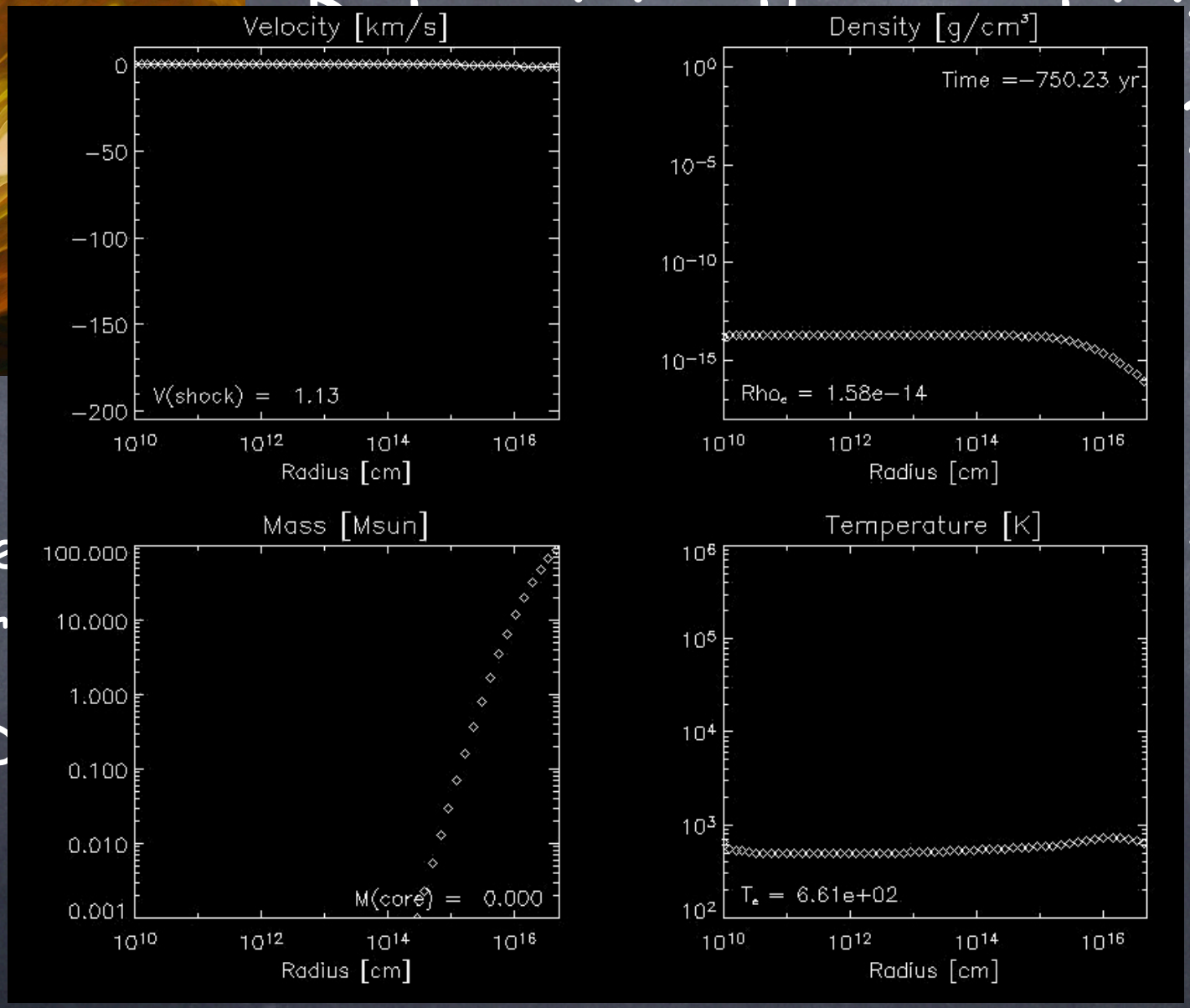

1D implicit adaptive radiation hydrodynamics Ripamonti & Abel

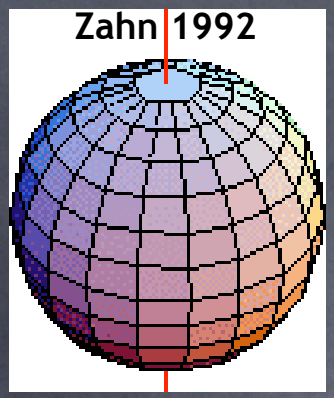

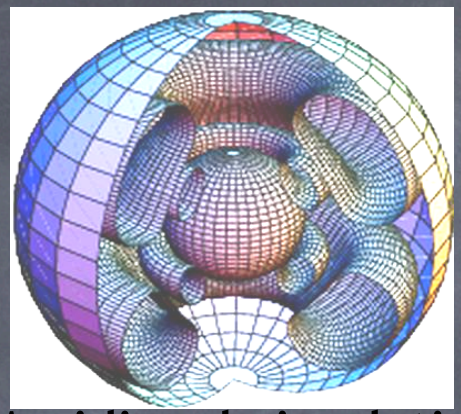

Meridional circulation

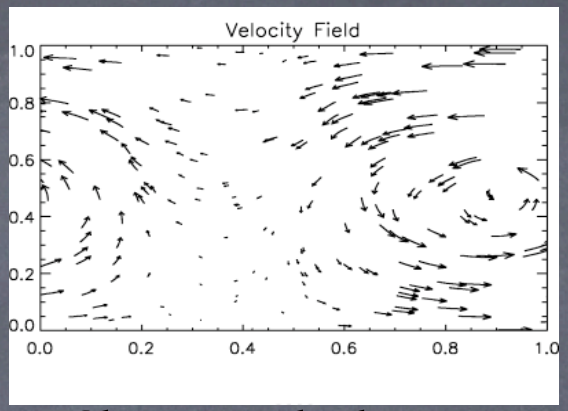

Shear turbulence

Transport of the angular momentum

$$\rho \frac{\partial (r^2 \Omega)}{\partial t} = \frac{1}{5r^2} \frac{\partial}{\partial r} \left(\rho r^4 U \Omega \right) + \frac{1}{r^2} \frac{\partial}{\partial r} \left(\rho r^4 D_{schear} \frac{\partial \Omega}{\partial r} \right)$$

Transport of the chemical species

$$\rho \frac{\partial X_i}{\partial t} = \frac{1}{r^2} \frac{\partial}{\partial r} \left[\rho r^2 (D_{eff} + D_{schear}) \frac{\partial X_i}{\partial r} \right]$$

- Effects of rotation?
- Rotation and perhaps even line driven winds?
- Dynamo? Yields, ...

Z = 0.020

60 M_{sol} V_{ini} = 300 km/s

$$\frac{\Omega}{\Omega_c} = 0.50$$

PopIII

60 M_{sol} V_{ini} = 300 km/s

$$\frac{\Omega}{\Omega_c} = 0.29$$

$$\frac{\Omega}{\Omega_c} = 0.50$$

V_{ini} ~ 800 km s^{-1}

Meynet & Maeder

Summary

- Massive isolated stars which are predicted by the simulations are so far are consistent with observations
- Rapidly expanding, “somewhat” new field
- Uses “all” of astrophysics to understand galaxy formation from the bottom up

Chemical Enrichment at $z=10^9$

An update of standard and nonstandard BBN

Kevork Abazajian
Los Alamos

Chemical Enrichment of the Early Universe
August 9 - August 13, 2004
Santa Fe, New Mexico

Do we know the chemical starting point?

- Observed abundances
- Standard success
- Extensions
  - neutrino overdensity (asymmetry)
  - multiple neutrinos (sterile?)
  - baryon inhomogeneity…

The Reaction Network

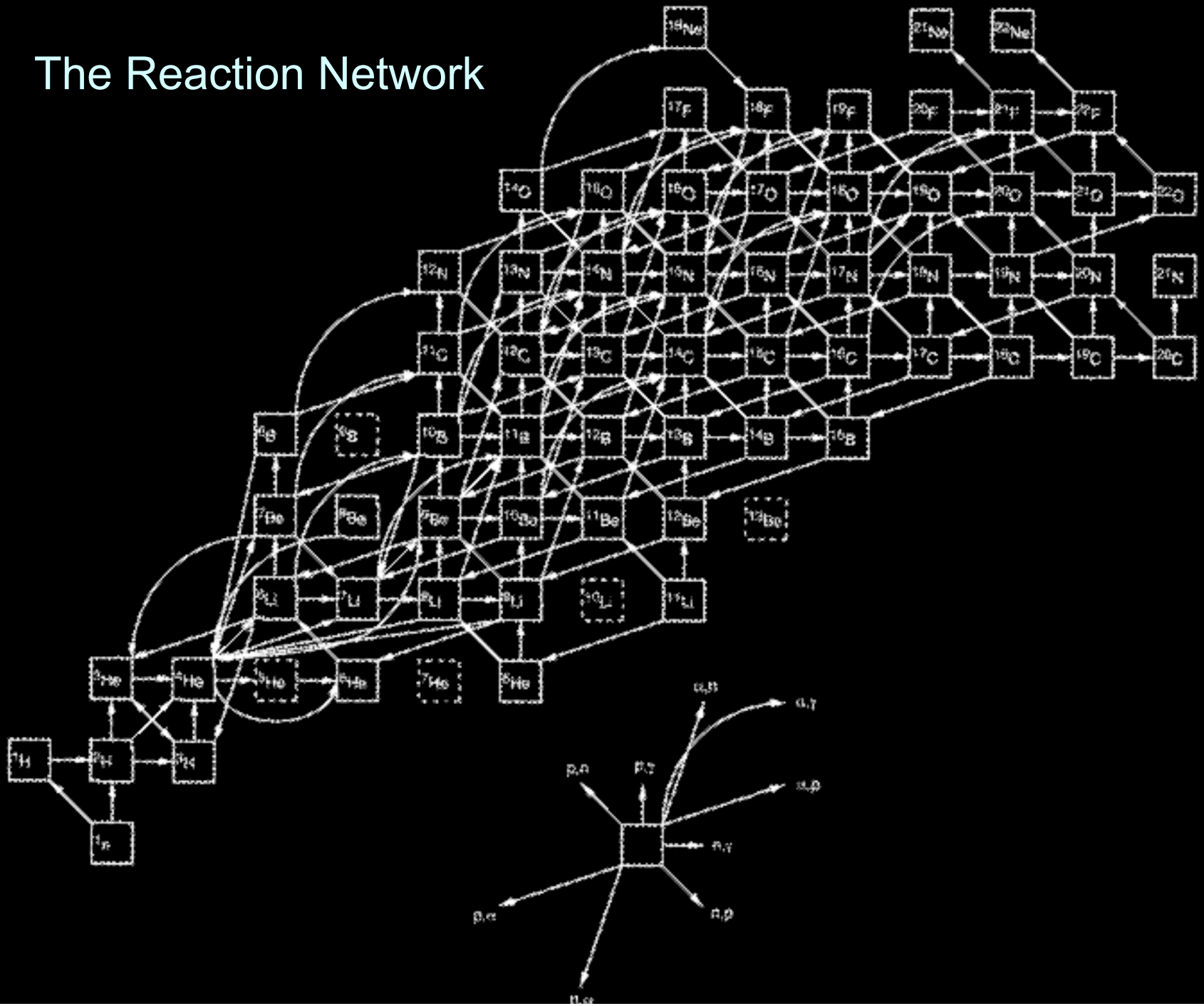

BBN Evolution

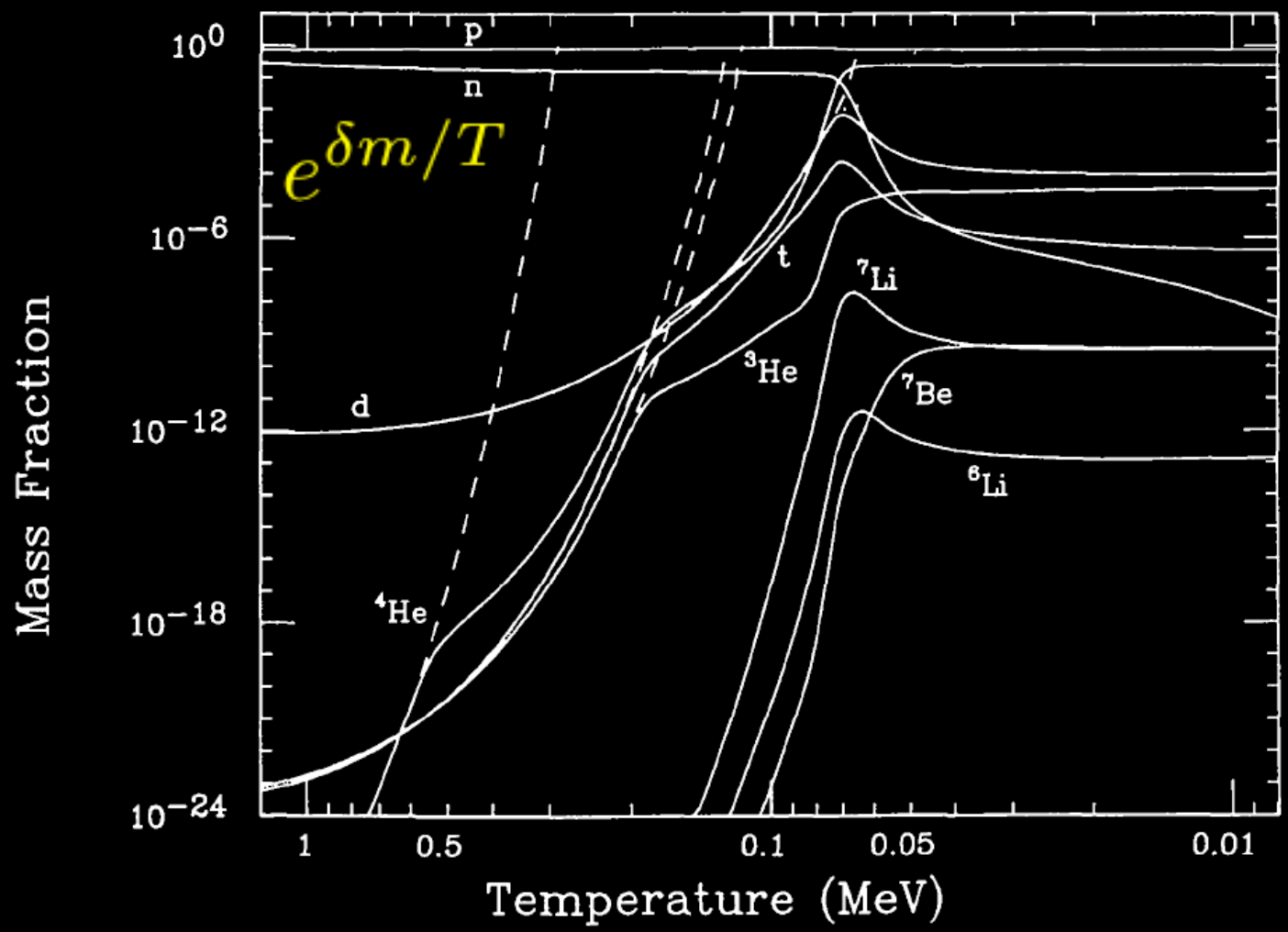

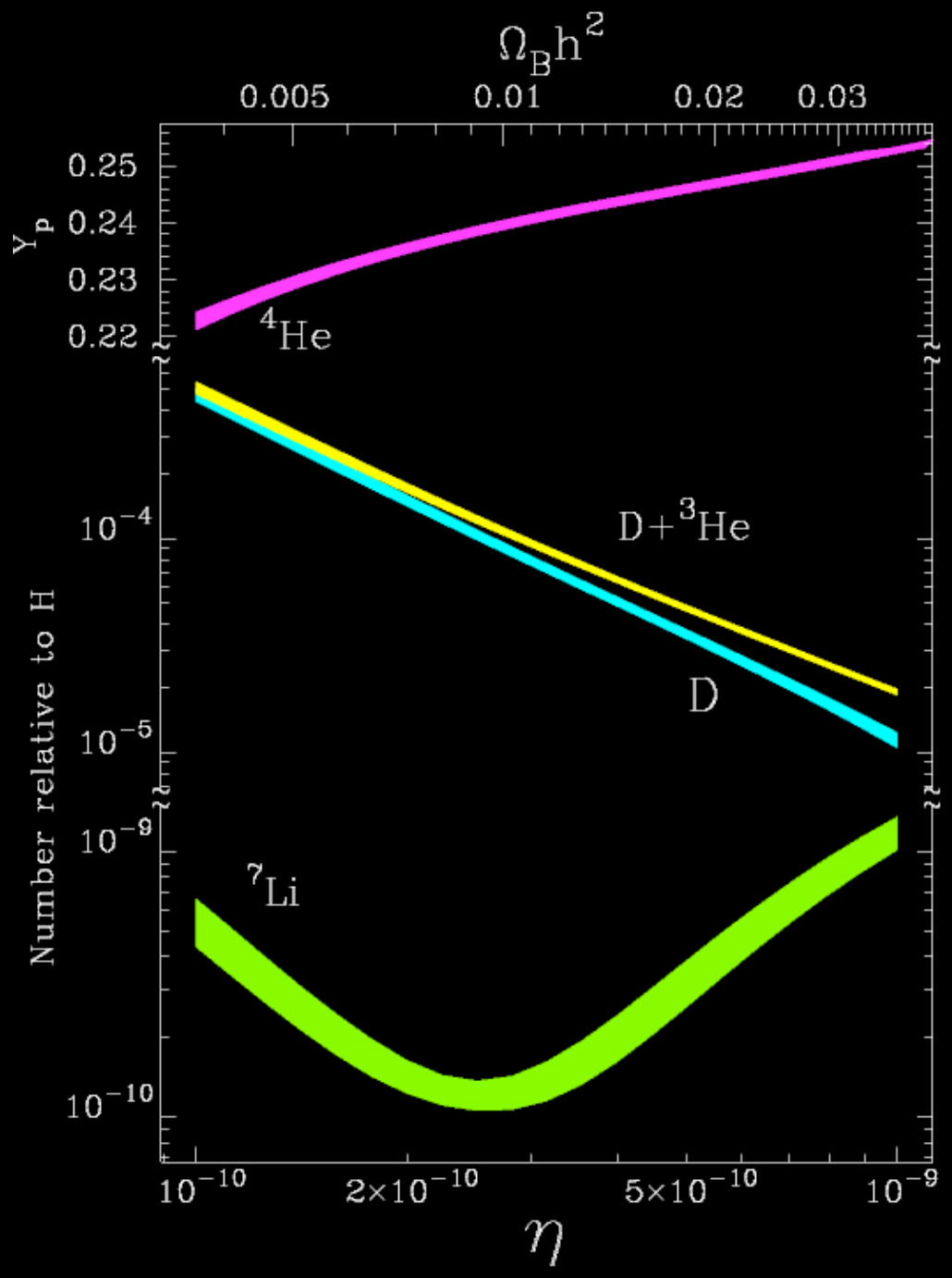
$\Omega_B h^2$
0.005
0.01
0.02
0.03
Y_p
0.25
0.24
0.23
0.22
^{4}He
10^{-4}
10^{-5}
10^{-9}
10^{-10}
D+^{3}He
D
^{7}Li
Number relative to H
10^{-10}
2×10^{-10}
5×10^{-10}
10^{-9}
η

Deuterium

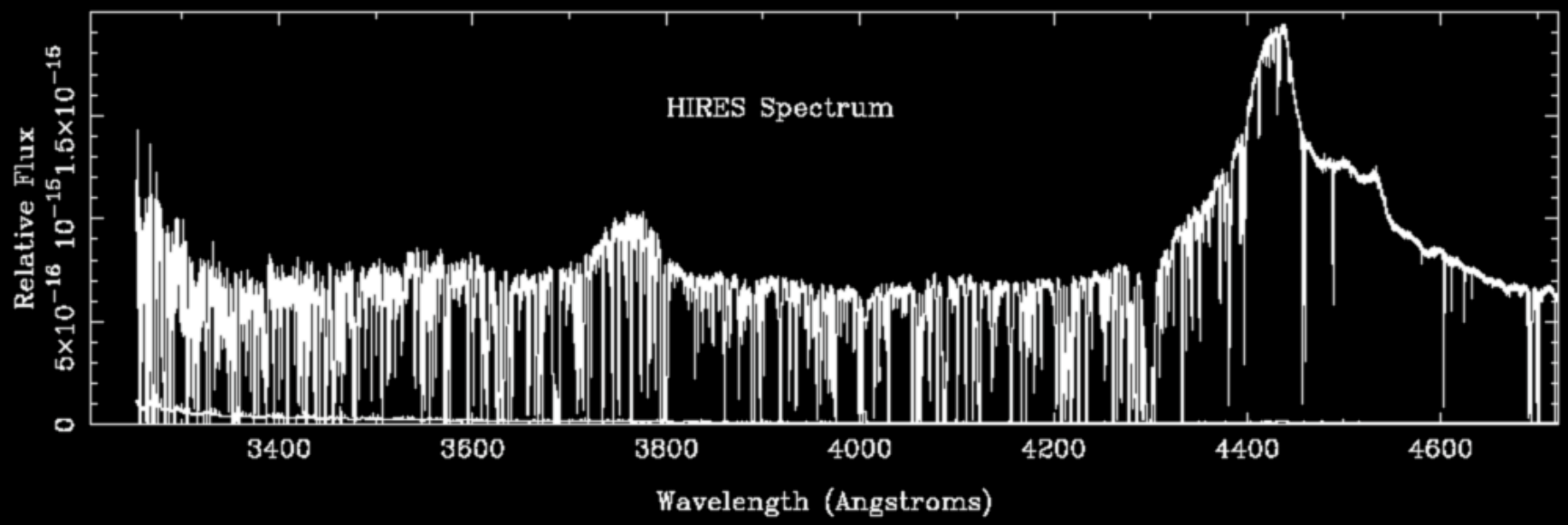
HIRES Spectrum
Relative Flux
0
5×10^-16
10^-15
1.5×10^-15
3400
3600
3800
4000
4200
4400
4600
Wavelength (Angstroms)

Deuterium

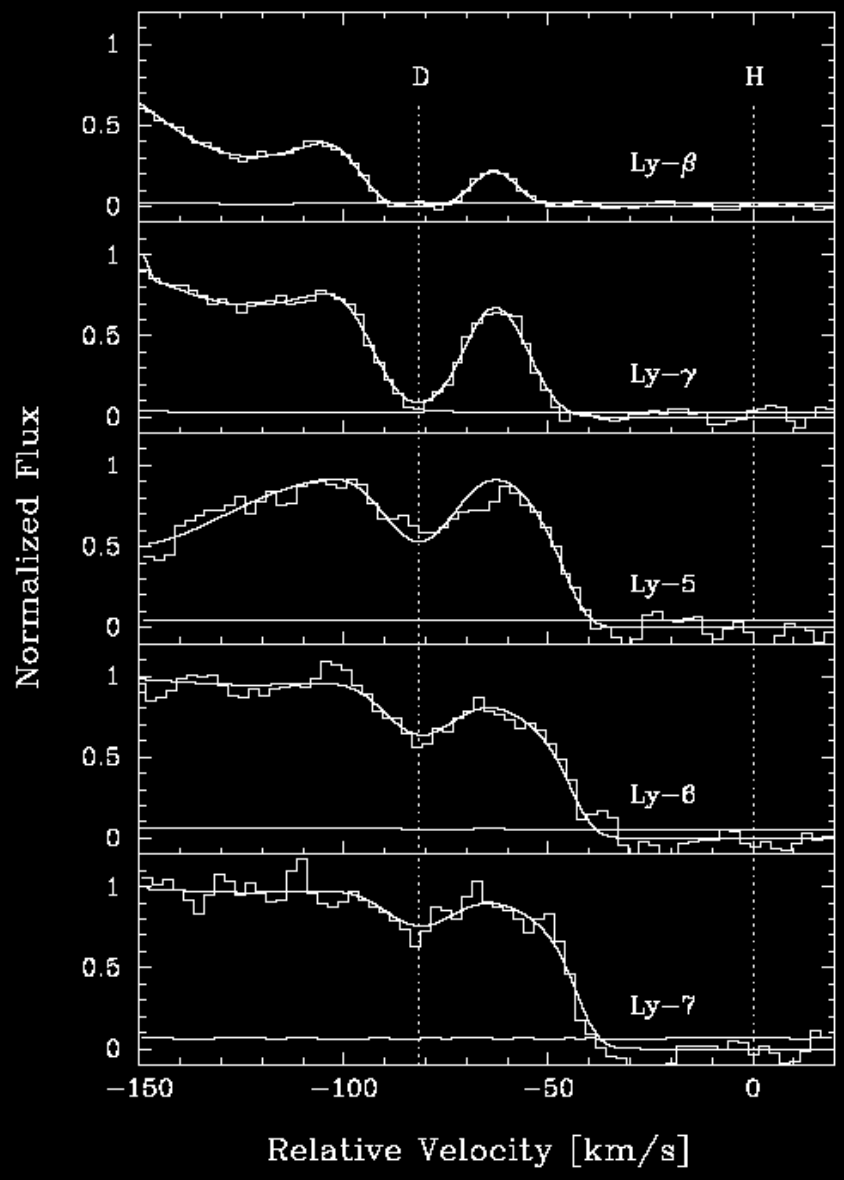

O'Meara et al 2001

Deuterium

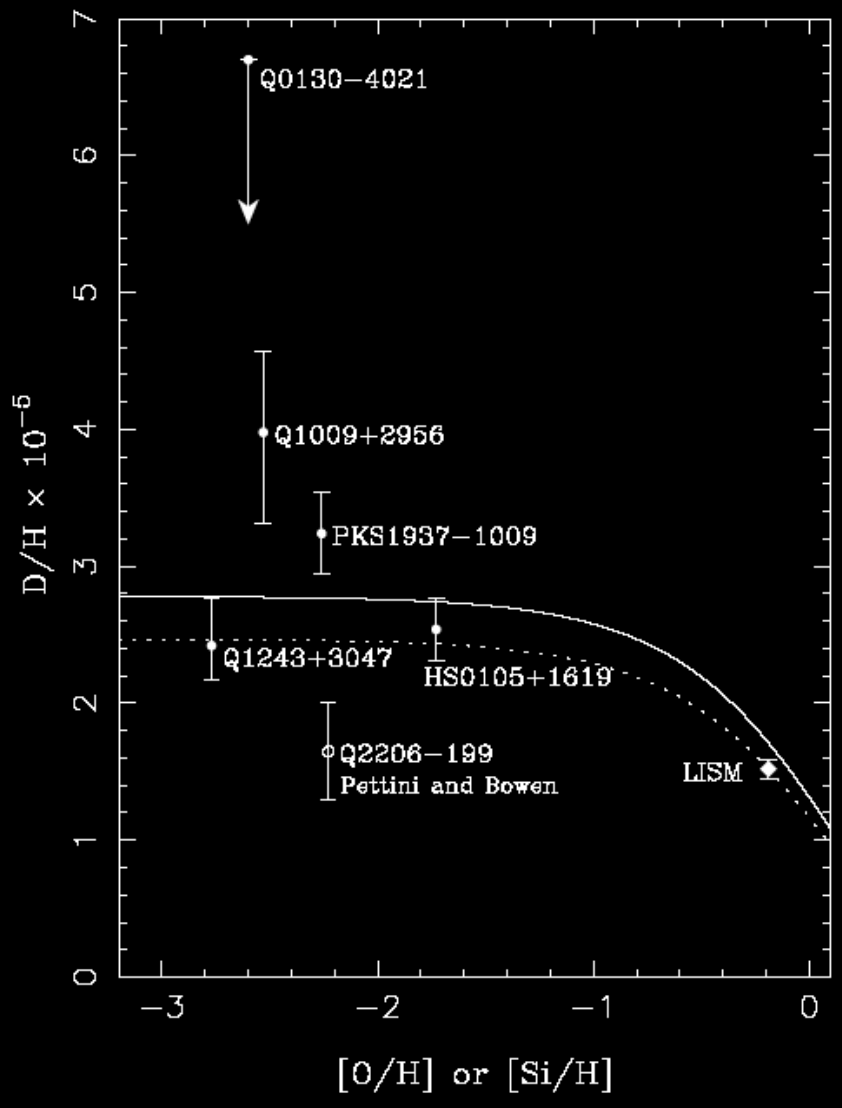

Kirkman et al 2003

$$\frac{\mathrm{D}}{\mathrm{H}} = 2.78^{+0.44}_{-0.38} \times 10^{-5}$$

Pop III population of intermediate mass stars? (Fields et al 2001)

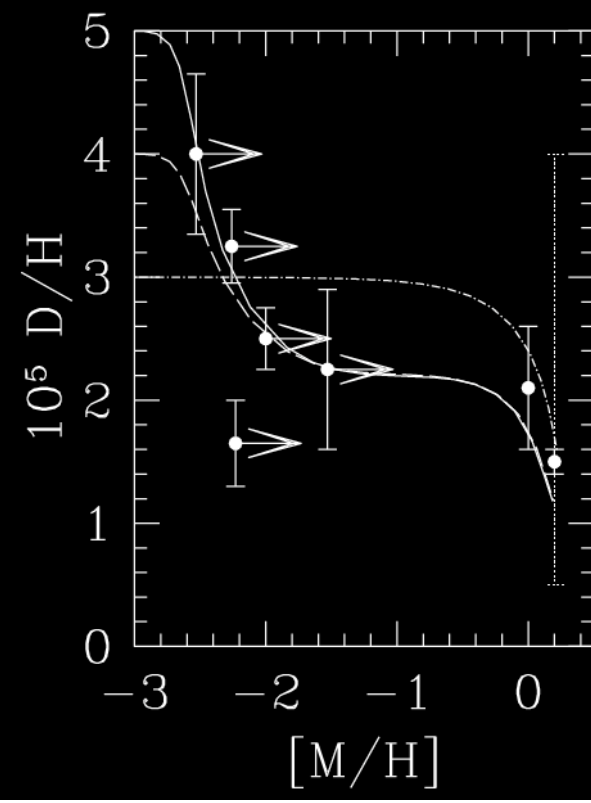

Helium - 4

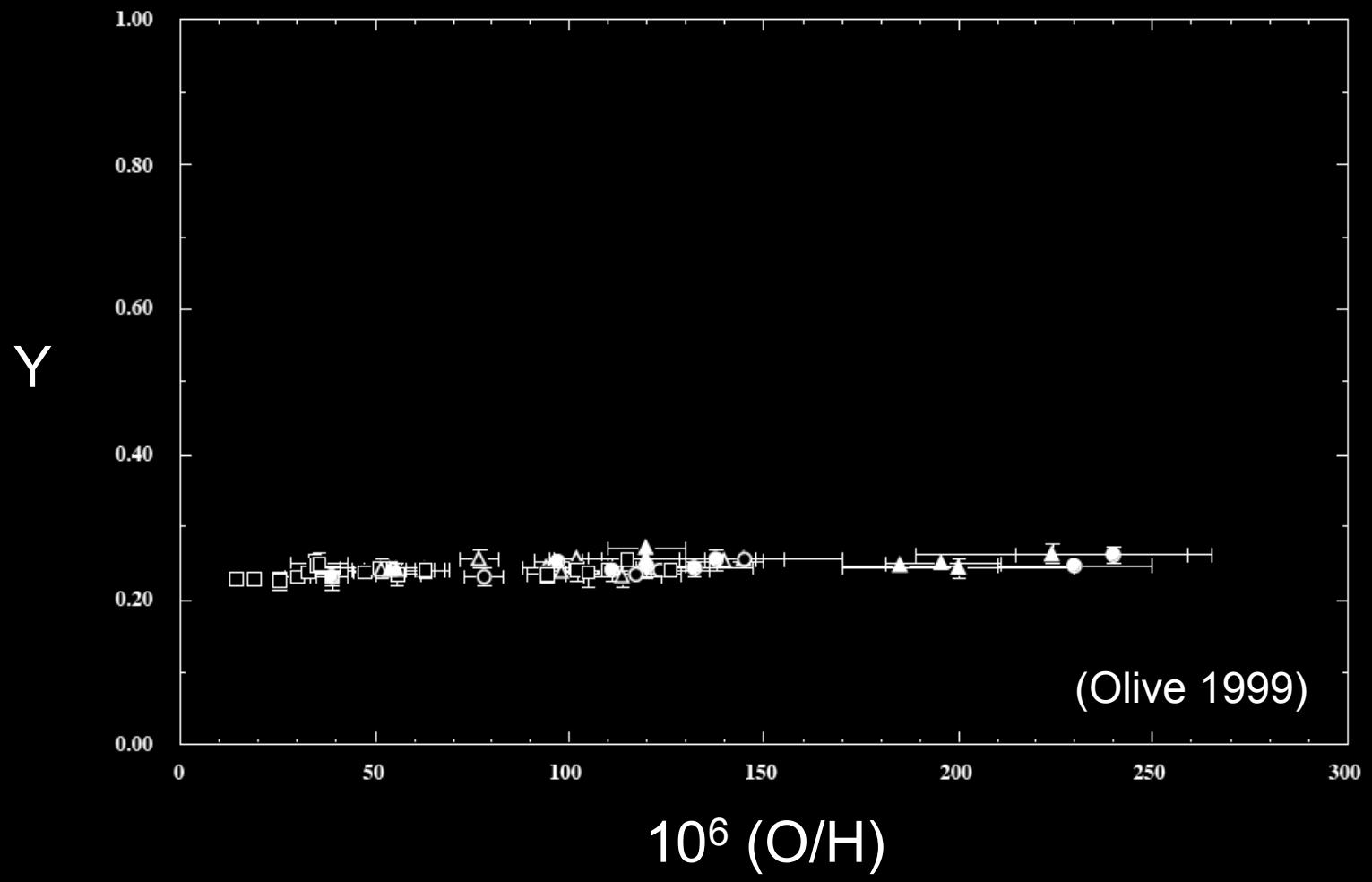

Observations of HII Regions in local metal poor compact blue galaxies

Helium - 4

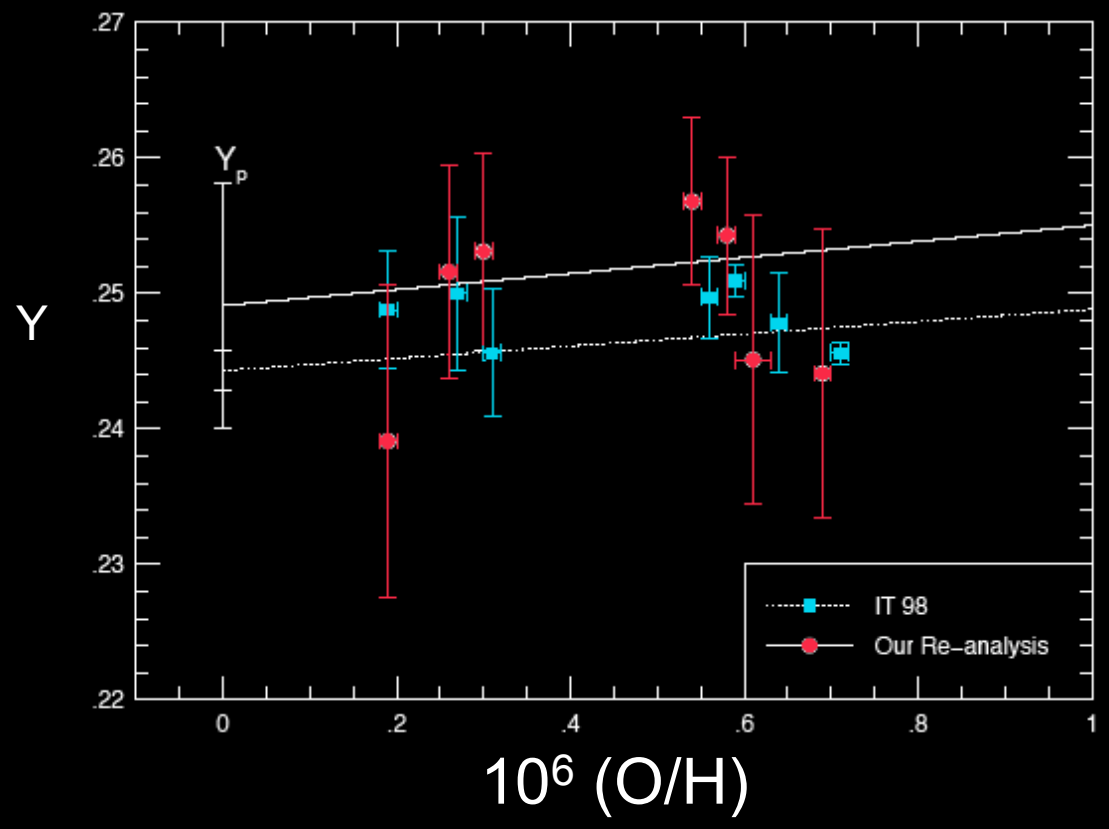

Olive & Skillman 2004:

Reanalyzed
Pagel et al 2000 and Izotov & Thuan 1998 spectra simultaneosly fitting H and He lines while varying temperature, density.

Use a Monte Carlo technique and find a second solution at low temperatures and high densities

$$0.232 \leq Y_p \leq 0.258$$

Lithium-7

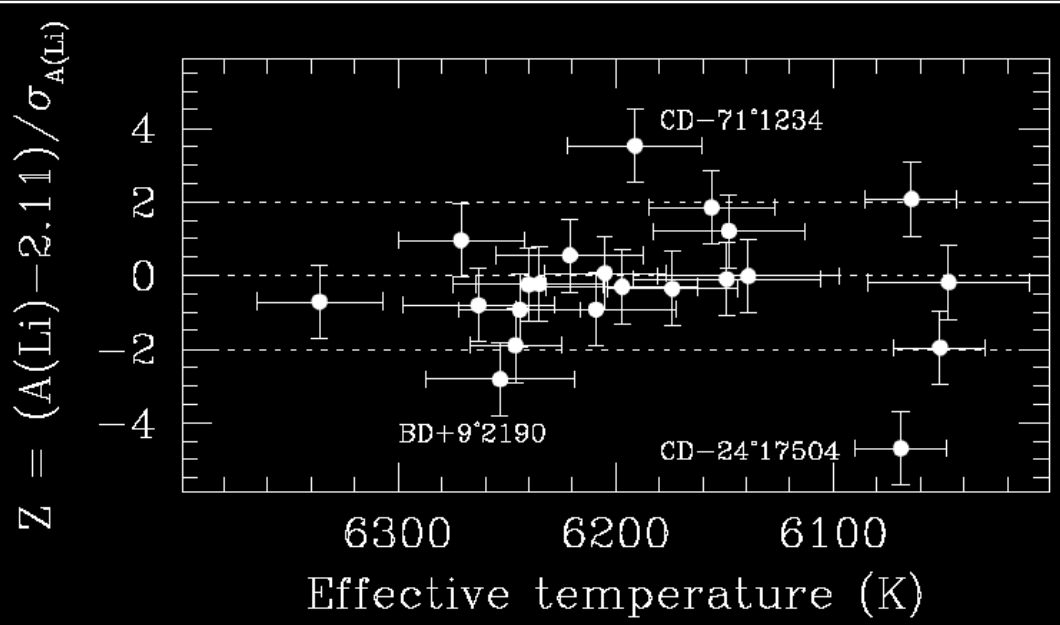

Ryan, Norris & Beers 1999

$$\frac{^7\mathrm{Li}}{\mathrm{H}} = 1.23^{+0.34}_{-0.16} \times 10^{-10}$$

Temperatures based on

$b-y, B-V, V-R, R-I, \beta$, and HP2

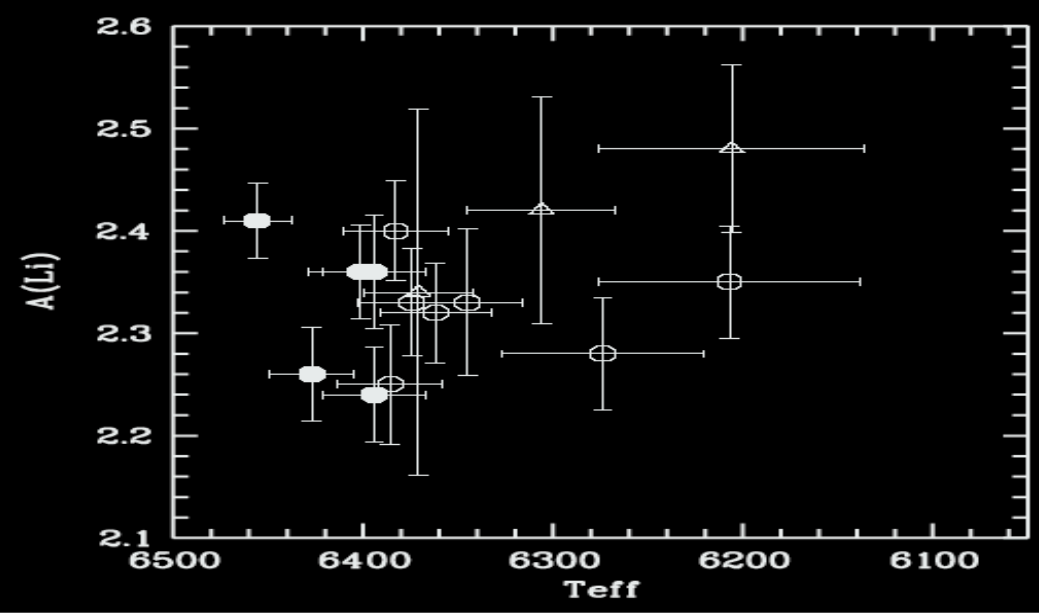

Bonifacio et al 2002

$$\frac{^7\mathrm{Li}}{\mathrm{H}} = (2.19 \pm 0.28) \times 10^{-10}$$

Temperatures based on Hα lines

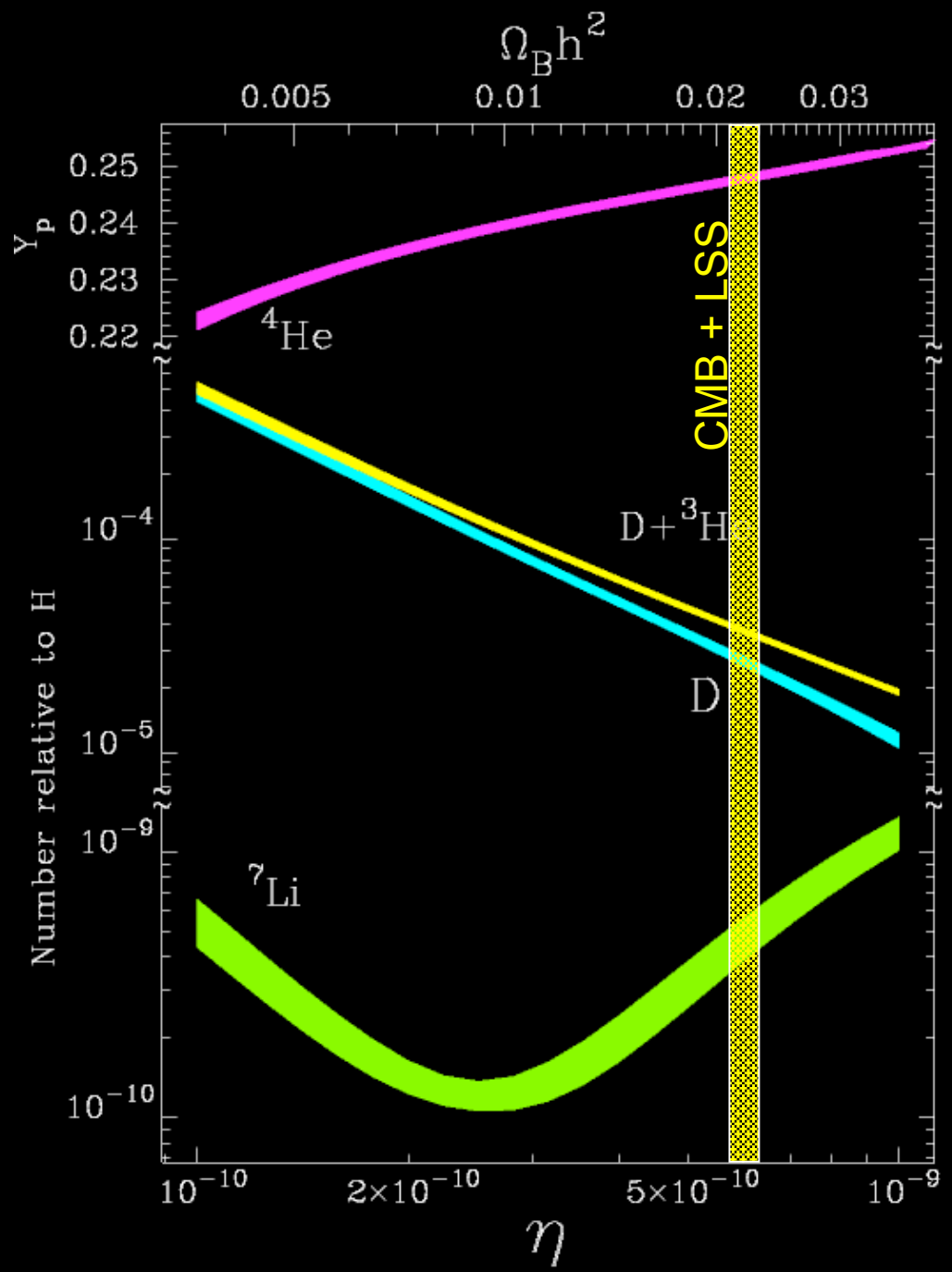

Standard
Big Bang Nucleosynthesis (BBN)
Predictions vs. Observations

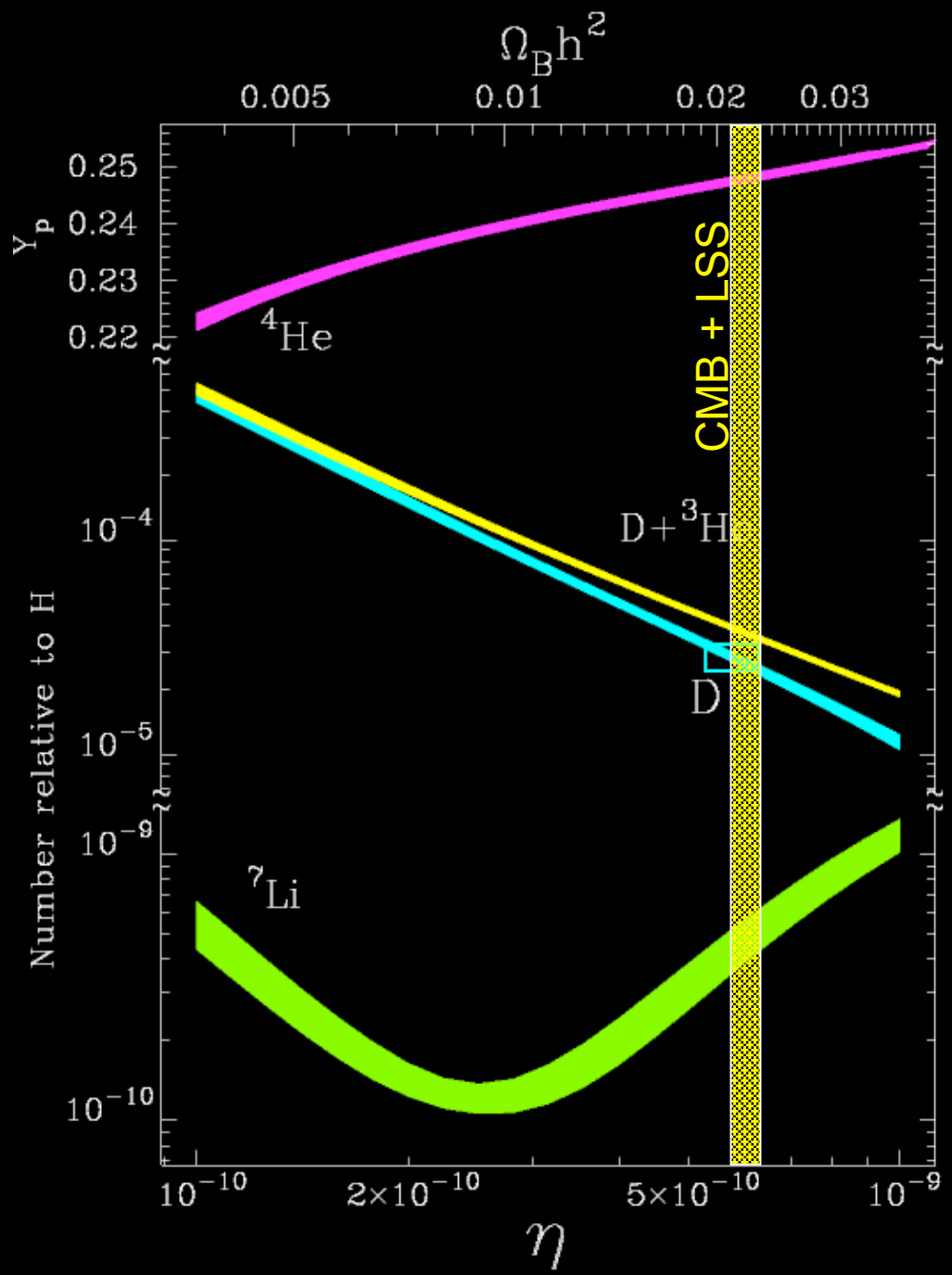

Standard
Big Bang Nucleosynthesis (BBN)
Predictions vs. Observations

Deuterium:

$$\frac{\mathrm{D}}{\mathrm{H}} = 2.78^{+0.44}_{-0.38} \times 10^{-5}$$

(Kirkman et al 2002)

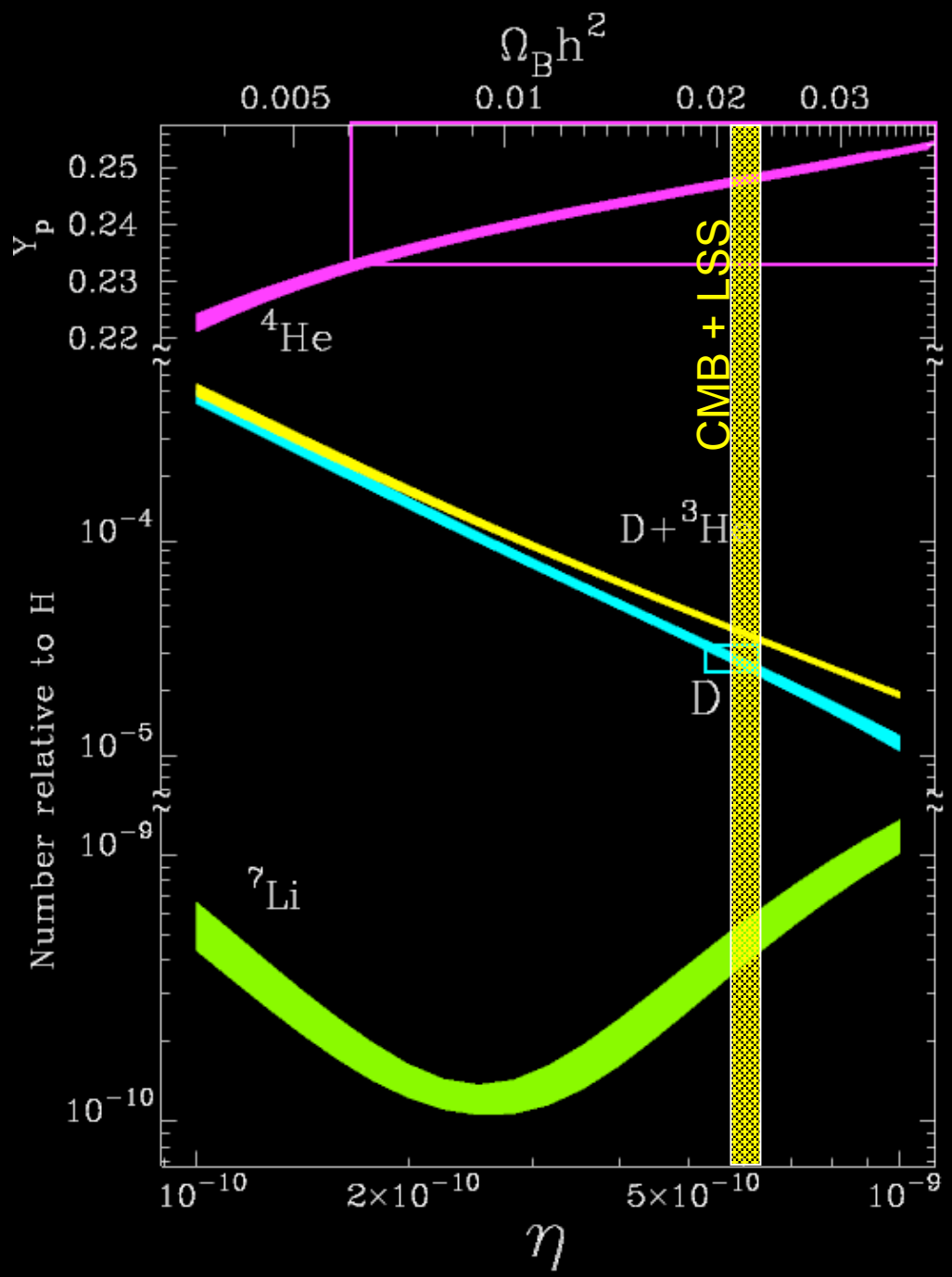

Standard
Big Bang Nucleosynthesis (BBN)
Predictions vs. Observations

Helium-4:

$$0.232 \leq Y_p \leq 0.258$$

(Olive & Skillman 2004)

Deuterium:

$$\frac{\mathrm{D}}{\mathrm{H}} = 2.78^{+0.44}_{-0.38} \times 10^{-5}$$

(Kirkman et al 2002)

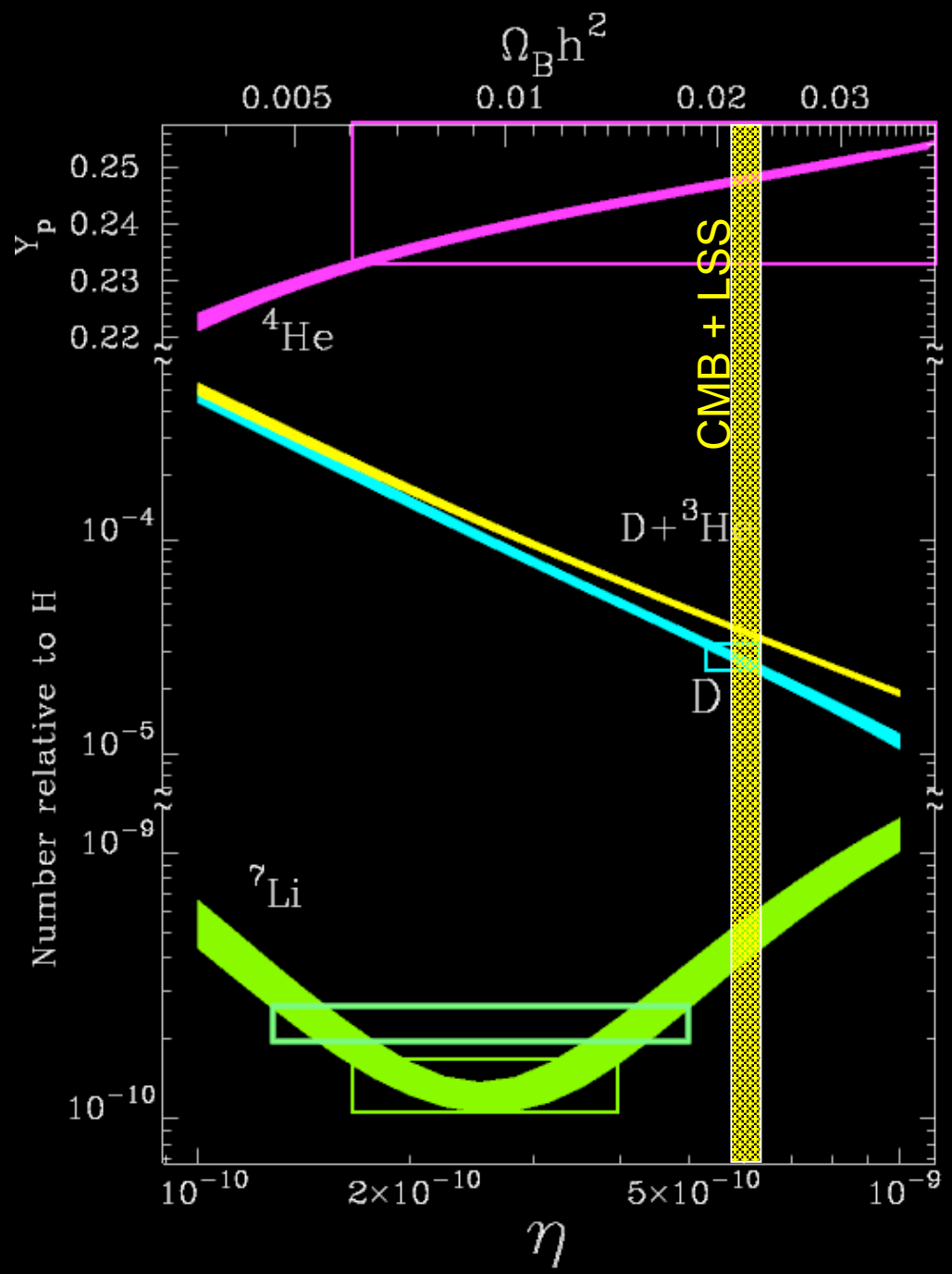

Standard
Big Bang Nucleosynthesis (BBN)
Predictions vs. Observations

Helium-4:

$$0.232 \leq Y_p \leq 0.258$$

(Olive & Skillman 2004)

Deuterium:

$$\frac{\mathrm{D}}{\mathrm{H}} = 2.78^{+0.44}_{-0.38} \times 10^{-5}$$

(Kirkman et al 2003)

Lithium-7:

$$\frac{^7\mathrm{Li}}{\mathrm{H}} = (2.19 \pm 0.28) \times 10^{-10}$$

(Bonifacio et al 2002)

$$\frac{^7\mathrm{Li}}{\mathrm{H}} = 1.23^{+0.34}_{-0.16} \times 10^{-10}$$

(Ryan et al 1999)

Neutrino energy density beyond the standard model (assumption) $N_\nu \equiv 3$

1. Neutrino Asymmetry: $\Delta N_\nu = \frac{30}{7}\left(\frac{\xi}{\pi}\right)^2 + \frac{15}{7}\left(\frac{\xi}{\pi}\right)^4$

$$f(p,\xi) = \frac{1}{e^{p/T-\xi} - 1}$$

$$\rho_\nu + \rho_{\bar{\nu}} = \frac{1}{2\pi^2}\int_0^\infty dp\, p^2 E_\nu \left[f_\nu(p) + f_{\bar{\nu}}(p)\right]$$

2. Extra Neutrino Flavors: ΔN_ν

   ν_s, $\nu_{s'}$, $\nu_{s''}$ …

   Models: 2+2, 3+1, 3+2, 3+N …

Constraints on New Physics: N_ν

BBN Alone

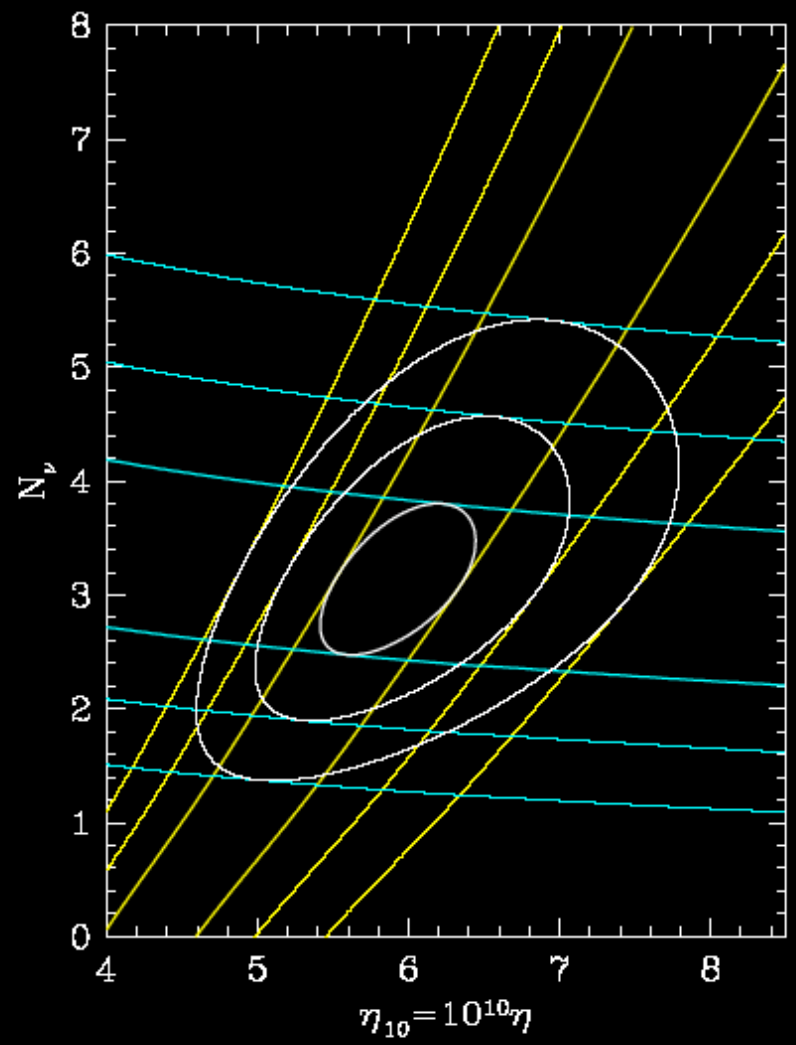

BBN + CMB η

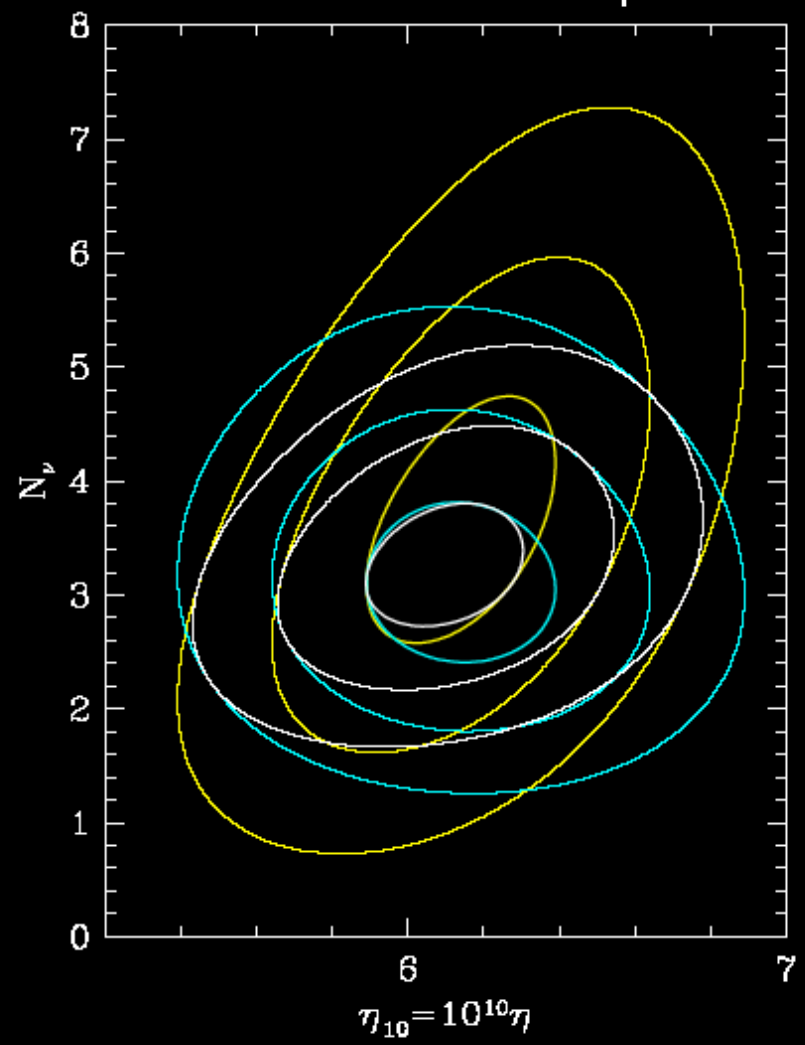

Cyburt et al 2004

Neutrino Asymmetries

"Degenerate" Big Bang Nucleosynthesis:

$$f(p,\xi) = \frac{1}{e^{p/T-\xi} - 1}$$

$\xi \neq 0$

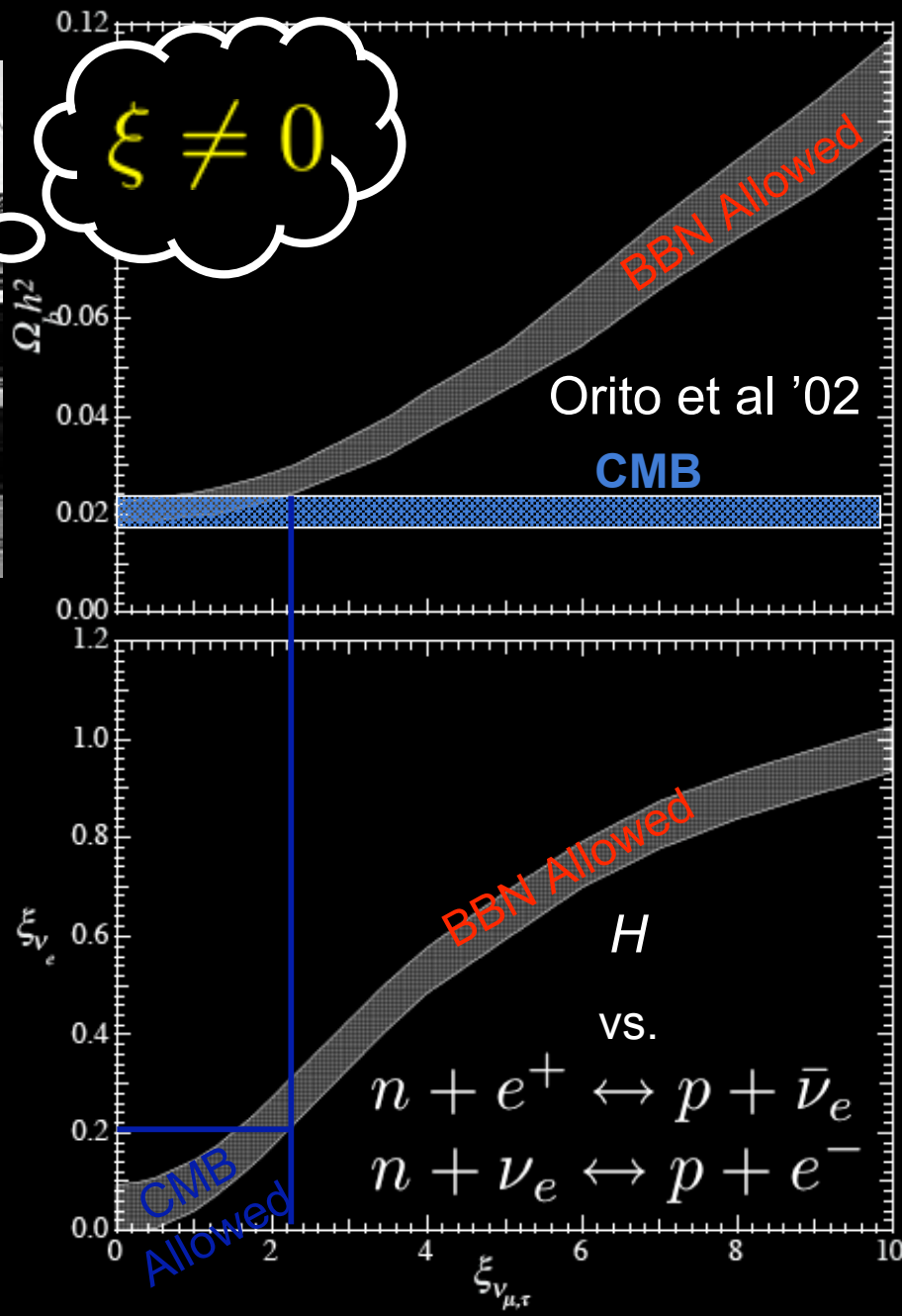

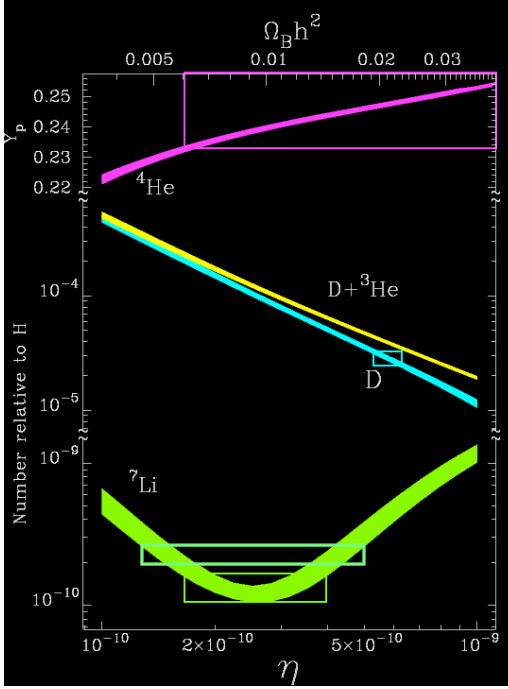

Using the observed abundances of D, ^{4}He, and ^{7}Li alone,

BBN is very pliable to allow large neutrino asymmetries

Due to canceling effects between $\nu_{\mu/\tau}$ and ν_e, and baryon density, $\Omega_b h^2$

$$e^{\delta m/T - \xi_e}$$

Neutrino Mixing is indisputable!

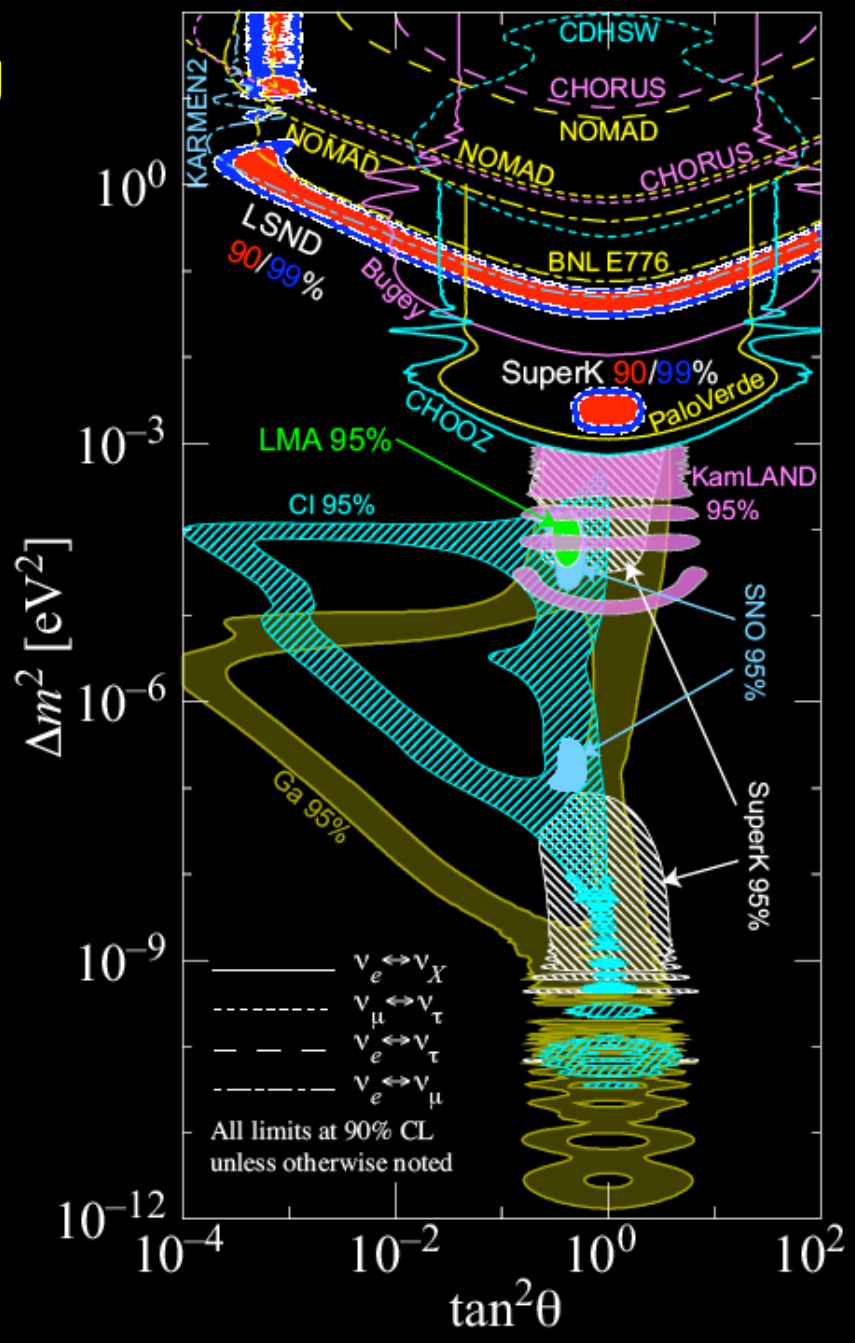

PDG, RPP 2004

Evolution of Neutrino Asymmetries in the Early Universe

$$\dot{\mathbf{P}}(p) = \mathbf{V}(p) \times \mathbf{P}(p)$$

$$\mathbf{V}(p) = \boldsymbol{\Delta}(p) + \left[V^B(p) + V^T(p)\right]\hat{\mathbf{z}} + \mathbf{V}^S(p)$$

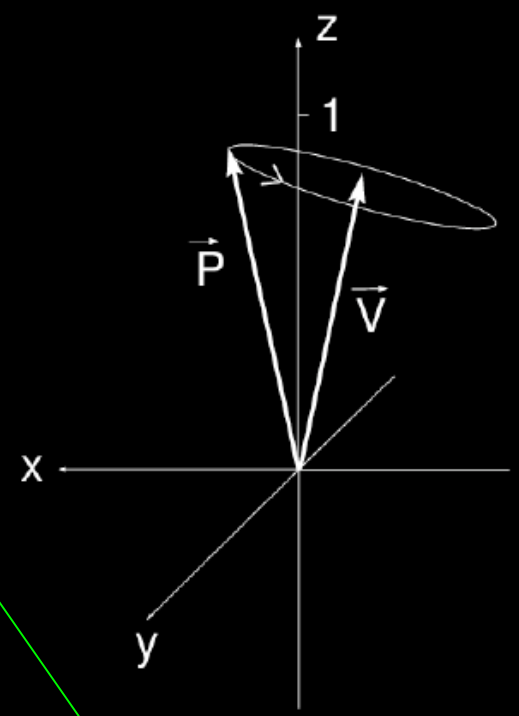

...dipole precession in a magnetic field

Vacuum Oscillation

$e^{+/-}$ / $\mu^{+/-}$ background

Thermal Potential

(finite temperature effects)

Neutrino Self-Potential

Conversion of Asymmetry

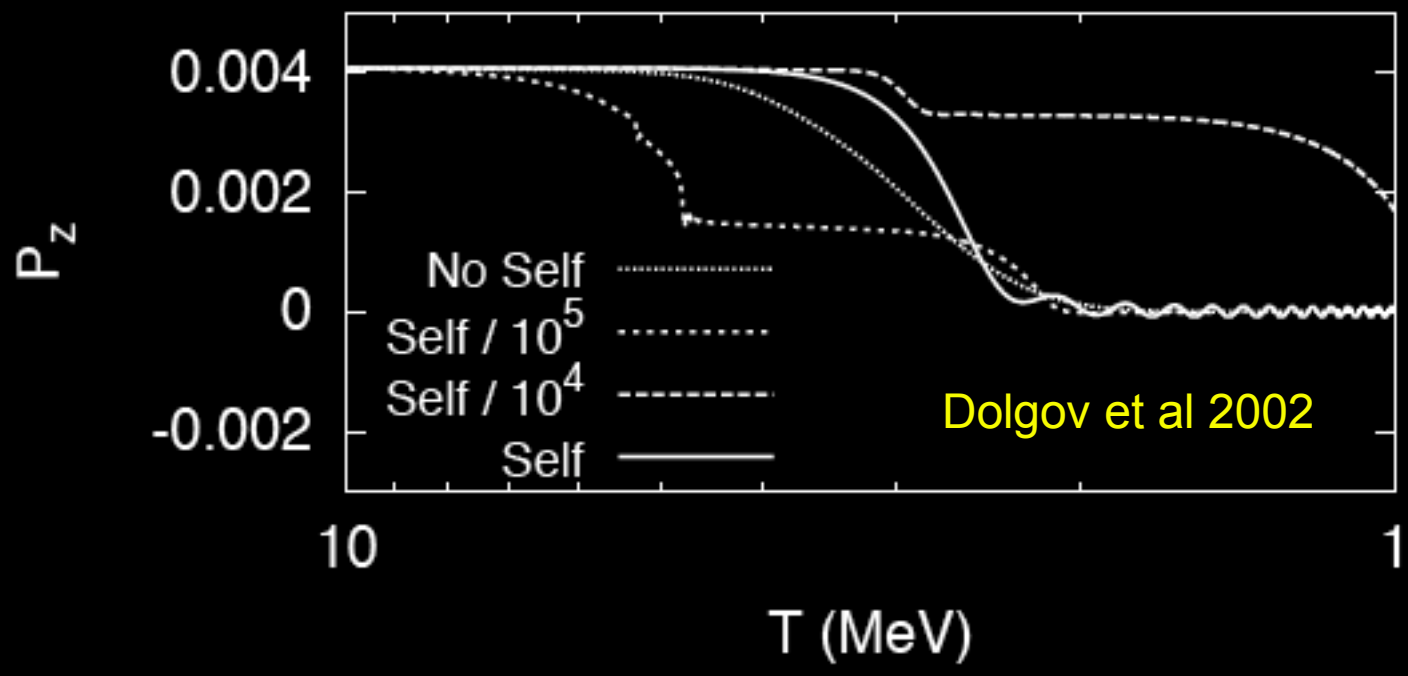

LMA solar + maximal ATM

➔Any chemical potential will alter the ^{4}He abundance.

ξ <<1

$$n + e^+ \leftrightarrow p + \bar{\nu}_e$$
$$n + \nu_e \leftrightarrow p + e^-$$

Art of Synchronization

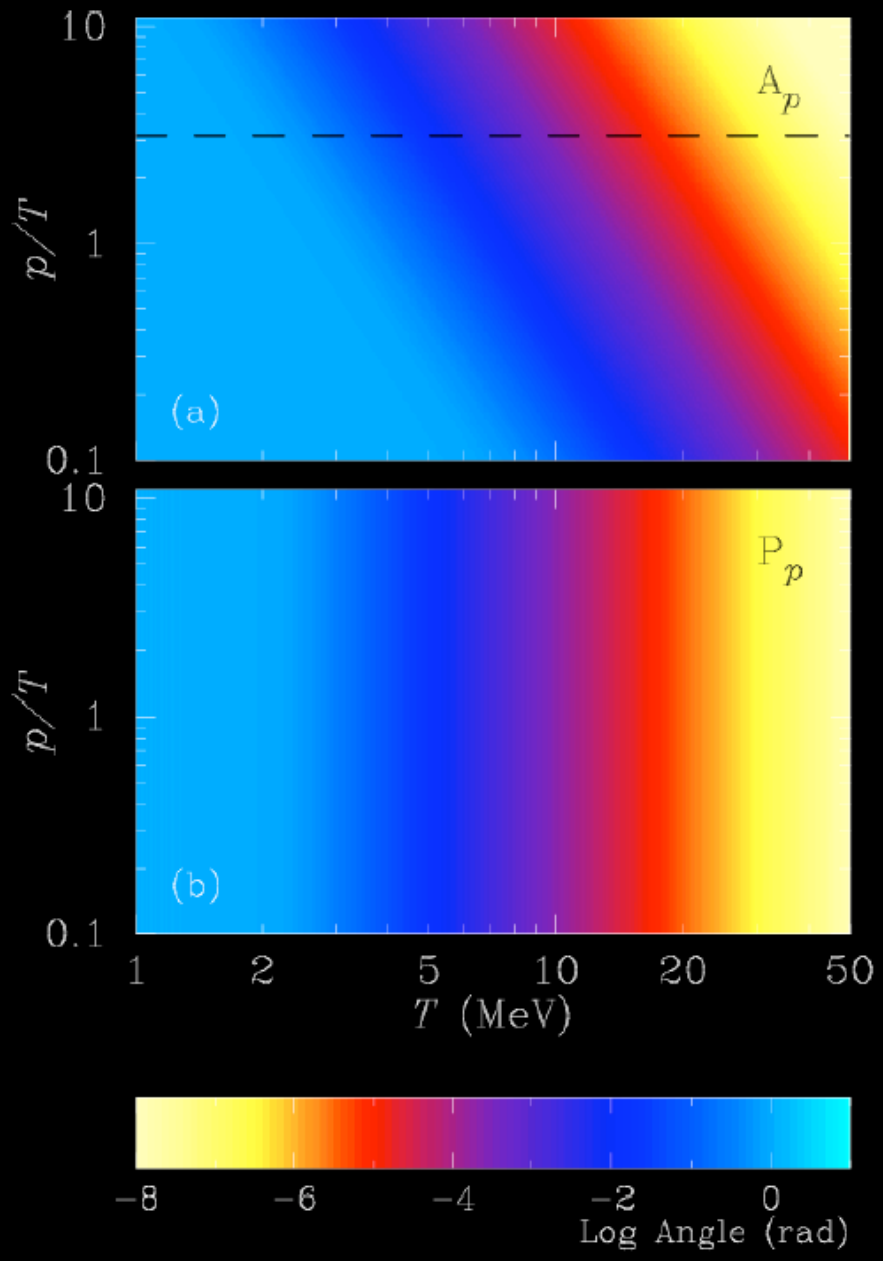

System evolves as:

$$\partial_t \mathbf{I} = \mathbf{A}_{\rm eff} \times \mathbf{I}$$

Assuming $\mathbf{I} || (\mathbf{P}_p + \bar{\mathbf{P}}_p)$:

$$\mathbf{A}_{\rm eff} \simeq \frac{1}{\mathbf{I}^2} \int \mathbf{A}_p (\mathbf{P}_p + \overline{\mathbf{P}}_p) \cdot \mathbf{I}.$$

follows...

$$\mathbf{A}_{\rm eff} \equiv \Delta_{\rm sync} \left(\sin 2\theta_{\rm sync} \hat{\mathbf{x}} - \cos 2\theta_{\rm sync} \hat{\mathbf{z}} \right),$$

$$\frac{p_{\rm sync}}{T} = \pi \sqrt{1 + \xi^2/2\pi^2} \simeq \pi.$$

while the average for a Fermi-Dirac distribution is

$$\langle p/T \rangle = \frac{7\pi^4}{180\zeta(3)} \simeq 3.15$$

Abazajian, Beacom & Bell 2002

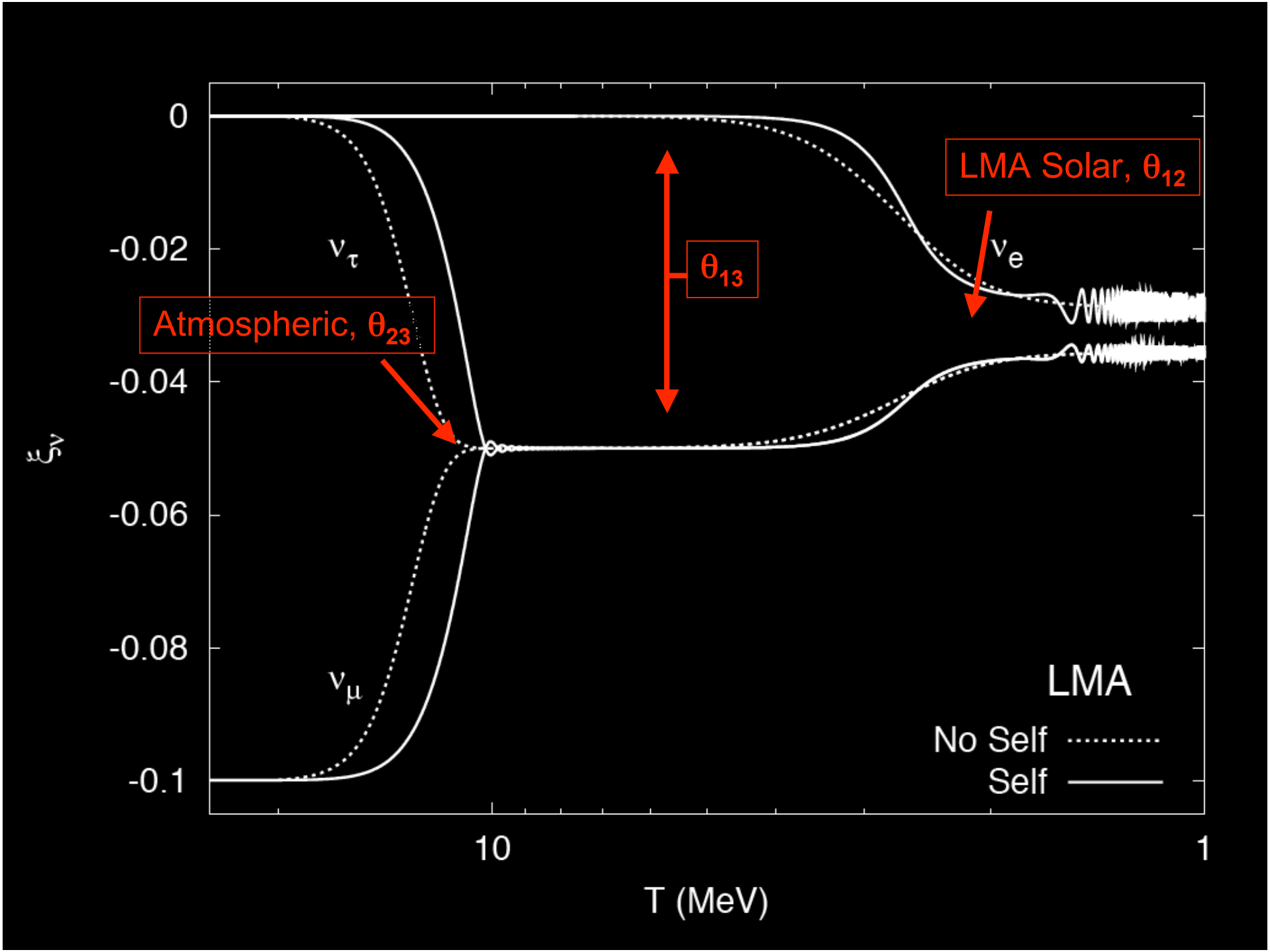
0
-0.02
-0.04
-0.06
-0.08
-0.1
ξ_ν
10
1
T (MeV)
ν_τ
ν_μ
ν_e
Atmospheric, θ_{23}
θ_{13}
LMA Solar, θ_{12}
LMA
No Self
Self

Non-zero: $\theta_{13} > 10^{-10}$

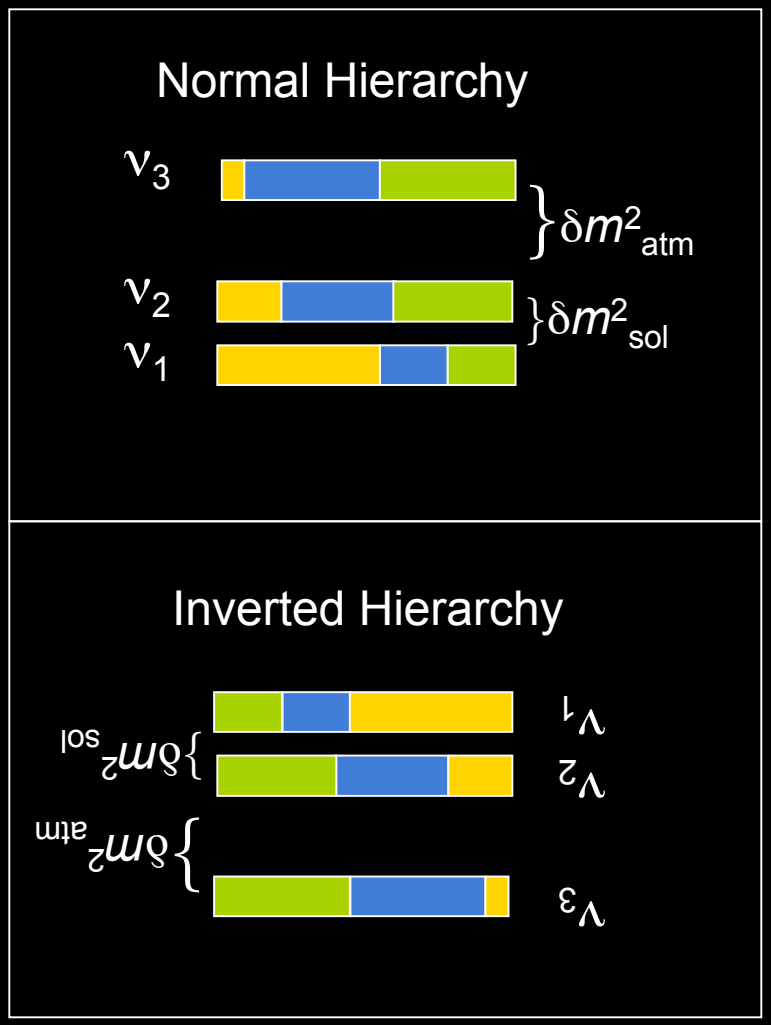

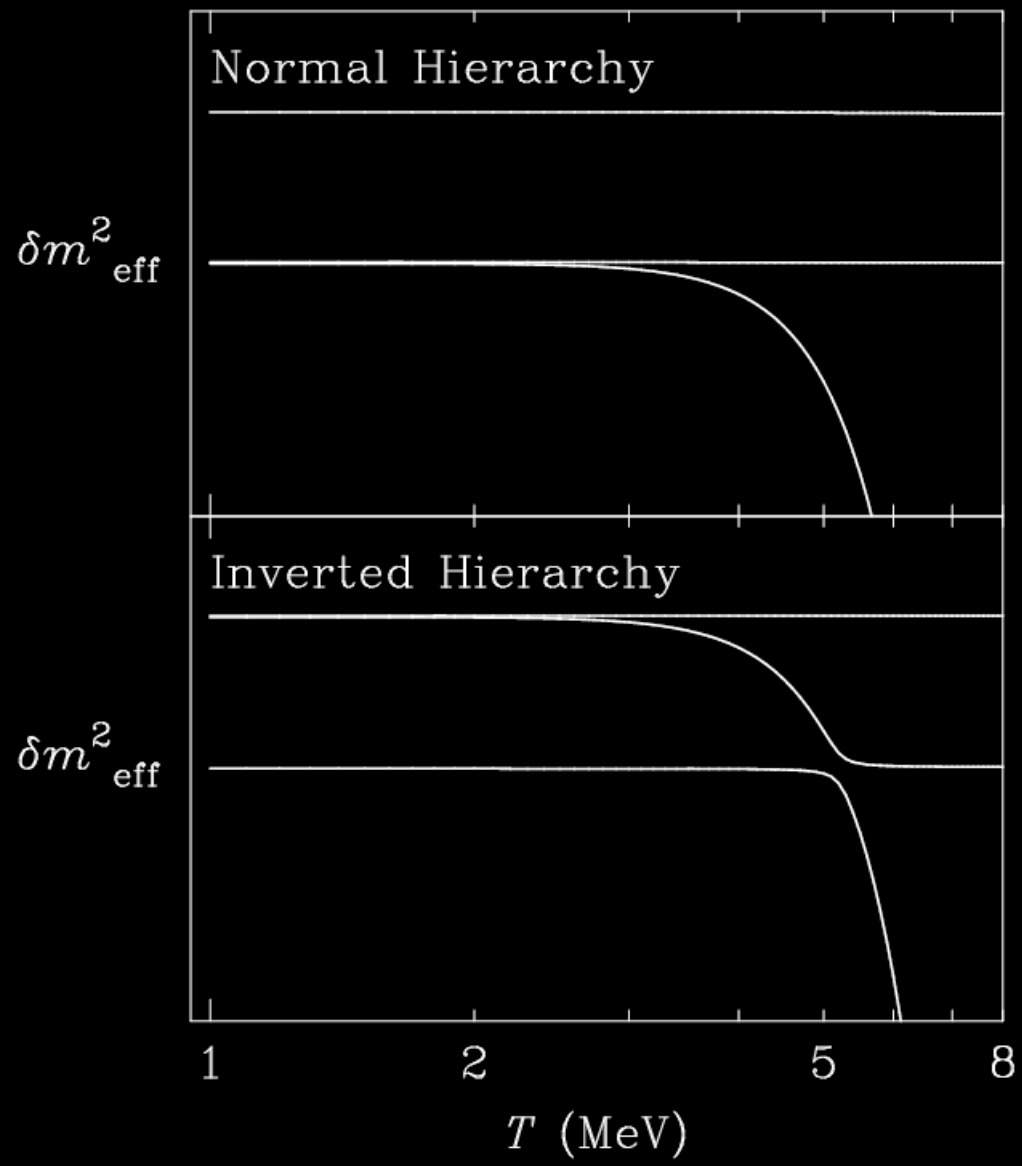

The End of Degenerate BBN & New Constraints on N_ν

The primordial helium abundance Y_p is determined by n/p at beta-equilibrium freeze-out.

$$\frac{n}{p} \propto e^{-\xi_e} \approx 1 - \xi_e$$

$$Y_p \propto \frac{n}{p}$$

$$\Downarrow$$

$$\Delta Y_p \approx -Y_p \xi_e$$

Conservatively, errors $\Delta Y_p / Y_p$ are of order 0.1, and thus $|\xi_e| \lesssim 0.1$

$$|\Delta N_\nu| < 0.1$$

(active neutrinos)

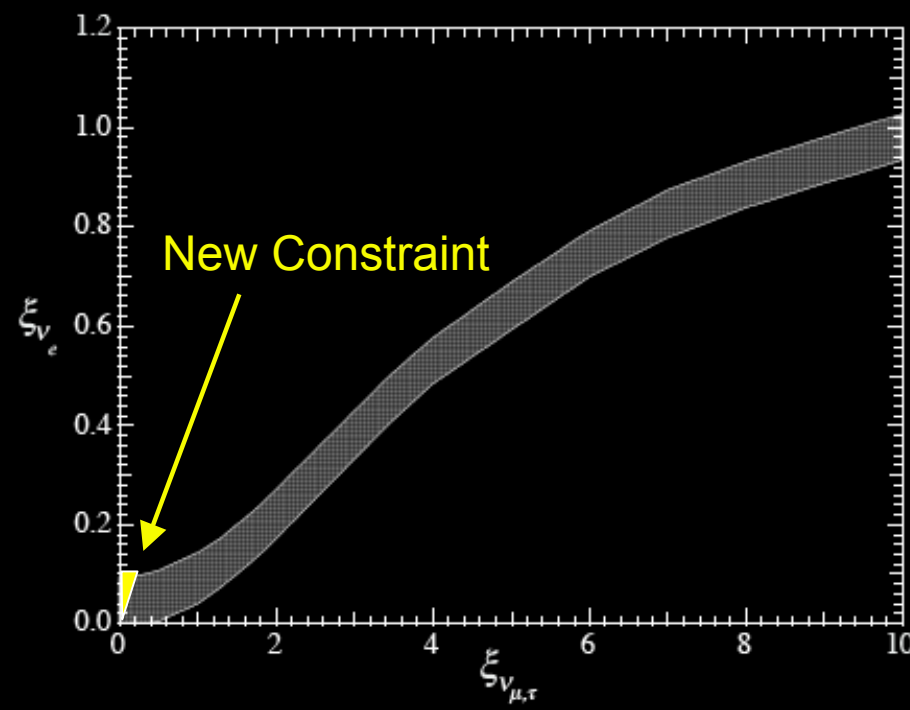

The only *known* relativistic cosmological components (ν,γ) are constrained *extremely well.*

Light Sterile Neutrinos

Neutrino Mixing
is
indisputable??

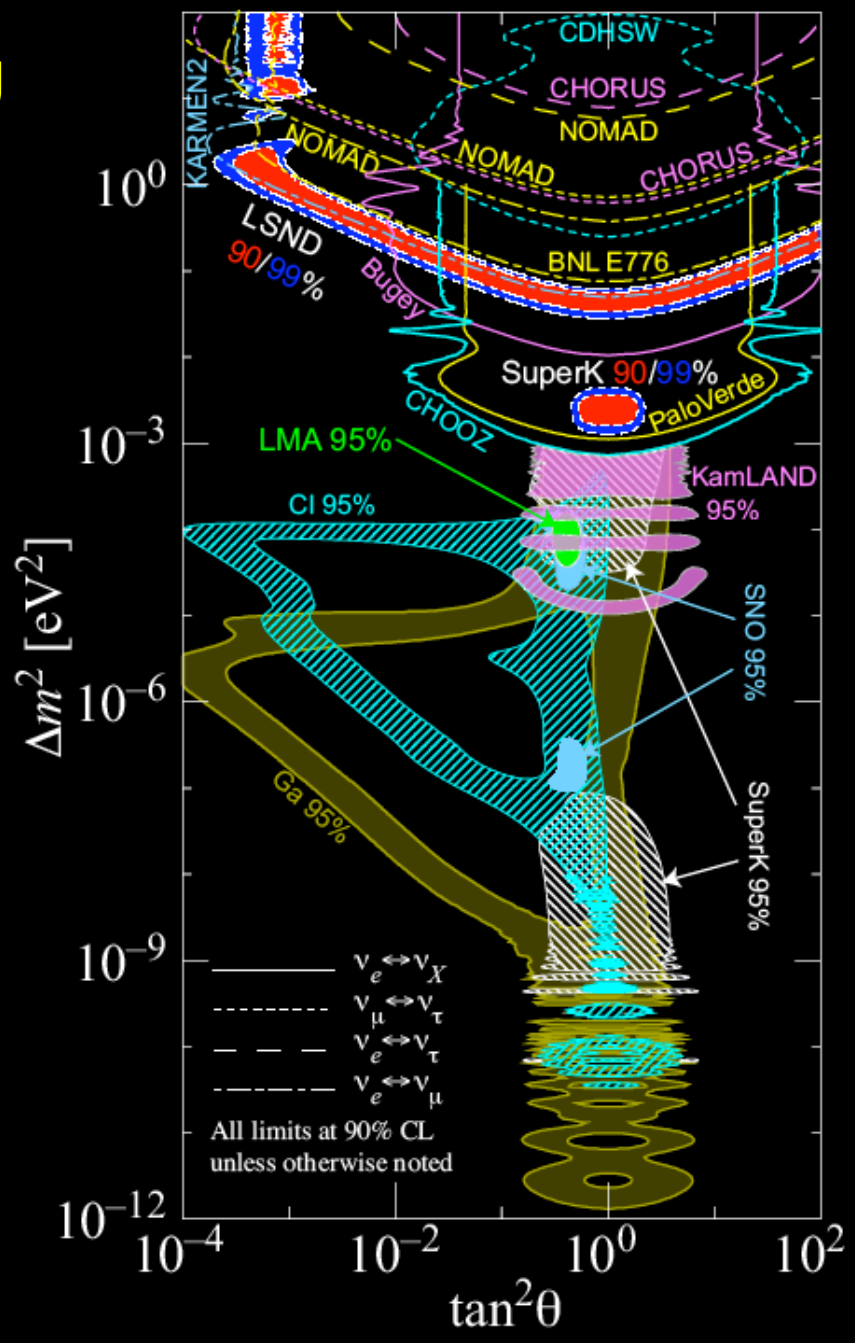

PDG, RPP 2004

4-Neutrino Mass-modelling

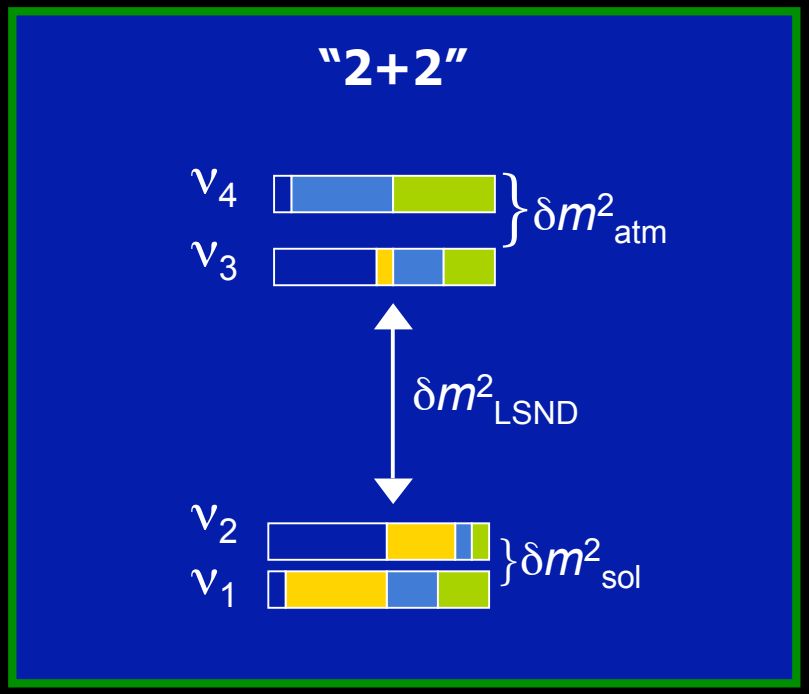

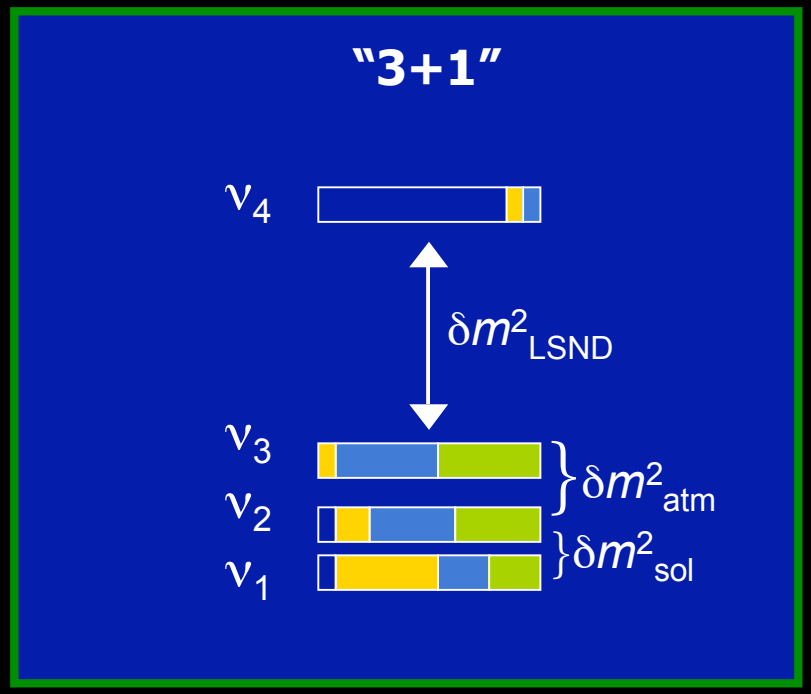

Constraints on New Physics: N_ν

BBN Alone

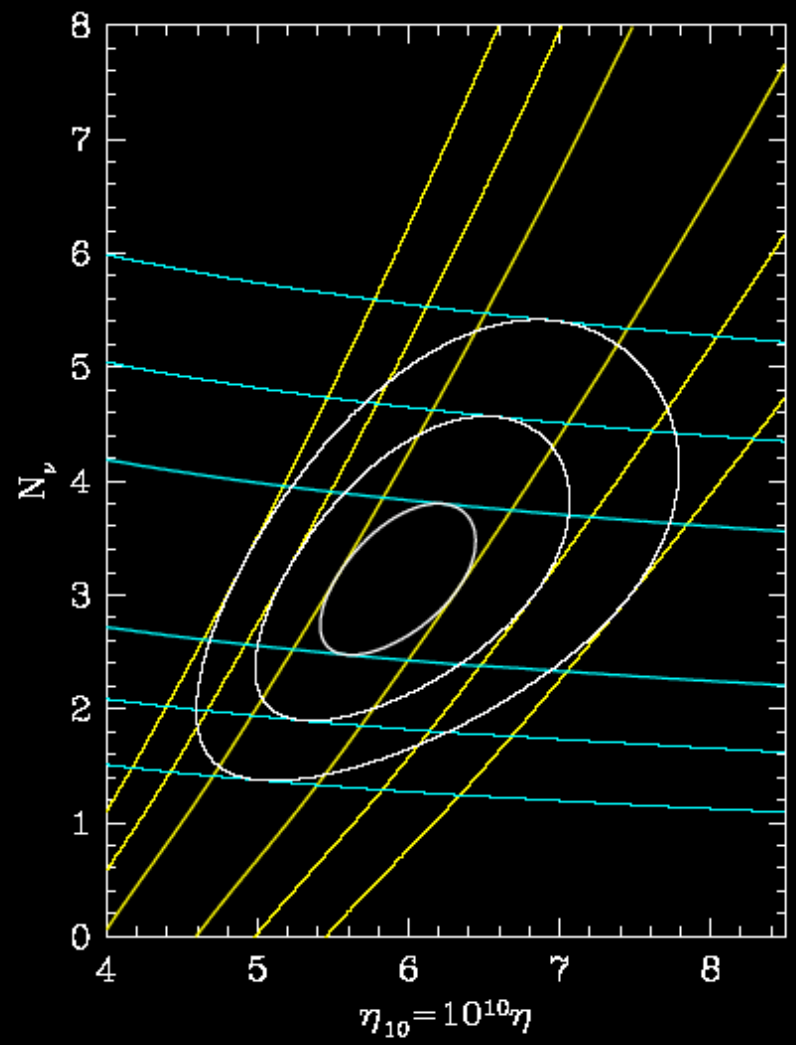

BBN + CMB η

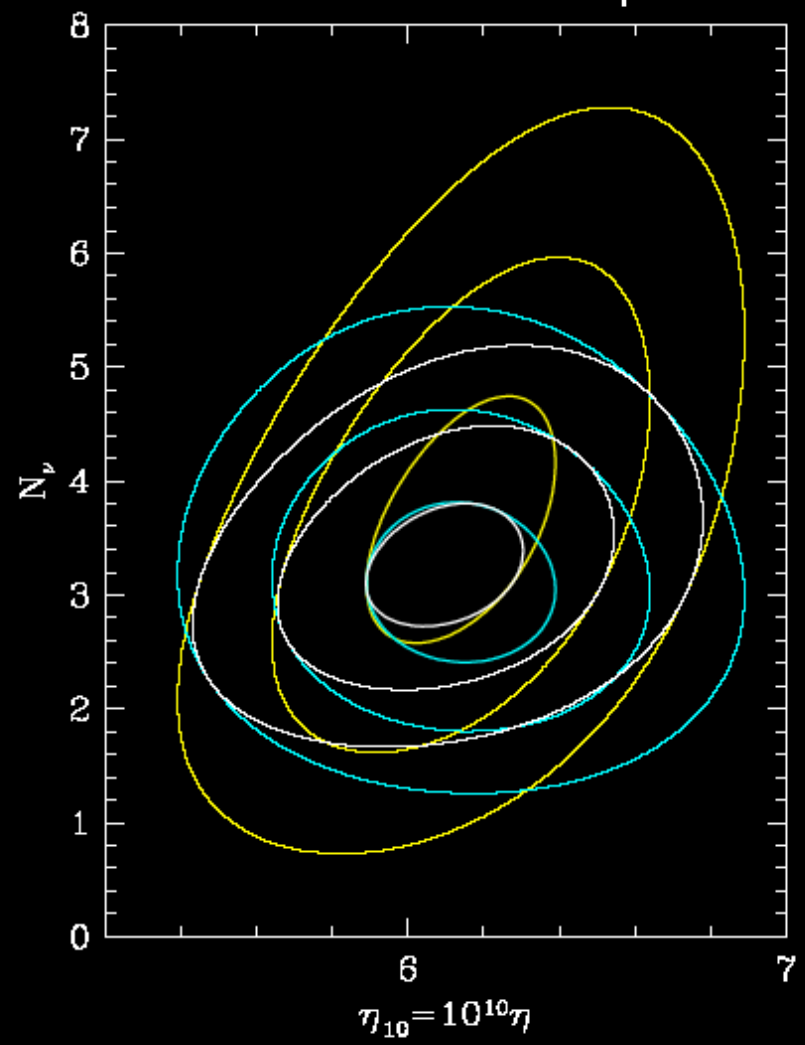

Cyburt et al 2004

Constraining Sterile Neutrino Mixing

- Collisions decohere neutrino gas and populate sterile neutrinos
- Requiring that ν_s are not equilibrated (N_ν<4)

$$\delta m^2_{\alpha s} \sin^4 2\theta_{\rm BBN} < \begin{cases} 5\times 10^{-6}, & \text{for } \alpha = e \\ 3\times 10^{-6}, & \text{for } \alpha = \mu, \tau \end{cases}$$

The relevant amplitude is simply:

$$A_{\alpha;s} = 4|U_{\alpha 4}|^2 |U_{s4}|^2 \simeq \sin^2 2\theta_{\rm BBN}\,.$$

- Which is violated by both the 3+1 and 2+2 models

(Abazajian 2002)

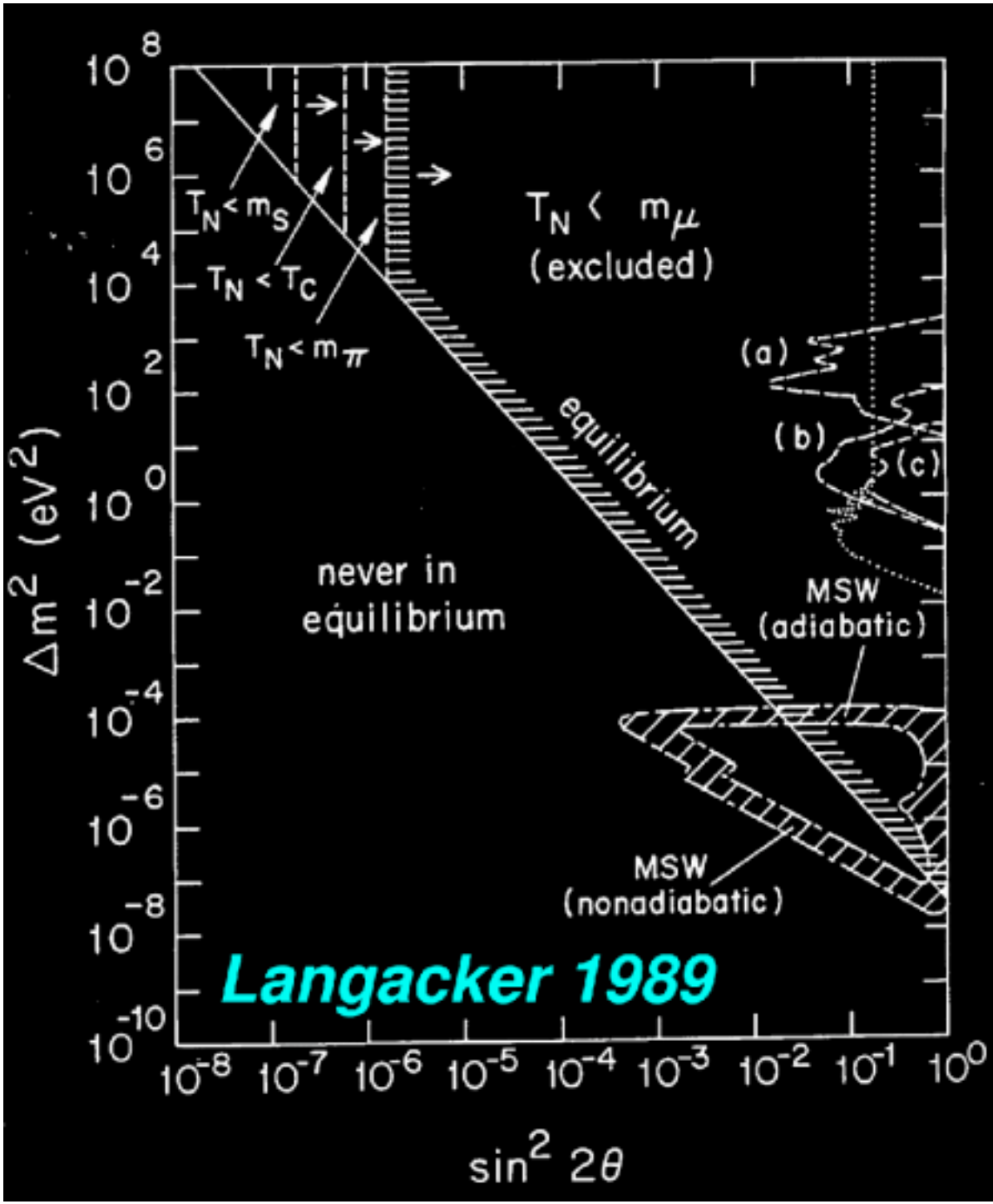

Original 2-neutrino limits:
Langacker 1989;
Barbieri & Dolgov 1990;
Enqvist, Kainulainen, Thomson 1992;
Shi, Schramm & Fields 1993

Application to all 4 neutrino models:
K. Abazajian, 2002;
P. Di Bari, 2002

SDSS Ly-a + galaxy bias HDM limits

Seljak et al 2004

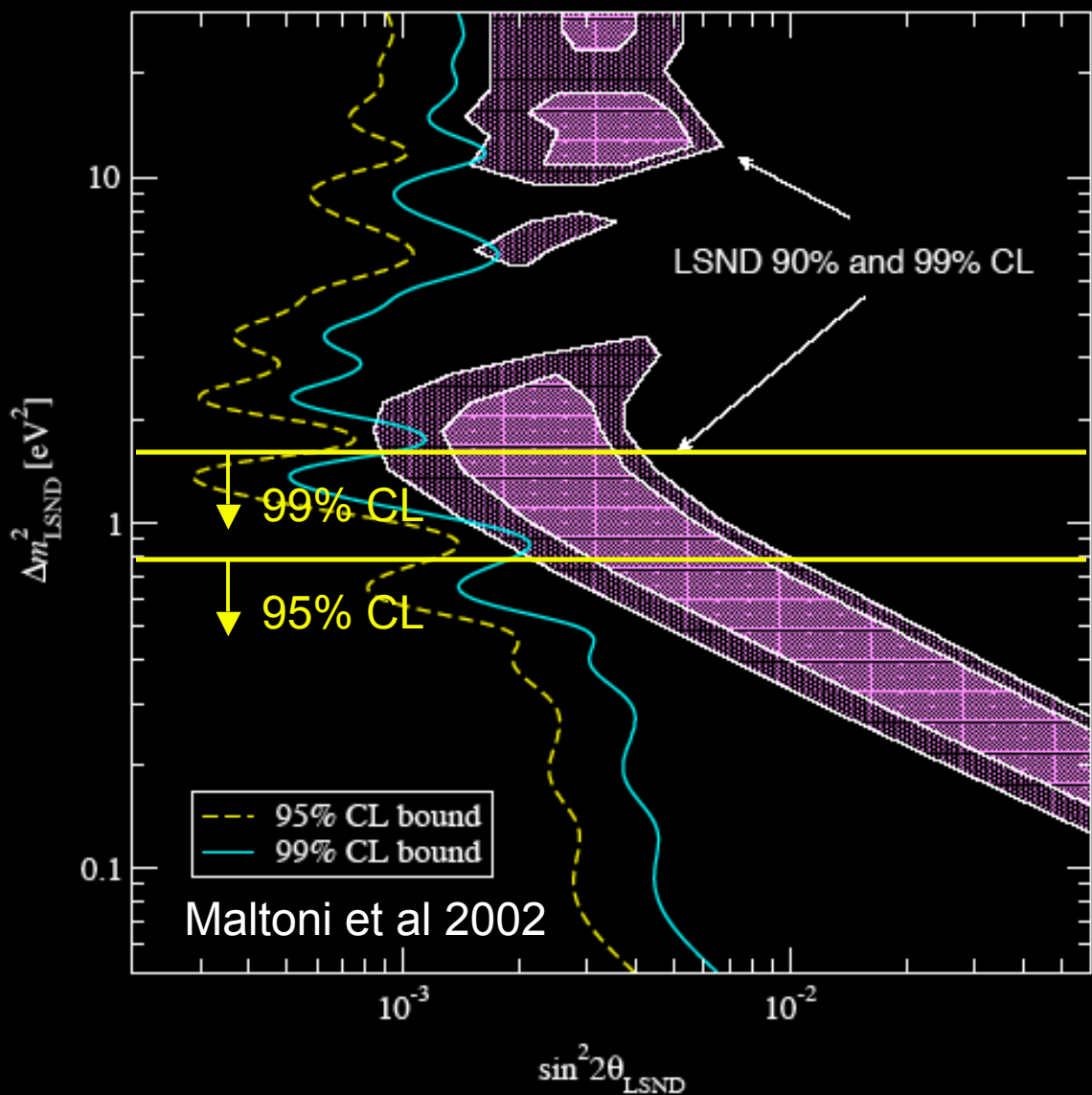

$$m_\nu < 0.79\,\mathrm{eV}(1.55\,\mathrm{eV})$$

95% C.L. (99% C.L.)

- for 3+1 models
- [2+2 more constrained]

The MiniBooNE Experiment @ Fermilab

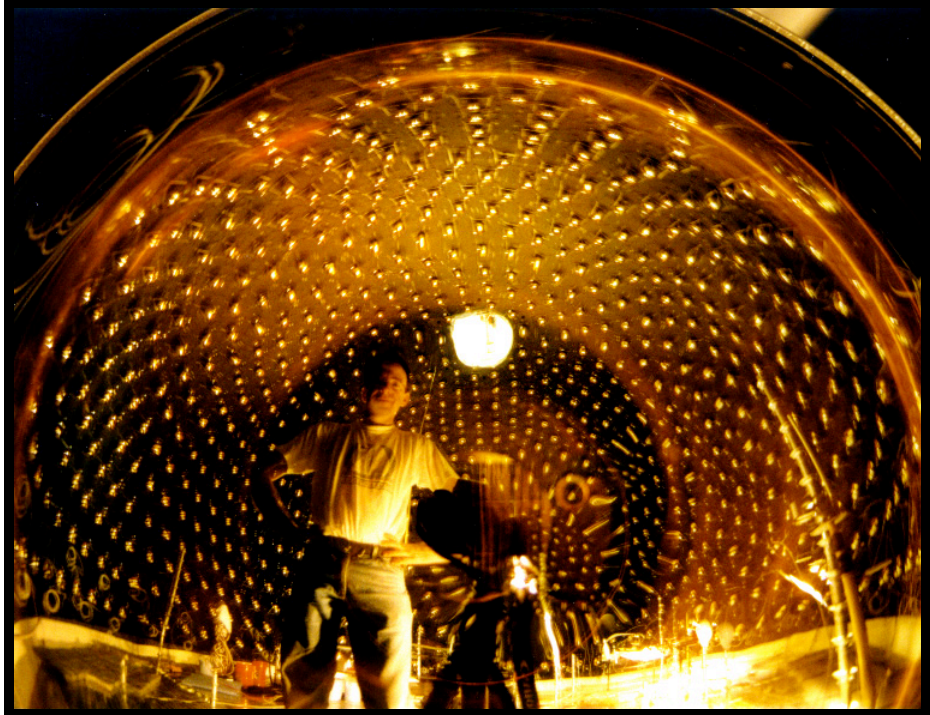

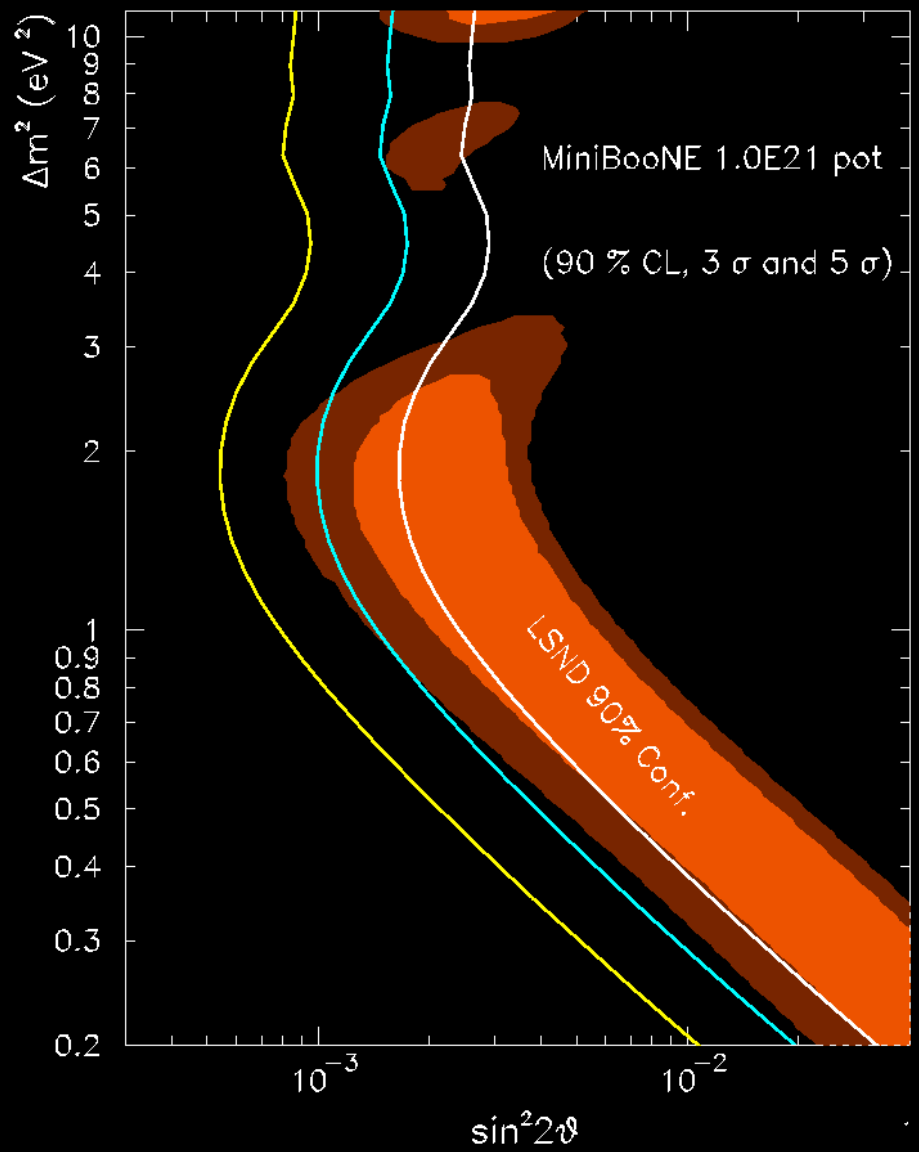

- Structure Formation
- Primordial Nucleosynthesis
- Neutrino Physics

Constraint Evasion & New Physics

1. Pre-existing lepton number (L ~ 10^5 B)
2. A fifth mass eigenstate, mostly sterile

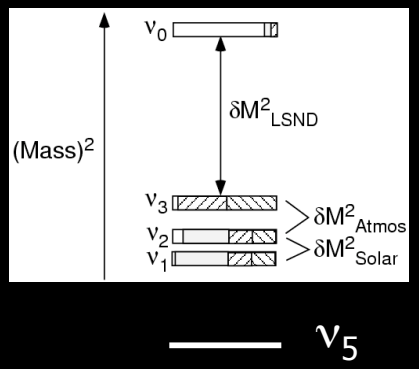

ν_5

may dynamically generate lepton number (Foot, Thomson & Volkas, 1996) sufficiently early

3. Generation of majoron fields (Berezinsky & Bento 2001)
4. Low reheating temperature (3 active neutrinos are not thermalized)
5. Baryon-Antibaryon inhomogeneities: $N_\nu < 7$ (Giovannini, Kurki-Suonio & Sihvola 2002)
6. Extended quintessence ("dark radiation") (Chen, Scherrer & Steigman 2001)
7. CPT violating Neutrinos (Murayama & Yanagida 2001; Barenboim, Borrisov, Lykken & Smirnov 2001)

What if there *are* 4 neutrinos??

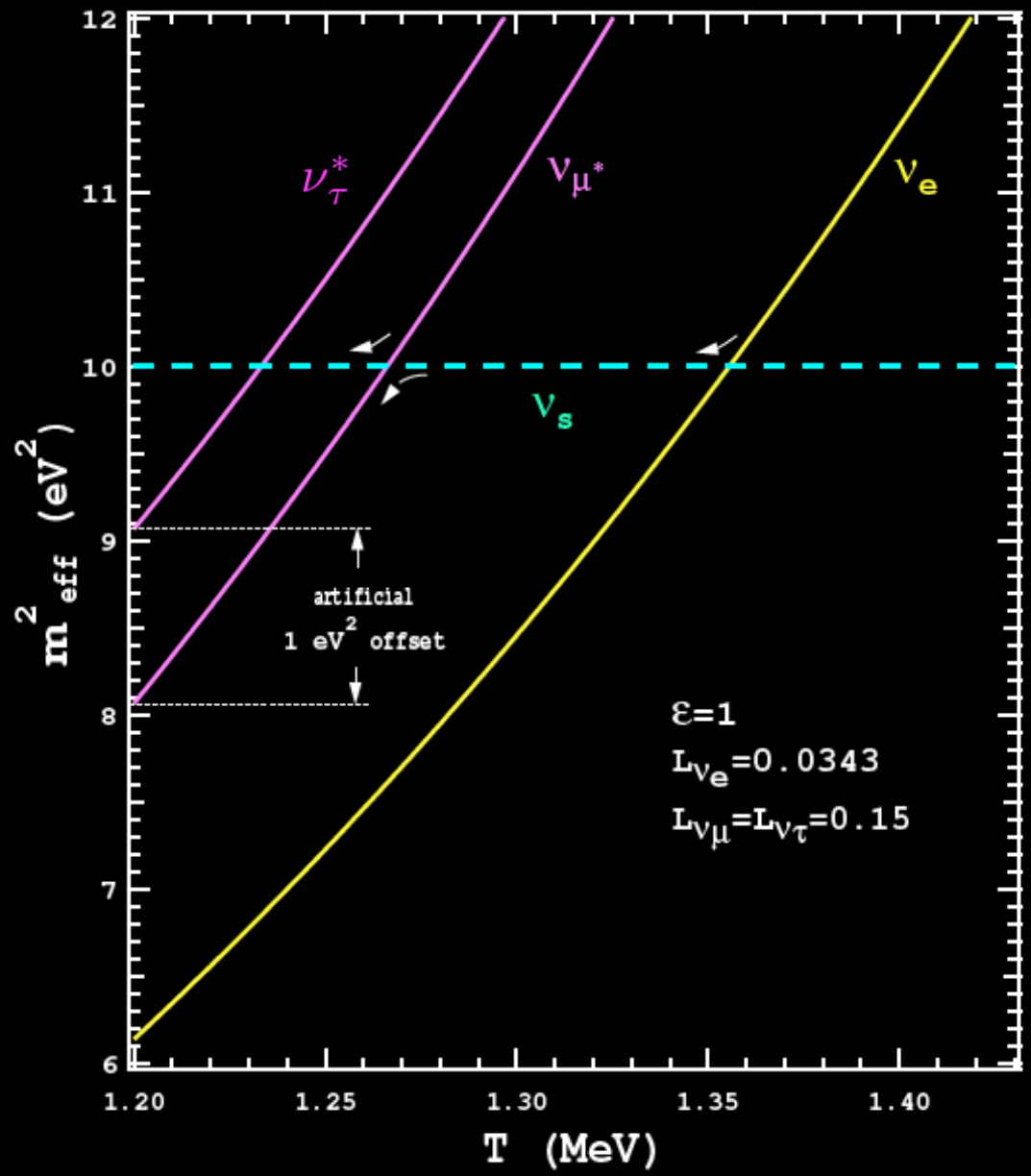

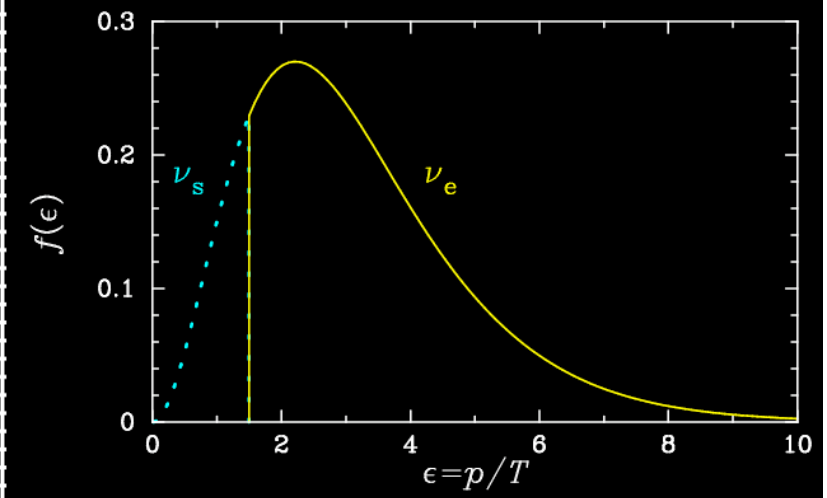

$$n + e^+ \leftrightarrow p + \bar{\nu}_e$$
$$n + \nu_e \leftrightarrow p + e^-$$

Abazajian, Bell, Fuller & Wong (in preparation)

Do we know the chemical starting point?

- Yes! the predicted CMB abundances:

$$(\mathrm{D/H})_p = 2.75^{+0.24}_{-0.19} \times 10^{-5}$$

$$^3\mathrm{He/H} = 9.28^{+0.55}_{-0.54} \times 10^{-6}$$

$$Y_p = 0.2484^{+0.0004}_{-0.0005}$$

$$^7\mathrm{Li/H} = 3.82^{+0.73}_{-0.60} \times 10^{-10}$$

- There can be no substantial neutrino asymmetries (no DBBN)
- *Unless*… a fourth (fifth?) neutrino is lurking in the neutrino sector…

The observed metallicity of the intergalactic medium

Starring:

Anthony Aguirre

UC Santa Cruz

Co-Starring:

Joop Schaye

IAS Princeton

QSO spectra by:

T.-S. Kim, W. Sargent, M. Rauch

Simulation provided by:

Tom Theuns

Metals in the IGM

Prime tool: QSO spectra

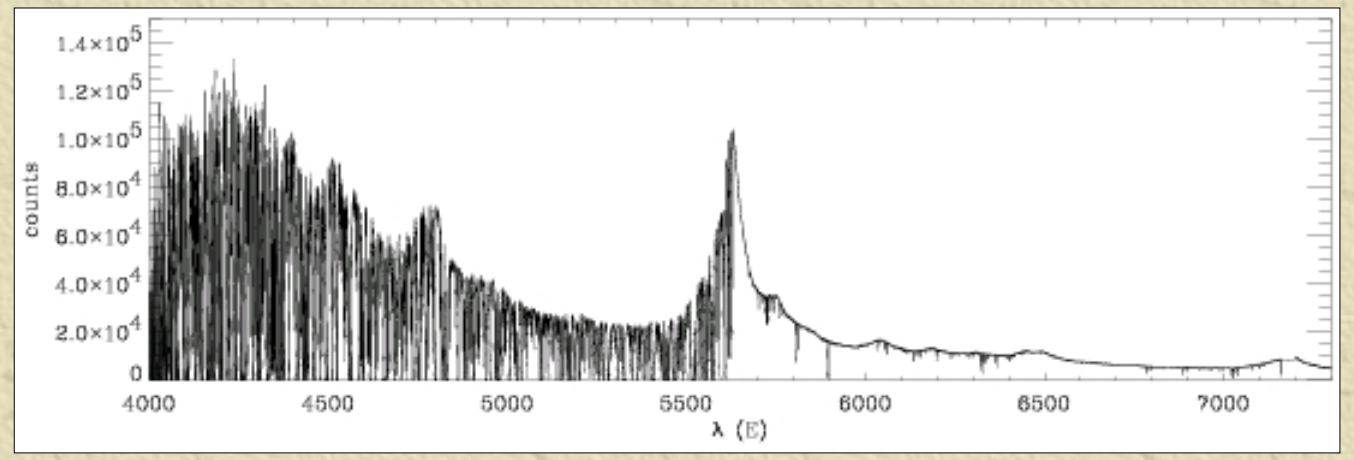

Keck HIRES, z = 3.62

Metals in the IGM

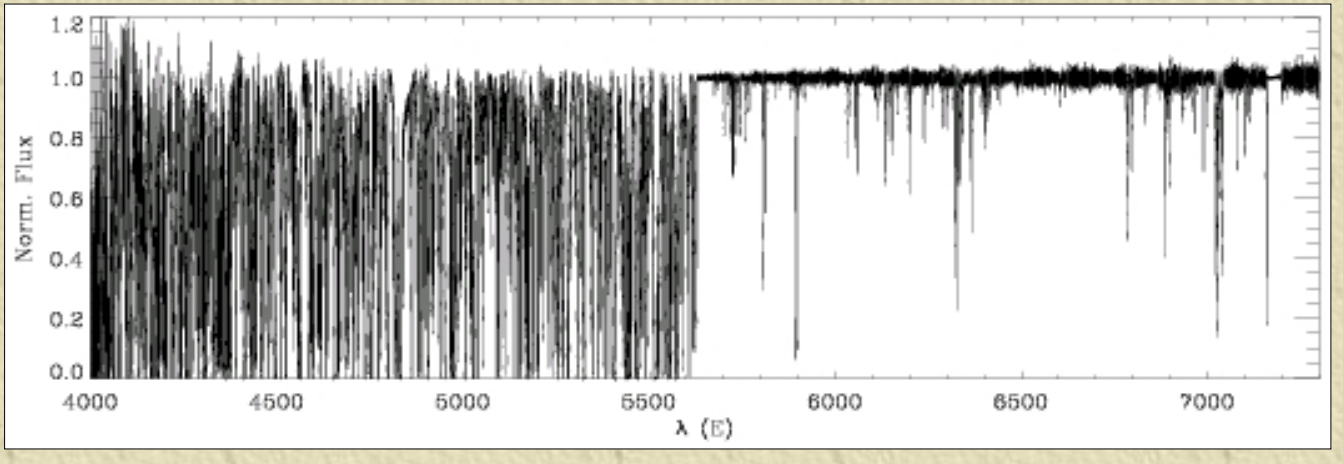

Keck HIRES, z = 3.62

Metals in the IGM

Compare metal lines to HI lines

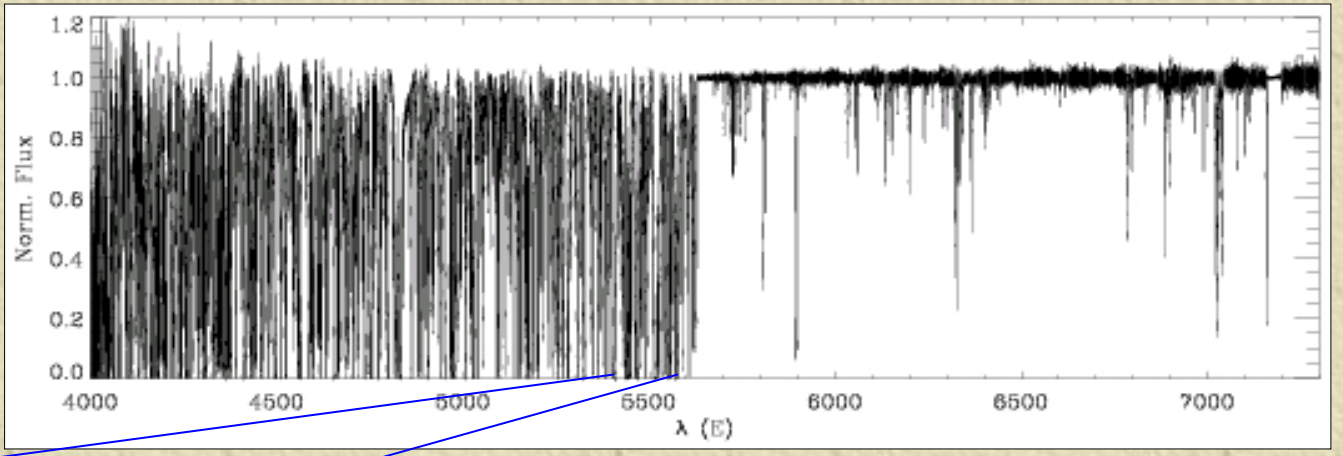

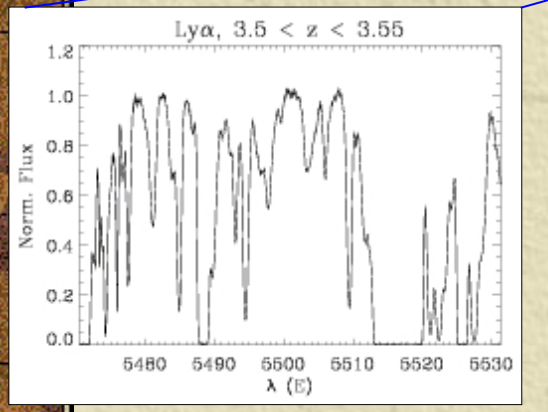

Keck HIRES, z = 3.62

Metals in the IGM

Compare metal lines to HI lines

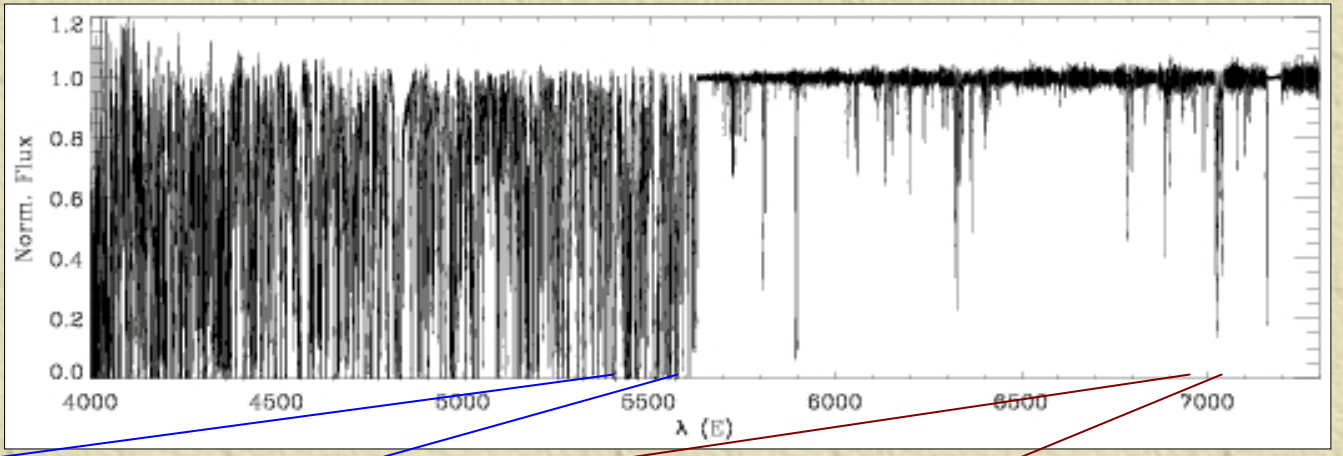

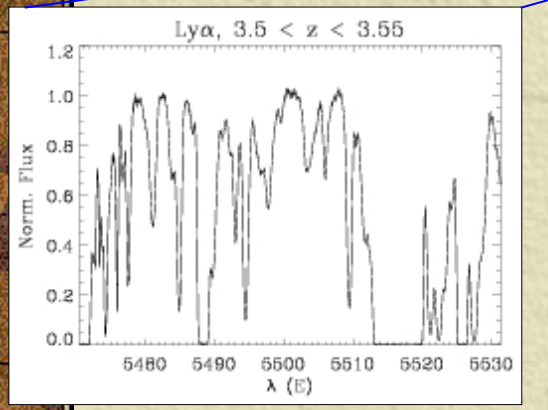

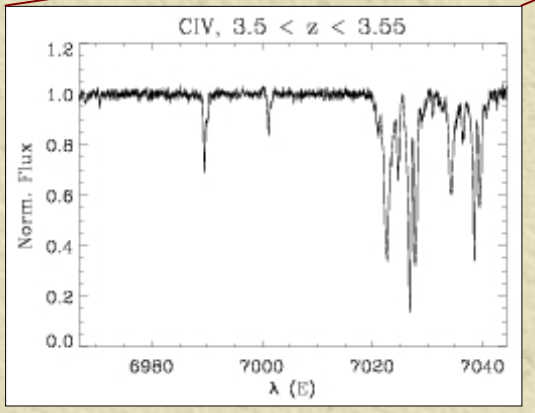

Keck HIRES, z = 3.62

IGM metallicity provides information on:

- History of star/galaxy formation.
- Formation of unobservably early stars/galaxies.
- UV ionizing background.
- Feedback in galaxy formation processes.

Enrichment scenarios:

1. Primordial enrichment at z >> 100

Enrichment scenarios:

1. Primordial enrichment at z >> 100
   - In principle, heavy elements could be primordial.
   - Nobody believes that the observed one are.
   - But: it can be tested!

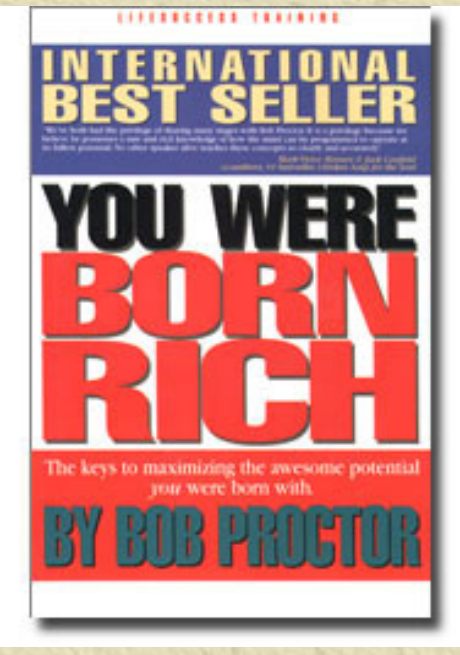

Enrichment scenarios:

2. “Early” enrichment by z >> 6 galaxies.

Features:

- Outflow from protogalaxies/Pop. III.
- Window into very high z.

Arguments for:

- Small wells easier to escape from.
- Low outflow velocities -> little heating.
- IGM has time to “recover.”

Enrichment scenarios:

2. "Early" enrichment by z >> 6 galaxies.

Features:

- Outflow from protogalaxies/Pop. III.
- Window into very high z.

Arguments for:

- Small wells easier to escape from.
- Low outflow velocities -> little heating.
- IGM has time to "recover."

Model as: no effect on IGM, metals sprinkled in.

Enrichment scenarios:

3. "Late" enrichment by $2 < z < 6$ galaxies.

Features:

- *Strong feedback* during galaxy formation.
- Heating of IGM.

Arguments for:

- Observed $z \sim 3$ galaxies drive strong winds.
- Galaxy formation theory: strong feedback seems necessary.
- Most of cosmic star formation at $z < 5$.

Signatures of early vs. late in observed IGM.

1. Look for *evolution* in Z at z < 5.
2. Check *temperature* of gas (late enrichment should come with/in hot gas).
3. Compare *amount* of metals with expectations.
4. Look at *spatial distribution* of metals.
5. Look at *abundance ratios* for info. on nucleosynthetic sources.

All this and more can be done with:

Pixel statistics

Pixel method in brief

19x

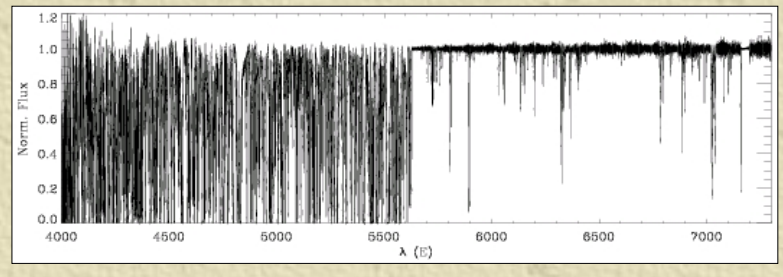

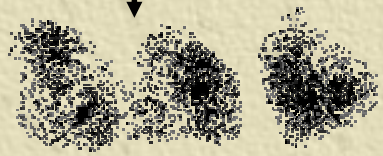

HI, CIV, SiIV pixel optical depths

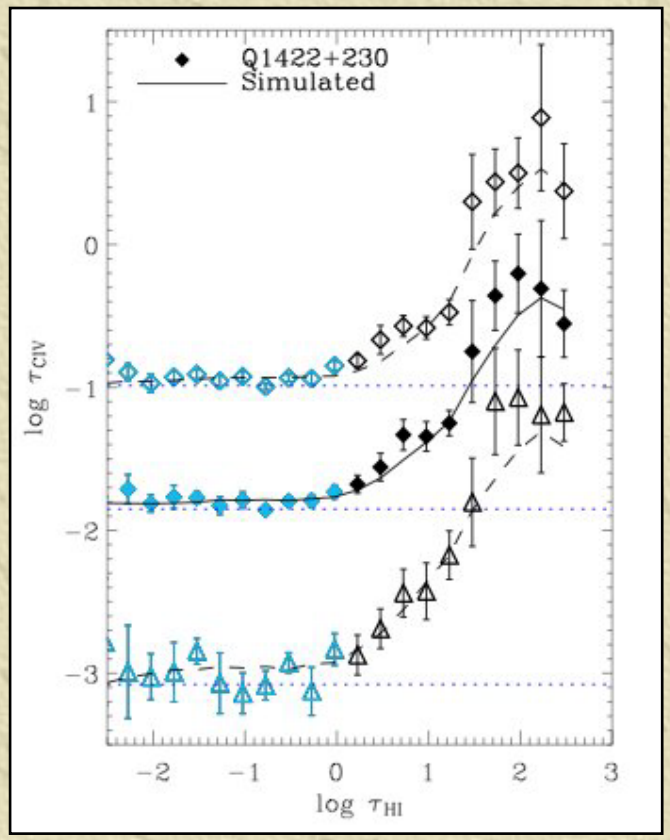

Correlations

Pixel method in brief

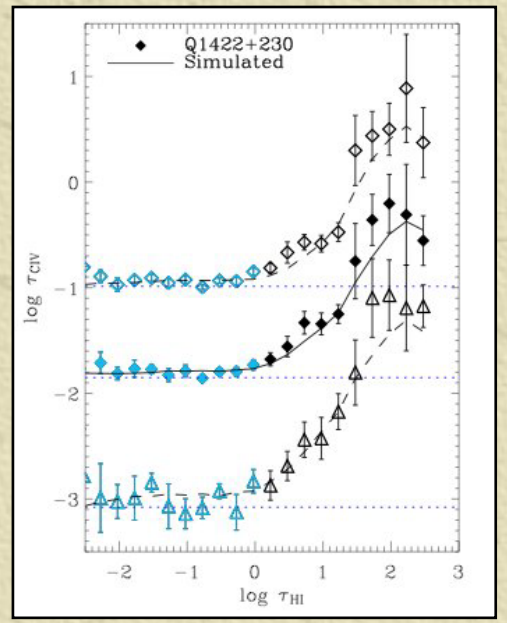

Correlations

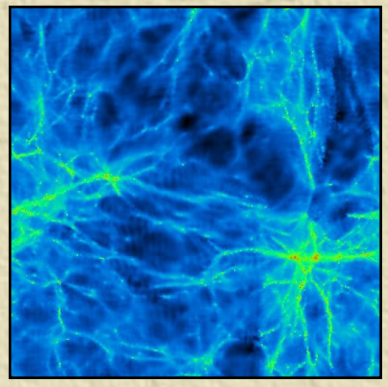

Hydro. simulations

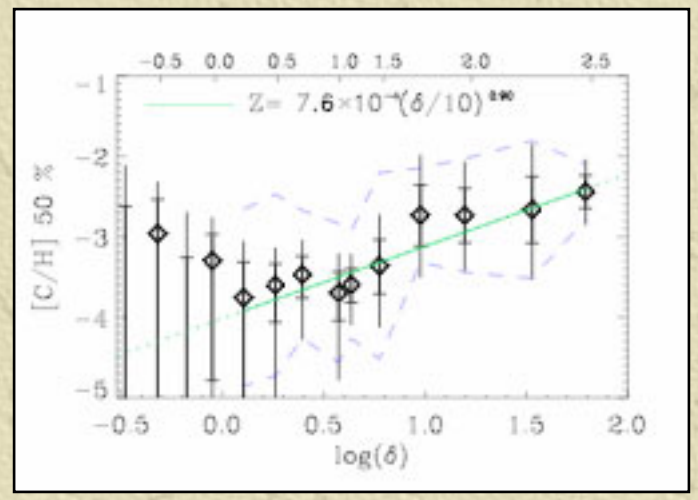

Metallicities

UVB model

Results: Carbon metallicities from CIV

1. The carbon metallicity is inhomogeneous.

- At fixed δ and *z*, p.d.f. for [C/H] is gaussian, i.e. carbon metallicity distribution is lognormal.

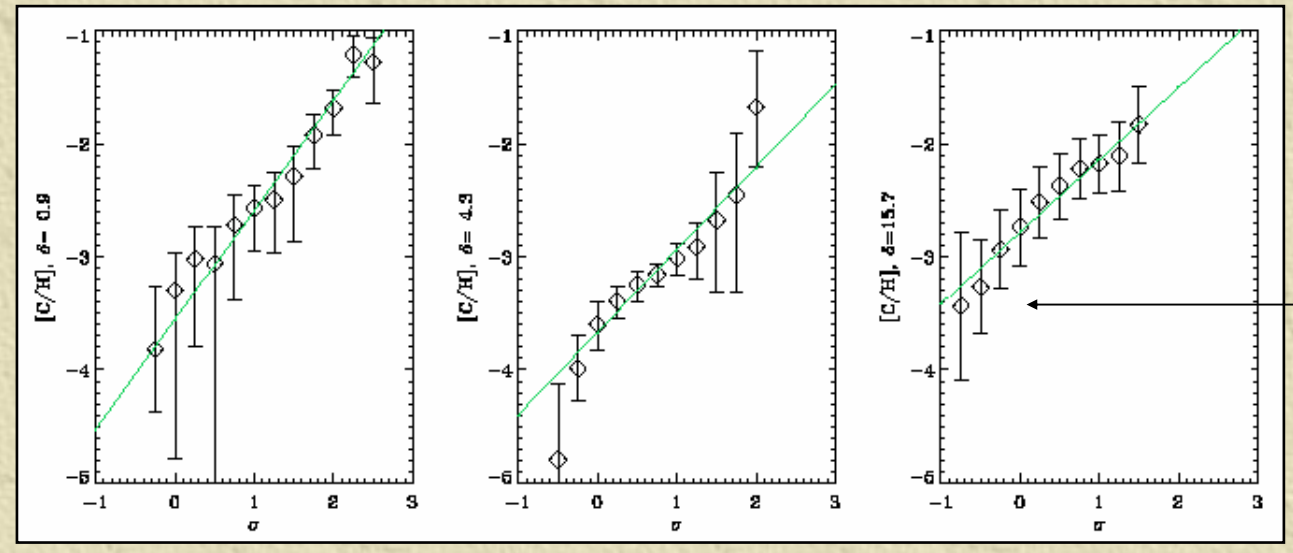

Note these

- Characterize by [C/H] and σ([C/H])

Results: Carbon metallicities from CIV

1. The carbon metallicity is inhomogeneous.

- Primordial enrichment is ruled out.
- But early vs. late will require detailed modeling.

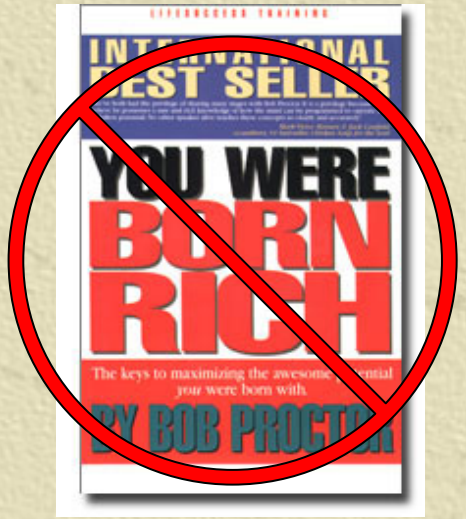

Results: Carbon metallicities from CIV

2. **The median carbon metallicity [C/H] changes with density.**

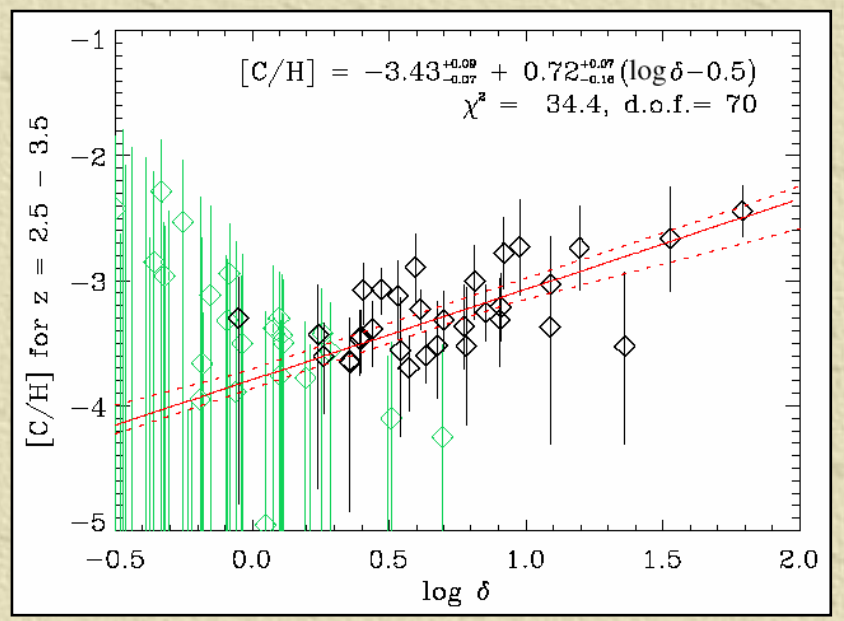

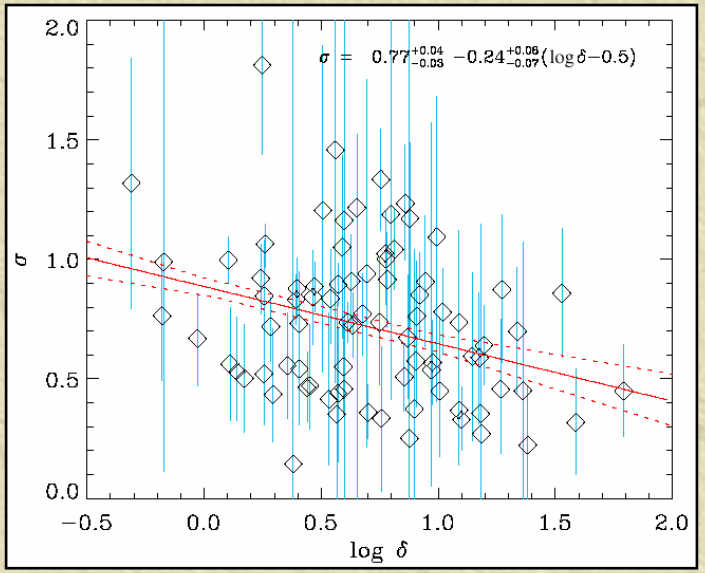

So does scatter σ([C/H])

Results: Carbon metallicities from CIV

2. **The median carbon metallicity [C/H] changes with density.**

- Expected and reasonable, but never observed.
- Metallicity more inhomogeneous at low-δ
- Primordial metals even more ruled out.

Results: Carbon metallicities from CIV

3. There is Carbon in *underdense* gas.

- 2.4σ detection in medians
- 3.4σ detection in higher percentiles.
- Most information from z > 3.5.

[C/H] ~ -3.5: lowest known carbon abundance?

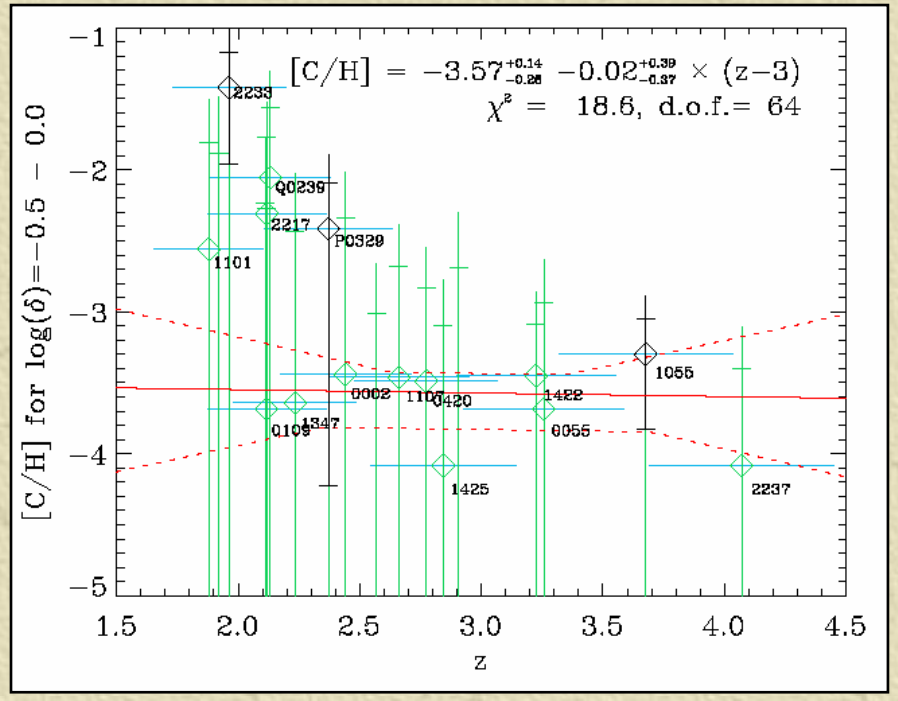

Results: Carbon metallicities from CIV

3. There is Carbon in *underdense* gas.

- The filling factor of metals is high: tens of percent (depending on metallicity threshhold).
- Difficult for late enrichment?

Results: Carbon metallicities from CIV

4. The median carbon metallicity [C/H] does not evolve (for our fiducial UVB) from z~4 to z~2.

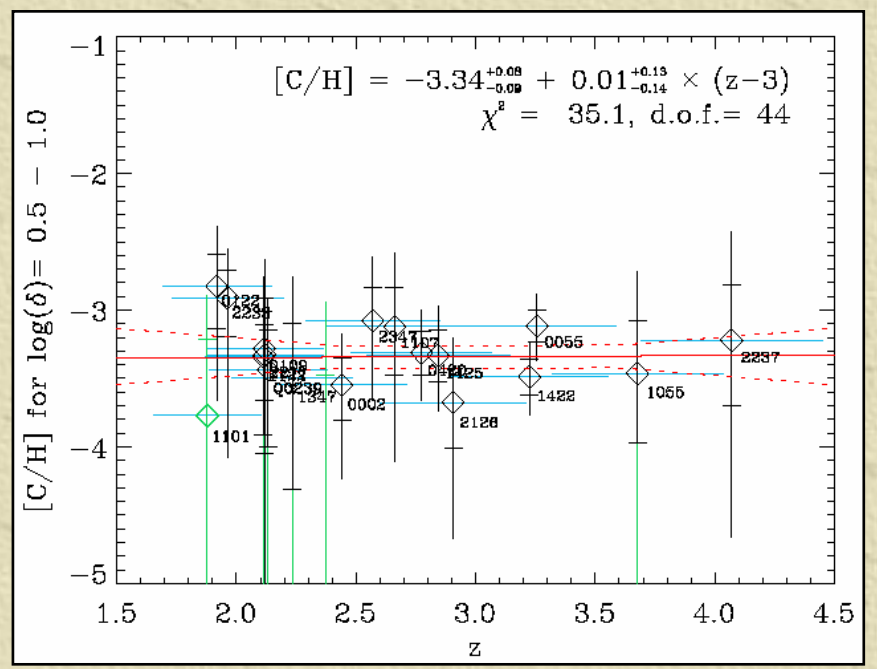

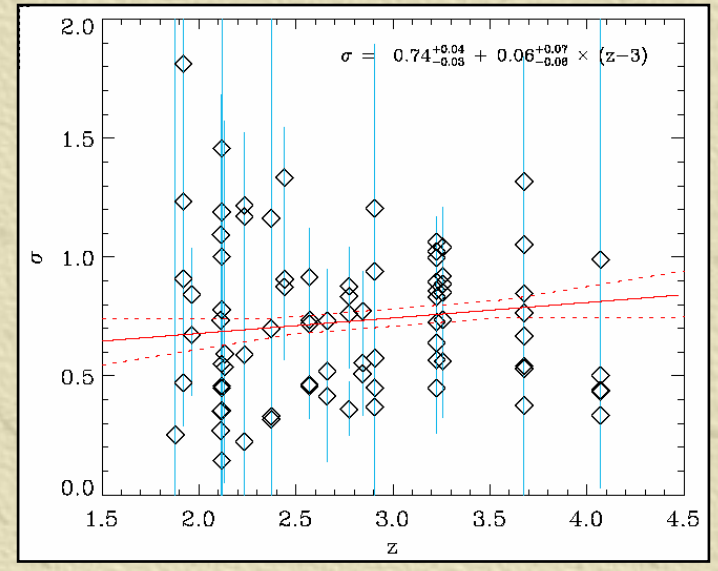

Neither does σ([C/H])

Results: Carbon metallicities from CIV

4. **The median carbon metallicity [C/H] does not evolve (for our fiducial UVB) from z~4 to z~2.**

- Clearly favors enrichment at z > 4.
- But: there is *some* room for more.

Results: Carbon metallicities from CIV

5. [C/H] depends on UVB model.

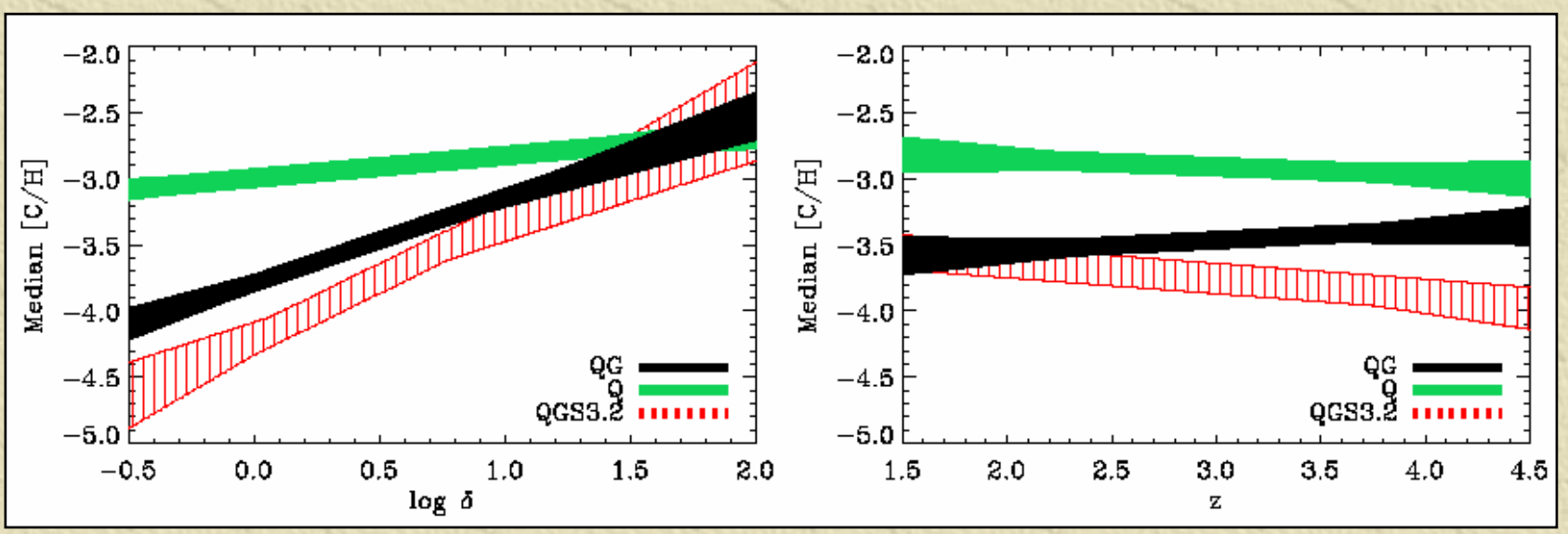

But very different UVBs can be ruled out.

Results: Carbon metallicities from CIV

5. [C/H] depends on UVB model.

- Inferences are sensitive to assumed UVB (and its history).
- But density-dependence, scatter are robust, and evolution *fairly* robust.

Gas temperature from CIII, SiIII

6. CIII/CIV, SiIII/SiIV provide thermometer.

- Bulk of SiIV gas at $T<10^{4.9}$K
- Little scatter in gas temp.
- But some evidence for hotter gas? (< 30%)
- Similar results using CIII/CIV.

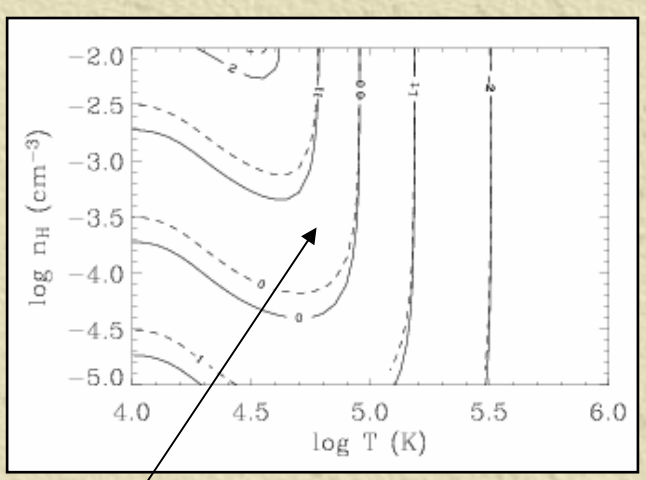

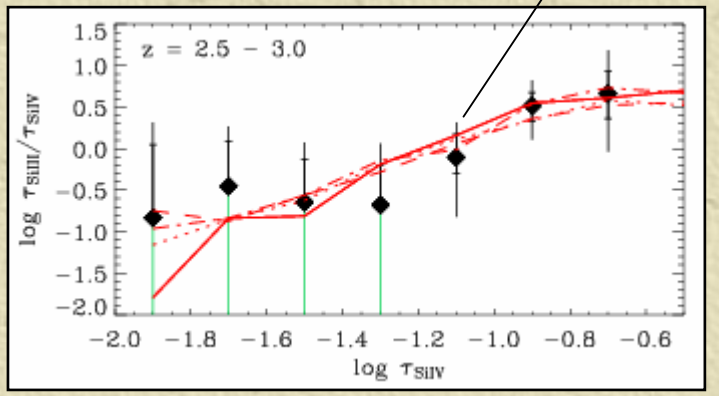

Gas temperature from CIII, SiIII

6. CIII/CIV, SiIII/SiIV provide thermometer.

- Observed metals are in photoionized, warm gas, *not* the collisionally ionized warm/hot gas expected from winds.

Gas temperature from CIII, SiIII

6. CIII/CIV, SiIII/SiIV provide thermometer.

- Observed metals are in photoionized, warm gas, *not* the collisionally ionized warm/hot gas expected from winds.
- But: slight evidence for some missing SiIII, and suggestions of collisionally ionized gas from OVI (in progress).

Silicon metallicities from SiIV, CIV

7. SiIV/CIV vs CIV: ratios depend on δ, reproduced by simulation.

- [Si/C]=0.77+/-0.05
- [Si/C] varies w/UVB hardness.
- *No scatter* in inferred [Si/C]

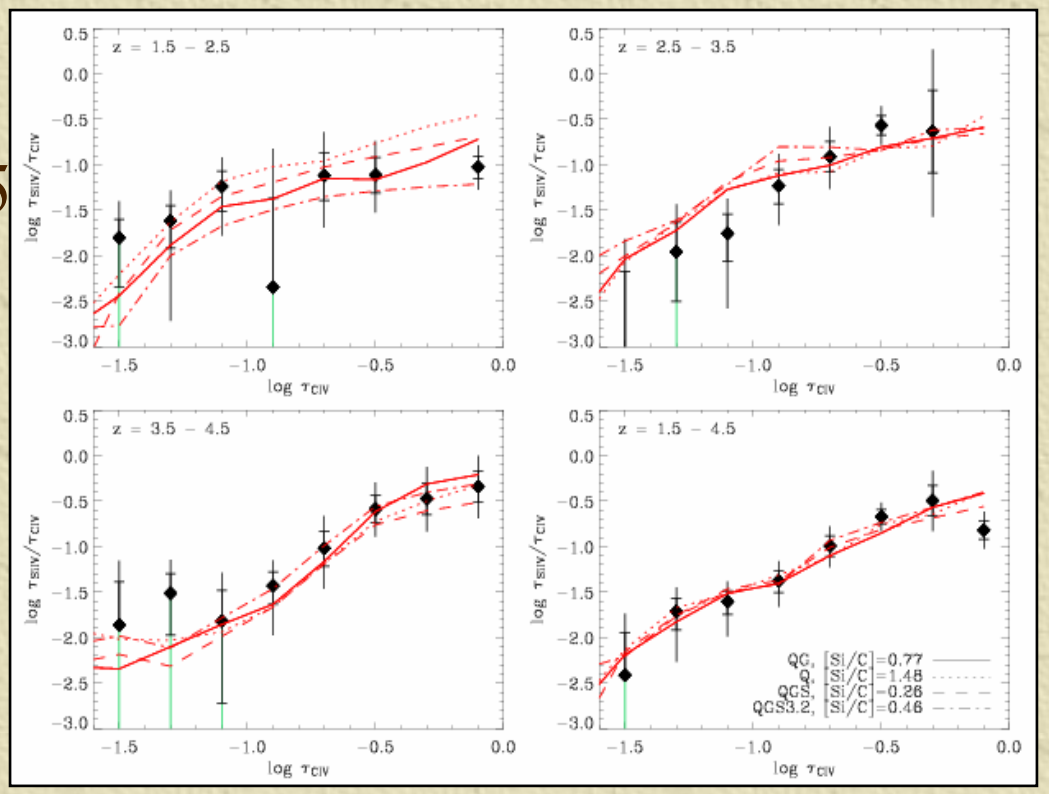

Silicon metallicities from SiIV, CIV

7. SiIV/CIV vs CIV: ratios depend on δ, reproduced by simulation.

- Suggests Pop. II enrichment, which can have [Si/C] ~ 0.5.
- If [Si/C]=0.77 taken seriously, could be more expotic (PISn a la Heger & Woosley?)
- Lack of scatter -> Si and C from same sources; later C production not important.

Silicon metallicities from SiIV, CIV

8. SiIV/CIV vs CIV: ratios depend little on z, reproduced by simulation.

- No jump in UVB hardness at z ~ 1
- No evolution in [Si/C] for usual UV

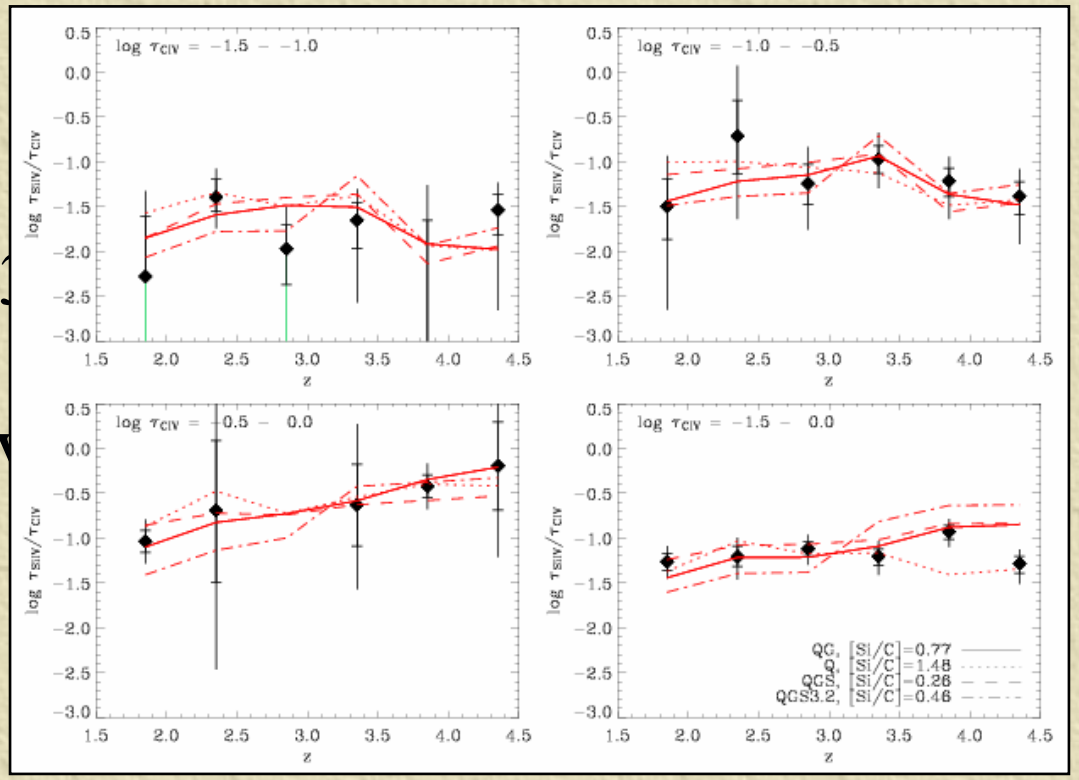

Silicon metallicities from SiIV, CIV

8. SiIV/CIV vs CIV: ratios depend little on z, reproduced by simulation.

- Again, more lack of evidence for anything evolving.

Adding up global C, Si abundances.

9. Median+scatter mean metallicity, and contribution to cosmic C, Si abundance.

- [C/H] = -2.8, [Si/H] = -2.0
- $\Omega_C = 2.7 \times 10^{-7}, \ \Omega_{Si} = 3.2 \times 10^{-7}$
- $\Omega_{\mathrm{Si},*} = 7.5 \times 10^{-7} \left(\frac{\Omega_*}{0.001} \right) Z_{\mathrm{Si}}$

$Z_\odot$ **stars hold only < 60-70% of cosmic Si; rest is in Lyα forest.**

- **Lots of metals in the forest!**

Adding up global C, Si abundances.

9. Lots of metals in the forest.

- Metal ejection is quite efficient before z ~ 3-4.
- Could z >> 6 enrichment provide enough metals?
- Also: clusters -> metallicity evolution and/or hidden metals in hot gas.

The scorecard

Test	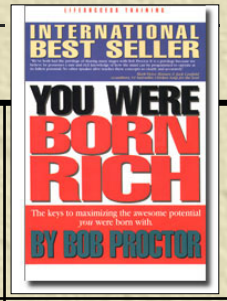		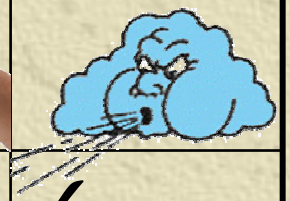
Inhomogeneous, ρ-dep. Z	X	✓	✓
No evolution in Z observed.	✓	✓	X
Warm, photoionized gas	✓	✓	X?
[Si/C] ~ 0.75	?	✓ ?	✓ ?
No evolution, scatter in [Si/C]	✓	✓	X?
Lots of metal in IGM	?	X?	✓

Real picture: a conundum. Early *and* late?

Some questions/considerations:

- Metals sprinked in non-feedback simulation reproduce all current observations. *But*…
- Do the observed winds escape? If so, where do the metals go?
- If not winds, how to we fix baryon fraction in galaxies?
- How do we close the cluster -- forest gap?
- Metal from late galaxies may be hidden in unobservably hot gas, with low filling factor (and avoiding the filaments?)
- Metal and H absorption does not *have* to come from same gas.
- Data allows some evolution, esp. using freedom in UVB.

To do/in progress:

1. Complete OVI analysis, look for NV:
   - UVB has “opposite” effect on O than on Si.
   - hotter gas can be seen in OVI.
2. Look at metallicity vs. “distance” from absorber.
3. Look at wavelenth-*correlations* in PODs.
4. Compare observed PODs in detail to hydro. simulations *with feedback.*
5. Try to connect these with simulations of individual galaxies.

Conclusions

- The observations are consistent with metals "sprinkled" at z > 5 with $[C/H] = \log[10^{-3}\,(\delta/10)^{0.7}]$ and σ ~ 0.75 dex, [Si/C] ~ 0.75.
- They are *in*consistent with:
  - Lots of C or Si in T ~ 10^5 - 10^6 K gas.
  - Evolution of C or [Si/C] in T < 10^6 K gas.
  - Homogeneous enrichment.
- Stronger constraints coming soon!
- For more detail, see: Aguirre et al. 2003, 2004; Schaye et al. 2004.

The Role of Early Intermediate Mass Stars on the Cosmological Evolution of α

T. Ashenfelter, G. J Mathews - Notre Dame

K. A. Olive - Minnesota

Ashenfelter, Mathews, & Olive, Phys Rev Lett (2004)

ApJ (2004), astro-ph/0404257

$$\alpha = e^2/(2\varepsilon_o hc)$$

Workshop on the Chemical Enrichment of the Early Universe, Santa Fe, NM Aug. 12

Why look for a varying α ?

- **α is a dynamical variable in GUTs that freezes to a vacuum expectation value**
- **Evolution of extra dimensions in multi-dimensional theories changes the properties of the vacuum**
- **Larger speed of light in the Early Universe to account for Inflation**
  - **Caution: Depends on the "definition" for c**

Observational Limits on α Variation

- **Big Bang Nucleosynthesis at a $z=10^{10}$**
  - $\Delta\alpha/\alpha$ **< few x 10^{-4}**

$\Delta\alpha/\alpha = -.54 \times 10^{-5}$ $.5<z<4.3$ from MM method

- **Meteoritic data of ^{187}Re β decay at $z<.45$**
  - $\Delta\alpha/\alpha$ **< 10^{-7} - 10^{-8}**
- **Oklo natural fission reactor at z = .15**
- **Atomic Clocks of ^{87}Rb and ^{133}Cs measured for a 5 year span vary less than 1.5 x 10^{-15} / year**

Many-Multiplet Method Results

- **Murphy et al. (2001 & 2003) measured spectral lines in 128 Damped Lyman-Alpha Clouds (DLAs) from a redshift range of z = .5 to 4.2**
  - **MM method compares separation of a line sensitive to α to one that is not (anchor).**
    - **Relies heavily on precise Atomic data**
  - **Heavier atoms have larger relativistic corrections than lighter atoms (ex. Fe vs. Mg)**
    - **Line shift proportional to $(Za)^2$**
- **Result in $\Delta\alpha / \alpha = (-.54 +/- .11) \times 10^{-5}$ → 4.7σ result!**

From John Webb's homepage

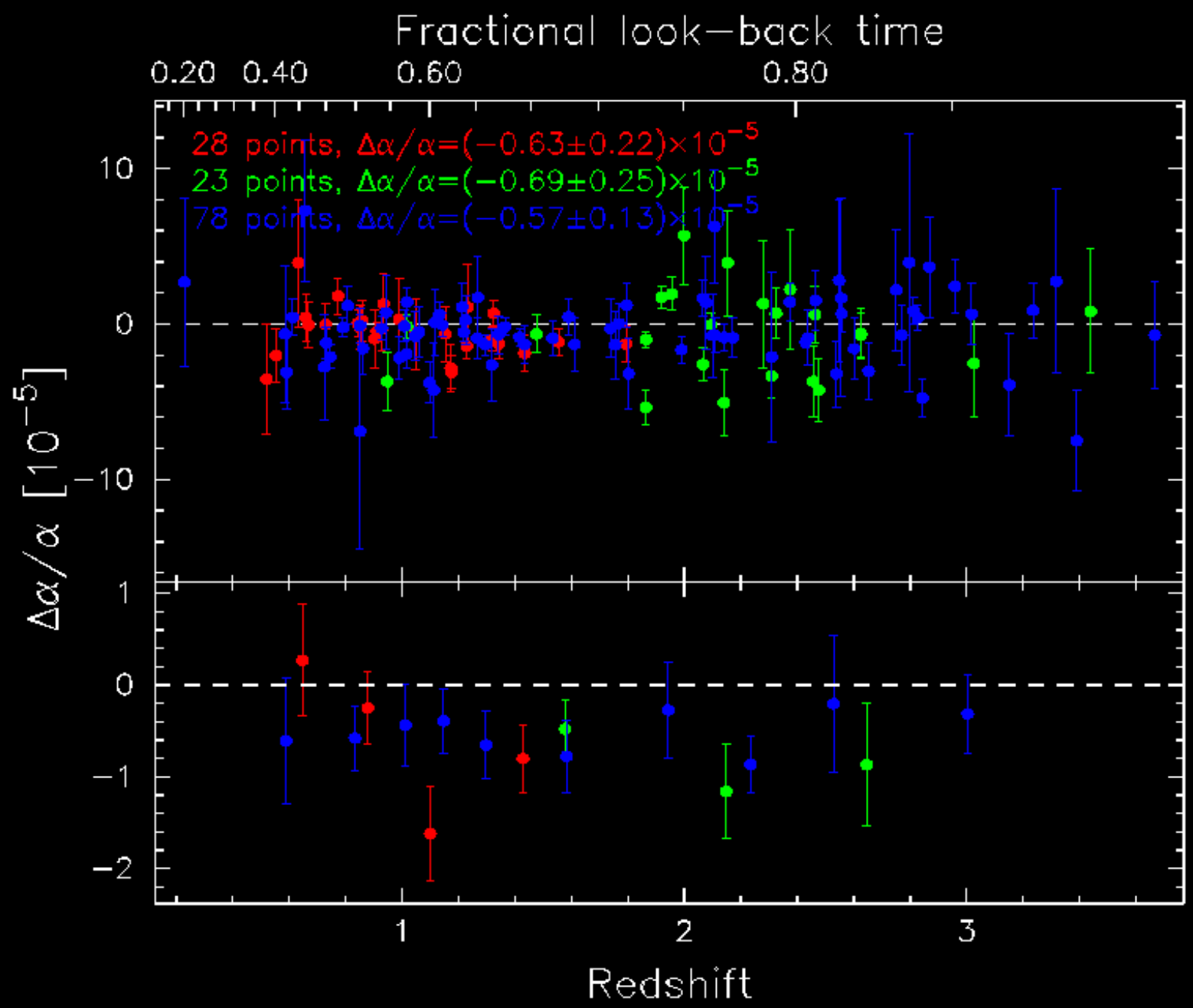

Sensitivity of MM method with Mg anchor on Isotopic Ratio

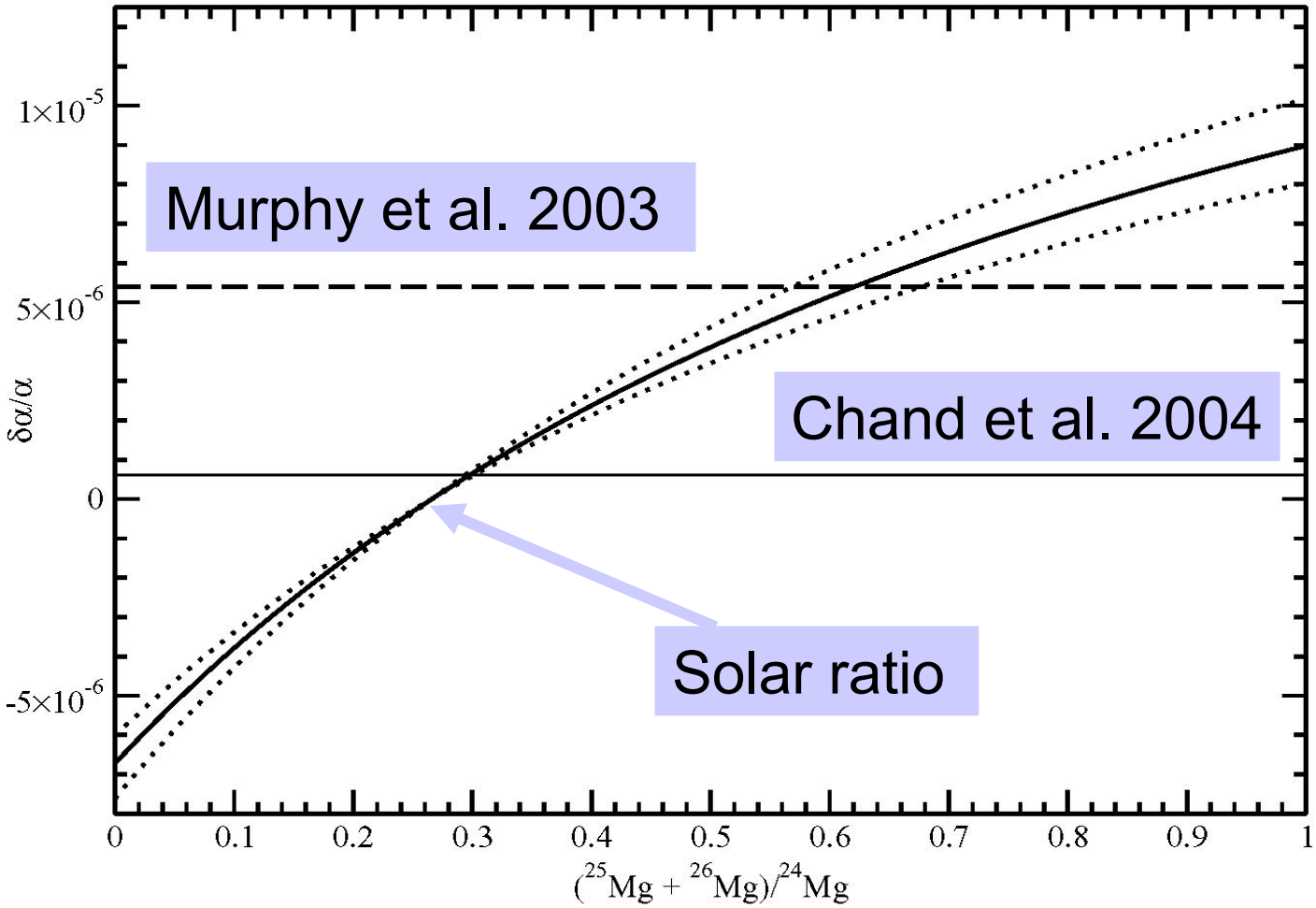

Evidence for enhanced $^{25,26}Mg$ Production

- **Sample of cool halo stars. Large ratios in halo/thick disk stars.**
- **As high as 60:20.**
- **(Yong et al. 2003 A&A 402, 985)**

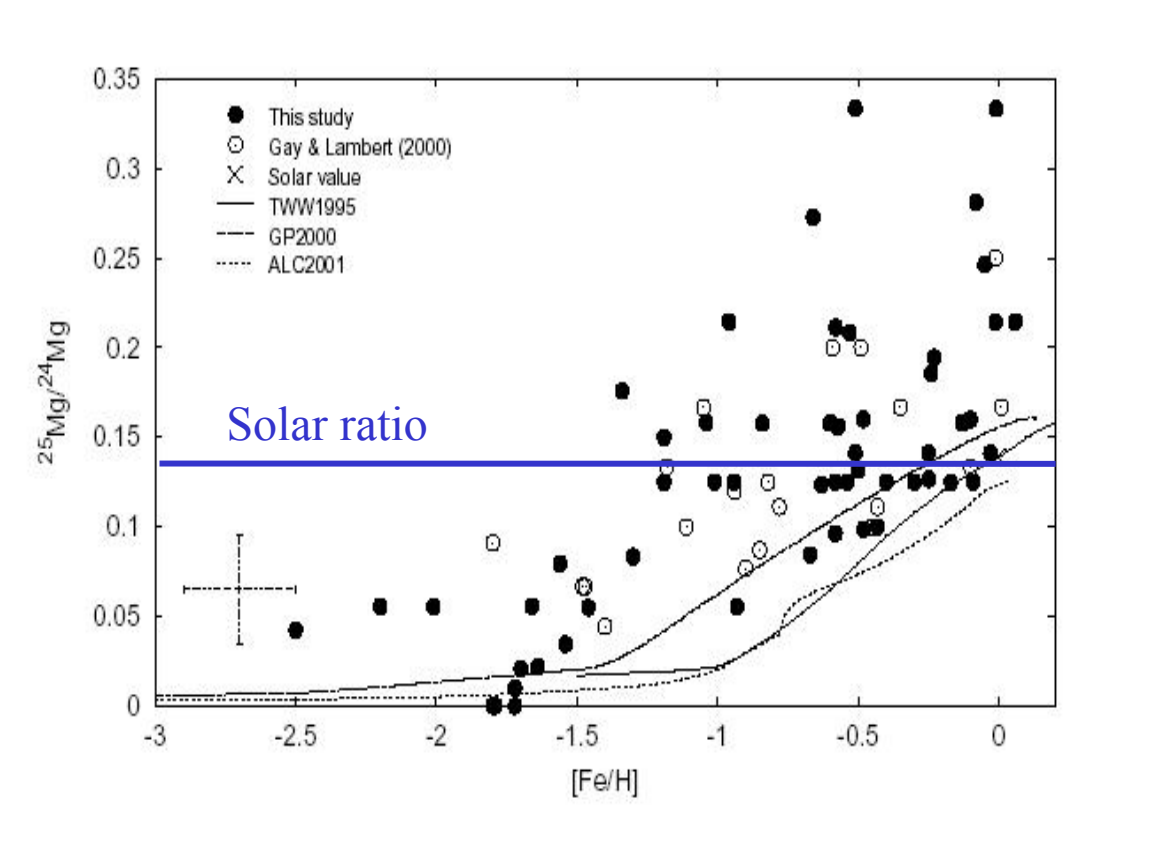

AGBs are a source of $^{25,26}Mg$

Hot-bottom burning from p capture: (secondary)

$^{24}Mg \Rightarrow {}^{25}Al$ or $^{26}Al \Rightarrow {}^{25}Mg$ or ^{26}Mg

He burning shell from α capture: (primary)

$^{14}N \Rightarrow {}^{22}Ne \Rightarrow {}^{25}Mg$ or ^{26}Mg

Chemical Evolution Model

- **Timmes, Woosley & Weaver(1995) model modified for DLA systems:**
  - **Updated AGB Yields for Mg,Al**

  [Karakas & Lattanzio (2003); Marigo (2001); Portinari (1998)]
  - **Cosmic Type Ia/II Supernova rates**

  (Kobayashi et al. 2001) metallicity constraint
  - **Early AGB enhanced IMF centered around 5-6 solar masses (most efficient Mg isotope producer)**

Enhanced Initial Mass Function

- Lognormal mass distribution on top of the standard power law distribution of masses
  - Center of lognormal around 5 solar masses
- IMF still is normalized to unity
- Coefficient exponentially decays rapidly as a function of time (.2-.4 Gyr timescale).

Clues for an AGB enhanced IMF

- **Populate the halo with MACHOs (white dwarfs)**
- **Bi-modal primordial IMF (Uehara et al. 1996)**
- **S-processing in metal poor stars**
- **C,N enhancements in metal poor stars**
- **Proximity to possible r-process site in 8-10 M_{sol}**
- **Observed Deuterium depletion w/o metal overproduction (Fields et al. 2001).**
- **Additional Mg source**

Chemical Evolution Model can imitate α variation

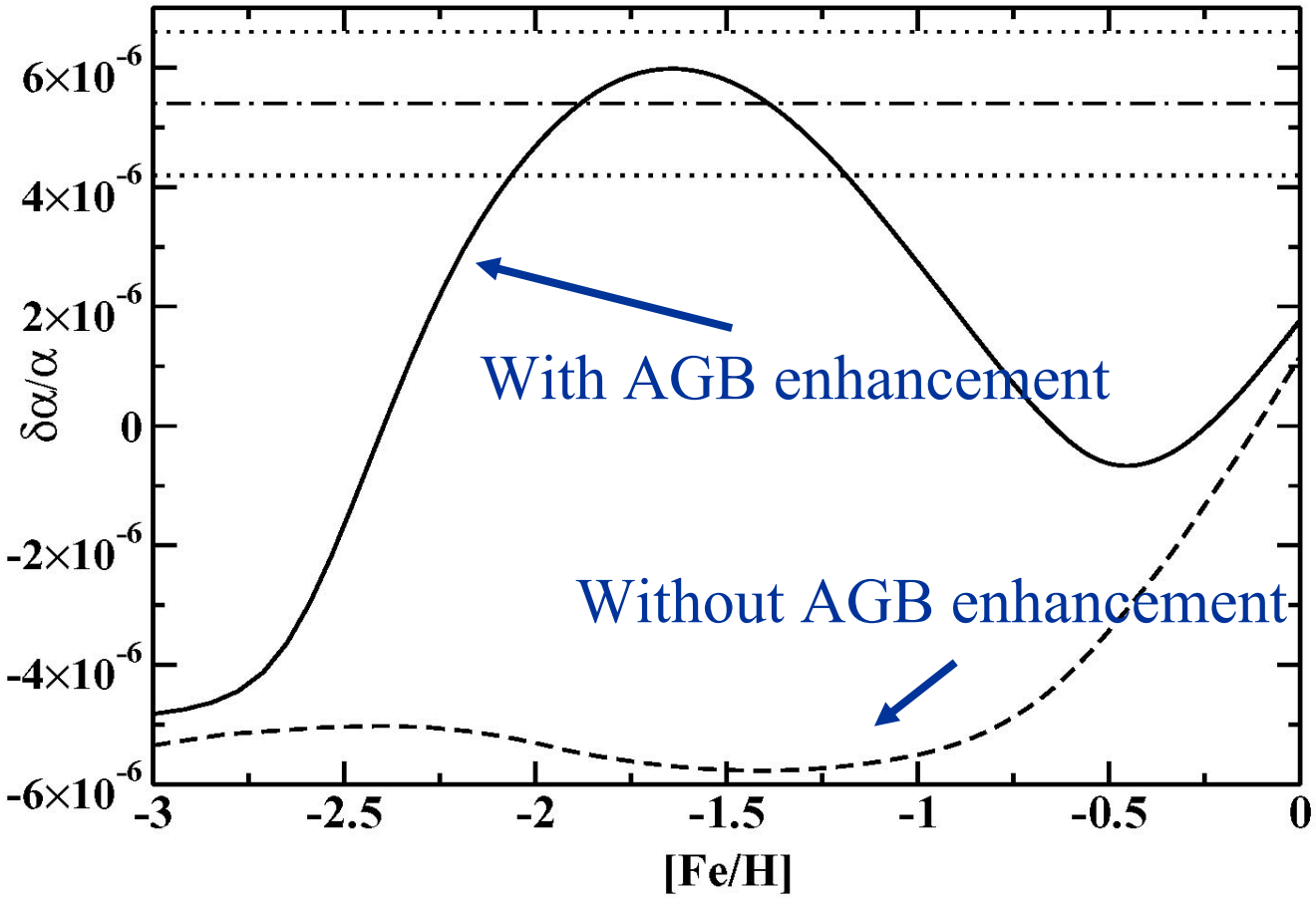

A Tale of Two Surveys

No AGB enhancement		Some AGB enhancement
	Murphy et al.	
$-.87 +/- .13 \times 10^{-5}$ ←	**$-.54 +/- .11 \times 10^{-5}$**	→ **$0 +/- .11 \times 10^{-5}$**
	Chand et al.	
$-.36 +/- .06 \times 10^{-5}$ ←	**$-.06 +/- .06 \times 10^{-5}$**	→ **$0 +/- .06 \times 10^{-5}$**

Must compare the 2 scenarios!

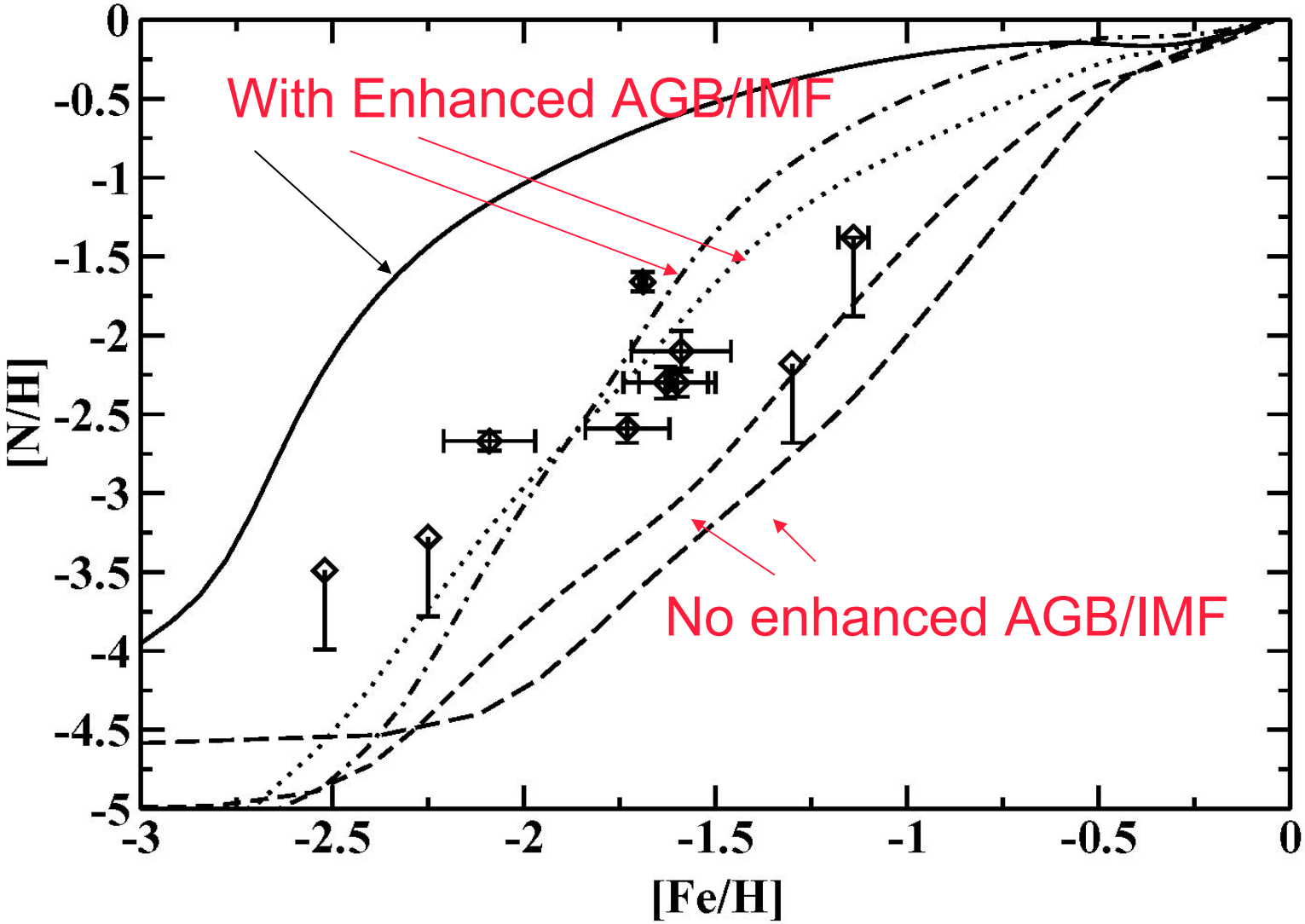
With Enhanced AGB/IMF
No enhanced AGB/IMF
[N/H]
[Fe/H]
0
-0.5
-1
-1.5
-2
-2.5
-3
-3.5
-4
-4.5
-5
-3
-2.5
-2
-1.5
-1
-0.5
0

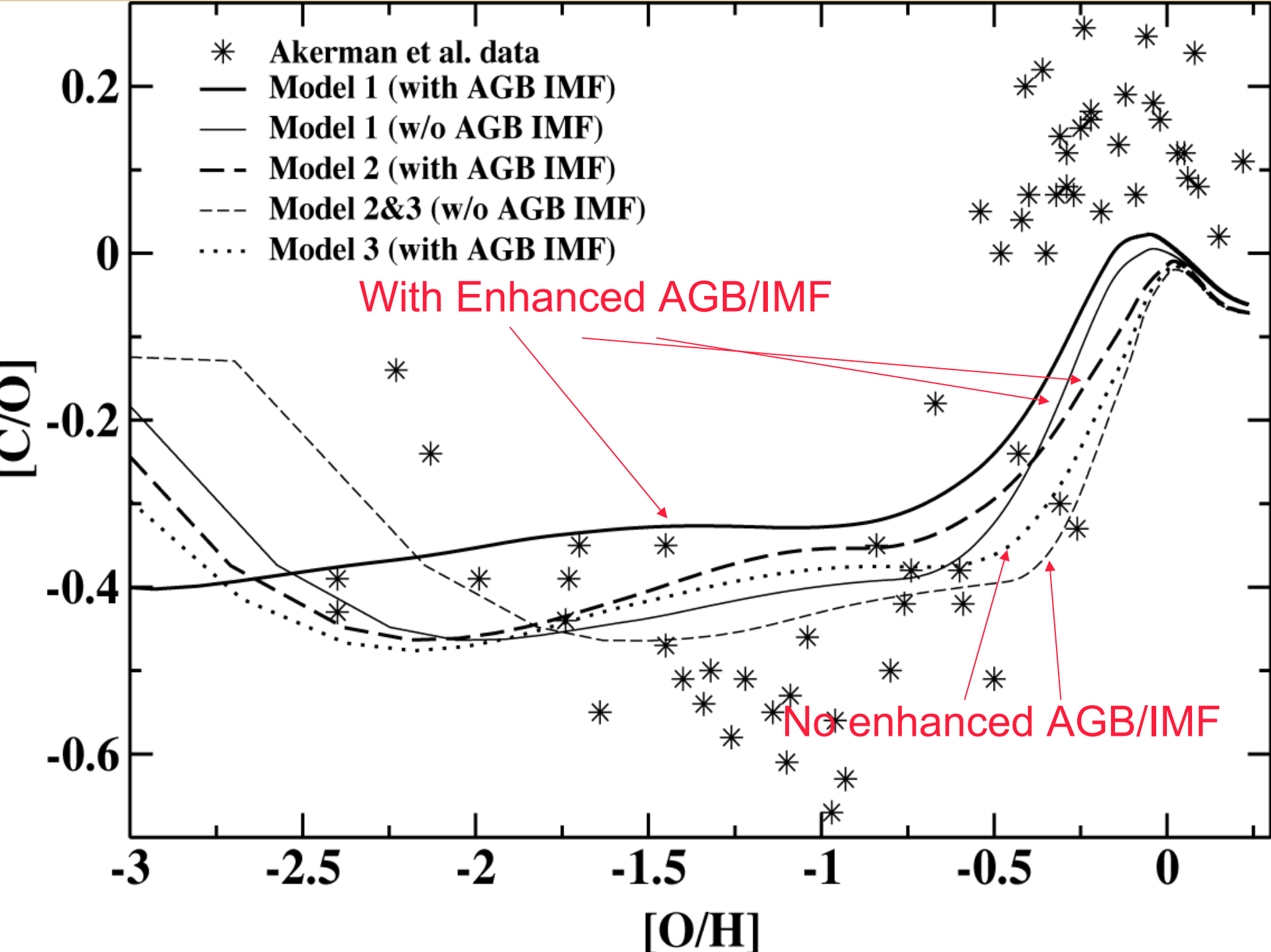
Akerman et al. data
Model 1 (with AGB IMF)
Model 1 (w/o AGB IMF)
Model 2 (with AGB IMF)
Model 2&3 (w/o AGB IMF)
Model 3 (with AGB IMF)
With Enhanced AGB/IMF
No enhanced AGB/IMF
[C/O]
[O/H]
0.2
0
-0.2
-0.4
-0.6
-3
-2.5
-2
-1.5
-1
-0.5
0

Conclusions

1). Chemical Evolution offers an alternate to α variation, but requires early AGB stars.

2). MM method can be an extremely useful statistical tool for determining abundances, especially isotopes.

3). An anchor insensitive to isotopic variations needs to be implemented for further fine structure analysis.

4) DLA abundances provide a great laboratory to test Hypotheses in chemical evolution

Avenues for Improvement

1). Improved Atomic data on oscillator strengths and effective isotopic shifts.

2) Stellar yield models for 7 – 12 solar masses of all metallicities.

3). More abundances of metal poor stars and DLAs.

4). Find highly correlated abundance ratios for unique enrichment scenarios.

5). Stellar yield models for low metallicity 40-160 solar masses.

6). AGB yield models that self-consistently follow CNO and Mg, Al, Si, and Li. Models for very low metallicity.

New Mg Isotope Yields

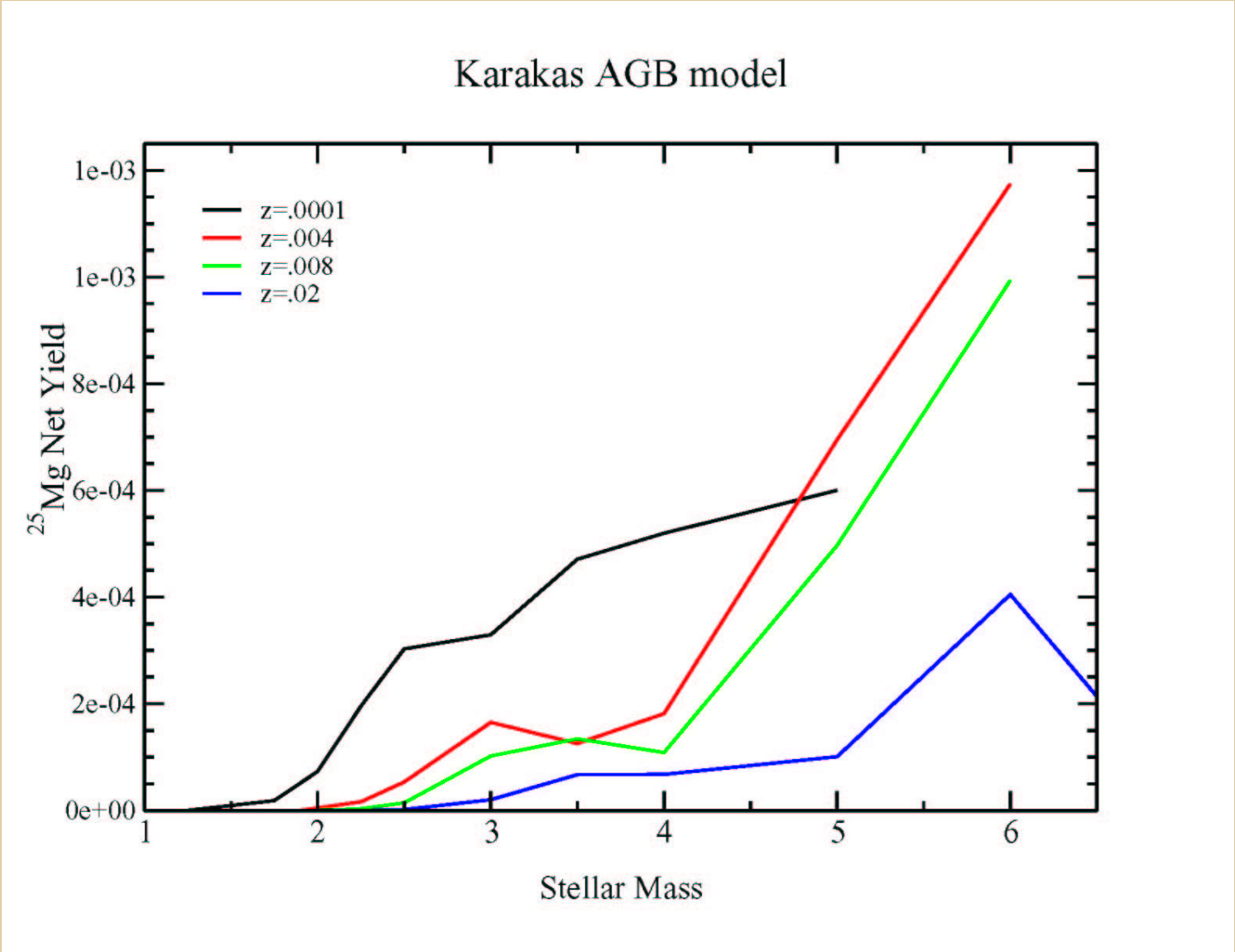

New Nitrogen Yields

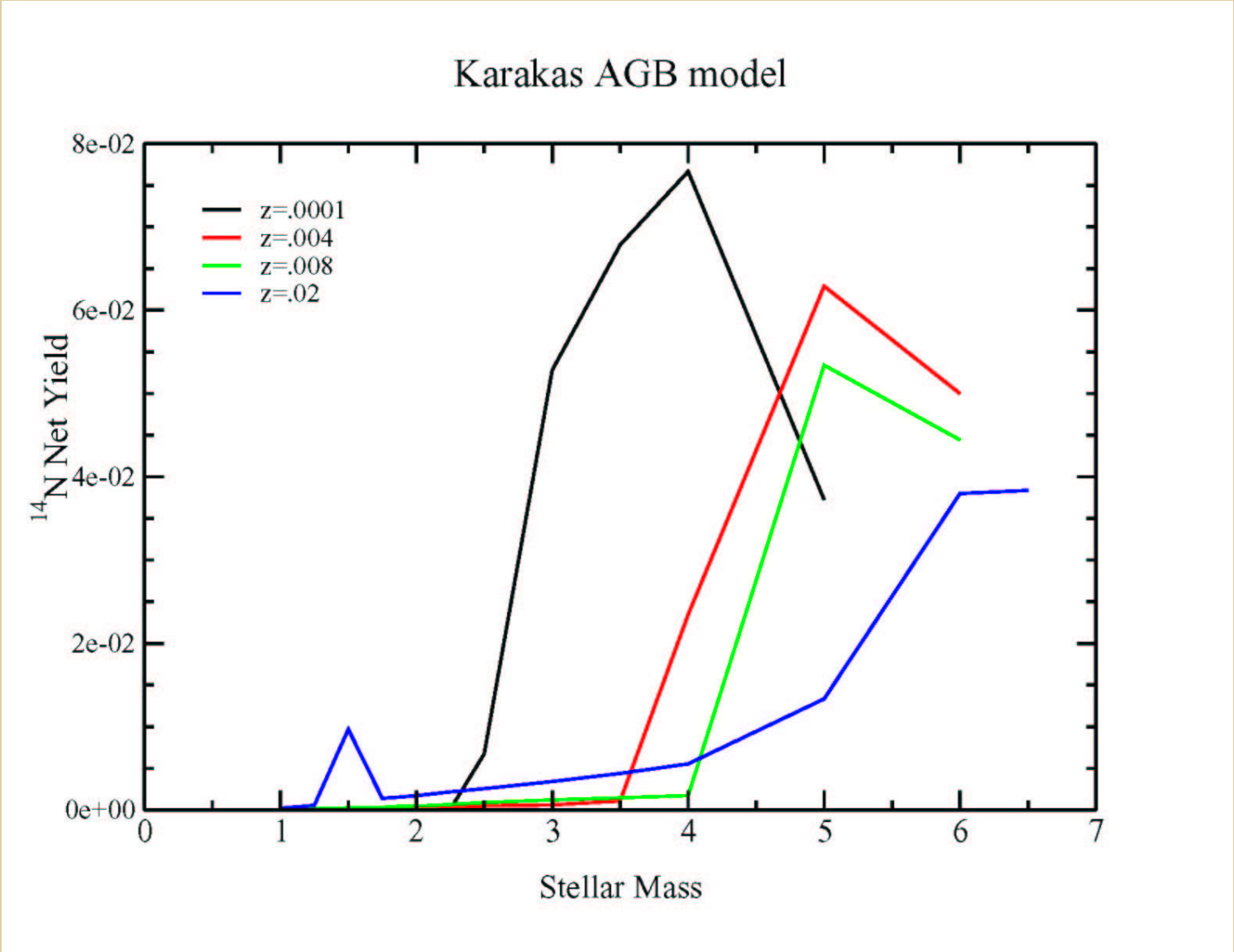

New Carbon Yields

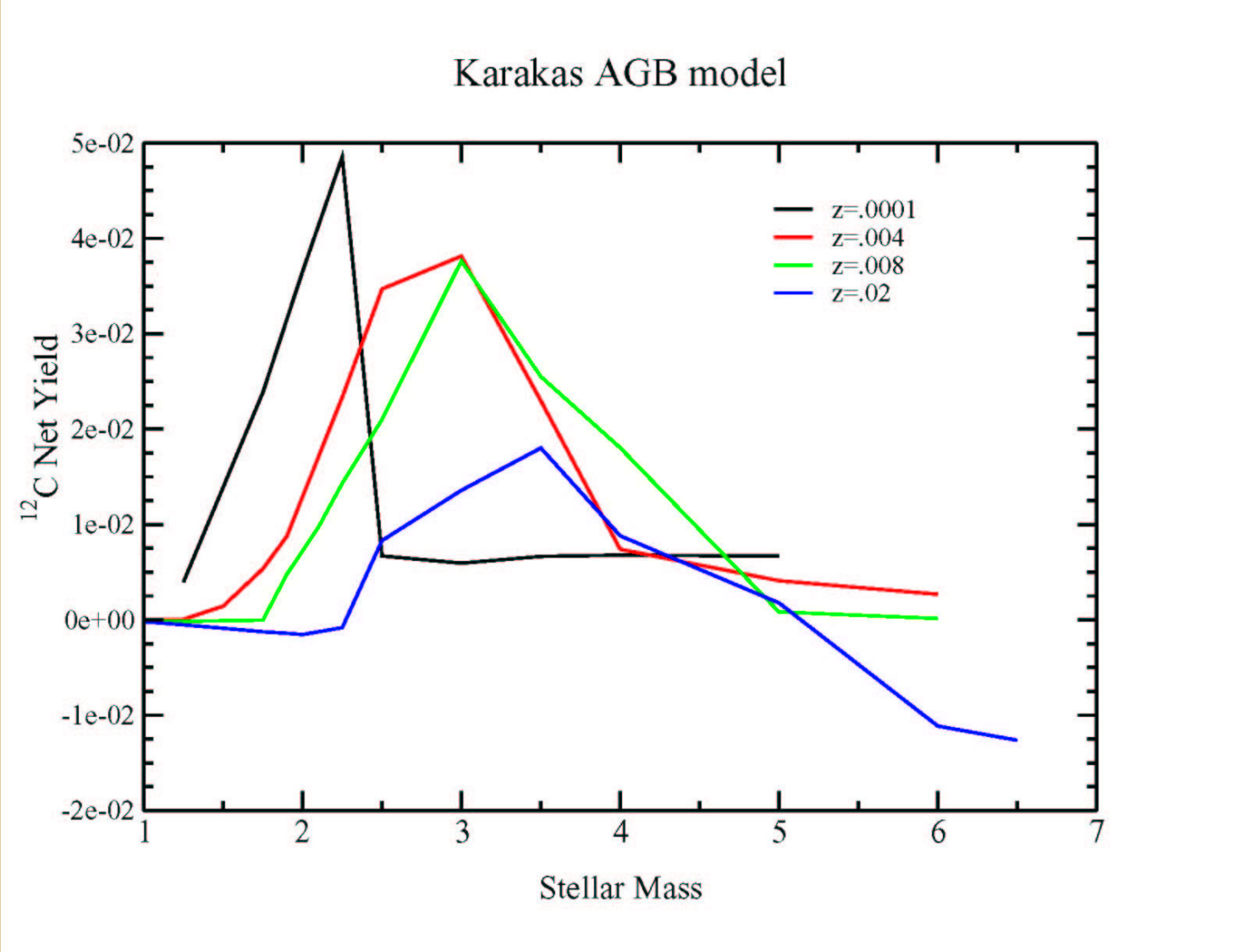

Frequency and Metallicity of Low-Z Stars – A Survey of Surveys

Timothy C. Beers

Department of Physics & Astronomy
and
JINA: Joint Institute for Nuclear Astrophysics
Michigan State University

Outline of Talk

- Results to Date
  - HK-I Survey
  - Hamburg/ESO Survey (Giants)
- Ongoing Surveys
  - HK-II Survey
  - Hamburg/ESO Survey (Dwarfs)
  - Hamburg/ESO Survey (SOS)
  - Hamburg/ESO Survey (UMP)
  - Hamburg/ESO Survey (HERES)
- Future Surveys
  - SDSS-II (SEGUE)

Selection of HK Survey Stars – HK-I (visual selection)

Initially, visually selected from wide-field (5° X 5°) objective-prism plates (6500 square deg, N+S) :

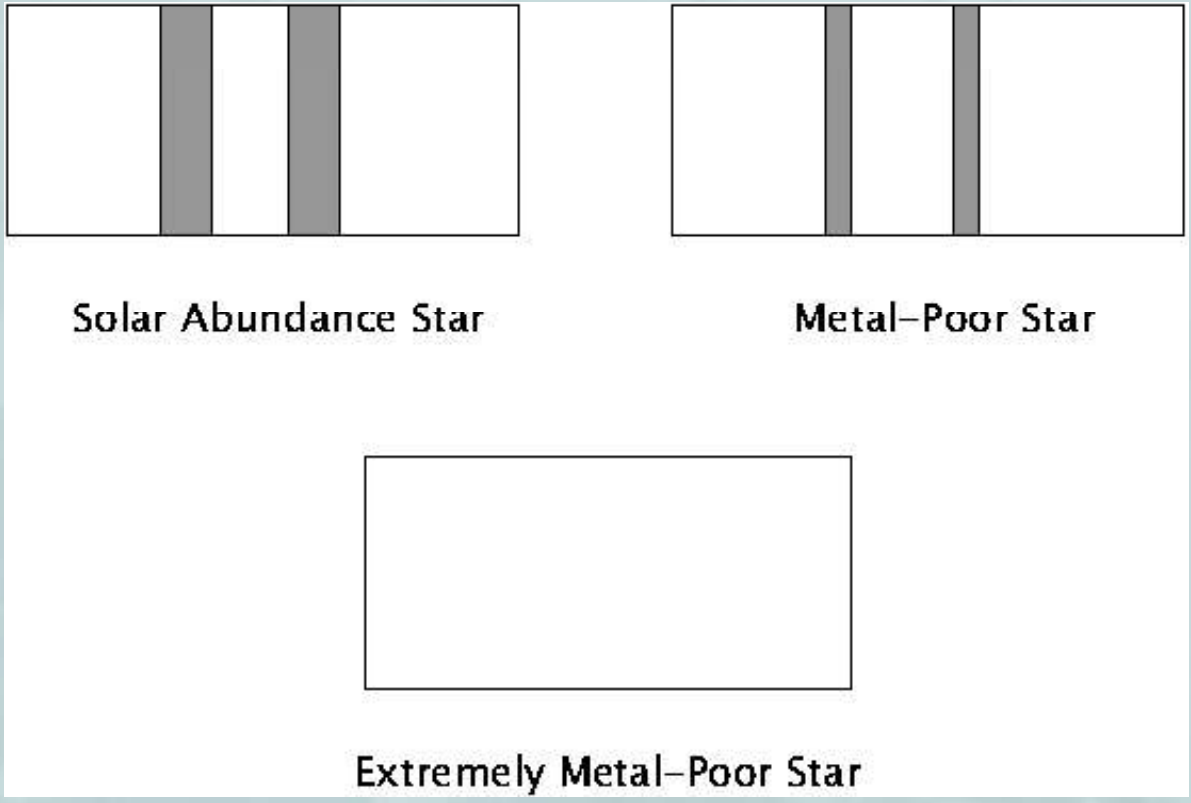

Results from HK-I Survey

- Medium-resolution (1-2 A) spectroscopy of some 7000 candidates, one at a time, over last 20 years
- N ~ 1000 stars with [Fe/H] < -2.0
  - 11.5 < B < 15.5
- MDF consistent with simple models of GCE, down to [Fe/H] ~ -4.0
- Discovery of large fraction (~20-25%) of [Fe/H] < -2.0 stars with carbon enhancement
- Unfortunately, visual selection leads to rather severe temperature-related bias (lack of giants)

The HK-I Metallicity Distribution

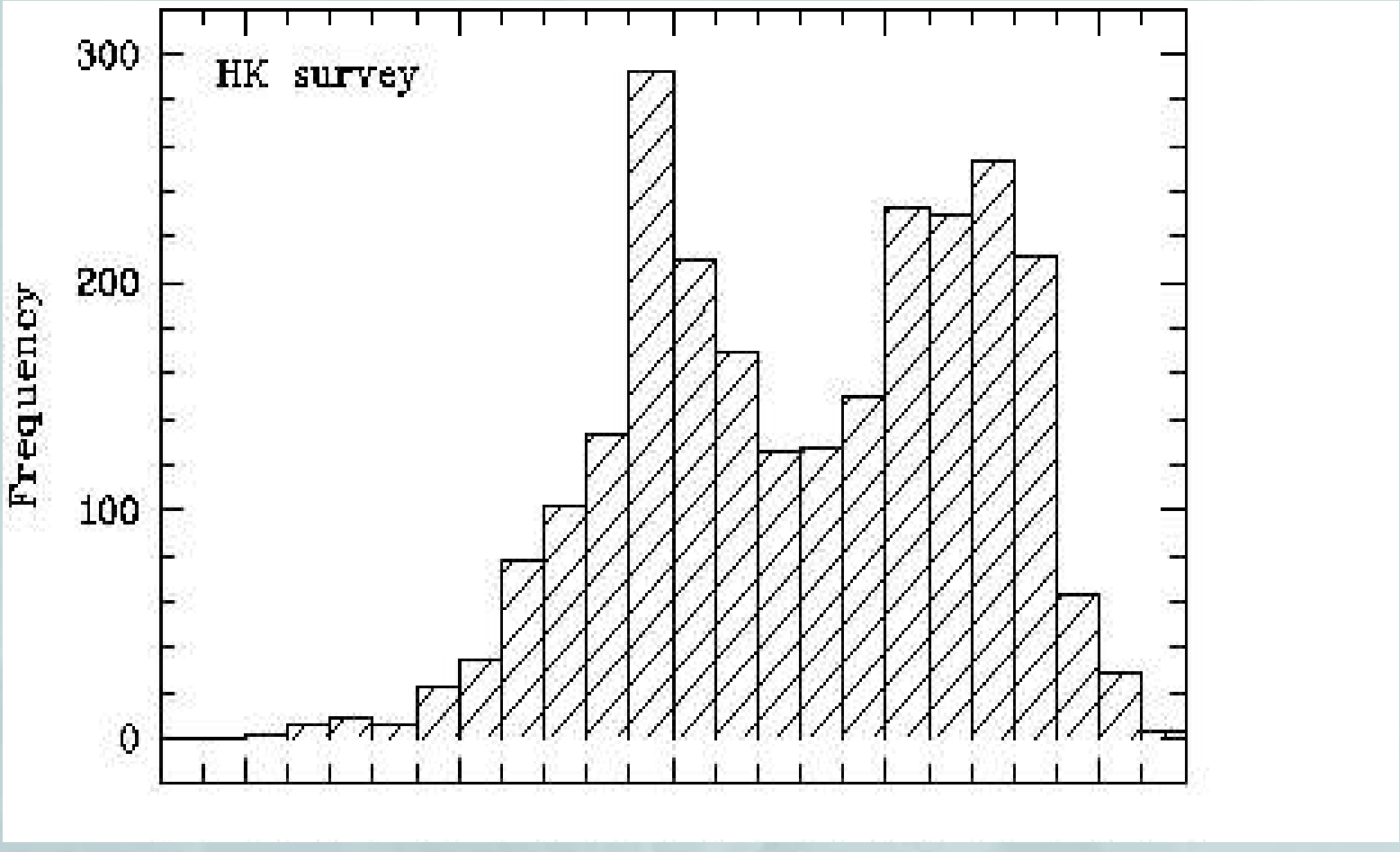

-4 -3 -2 -1 0

[Fe/H]

Examples of Low Metallicity Trends Based on HK Survey Giants – Cayrel et al. (2004)

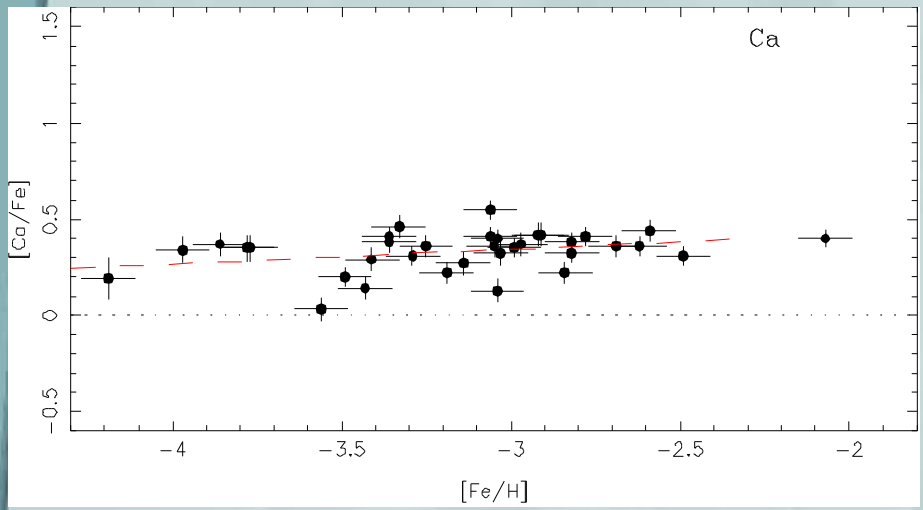

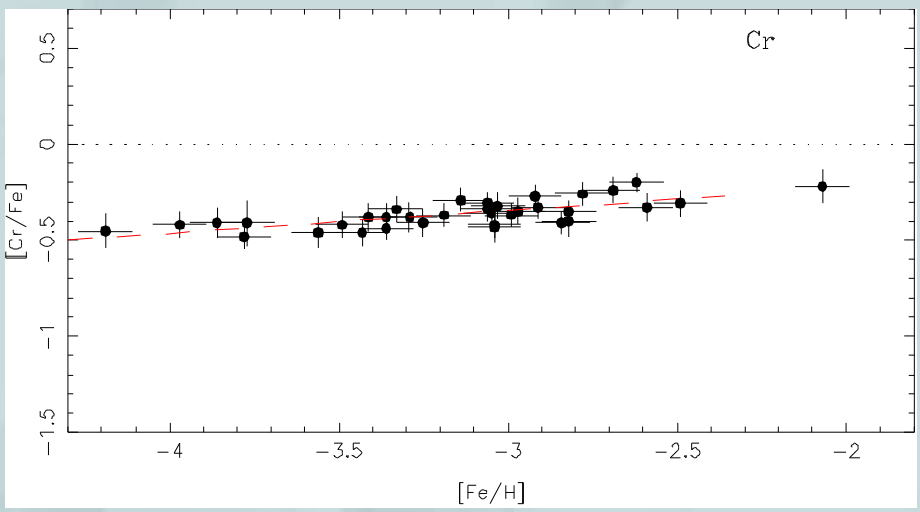

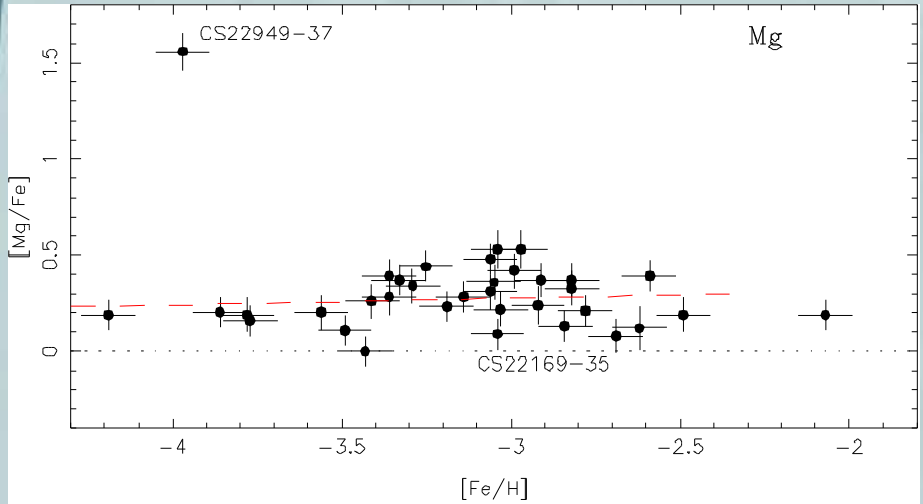

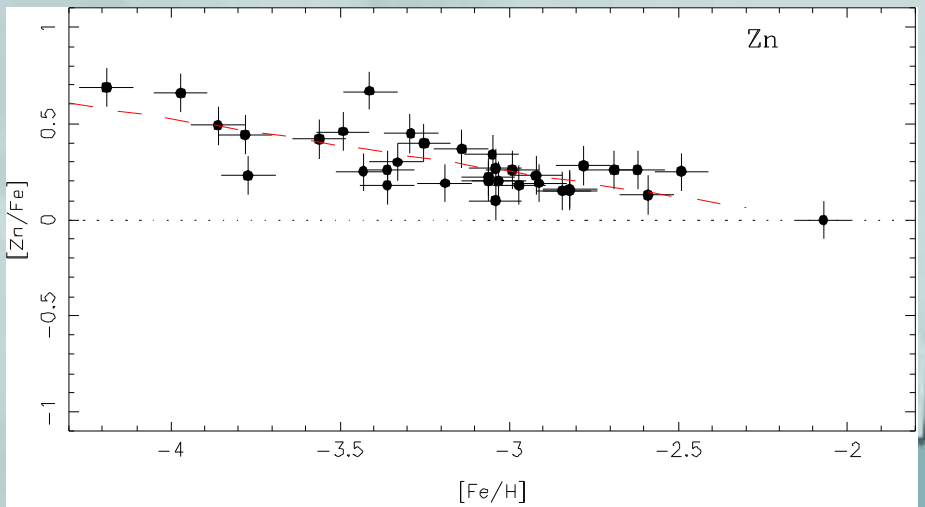

The New Kid on the Block – The Hamburg/ESO Survey

- Deep wide-field objective prism survey of the southern sky (7500 square deg.) $|b| > \pm 30^{o}$ $13.5 < B < 17.5$
- Machine scanned and automatically classified (4,000,000 stellar spectra)
- Highly efficient selection of metal-poor, FHB/A stars, carbon-enhanced stars, etc.

Comparison of the HK & HES Surveys

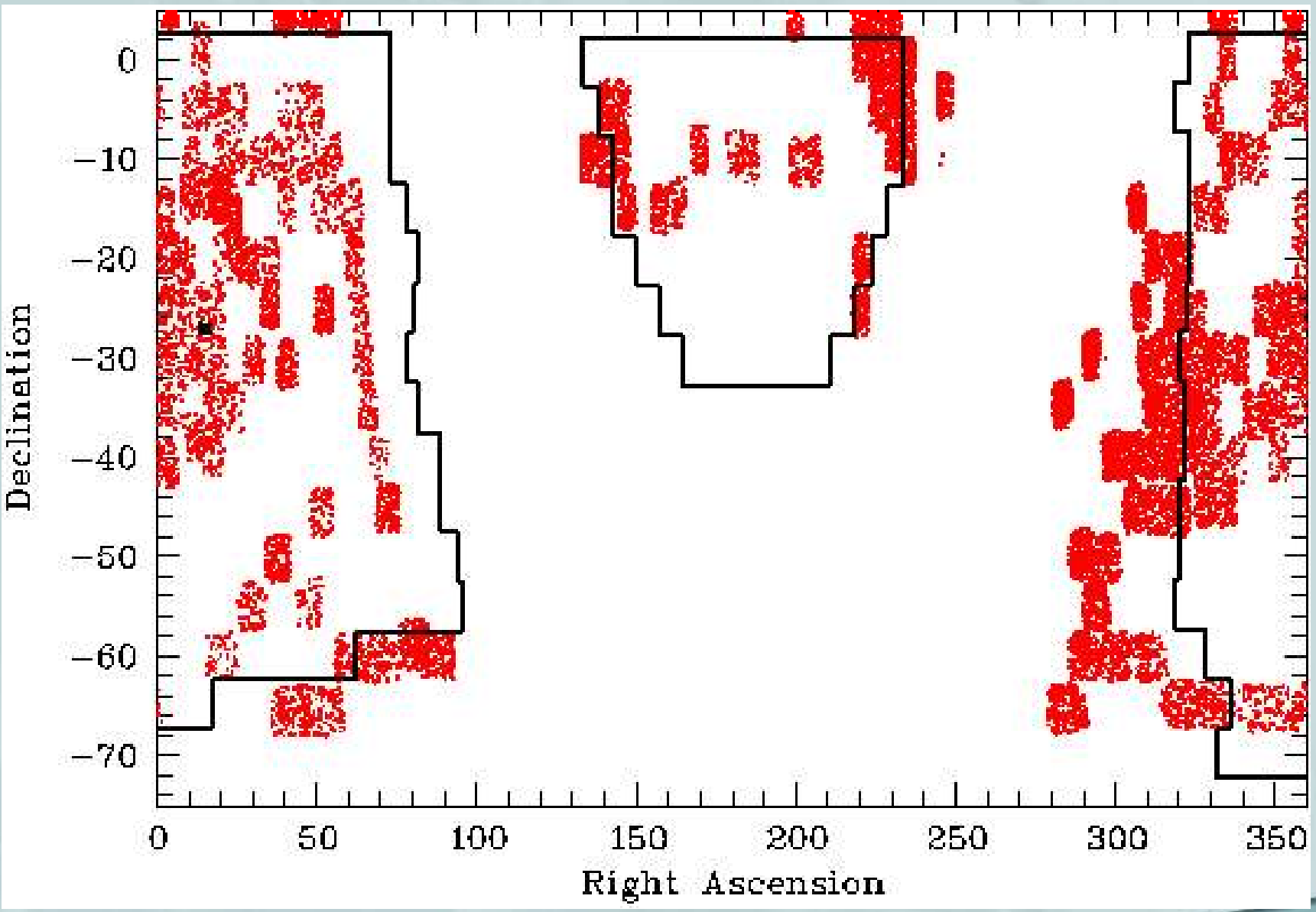

Example HES Spectra of MP Stars

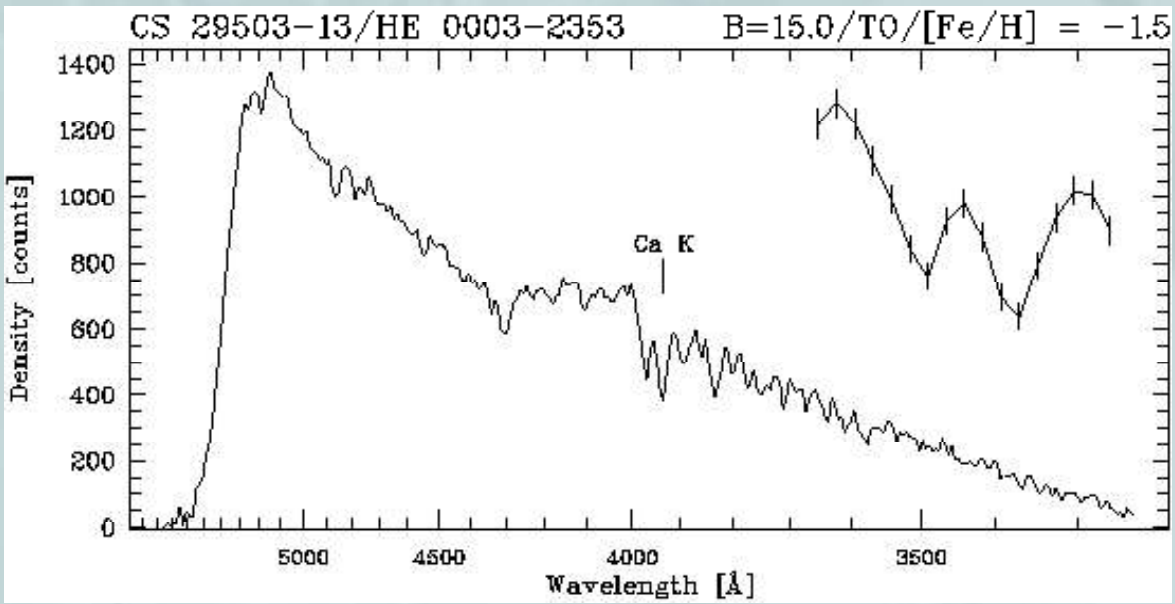

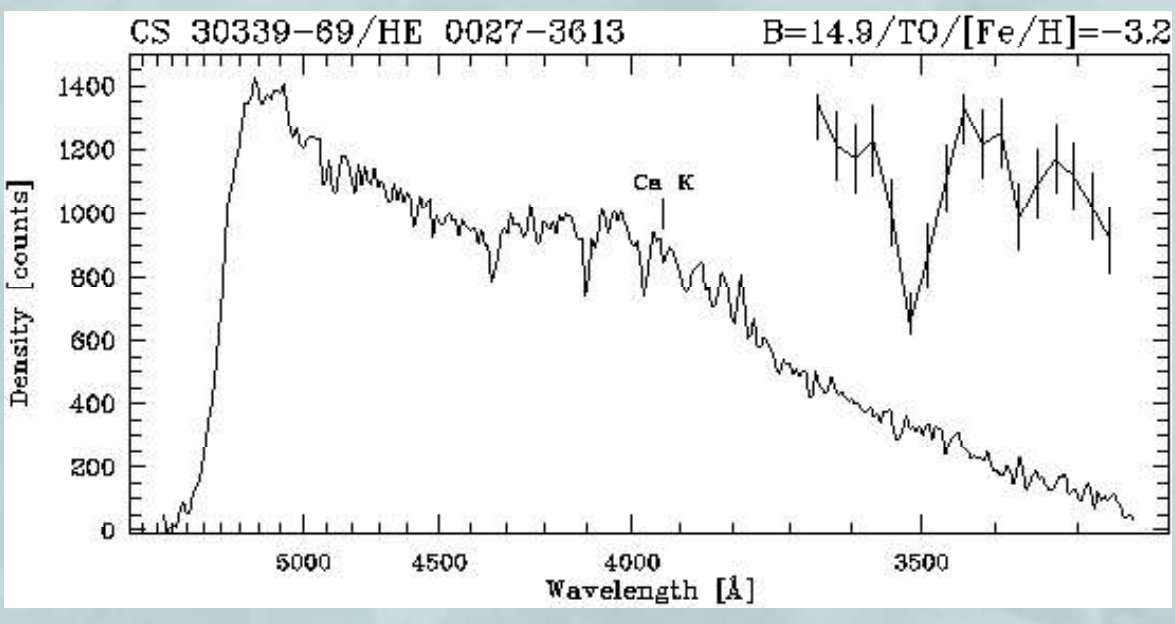

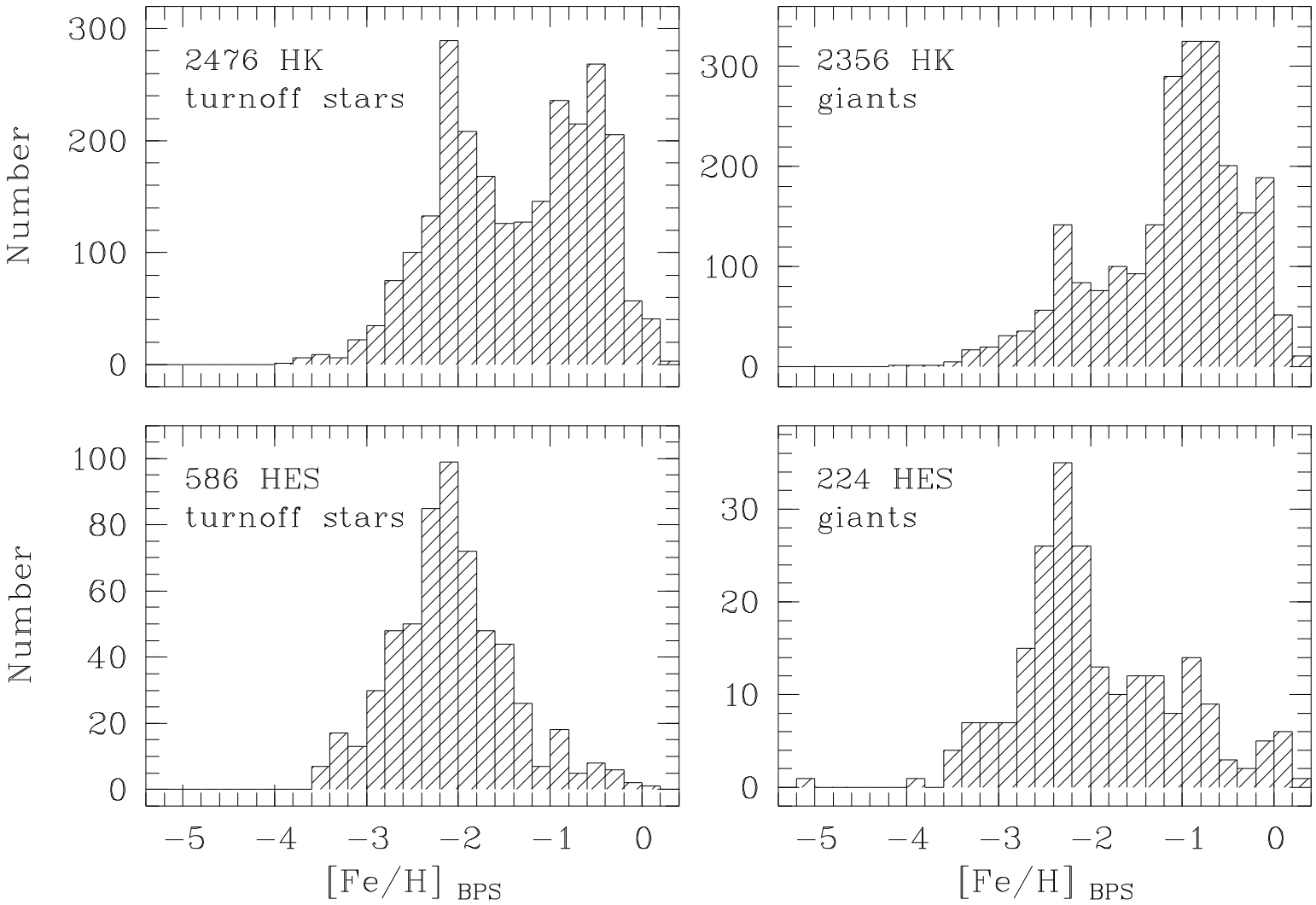
2476 HK
turnoff stars
2356 HK
giants
586 HES
turnoff stars
224 HES
giants
Number
Number
[Fe/H] BPS
[Fe/H] BPS

Results from HES

- Medium-resolution (1-2 A) spectroscopy of some 3000 candidates, concentrating primarily on giants, more recently on turnoff stars
- N ~ 1000 stars with [Fe/H] < -2.0
- MDF consistent with HK-I, e.g., simple models of GCE, down to [Fe/H] ~ -4.0
- Confirmation of large fraction (~20-25%) of [Fe/H] < -2.0 stars with carbon enhancement
- Discovery of most iron-deficient star yet known, HE 0107-5240, with [Fe/H] = -5.3

Ongoing Surveys

- HK-II Survey (Rhee)
  - Automated scans of HK survey plates + 2MASS JHK
  - Designed to eliminate temperature bias in HK-I
- Hamburg/ESO Survey (Dwarfs)
  - Renewed effort on warmer stars
  - N ~ 2000-3000 candidates planned to be observed
- Hamburg/ESO Survey (SOS; Frebel)
  - Saturated Object Survey
  - N ~ 1700 HES stars with $10 < B < 14$
- Hamburg/ESO Survey (UMP)
  - Ultra Metal-Poor Survey: HK/HES objects with $[Fe/H] < -3.5$
  - N ~ 20, being observed at high-resolution with Subaru/HDS + VLT/UVES

HERES: The Hamburg/ESO R- Process Enhanced Star Survey

- Based on 15-20 minute "snapshot" spectra of ~ 375 validated [Fe/H] < -2.5 giants with VLT/UVES
  - 350 hours (~ 44 nights of time) already assigned; last scheduled observations taking place now
  - R = 20,000; S/N ~ 30/1 obtained (suitable for poor seeing conditions, queue mode)
  - Should find 10-15 r-II stars, perhaps 20-30 r-I stars, and additional r-s stars (enhanced in BOTH r- and s-process elements
- Searching for detectable absorption of Eu II 4129 A
- Obtain elemental abundances of ~ 20 additional elements, even for non r-process-enhanced stars

Sample Spectra in the Region of Europium (for an r-I Star)

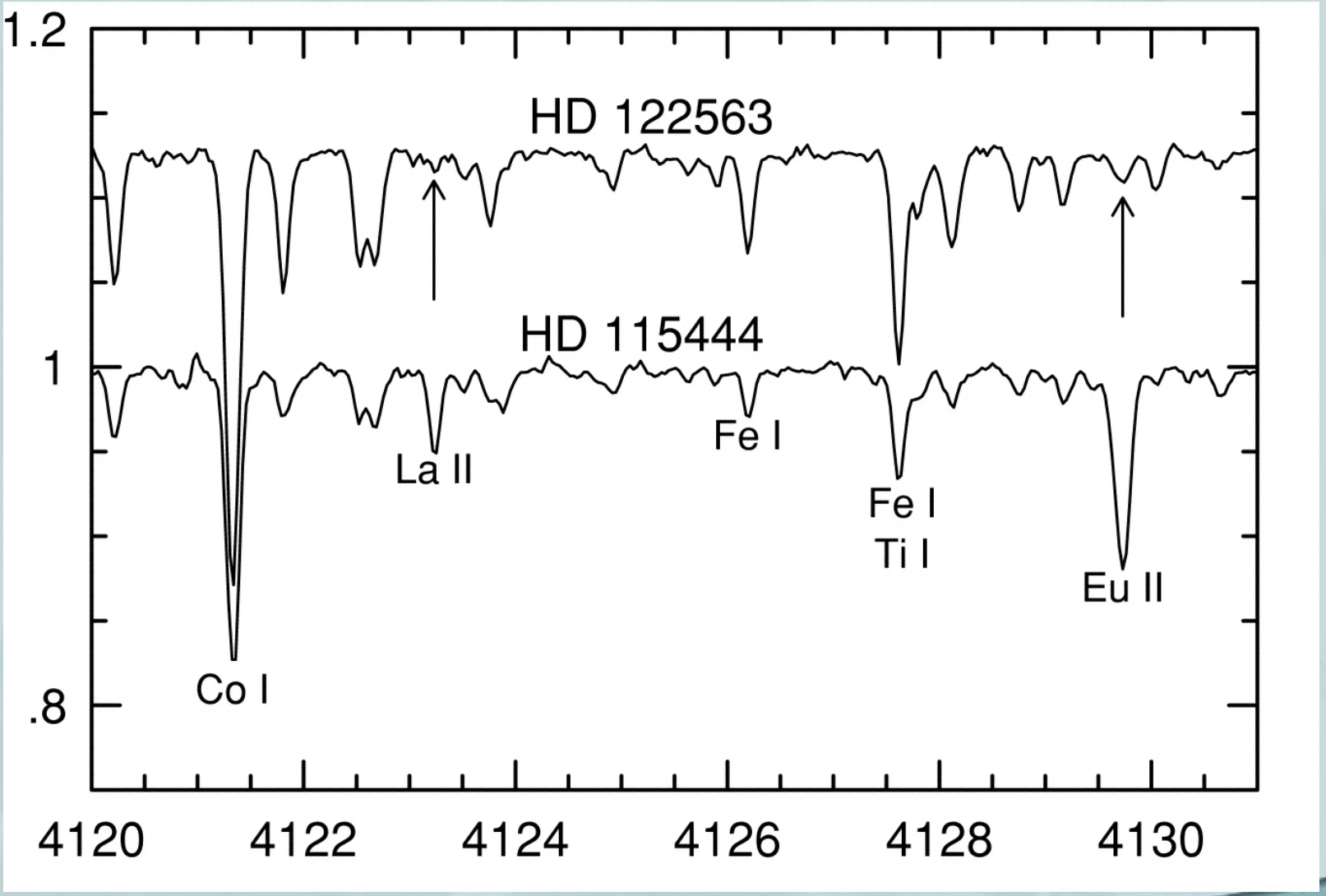

Example HERES Survey Spectra and Results to Date

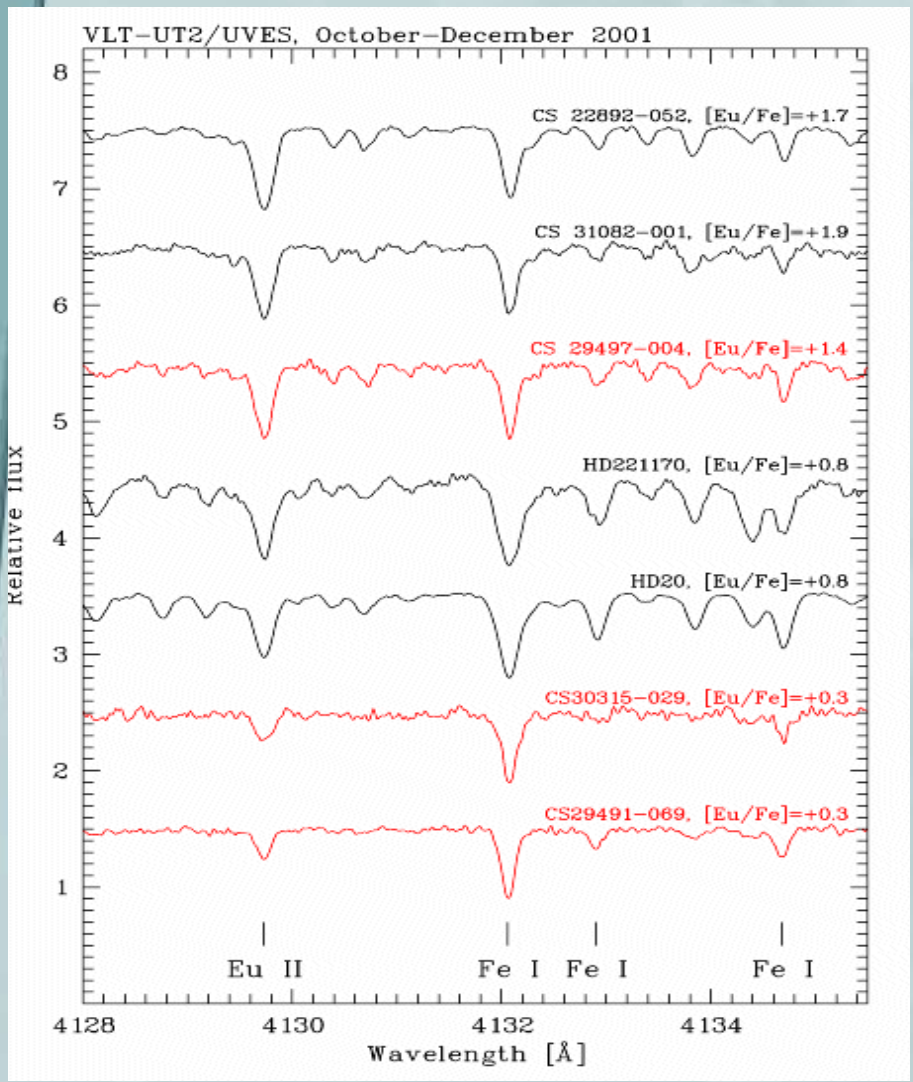

Thus far, a total of ~ 230 spectra have been examined. Among these are found:

25 stars: +1.0 < [Eu/Fe]
23 stars: +0.5 < [Eu/Fe] ≤ +1.0

Some of these are s-process enhanced as well, some r-process enhanced. From detailed inspection to date, we have:

- 10 new stars with [r/Fe] > +1.0 (all except 1 have [Fe/H] < -2.5)
- 15 new stars with +0.5 ≤ [r/Fe] ≤ +1.0 (all have -2.7 < [Fe/H] < -2.0)

The apparent frequency of r-II stars is roughly consistent with preliminary estimate of ~ 3% of giants with [Fe/H] < -2.5

A New R-Process Enhanced Star with Uranium Detected: CS 29497-004 !

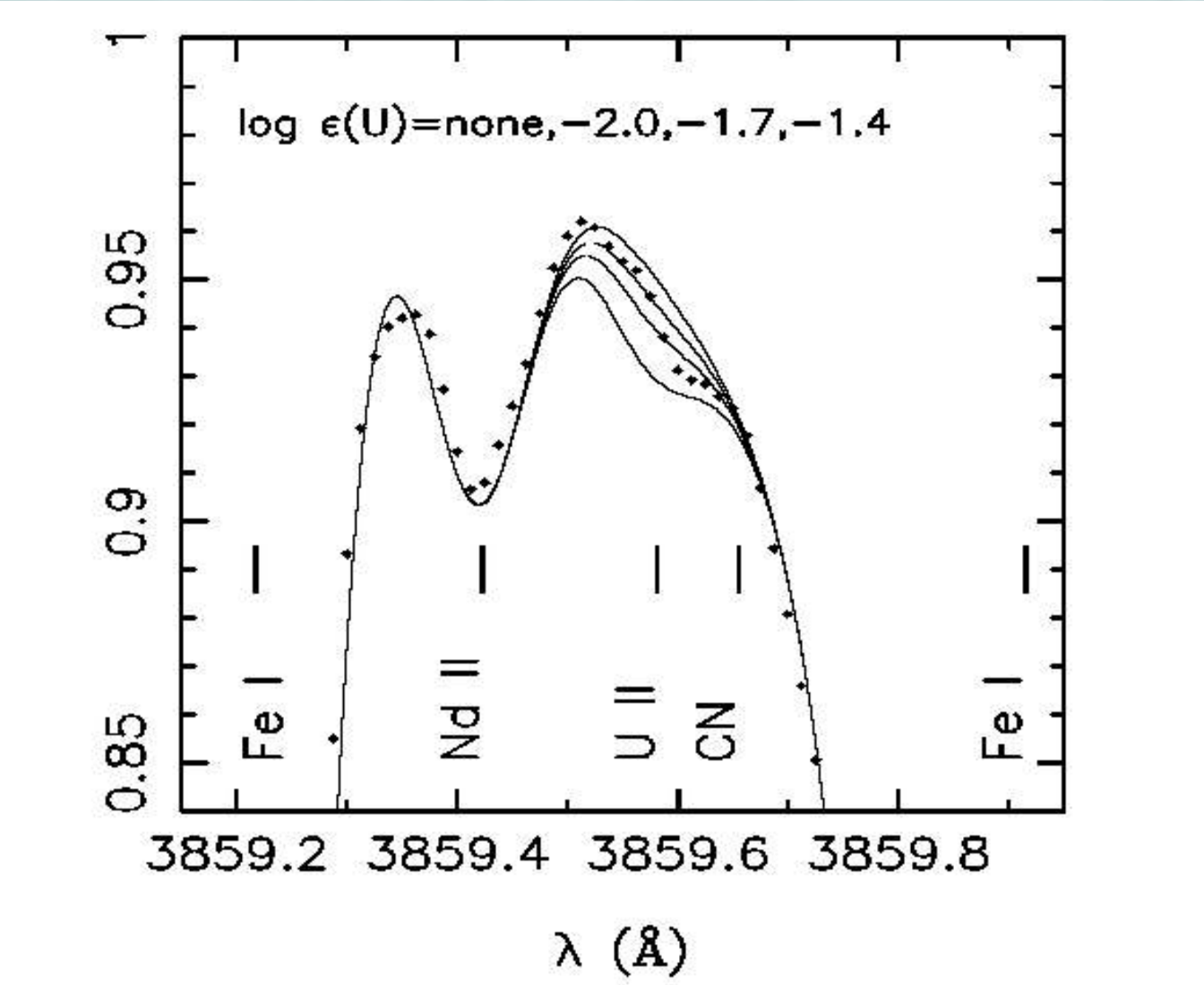

HERES Survey: Other Elements !

CS 31082-001: [Fe/H] = -2.9 HERES Blue Spectrum

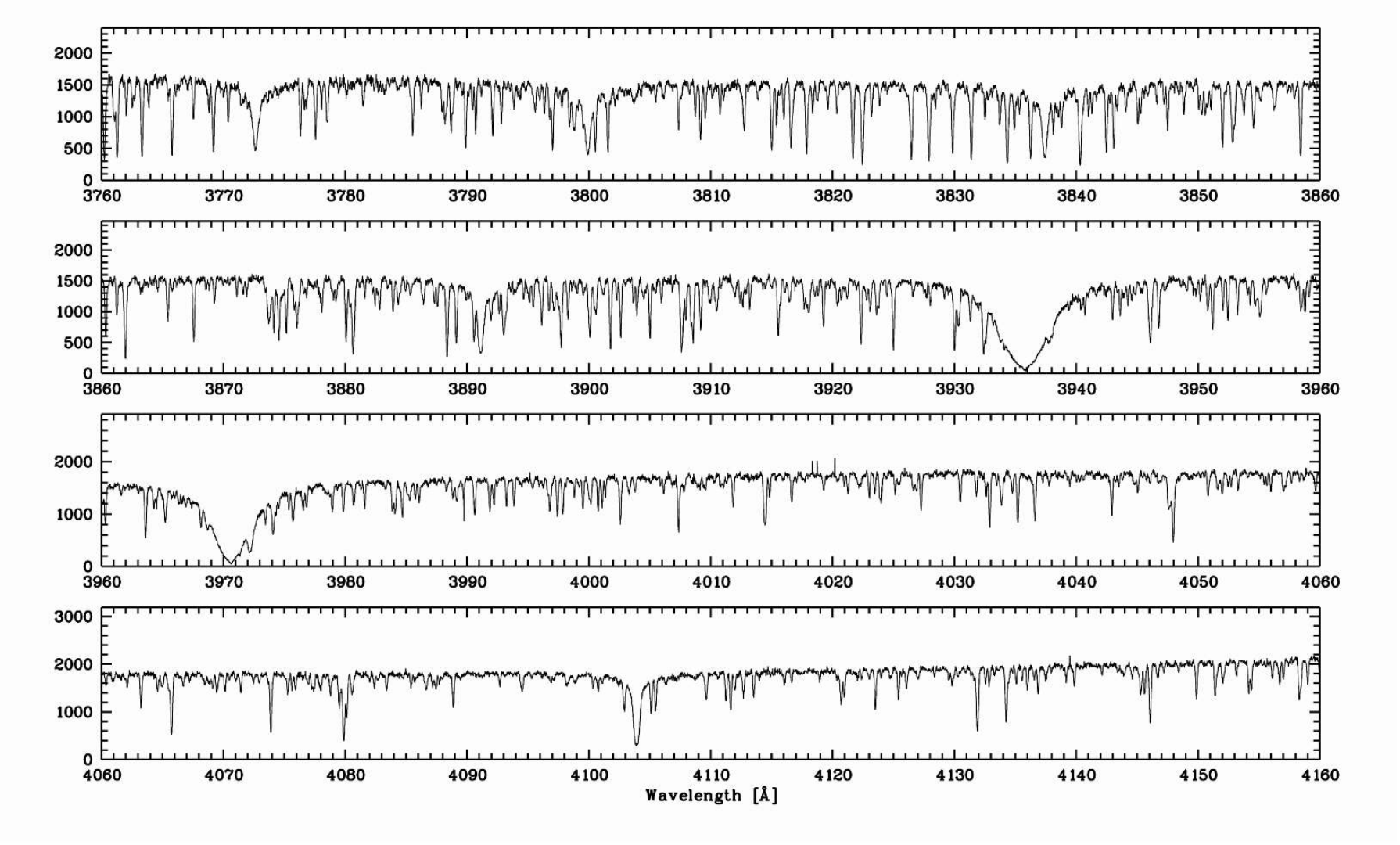

HERES Pilot Survey Results (N ~ 35 Stars Fully Analyzed to Date)

- There are already some 350 total stars with [Fe/H] < -2.5 observed on this program, with another ~ 25 to go
- Derive (relative) abundances for N ~ 20 elements per star, with accuracies on the order of 0.15 to 0.25 dex
- Definitive determinations of abundance patterns, scatter, below [Fe/H] = -2.5

Trends and Scatter of Light, Alpha- and Fe-Peak Elements for HERES Pilot Survey

- Estimates of individual elemental abundances obtained from automated analysis procedure (Barklem et al. 2004, A&A submitted)

- Behavior of trends is as expected, when compared with higher S/N spectroscopic surveys conducted to date, e.g., the "First Stars" program of Cayrel et al. (2004)

- Final database will provide unprecedented detail for the largest sample of [Fe/H] < -2.5 stars yet assembled

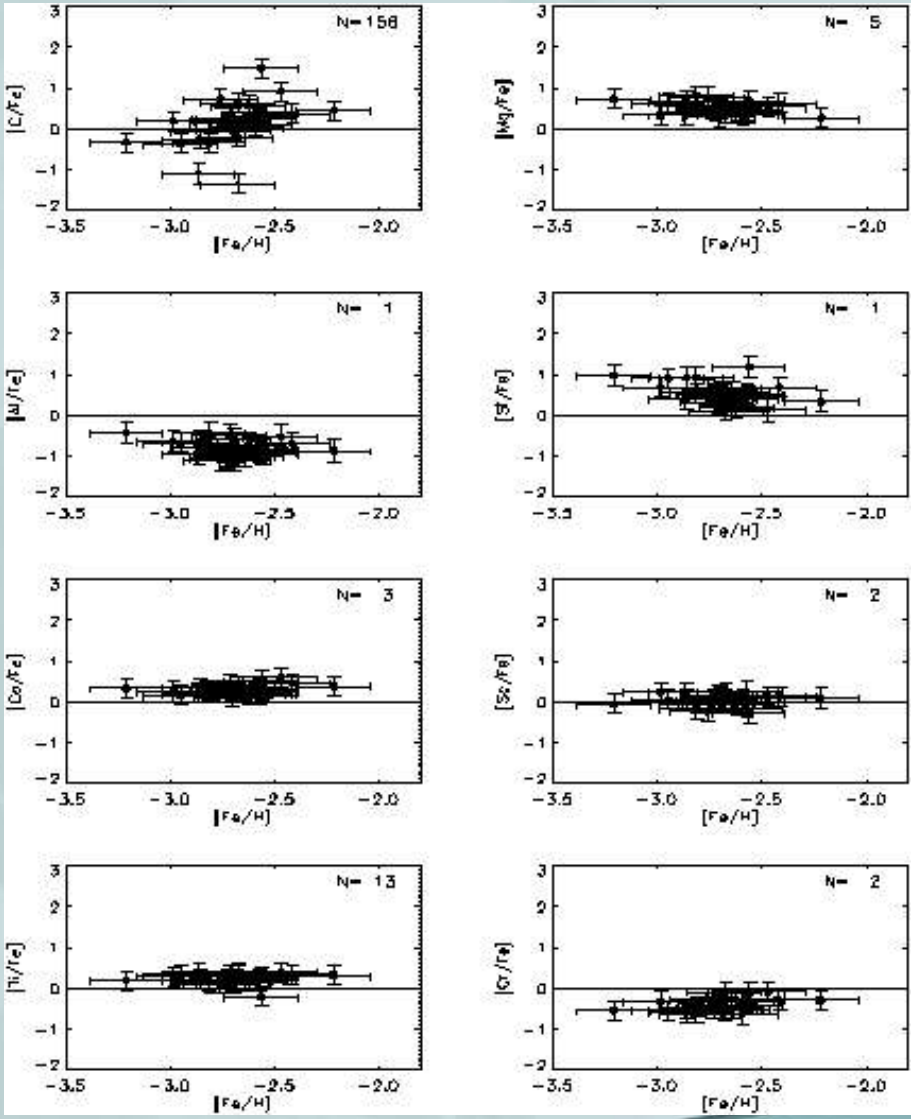

Iron-Peak and Neutron-Capture Elements for HERES Pilot Survey Stars

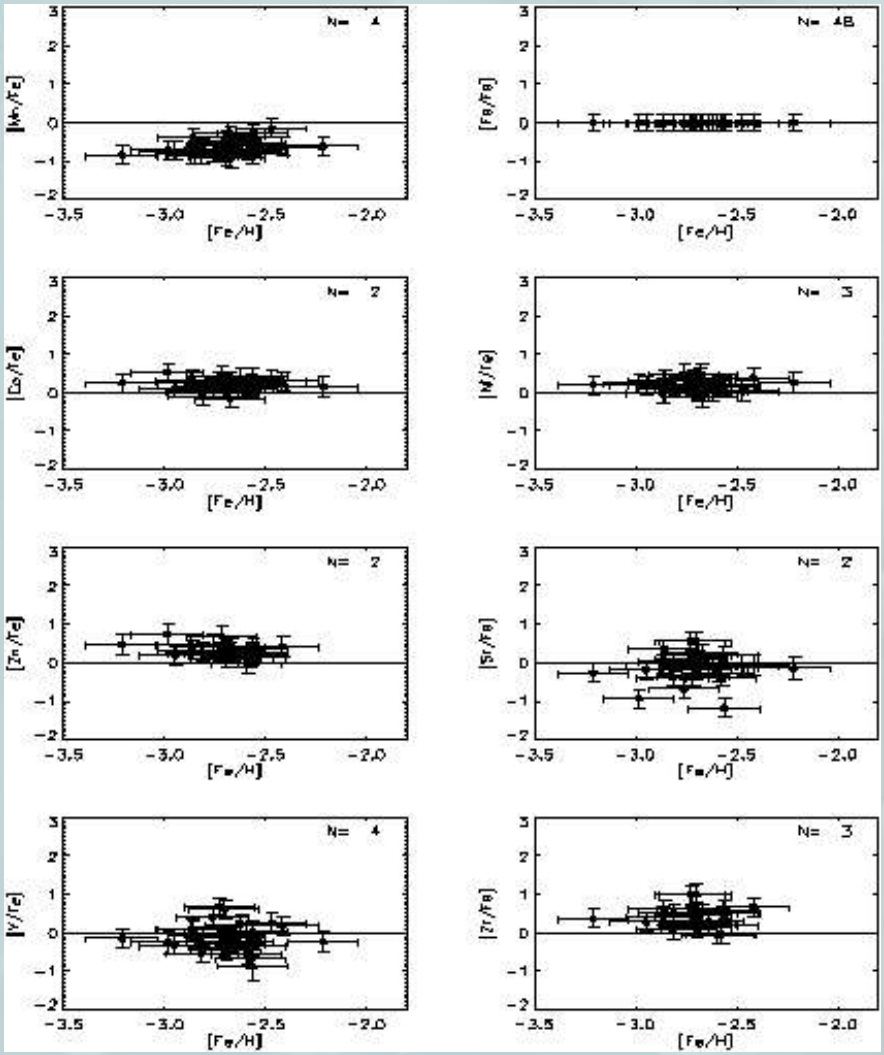

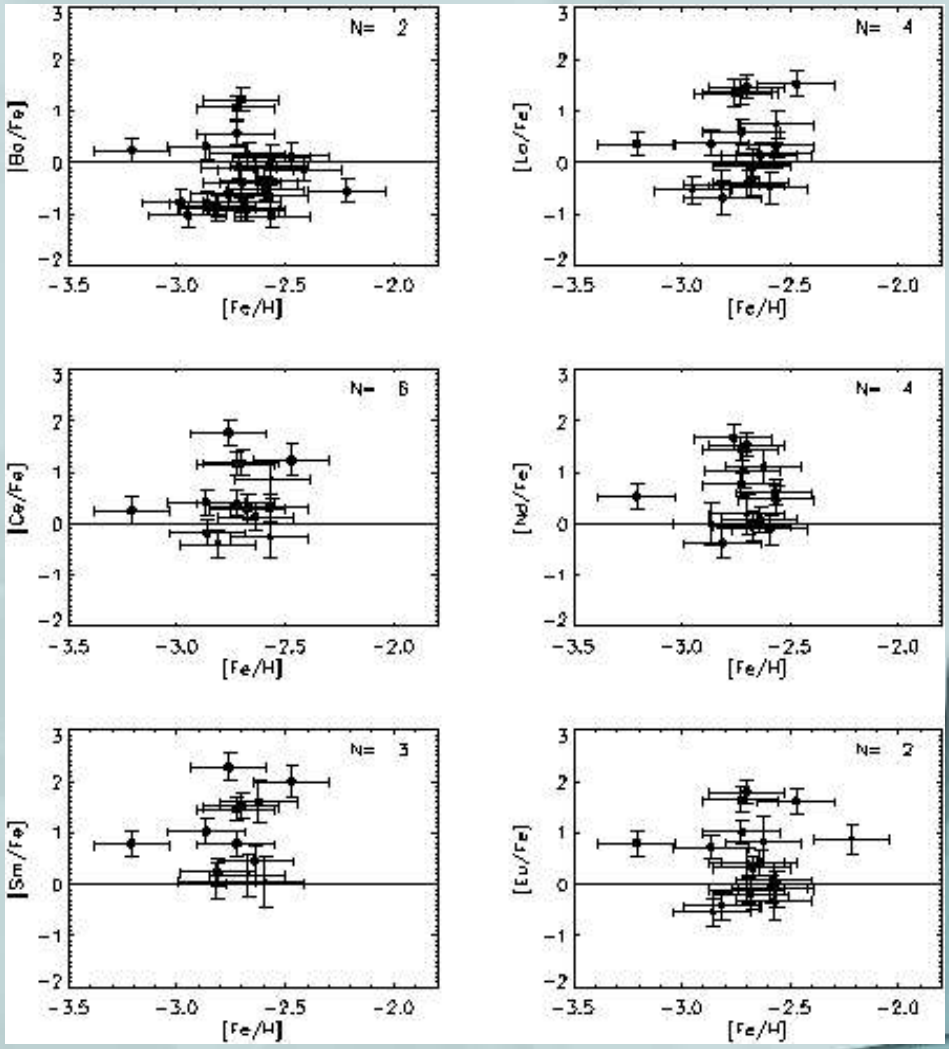

A Few “Close Ups”

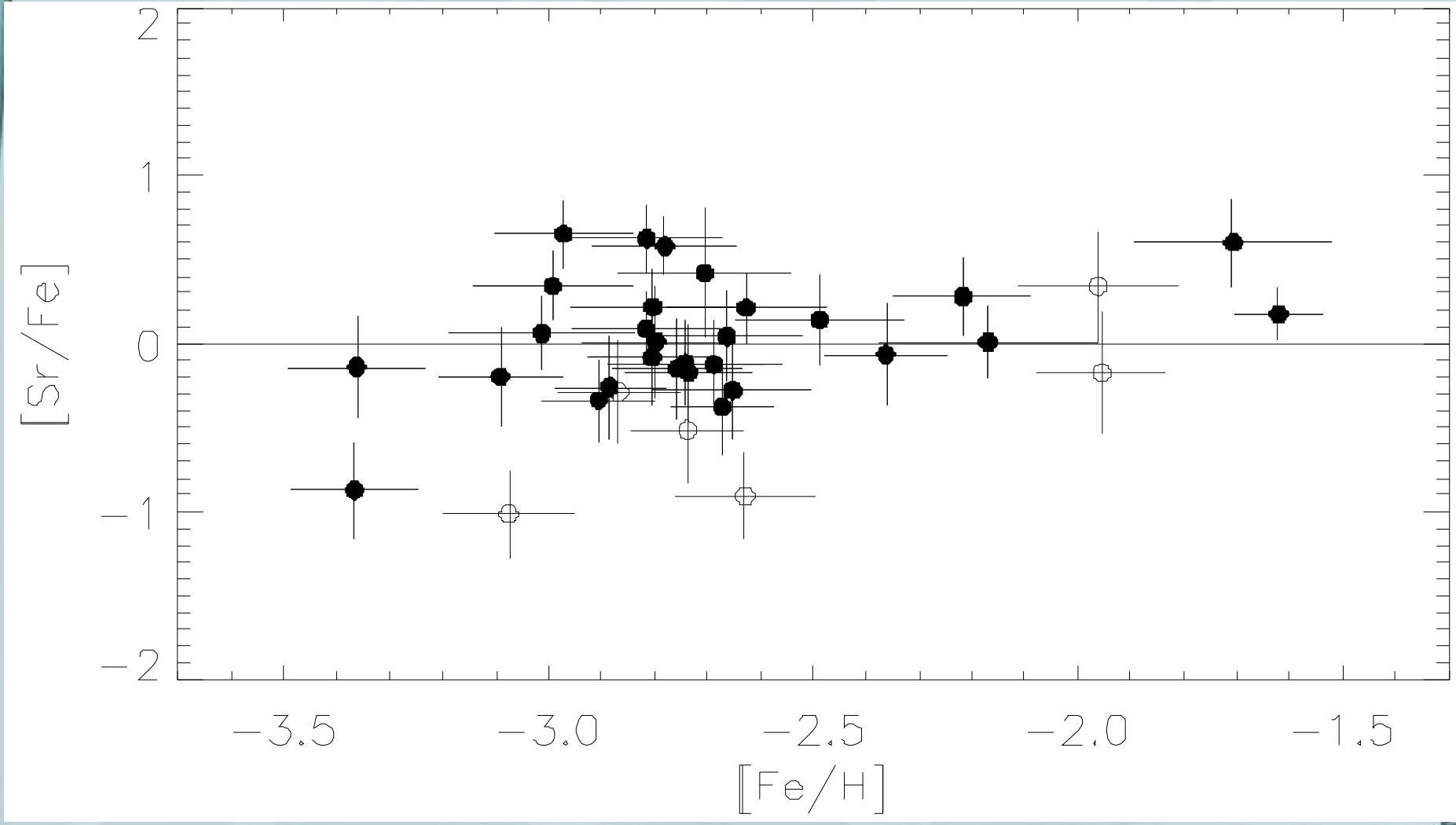

Plans for the Immediate Future

- Complete “snapshot” search for r-I, r-II, and r-s stars and derive frequencies of the phenomena as a function of [Fe/H]
- Obtain higher S/N spectra of clear r-process-enhanced stars, and obtain required information on scatter (if any) amongst r-process patterns, as well as chronometric age estimates
- Derive estimates of trends and scatter for N ~ 20 elements per star, yielding definitive information on patterns for [Fe/H] < -2.5
- Perform statistical analysis of elemental abundance patterns, looking for “natural groups” that might be associated with specific astrophysical sites

A Path to Understanding

- Full understanding of elemental production mechanisms requires:
  - Precise determinations of frequencies of distinctive patterns as f (]Fe/H]) – coming from HERES and other follow-ups
  - Association of patterns with astrophysical scenarios – presently being explored
  - New measurements of nuclear properties of heavy isotopes (Rare Isotope Accelerator) – critical for neutron-capture predictions
  - Comparison with self-consistent models of GCE incorporating IMFs and SN-II yields capable of predicting correct dispersions and frequencies of elemental patterns

What Comes Next ?

- SEGUE – Sloan Extension for Galactic Understanding and Evolution
- Starting NOW – obtaining 3.5 A resolution spectra of 250,000 MW stars
- Expect (conservatively) ~ 50,000 stars with [Fe/H] < -2.0
- High-Res follow-up spectroscopy with HET and Subaru of ~ 1000 brightest < -2.0 stars will reveal the history of chemical evolution in the first ~ 1-2 Gyr since star formation began

A Little Closer Look at a Slice of SDSS Redshift Space

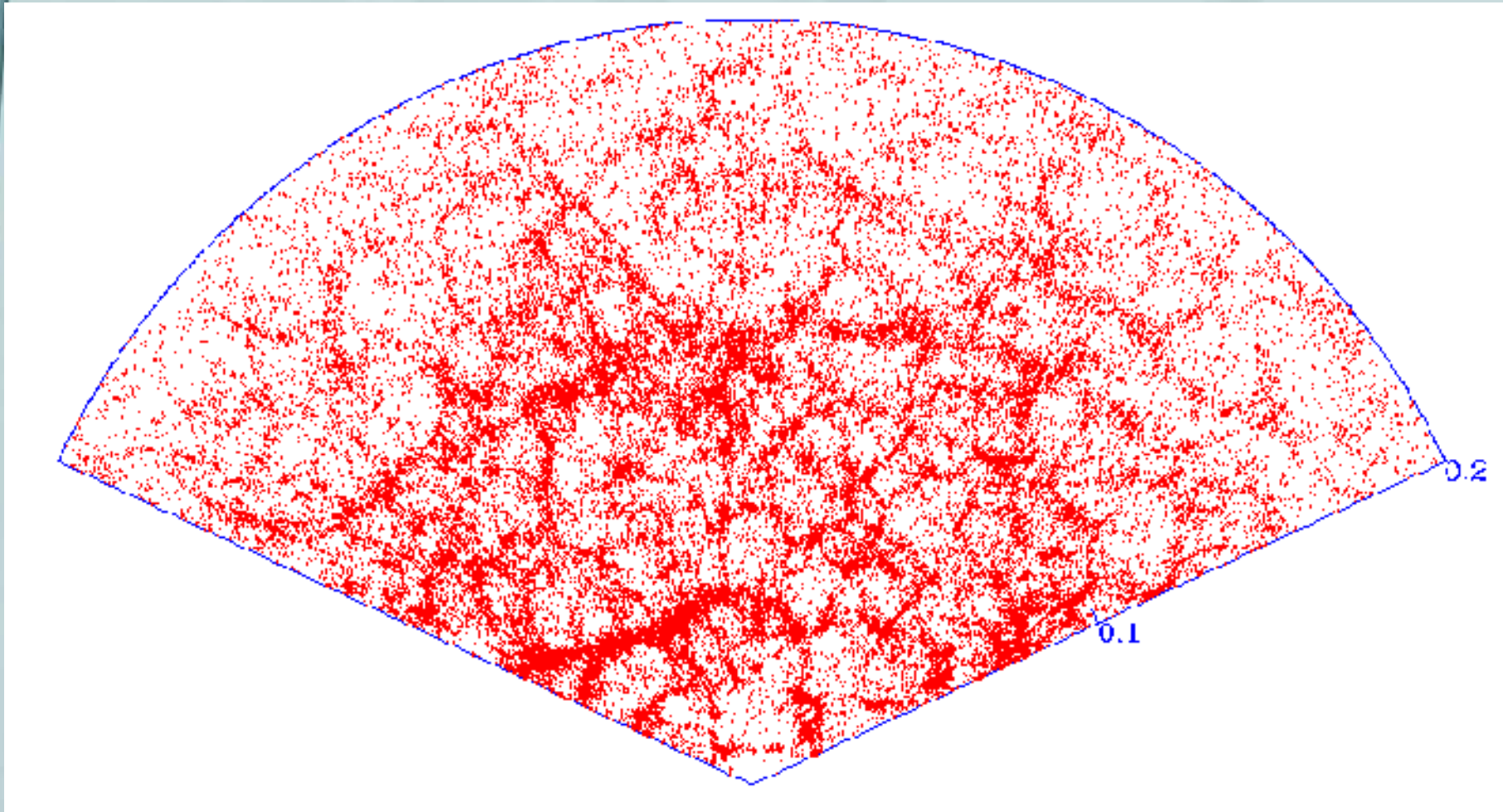

One Galaxy Left Behind…

A Proposed Sloan Extension

- Beyond 2005, a proposal has been made (Sloan/NSF/Institutional Partners) to conduct additional SDSS observations for three years (2005-2008)
  - Legacy: Close the Imaging Gap
  - Supernovae Survey
  - SEGUE
- Already received commitment of $5.4 Million from Sloan Foundation
- Similar amount proposed to NSF (June 2004)
- N ~ 10 Institutional Partners
  - JINA is included among these partners

SEGUE: Sloan Extension for Galactic Understanding and Evolution

- An imaging and spectroscopic survey to unravel:
  - Structure
  - Formation history
  - Kinematical and dynamical evolution
  - Chemical evolution
  - Dark matter distribution in the Galaxy
  - Proposal is to complete within three years using existing SDSS 2.5m

Technical Details – The SEGUE Plan of Attack

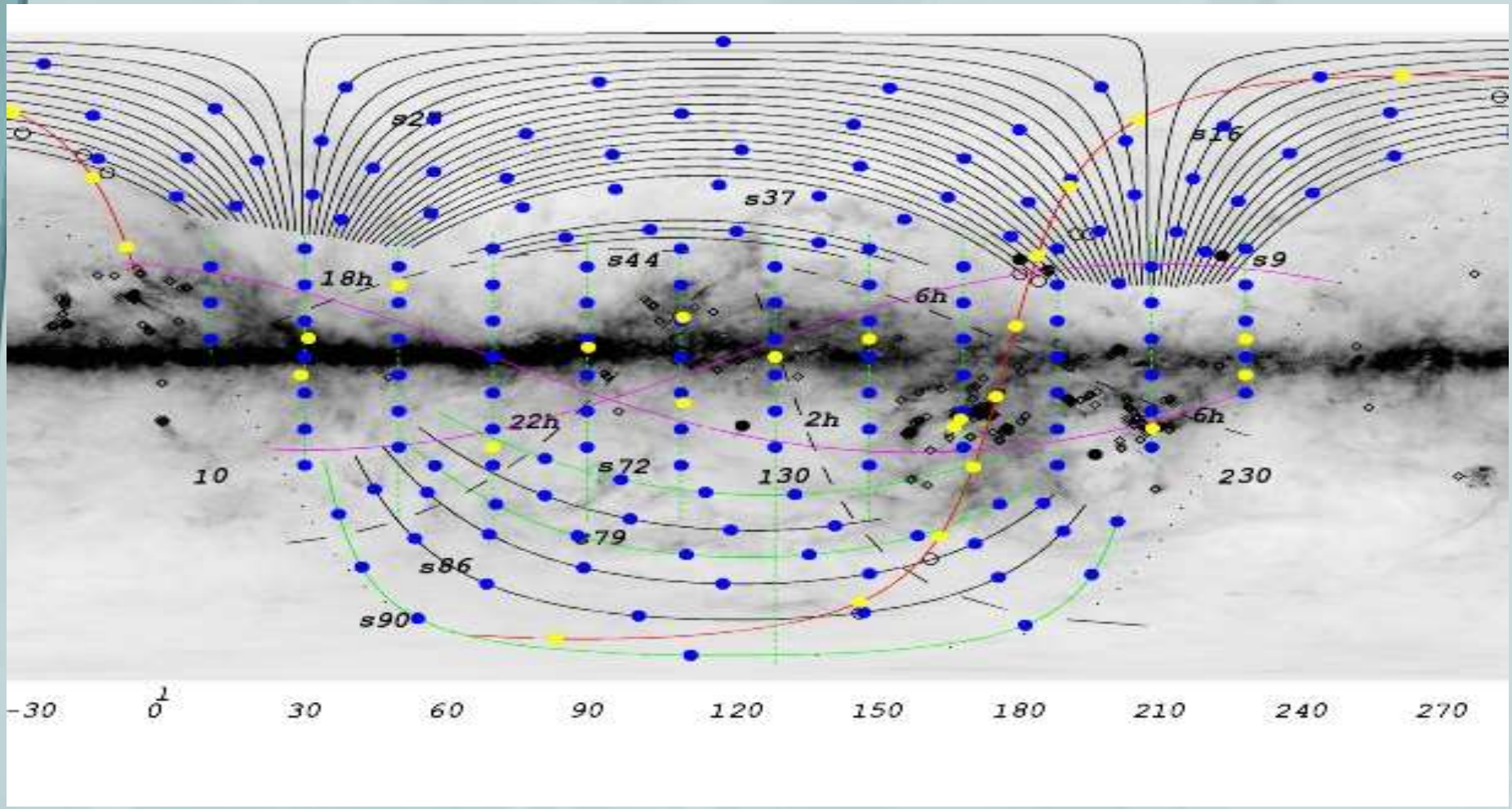

The Allure of Color-Selection

- Spectroscopic survey of N~ 250,000 Galactic stars, 14 < B < 20, which has been designed to include:

- 50,000 stars, color-selected for [Fe/H] < -2.0

- 5,000 stars with [Fe/H] < -3.0

- 500 (?) stars with [Fe/H] < -4.0

Results "Without Even Trying" -- The SDSS Early Data Release Stellar Spectra

- QSO = 1461
- BHB = 1242
- Reddening Std = 714
- Spectrophot Std = 706
- Galaxy = 628
- Other = 853

- TOTAL = 5604

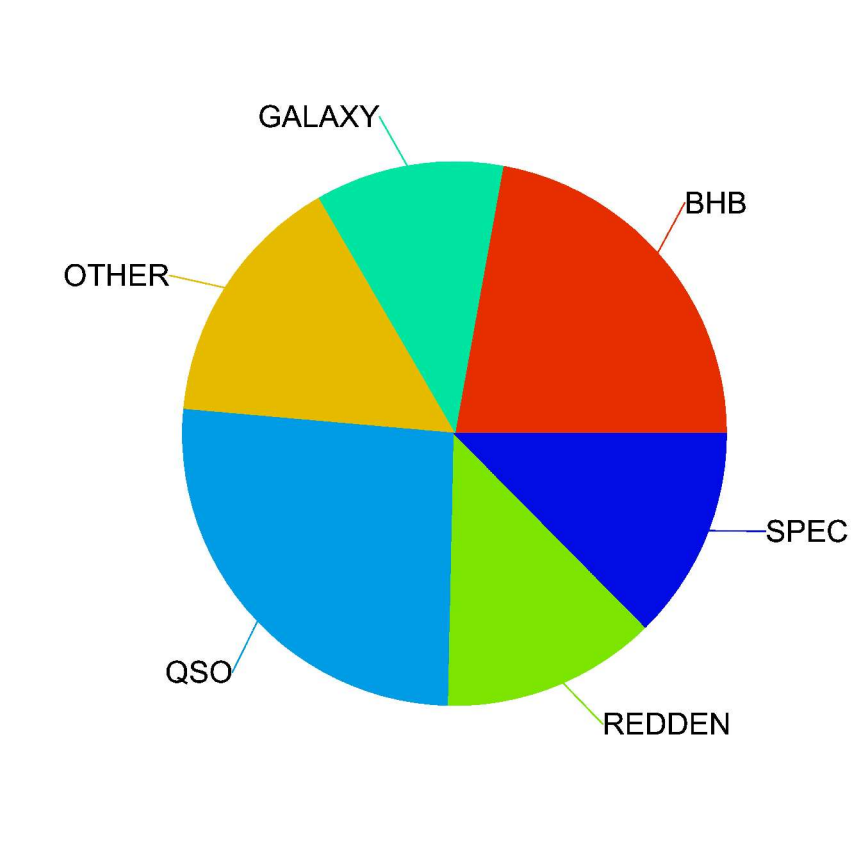

A [Fe/H] = -3.3 Star from EDR

EDR 3907: SDSS 2.5m Spectrum

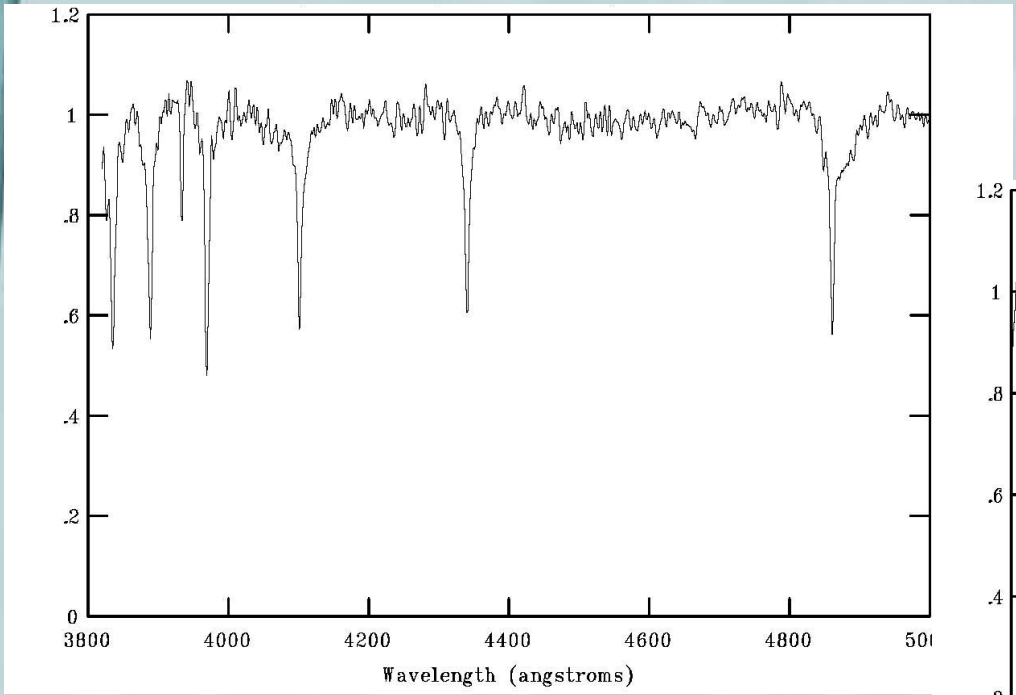

EDR 3907: CTIO4m Spectrum

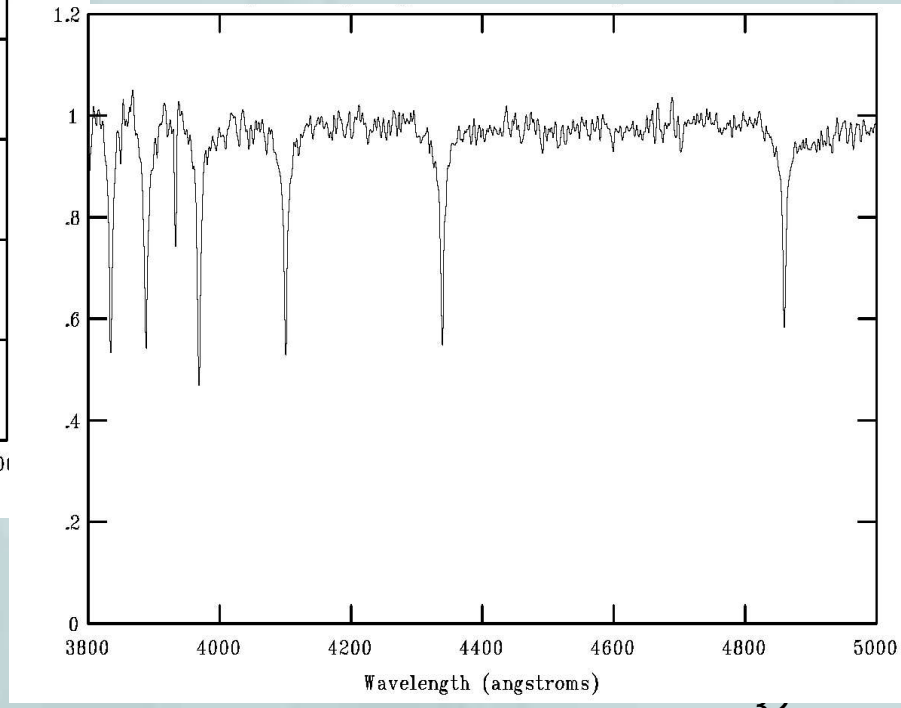

RESULTS – Metallicity Distributions

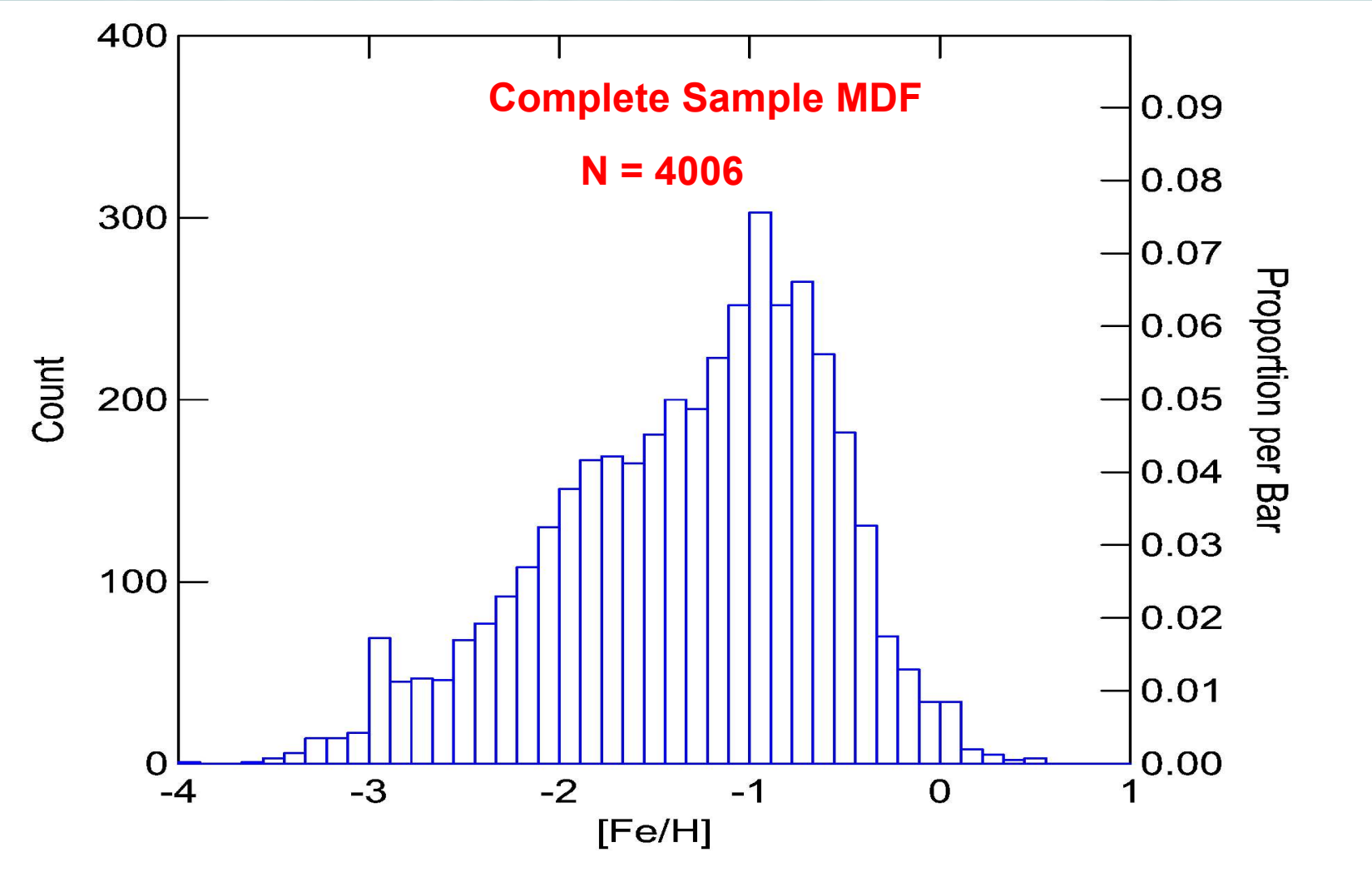

RESULTS – Distance Distributions

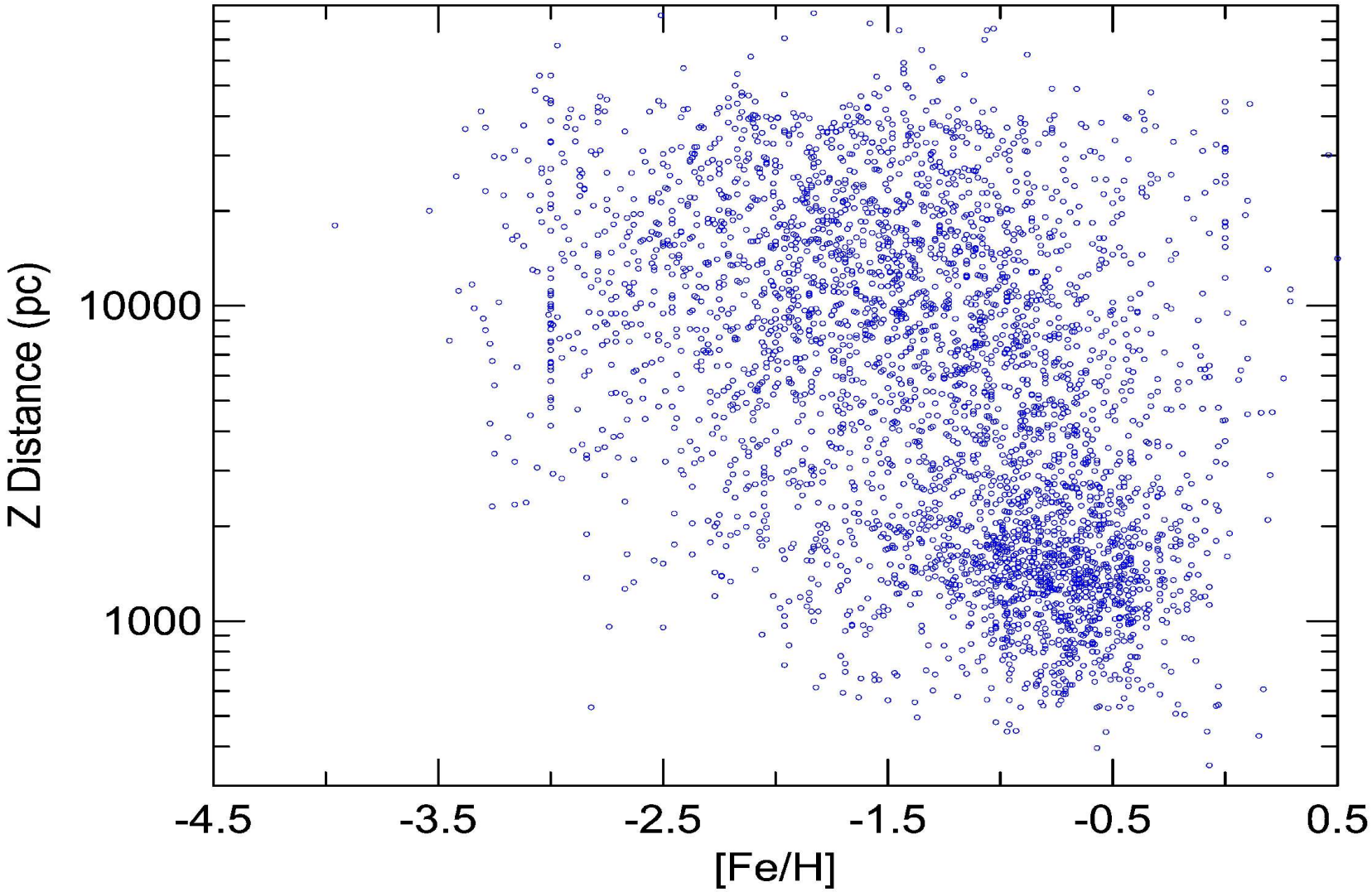

HET-RES and SALT-RES

- Conduct a similar survey as HERES, but using input bright stars from HK-II + SEGUE discoveries
  - 14.0 < B < 17.0
- HET-RES: Hobby-Eberly 9.2m Telescope (Texas)
- SALT-RES: South African Large (9.2m) Telescope
- Each target N ~ 1000 candidates with [Fe/H] < -2.0
- High S/N Follow-up with SUBARU 8m Telescope (Hawaii)
- Should result in (at least) ~ 50-60 new r-II stars, ~ 100-120 new r-I stars, a host of other neutron-capture-rich stars, other "peculiar" abundance pattern stars, and definitive data on abundance patterns and scatter at low metallicity

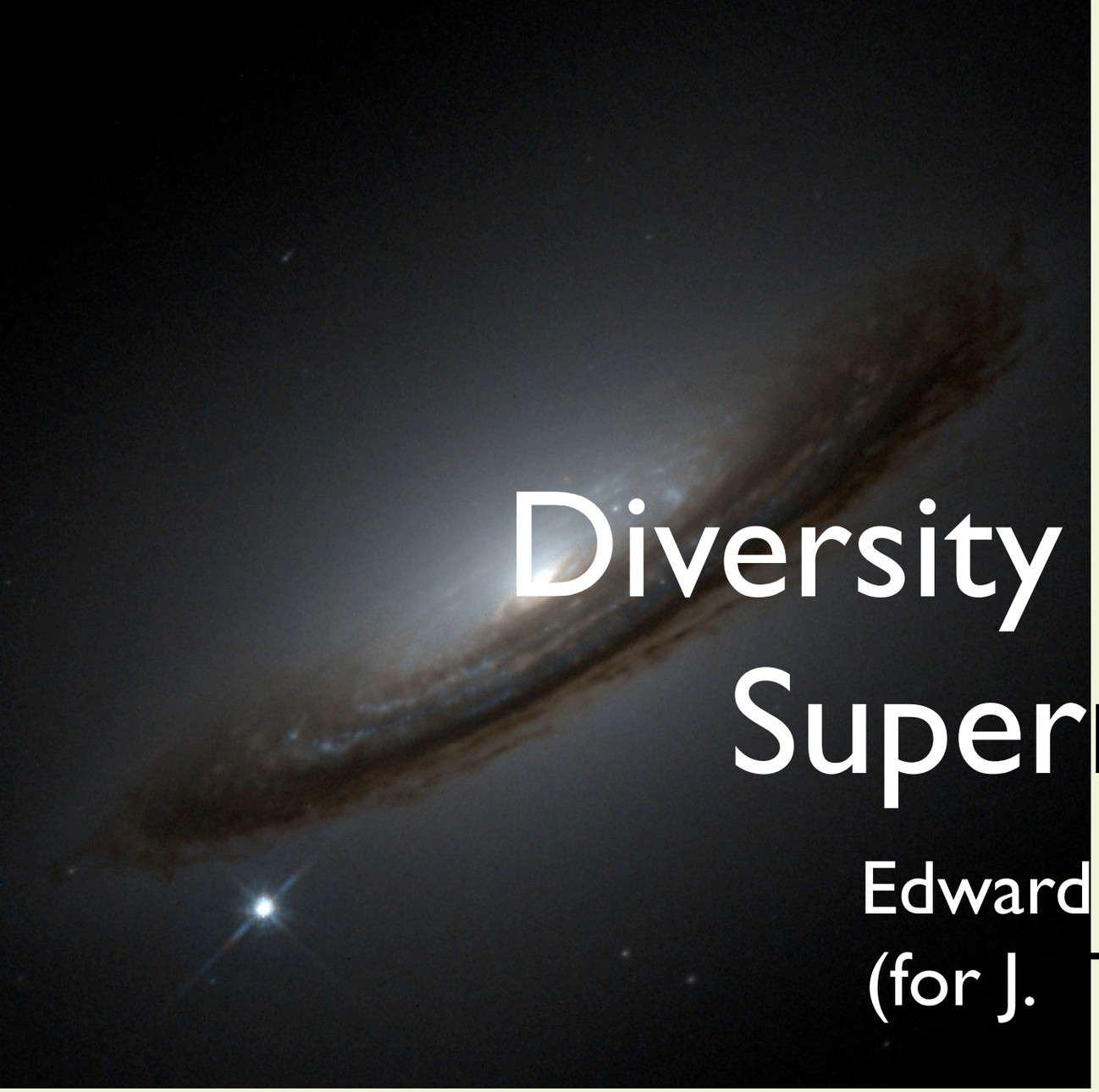

Diversity in Type Ia Supernovae

Edward Brown
(for J. Truran)

Department of Physics and Astronomy
MICHIGAN STATE UNIVERSITY
JINA

SNe Ia Peak Luminosities

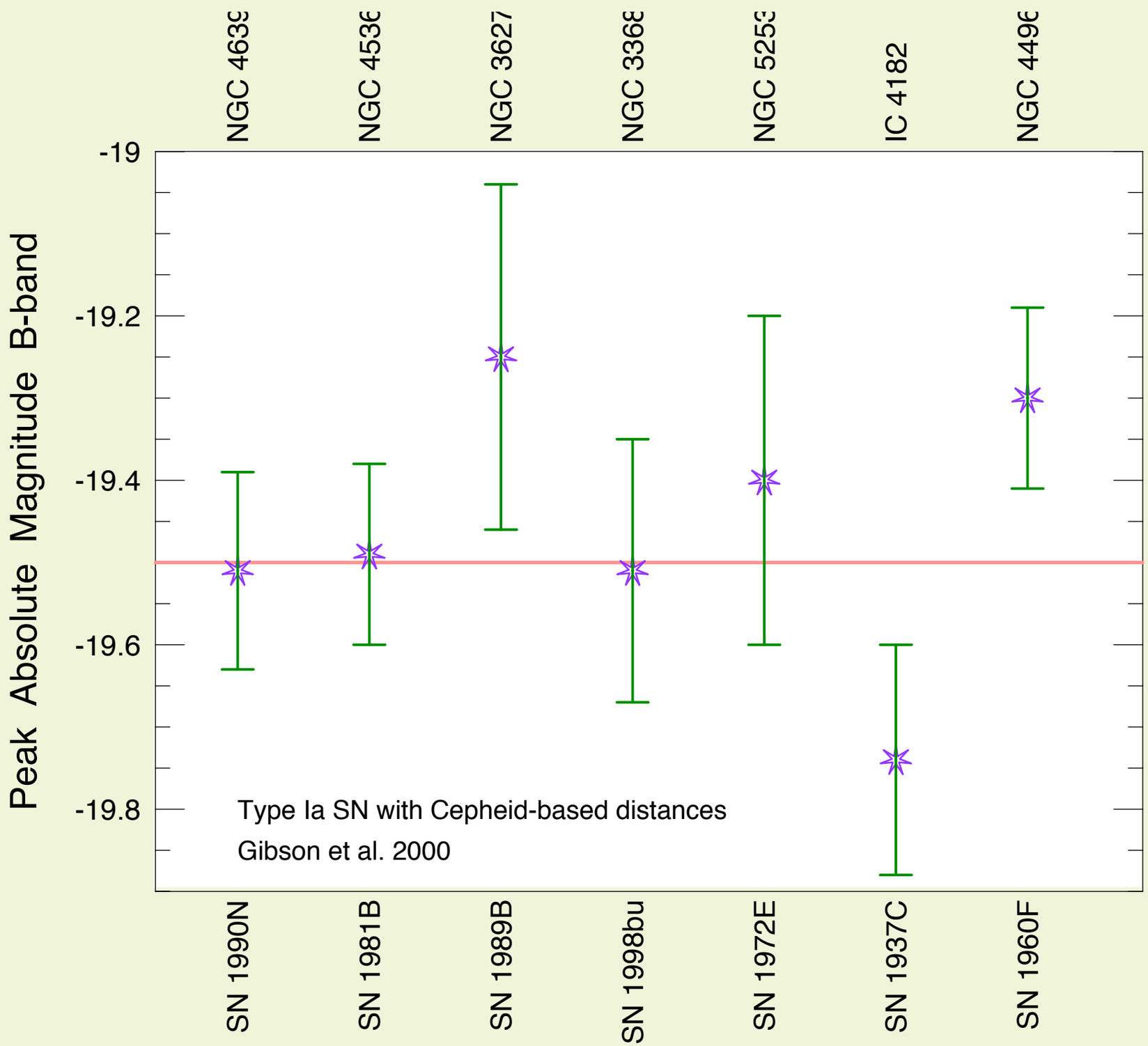

Plot courtesy F. Timmes

Outline

- How does the progenitor's composition influence the SNe?
  - C:O ratio (Höflich et al. 1998, Umeda et al. 1999, Iwamoto et al. 1999, Domínguez et al. 2001, Röpke & Hillebrandt 2004)
  - *Metallicity* (Timmes, Brown & Truran 2003)
- Multi-dimensional simulations with tracer particles
  - Garching: Röpke et al. 2004, Travaglio et al. 2004
  - Chicago

Type Ia SNe

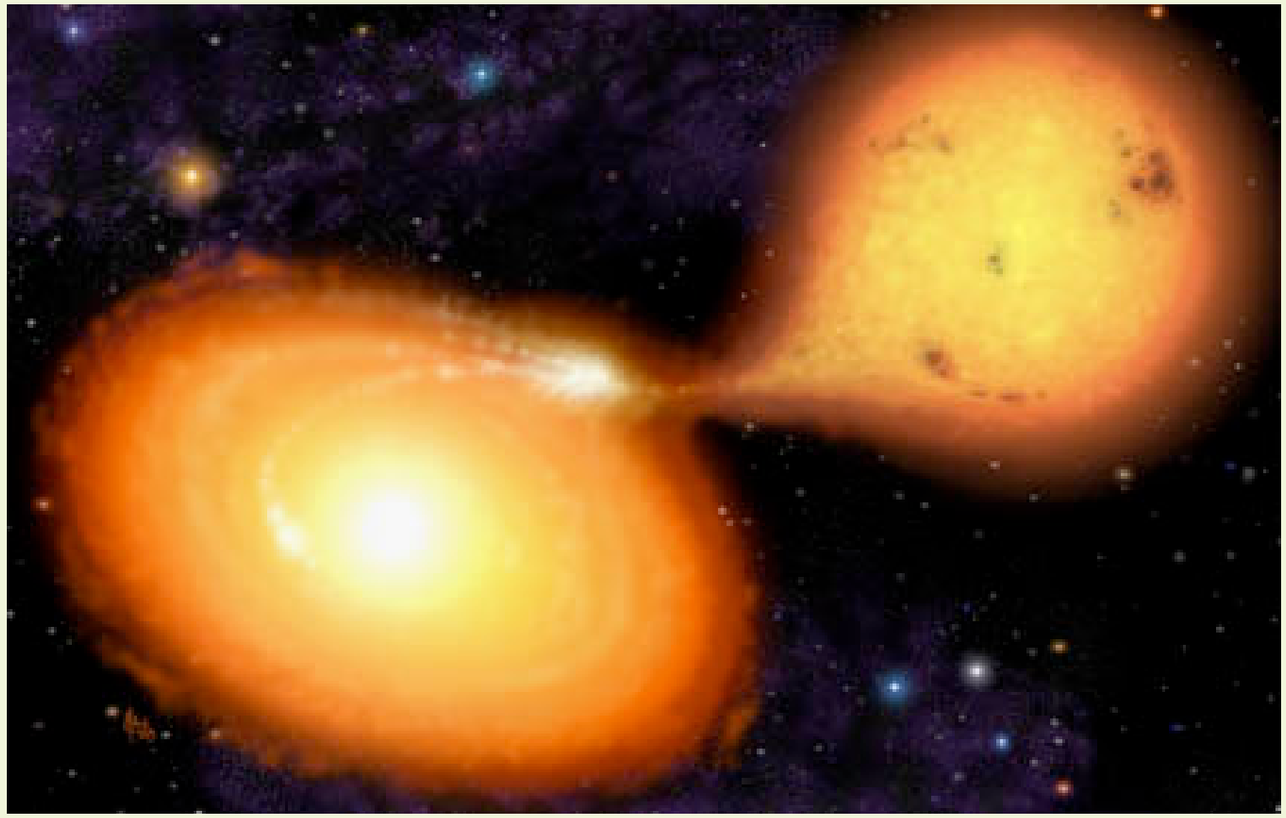

Mark A. Garlick

Scenario

- C/O white dwarf accreting from companion
- When M is nearly M_{ch}, ^{12}C ignites in center

$X(\mathrm{CNO})$ & $X(^{56}\mathrm{Ni})$

During H burning, CNO catalysts pile up in ^{14}N; as the progenitor core burns to C/O, the aboriginal CNO is converted to ^{22}Ne via

$$^{14}\mathrm{N}(\alpha,\gamma)^{18}\mathrm{F}(\beta^+,\nu_\mathrm{e})^{18}\mathrm{O}(\alpha,\gamma)^{22}\mathrm{Ne}$$

Outside innermost $0.2\,M_\odot$,

$$\left(\frac{d\eta}{dt}\right)^{-1} > t_\mathrm{expand}$$

$$\eta = \frac{N_n - N_p}{N_n + N_p} = \mathrm{const}$$

^{22}Ne and ^{58}Ni have N_n-N_p = 2, so $N(^{22}\mathrm{Ne})$ = $N(^{58}\mathrm{Ni})$

$$X(^{56}\mathrm{Ni}) = 1 - X(^{58}\mathrm{Ni}) = 1 - \frac{58}{22}X(^{22}\mathrm{Ne})$$

The abundance of $^{56}\mathrm{Ni}$ depends *linearly* on Z

$$X\left(^{56}\mathrm{Ni}\right) = 1 - \frac{58}{2}\eta$$
$$= 1 - 0.057\left(\frac{Z}{Z_\odot}\right)$$

Adding in more isotopes, eg, ^{54}Fe changes this relation only slightly

Take $\langle M(^{56}\mathrm{Ni})\rangle \approx 0.6$ (W7 & $\langle L_{\mathrm{peak}}\rangle$),

$$M(^{56}\mathrm{Ni}) \approx 0.6\left(1 - 0.057\frac{Z}{Z_\odot}\right)$$

for 1-d models!

Solar Neighborhood Age-Metallicity Relationship

- Scatter in CNO is ~0.5 dex about the mean

- [Fe/H] changes slightly (less than scatter) for the last ~10 Gyr ($z < 1$)

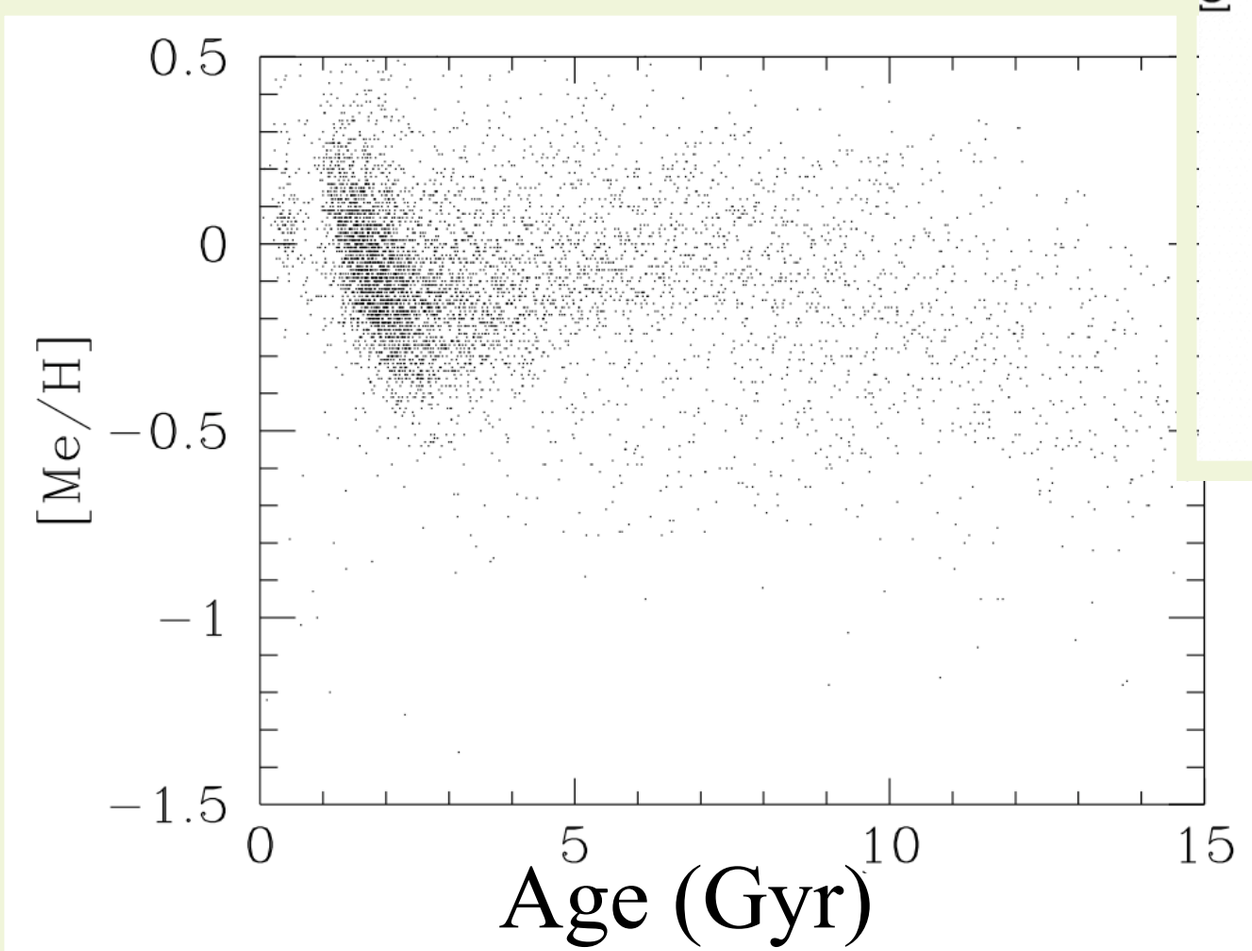

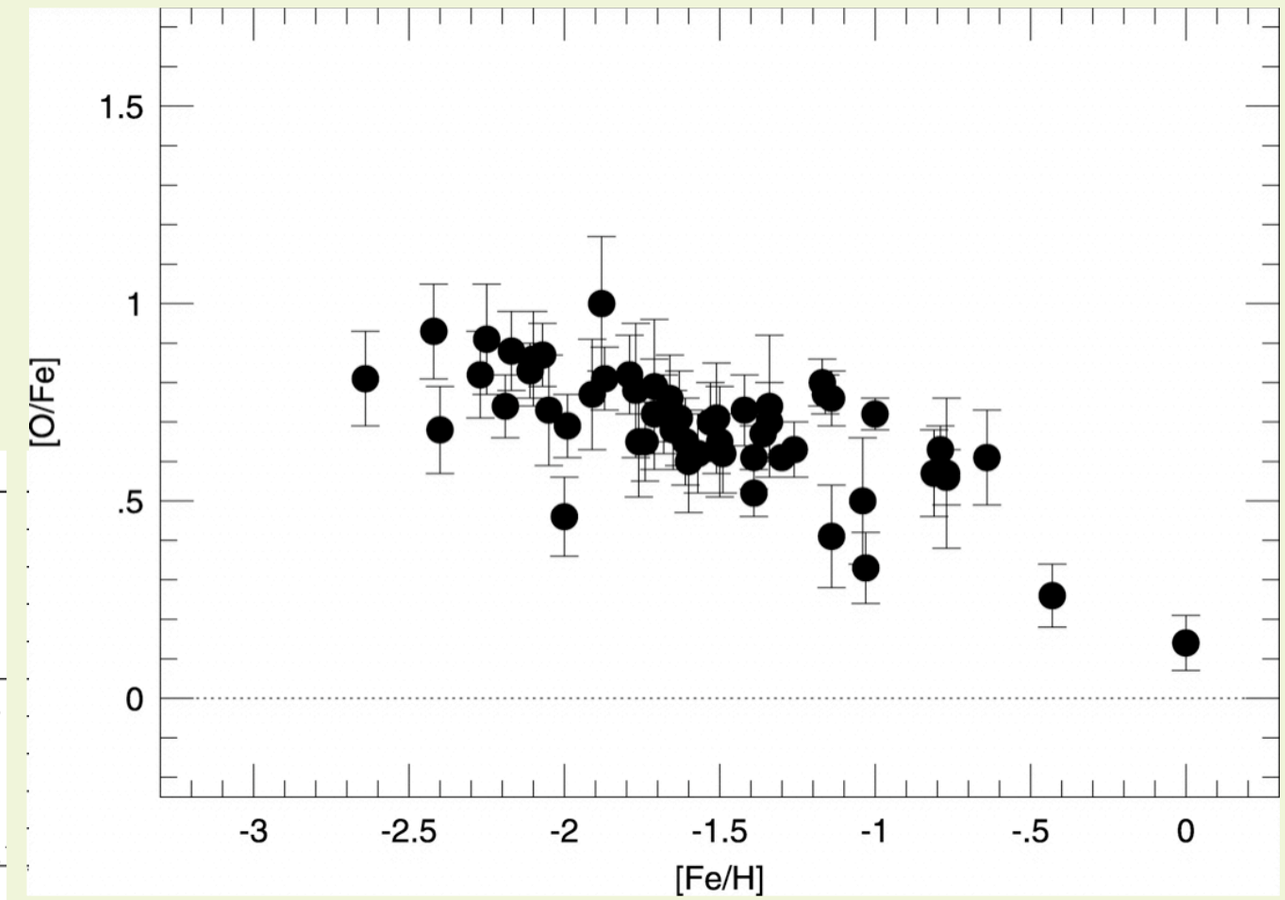

Fulbright & Johnson 2003

Hipparcos data
Feltzing, Holmberg & Hurley 2001

≈0.5 dex scatter about the mean in CNO abundances induces a effective range, in $X(^{22}\mathrm{Ne})$ from 0.8% to 7.5%

This, by itself, produces $\Delta M(^{56}\mathrm{Ni})\approx 25\%$,...

...or $\Delta V \approx 0.2$ mag, using $V(M_{\mathrm{Ni}})$ from Pinto & Eastman (2001)

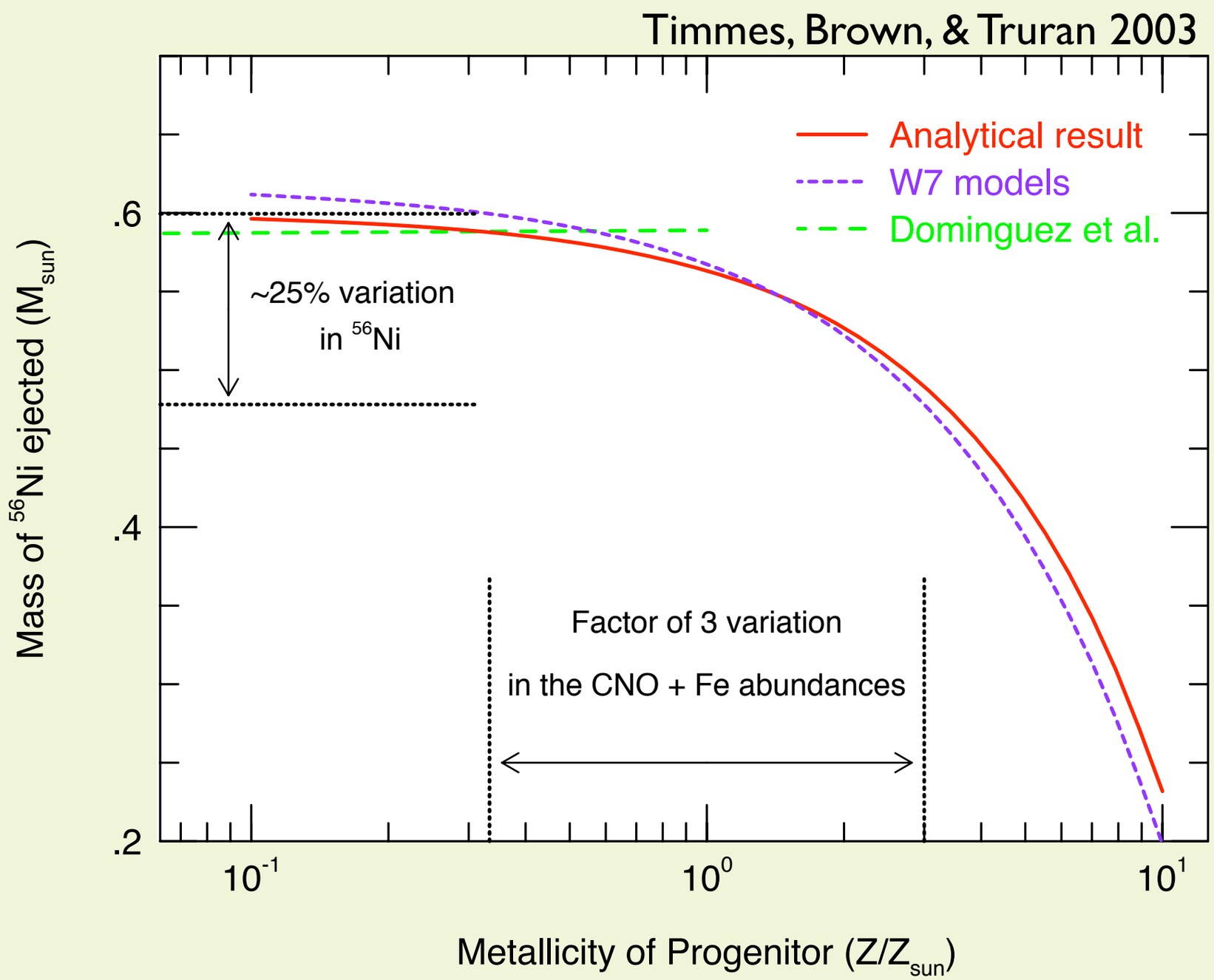

Higher metallicity progenitors should make intrinsically dimmer SNe Ia, all else being equal

Self-consistency of 1-d calculations

- Flame speed

  During Si-burning (Hix & Thielemann 1996, 1999)

  $$\frac{d\dot{S}}{d\eta} > 0$$

- Progenitor structure: correlations between $X(^{22}\mathrm{Ne})$ and $X(^{12}\mathrm{C})/X(^{16}\mathrm{O})$ (Umeda et al. 1999, Domínguez et al. 2001)

- Sedimentation of $^{22}\mathrm{Ne}$ (e.g., Bildsten & Hall 2001)

≈0.5 dex scatter about the mean in CNO abundances induces a effective range, in $X(^{22}\mathrm{Ne})$ from 0.8% to 7.5%

This, by itself, produces $\Delta M(^{56}\mathrm{Ni})\approx 25\%$,...

...or $\Delta V \approx 0.2$ mag, using $V(M_{\mathrm{Ni}})$ from Pinto & Eastman (2001)

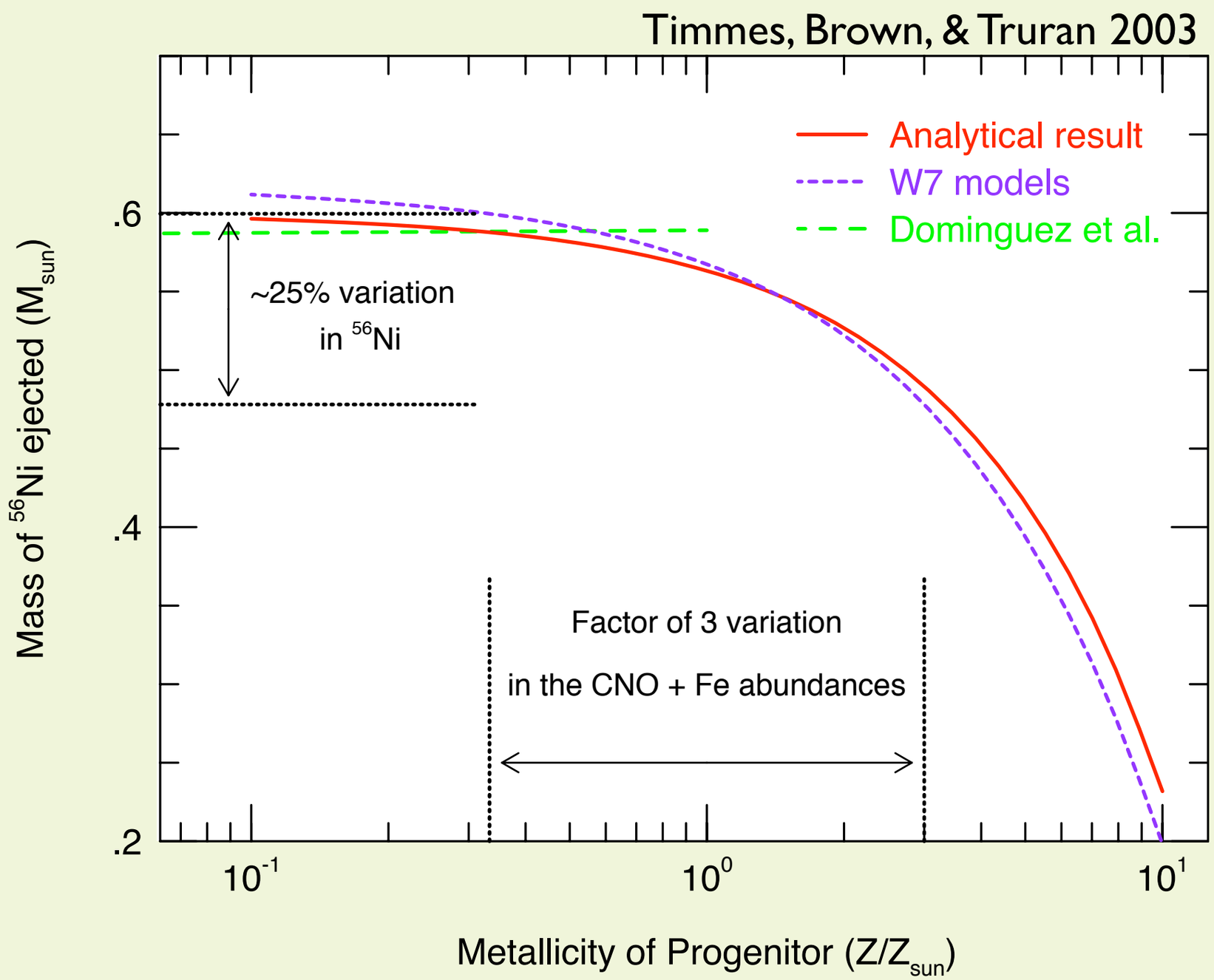

Higher metallicity progenitors should make intrinsically dimmer SNe Ia, all else being equal

Observations

- Absence of fast-declining (dimmer) SNe Ia in bluer galaxies (Hamuy et al. 1996, 2000; Riess et al. 1999)
- BUT...no correlation of $\Delta m_{15}(B)$ with normalized radial distance in elliptical galaxies (Ivanov et al. 2000)
- More obs. needed; both for SNe and host galaxies

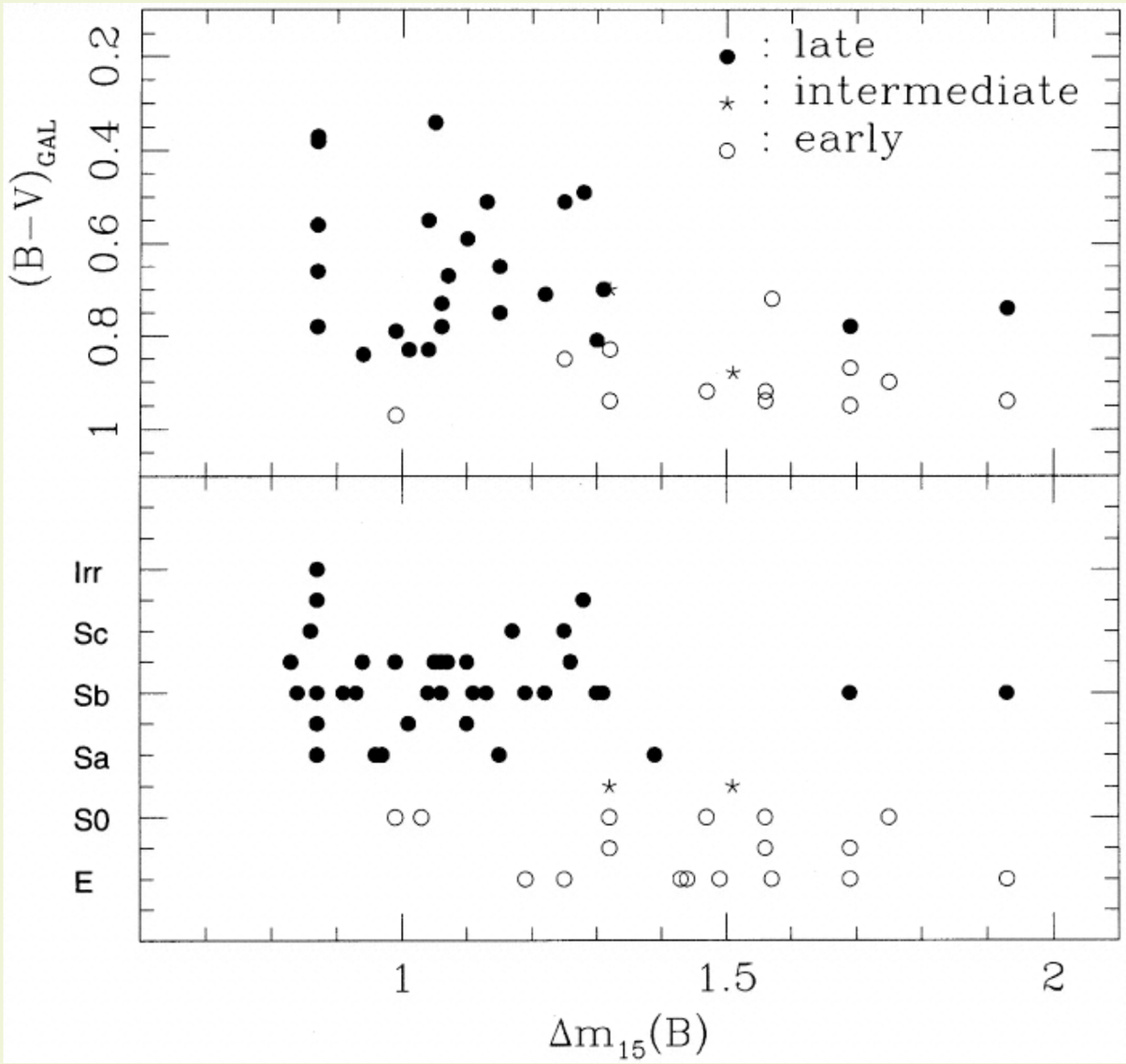

Hamuy et al. 2000, fig. 1

Simulations & Tracers

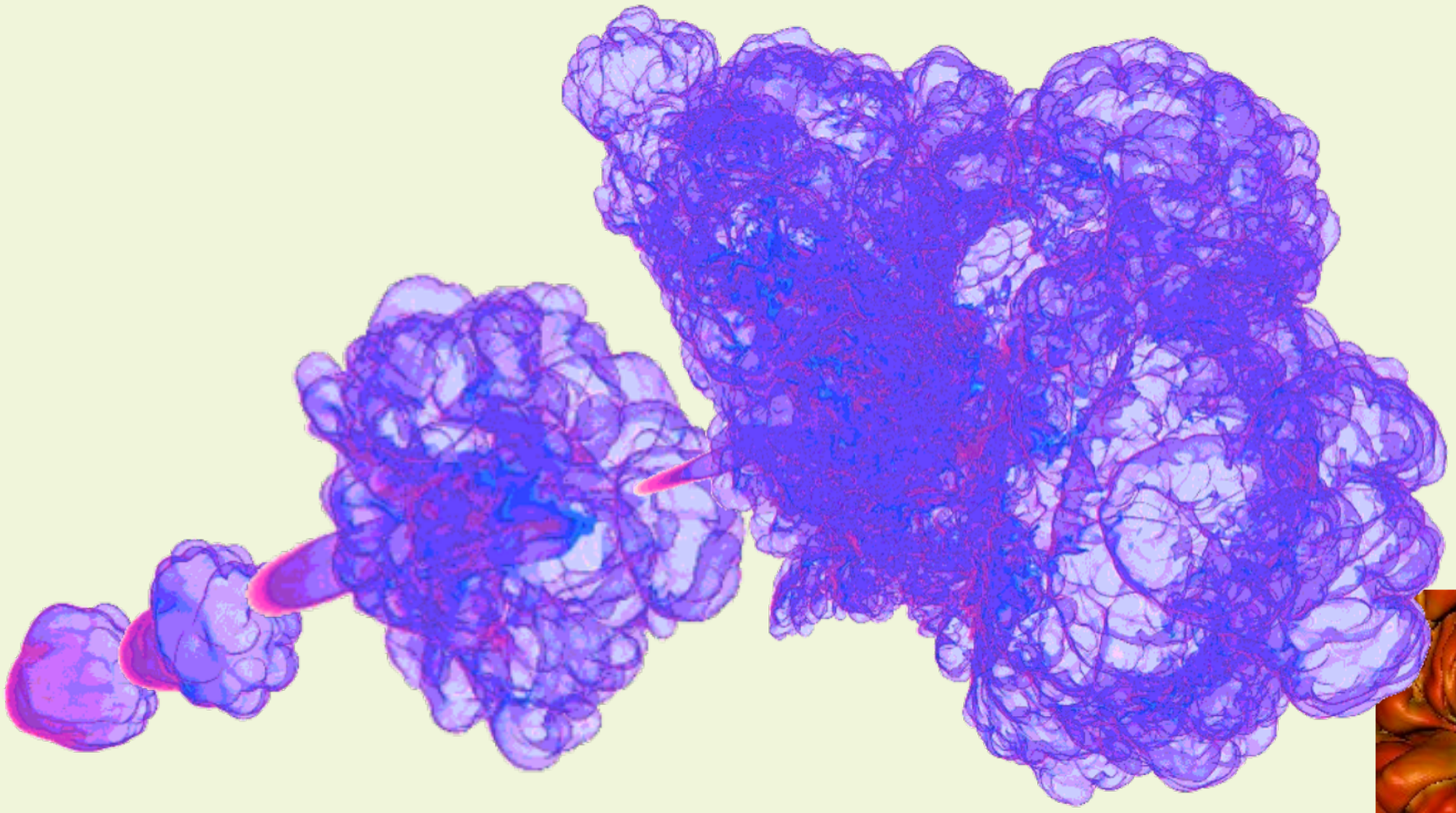

Plewa et al. 2004; images courtesy A. Calder

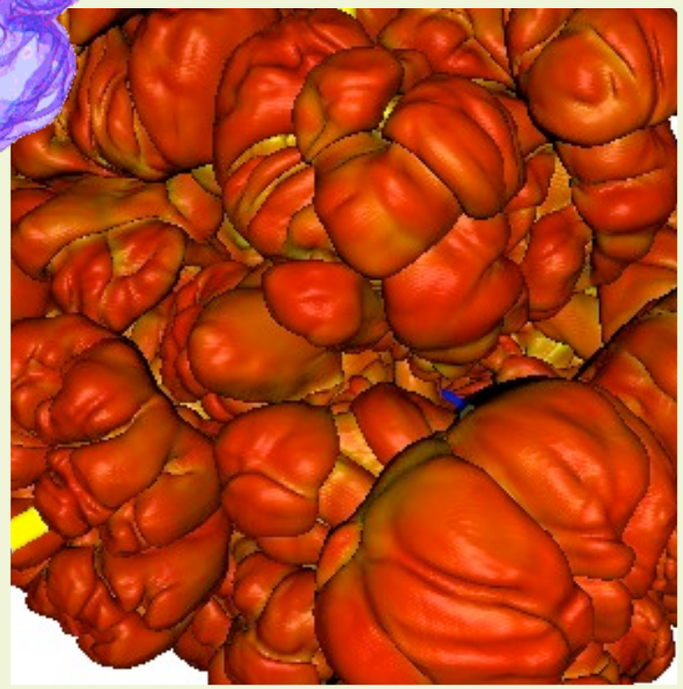

Reinecke et al. 2003

Variation with Composition

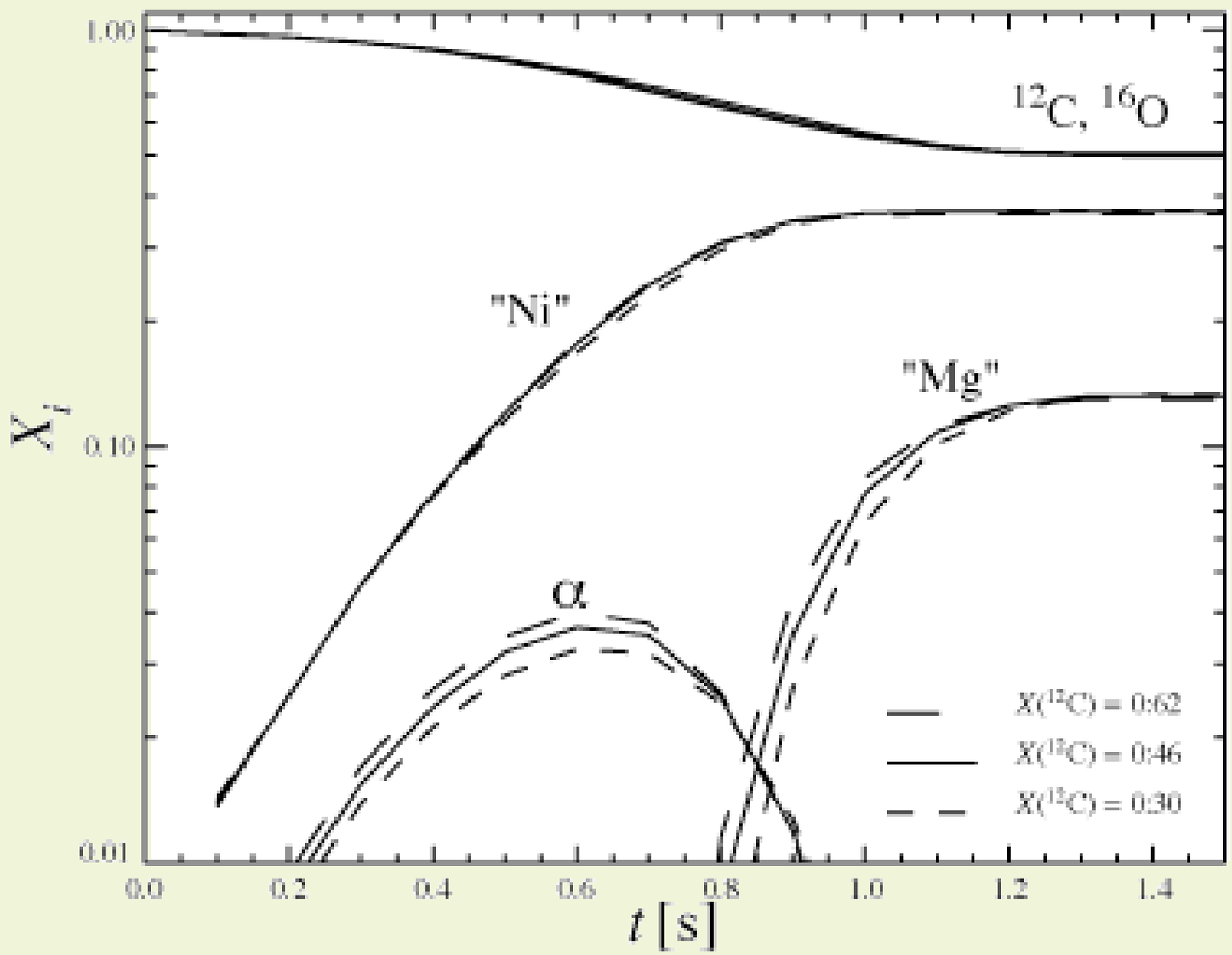

Mass of ^{56}Ni synthesized is independent of C:O ratio

plot from Röpke & Hillebrandt (2004) A&A, astro-ph/0403509

Simulations with the FLASH code

A Calder, T Plewa, P Ricker, K Robinson, JB Gallagher

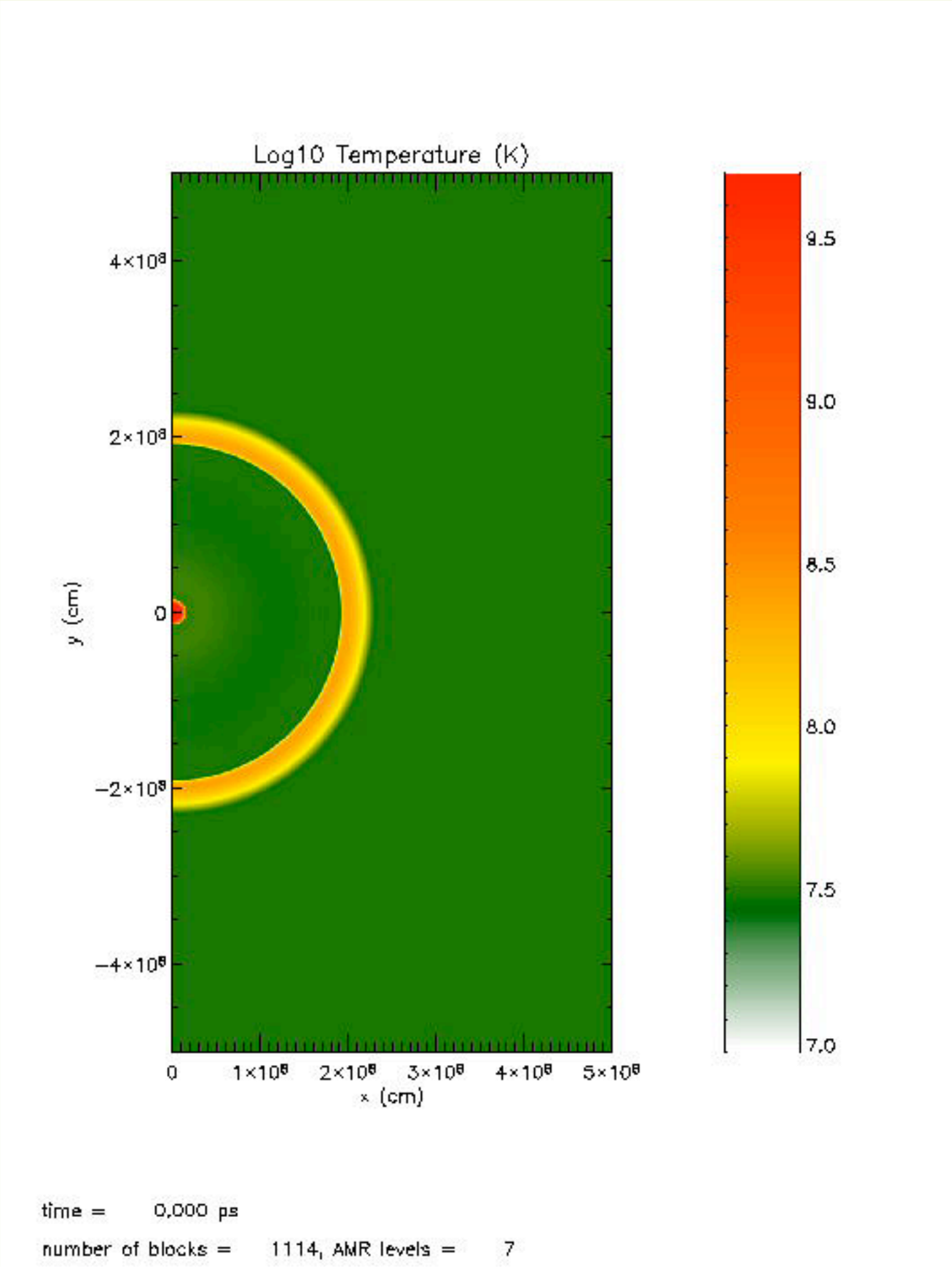

Centered ignition in cylindrical geometry

Flame model: evolution of progress variable and 5-isotope scheme (Khokhlov 1995)

Movie credit
K. Robinson

Embedded Tracer Particles (*first results*)

Brown, Calder, Plewa, Ricker, Robinson & Gallagher 2004

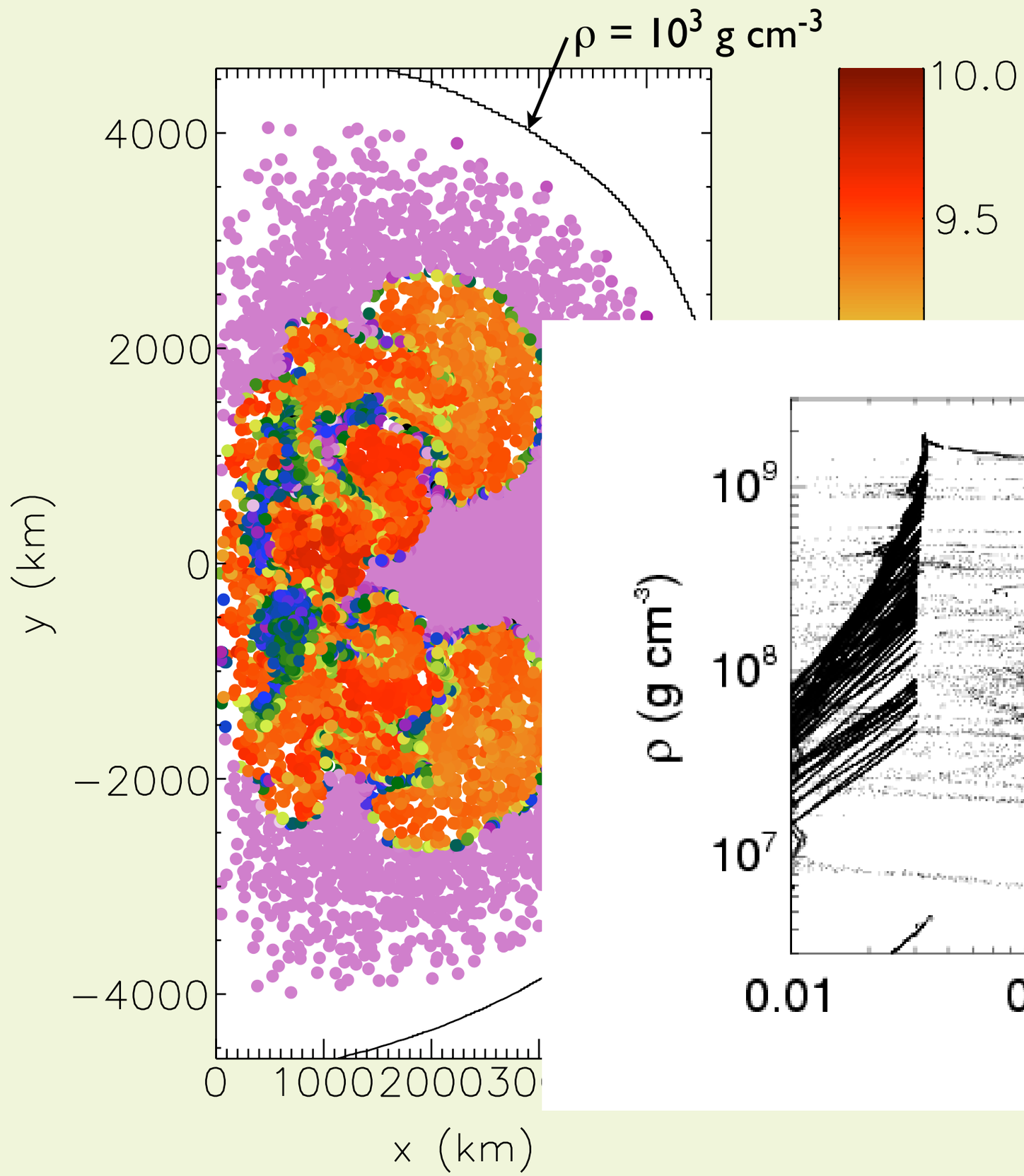

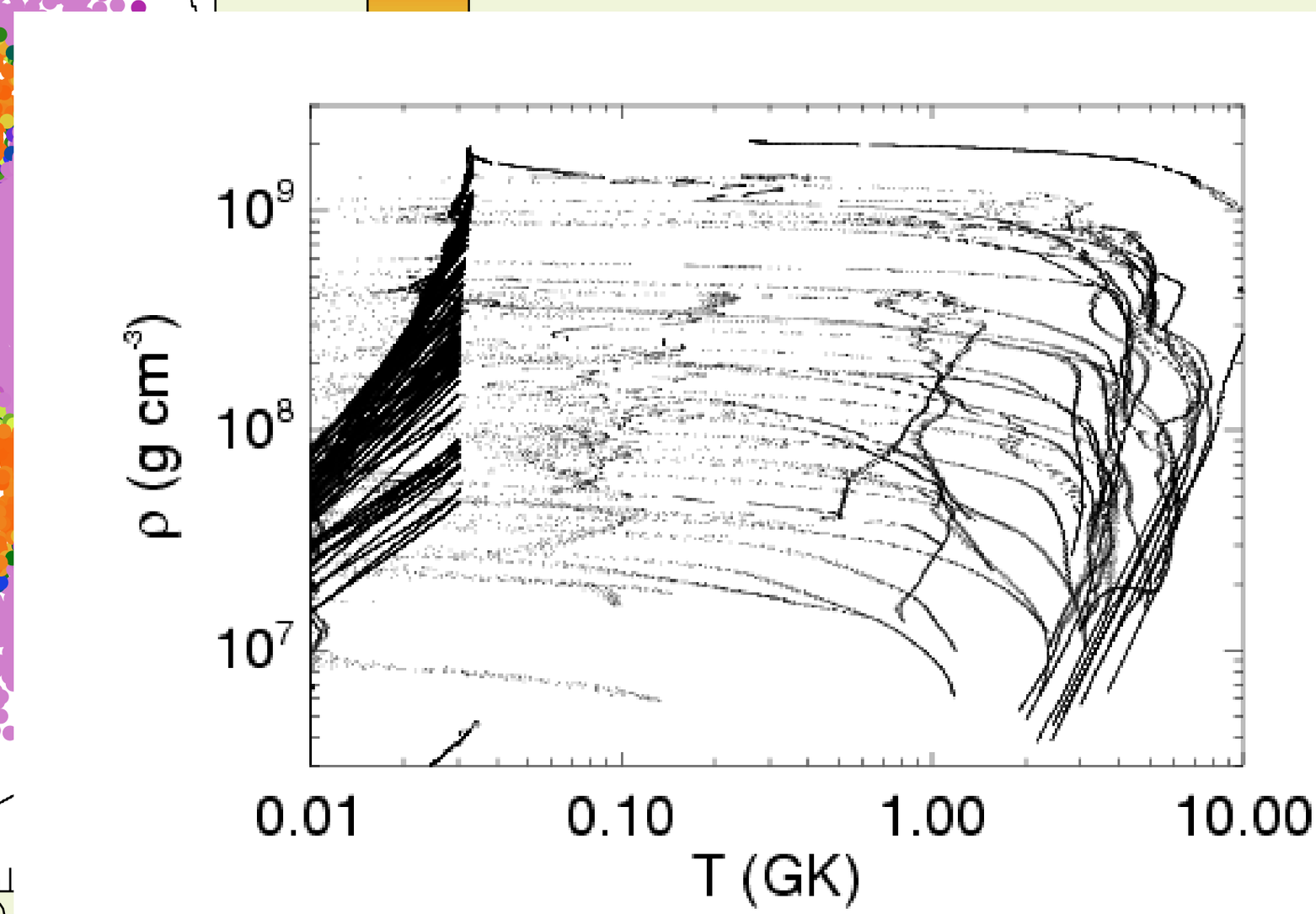

Yields

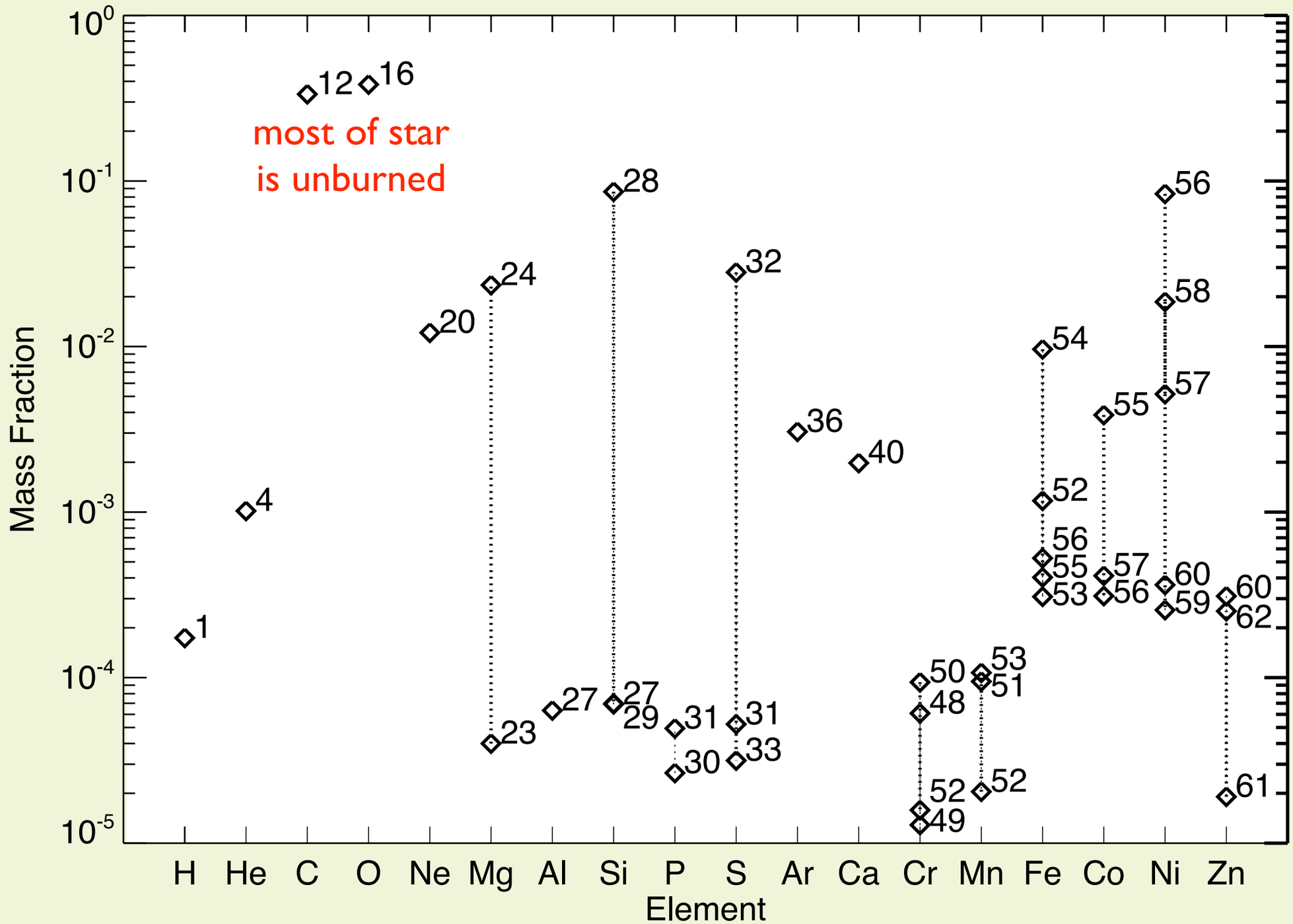
most of star
is unburned
Mass Fraction
Element
H He C O Ne Mg Al Si P S Ar Ca Cr Mn Fe Co Ni Zn

Ashes are mixed...

see also Gamezo et al. (2004) PRL

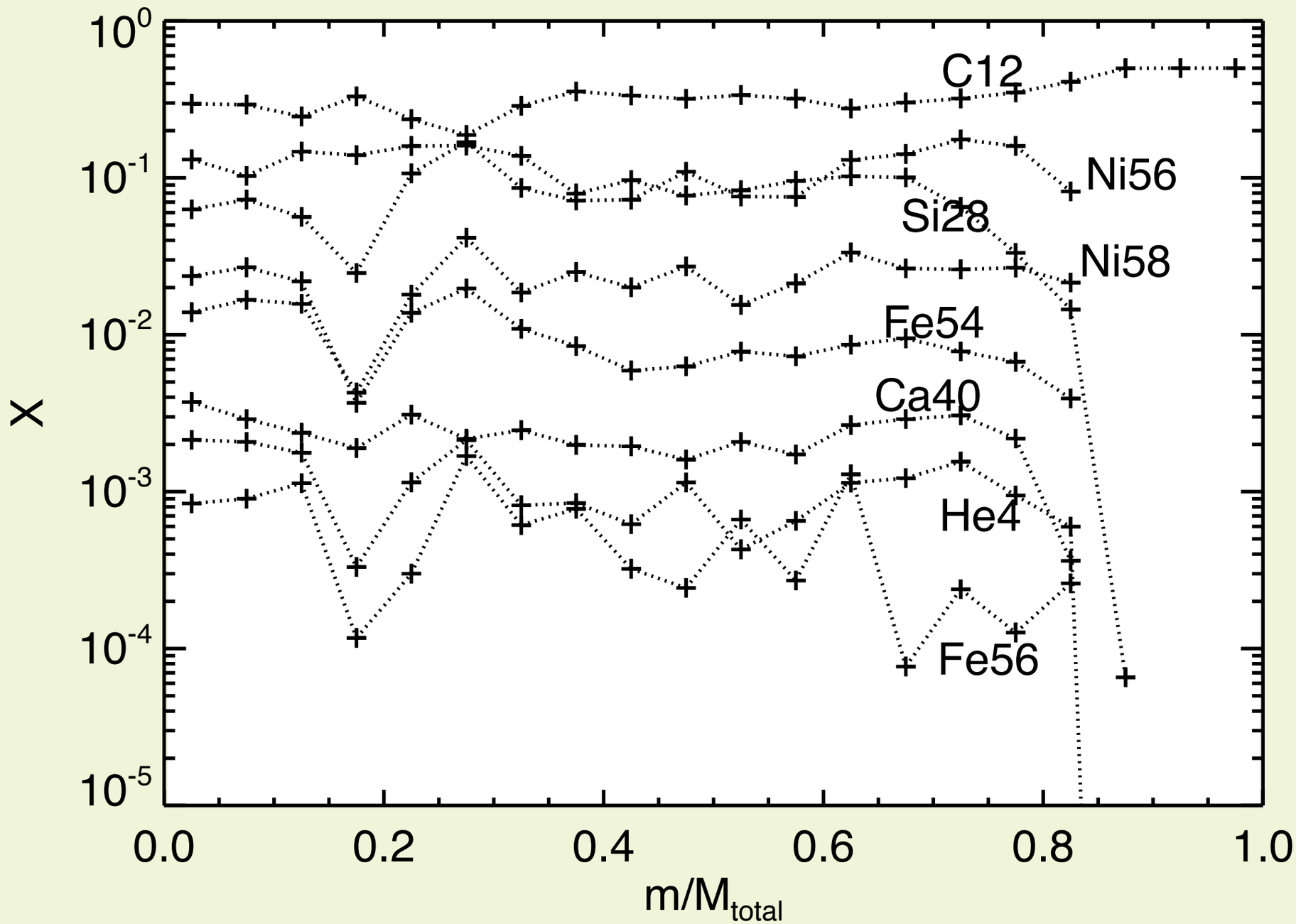

A 1-D Burn (W7)

Peak luminosity and decay rate set by mass of ^{56}Ni synthesized

1-dimensional models (W7-like) produce ^{56}Ni in the mass shell

$0.2\,M_\odot \lesssim M \lesssim 0.8\,M_\odot$

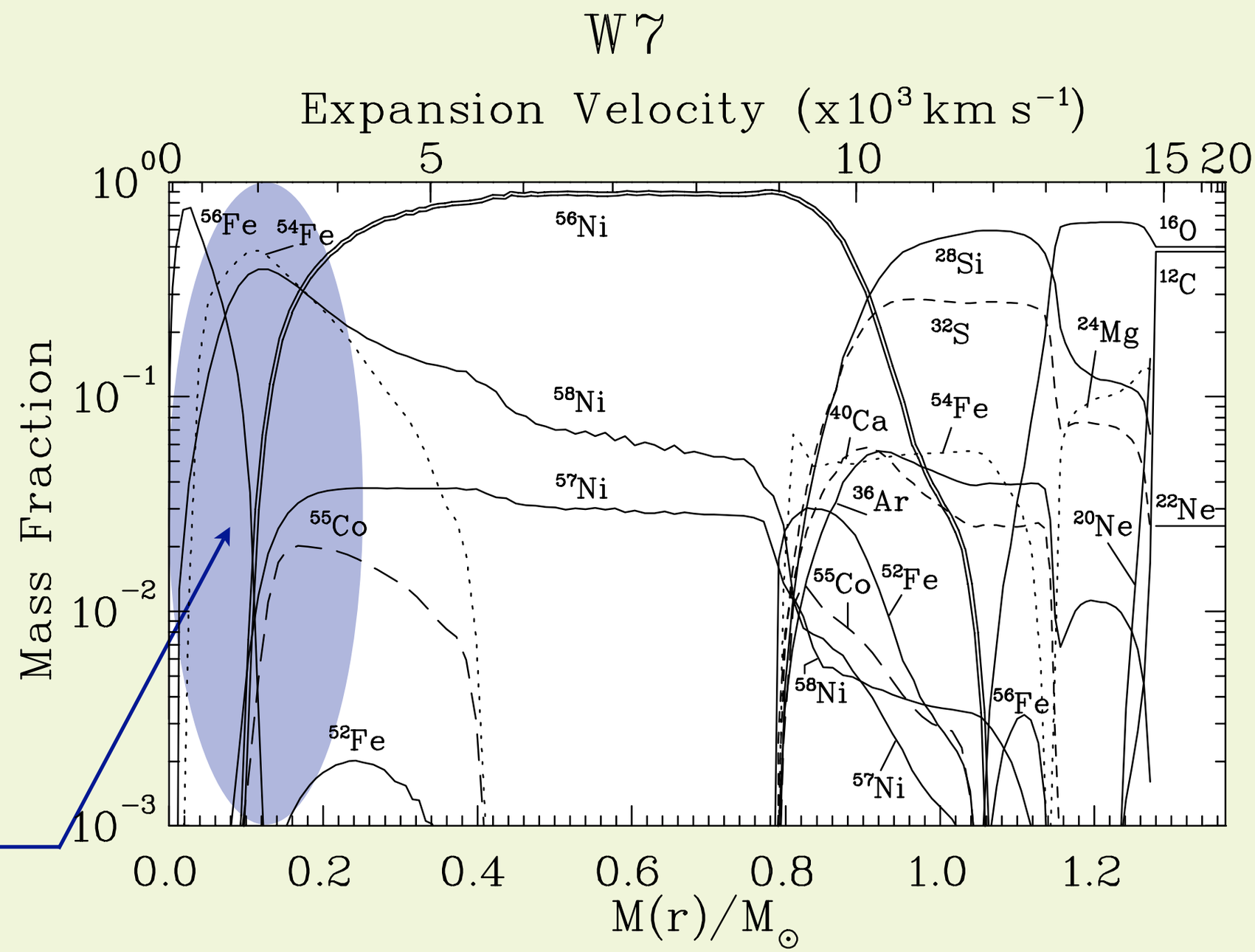

Y_e reduced by electron captures

Iwamoto et al. 1999

^{56}Ni production & ^{22}Ne

see also Travaglio et al. 2004

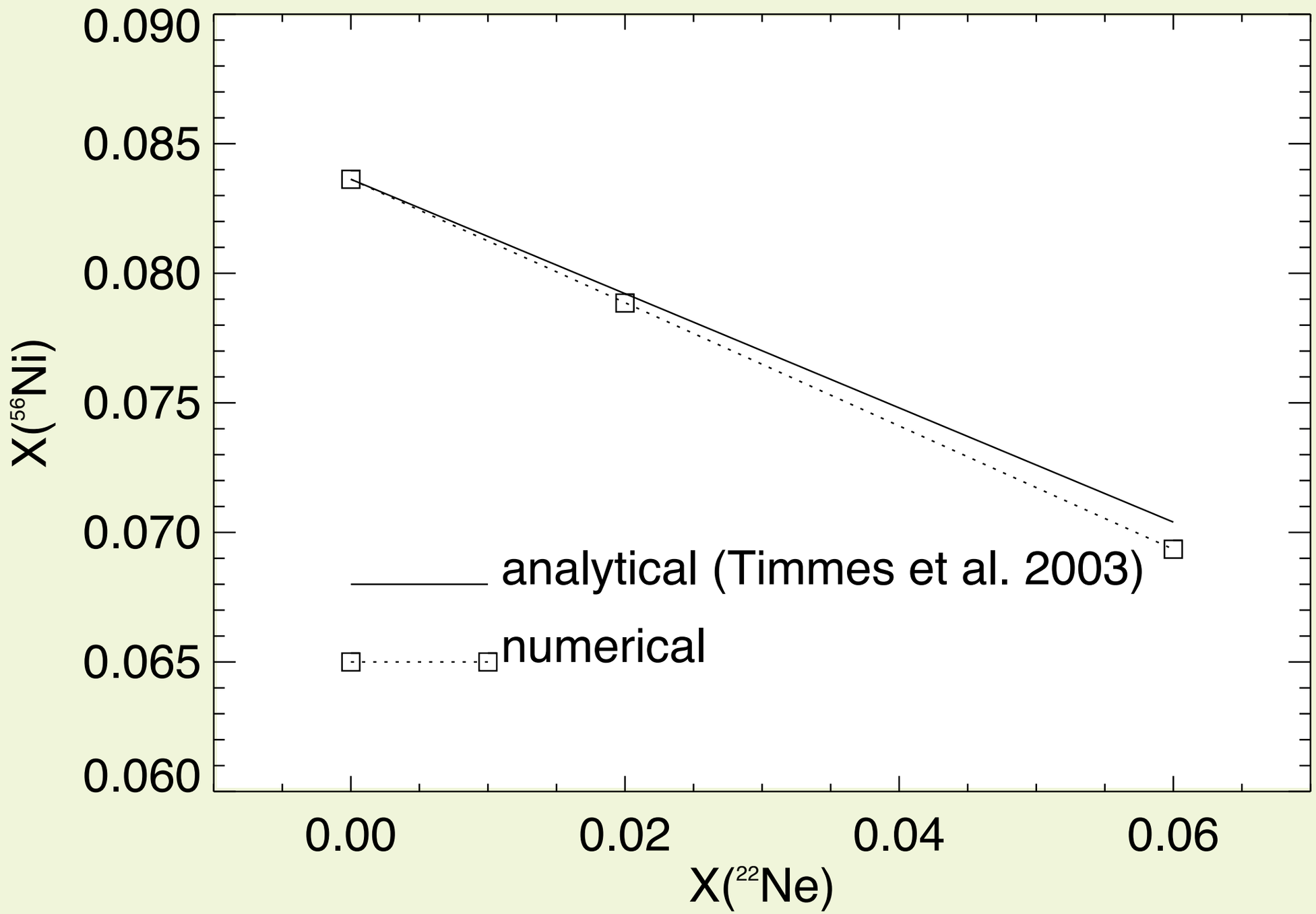

Summary

- $M(^{56}\mathrm{Ni})$ varies by ≈25% for $Z = [0.3\ Z_\odot, 3\ Z_\odot]$
  - Metallicity affects $M(^{56}\mathrm{Ni})$ more than C:O, ρ_c
  - Induces variation in peak brightness by ≈0.2 mag
- Questions
  - Is the Phillips relation truly unaffected?
  - Observations: SNeIa properties—host galaxy correlations
  - ***Progenitors & Ignition***

These Powerpoint slides were made
by Judy Cohen
for a talk at Santa Fe in August, 2004

THE LOCAL HIGH REDSHIFT UNIVERSE – THE EXTREMELY METAL POOR STARS IN THE GALACTIC HALO

Why study very metal poor stars ?

We can study the early epochs of the Galaxy, the local equivalent of the z ~ 5 Universe, with objects that are bright enough to be found in large numbers and to be analyzed in considerable detail.

We can study the kinematics of the early Galaxy and its halo.

We can study the onset of chemical evolution in the Galaxy, the possible stellar sources which produced many elements at very early epochs (very massive stars and SNII).

We can probe the age of the galaxy (Th and U dating) and the relationship between the halo field stars and the Galactic globular clusters.

The 0Z Project Team

Core group: Norbert Christlieb (Hamburg), Judy Cohen (Caltech) Andy McWilliam, Steve Shectman and Ian Thompson (Carnegie)

Associates/ Keck Pilot Project: E. Carretta, R.Gratton, T.Beers

Past & Present Postdocs: Innocenza Busa, Franz-Joseph Zickgraf, Inese Ivans, Jorge Melendez & Solange Ramirez, Torgny Karlsson & Mattias Dehn

Undergrad: Amber Swenson (Caltech)

Theoretical Support: G. Wasserburg & Y.Qian

Also: Model atmospheres – Bob Kurucz, MOOG (abund. anal. Code) – Chris Sneden, MAKEE (HIRES anal. code) –Tom Barlow, atomic data – NIST and Bob Kurucz, HIRES at Keck – Steve Vogt, Jerry Nelson, Gerry Smith and their teams.

Goals (Observational) for the 0Z Project

Isolate a sample of new EMP stars with [Fe/H]<-3 dex from the HES with a 2 step process, select from HES, vetting with moderate resolution spectra at 5-m class telescope. Step 1: selection from HES by N. Christlieb.

Step 2: Obtain moderate resolution spectra of all EMP candidates from the HES over about 5000 deg2,**

(This is about 2200 stars)

After 3 years and many nights at P200 and at Magellan, we have 1500+ spectra of EMP candidates.

Step 3: Obtain high dispersion spectra of all stars found from follow up mod res spectra to have [Fe/H] < -3 dex.

(Keck Pilot Project, also involving Gratton and Carretta from Padua, Italy, verified some of the techniques we are using)

Current Status of the 0Z Project - Analysis

- About 40 Keck/HIRES spectra of HES EMP candidates have been analyzed.
- So far, there are 19 new stars with [Fe/H] < -3 dex.
- So far, there are 8 with [Fe/H] < -3.5 dex.
- So far, there is 1 new extreme r-process star.
- A new calibration of the moderate res. [Fe/H] scale has been completed by Steve Shectman.
- Thompson and Shectman are working on the metallicity distribution in the halo from the 1500 mod res spectra.

Suggested phenomenological model:

N(elem E)=A x p(E,light) + B x p(E,Fe-peak) + C x p(E,r,Fe-seed) + D x p(E,s,Fe-seed)

A, B, C, and D are independent !

Key elements in each process:

Light – CNO through Mg - SNII

SNIa, Fe-peak - Fe, Ni (Ca to Zn)

s process – Ba, La

r process – Eu (hard to observe all r-process elements)

Relative yields of these processes

- **Patterns (based on looking at many spectra of very metal poor stars)**

- **Light elements: when C is high, N can range from normal to high, abundance pattern is highly variable. If C is normal, N is also normal.**

- **All the processes producing heavier elements (Fe-peak, r and s process) – fixed relative ratios for all relevant elements, at least through the Ba peak. s yield depends on abundance of Fe-seeds, i.e. Pb/Ba.**

- **s-process excess exists only with C excess, while r-process excess does not require a C excess.**

The 0Z Project – Keck Observations

- **Keck/HIRES spectra of 55 stars from the HES, 8 from the HK Survey and 26 bright metal poor field stars beginning Sep 2000 through May 2004**

- **Spectra mostly have $\Delta\lambda$=43,000 (for B>16, some have 34,000) and cover 3820-5320 A.**

- **Most have SNR of 100/spec. res. element**

- **Sample selection: [Fe/H](HES) < -3.0 dex, or strongly C-enhanced with [Fe/H](HES) < 2.5 dex.**

- **Uniform determination of stellar parameters (Teff V-J, V-K; log(g) from isochrones, E(B-V) from Schlegel et al all sky maps, grid of predicted colors from Houdashelt et al.**

- **Spectrum is not used in setting stellar parameters.**

Analysis procedures

- **Only freedom is above or below turnoff for stars near MSTO.**
- **Use automatic eq. width program of Ramirez & Cohen, then a well defined procedure of manual checks for weak lines.**
- **Fixed template list of lines, gf values, HFS corrections, damping constants. Fixed list of molecular lines for C and N abundances.**
- **Use MOOG code of Sneden modified for batch operation.**
- **v_t determined for some stars, v_t –Teff relation used for most**
- **Except for the Keck Pilot Project (Sep 2000 run), I have done all the observing, data reduction and analysis thus far myself.**
- **For the Keck Pilot Proj., E. Carretta and R. Gratton did the analysis. I did the stellar parameters and data reduction.**

Analysis Errors:

Random – Teff errors from uncertainties in photometry

measurement errors in absorption line strengths

uncertainties in gf values

Systematic errors:

Do the model atmospheres have the correct T/optical depth ?

Systematic errors in gf values

non-LTE corrections

Current Status of the 0Z Project - Observations

Selection of EMP candidates from the HES (complete; done by N.Christlieb)

Follow up spectra - ~1500 from 5m Hale or 6.5m Magellan, effort ~80% complete

High res spectra of suspected [Fe/H]< -3 stars, ~50 (Keck/HIRES), ~15 (Mike/Magellan). 75% complete at Palomar, just starting at Las Campanas.

Best possible high res spectra of new [Fe/H] < -3.5 stars; this effort is just starting.

Supporting photometry: IR-2MASS, opt. C40, now using 1.3m Andicam queue at CTIO. ~150 stars observed so far.

Examples of HES objective prism spectra of candidate metal poor stars from the HES (digitized photographic plates) (from Christlieb 2003)

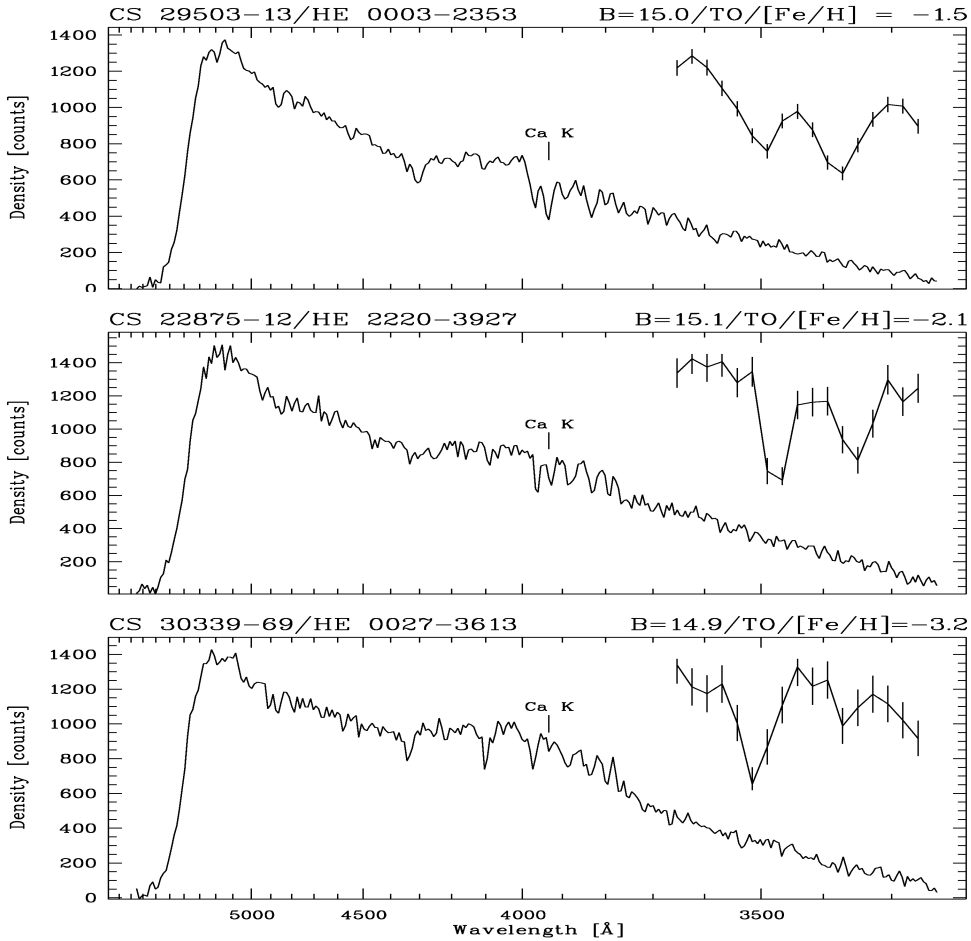

Examples of highly carbon enhanced metal poor stars (based on G band of CH) selected from the HES (from Christlieb 2003)

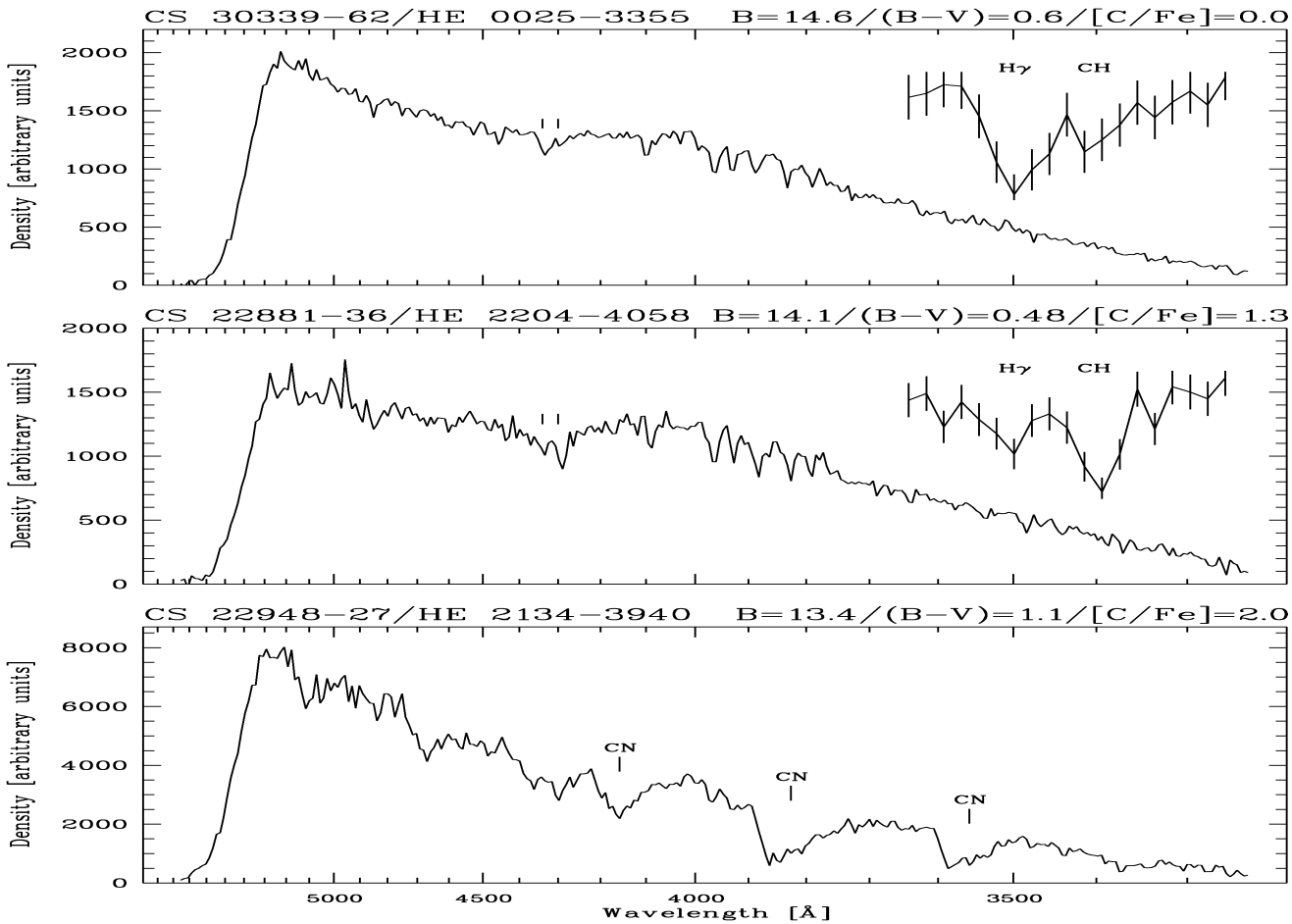

Sample Mod. Res. Follow Up Spectra of HES EMP candidates from 200-inch Hale Telescope. Measure Call and Balmer line indices.

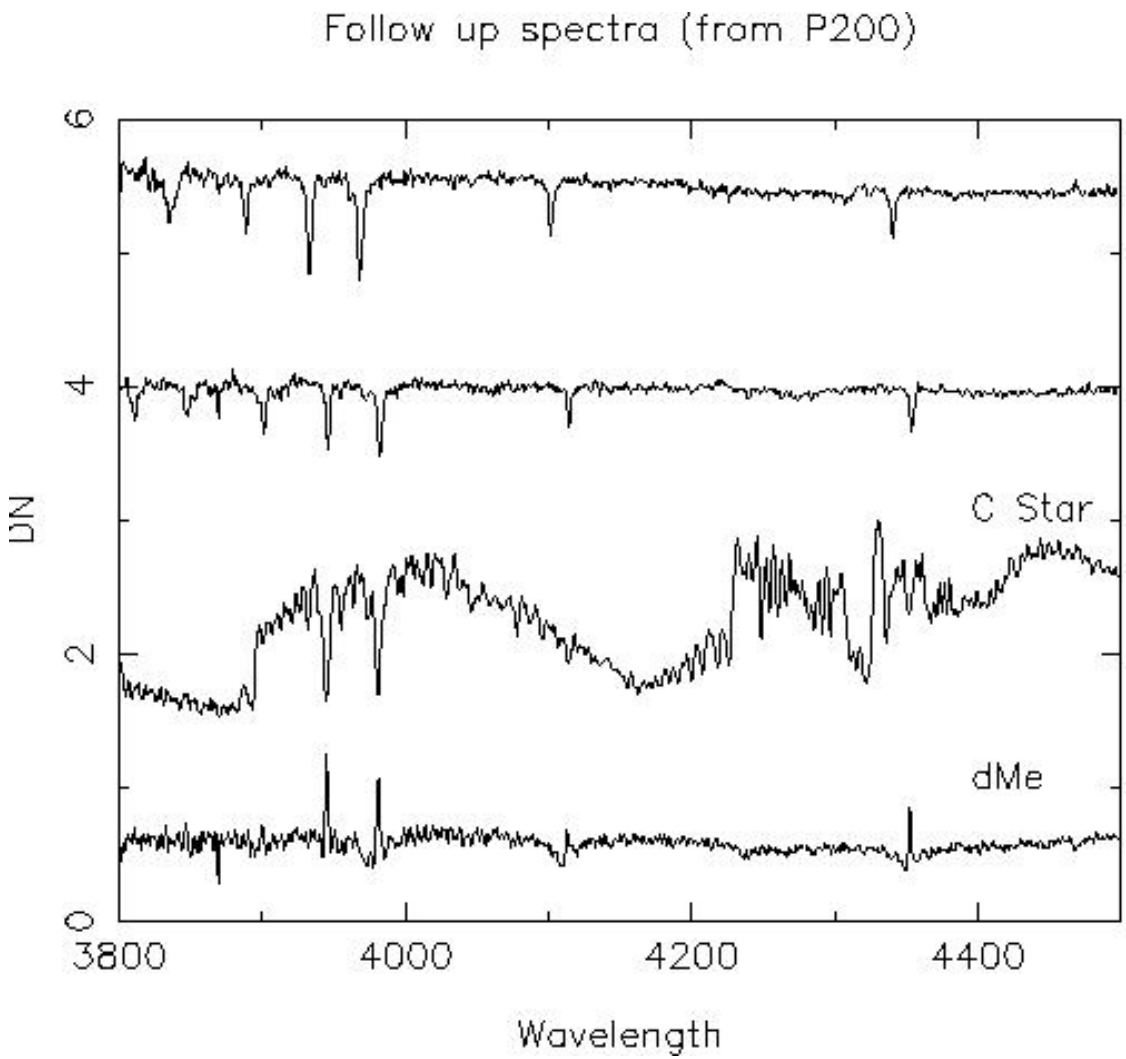

3933/CaII index versus Hdelta index for ~800 stars from the HES with mod. res. specta from Magellan (from Ian Thompson)

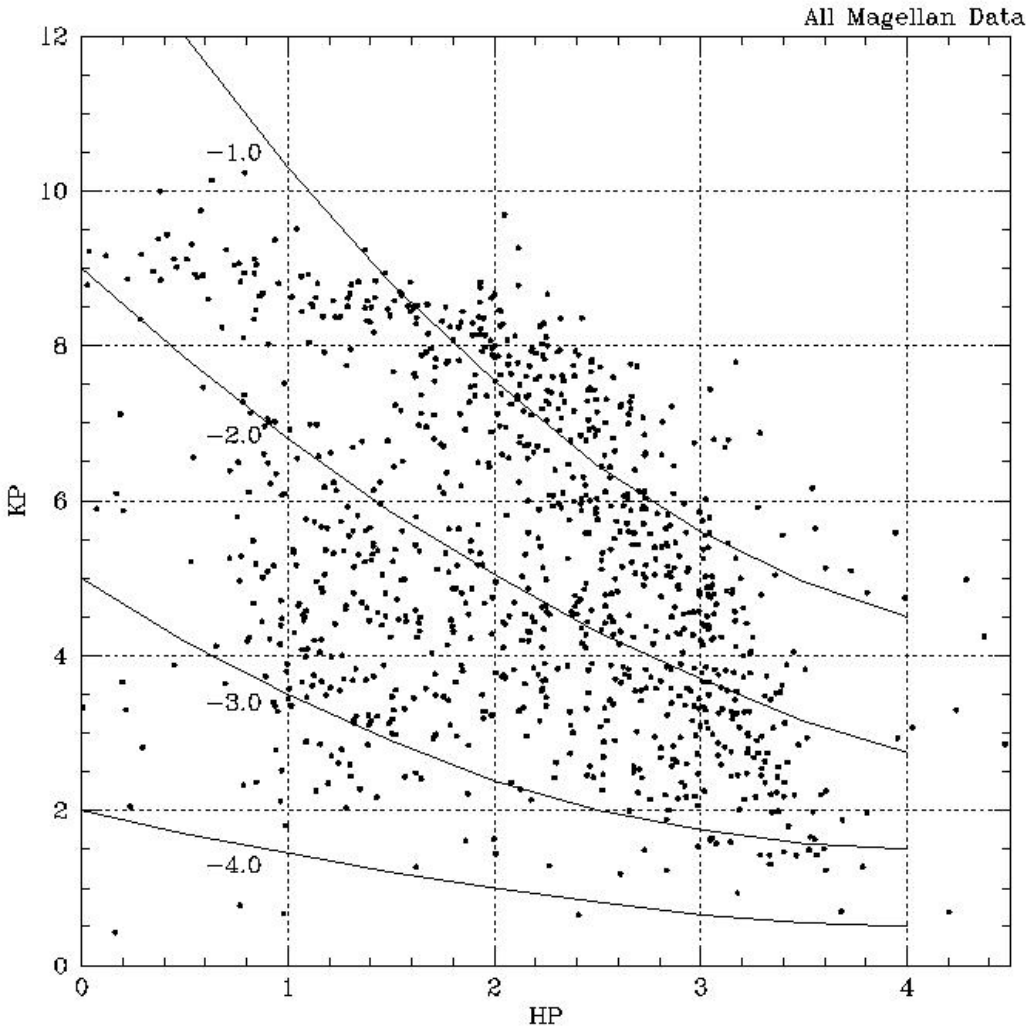

The observed metallicity distribution from mod. Resolution spectra of the HES and HK turnoff stars (left panel) and giants (right panel)

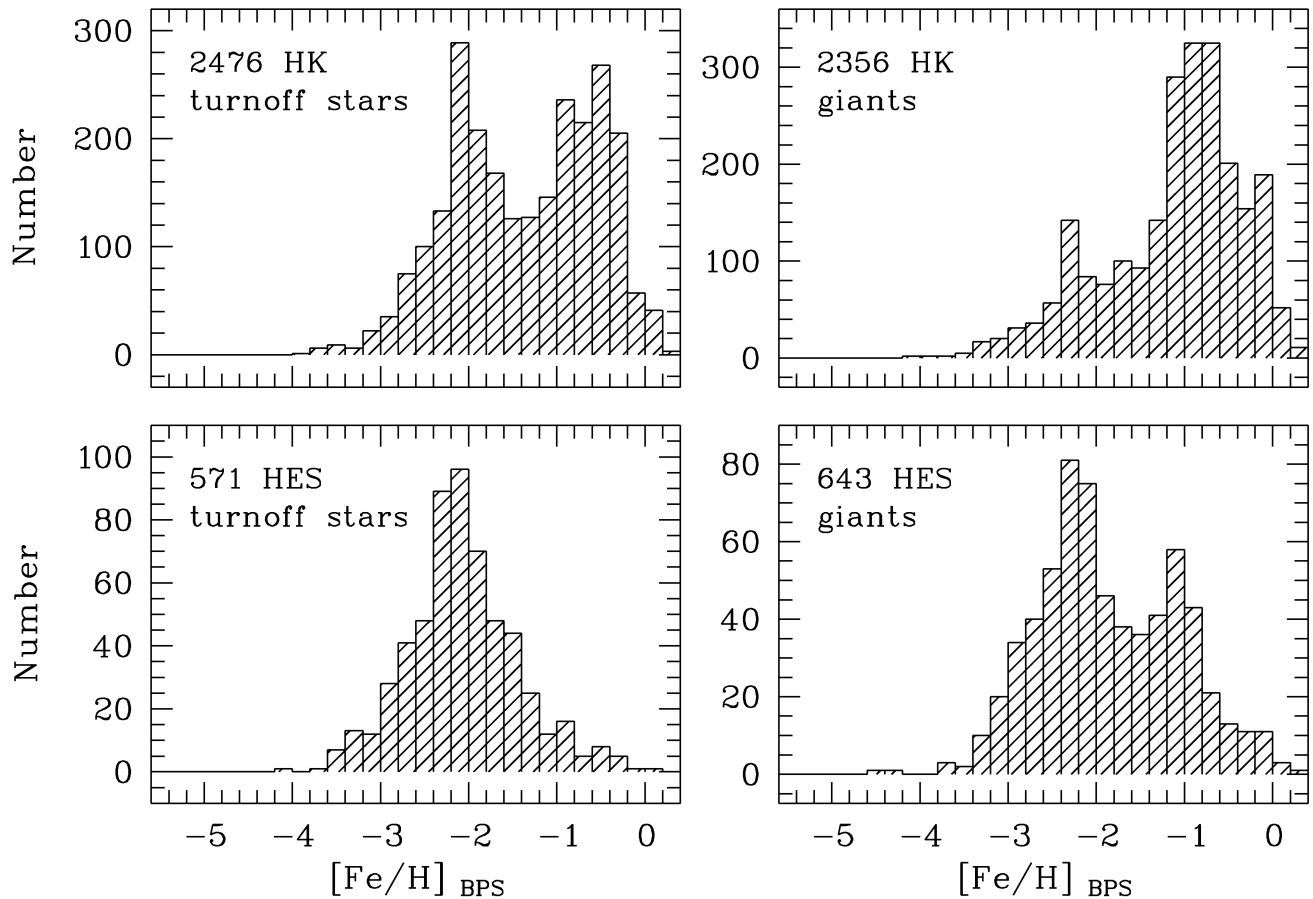

The Accuracy of the [Fe/H] From the Mod. Res. Spectra (algorithm of Beers applied by Christlieb)

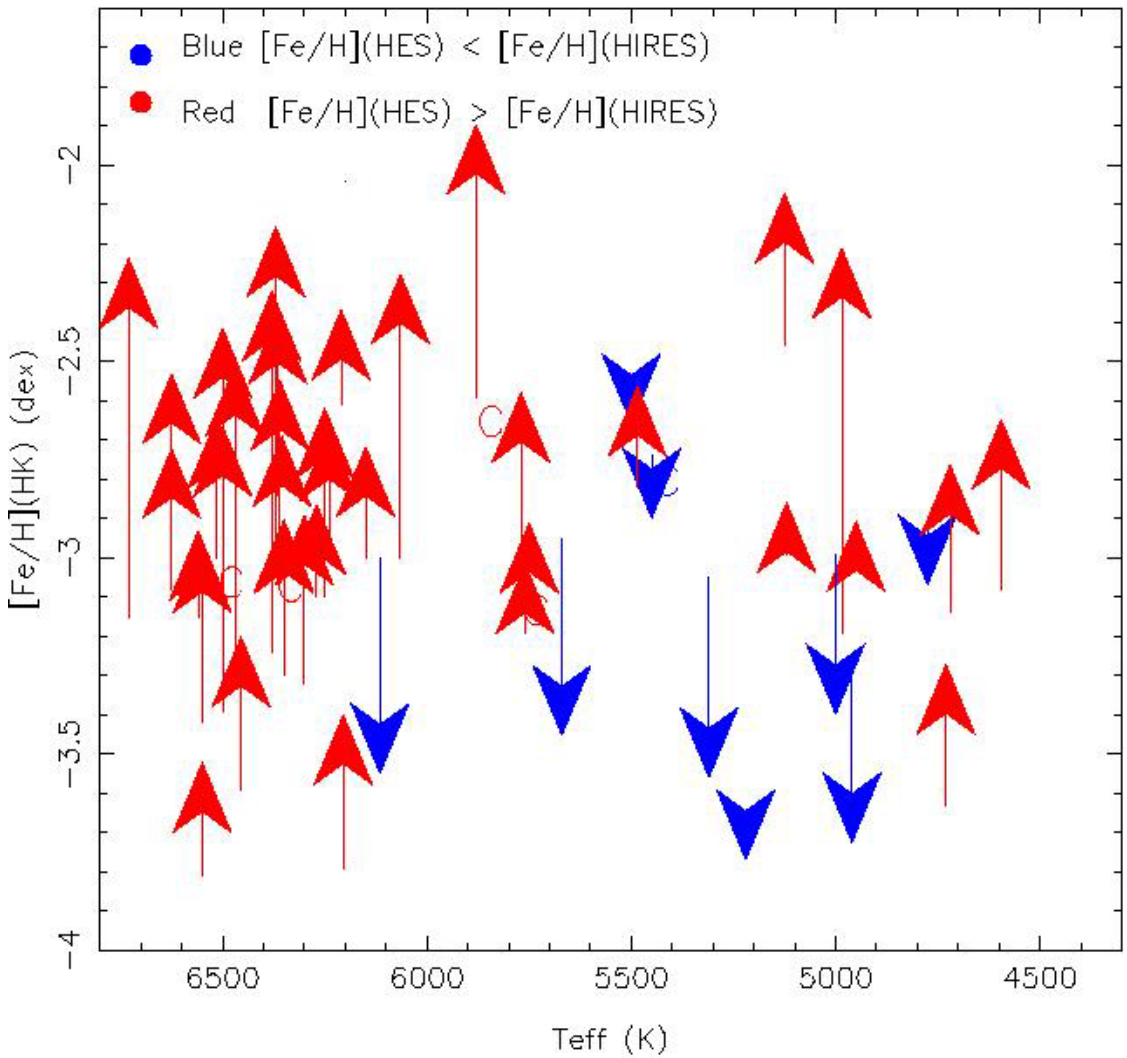

Comparing the HIRES/Keck echelle abundances with those inferred from the mod. res. spectra

Table 1. The Accuracy of the HK Metallicity Scale

Set of Stars	No. Stars	Δ[Fe/H](High Res – HK) (dex)	$\sigma\Delta$[Fe/H] (dex)
Dwarfs			
All	28	+0.42	0.32
No C-enh	20	+0.39	0.32
C-enh	4	+0.62	0.31
Giants			
All	20	+0.12	0.41
No C-enh	14	+0.06	0.33
C-enh	6	+0.24	0.57

Fe/H distribution for the 28 dwarfs in the sample (22 from the HES, 3 from the HK Survey, and 3 bright halo field stars) from Cohen et al (2004)

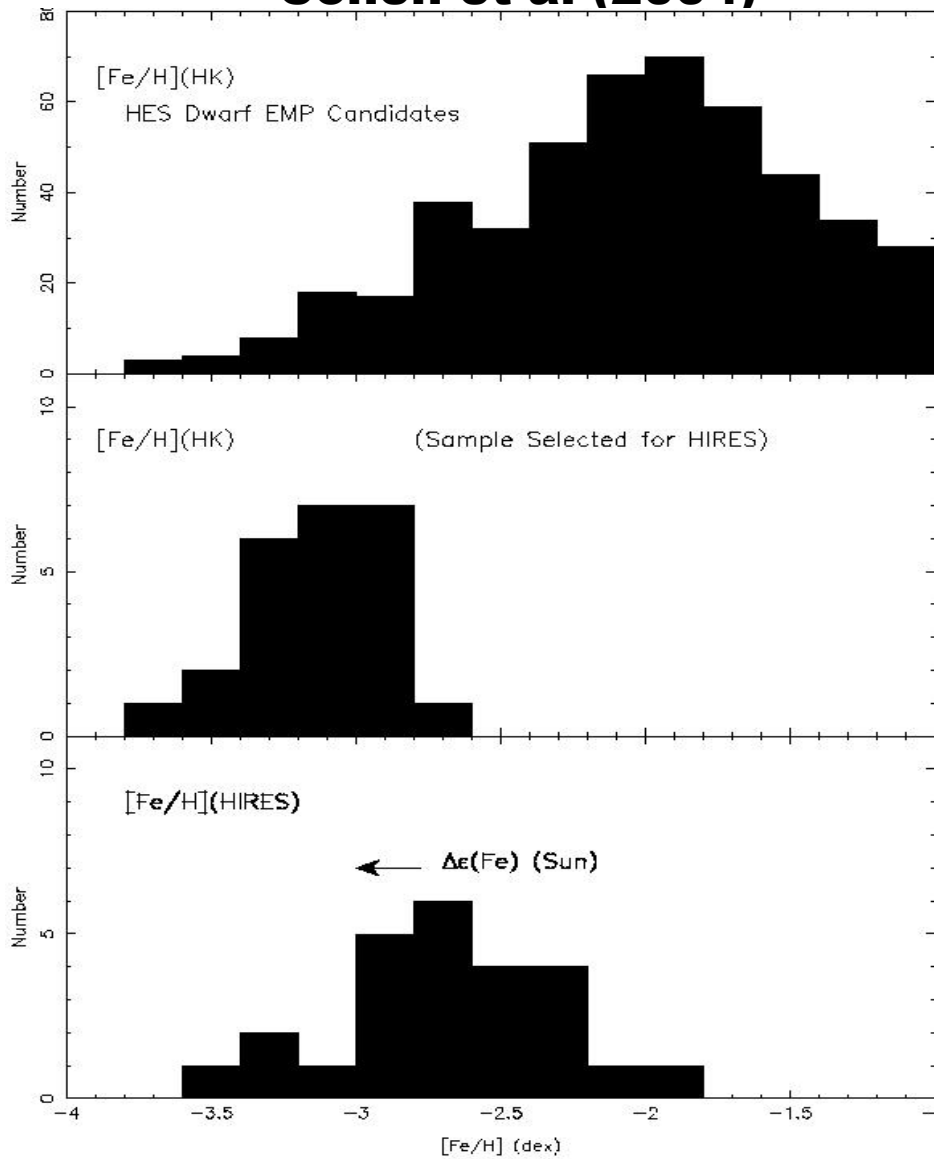

Dwarfs versus Giants/sub-giants

Dwarfs versus Giants

Dwarfs (define as Teff $\geq$ 6000 K) are hotter (hence have weaker lines for a given [Fe/H]) and less luminous (so closer for a given V mag). They are unevolved, hence their surface abundances should be those of the material from which they formed.

Giants (including subgiants) (define as Teff $<$ 6000 K) are much cooler, hence have much stronger lines. Many more elements can thus be measured in these stars. However, they are more evolved, and may have had internal nuclear processing and dredge up to the surface.

Overall, its much easier to isolate EMP giants and the determine their chemical abundances than it is to do such for EMP dwarfs.

Keck/HIRES Spectra of Several EMP dwarfs (and 1 EMP giant) in the region of the CH G band

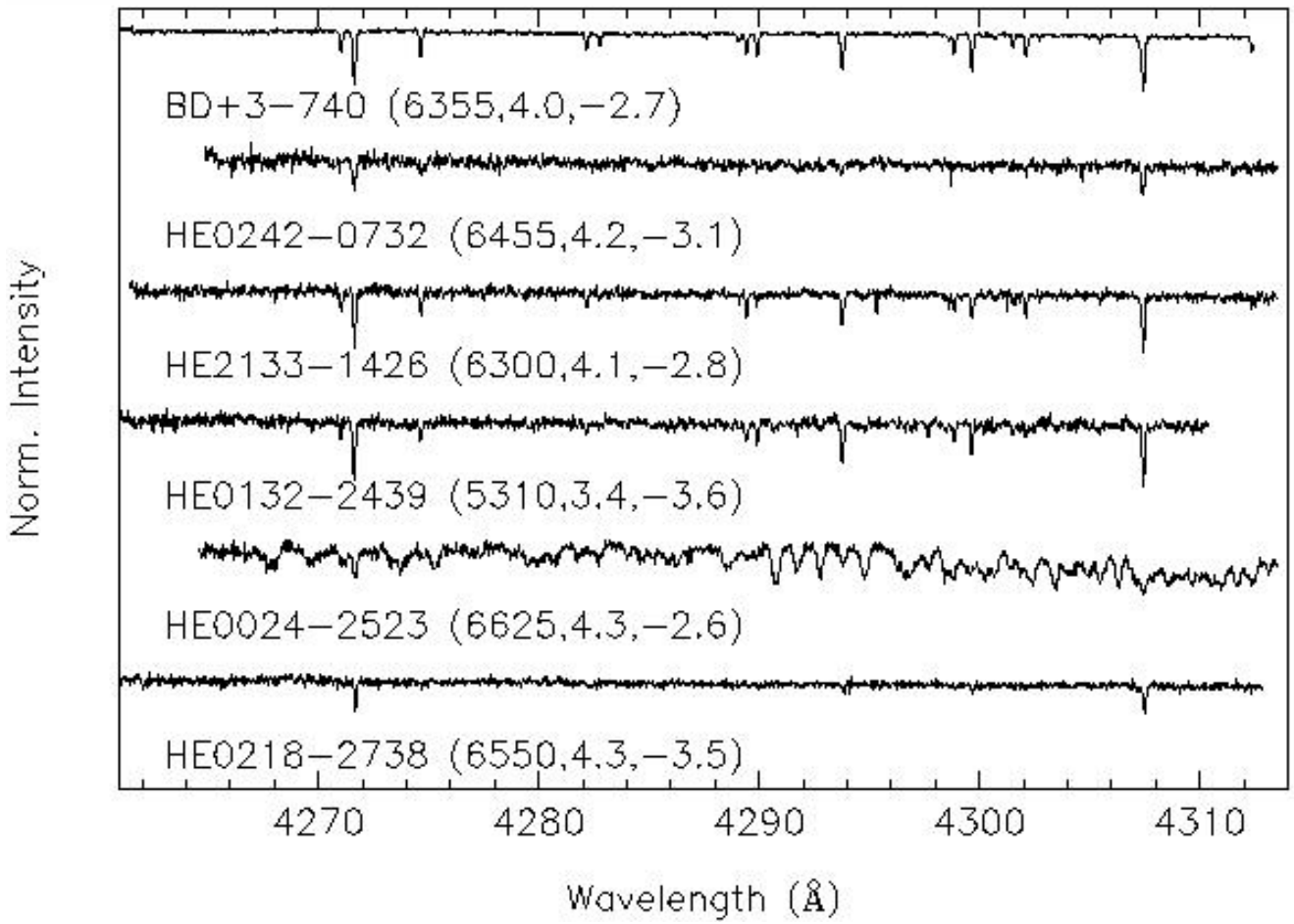

Spectra of several EMP dwarfs (and 1 EMP giant) in the region of the 4215 A SrII line

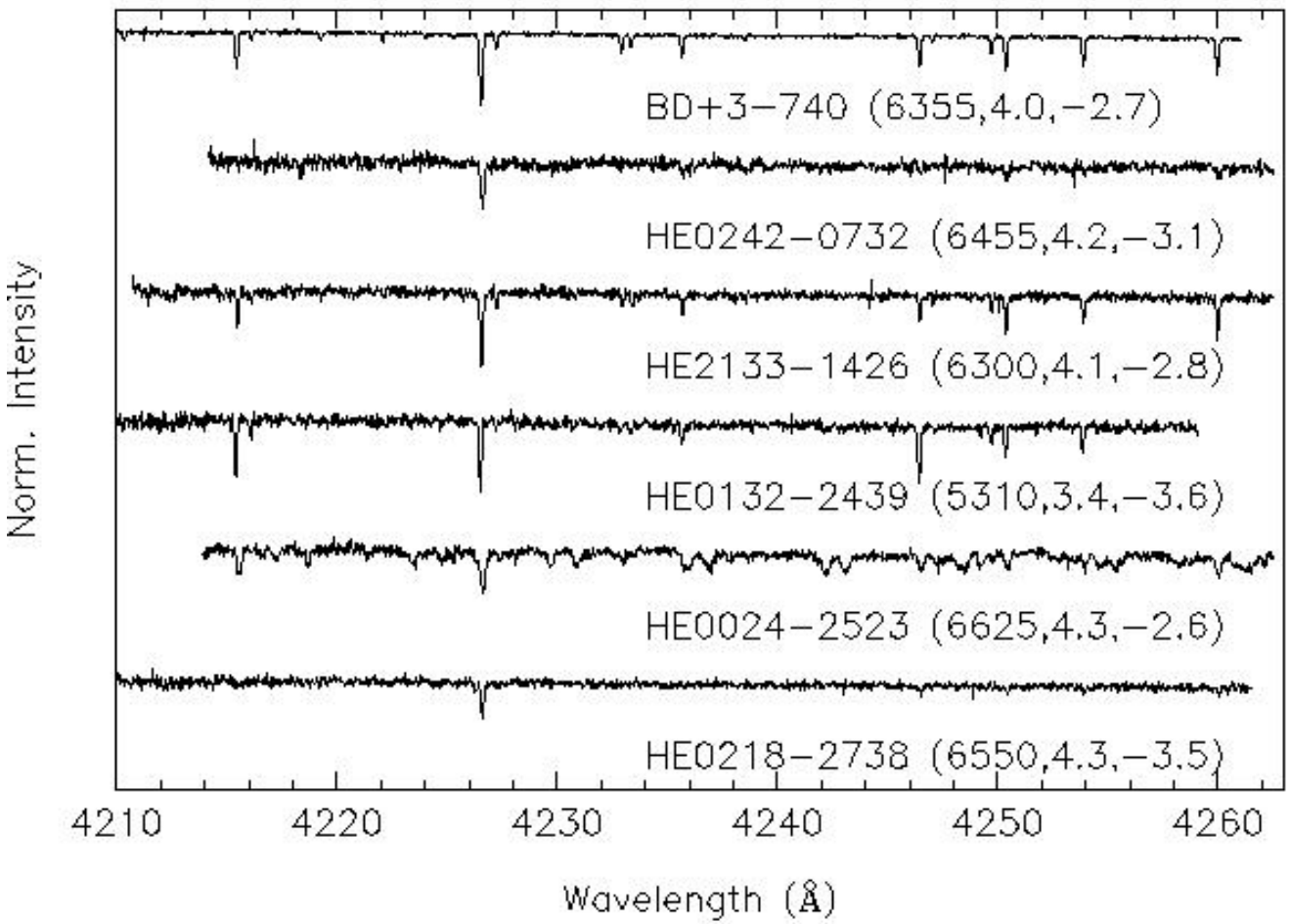

Spectral synthesis of the region of the CH and C2 bandheads in the dwarf carbon star HE0007-1832

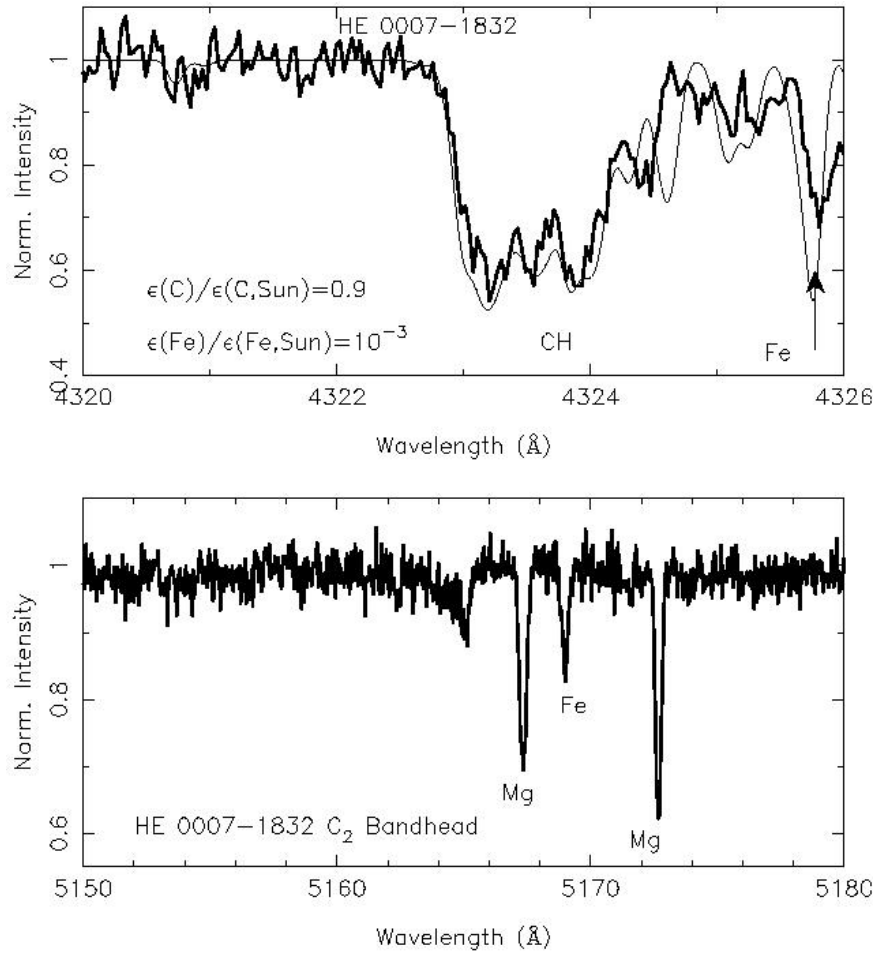

Spectra of two similar C stars (subgiants) from the HES, one of which has much stronger CN than the other. Note the "busy" nature of the spectrum compared to dwarfs.

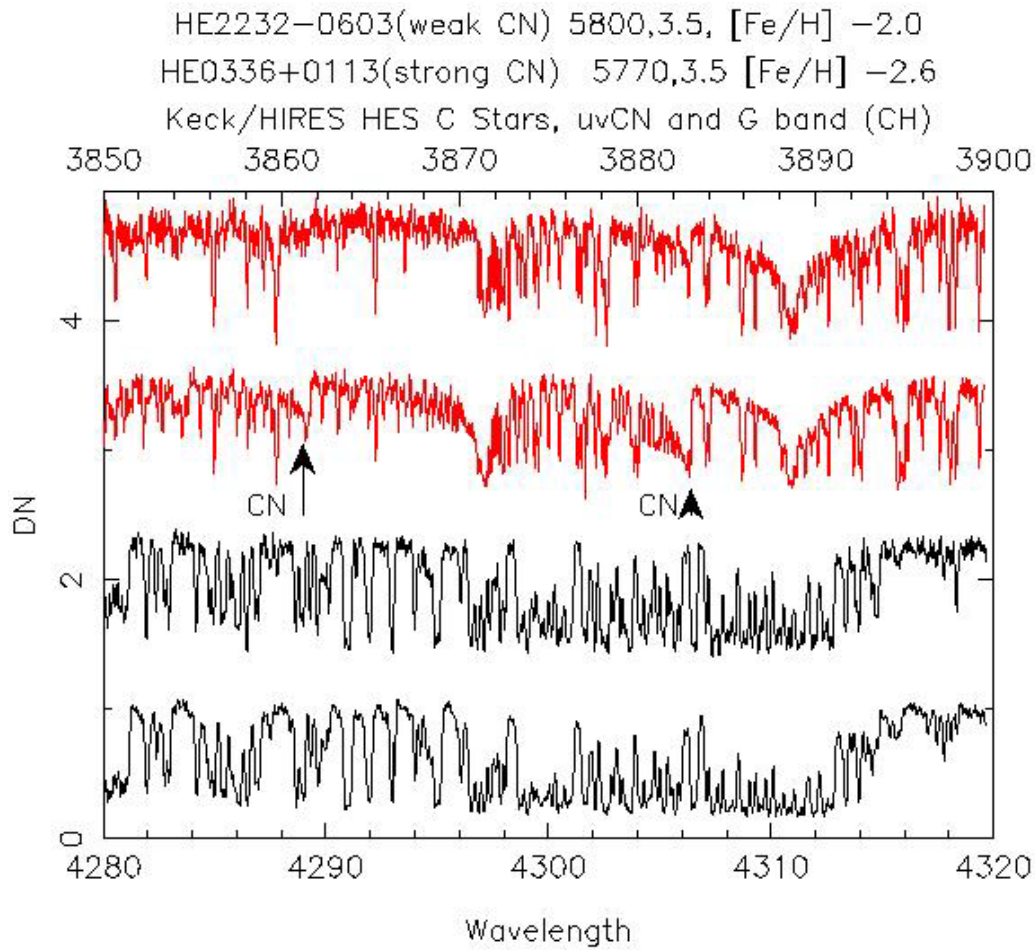

Searching for Eu enhanced stars to find more r-process stars, to search for Th and U for age dating (after Christlieb et al, 2004)

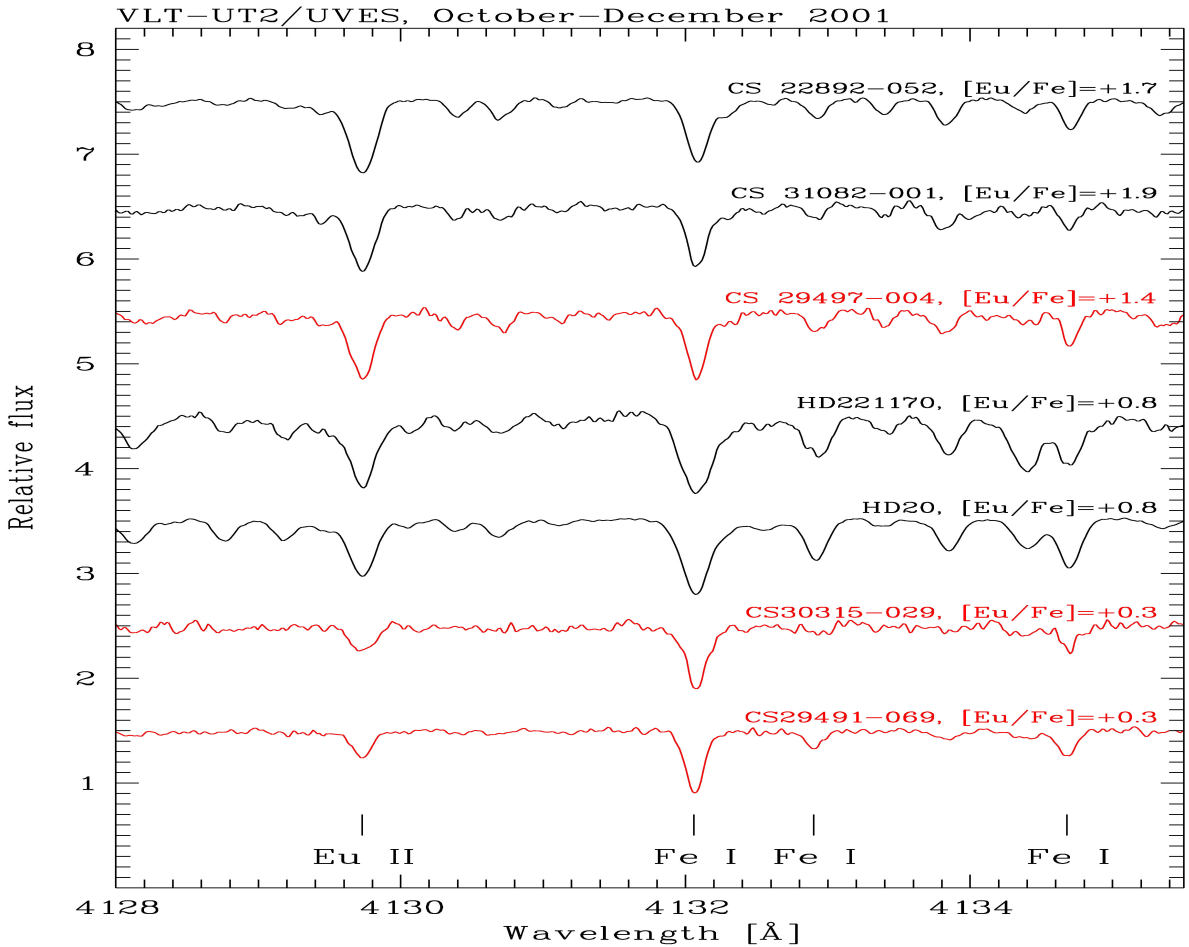

CMD diagram for sample of 53 stars from the HES with HIRES/Keck spectra thus far (note: log(g) determined from isochrone)

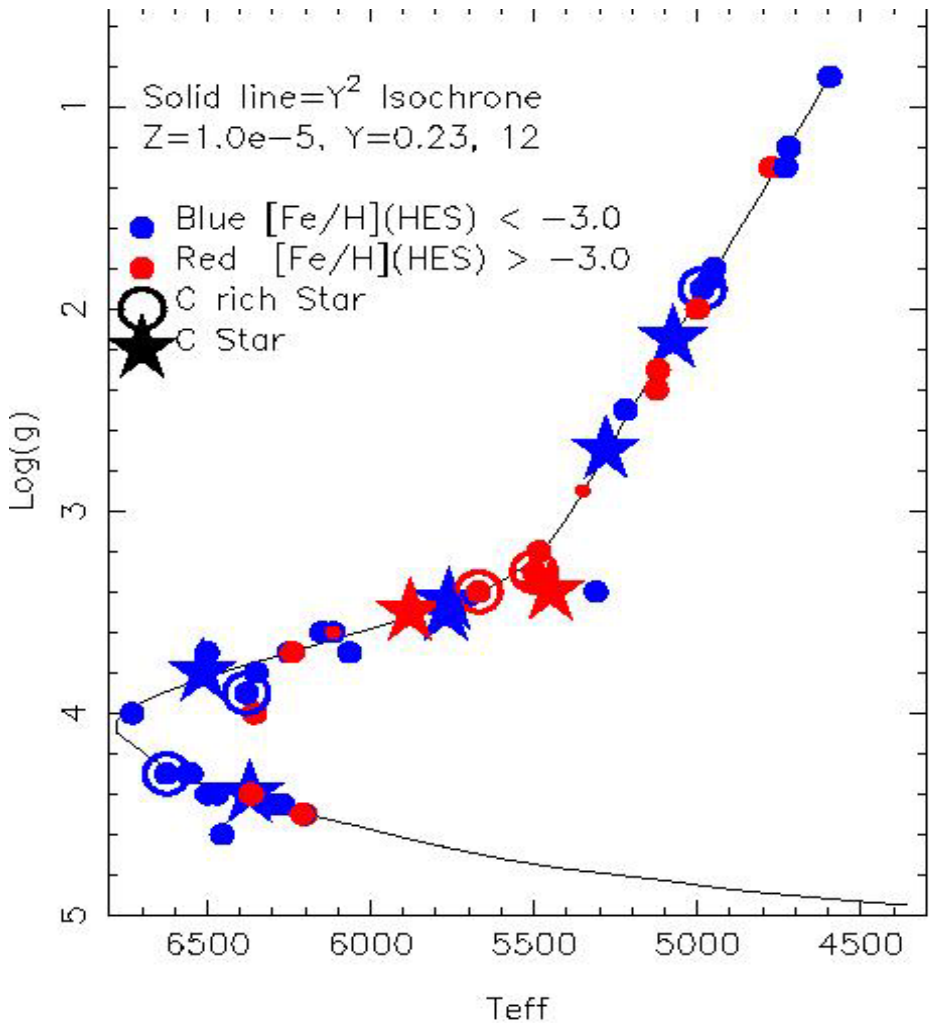

Fe ionization eq., 47 stars from HES, Keck/HIRES.
<[Fe/H](FeI)-[Fe/H](FeII).=+0.039, σ=0.126 dex,
Teff>6000 K blue, Teff<,red, open blue=below MSTO

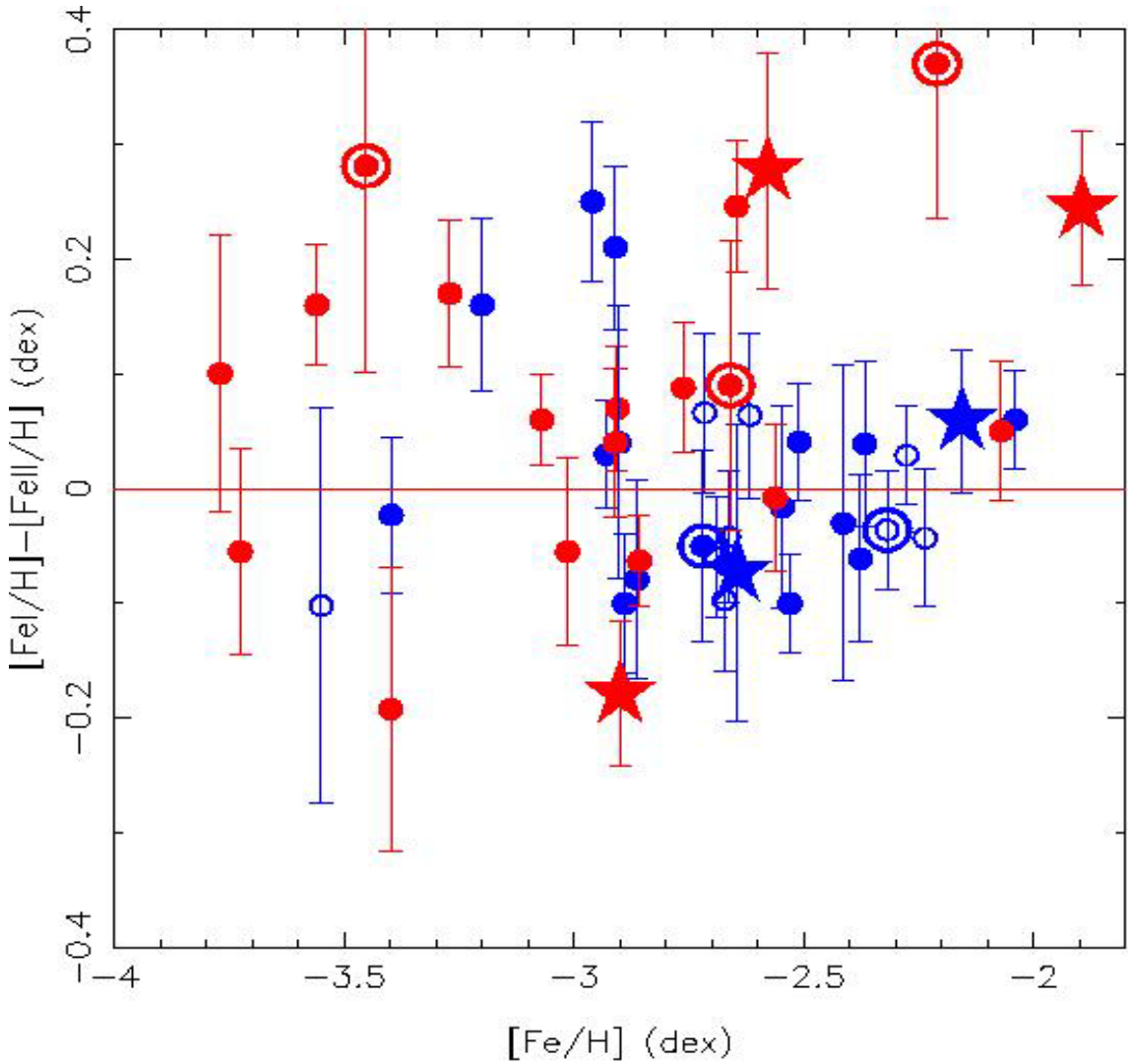

Ca, Sc, Ti/Fe versus metallicity for 47 HES dwarfs and giants. σ([Ca/Fe], [Sc/Fe], [Ti/Fe]) < 0.15 dex

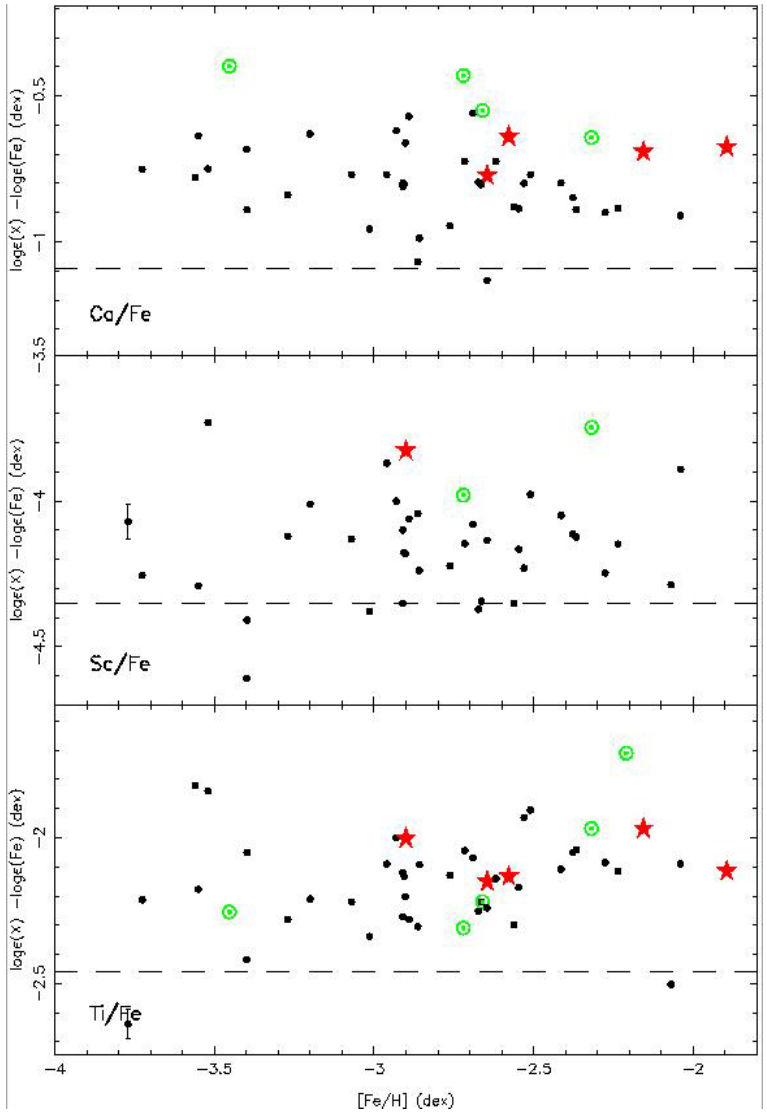

Si, Mn/Fe versus metallicity [Fe/H] for 28 EMP dwarfs, showing all outliers, from Cohen et al (2004)

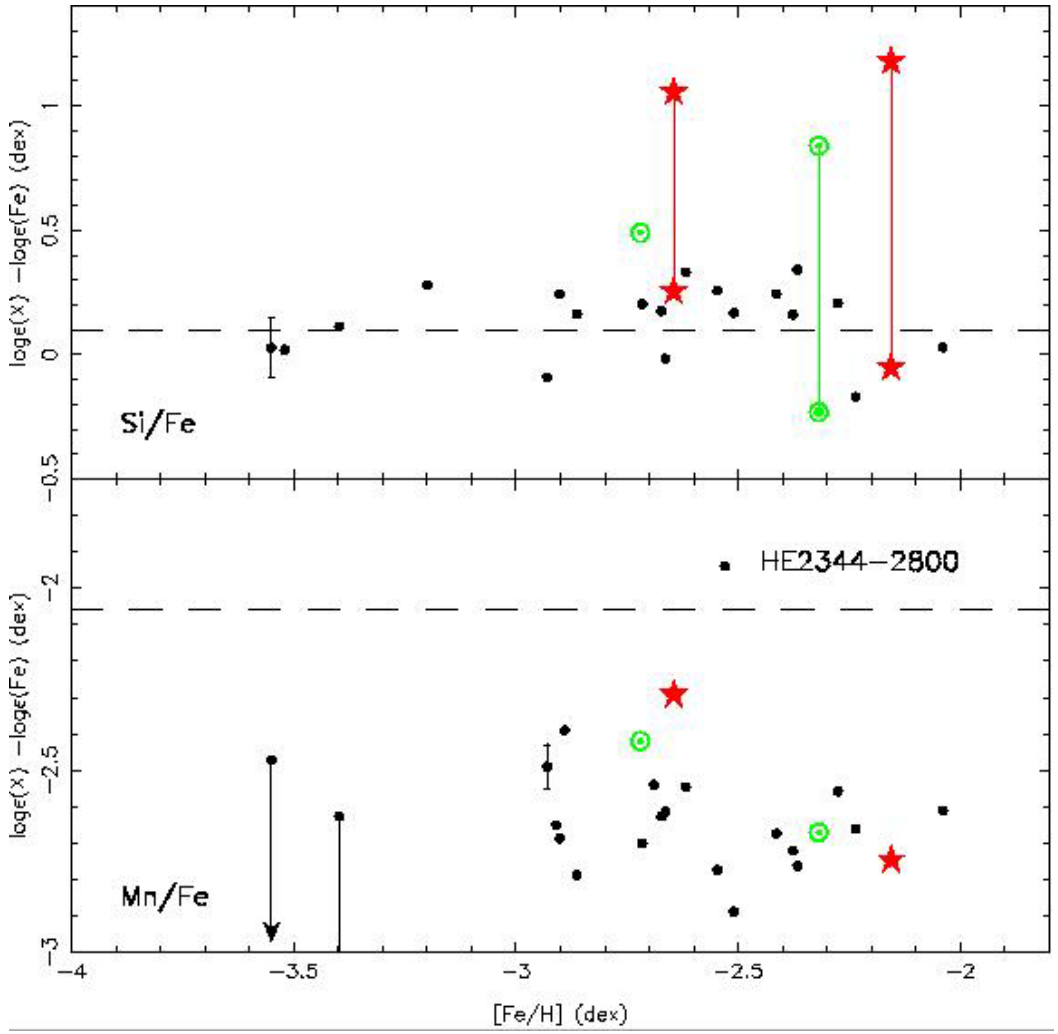

Sr,Ba/Fe as a function of [Fe/H] for 47 HES dwarfs and giants. Note the tremendous Y range.

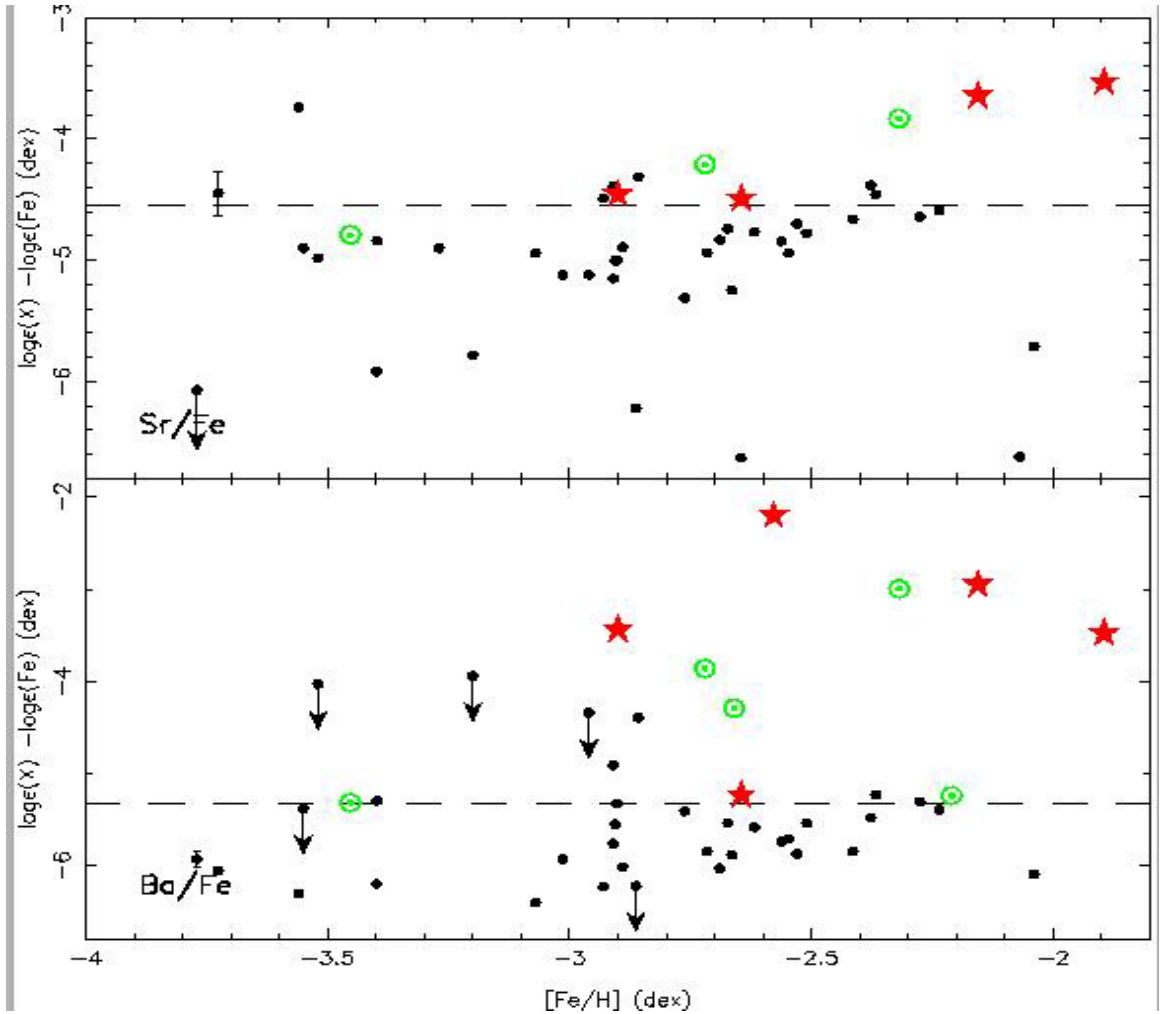

Mean abundance ratios and their dispersions for 28 candidate EMP dwarfs (from Cohen et al 2004)

Table 8. Mean Abundance Ratios [X/Fe] and Their Dispersions for the 28 Candidate EMP Dwarfs

Species	All Stars			No C-enh. Stars			Special Cases		
	<[X/Fe]> (dex)	σ (dex)	Num. Stars	<[X/Fe]> (dex)	σ (dex)	Num. Stars	<[X/Fe]> (dex)	σ (dex)	Num. Stars
Mg/Fe	+0.42	0.22	28	+0.39	0.21	24	+0.56[b]	0.12	20
Mg/Fe[h]	+0.56	0.18	19	+0.52	0.21	19	+0.56[i]	0.15	16
Al/Fe[a]	−0.10	0.19	28	−0.09	0.16	24	...	...	...
Si/Fe	+0.14	0.17	23	+0.04	0.14	19	...	...	...
Ca/Fe	+0.33	0.13	28	+0.31	0.12	24	...	...	...
Sc/Fe[c]	+0.28	0.21	26	+0.24	0.16	23	...	...	...
Ti/Fe[c]	+0.36	0.12	28	+0.36	0.12	24	...	...	...
Cr/Fe	−0.23	0.13	27	−0.21	0.13	24	−0.23[d]	0.09	23
Mn/Fe	−0.54	0.20	23	−0.55	0.20	19	−0.59[d]	0.13	18
Co/Fe	+0.43	0.14	16	+0.42	0.12	13	...	...	...
Ni/Fe	−0.03	0.13	18	−0.02	0.12	15	...	...	...
Zn/Fe	0.52	0.01	2	+0.52	...	1	...	...	...
Sr/Fe[c]	−0.24	0.53	28	−0.37	0.45	24	−0.19[e]	0.25	21
Y/Fe[c]	+0.68	0.24	3	+0.40	...	1	...	...	...
Ba/Fe[c]	+0.01	0.89	23	−0.32	0.35	19	−0.20[f]	0.28	16
La/Fe[c]	+2.02	0.22	3[g]	...	...	...	...	...	...
Eu/Fe[c]	+1.83	0.17	2[g]	...	...	...	...	...	...
Pb/Fe	+3.32	0.17	3[g]	...	...	...	...	...	...

[a]A constant non-LTE correction is assumed for Al.

[b]The four stars with Solar Mg/Fe have been excluded.

[c]Fe II is used in determining the abundance ratio instead of Fe I.

[d]HE2344−2800 is excluded.

[e]Three stars (LP-831−070, G138−9 and HE0242−0732) with very low Sr/Fe omitted.

[f]Three stars (LP-831−070, G138−9 and HE0130−2303) with very low Ba/Fe omitted. HE0242−0732 has no detected Ba lines.

[g]Only detected in some of the C-enhanced stars.

[h]The stars for which only the Mg triplet was detected are excluded.

[i]The outlier G139−8 is also excluded.

Roads to Peculiar Abundances

- **These stars are very metal poor. A very small amount of additional material of a relatively rare element can produce a big change in its abundance, assuming the material does not diffuse into the interior.**

- **Mass transfer in a binary system where the primary is more massive, in the AGB phase, and transferring material onto the low mass secondary. Today the primary is a WD, and the secondary, which we see, has a surface contaminated with enhanced C and s-process elements.**

Sr,Pb(lead)/Fe versus metallicity for 47 dwarfs and giants from the HES. Note the large Y range.

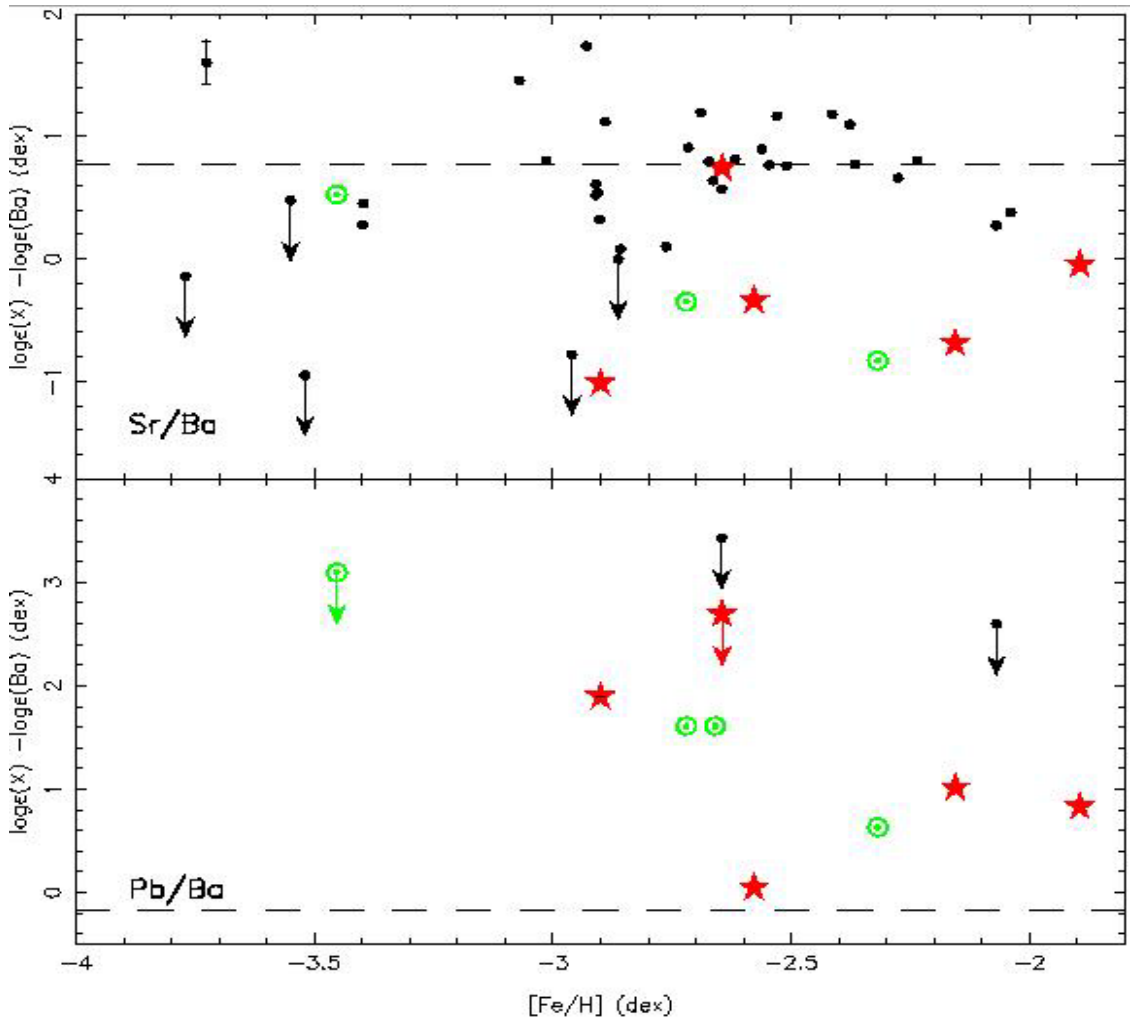

Ba/Fe is enhanced in the C-enh stars, and Solar or lower in the rest of the stars.
Ba/Eu is that of the r-process for the two stars with the lowest Ba, lies near the s-process for two more, and in between for 3 stars.

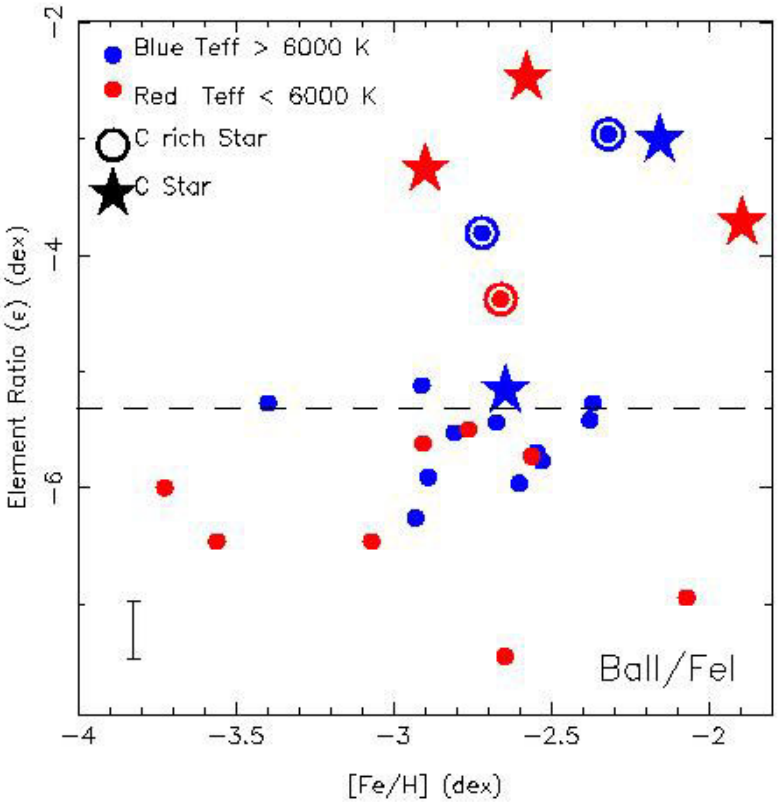

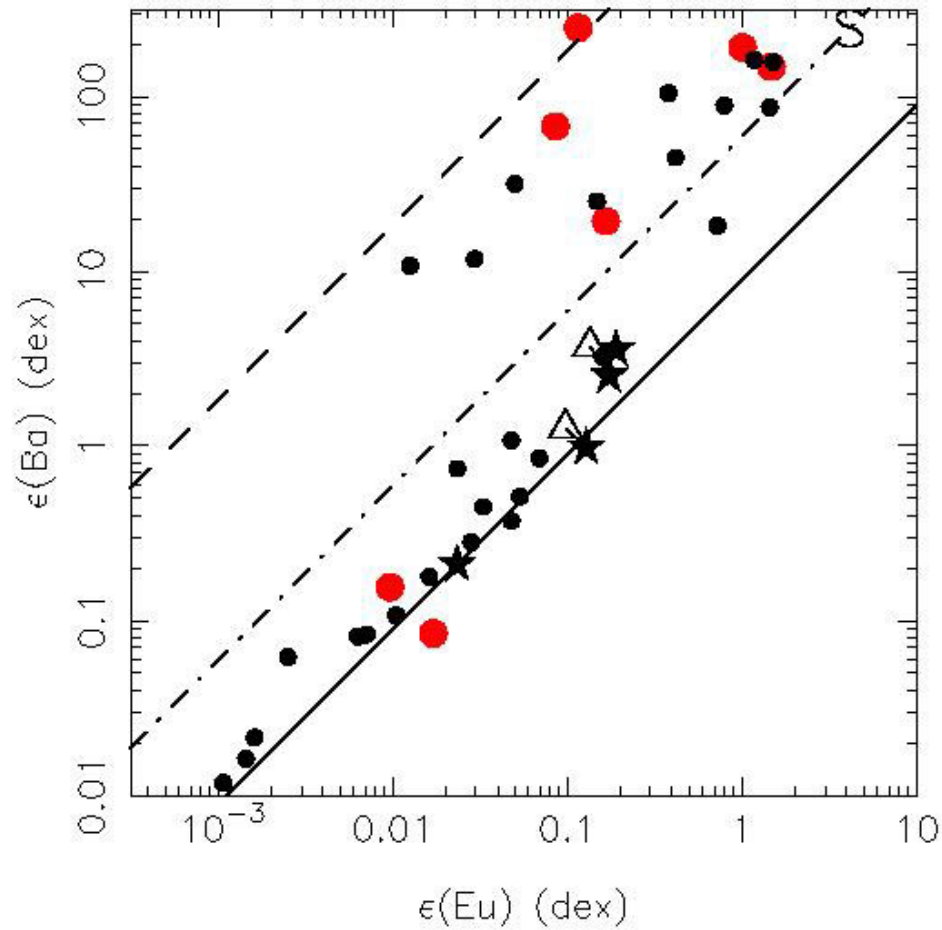

The Newly Discovered Extreme r-process star from the HES

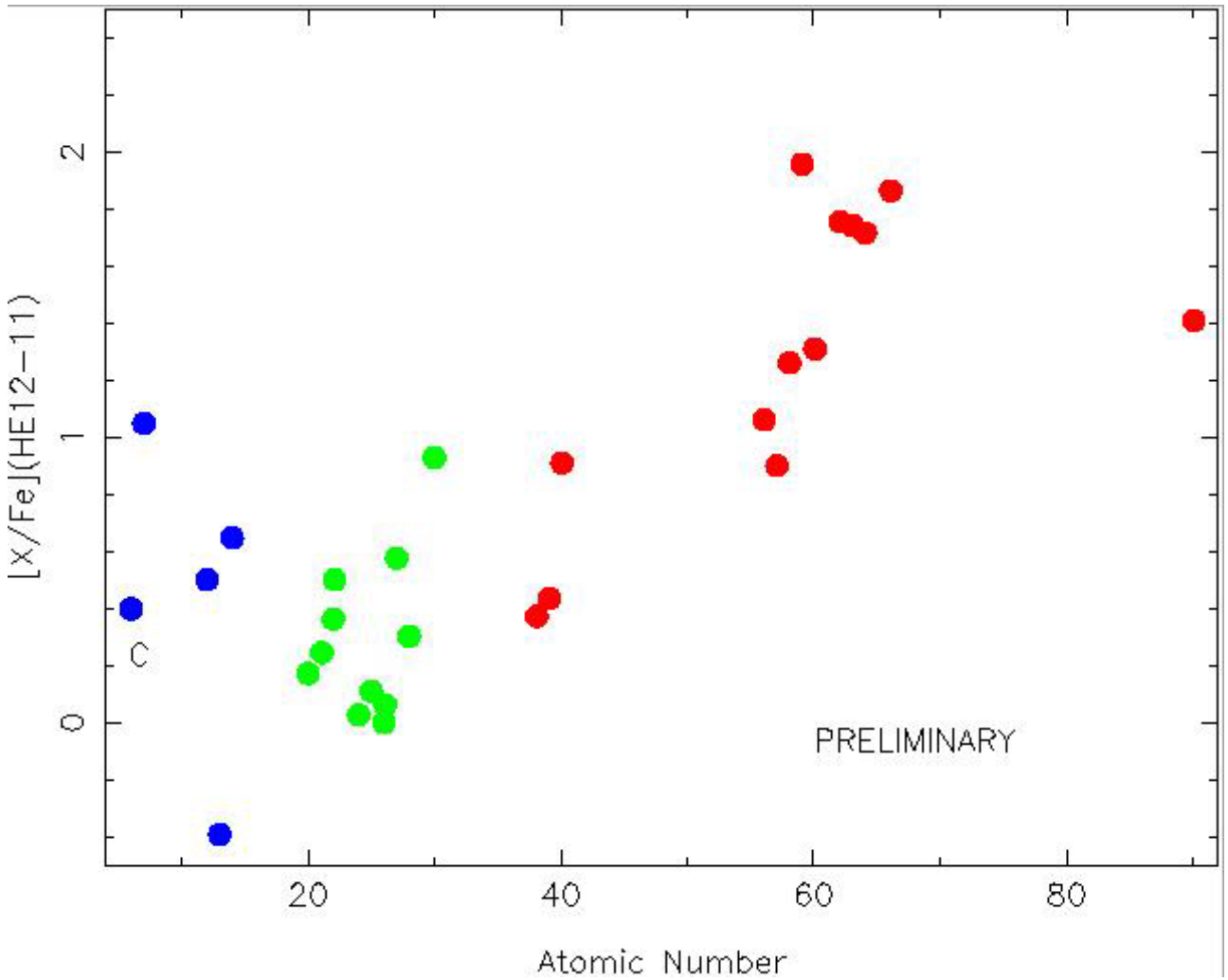

Comparison of the newly discovered extreme r-process star with CS 2289-052, the canonical extreme r star.

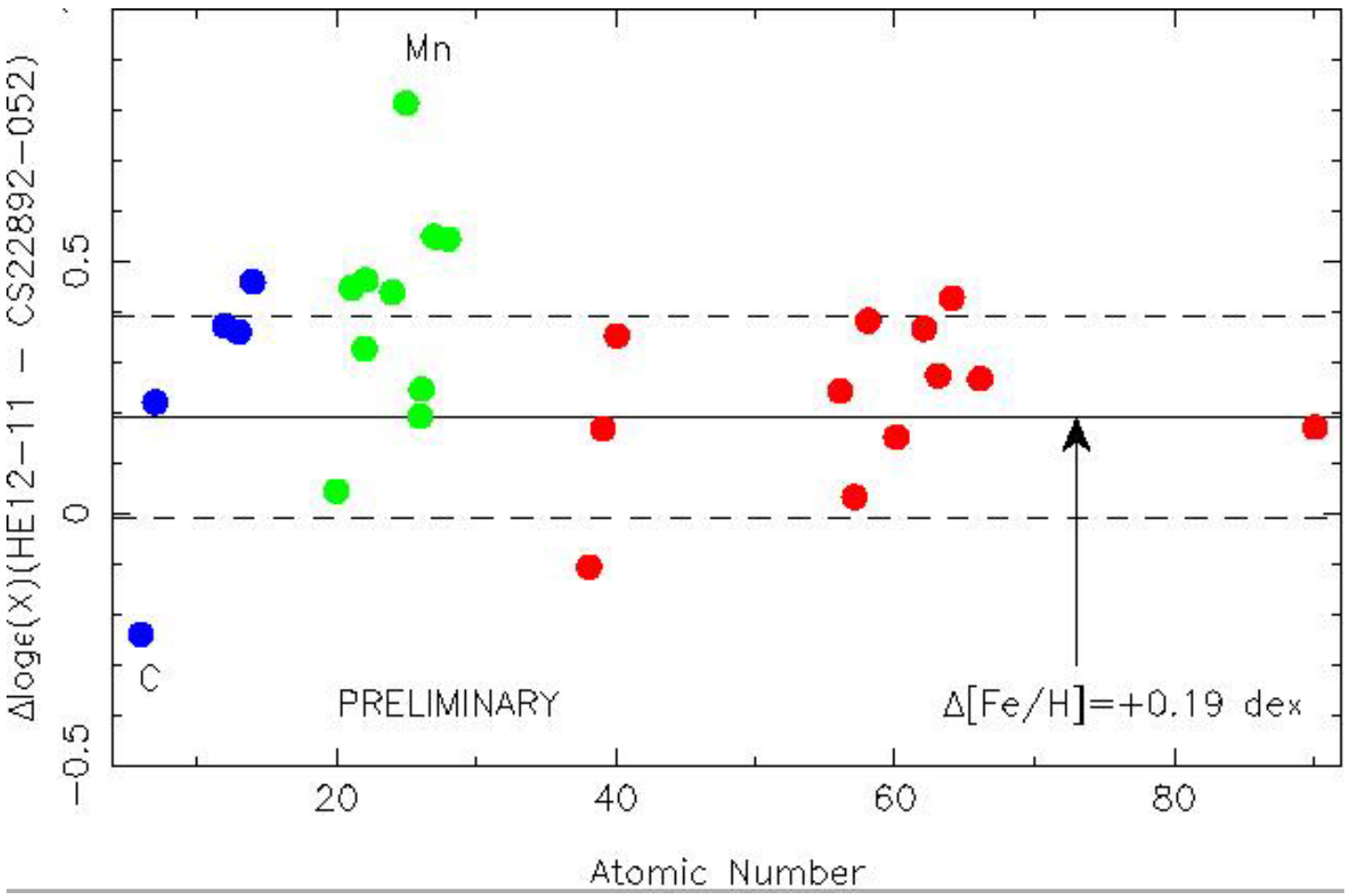

Deviations from the mean for Ca/Fe versus Ti/Fe. Circular distribution suggests random errors. From Cohen et al (2004)

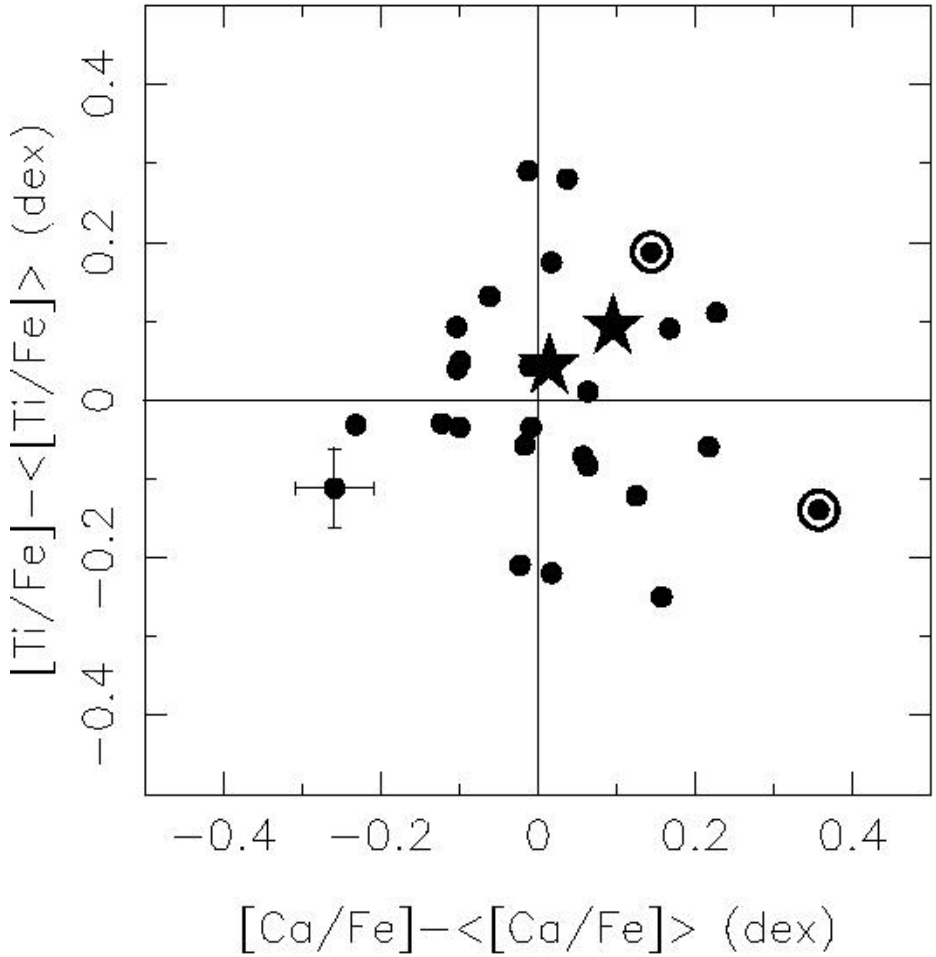

Deviations from the mean for Cr/Fe versus those for Ti/Fe. Circular distribution suggests random errors. (Cohen et al 2004)

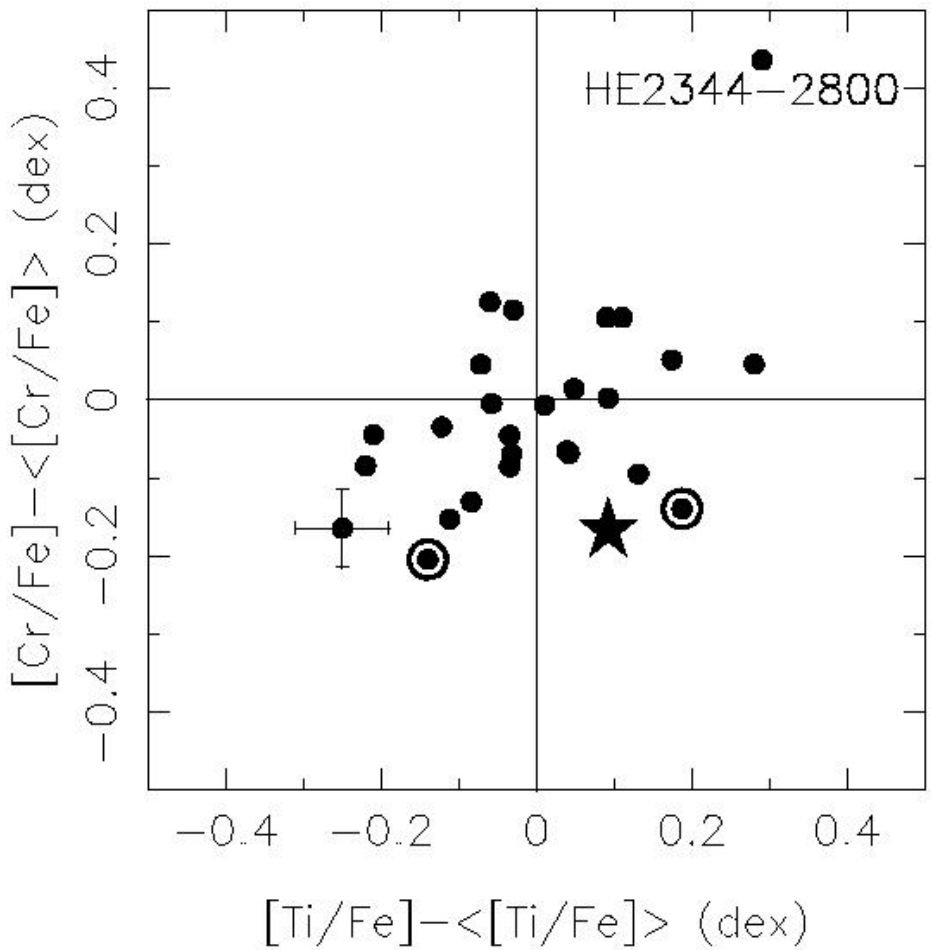

Deviations from the mean for Mg/Fe vs those of Ca/Fe. Apparent variation in Mg/Fe is probably due to systematic effects.

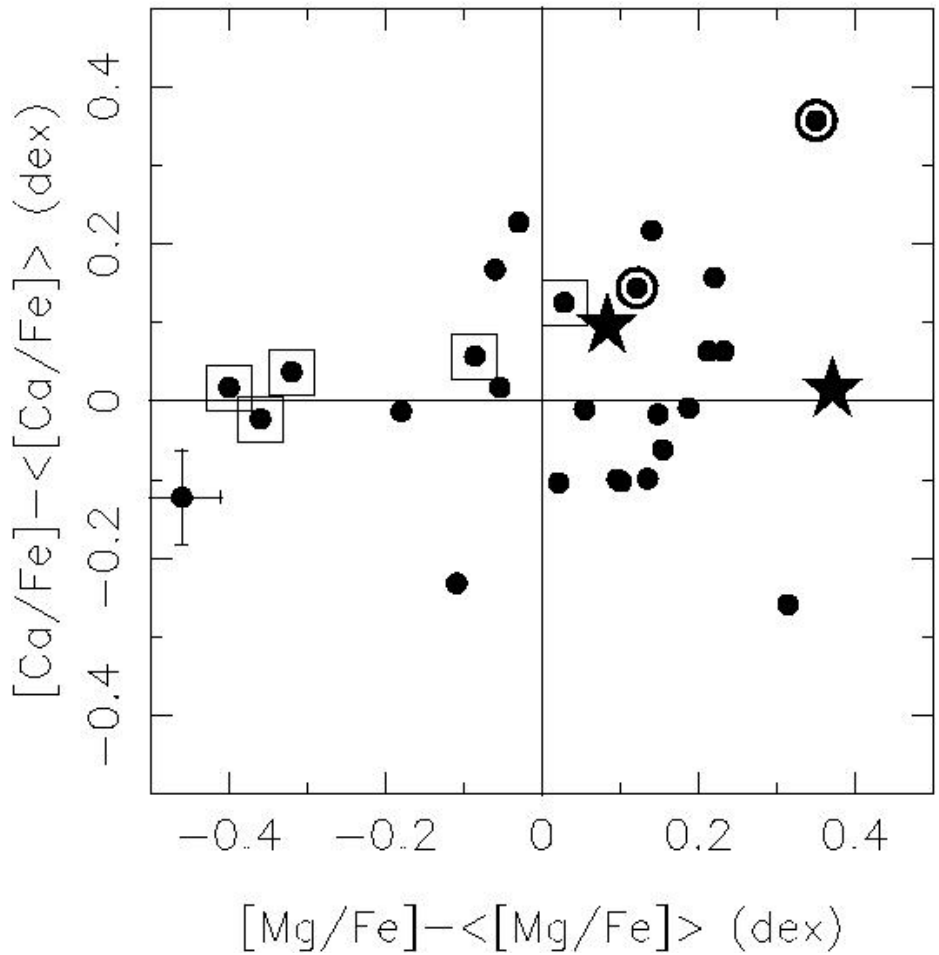

Comparison of independent analyses of dwarfs (0Z project/Keck) and giants (First Stars/Cayrel/VLT)

Table 10. Comparison of Mean Abundance Ratios and Dispersions With Those of Cayrel *et al.* (2003)

Species	Mean [X/H] EMP Dwarfs[b] (dex)	Mean [X/H][a] Cayrel Giants[c] (dex)	Δ^a (Dwarfs-Giants) (dex)	σ EMP Dwarfs (dex)	σ Cayrel Giants (dex)
Mg/Fe	+0.39	+0.28	+0.11	0.13[d]	0.13
Al/Fe	−0.09	−0.08[e]	−0.01	0.16	0.18
Si/Fe	+0.04	+0.45	−0.41	0.14	0.15
Ca/Fe	+0.31	+0.34	−0.03	0.12	0.10
Sc/Fe	+0.24	+0.08	+0.16	0.16	0.11
Ti/Fe	+0.36	+0.23	+0.13	0.12	0.09
Cr/Fe	−0.21	−0.35	+0.14	0.09[f]	0.05
Mn/Fe	−0.55	−0.44	−0.11	0.13[f]	0.12
Co/Fe	+0.42	+0.27	+0.15	0.12	0.13
Ni/Fe	−0.02	−0.04	+0.02	0.12	0.11

[a]Cayrel *et al.* (2003) adopt $\log\epsilon(\mathrm{Fe}) = 7.50$ dex, 0.05 dex higher than we do. No correction for this difference has been applied.

[b]The C-rich stars in our sample are excluded.

[c]Calculated from the fits given in Cayrel *et al.* (2003) at [Fe/H] = −3.0 dex.

[d]We use the value from Table 6 ignoring the C-rich stars and the four stars with Solar Mg/Fe.

[e]We adjust the value from Cayrel *et al.* (2003) to the slightly smaller non-LTE correction for Al I adopted here.

[f]We ignore the discrepant star HE2344−2800 as well as the C-rich stars.

Ti/Fe as a function of metallicity ([Fe/H]) for halo field stars and for Galactic globular clusters – for Ti, the chemical history appears identical, for [Fe/H] > -2.5 dex

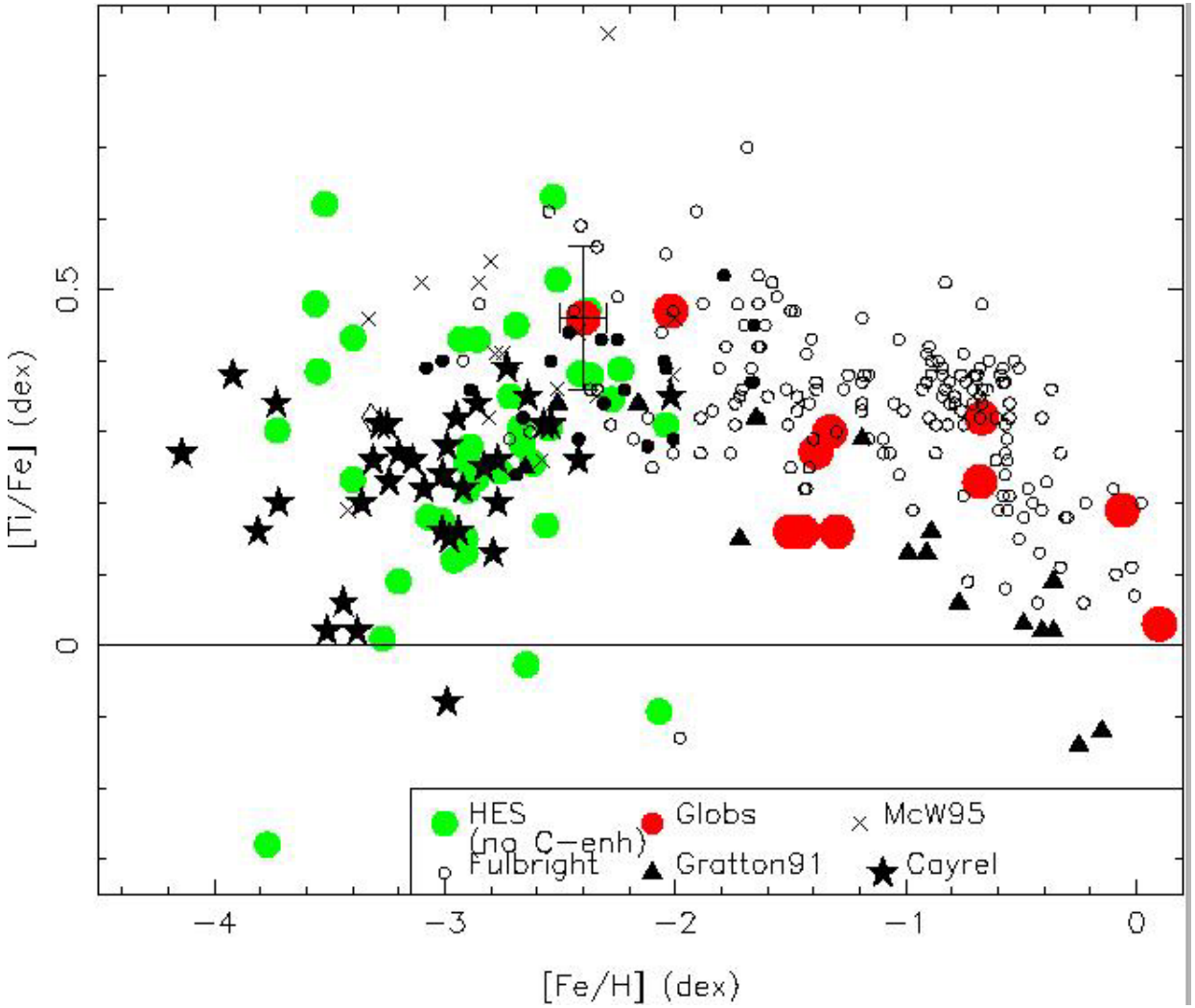

Ni/Fe as a function of metallicity ([Fe/H]) for halo field stars and for Galactic globular clusters, for Ni the chemical history appears identical for [Fe/H] > -2.5 dex.

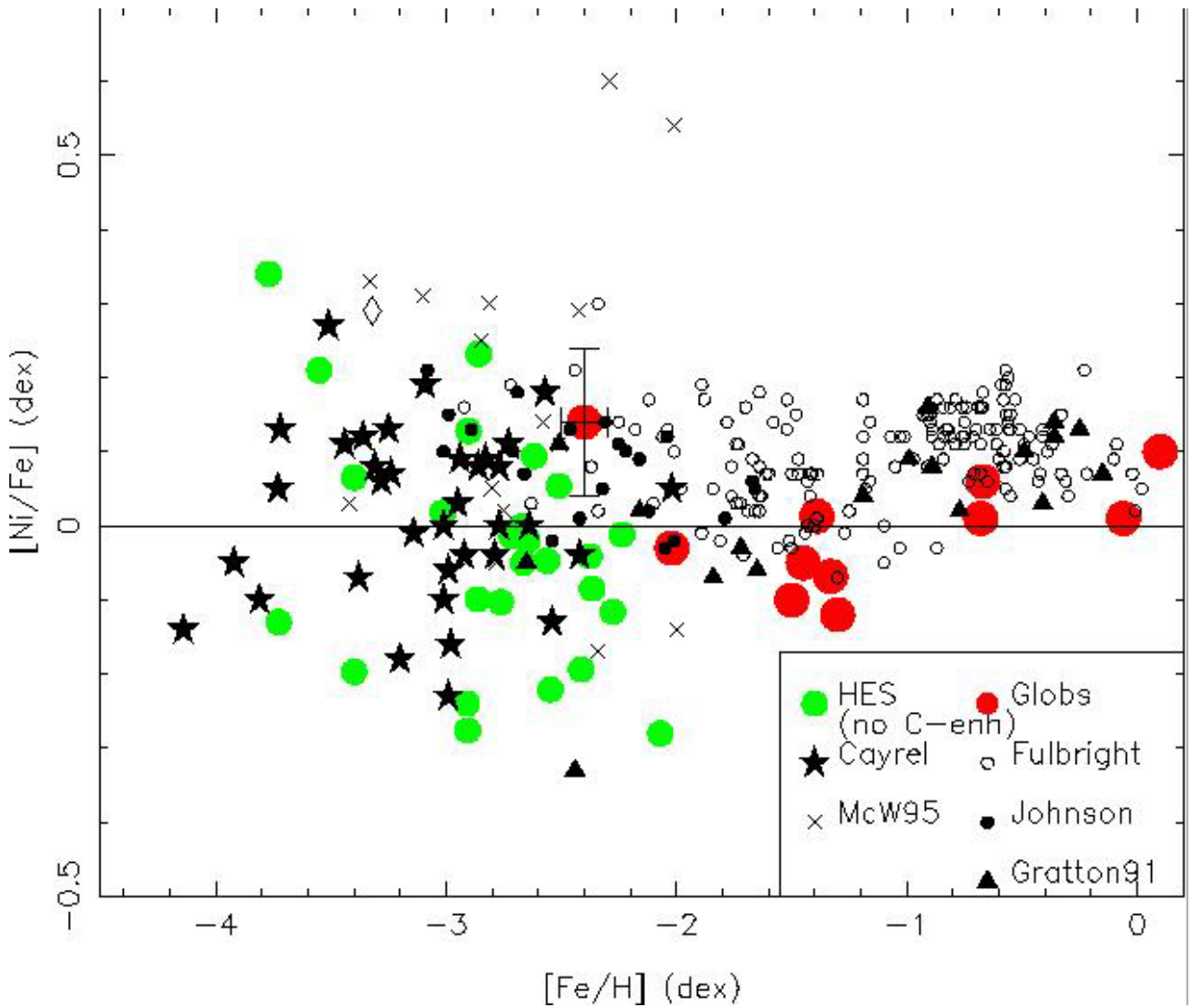

Ba/Fe as a function of metallicity ([Fe/H]) for halo stars and for Galactic globular clusters. For Ba, the chemical history appears identical for [Fe/H] > -2.5 dex.

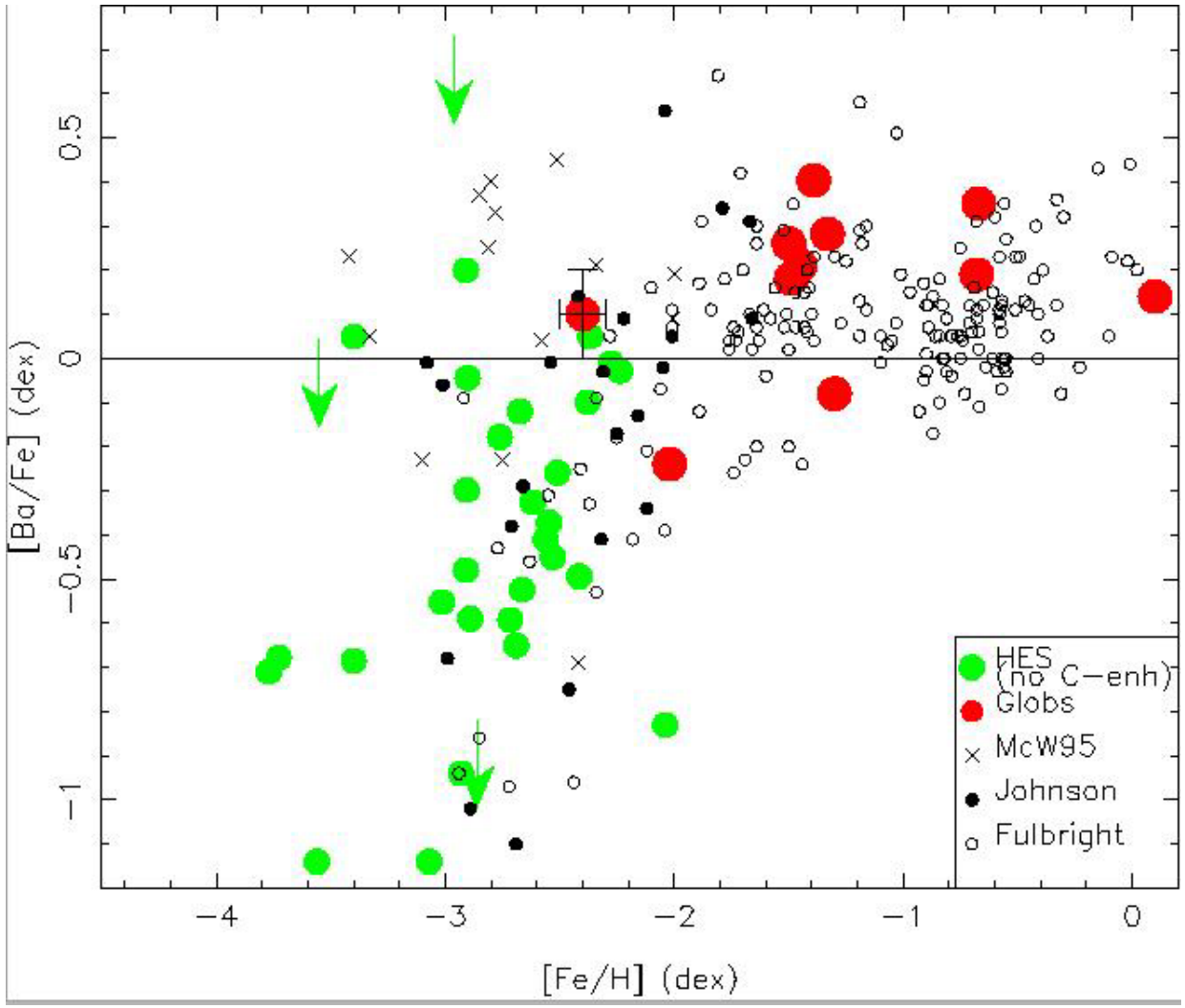

Ca/Fe versus metallicity ([Fe/H]) for halo field stars and Galactic globular clusters. There may be a slight difference in the chemical history.

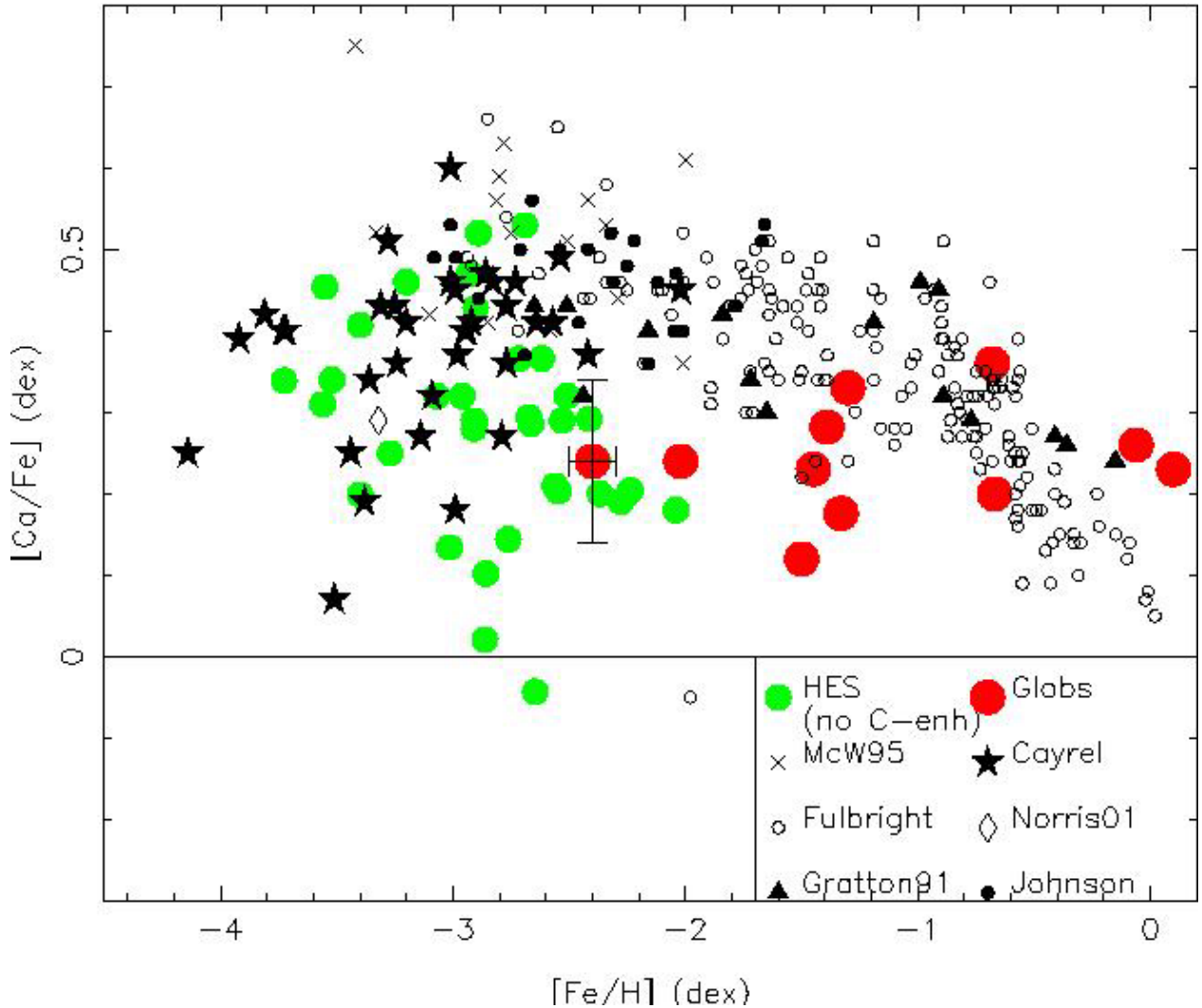

Mg/Fe versus metallicity ([Fe/H]) for halo field stars and for galactic globular clusters. There may be a slight difference in chemical history.

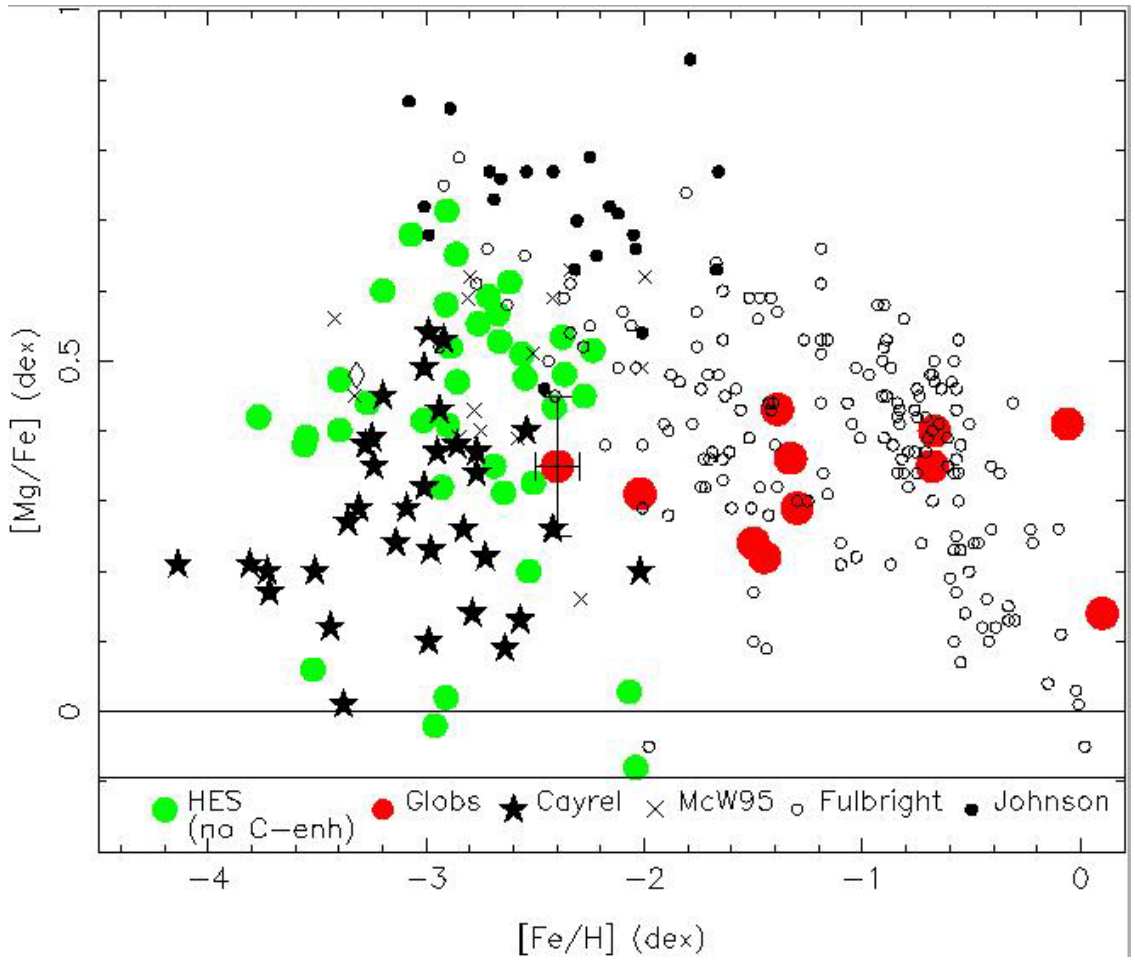

Test for binaries in the HES via cross-correlations, from Cohen et al (2004)

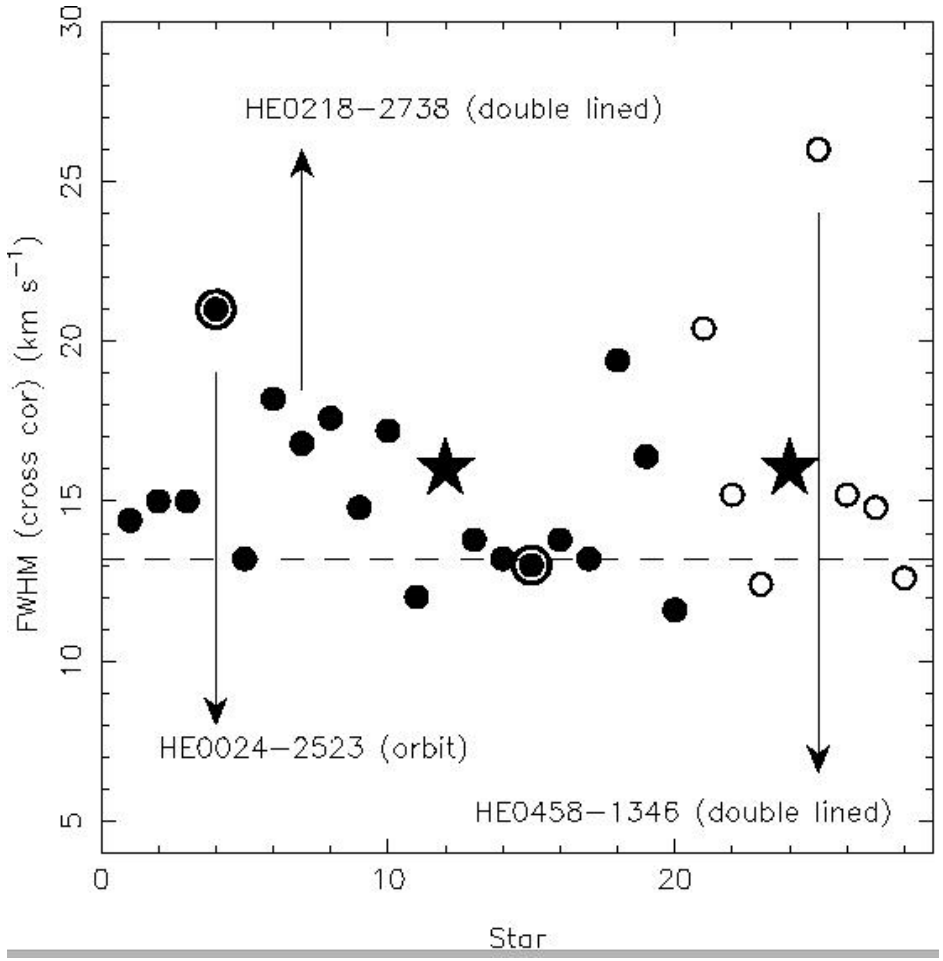

Comparison with the phenomenological model for yields of SNII of Qian and Wasserburg (Cohen et al 2004)

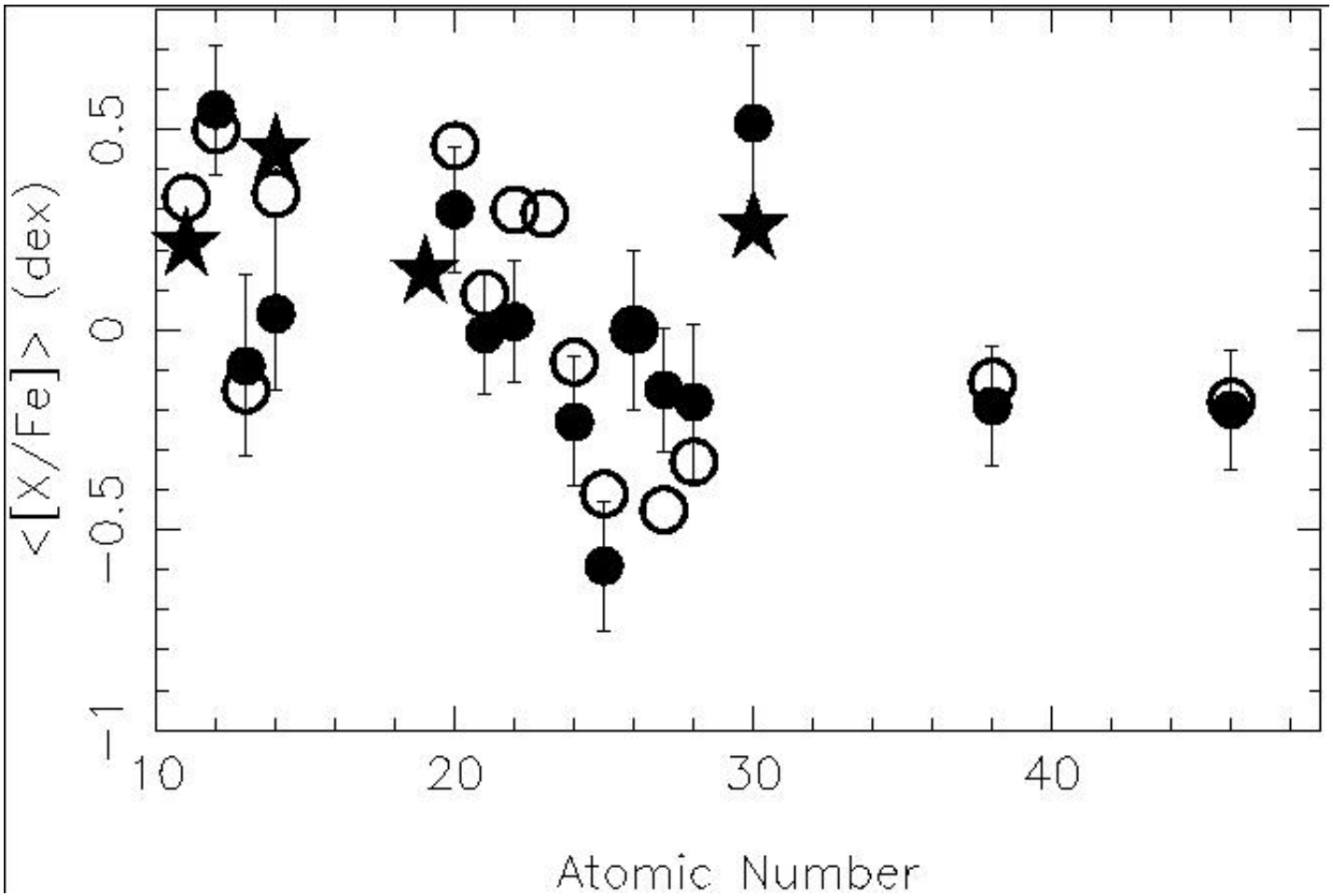

Comparison of our results with the SNII yields of Umeda & Nomoto for a range of progenitor mass and explosion energy, from Cohen et al (2004). Note odd-even problems.

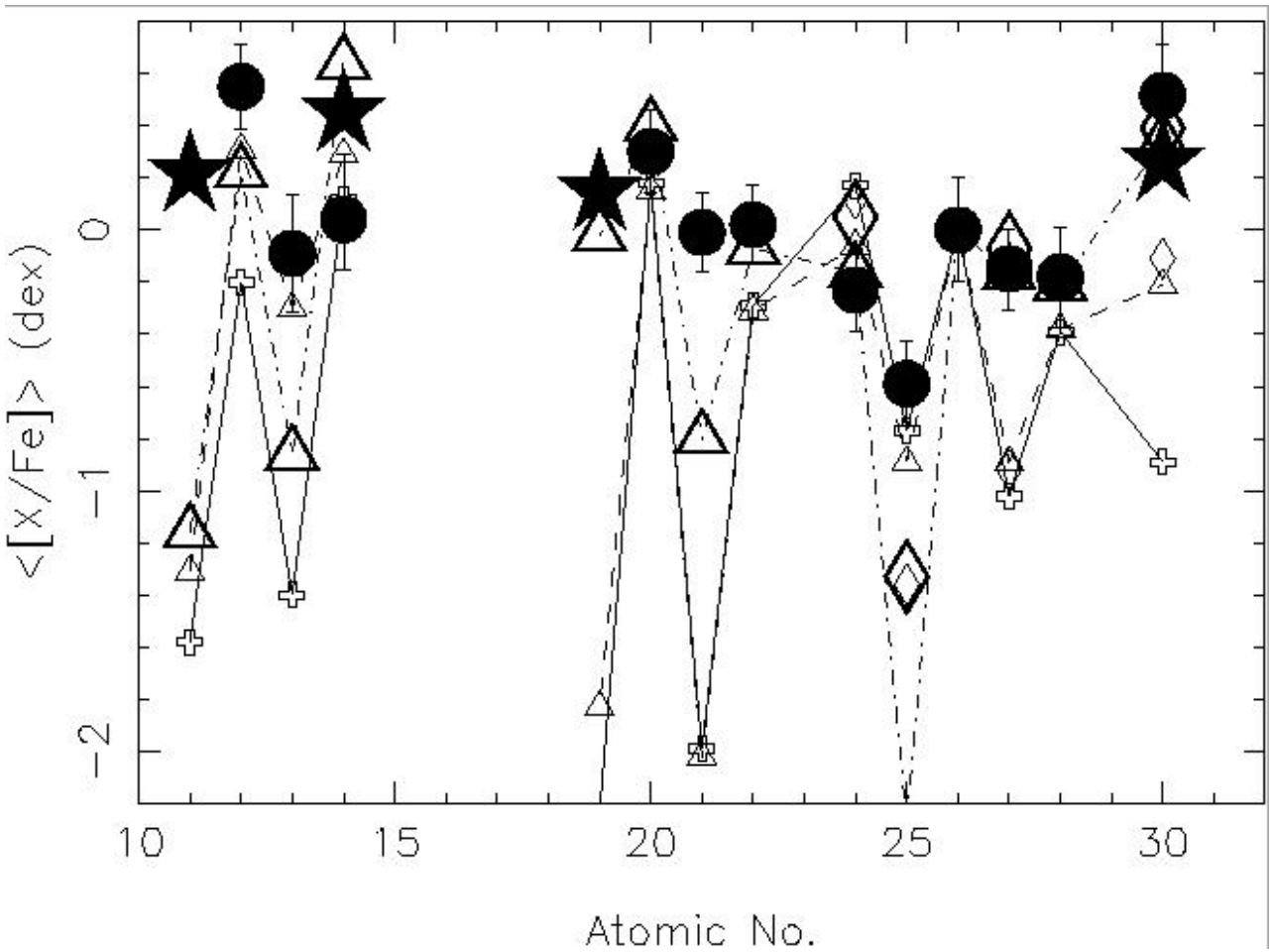

C-enhanced stars

- **Most, but not all, C-enhanced stars also show large enhancements of Ba, the rare earths, and lead.**

- **The rare earths in these stars appear to be predominantly of s-process origin.**

- **These stars show smaller enhancements of Sr and Y than of Ba or the rare earths.**

- **At least one highly C-enhanced star shows a "normal" pattern for the heavy elements, no enhancement of Ba nor of the rare earths and no detected lead.**

- **A second star, almost identical to HE2148-1247, with a large C enh, v. large Ba and rare earths enh, and Ba/Eu intermediate between the pure r- and s-ratios, has been found.**

r-process Enhanced Stars

- A highly r-process enhanced star has been found. Frequency is about 1 in 30 very metal poor giants observed at high resolution and SNR.

A second, less highly enhanced star has also been found.

- r-process stars can have normal or enhanced C.

Conclusions

The σ[X/Fe] < 0.15 dex for all elements between Mg and Ni when C-enh stars excluded. These are VERY SMALL, and are probably still dominated by systematic errors, not by real star-to-star variations in abundance ratios.

The X/Fe ratios hit a plateau below -2 for field halo stars. The X/Fe found in EMP stars are identical to those found in globular clusters ranging up to [Fe/H] = -0.7.

A SINGLE NUCLEOSYNTHESIS CHANNEL, PRESUMABLY SNII, PRODUCED ALL THE CHEMICAL INVENTORY THROUGH THE FE-PEAK SEEN IN OLD HALO STARS.

Explanation: many SNII contributing, or somehow narrowing the range of progenitor mass and explosion characteristics to maintain uniformity ?

There are definite trends with [Fe/H] for Mn/Fe and Co/Fe, which are rare nuclei compared to Fe. The relative yields for these nuclei depend on the metallicity.

The range of Sr/Fe and Ba/Fe is much larger than for the lighter elements, but is reduced by eliminating C=enh. stars, i.e. s-process material.

We suggest that C-enhancement is a sign of binarity. Is the fraction of binaries as high as we suspect ? Can we confirm more binaries in an efficient manner ?

What will the spectra of the giants, which are much richer than the dwarfs for a given metallicity as they are hotter, show ?

Publications by the 0Z Project

Publications from the 0Z Project

Stellar Archeology: a Keck Pilot Program on Extremely Metal Poor Stars from the HES. I. Stellar Parameters, Cohen, J. G., Christlieb, N., Beers, T. C., Gratton, R. G., Carretta, E., 2002, AJ, 124, 470

Stellar Archeology: a Keck Pilot Program on Extremely Metal Poor Stars from the HES. II. Abundance Analysis, Carretta, E., Gratton, R. G., Cohen, J. G., Beers, T. C., Christlieb, N., 2002, AJ, 124, 481

Stellar Archeology: a Keck Pilot Program on Extremely Metal Poor Stars from the HES. III. The Lead Star HE0024–2523, Lucatello, S., Gratton, R., Cohen, J. G., Beers, T. C., Christlieb, N., Carretta, E. & Ramírez, S., 2003, AJ, 125, 875

Abudance Analysis of HE 2148–1247, a Star with Extremely Enhanced Neutron Capture Elements (This is a star which apparently has both an r and a s process enhancement.) Cohen, J. G., Christlieb, N., Qian, Y. Z. & Wasserburg, J. G., 2003, ApJ, 588, 1082

Abundances In Very Metal Poor Dwarf Stars, Judith G. Cohen, Norbert Christlieb, Andrew McWilliam, Steve Shectman, Ian Thompson, G.J. Wasserburg, Inese Ivans, Matthias Dehn, Torgny Karlsson & J.Melendez, 2004, ApJ, in press,

PROBING THE NUCLEOSYNTHESIS PRODUCTS OF THE FIRST STARS

J. J. COWAN
University of Oklahoma

Chemical Enrichment of the Early Universe

Abundance Clues and Constraints

- New observations of n-capture elements in low-metallicity Galactic halo stars providing clues and constraints on:
  1. Synthesis mechanisms for heavy elements early in the history of the Galaxy
  2. Identities of earliest stellar generations, the progenitors of the halo stars
  3. Suggestions on sites, particularly site or sites for the r-process
  4. Galactic chemical evolution

Most Likely Site(s) for the r-Process

- Supernovae: The Prime Suspects
  - → Regions just outside neutronized core: (Woosley et al. 1994; Wanajo et al. 2002)
  - → Prompt explosions of low-mass Type II SNe (Wheeler, JC, Hillebrandt 1998)
  - → Jets and bubbles (Cameron 2001)
- NS & NS-BH mergers (Rosswog et al. 1999; Freiburghaus et al. 1999)

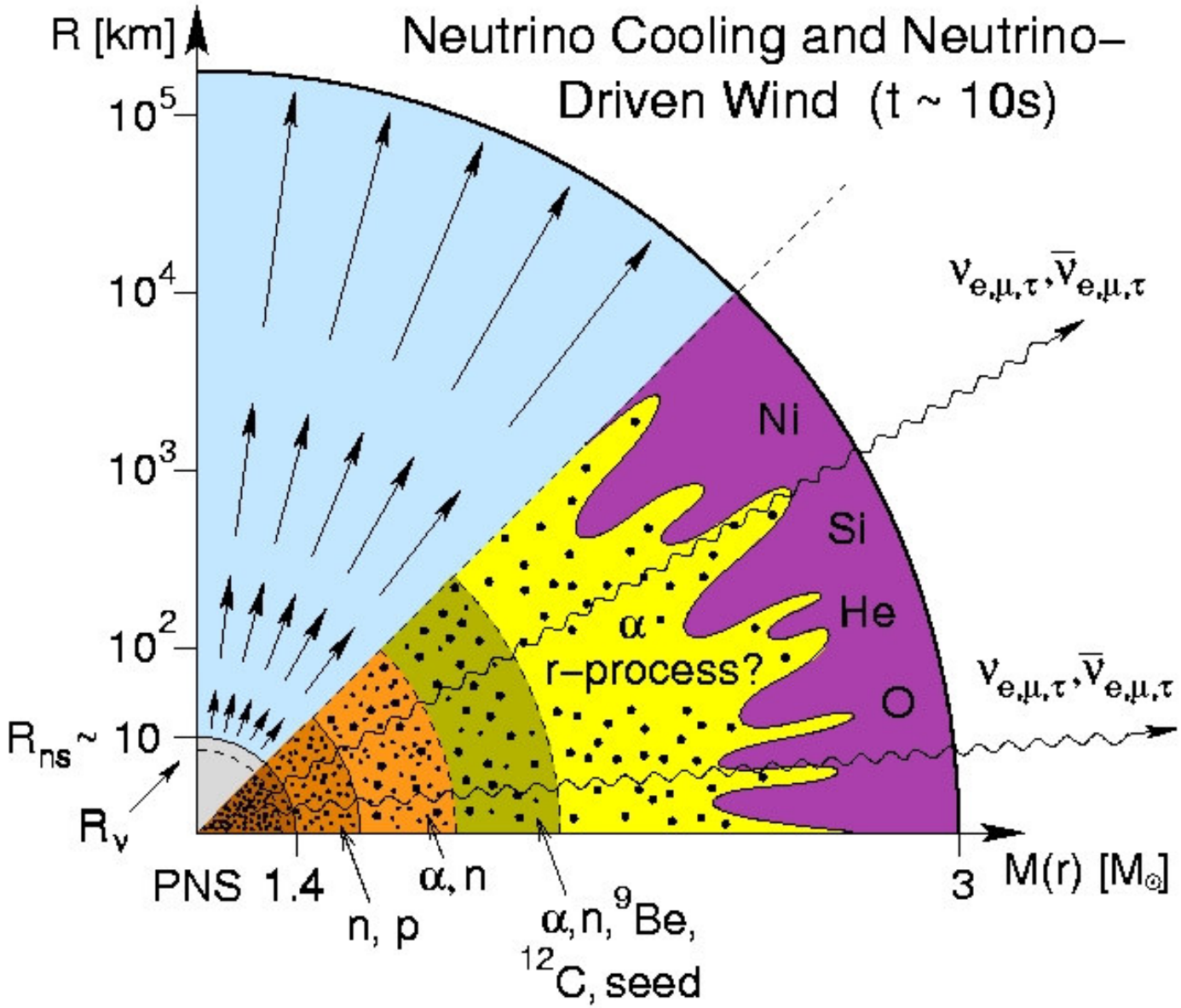
Neutrino Cooling and Neutrino–
Driven Wind (t ~ 10s)
R [km]
10^5
10^4
10^3
10^2
R_{ns} ~ 10
R_ν
PNS 1.4
n, p
α, n
α, n, ^{9}Be,
^{12}C, seed
3
M(r) [$M_\odot$]
$\nu_{e,\mu,\tau}, \bar{\nu}_{e,\mu,\tau}$
$\nu_{e,\mu,\tau}, \bar{\nu}_{e,\mu,\tau}$
Ni
Si
He
O
α
r–process?

Solar System Abundances

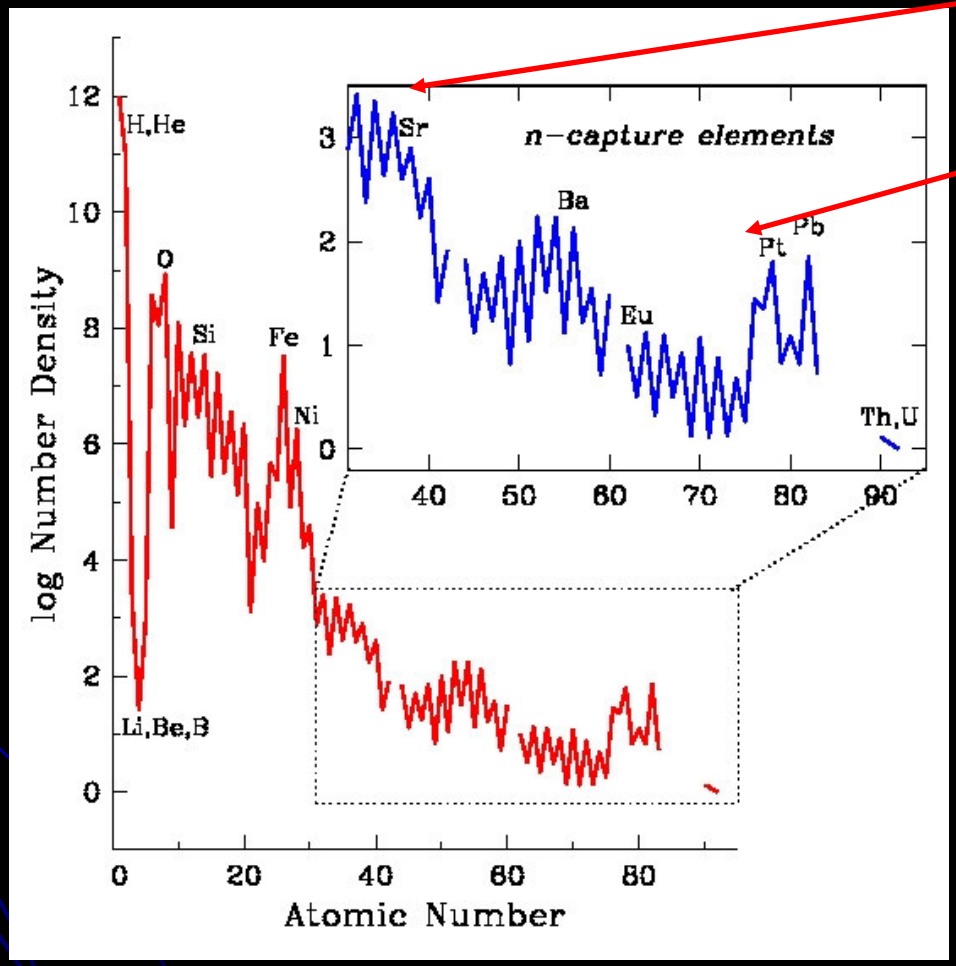

Ge, Zr

Os, Pt

Sneden & JC (2003)

Focus On Individual Elements: Nd

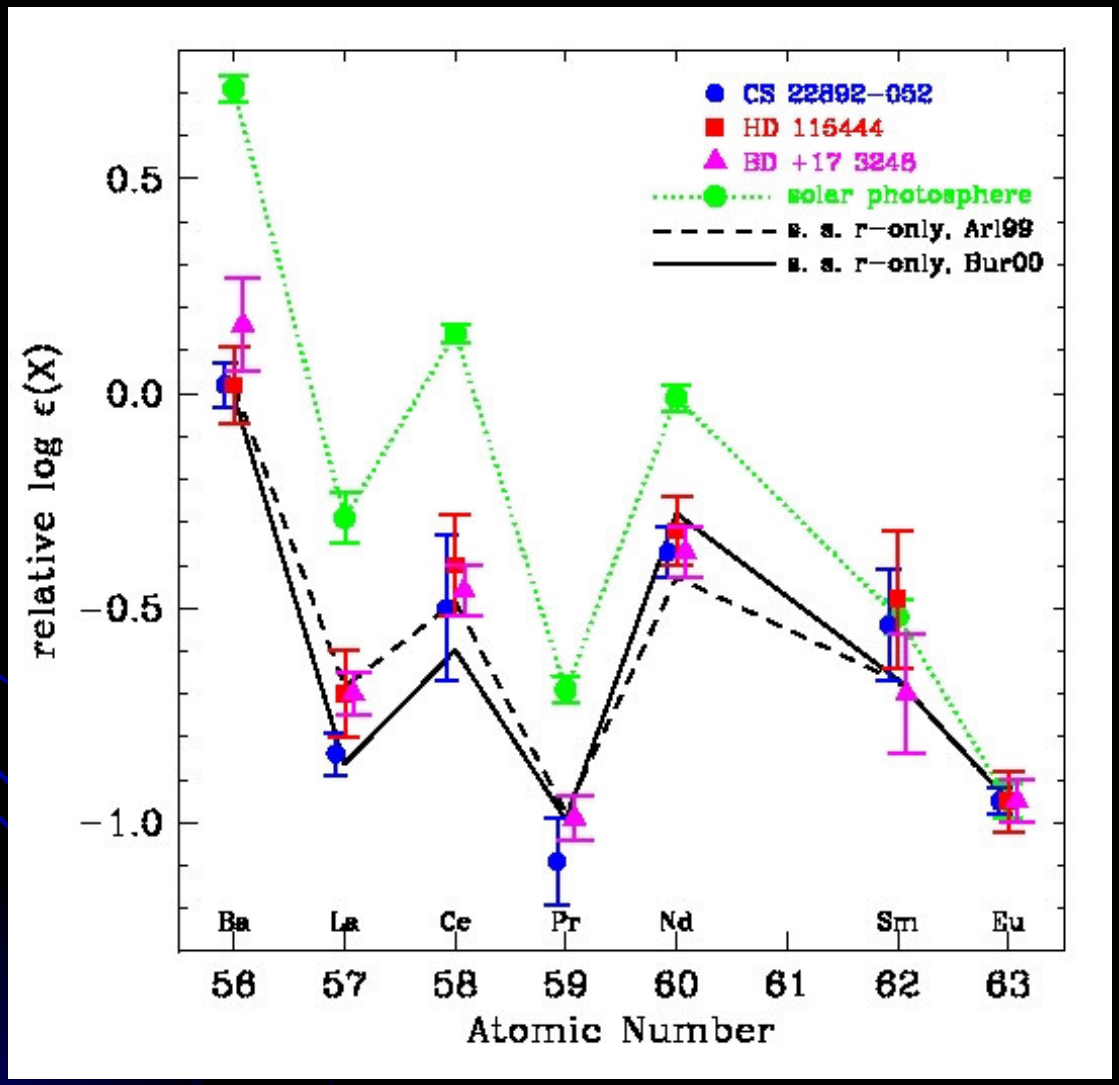

New experimental atomic physics data.
Den Hartog et al. (2003).

Focus On Individual Elements: Ho

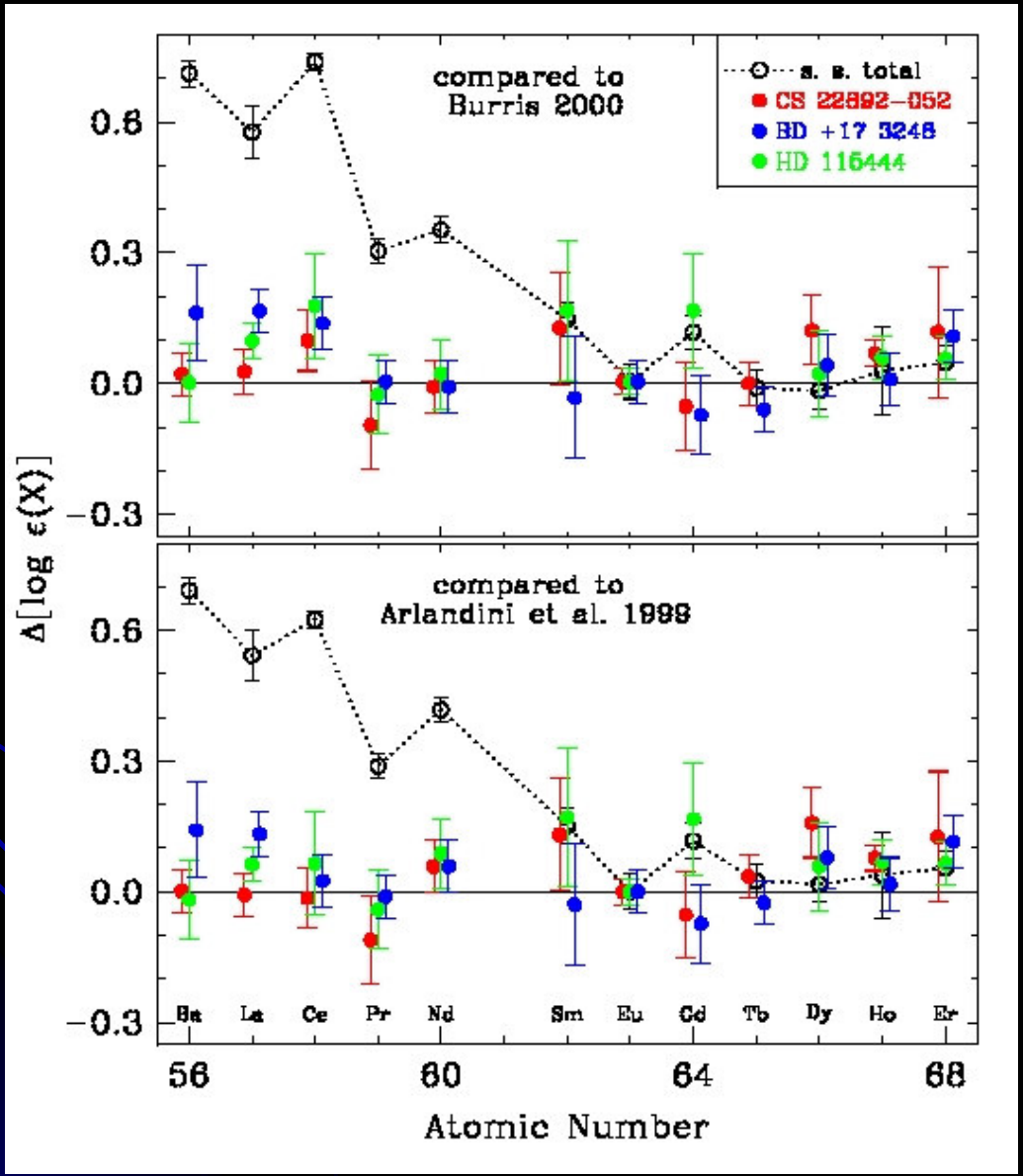

New experimental atomic physics data. Lawler et al. (2004).

Working our way through the Periodic Table!

CS 22892-052 Abundances

Cowan et al. (2004)

Germanium

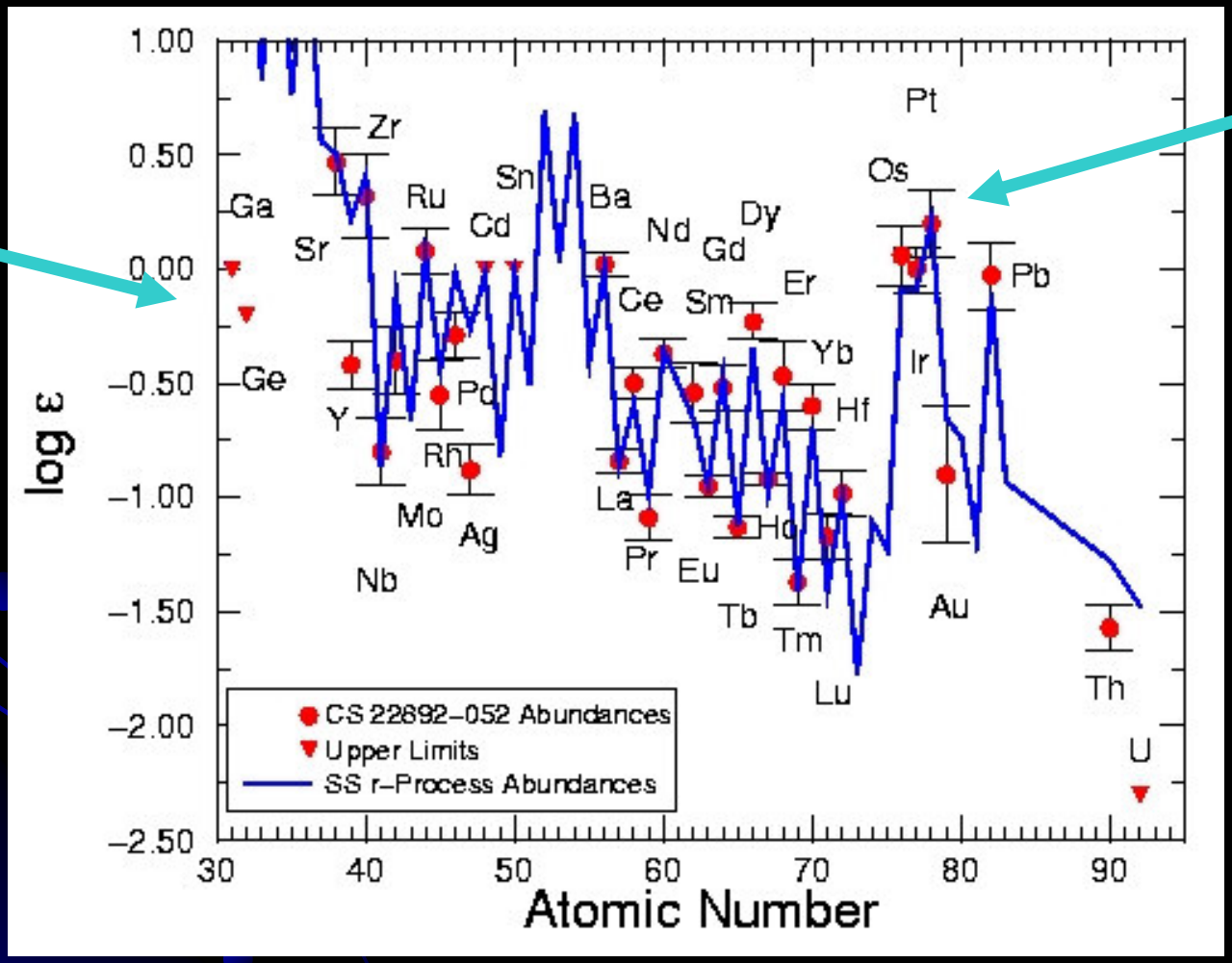

Platinum

57 elements observed. More than any star except the Sun.

$$\text{Log } \varepsilon(A) = \log_{10}(N_A/N_H) + 12$$

Halo Star Abundances

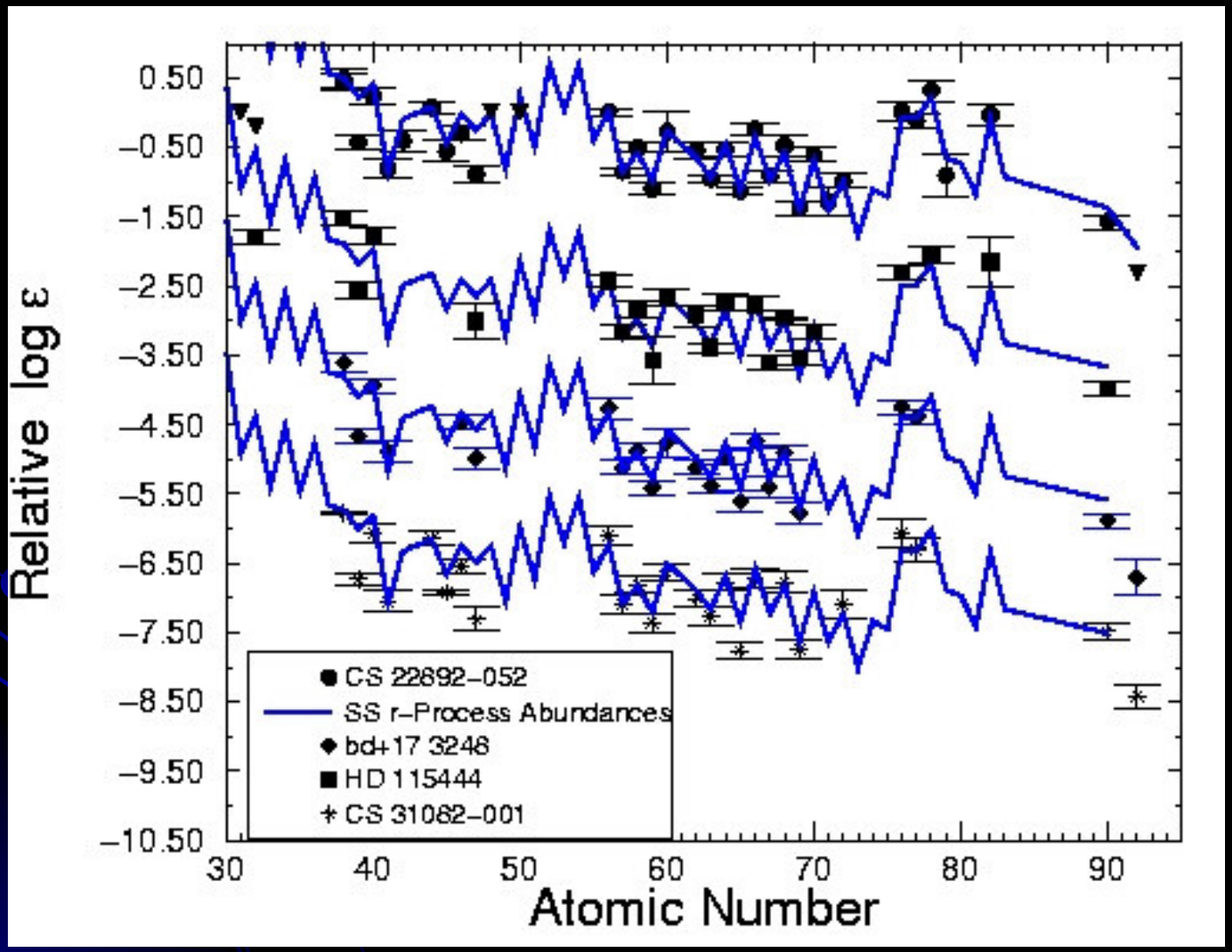

4 r-process rich stars

Light n-Capture Elements: Evidence for a Second r-process ?

- Only recently any detections of elements, Z = 40-50
  → Best evidence CS 22892-052
- Heavier element (Z ≥ 56) abundances seem to follow SS r-process curve, not so for the lighter elements
  → Same pattern appears in several other r-process rich stars
- Two separate sites (Wasserburg, Busso & Gallino): strong and weak r-process (2 types of SNe or SNe and NS mergers) or
- One site (different epochs or regions)

New HST Abundance Observations

- Dominant transitions for elements such as Ge, Os and Pt in NUV requires HST
- New abundance determinations of these elements (and Zr) in 11 metal-poor halo stars
- Attempt to identify abundance trends and correlations

NUV HST STIS Spectra

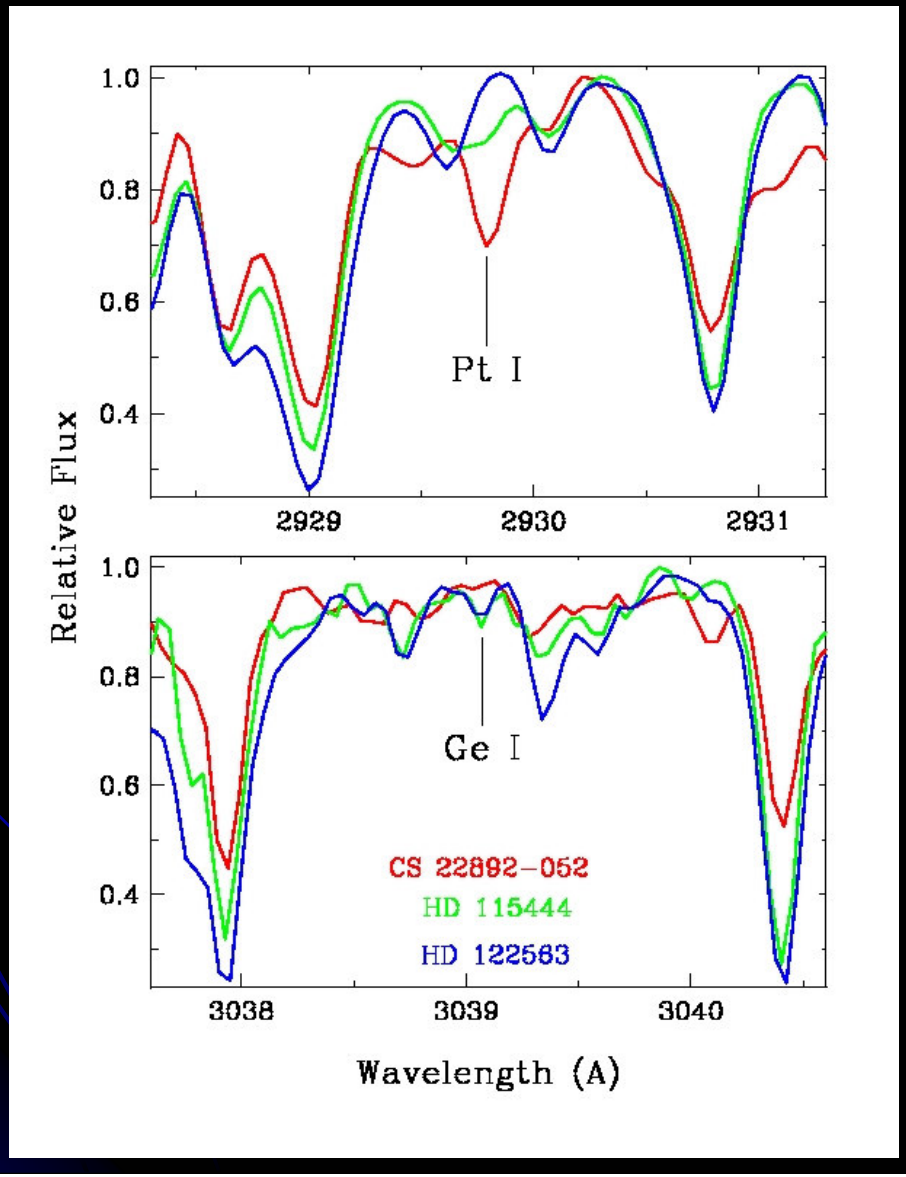

Ge Abundances in Halo Stars

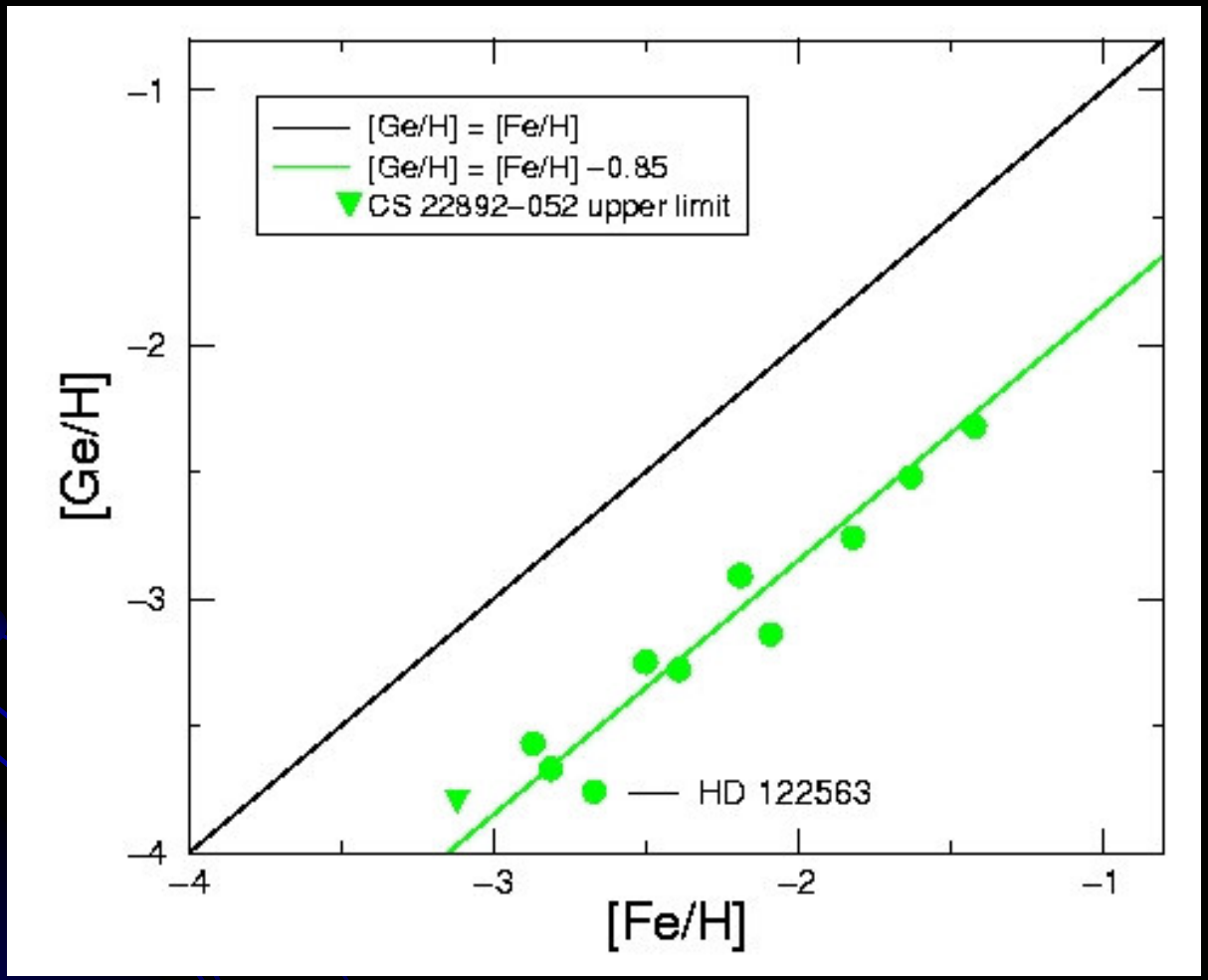

Ge ∝ Fe

JC et al. (2004)

$$[A/B] = \log_{10}(A/B)_{star} - \log_{10}(A/B)_{sun}$$

Ge vs. Eu in Halo Stars

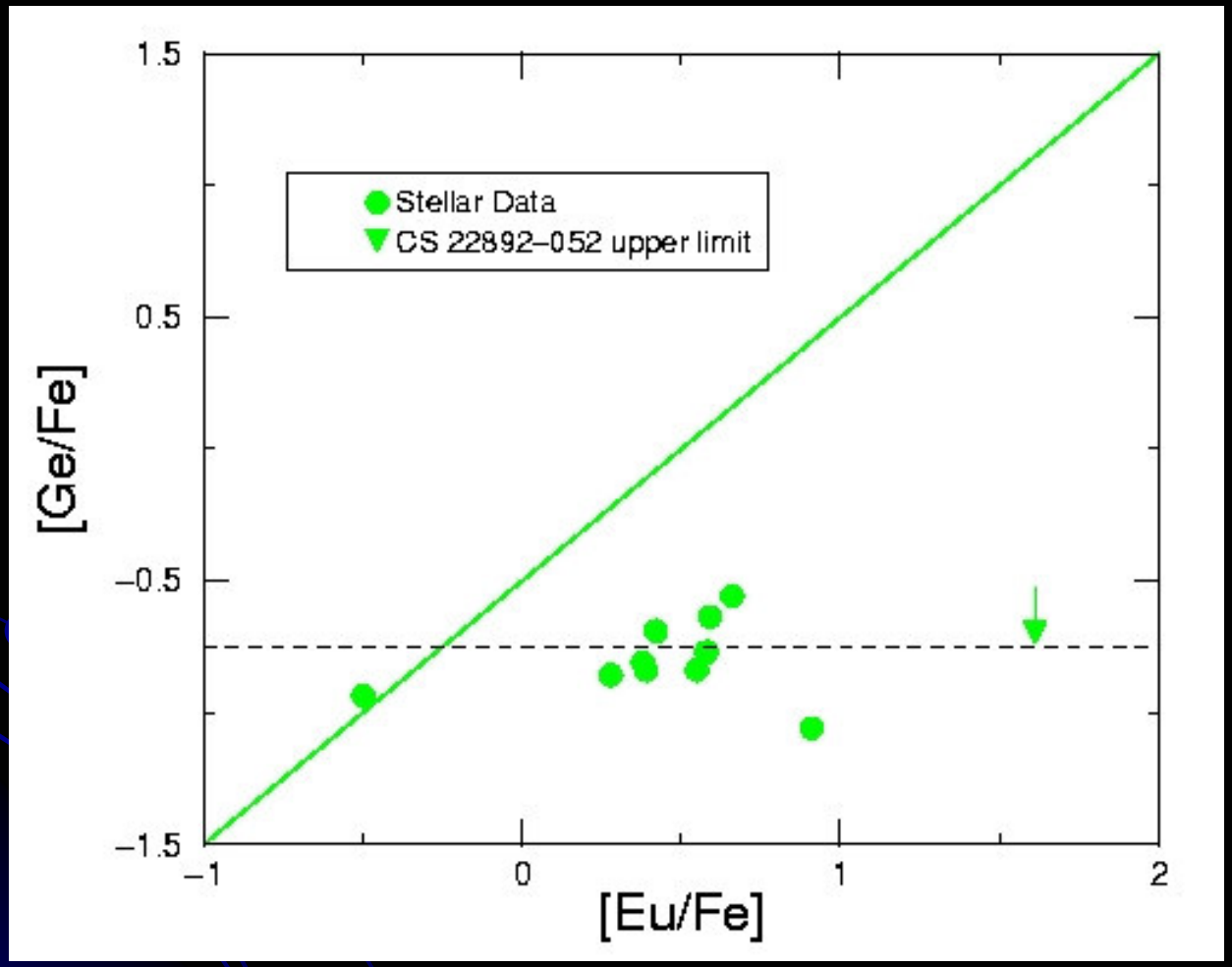

Ge $\not\propto$ Eu

JC et al. (2004)

$$[A/B] = \log_{10}(A/B)_{star} - \log_{10}(A/B)_{sun}$$

Zr as a Function of Metallicity

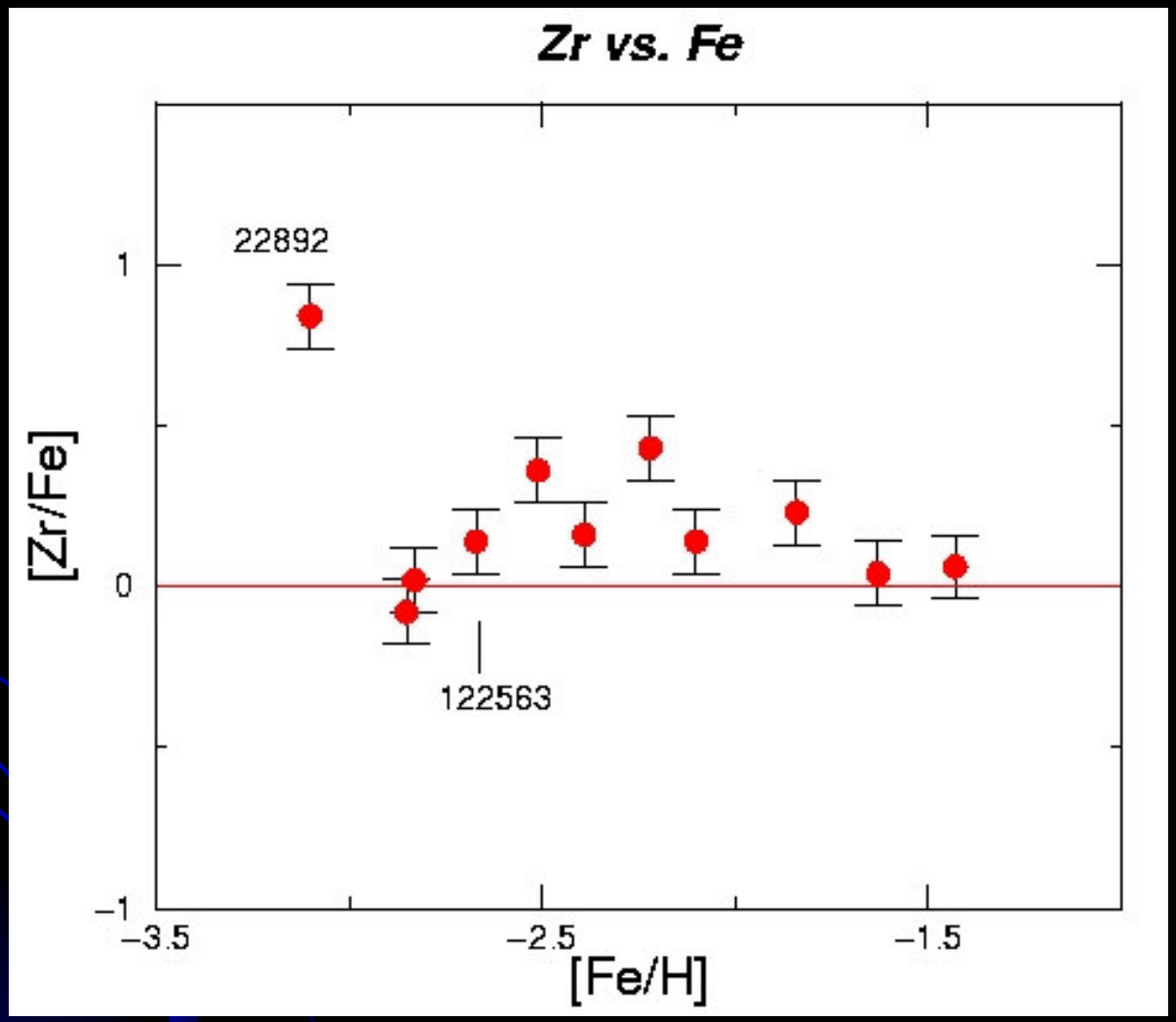

Zr independent of [Fe/H], as shown already by Travaglio et al. (2004).

Zr and Eu Abundances in Halo Stars

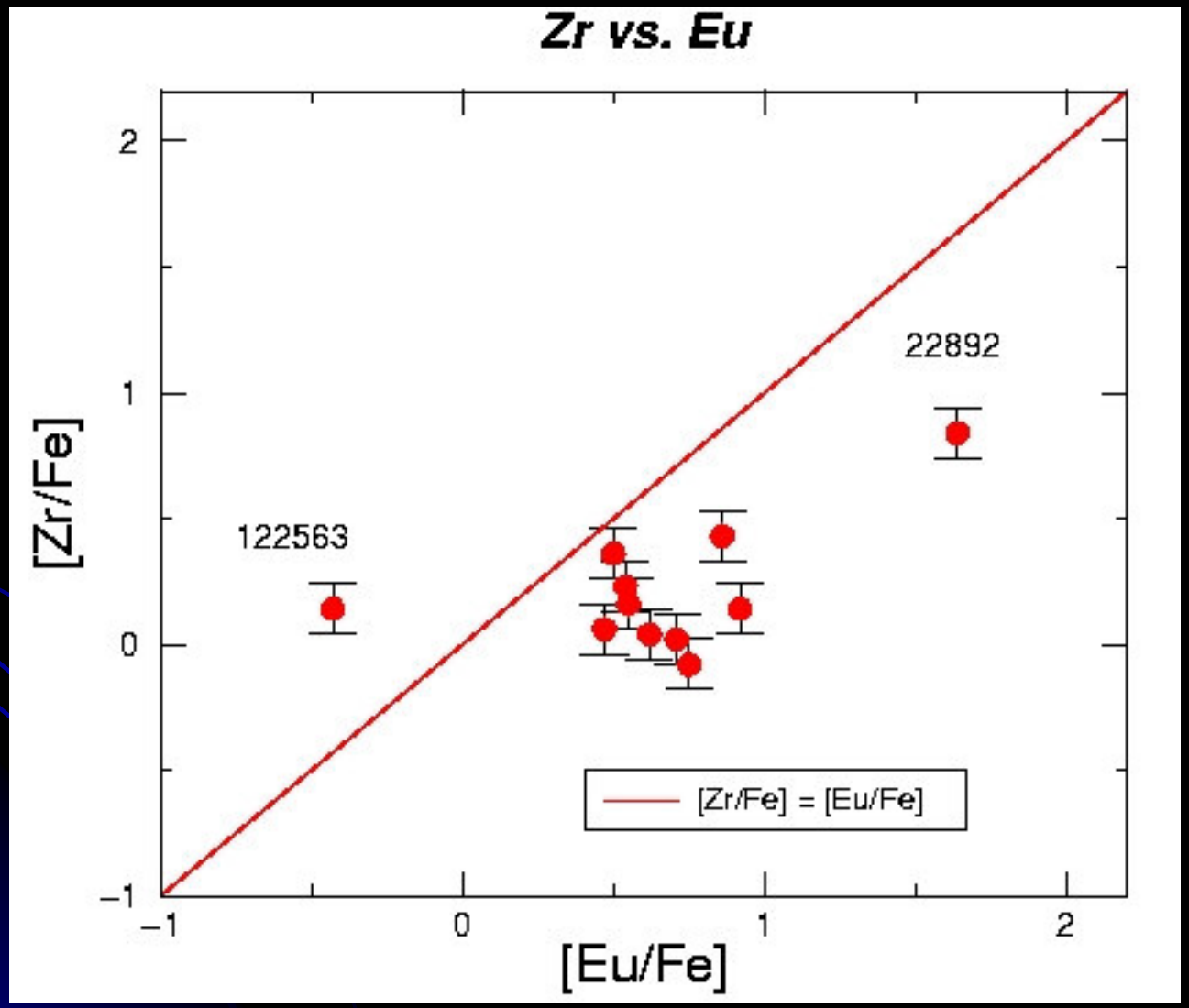

Zr ≠ Eu

N-Capture Element Correlations

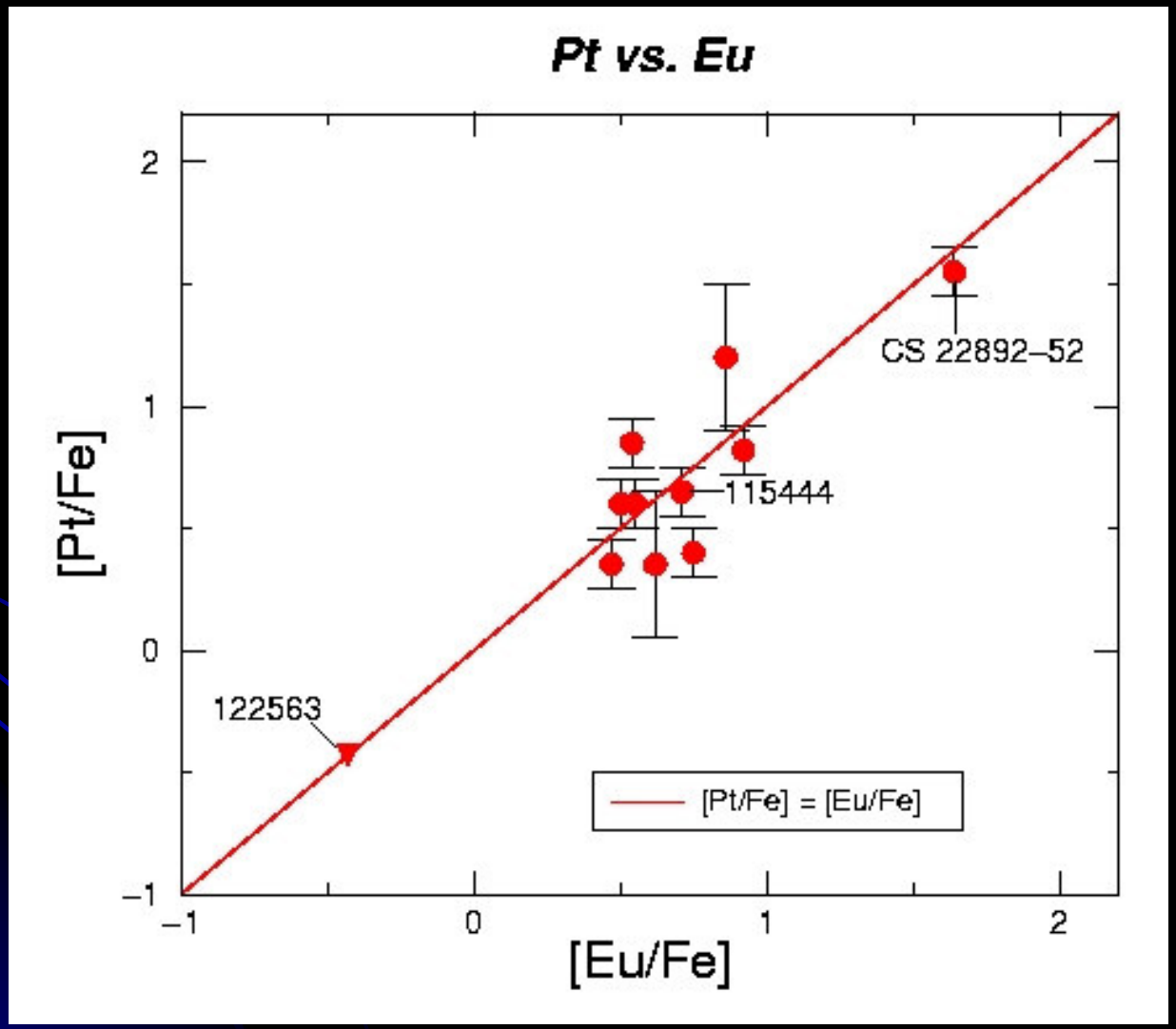

Pt ∝ Eu

N-Capture Element Correlations

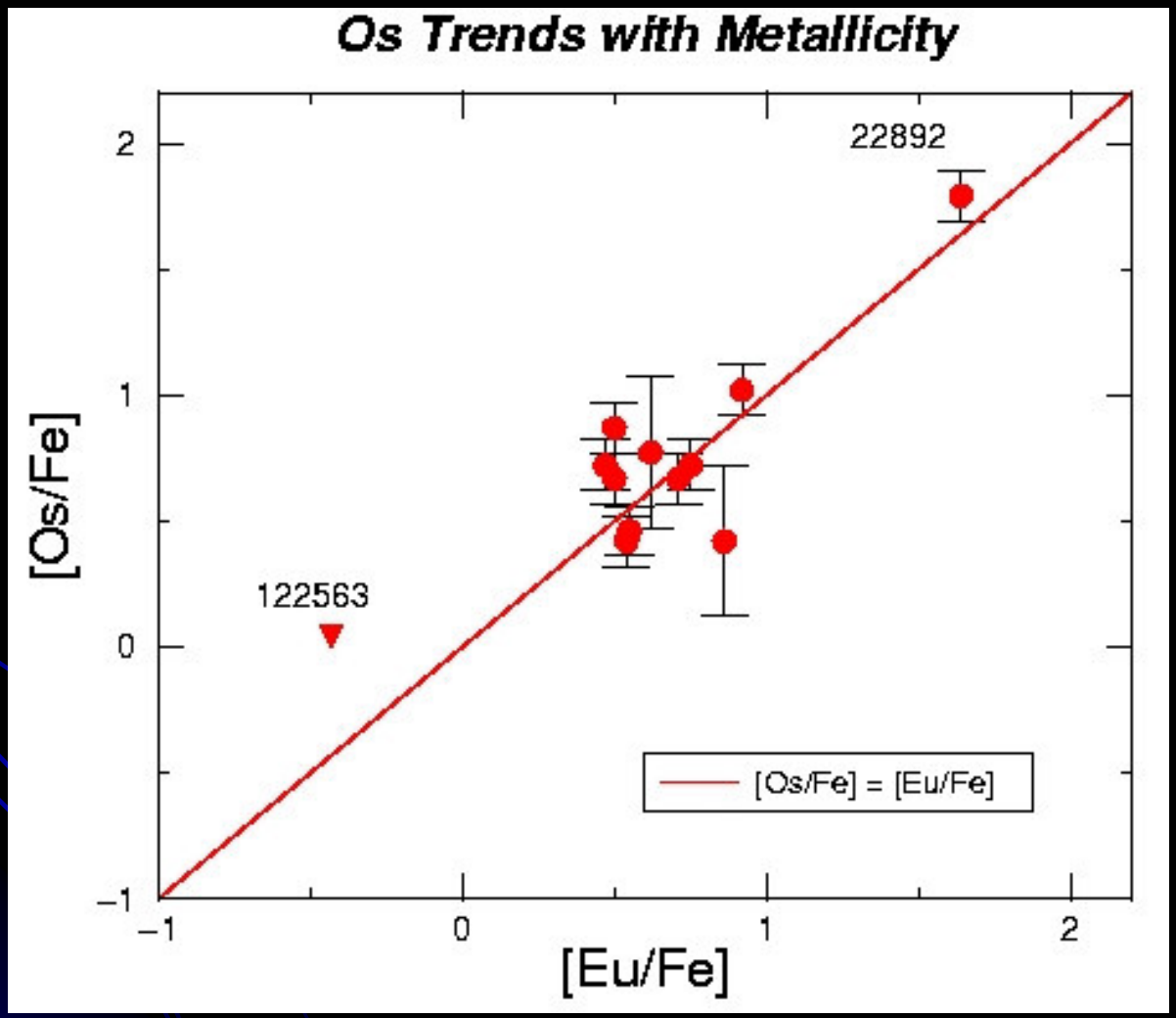

Os ∝ Eu

N-Capture Element Correlations

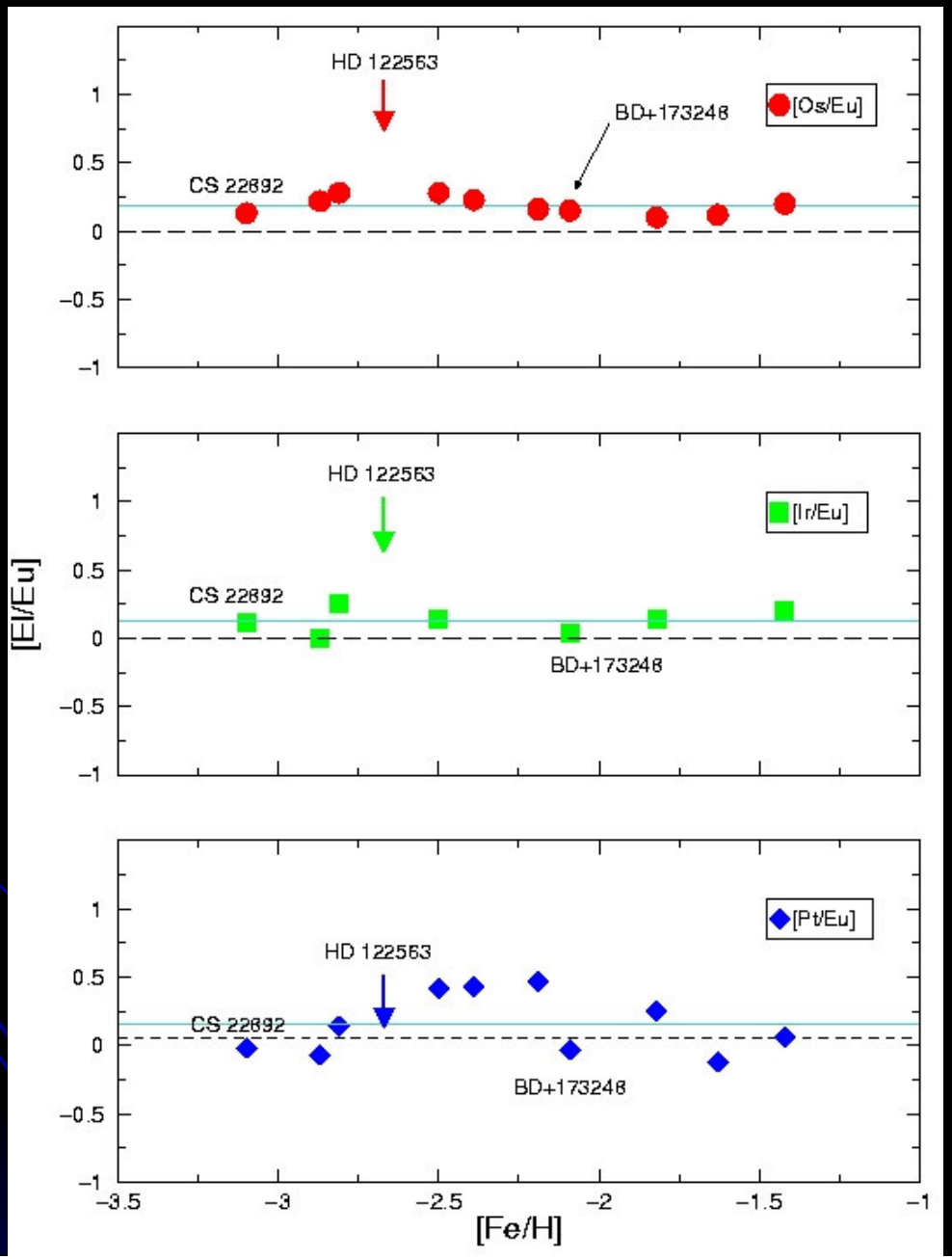

Eu Abundance Scatter in the Galaxy

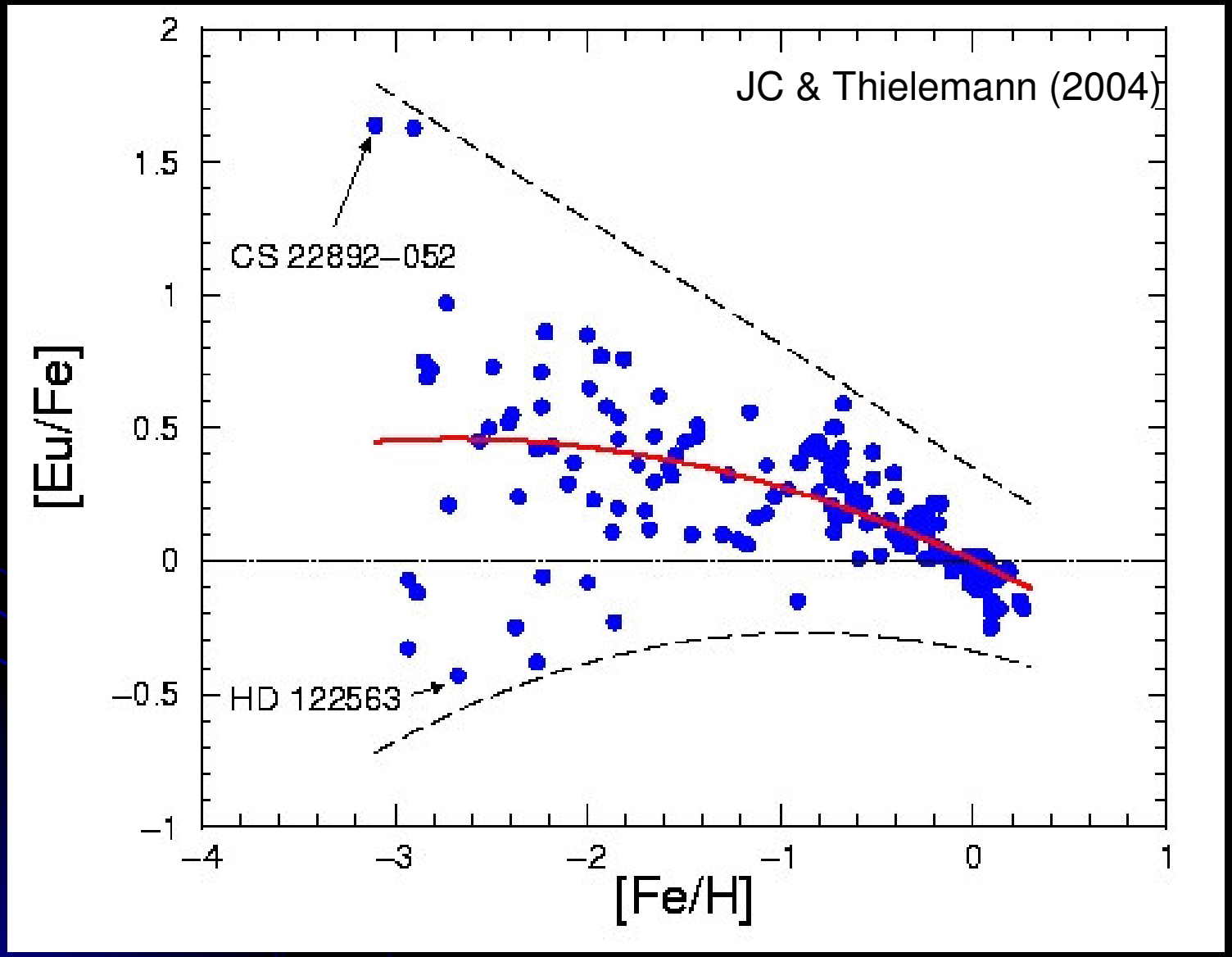

N-Capture Element Abundance Trends

Os-Pt & Eu correlated and show similar scatter with [Fe/H]

RARE

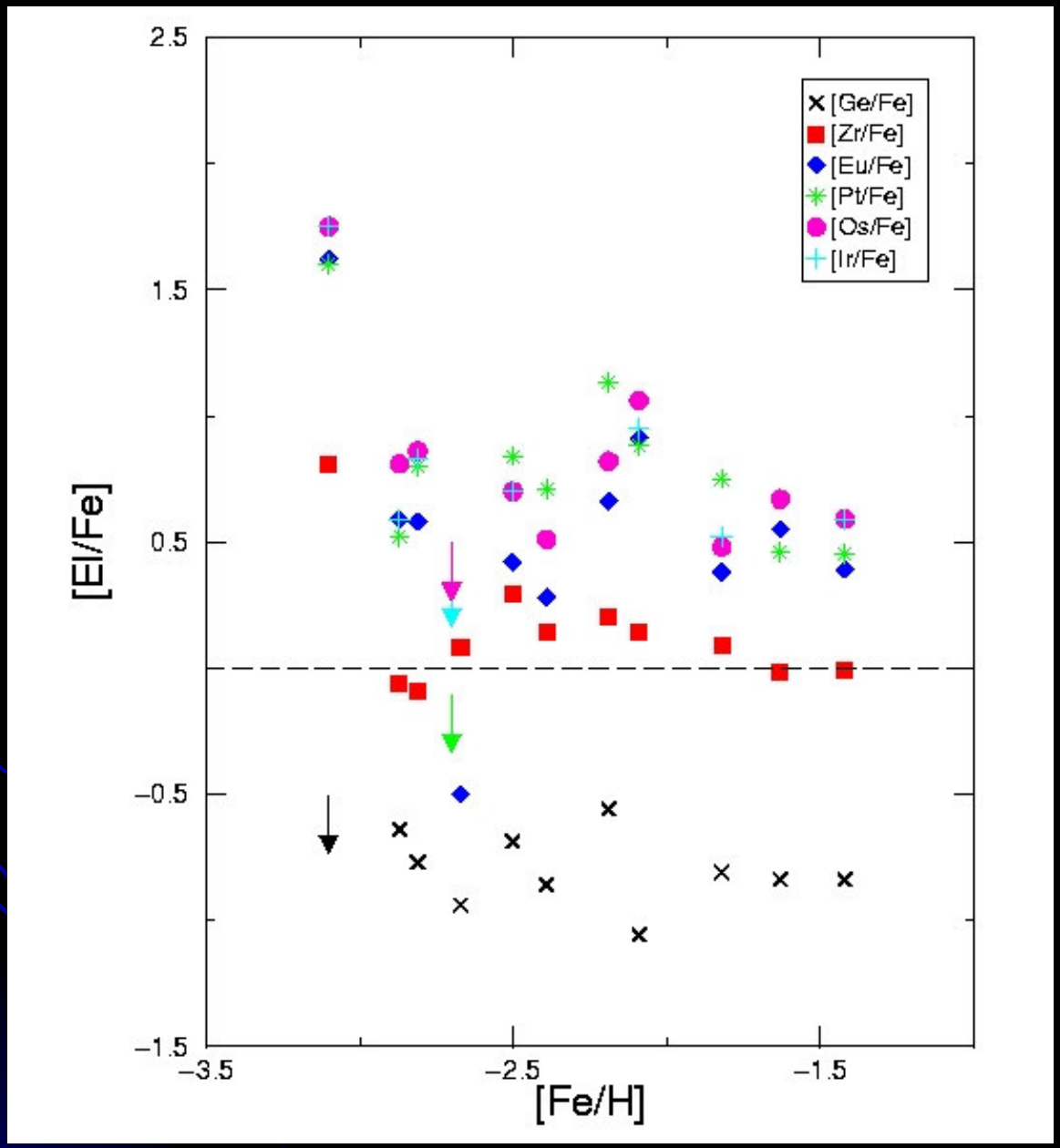

Ge & Zr Show little Scatter.

COMMON

R- and S-Process Abundance Trends

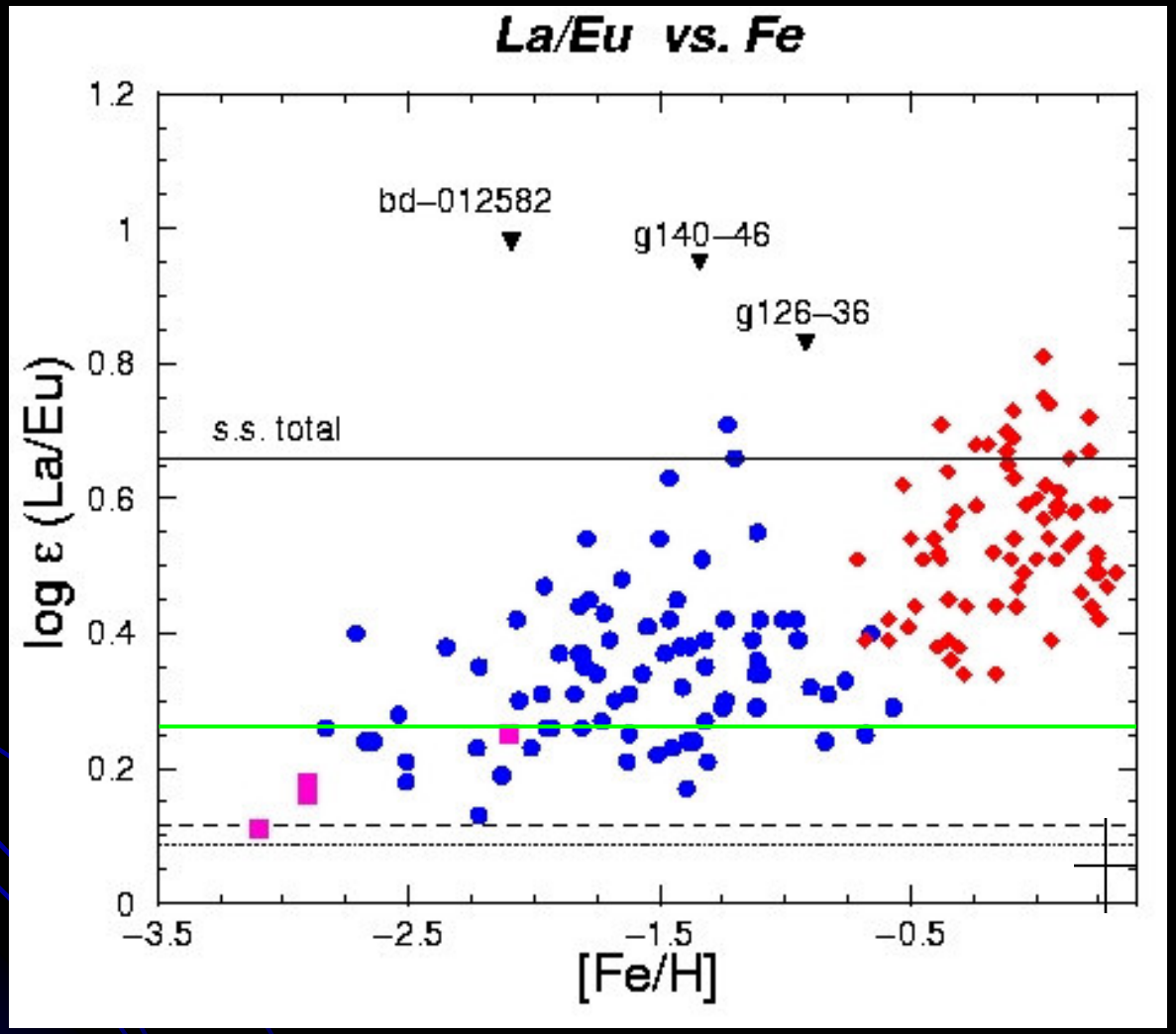

Simmerer et al. (2004)

O'Brien et al. (2003)

Burris et al. (2000)

r-process only

Some Concluding thoughts on: Element Synthesis

- Ge, thought of as an n-capture element, appears to be correlated with Fe
- Zr (like Sr & Y) complicated:
  - → not correlated with metallicity or with heavier n-capture element abundances
  - → not same origin as Eu, some primary (Travaglio et al. 2004)
- Element abundances from Z = 40-50 may be uniform in r-process rich stars, but below upper end
- Os,Ir,Pt correlated with Eu abundances

Some Concluding Thoughts on: Abundance Trends in the Galaxy

- New Os-Pt abundance values show same scatter as [Eu/Fe] at low metallicity
- New La/Eu ratios more reliable than Ba/Eu:

1. Show scatter
2. Only most metal-poor stars show r-process only ratio
3. Stresses importance of nuclear measurement
4. Some “dusting” of s-process even at [Fe/H] < -2 ?

Some Concluding thoughts on: Nucleosynthesis Early in the Galaxy

- R-process elements observed in very metal-poor halo stars
- Implies that r-process sites, earliest stellar generations,

→ rapidly evolving : live and die, eject r-process material into ISM prior to formation of halo stars

- Elements (even s-process ones like Ba) produced in r-process early in Galaxy
- Robust for heavy end :

→ places constraints on sites for the r-process

GALACTIC METALLICITY GRADIENTS FROM OB STARS

Katia Cunha
Observatório Nacional – BR/
University of Texas at El Paso

Simone Daflon (Observatorio Nacional - BR)

+

Keith Butler (UMS)

Radial Metallicity Gradients ➡ Provide important observational constraints for models of Galaxy formation and Chemical Evolution

Abundance gradients : Seem to be a feature commonly observed in galaxies > metallicity decreases outwards from the galactic center

General Trend: Gradients shallower in ellipticals; progressively steeper gradients in spirals

Spiral Galaxies: between -0.03 and -0.07 dex kpc^{-1}

non-barred: steeper gradients

barred: flatter gradients, depending on size of the bar

Ellipticals: mean gradient ~ -0.02 dex kpc^{-1}

(Henry & Worthey 1999)

Gradients Across the MW Disk; Observations

- **Present Day Gradients** : H II regions (ionized gas; gas phase abundances), OB stars (stellar atmospheres) > their abundances should reflect the current ISM composition

- **Gradients from more evolved objects > used to study disk evolution:** **PNe** (ionized gas; span a large fraction of the age of the Galaxy) , **Cepheids** (stellar atmospheres; more evolved but still young!), **Open Clusters** (a few Myr old to several Gyr old; typically, Fe/H derived from photometry or medium res. spectra + some high res. studies)

- So far… there is not a consensus on what the metallicity gradients derived from these samples actually are
- Do gradients flatten or steepen with time? > trace the history of the Galactic Disk

Summary of Milky Way Gradients

Ionized Gas:

	Studies	ΔR_g(kpc)	N	O	S
			Slopes (dex kpc^{-1})		
H II Regions	Shaver *et al.* (1983)	$3.5<R_g<13.7$	-0.09	-0.07	-0.01
	Henry & Worthey (1999)	$5.9<R_g<13.7$	-	-0.05	-
	Afflerbach et al. (1997)	$0<R_g<11.4$	-0.072	-0.064	-0.063
	Vílchez & Esteban (1996)	$11.7<R_g<18$	-0.01	-0.036	-0.04
	Deharveng et al. (2000)	$5<Rg<15$	-	-0.039	-
	Pilyugin et al. (2003)	$6.6<R_g<14.8$	-	-0.048	-
PNe II	Pasquali & Perinotto (1993)	$1<R_g<16$	-0.03	-0.05	-
	Maciel & Quireza (1999)	$4.5<R_g<12$	-	-0.069	-0.067
	Maciel & Quireza (1999)	$3.5<R_g<13.5$	-	-0.058	-0.077
	Martins & Viegas (2000)	$4.8<R_g<12.4$	-	-0.054	-0.064
	Henry et al. (2004)		-	-0.037	-0.048

Cepheids : Andrievski et al. (2002); Luck et al. (2003)
Rg ~ between 4 - 15 Kpc

Abundance distributions for inner and outer Disk > an offset of ~ 0.2 dex → outer disk ~ lower abundances

- Mean gradient for all elements: -0.03 dex kpc^{-1}

Open Clusters : Twarog et al. (1997) > DDO photometry + moderate disp. spec. of 76 Open Clusters between 6.5 -15 Kpc

- [Fe/H] ~ 0 +- 0.15 dex for R_g=6.5-10 Kpc > at best a weak evidence for a **shallow** abundance gradient in this range: FLAT

- **Discontinuity** @ 10 Kpc > Conclude that "Outer" disk (beyond 10 Kpc) ~ lower abundances by -0.3 dex + larger scatter

- IF considered all clusters > -0.07 dex/Kpc; however, they do **NOT** favor single line slope but a **step function**

Friel et al. (2002) : 39 Open Clusters with ages > 700 Myr (7-16 Kpc)

Fe grad : -0.06 +- 0.01 dex/Kpc (linear relation)

But also breaks sample in 4 age intervals : < 2Gyr [-0.023]; 2-4 Gyr [-0.053]; 4-6 Gyr [-0.057]; > 6 Gyr [-0.096]

- Gradients get shallower over time

Chen et al. (2003) : 118 Open Clusters (6-16 Kpc)

ALL OC > Fe: -0.063 dex/Kpc (shallower inside 10 Kpc)

80 clusters with ages < 0.8 Gyr (~ age Hyades)

Fe grad: -0.024 +- 0.01 dex/Kpc

38 clusters with ages > 0.8 Gyr

Fe grad: -0.075 +- 0.013

Gradients Obtained from Young OB stars

- Early studies of OB stars (Gehren et al. 1985, Fitzsimmons *et al.*, 1992; Kaufer *et al.*,1994; Kilian-Montenbruck *et al.* 1994): **Gradients ~ zero**

- Smartt & Rolleston (1997) : first to report detection of significant grads
  - Gummersbach et al. (1998): Non-LTE analysis (Kaufer '94 dataset) 16 OB stars between 5 and 14 kpc (11 positions)

C	N	O	Mg	Al	Si
-0.035 ±0.014	-0.078 ±0.023	-0.067 ±0.024	-0.082 ±0.026	-0.045 ±0.023	-0.107 ±0.028

  - Rolleston et al. (2000): same dataset as Smartt & Rolleston '97 Compilation values of T_{eff}, log g, EQW (not homogeneous) 73 OB stars; $6<R_G<18$ kpc, LTE analysis

C	N	O	Mg	Al	Si
-0.07 ±0.02	-0.09 ±0.01	-0.067 ±0.008	-0.07 ±0.01	-0.050 ±0.015	-0.06 ±0.01

(Note different carbon and silicon gradients + very steep N grad.)

•What is the Radial Metallicity Gradient of the Galaxy?

Our goal:

- Construct a homogeneous database of OB-star abundances
  - Homogeneous T_{eff} -scale
  - Non-LTE abundance calculations (line formation)
- The "way to go" if you want to look at trends

Why OB Stars?

- $M \geq 10M_{\odot}$, Ages ~10^7 years
- OB Associations: tracers of Spiral Arms
- Close to their place of birth
- On the MS: original abundances of the gas

Our Sample

70 main-sequence O9-B3 stars, members of
25 Open Clusters, OB Associations & H II Regions

Cluster/Observ		R_g	N
Sh2 47	ESO	4.7 (0.5)	1
Ser OB1	ESO	5.8 (0.5)	4
Sh2 32	ESO	5.9 (0.4)	2
NGC 6204	ESO	6.0 (0.6)	1
Tr 27	ESO	6.0 (0,3)	2
NGC 6231	ESO	6.2 (0.3)	4
NGC 6604	ESO	6.5 (0.7)	1
Ara OB1	ESO	6.6 (0.3)	2
Vul OB1	ESO/MCD	6.9 (0.3)	2
Stock 16	ESO	6.9 (0.3)	1
Sct OB2	ESO	7.1 (0.3)	2
NGC4755	ESO	7.1 (0.4)	4
IC 2944	ESO	7.3 (0.3)	2

Cluster		R_g	N
Cyg OB3	MCD	7.6 (0.3)	5
Cyg OB7	MCD	7.9 (0.3)	3
Lac OB1	MCD	8.0 (0.3)	5
Cep OB2	MCD	8.1 (0.3)	17
Cep OB3	MCD	8.2 (0.3)	3
Mon OB2	ESO	9.4 (0.3)	1
Sh2 247	ESO	10.7 (0.9)	1
NGC 2414	ESO	10.9 (0.3)	2
Sh2 253	ESO	12.2 (0.5)	1
NGC 1893	ESO	12.4 (0.9)	2
Sh2 284	ESO	12.8 (0.3)	1
Sh2 285	ESO	13.2 (1.3)	1

ESO : 1.52m

McDonald : 82″ + 107″

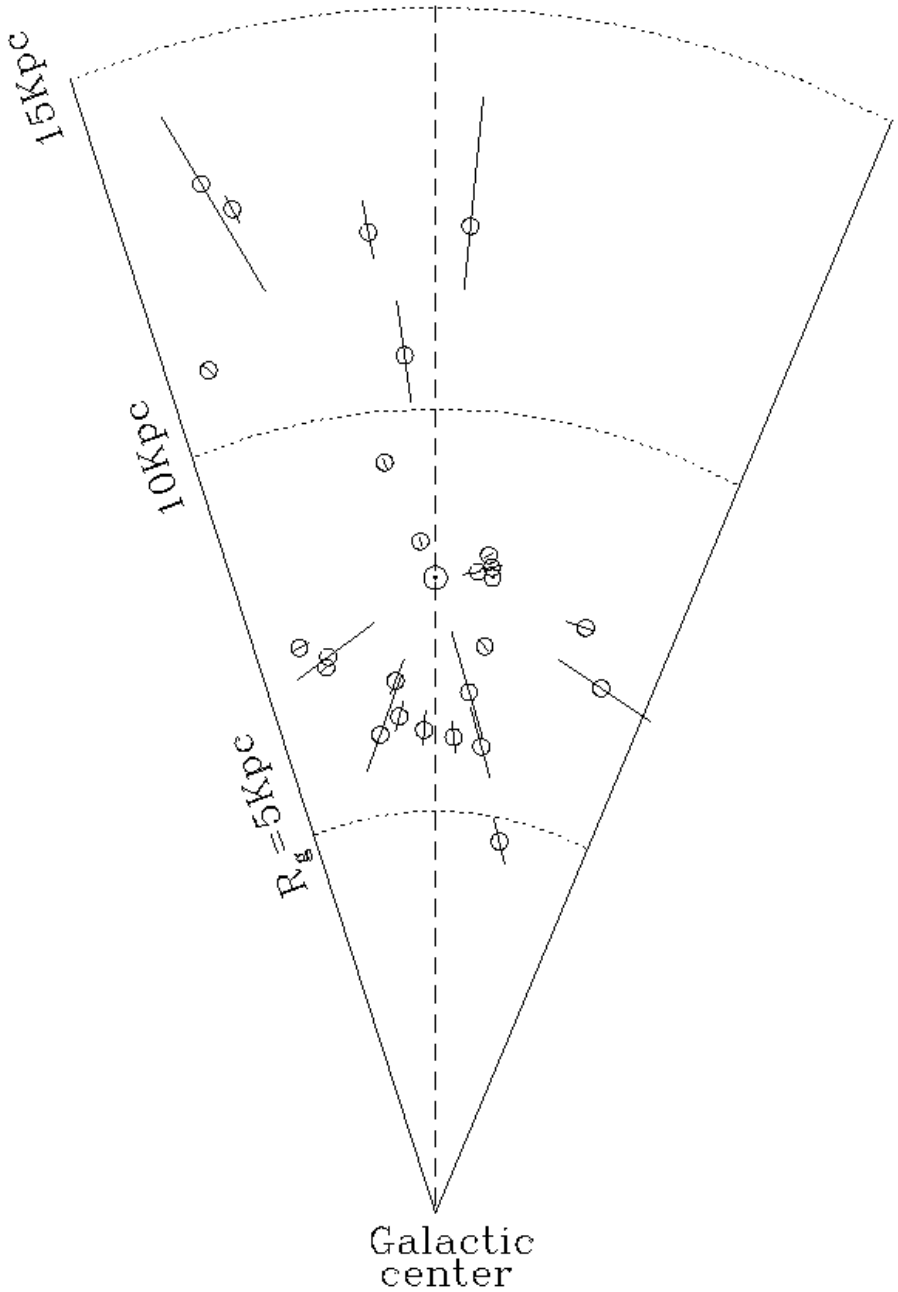

Part of Galaxy we sampled …

$4.7 < R_G < 13.2$ Kpc

The Sun: $R_{\odot}$=7.9 kpc
(McNamara et al. 2000)

Northern Sample : McDonald Observatory

HD197512

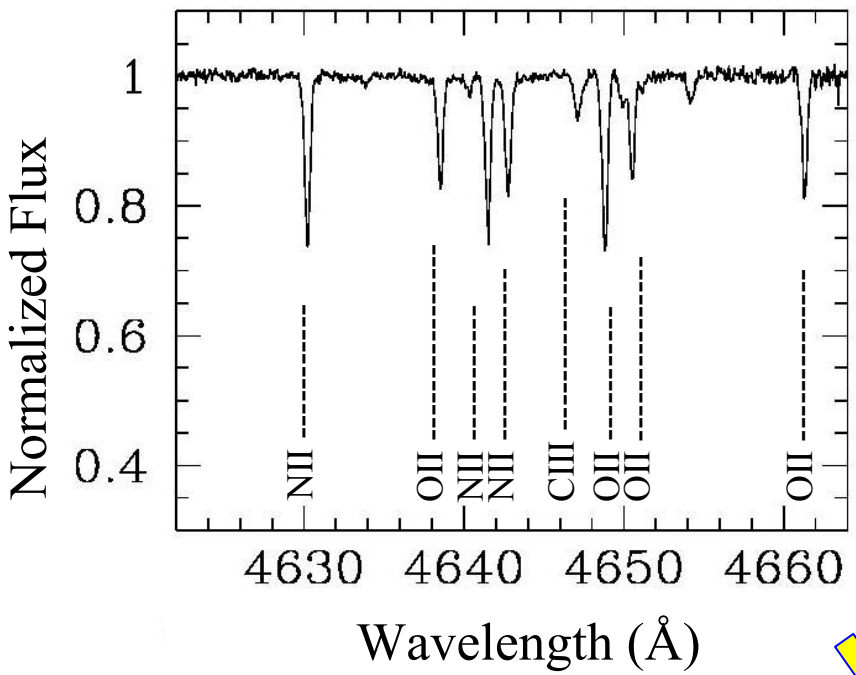

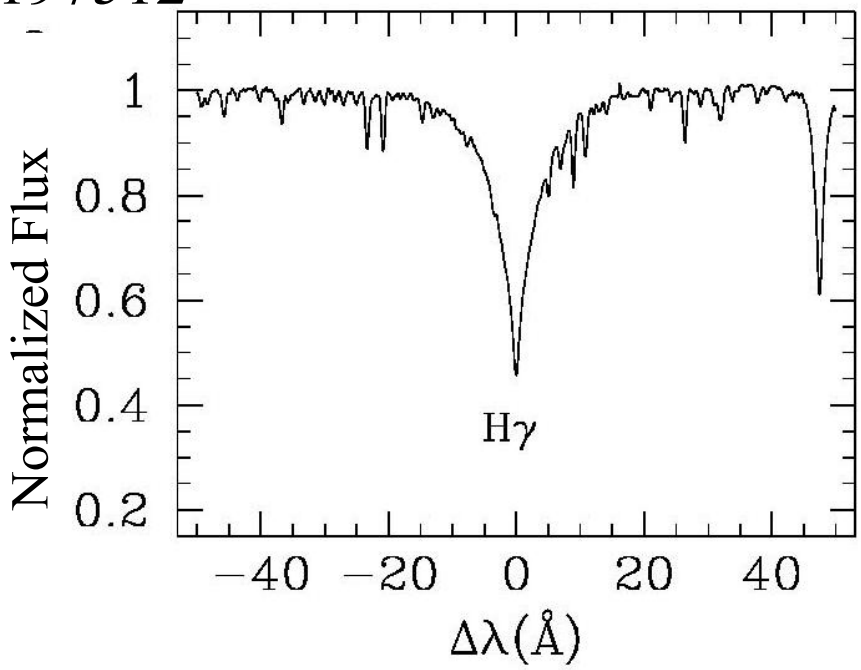

Telescope	2.1 m+ Sandiford	2.7 m Coude'
Nominal Resolution	60.000	12.000
# orders	18 – 23	1
Spectral coverage	500Å – 850Å	~150Å
S/N	150 – 300	>50

Southern Sample: ESO

1.52 m + FEROS, R=48,000, 3900-9200Å, S/N > 100

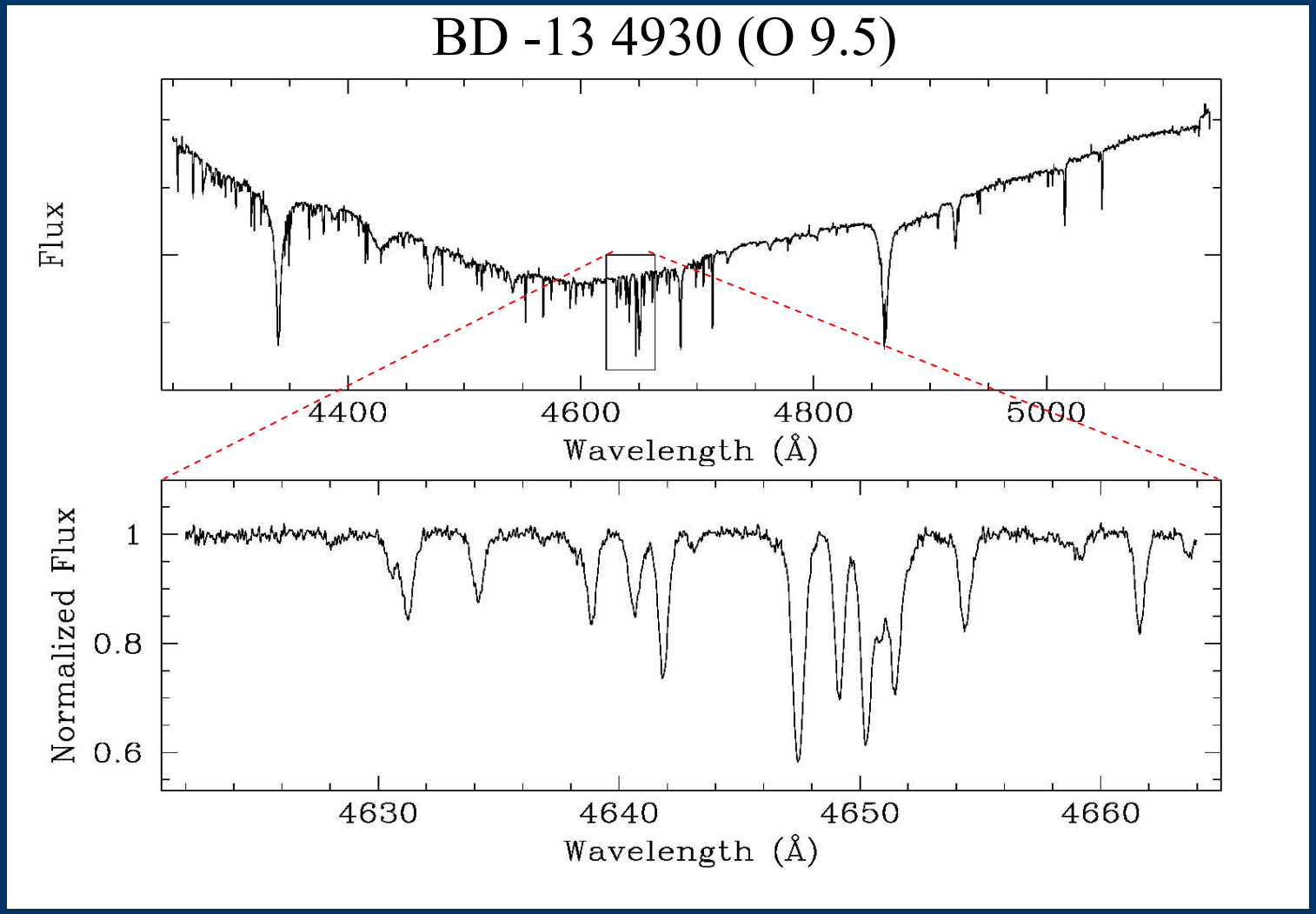

Stellar Parameters

> Method : Gies & Lambert (1992)

• Effective temperatures + surface gravities: derived iteratively from photometric calibrations for the indices c_1 and β, coupled to fits of the wings of $H\gamma$ profiles

Initial guess T_{eff}
Balona (1984): $T=f(c_o, \beta)$ +5.2%
LGK (1986): $T=f([c_1],\beta)$ +4.2%

① $C_1, \beta^{(1)} \rightarrow T_{eff}^{(1)}$
$H\gamma \rightarrow \log g^{(1)}$

② $\log g^{(1)} \rightarrow \beta^{(2)}$

③ $C_1, \beta^{(2)} \rightarrow T_{eff}^{(2)}$
$H\gamma \rightarrow \log g^{(2)}$

• Only for stars with Stromgren photometry available ….

< For most of sample stars > No Strömgren photometry .... >

Q -calibration

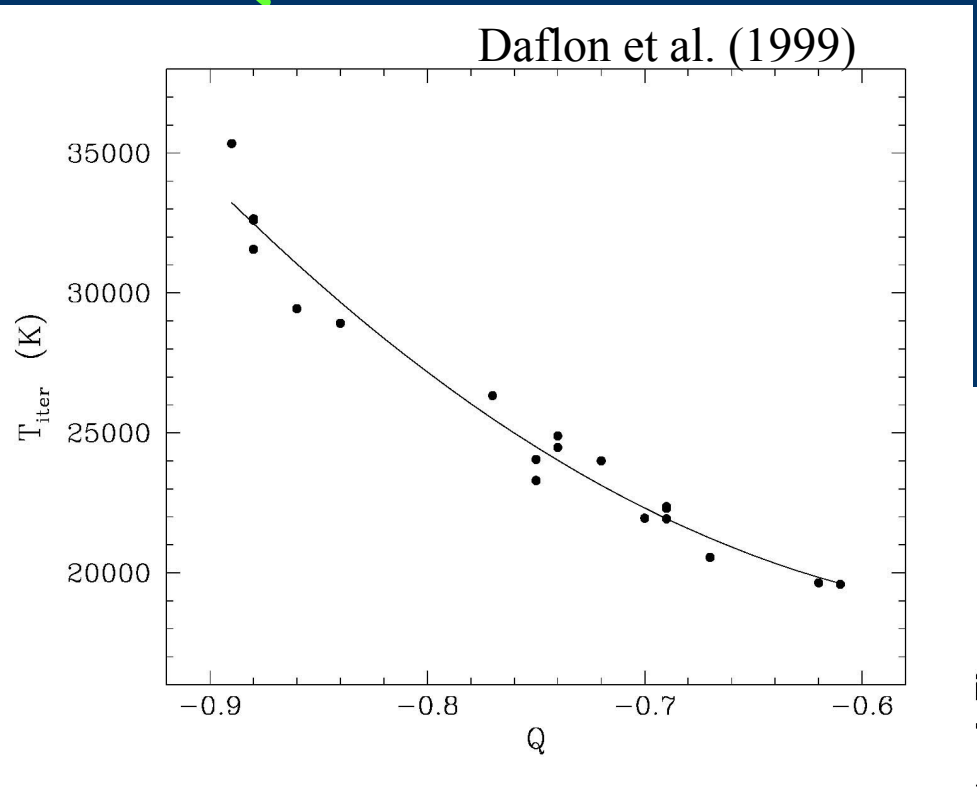

- Effective temperatures: derived from calibration of Q vs T_{iter}
- Surface gravities: fits of the wings of Hγ profiles

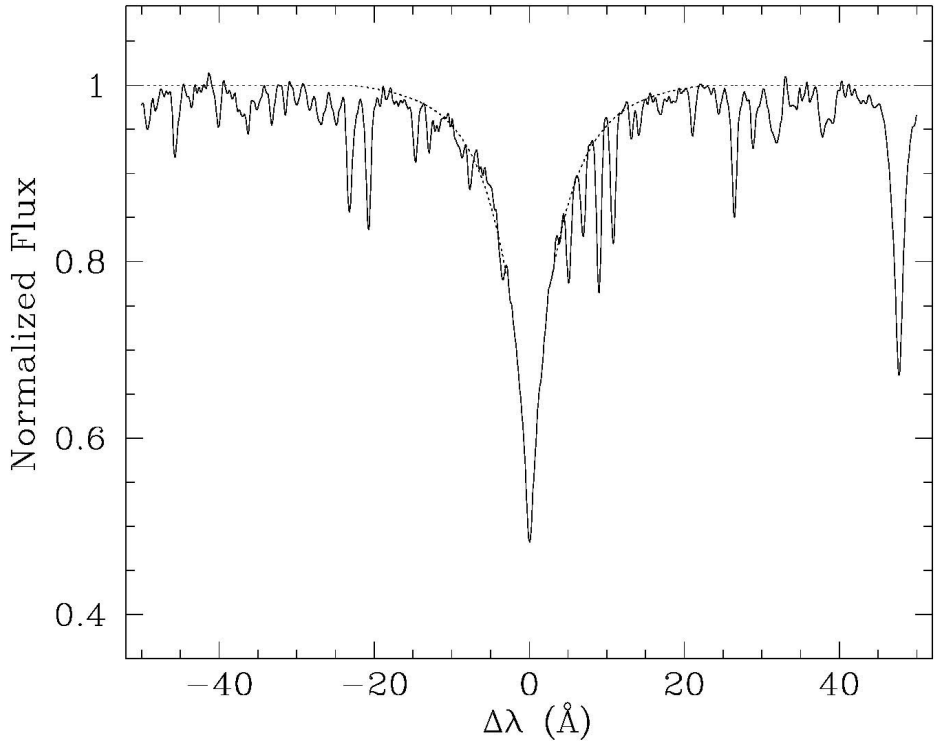

Sample T_{eff} and log g ranges:

19,000 < Teff < 33, 000K

4.4 < log g < 3.6

Abundance Analysis

- **Model atmospheres**: LTE, 1d plane-parallel models (ATLAS9)
- **Non-LTE Synthesis**: theoretical profiles calculated assuming non-LTE line formation theory (DETAIL + SURFACE)

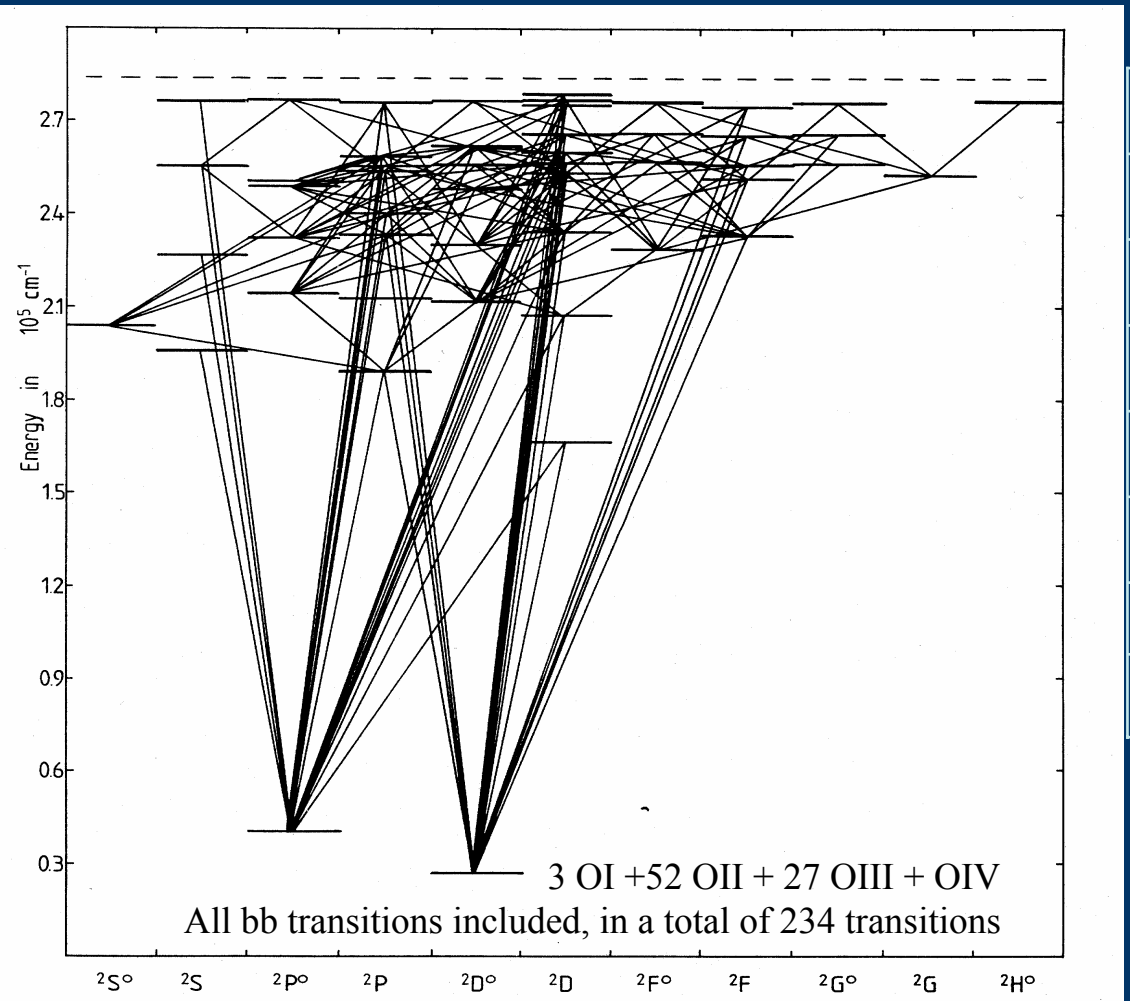

Ion	Model Atoms
C II	Eber & Butler (1988)
N II	Becker & Butler (1989)
O II	Becker & Butler (1988)
Mg II	Przybilla et al. (2001)
Al III	Dufton et al. (1986)
Si III	Becker & Butler (1990)
S III	Vrancken et al. (1996)

- **Abundance analysis of homogeneous sets of lines**

Synthetic profiles & observed spectra for BD-00 1491

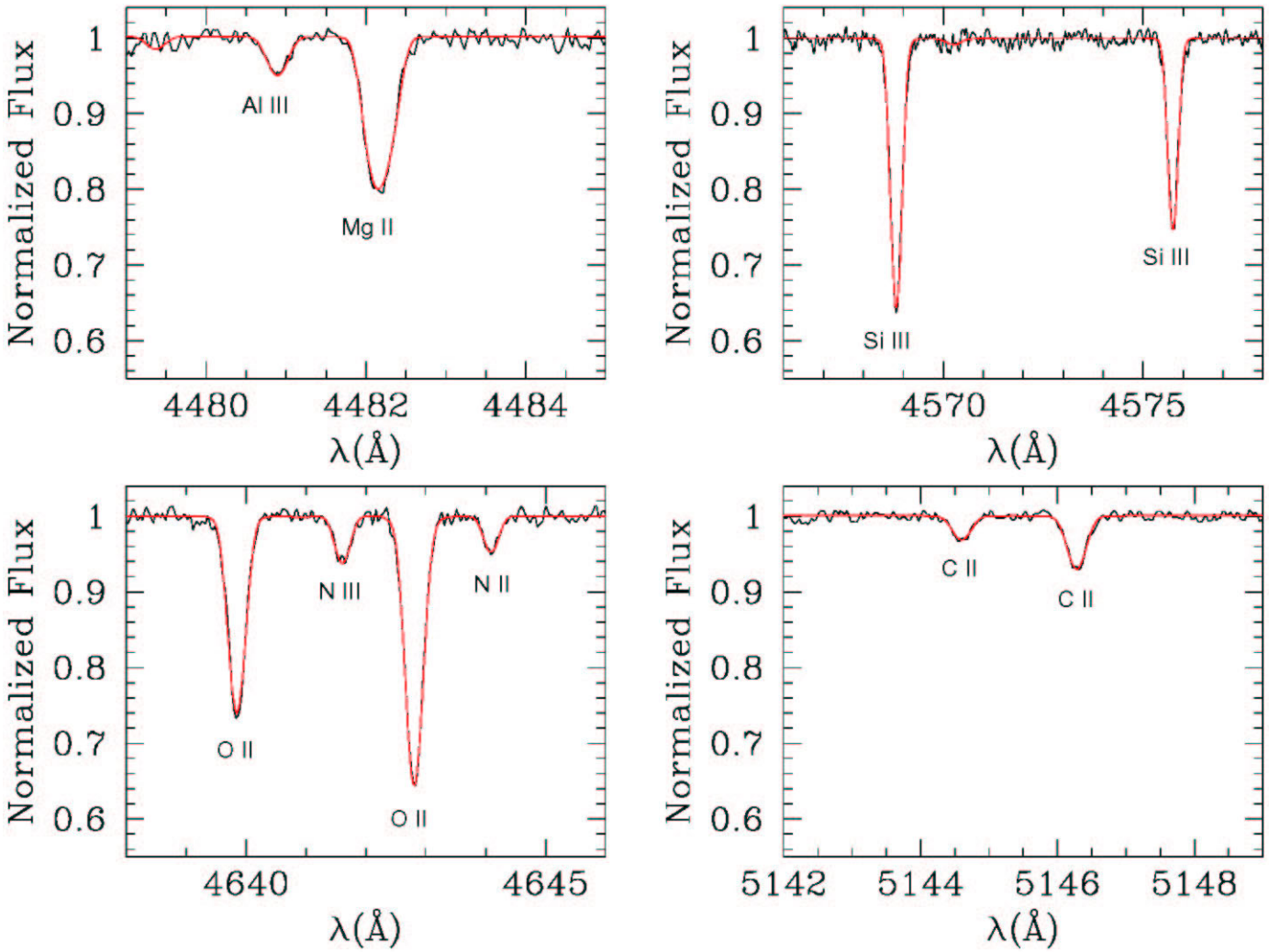

- Large Teff interval for the sample stars

- Important to look at trends that might indicate presence of systematic errors in the 'observed' abundances

- For most elements: No significant trends

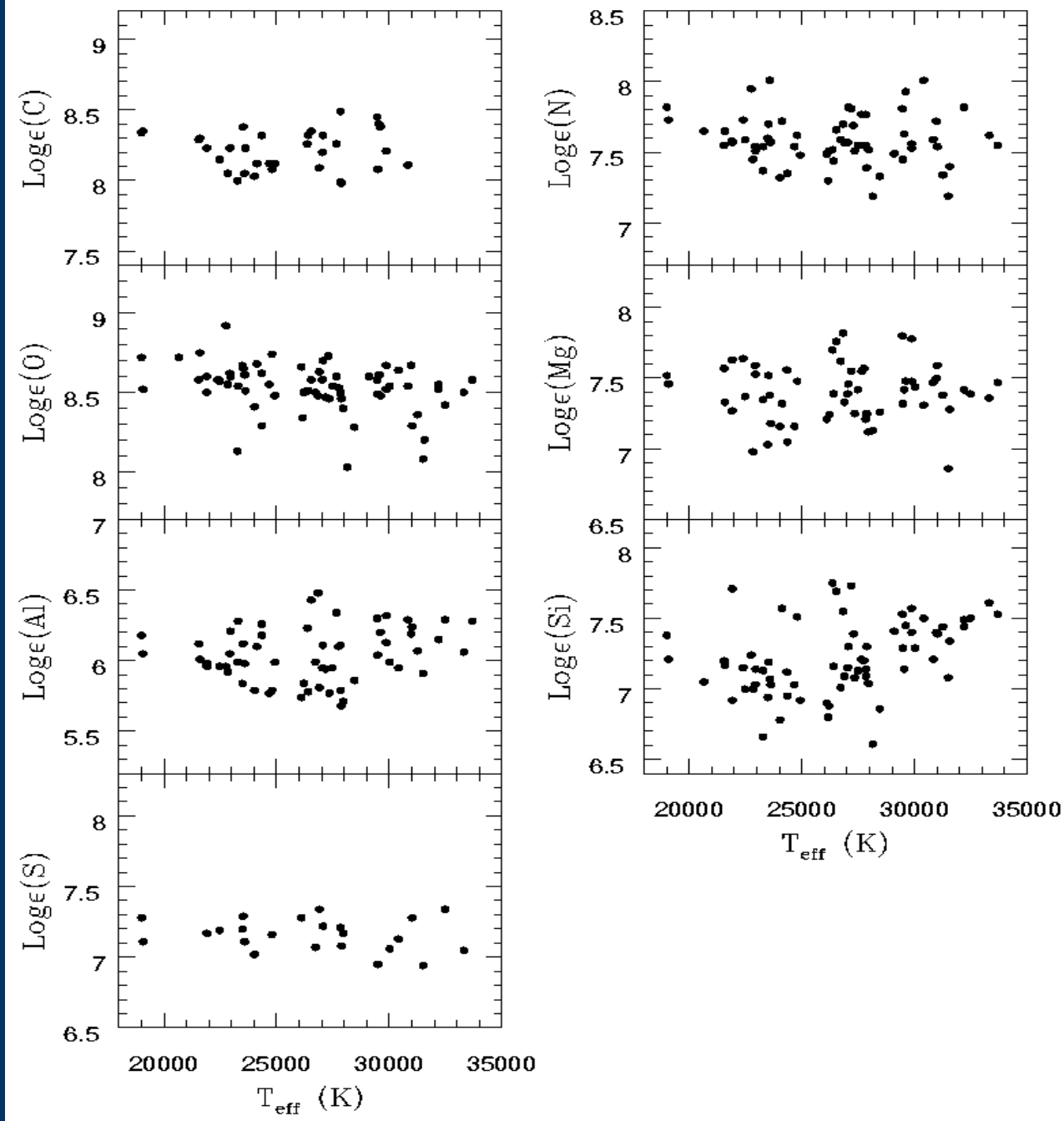

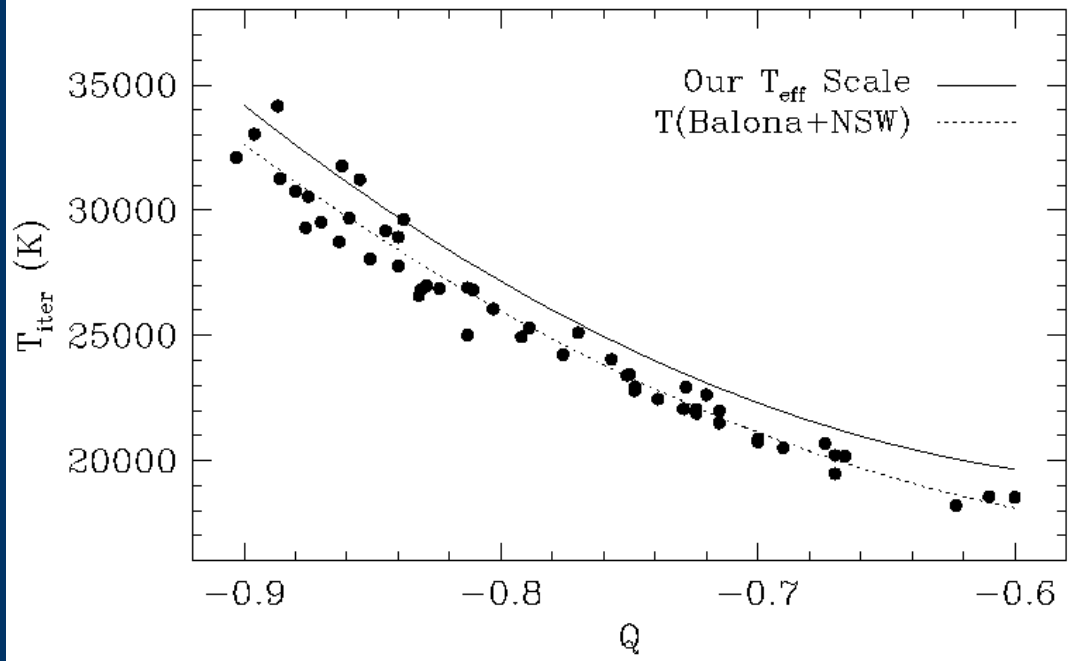

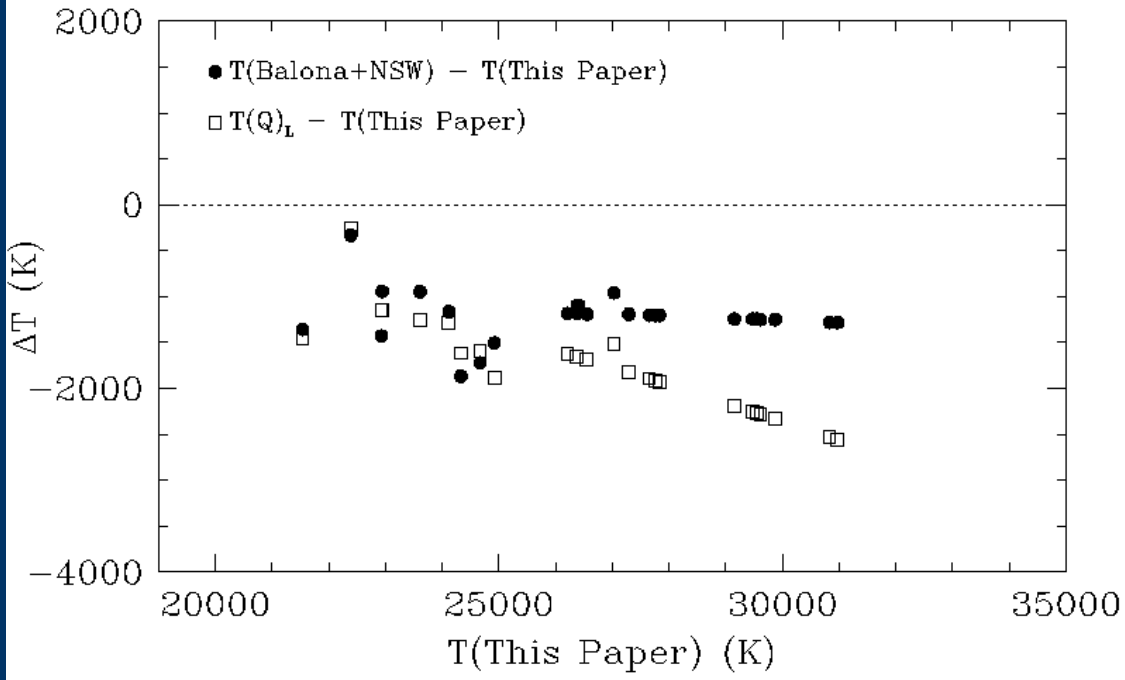

What if we used other T_{eff} - Calibrations?

- Our T_{eff}s lower than those from Si III/Si IV ionization balance

Other possibilities:

1. Use Napiwotski et al. (1993, NSW)
2. New T(Q) calibration derived for Balona+NSW → lower T_{eff}s by ~1300K

2. T(Q) from Lyubimkov et al. (2002)
- lower T_{eff}s by ~1700K

→ larger difference for higher T_{eff}

Oxygen abundances as a function of T_{eff}

OII EQW are maximum for T_{eff}~27 000K

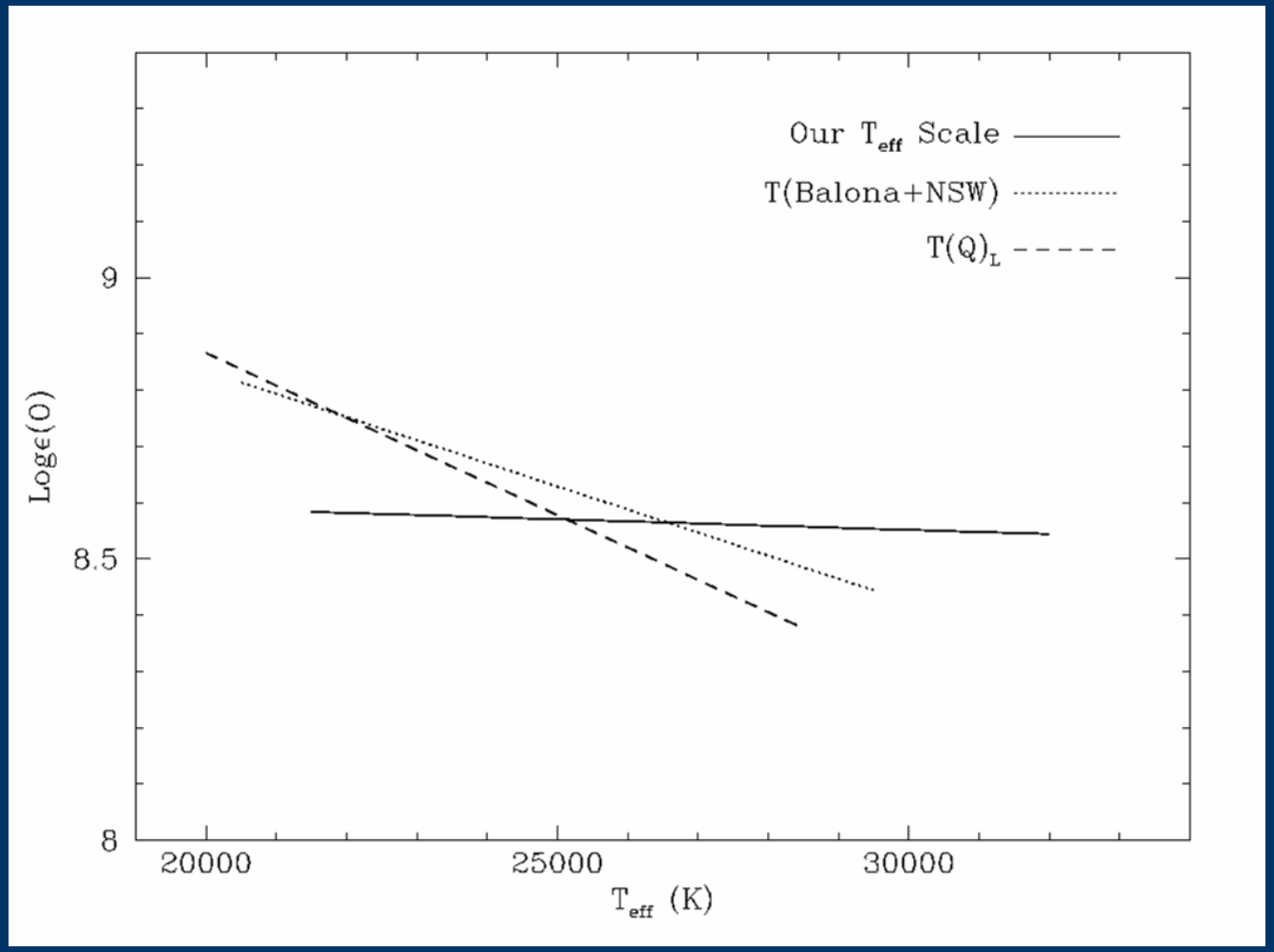

Lower T_{eff} scales

- T<27 000 K: Logϵ(O) ↗
- T>27 000 K: Logϵ(O) ↘
- O abundances become dependent of T_{eff}
- Similar effect is observed for N and Si;
- The opposite for Mg

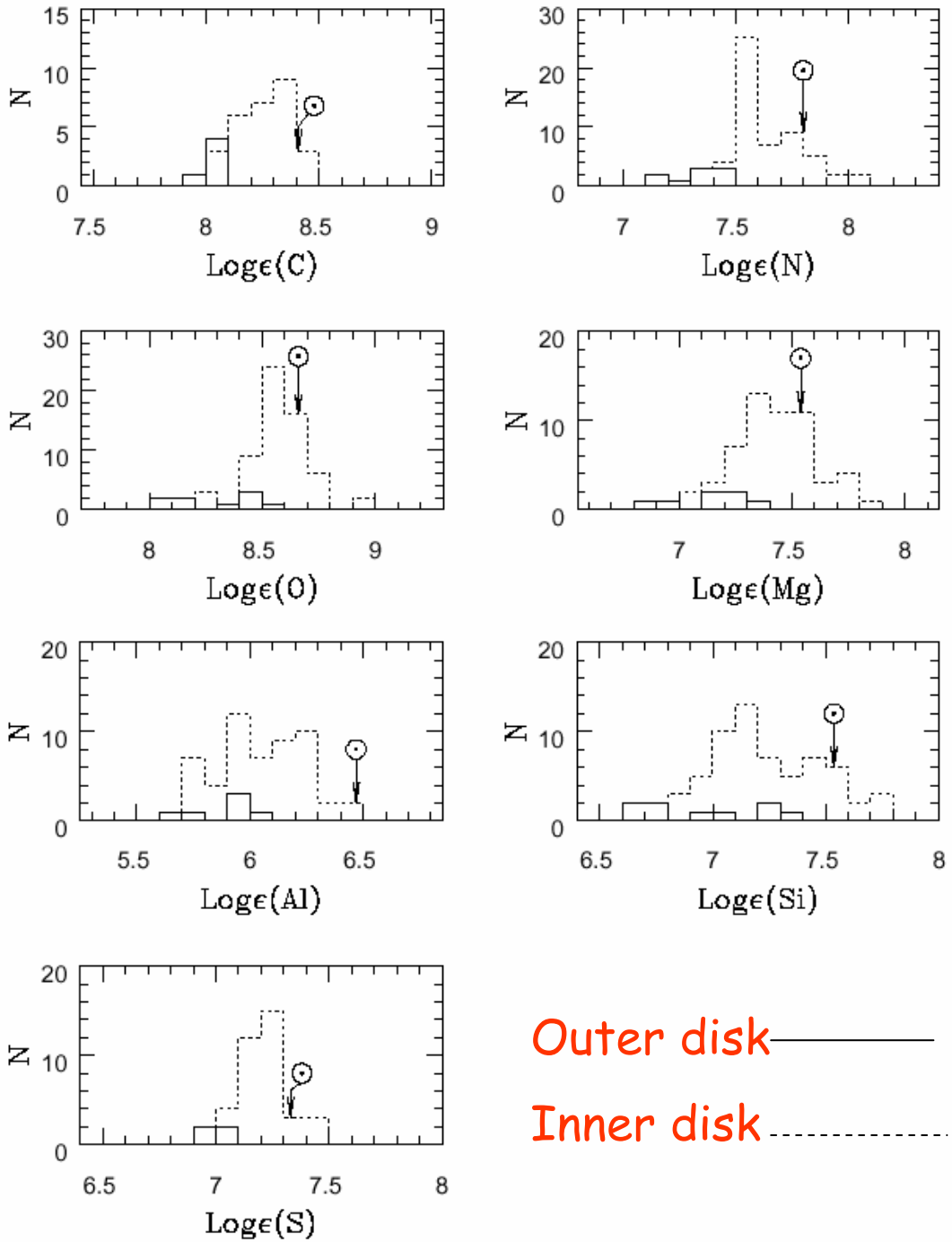

- 61 stars inside the Solar circle ("INNER" DISK) + 9 stars from "OUTER" DISK.
- Tendency: Abundances for outer disk are lower than inner Disk stars
- Solar abundances fall within upper envelope of abund. distribution of inner Disk stars
- Oxygen: Solar value close to peak of inner Disk distribution:

<inner disk>= 8.60 +- 0.06

<outer disk>= 8.30 +- 0.19

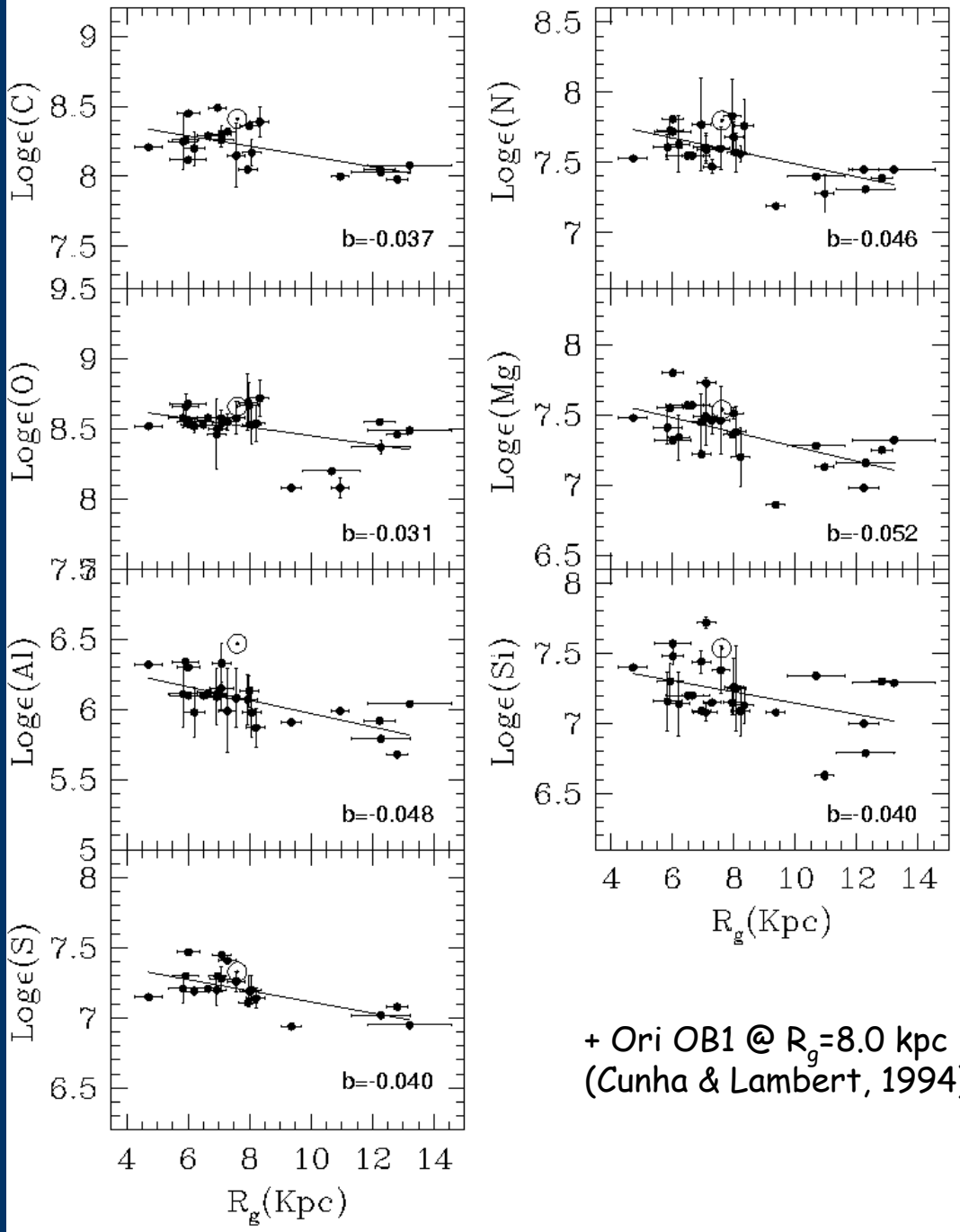

+ Ori OB1 @ R_g=8.0 kpc
(Cunha & Lambert, 1994)

Resulting Gradients:

1) 'Cluster' Abundances

> average of stellar abundances in a cluster

Simplest way > Assume that the distributions can be represented by straight lines

Element	Gradients (dex kpc^{-1})
C	-0.037±0.010
N	-0.046±0.011
O	-0.031±0.012
Mg	-0.052±0.014
Al	-0.048±0.010
Si	-0.040±0.017
S	-0.040±0.011
Mean	-0.042+0.007

<Grad> -0.042 +- 0.007

Gradients from Individual Stellar Abundances

Advantages:

Possibility to isolate sub-samples of stars + investigate systematic effects from sample selection on the calculated gradients

- **T_{eff}** : Select sub-samples with stars spanning a very narrow range in T_{eff} (whole sample T_{eff} range between 19000 and 34000K)

- **Rotation** :Mostly OB stars are fast rotators; mixing effects

Our abundance database includes mostly low v sin i stars (sharp lined) but also 26 stars with v sin i > 60 km/s

> Select sub-samples of stars with sharp lines and broad lines

2) Individual Stellar Abundances

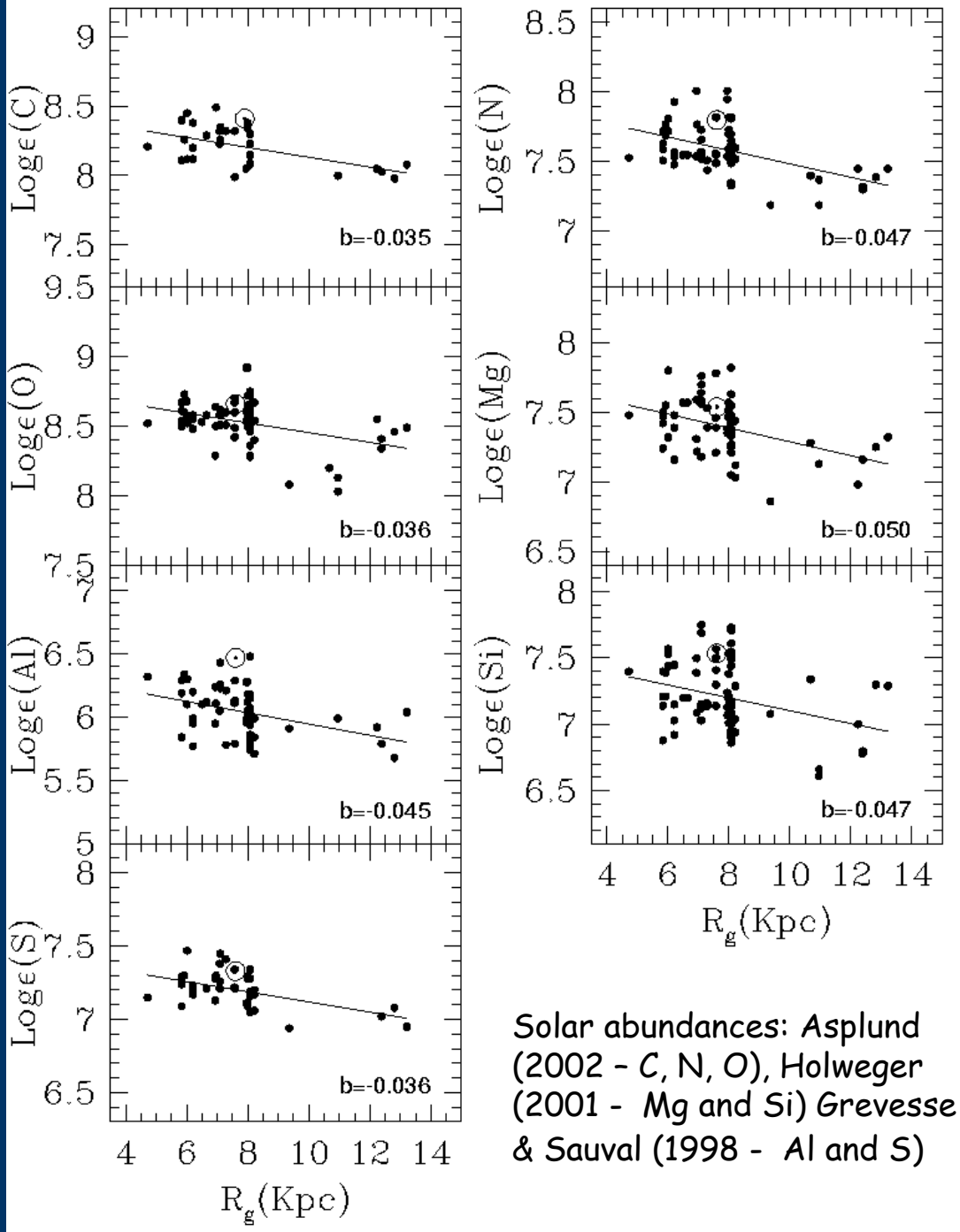

Solar abundances: Asplund (2002 – C, N, O), Holweger (2001 - Mg and Si) Grevesse & Sauval (1998 - Al and S)

- Using whole abundance database

Elem	Grad (dex kpc^{-1})
C	-0.035±0.013
N	-0.047±0.012
O	-0.036±0.012
Mg	-0.050±0.016
Al	-0.045±0.014
Si	-0.047±0.016
S	-0.036±0.010

<Grad> = -0.042 +- 0.006

➢Similar to grads obtained from mean cluster abunds (expected)

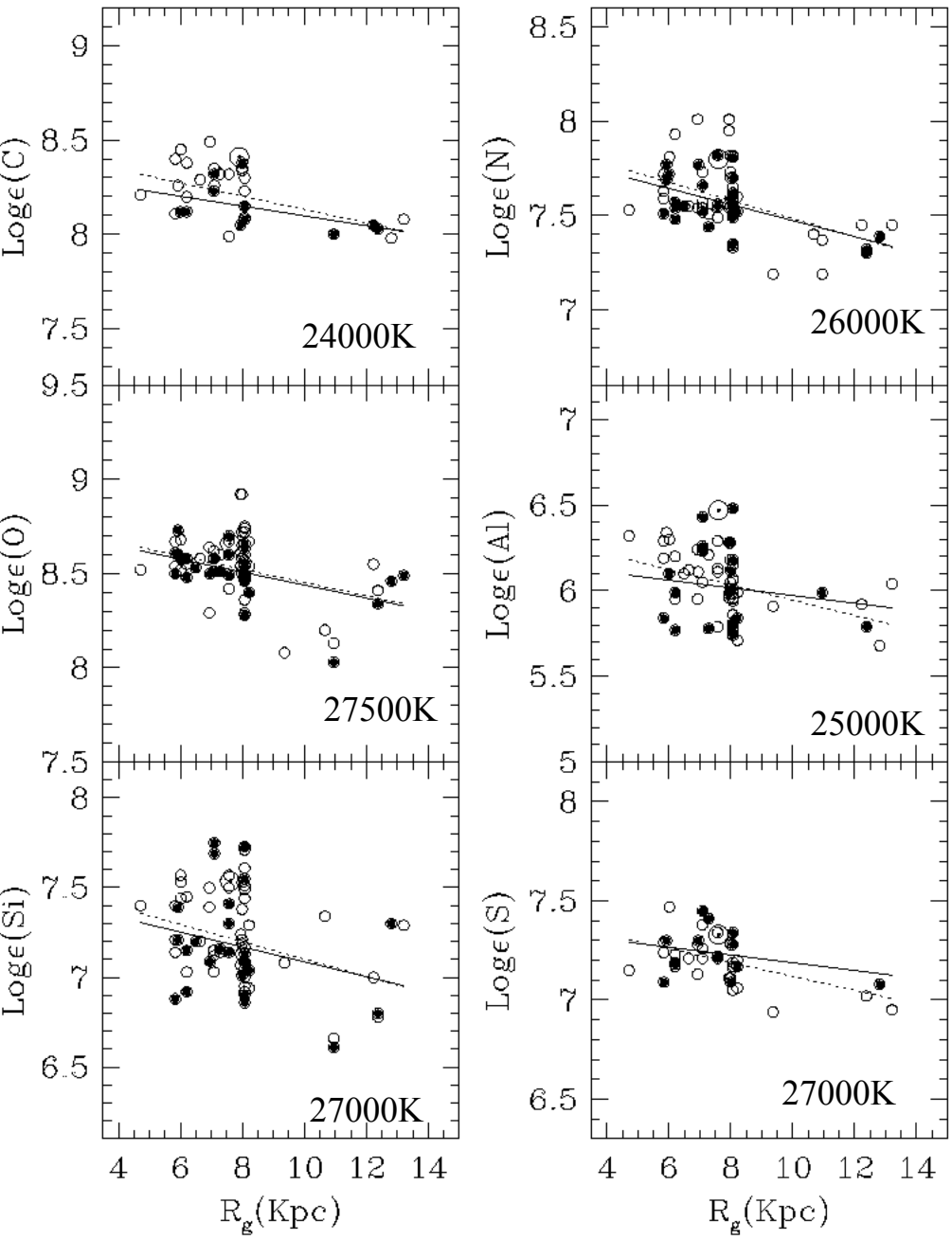

Sub-sample of stars within a restricted range in T_{eff}

- Centered @ ~T_{max}'s (line strengths reach maximum); within a 2-σ interval (+- 4%)

➢ Adopted sub-samples : **most reliable abundances** (filled circles; solid lines)

➢ span ~ original interval in R_g

➢ Differences in the derived gradients : oxygen ~ no difference (robust result)

➢ Tendency of finding slightly flatter gradients

Segregating the Sample in High & Low V sin i

Database : 7< v sin i < 190 Km/s

- V sin i distribution is biased towards low values ➔

- Selected stars that are preferencially sharp lined + also included high - v sin i stars (synthesis)

- Surface abundances may be altered by rotation : ^{14}N is enriched at the surface by a factor 2-3 (at the expense of ^{12}C and ^{16}O)

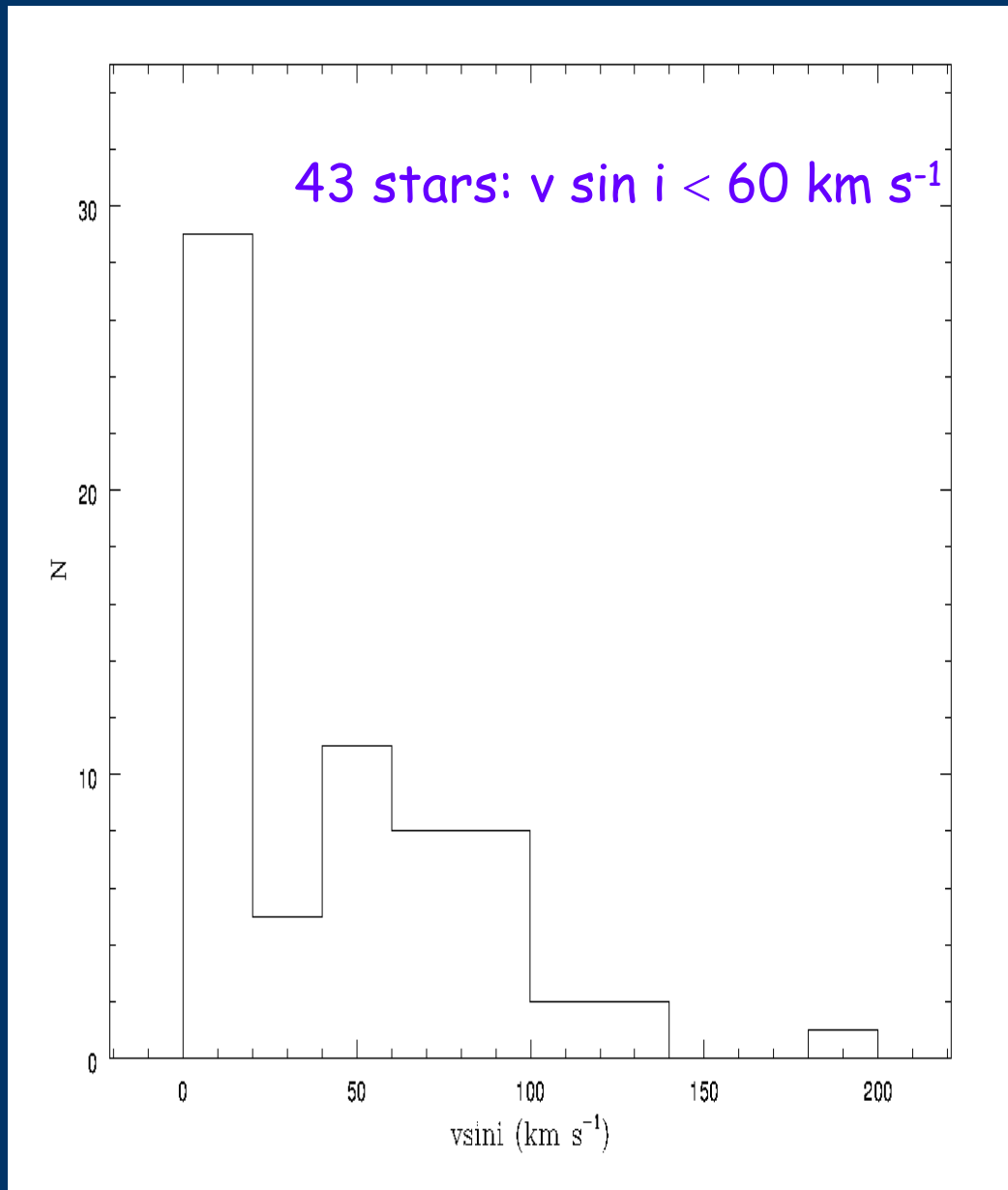

Sample high v sin i spectra

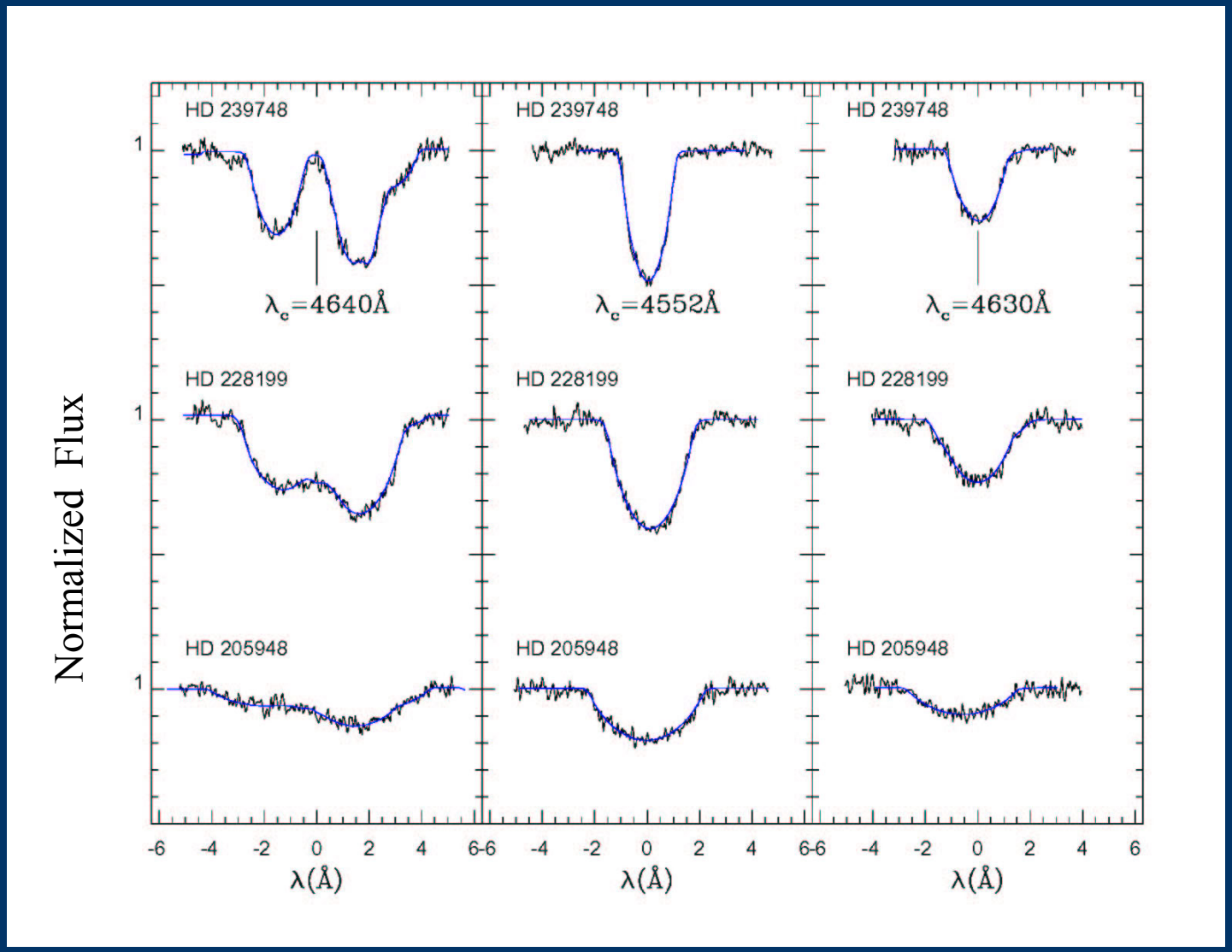

V sin i

(km s^{-1})

68

104

144

Line blending + rotationally induced mixing: Systematically different abundances?

• Oxygen abundance distribution for stars w/ high and low v sin i : ~ SAME

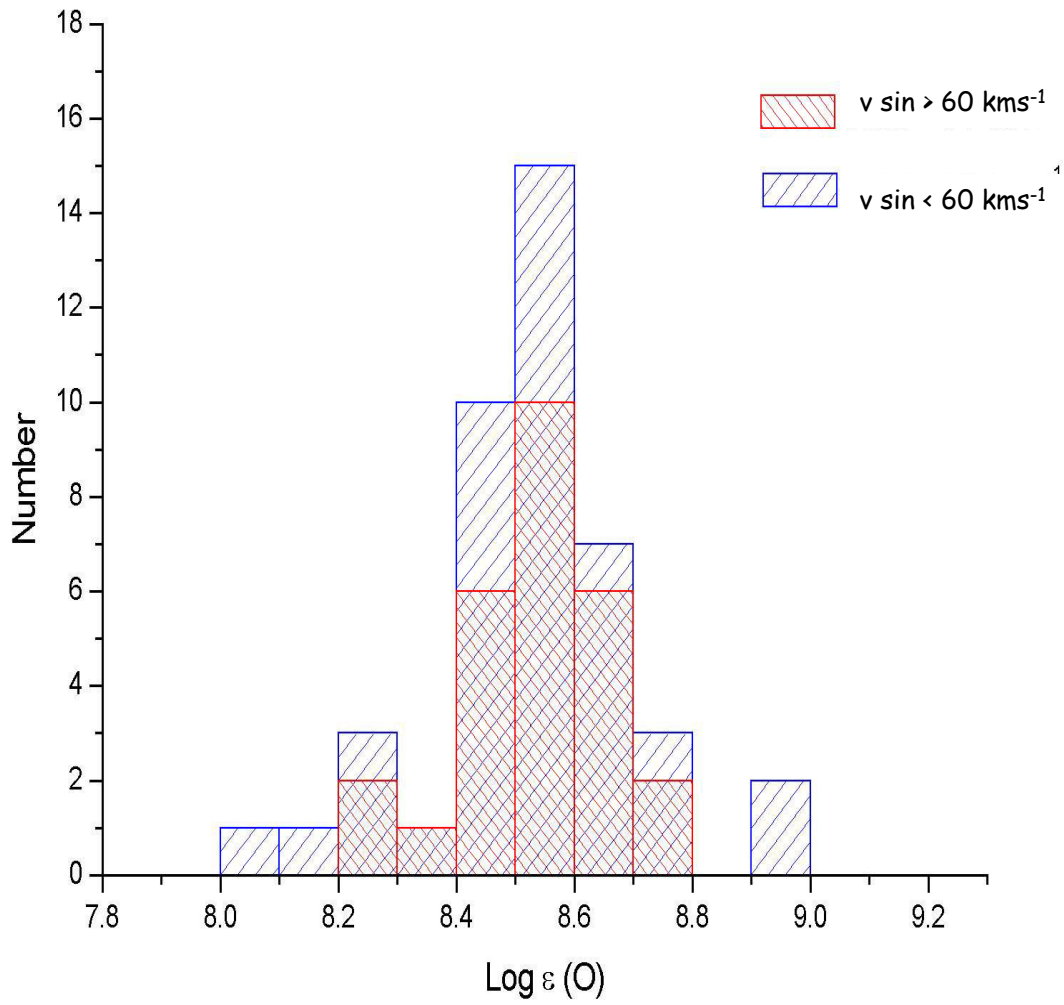

•→ No evidence of

a systematic trend:

No offsets

(Of course: Low v sin i is not a guarantee of slow rotation!)

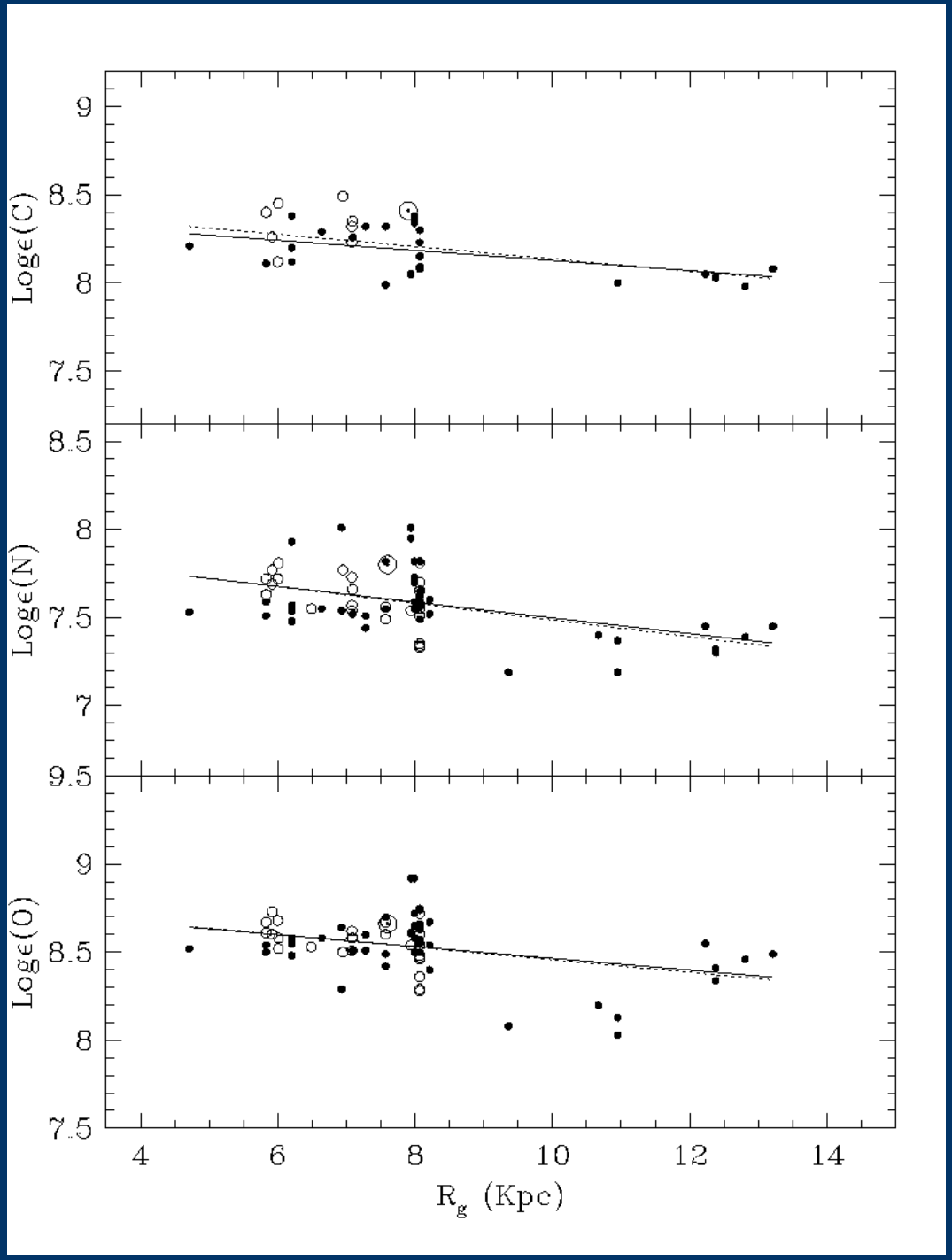

New gradients: Sub-sample of sharp lined stars (low v sin i)

• No significant differences in C,N, O gradients.

- Open circles > high v sin i
- Filled circles > low v sin i
- Solid line : grad with low v sin i stars only

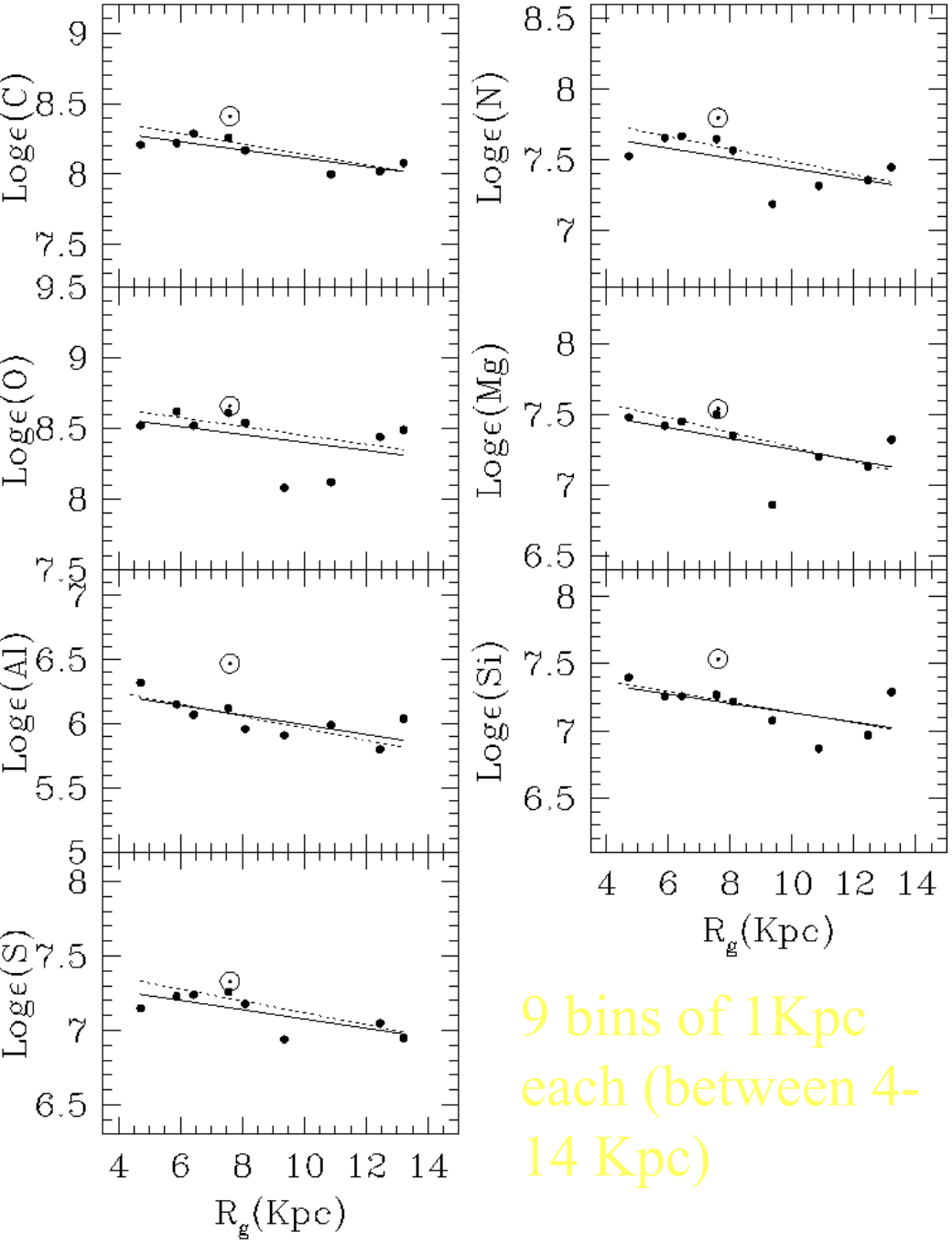

9 bins of 1Kpc each (between 4-14 Kpc)

Gradients from a sample Binned in Rg

- Our database contains 26 positions on the galactic disk
- Target stars are not homogeneously distributed along the disk >>> Heavily weighted towards the inner disk + scarcely sampled outwards

> Binned sample > Results in similar gradients (~ a little flatter)

Extending the sample [Oxygen]

Inclusion of 10 targets from other studies in the literature

- Abundances not directly taken from the literature
- Used Q-calib
- Published eqws (no spectra available)
- Average distances (+ Sun @7.9 Kpc)

- -0.045dex/kpc + Bigger dispersion [Not as steep as -0.07 dex/Kpc…]

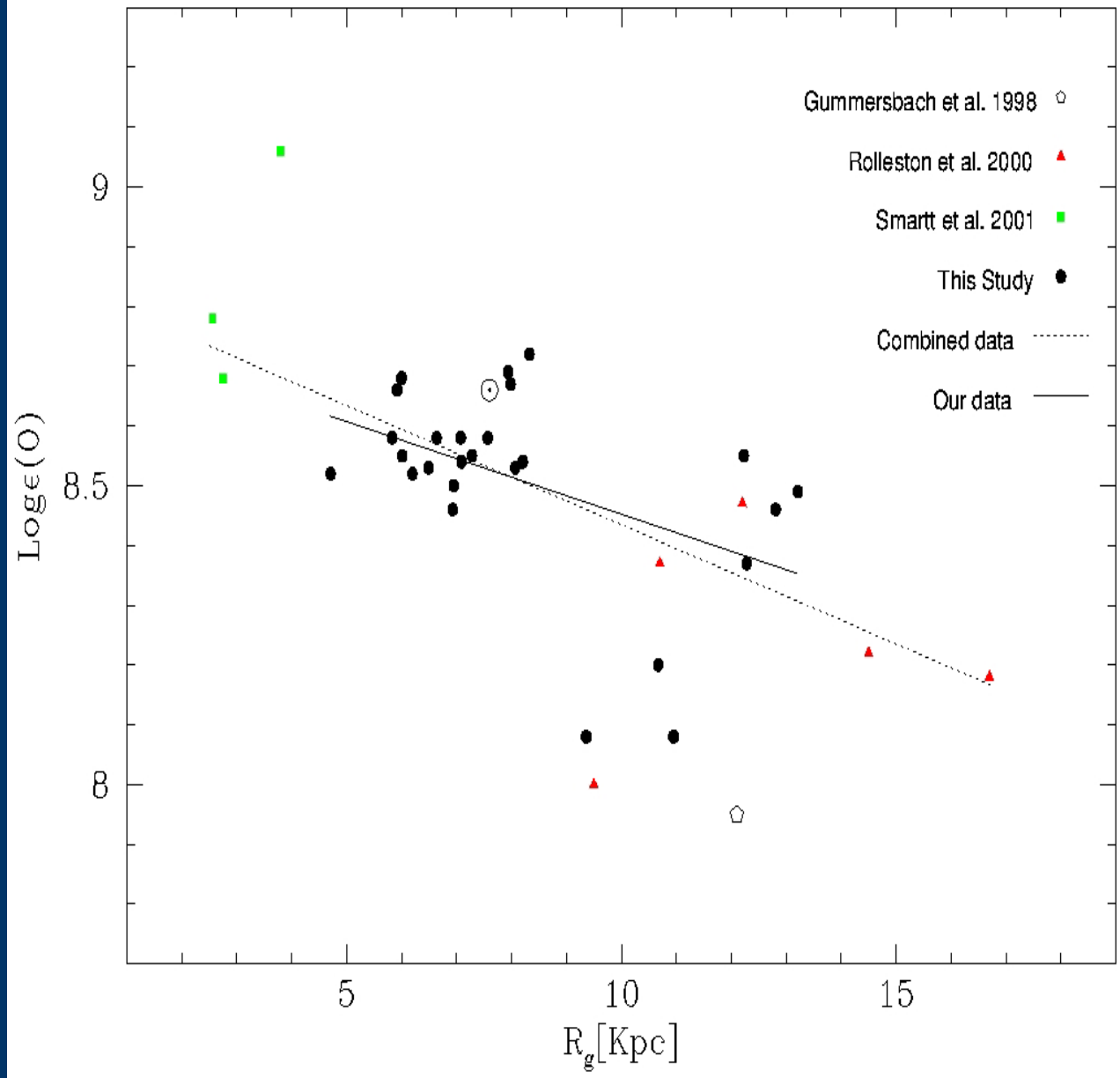

Galactic Chemical Evolution Models

- Several chemical evolution models are available in the literature > Must reproduce trends of abundances with R_g

- 3 models > that consider infall of external material in early phases of formation of the MW

- Chiappini et al. (2001) + private communication

  – Four different scenarios, according to halo evolution: **affect mainly the outer disk gradients**

- Hou et al. (2000)

  – Yields of massive stars only

- Alibés et al. (2001)

  - Infall of external material:

  1) primordial (grad (O)=-0.053)
  2) enriched (flatter grads; grad (O)=-0.047 dex/ Kpc)

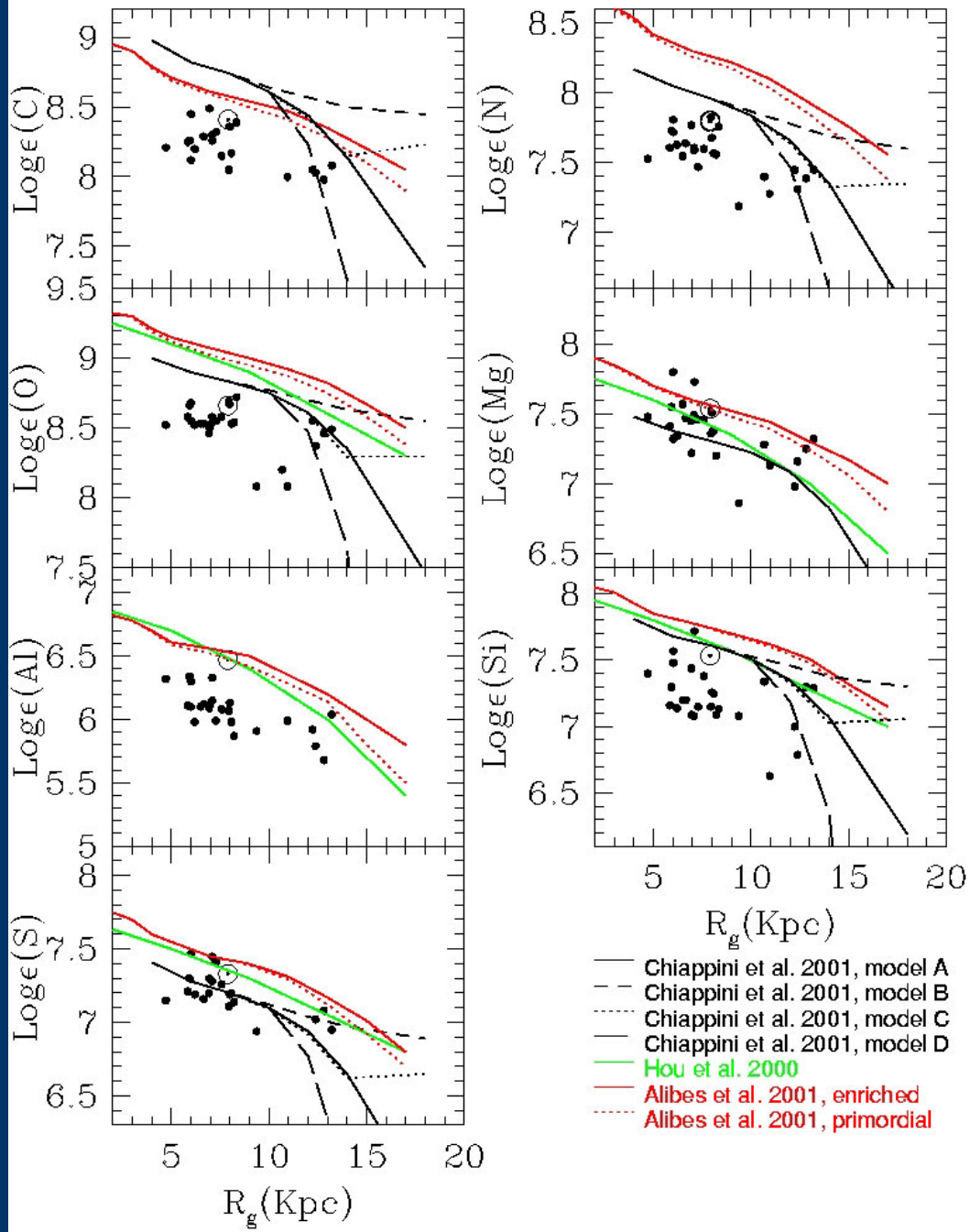

Abundance gradients > a tool for understanding the formation of the MW

- There is an offset between chemical evolution models and Solar CNO abundances

- In general, models do not seem to reproduce OB stars abundances either
  - ➢Models fall above

- Most recent HII region abundances also fall below models

- Note **low oxygen** results around 10Kpc

Galactic Chemical Evolution Models

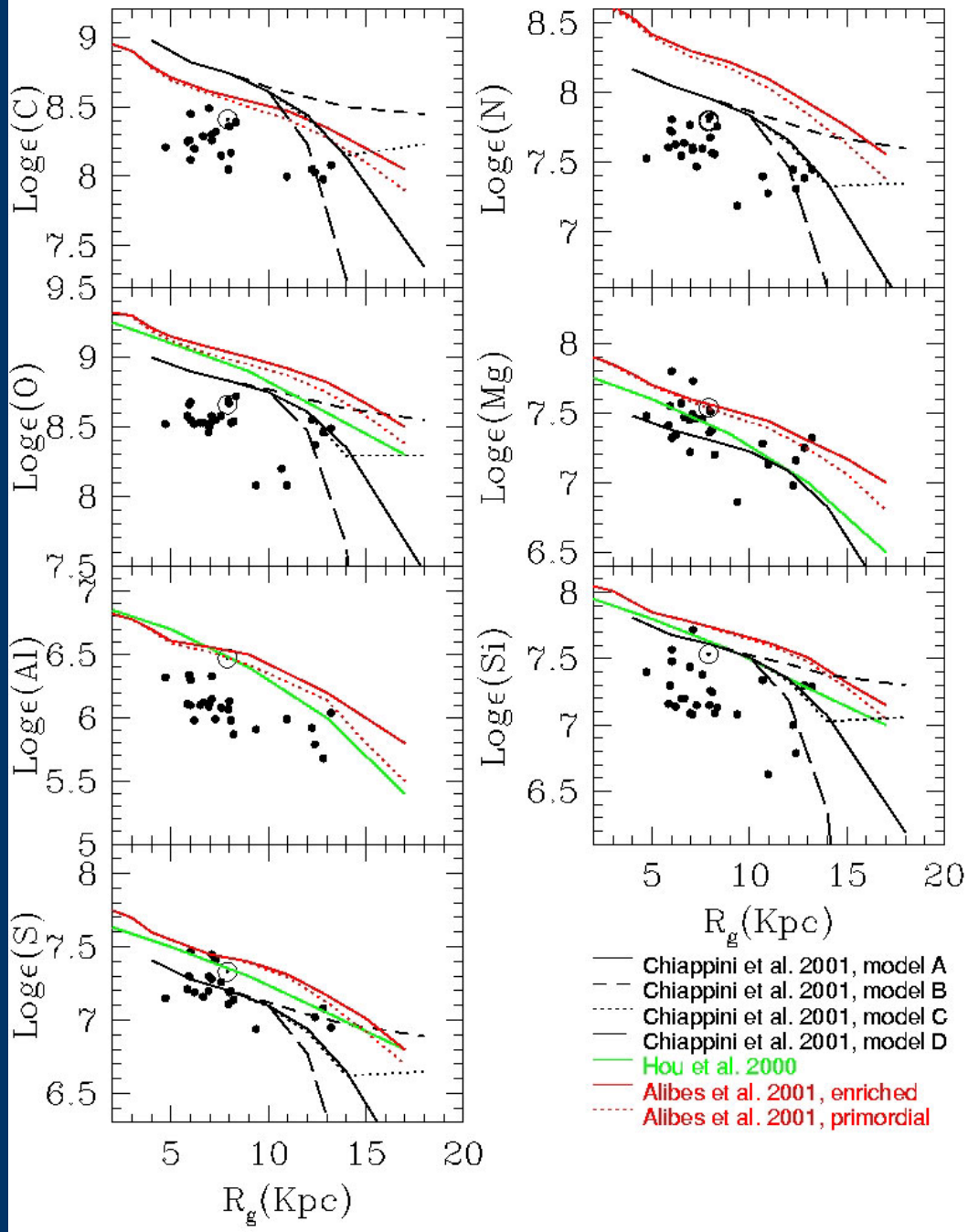

Time Evolution of the Abundance Gradients

Where do the young OB stars fit in?

(Previous gradients : -0.07 to -0.1 dex/Kpc)

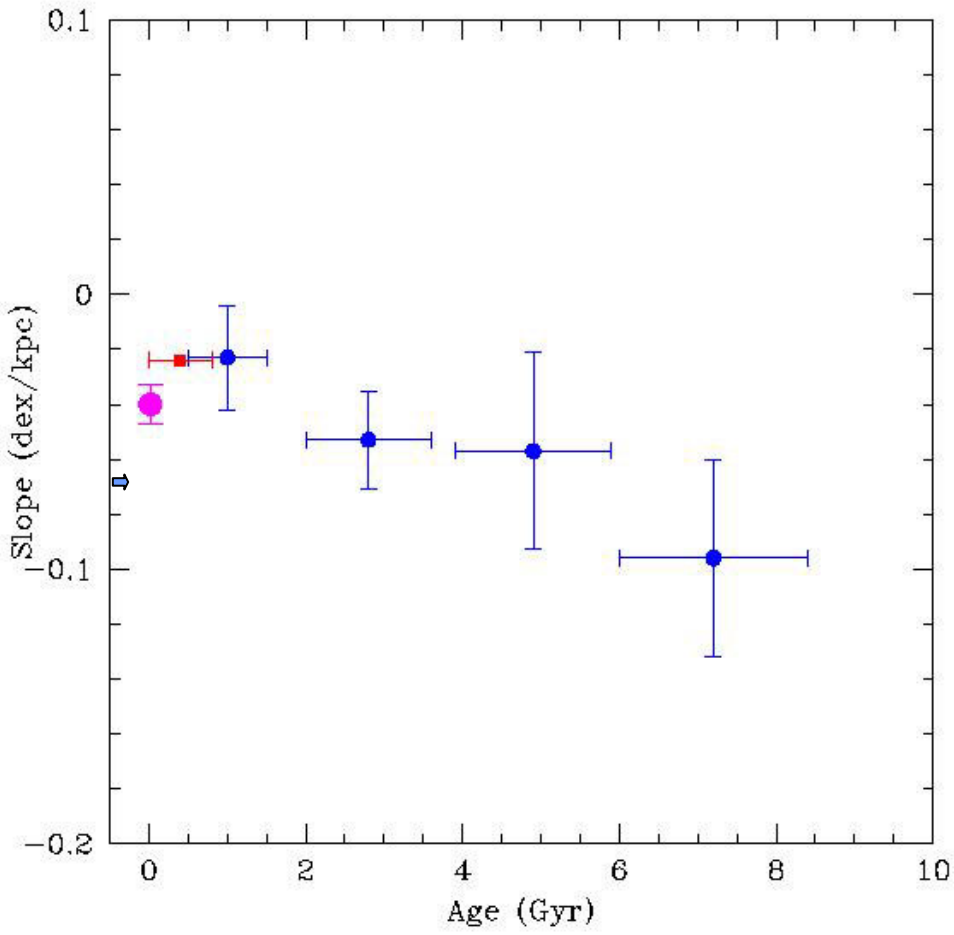

Open cluster data: Friel et al. (2002) + Chen et al. (2003)

Conclusions

- Abundance databases derived homogeneously provide an excellent means of investigating spatial and radial abundance variations in the Galaxy.

- We constructed a database of non-LTE abundances for a large sample of OB stars, between 4.7 and 13.2 Kpc away from the Galactic center.

- Results in : metallicity gradients for the Galactic disk of ~-0.04 dex/Kpc (for oxygen, in particular > -0.031 dex/Kpc)

- Metallicity Gradients obtained are flatter than results from recent studies of OB stars

....Conclusions....

- **Flatter:** More in line with gradients for a barred spiral Galaxy (almost no spirals with metallicity gradients around -0.07 dex/Kpc)

- Also more in line with open cluster results of flattening of gradients with time

- Also in line with results for 4 B stars within 2.5-5 Kpc analyzed by Smartt et al (2001) + results for 2 stars around 4 Kpc by Munn et al (2004) that find ~ solar oxygen (inconsistent with simple extrapolation of steep grads around -0.07 dex/Kpc...)

…. Conclusions …

- These flatter gradients are in ~ agreement with the most recent H II abundance results by Deharveng et al. (2000) and abundance re-assessments by Pilyugin et al. (2003)

- Also in rough agreement with average metallicity gradients found in studies of Cepheid stars

- Comparisons between OB abundance results and current chemical evolution models of the Galaxy show apparent offset, although flatter metallicity gradients are obtained for selected models

The CORALS Survey: Dust and Metals at 0.5<z<3.5

Sara Ellison

University of Victoria

Why Worry About Dust Bias?

Simple calculation based on local extinction laws.

E.g., in the SMC:

$$A_{1500}=12.5 \times E(B-V)$$

$$\longrightarrow \quad A_{1500}=12.5 \times N(HI)/4.4\times10^{22}$$

E.g., a z=3 QSO with an intervening DLA of N(HI)= 1×10^{21} atoms/cm^2 would suffer about 0.3 mags of extinction in the optical.

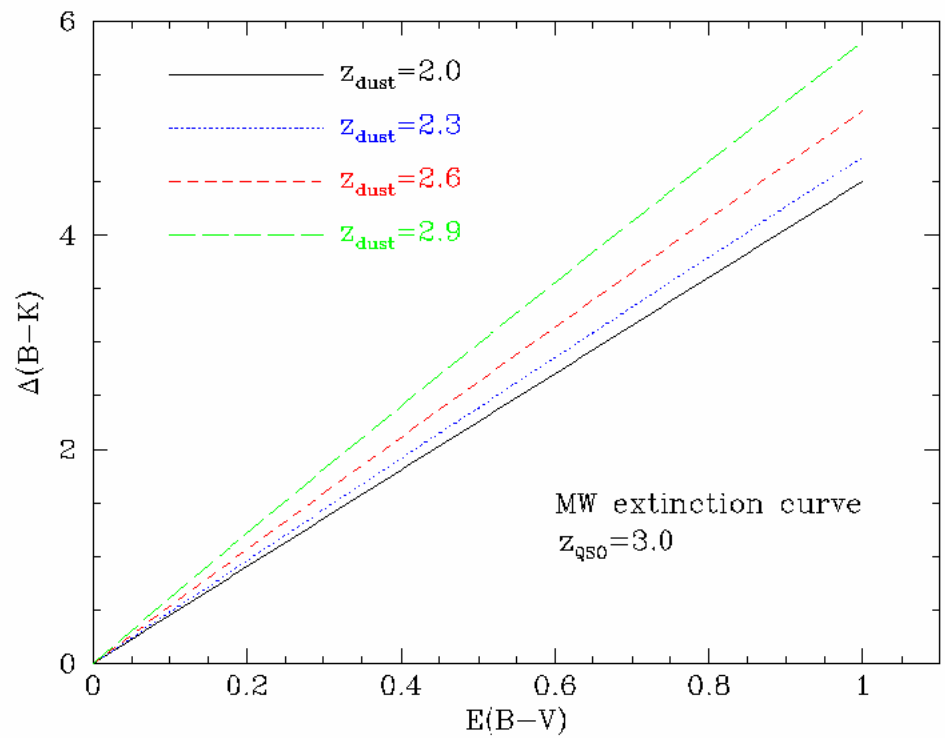

Why Worry About Dust Bias?

Theoretical motivation:
Several studies have investigated the effects of dust on QSO detection, either analytically (e.g. Fall & Pei 1993) or with simulations (e.g. Churches et al 2004).

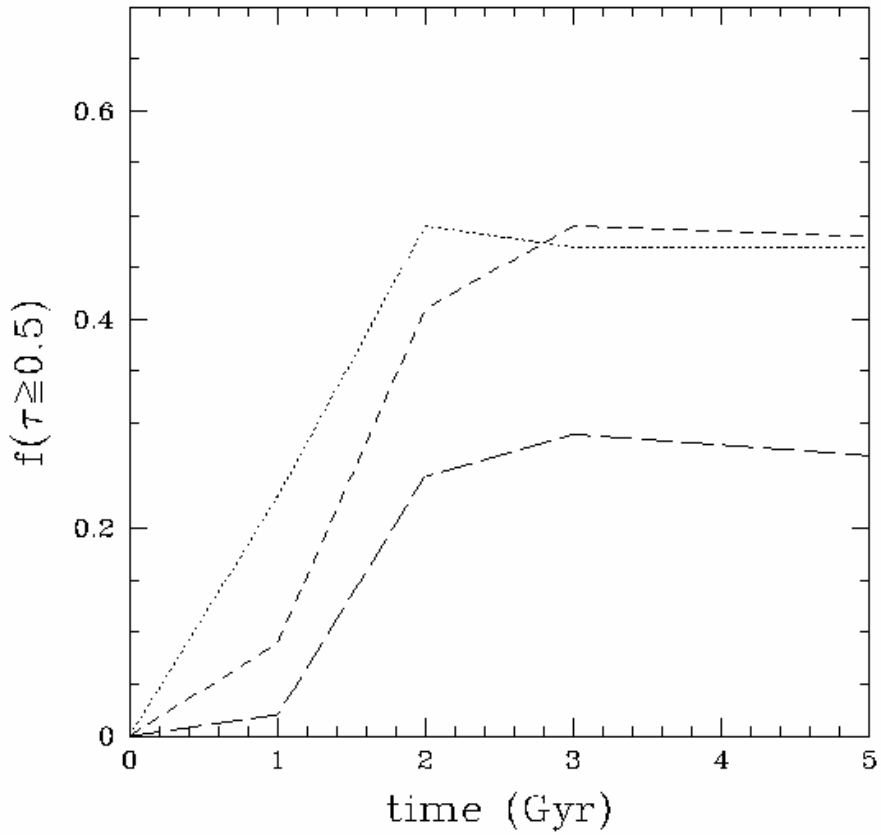

Why Worry About Dust Bias?

Observational motivation:

1) [Zn/Cr] ratios

- Anti-correlation of N(HI) and [Zn/H]
- Lack of [M/H] evolution

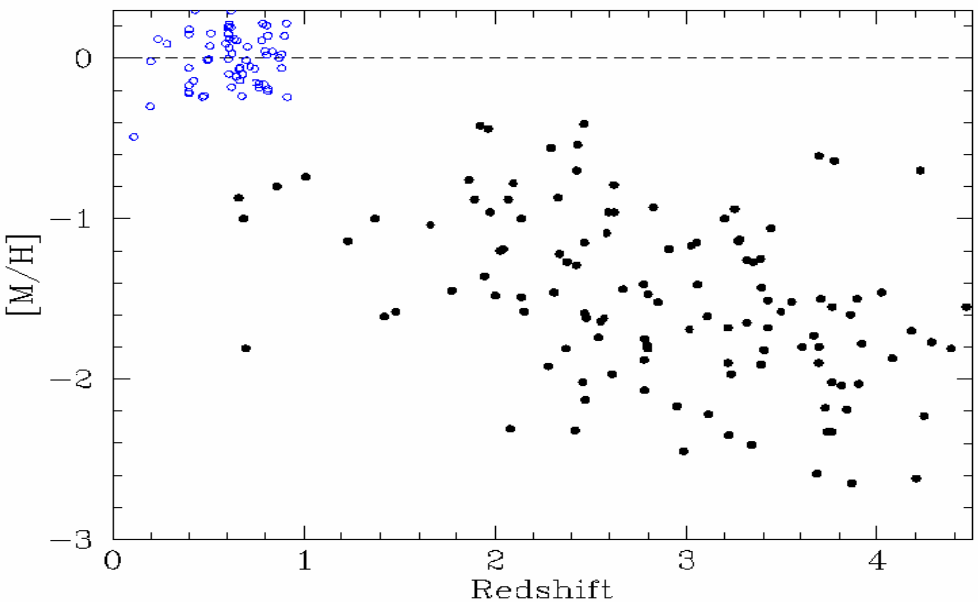

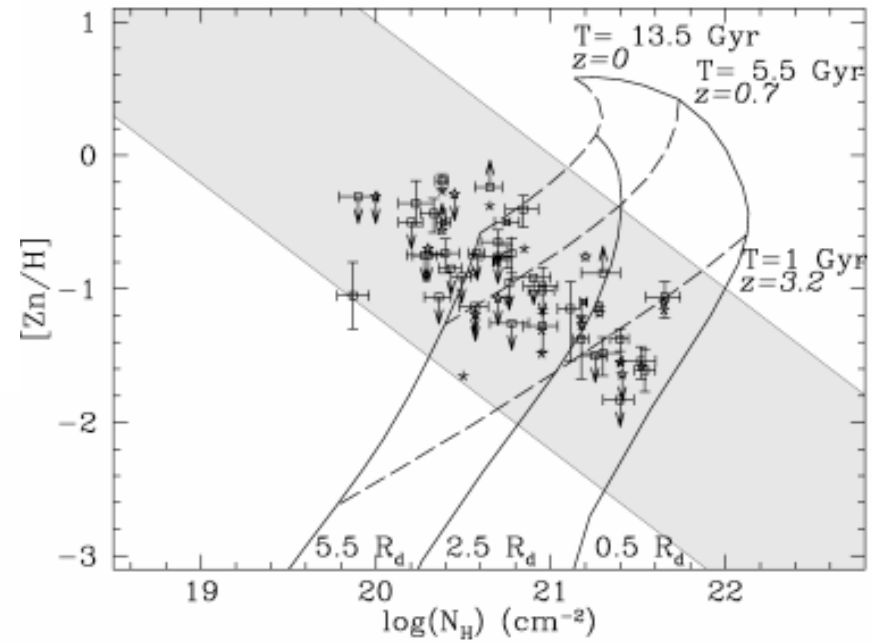

DLA metallicities and z<1 emission line galaxy abundances.

Are DLA surveys missing a lot of gas and metals??

The Complete Optical and Radio Absorption Line System (CORALS) Survey:

Lin Yan, Isobel Hook, Max Pettini, Jasper Wall, Peter Shaver

Strategy: Select radio loud quasars from the PKS catalogs (>0.25 Jy) and obtain complete optical identifications. Obtain moderate resolution optical spectroscopy for *every* QSO regardless of optical magnitude.

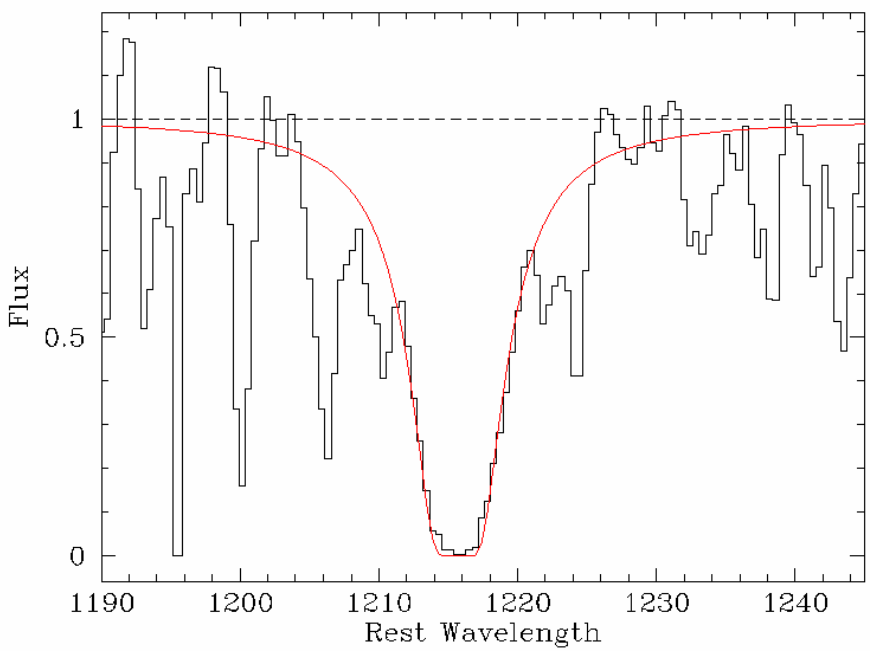

Vital Statistics:

66 QSOs $z_{em} > 2.2$

$16.5 < B\ mag < 24$

$\Delta z = 56$

19 DLAs

$1.8 < z_{abs} < 3.8$

Ω_{DLA}, the mass density of neutral gas in good agreement.

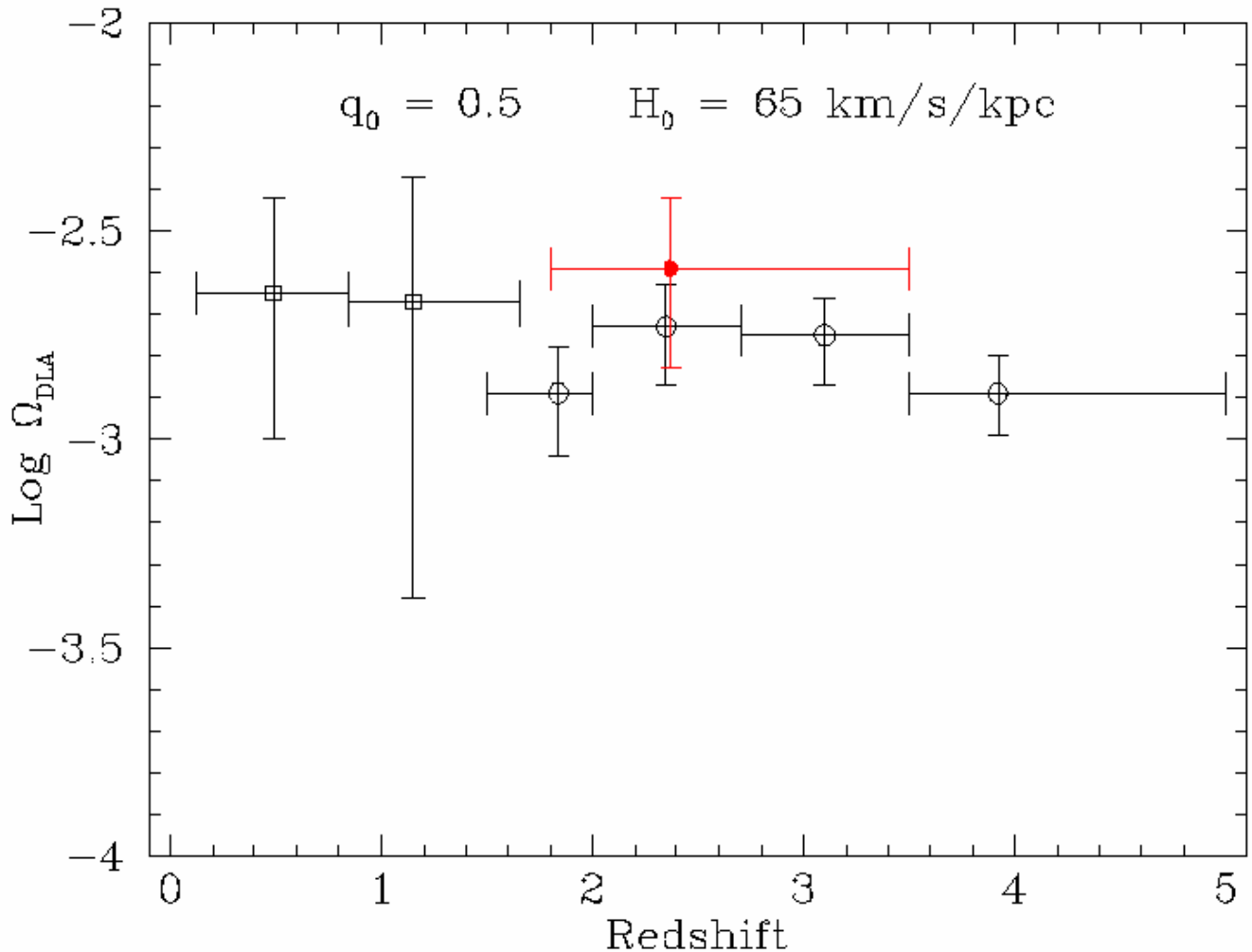

Ellison et al. (2001)

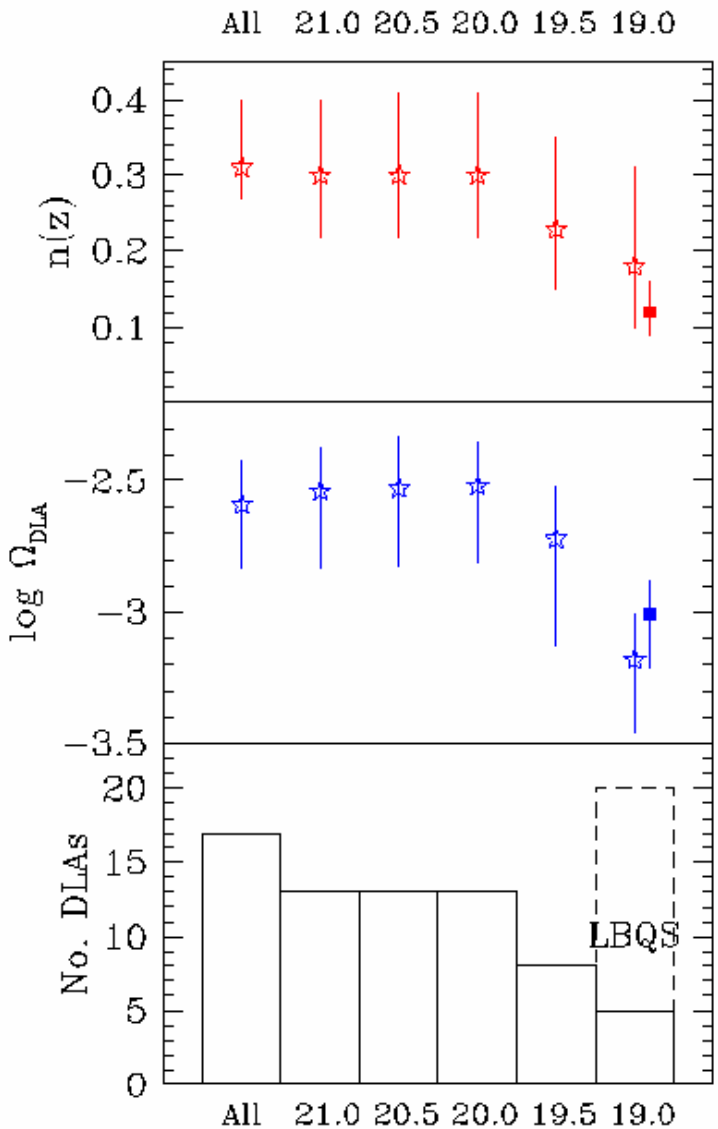

Statistics as a function of cumulative B band magnitude. Seem to reach asymptote by about B~20: Eddington bias?

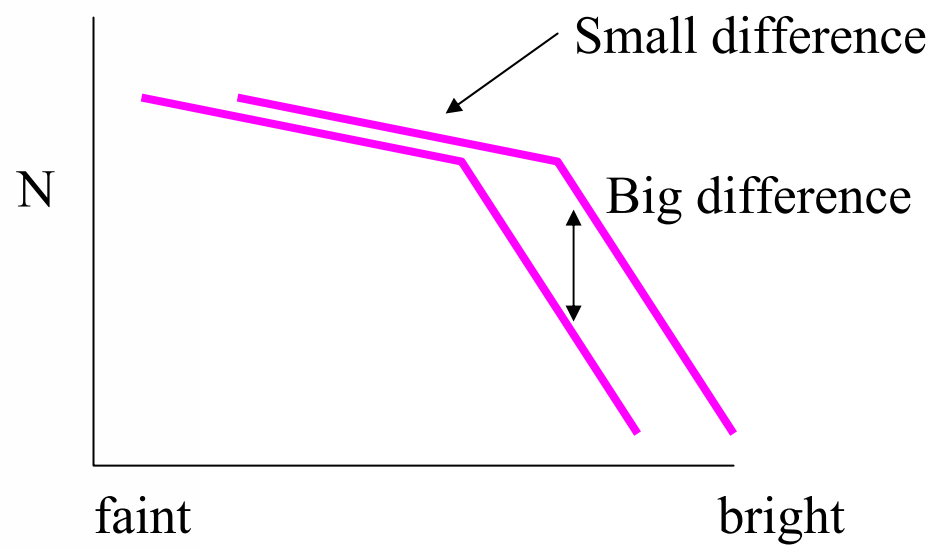

CORALS II: The Low Redshift Sequel.

Chris Churchill, Sam Rix, Max Pettini

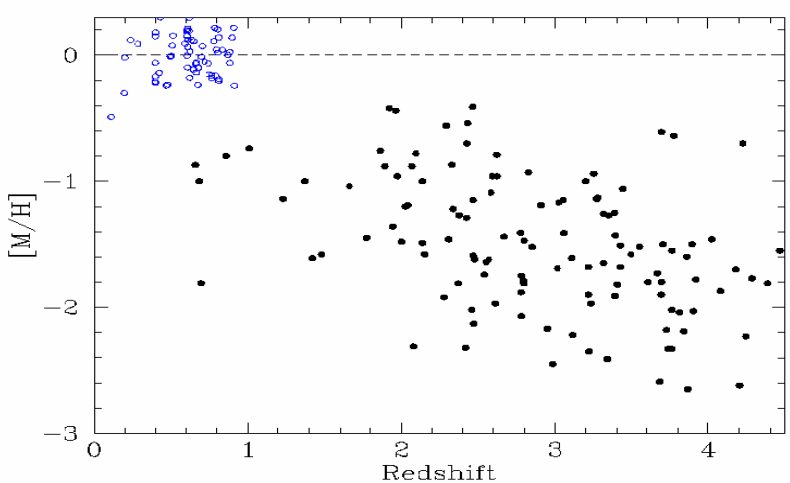

However, perhaps the more serious issue is at low z when most of the stellar mass has assembled and stars are major contributors of dust.

At z<1.5 select DLAs by MgII and FeII. DLA 'candidate' if EW(MgII, FeII)>0.5 Å. 50% confirmation rate.

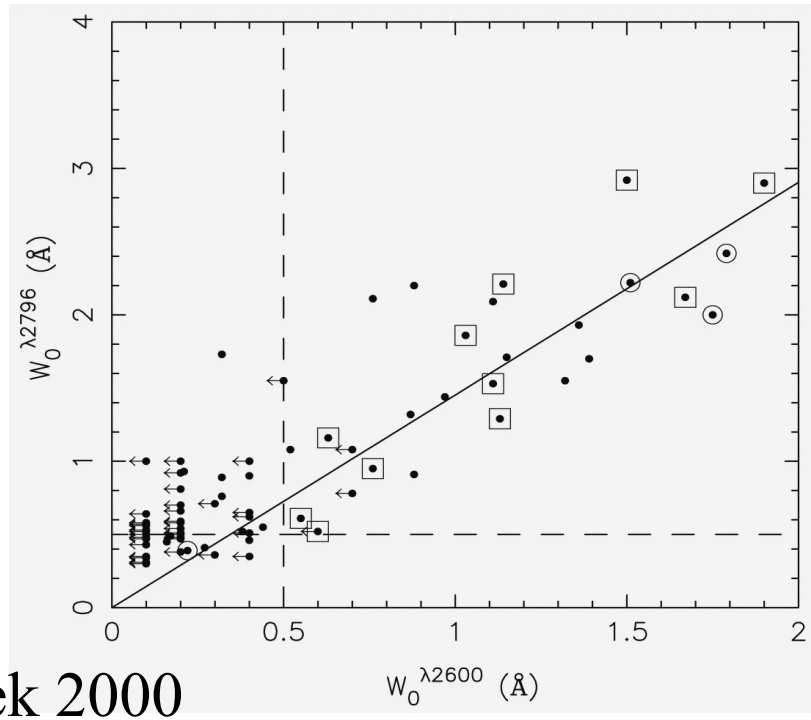

Rao & Turnshek 2000

Similar strategy to CORALS I: optically complete, radio selected sample. Line identification and fit via automated search

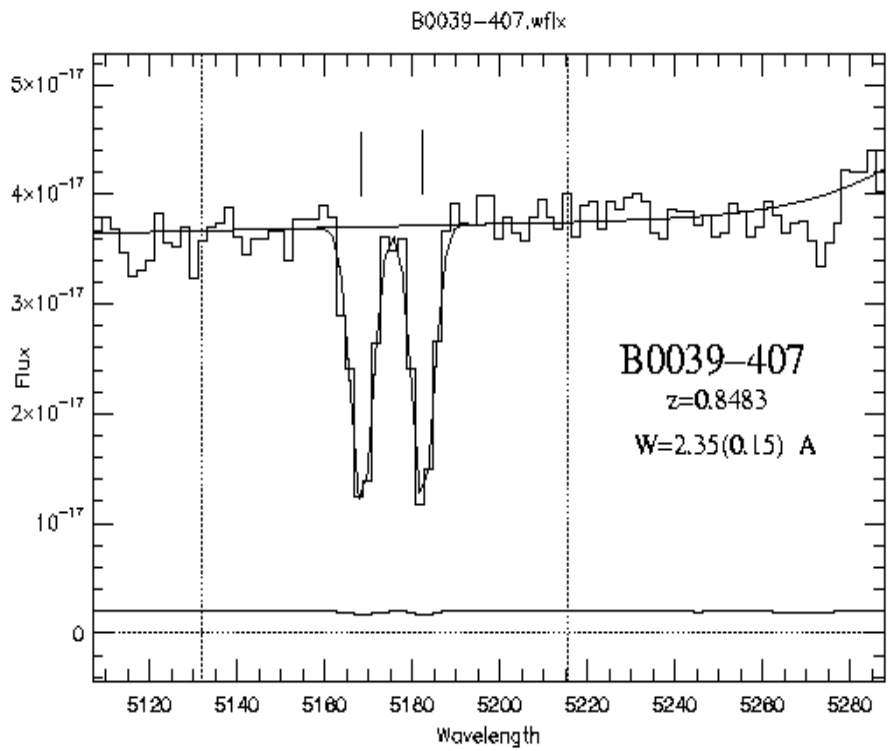

Vital Statistics

73 QSOs

Δz=58.2 (0.6 Å)

47 MgII systems

$0.6 < z_{abs} < 1.7$

14 DLA candidates

Calculate the number density of MgII absorbers above a certain EW threshold and compare with previous surveys.

Excellent agreement with the large SDSS sample of absorbers (Nestor et al.)

No evidence for a previous systematic under-estimate of MgII absorption systems.

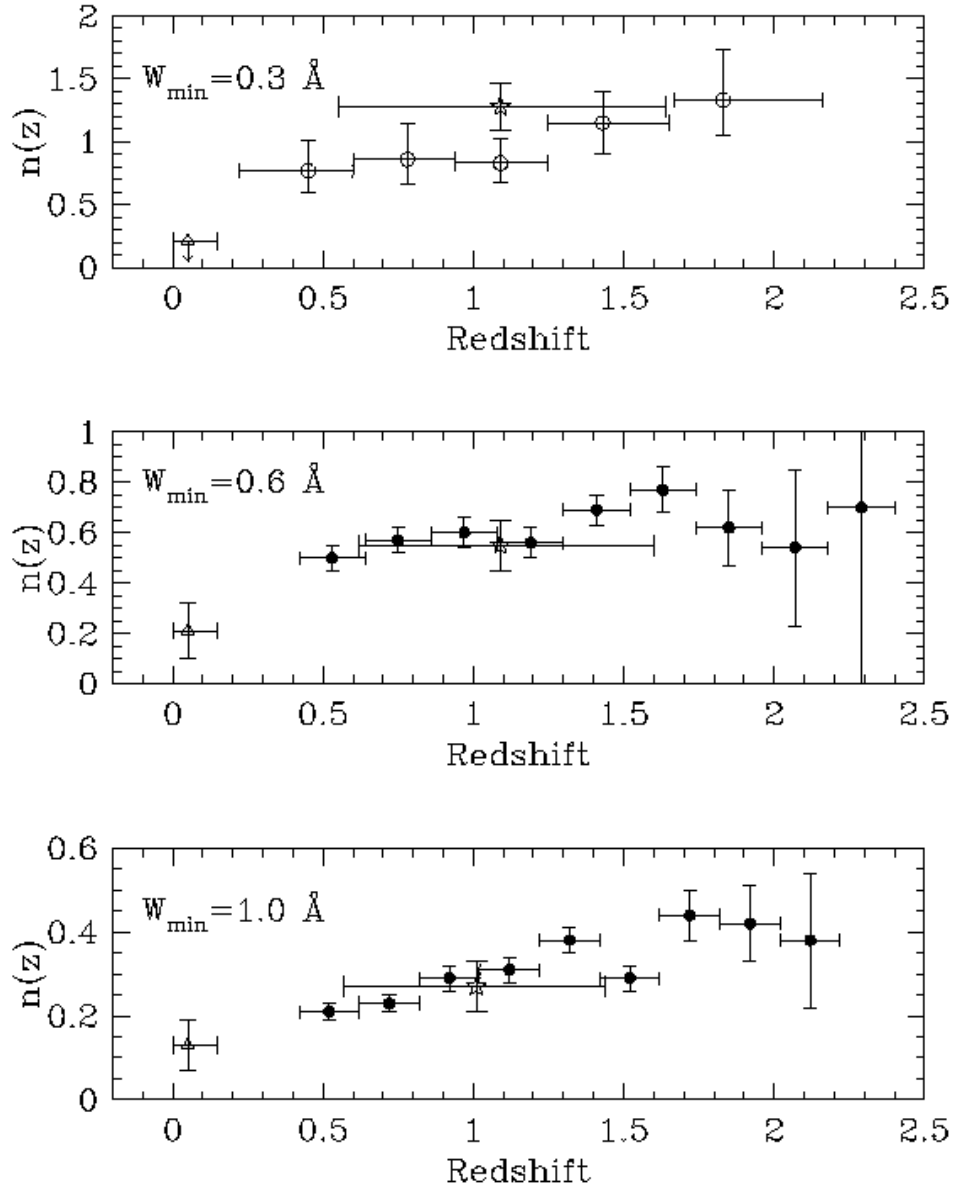

Ellison et al. 2004

Inferences on $n(z)_{DLA}$ at Low z

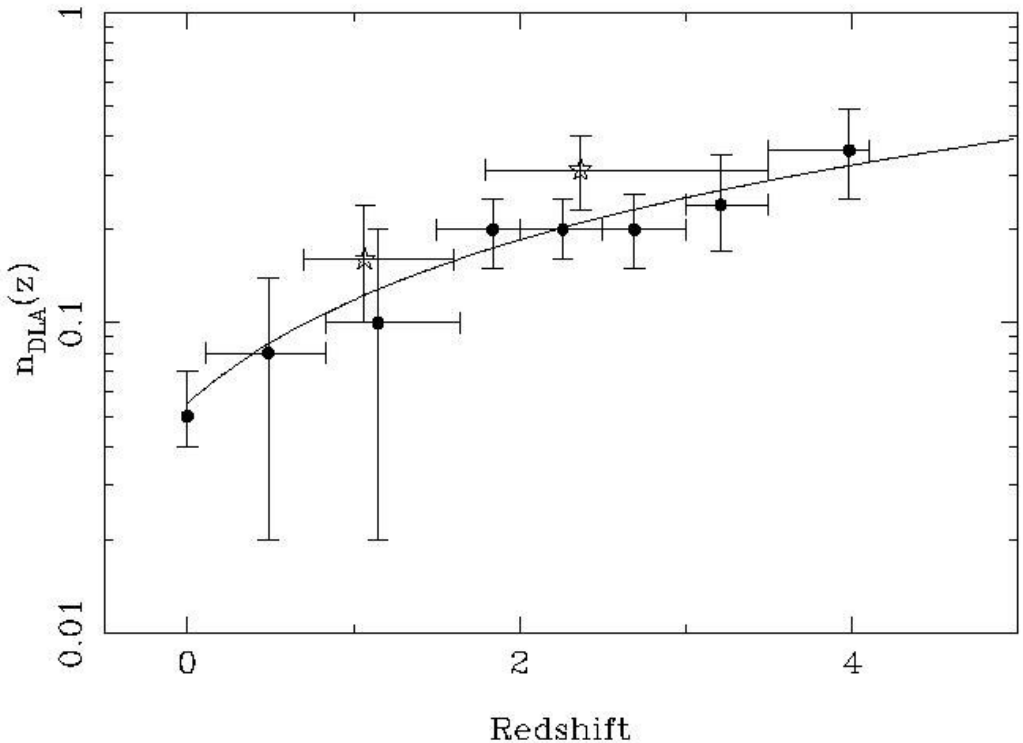

Ellison et al. 2004

Assuming that 50% of our MgII selected DLA candidates will be confirmed, we infer a number density of DLAs at 0.6<z<1.6 consistent with previous studies (but need HST follow-up).

CORALSZ: Metallicity Follow-up

Chris Akerman, Max Pettini, Chuck Steidel

High resolution follow-up (mostly with either VLT/UVES or Keck/ESI) of the DLAs in the high z CORALS I sample.

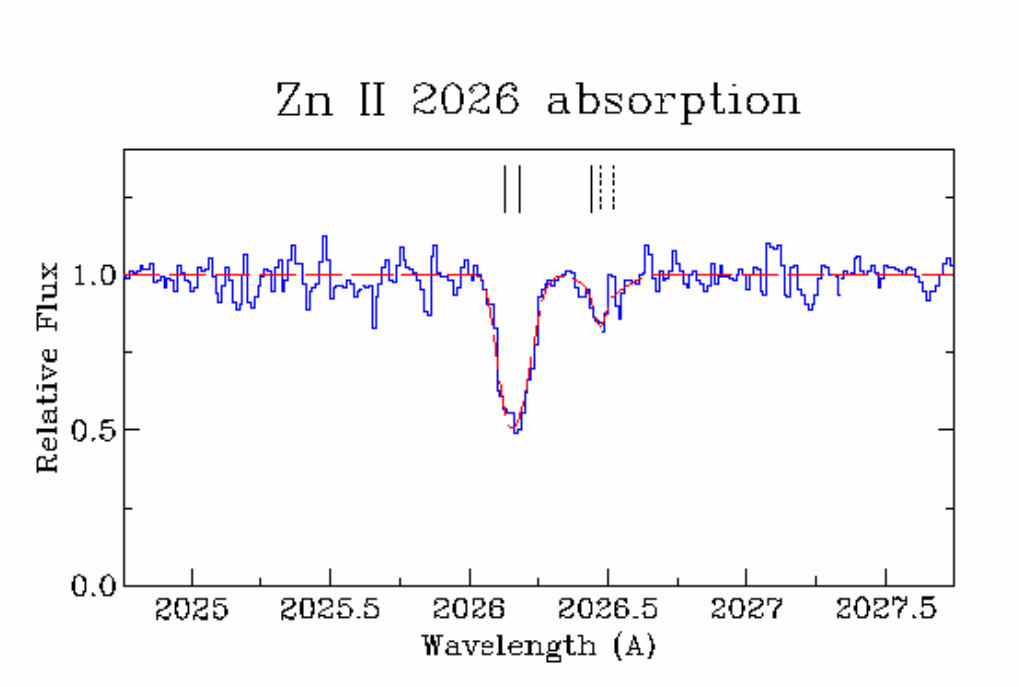

Vital Statistics

14/19 DLAs observed

<[Zn/H]> ~ -0.9

[<Zn/H>] ~ -1.1

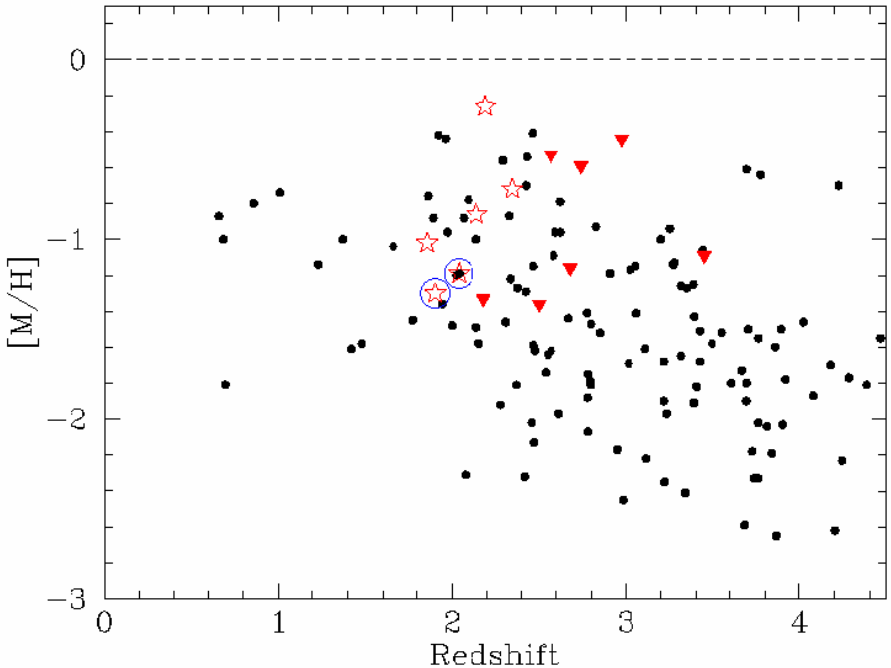

Metallicity of individual literature DLAs and CORALS DLAs.

Binned, weighted metallicities. CORALS point consistent with literature DLAs

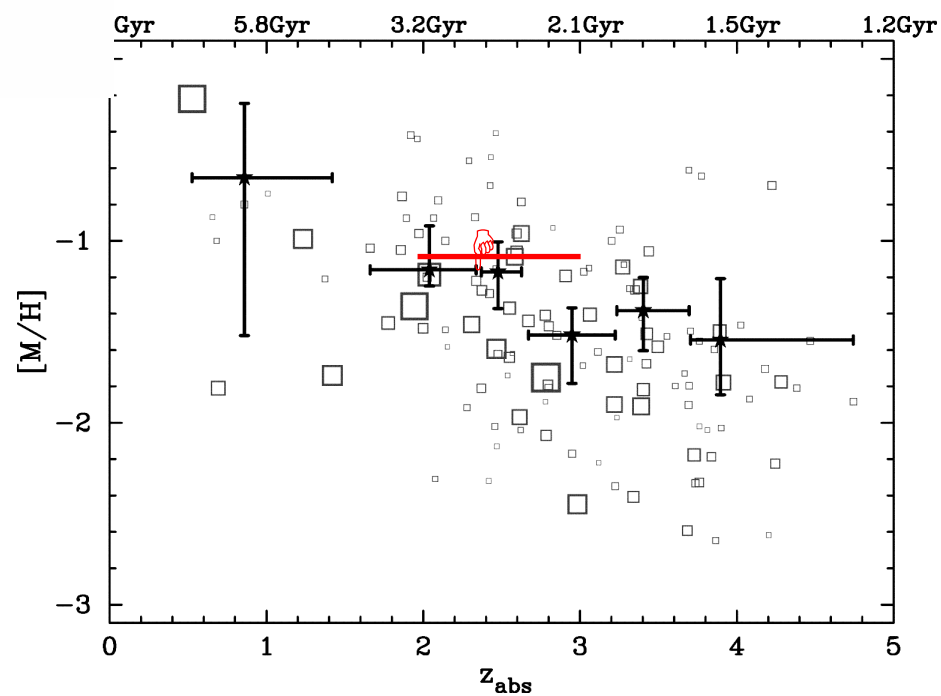

Prochaska et al (2003)

CORALS Summary

1. At z>2, the number density and gas content of CORALS DLAs is in good agreement with magnitude limited surveys.
2. Evidence of Eddington bias, indicating that completeness only necessary up to LF's knee (B~19.5)
3. At 0.6<z<1.7, the number density of CORALS MgII in excellent agreement with SDSS.
4. Inferences on DLA statistics in this low z interval indicate reasonable agreement with DLA n(z).
5. The weighted metallicity of the high redshift CORALS DLA sample is in good agreement with literature DLAs.

Overall: no evidence for missing a significant amount (more than about x2) of gas or metals due to dust bias

Is There a Missing Metals Problem?

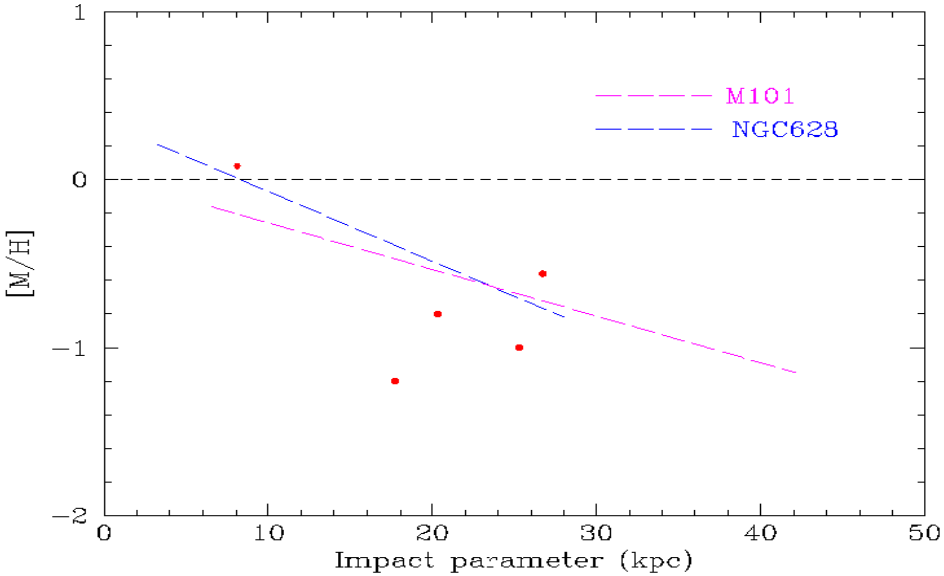

Look at DLA metallicities versus impact parameter. Metallicities low because they sample galaxy far out?

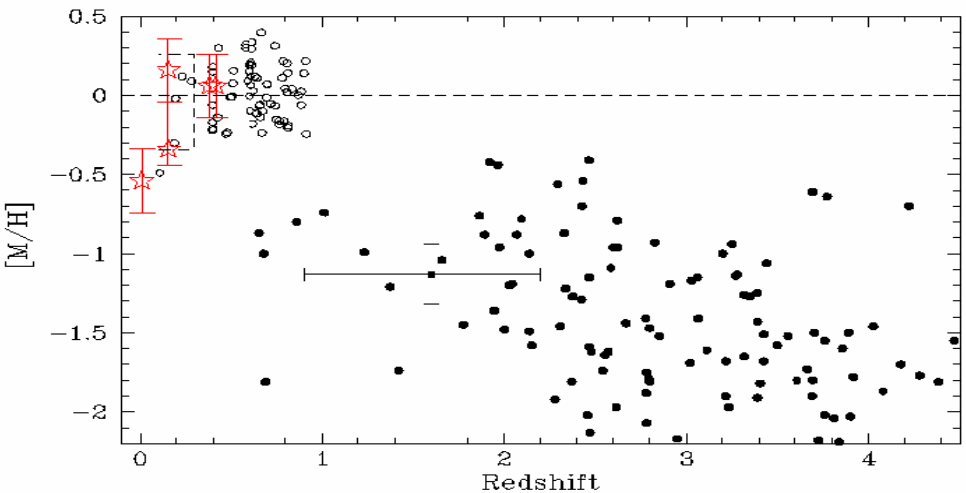

Determine emission line spectra of absorption (MgII) selected galaxies (central few kpc): solar metallicity.

Lead & s-process elements in stars of various metallicities: AGB predictions and observations

Roberto Gallino

Debora Delaude

Sergio Cristallo

Laura Husti

Sean Ryan

Oscar Straniero

THE AGB PHASE

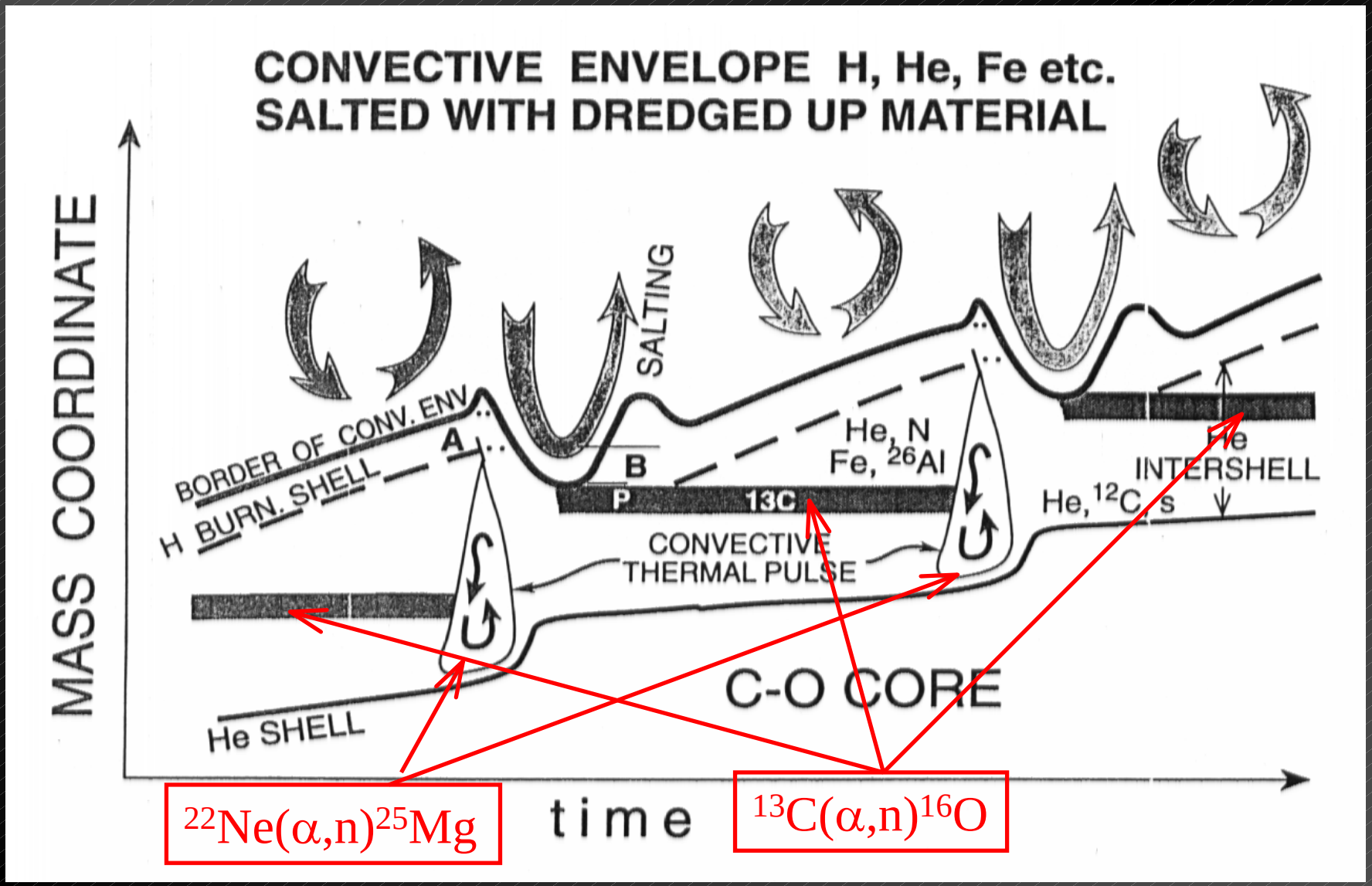

N-capture nucleosynthesis

Straniero et al. 95, Gallino et al. 98

Neutron source: $^{12}C(p,\gamma)^{13}N(\beta^+)^{13}C(\alpha,n)^{16}O$

Type: primary

When: interpulse T_6>90.

Where: intershell zone in LMS & IMS.

Density: 10^6-10^7 (neutrons/cm^3)

Iben 1974, Truran & Iben 1977

Neutron source: $^{22}Ne(\alpha,n)^{25}Mg$.

Type: secondary/primary

When: TP T_6>300.

Where: bottom of convective pulse of IMS.

Density: up to 10^{11} (neutrons/cm^3)

CNO→ ^{14}N $^{14}N(\alpha,\gamma)^{18}F(\beta+)$ $^{18}O(\alpha,\gamma)^{22}Ne$

Primary ^{22}Ne (due to the C dredge up) is probably the main n-source in low metallicity massive AGB.

Lead stars

- s-enhanced and lead-rich stars in the Galaxy. Few observations, lead requires HRS (R≥50000).

- Classical analysis ascribes most of Pb production to the *Strong component;* however, the astrophysical site is unknown.

- Predictions of AGB nucleosynthesis models (Gallino et al. 1998): a large Pb production is expected in AGB stars of low metallicity.

Why?

- Lead (^{208}Pb) and Bi are at the termination point of the s-fluence.

- With a primary-like neutron source, the amount of neutrons per seed increases with decreasing Z and lead becomes the major s-process product at low metallicity.

Nucleosynthesis (post-process)

From stellar models:

- Temperature and density in the PDCZ.
- Mass of dredge up.
- Envelope mass.
- N. of TPs with TDU.

Assumptions:

- Extension of the ^{13}C pocket.
- An average neutron density is used within the PDCZ, when the ^{22}Ne neutron source is marginally activated giving rise of a short neutron burst (- 6 yr) with a low neutron exposure, but a large neutron density (10^{10} cm^{-3})

see Gallino et al. 1998 for details

s-process versus metallicity.

[ls/Fe] vs [Fe/H] ls =(Y, Zr)

envelope last pulse condition

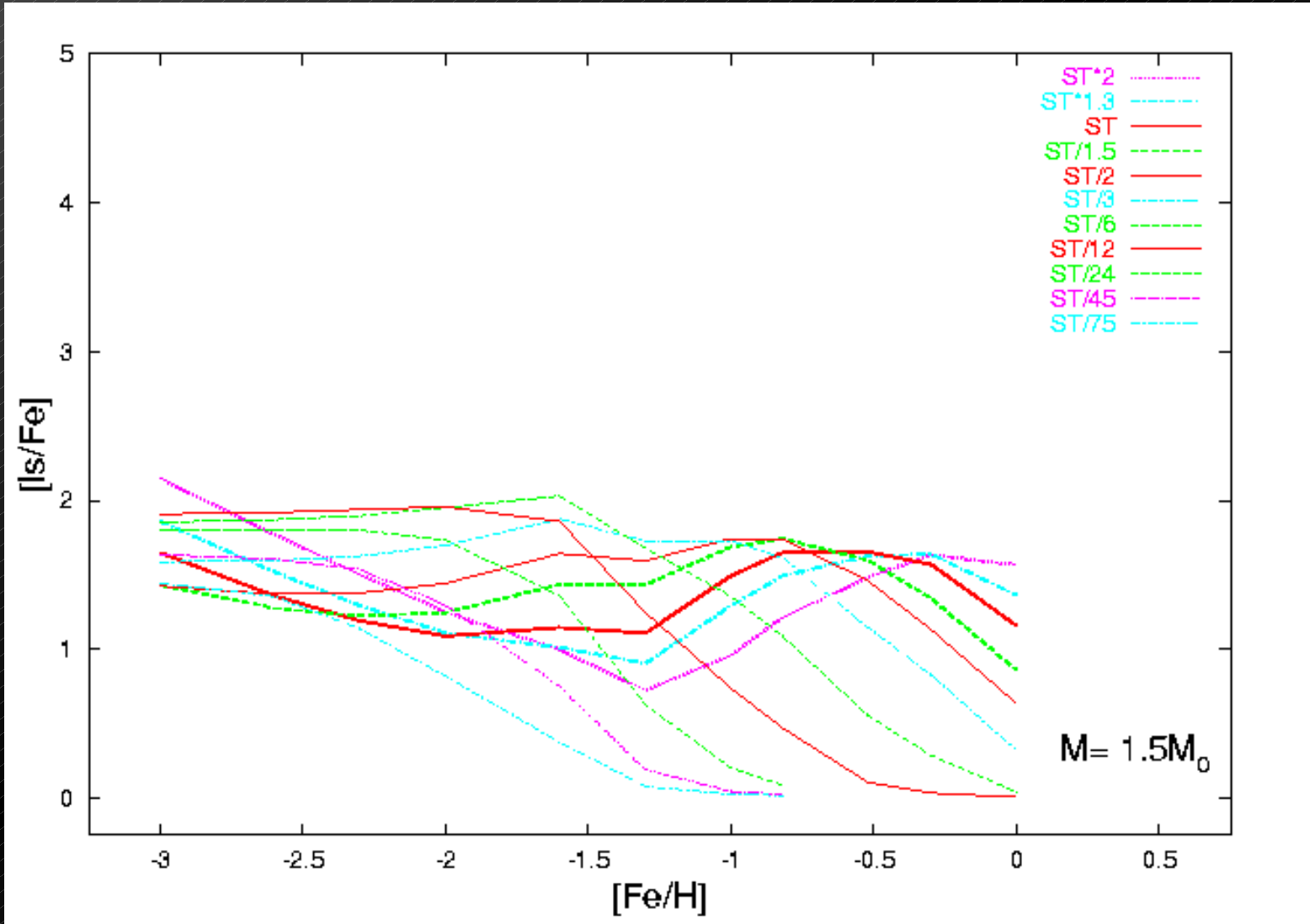

[hs/Fe] vs [Fe/H] hs =(Ba, La, Nd, Sm)
envelope last pulse condition

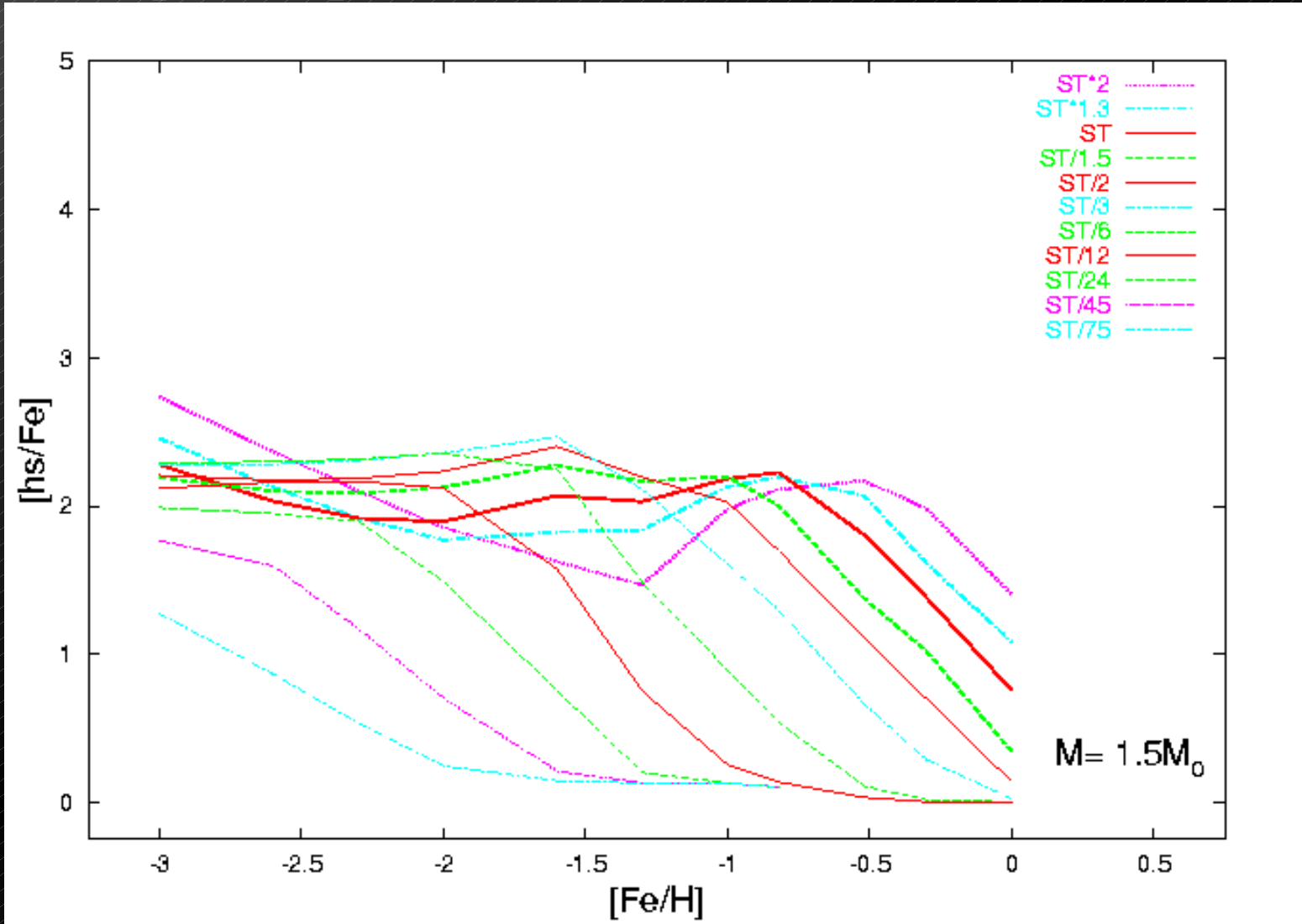

[Pb/Fe] vs [Fe/H]
envelope last pulse condition

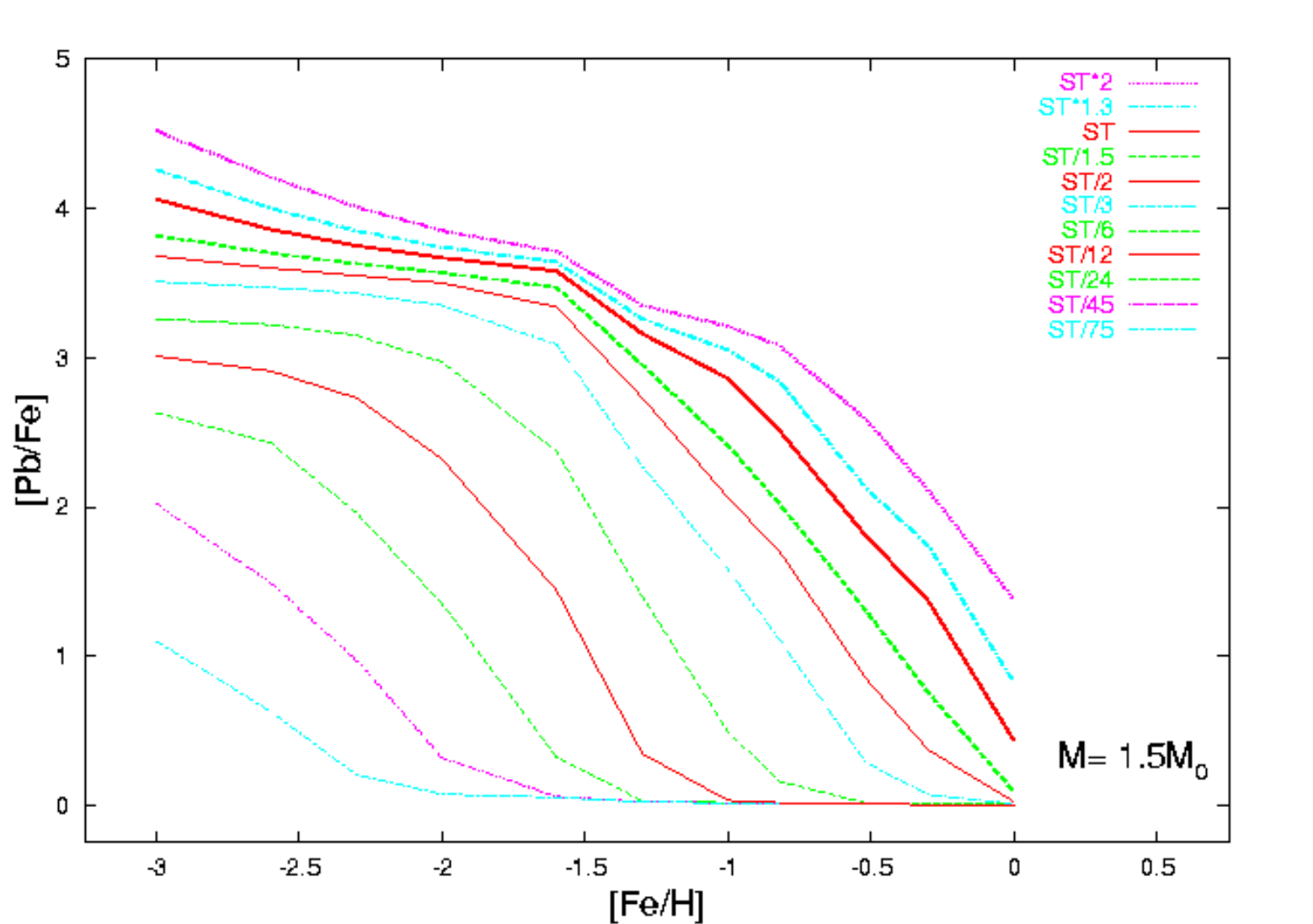

[hs/ls] vs [Fe/H] First intrinsic indicator envelope last pulse condition

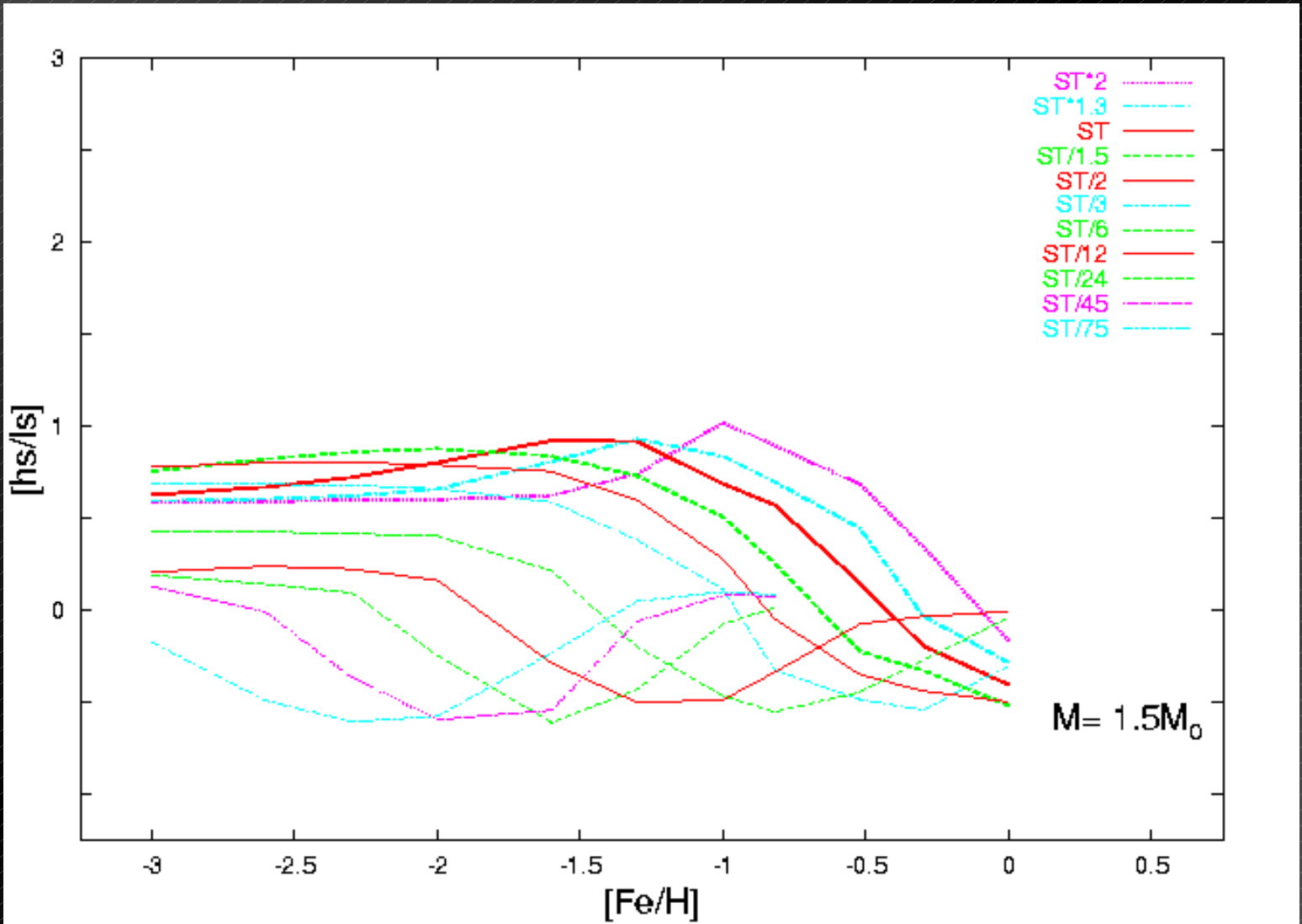

[Pb/ls] vs [Fe/H] intrinsic indicator
envelope last pulse condition

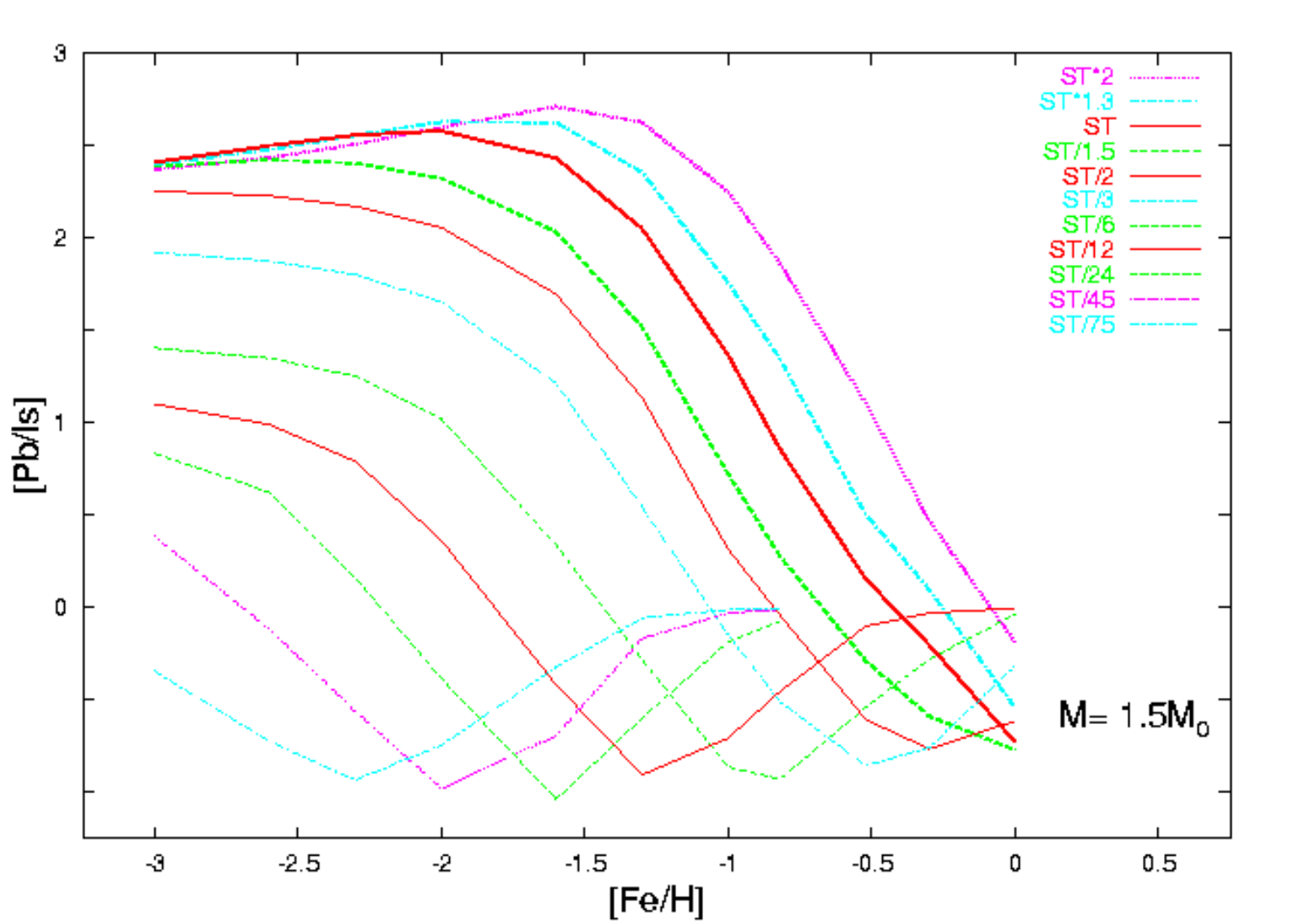

[Pb/hs] vs [Fe/H] intrinsic indicator
envelope last pulse condition

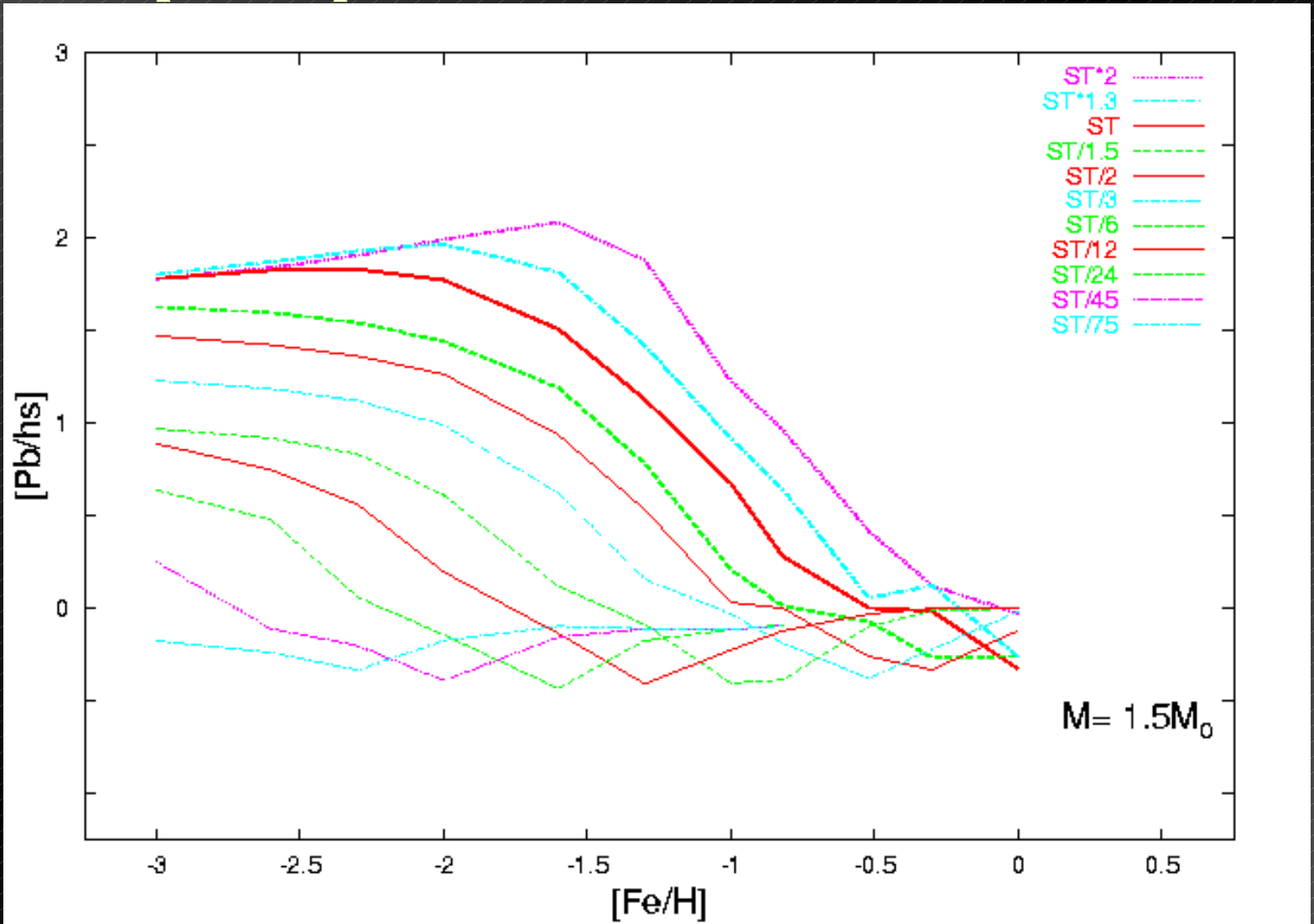

The 2 relative indexes [hs/ls] and [Pb/ls] (or [Pb/ls]) are intrinsic indicators of the s-process efficiency

They reflect the physical conditions at the s-process site

Working hypothesis:

Pb-stars are extrinsic C-stars: C and s enhancements are the result of an accretion process from an AGB companion, now a WD, occurred a few Gyrs ago.

Unknowns:

1. Main Sequence mass of the companion
2. Dilution factor
3. Pristine composition (especially r-process isotopes abundances)

Europium spread in the Galaxy (from Travaglio et al. 1999)

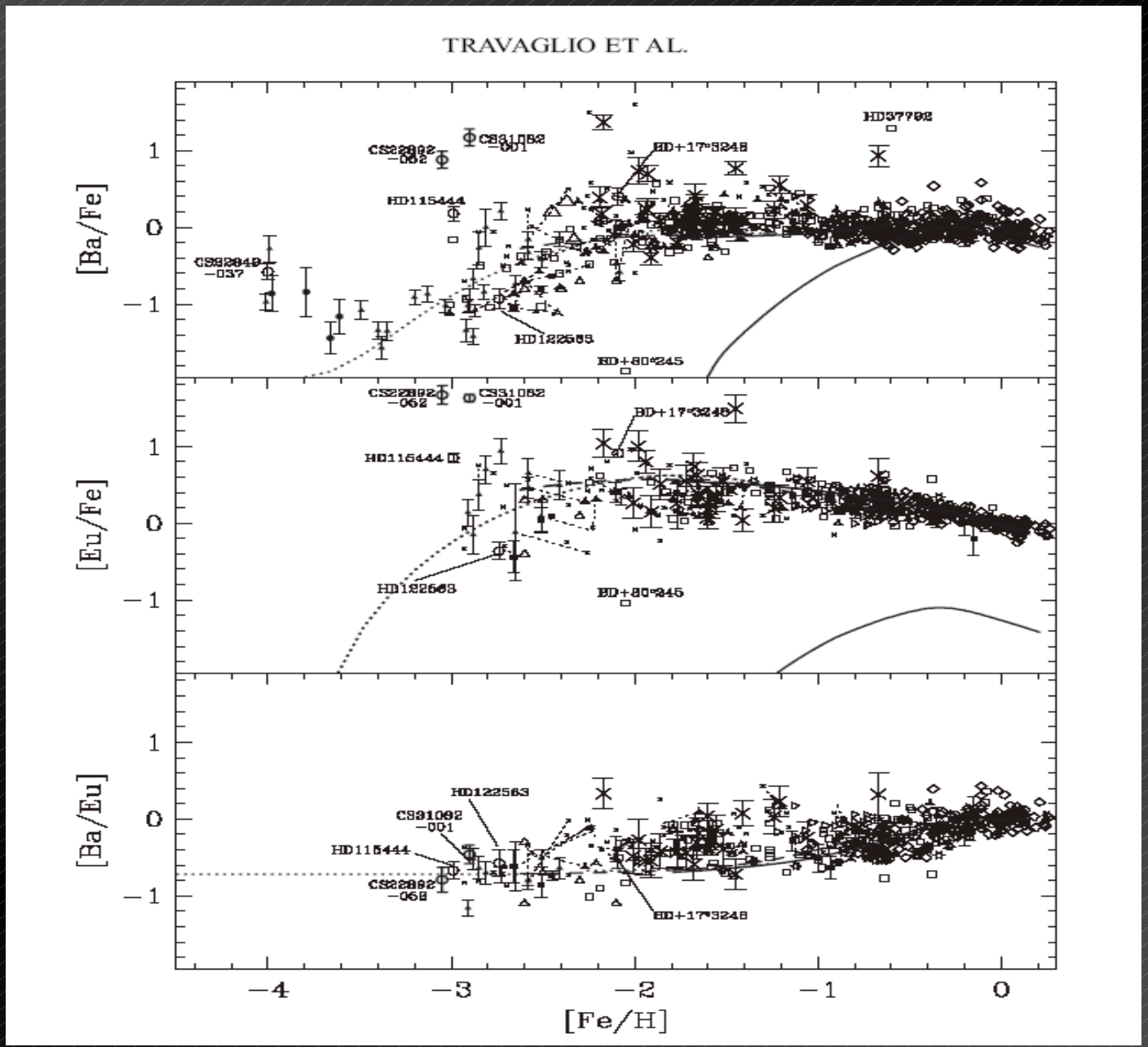

THE SAMPLE OF STARS

Object	T_{eff}	log g	[Fe/H]	[Pb/Fe]	Binary	Ref.	$M/M_{\odot}$	^{13}C pocket	dil	[Eu/Fe]
CS 22183-015	5200	2.5	-3.12	3.17	...	1	1.5	ST/1.5	0.65	1.0
CS 22880-074	5850	3.8	-1.93	1.90	no	2	1.2	ST/6	0.8	0.5
CS 22898-027	6250	3.7	-2.26	2.84	no	2	1.5	ST/3	0.3	1.5
CS 22942-019	5000	5.24	-2.64	≤1.6	yes	2	1.5	ST/45	0	0.5
CS 29497-030	6650	3.5	-2.70	3.55	yes	3	1.3	ST*2	0.4	0.5
CS 29526-110	6500	3.2	-2.38	3.3	yes	2	1.5	ST/1.5	0.2	1.5
CS 30301-015	4750	0.8	-2.64	1.7	...	2	1.3	ST/12	1.25	0.0
CS 31062-012	6250	4.5	-2.55	2.4	...	2	1.2	ST/18	0	1.5
CS 31062-050	5600	3.0	-2.31	2.9	...	2	1.3	ST/6	0	1.5
	5500	2.7	-2.41	2.81	...	4	1.3	ST/6	0.2	1.5
LP 625-44	5500	2.8	-2.71	2.6	yes	5	1.3	ST/12	0	1.5
HD 26	5170	2.2	-1.25	1.9	...	6	1.5	ST/2	0.8	0.5
HD 187861	5320	2.4	-2.3	3.3	...	6	1.5	ST/2	0.25	0.5
HD 189711	3500	0.5	-1.80	0.7	...	6	1.3	ST/24	0.4	0.5
HD 196944	5250	1.8	-2.25	1.7	...	2	1.5	ST/6	1.4	0.0
	5250	1.7	-2.4	2.1	...	6	1.5	ST/3	1.3	0.5
HD 198269	4800	1.3	-2.20	2.2	...	6	1.2	ST/9	0.4	0.5
HD 201626	5190	2.25	-2.10	2.4	...	6	1.5	ST/3	0.7	0.5
HD 224959	5200	1.9	-2.2	3.1	...	6	1.5	ST/2	0.35	0.5
HE 0024-2523	6625	4.3	-2.72	3.3	yes	7	1.5	ST	0.5	0.5
HE 2148-1247	6380	3.9	-2.30	3.12	yes	8	1.5	ST/3	0.15	2.0
V-Ari	3580	-0.2	-2.40	1.0	...	6	1.2	ST/30	0.05	0.5
HD 202109	5050	2.8	+0.01	≤0.19	...	9	1.5	ST*2	1.0	0.5

(1)Johnson et al. 2002; (2)Aoki et al. 2002; (3)Sivarani et al. 2003; (4)Johnson et al. 2004; (5)Aoki el al. 2001; (6)Van Eck et al. 2003;(7)Lucatello et al. 2003; (8)Cohen et al. 2003; (9)Yushchenko et al. 2004

Global fit

HE 0024-2523

CS 29497-030

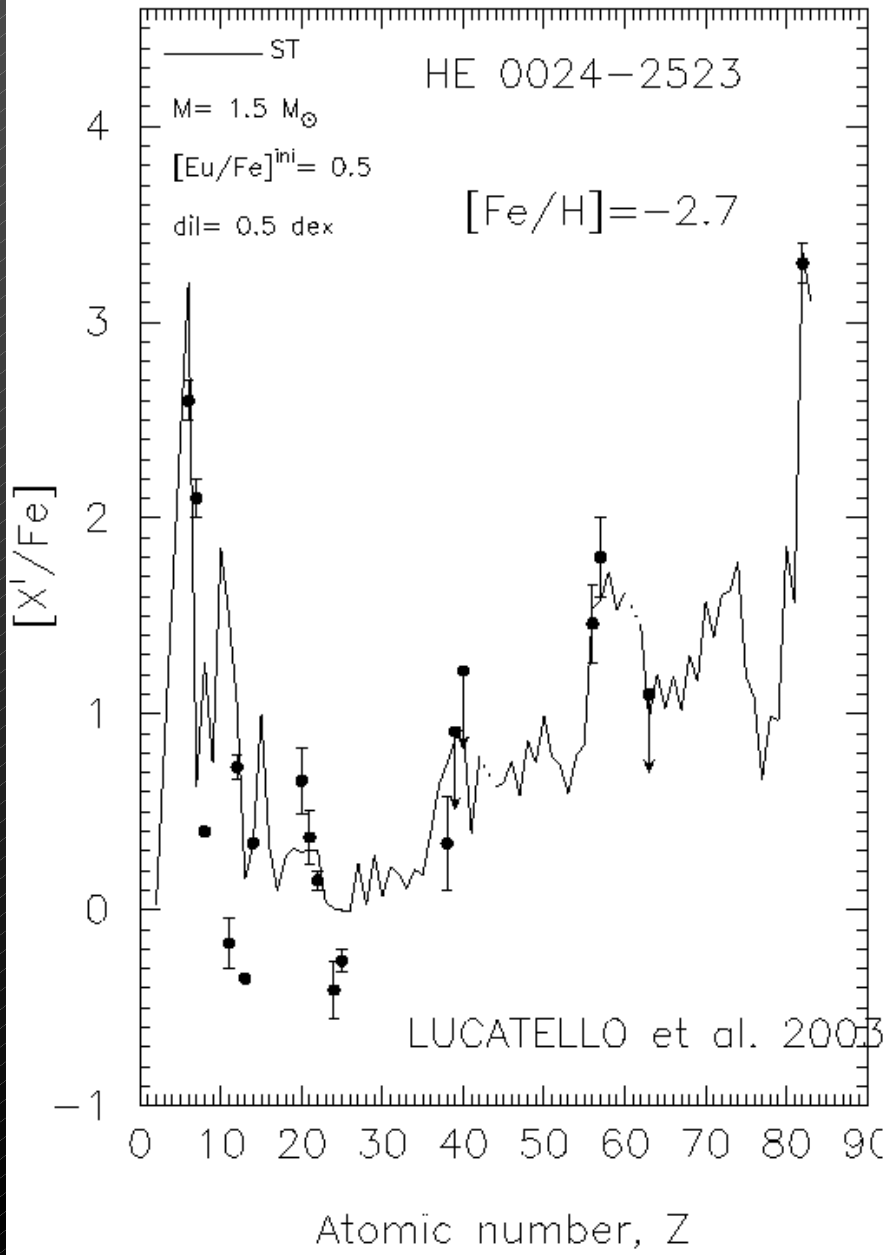

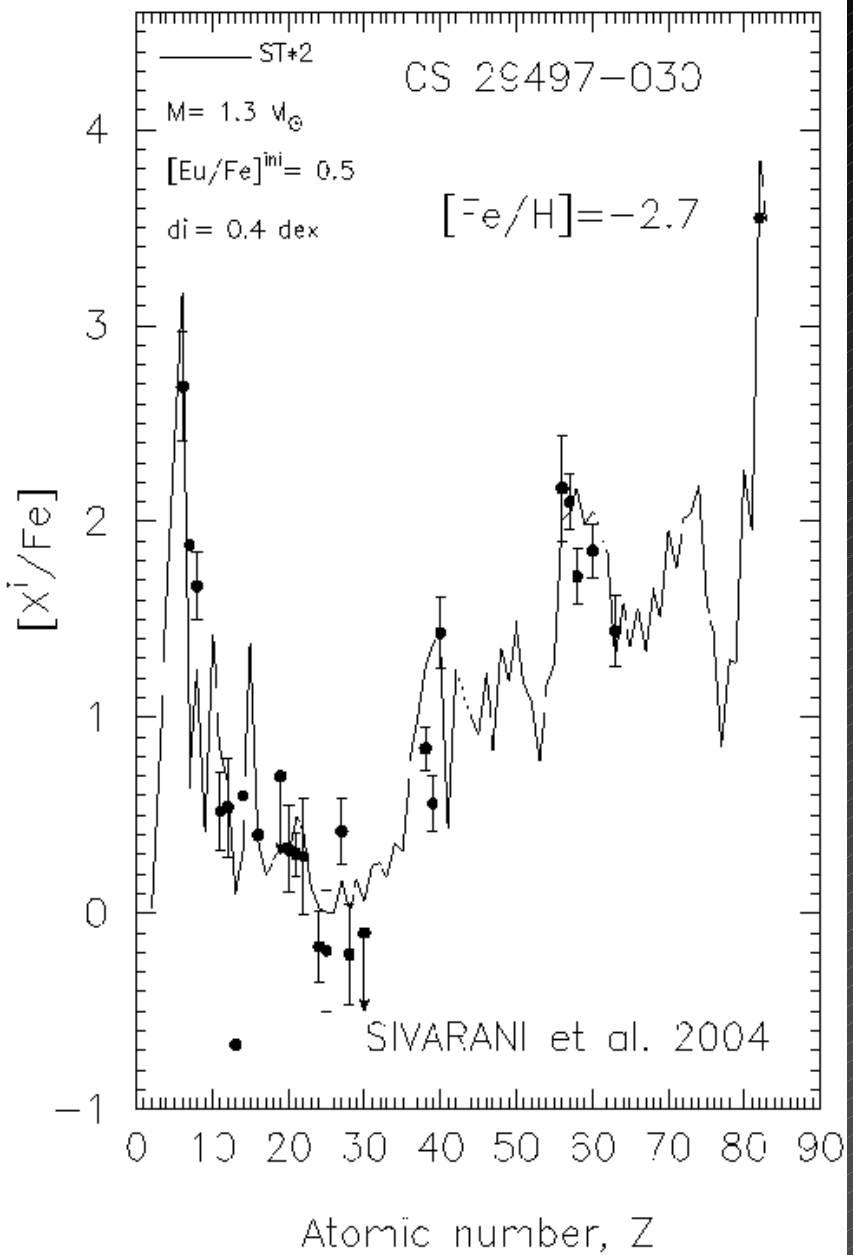

CS 22183-015

$[Eu/Fe]_{initial} = 0.5$

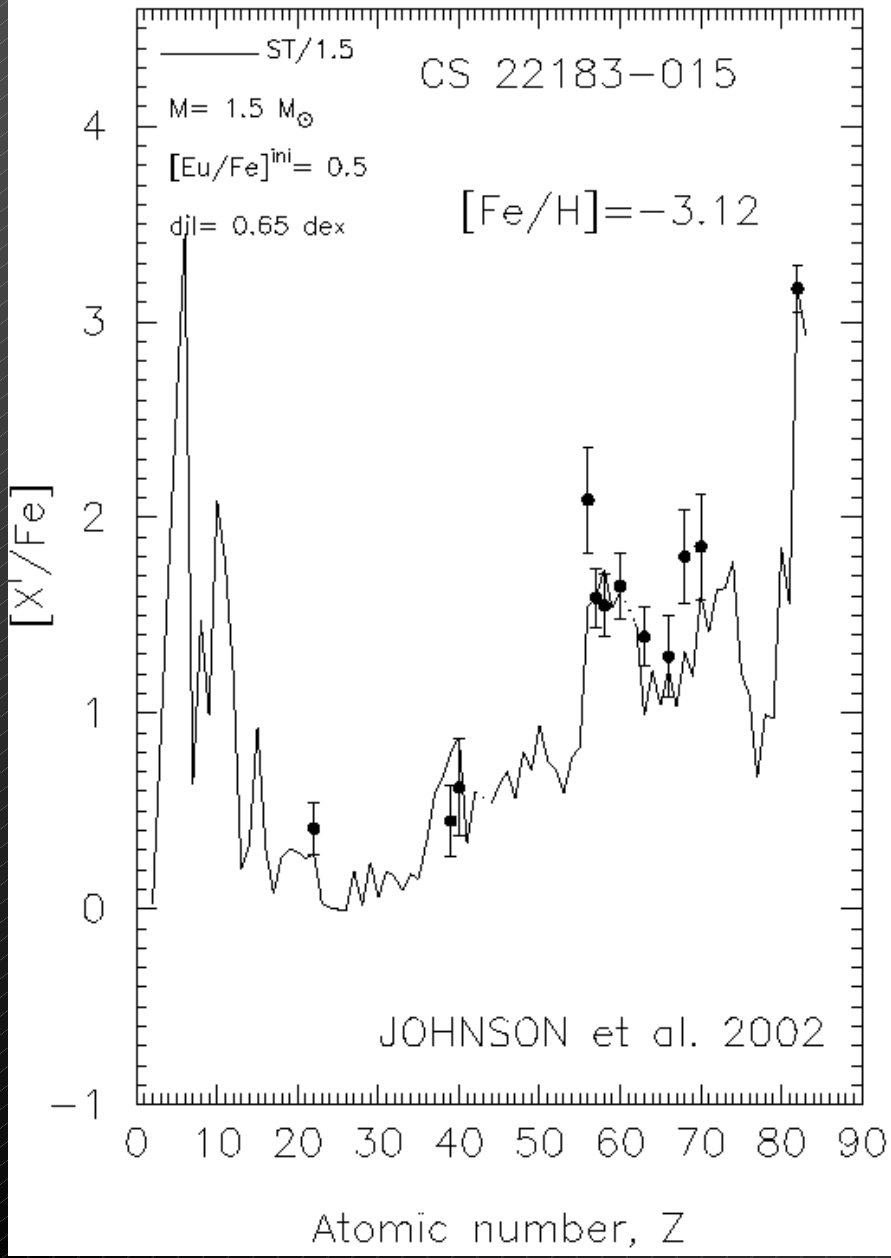

$[Eu/Fe]_{initial} = 1.0$

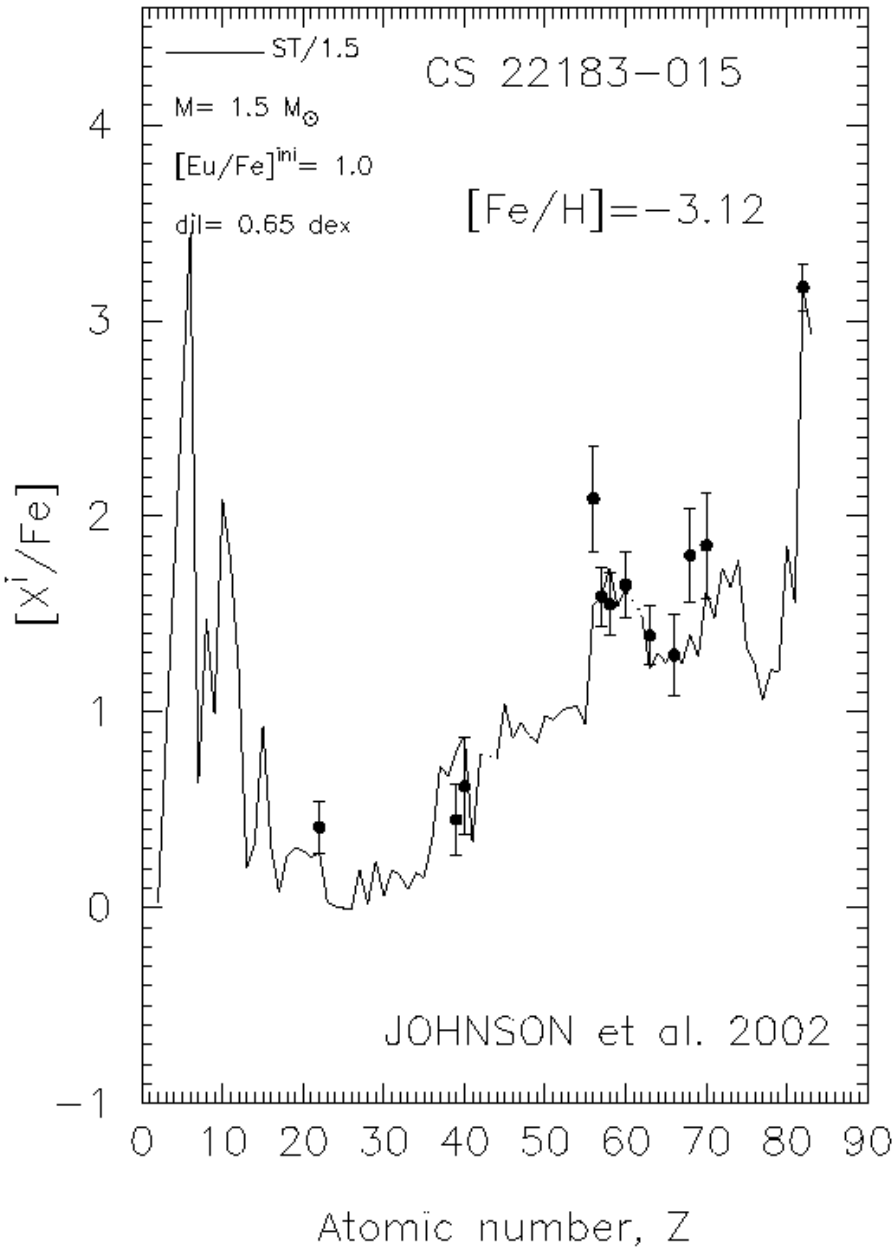

HD 196944 $[Eu/Fe]_{initial} = 0.0$

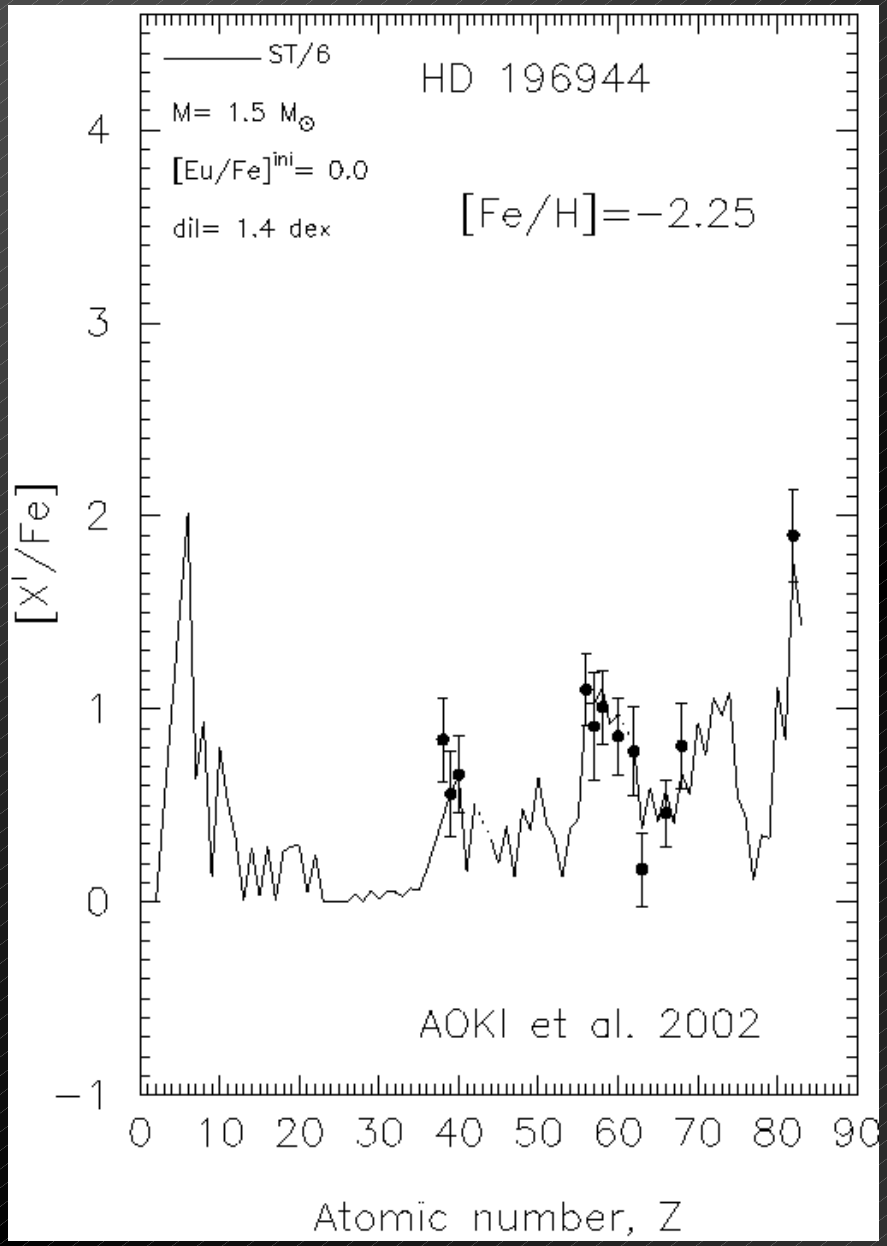

HE 2148-1247 $[Eu/Fe]_{initial} = 2.0$

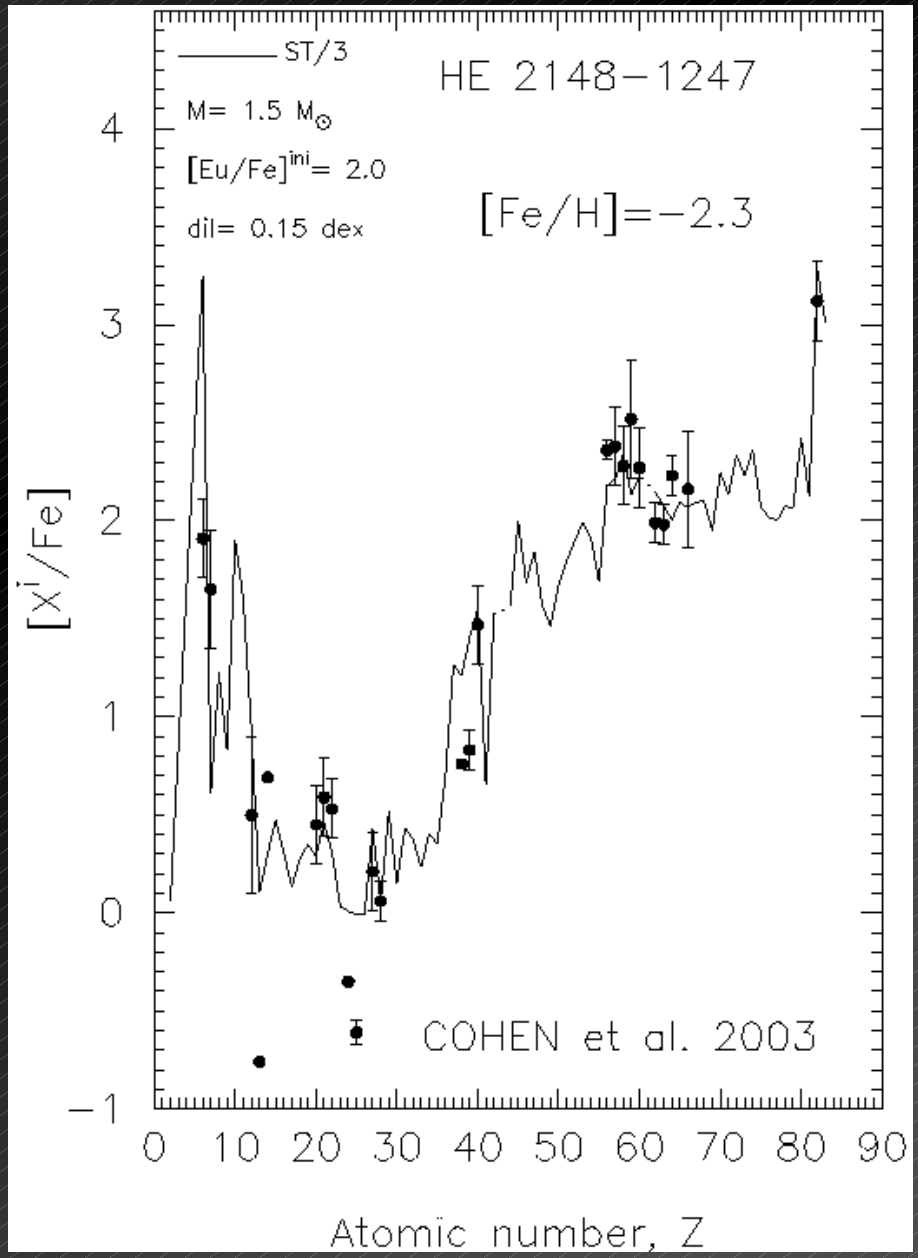

Pb/Hs and ^{13}C pocket

CS 29526-110

LP 625-44

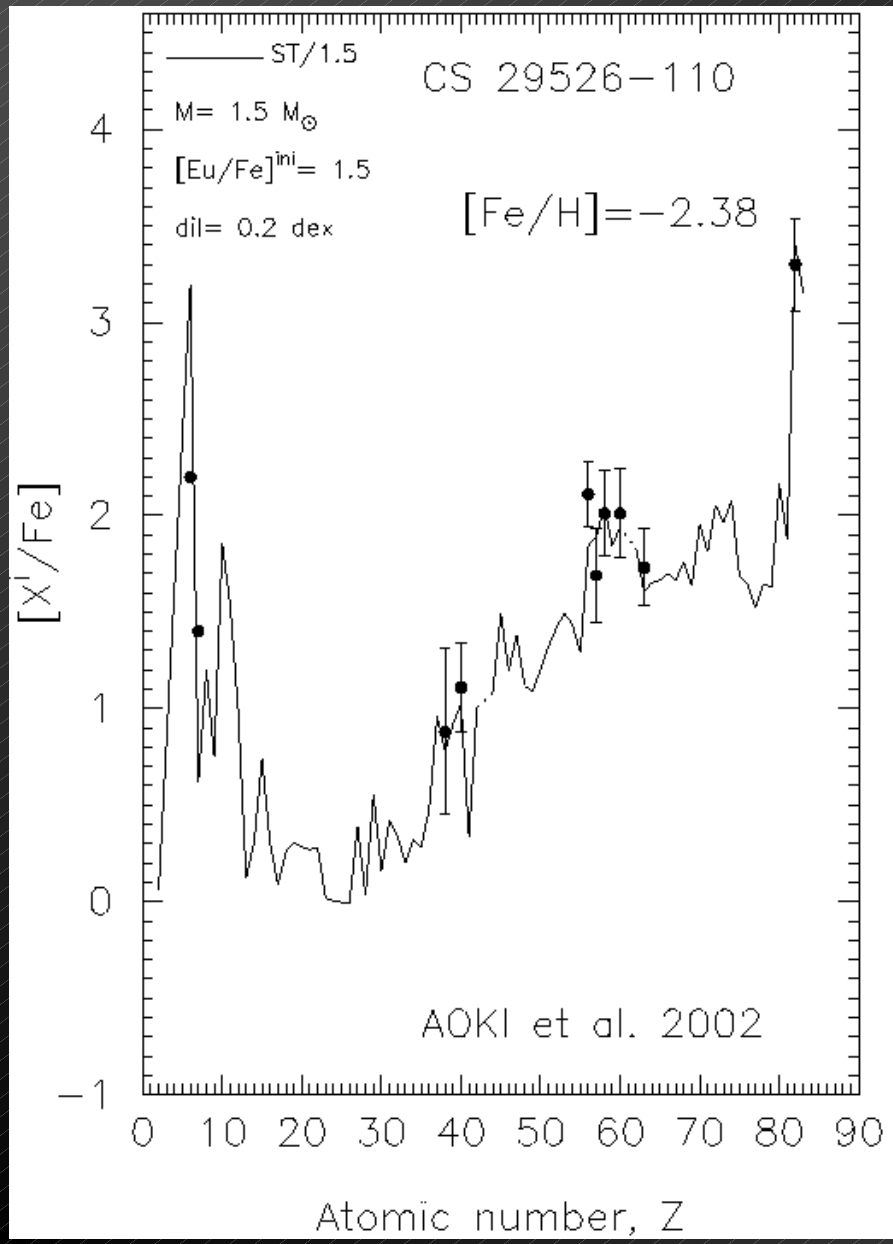

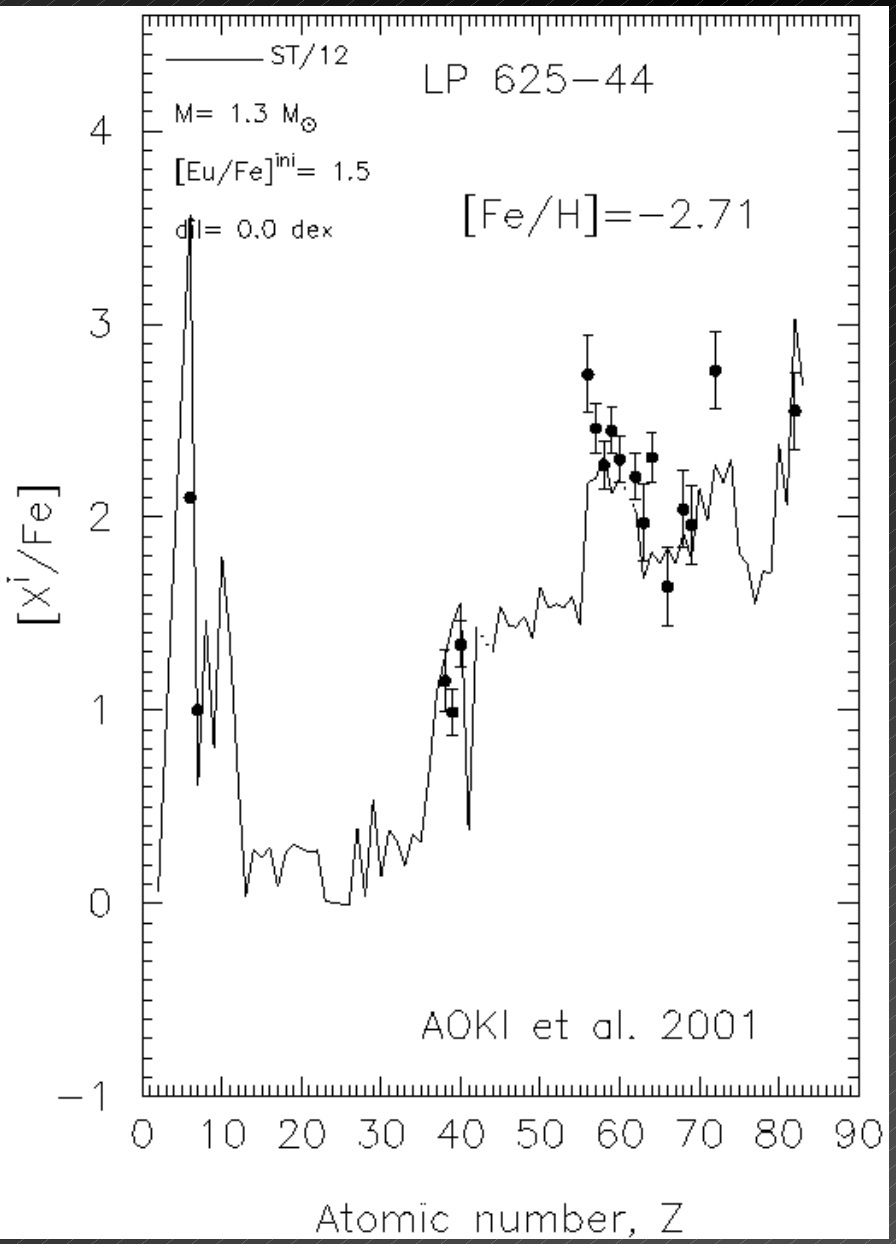

CS 31062-050. Ba?

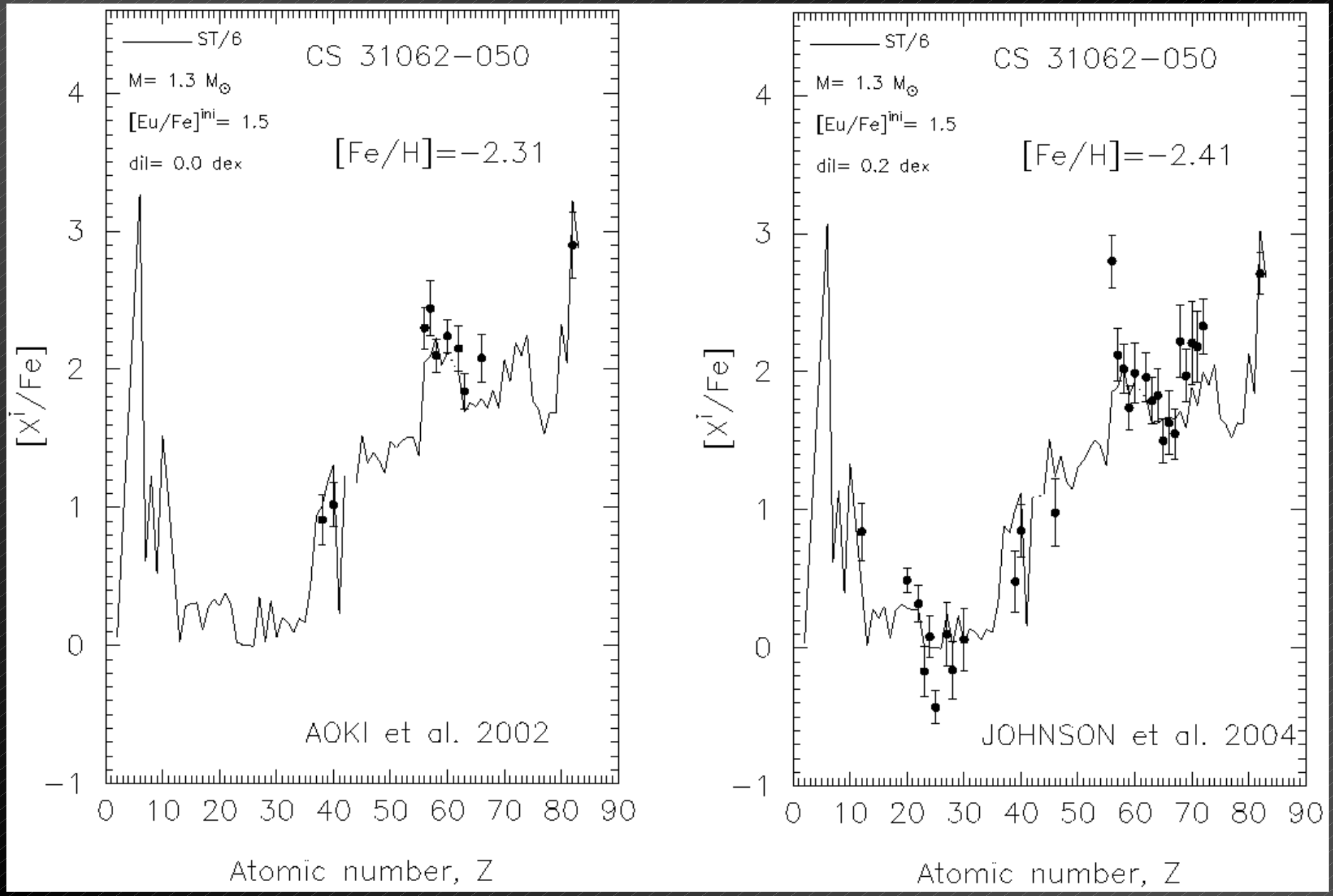

Concluding Remarks

- A large spread of $[r/Fe]_{initial}$ is found.
- The observed spread of [Pb/hs] implies a large spread of the ^{13}C pocket efficiency.
- For a given [Pb/hs], the lower the initial mass the lower the [ls/hs] (but the same can be also obtained by increasing the mass loss rate).

Open Questions

A best reproduction of all the observed elements is required

- In some cases Ba seems underestimated, while La, Ce, Pr, Nd are well reproduced.

- Predicted values of Sr, Y and Zr are very similar. On the contrary, observations show significant differences.

Problems for: nuclear physics, stellar spectroscopy or nucleosynthesis models??? The debate is open.

Other Questions

- Indication of huge N enhancements, in many Pb-stars: H flash driven by a protons ingestion in the PDCZ (Fujimoto et al) or cool bottom process (Nollet et al.) ??? Wait for the next talk.

- Spread in r-process isotopes. For HE 2148-1247 the increase of $[Eu/Fe]_{ini}$=2 dex appears exceptional. Alternative solutions are discussed in Cohen et al. 2003.

Thanks!!!!

Questions to: gallino@ph.infn.it

Roberto

TOP TEN

slides on Globular Cluster Formation

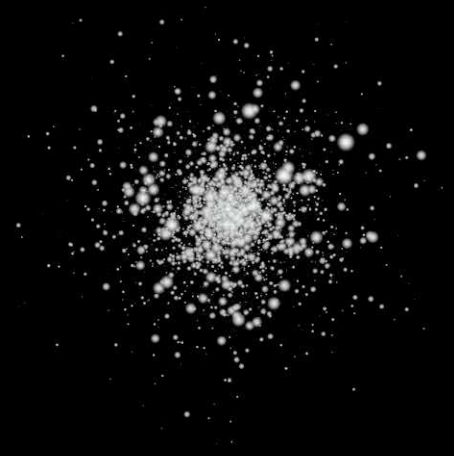

Oleg Gnedin
STScI

Slide 10: stars

Observations tell us that stars form in self-gravitating cores of molecular clouds, which have filamentary structure…

Williams et al. (2000)
Hartmann et al. (2001)
Larson (2003)

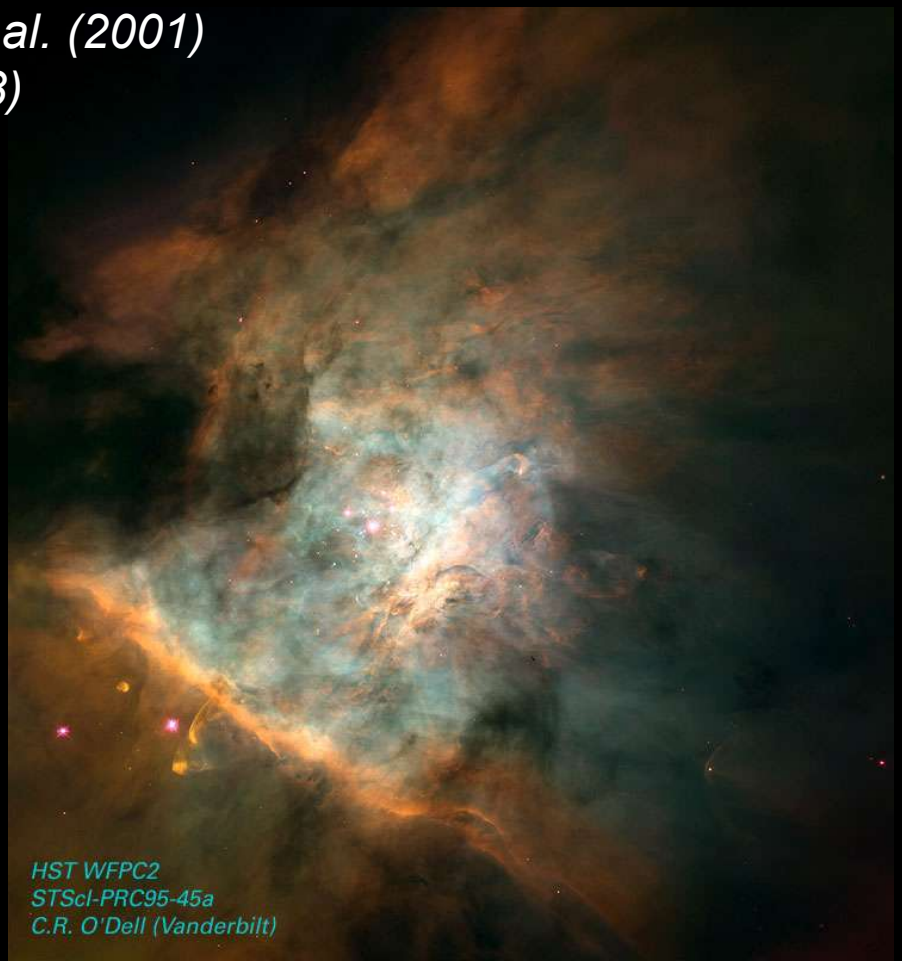

Slide 10: star clusters

Observations tell us that star clusters form in self-gravitating cores of giant molecular clouds, which have filamentary structure…

Elmegreen (2000)
Clarke et al. (2000)

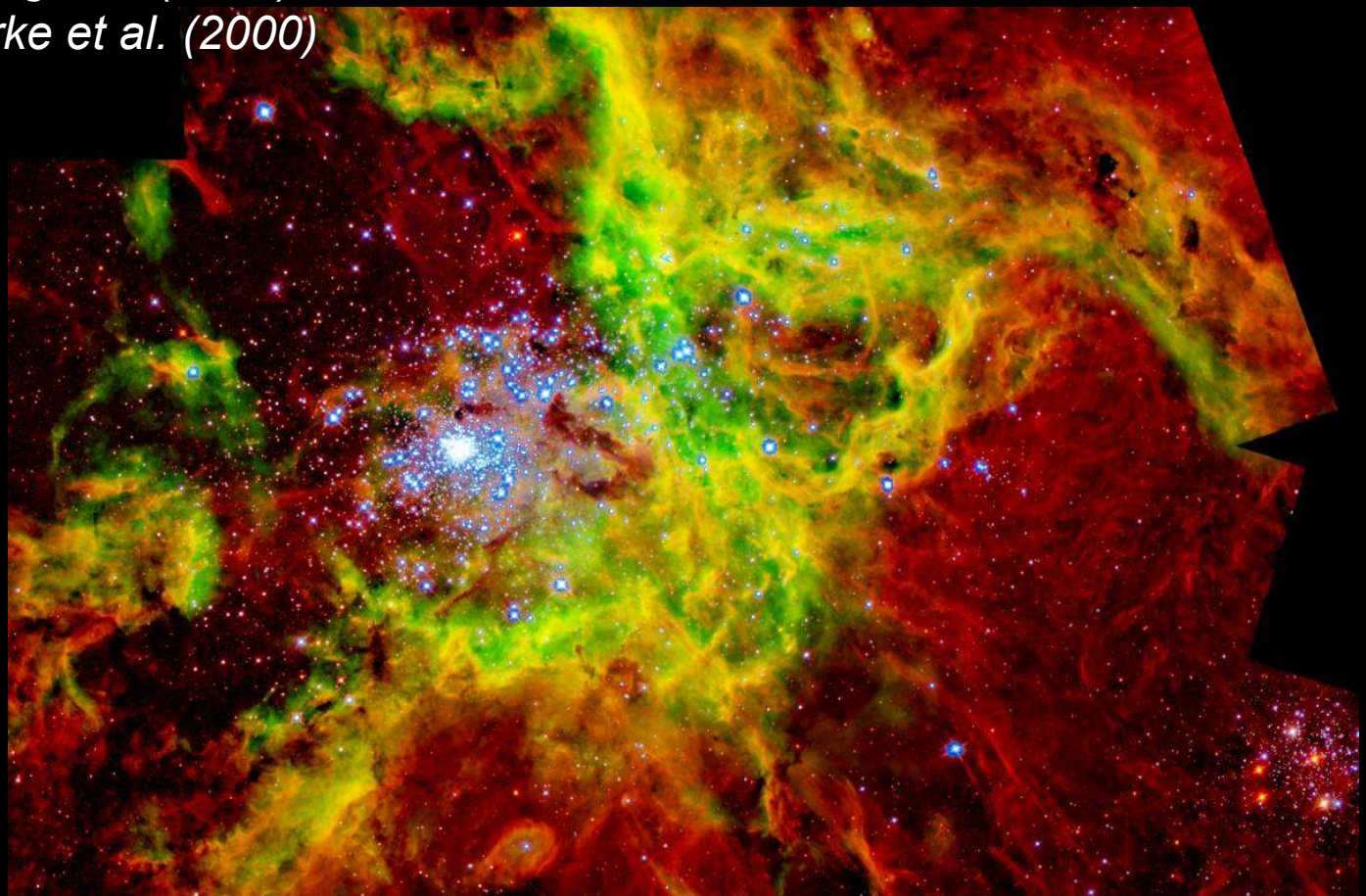

Slide 10: globular clusters

Observations tell us that globular clusters form in self-gravitating cores of supergiant molecular clouds, which have filamentary structure…

Whitmore et al. (1999)
Zepf et al. (1999)
de Grijs et al. (2003)
Anders et al. (2004)

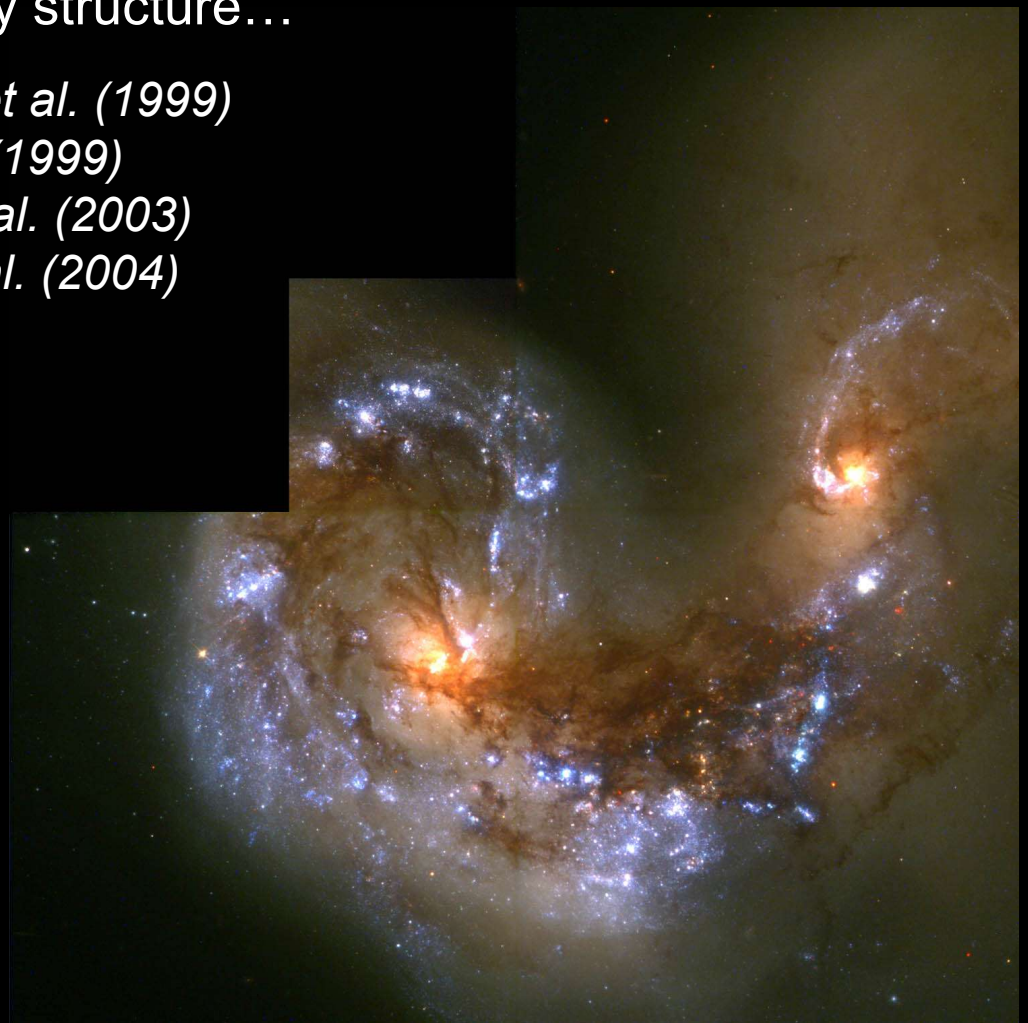

Slide 9: this is a problem

star formation rate in the Galactic disk ~ 1 M yr^{-1} efficiency of star formation in GMCs ~ 1-10%

to form globular clusters, need supergiant molecular clouds

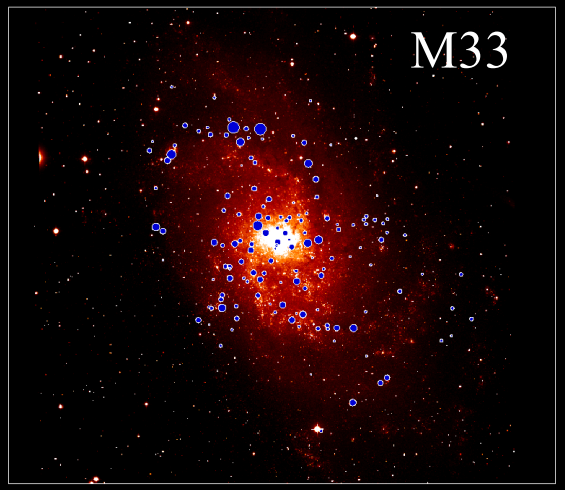

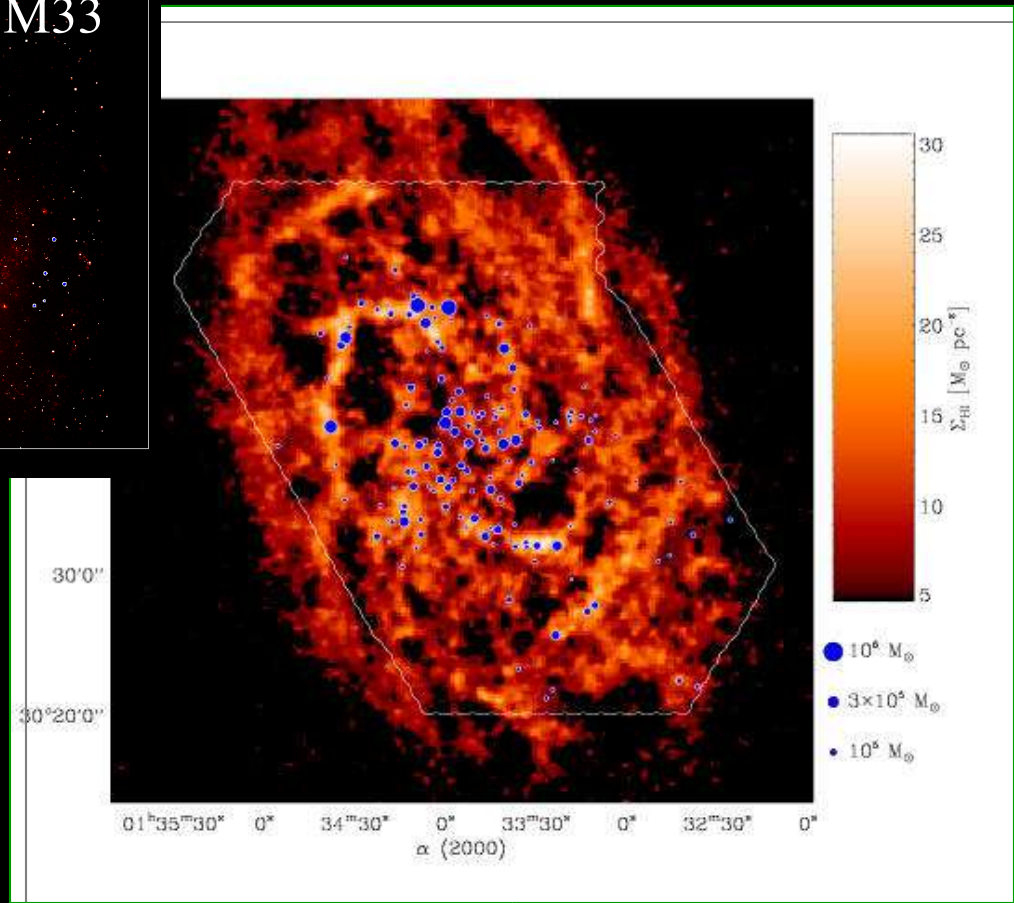

Molecular clouds form in spiral arms of disk galaxies, globular clusters are in the halo

H_2: *Engargiola, Blitz et al. (2003)*
HI: *Deul & van der Hulst (1987)*

Slide 8: is this a problem?

In interacting galaxies there is enough molecular gas and young globular clusters are forming now in the Antennae and other nearby galaxies

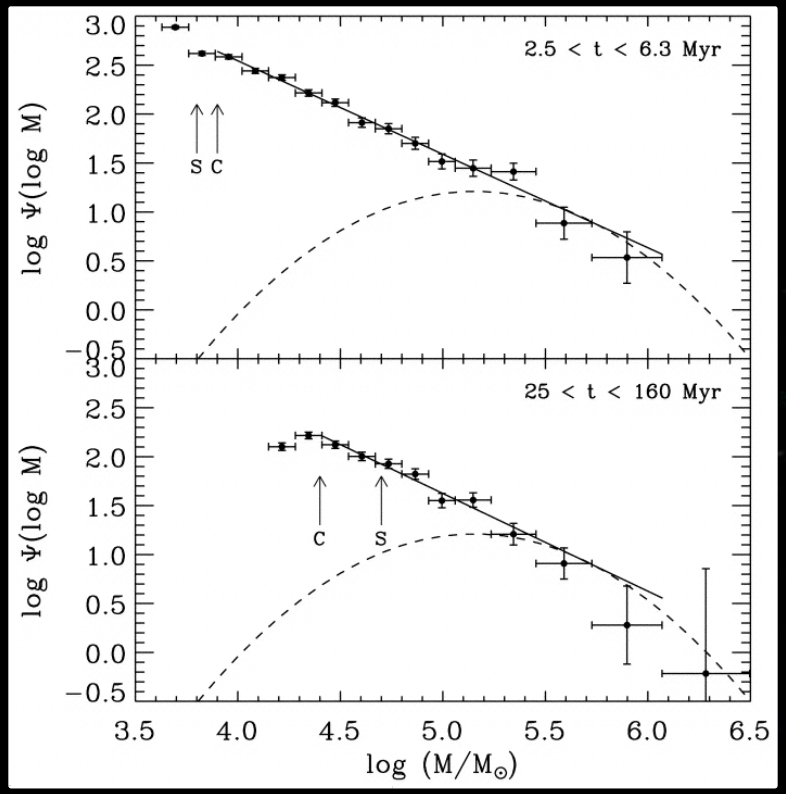

Zhang & Fall (1999)

Wilson et al. (2000)

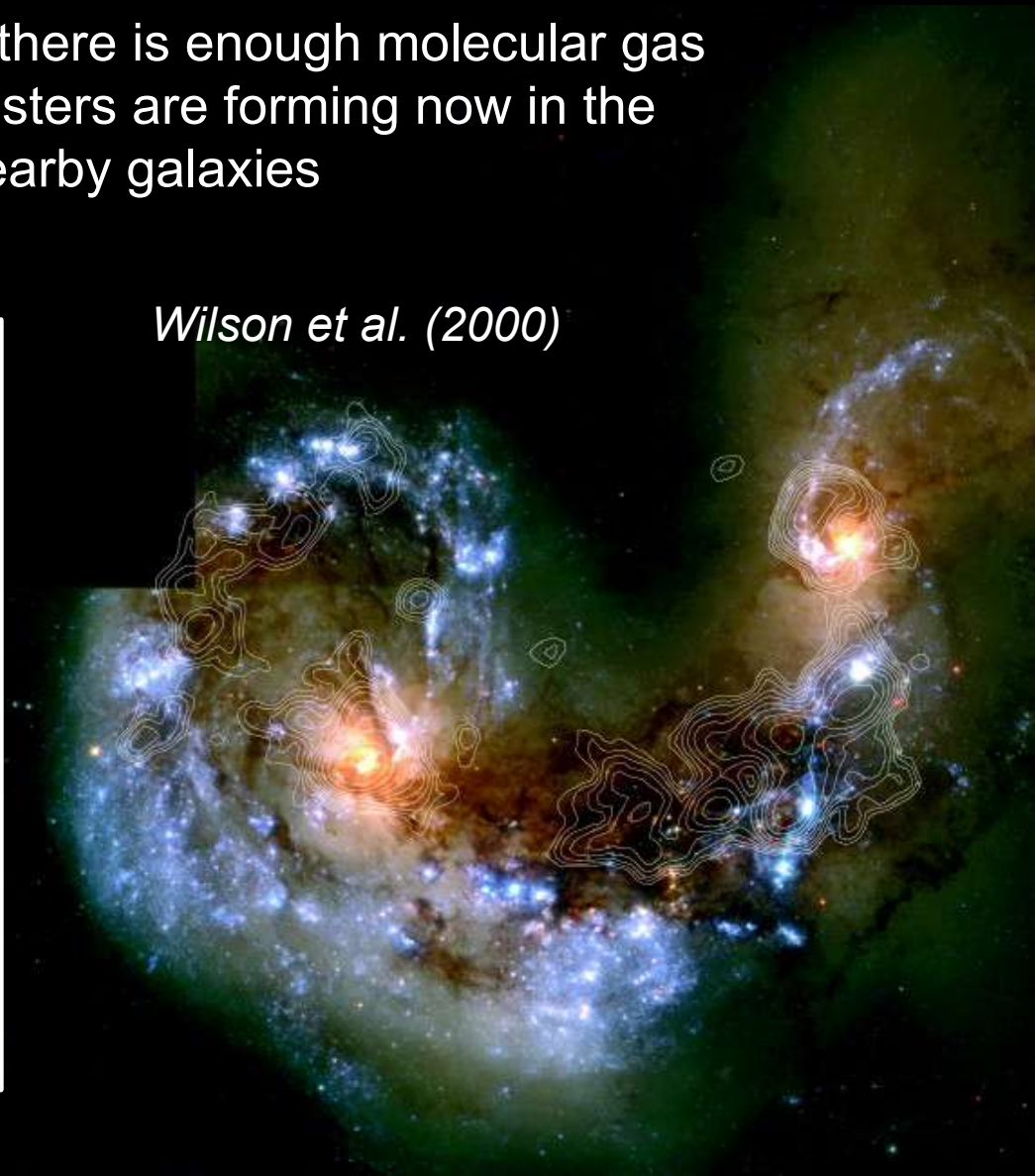

Slide 7: this is not a problem

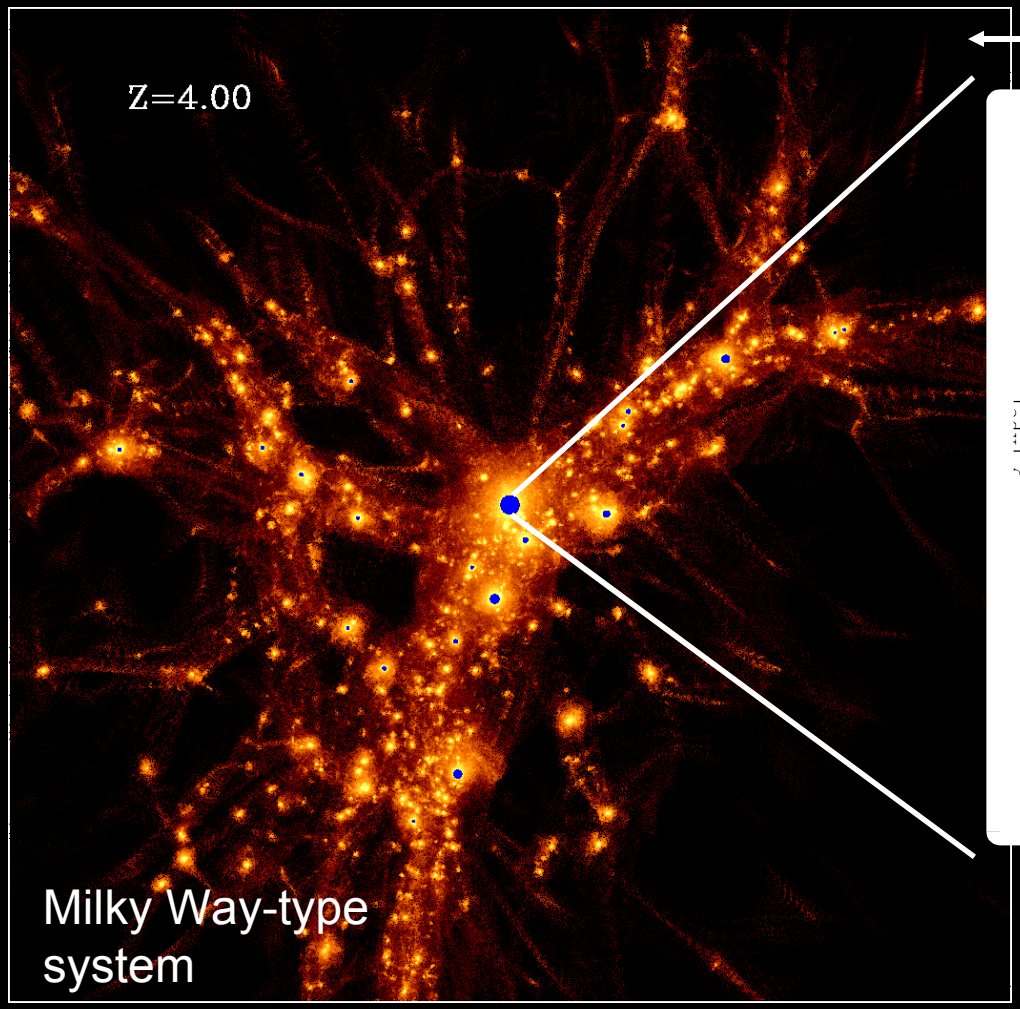

300 kpc (physical)

14 kpc

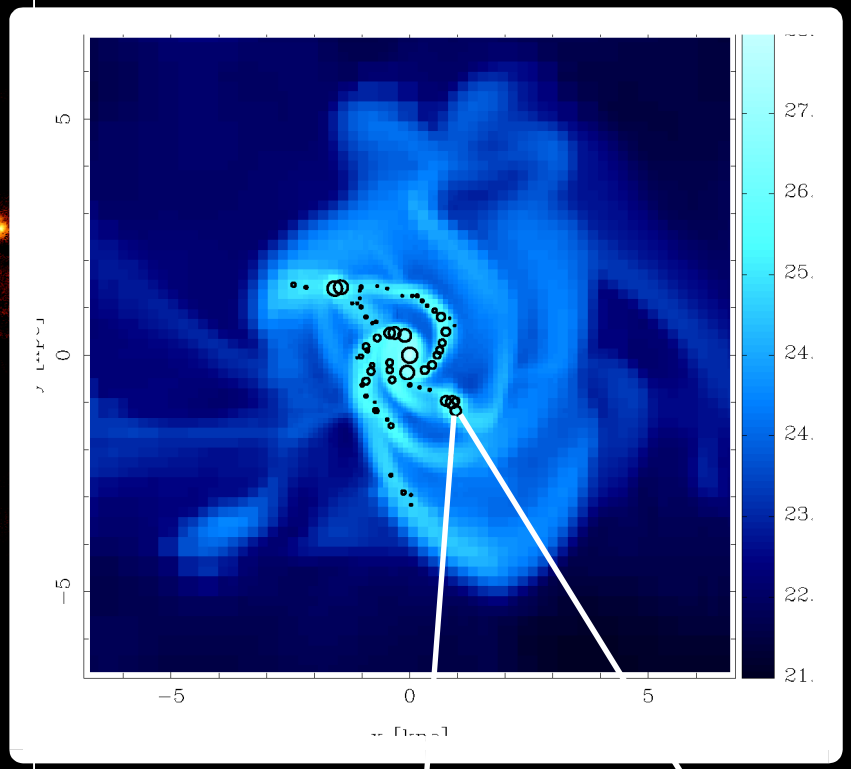

?

20 pc

ART simulation, Kravtsov & Gnedin (2003)

Slide 6: stars form in clusters

and so they should in simulations…

Larson, Harris & Pudritz: massive star clusters form in the same way as the smaller open clusters, in self-gravitating cores of molecular clouds

Elmegreen (2002): young star clusters in the Galaxy form wherever $\rho_{gas} > 10^4$ M pc^{-3}

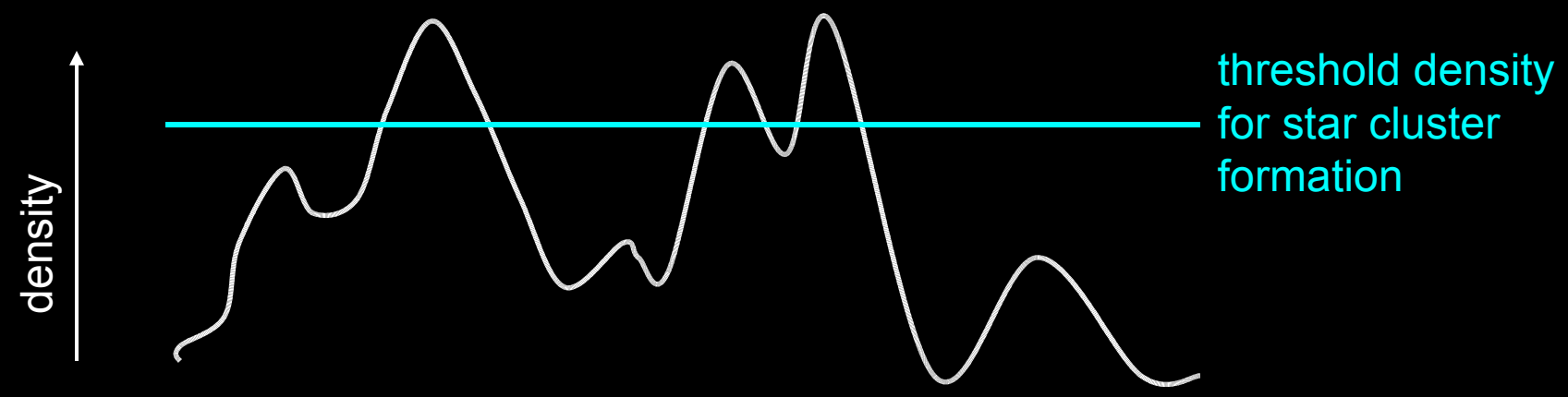

Slide 5: do the numbers work out?

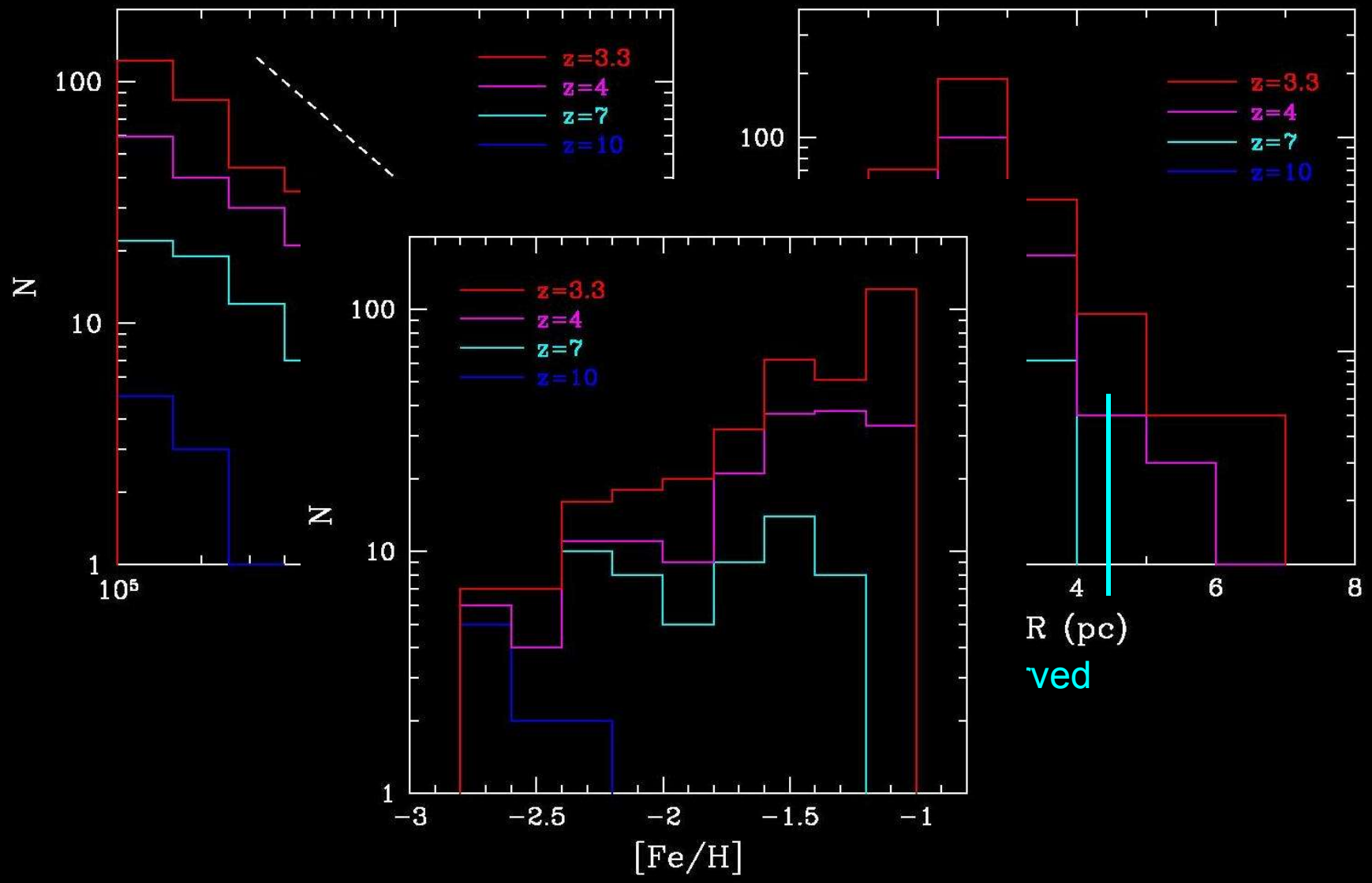

Slide 4: this is a problem

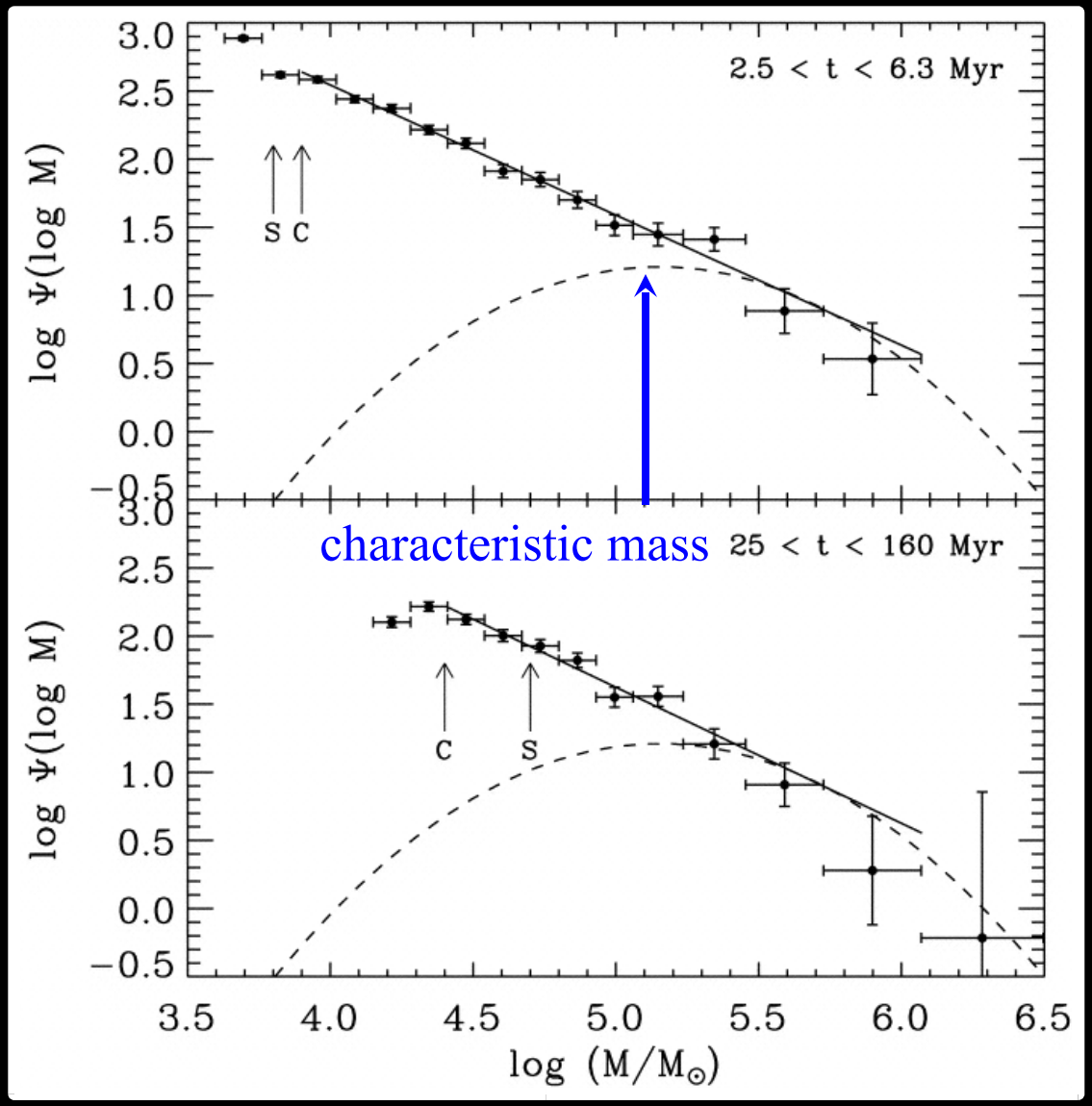

Zhang & Fall (1999)

Slide 3: is this a problem?

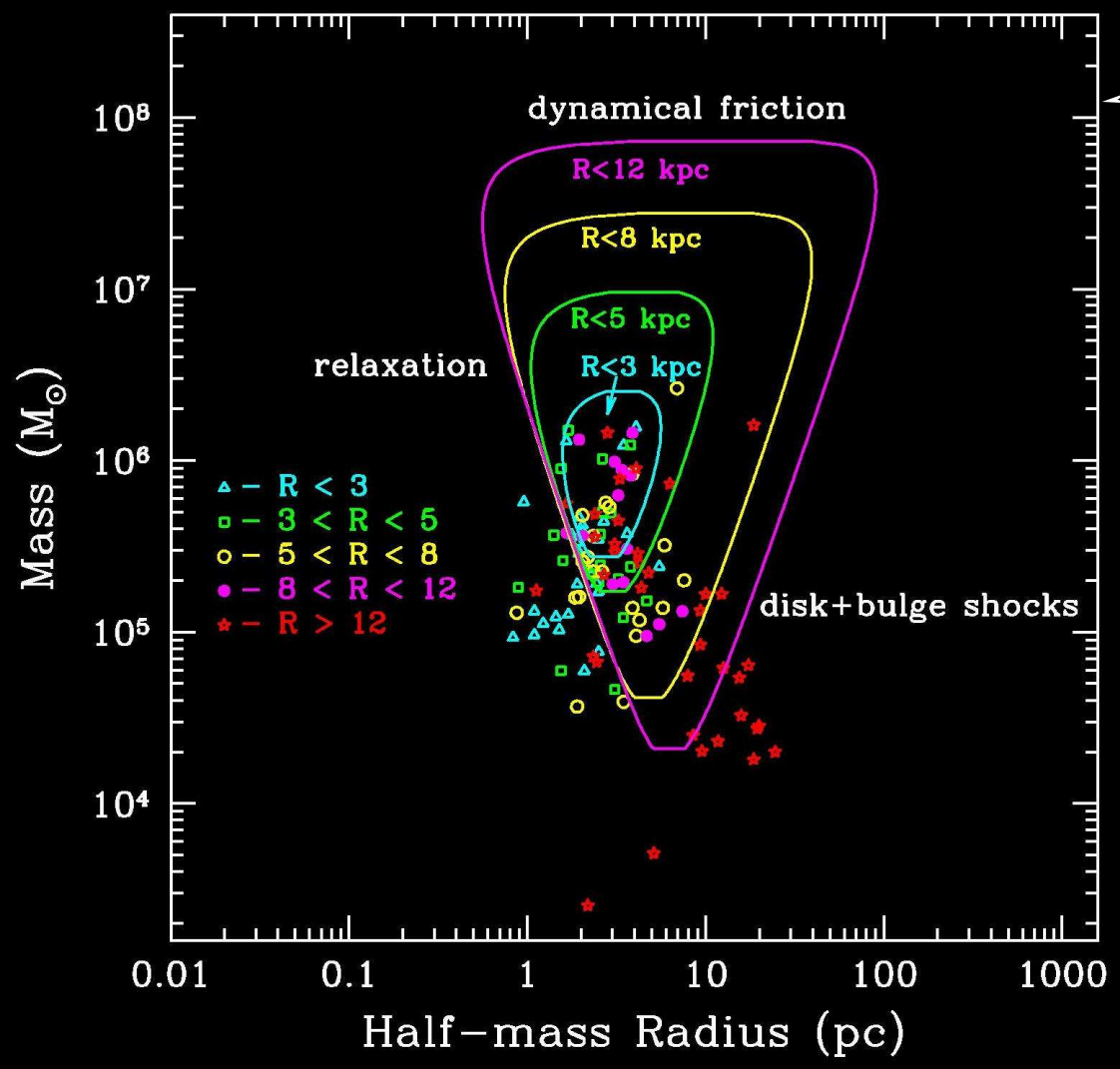

Gnedin & Ostriker (1997)

Fall & Rees (1977)
Spitzer (1987) + collaborators
Chernoff & Weinberg (1990) Murali & Weinberg (1997) Vesperini & Heggie (1997) Ostriker & Gnedin (1997) Gnedin, Lee & Ostriker (1999) Fall & Zhang (2001)

DYNAMICAL EVOLUTION:
Low-mass and low-density clusters are disrupted over the Hubble time by two-body relaxation and tidal shocks.

Slide 2: this is not a problem

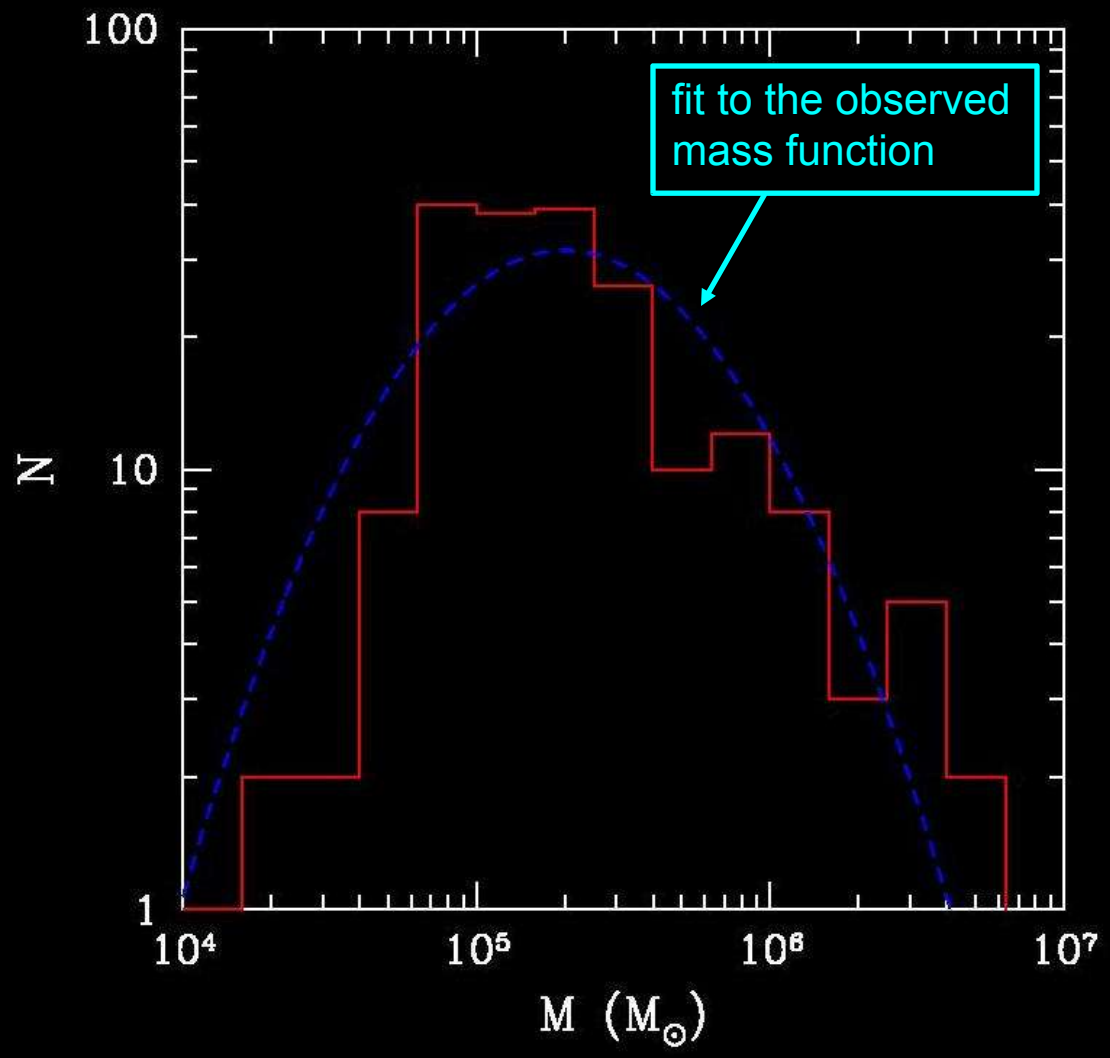

Slide 1: can we see GCs at z=4 ?

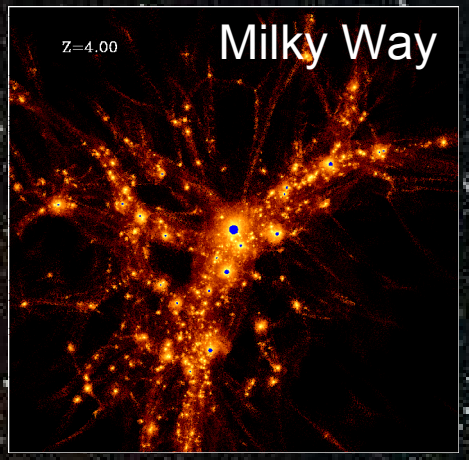

1 h^{-1} Mpc comoving (41″)

Star clusters in spiral arms of high-redshift disks

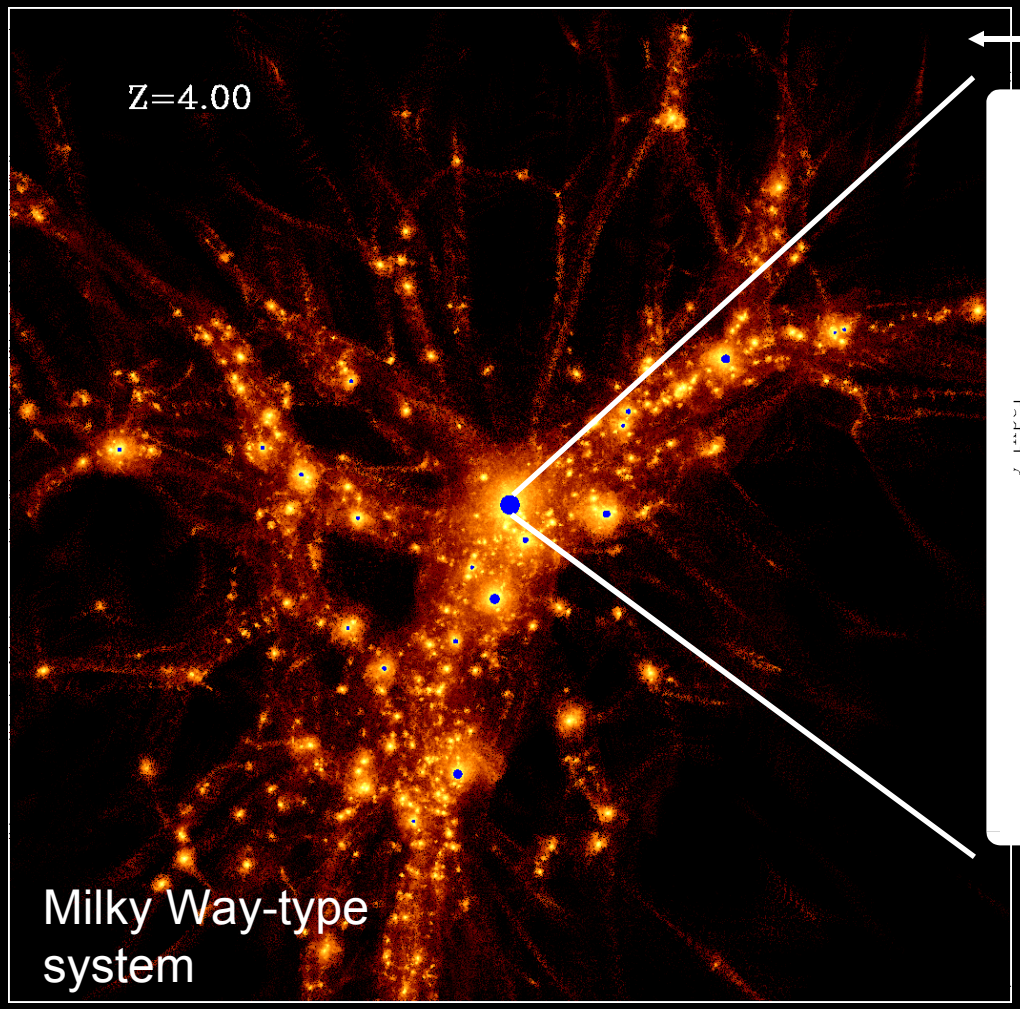

300 kpc (physical)

14 kpc

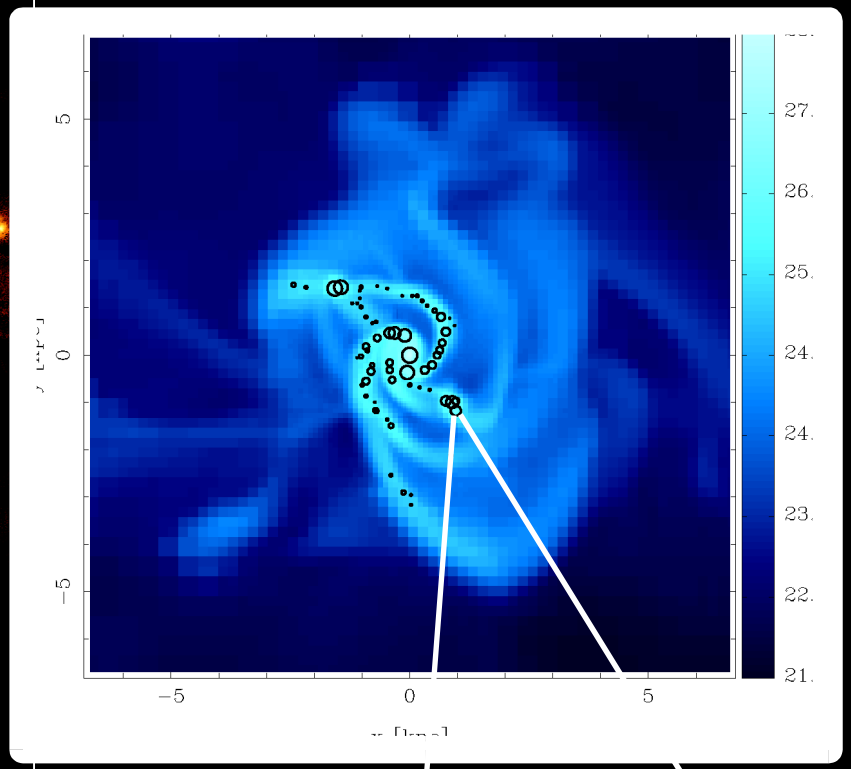

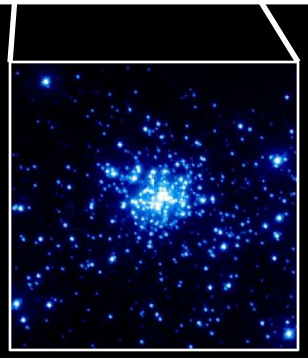

20 pc

cold gas always forms thin disks
stellar disks are quickly heated by mergers

The Role of Pulsations in Mass Loss from Massive Blue Stars

Joyce A. Guzik, Benjamin A. Austin, Arthur N. Cox, and Kate M. Despain

X-2, Applied Physics Division

Los Alamos National Laboratory

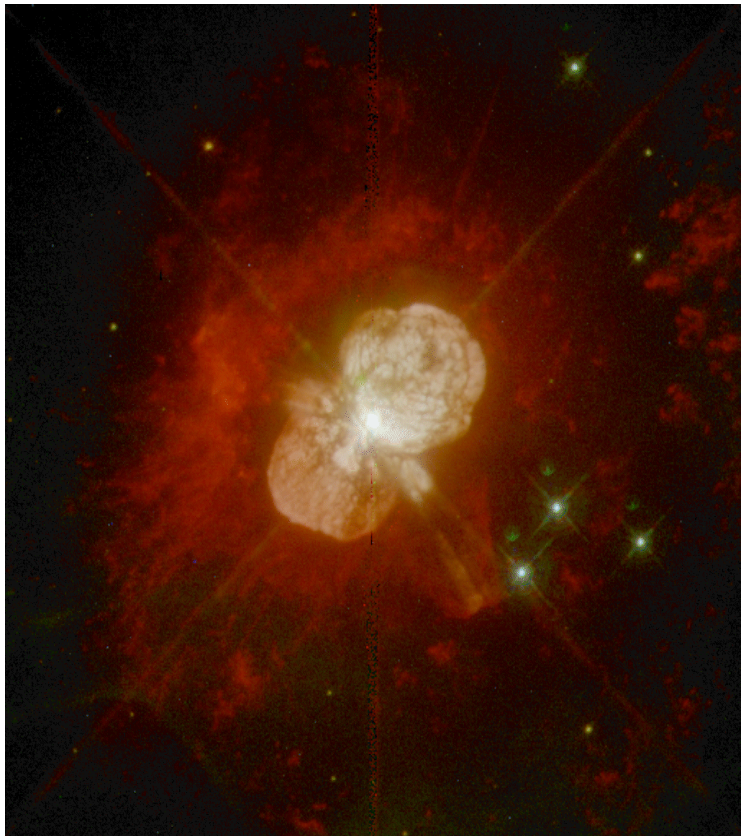

Chemical Enrichment of the Early Universe

Santa Fe, NM 9-13 August 2004

LA-UR-04-6002

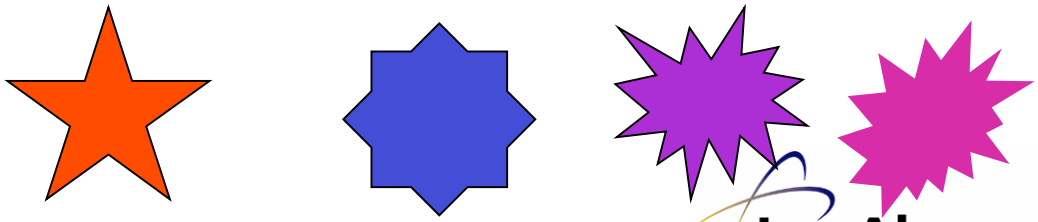

Los Alamos NATIONAL LABORATORY

Massive Stars on the HR Diagram

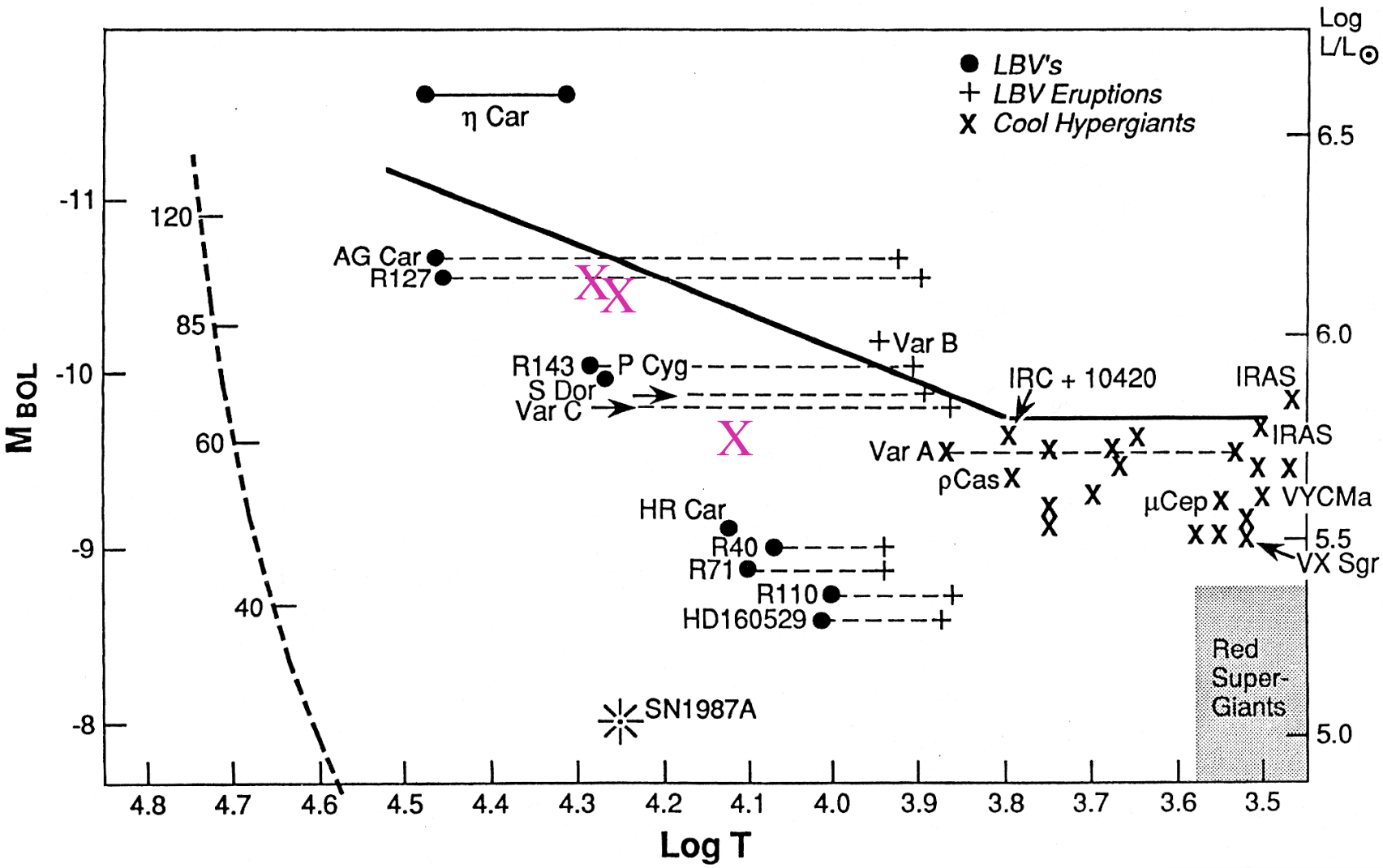

HR Diagram from Humphreys & Davidson 1994

Los Alamos NATIONAL LABORATORY

Main points of talk:

Massive hot stars are predicted under certain conditions to be pulsationally unstable.

Pulsation instability is due to kappa-effect driving from Fe ionization at 200,000 K in the envelope

Pulsation instability and amplitude depends critically on Fe abundance, and is reduced for less chemically-enriched stars.

Pulsation can extend envelope and enhance mass loss, thereby affecting stellar yields.

Pulsation can also trigger envelope instability and possibly 'normal' LBV outbursts accompanied by larger mass loss. Outbursts are caused by exceeding Eddington limit in deep layers due to time-dependence of convection.

A different mechanism is needed to explain the rare giant eruptions, with ejections of several solar masses, seen in Eta Car or P Cyg.

Los Alamos NATIONAL LABORATORY

Questions to Discuss

What are the consequences of pulsation of hot massive luminous stars for chemical enrichment?

How do pulsation properties that affect mass loss depend on initial mass function and stellar composition (Helium abundance and metal abundance Z)?

Have these implications been accounted for adequately (at all?) in stellar mass loss rates and nucleosynthetic yield models?

Los Alamos NATIONAL LABORATORY

Pulsation Simulations

- Models based on first crossing evolution models of initial mass 80 and 50 M_{sun} that lose mass at different mass-loss rates resulting in different surface Y abundances.
- 1-D Nonlinear hydrodynamics code of Ostlie & Cox (1990)
- Includes nonlocal time-dependent convection treatment
- No rotation included
- Model *envelope* only in hydro: 60-120 zones from above photosphere down to a few million K (95% of radius, but only 0.001% of mass!)
- Pulsation driving of radial (and nonradial) modes due to kappa effect driving from Fe ionization ~ 200,000 K.
- Hydro initiated with radial velocity amplitude 1 km/sec outward in one unstable mode (F, 1H, 2H)

Los Alamos NATIONAL LABORATORY

Evolution tracks of 80 and 50 M_{sun} models with mass loss

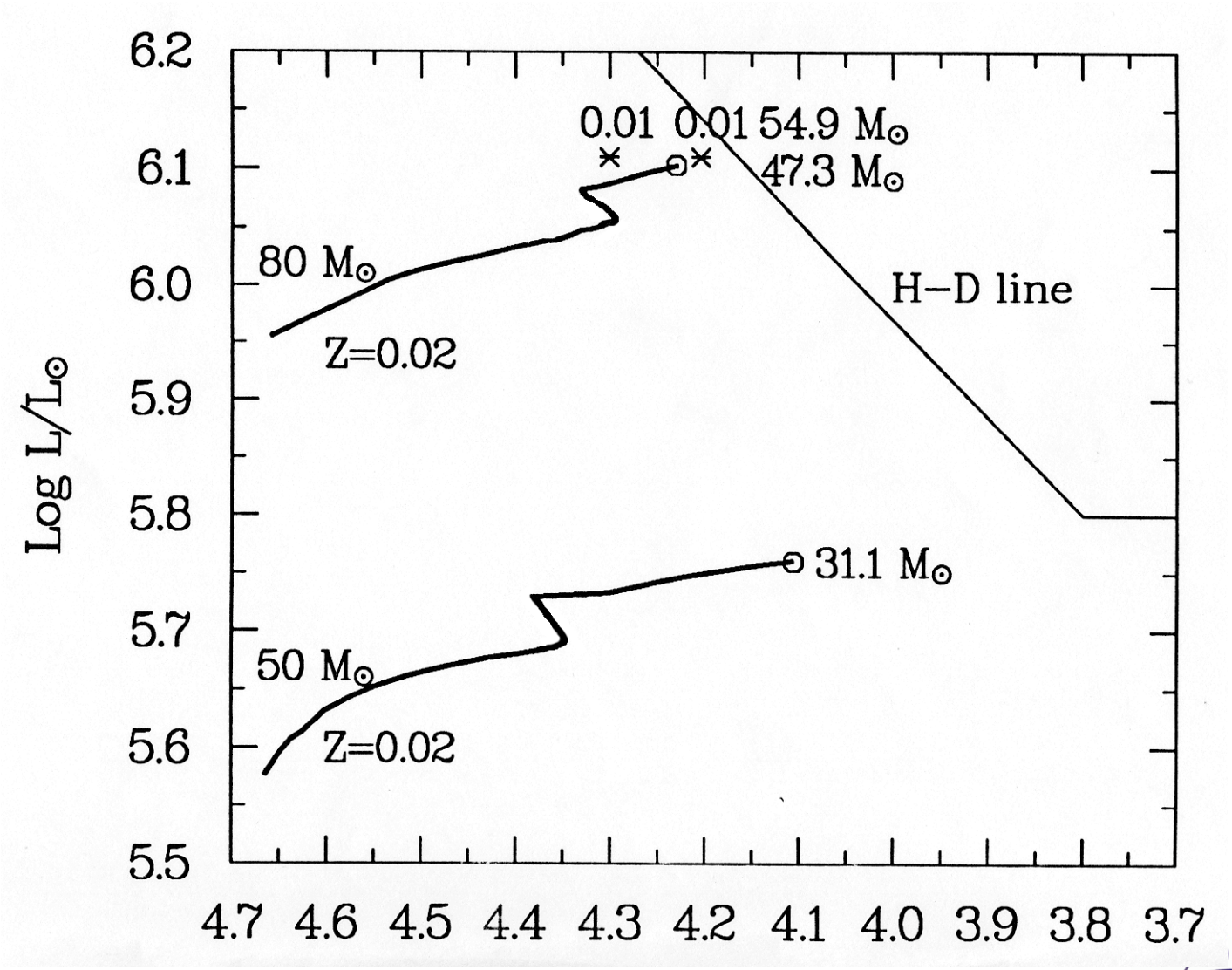

For Y=0.38 and 0.48, model shows large abrupt increase in outward radial velocity

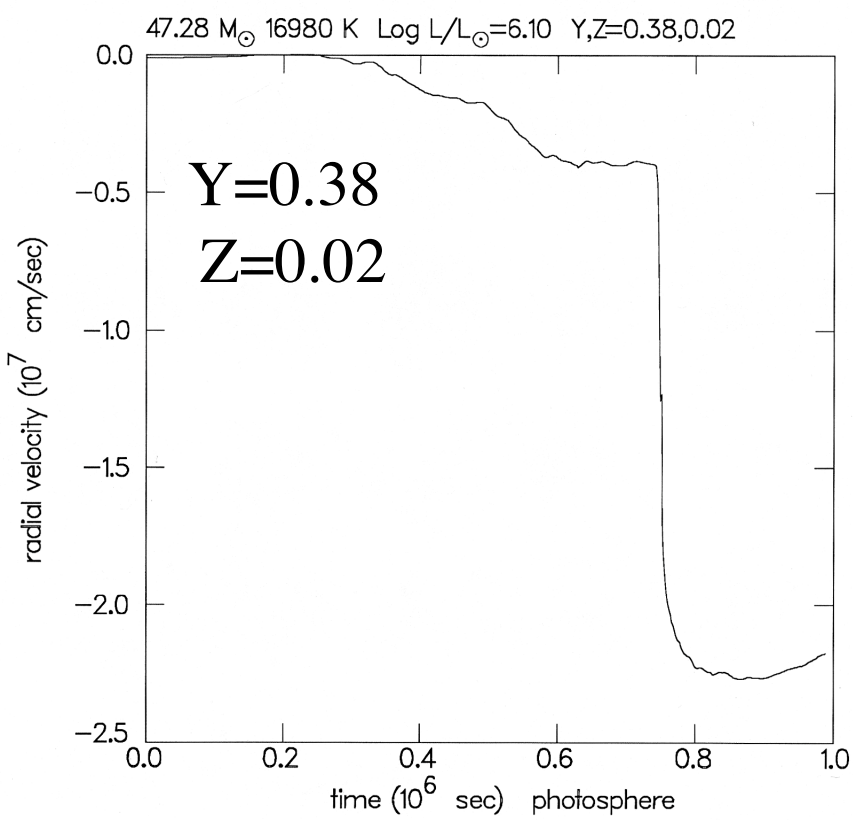

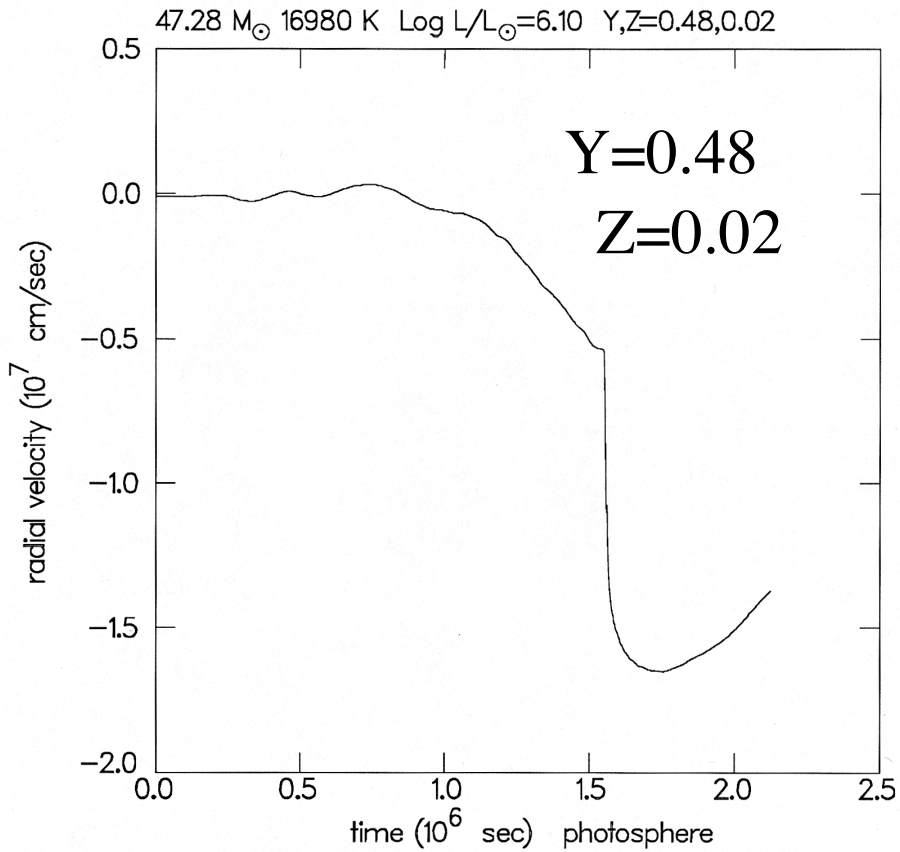

$V_{esc} \sim 370$ km/sec

Increase in Y abundance (to 0.58) stabilizes 'outburst' behavior

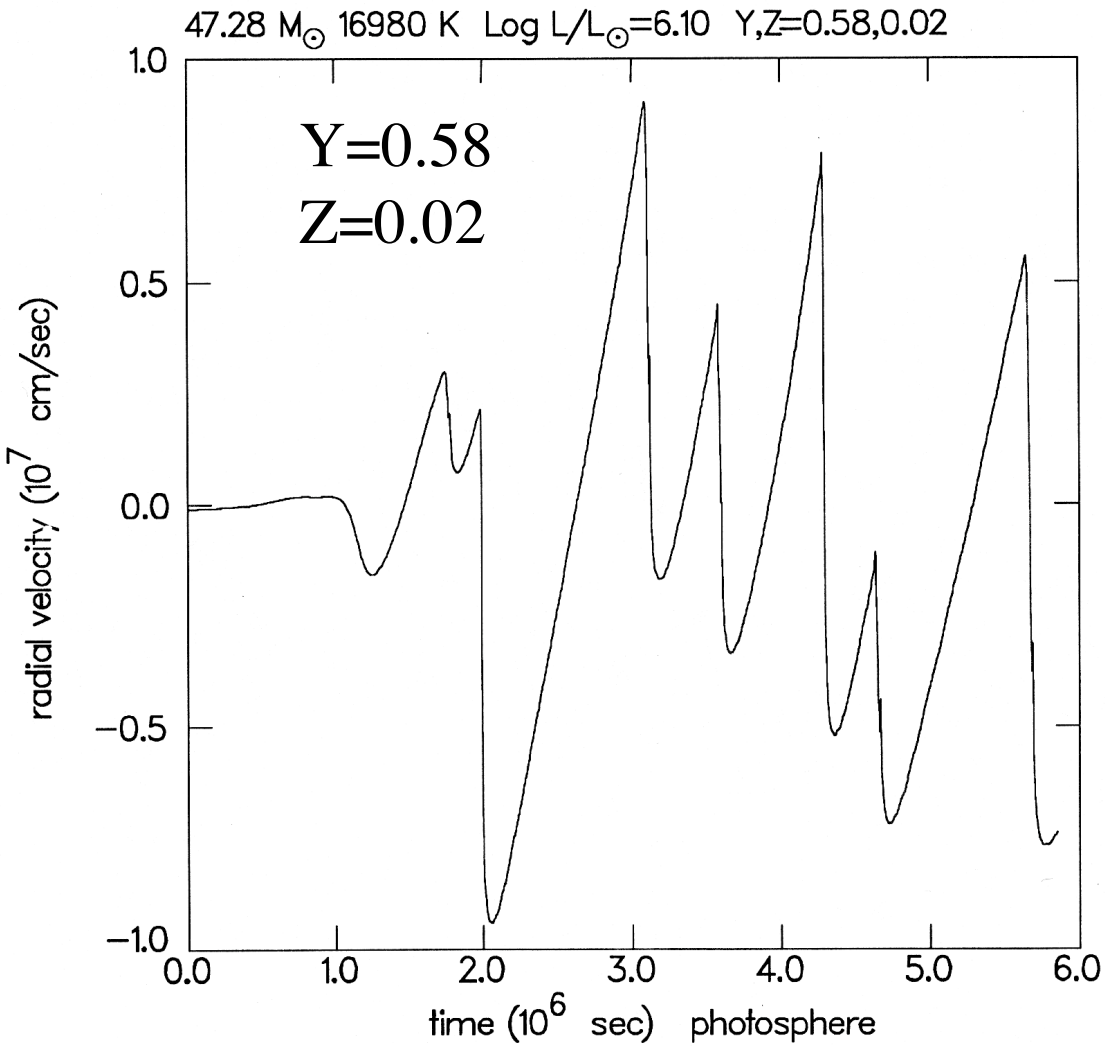

Amplitude ~100 km/sec

V_{esc} ~ 370 km/sec

For Y=0.29, lower Z model shows large abrupt increase in radial velocity

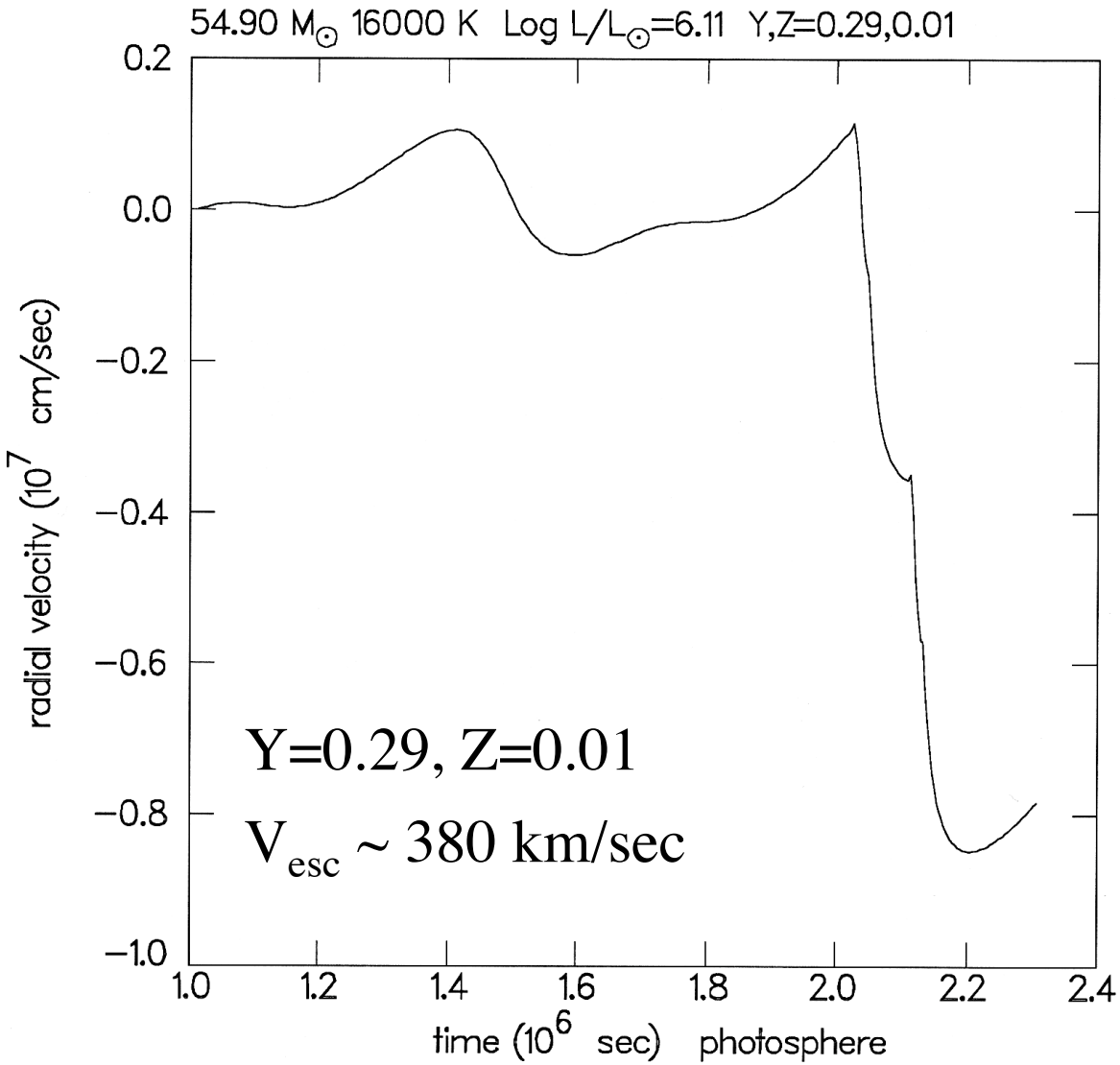

For Y=0.39, model shows steady multimode pulsations

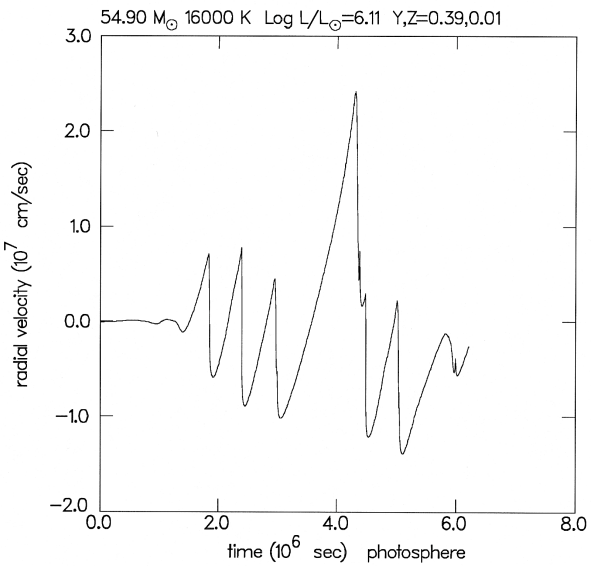

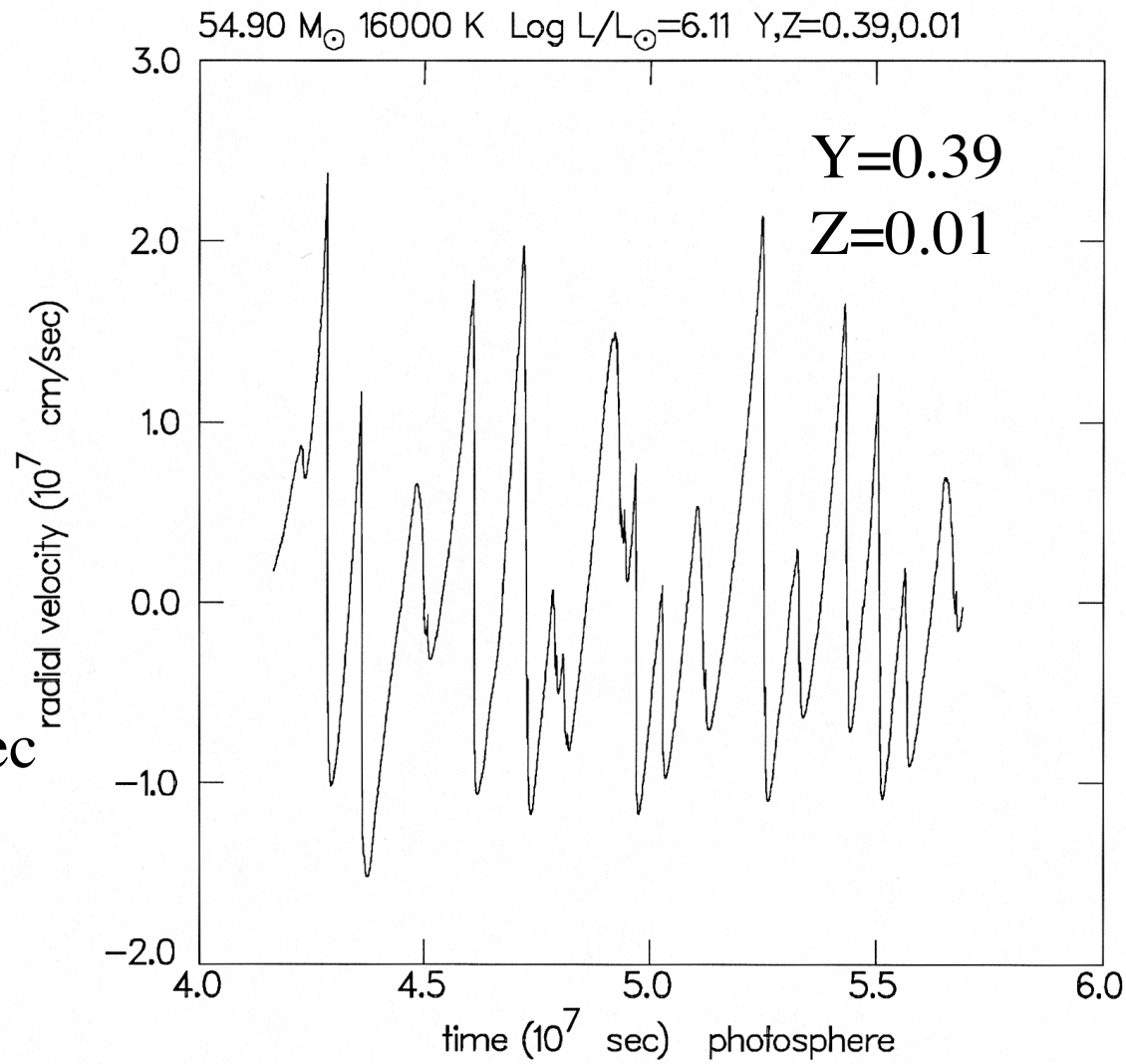

Amplitude ~200 km/sec

V_{esc} = 380 km/sec

For Y=0.49, model shows steady multimode pulsations at lower amplitude

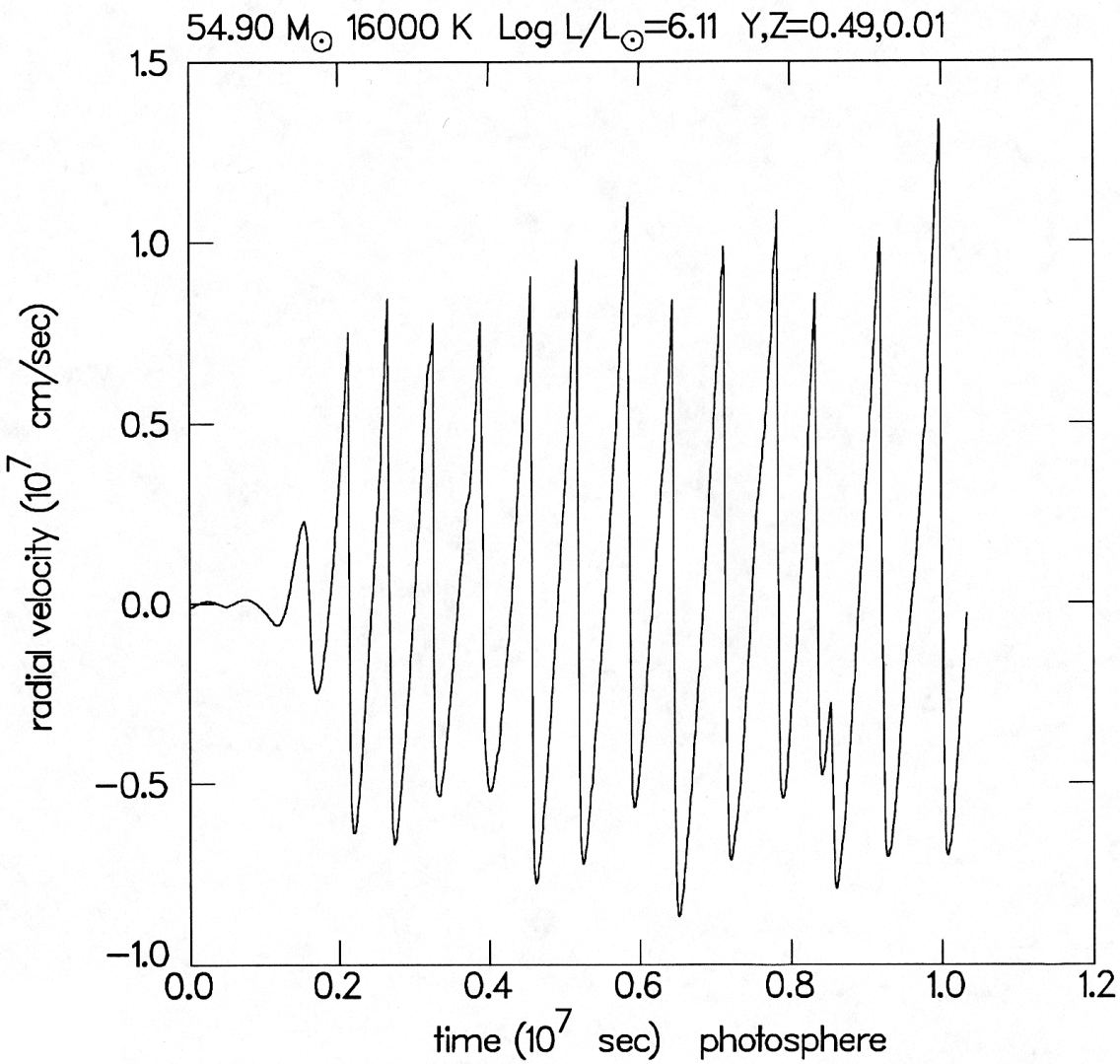

Y=0.49
Z=0.01

P ~ 7.6 d
Amplitude ~150 km/sec
V_{esc} ~ 380 km/sec

Lower-mass and luminosity models exhibit steady pulsations

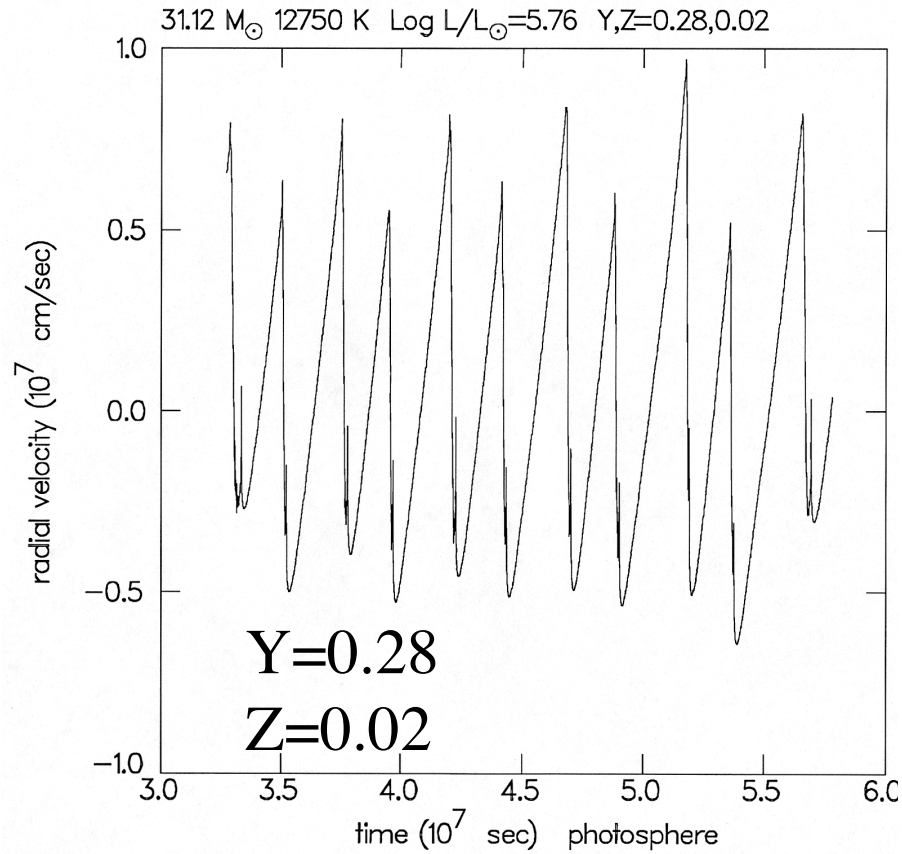

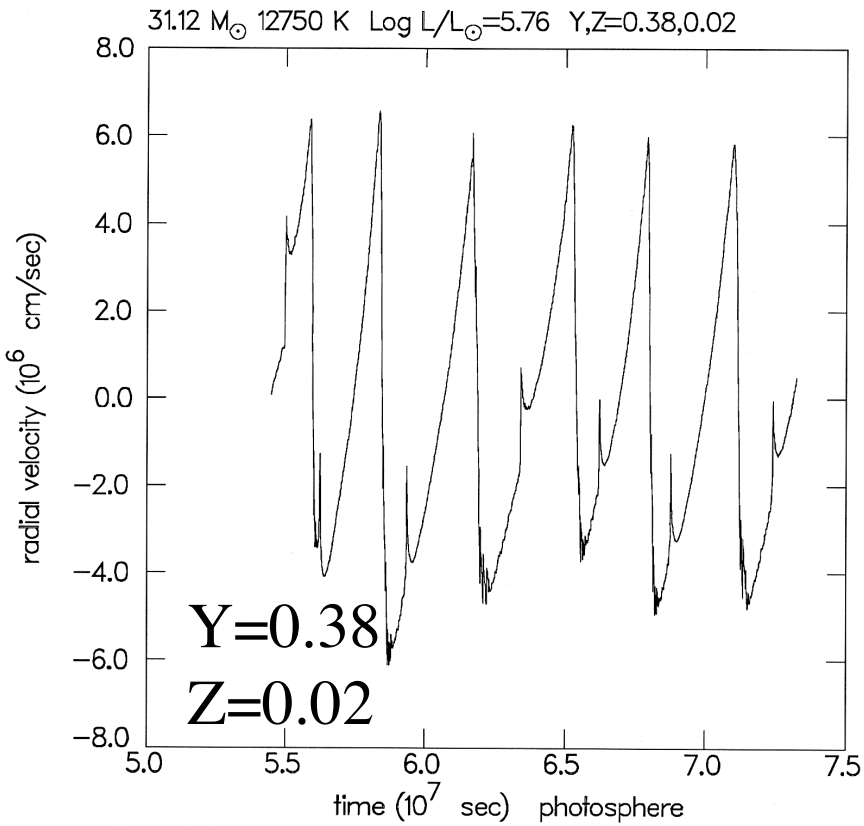

P ~ 26 d
Amplitude ~90 km/sec
V_{esc} ~ 280 km/sec

P ~ 35 d
Amplitude ~ 60 km/sec
V_{esc} = 280 km/sec

Summary of Nonlinear Pulsation Results

Y	Optically Thick Zones with $L_{rad} > L_{Edd}$	Result
47.28 M_{sun}, 16980 K, Z=0.02		
0.38	17, 30-34	"Outburst"
0.48	3, 29-32	"Outburst"
0.58	32-35	V_{max} 100 km/sec
54.9 M_{sun}, 16000 K, Z=0.01		
0.29	15-16	"Outburst"
0.39	None	V_{max} 200 km/sec
0.49	None	V_{max} 100 km/sec
31.1 M_{sun}, 12750 K, Z=0.02		
0.28	None	V_{max} 90 km/sec
0.38	None	V_{max} 60 km/sec

Los Alamos NATIONAL LABORATORY

The Eddington Limit

•An important characteristic that seems to determine whether models "outburst" appears to be whether the RADIATIVE LUMINOSITY of DEEP ZONES (temperatures > 100,000 K) exceeds the Eddington Luminosity limit at some point during the pulsation cycle.

Eddington Luminosity = $4\pi GMc/\kappa$

•At this limit, the force due to radiation pressure outward exceeds the force due to gravity.
•In a static non-pulsating model, convection turns on to transport the required luminosity, so the model avoids exceeding the Eddington limit.
•However, in a pulsating model, convection takes some time to turn on during pulsation cycle, so the Eddington limit can be periodically exceeded.

Los Alamos NATIONAL LABORATORY

Due to lag in convective luminosity increase during pulsations, deep layers can exceed L_{edd}

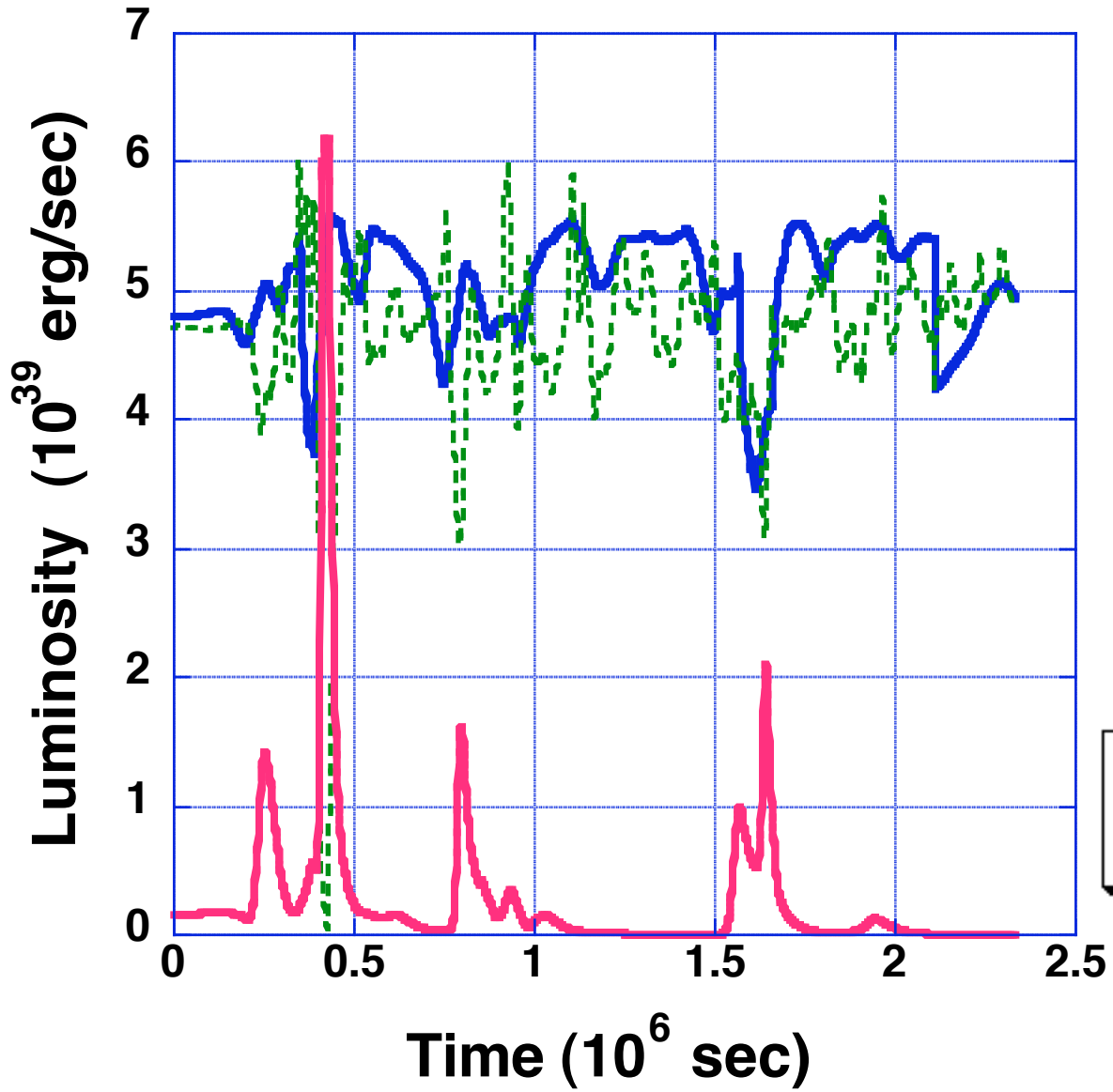

47 solar masses,
T_{eff} = 16,980 K
zone 25

Eddington Luminosity
Radiative Luminosity
Convective Luminosity

Los Alamos NATIONAL LABORATORY

Radiative luminosity exceeds L_{edd} until convection turns on to transport some luminosity

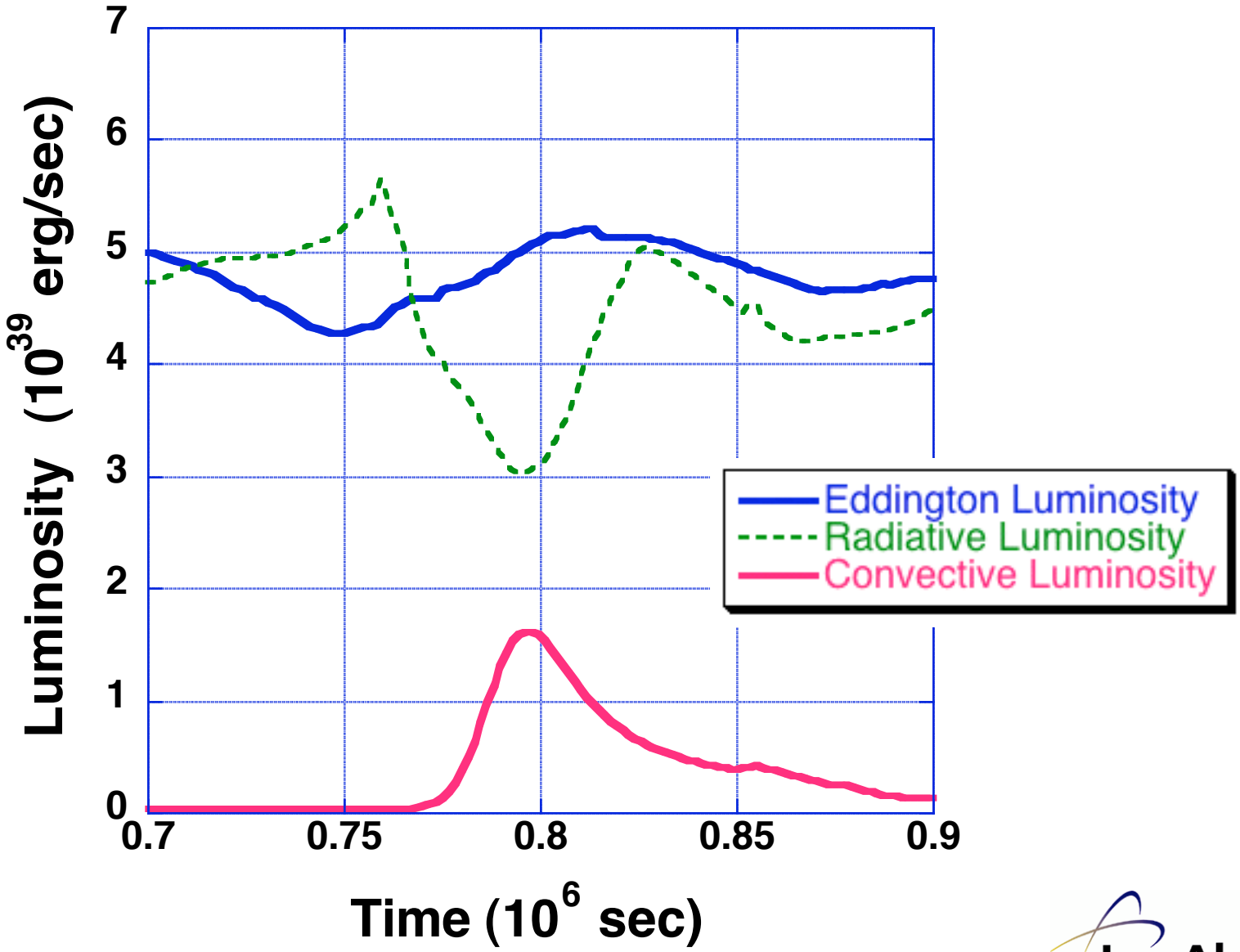

Los Alamos NATIONAL LABORATORY

Convective luminosity increase can lag radiative luminosity decrease

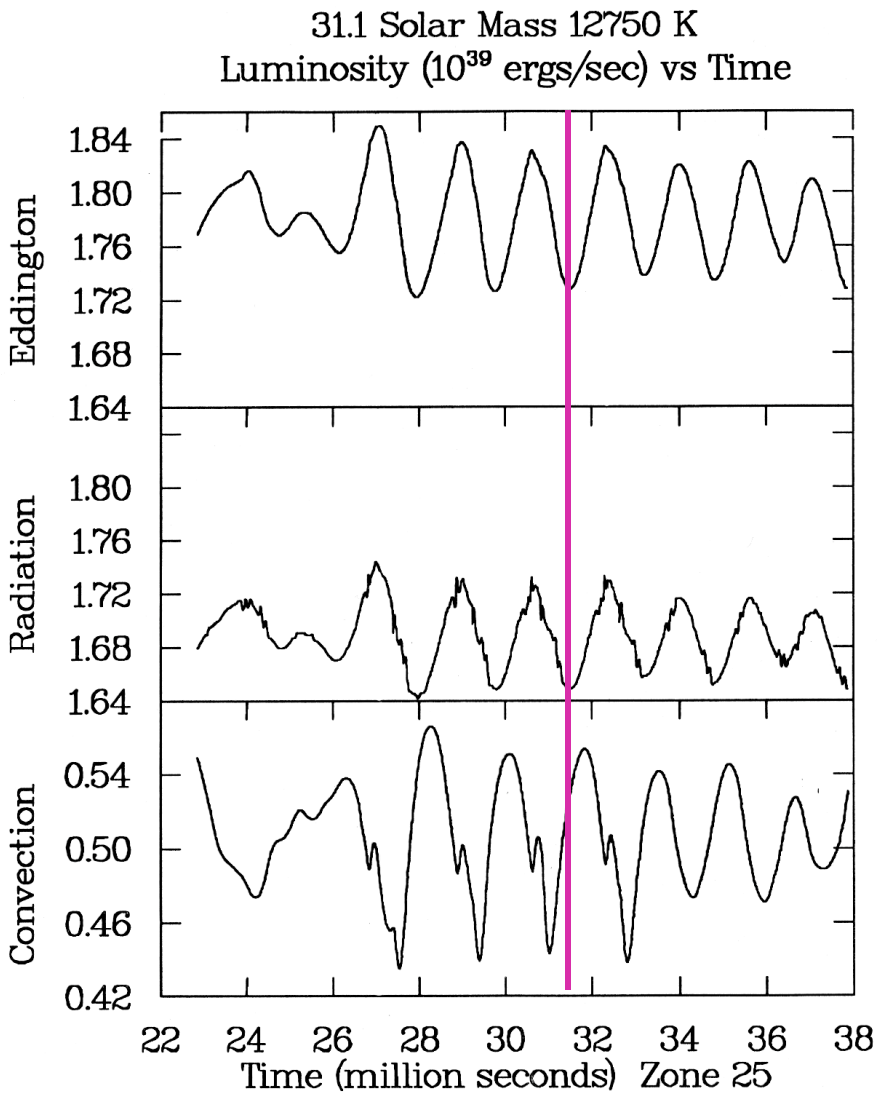

Even though for 31 M_{sun} model radiative luminosity is below Eddington luminosity, this model illustrates clearly lag of convective luminosity increase as radiative luminosity decreases.

Los Alamos NATIONAL LABORATORY

Winds or Outbursts?

- **We have shown ONLY that pulsations can trigger instability, and cause the outer layers of the star to move outward**

- Perhaps pulsation initiates flow, and shocks and and line-driven wind accelerate it (Bjorkman 1999).

- Our envelope models encompass only ~10^{-4} solar masses, whereas in observed outbursts much more mass can be lost

- Considering pulsation period, recovery time, winds produce at most 0.004 M_{sun}/year (10^{-4} M_{sun} every 10 days at best)

- Also, the calculated "outbursts" are generated within a few pulsation cycles (< 1 year) beginning from a near-static configuration, whereas the observed time between major outbursts is years or decades

Los Alamos NATIONAL LABORATORY

What is the origin/cause of empirical upper luminosity boundary?

Stars of $M_o > 50\ M_{sun}$ repeatedly outburst and lose mass until their envelopes are enriched in helium and outbursts are stabilized. These stars never evolve past the H-D line.

e.g. AG Car, S Dor

Pulsation-driven winds give rise to high mass loss rate that keeps stars to blue of H-D line

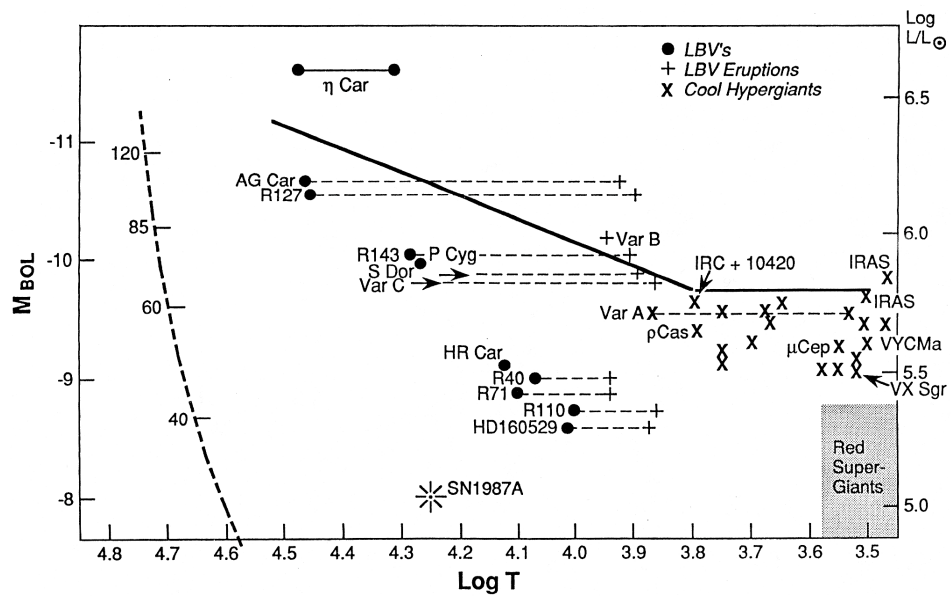

What is the origin/cause of empirical upper luminosity boundary?

Stars of $M_o < 50\ M_{sun}$ pulsate on first crossing of HR diagram, but do not outburst. These stars are able to evolve to become Red Supergiants.

After they have lost considerably more mass as RSGs and evolve back to the blue, their increased L/M ratio may cause them to exceed the Eddington limit and experience outbursts.

e.g. HR Car, R40, R71

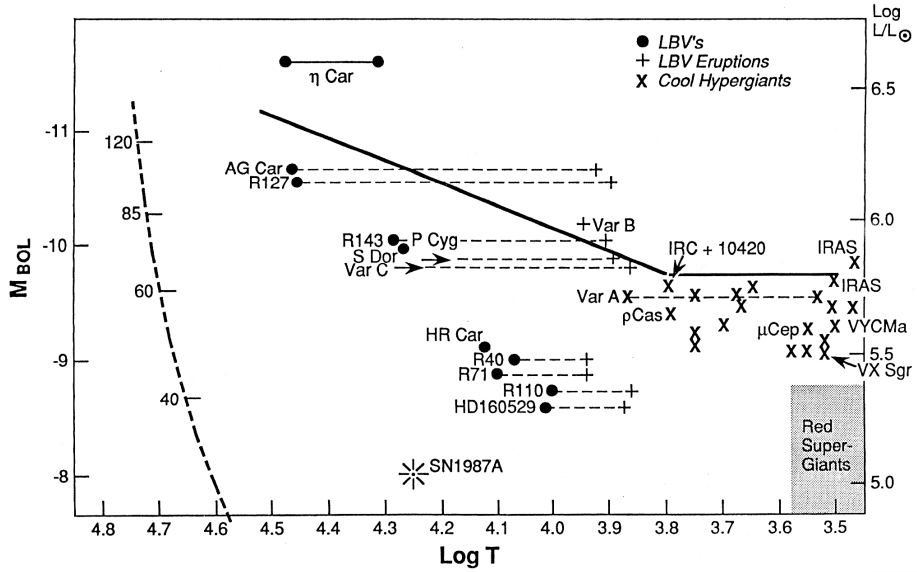

β Cephei and SPB stars in the Hertzsprung-Russell Diagram

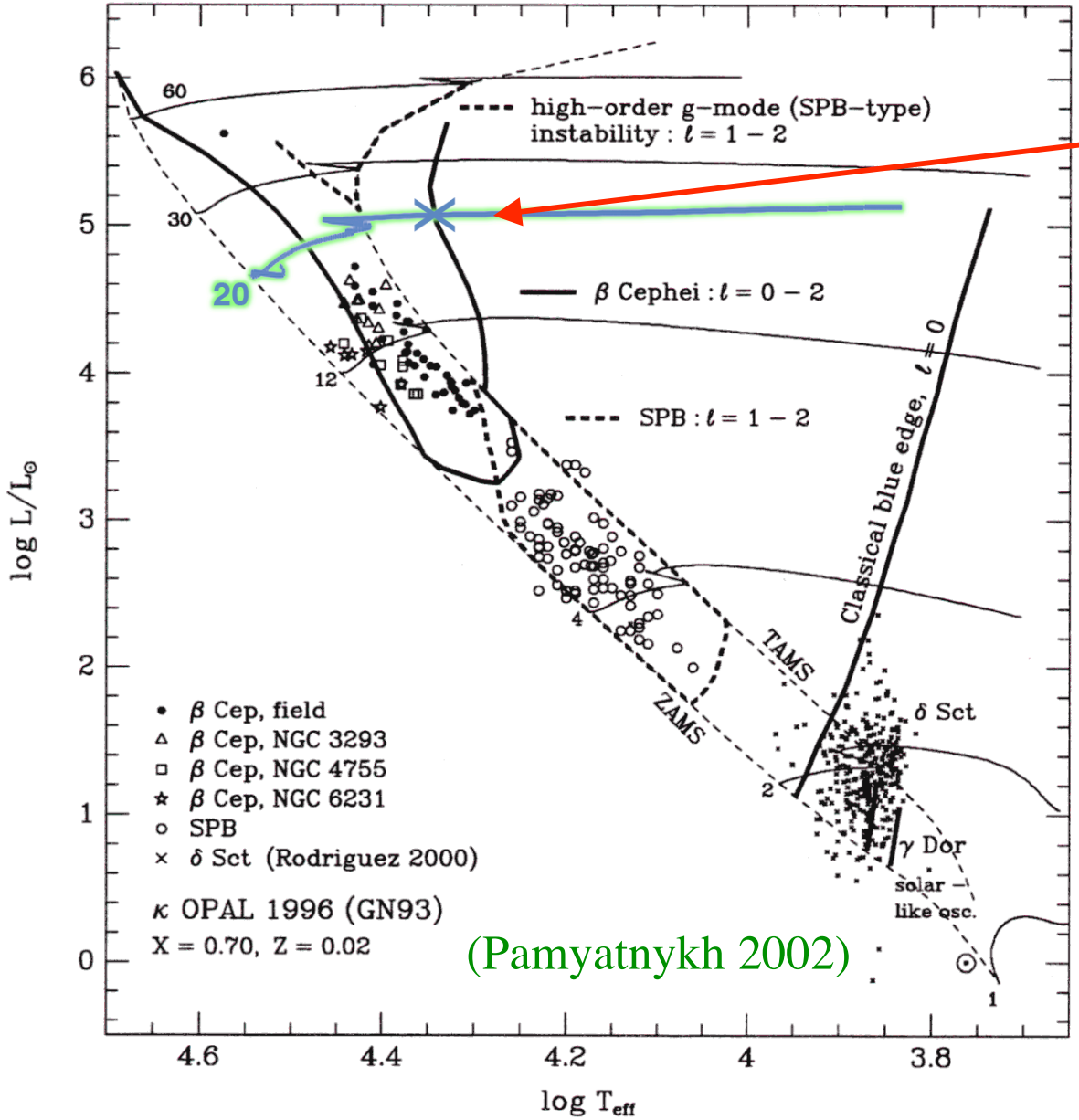

(Pamyatnykh 2002)

Our evolution track with Iben code for (X, Y, Z = 0.70, 0.28, 0.02), X marks ~22,000 K models we studied

20 M_{sun} model radius increases from 6 R_{sun} on ZAMS to 15 R_{sun} before 'blue hook' to 23 R_{sun} after 'blue hook'

Los Alamos NATIONAL LABORATORY

Linear pulsation behavior for 20 M_{sun} models

For fixed temperature, radius (~23 R_{sun}), and luminosity, the pulsation driving increases with increasing Z.

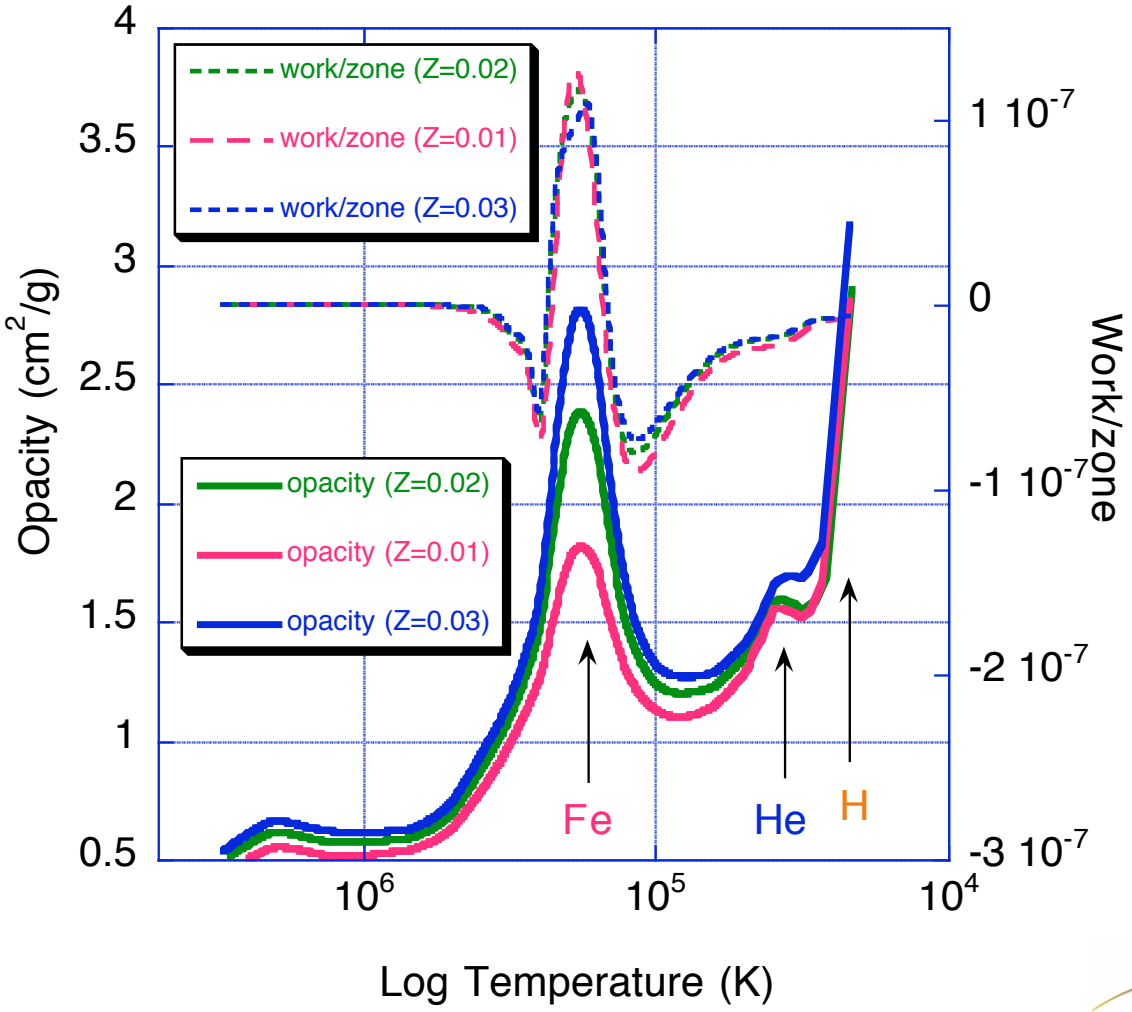

Linear pulsation behavior of 20 M_{sun} models with T_{eff} = 22,139 K

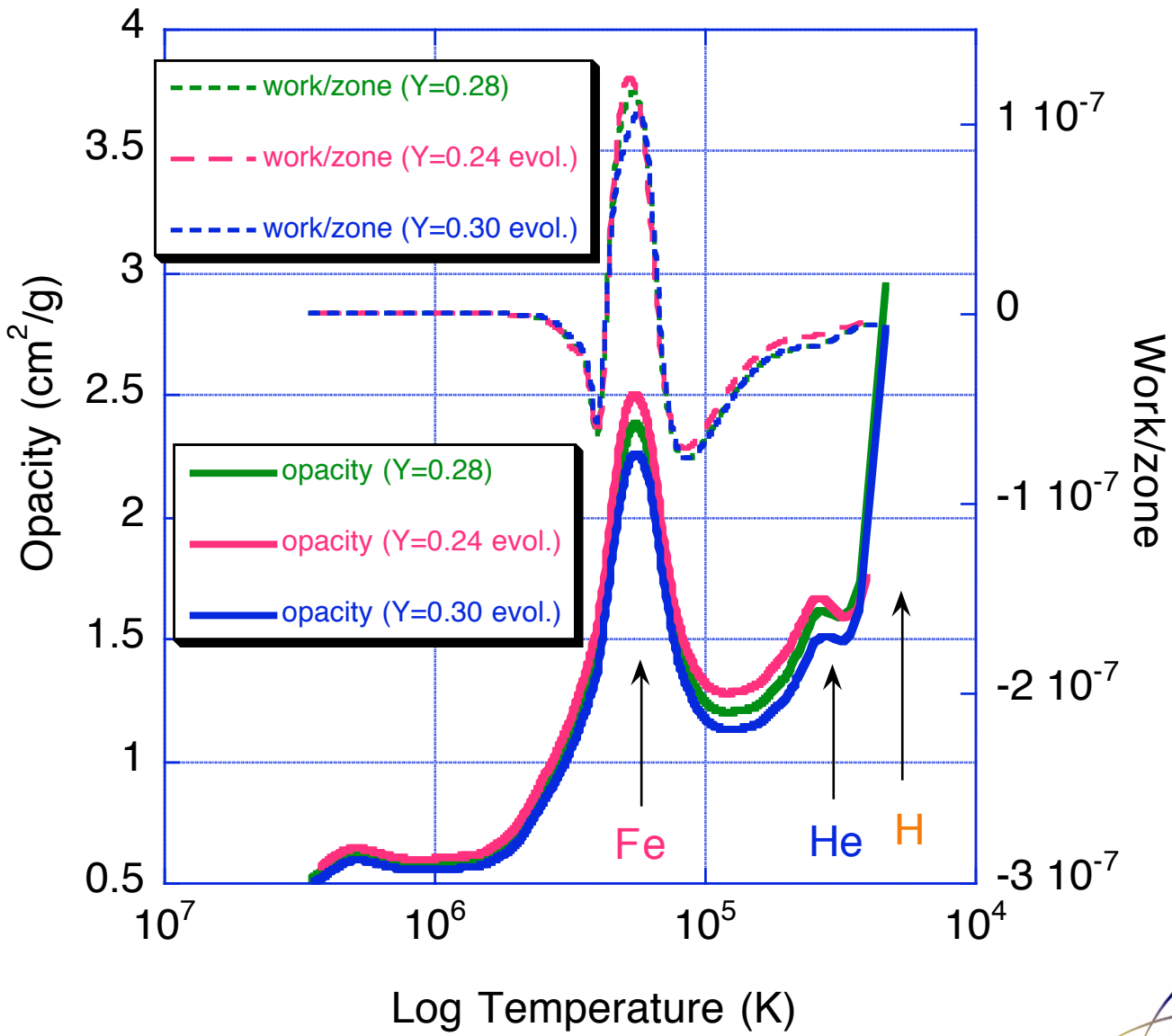

Linear pulsation behavior of 20 M_{sun} models

Y, Z	T_{eff} (K)	Fund. Mode Period(days)	Growth rate/period (+ = unstable)
0.24, 0.02	22,000	0.888	-0.0318
0.28, 0.02	22,000	0.877	-0.0236
0.32, 0.02	22,000	0.868	-0.0160
0.28, 0.01	22,000	0.833	-0.0556
0.28, 0.02	22,000	0.877	-0.0236
0.28, 0.03	22,000	0.916	+0.0186
0.28, 0.02	24,000	0.644	+0.0374
0.28, 0.02	22,000	0.877	-0.0236
0.28, 0.02	20,000	1.227	-0.1028

Los Alamos NATIONAL LABORATORY

Nonlinear Hydrodynamic Models

Models initiated in fundamental mode with radial velocity amplitude 5 km/sec.

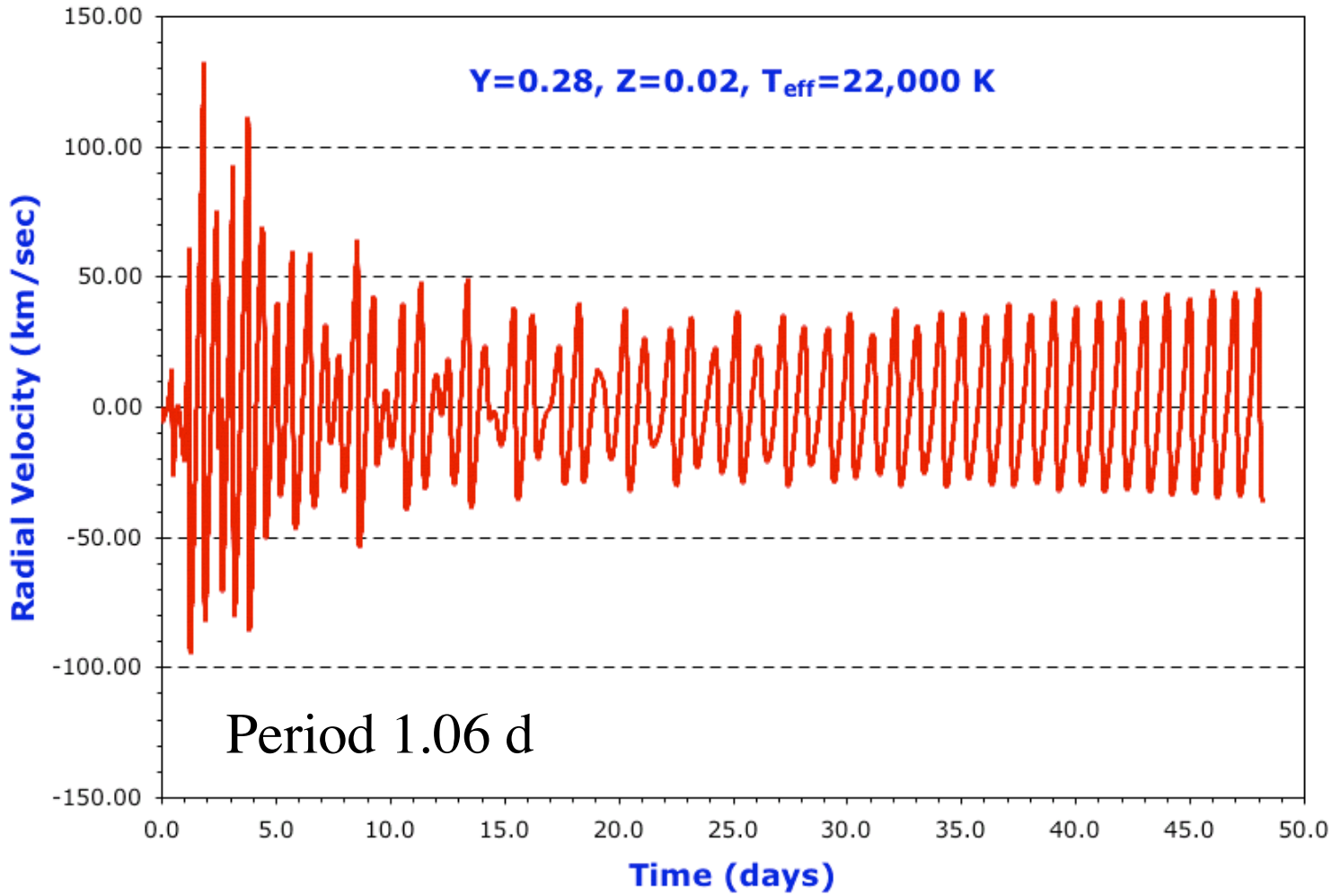

Los Alamos NATIONAL LABORATORY

Pulsations damp with lower photospheric T_{eff}

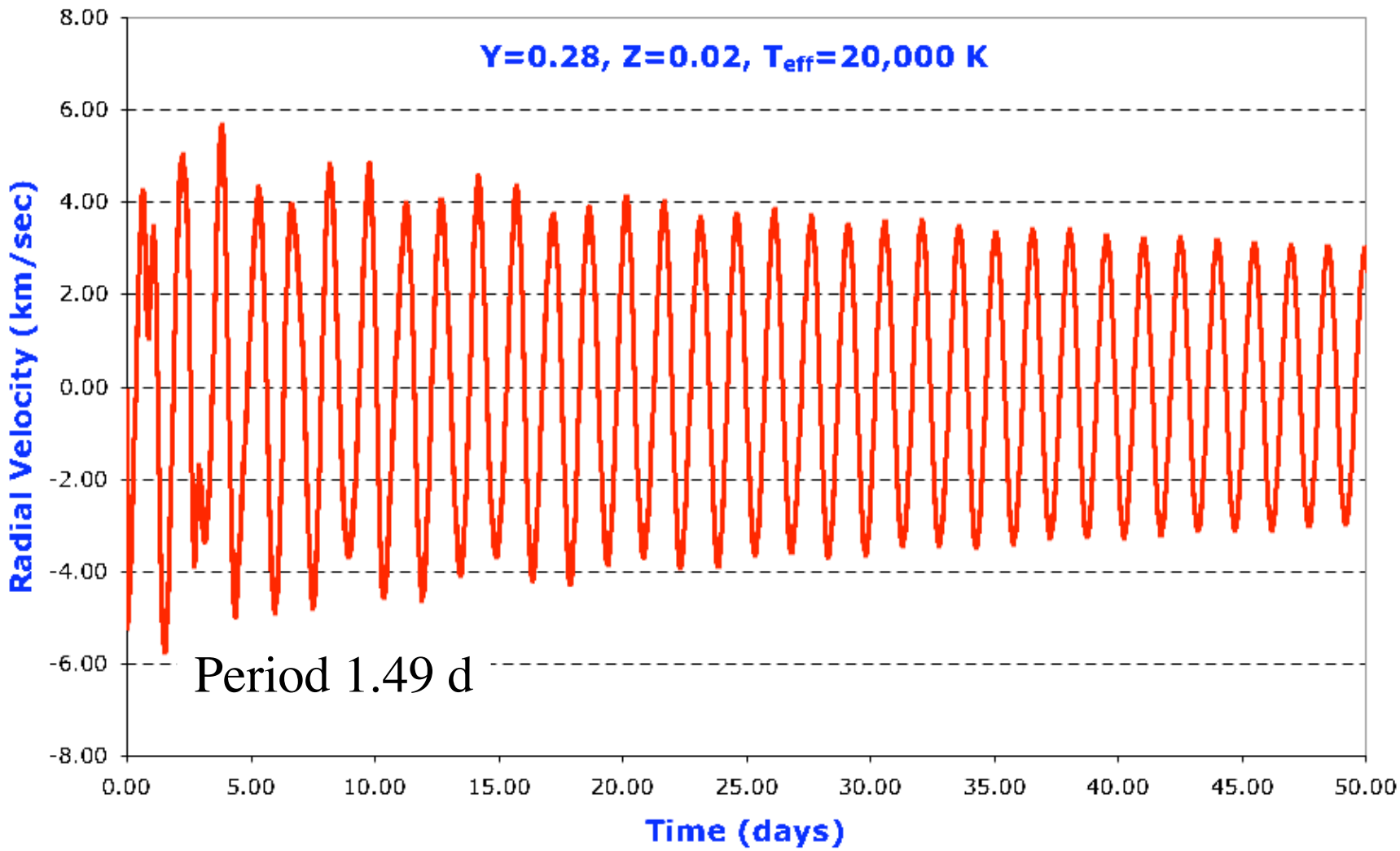

Los Alamos NATIONAL LABORATORY

Pulsations grow with higher photospheric T_{eff}

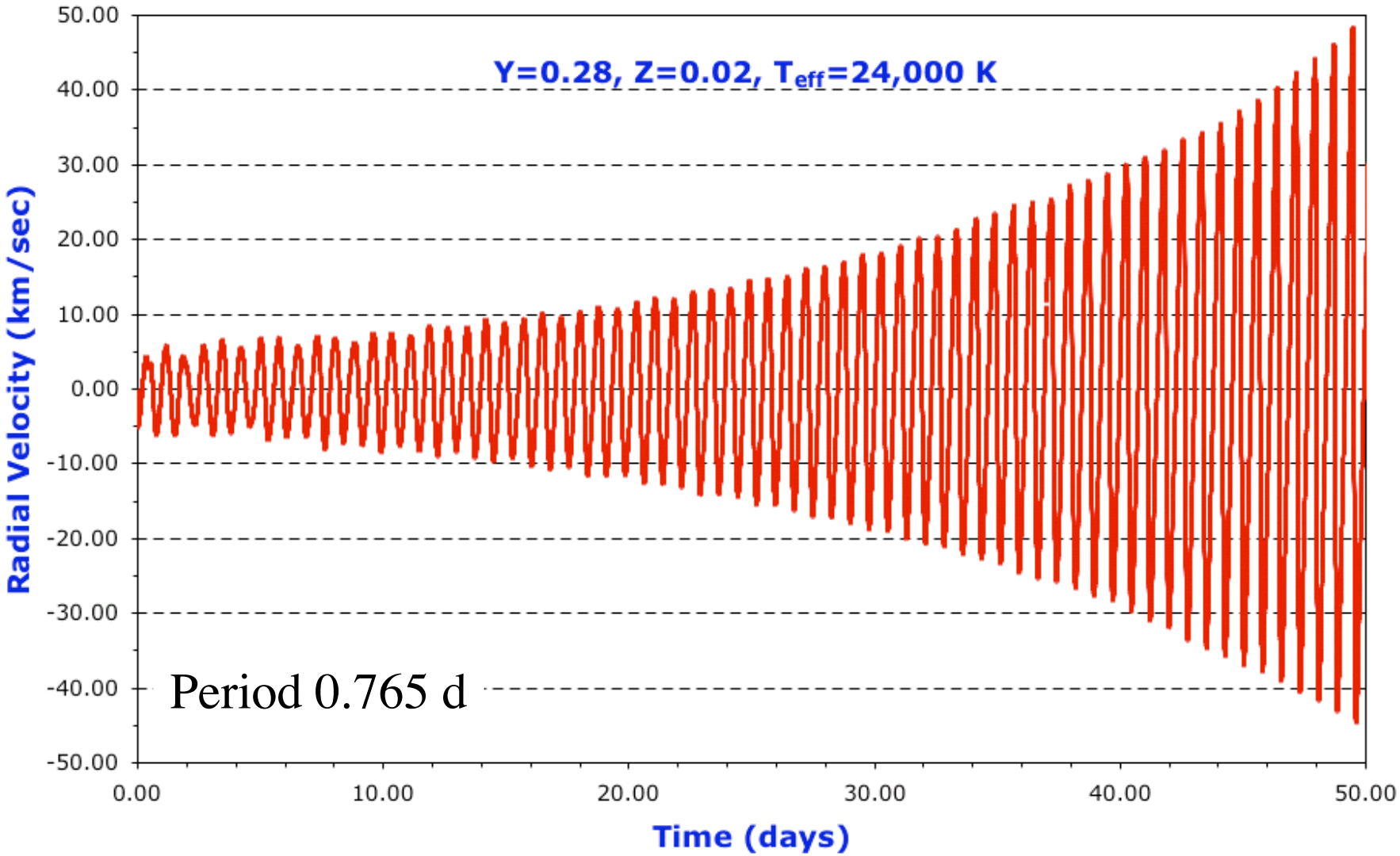

Pulsations damp quickly with decreased Z (Fe) abundance

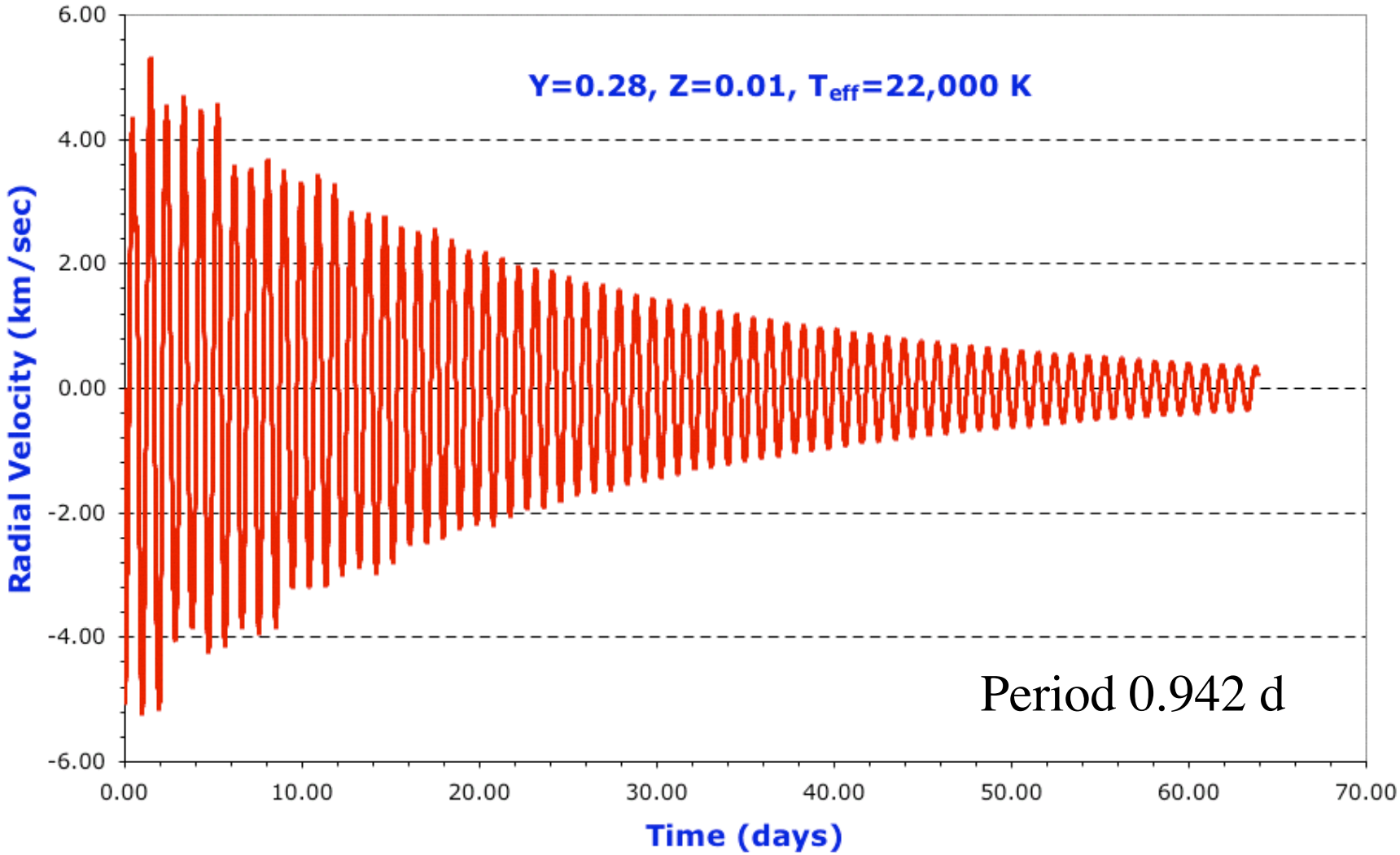

Los Alamos NATIONAL LABORATORY

Pulsations grow rapidly with increased Z (Fe) abundance

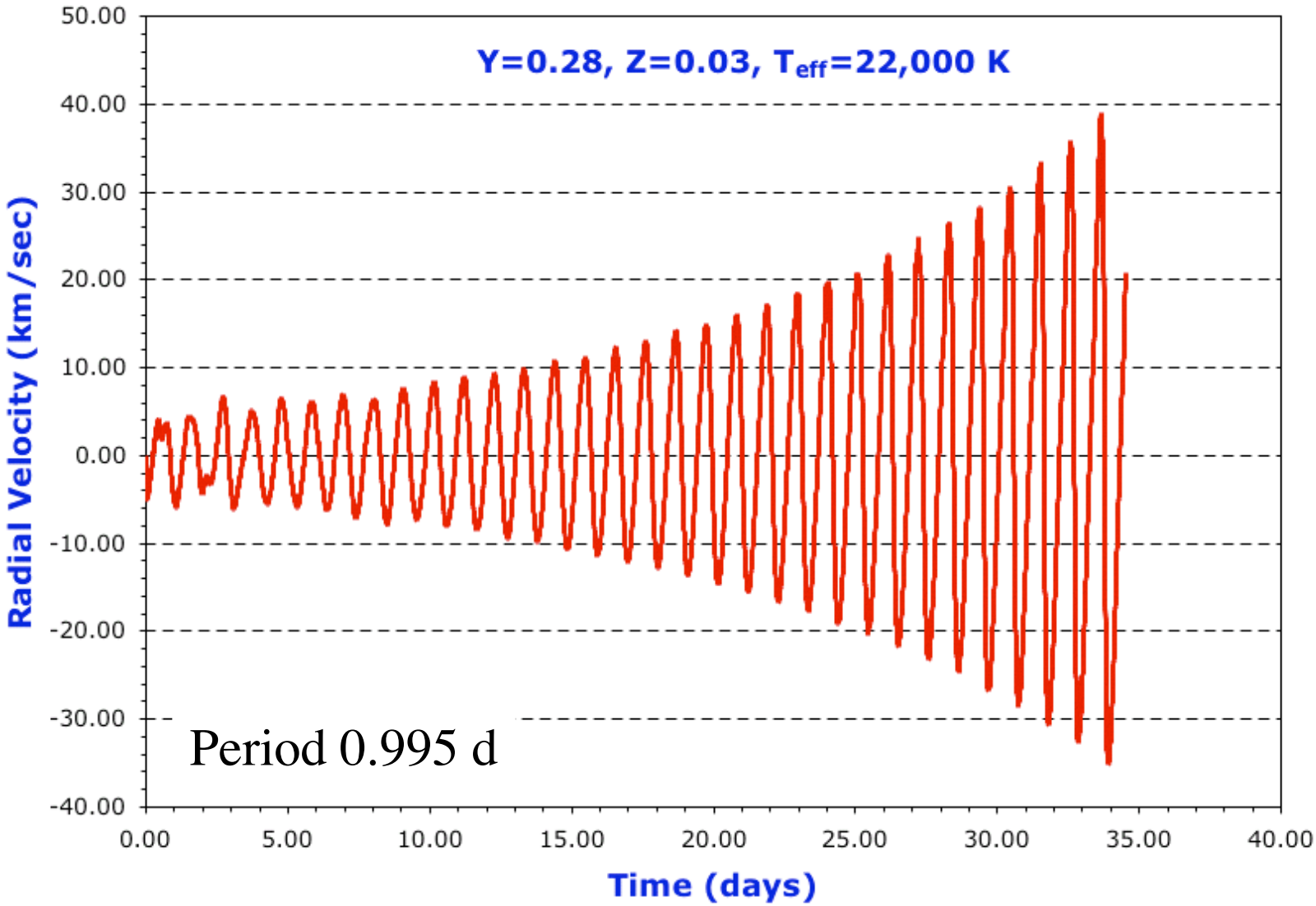

Los Alamos NATIONAL LABORATORY

Pulsations grow slowly with decreased He abundance

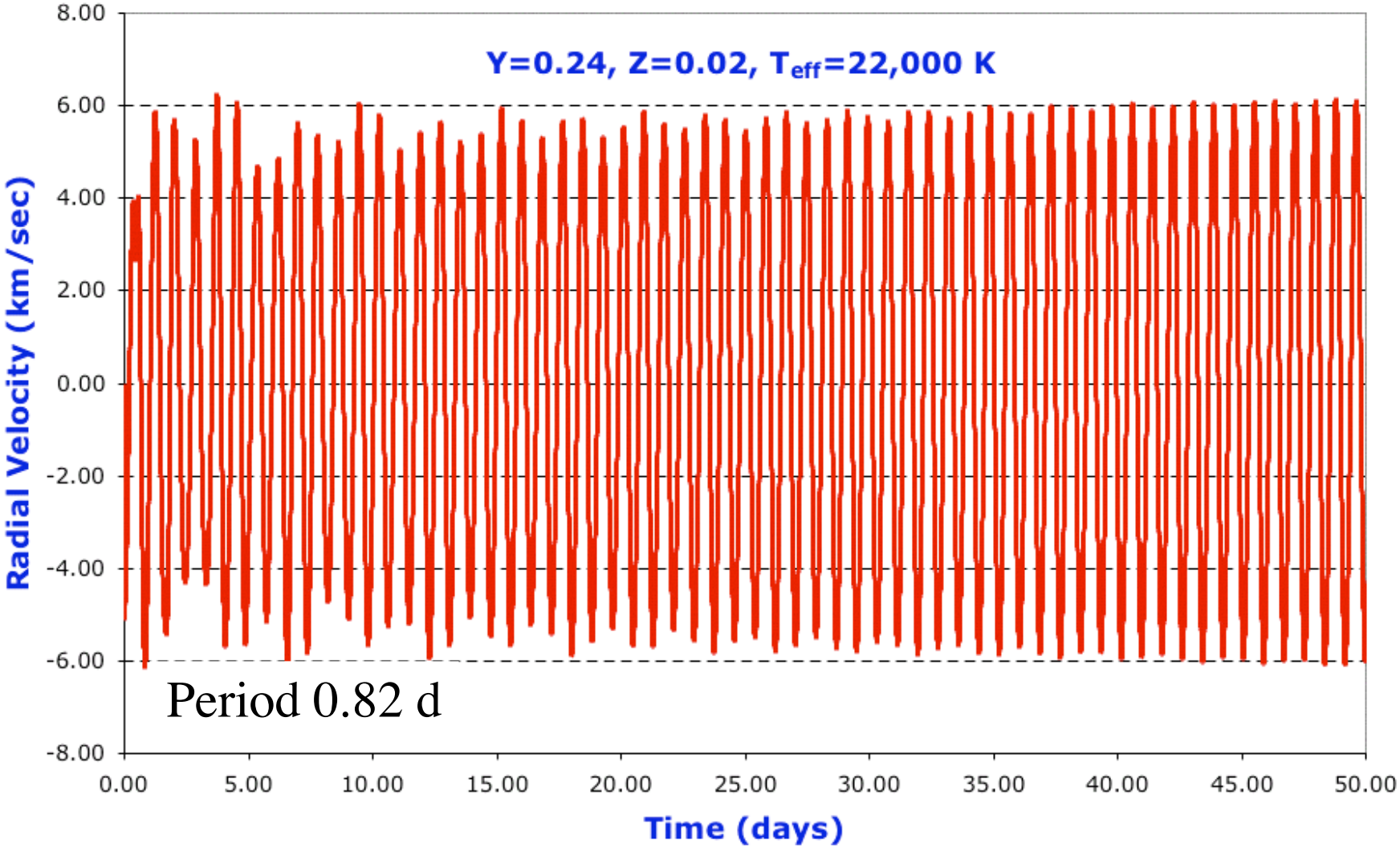

Los Alamos NATIONAL LABORATORY

Pulsations damp rapidly with increased He abundance

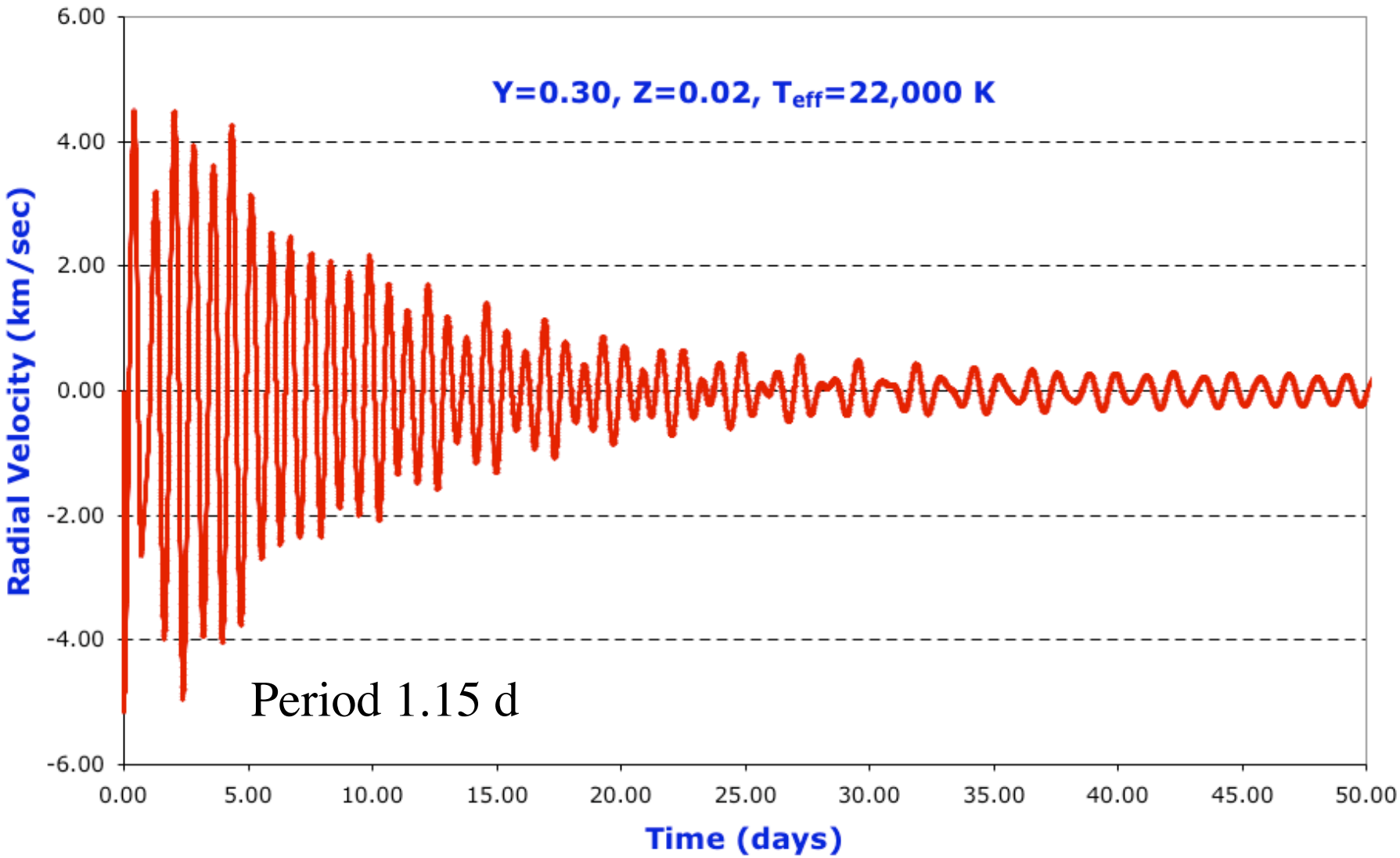

Los Alamos NATIONAL LABORATORY

Conclusions of talk:

Massive hot stars are predicted under certain conditions to be pulsationally unstable.

Pulsation instability is due to kappa-effect driving from Fe ionization at 200,000 K in the envelope

Pulsation instability and amplitude depends critically on Fe abundance, and is reduced for less chemically enriched stars.

Pulsation can extend envelope and enhance mass loss, thereby affecting stellar yields.

Pulsation can also trigger envelope instability and possibly 'normal' LBV outbursts accompanied by larger mass loss. Outbursts are caused by exceeding Eddington limit in deep layers due to time-dependence of convection.

A different mechanism is needed to explain the rare giant eruptions, with ejections of several solar masses, seen in Eta Car or P Cyg.

Los Alamos NATIONAL LABORATORY

Questions to Discuss

What are the consequences of pulsation of hot massive luminous stars for chemical enrichment?

How do pulsation properties that affect mass loss depend on initial mass function and stellar composition (Y, especially Z)?

Have these implications been accounted for adequately in stellar mass loss rates and nucleosynthetic yield models?

Los Alamos
NATIONAL LABORATORY

References

Austin, B.A., Guzik, J.A., Templeton, M.R., and Despain, K.M, 2004, in Variable Stars in the Local Group, ASP, ed. D.W. Kurtz and K. Pollard.

Cox, A.N., 1990, in Nonlinear Astrophysical Fluid Dynamics, ed. J.R. Buchler and S.T. Gottesman (New York Acad. Sci.), p. 54

Despain, K.M., Guzik, J.A., Cox, A.N. 1998, in A Half Century of Stellar Pulsation interpretations, ed. P.A. Bradley and J.A. Guzik, ASP, p 307

Guzik, J.A., Cox, A.N., & Despain, K., 1998, in *Variable and Non-Spherical Winds in Luminous Hot Stars*, Heidelberg, Germany, June 15-19, 1998, eds. B. Wolf, O.Stahl, and A.W. Fullerton, Lecture Notes in Physics #523, (Springer, Berlin, 1999), pp. 337-344.

Guzik, J.A., Cox, A.N., & Despain, K. in *Eta Carinae at the Millenium*, July 20-23, 1998, Gallatin Gateway, Montana, eds. J. Morse, R. Humphreys, and A. Damineli, (ASP Conf. Ser. Vol. 179, 1999), pp. 347-353.

Humphreys, R.M. & Davidson, K. 1994, PASP 106, 1025

Iben, I., 1963, ApJ, 138, 452; 1965a, ApJ, 141, 993; ApJ, 142, 1447

Iglesias, C.A. & Rogers, F.J., 1996, ApJ, 464, 943

Pesnell, W.D., 1990, ApJ, 363, 227

Ostlie, D.A & Cox, A.N., 1993, Ap&SS, 210, 311

Ostlie, D.A. 1990, in Numerical Modelling of Nonlinear Stellar Pulsations: Problems and Prospects, ed. J.R. Buchler (Kluwer Academic, Dordrecht, p. 89)

Pamyatnykh, A.A. 2002, Comm. Asteroseismology, 142, 10

Pesnell, W.D. 1990, ApJ, 363, 227

Los Alamos NATIONAL LABORATORY

Evolution of Massive Pop III Stars

Alexander Heger
Stan Woosley

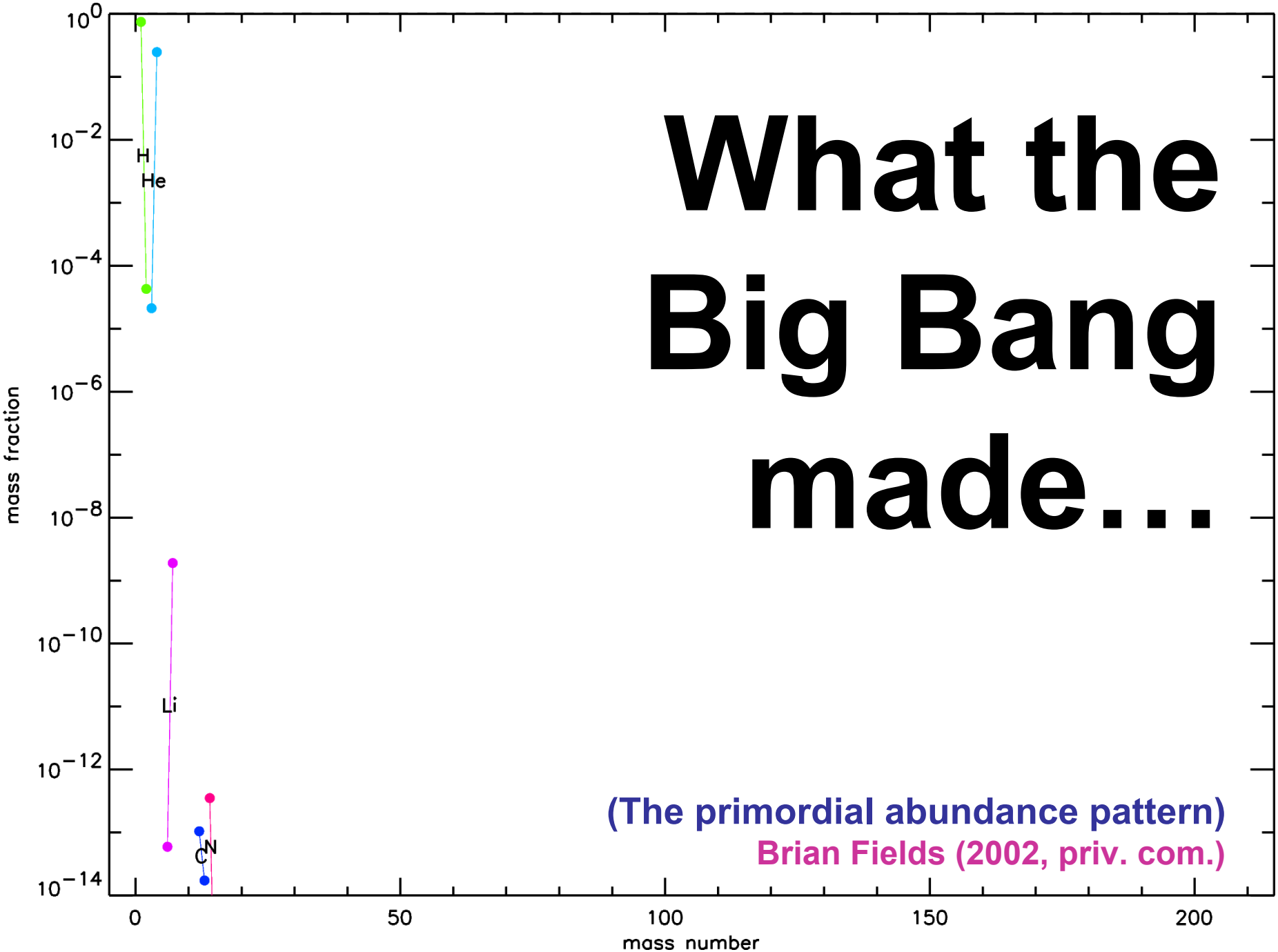

What the Big Bang made…

(The primordial abundance pattern)

Brian Fields (2002, priv. com.)

What We Find Today

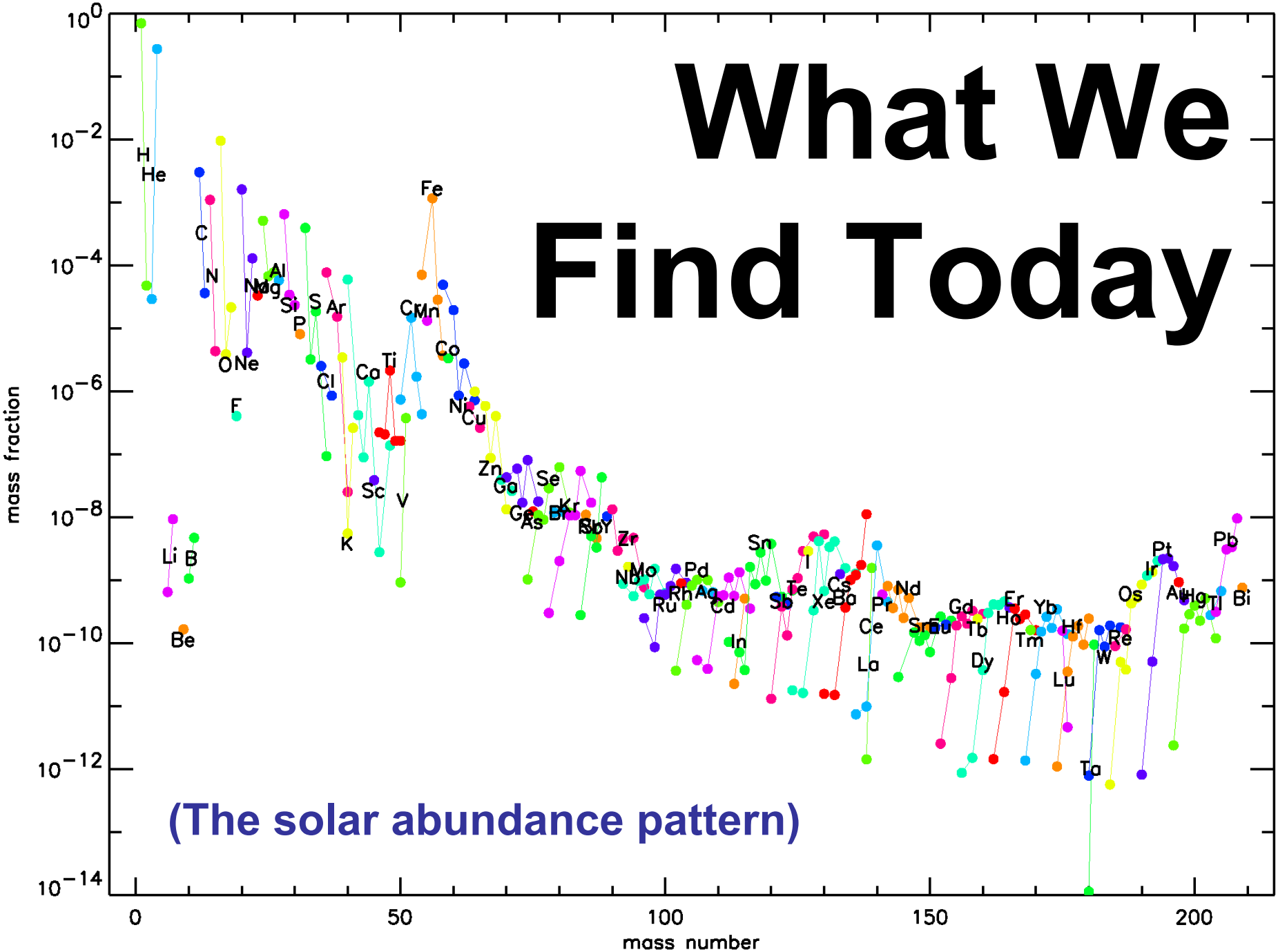

(The solar abundance pattern)

Overview

- Basics of massive star evolution and nucleosynthesis
- What comes out…?
- Nucleosynthesis in *massive* Pop III stars (10–100 $M_\odot$)
- Nucleosynthesis in *very massive* Pop III stars (100–1000 $M_\odot$)
- Can UMP star abundances constrain Pop III IMF?

Once formed, the evolution of a star is governed by gravity:

continuing contraction

to higher central densities and temperatures

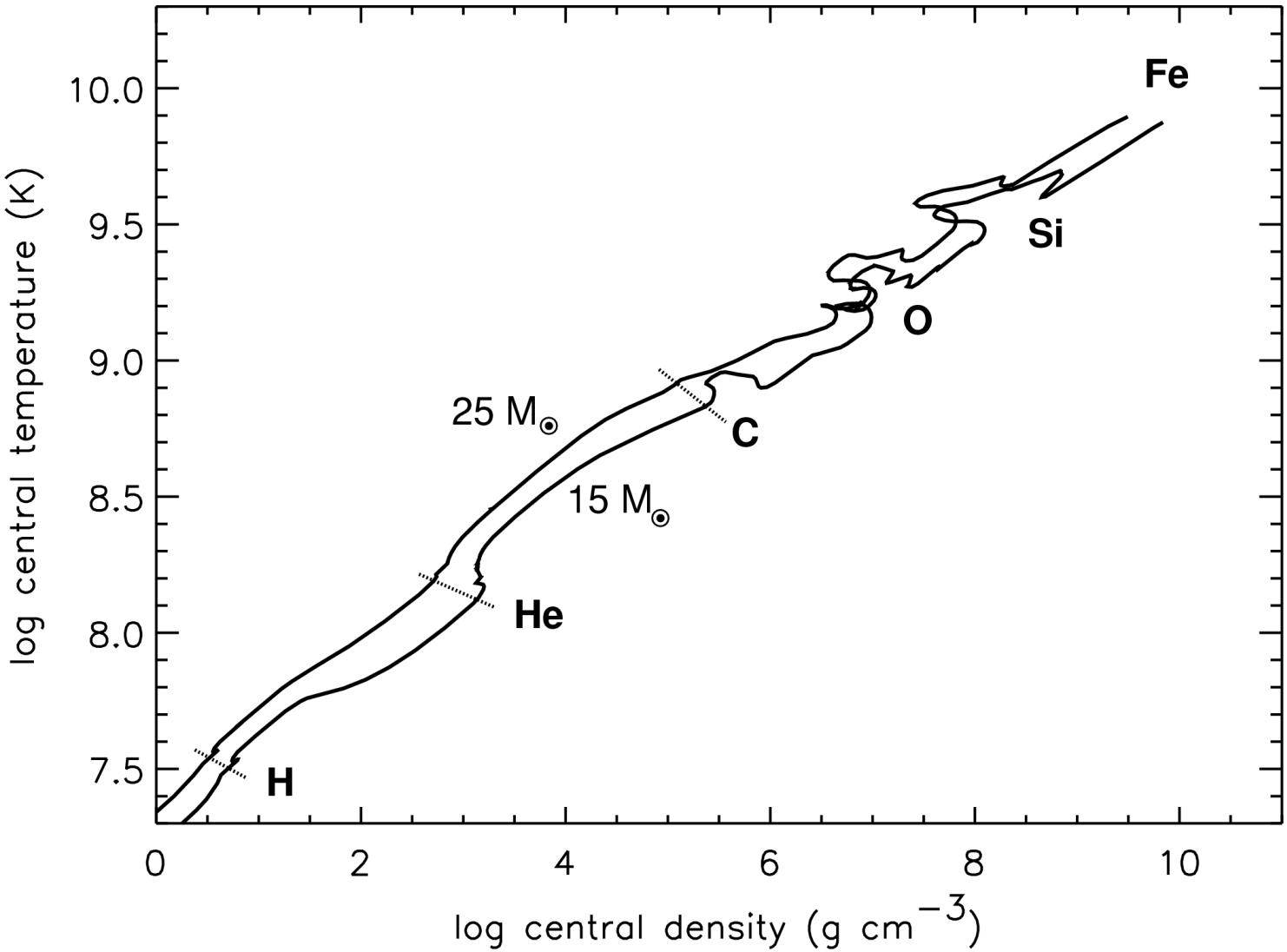

Evolution of central density and temperature of 15 $M_\odot$ and 25 $M_\odot$ stars

Nuclear burning stages

(e.g., 20 solar mass star)

Fuel	Main Product	Secondary Product	T (10^9 K)	Time (yr)	Main Reaction
H	He	^{14}N	0.02	10^7	$4\ H \xrightarrow{CNO} {}^4He$
He	O, C	^{18}O, ^{22}Ne s-process	0.2	10^6	$3\ He^4 \rightarrow {}^{12}C$ ${}^{12}C(\alpha,\gamma){}^{16}O$
C	Ne, Mg	Na	0.8	10^3	${}^{12}C + {}^{12}C$
Ne	O, Mg	Al, P	1.5	3	${}^{20}Ne(\gamma,\alpha){}^{16}O$ ${}^{20}Ne(\alpha,\gamma){}^{24}Mg$
O	Si, S	Cl, Ar, K, Ca	2.0	0.8	${}^{16}O + {}^{16}O$
Si	Fe	Ti, V, Cr, Mn, Co, Ni	3.5	0.02	${}^{28}Si(\gamma,\alpha)$…

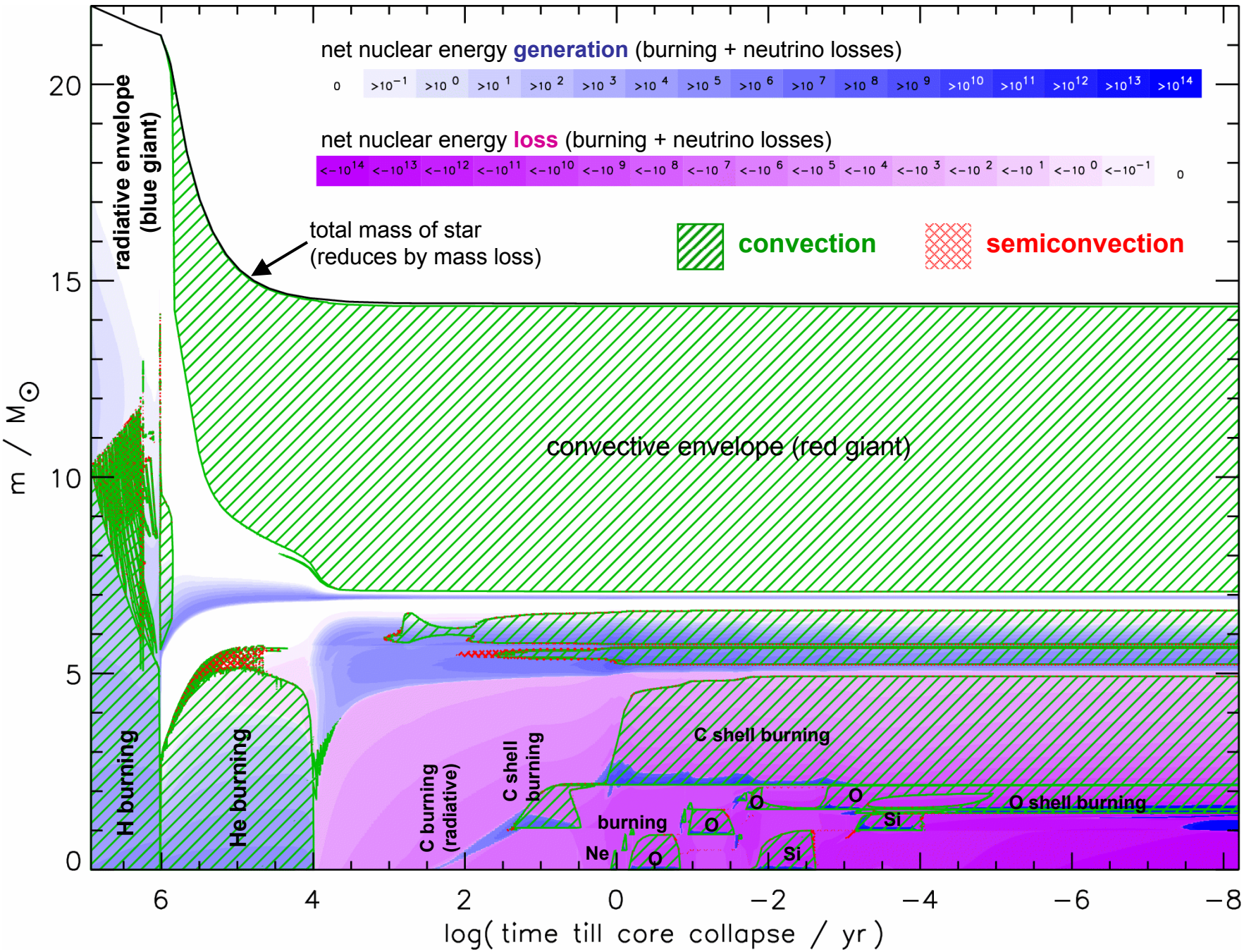
net nuclear energy generation (burning + neutrino losses)
0
>10^−1
>10^0
>10^1
>10^2
>10^3
>10^4
>10^5
>10^6
>10^7
>10^8
>10^9
>10^10
>10^11
>10^12
>10^13
>10^14
net nuclear energy loss (burning + neutrino losses)
<−10^14
<−10^13
<−10^12
<−10^11
<−10^10
<−10^9
<−10^8
<−10^7
<−10^6
<−10^5
<−10^4
<−10^3
<−10^2
<−10^1
<−10^0
<−10^−1
0
total mass of star
(reduces by mass loss)
convection
semiconvection
radiative envelope
(blue giant)
convective envelope (red giant)
H burning
He burning
C burning
(radiative)
C shell
burning
C shell burning
burning
Ne
O
O
O
Si
Si
O shell burning
m / M⊙
log(time till core collapse / yr)
20
15
10
5
0
6
4
2
0
−2
−4
−6
−8

Explosive Nucleosynthesis

in supernovae

Fuel	Main Product	Secondary Product	T (10^9 K)	Time (s)	Main Reaction
Innermost ejecta	*r*-process	-	>10 low Y_e	1	(n,γ), β^-
Si, O	^{56}Ni	iron group	>4	0.1	(α,γ)
O	Si, S	Cl, Ar, K, Ca	3 - 4	1	^{16}O + ^{16}O
O, Ne	O, Mg, Ne	Na, Al, P	2 - 3	5	(γ,α)
		p-process ^{11}B, ^{19}F, ^{138}La, ^{180}Ta	2 - 3	5	(γ,n)
		ν-process		5	(ν, ν'), (ν, e$^-$)

IMF of the First Stars

Predicted to be heavy to very heavy

by theory – insufficient cooling due to lack of metal (e.g., Larson 1999)

and by numerical simulations

(Bromm, Coppi, & Larson 1999, 2002;

Abel, Bryan, & Norman 2000, 2002;

Nakamura & Umemura 2001)

with a typical mass scale of ~100 $M_\odot$

➔The first stars *may* have had a significant very massive population

Ionizing Photon Fluxes

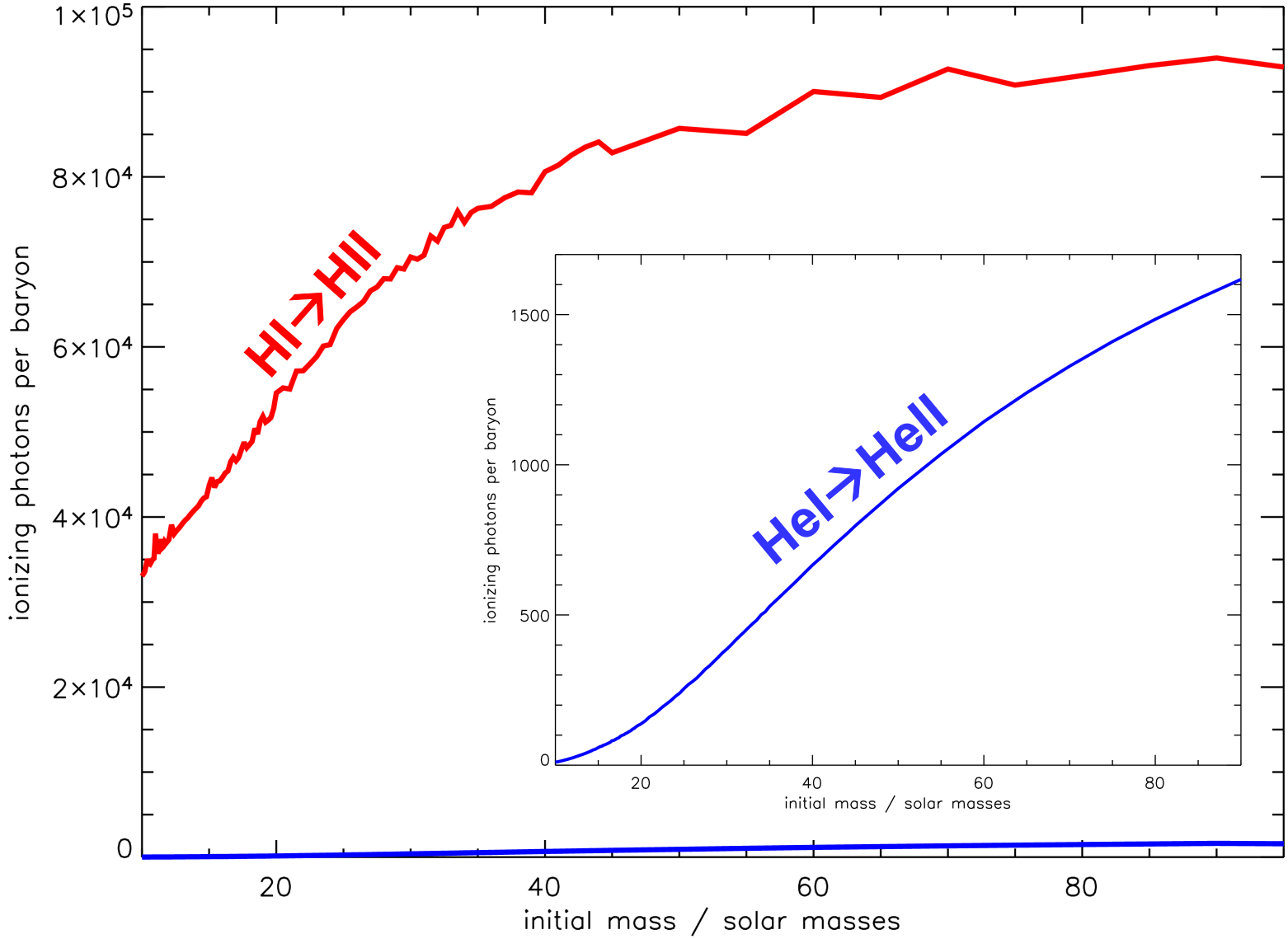

The number of ionizing photons per baryon strongly depends on the initial stellar mass at low mass, but levels off at high stellar mass (constant stellar temperature).

Additional Ingredient

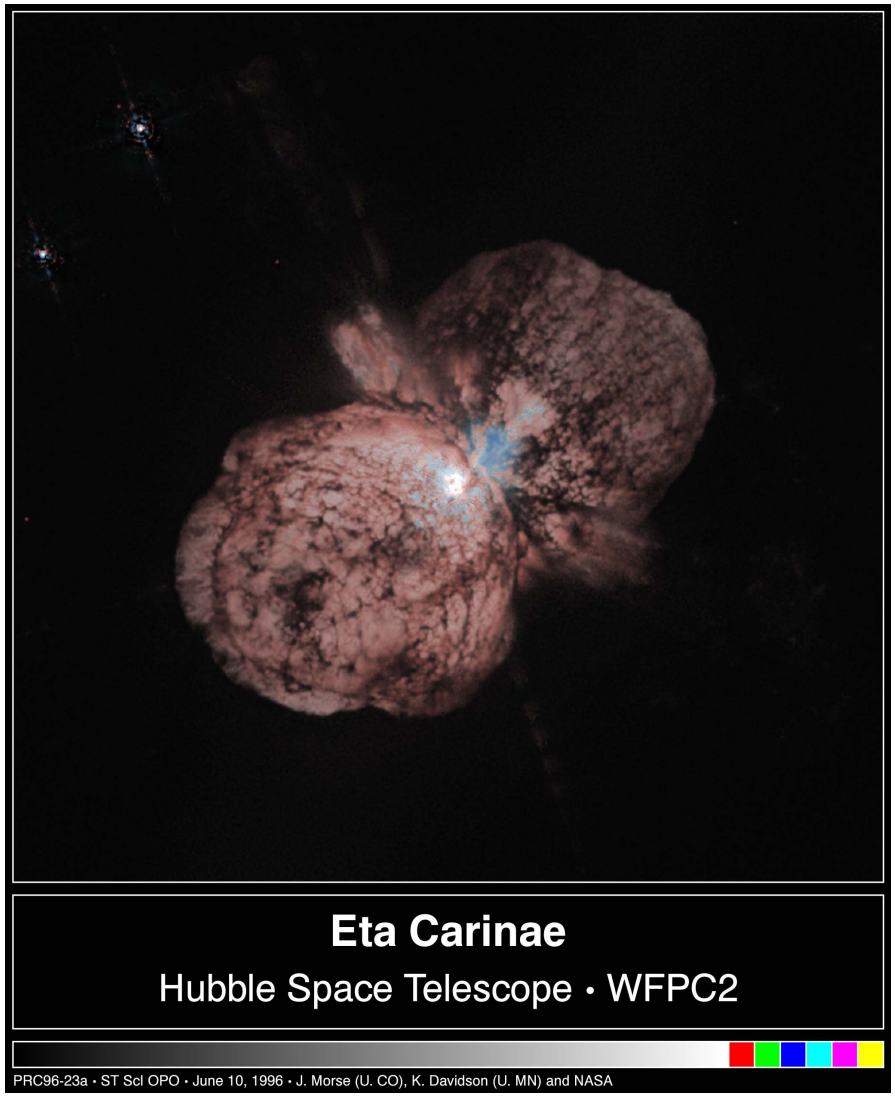

Essentially negligible mass loss in Pop III stars

in contrast:

Eta Carina

- Galactic star / solar+ metallicity
- Extremely high mass loss rate
- Initial mass: 150-200 $M_\odot$ (?)
- Will likely die as much less massive object

Mass Loss in Very Massive Primordial Stars

- Negligible line-driven winds
  (mass loss ~ metallicity$^{>1/2}$ – Kudritzki 2002)
- No opacity-driven pulsations (no metals – Baraffe, Heger & Woosley 2001)
- Continuum-driven winds @ $L \sim L_{Edd}$ have to be explored
  (talks by Owocki, Shaviv, *et al.*)
- Epsilon mechanism inefficient in metal-free stars below ~1000 $M_\odot$
  from pulsational analysis we estimate:
  - 120 solar masses: < 0.2 %
  - 300 solar masses: < 3.0 %
  - 500 solar masses: < 5.0 %
  - 1000 solar masses: < 12. %

  during central hydrogen burning
- Red Super Giant pulsations could lead to significant mass loss during helium burning for stars above ~500 $M_\odot$
- Rotationally induced mass loss?

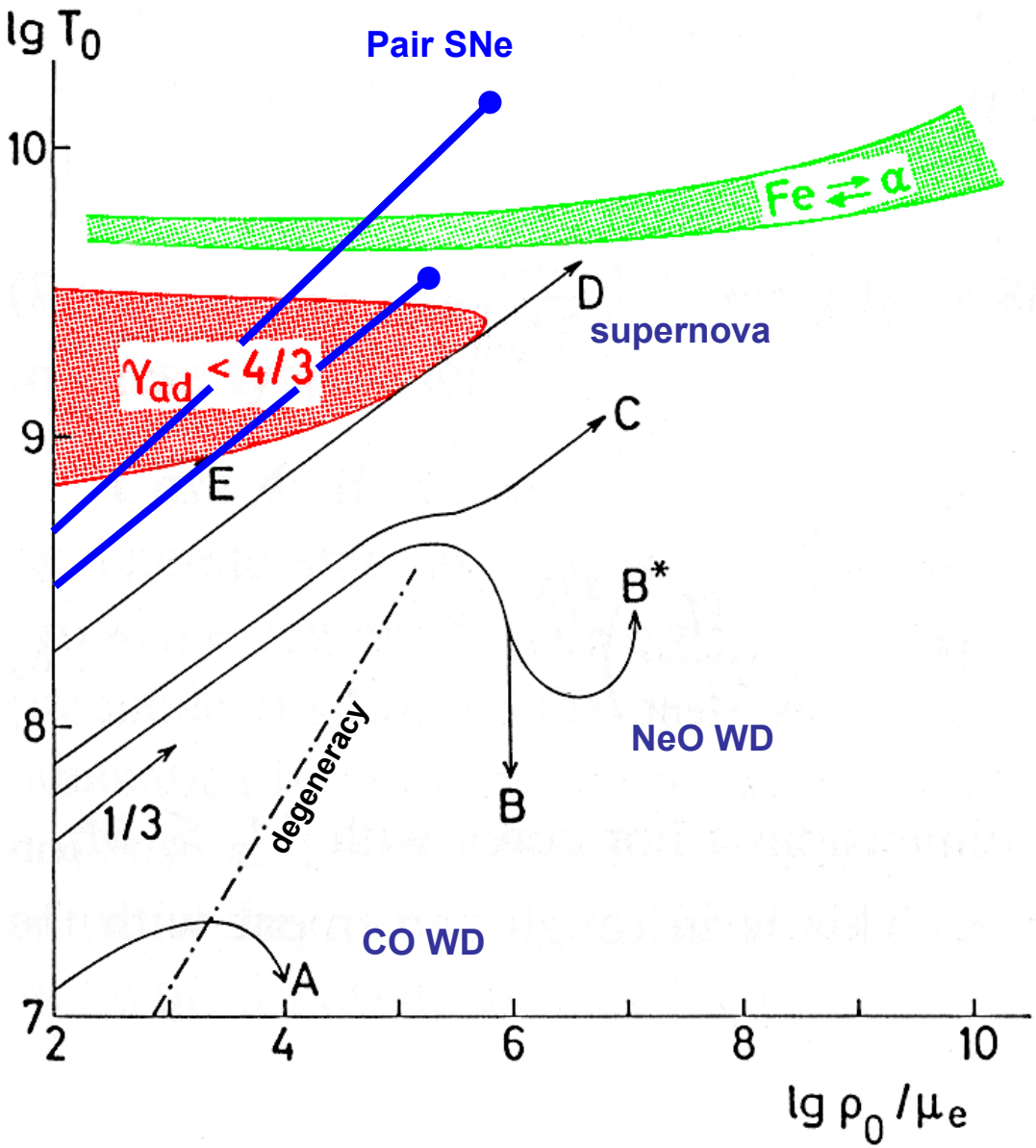

Kippenhahn & Weigert (1990)

Instability Regimes

adiabatic index < 4/3

Compression does not result in sufficient increase in pressure (gradient) to balance higher gravity at lower radius

e^+/e^--Pair Instability

Internal gas energy is converted into e^+/e^- rest mass (hard photons from tail of Planck spectrum)

Photo disintegration

Internal gas energy is used to unbind heavy nuclei into alpha particles and at higher temperature those into free nucleons

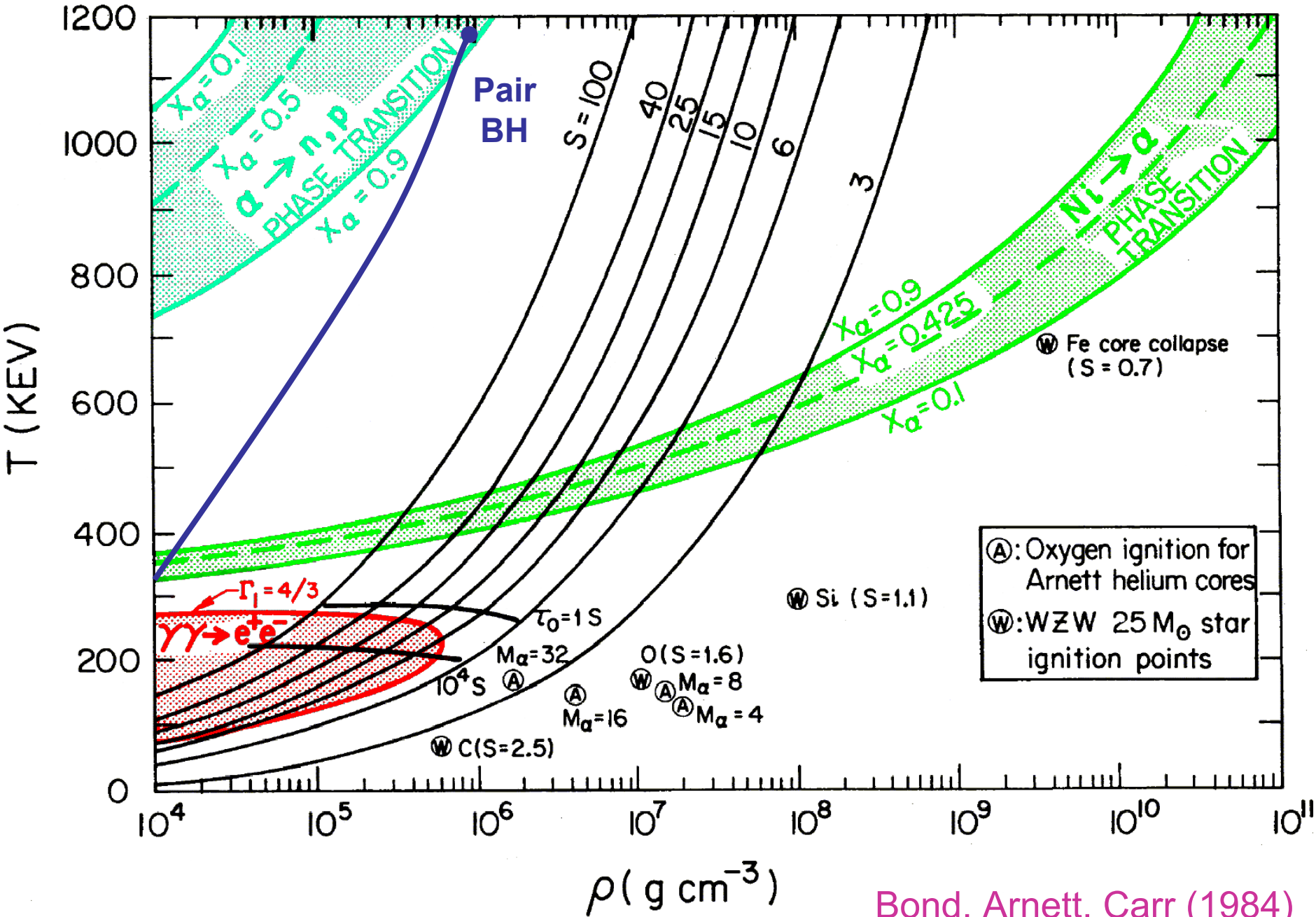

Bond, Arnett, Carr (1984)

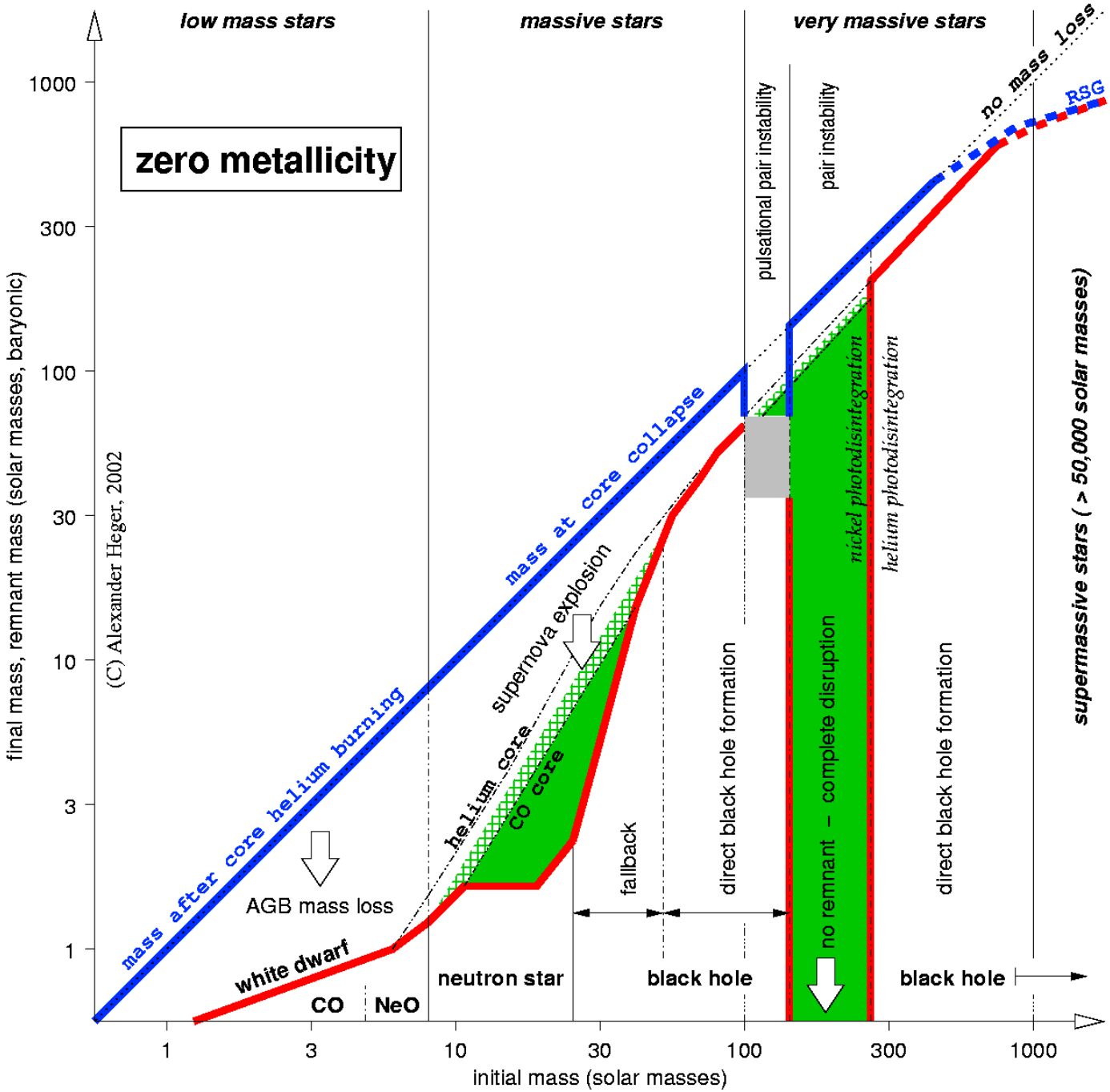

Ejected "metals"

Model Calculations

- 100 Pop III stellar model from 10-100 $M_\odot$
- Parametric piston supernova
- Piston located at S=4 entropy jump (base of the O shell)
- Fallback determined self-consistently with nucleosynthesis from 1-D hydro calculation

Pop III remnants for 0.6 foe explosion

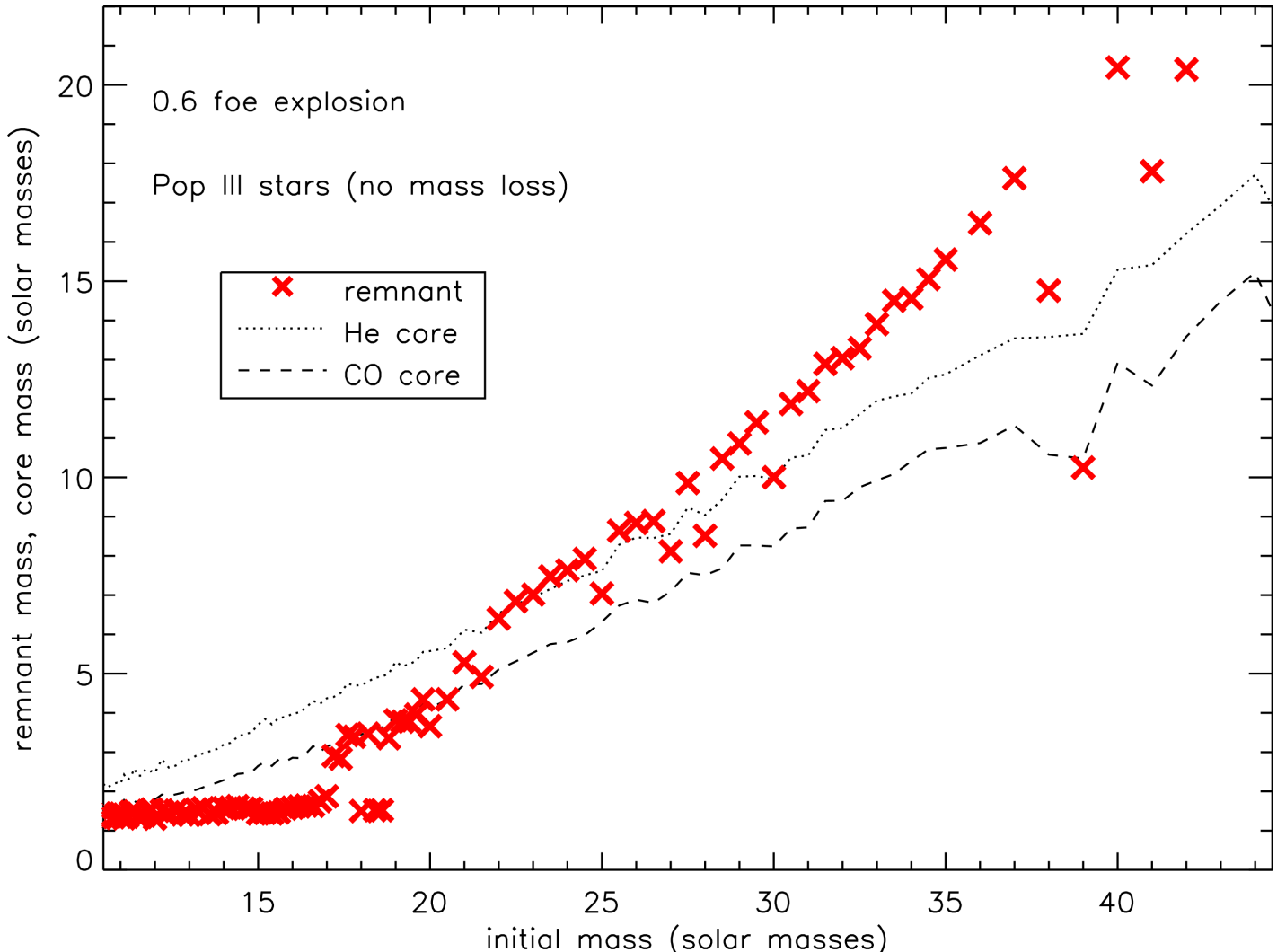

Pop III remnants for 1.2 foe explosion

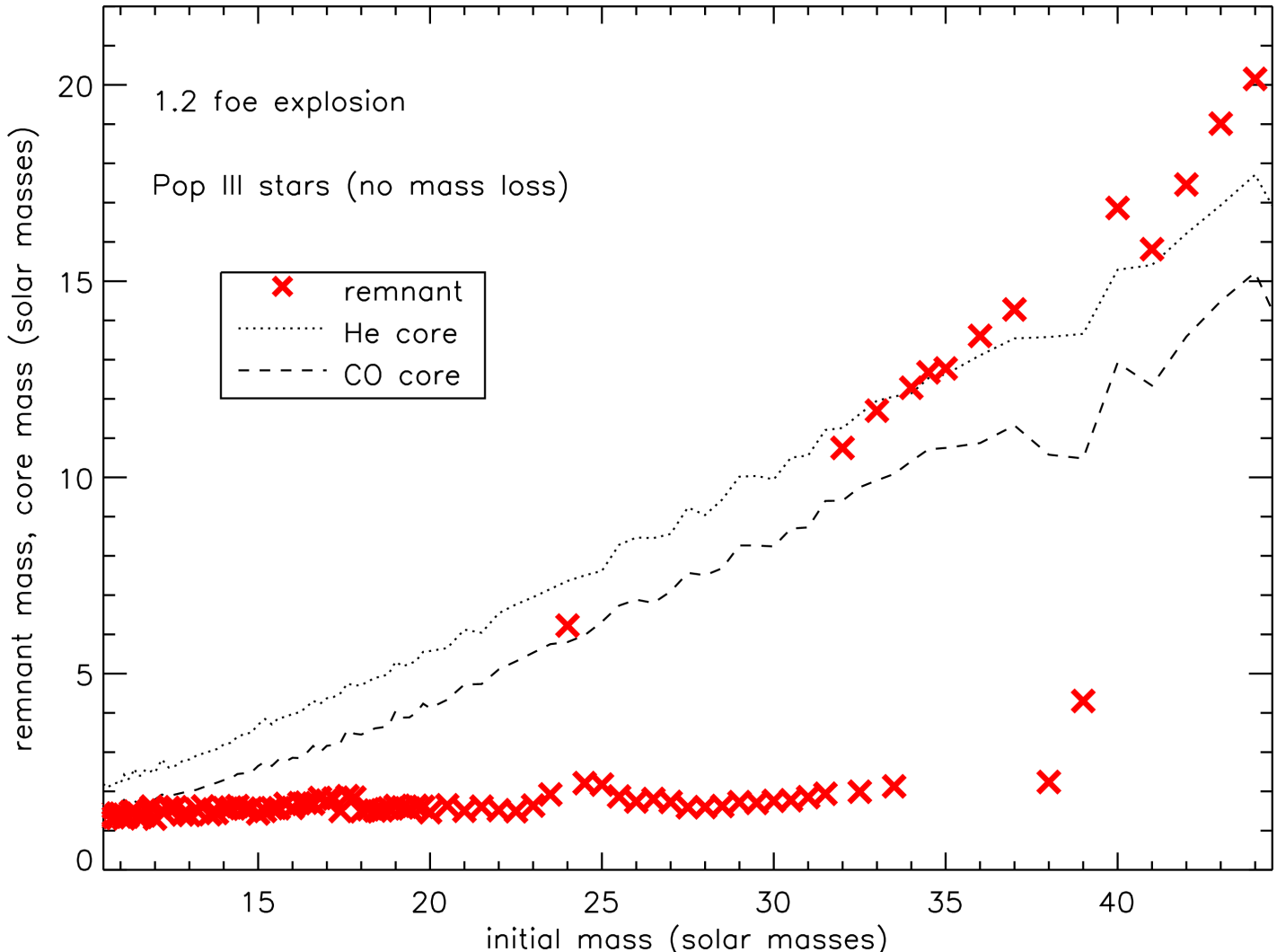

Pop III remnants for 1.8 foe explosion

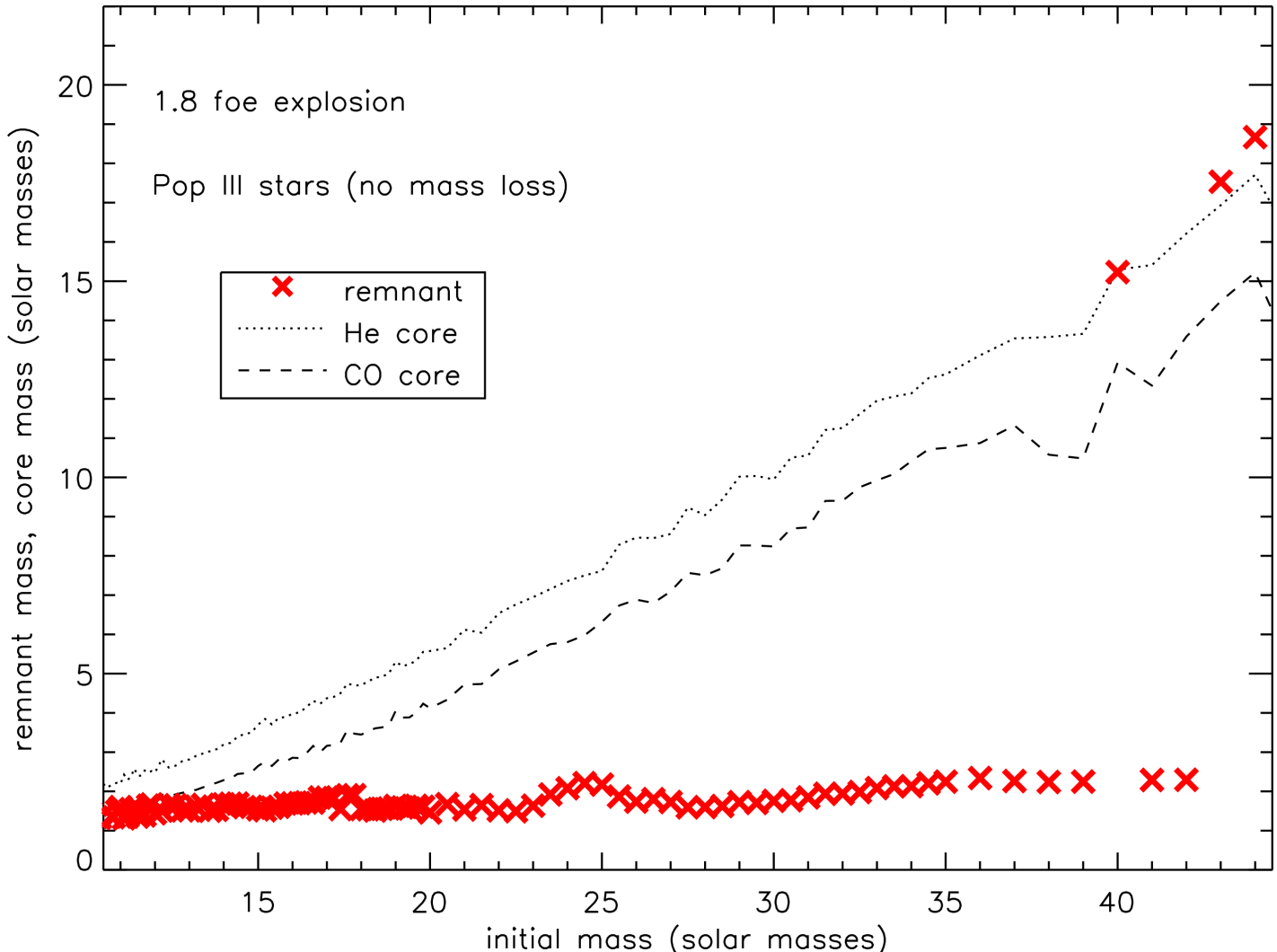

Elemental production factor in a 15 $M_\odot$ star

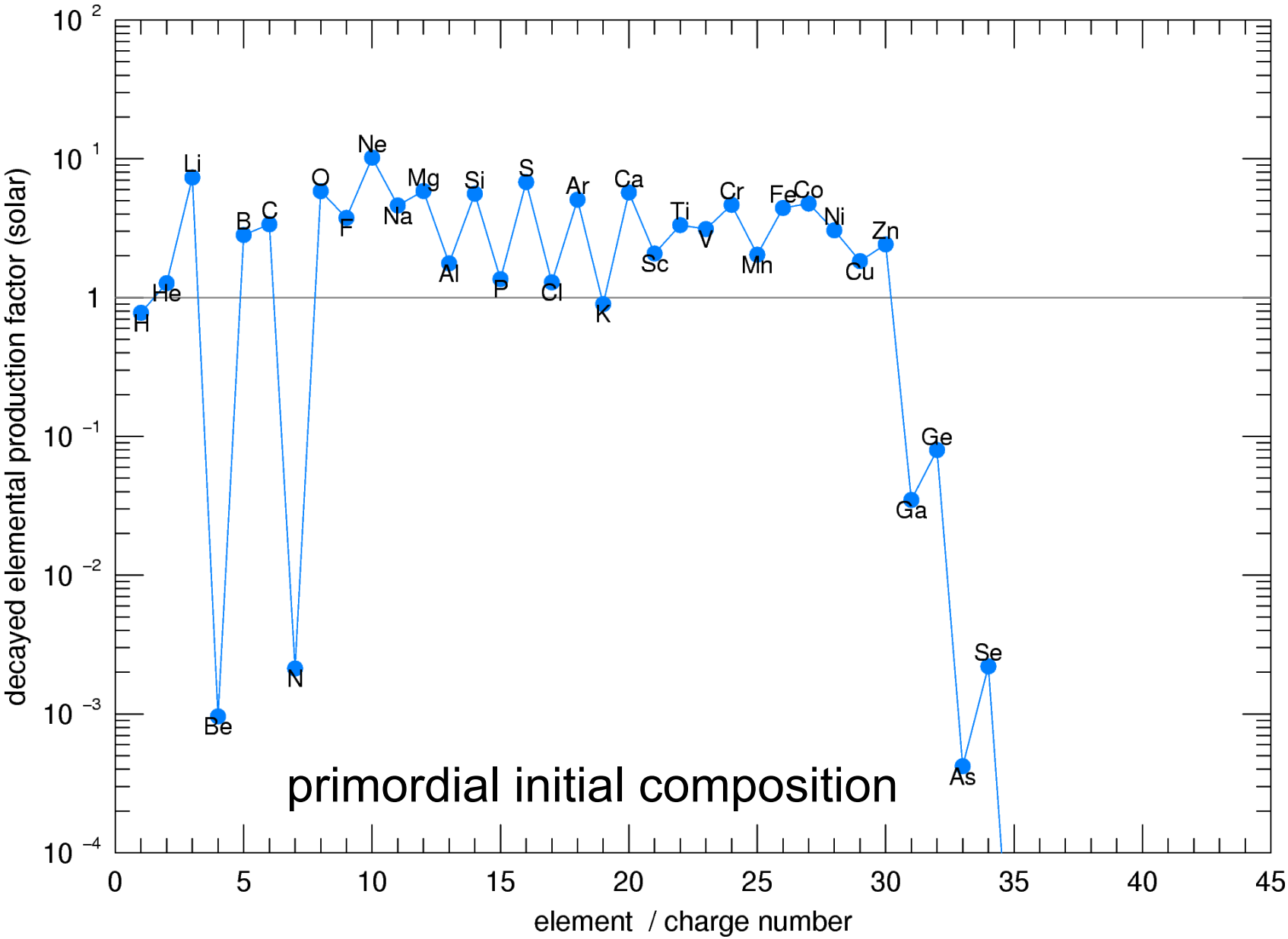

Elemental production factor in a 25 $M_\odot$ star

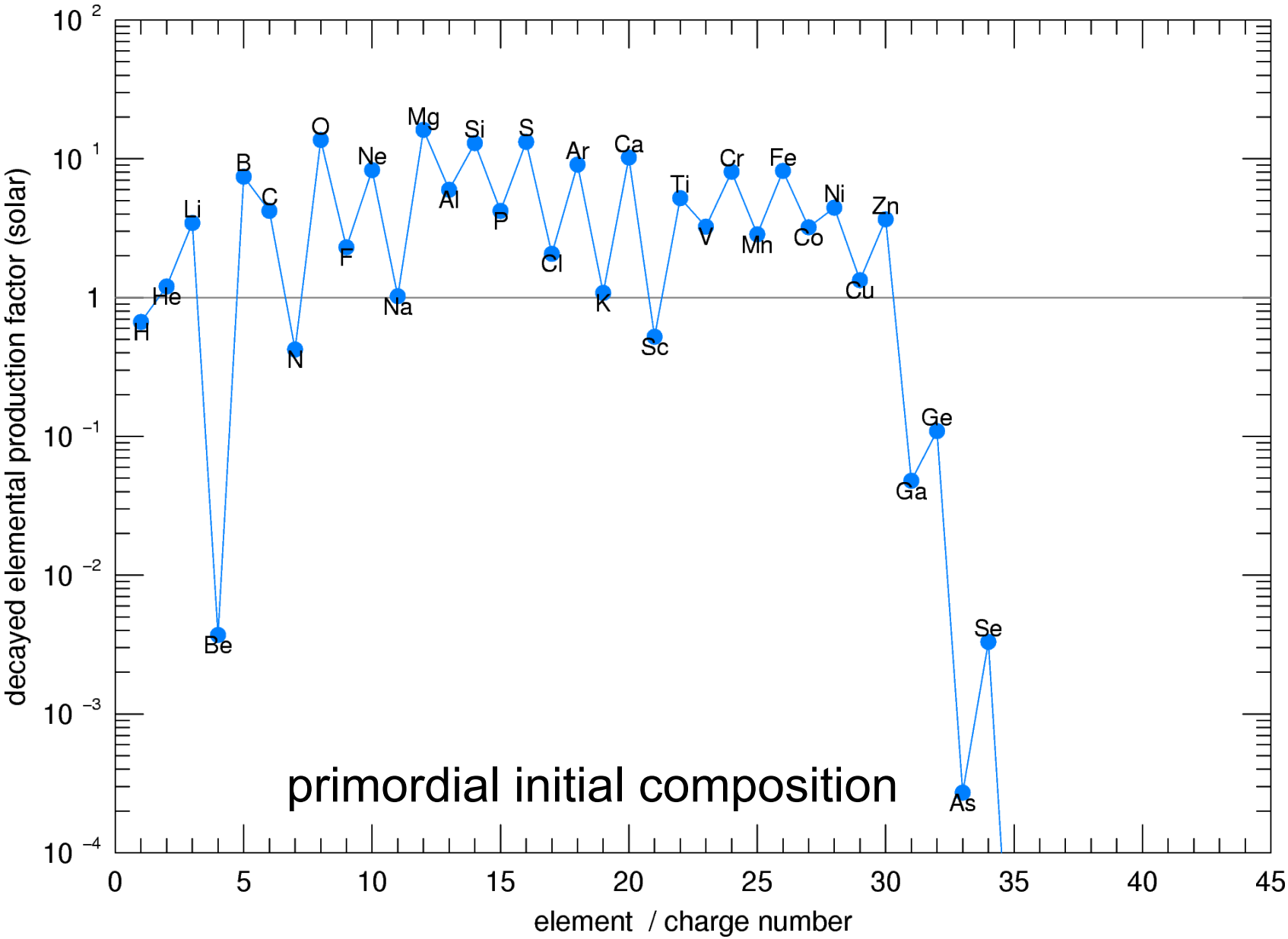

Elemental production factor in a 35 $M_\odot$ star

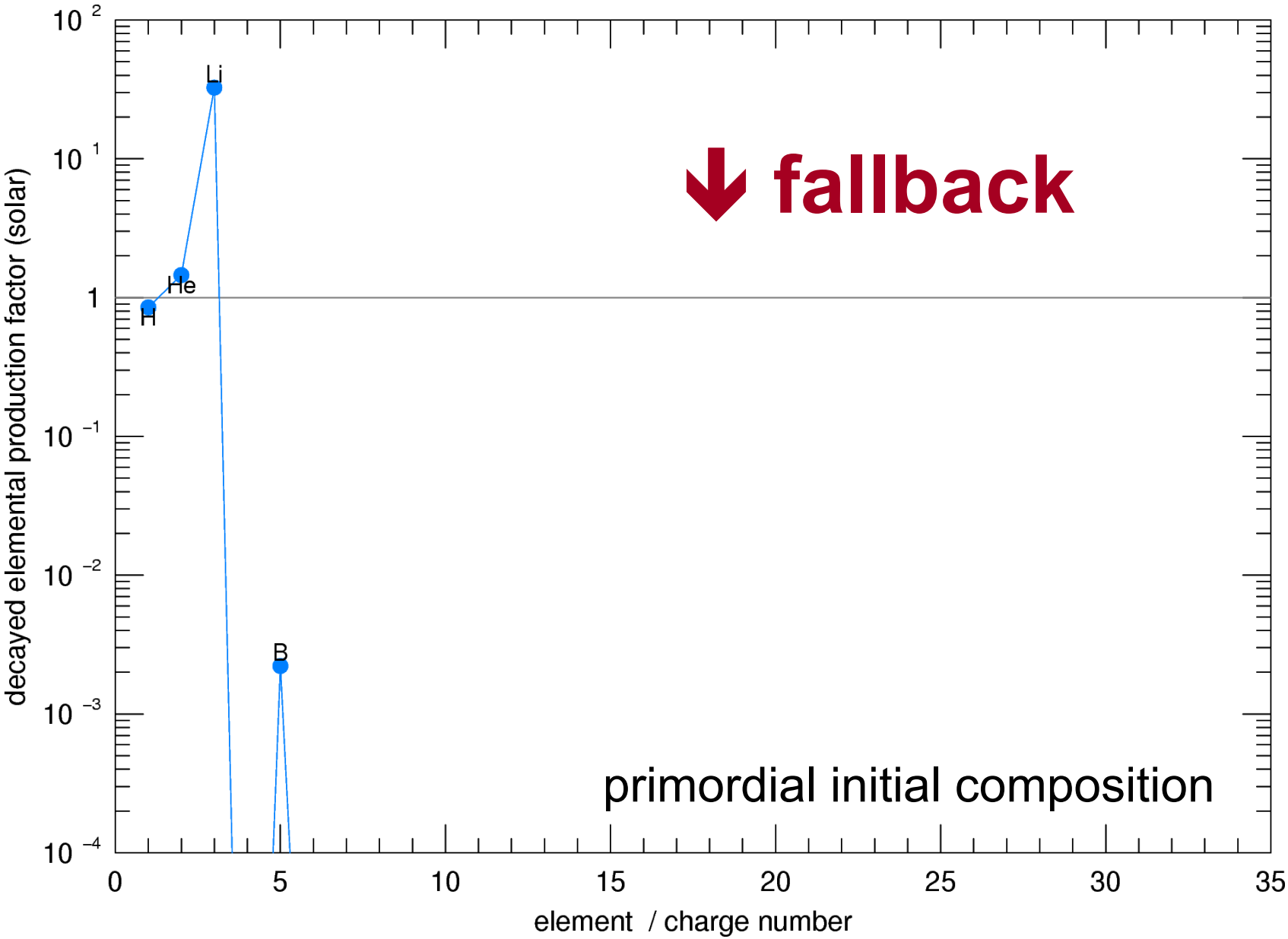

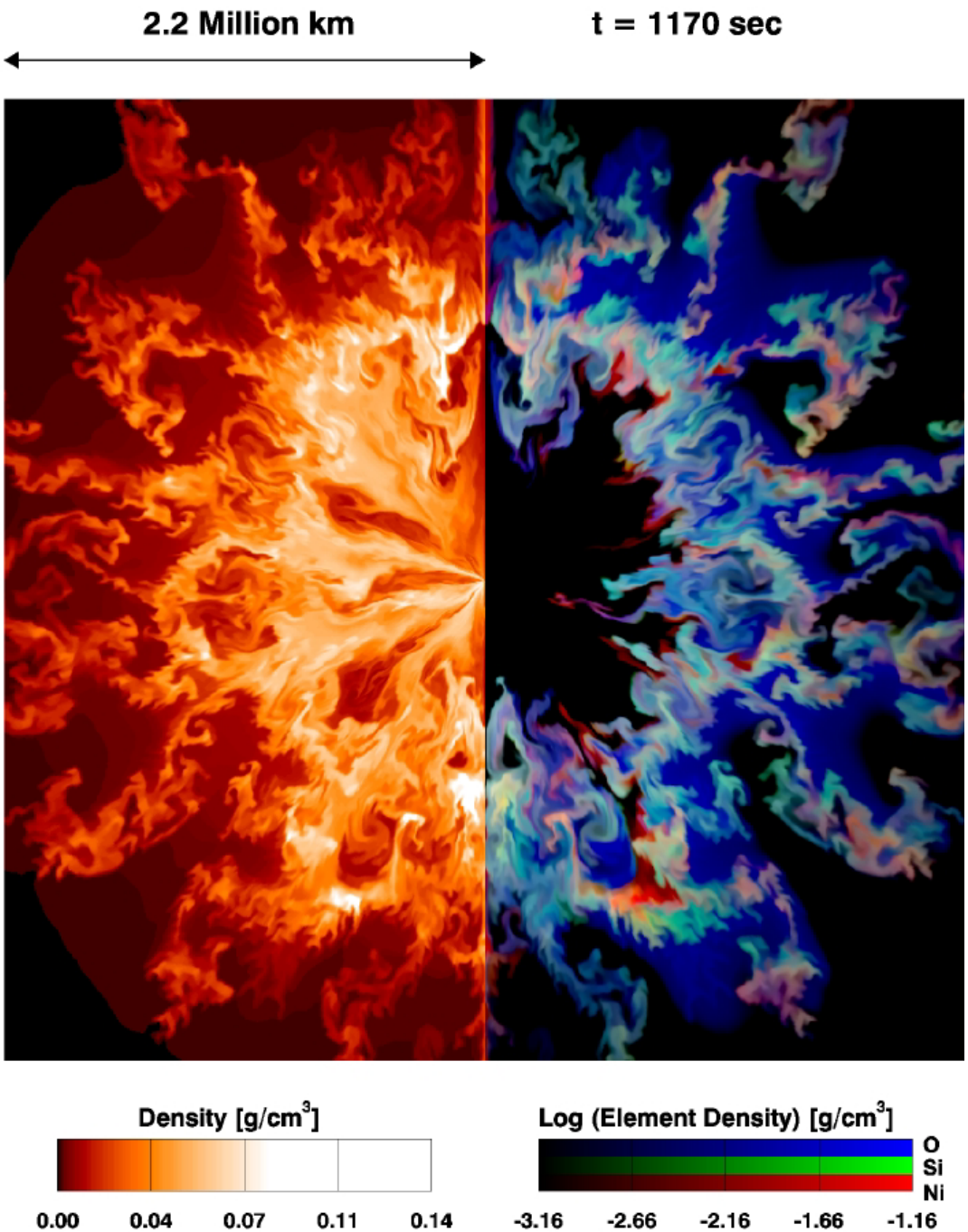

Mixing

early during the supernova explosion may allow materiel from the bottom of exploding star come out
-- even if most of the core falls back to form a black hole.

(Kifonidis et al. 2000)

Elemental production factor in a 35 $M_\odot$ star

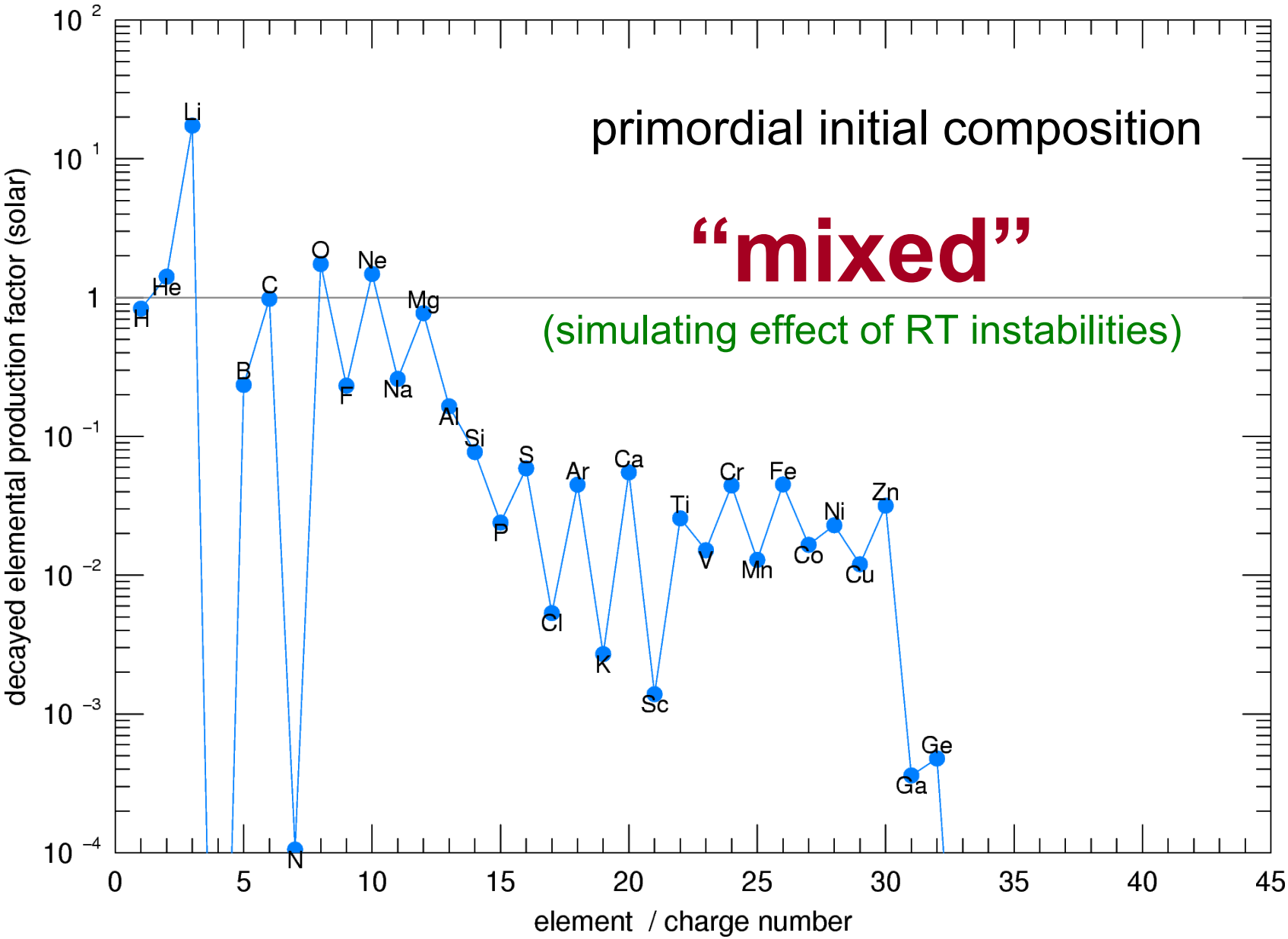

Comparison of the very metal-poor star CS 22949-037 with a "mixed" 35 $M_\odot$ model with fallback from Woosley & Weaver (1995) (Depagne et al. 2002)

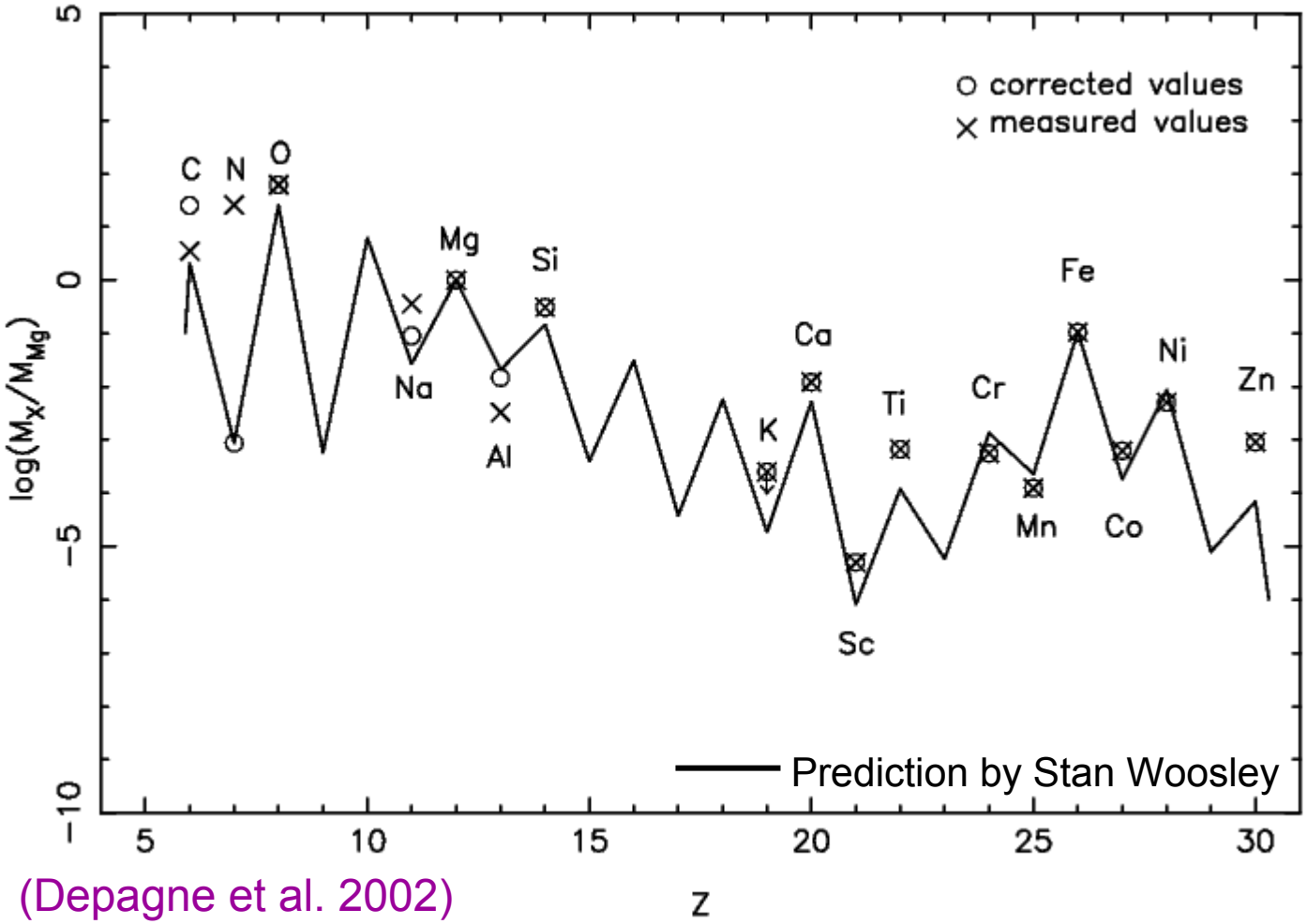

(Depagne et al. 2002)

➔reasonably good agreement for many elements!

(except nitrogen which could have been made in the observed star itself)

Mixing and Fallback

may explain some ultra metal-poor star abundance pattern

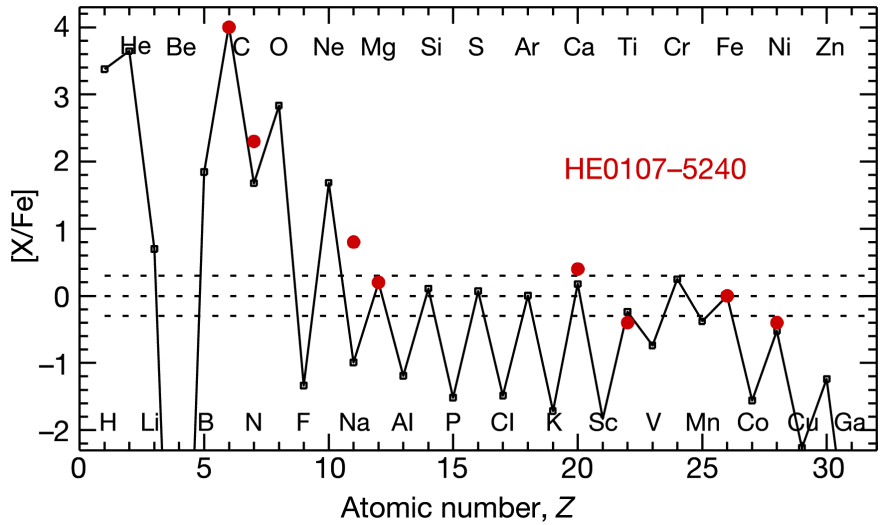

weak explosion (0.3 foe) and significant fallback

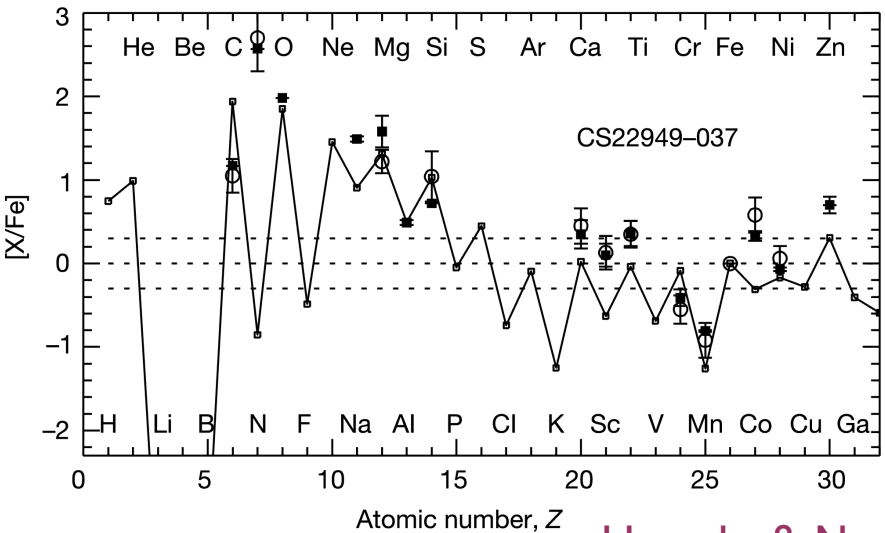

strong explosion (20 foe !!!) ***but*** (?) significant fallback

A combination of mixing and significant fallback *may* explain observed abundance pattern.

However:
detailed modeling and understanding of the mechanism is (still) required!

Umeda & Nomoto (2003)

Production factor of massive Pop III stars: w/ - w/o mixing

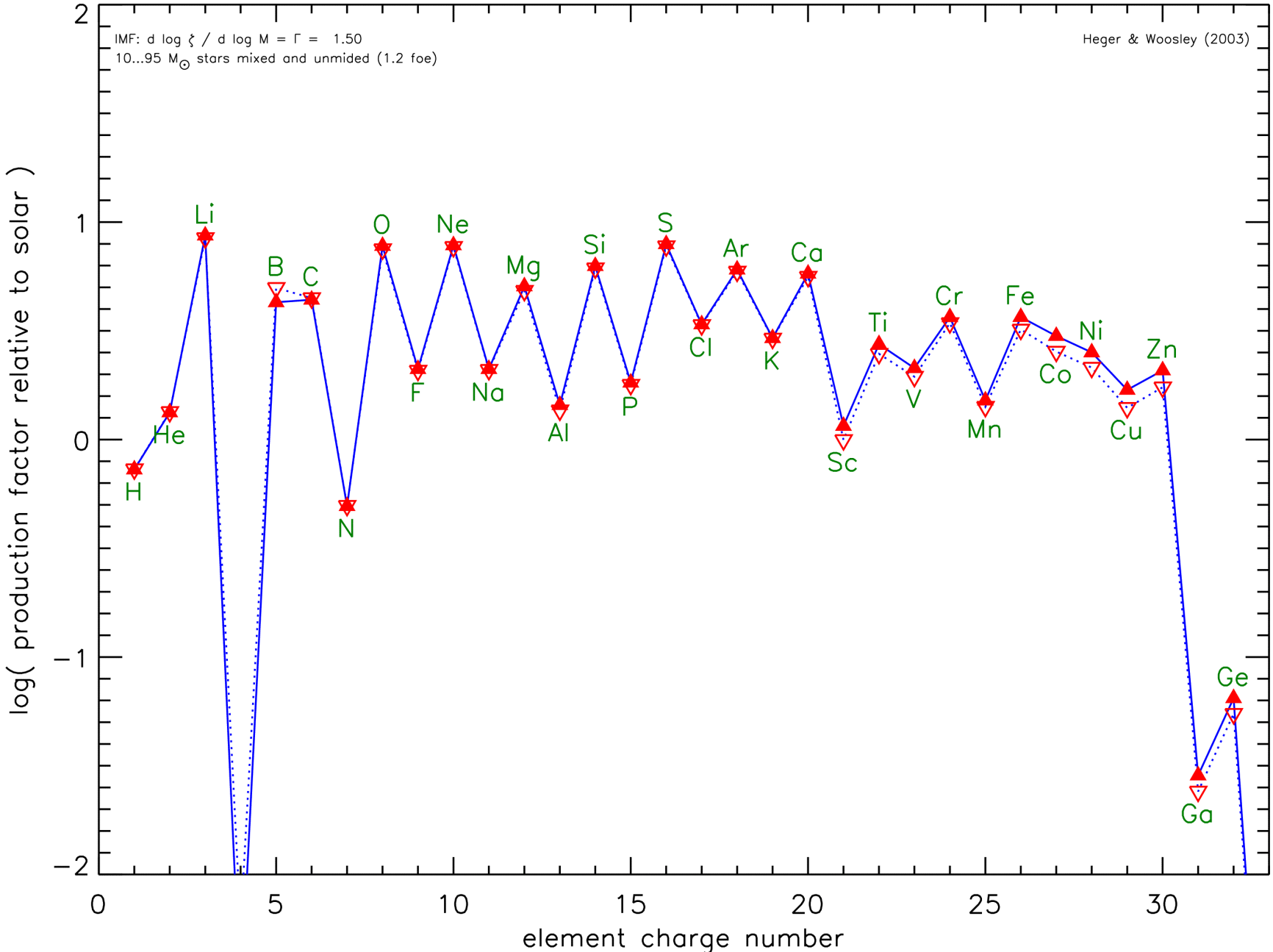

Production factor of massive Pop III stars – explosion energy

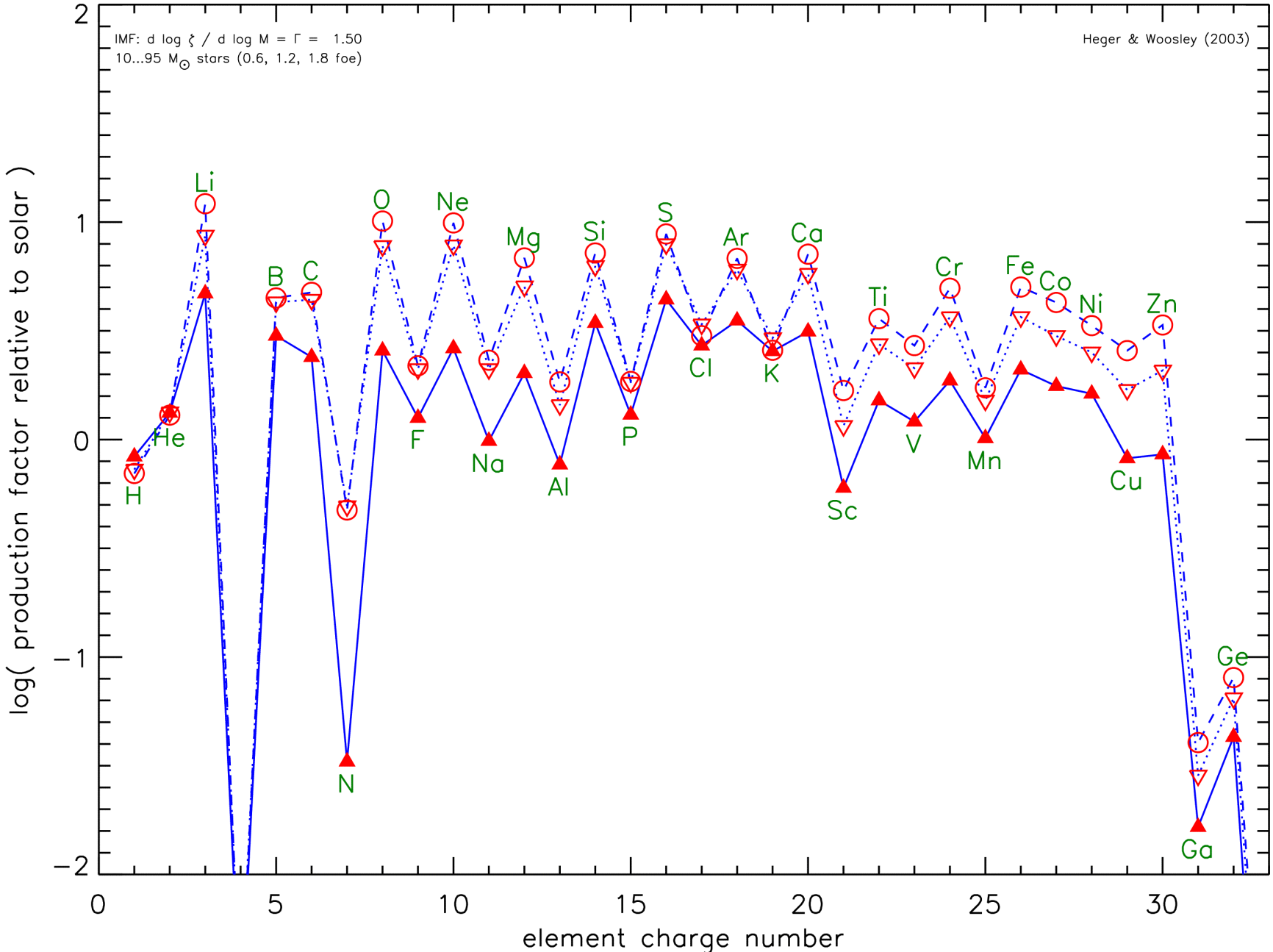

1.2 foe and 10 foe explosions

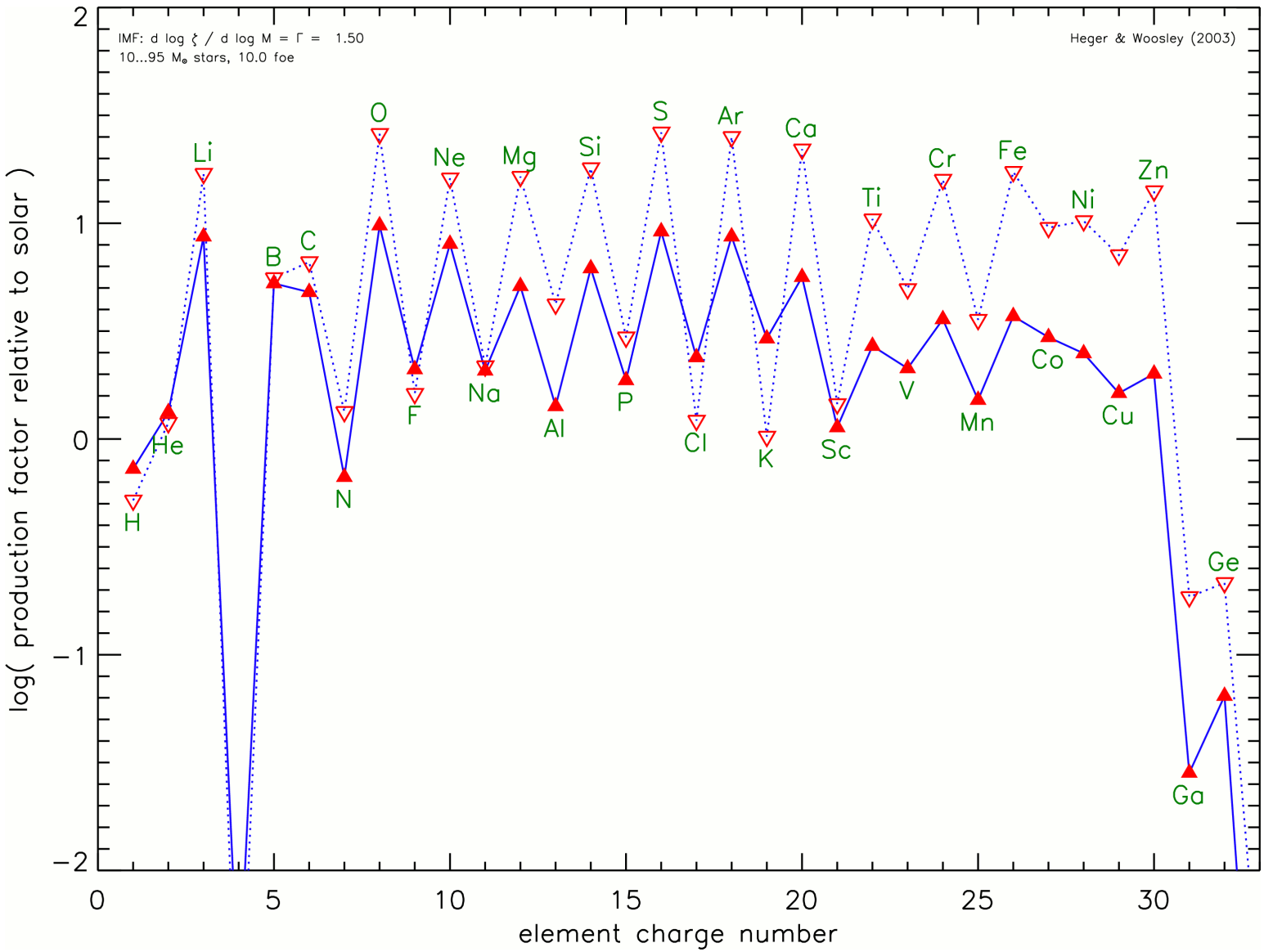

Pair-Instability Supernovae

Many studies in literature since more than 3 decades, e.g.,
Rakavey, Shaviv, & Zinamon (1967)
Bond, Anett, & Carr (1984)
Glatzel, Fricke, & El Eid (1985)
Woosley (1986)

Some recent calculations:
Umeda & Nomoto 2001
Heger & Woosley 2002

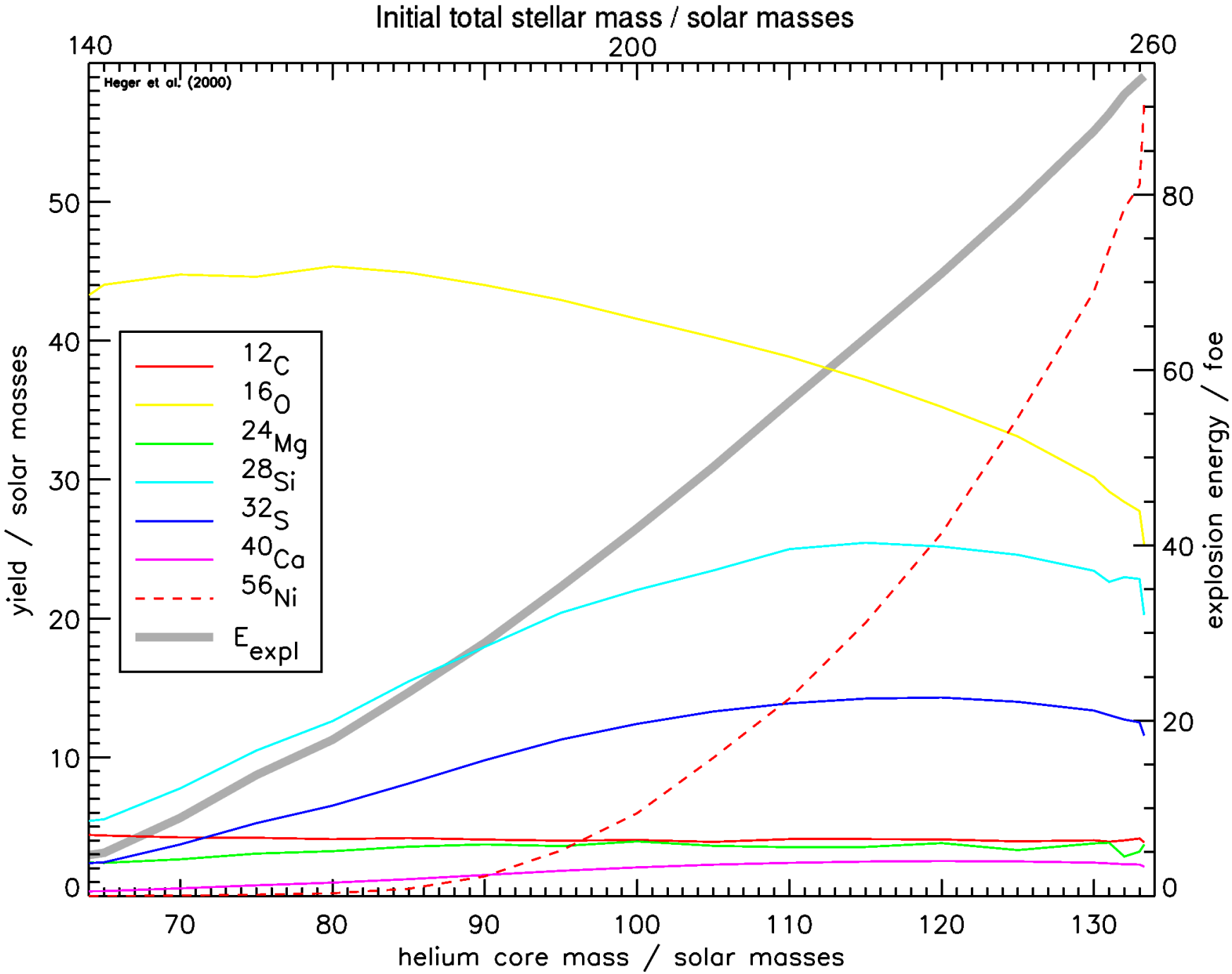
Initial total stellar mass / solar masses
140
200
260
Heger et al. (2000)
yield / solar masses
explosion energy / foe
helium core mass / solar masses
0
10
20
30
40
50
0
20
40
60
80
70
80
90
100
110
120
130
12C
16O
24Mg
28Si
32S
40Ca
56Ni
Eexpl

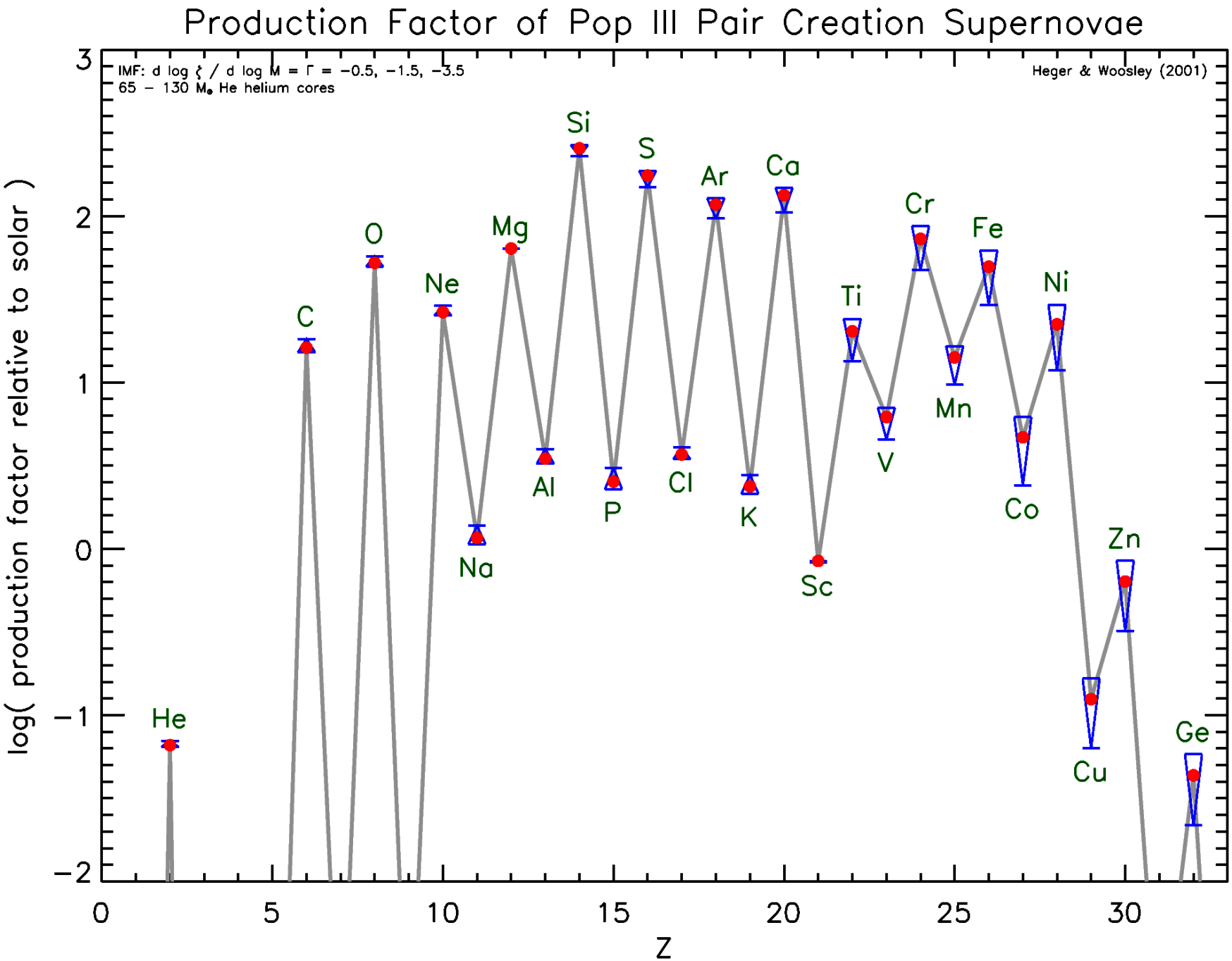
Production Factor of Pop III Pair Creation Supernovae
IMF: d log ξ / d log M = Γ = −0.5, −1.5, −3.5
65 − 130 M☉ He helium cores
Heger & Woosley (2001)
log(production factor relative to solar)
Z
He
C
O
Ne
Na
Mg
Al
Si
P
S
Cl
Ar
K
Ca
Sc
Ti
V
Cr
Mn
Fe
Co
Ni
Cu
Zn
Ge

Production factor of massive and very massive Pop III stars

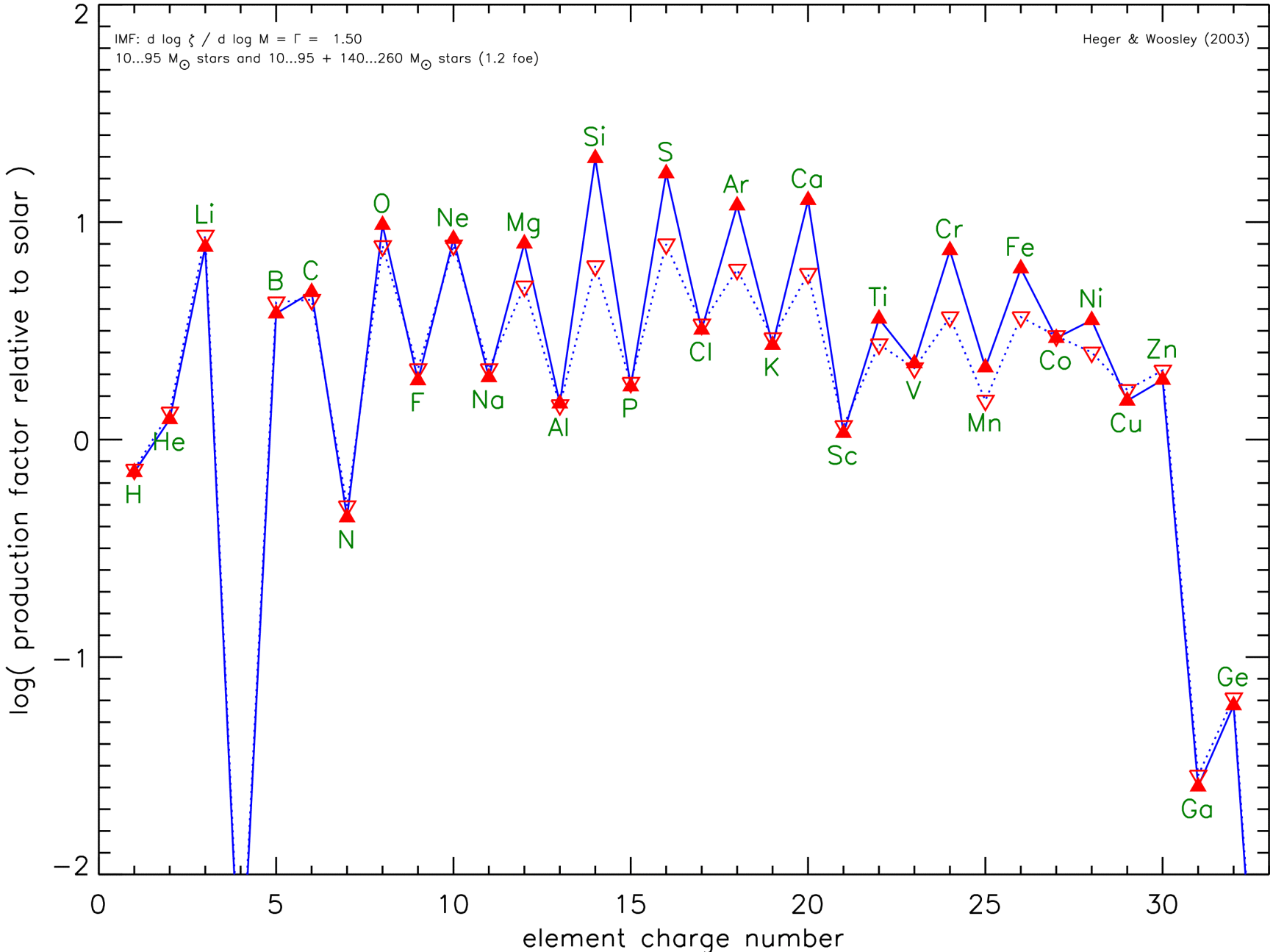

Problem:

Pair-Instability Supernovae do not reproduce the abundances as observed in very metal poor halo stars!

How to blow up those massive stars?

The "Collapsar Engine"

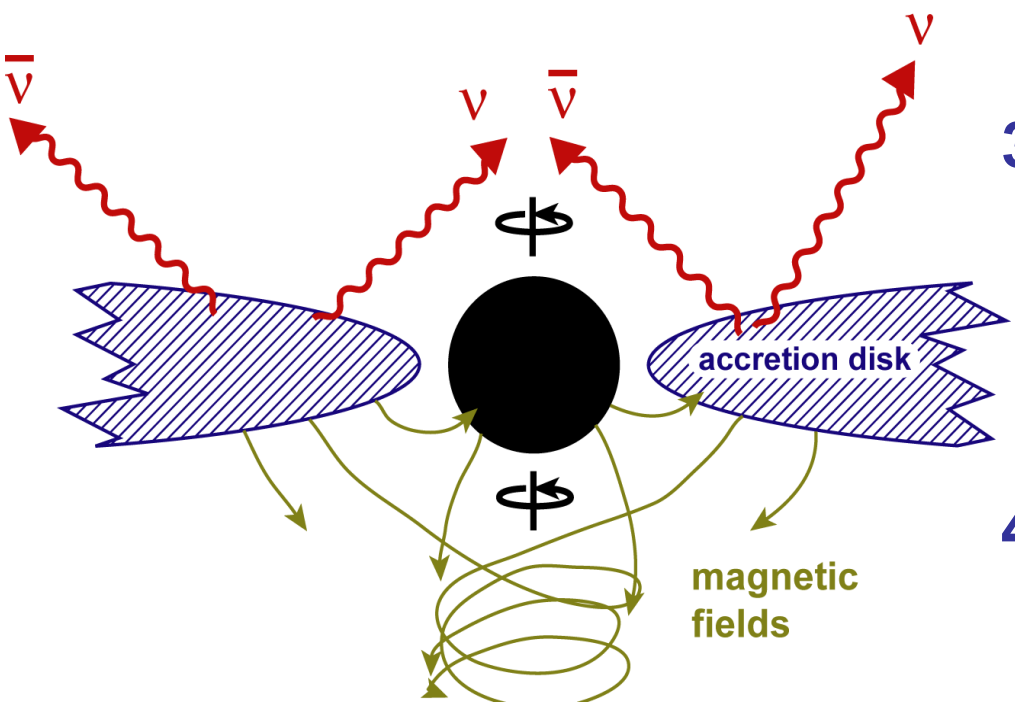

1. black hole forms inside the collapsing star
2. The infalling matter forms and accretion disk
3. The accretion disk releases gravitational energy (up to 42.3% of rest mass for Kerr BH)
4. Part of the released energy or winds off the hot disk explode the star

Accretion of 100 $M_\odot$ at up to ~100 $M_\odot s^{-1}$

➔ long duration X-ray transient may result *if*

- jet is made
- jet escapes the star

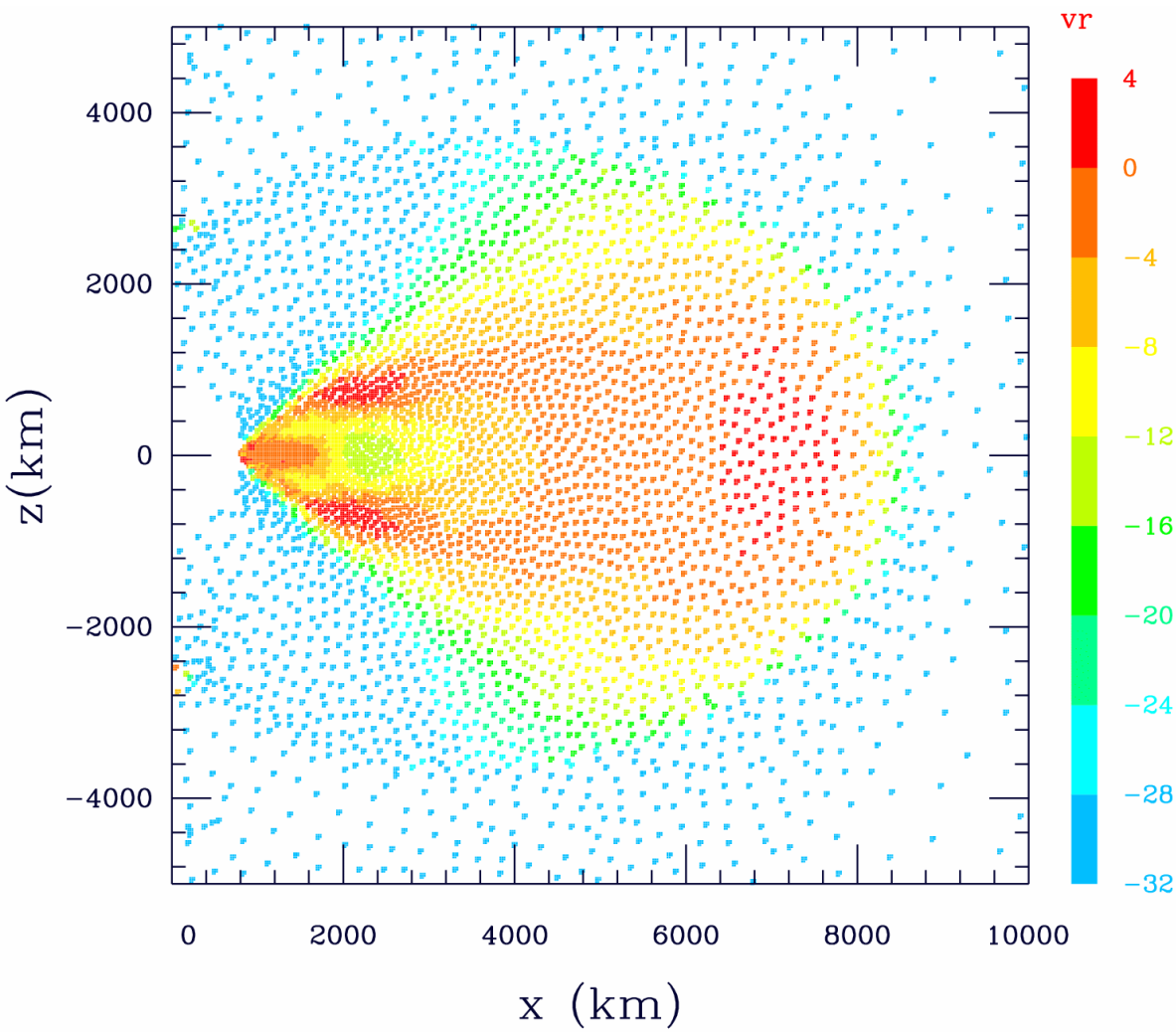

(long duration due to high redshift and big mass & radius scale)

(Fryer, Woosley, & Heger 2000)

Summary

Due to their unique composition, the birth, life and death of the first stars is very different from later generations:

- Even stars of several 100 solar masses might survive (no winds, no pulsational instability)
- They can encounter the pair-instability:
  - strong odd-even effect that has not been observed to date
  - No heavy elements beyond iron group produced
  - No *r*-process, no *s*-process – **not *directly* observed to date**
- Strong odd-even abundance pattern, especially in pair-SNe
- Salpeter IMF cannot reproduce UMP star abundances
  - Enrichment by individual events
  - IMF with peak or lower cut-off in massive SNe (~35 $M_\odot$) regime
  - massive SNe with mixing and fallback

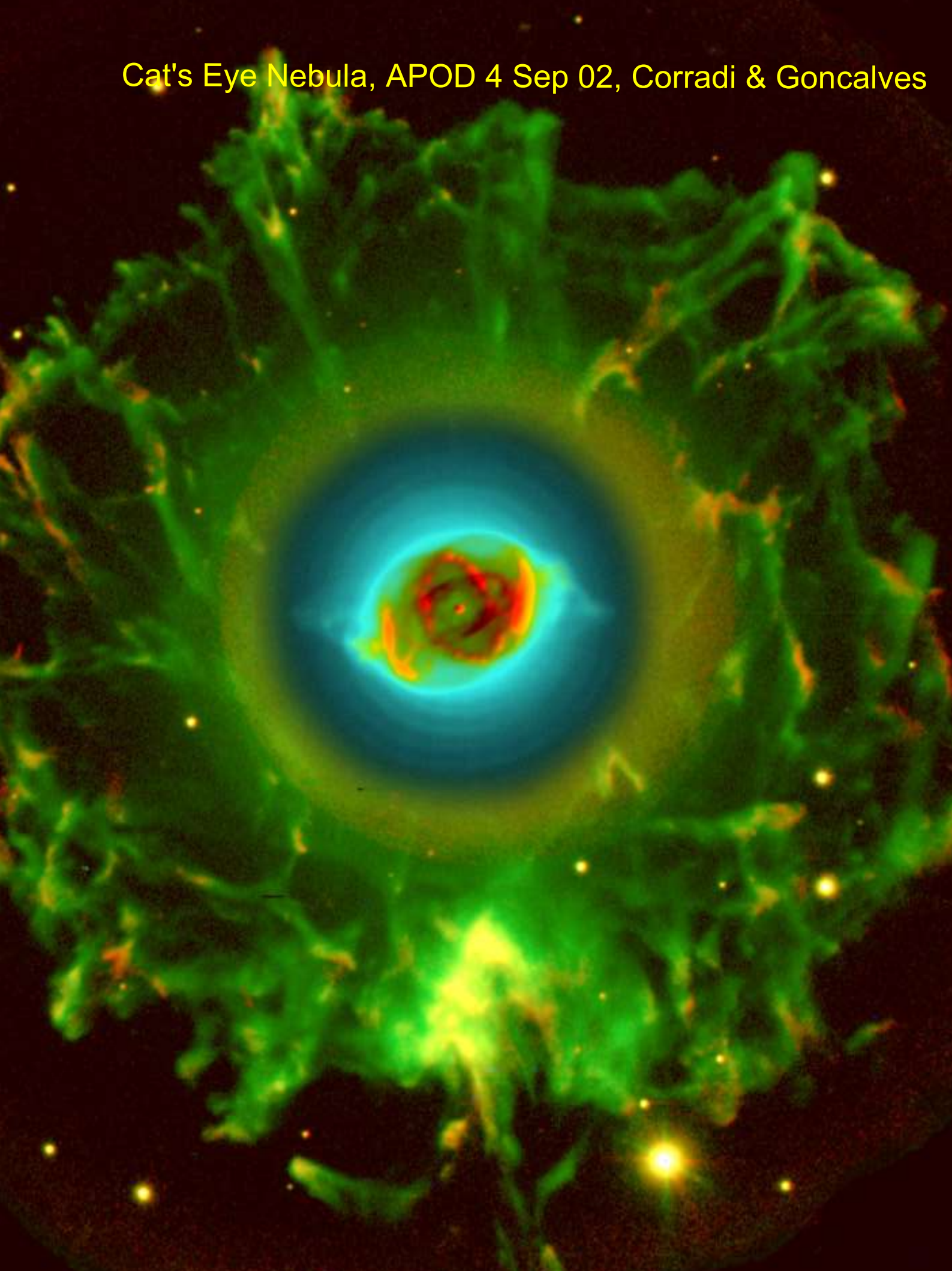
Cat's Eye Nebula, APOD 4 Sep 02, Corradi & Goncalves

The Second Stars

Falk H Herwig
Los Alamos National Laboratory

Theoretical Astrophysics (T-6) and
Los Alamos Neutron Science Center (LANSCE-3)

The Second Stars

- What are they?
- Why are they important?
- What do we know about them?
- What can we do to learn more about them?

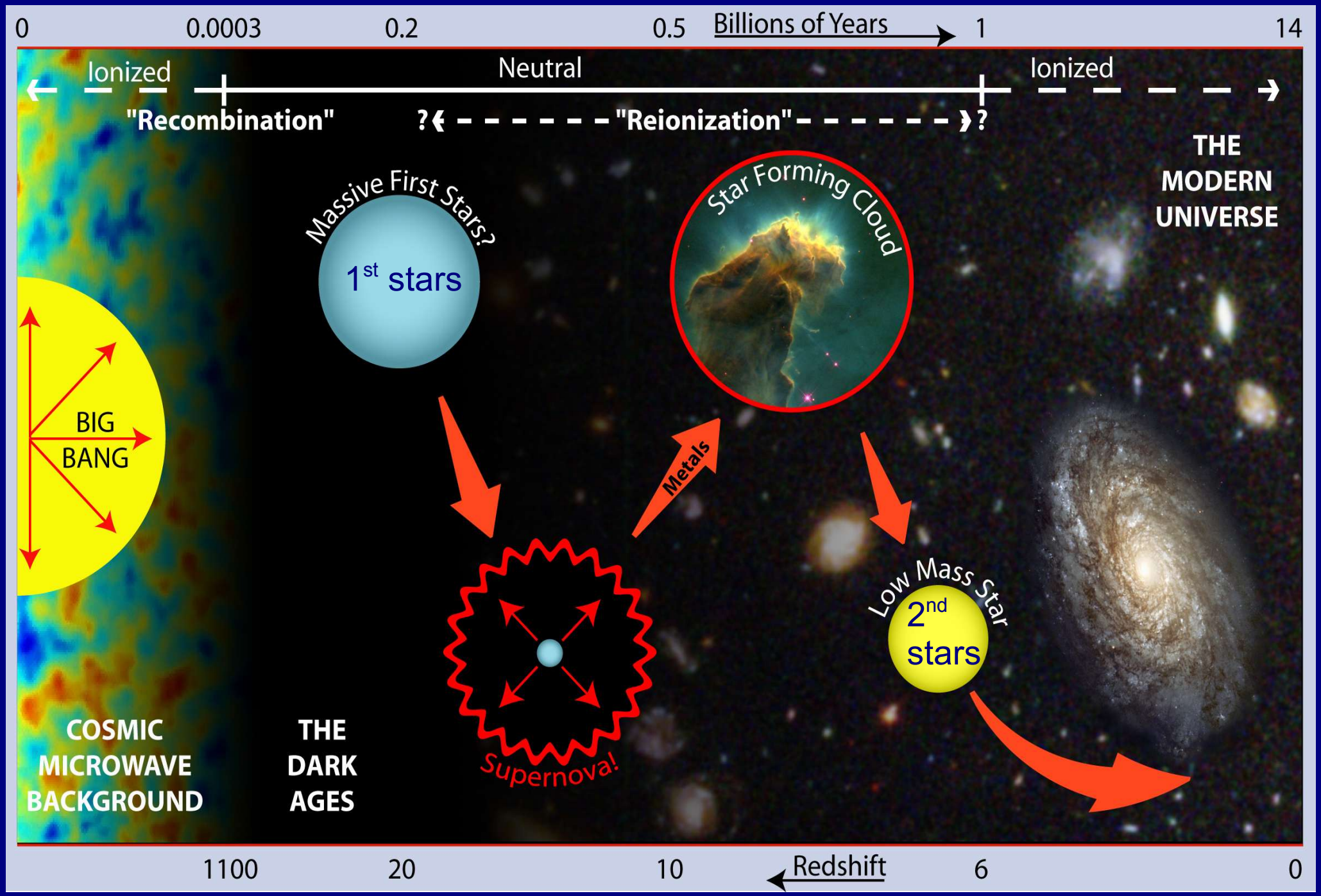
0
0.0003
0.2
0.5
Billions of Years
1
14
Ionized
Neutral
Ionized
"Recombination"
?"Reionization"?
THE MODERN UNIVERSE
Massive First Stars?
1st stars
Star Forming Cloud
BIG BANG
Metals
Supernova!
Low Mass Star
2nd stars
COSMIC MICROWAVE BACKGROUND
THE DARK AGES
1100
20
10
Redshift
6
0

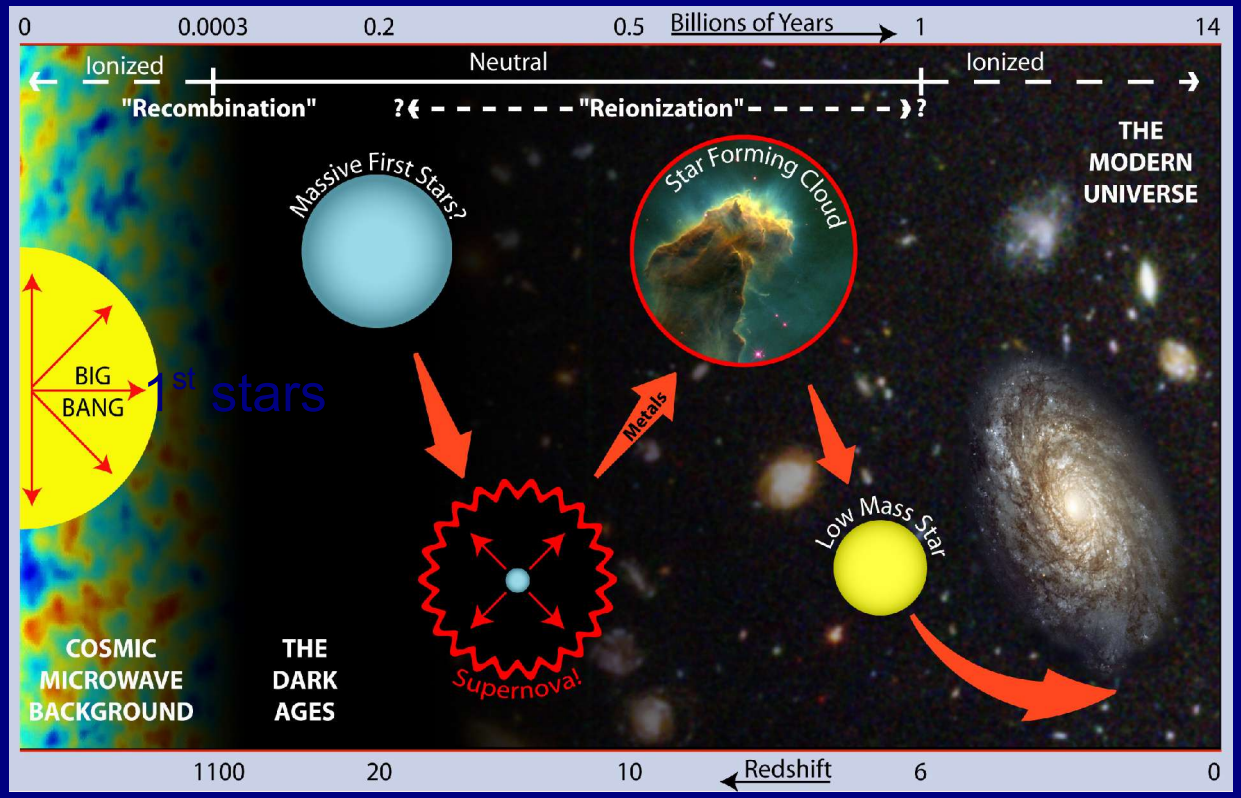

(mix of?) 1st stars
+
self polution

= Obs 2nd stars

What do we know about the 2nd stars?

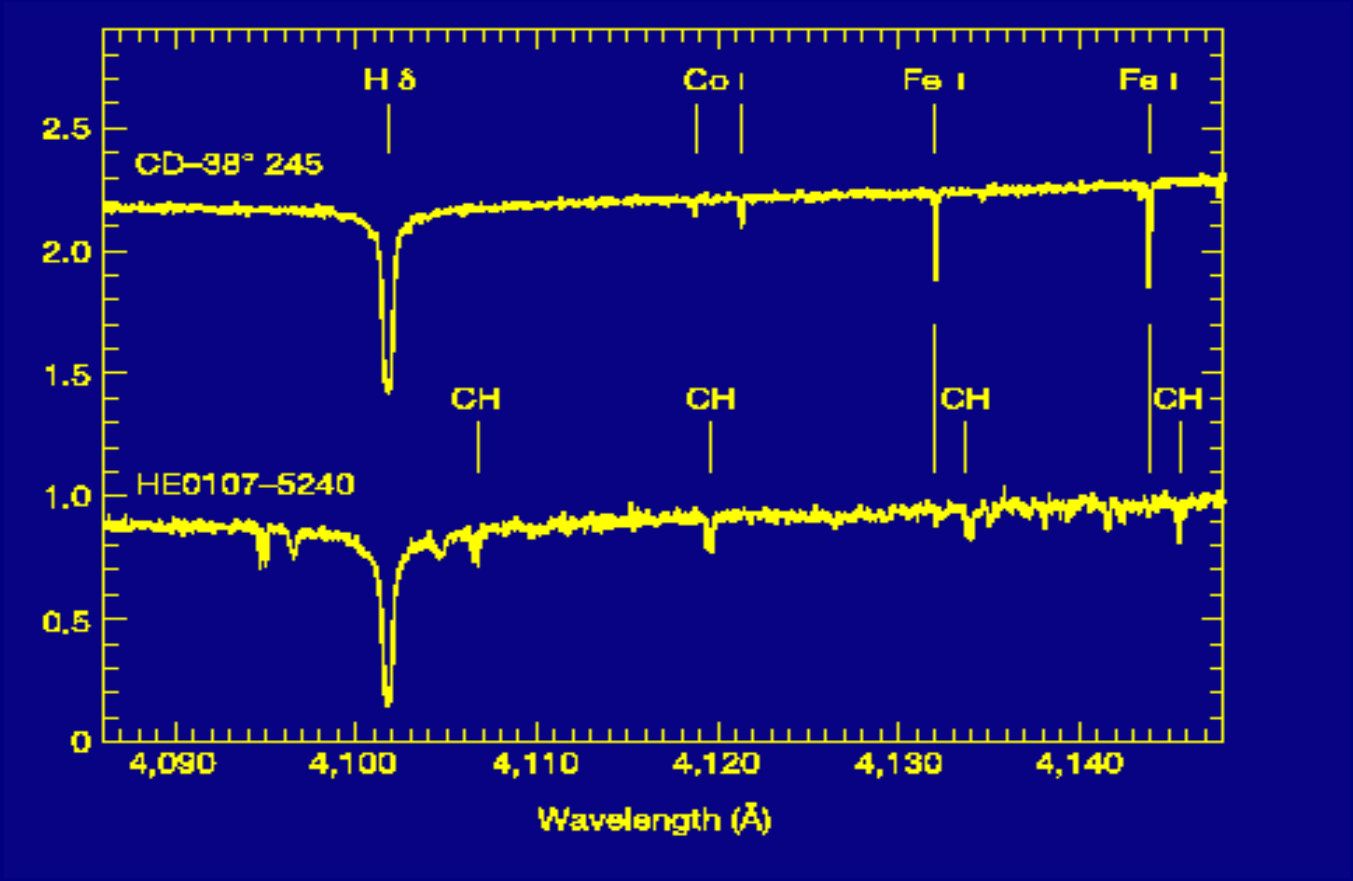

HE 0107-5240
Christlieb etal 2002

[Fe/H]=-5.3
[C/Fe]=4.0
[N/Fe]=2.3

- many UMP/EMP stars are C- *and* N
- need to understand why!

Table 3. Properties of EMP stars with radial velocity variations, *s*-process enhancements and CNO-overabundance

	[Fe/H]	[C/Fe]	[N/Fe]	[(C+N)/Fe]	[O/Fe]	[Na/Fe]	P_{orb}
LP 625-44[a]	−2.7	2.25	0.95	2.15	1.85	1.75	13yr[b]
HE 0024-2523[c]	−2.7	2.6	2.1	2.53	0.4	−0.17	3d
CS29497-030[d]	−2.8	2.38	1.88	2.31	1.67	0.52	346d

[a]Aoki et al. (2002), O abundance uncertain by a few tenth of dex; [b]Tsangarides et al. (2003); [c]Lucatello et al. (2003); [d]Sivarani et al. (2003)

Los Alamos NATIONAL LABORATORY

Z=0: s-process

- no Fe-seed
- in He-shell plenty of primary ^{12}C, can act as seed
- Neutron source (both ^{12}C and ^{22}Ne) primary

one-zone calculation, initial abundance:

$X(^{4}He)=0.72$

$X(^{12}C)=0.23$

$X(^{13}C)=0.03$

$X(^{16}O)=0.02$

all other X=0

$T_8=0.9$

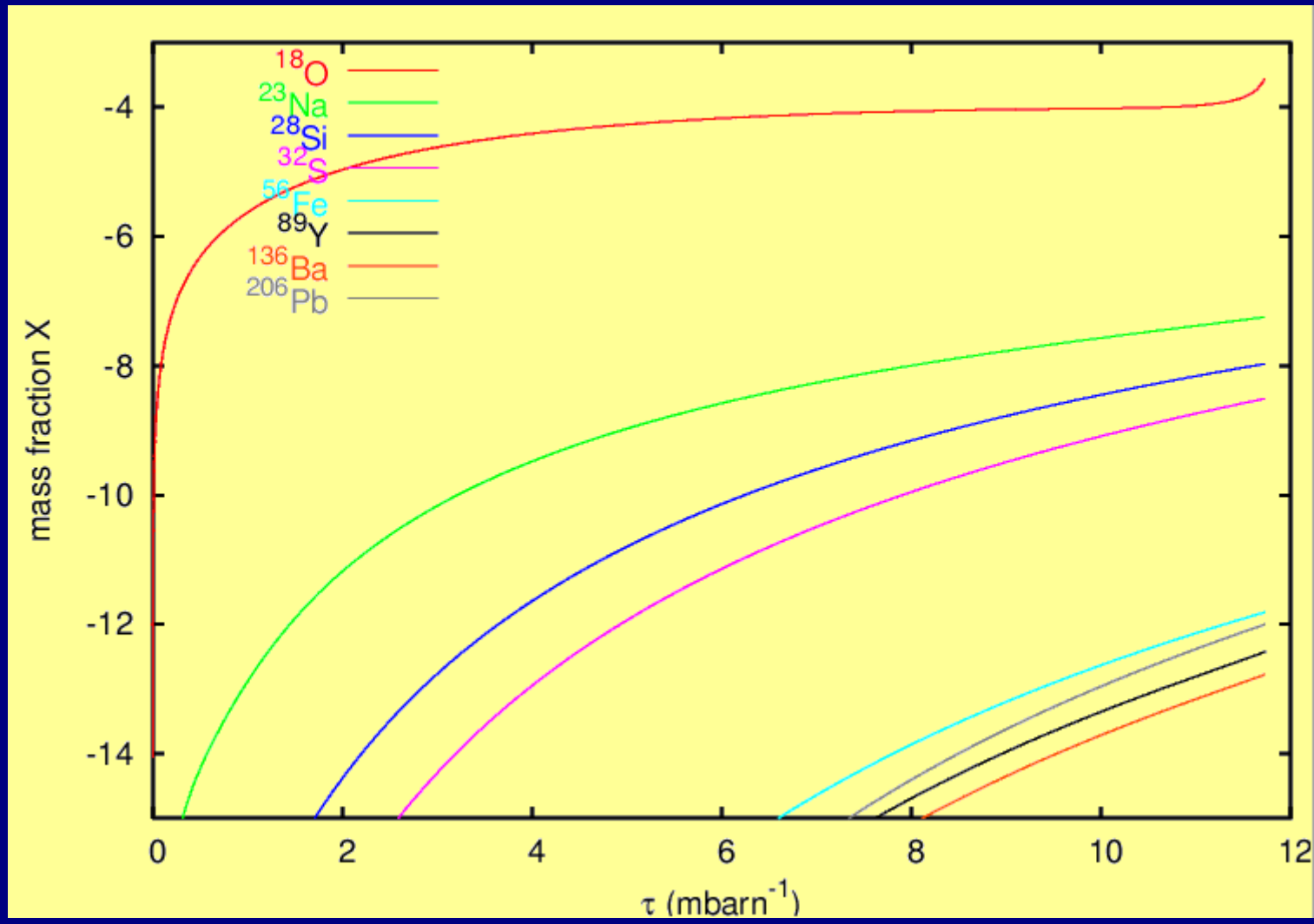

What do we know about the 2nd stars?

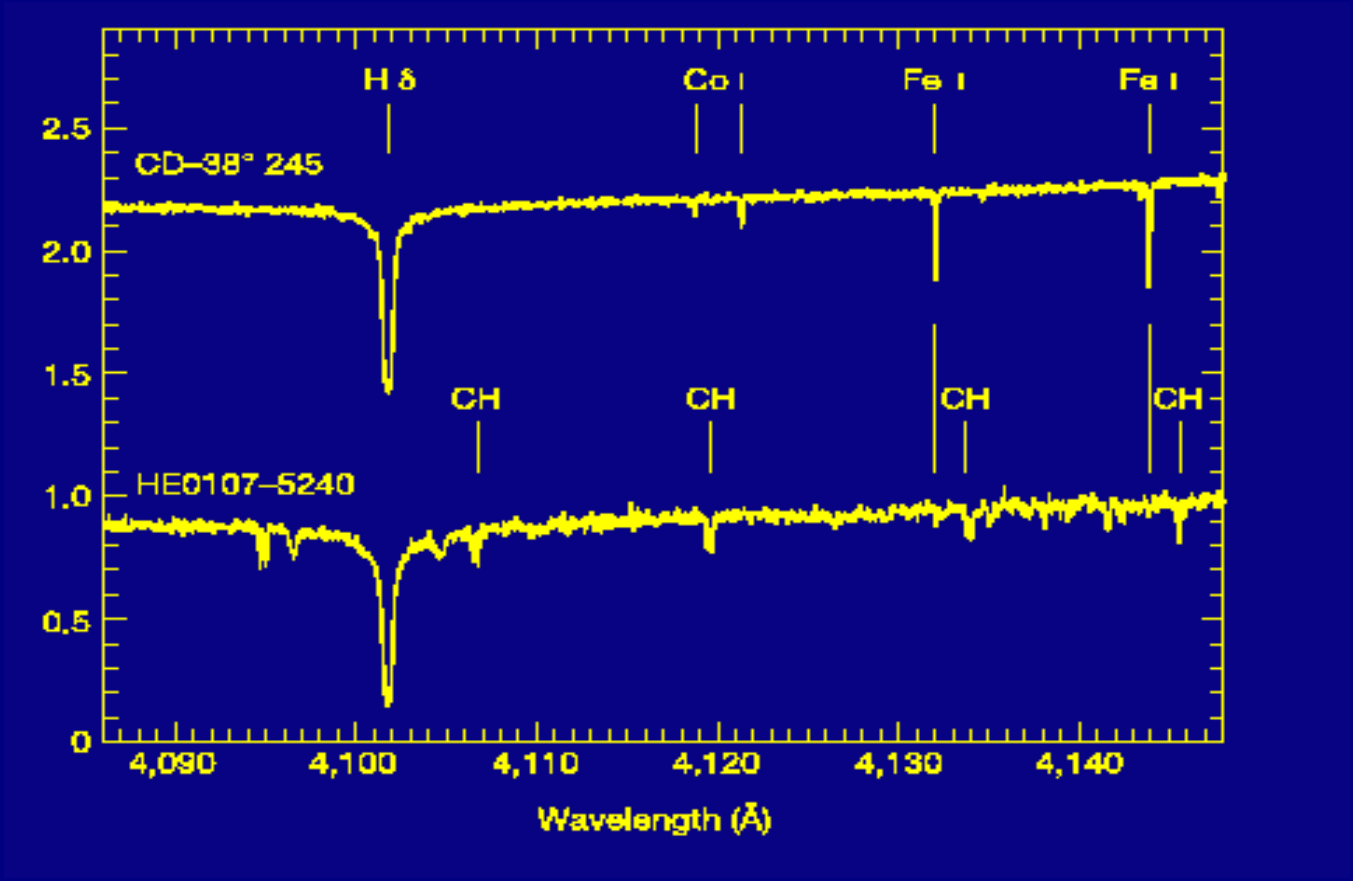

HE 0107-5240
Christlieb etal 2002
Nature

[Fe/H]=-5.3
[C/Fe]=4.0
[N/Fe]=2.3

[Ni/Fe]=-0.2

- many UMP/EMP stars are C- *and* N
- need to understand why!

Table 3. Properties of EMP stars with radial velocity variations, *s*-process enhancements and CNO-overabundance

	[Fe/H]	[C/Fe]	[N/Fe]	[(C+N)/Fe]	[O/Fe]	[Na/Fe]	P_{orb}
LP 625-44[a]	−2.7	2.25	0.95	2.15	1.85	1.75	13yr[b]
HE 0024-2523[c]	−2.7	2.6	2.1	2.53	0.4	−0.17	3d
CS29497-030[d]	−2.8	2.38	1.88	2.31	1.67	0.52	346d

[a]Aoki et al. (2002), O abundance uncertain by a few tenth of dex; [b]Tsangarides et al. (2003); [c]Lucatello et al. (2003); [d]Sivarani et al. (2003)

Los Alamos NATIONAL LABORATORY

C-rich extremely metal poor stars

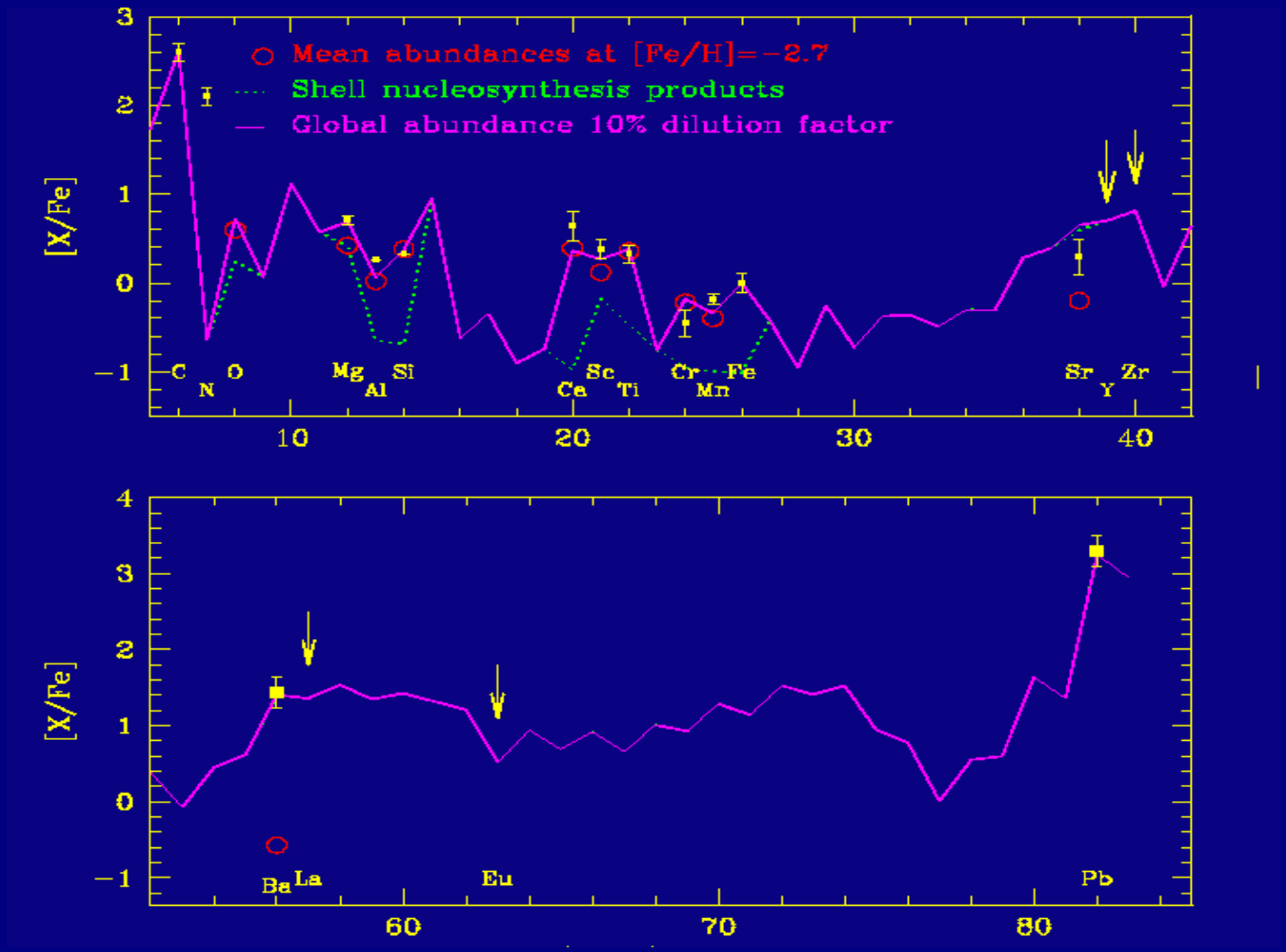

HE0024-2523:

[Fe/H]=-2.7, [C/Fe]=+2.6
[N/Fe]=+2.1

This star is a lead star:
[Pb/Ba]>1.5

(Lucatello etal 2003)

Origin of N and C enrichment in EMP/UMP stars
(with Johnson, Beers & Christlieb)

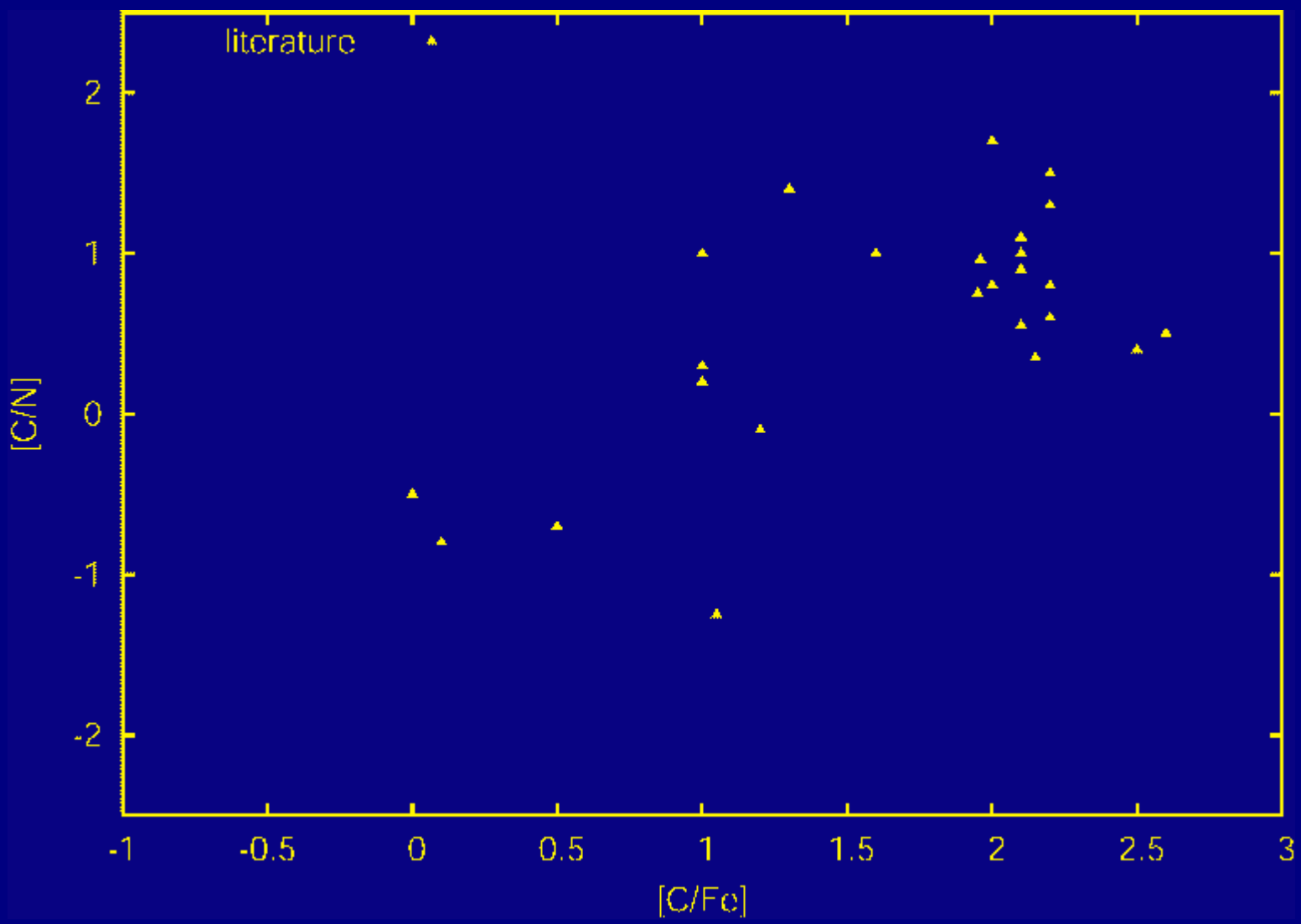

(Barbuy etal 1997, Aoki etal 2001a,b, Preston & Sneden 2001, Lucatello etal 2003)

Origin of N and C enrichment in EMP/UMP stars
(with Johnson, Beers & Christlieb)

new model set of EMP IMS stars Z=0.0001 Herwig 2004, ApJS, astro-ph

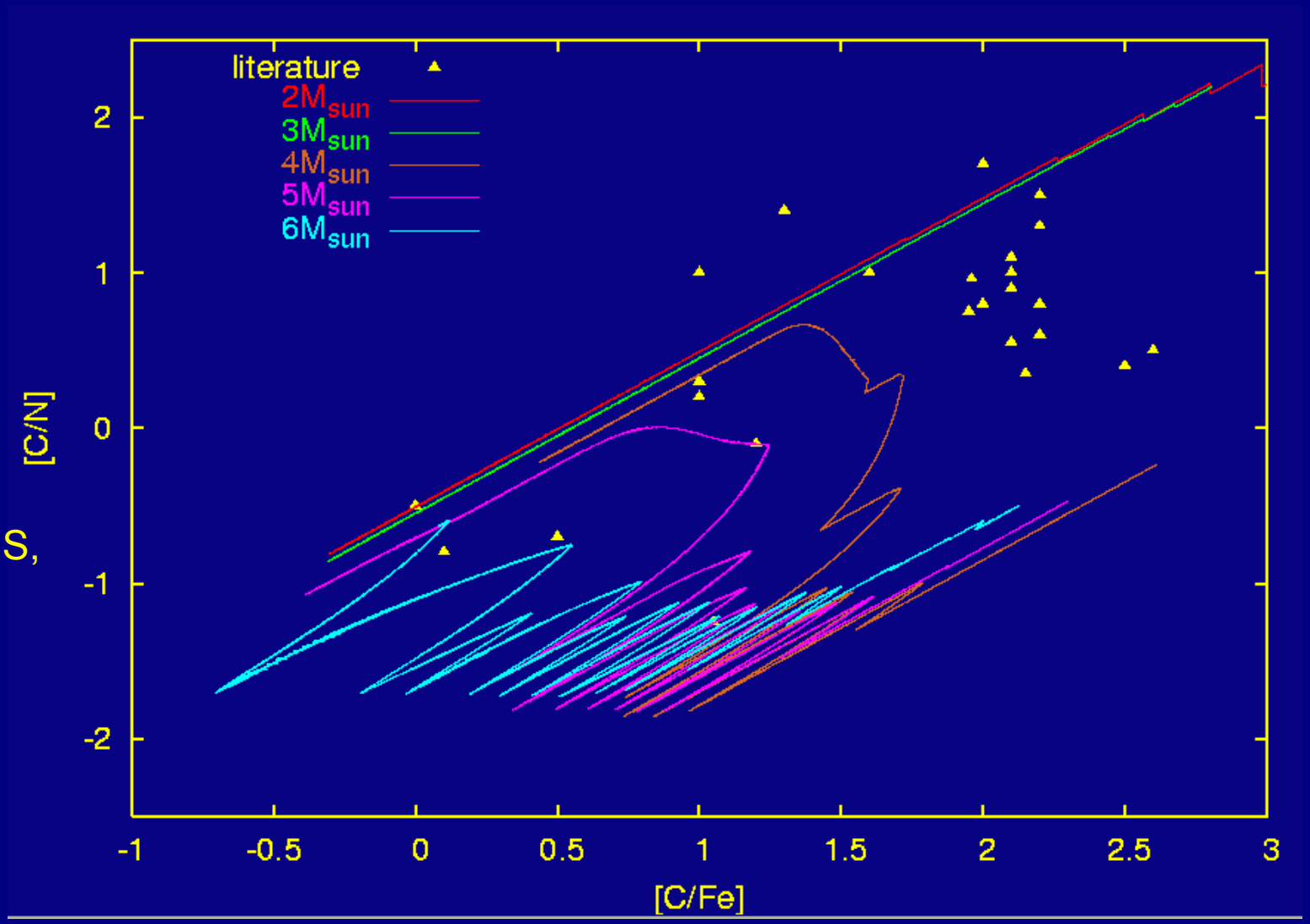

Origin of N and C enrichment in EMP/UMP stars
(with Johnson, Beers & Christlieb)

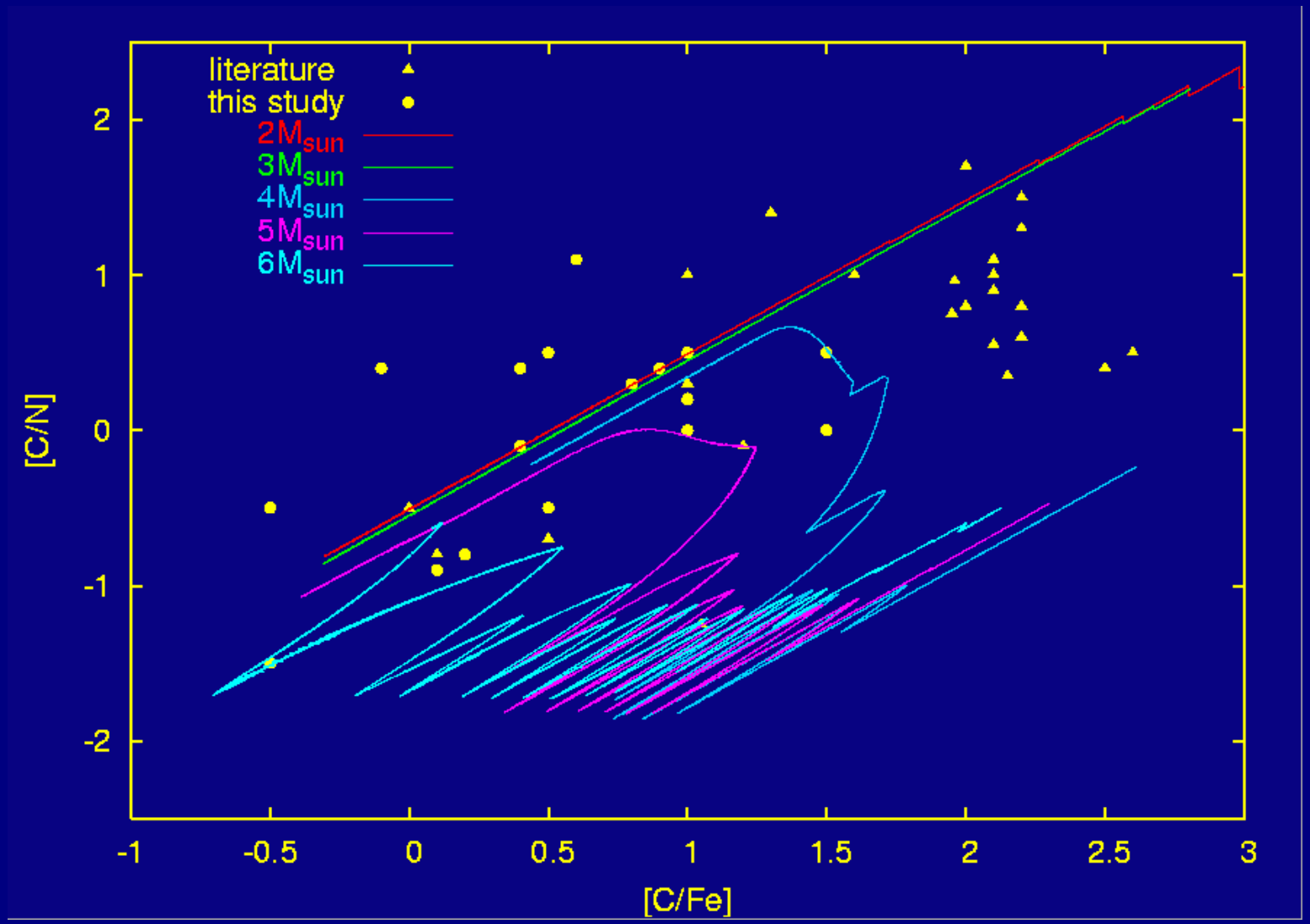

Origin of N and C enrichment in EMP/UMP stars
(with Johnson, Beers & Christlieb)

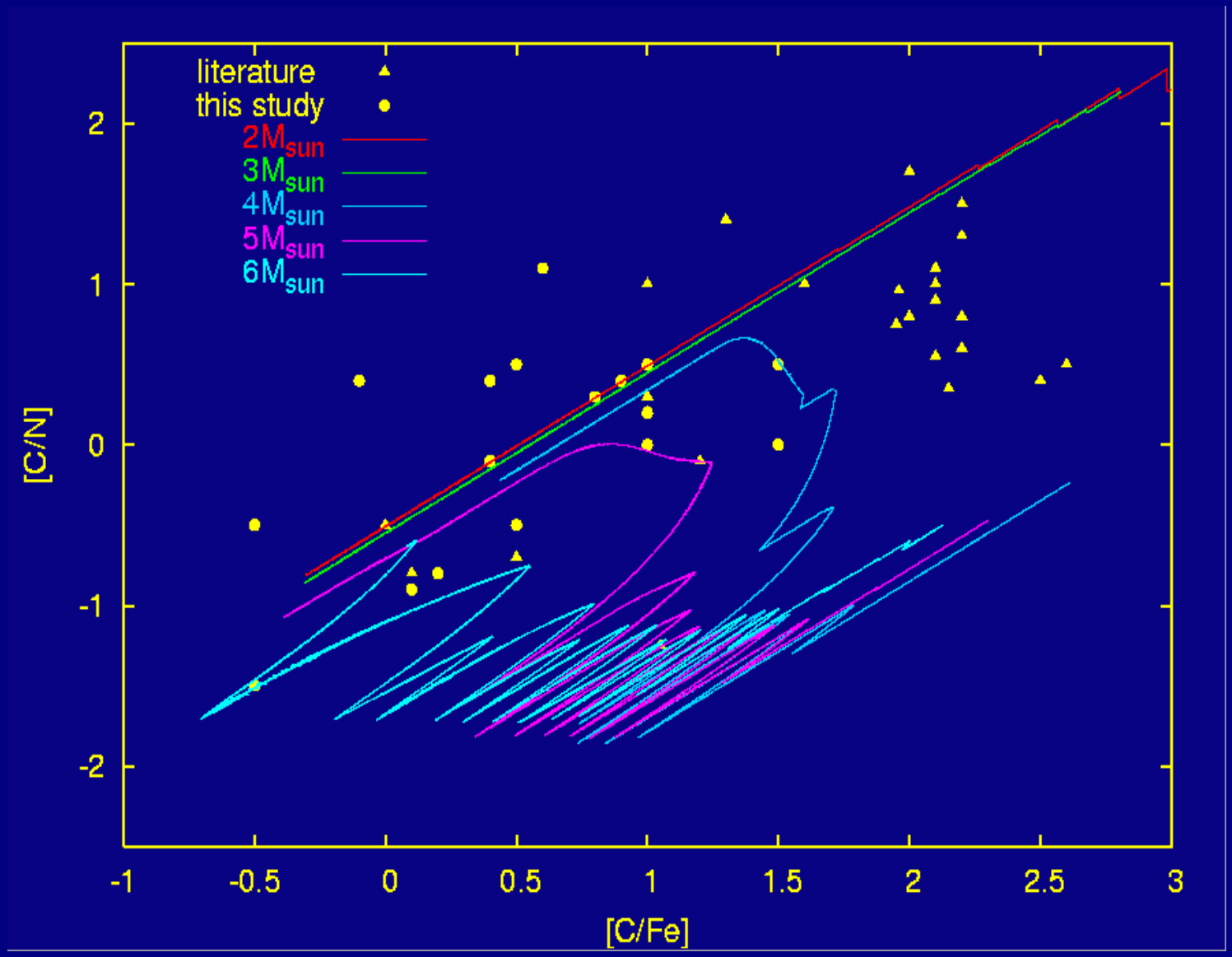

There are in fact two problems:

1. Where does the N in the C-rich stars come from?

2. Where are the EMP stars poluted by the N-rich IMS?

Nitrogen-period anti-correlation in EMP binary members with s-process:

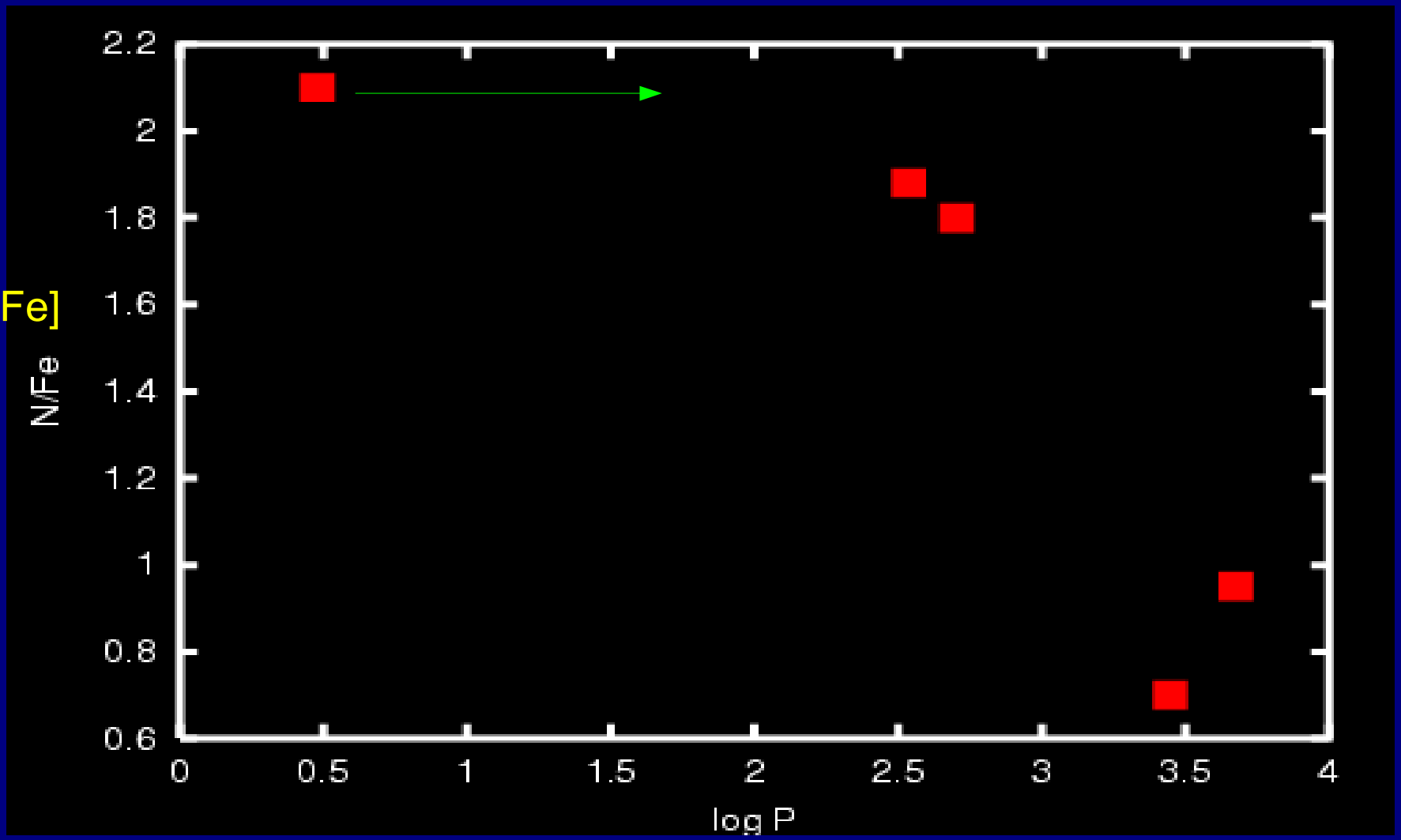

binary period

Na-period correlation of s-process rich EMP binary members:

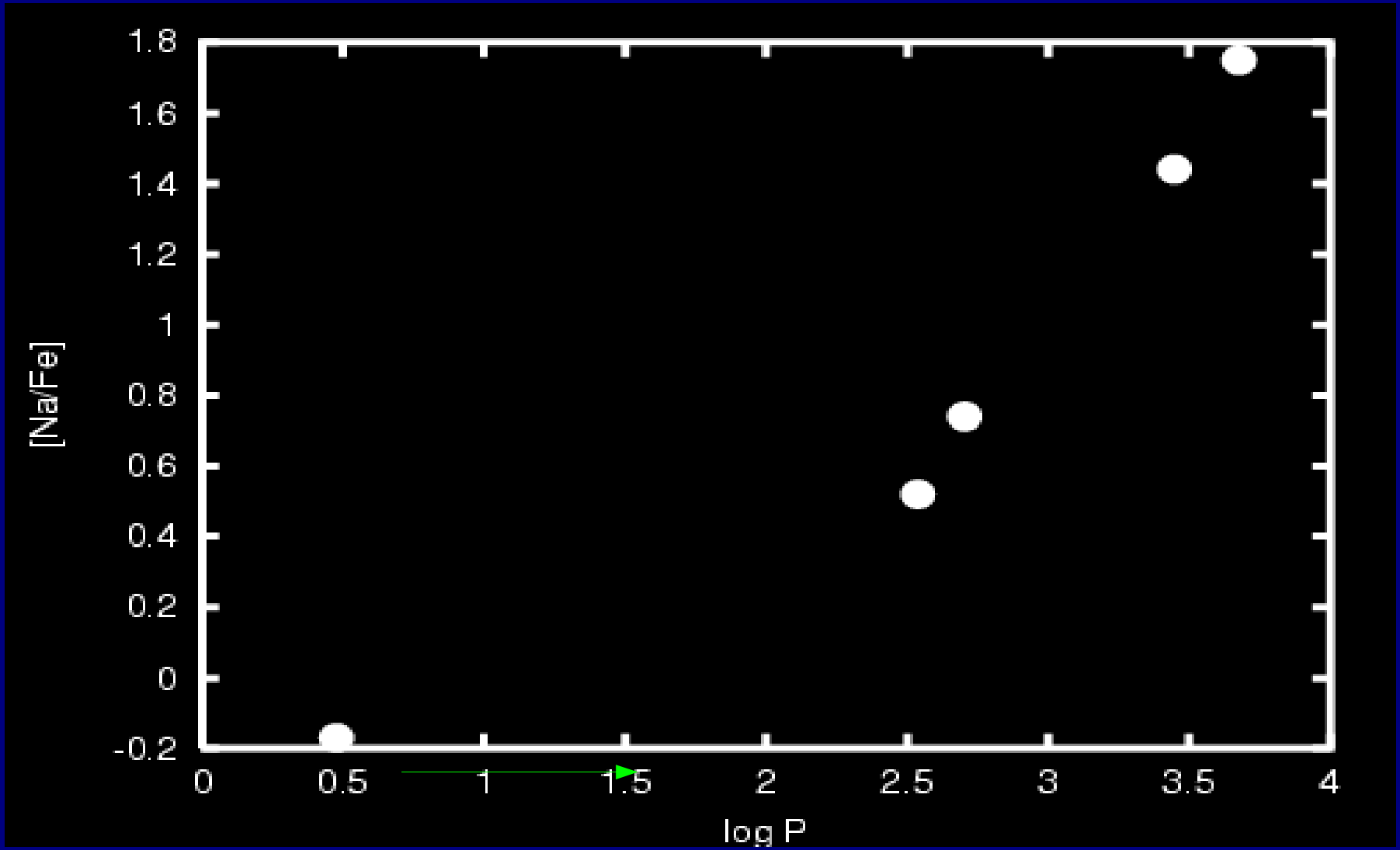

HE0024-2523 (Lucatello etal 2003), CS29497-030 (Sivarani etal 2003)
CS22948-027, CS22942-019 (Preston & Sneden, 2001)
LP625-44 (Aoki etal 2002)

Origin of the Mg isotopic ratios in the Early Universe

Yong etal 2003, ApJ: Mg isotopic ratios in members of GC NGC6752 (60/10/30)

Denissenkov & Herwig 2003: HBB IMS can not be the primordial source
ApJL of GC abundance correlations because they produce $^{25}Mg > ^{26}Mg$ (calculations without mass loss)

Herwig 2004: $Z=10^{-4}$, AGB evolution with mass loss:
ApJS ^{22}Ne s-process in intershell makes $^{25}Mg < ^{26}Mg$! mainly because
astro-ph of large np-capture X-section of ^{25}Mg.

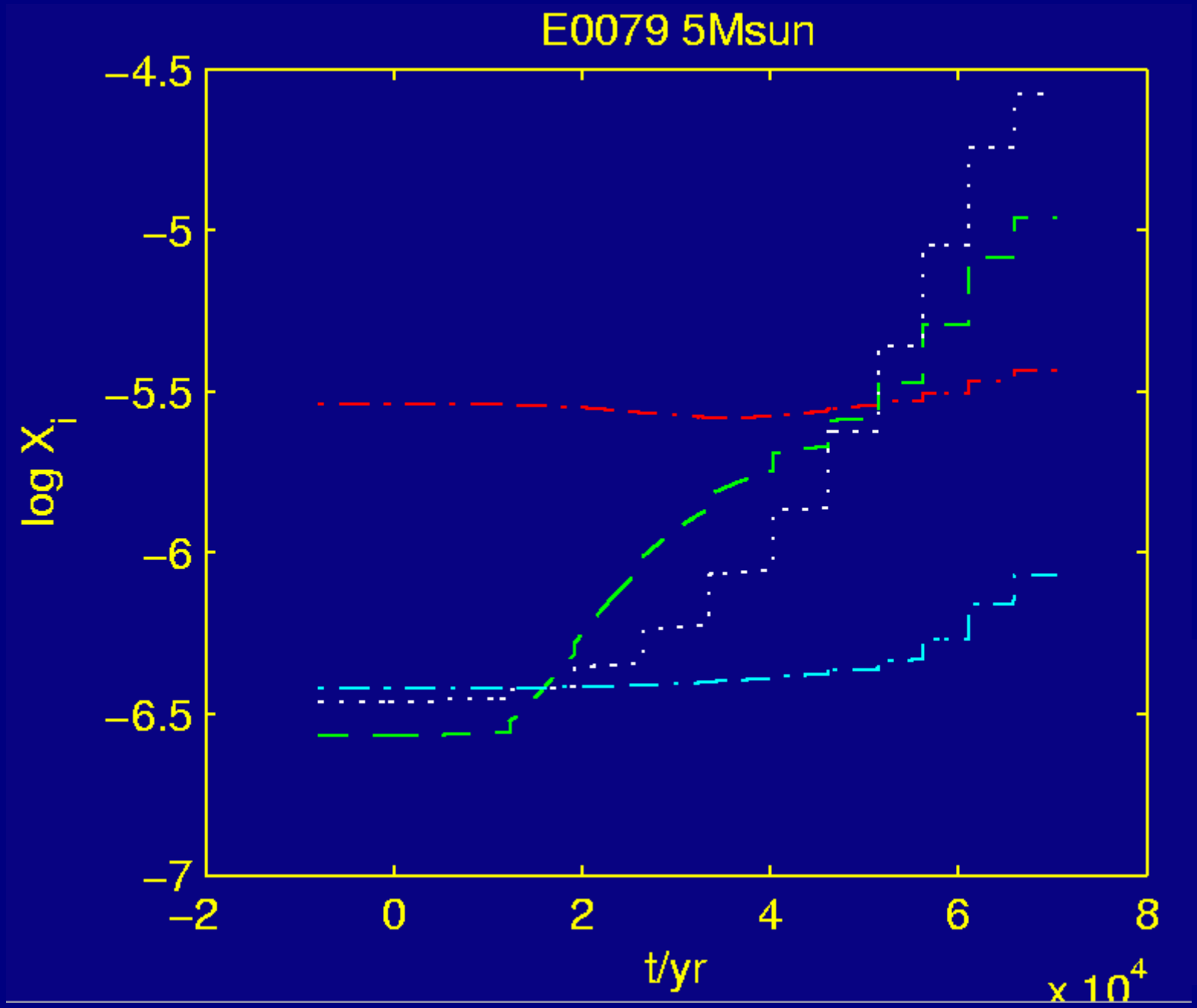

Surface evolution of IMS AGB star Mg and Al

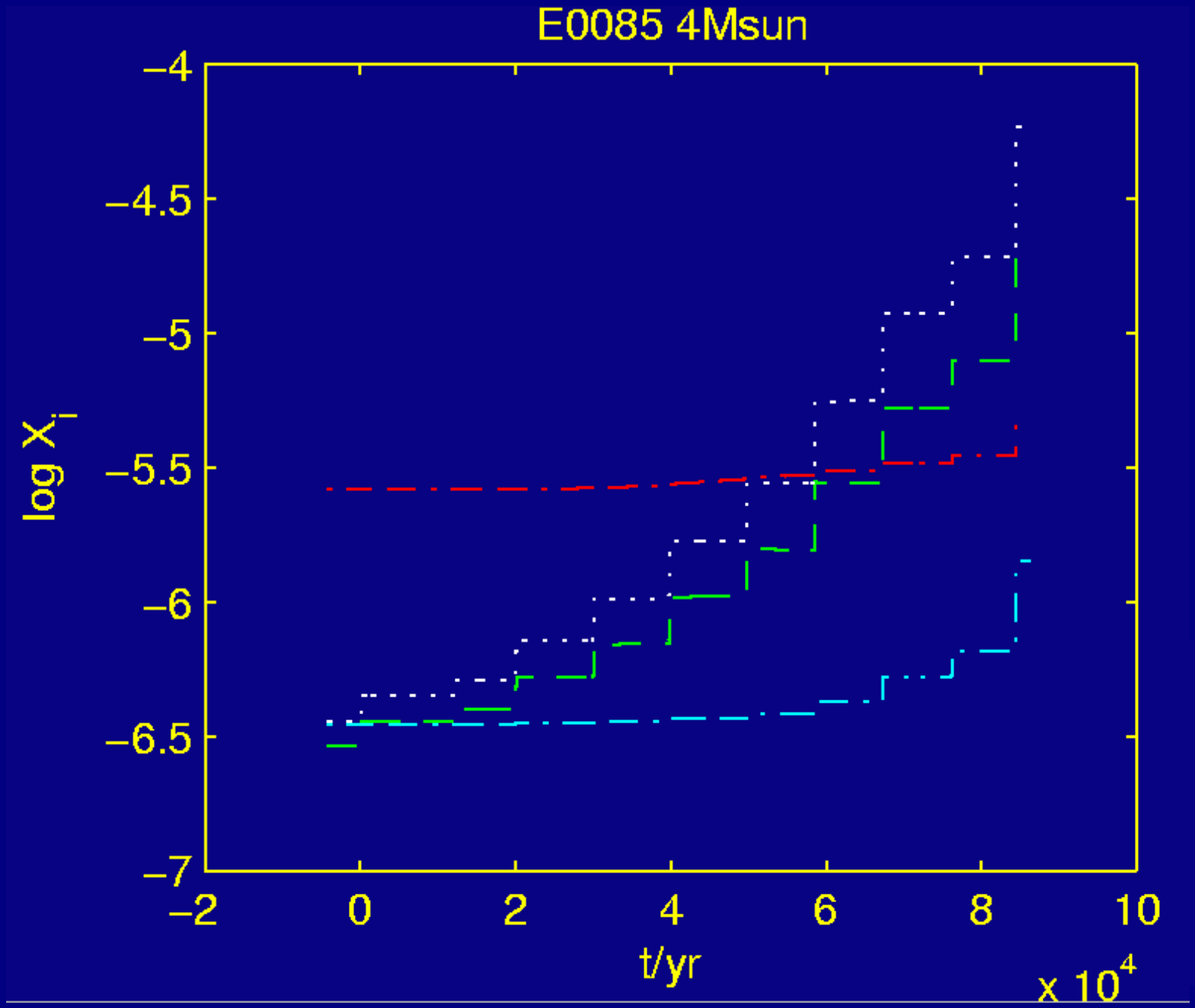

Surface evolution of IMS AGB star Mg and Al

Origin of the Mg isotopic ratios in the Early Universe

Yong etal 2003, ApJ: Mg isotopic ratios in members of GC NGC6752 (60/10/30)

Denissenkov & Herwig 2003: HBB IMS can not be the primordial source
ApJL of GC abundance correlations because they produce $^{25}Mg > ^{26}Mg$ (calculations without mass loss)

Herwig 2004: $Z=10^{-4}$, AGB evolution with mass loss:
ApJS ^{22}Ne s-process in intershell makes $^{25}Mg < ^{26}Mg$! mainly because
astro-ph of large np-capture X-section of ^{25}Mg.

Typical ratio in ejecta of these models: $^{25}Mg:^{26}Mg \sim 1:2$

The s-process

Where and how does the s-process operate in EMP, UMP or (if they exist?!?) Z=0 AGB stars?

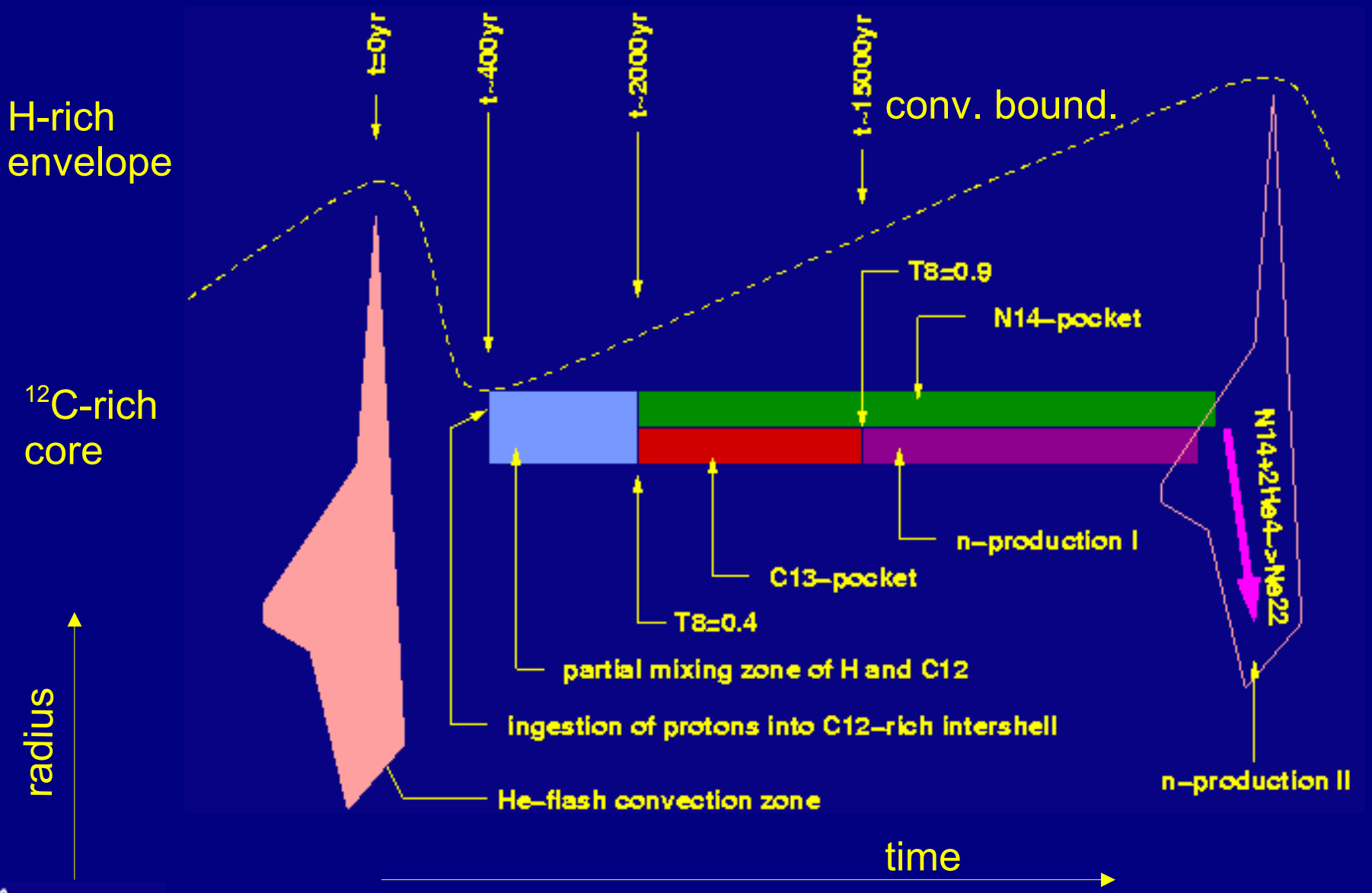

$Z=10^{-4}$: evolution

- Herwig 2004, ApJ, v605
- overal *normal* AGB evolution, TPs etc
- corrosive H-burning during DUP phase
  -> may lead to termination of AGB phase

Herwig 2004, ApJ, v605.

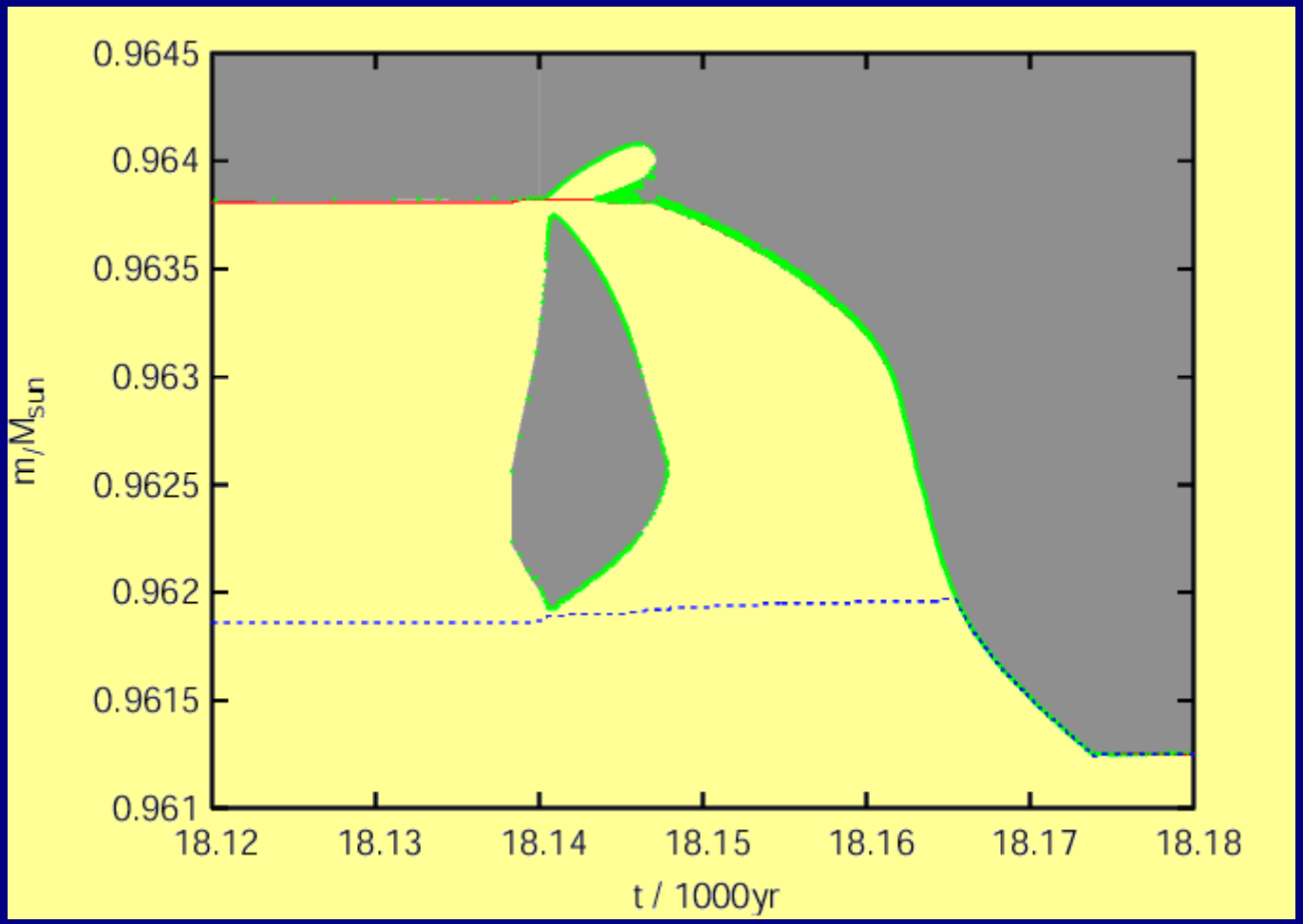

Early TP during $5M_{sun}$ sequence.

f_{OV}=0.016 (=10x smaller than what would be required for ^{13}C-pocket).

AGB evolution at extremely low metallicity: the interplay of DUP and HBB (Herwig, 2004, ApJ, April 10 issue):

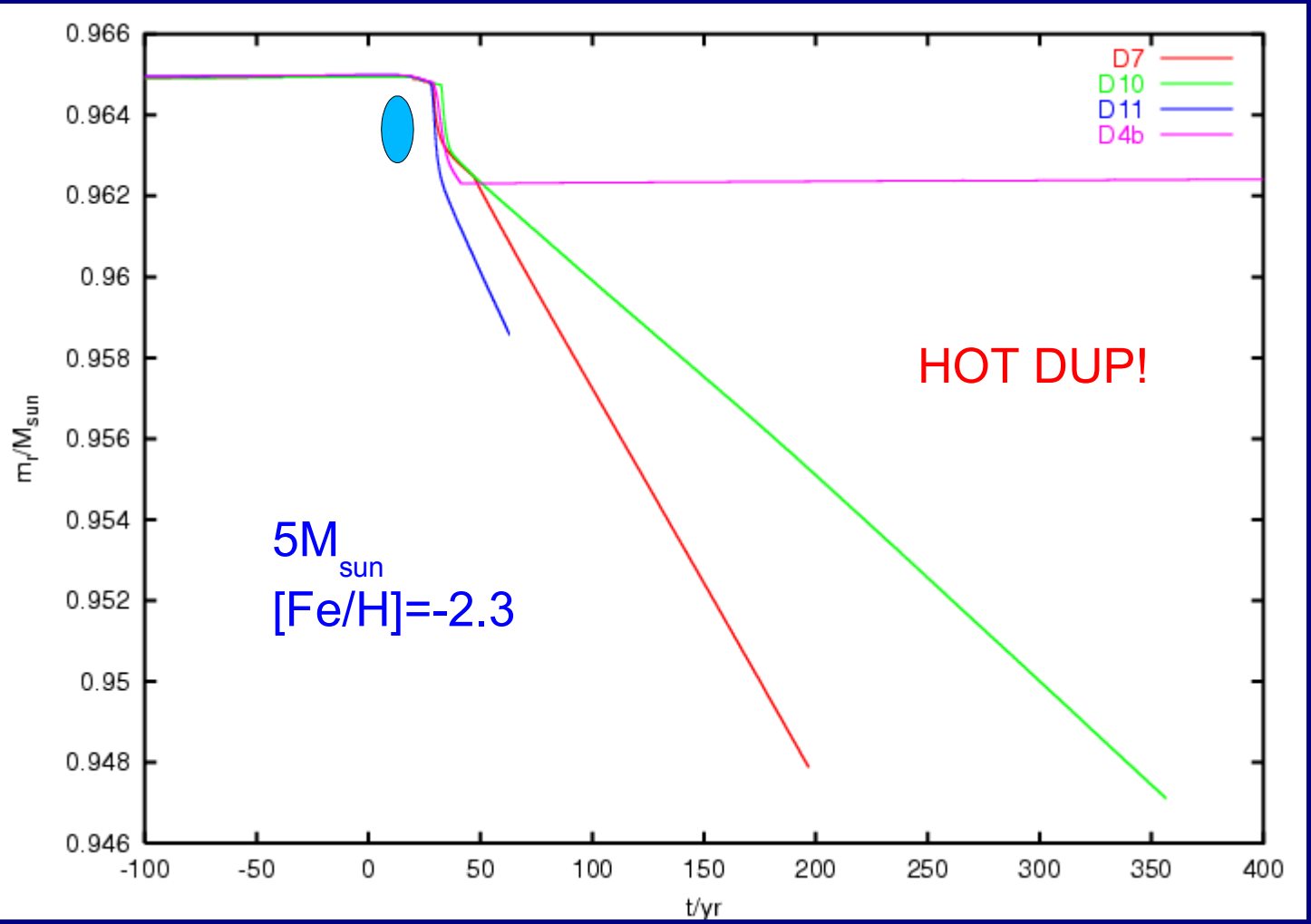

Calculations with exponential overshooting at the bottom of the envelope: f=0.032

for s-process ^{13}C-pocket in low-mass stars at solar Z: f=0.13-0.16

Ultra-metal poor or Z=0 evolution:

- no CNO for CNO cycle
- H-shell very hot
- may show HIF (Hydrogen-ingestion flash)

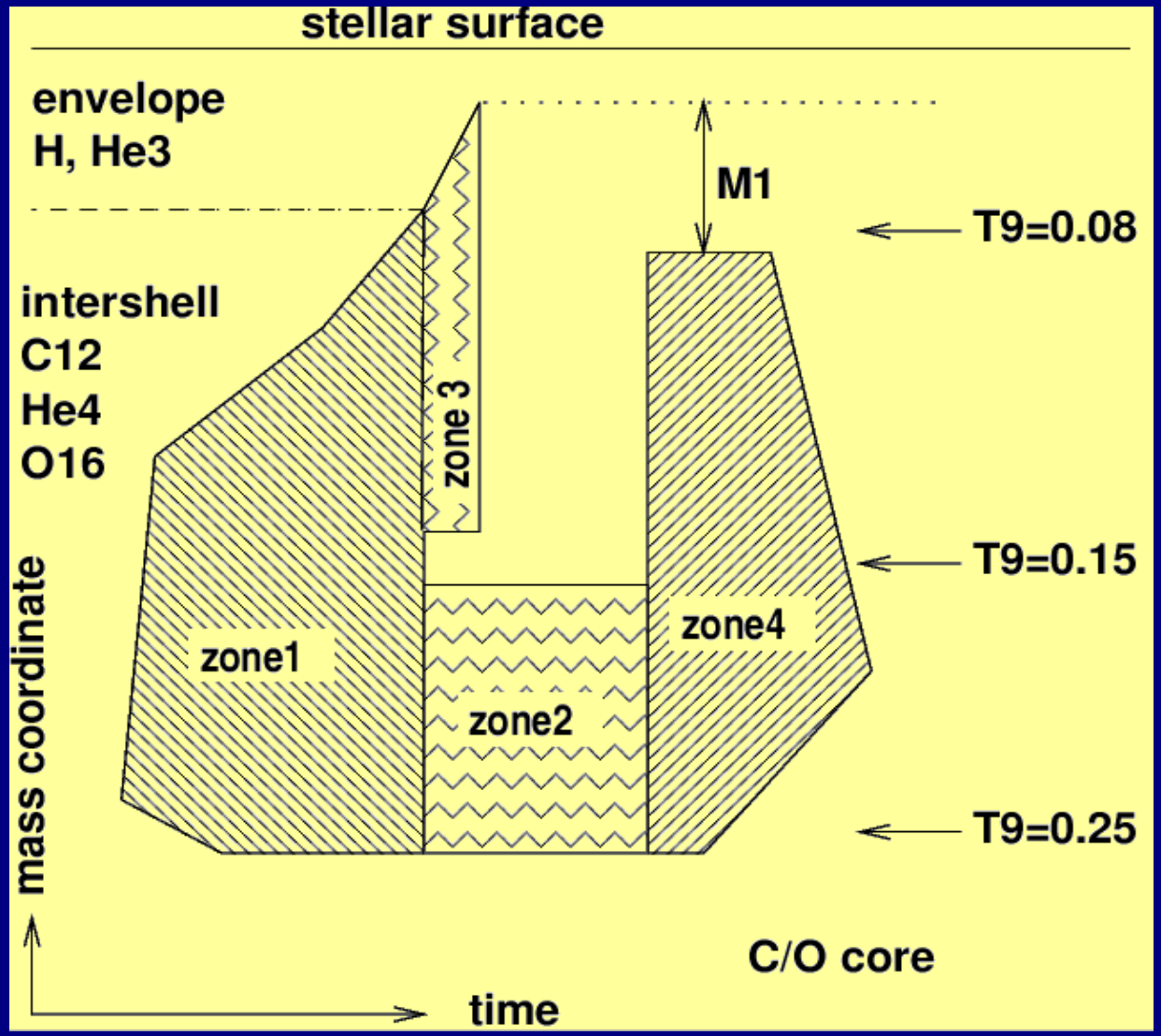

- Ingestion of H into He-flash convection (Fujimoto etal 2000, Herwig 2002, Iwamoto etal 2004)
- Known or suspected to happen in several other situations, e.g. young WDs (born again AGB stars)

Herwig etal 1999, Herwig 2001

- whether or not HIF occurs depends on excact interplay of convection, rotation and likely also magnetic fields
- and so does the exact morphology of the different zone
- this determines the nuclear evolution

$M=5M_{sun}$, Z=0.0, time sequence of profiles in H-flash region (on top of He-shell flash convection zone)

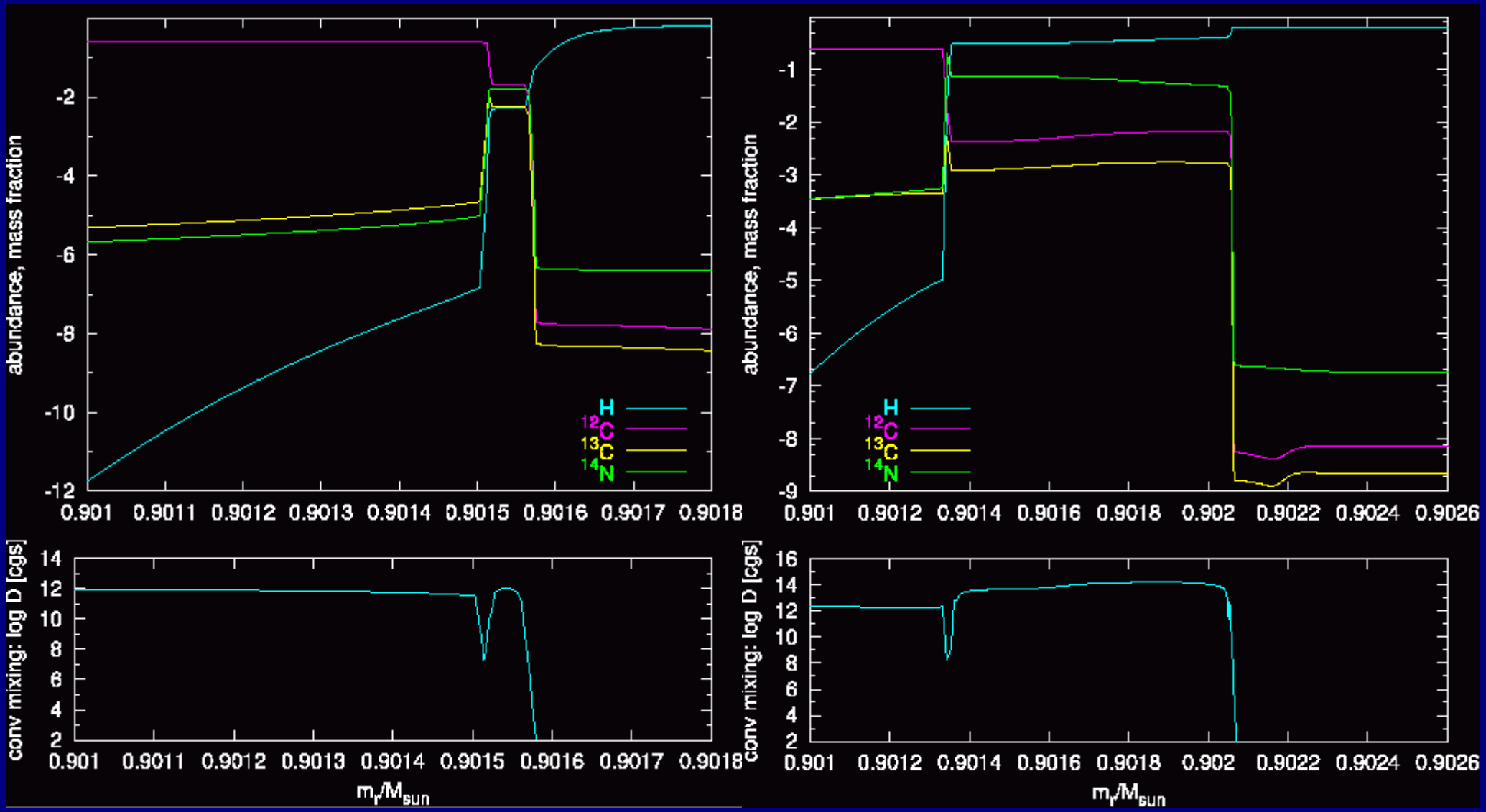

The Second Stars

- What are they?
- Why are they important?
- What do we know about them?
- What can we do to learn more about them?

What can we do to lear more about the second stars?

Nuclear Physics input

✔ C-star formation very sensitive to nuclear physics input. Revised reaction rate for $^{14}N(p,\gamma)^{15}O$ (factor 0.6 * NACRE in T-range of H-shell burning) leads to more efficient dredge-up (Herwig & Austin 2004, ApJ Let, in press)

Improving the mixing models for stellar interior evolution:

✔ Rotating AGB models fail to produce s-process (Herwig, Langer, Marigo ApJ 2003; confirmed by Siess etal 2004) ... what is wrong?

- direct hydrodynamic simulations of mixing and burning in stellar interior nuclear production site, new program with ASC codes at LANL(T-6/X-2)
- s-process as a diagnostic tool, relies on better Nuclear Physics data, new Nuclear Astrophysics program with LANL/LANSCE

Rate selections for stellar evolution TP–AGB calculations

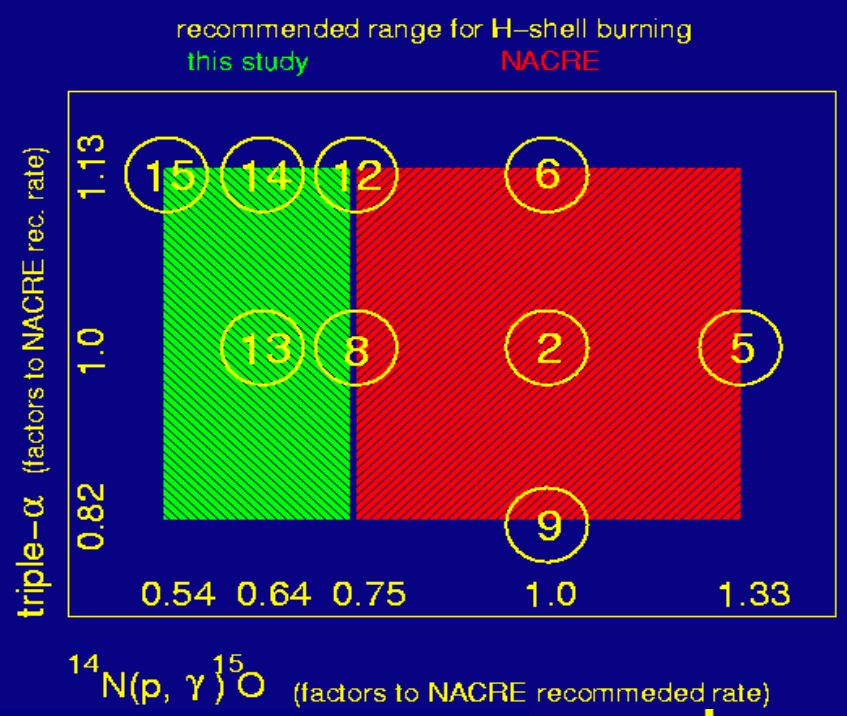

C-surface abundance evolution of complete $M=2M_{sun}$, $Z=0.01$ for a range of rate selections

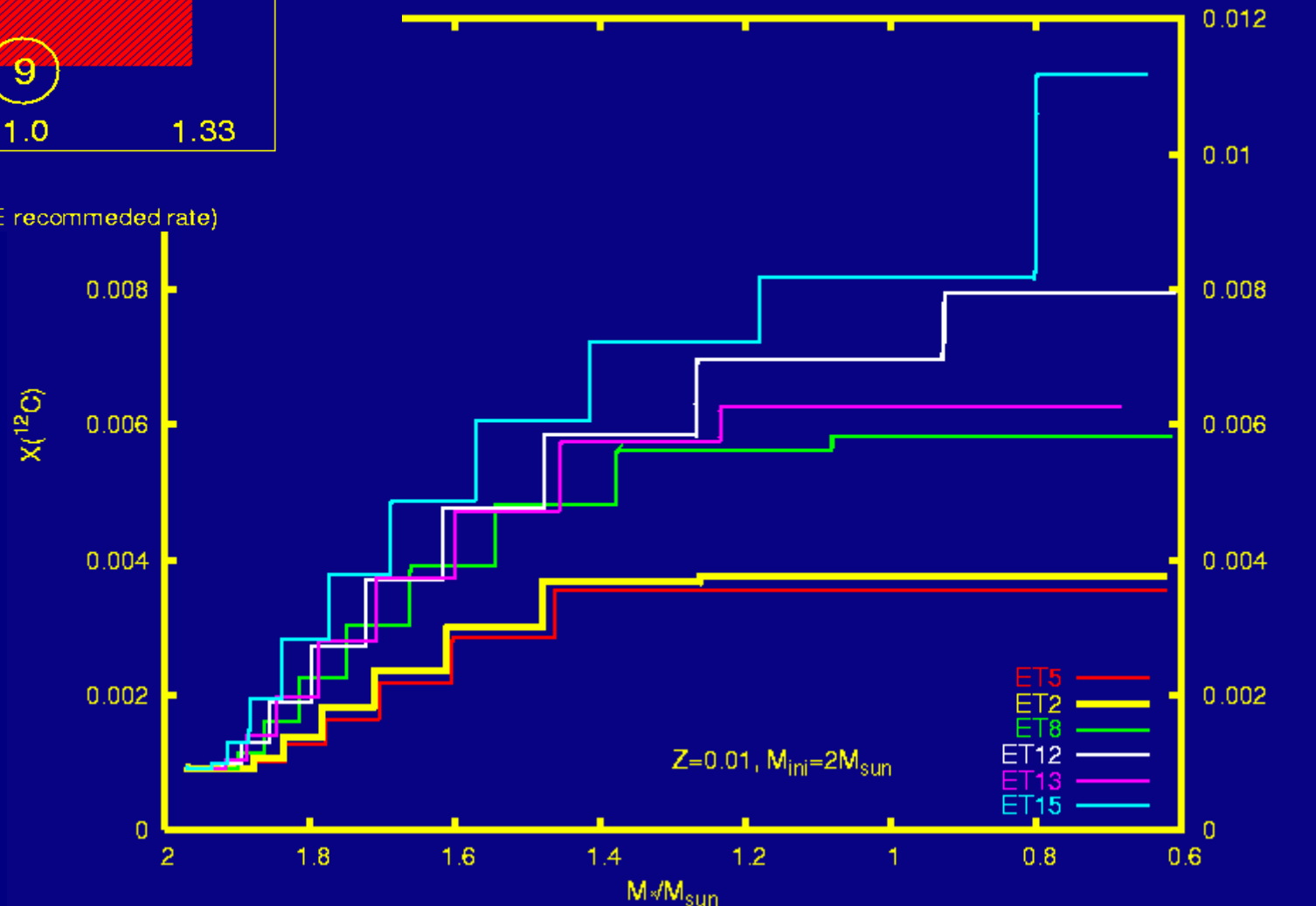

Los Alamos NATIONAL LABORATORY

What can we do to lear more about the second stars?

Nuclear Physics input

✔ C-star formation very sensitive to nuclear physics input. Revised reaction rate for $^{14}N(p,\gamma)^{15}O$ (factor 0.6 * NACRE in T-range of H-shell burning) leads to more efficient dredge-up (Herwig & Austin 2004, ApJ Let, in press)

Improving the mixing models for stellar interior evolution:

✔ Rotating AGB models fail to produce s-process (Herwig, Langer, Marigo ApJ 2003; confirmed by Siess etal 2004) ... what is wrong?

- direct hydrodynamic simulations of mixing and burning in stellar interior nuclear production site, new program with ASC codes at LANL(T-6/X-2)
- s-process as a diagnostic tool, relies on better Nuclear Physics data, new Nuclear Astrophysics program with LANL/LANSCE

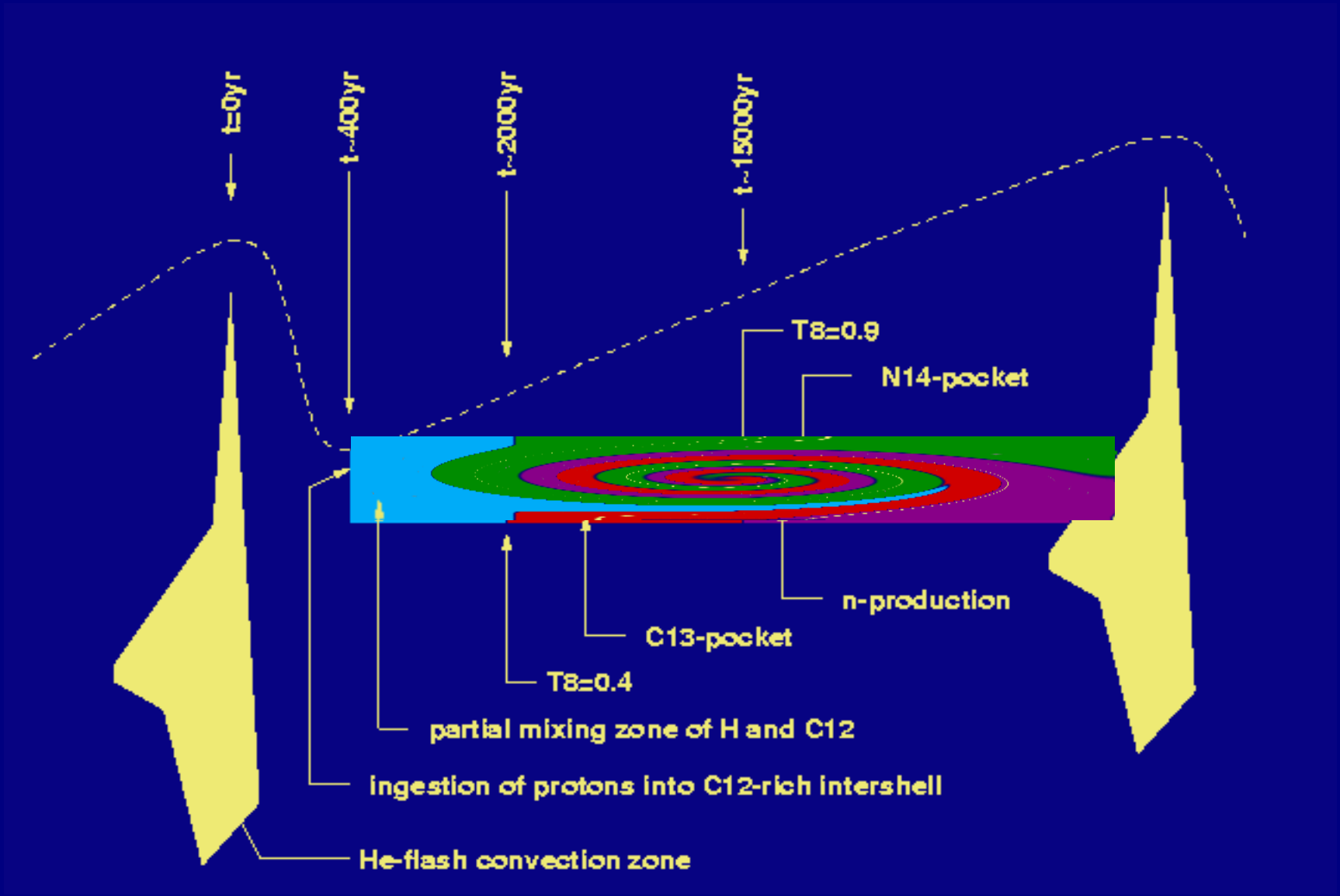

$^{14}N(n,p)^{14}C$ neutron poison

What can we do to lear more about the second stars?

Nuclear Physics input

✔ C-star formation very sensitive to nuclear physics input. Revised reaction rate for $^{14}N(p,\gamma)^{15}O$ (factor 0.6 * NACRE in T-range of H-shell burning) leads to more efficient dredge-up (Herwig & Austin 2004, ApJ Let, in press)

Improving the mixing models for stellar interior evolution:

✔ Rotating AGB models fail to produce s-process (Herwig, Langer, Marigo ApJ 2003; confirmed by Siess etal 2004) ... what is wrong?

- direct hydrodynamic simulations of mixing and burning in stellar interior nuclear production site, new program with ASC codes at LANL(T-6/X-2)
- s-process as a diagnostic tool, relies on better Nuclear Physics data, new Nuclear Astrophysics program with LANL/LANSCE

s-process branchings as a diagnostic tool to probe stellar interior physics

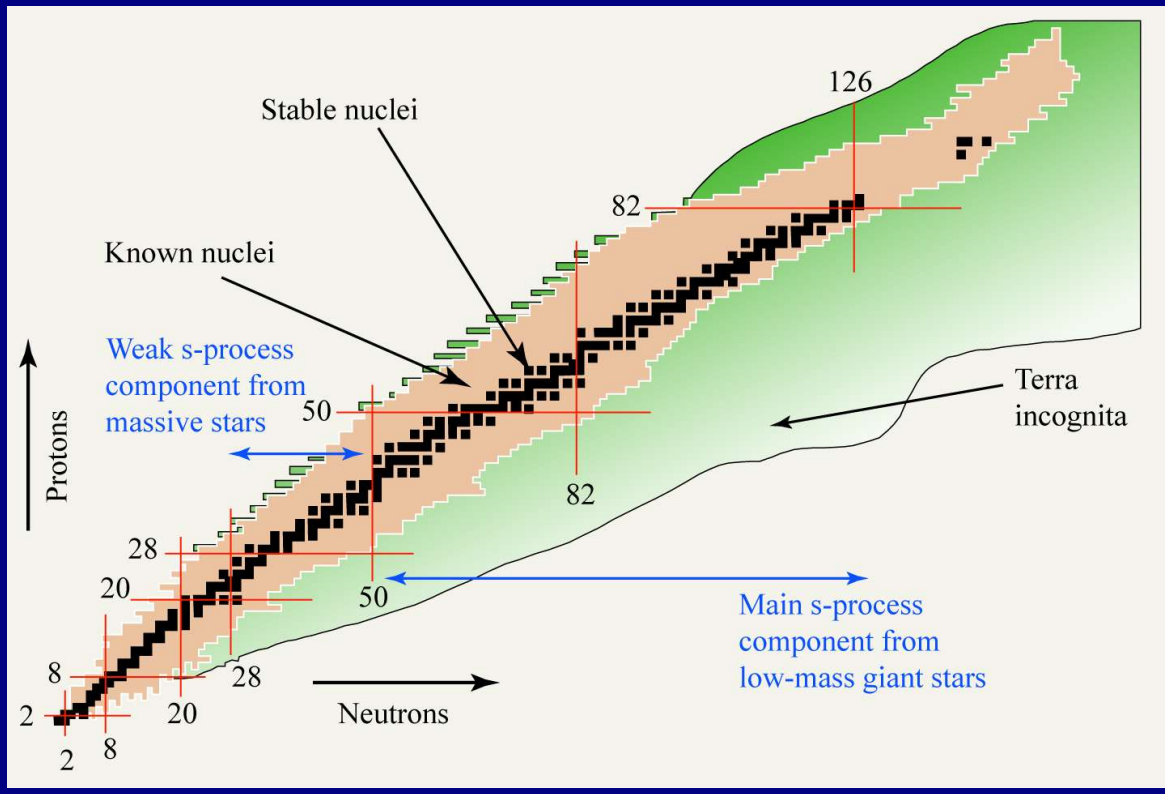

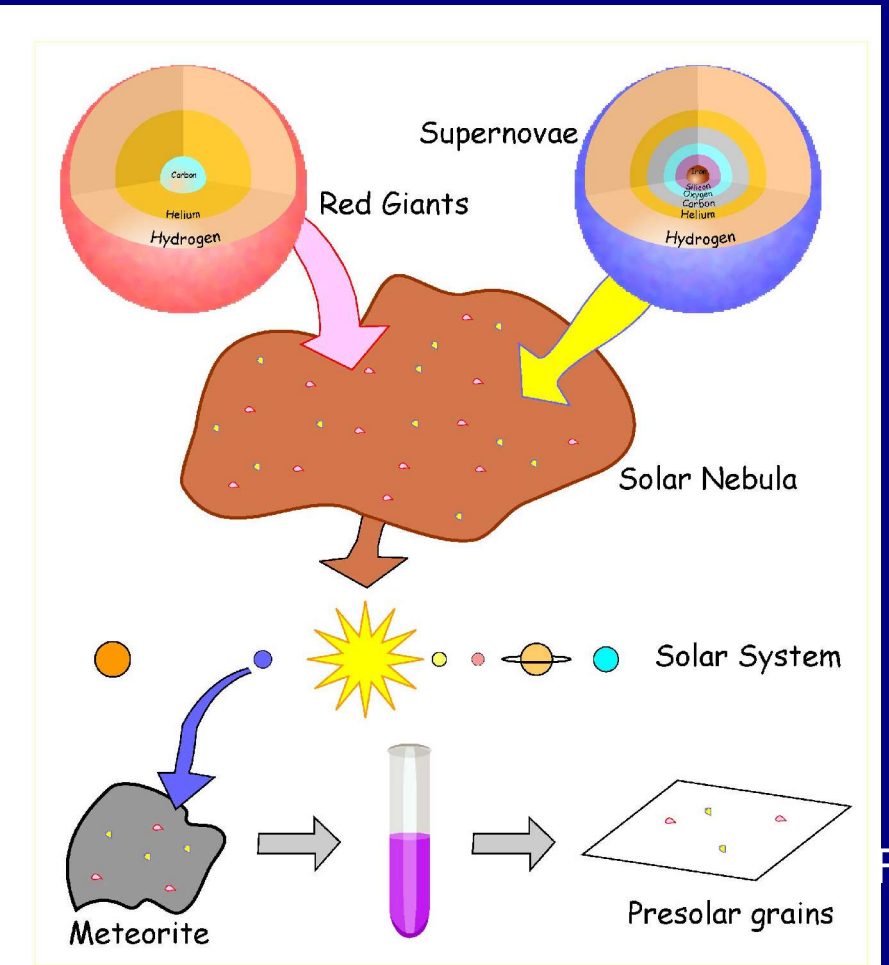

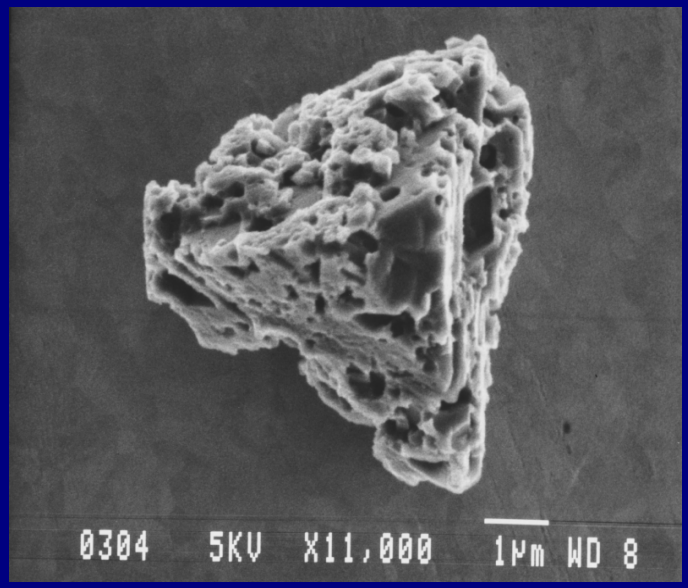

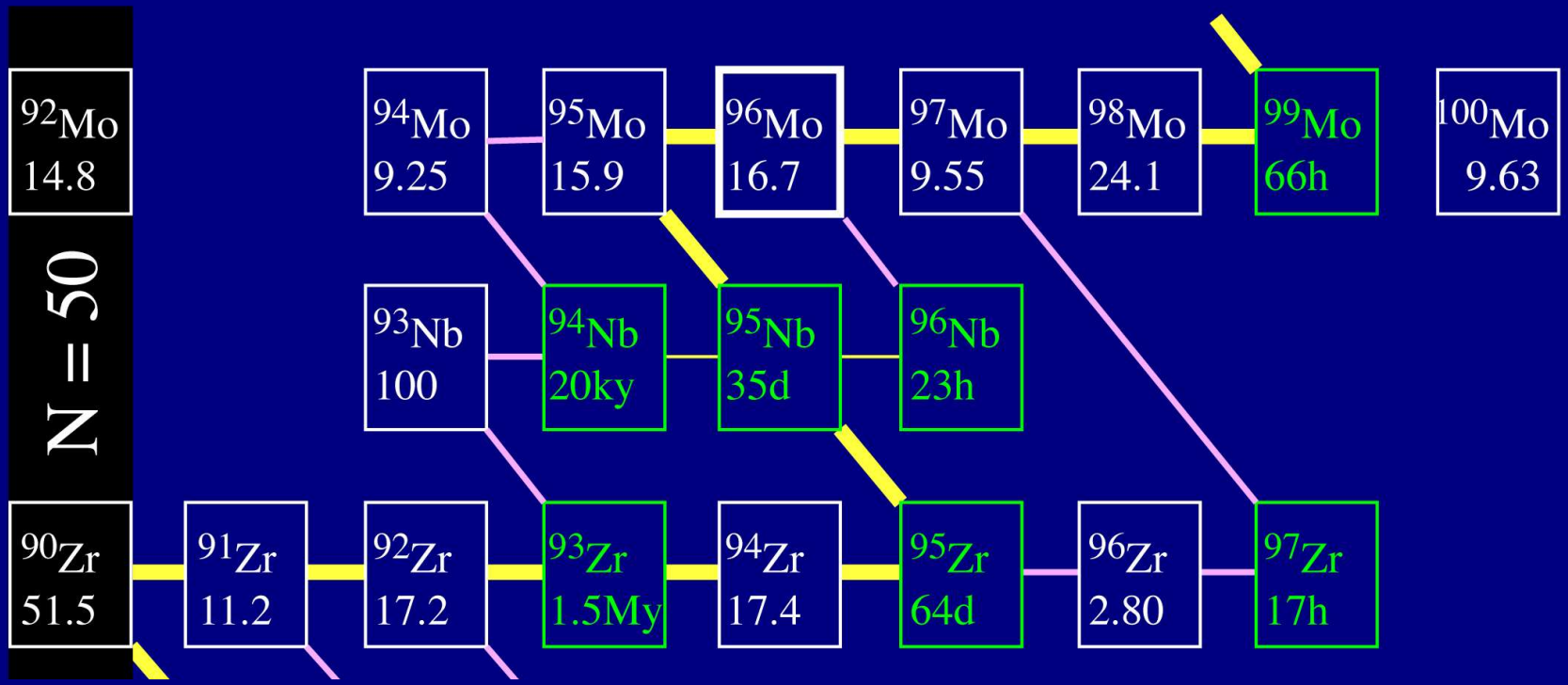
N = 50
92Mo 14.8
94Mo 9.25
95Mo 15.9
96Mo 16.7
97Mo 9.55
98Mo 24.1
99Mo 66h
100Mo 9.63
93Nb 100
94Nb 20ky
95Nb 35d
96Nb 23h
90Zr 51.5
91Zr 11.2
92Zr 17.2
93Zr 1.5My
94Zr 17.4
95Zr 64d
96Zr 2.80
97Zr 17h

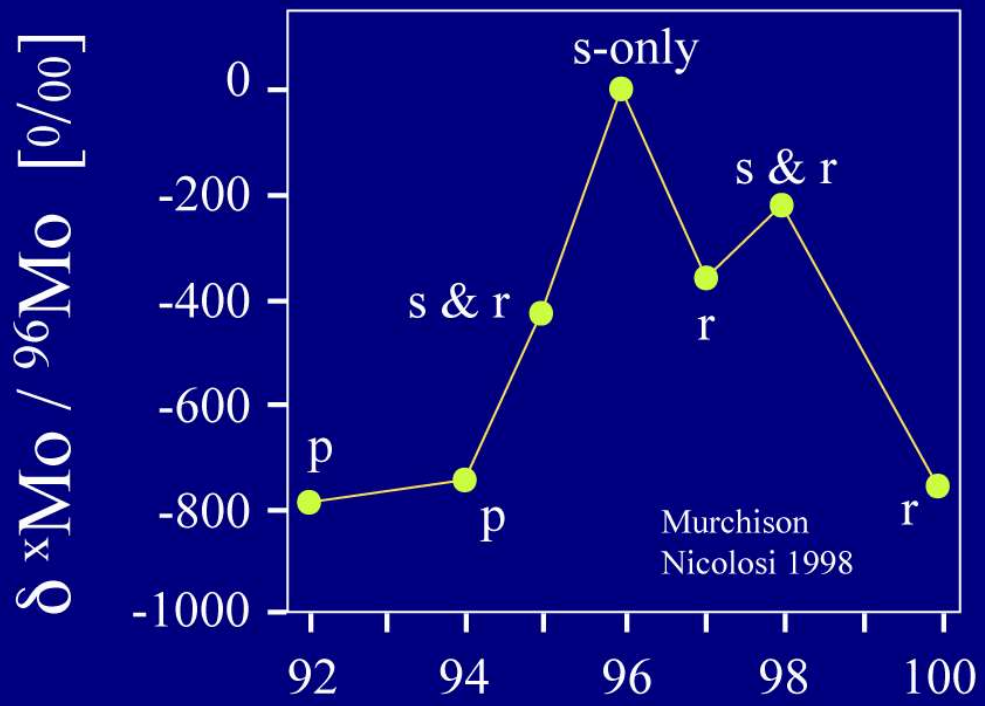
δ xMo / 96Mo [0/00]
0
-200
-400
-600
-800
-1000
92
94
96
98
100
s-only
s & r
s & r
r
p
p
r
Murchison
Nicolosi 1998

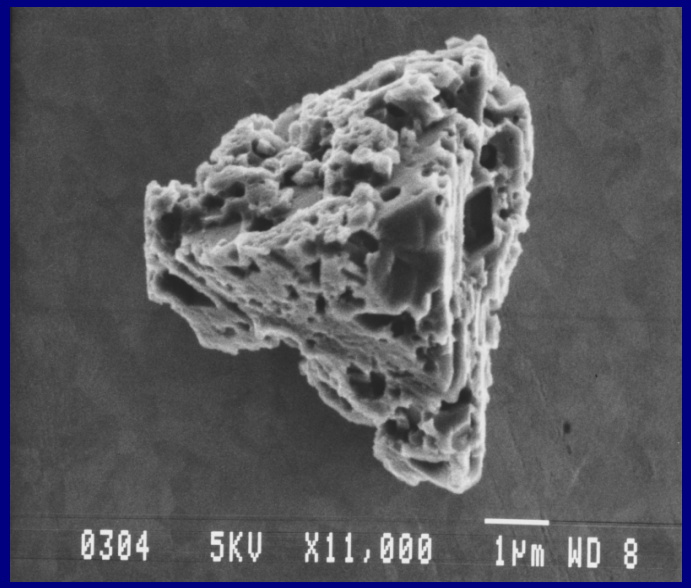
0304 5KV X11,000 1μm WD 8

Convection

Schematic of He-shell flash

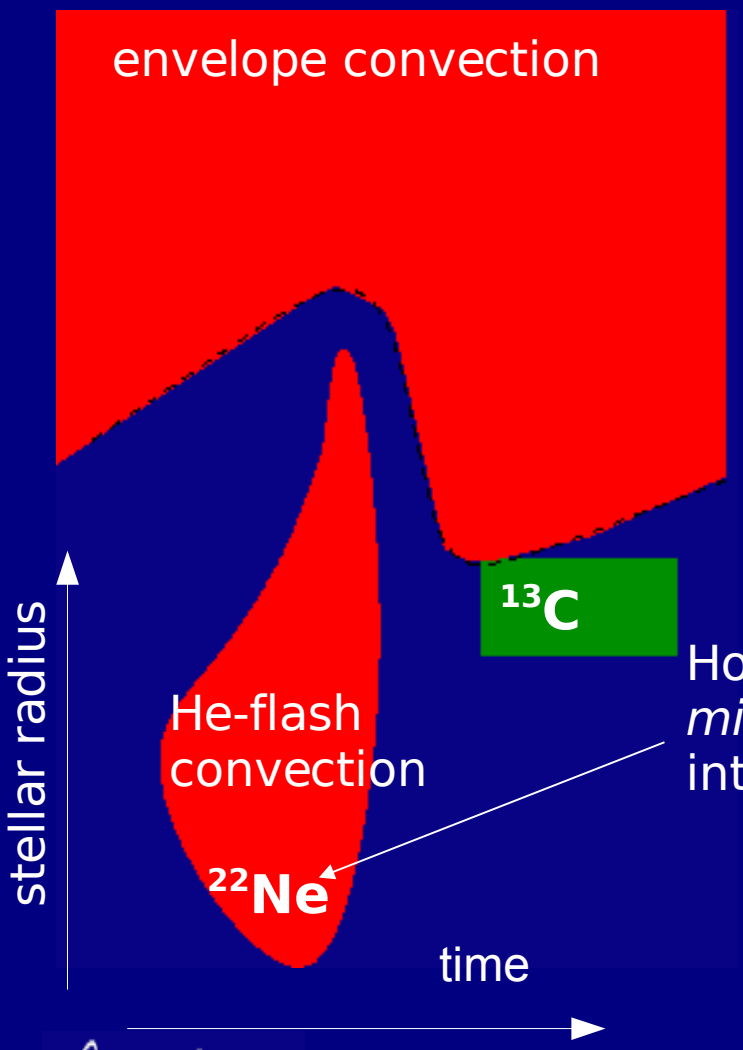

How efficient is *extra mixing* in deep stellar interior?

2D-simulation of White Dwarf convection zone

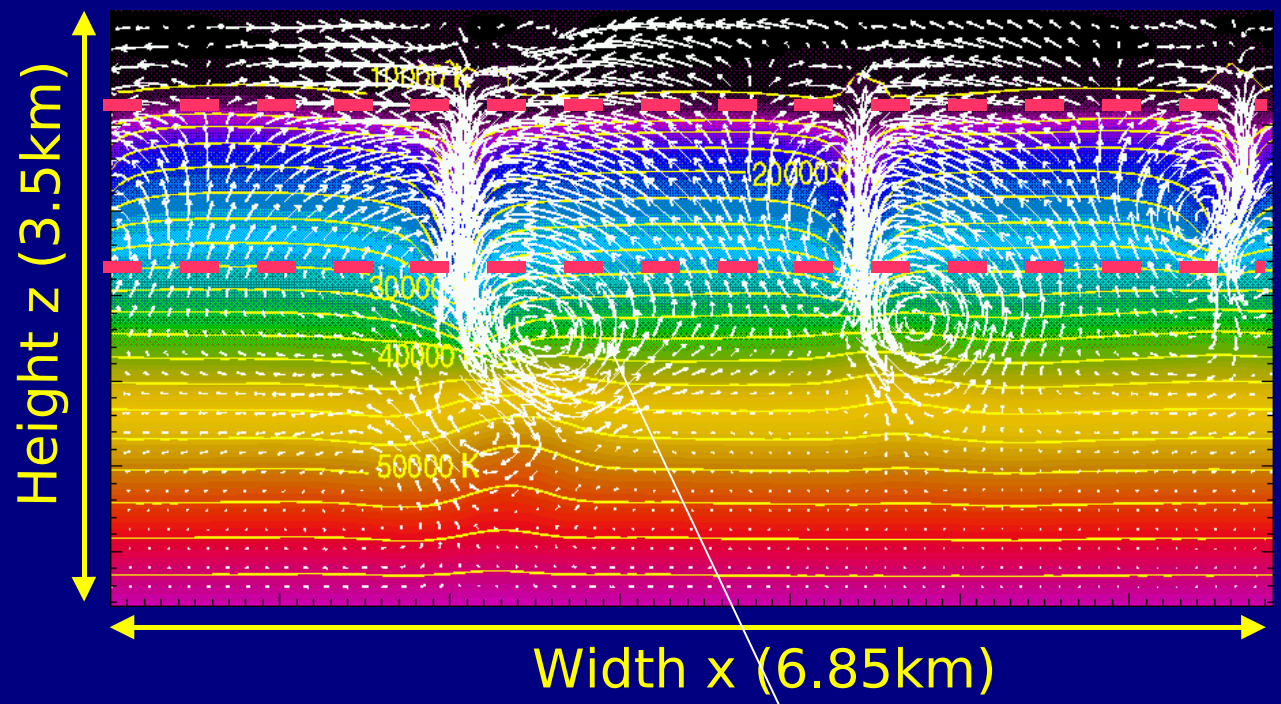

Mixing extends into stable layers -> *extra mixing*.

Test with 1D exponential diffusion approximcation, efficiency parameter f.

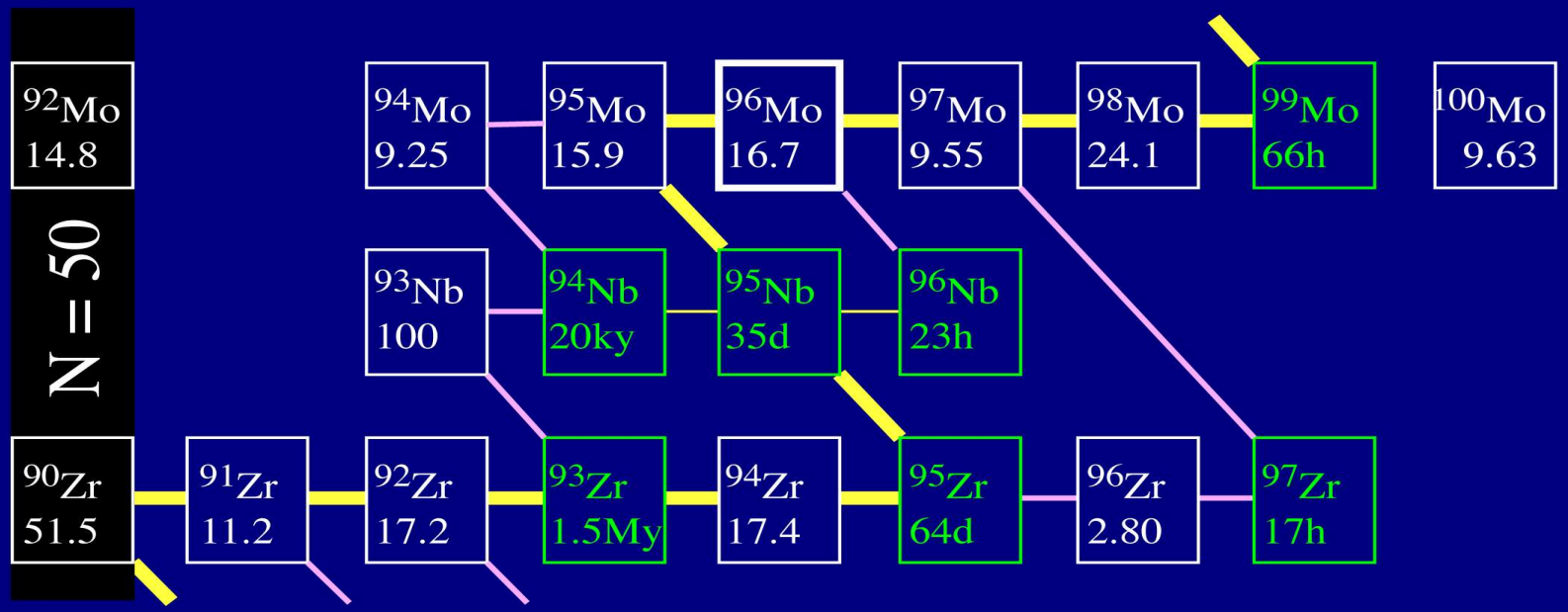
N = 50
92Mo 14.8
94Mo 9.25
95Mo 15.9
96Mo 16.7
97Mo 9.55
98Mo 24.1
99Mo 66h
100Mo 9.63
93Nb 100
94Nb 20ky
95Nb 35d
96Nb 23h
90Zr 51.5
91Zr 11.2
92Zr 17.2
93Zr 1.5My
94Zr 17.4
95Zr 64d
96Zr 2.80
97Zr 17h

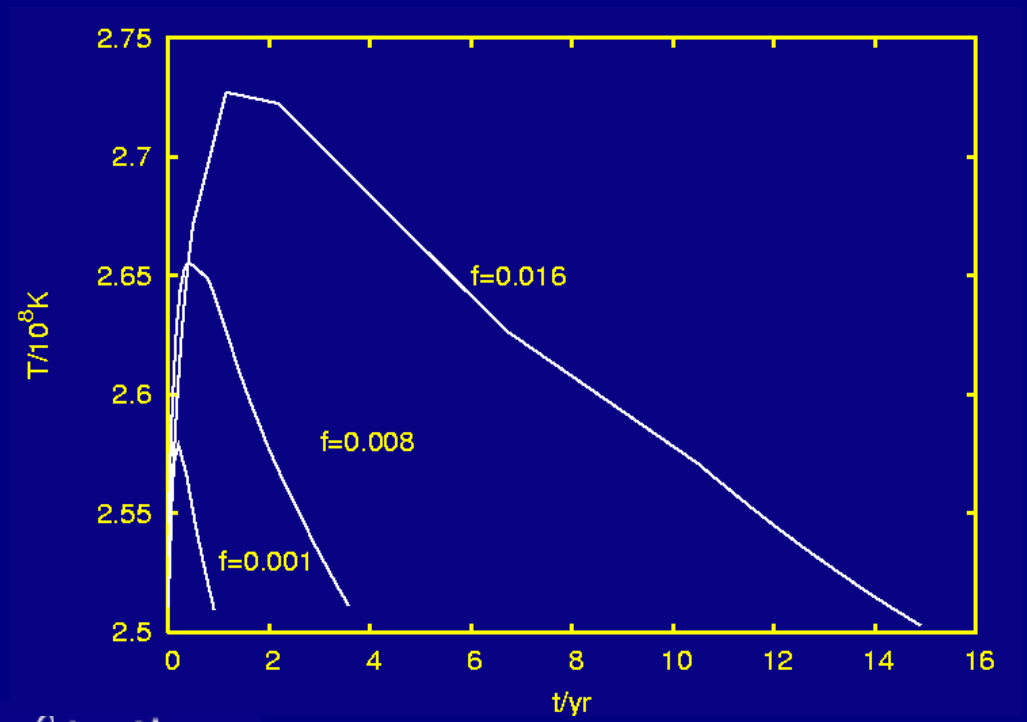
T/10^8K
t/yr
f=0.016
f=0.008
f=0.001
2.75
2.7
2.65
2.6
2.55
2.5
0
2
4
6
8
10
12
14
16

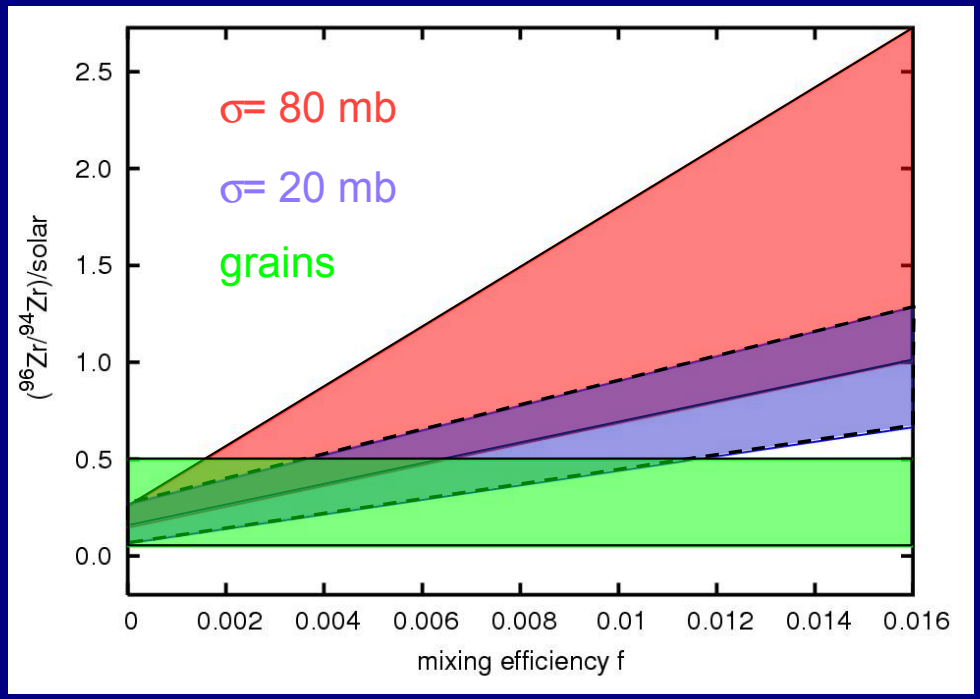
σ= 80 mb
σ= 20 mb
grains
(96Zr/94Zr)/solar
mixing efficiency f
2.5
2.0
1.5
1.0
0.5
0.0
0
0.002
0.004
0.006
0.008
0.01
0.012
0.014
0.016

Neutron capture experiments with unstable isotopes and fundamental stellar physics evaluations

Isotope	Half-Life	Facility	Observable	Stellar Physics	Comment
^{151}Sm	93 yr	DANCE: experiment finished	^{152}Gd in solar distribution ^{151}Eu/^{153}Eu ratio hyperfine line split	Timescale of hot Helium-shell flash s-process in very old stars	Pre-DANCE uncertainty: ± 30%
^{134}Cs	2 yr	DANCE: planned	Ba isotope ratios from presolar grains	Sets ^{12}C abundance of He-shell flash	Pre-DANCE uncertainty: ± 30%
^{135}Cs	2×10^6 yr			Amount of rotation	± 10%
^{95}Zr	64 d	RIA	^{96}/Zr/^{94}Zr ratio presolar grains	Temperature at bottom of He-shell flash region	Current uncertainty: 20 - 80 mb

s-Process as a diagnostic tool for better models for the first and second stars

Pre-solar grains:
- Isotopic ratios

Physical processes in stars:
- Convection
- Rotation
- Magnetic Fields

Spectroscopic observables:
- Solar-like metallicity stars
- Extremely metal-poor stars
- Central stars of PN

N-capture nuclear physics:
- X-sections
- T-dependence

Predicting observables

Computational modelling:
- Large network and mixing codes
- High-resolution stellar structre and evolution
- Hydrodynamic processes in stars

- ✓Apply improved physics modules to evolution of 1st and 2nd stars
- ✓Model the first s-process in the Early Universe
- ✓Decipher the information locked in the EMP stars

Conclusions

I. The second stars as a window into the Chemical Enrichment in the Early Universe.

II. s-process in low-mass stars to verify modelling of physical processes (convection, rotation, magnetic fields).

III. Accurate nuclear reactions for validation and model prediction.

Neutrino Background from Population III stars

Fabio Iocco[*]
(iocco@na.infn.it)

Santa Fe 8/9-13/2004
"Chemical Enrichment of the Early Universe"

*

Università di Napoli "Federico II"
& INFN, Sezione di Napoli

in coll. with G. Mangano, G. Miele, G. Raffelt and P.D. Serpico

Why neutrinos?

- Neutrinos are weakly interacting with matter:

(they should be the most direct probe, getting to us in quite an unmodified way)

- Possible probe for PopIII

very high SNR/SFR

(do they **all** end their life with huge ν emission?)

- Actually much effort to understand the whole range neutrino spectra

(and expecially the cosmic background from SN explosions)

- Estimate of decay lifetime of νs

(detectable neutrinos from *cosmic* epochs)

What do we see today from a cosmic source?

$$\frac{dF}{dE} = c \int_{z_i}^{z_f} \Psi(z) \left| \frac{dN(E')}{dE} \right|_{E'=(1+z)E} (1+z) \left| \frac{dt}{dz} \right| dz$$

$$\Psi(z) = SFR(z)$$

$$E' = E_{emission}$$

$$E = E_{today} = \frac{E'}{1+z}$$

The energy is redshifted by a factor (1+z)

Actually there is an intrinsic dependence upon IMF…

Stellar mass affects stellar fate:

$$\frac{dN(E')}{dE}$$

Depends upon IMF (and SFR) in thermonuclear, thermal and final stage spectrum (SN explosion/BH formation)

To get a first estimate of the flux

We assume a delta-like IMF:
300 solar mass rotating star.

This is not very likely, unfortunately the only explicit good estimate of neutrino fluxes for a PopIII we are aware of has been performed for such a star.

Assuming that $f = 5*10^{-4}$ of baryonic matter forms only 300 solar masses popIII at a given redshift (again not very likely, but time-extended SF results are shown in the following)…

$$\frac{dF}{dE} = c f \eta n_\gamma^0 (1+z) \frac{m_B}{M_{III}} \frac{dN(E(1+z))}{dE}$$

$\eta = n_b/n_\gamma$ baryon to photon ratio

f fraction of baryonic content into popIII

M_{III} average popIII mass

m_B average baryon mass

Thermonuclear MS neutrinos from popIII

Quite independent of IMF
much more sensitive to *f*:
each star burns almost half of
initial H mass into ^{4}He.
For each converted proton
there is a ν_e emission.

Which is the energy spectrum?

to pp or to CNO
this is the question

We observe MeV (at emission)
neutrinos redshifted:
CNO or pp spectra redshifted
into the 10-100 keV range

Under previous
assumptions, at fixed
redshift z = 17

whole pp burning:
up to 4 events cm^{-2} s^{-1}
E < 100 keV

CNO burning:
up to 20 events cm^{-2} s^{-1}
E < 20 keV

Dominant **cosmic** sources
in this energy range

Overall neutrino luminosity

Neutrino luminosity for a 300 solar masses rotating star at the time of BH formation.

Notice how μ and τ neutrino luminosity (dotted curve) drops to zero at earlier times: inner neutrinosphere

↓

Higher emission energy

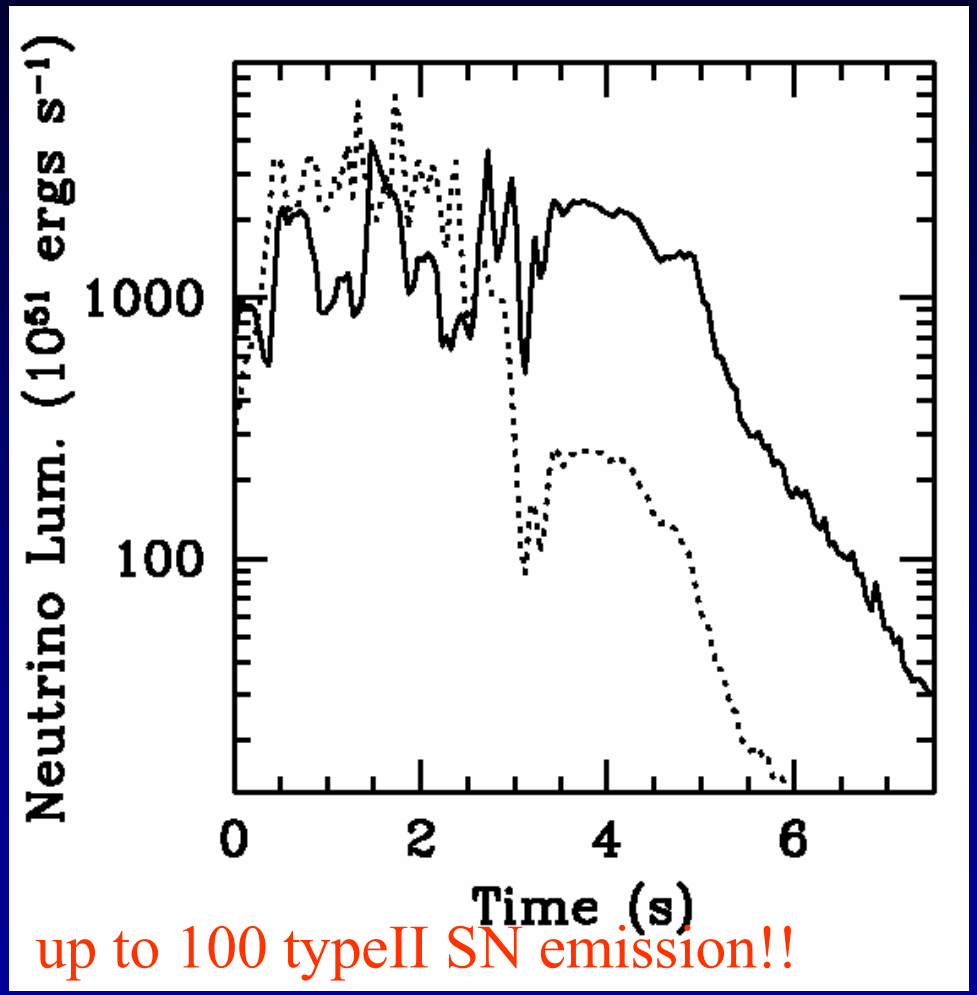

Fryer, Woosley, Heger; ApJ 550: 372-382,2001

Neutrino energy at emission

Core Collapse neutrinos form during deleptonization of the star at time of core collapse and propagate through the star:

how to estimate their emission energy?

$$E_{\nu_e} \propto \frac{M_c}{R_c} \sim 13 MeV$$

$$E_{\nu_x} \sim 2.3 E_{\nu_e}$$

$$E_{\overline{\nu}_e} \sim 1.4 E_{\nu_e}$$

For type II SN effective neutrino transport simulations available: scaling relations for that regime

(take care: SN do NOT explode!?!?)

This estimates cannot be *blindly* applied to any mass and radius regime but…

we have first used it to get an order-of-magnitude estimate of energies at emission

Summary of our model for "final stage" ν flux

Best estimates come from simulations:
C.L. Fryer kindly provided emission energies of the three species for the 300 solar mass star ; at different times in the previous figure:

$$E_{\nu_e} = 10 \div 15 MeV$$
$$E_{\overline{\nu}_e} = 12 \div 17 MeV$$
$$E_{\nu_x} = 9 \div 20 MeV$$

Same order of magnitude estimate as from previous scaling relations

The most important parameters are f and E_{ν_e}:
IMF dependence to be taken into account (effects on E_{ν_e})

Assuming a thermal FD distribution at emission:

$$\frac{dN}{dE} = \frac{E^2}{1 + e^{E/T_\nu}}$$

$$\langle E_\nu \rangle = \int_0^\infty \frac{E^3}{1 + e^{E/T_\nu}} dE = \frac{7\pi^4 T_\nu}{180\zeta(3)} \simeq 3.15 T_\nu$$

Emission energy dependence of ν flux

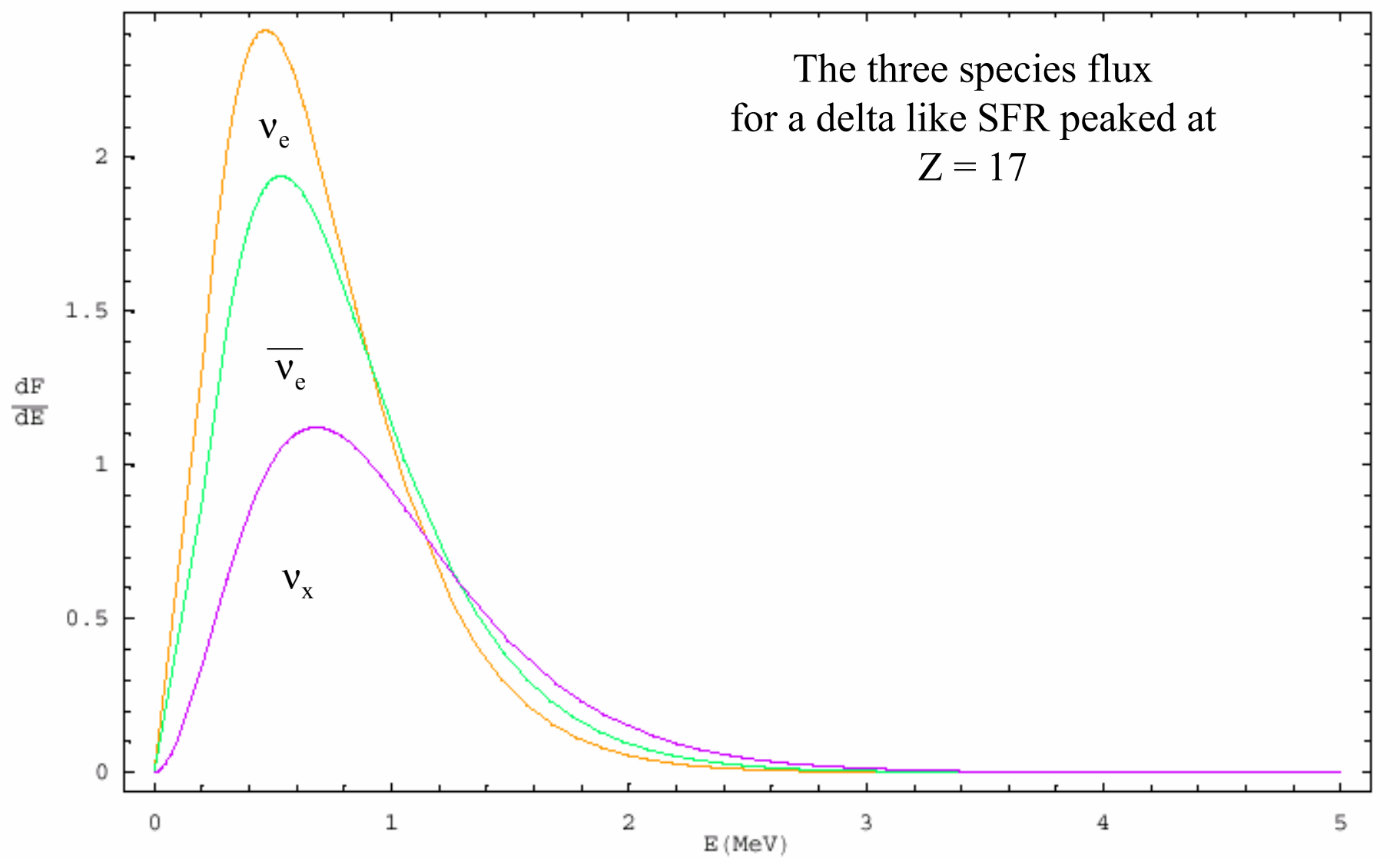

Redshift dependence of ν flux

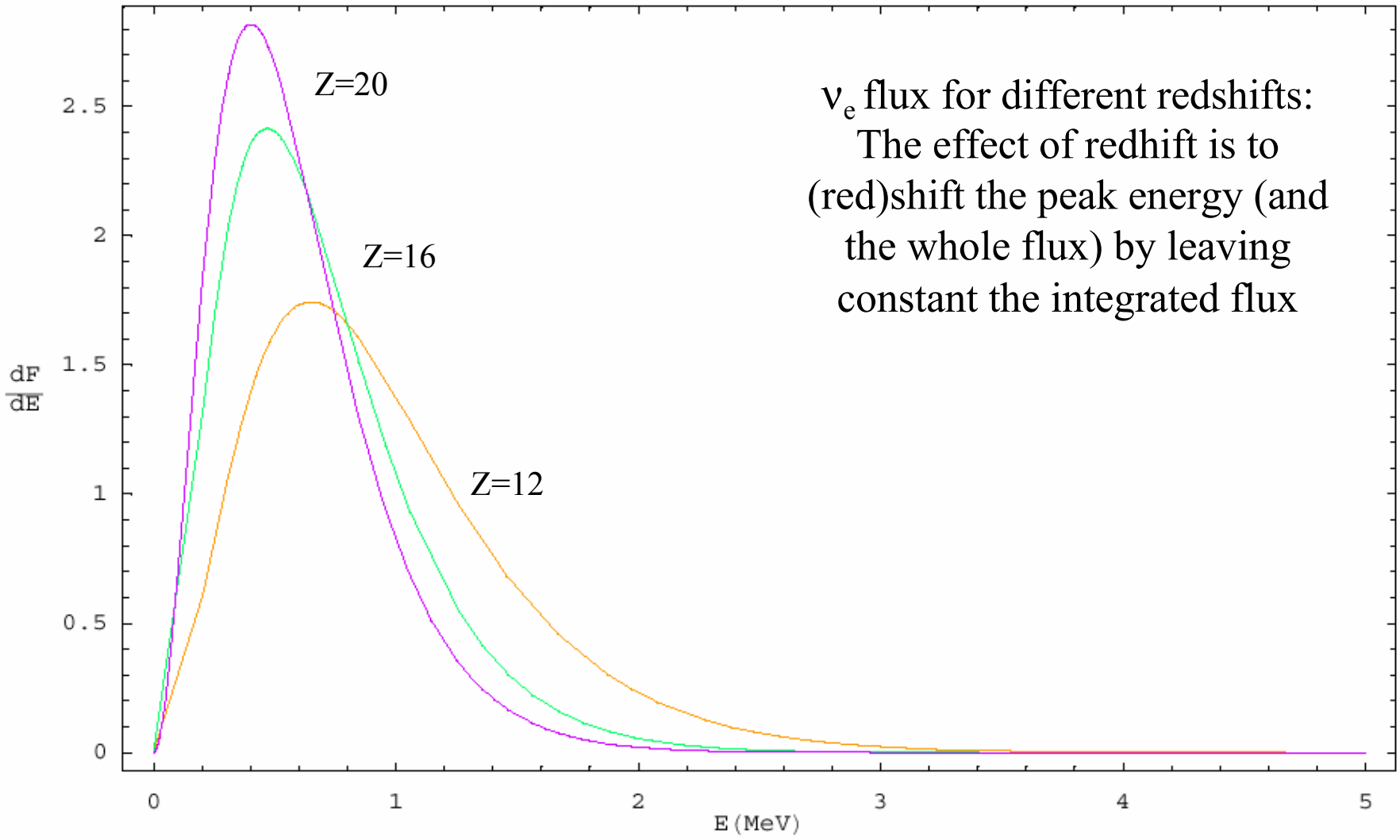

ν_e flux for different redshifts: The effect of redhift is to (red)shift the peak energy (and the whole flux) by leaving constant the integrated flux

Different redshift formation histories

(constant formation rates)

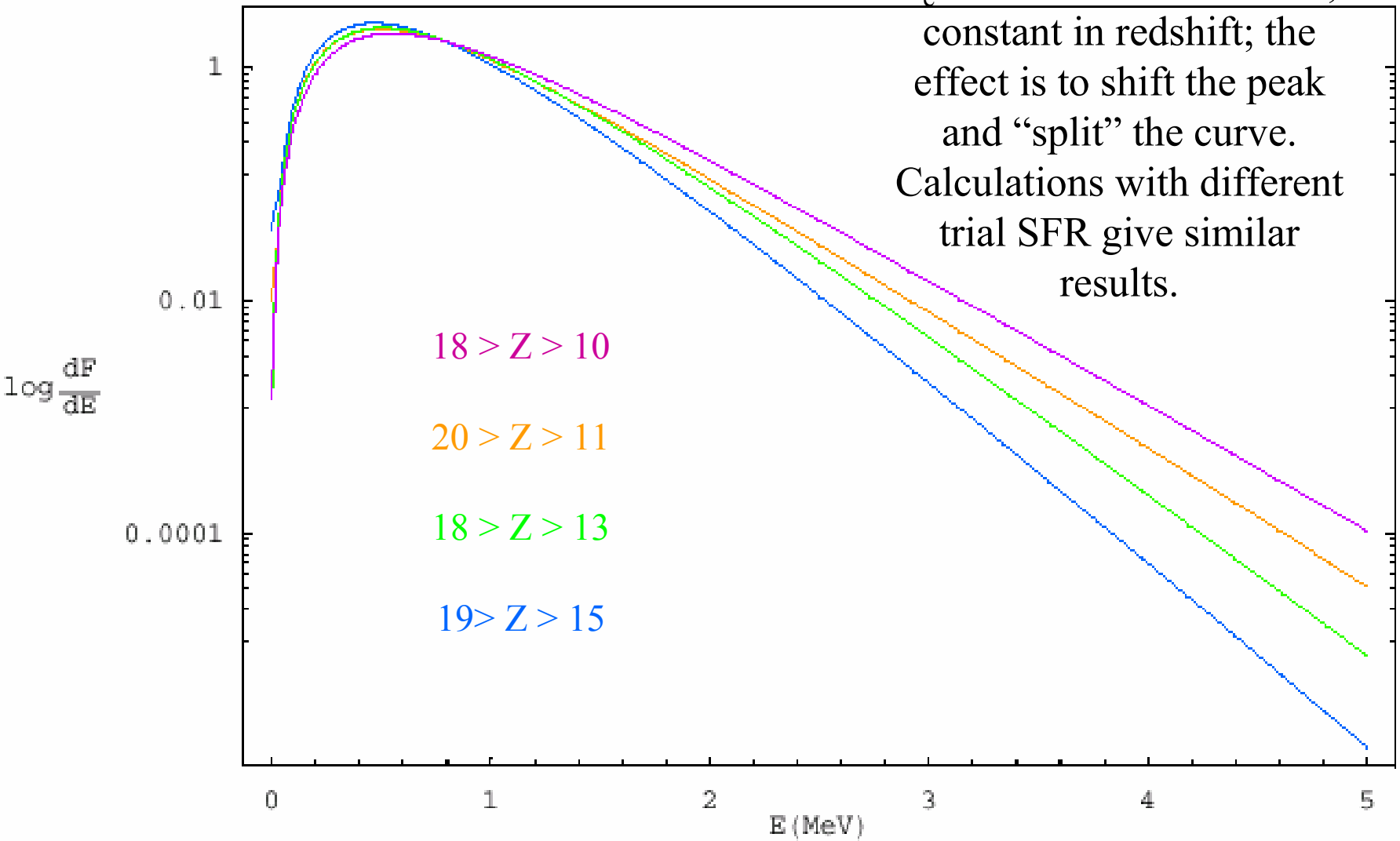

ν_e flux for different SFRs, constant in redshift; the effect is to shift the peak and "split" the curve. Calculations with different trial SFR give similar results.

What do we expect from different IMFs? (some qualitative considerations)

Higher spectra sensitivity to E_ν than to z:
relations between E_ν and M are needed in the whole mass range.

$$\begin{array}{rcl} \text{if } M & \sim & few 100 M_\odot \\ 1MeV & < & E_{\nu_e} < 15MeV \end{array}$$

Same order-of-magnitude ν luminosity and E_ν for CC neutrinos

The post-MS nuclear and thermal spectra are extremely sensitive to IMF: different paths in $T_c - \rho_c$ strongly characterize the nuclear burning and thermal rates.
A delta like IMF based calculation is completely meaningless.

Thermonuclear neutrino background from cosmic population II and I

Diffuse cosmic neutrino background (no angular dependence) from

Porciani, Petroni, Fiorentini; Astropar.Phys.20: 683-701; 2004

Superimposed on it PopIII spectra for the 3 different species assuming a constant formation rate at 18 > z > 10

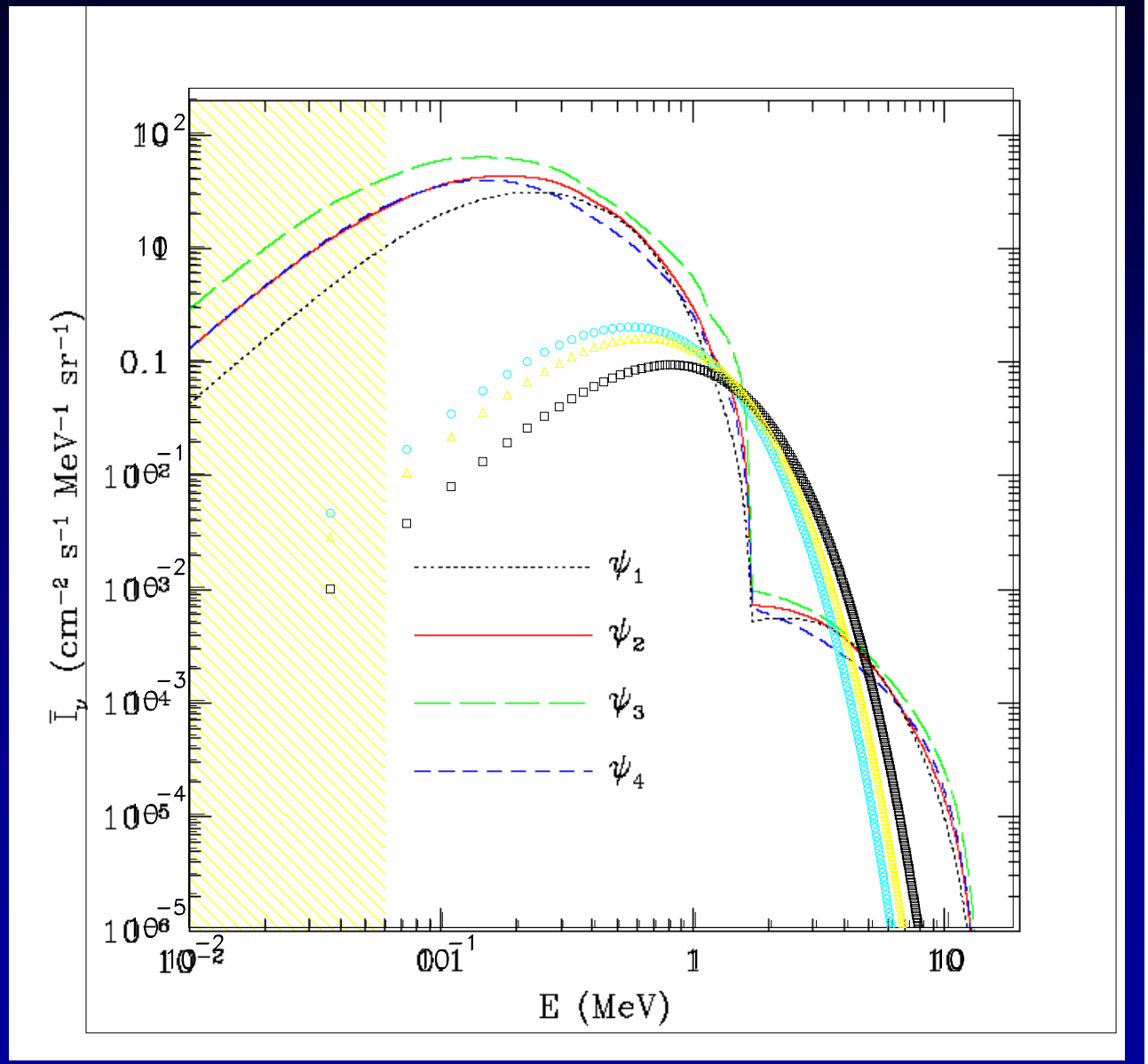

Thermonuclear neutrino background from galactic stars

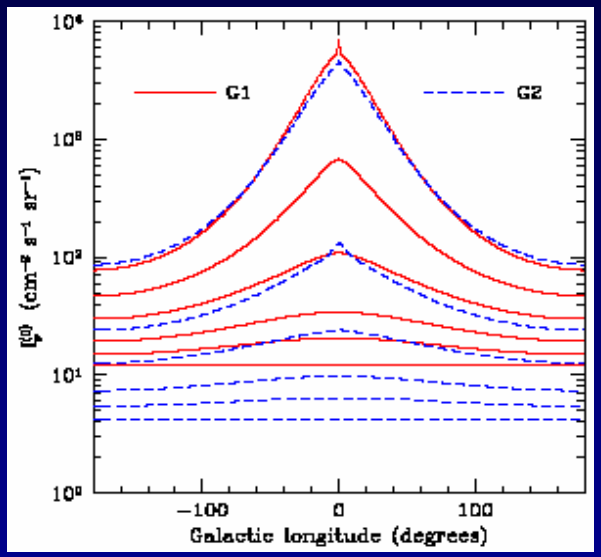

Intensity profile of galactic neutrino flux

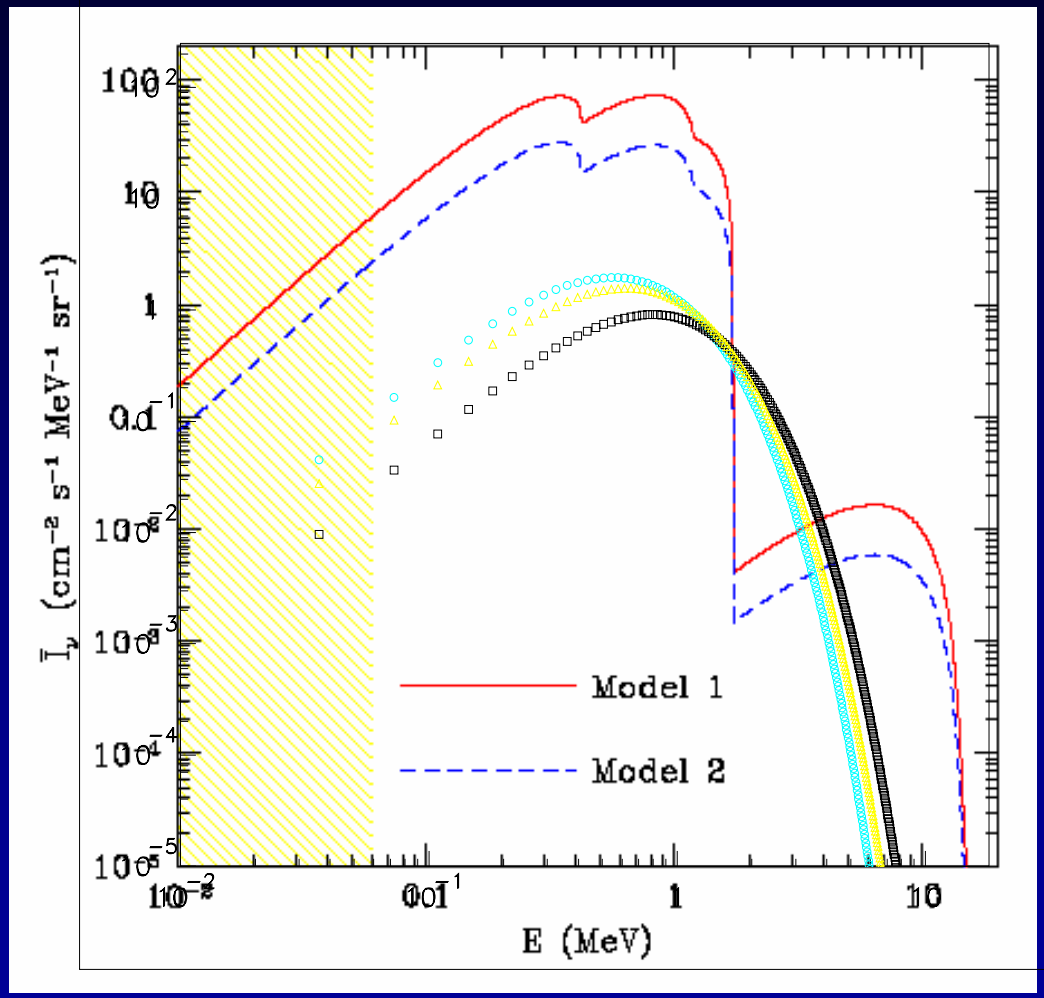

Flux averaged over the whole sky

Porciani, Petroni, Fiorentini; Astropar.Phys.20: 683-701; 2004

What's the overall background?

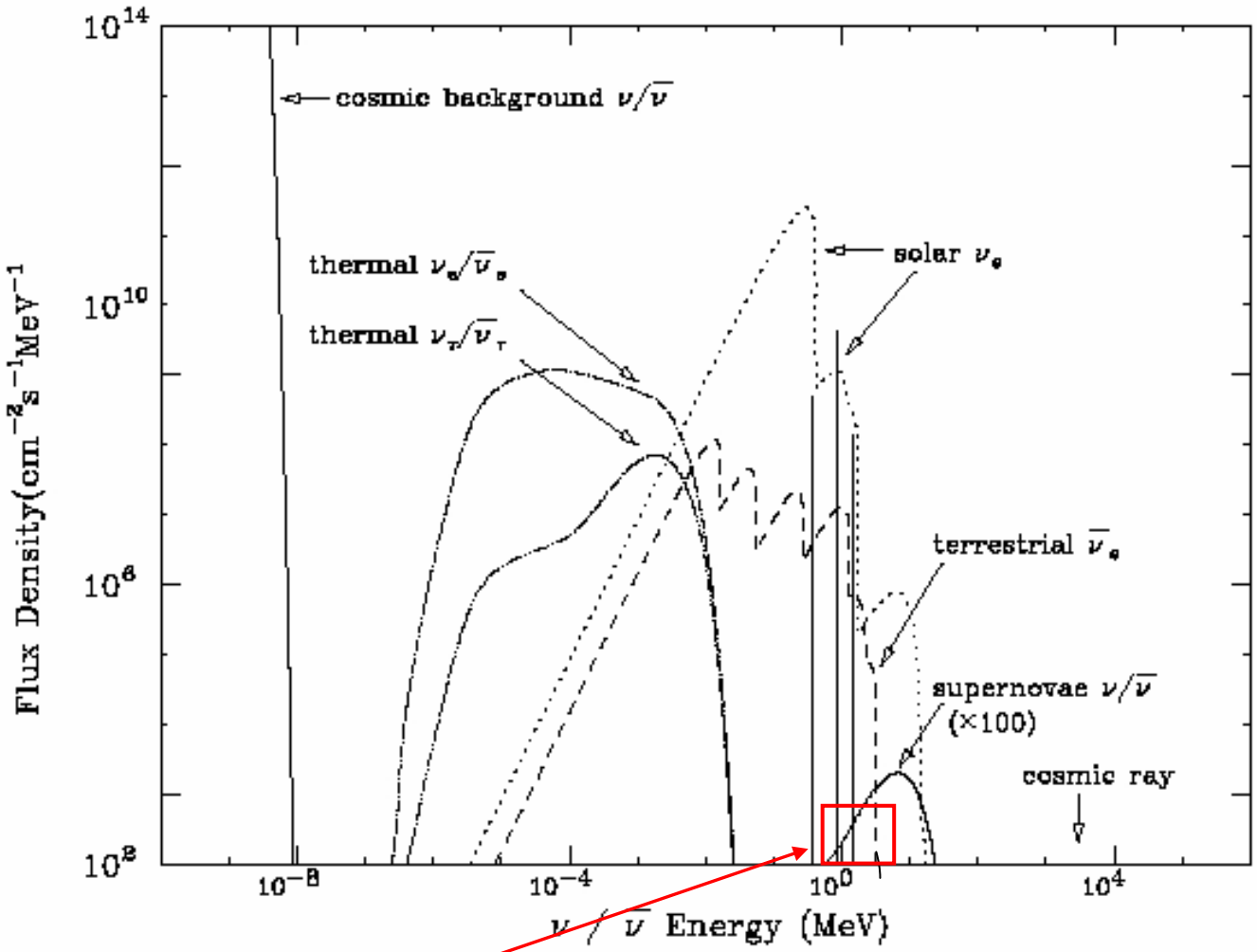

Unfortunately popIII ν flux is overwhelmed from other sources:
solar ν_e, terrestrial $\bar{\nu}_e$

Conclusions

The model is still quite rough (no IMF dependence, flat SFR(z))

IMF is crucial in determining the exact flux.

In particular the thermal and nuclear ν background are extremely sensitive to the stellar evolutionary path.

ν_i flux comparable with thermonuclear pop I & II νs,

but overwhelmed by solar flux and geoneutrinos: only a hypothetical low energy directional detector could distinguish it.

At the moment no direct detection seems to be possible.

A possible detection seems to be possible for TeV ν powered by GRB

PopIII are the only cosmic source of $\overline{\nu}_e$ in the 0 – 2 MeV range

Aknowledgements

I would really like to thank the organizers and sponsors of the workshop, and in particular A. Heger, for support given, kind ospitality and, of course, for giving me the chance to participate.

I would also like to thank T. Abel for useful discussions and C.L. Fryer for providing me unexpected details and values about the 300 solar mass star simulation.

(some) References

- T. Abel, G.L. Bryan and M.L. Norman; ApJ **540**, *2000*, 29
- A. Heger and S. E. Woosley; ApJ **543**, *2002*, 532
- C. L. Fryer, S. E. Woosley and A. Heger ; ApJ **550** ,*2001*, 372
- G. Raffelt; "Stars as Laboratories for Fundamental Physics", *1996*, University Of Chicago Press, Chicago, USA
- C.Porciani, S. Petroni and G. Fiorentini; Astropar. Phys. **20**, *2004*, 683
- J.N. Bahcall; "Neutrino Astrophysics", *1989*, Cambridge University Press, Cambridge, UK
- R. Schneider, D. Guetta and A. Ferrara; MNRAS **334**, *2002*, 173
- F. Iocco et al; astro-ph/041xxxx, in preparation

R-Process Data

Karl - Ludwig Kratz
Kernchemie Mainz—VISTARS

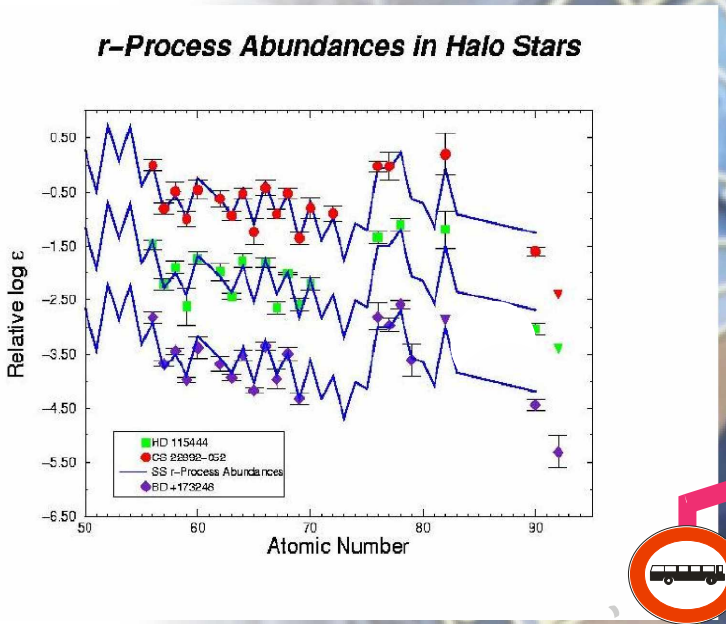

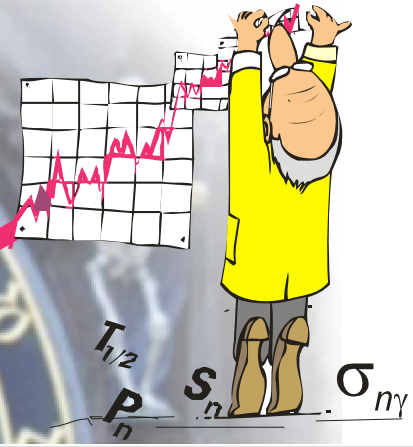

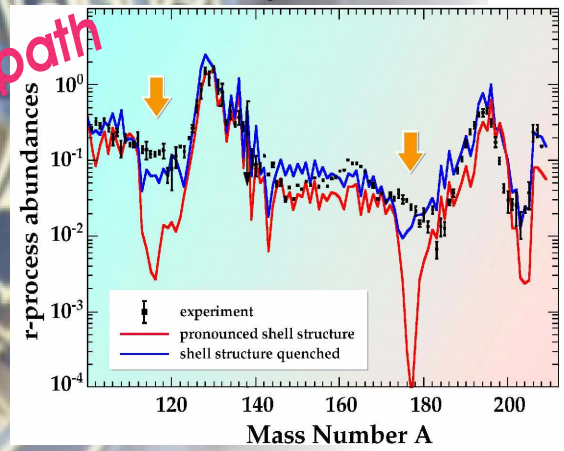

r-process path

waiting point

CEoEU
August 9-13, 2004
Santa Fe, New Mexico

g the
ven Greatest Unanswered Questions of Physics Discover Magazine, 2002)

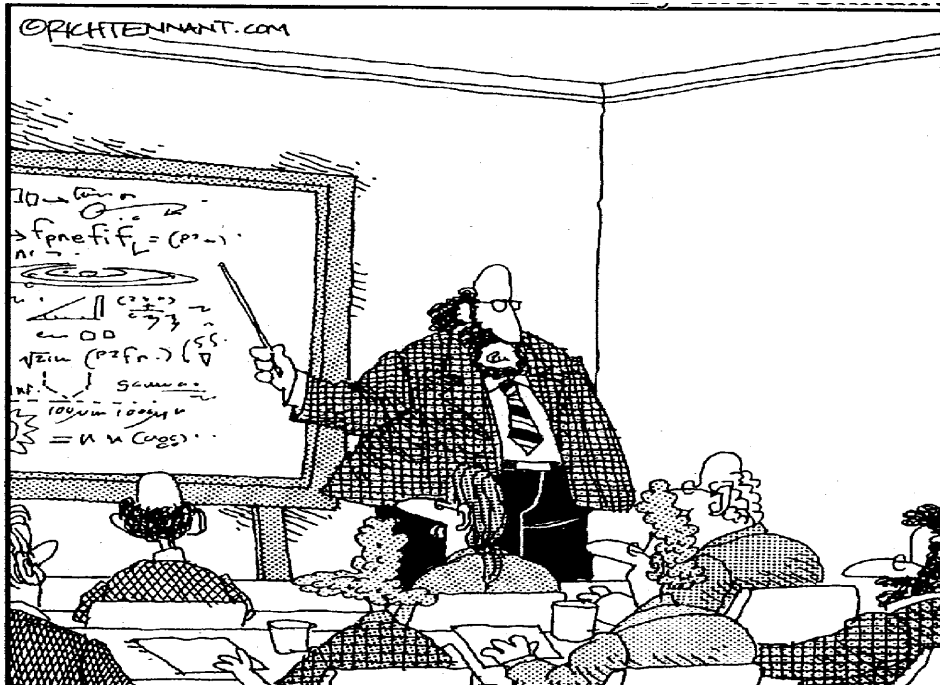

"After the discovery of "antimatter" and "dark matter", we have recently found the existence of "doesn't matter", which seems to have no effect on the Universe whatsoever."

… How were the heavy elements from Fe to U made?

Motivation:

R - abundances ⇌ Nuclear structure

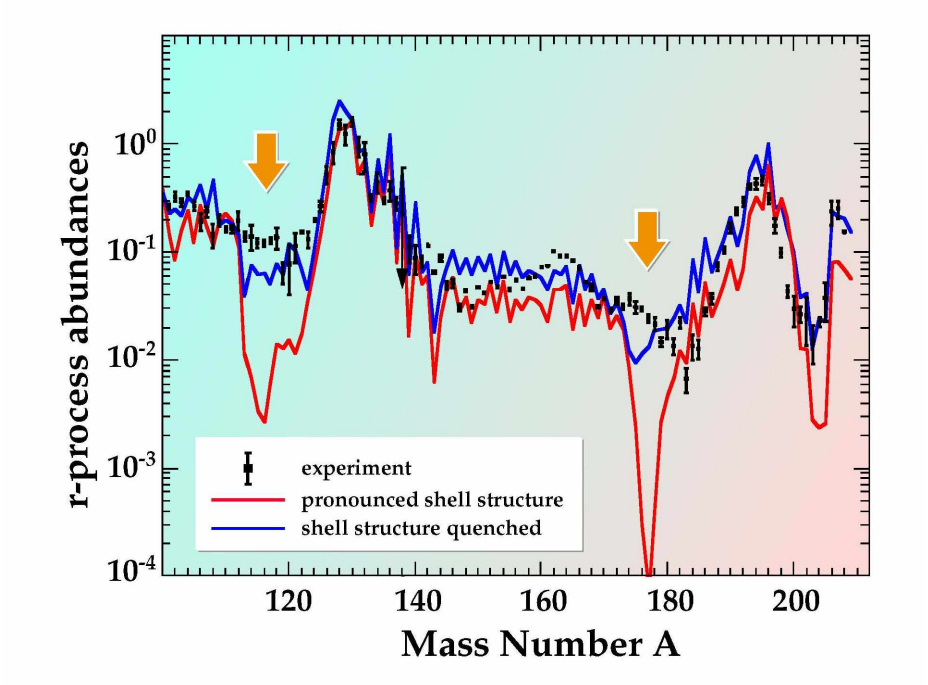

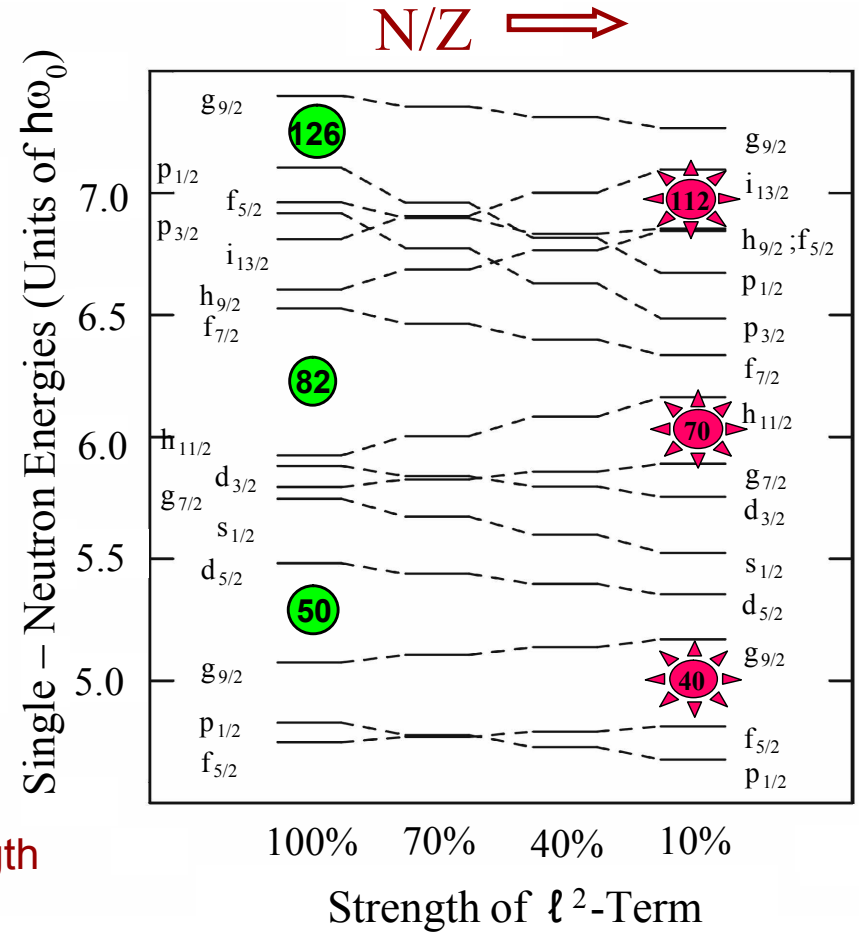

FK²L (Ap.J. 403 ; 1993)

"..the calculated r-abundance 'hole' in the A ≅ 120 region reflects ... the weakening of the shell strength ... below $^{132}_{50}Sn_{82}$ "

B. Pfeiffer et al.,
Acta Phys. Polon. **B27** (1996)

R-abundance peaks and neutron-shell numbers

already B²FH (Revs. Mod. Phys. 29; 1957)
C.D. Coryell (J. Chem. Educ. 38; 1961)

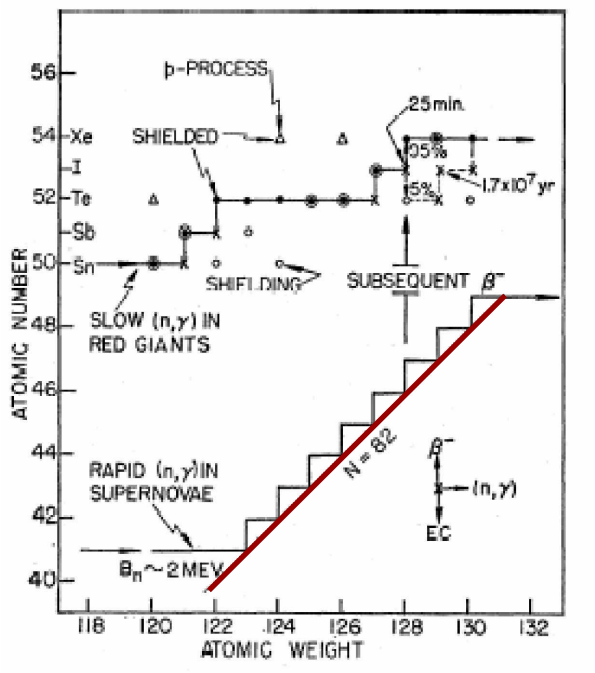

"climb up the staircase" at N=82;
major waiting point nuclei;
"break-through pair" ^{131}In, ^{133}In;

"association with the rising side of major peaks in the abundance curve"

...still today important r-process properties to be studied experimentally and theoretically.

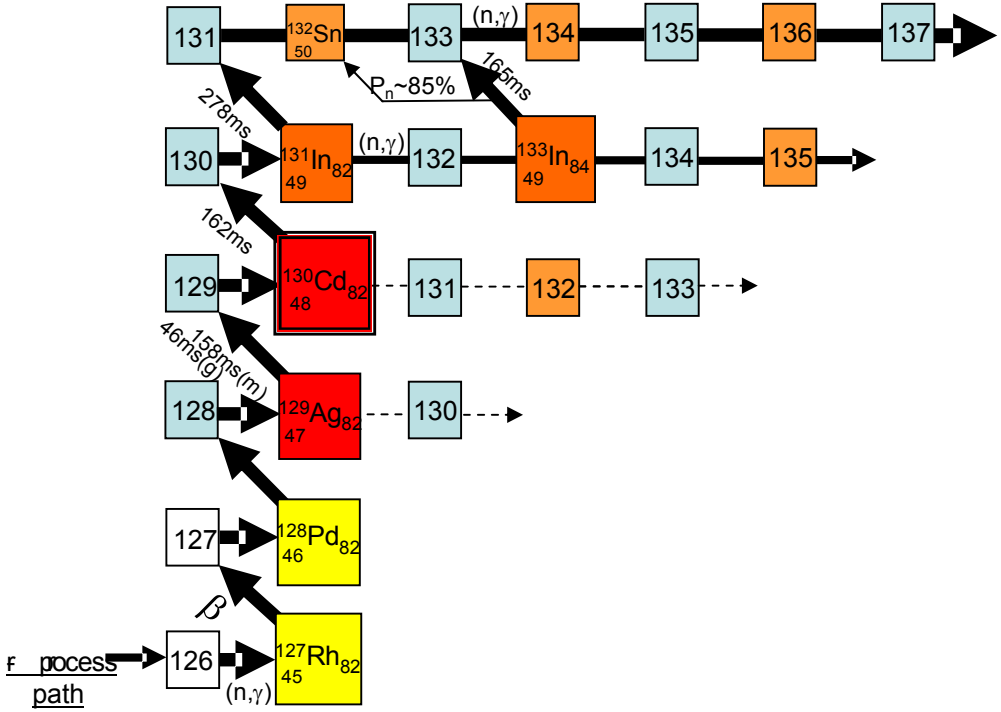

K.-L. Kratz (Revs. Mod. Astr. 1; 1988)

climb up the N= 82 ladder ...

A ≅ 130 "bottle neck"

⇨ **total r-process duration τ_r**

What we knew already in 1986 ...

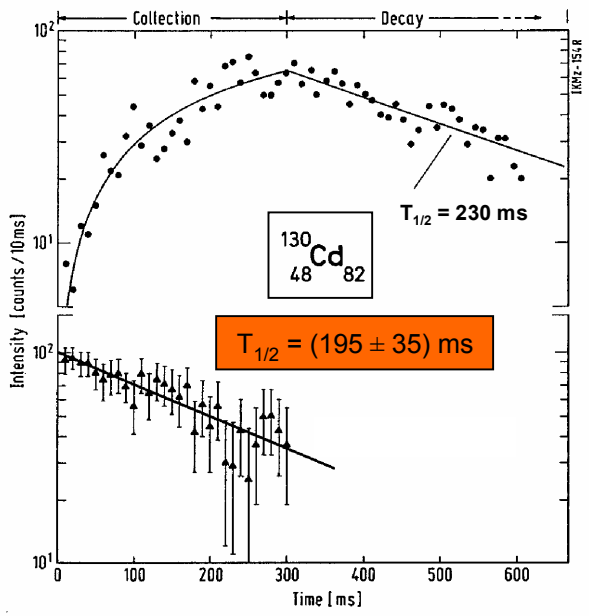

K.-L. Kratz et al (Z. Physik A325; 1986)

Exp. at old SC-ISOLDE
with plasma ion-source
and βdn counting

Problems:
high background from
-surface ionized ^{130}In, ^{130}Cs
-molecular ions $[^{40}Ca^{90}Br]^+$

Request: **SELECTIVITY !**

Shell-model (QRPA; Nilsson/BCS) prediction

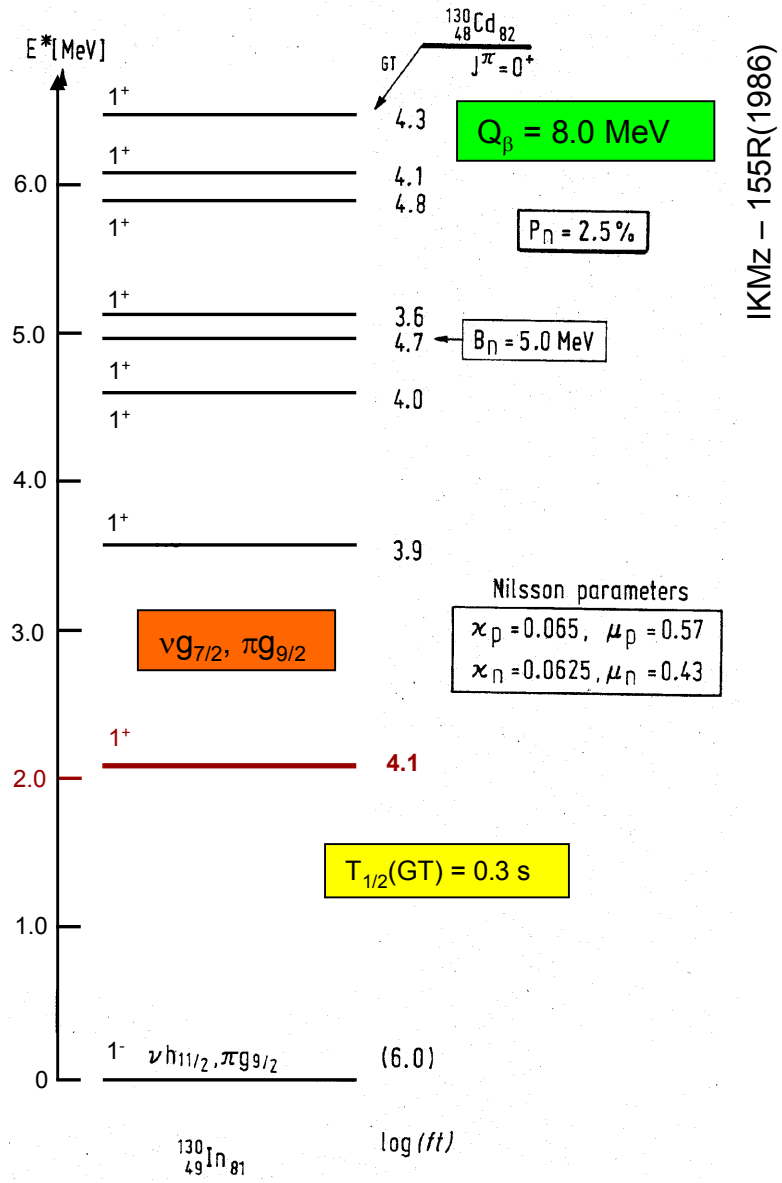

K.-L. Kratz CEoEU

Request: **Selectivity !**

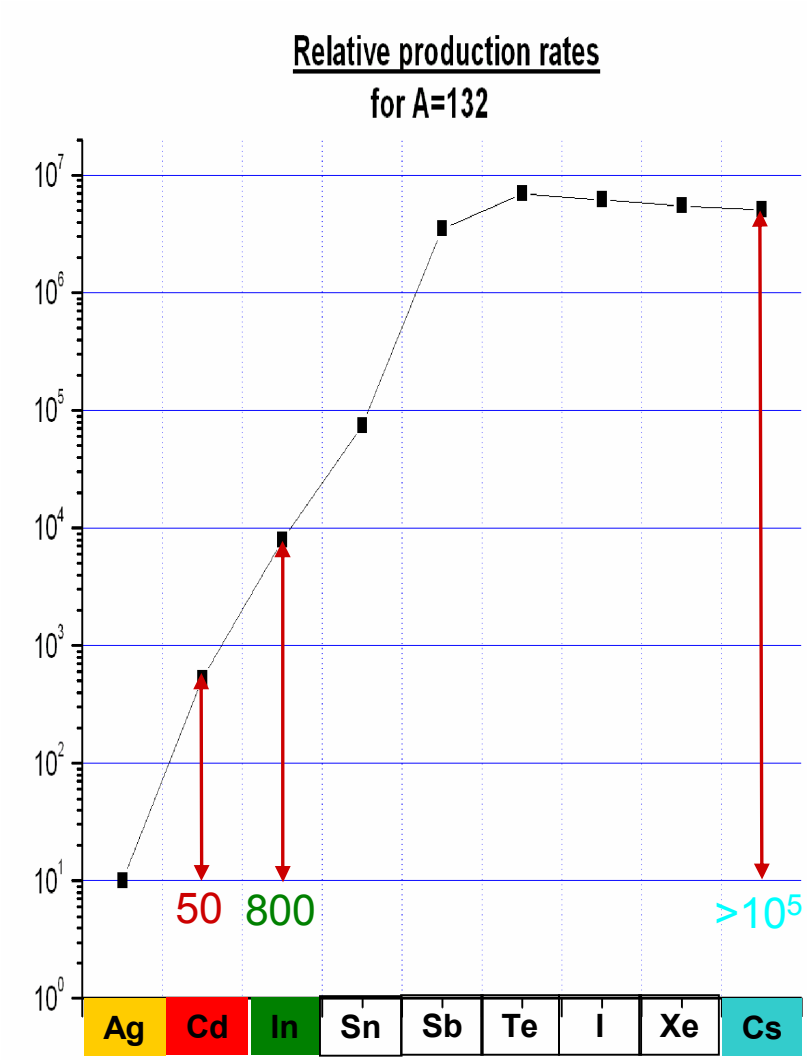

today, at PSB-ISOLDE

- Fast UC_x target
- Neutron converter
- Laser ion-source (RILIS)
- Hyperfine splitting
- Isobar separation (HRS)
- Multi-coincidence setup

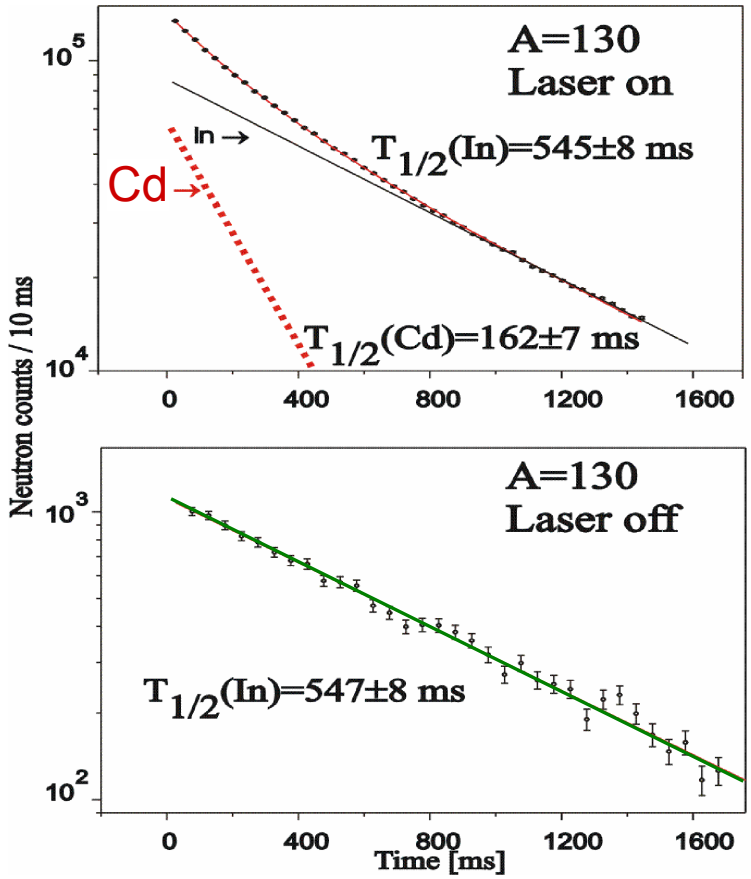

K.-L. Kratz CEoEU

The r-process "waiting-point" nucleus ^{130}Cd

...obtain a physically consistent picture!

Nilsson model (BCS)

$^{130}_{48}Cd_{82} \rightarrow {}^{130}_{49}In_{81}$

Important ingredients:

$T_{1/2}$, Q_β, $E(1^+)$, $I_\beta(1^+)$, log ft

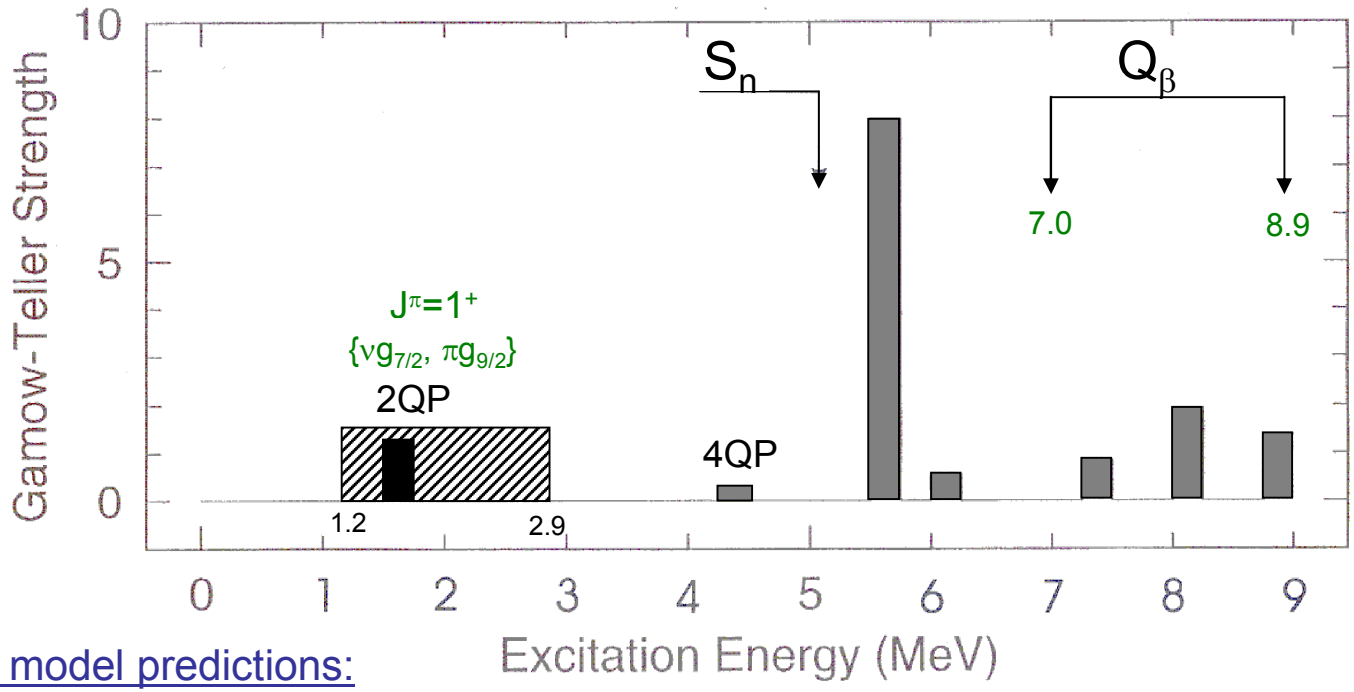

Various model predictions:

P. Möller et al. (FY/LN) $T_{1/2}$(GT) = 1.08 s, log ft = 4.4, $E(1^+)$ = 2.87 MeV

(Nils./BCS) $T_{1/2}$(GT) = 233 ms, log ft = 4.1, $E(1^+)$ = 1.19 MeV

Engel et al. $T_{1/2}$(GT) ≅ 250 ms

Martinez-Pinedo et al. $T_{1/2}$(GT) = 146 ms, log ft = 3.8, $E(1^+)$ = 1.55 MeV

A. Brown et al. "old" $T_{1/2}$(GT) = 180 ms, log ft = 4.2, $E(1^+)$ = 1.38 MeV

"new" $T_{1/2}$(GT) = 233 ms, log ft = 4.2, $E(1^+)$ = 2.18 MeV

Spectroscopy $^{130}Cd_{82}$ β-decay

γ-singles spectrum

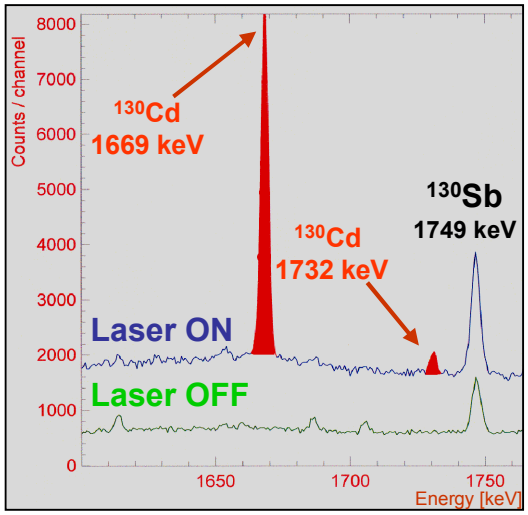

γγ t-coincidences

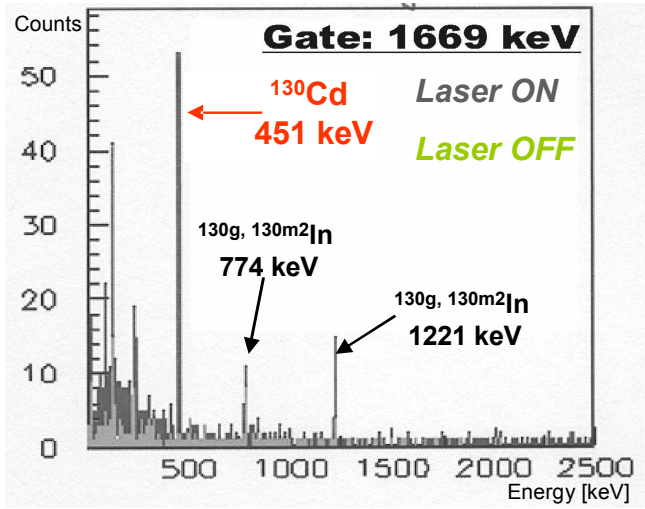

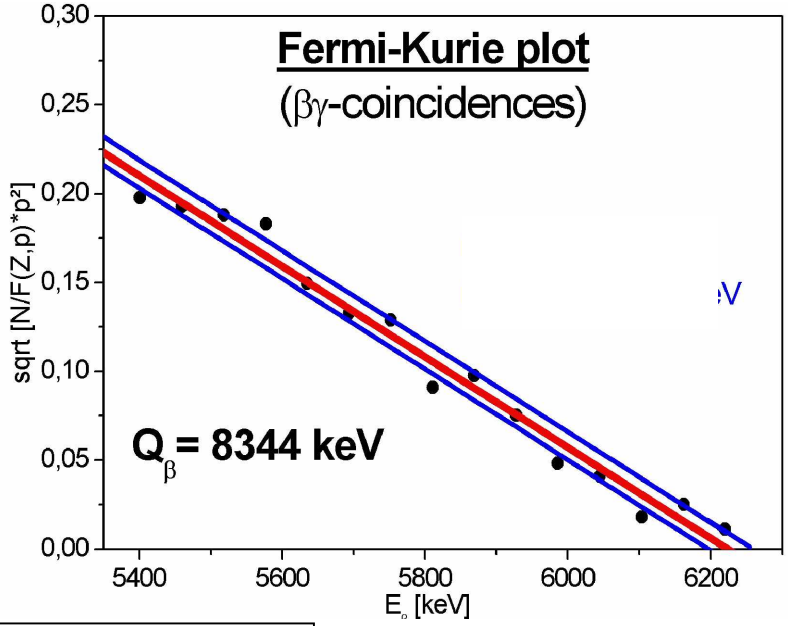

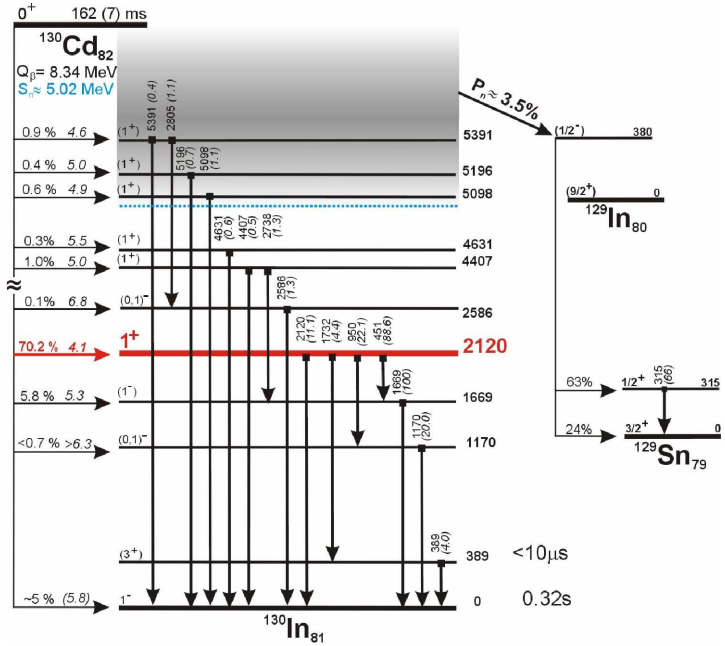

K.-L. Kratz CEoEU

^{130}Cd decay spectroscopy

ISOLDE experiment – Q_β from measurement of β-spectrum endpoint energy:

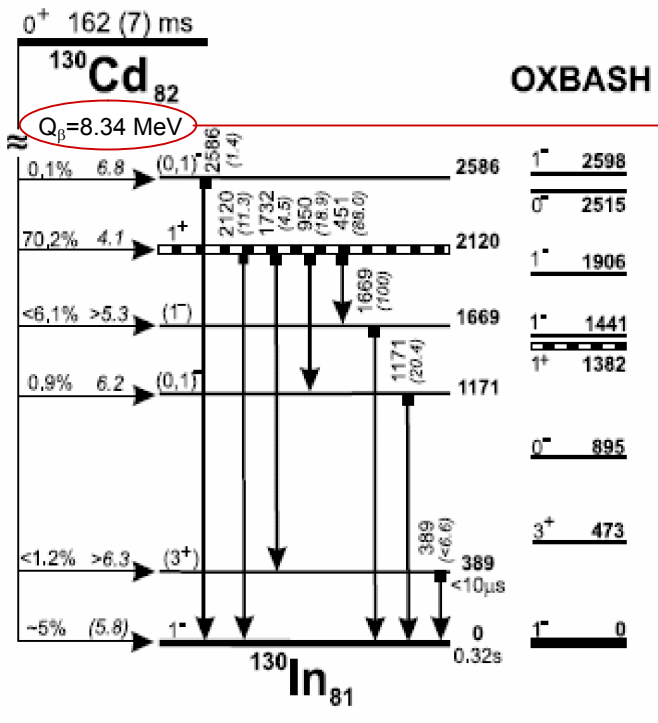

Large Q_β value best reproduced by mass models with N=82 shell quenching

Mass model predictions	Q_β
Hilf et al. (*GTNM*, 1976)	7.57 MeV
Möller et al. (*FRDM*, 1995):	7.43 MeV
Aboussir et al. (*ETFSI*, 1995):	7.87 MeV
Duflo & Zuker (1995)	7.56 MeV
Dobaczewski et al. (*HFB/SkP*, 1996):	8.93 MeV
Pearson et al. (*ETFSI-Q*, 1996):	8.30 MeV
Audi & Wapstra (*Mass Eval.*, 1997):	8.50 MeV
Goriely et al. (*HFBCS*, 2001)	7.00 MeV
Samyn et al. (*HFB-2*, 2002)	7.64 MeV
Brown et al. (*local OXBASH*, 2003):	8.75 MeV

Normalized mass deviations of $_{50}$Sn and $_{48}$Cd isotopes
relative to the „unquenched“ FRDM

Comparison to mass model predictions with „shell quenching“

HFB/SkP

ETFSI-Q

HFB-2

and Audi & Wapstra Evaluation (AMDC, 2003)

⇨ Different behavior beyond N=82 in Cd chain

⇨ Need for experimental masses of ^{129}Cd, ^{131}Cd, ^{132}Cd

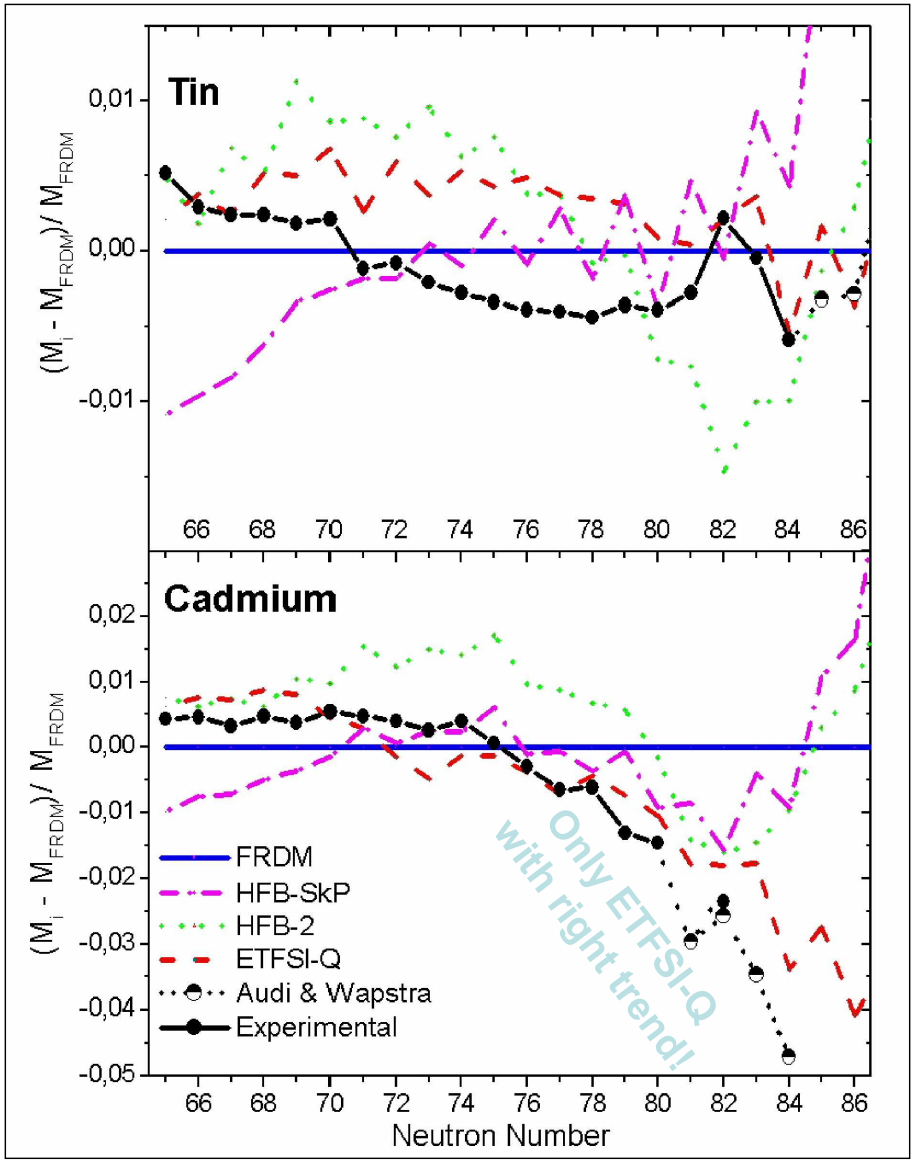

N=82 Shell Gap

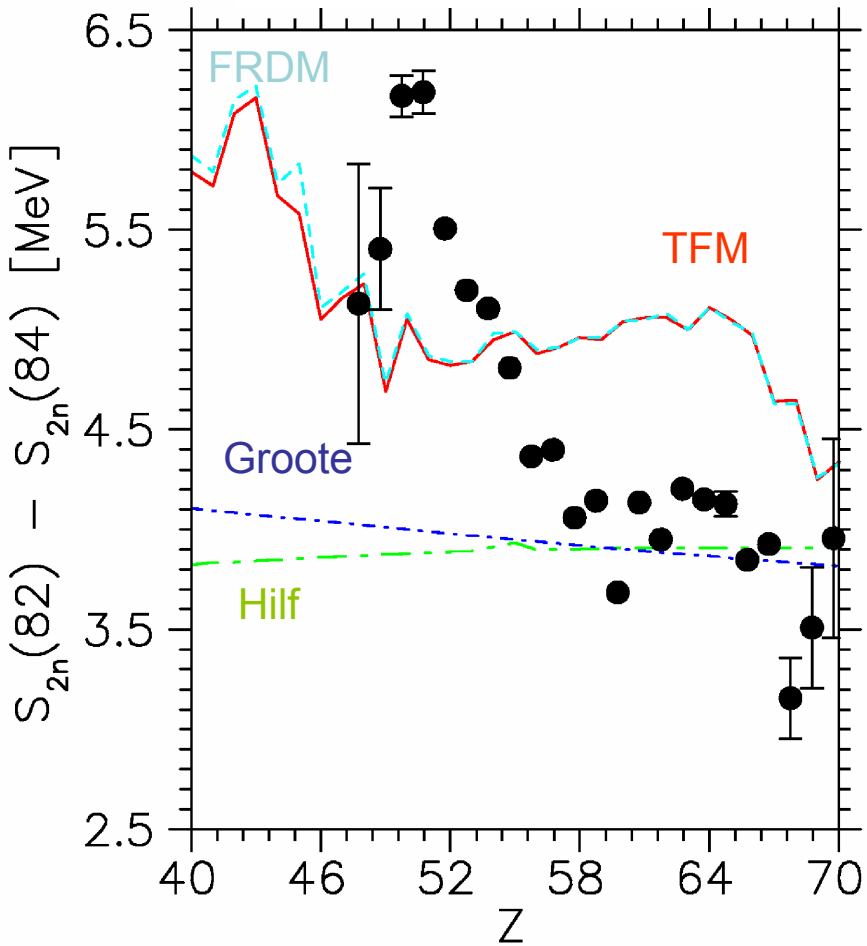

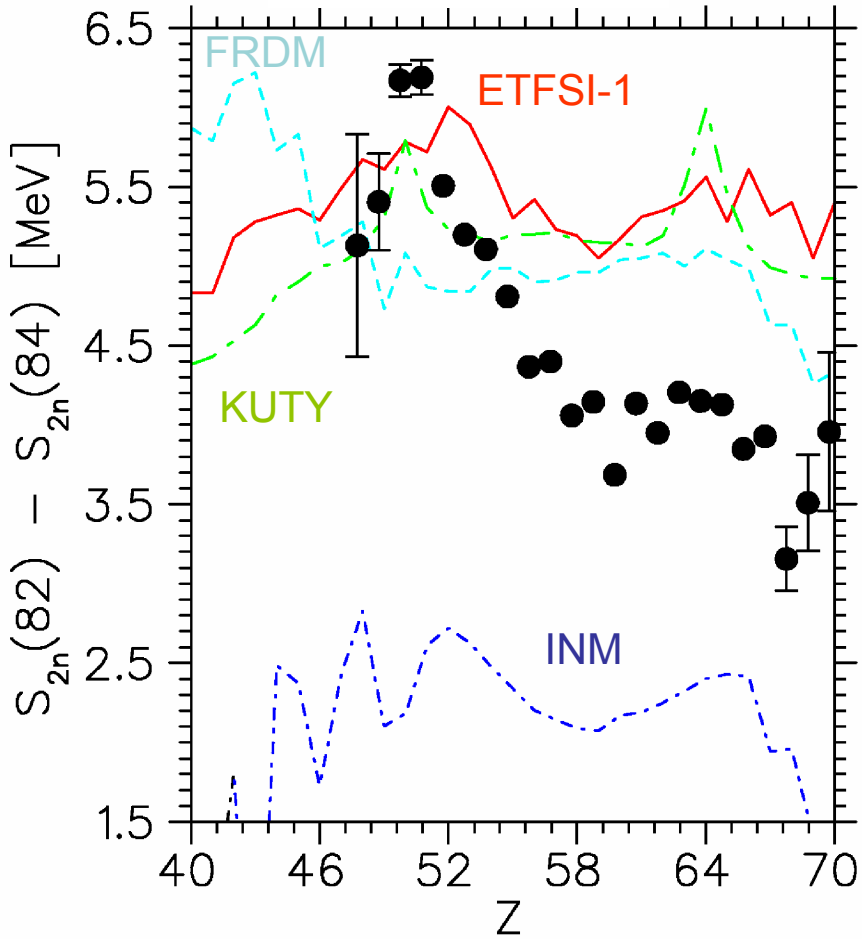

TFM: Thomas-Fermi model (1994)
Myers, Swiatecki, LBL-36803

KUTY: Kuora et al., NP A674 (2000) 47
INM: Infinite Nuclear Matter Model

N=82 Shell Gap

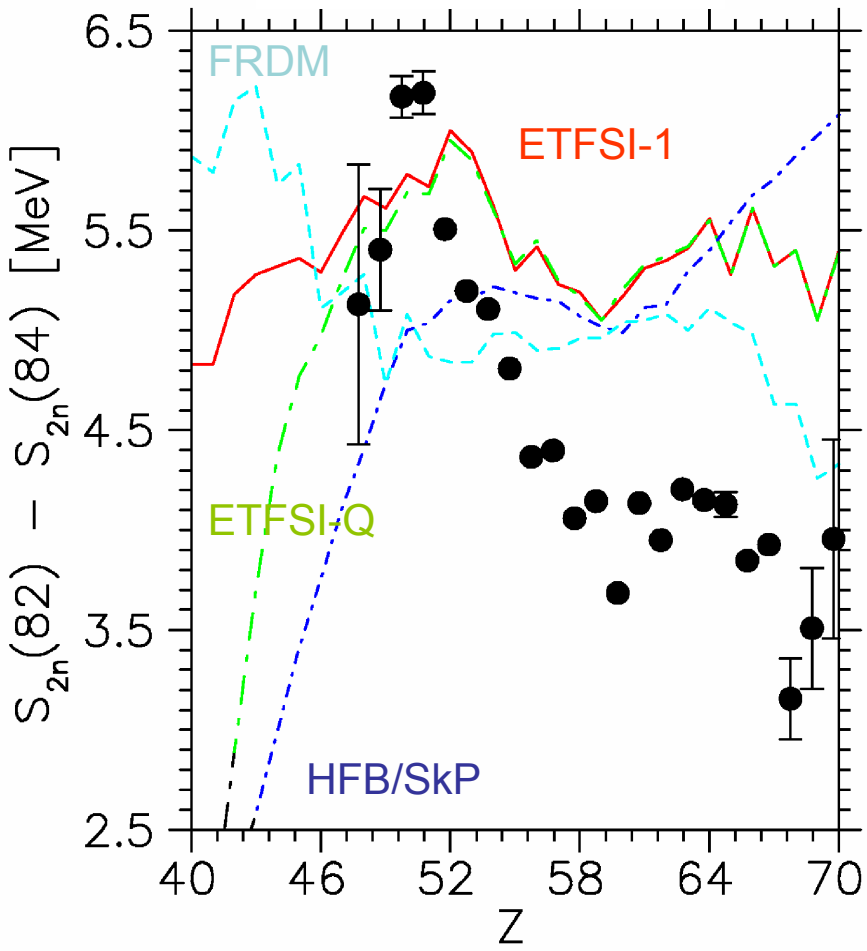

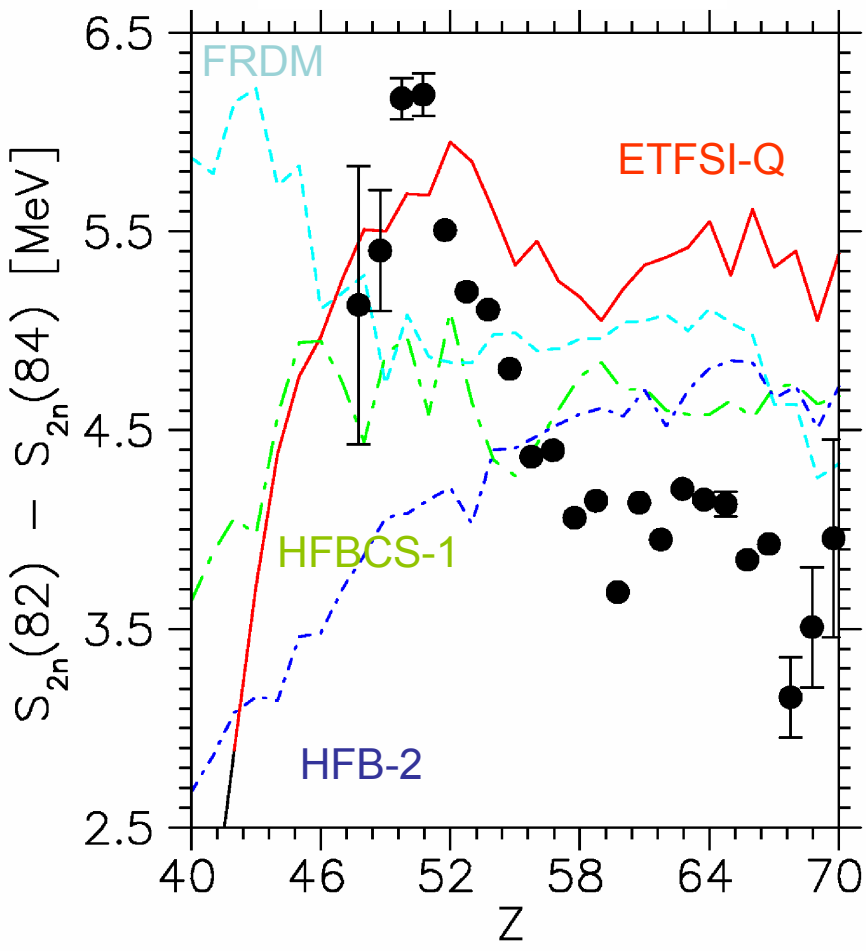

K.-L. Kratz CEoEU

The N=82 shell gap

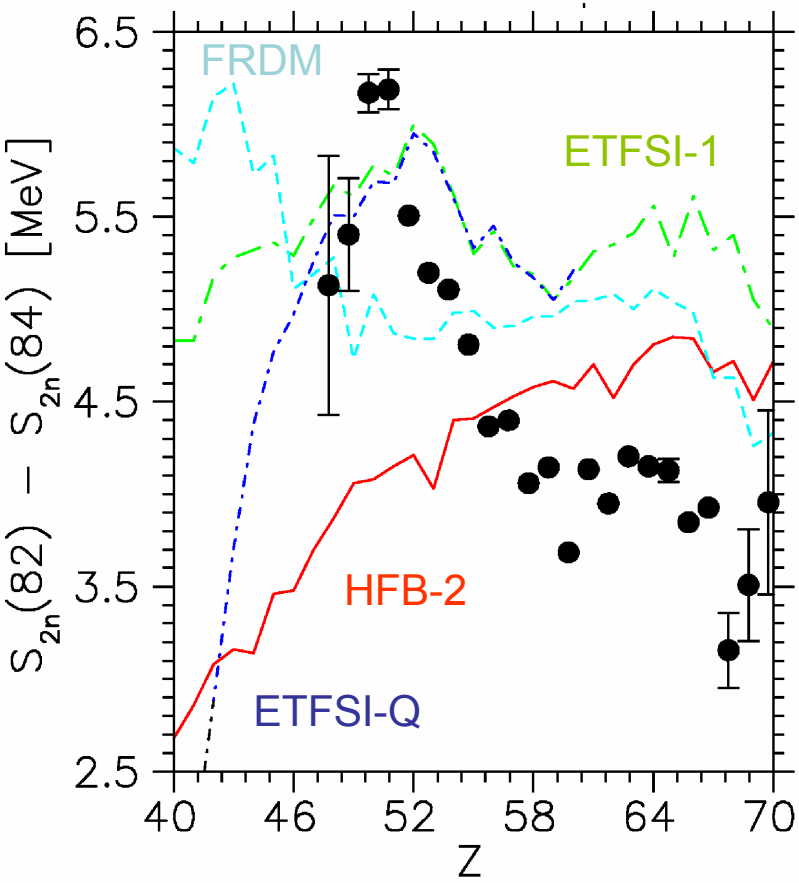

NONE of the mass models predicts the trend correctly!

Astrophysical consequences

...mainly resulting from new nuclear-structure information:

- **better understanding of formation and shape of as well as r-process matter flow through** } **the A≈130 $N_{r,\odot}$ peak**
- **no justification to question waiting-point concept (Martinez-Pinedo et al., PRL 83, 1999)**
- **no need to request sizeable effects from ν-induced reactions (Qian et al., PRC 55, 1997)**

⇨ **r-process abundances in the Solar System and in UMP Halo stars...**

...are governed by nuclear structure!

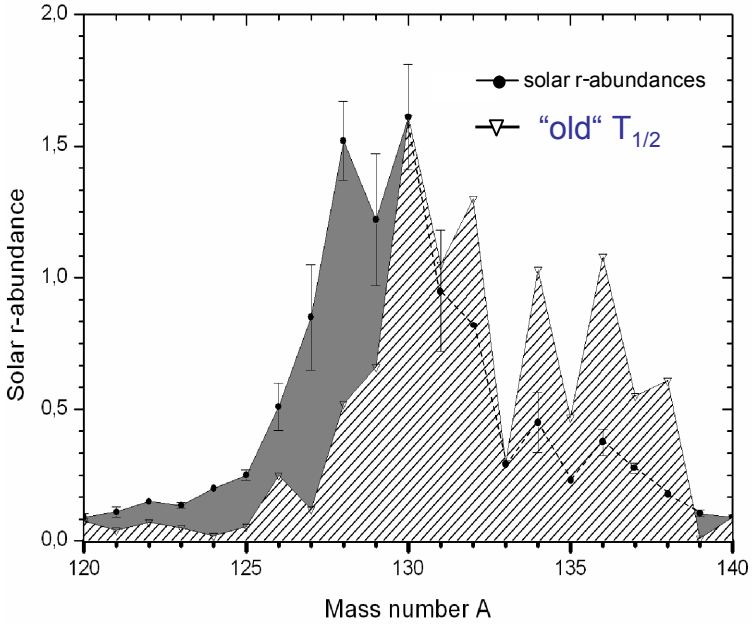

Nuclear masses from AMDC, 2003 & ETFSI-Q

Normalized to $N_{r,\odot}$ (^{130}Te)

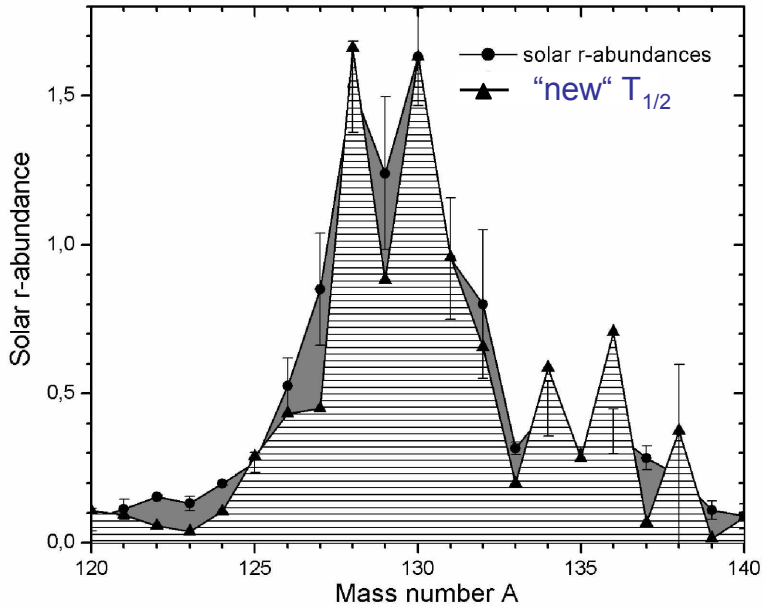

K.-L. Kratz CEoEU

Nuclear masses

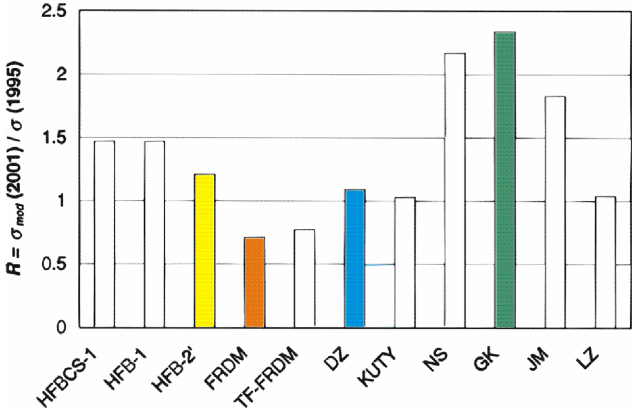

FIG. 13. A comparison of the predictive power of the various models (the quantity R in Table I): DZ, Duflo-Zuker; FRDM, finite-range droplet model; GK, Garvey-Kelson; JM, Jänecke-Masson; KUTY, Koura *et al.*; LZ, Liran-Zeldes; NS, Nayak-Satpathy; TF-FRDM, Thomas-Fermi finite-range droplet model.

(D. Lunney et al. Rev of Mod. Phys., Vol. 75, No. 3, July 2003)

Total Error = 3.73 for 184 nuclei, $T_{\beta,exp}$ < 1s

Half-lives

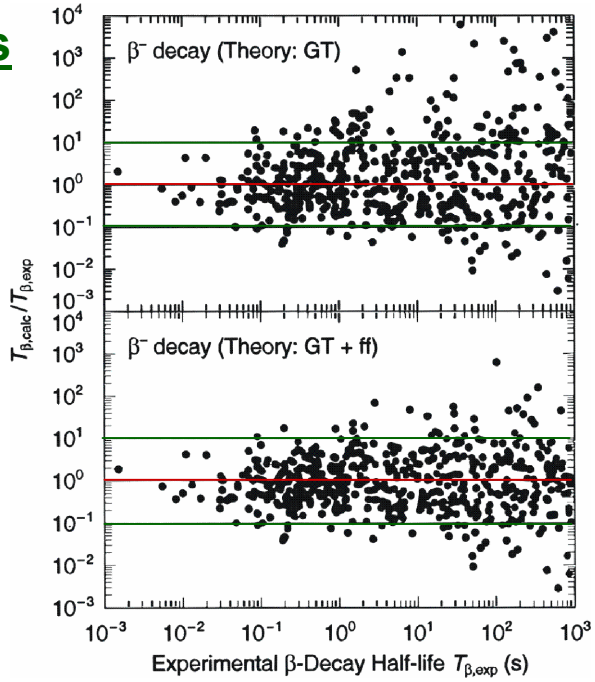

Total Error = 3.08 for 184 nuclei, $T_{\beta,exp}$ < 1s

P_n-Values

Total Error = 5.54

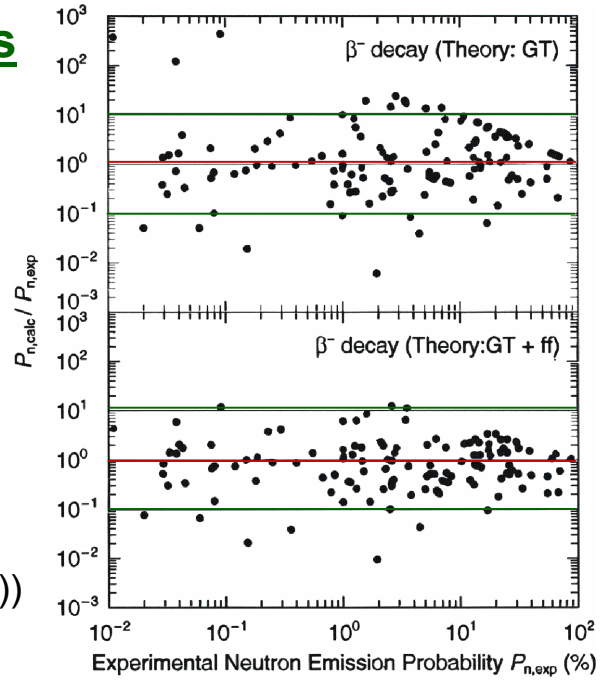

Total Error = 3.52

(P. Möller et al., PR **C67**, 055802 (2003))

K.-L. Kratz CEoEU

Experimental situation 2004 for $T_{1/2}$, P_n

Isotopes	Mass units away from β-stability	r-process path
$^{70}Fe_{44}$	12	-6
$^{78}Ni_{50}$	14	in
$^{79}Cu_{50}$	14	in
$^{81}Zn_{51}$	11	in (+1)
$^{84}Ga_{53}$	13	in (+1)
$^{85}Ge_{53}$	9	-3
$^{94}Br_{59}$	13	-3
$^{99}Kr_{63}$	13	in (+3)
$^{102}Rb_{65}$	15	-1
$^{105}Zr_{65}$	9	-7
⋮		
$^{120}Pd_{74}$	10	-8
$^{130}Ag_{83}$	21	in (+1)
$^{133}Cd_{85}$	17	in (+3)
$^{135}In_{87}$	21	in (+4)
$^{138}Sn_{88}$	14	in (+2)
$^{139}Te_{87}$	9	in (+1)
$^{147}Xe_{93}$	11	in (+1)
$^{162}Eu_{99}$	9	-27
$^{177}Tm_{107}$	8	-18
$^{215}Pb_{133}$	7	-39

What do we calculate?

Reproduce isotopic $N_{r,\odot}$ distribution using waiting-point approach (lsq-fits; A ⩾ 80, A ⩾ 120)

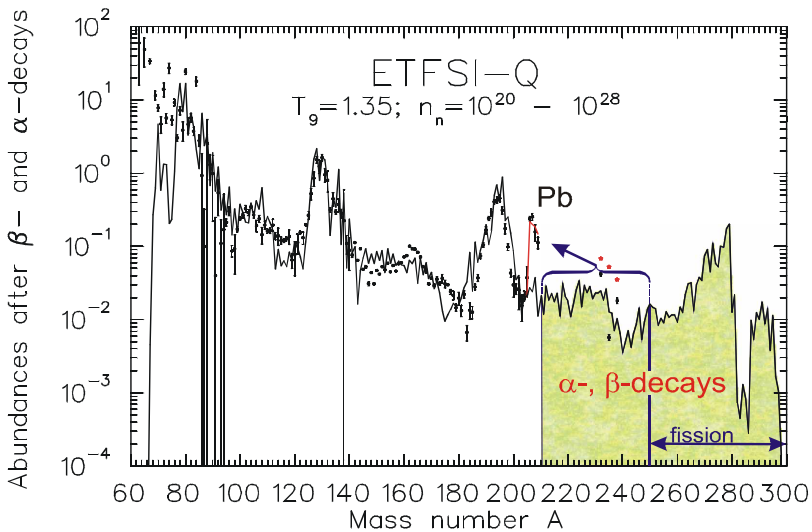

3rd $N_{r,\odot}$ peak and Pb abundances as reliability criterion for Th,U region!

Convert to elemental $N_{r,\odot}$ curve(–), and scale to halo abundances (■)

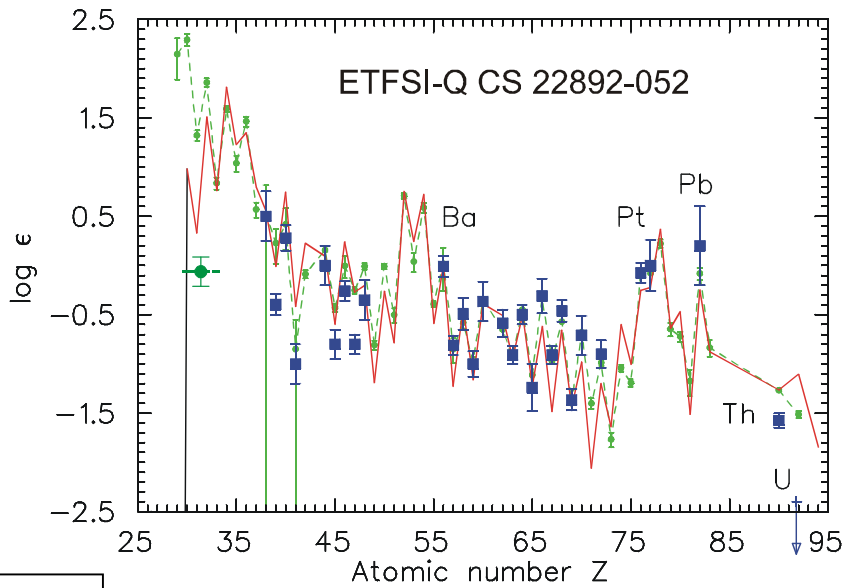

comparision to $N_{r,\odot}(Z)$

⇒ excellent agreement above Ba

⇒ Th, U cosmochronometry

K.-L. Kratz CEoEU

Cosmochronology with Thorium

Several UMP halo stars consistently show solar elemental abundance pattern, among them

CS 22892-052

with 17 elements between Ba and Ir, plus Pb and ^{232}Th ($T_{½}$ = 14·10^{9} a)

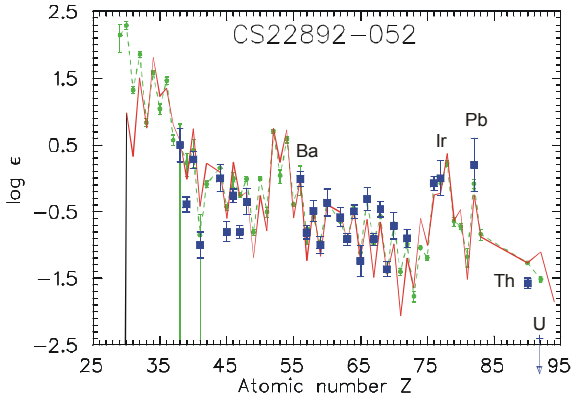

⟹ age from average of Th/Ba-Ir

14.6 ± 3.0 Gyr

≈ age of the Universe

Tuning the clock with Uranium

Because of shorter half-life ($T_{½}$ = 4.5 · 10^{9} a), ^{238}U may yield more precise age.
Recently, first observation of U in CS 31082-001

(Cayrel et al., 2001)

⟹ age from U/Th

15.0 ± 3.0 Gyr

(Schatz et al., 2002)

In the meantime, second observation of U in BD +17°3248 ⟹ age from U/Th and U,Th/3rd peak

13.8 ± 4.0 Gyr

(Cowan et al., 2002)

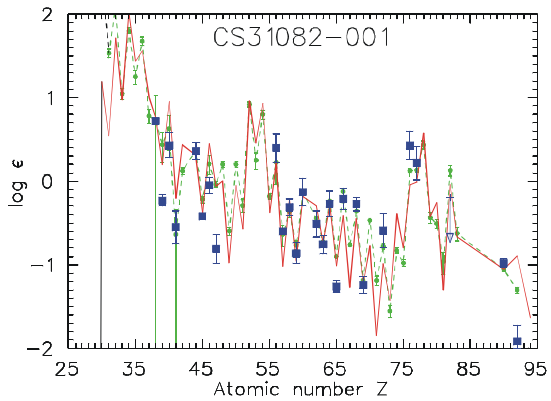

Reach of radioactive beam facilities

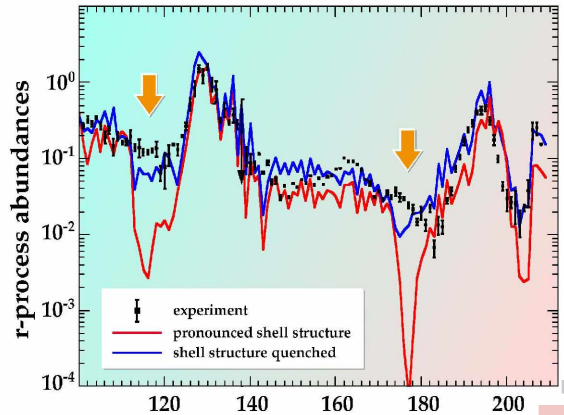

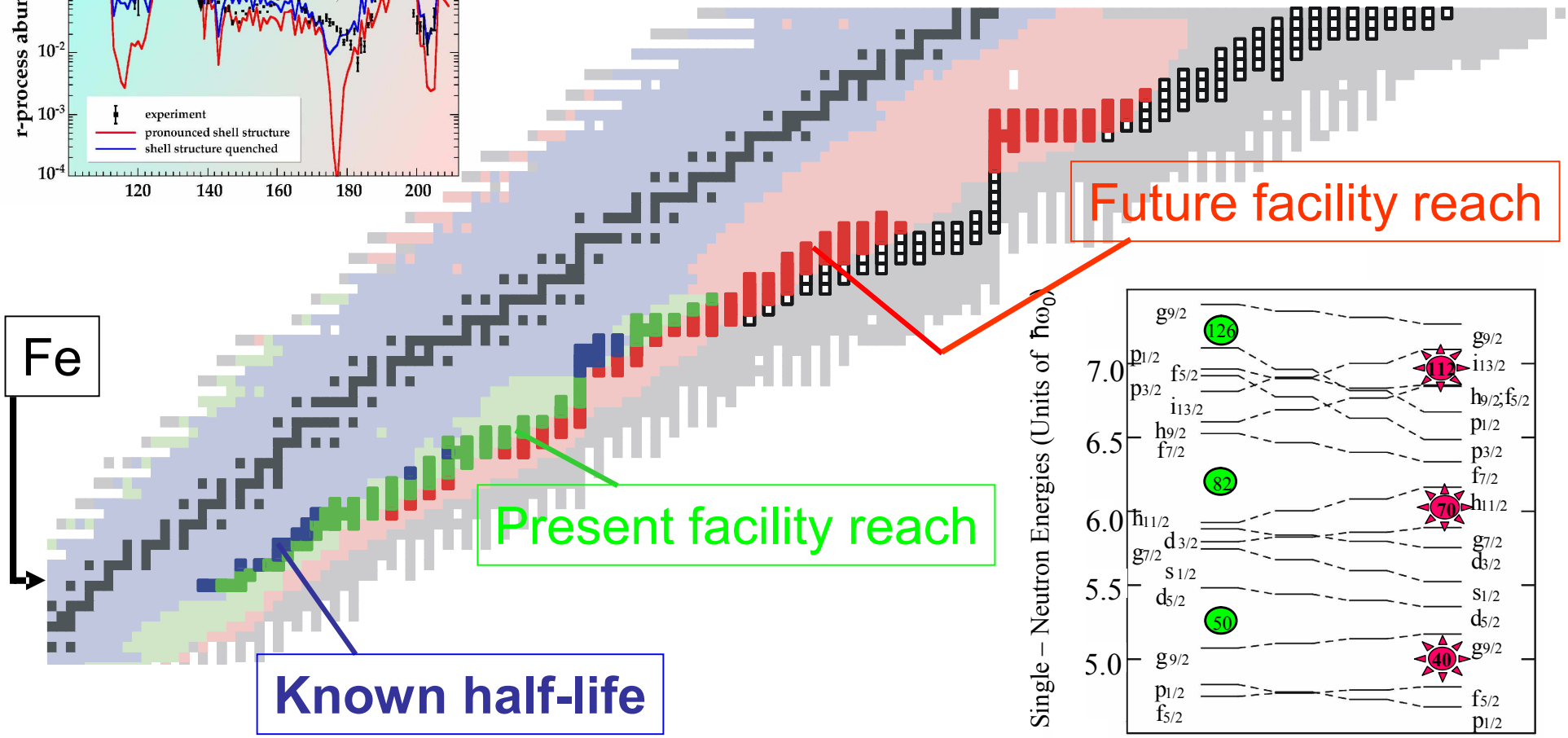

New magic numbers ?

From K.-L. Kratz (KCh MZ) and H. Schatz (MSU)

Reach for at least a half-life measurement

K.-L. Kratz CEoEU

Conclusions

Direct comparison between astronomical and nuclear structure observations and astro-model predictions

- information about stellar parameters
  - ⇒ temperatures,
  - ⇒ particle (e.g. p, α, n) and matter densities,
  - ⇒ ν–fluxes,
  - ⇒ time scales,
  - ⇒ hydrodynamical conditions.

- possible information on nuclear physics far from stability
  - ⇒ position of particle drip-lines,
  - ⇒ regions of shape-transition,
  - ⇒ $\pi\nu$ residual interaction,
  - ⇒ shell quenching.

It is clear that also in the future astrophysics will have to rely on nuclear physics input;
mainly from nuclear theories,
still not sufficiently well understood.

Therefore, continued **request** for
radioactive-beam
nuclear mass
β-decay

experiments

Present ISOL-RIB facilities (ISOLDE, SPIRAL, ...) → TARGISOL → EURISOL, RIA, upgrades GSI, RIKEN

K.-L. Kratz CEoEU

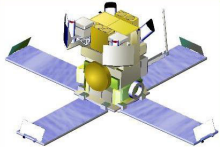

GRBs as a Probe of the Elemental Abundance History of the Universe

D. Q. Lamb (U. Chicago)

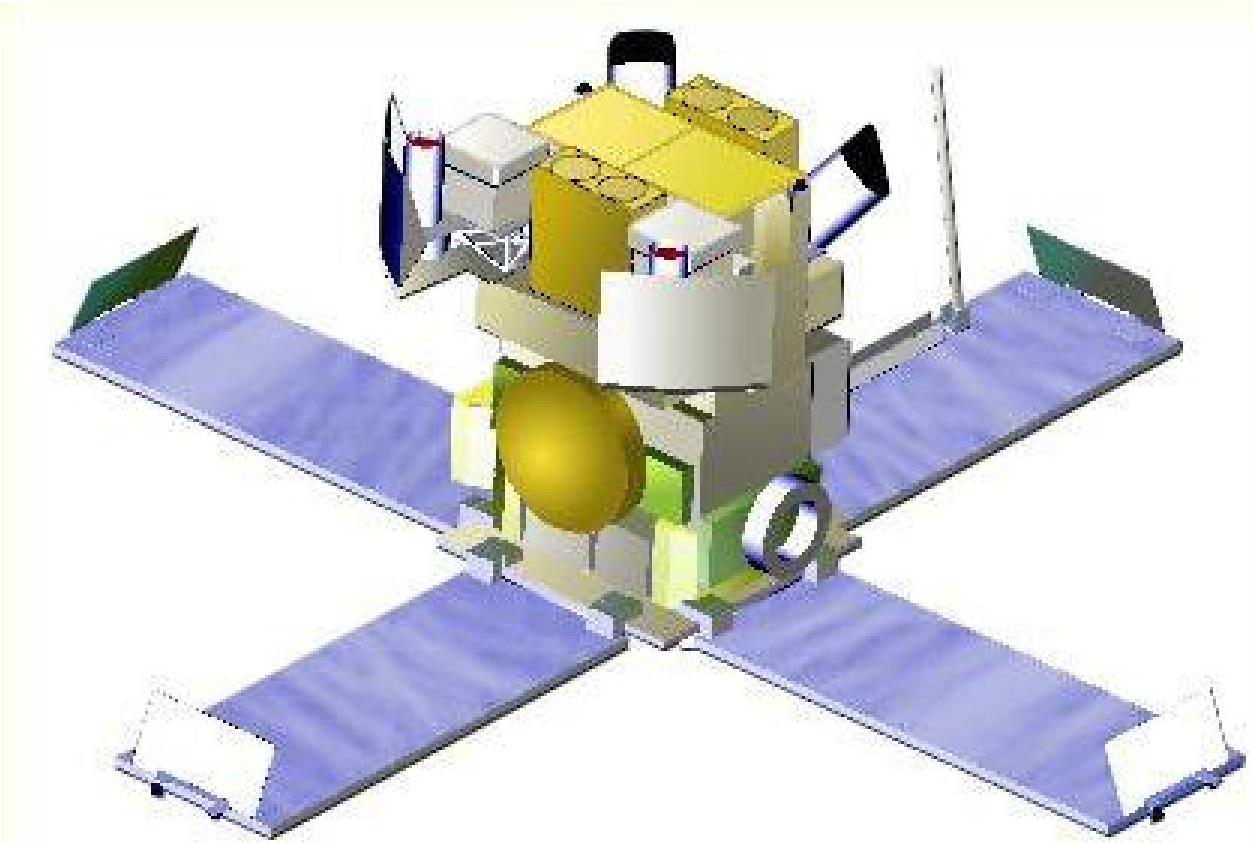

Workshop on Chemical Enrichment of the Early Universe
Santa Fe, NM, 13 August 2004

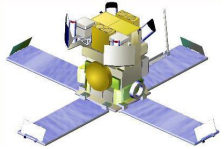

Outline of This Talk

- HETE-2 is “going great guns:”
  - It is currently localizing ~ 25 - 30 GRBs yr^-1
  - It has localized 68 GRBs so far
  - 25 of these localizations have led to the detection of X-ray, optical, or radio afterglows
  - 15 of these afterglows have led to redshift determinations
- In this talk, I will discuss:
  - GRB-SN Connection
  - Detectability of GRBs and their optical/NIR afterglows out to very high redshifts ($z > 5$)
  - GRBs as (possible) powerful probes of cosmology and the early universe

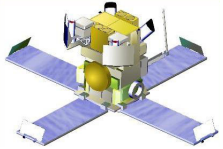

GRB030329: HETE "Hits a Home Run"

Vanderspek et al. (2004)

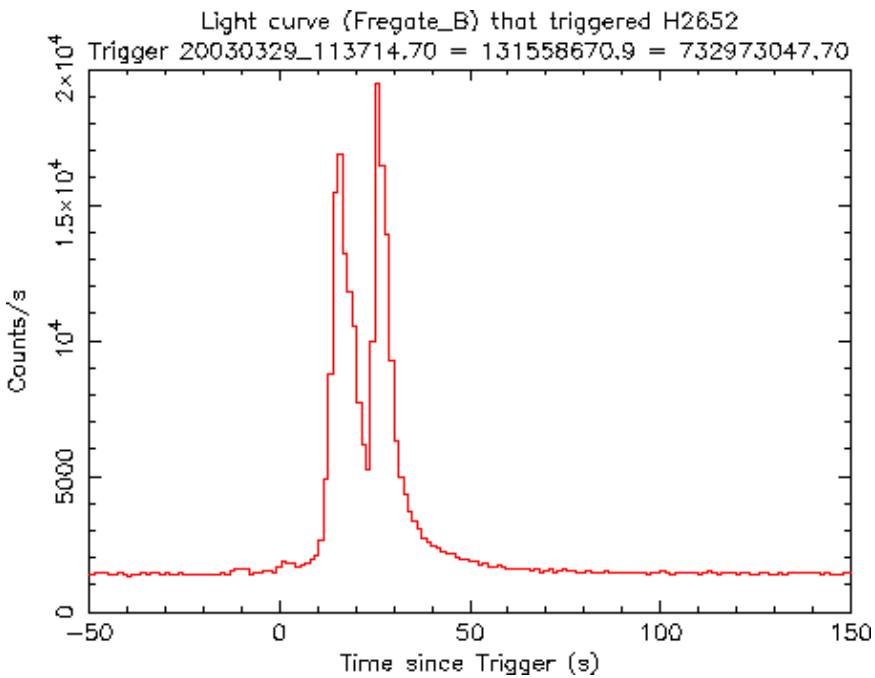

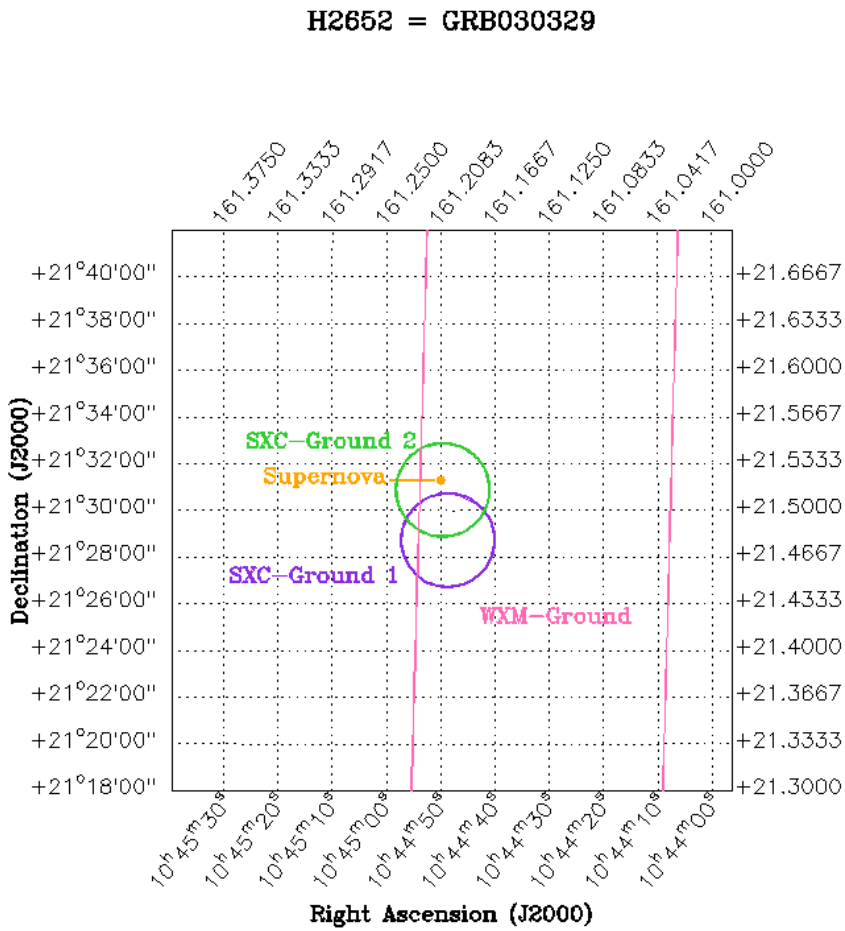

z = 0.1675 ⇔ probability of detecting a *bright* GRB this close by is ~1/3000 => unlikely that HETE-2 or *Swift* will see another such event

GRB030329:Spectrum of SN 2003dh

Stanek et al. (2003)

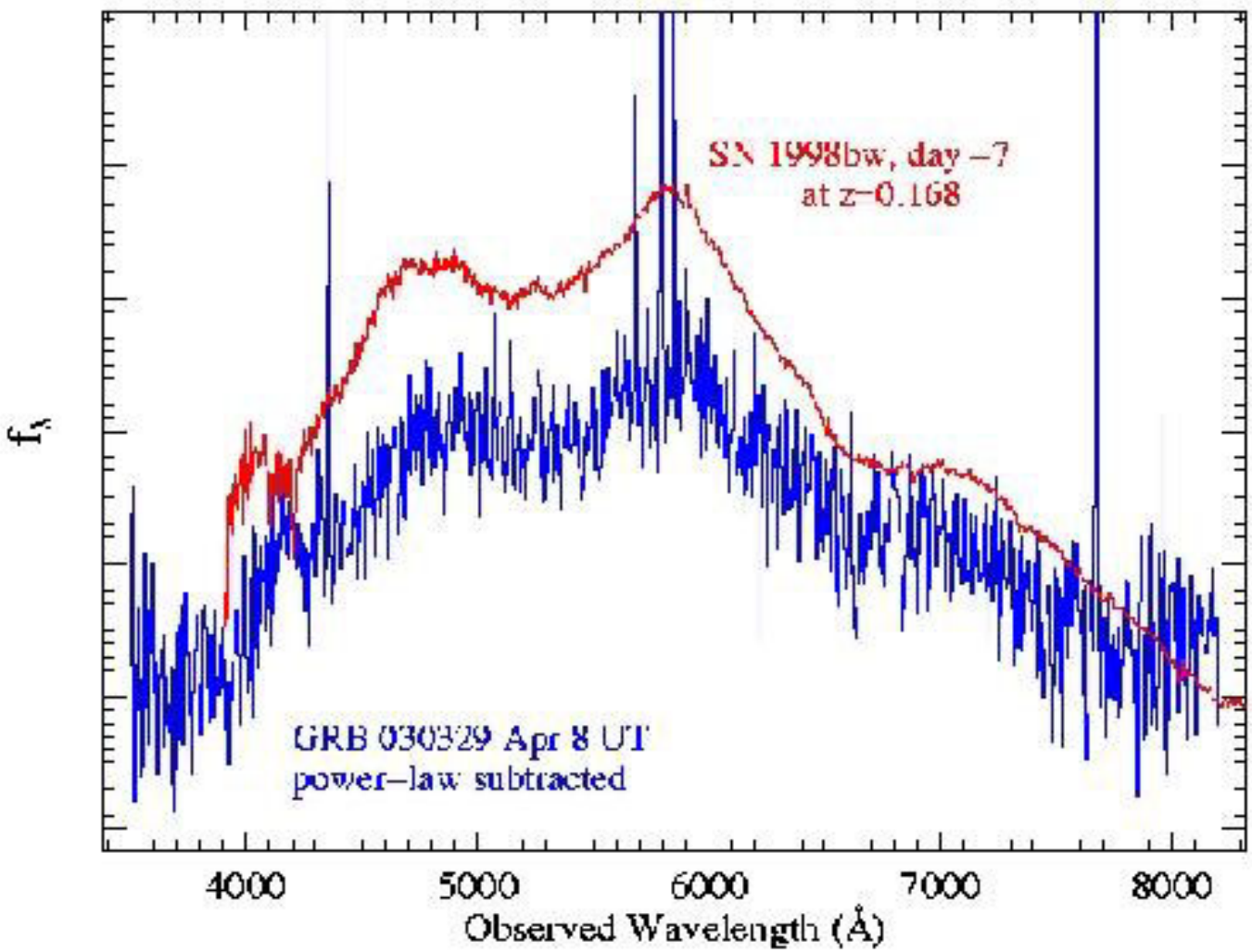

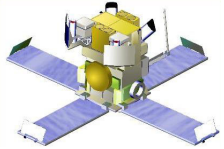

GRB030329: Implications

- HETE-2—localized burst GRB030329/SN 2003dh confirms the GRB – SN connection

- Implications:
  - We must understand Type Ib/Ic core collapse SNe in order to understand GRBs
  - Conversely, we need to understand GRBs in order to fully understand Type Ib/Ic core collapse SNe
  - Result strengthens the expectation that GRBs occur out to $z \sim 20$, and are therefore *a powerful probe of cosmology and the early universe*

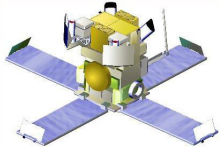

Detectability of GRBs

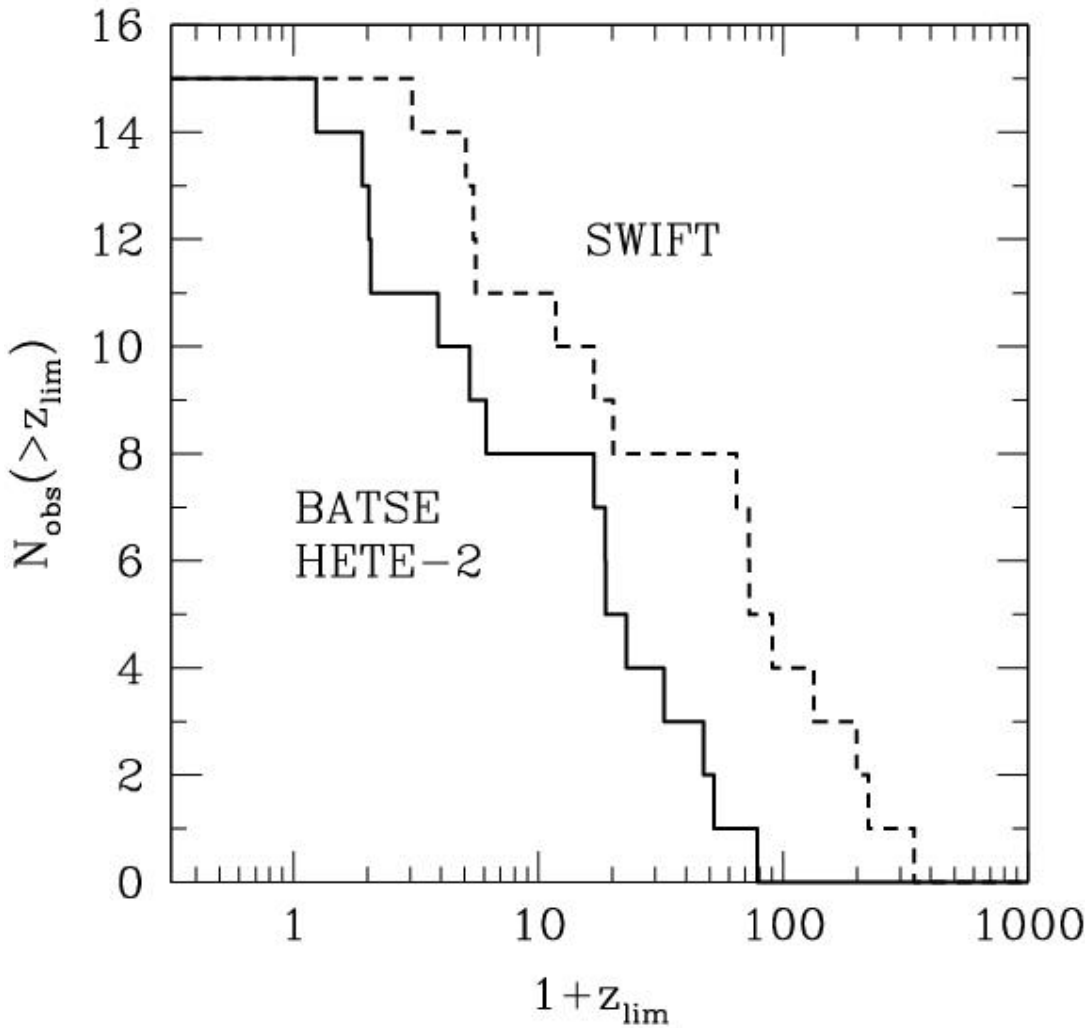

Lamb and Reichart (2000)

Detectability of GRB Optical Afterglows

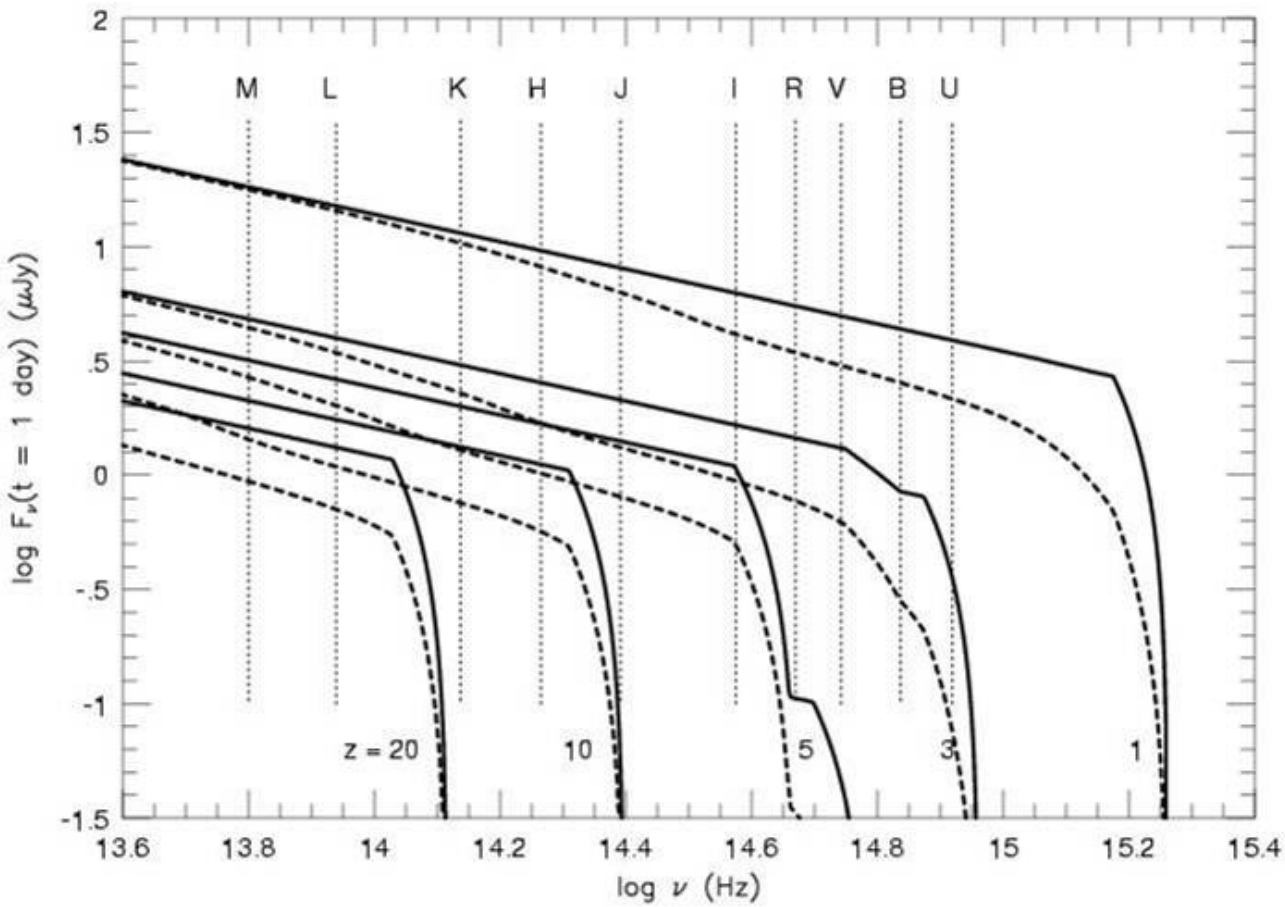

Lamb and Reichart (2000)

Evidence for Evolution of GRBs with Redshift

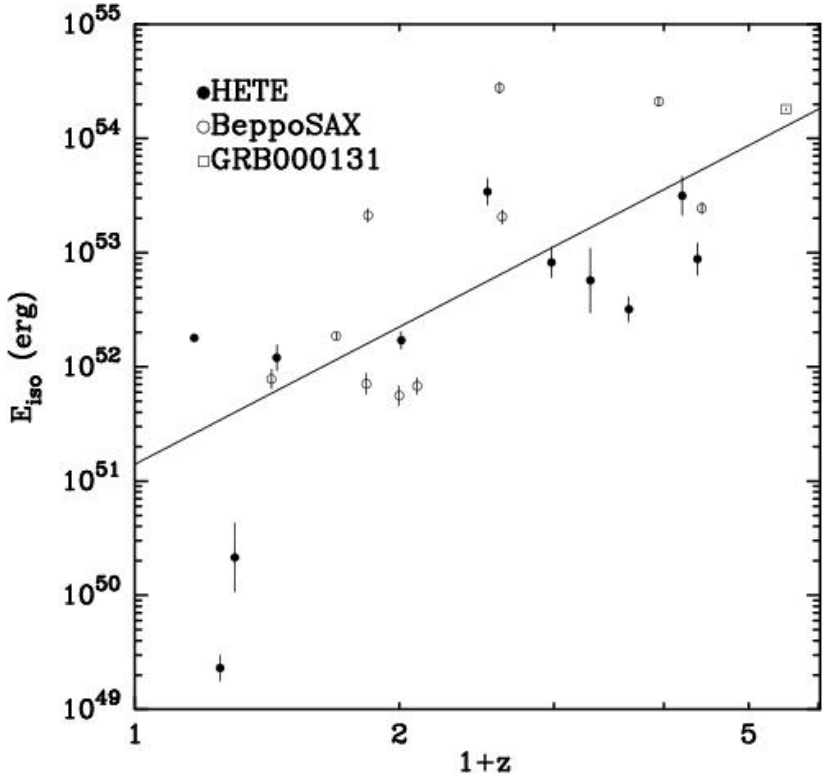

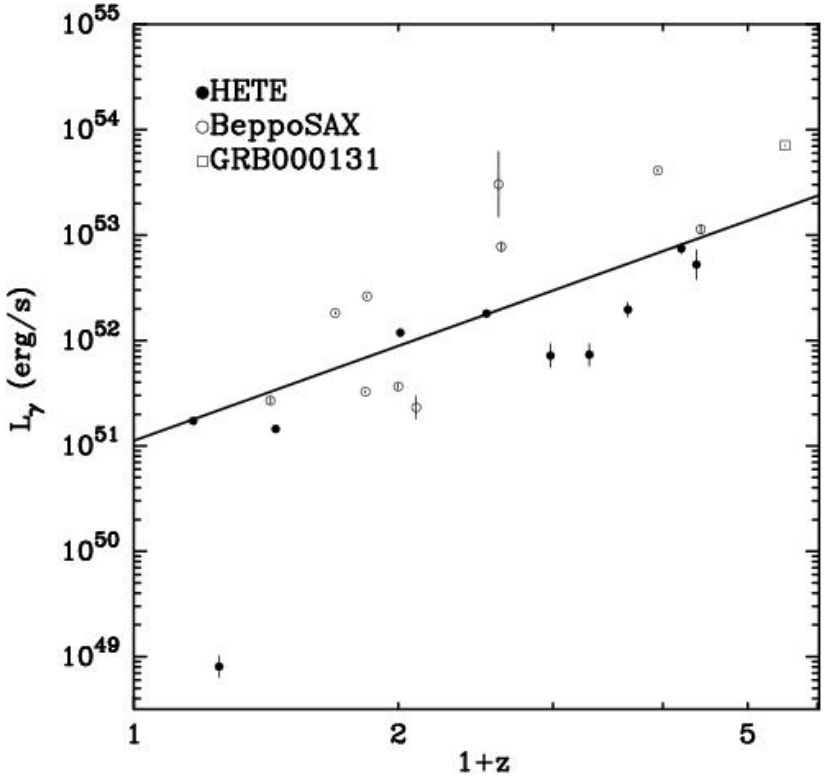

Graziani, Lamb, and Donaghy (2004)

Possible Star-Formation Rate

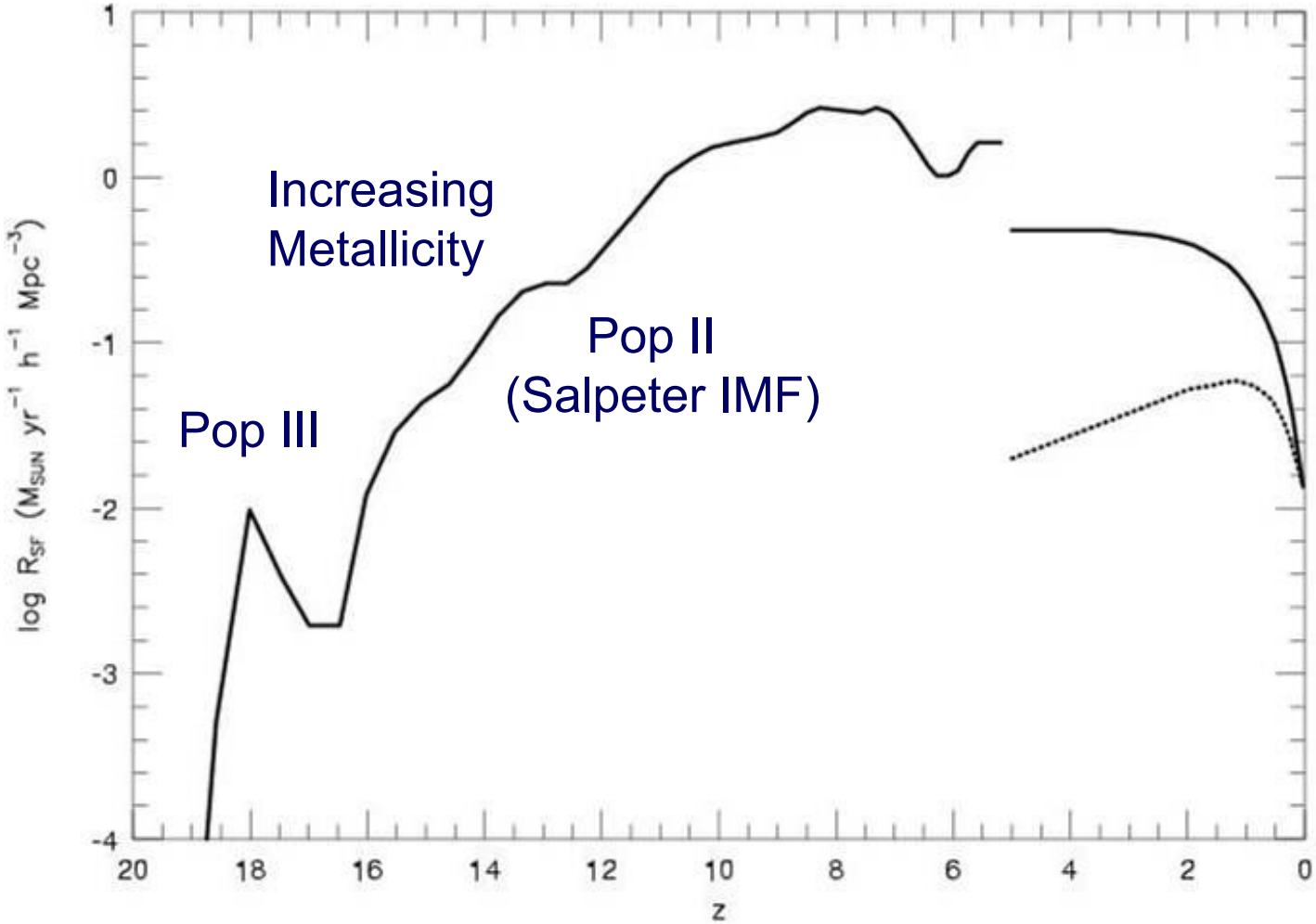

Lamb and Reichart (2000)

Possible Differential and Cumulative Distributions of GRBs

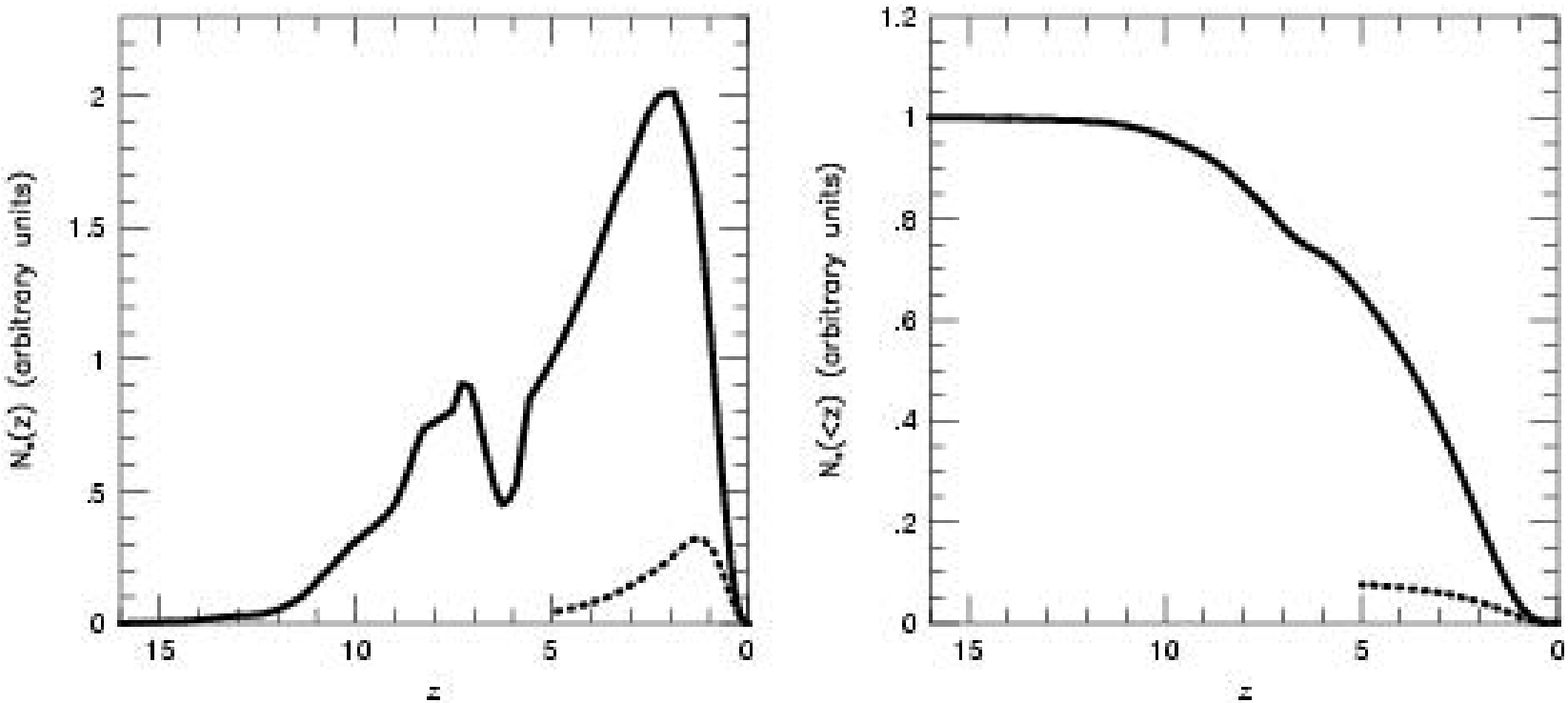

- 15-25% of GRBs May Lie at $z > 5$

Lamb and Reichart (2000)

GRBs in Cosmological Context

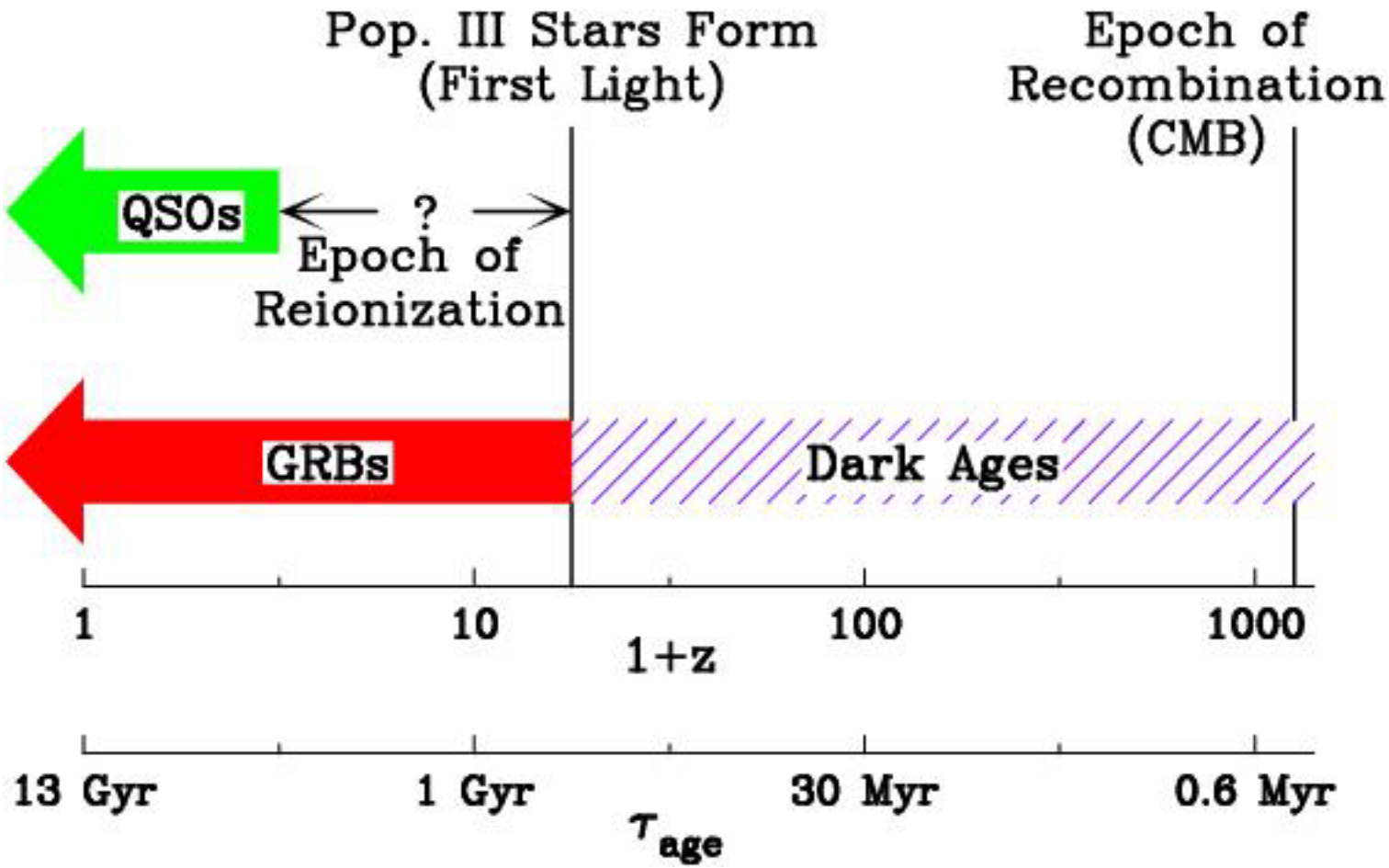

Lamb (2000)

Predicted Elemental Abundances as Function of Redshift

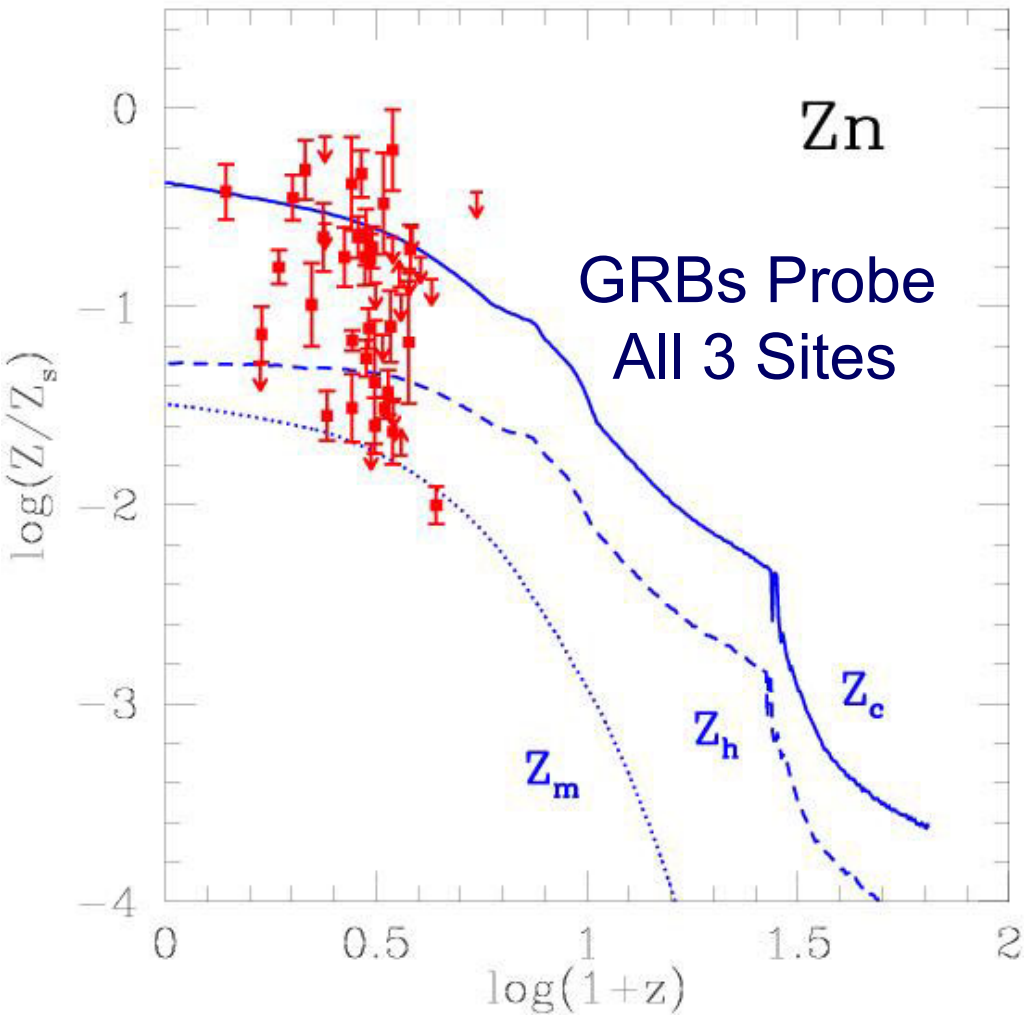

Predictions from Valageas and Silk (1999)

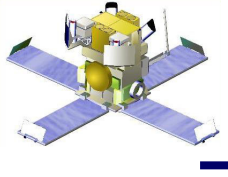

GRBs as Probe of Elemental Abundance History of Universe

- High-resolution IR and near-IR spectra can measure column density and thermal velocity of clouds within GRB host galaxy – perhaps even within the star-forming region in which GRB occurs
- EWs of absorption lines provide an estimate of the total star formation that has occurred in damped Ly-alpha and Ly-alpha forest clouds as a function of column density N_H of the cloud and redshift z
- EWs of absorption lines trace history of heavy element production in universe as function of redshift

GRB 021004

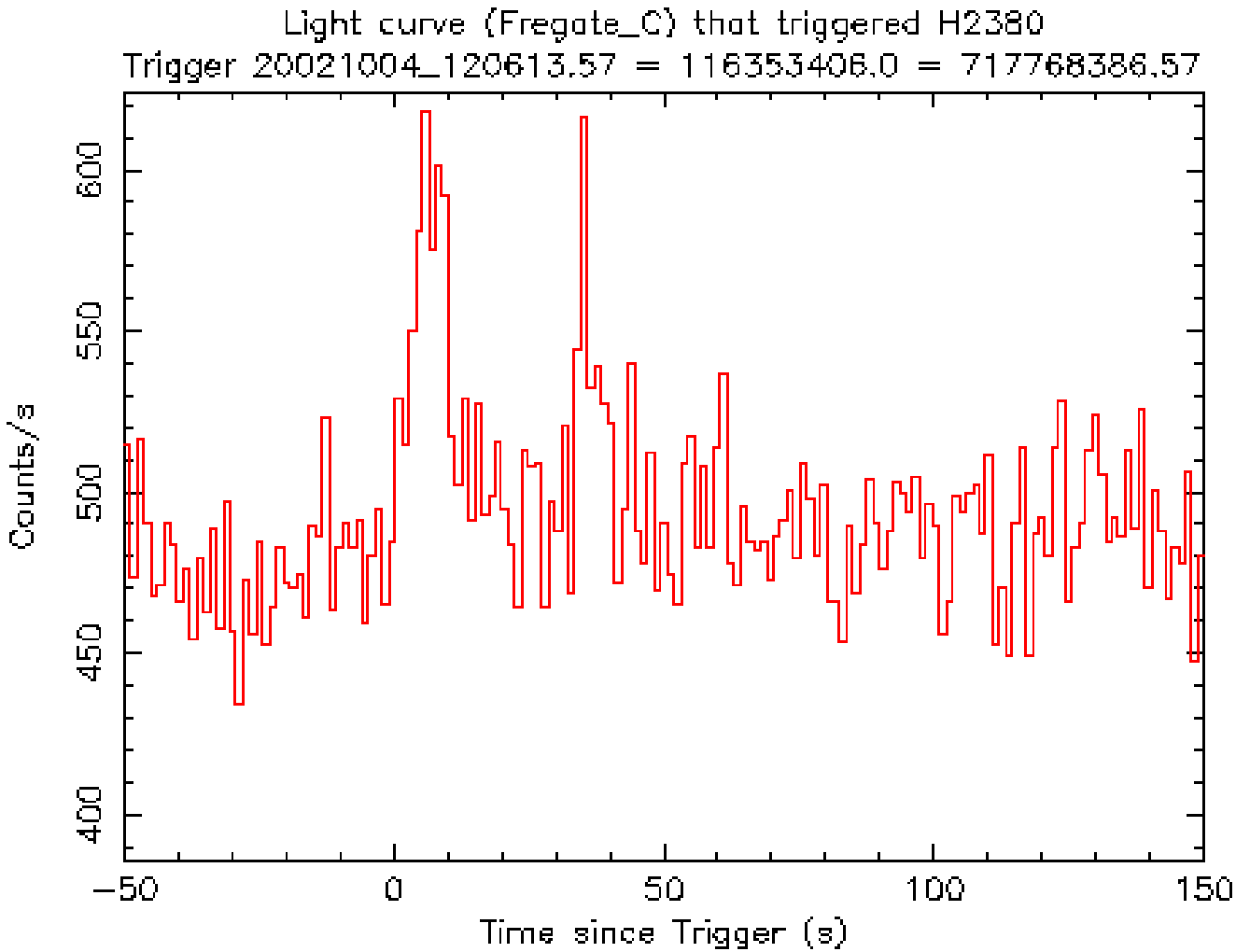
Light curve (Fregate_C) that triggered H2380
Trigger 20021004_120613.57 = 116353406.0 = 717768386.57
Counts/s
400
450
500
550
600
−50
0
50
100
150
Time since Trigger (s)

GRB021004: T + 43 sec

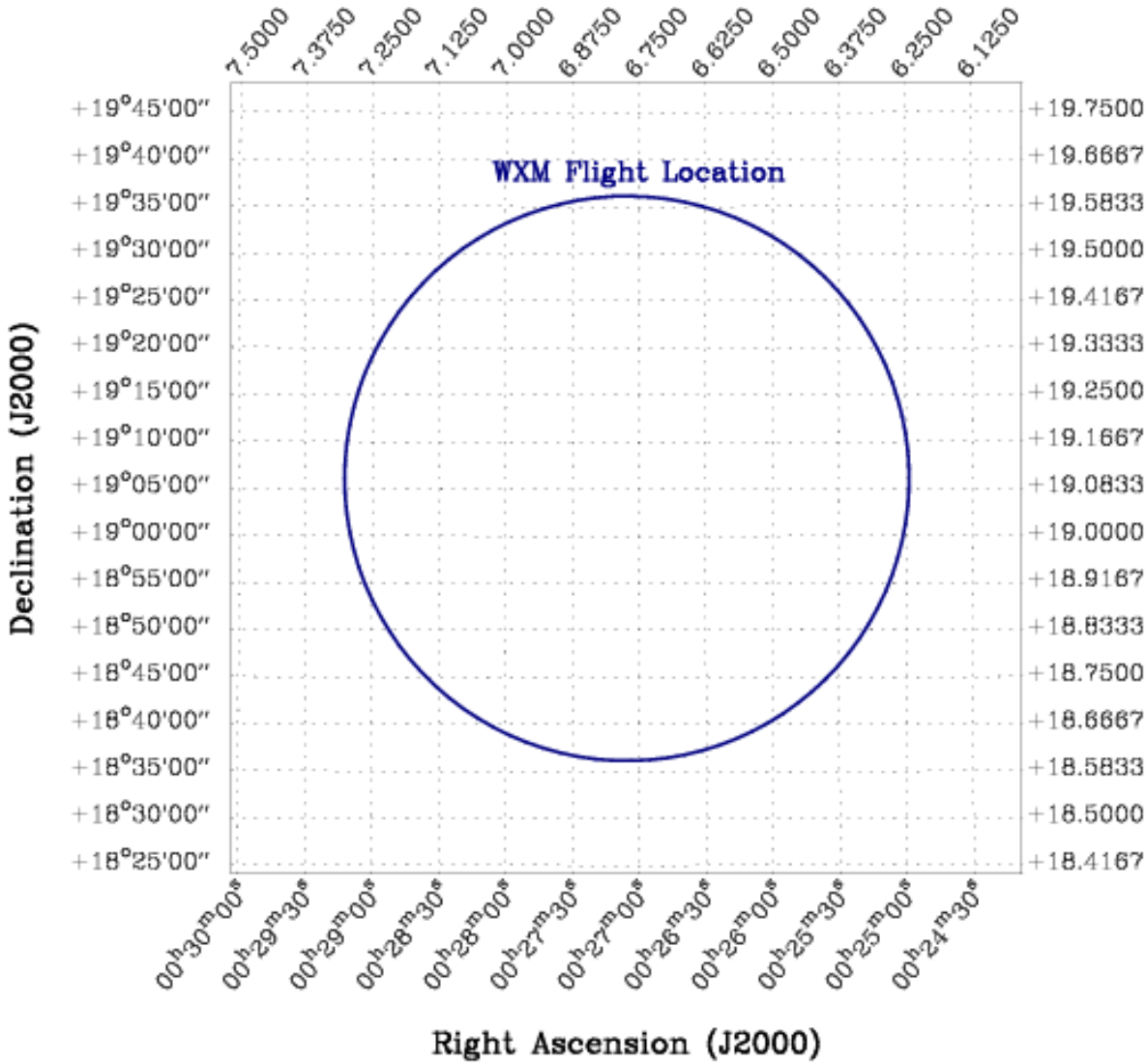

GRB021004: T + 73 min

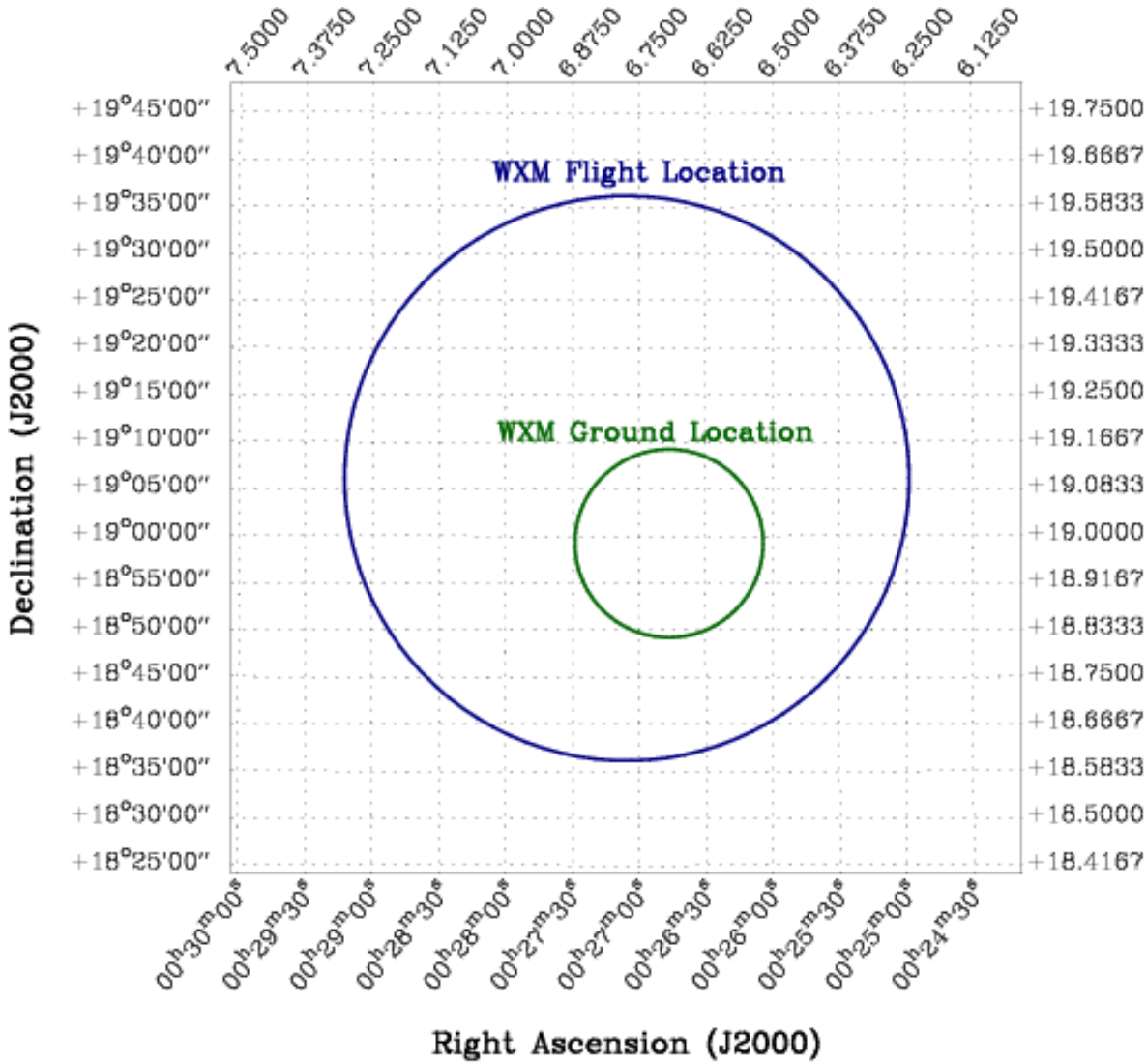

GRB021004: T + 154 min

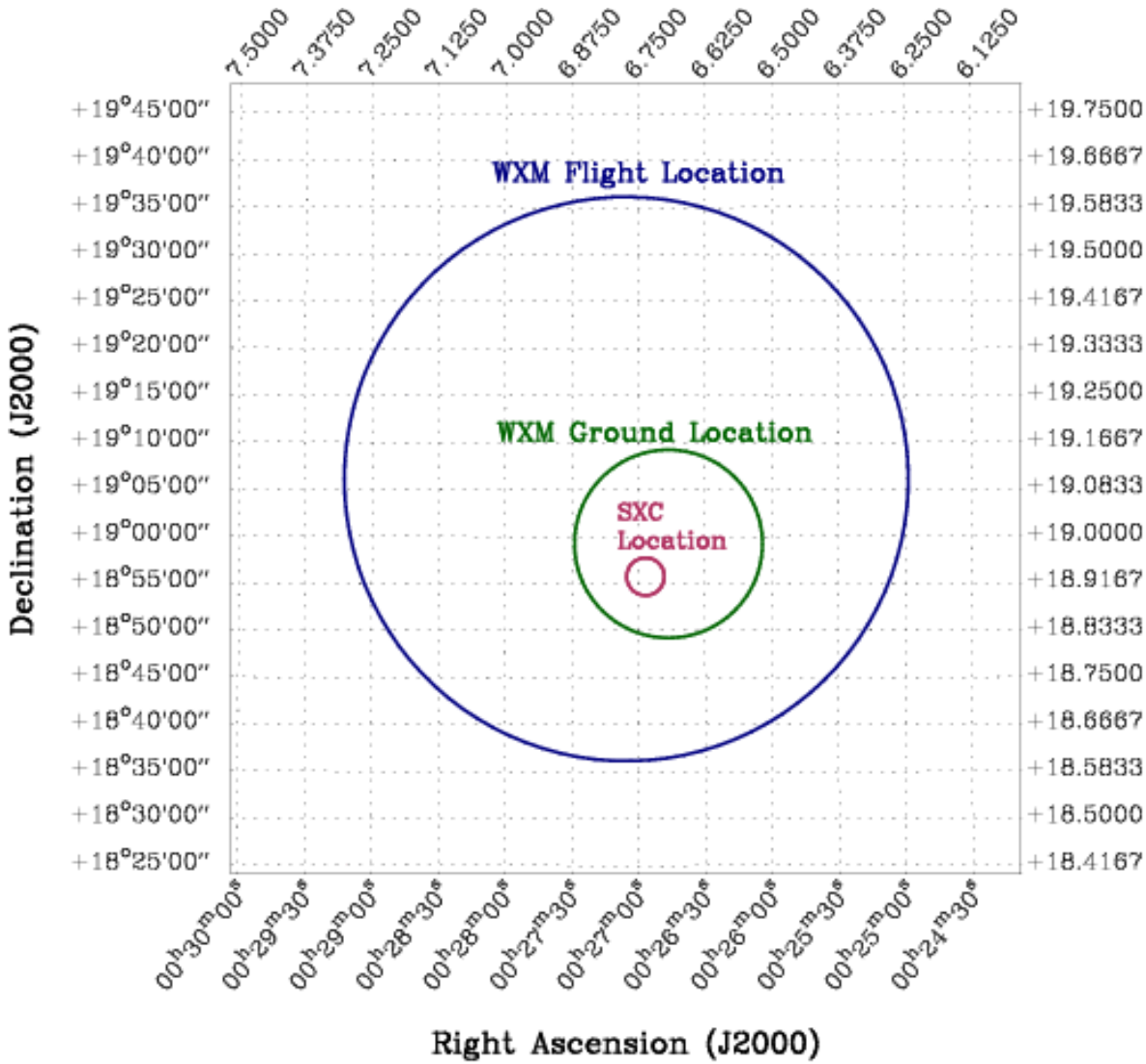

GRB021004: T + 180 min
(Optical Transient Detected at T + 9 min)

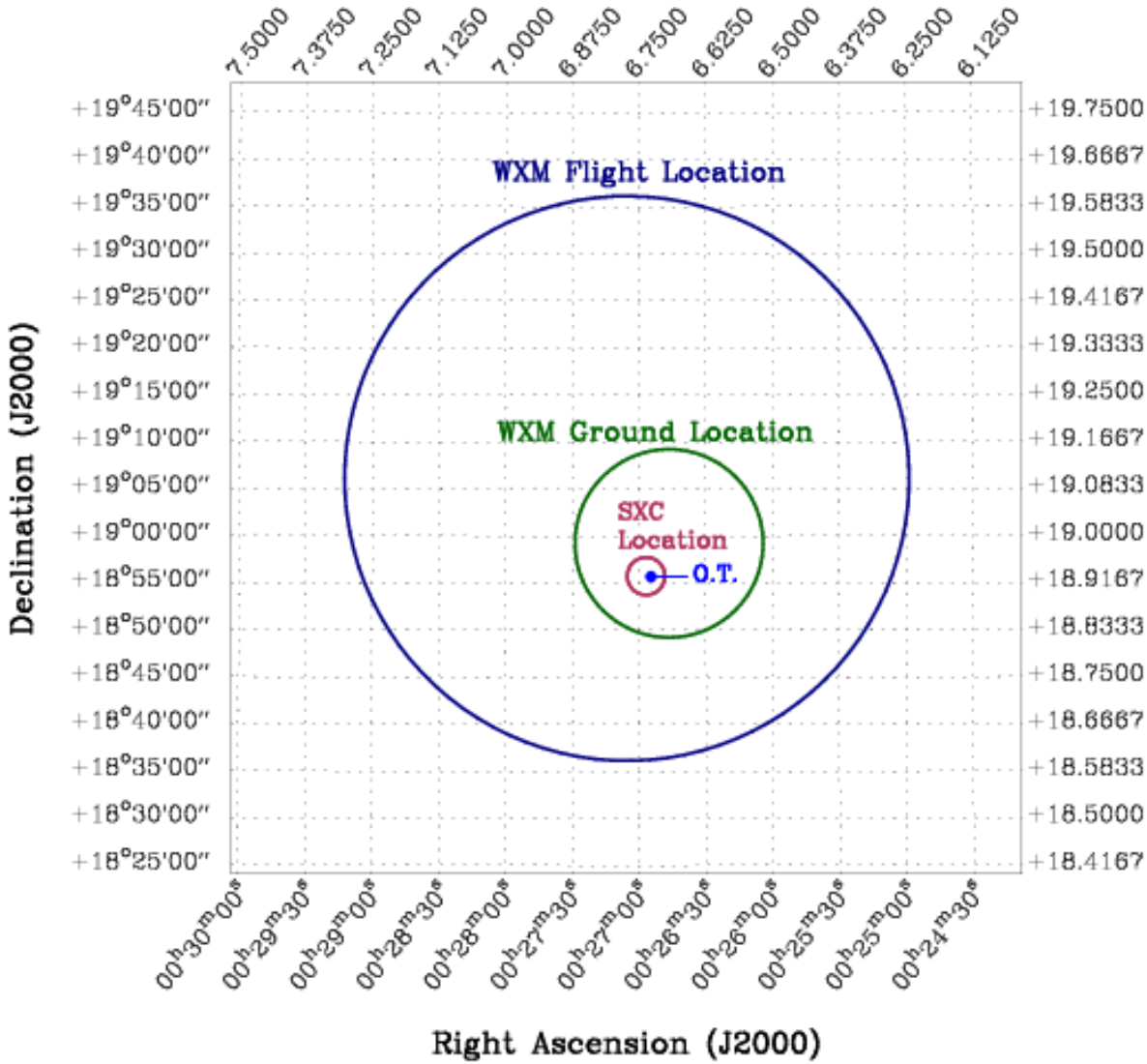

Discovery of GRB 021004 Optical Afterglow

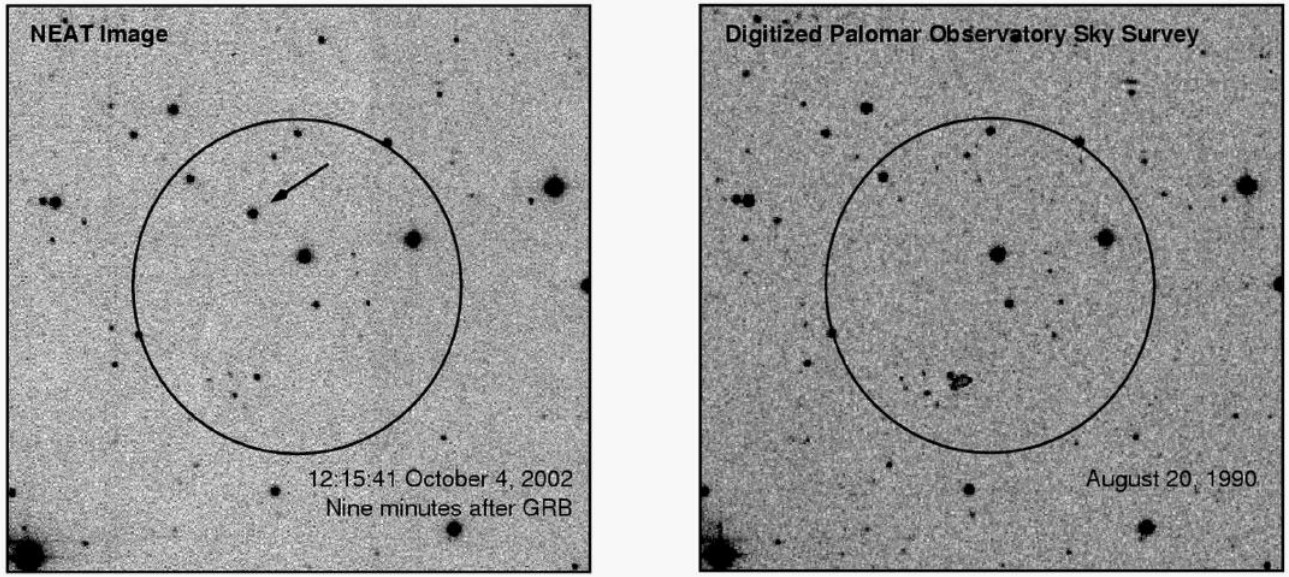

The Nine Minute–Old Gamma–Ray Burst

Palomar Oschin Telescope + Near–Earth Asteroid Tracking Camera (NEAT)

Derek Fox for the Caltech–NRAO GRB Collaboration

- Spectroscopic observations < 3 hours later gave first redshift info ($z > 1.6$)
- Optical afterglow *very* bright (R = 15.4) at discovery

GRB 021004 Optical Afterglow

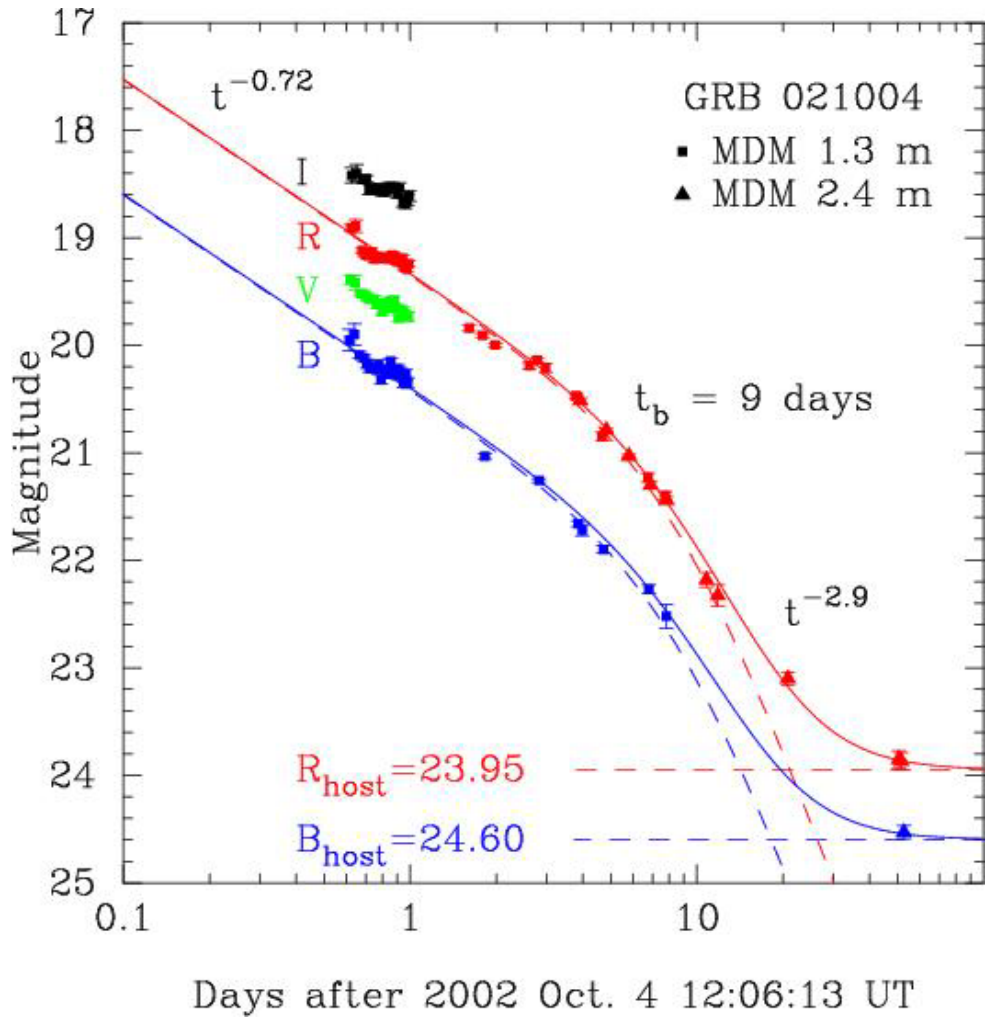

Mirabal et al. (2003)

ALS in Optical Afterglow Spectrum of GRB 021004

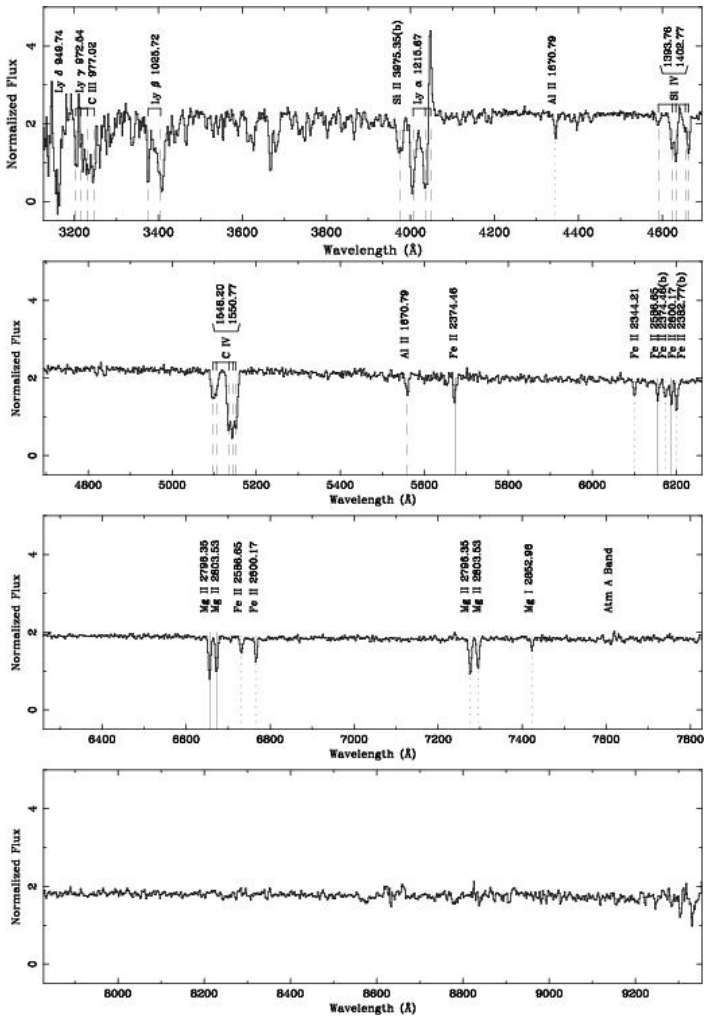

- LRIS spectrum taken 2002 Oct. 8.507
- Three ALS seen:
  - $z_1 = 1.380$
  - $z_2 = 1.602$
  - $z_3 = 2.328$

Mirabal et al. (2003)

Fragmented Circumburst Nebula Model

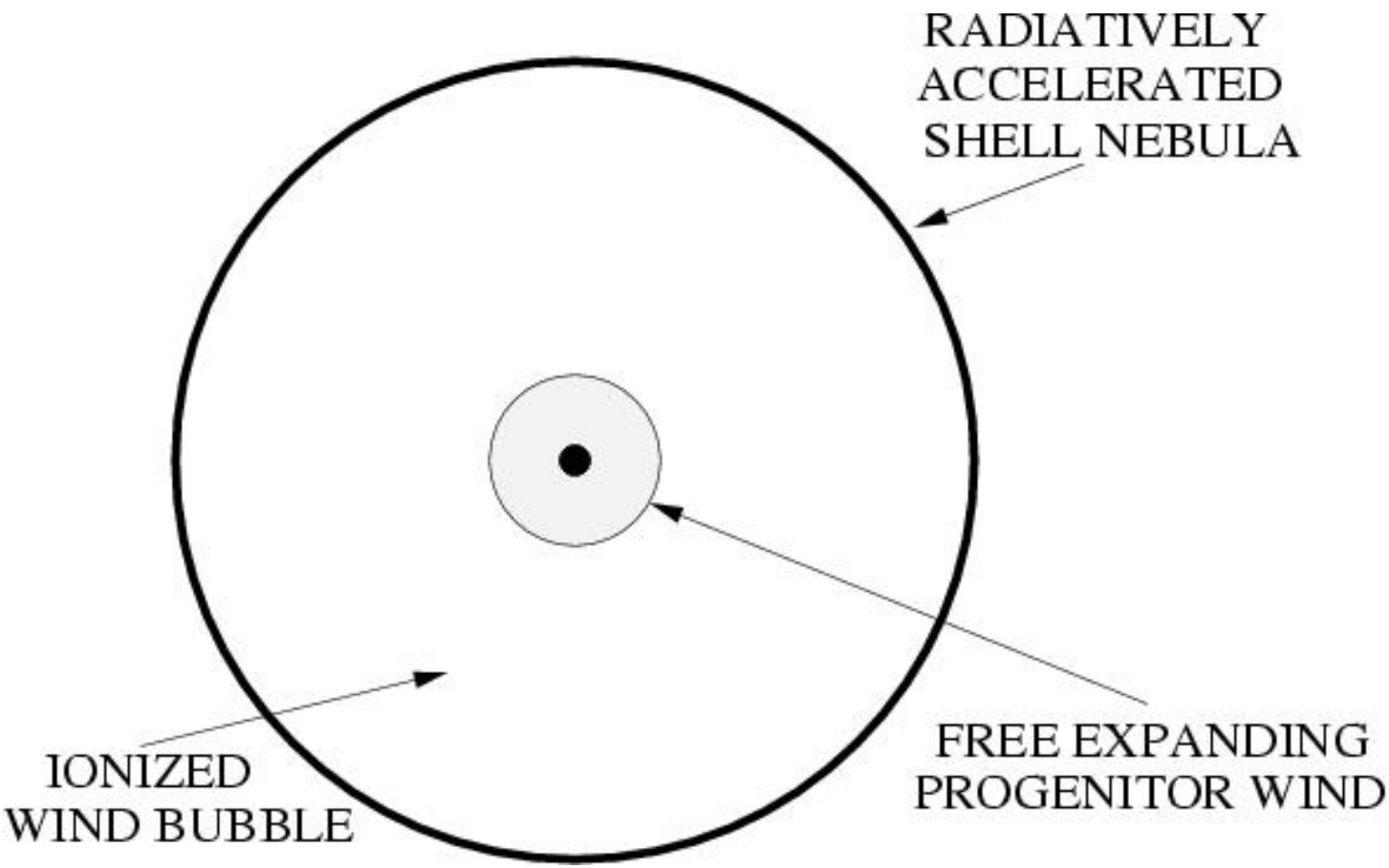

Mirabal et al. (2003)

Redshift Sub-Components in Optical Afterglow Spectrum of GRB 021004

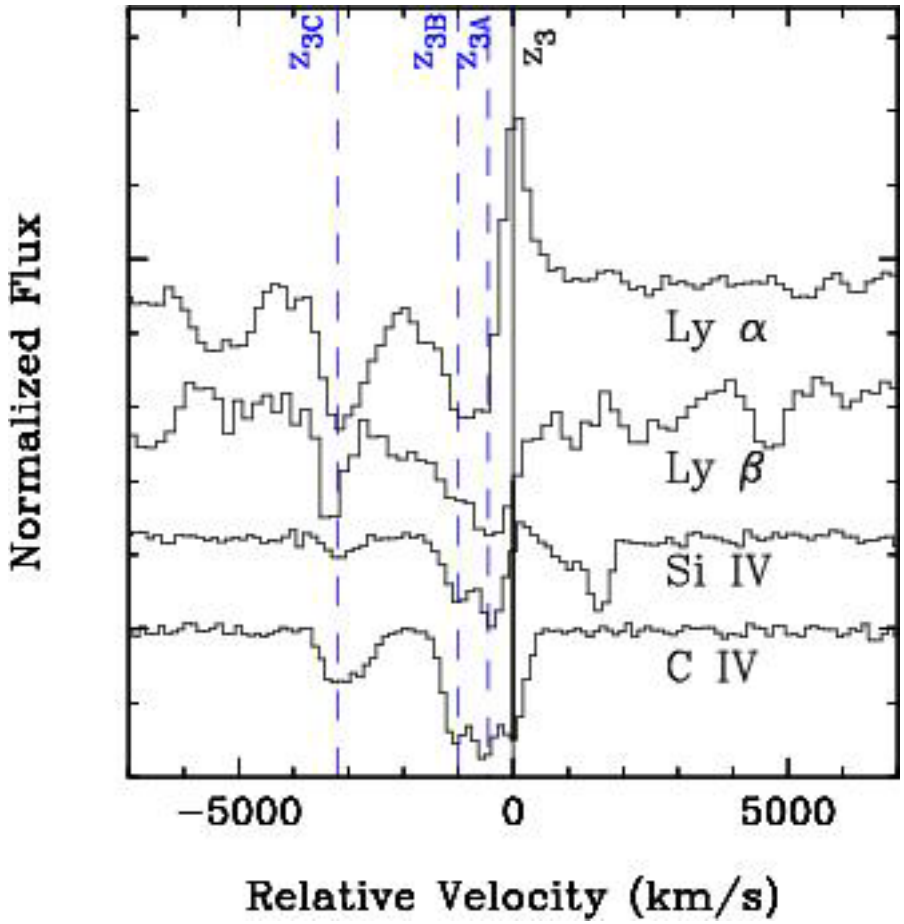

Mirabal et al. (2003)

Column Densities of Elements

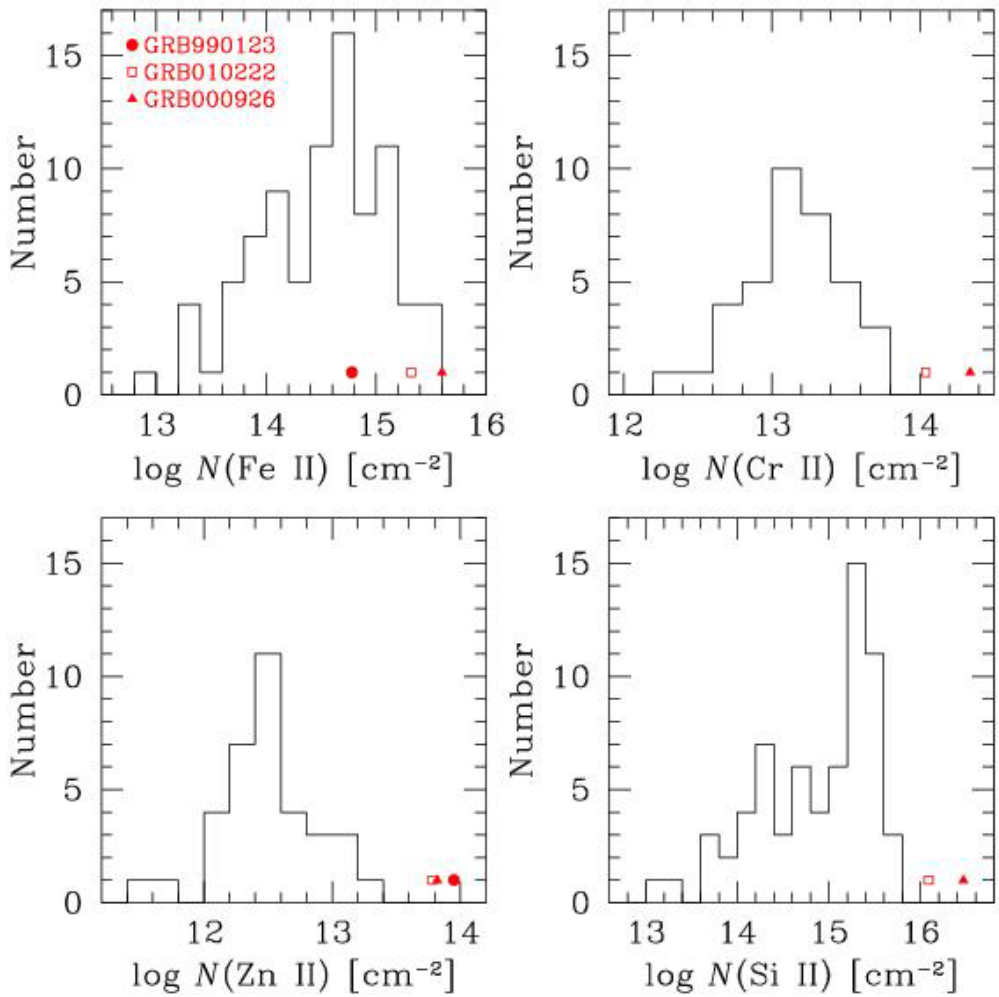

Savaglio, Fall and Fiore (2003)

Observed Mass of C IV as Function of Redshift

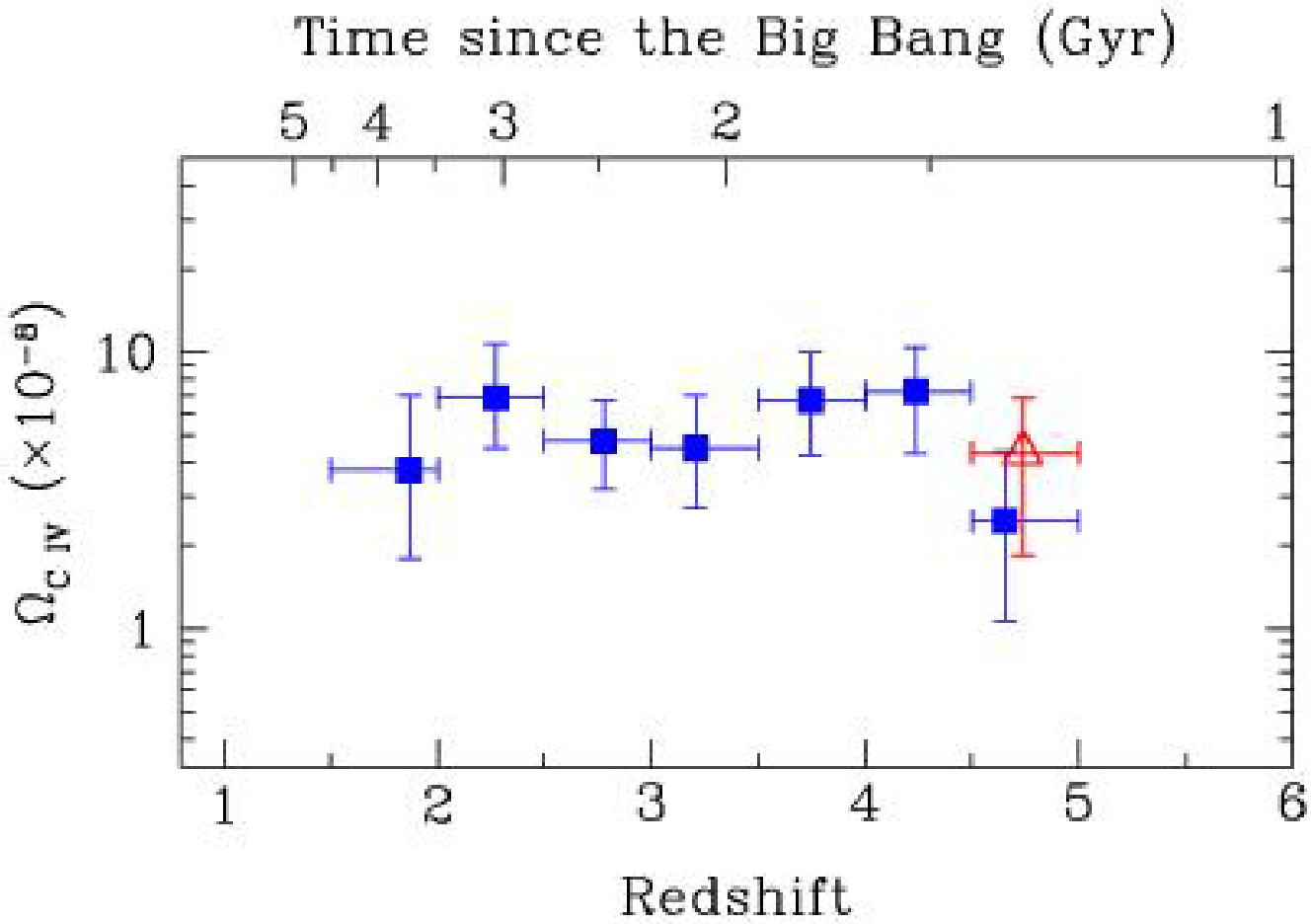

Pettini et al. (2003)

Possible Ionization Histories of the Universe

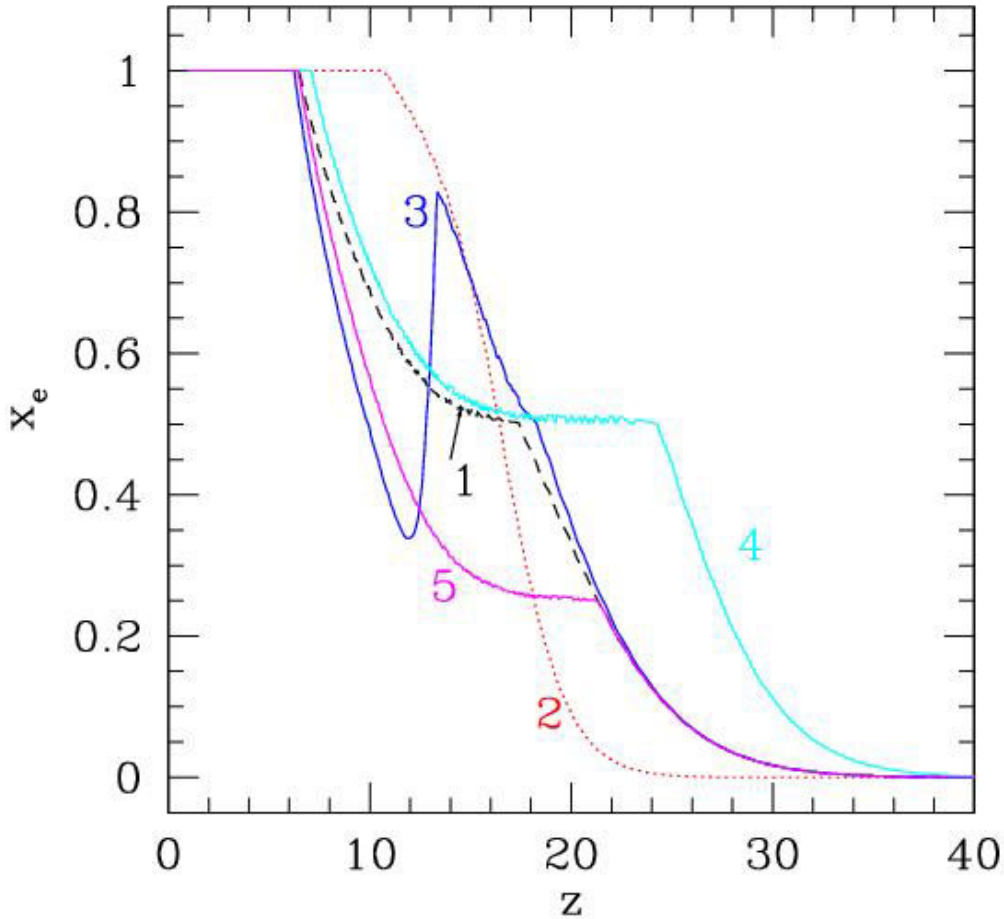

Holder et al. (2003)

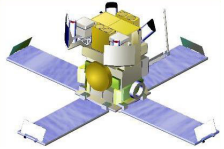

Advantages of GRBs as Probes of Reionization

- GRBs are by far the most luminous events in the universe and are therefore easy to find
- GRBs are expected to lie at very high redshifts ($z > 5$)
- Optical and NIR/IR afterglows of GRBs are detectable out to very high redshifts
- GRBs produce no “proximity effects” (i.e., no dynamical disturbance or ionization of the IGM)
- GRBs have simple power-law spectra and dramatically outshine their host galaxies, making it relatively easy to determine the shape of the red edge of the Gunn-Peterson trough

Reionization Signature in GRB NIR Afterglows

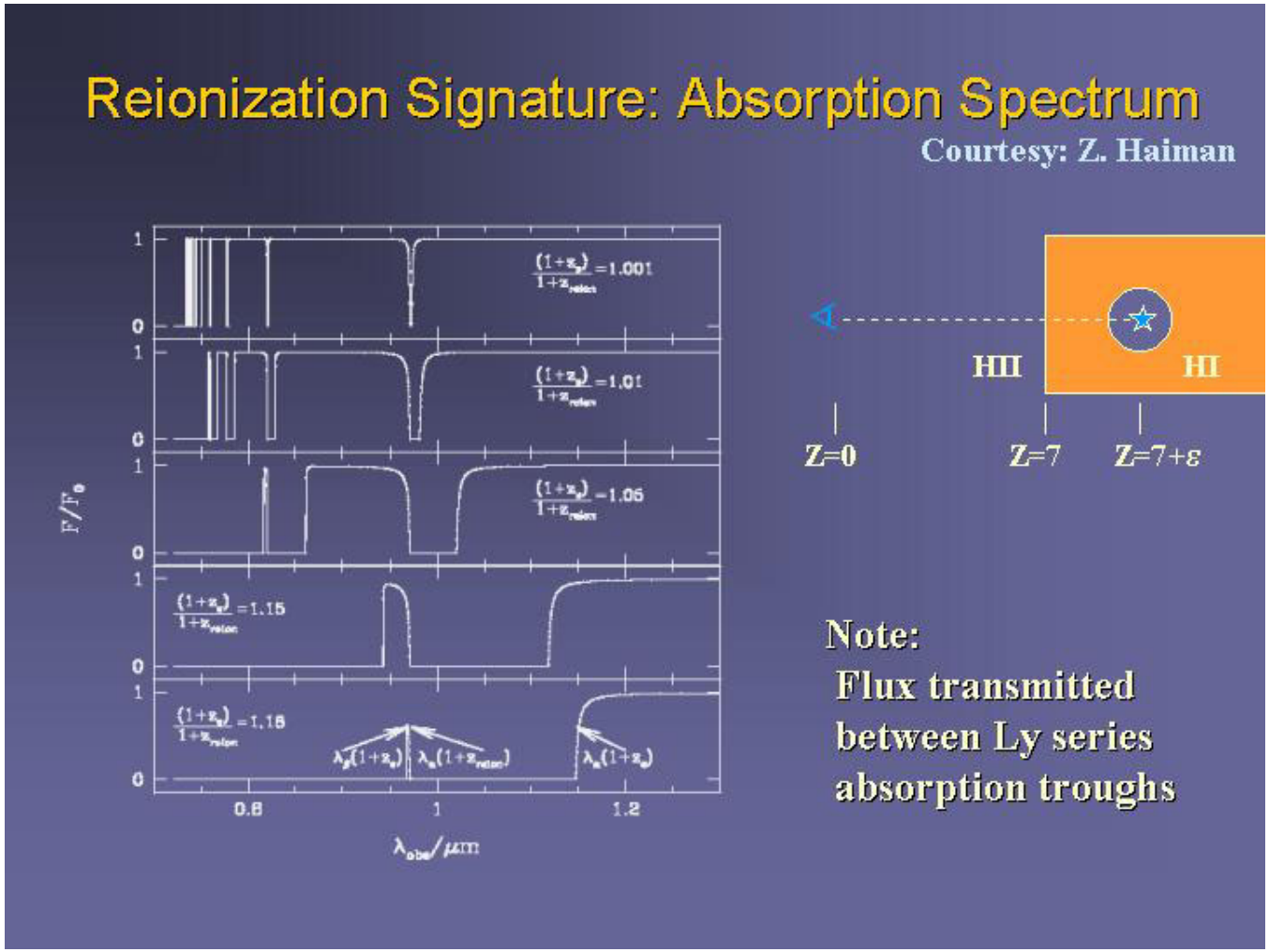

NIR Spectra of GRBs as Probe of Reionization

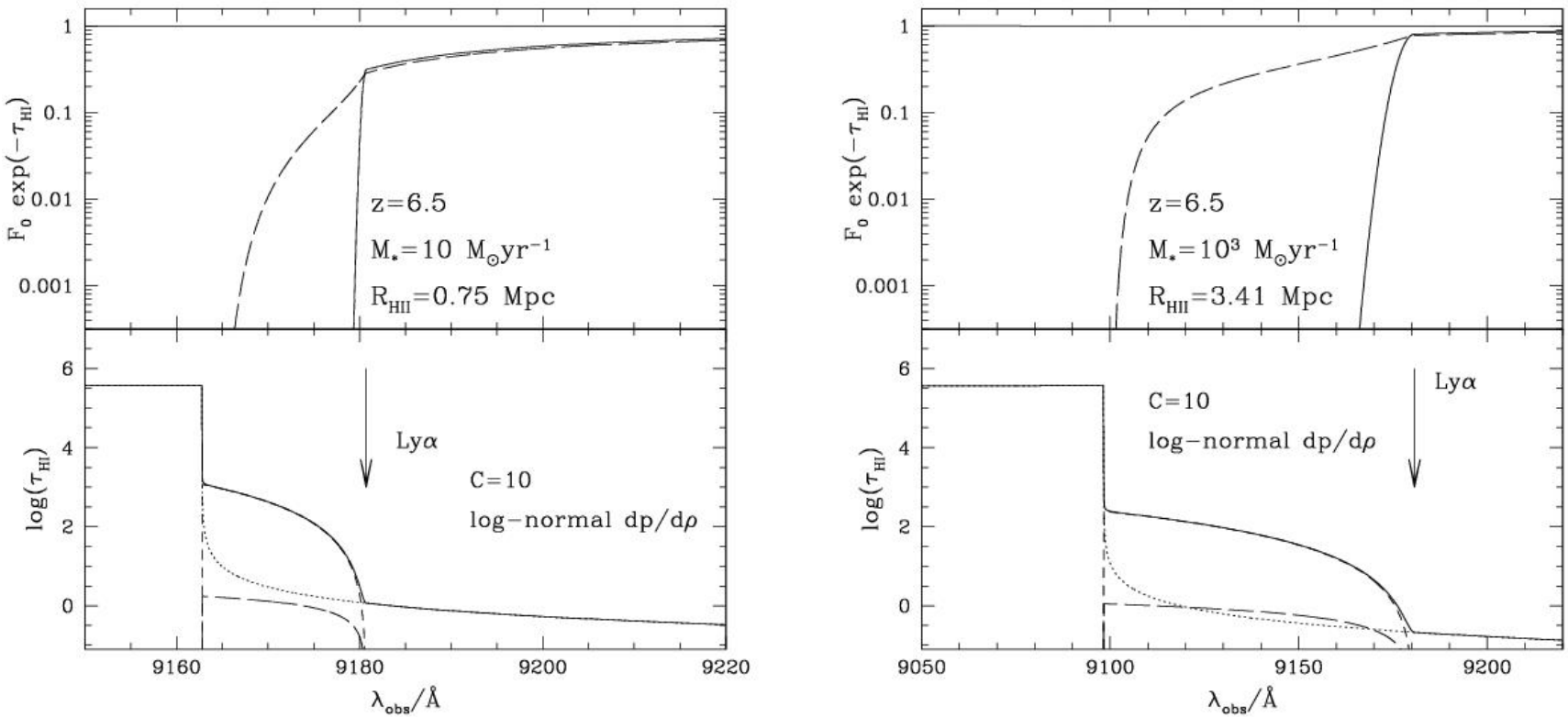

Lamb and Haiman (2004)

NIR Spectra of GRBs as Probe of Reionization

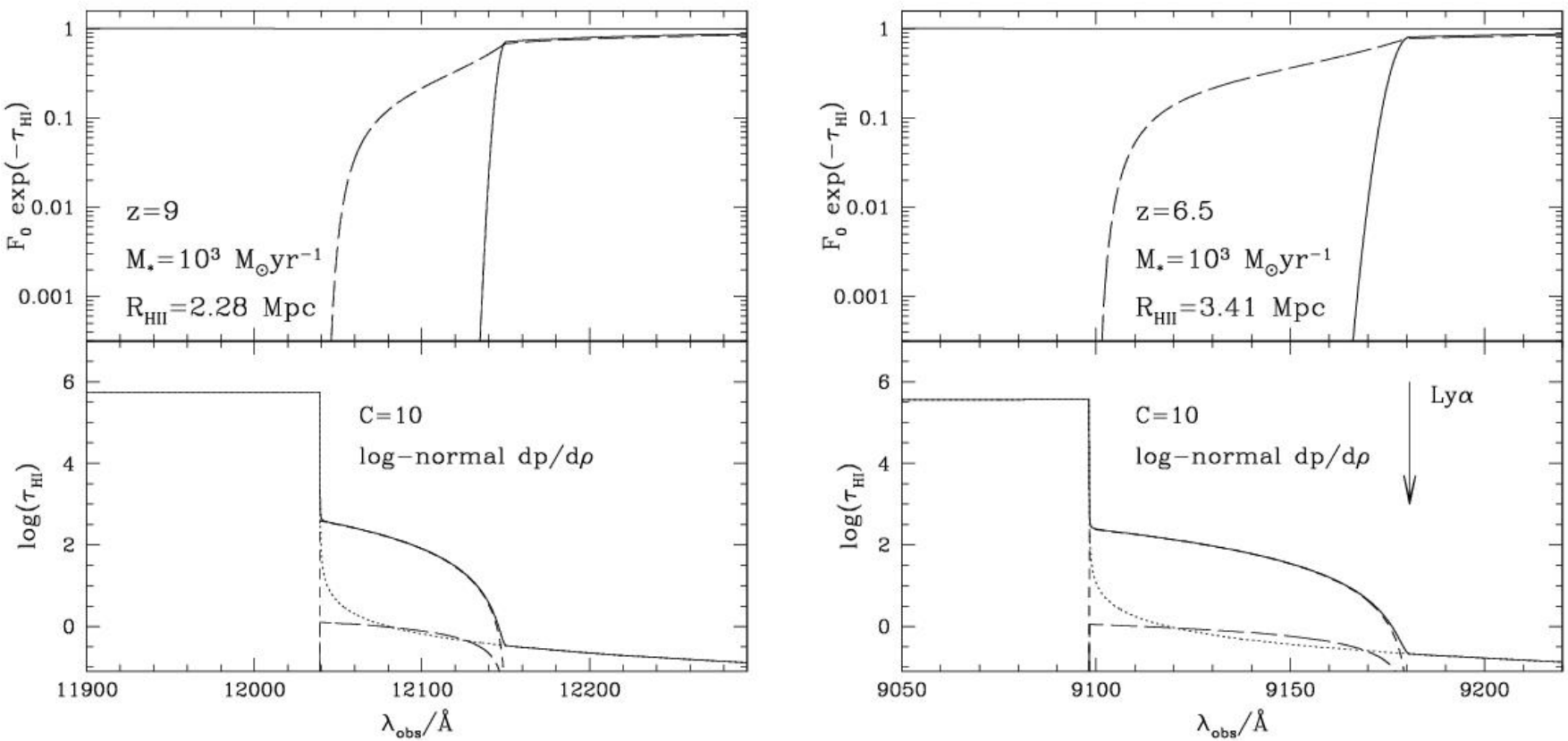

Lamb and Haiman (2004)

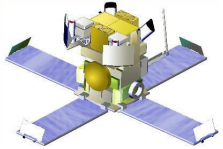

Conclusions

- HETE-2 and follow-up observations have confirmed the connection between GRBs and core-collapse supernovae
- This strengthens likelihood that GRBs exist out to very high redshifts ($z > 5$)
- GRBs and their optical/NIR afterglows are easily visible out to redshifts $z \sim 20$
- GRBs may therefore provide a powerful probe of
  - Moment of first light
  - Star-formation history of the universe
  - Elemental abundance history of the universe
  - Reionization history of the universe

The Colors and Metallicities of Dwarf Elliptical Galaxy Globular Cluster Systems, Nuclei and Stellar Halos

Jennifer Lotz
UC Santa Cruz

with Bryan Miller *(Gemini)*
and Harry Ferguson *(STScI)*

The Colors of dE Globular Cluster Systems

- Motivation
- Background
  - Globular Clusters in Local Group dwarfs
- HST Dwarf Elliptical Snapshot Survey
- Implications for GC formation and enrichment

Why study dwarf galaxy GCs?

fossil record of early star-formation in smallest galaxies

Dwarf-sized DM halos among first objects to collapse
→ local dwarfs are "survivors" of hierarchical mergers
GC formation in dwarfs predicted at z~10-20
(Bromm & Clarke 2002)

Dwarf galaxies unlikely to have had recent mergers
→ old globular cluster systems?

Milky Way halo, GCS built up by accretion of dwarfs?
(e.g. Sagittarius; Searle & Zinn 1978, Cote et al 1998)

Dwarf Elliptical Galaxies (dEs)

- low-mass ($M_* < 10^{10} M_\odot$), faint ($M_B > -18$)
- gas-poor, old/intermediate age stellar pops (4-13 Gyr)
  (Geha et al 2003, Conselice et al 2003)
- highly clustered (in clusters or as satellites)
  → collapsed early, formed stars before re-ionization?
  (Tully et al. 2002)
- potentially fragile systems
  - star-formation delayed/halted by re-ionization, supernovae-driven winds, gas-stripping via tides..
  (Dekel & Silk 1986, Efstathiou 1992, Bullock et al 2000, Moore et al 1998, Kravtsov et al 2004)

Local Group dSph/dE GCS

5 Local Group dE/dSph possess globulars clusters:
dEs -- NGC 205 (7 GCs),
NGC185 (5),
NGC147 (2)
dSphs – Fornax (5), Sagittarius (4)

dSph GC <Ages> = 12-13 Gyr, <[Fe/H]> < -1.5
(few intermediate age, more metal-rich GCs, eg. Terzan 7)
Strader et al 2004, 2003, Buonanno et al 1999, da Costa & Mould 1988

GCs ~ 0.5- 1.0 dex more metal-poor than field stars
(da Costa & Mould 1988)

small number statistics → need larger sample

Extragalactic Globular Cluster Systems

galaxies with $M_* > 10^{10} M_\odot$ often have bi-modal GCS

metal-poor GC <V-I> = 0.95, [Fe/H] ~ -1.5
metal-rich GC <V-I> = 1.15, [Fe/H] ~ -0.5

metal-poor GC – "pregalactic"? (Peebles & Dicke 1968)
accreted from dwarfs? (Cote et al 1998)
multi-phase collapse?

metal-rich GC – formed in major mergers (Ashman & Zepf 1992)
multi-phase collapse
associated with bulge formation?

HST WFPC2 dE Snapshot Survey

with Bryan Miller (Gemini), Harry Ferguson (STScI)

~70 dE in the Virgo + Fornax Clusters observed in V+I
dE luminosities: $-12 < M_B < -18$

GOALS:

- detect globular clusters candidates
- calculate dE GCS specific frequency, luminosity function (Miller et al. 2001)
- study nature of dE nuclei (Lotz et al 2001)
- study dE GC colors, stellar halo colors
  Lotz, Miller, & Ferguson astroph/0406002

Globular Cluster Candidates

GCC:
0.5< V-I < 1.5,
FWHM < 2.5 pix
radius < 5 r_0

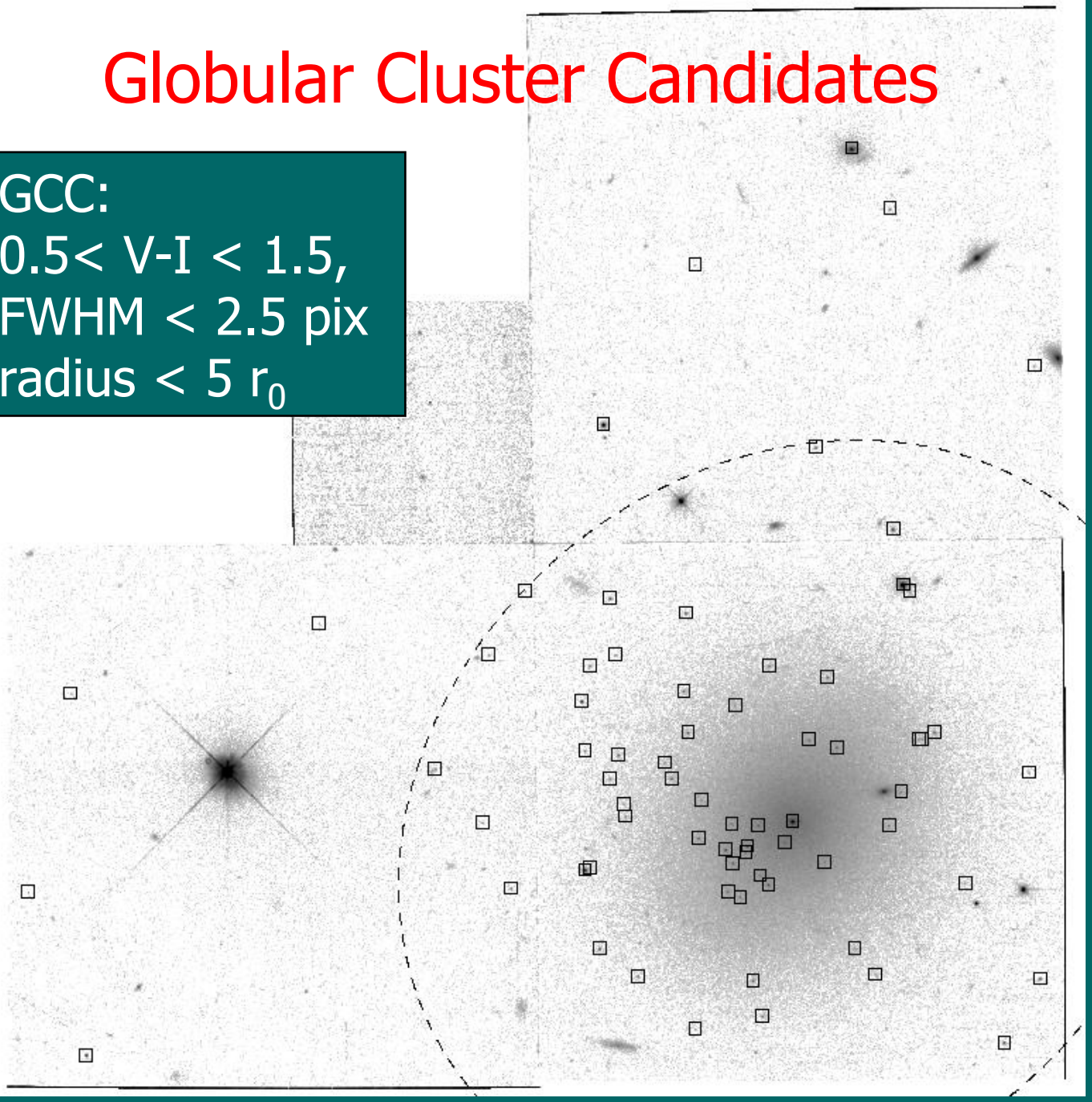

GC Color Distribution

small N_{GCC} per dE
→to correct for backgnd objects, we bin GCs by dE luminosity

GC <V-I> ≤ metal-poor GCs (0.95)

min. GC V-I consistent with Milky Way GC min [Fe/H] ~ -2.5

dE GC average color, σ
~ host dE luminosity
→ bright dEs host redder GCS

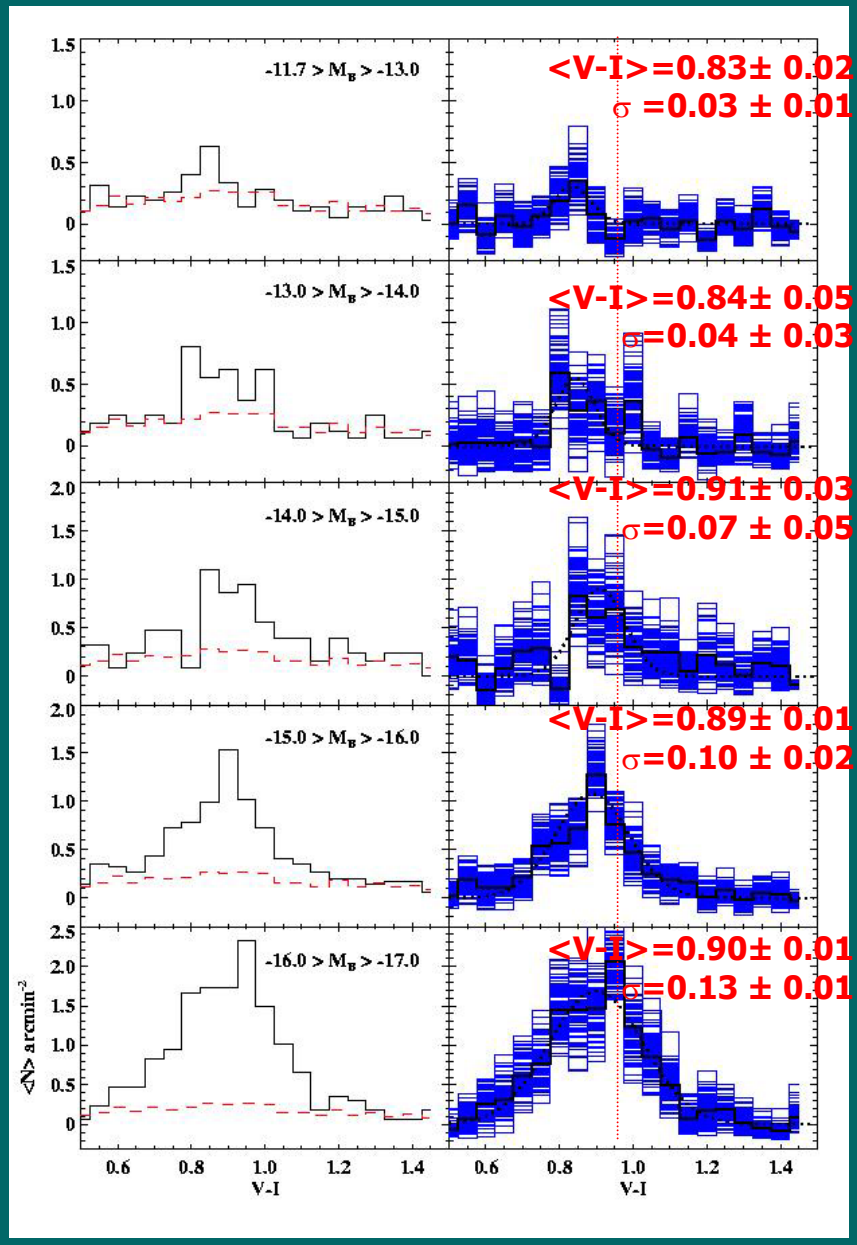

GC <V-I> v. Galaxy Luminosity

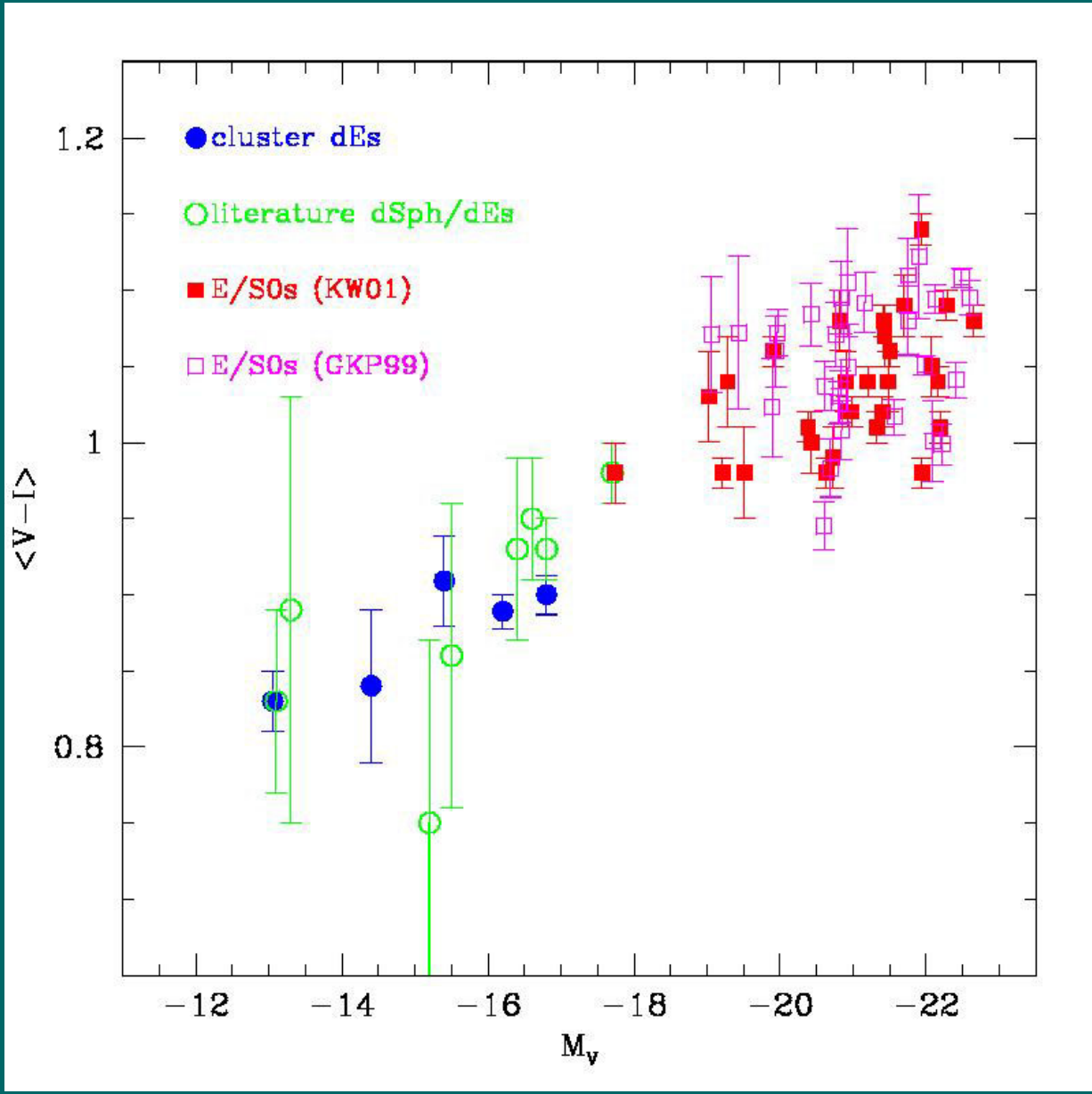

GC <V-I> v. Galaxy Luminosity

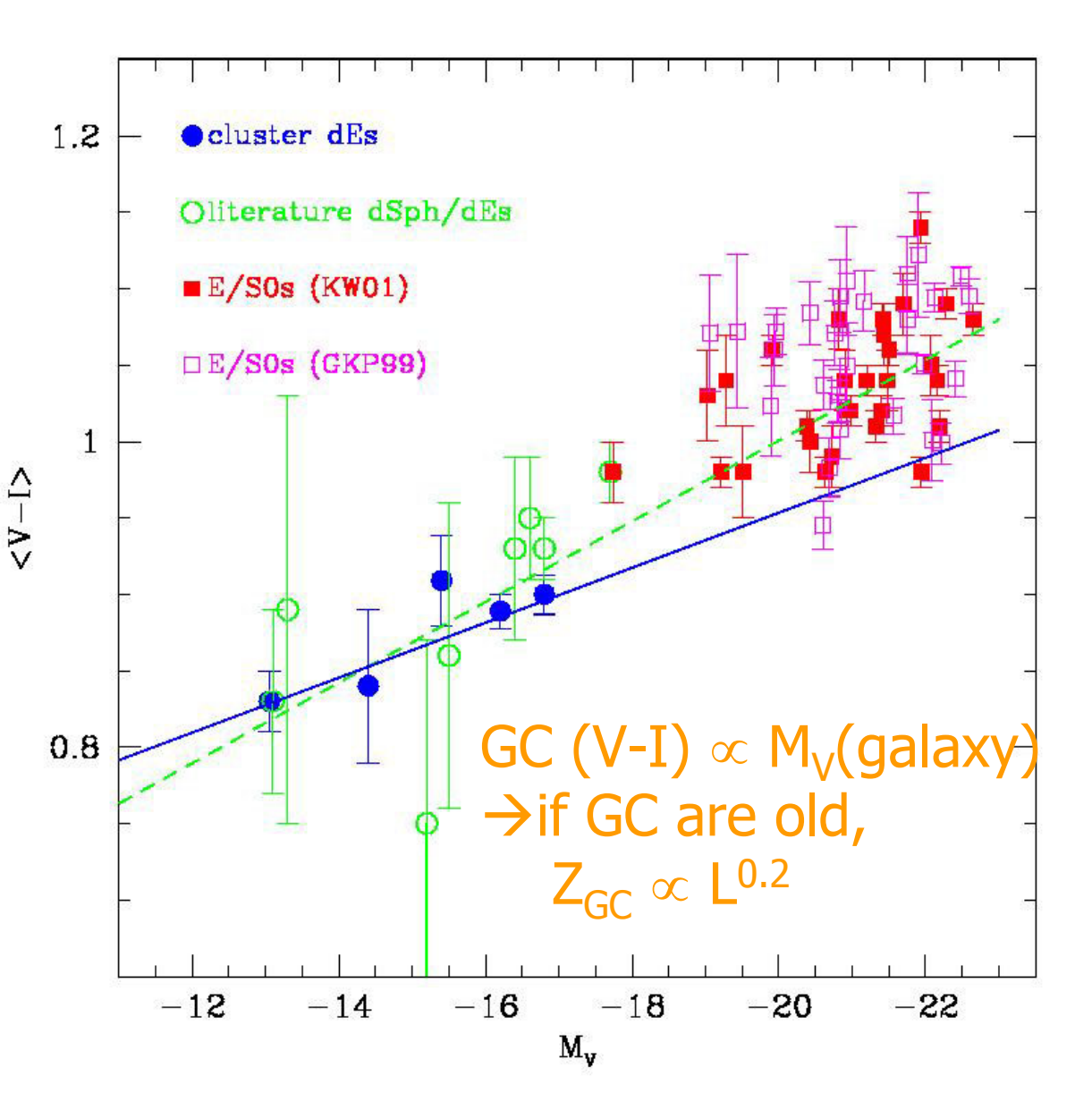

Globular Cluster Color Bi-Modality

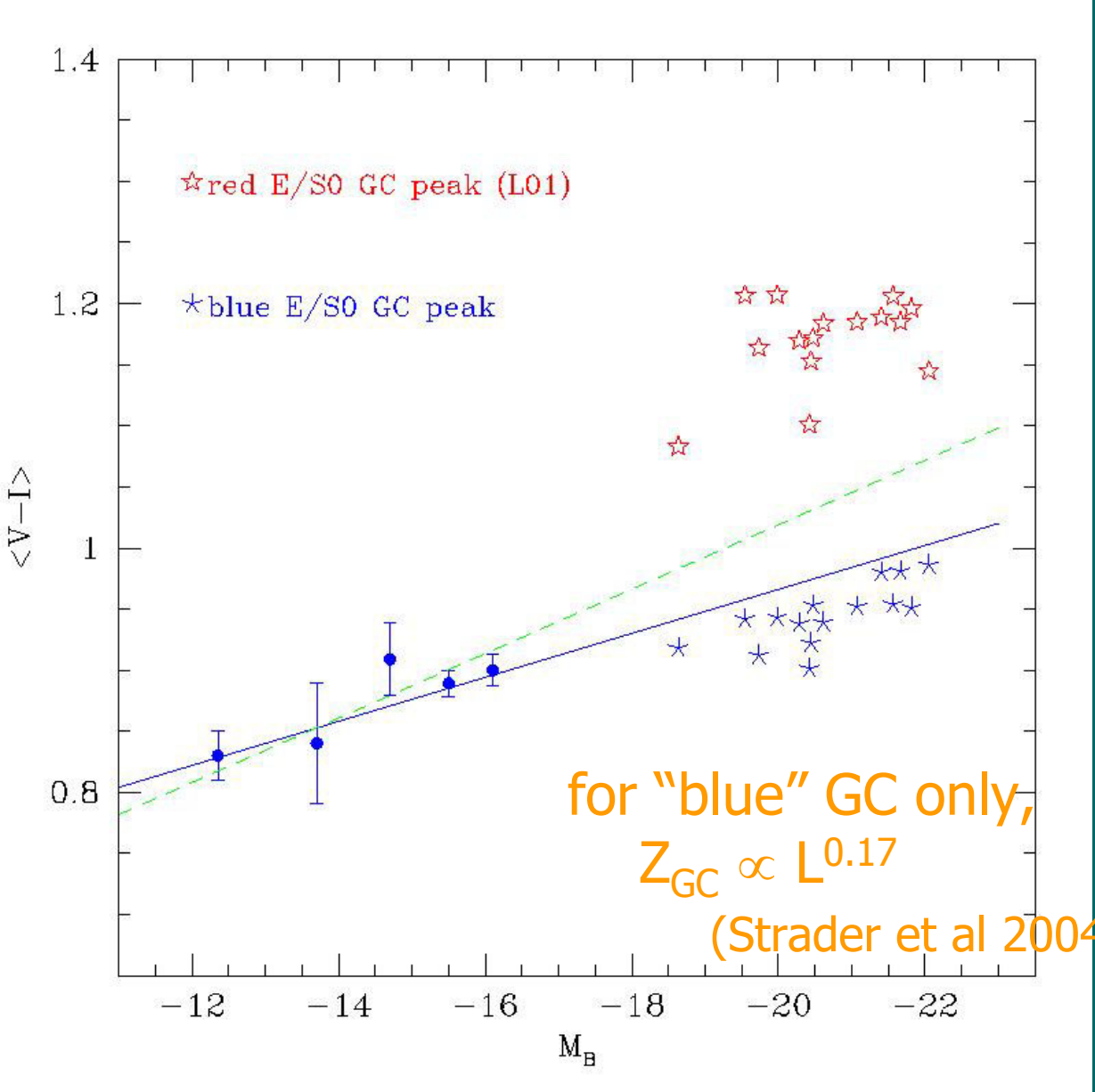

for "blue" GC only,

$Z_{GC} \propto L^{0.17}$

(Strader et al 2004)

Implications for GC enrichment

GC "know" about dE host → NOT "pre-galactic"

if GC are old →

GC [Fe/H] ~ dE luminosity ($Z_{GC} \sim L^{0.20 \pm 0.05}$)

GC σ([Fe/H]) ~ dE luminosity

blue metal-poor GCs in giant galaxies slightly redder

→ not assembled via accretion of present-day dwarfs?

GC vs. Field Star Colors

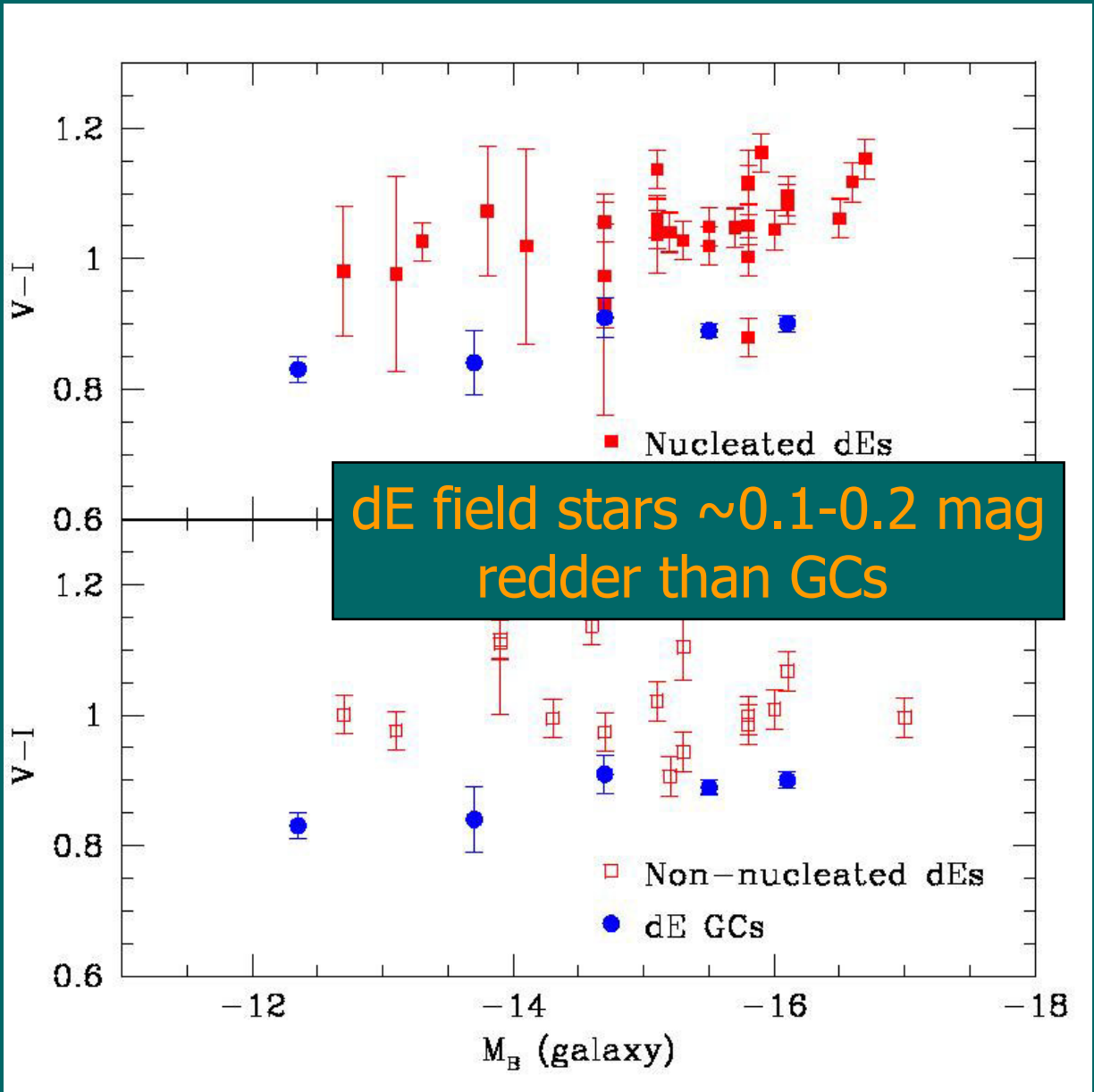

dE field stars ~0.1-0.2 mag redder than GCs

dE Field Star [Fe/H] vs. Luminosity

Local Group dSph/dE $Z_{FS} \sim L^{0.4}$

→ supernovae-wind metal loss (Dekel & Silk 1986, Dekel & Woo 2003)

if dE field stars are roughly coeval with GCs,

<V-I> ~ 1.05 → dE [Fe/H] ~ -0.8

→ ≥ 0.5 dex more metal-rich than GCs

Virgo dE/Local Group dSph

[α/Fe] <~ solar (Geha et al 2003,Tolstoy et al 2003)

→ star-formation epoch > 1 Gyr (SnI enrichment)

dE $Z_{GC} \sim L^{0.2}$ → different chemical enrichment process?

dE Nuclei

compact, bright star-clusters in dE centers
-- HST WFPC2 resolution → size < 10 pc

Nuclei are *bluer* than dE field stars
+ marginally redder than GCs (<V-I> = 0.98)

Several nuclei are very blue (like NGC205)
→ages ~ 1 Gyr

Some nuclei are old massive globular clusters?
or later generation of stars (young, metal-rich)

dE Nuclei

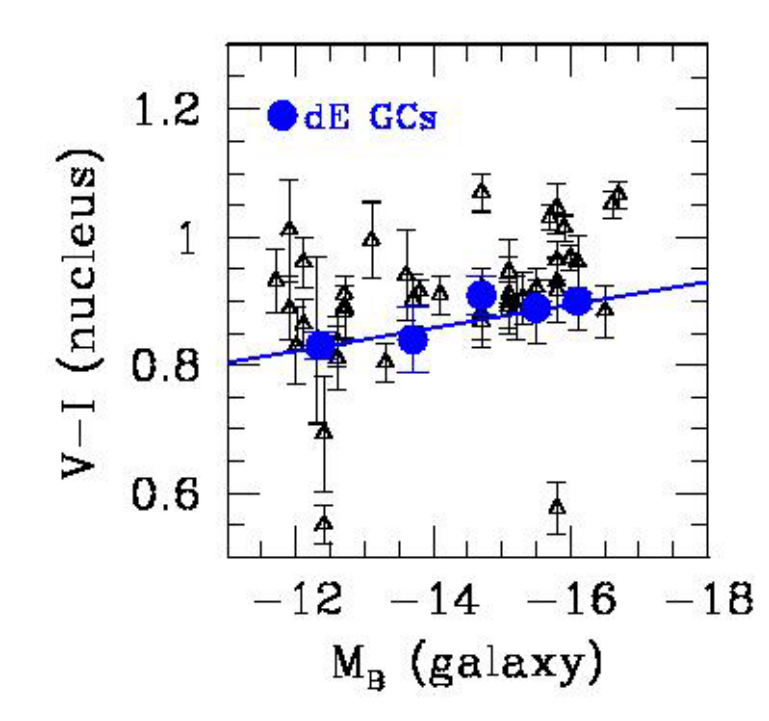
dE GCs
V−I (nucleus)
1.2
1
0.8
0.6
−12
−14
−16
−18
M_B (galaxy)

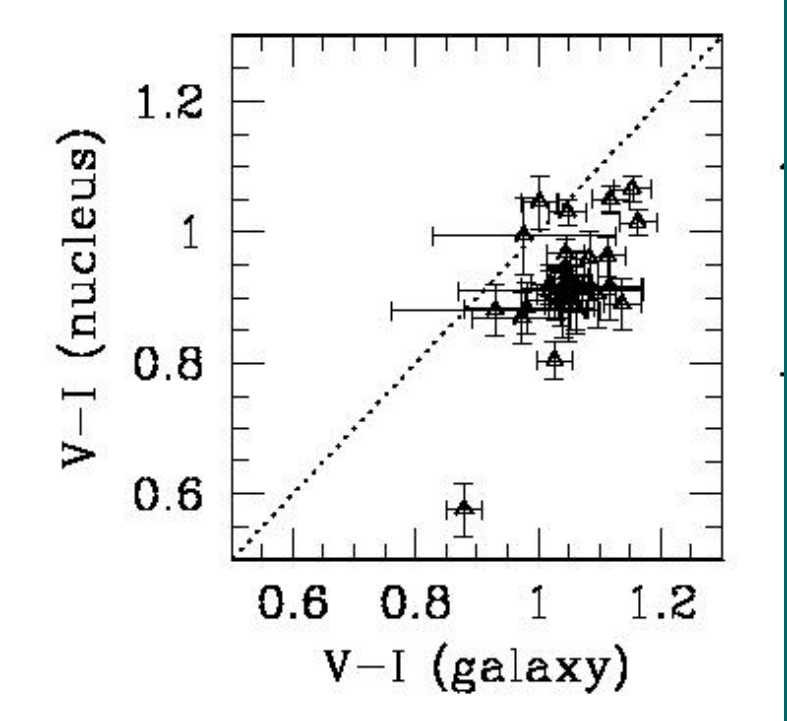
V−I (nucleus)
1.2
1
0.8
0.6
0.6
0.8
1
1.2
V−I (galaxy)

Summary

- dE GCS colors ~ dE luminosity
  → dE GCs are formed in proto-dE halos
  not "pre-galactic" (Peebles + Dicke 1968)
- if most dE GCs are old, then
  $Z_{GC} \sim L_{galaxy}^{0.20 +/- 0.05}$
- dE field stars are redder than GCS
  → GC and field stars formed in separate events
- Local Group dSph $Z_{FS} \sim L^{0.4}$ (supernovae winds)
  → GC chemical enrichment significantly different

Questions...

Why the difference in colors/chemical enrichment of dE GCS and dE field stars?

→ metal-poor GC formed prior to re-ionization and/or strong SN wind feedback ?

Why no (few) metal-rich GCs in galaxies < 10^{10} $M_{\odot}$?

→ GC production/survival in dwarfs much lower at later times

Is this related to bi-modality in GC for "giant" galaxies?

GMOS Spectroscopy of dE GC Systems

with Bryan Miller (Gemini), Michael Hilker (Bonn),
Markus Kissler-Patig (ESO), Thomas Puzia (STScI)

Goals:

confirm GC membership in galaxies

kinematics (rotation, velocity dispersions, M/L

ages/metallicities from line ratios

Sample:

4 of the brightest dE,N with largest numbers of GCs

First Results – candidate confirmation

FCC136

8 candidates + Nuc with 1000 km/s $<V_{obs}<$2500 km/s

4 GCs within 200 km/sec and 1 kpc of nucleus

σ(r<1kpc) ~ 54 km/sec

No evidence of rotation

2 candidates at radii up to 7 kpc

20 arcminutes from NGC1379

First Results – candidate confirmation

FCC1

8 ca

4 G

2 ca

20 a

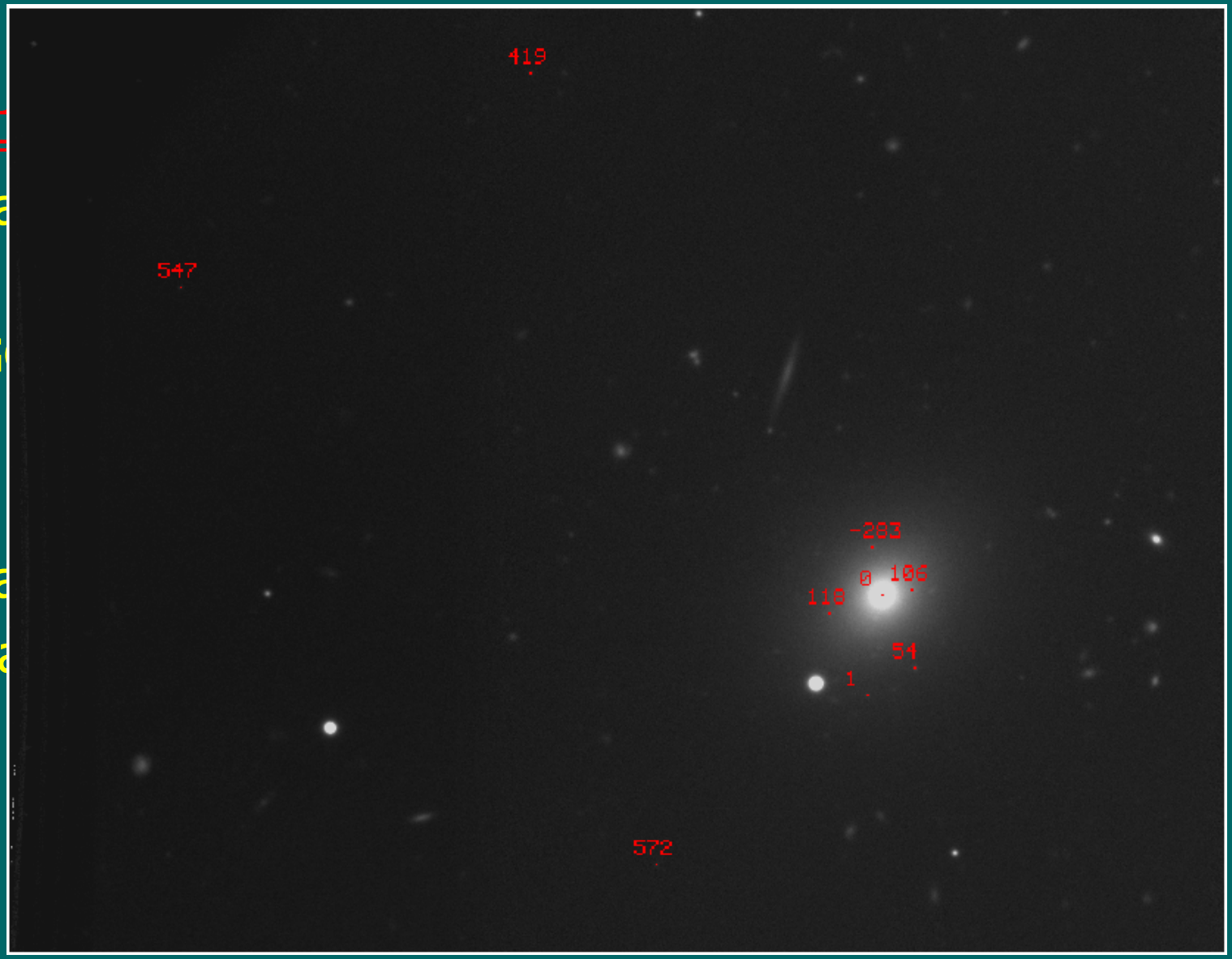

Global Nuclear Structure Calculations for Astrophysics, Recent Developments

Peter Möller
Nuclear Physics Group, T-16
Theoretical Division
Los Alamos National Laboratory
(LA-UR-04-3849)

Slide layout by Alexander Heger

Comparison of the FRDM (1992) mass model to (published) new experimental data that was not known when the model was published. The model actually agrees **better** with the mass data that was unknown at the time of publication.

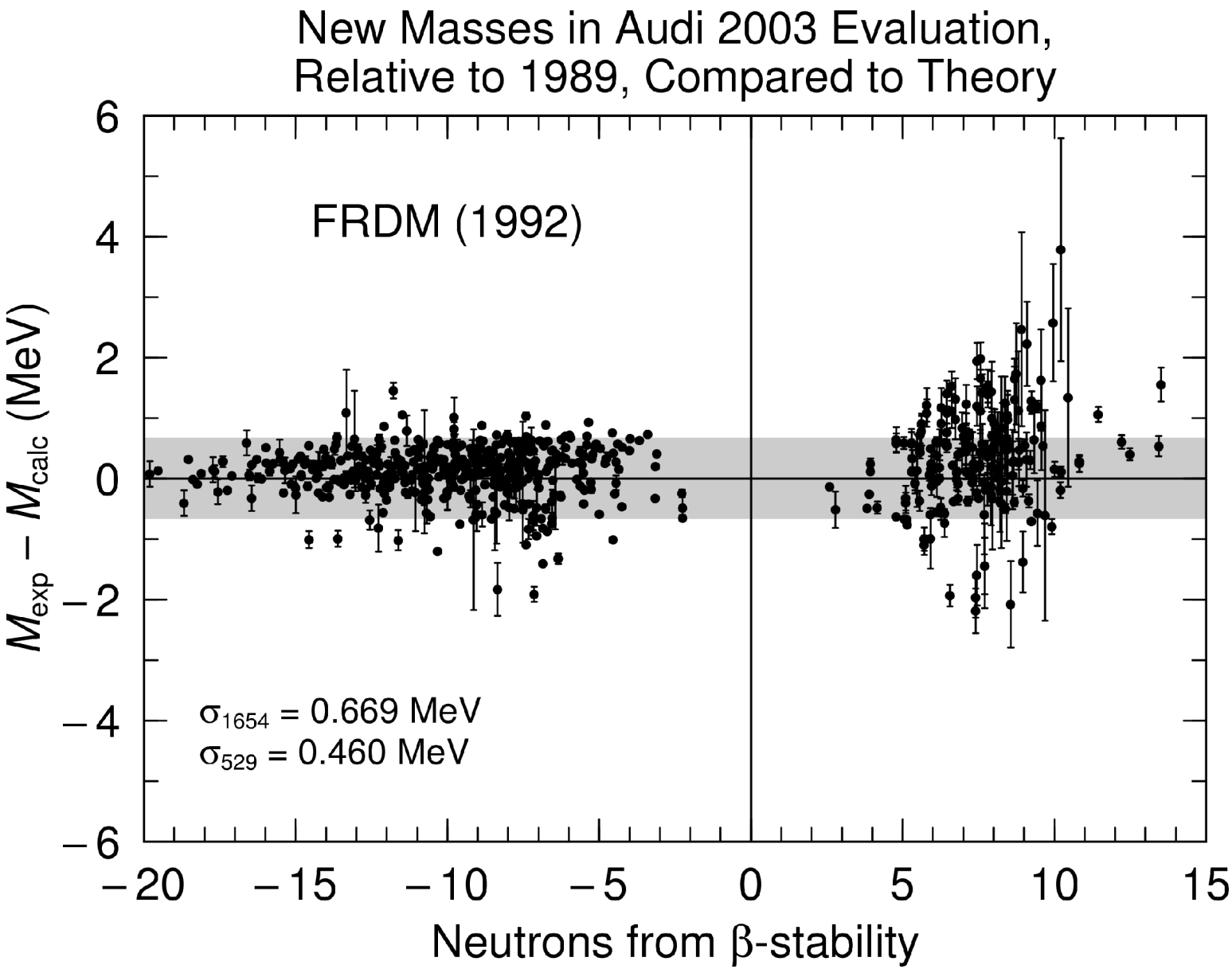

Comparison of calculated beta-decay half-lives and delayed neutron-emission probabilities to experimental data.

The figures are from Physical Review C 67 (2003) 055802

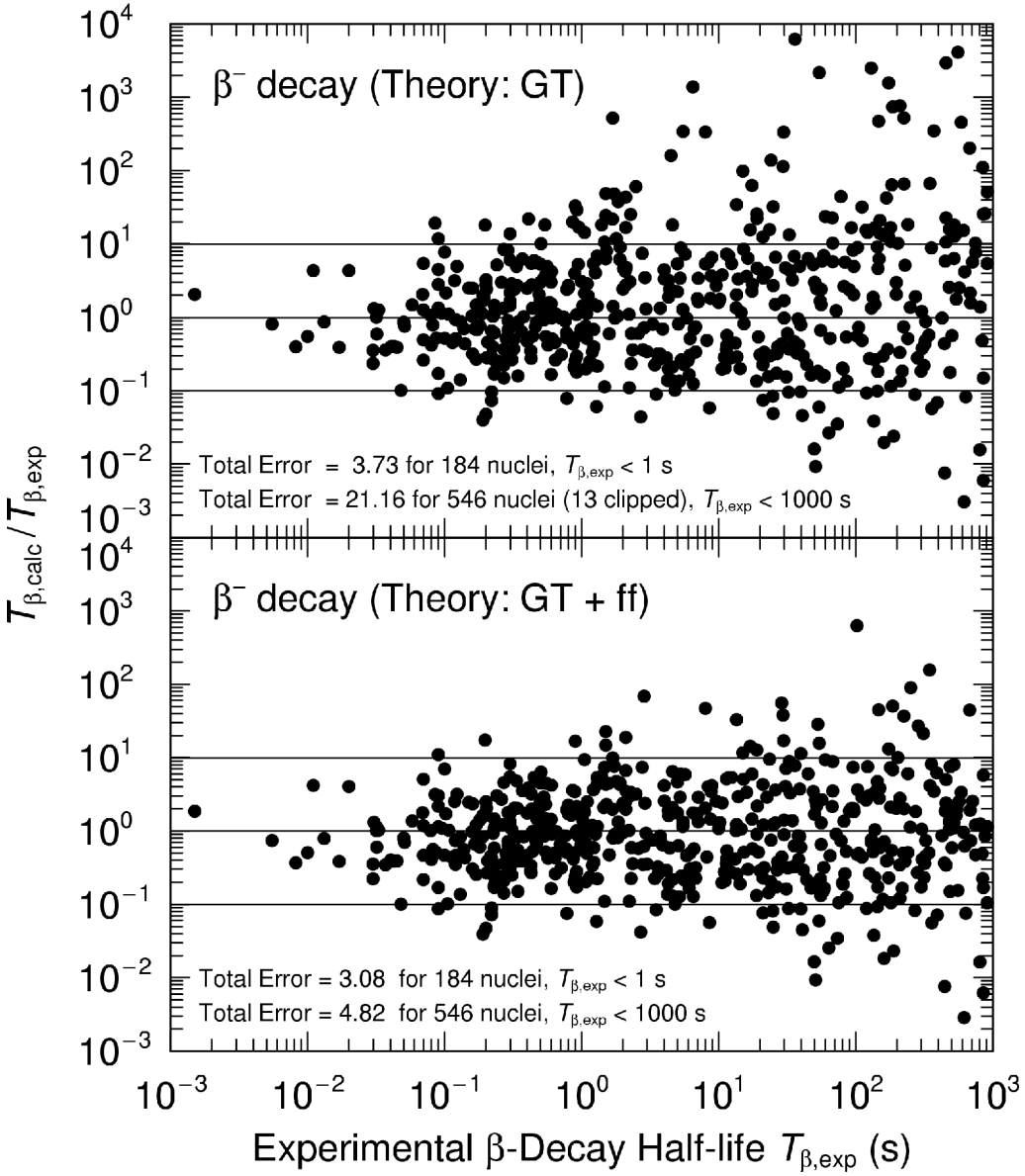

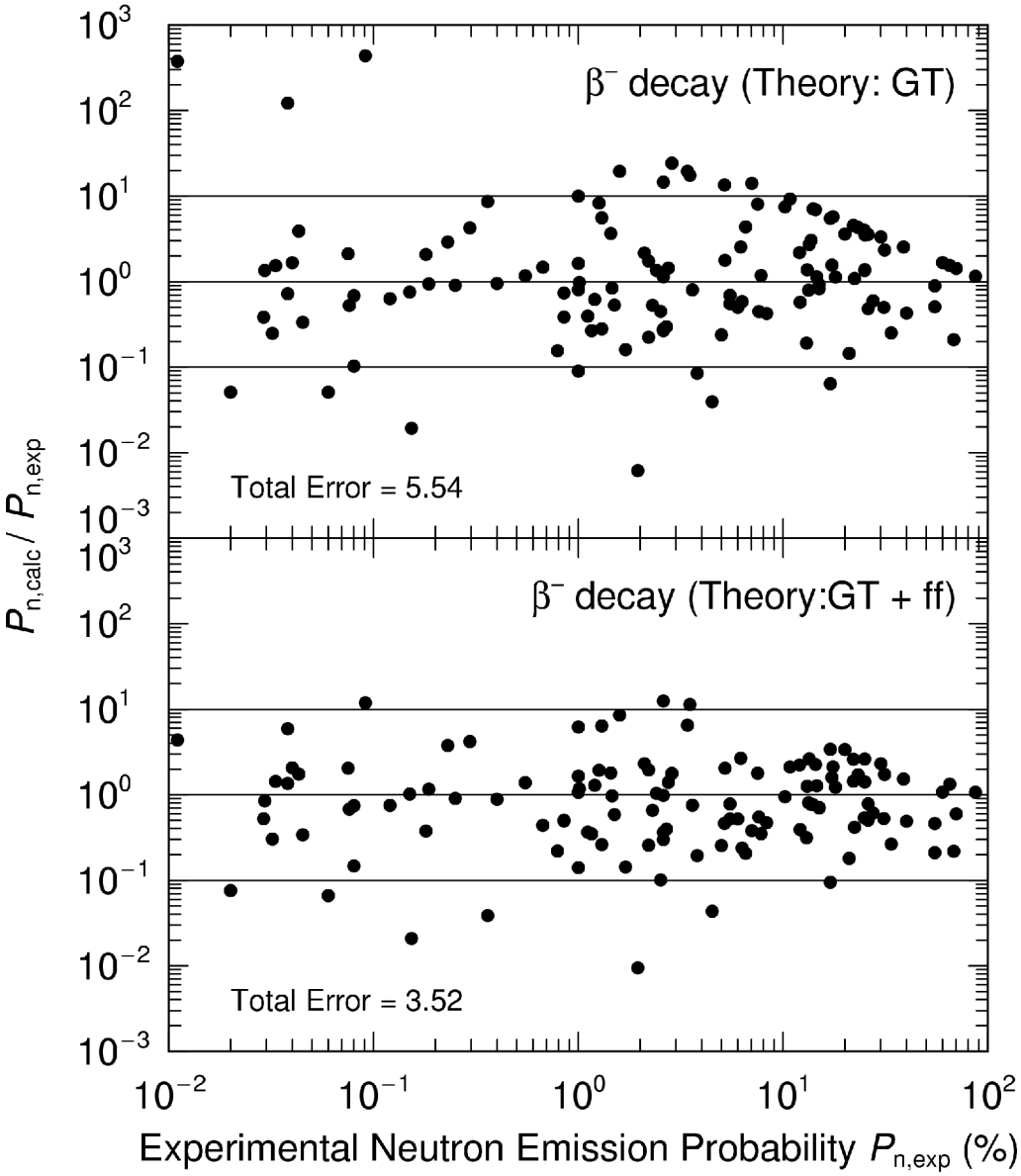

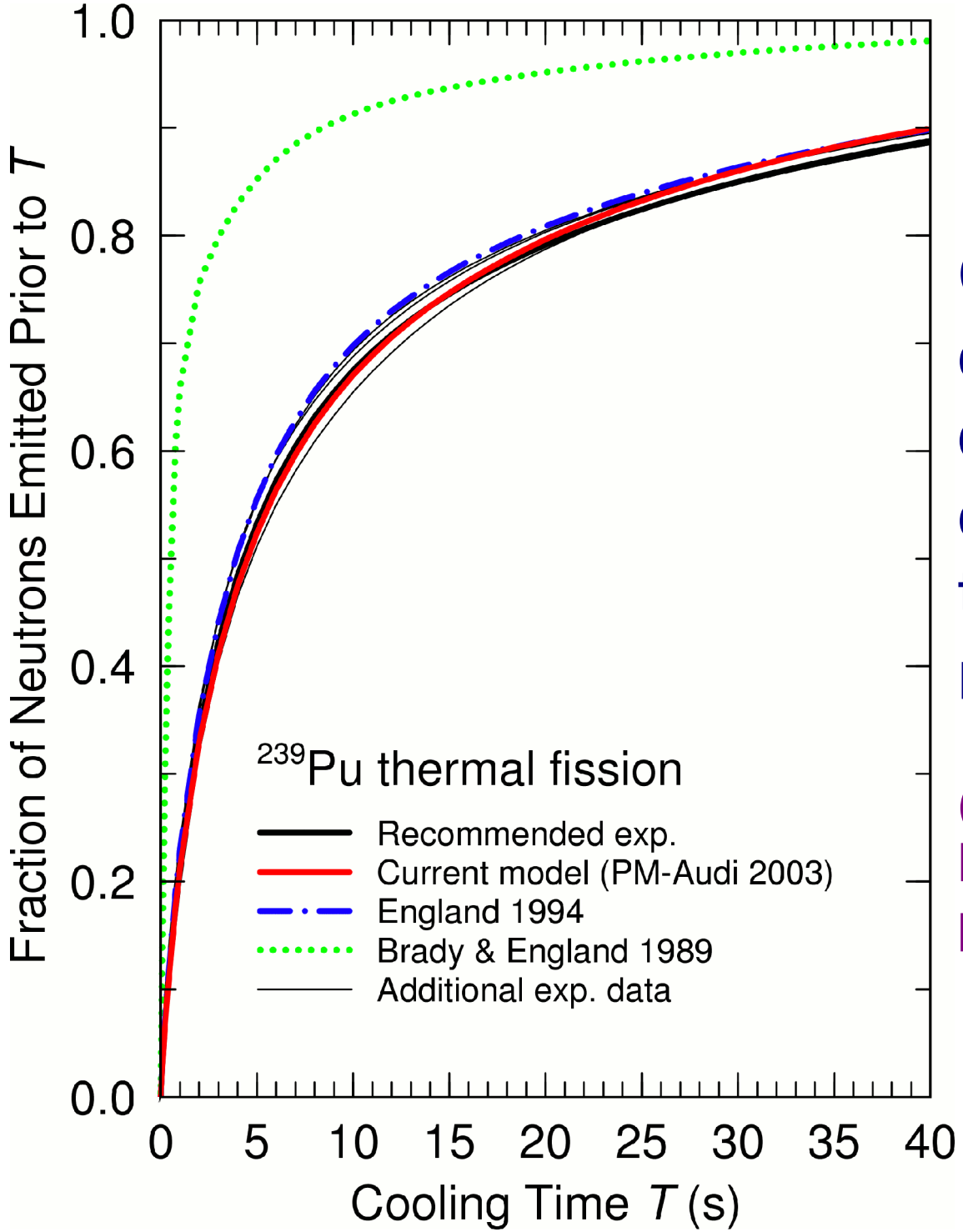

Comparison of various experimental data for delayed neutrons emitted after a pulse of thermal neutrons in a reactor to calculations

(similar to figures in LA-UR-03-0001, pages 56 forward)

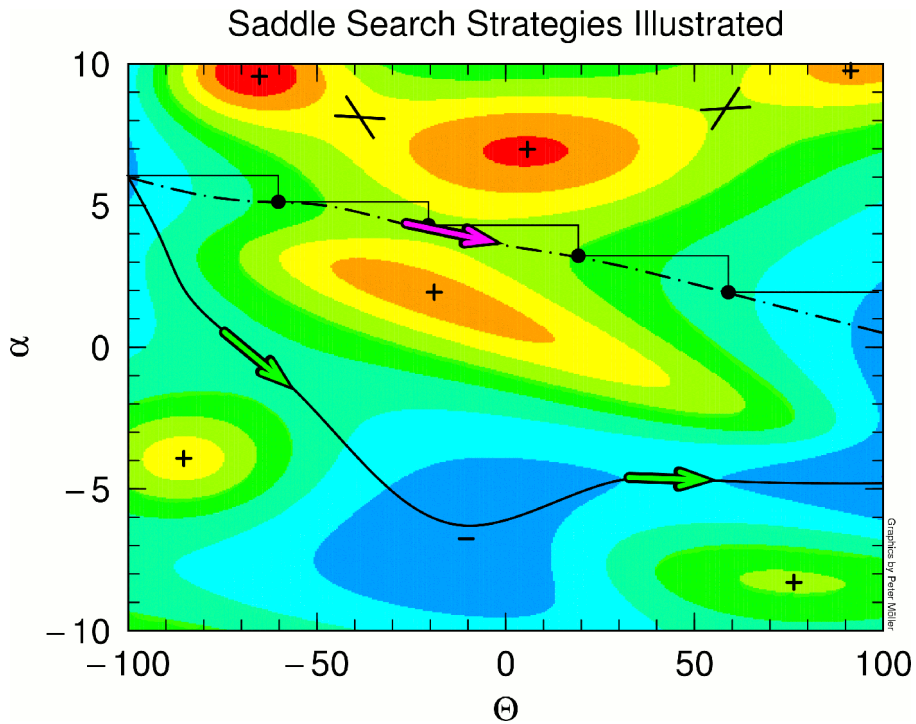

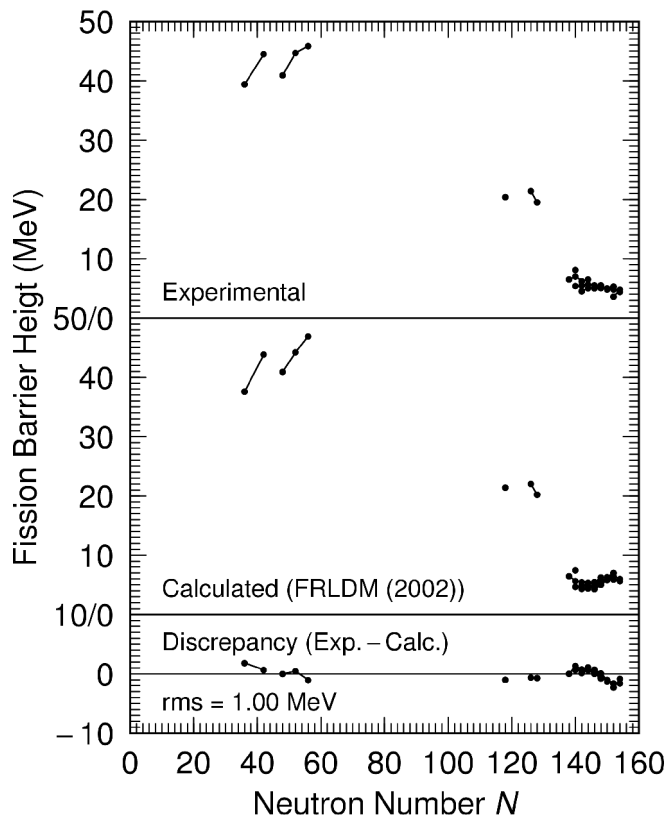

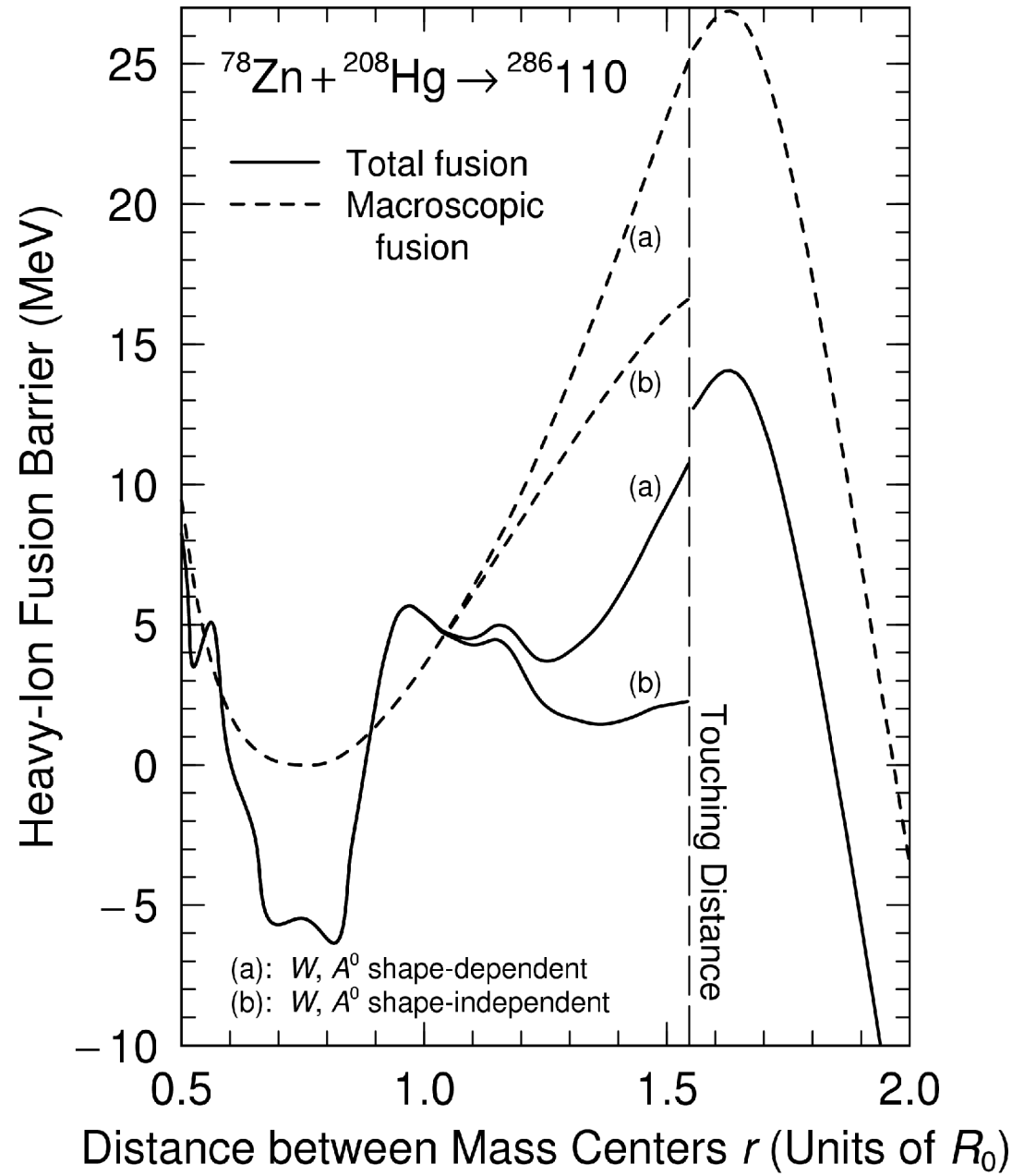

Figures 9-11 from Physical Review Letters 92 (2004) 072501

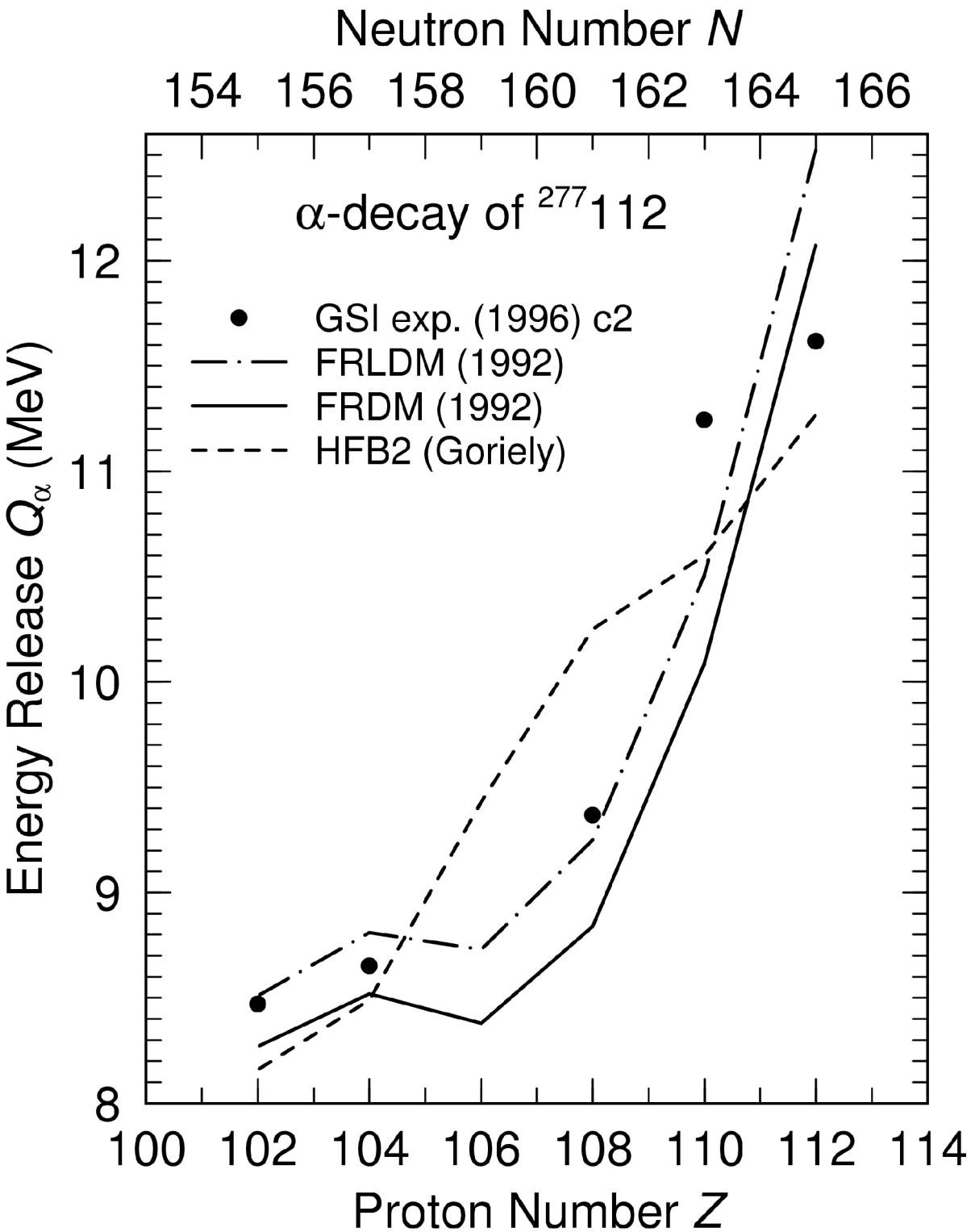

Comparison of observed Q-alpha decay energies in the decay chain of element 112 with calculated values. The calculated values are obtained from mass differences in three mass models. The HFB2 model does not reproduce the kink in the data which is a manifestation of increased stability (shell gaps) near Z=108-110 and N = 162.

Nucleosynthesis in Hypernovae and Abundance Patterns of Extremely Metal Poor Stars

GRB030329/SN 2003dh

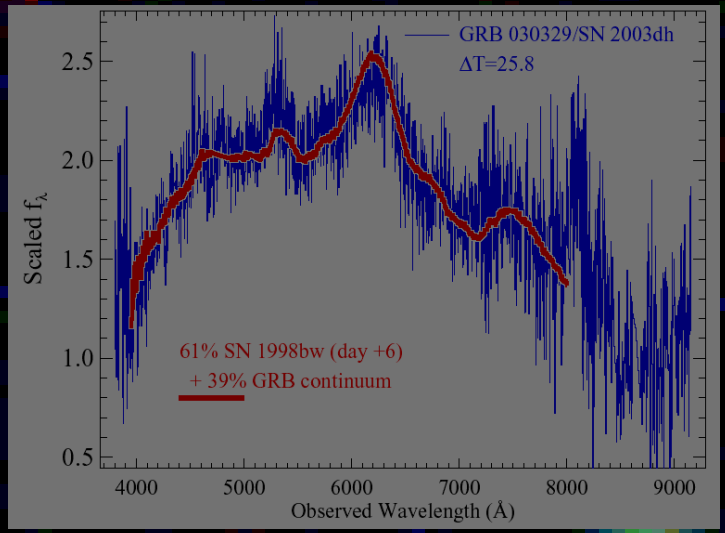

K. Nomoto (Univ. of Tokyo)

The First Stars ?

- **First Stars (IMF ?)** ⇨ **Reionizing Source**

⇩

- **First Supernovae** (Type II, Ibc, Hypernovae, Pair)

⇩

- **Metal-Enrichment**

⇩

- **Abundance Ratios @high z, low Z**
  - EMP (Extremely Metal-Poor) Stars: Halo, dSph
  - DLA, ICM, …
  - **α-elements: [(C, N, O, Mg, Si, Ca)/Fe], [Si/O]**
  - **Fe-peak elements: [(Ti, Cr, Mn, Co, Ni, Zn)/Fe]**
  - **R-process, s-process elements**

The First Stars ?

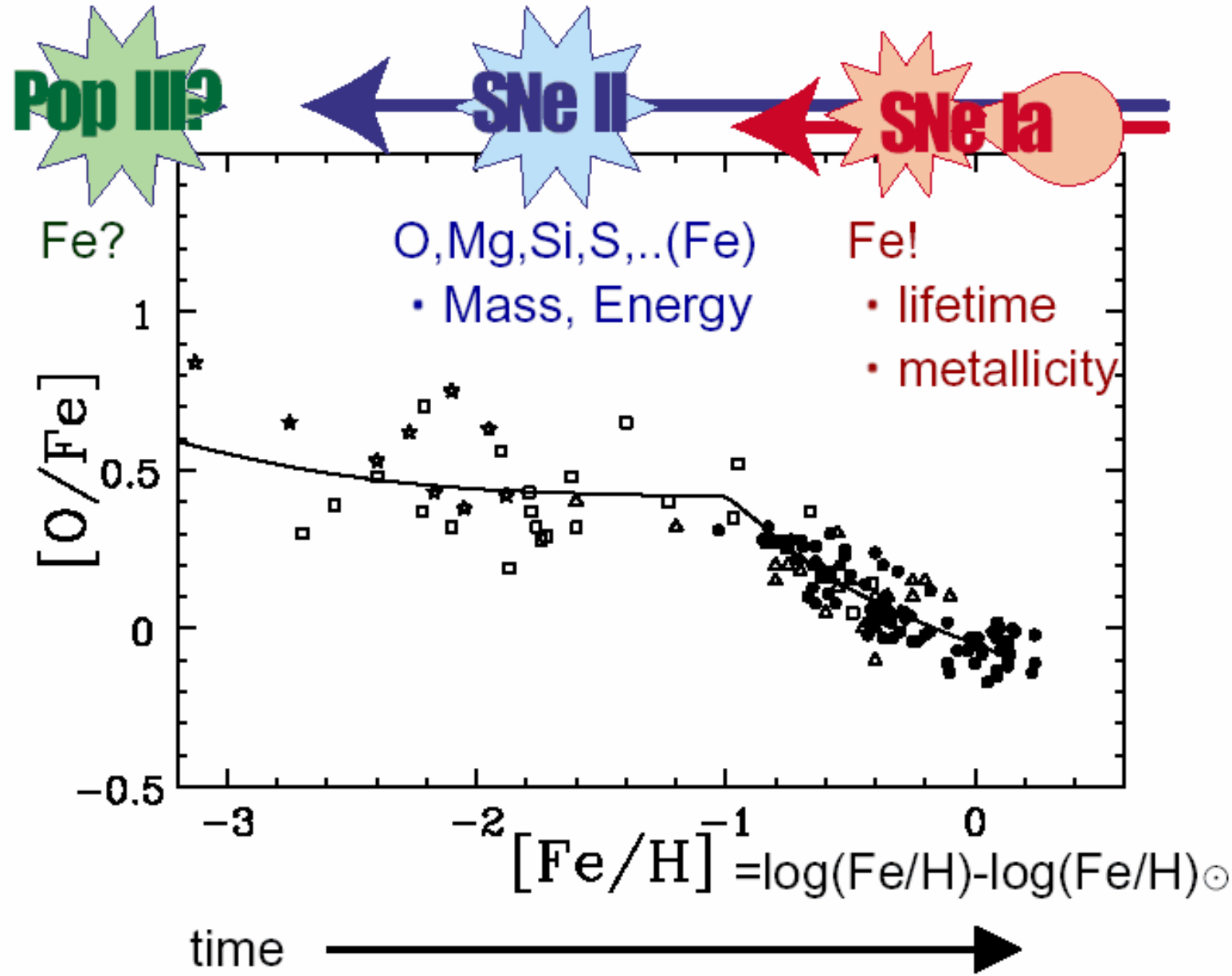

McWilliam, Ryan

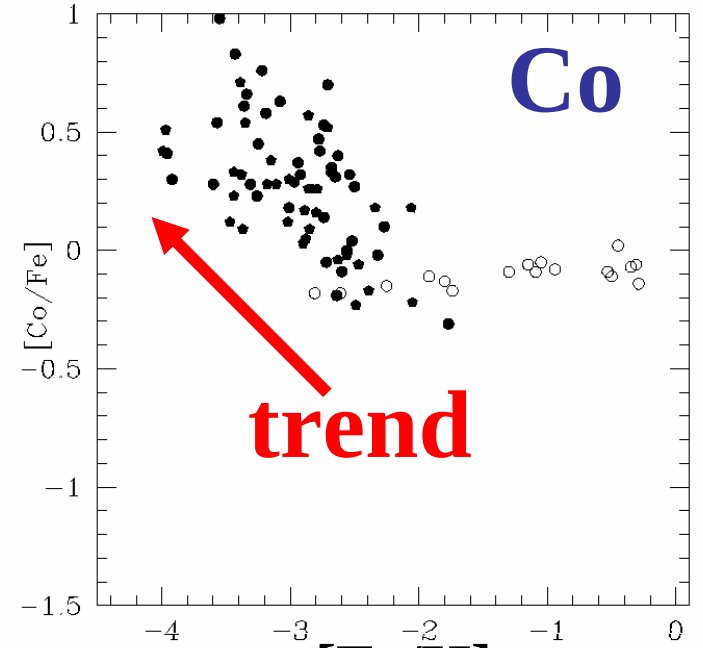

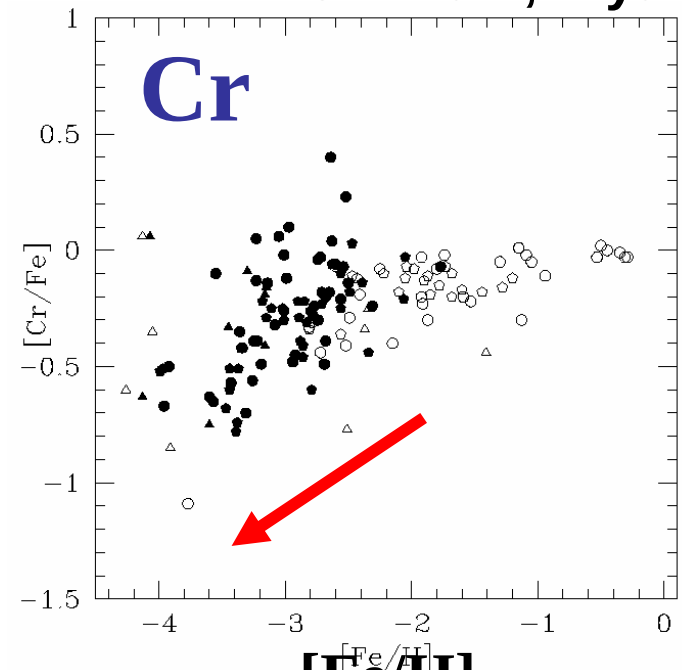

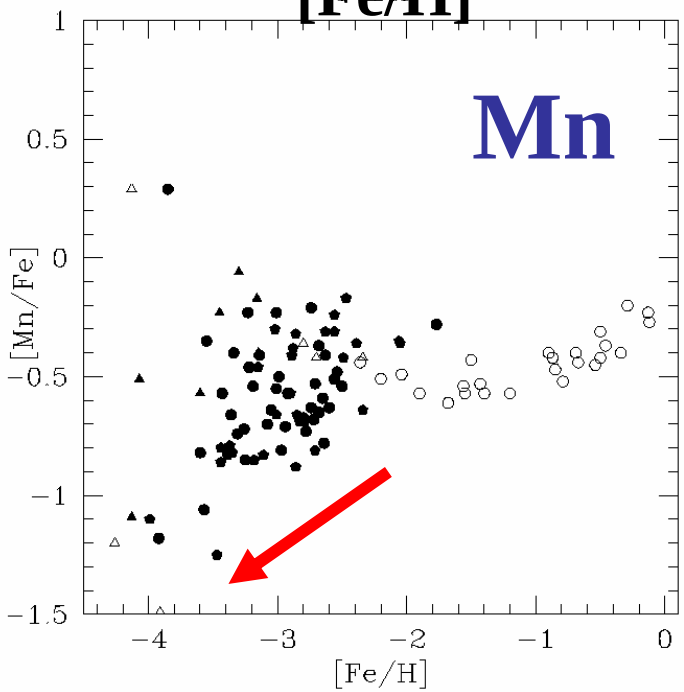

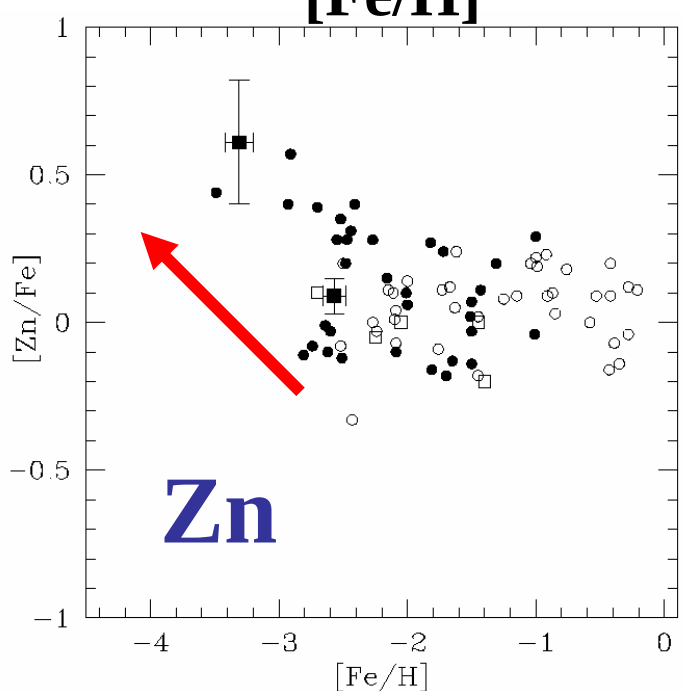

[Zn/Fe]: Cayrel et al. (2003)

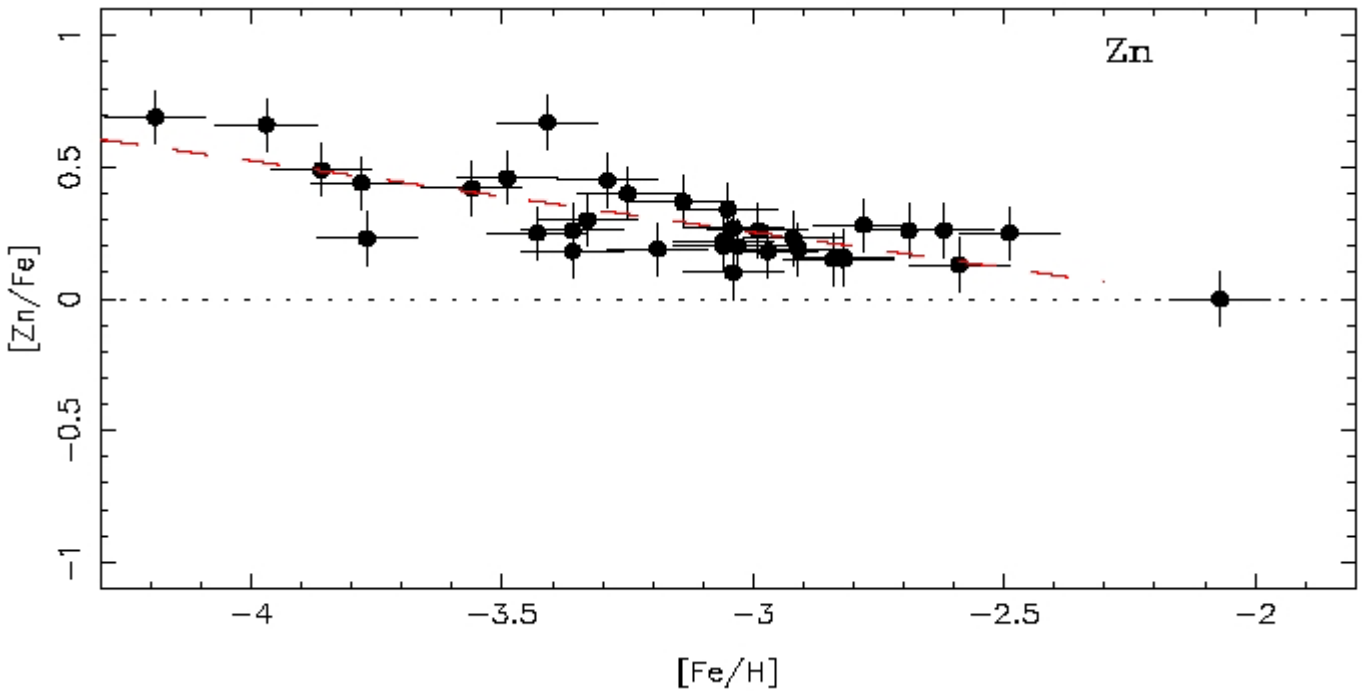

C-rich EMP Stars

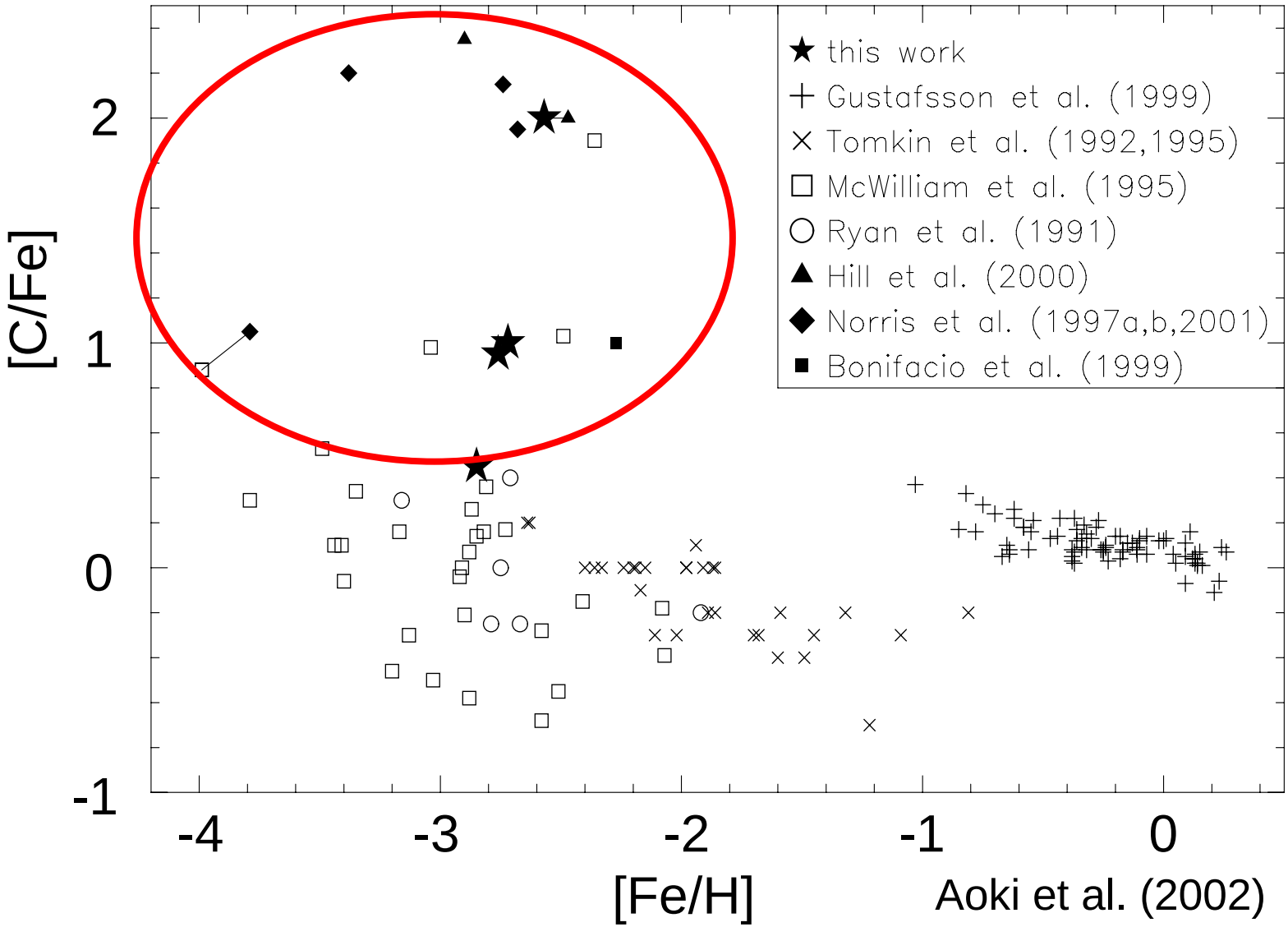

Aoki et al. (2002)

The most Fe-poor star: HE0107-5240

- Discovery : Oct 31,2002 (Christrieb et al, Nature)
- Red-giant, about 0.8 $M_{\odot}$
- [Fe/H] ~ -5.3
- Quite unusual abundance ratios:e.g., [C/Fe] ~ +4
- Is this star Pop III (first generation) or Second generation?

  --- Pop III Low mass Star formation is predicted to be inefficient in the typical (simplest?) star formation theory.

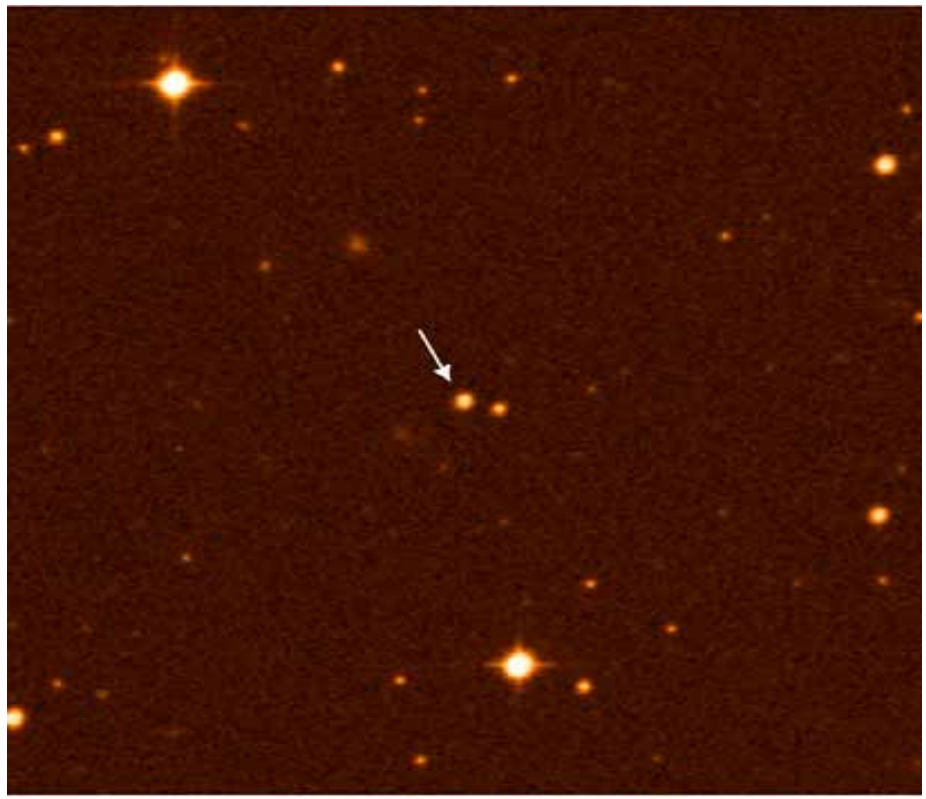

The Very Metal-Deficient Star HE 0107-5240

ESO PR Photo 25a/02 (30 October 2002)

©European Southern Observatory

The First Star Candidates

$M > 10^5 M_\odot$: SMS (Super Massive Stars)

→ GR instability → Collapse

$M \sim 300 - 10^5 M_\odot$:

→ Collapse

$M \sim 130 - 300 M_\odot$:

→ Pair Creation Instability

→ Nuclear Explosion

$M \sim 8 - 130 M_\odot$:

→ Fe core Collapse → **Hypernovae ?**

→ **SNe II**

Hypernova Candidates

$E_{kinetic} > (5\text{-}10) \times 10^{51}$ ergs

SNe Ic	
SN	GRB
1998bw	980425
1997ef	(971115)
2002ap	
2003dh	030329
2003lw	031203
1997dq	
1998ey	
1992ar	

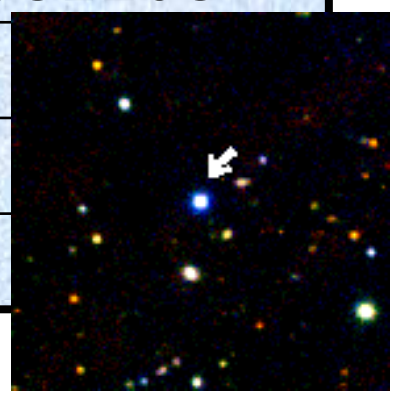

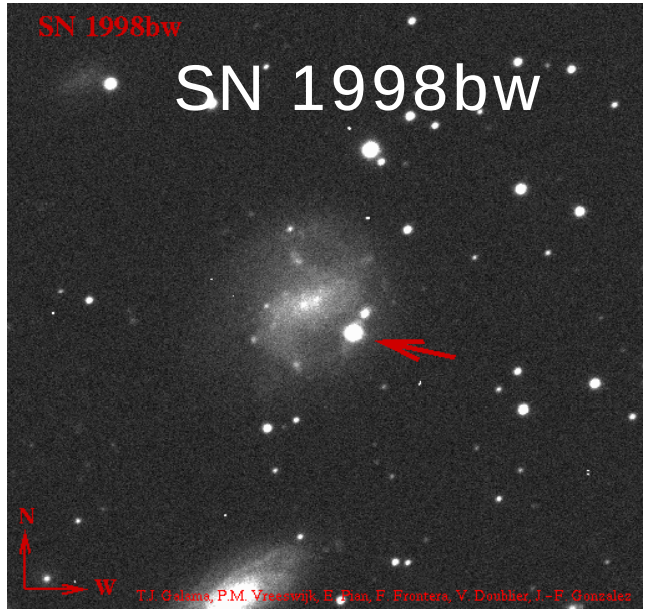

Spectra of Supernovae & Hypernovae

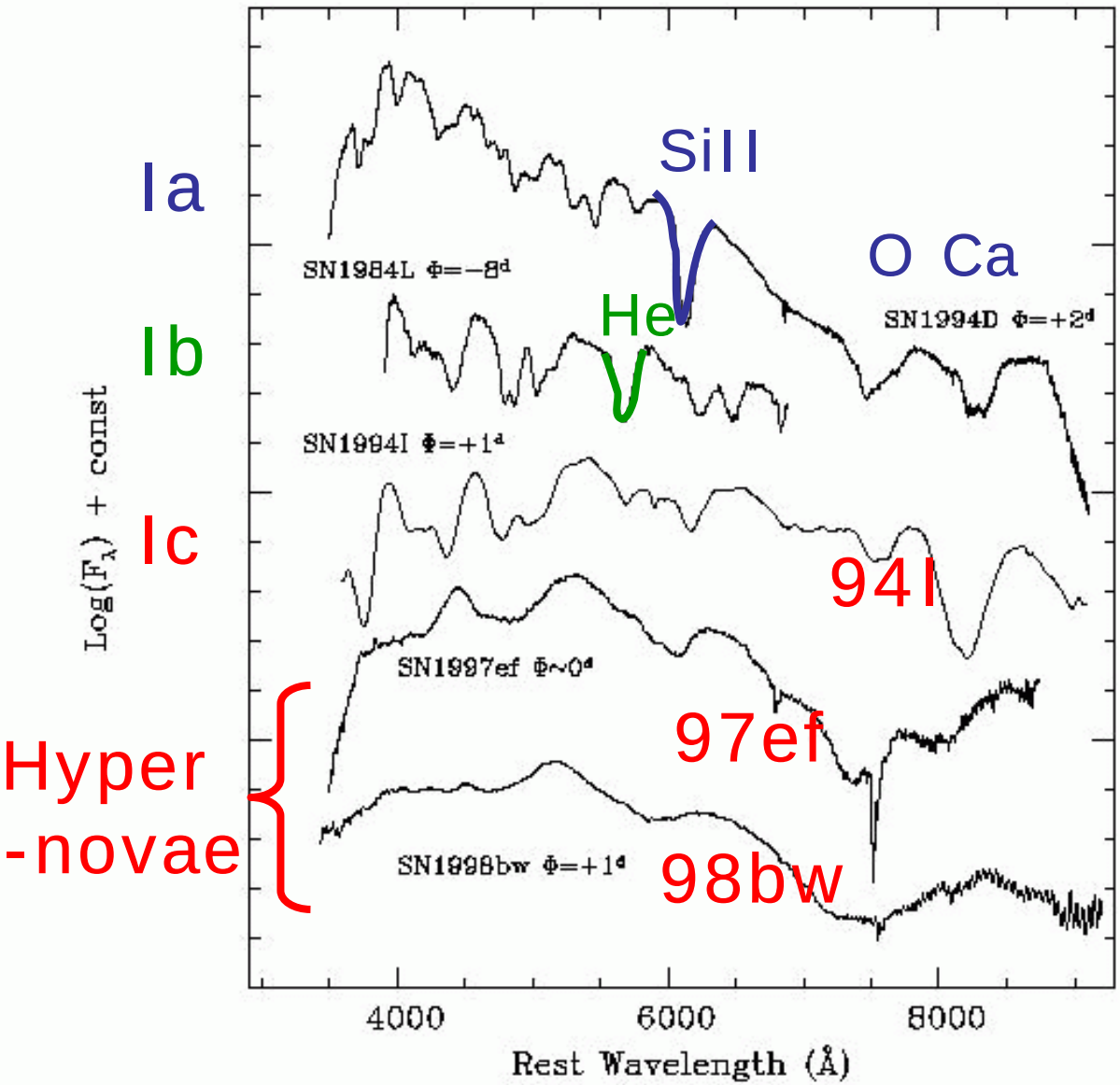

Ic: no H,

no strong He,

no strong Si

Hypernovae:

broad features

↑

blended lines

↑

"Large mass at high velocities"

^{56}Co-decay

$$^{56}\mathrm{Ni} \xrightarrow[6.6\mathrm{d}]{\gamma} {}^{56}\mathrm{Co} \xrightarrow[78\mathrm{d}]{\gamma} {}^{56}\mathrm{Fe}$$

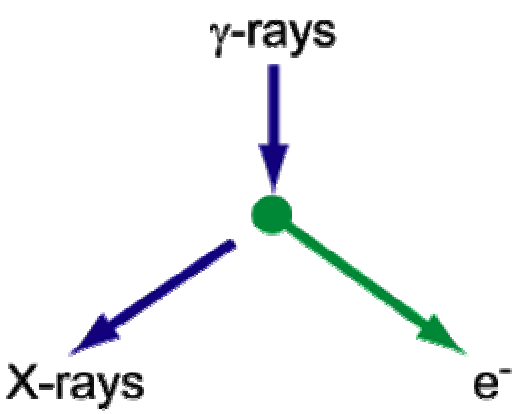

Photoabsorption Excitation/Ionization

$$\begin{cases} L \propto M(^{56}\mathrm{Ni}) \\ \mathrm{Shape}: M_{ej} \end{cases}$$

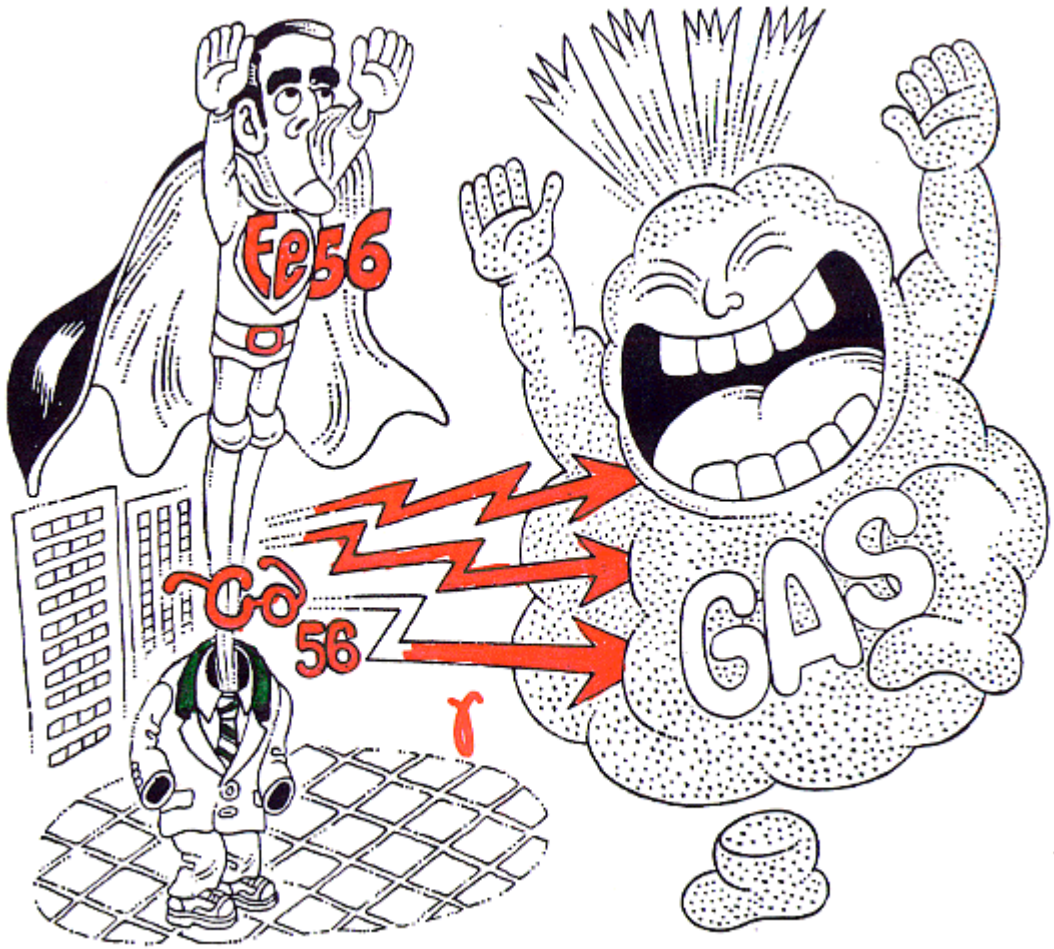

© Haruyo Nomoto

CO Star Models for SNeIc

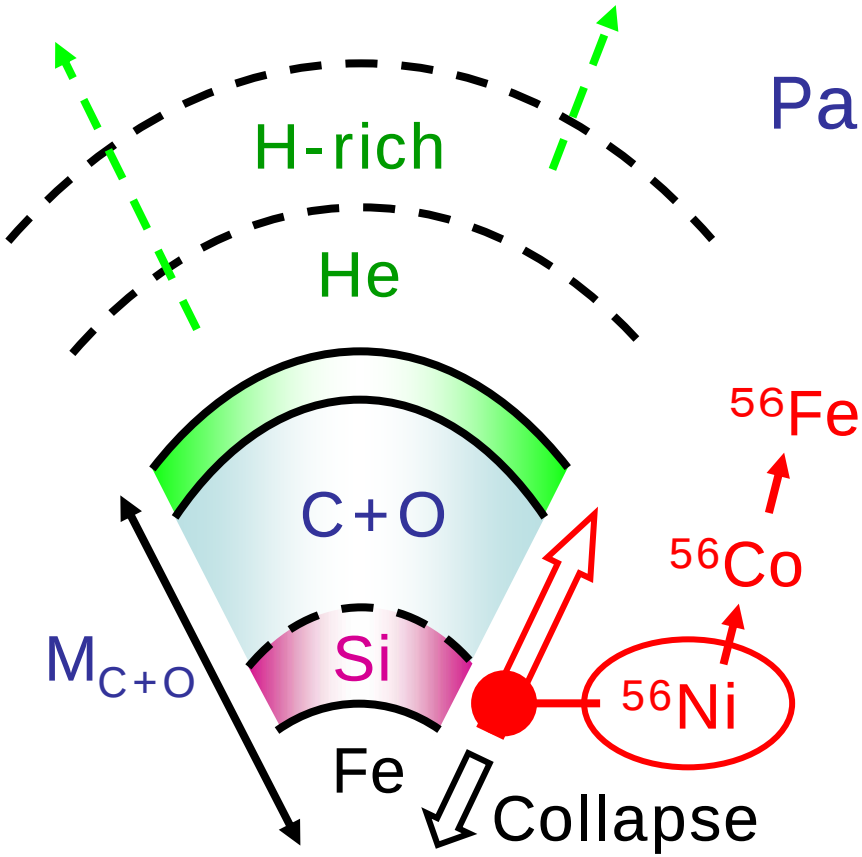

$M_{ms}/M_\odot$	$M_{C+O}/M_\odot$
~ 40	13.8
~ 35	11.0
~ 22	5.0

Parameters [M_{ej}, E, M(^{56}Ni)]

Light Curve | Spectra

$$\tau \sim [\tau_{dyn} \bullet \tau_{diffusion}]^{1/2}$$

$$\sim \left(\frac{R}{V} \bullet \frac{\kappa M_{ej}}{R\ c}\right)^{1/2}$$

$$\propto \kappa^{1/2} M_{ej}^{3/4} E^{-1/4}$$

$E \propto M_{ej}$

$E \propto M_{ej}^3$

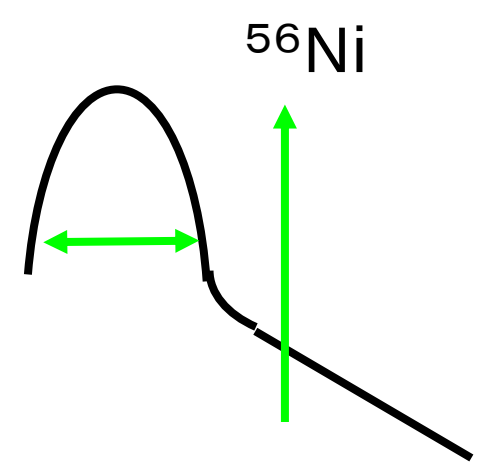

Spectral Fitting: SN1997ef

Iwamoto et al. 2000

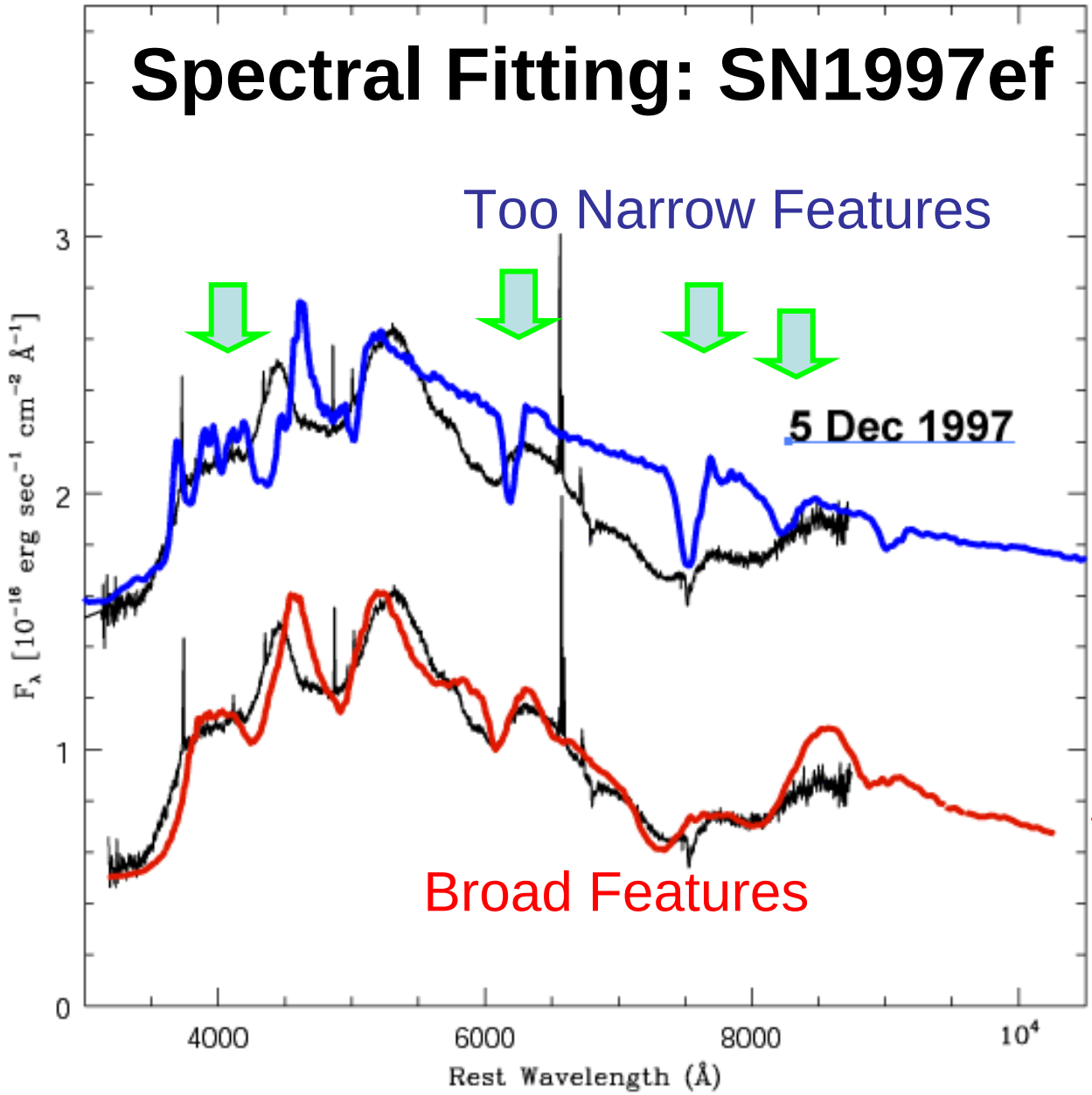

Normal SN
(**E_{51}=1**)

Small M_{ej}

Hypernova
(**E_{51}=20**)

Large M_{ej}
at High Vel.

Light curves of Hypernovae & SNeIc

C+O Star Models			
	98bw	97ef	94I
M_{ms} ($M_\odot$)	40	35	15
M_{C+O} ($M_\odot$)	13.8	10.0	2.1
E_K (10^{51}erg)	30	20	1
$M(^{56}Ni)$ ($M_\odot$)	0.5	0.15	0.07

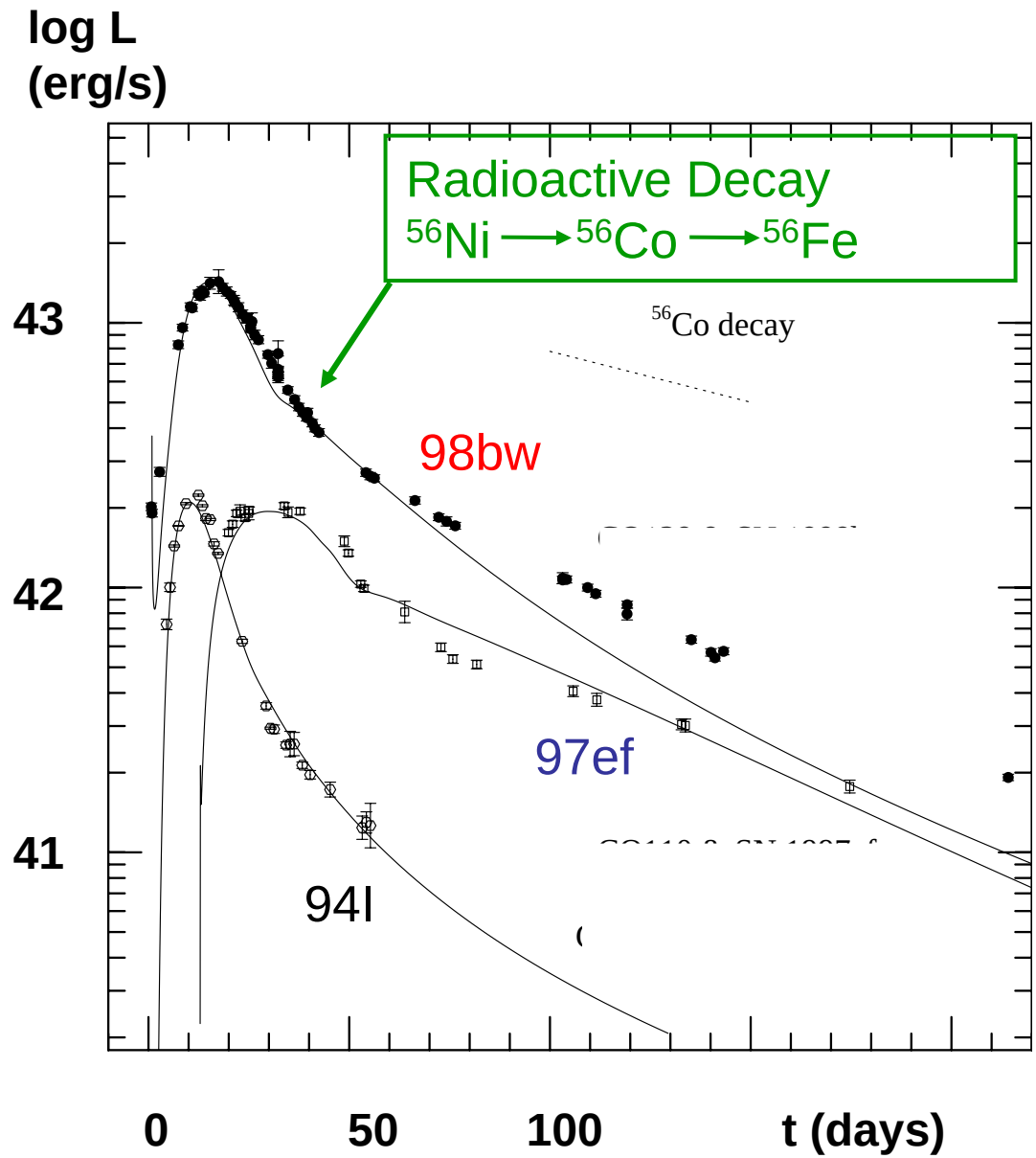

SN II 1997D: Faint SN

Turatto, Mazzali, Young, Nomoto, Iwamoto et al. (1998)

m－M=30.64 (NGC1536)

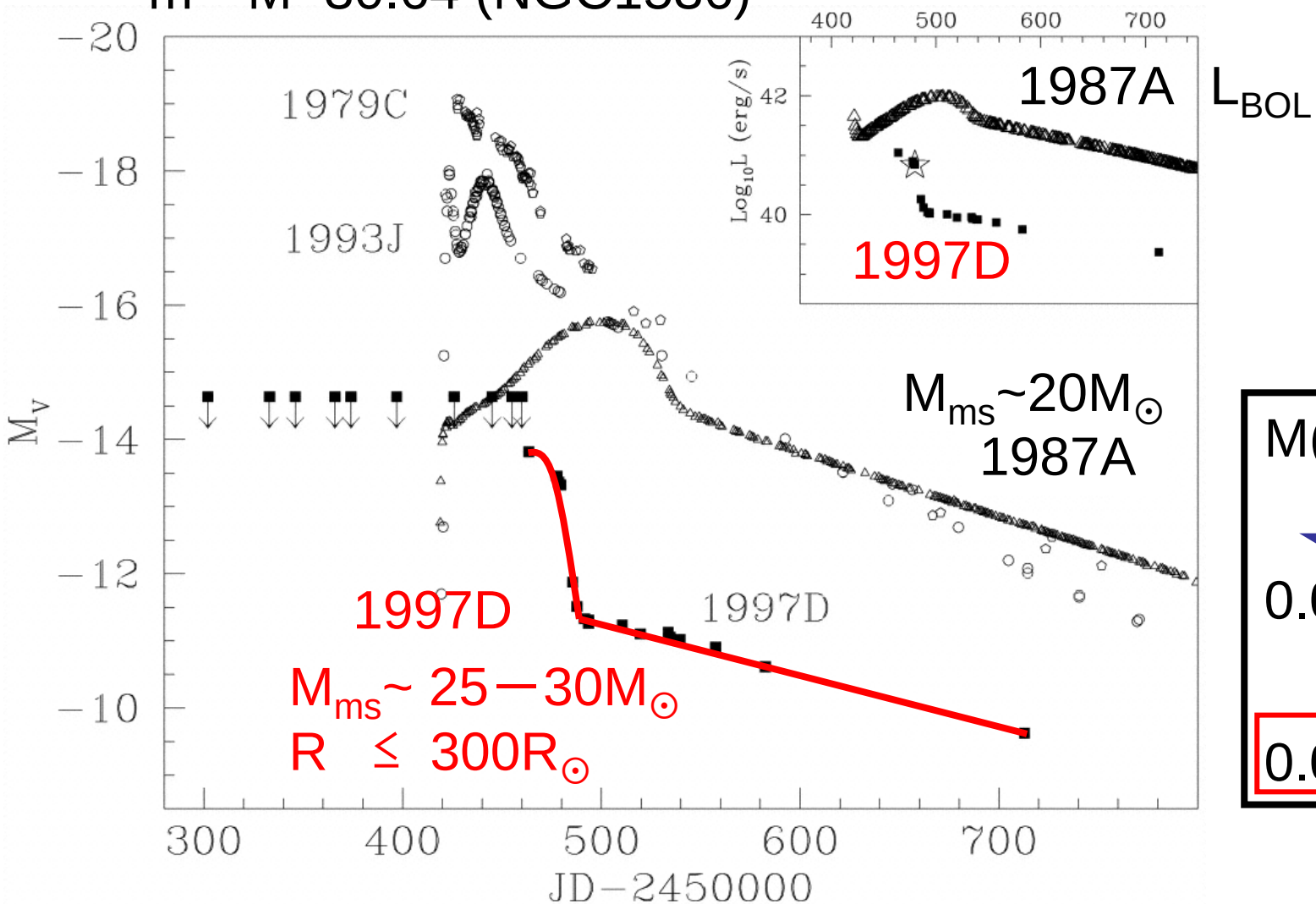

M(^{56}Ni)

0.07$M_\odot$

0.002$M_\odot$

E~4×10^{50}erg

narrow lines

Hypernovae/Faint SNe

Nomoto et al. (2003)

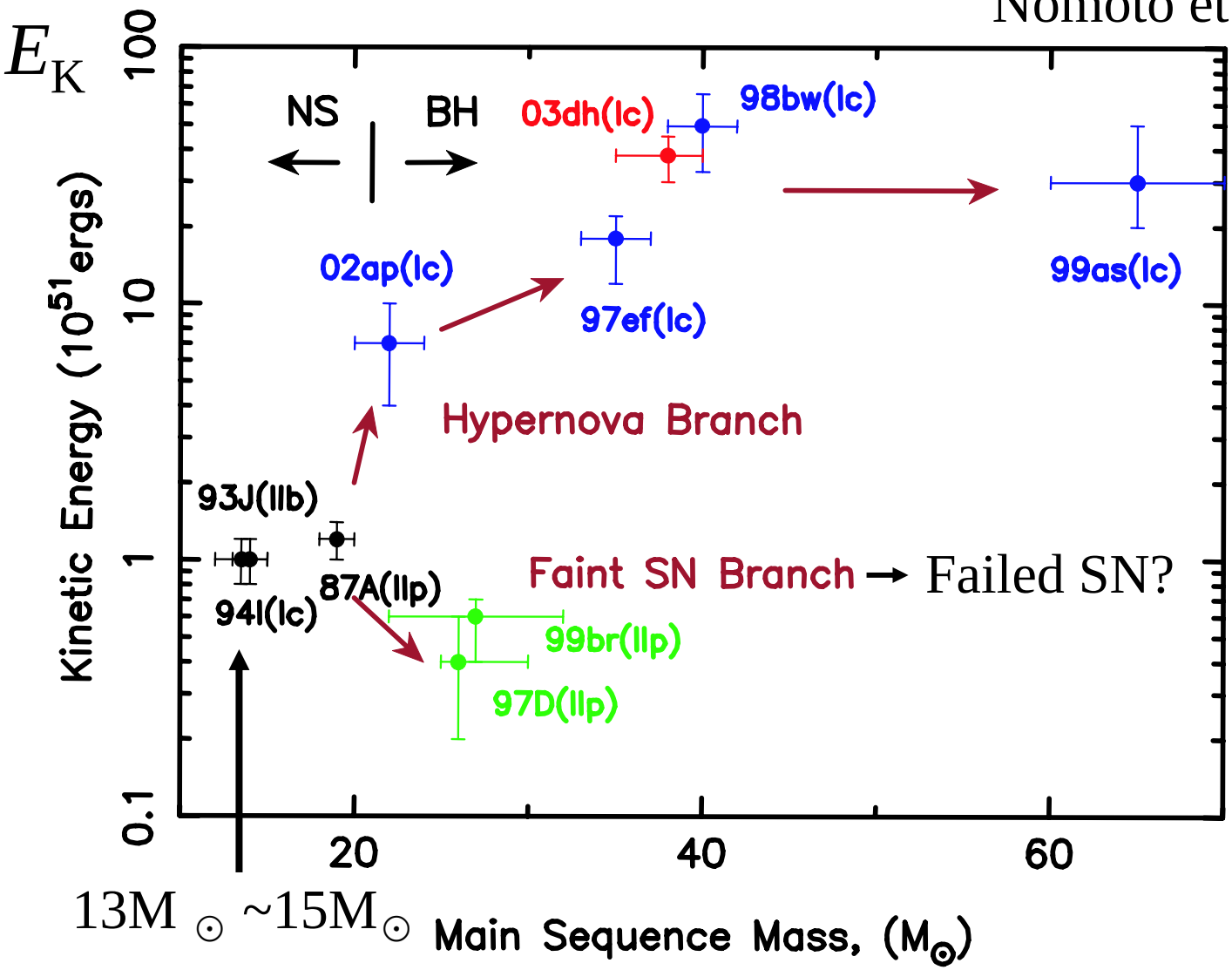

$M(^{56}\mathrm{Ni})/M_\odot$

Nomoto et al. (2003)

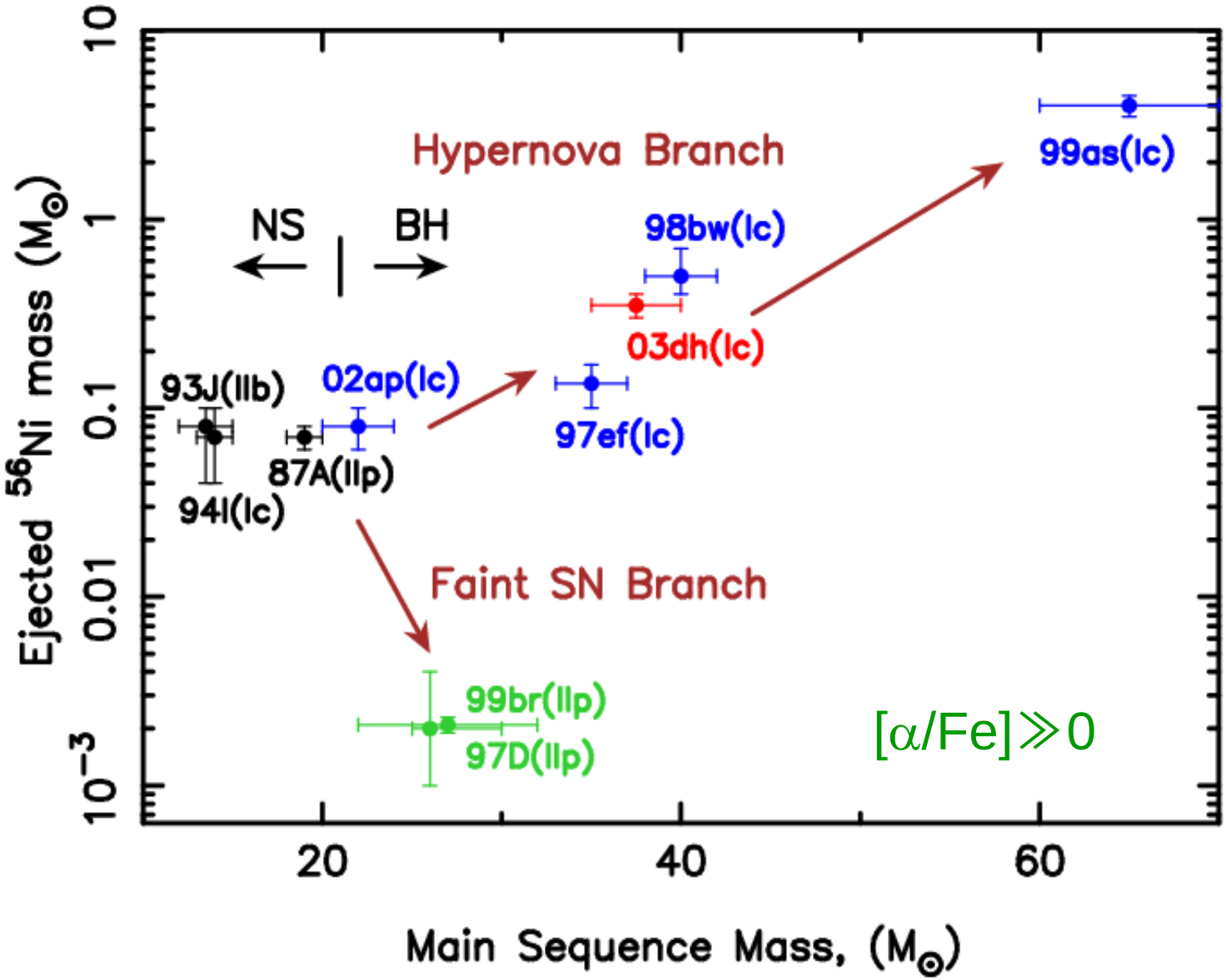

The Most Metal-Poor Star: HE0107-5240 (Chriestlieb et al. 2002)

[Fe/H] = −5.3

[C/Fe] = 4.0

[Mg/Fe] = 0.2

[Ti/Fe] = −0.4

[N/Fe] = 2.3

[Ca/Fe] = 0.4

[Ni/Fe] = − 0.4

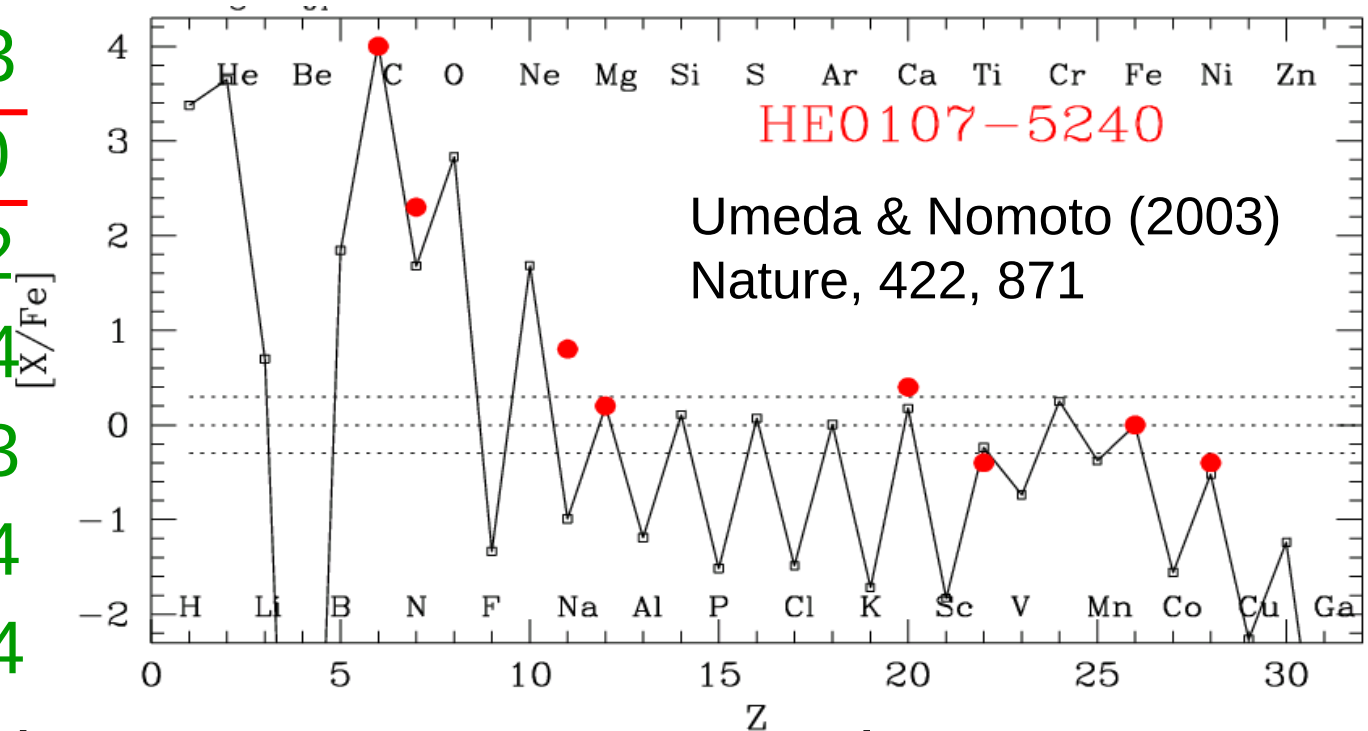

no s-, r- enhancement : no companion star

$M = 25M_\odot$ $E = 3 \times 10^{50}$ergs

$M_{He} = 8M_\odot$ → C+N from He layer

$M_{CO} = 6M_\odot$ → M_{BH}

$M(Fe) \sim 10^{-5}M_\odot$

$M=25M_\odot$, $E=3\times10^{50}$erg [Fe/H]=−5.3

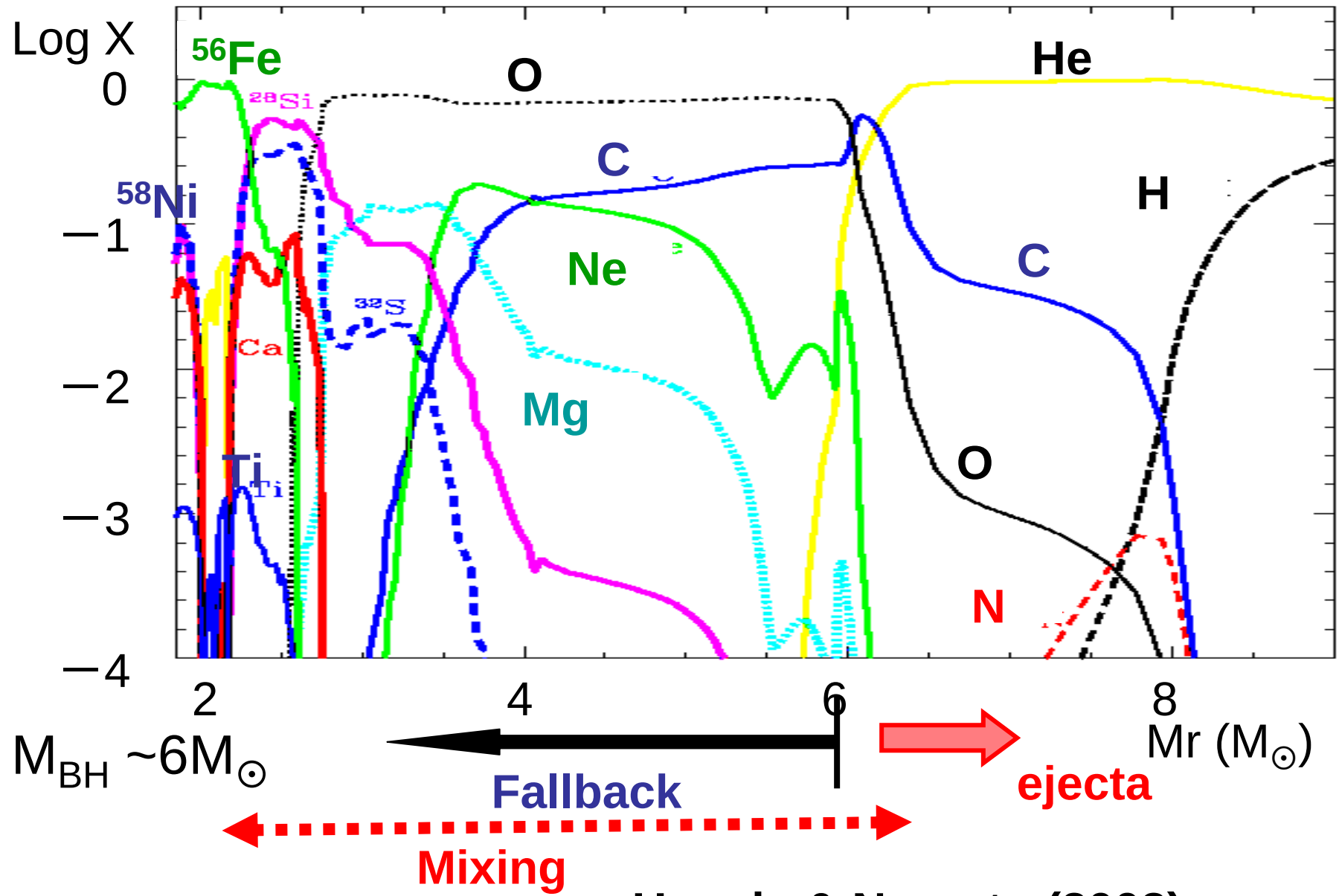

Umeda & Nomoto (2003)

SN1987A

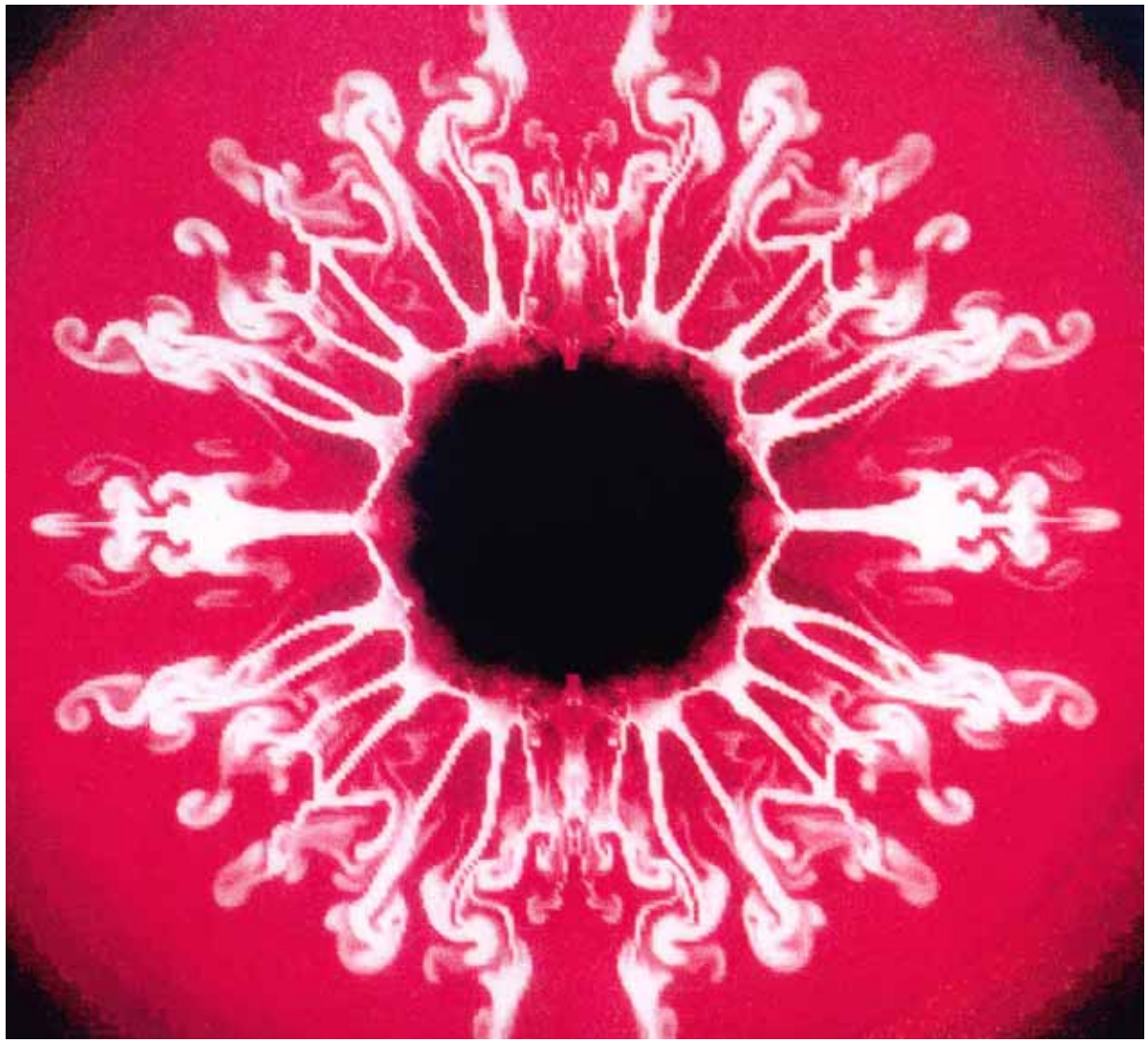

Hachisu, Nomoto et al.

HE0107-5240

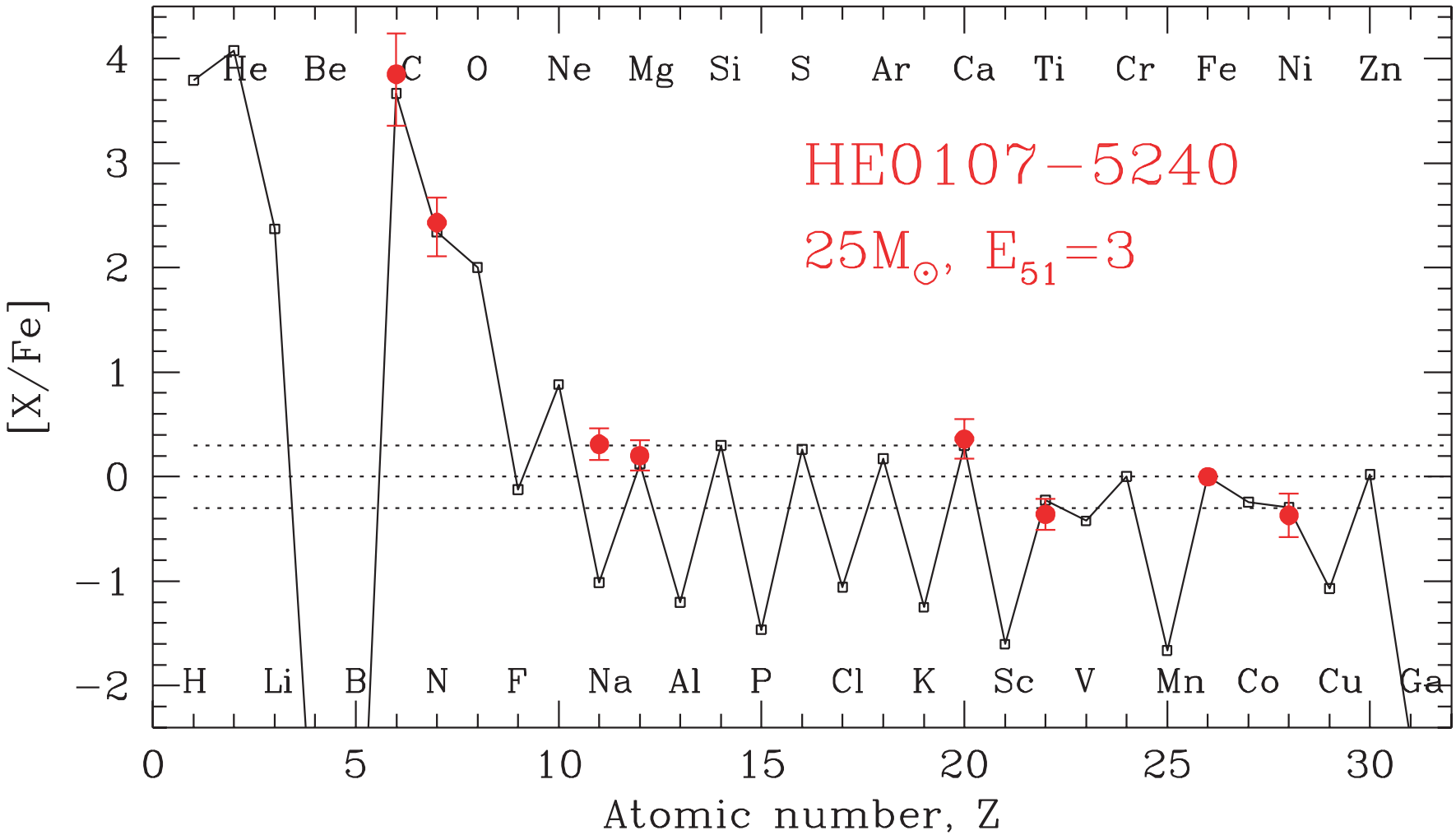
HE0107−5240
25M⊙, E51=3
He Be C O Ne Mg Si S Ar Ca Ti Cr Fe Ni Zn
H Li B N F Na Al P Cl K Sc V Mn Co Cu Ga
[X/Fe]
Atomic number, Z
4
3
2
1
0
−1
−2
0
5
10
15
20
25
30

C, N-Rich Star

[Fe/H] ~ -4.0 (Norris et al.: Depagne et al.)

$30M_\odot$

$E=2\times10^{52}$erg, [Zn/Fe]~0.7 ⟶ Hyper

$M(^{56}Ni)\sim3\times10^{-3}M_\odot$, $M(BH)\sim8M_\odot$

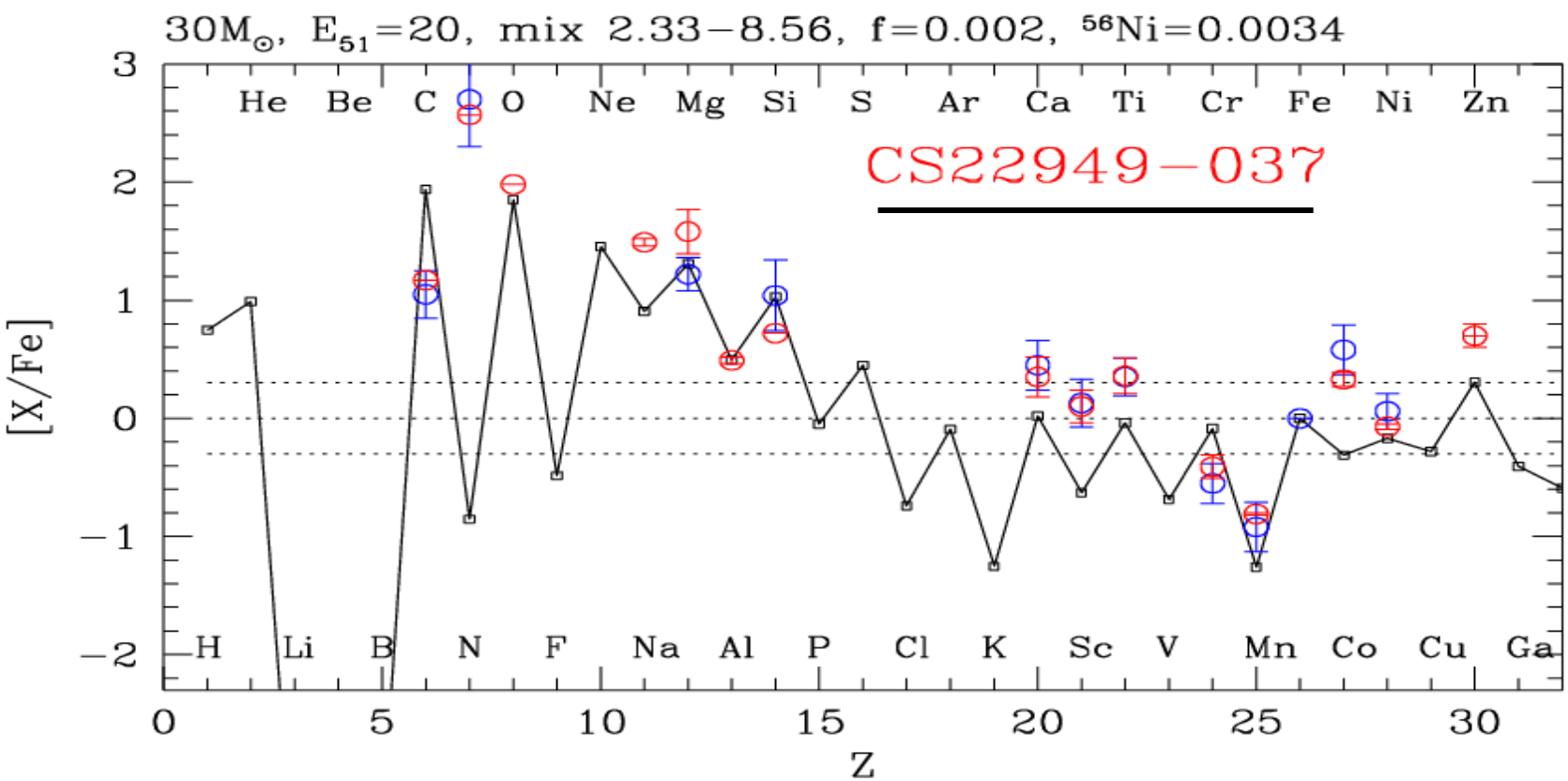

C,N rich – Extremely Metal-Poor Stars

CS 22957-027, [Fe/H]~ −3.1 (Aoki et al. 2002)

$25M_\odot$, E_{51}=1, Mixing=2.16 - 4.84$M_\odot$, f= 0.003

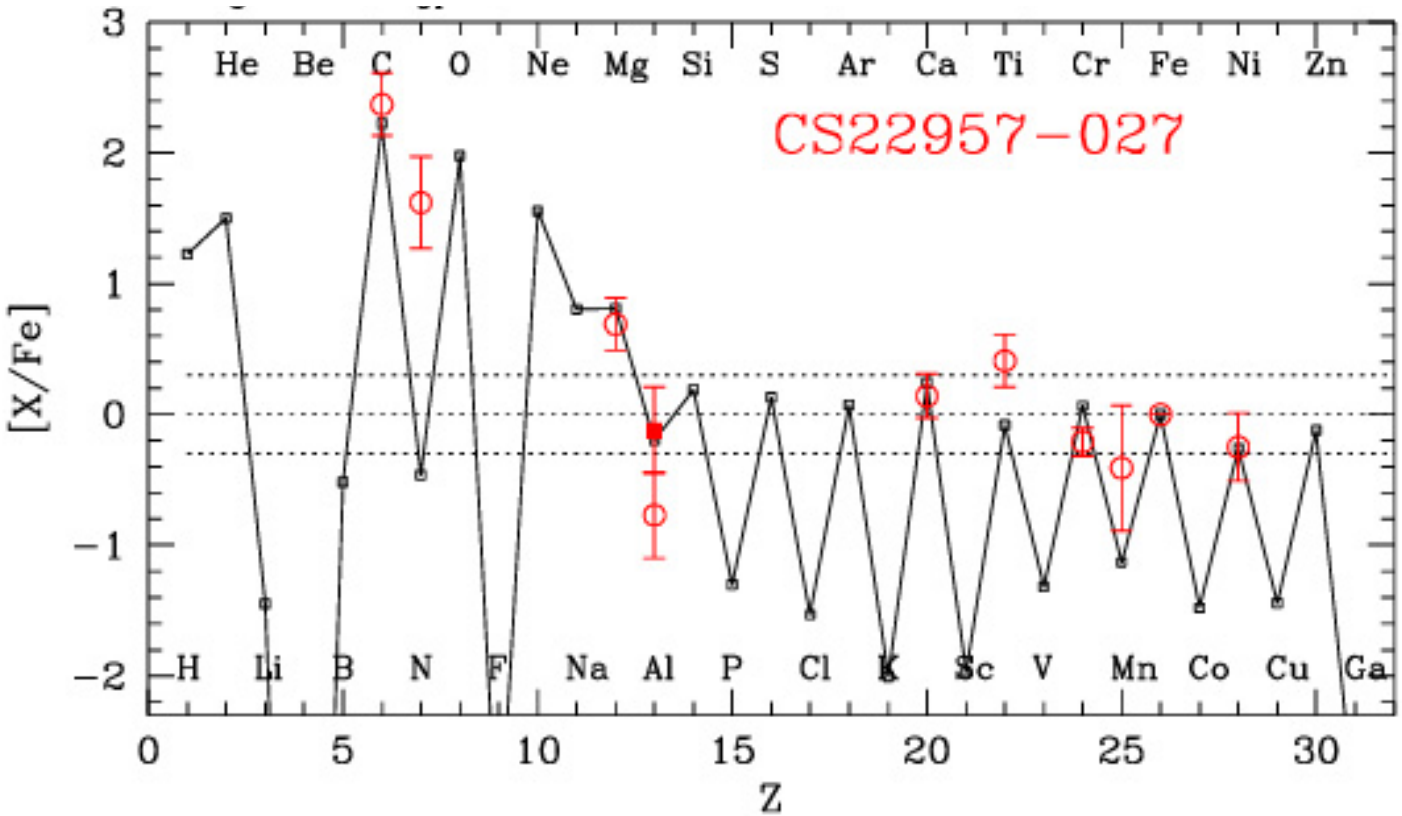

Little Fe（56Ni) ⇒ C,N,O/Fe ↗

C/Mg ↗ ⇒E ↘、M_{cut}(f) ↗

Other C,N-rich Stars

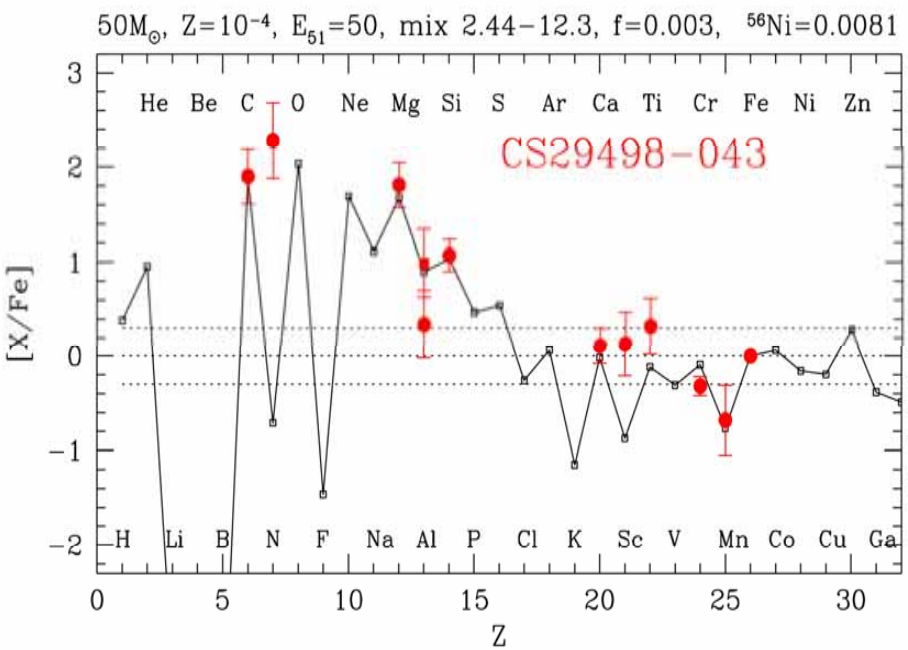

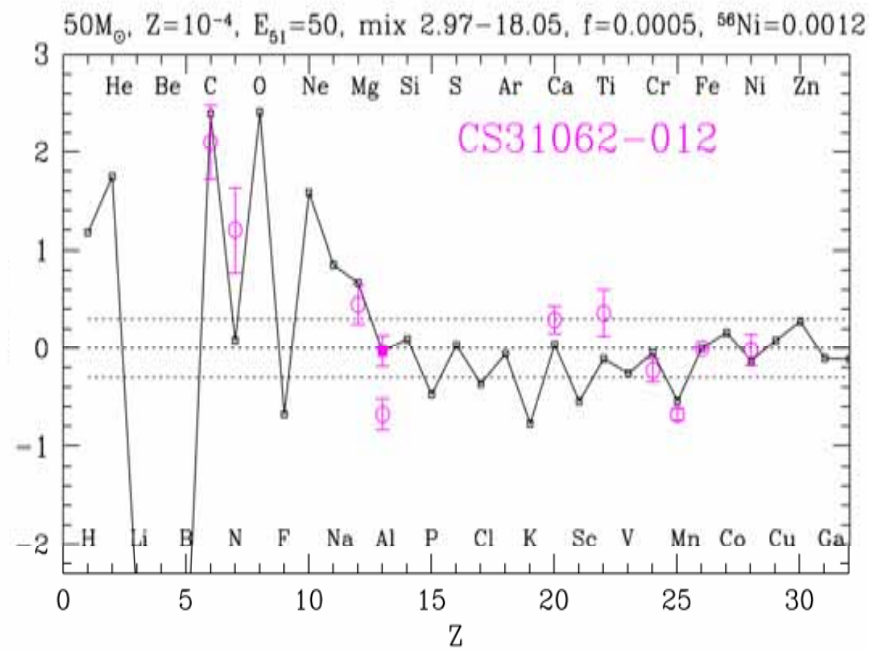

$M_{BH}=12M_{\odot}$
$M_{MS}=50M_{\odot}$
$E_{51}=50$
Mixing 2.44 – 12.3$M_{\odot}$
f=0.003
$M(^{56}Ni)=0.0081M_{\odot}$

$M_{BH}=18M_{\odot}$
$M_{MS}=50M_{\odot}$
$E_{51}=50$
Mixing 2.97 – 18.05$M_{\odot}$
f=0.0005
$M(^{56}Ni)=0.0012M_{\odot}$

Hypernova Nucleosynthesis

$E \sim 10^{51}$erg → $E/10^{52}$erg

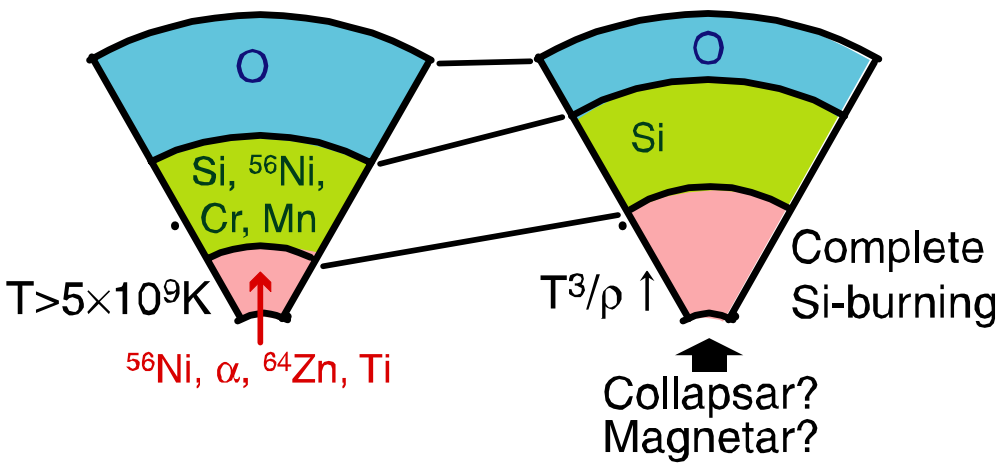

Low energy High energy

(1) M(Complete Si-burning) ↗

(Zn, Co)/Fe ↗

(Mn, Cr)/Fe ↘

Fe/(O, Si) ↗

(2) More α-rich ⇦ entropy ↗

Zn/Fe ↗ ⇦ ^{64}Ge

Ti/Fe ↗

(3) More O burns

(Si, S, Ca)/O ↗

Normal SNe vs Hypernovae

Normal SNe

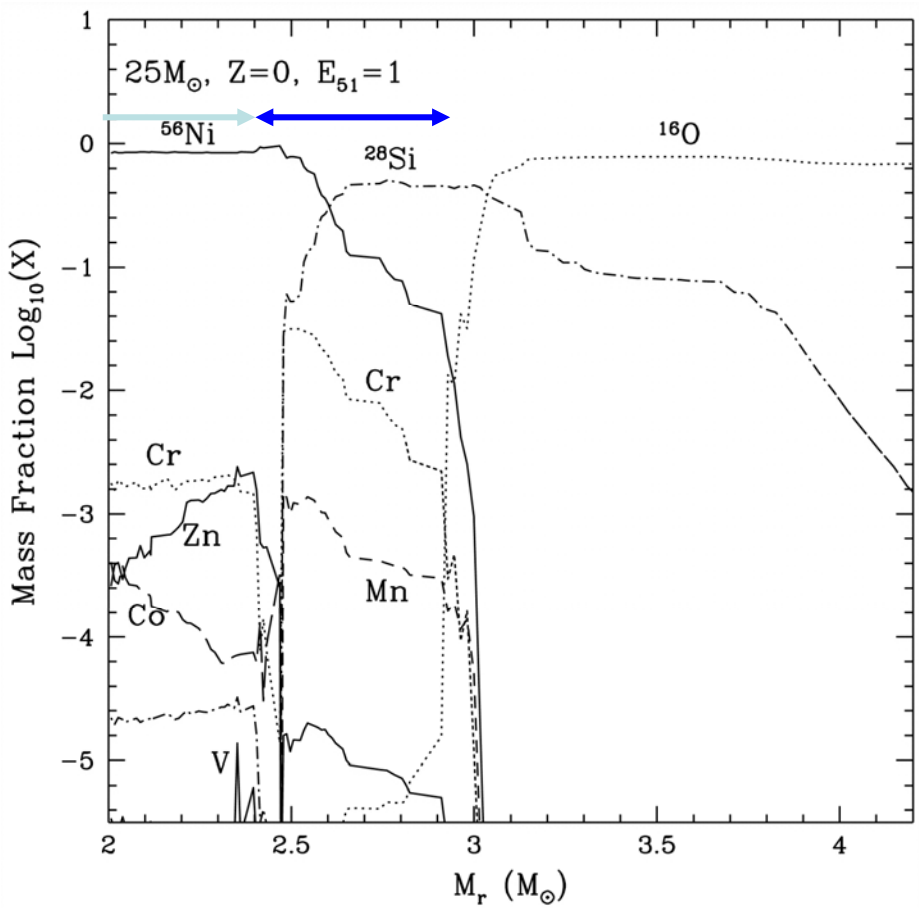

Hypernovae

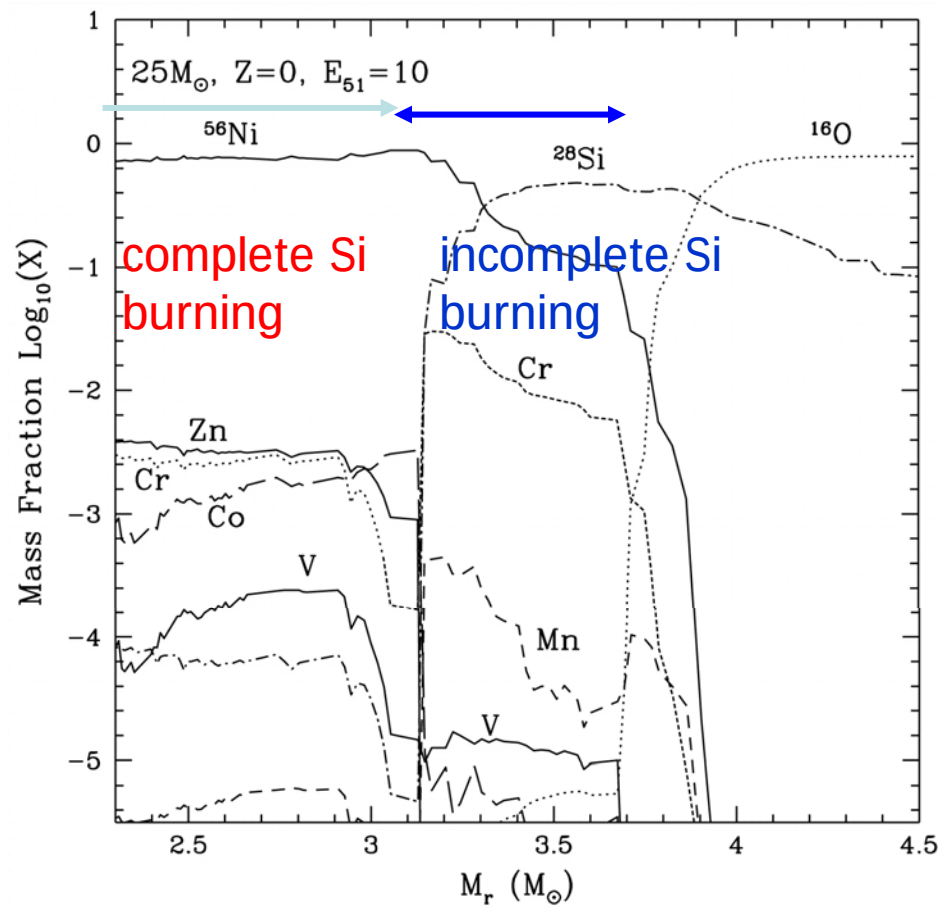

Umeda et al. 2002

Supernova-induced Star Formation

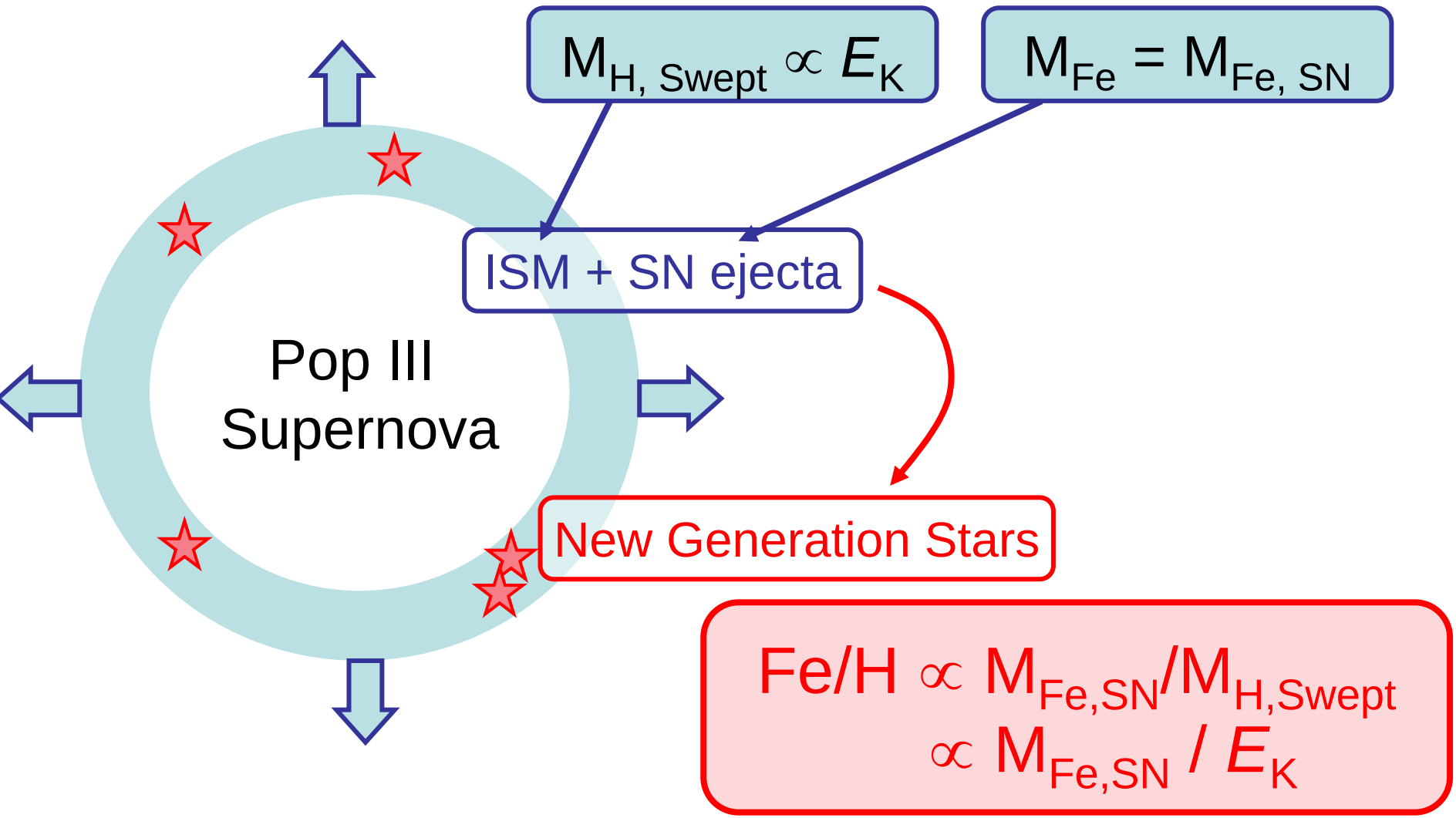

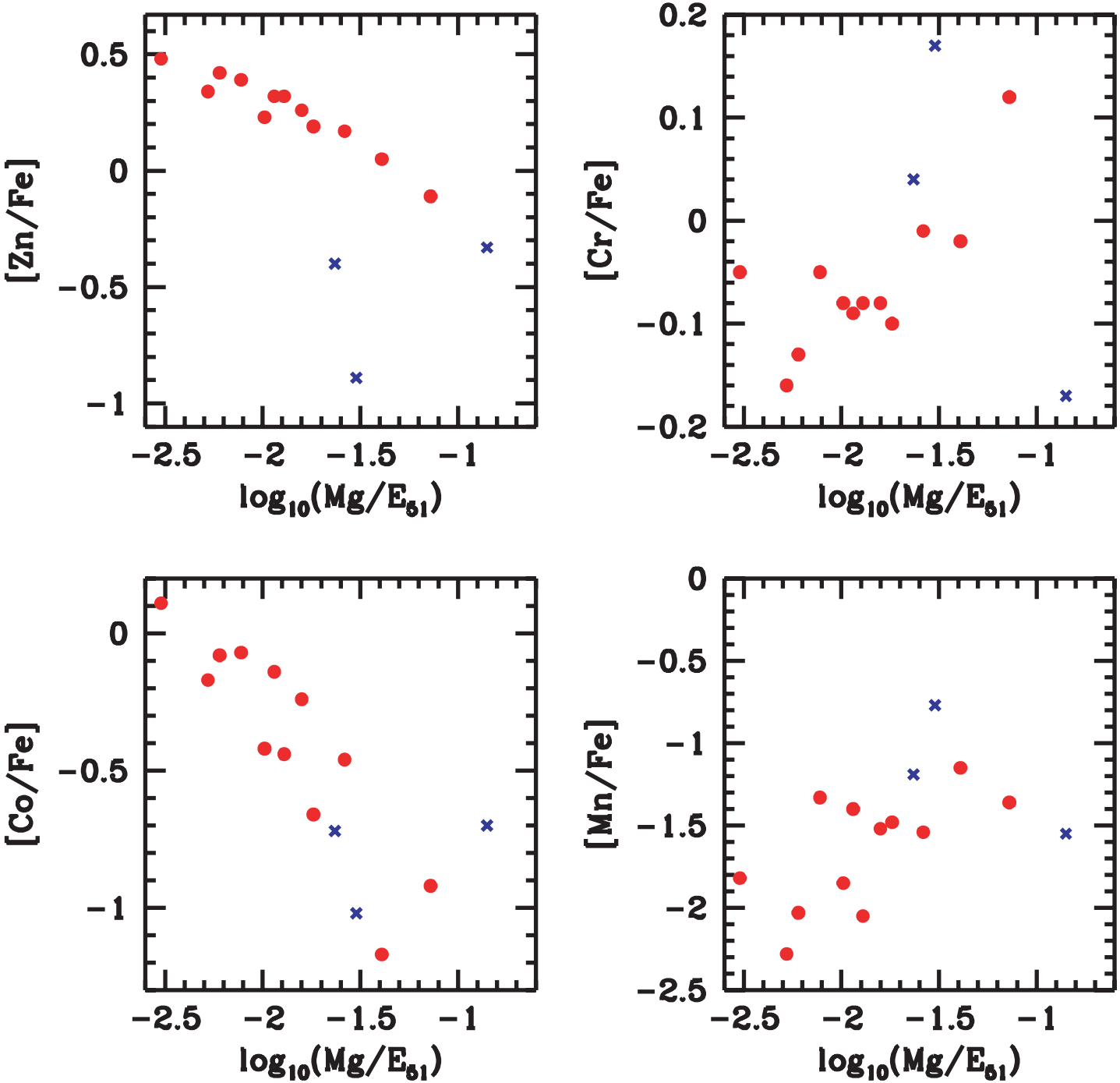
[Zn/Fe]
0.5
0
−0.5
−1
−2.5
−2
−1.5
−1
log10(Mg/E51)
[Cr/Fe]
0.2
0.1
0
−0.1
−0.2
−2.5
−2
−1.5
−1
log10(Mg/E51)
[Co/Fe]
0
−0.5
−1
−2.5
−2
−1.5
−1
log10(Mg/E51)
[Mn/Fe]
0
−0.5
−1
−1.5
−2
−2.5
−2.5
−2
−1.5
−1
log10(Mg/E51)

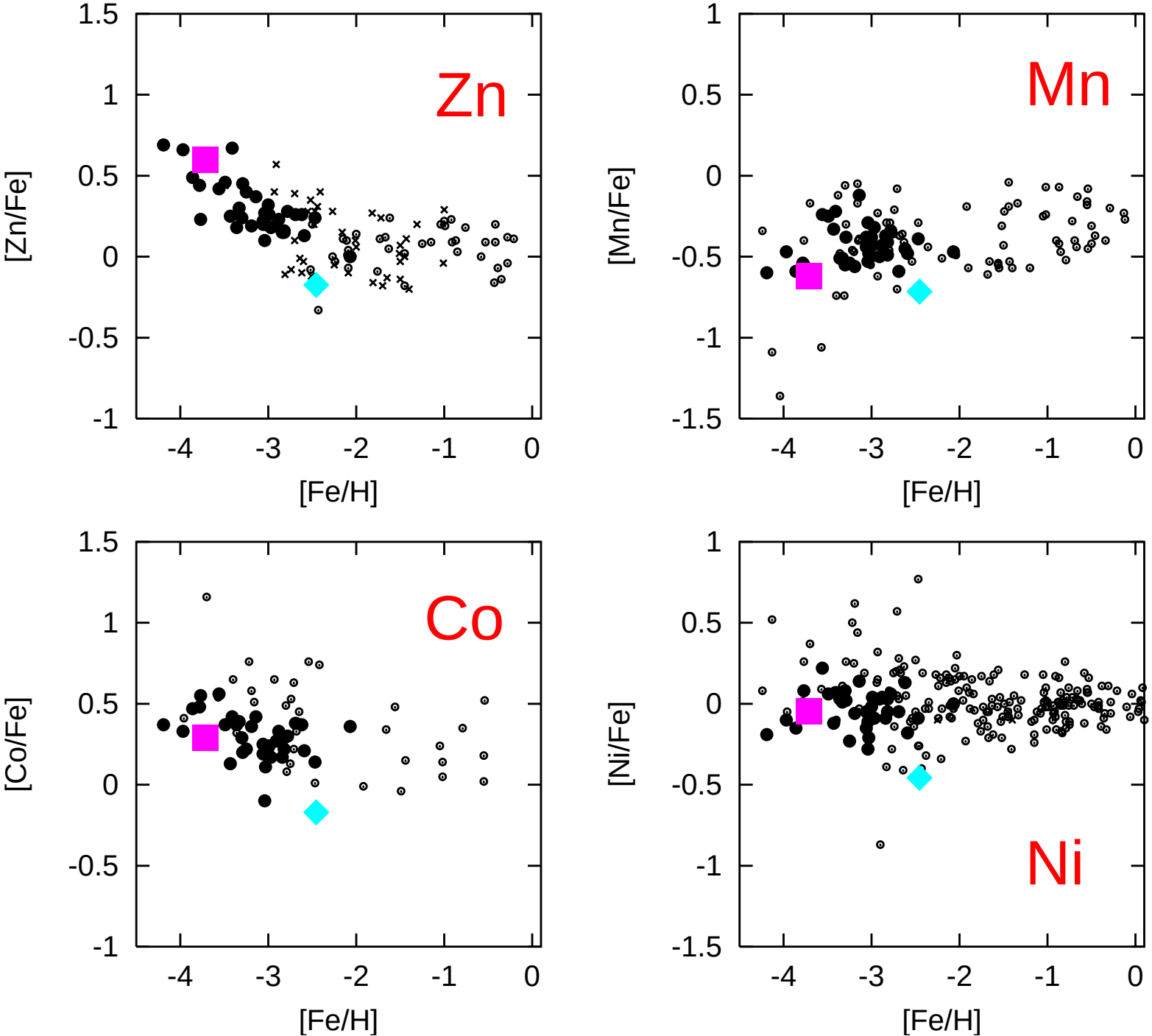
Zn
[Zn/Fe]
[Fe/H]
Mn
[Mn/Fe]
[Fe/H]
Co
[Co/Fe]
[Fe/H]
Ni
[Ni/Fe]
[Fe/H]

$M_{MS}=40M_{\odot}$

Hydrodynamic Models

Spherical
$E_{51}=30$

Aspherical
Vz/Vr=1.5
$E_{51}=30$

$2M_{\odot}$

Final mass of BH

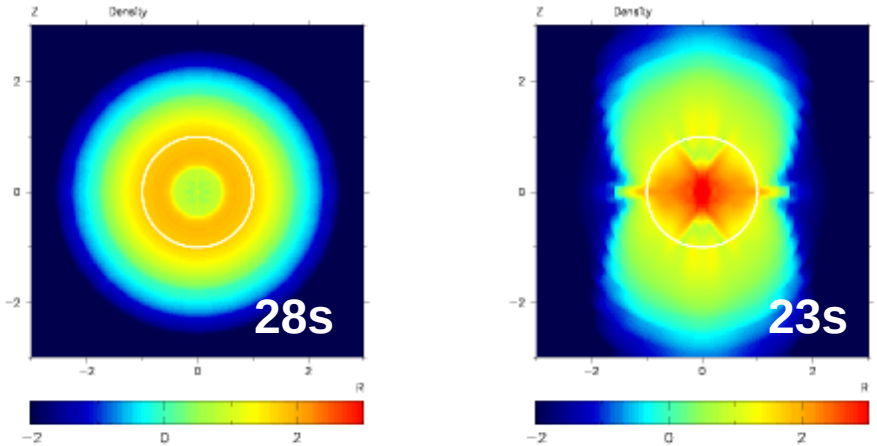

$2M_{\odot}$

$9M_{\odot}$

$10M_{\odot}$

Aspherical
Vz/Vr=1.5
$E_{51}=5$

Jet-like
$E_{51}=10$

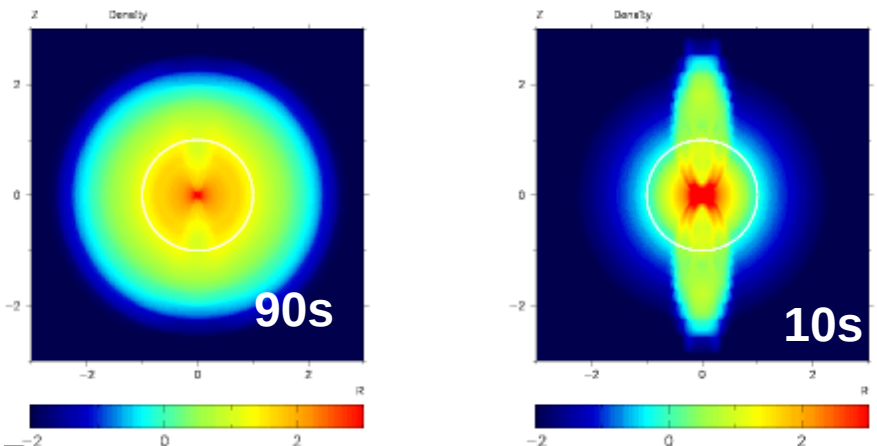

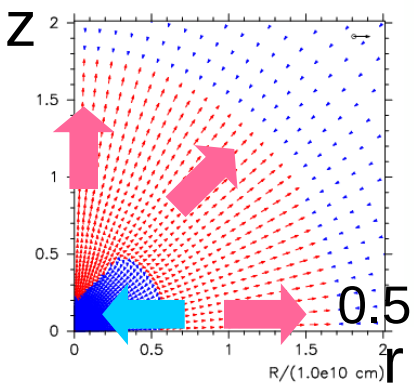

$0.5R_{*}$

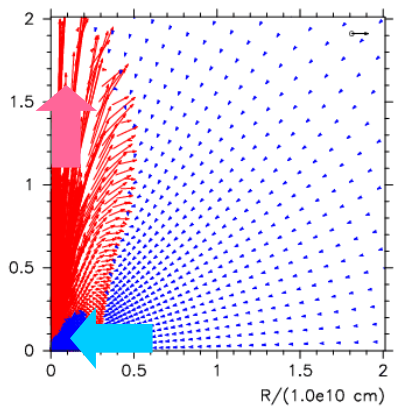

Element Distribution in Bipolar Explosion

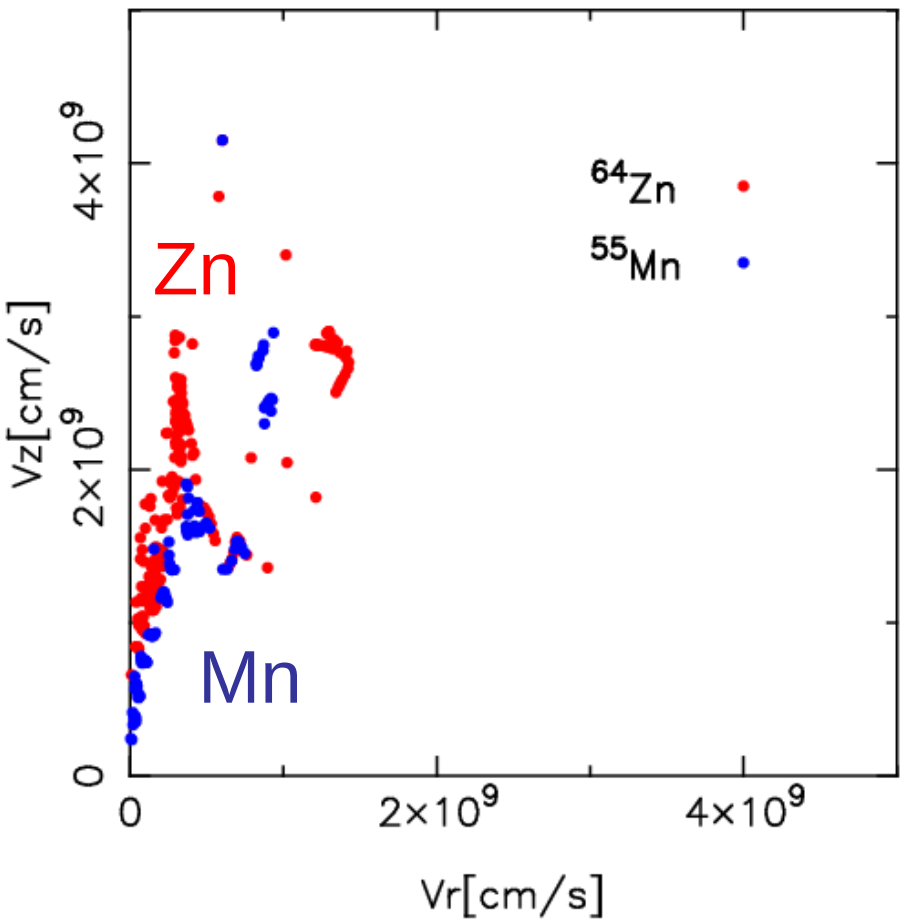

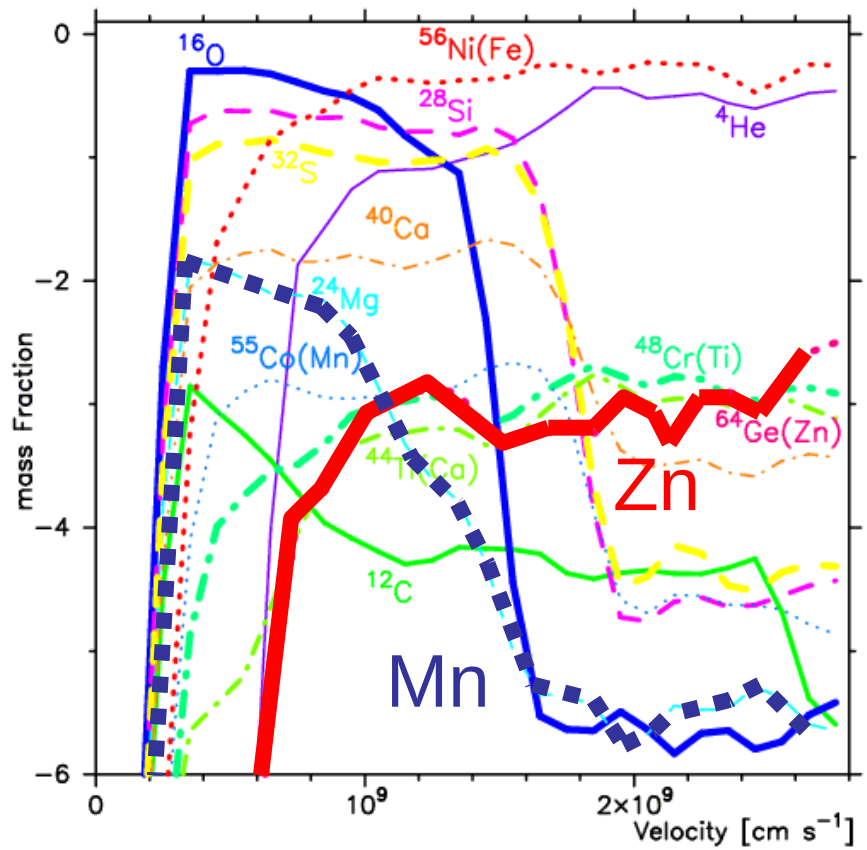

Maeda & Nomoto (2003), ApJ, 598, 1163

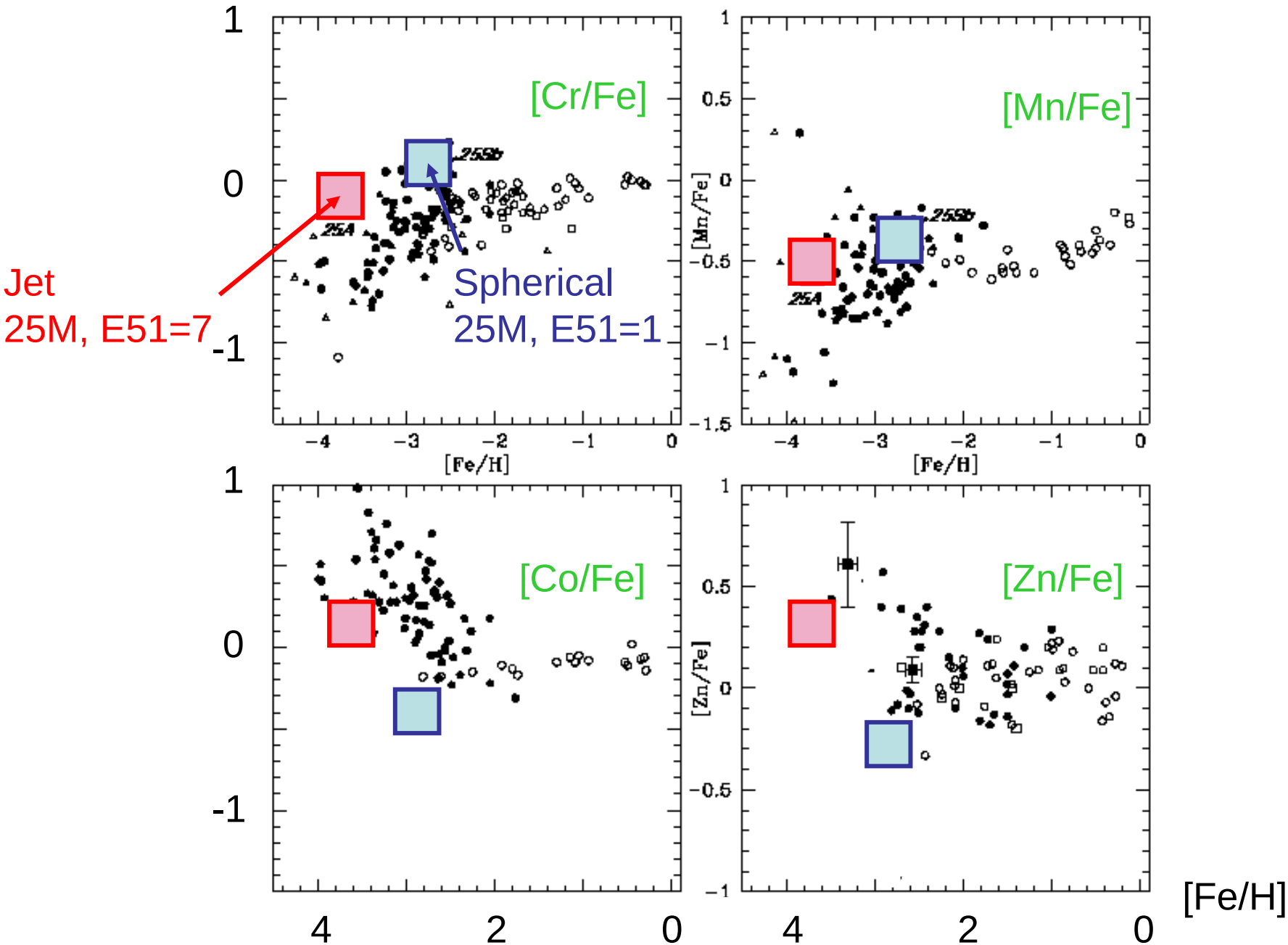
[Cr/Fe]
[Mn/Fe]
[Co/Fe]
[Zn/Fe]
Jet
25M, E51=7
Spherical
25M, E51=1
25A
25Sb
[Fe/H]
[Mn/Fe]
[Zn/Fe]
1
0
-1
0.5
-0.5
-1.5
-4
-3
-2
-1
4
2

Pair Instability Supernovae (130M$_\odot$ — 300M$_\odot$)

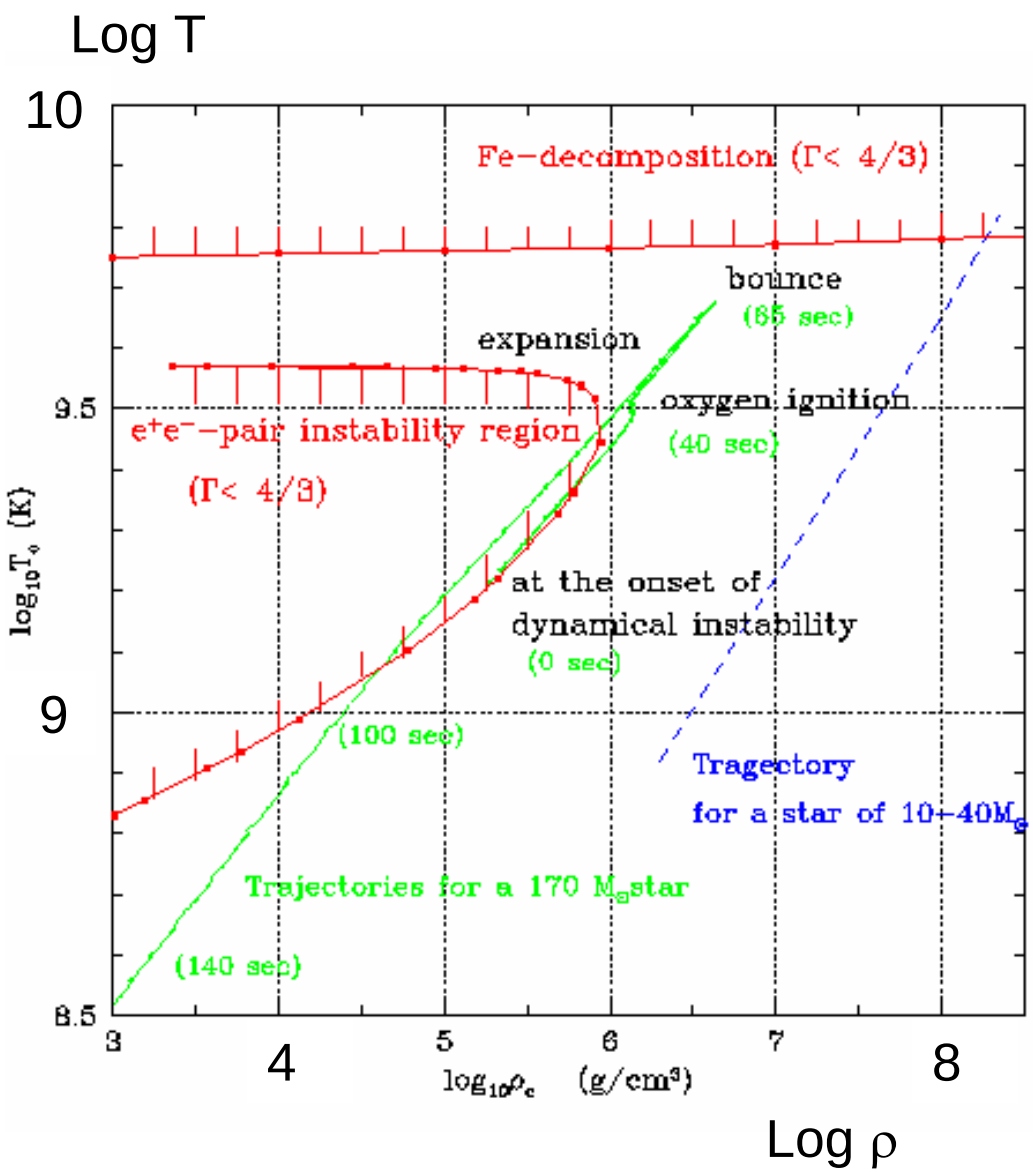

Complete Si-burning ↘

⇩

[Zn/Fe] < −0.8

[Co/Fe] < −0.2

[C/Fe] < 0

[Si/Fe] > 0.7

Umeda & Nomoto 2002, ApJ, 565, 385

Heger & Woosley 2002, ApJ, 567, 532

First Supernovae

[Fe/H] :	-5	-4	-3	-2.5
	Faint SNe			
	Hypernovae			
			Normal SNe	

Black-Hole Forming Supernovae (20-130$M_\odot$)

⇒ **First Black Hole** > 2~6$M_\odot$

Faint SNe **(High and Low energy)** ⇒ **C,O-rich ejecta**

⇒ **Efficient Cooling of ISM**

⇒ **Formation of Low Mass C,O-rich 2nd Generation Stars**

Reionizing Source: 20 – 130 $M_\odot$ (Tumlinson et al)

Possible Types of SN-HN

- **Hyper-Energetic SN II ?**
  - Rotating Black-Hole + H-rich Envelope (low metallicity?)

    SN IIn 1997cy ?（but SN 2002ic Ia => IIn）

Faint SN Ibc ?

- Small ^{56}Ni (fallback) + No Shock Heating

Hyper-Energetic but Faint SN Ibc ?

(fallback of ^{56}Ni)

Early Enrichment of the Lyman α Forest

Michael Norman, Brian O'Shea, Pascal Paschos
Laboratory for Computational Astrophysics
UC San Diego

1. Pollution by Very Massive Pop III Stars
2. Pollution by High-z Dwarf Galaxies
3. Signatures of Pop III in quasar absorption lines
4. Future: Gigazone Simulations

1. Pollution by Massive Pop III

Summary of AMR results

- 1 massive Pop III star per DM halo with M >5 x 10^5 $M_\odot$ at 15 < z < 25 (Abel, Bryan & Norman 2002)
- Baryons driven out of halo by photo-evaporation by UV heating from PopIII star (Whalen, Abel & Norman 2004)
- Metals dispersed to r ~ 1 kpc by supernova explosion in UV preprocessed halo

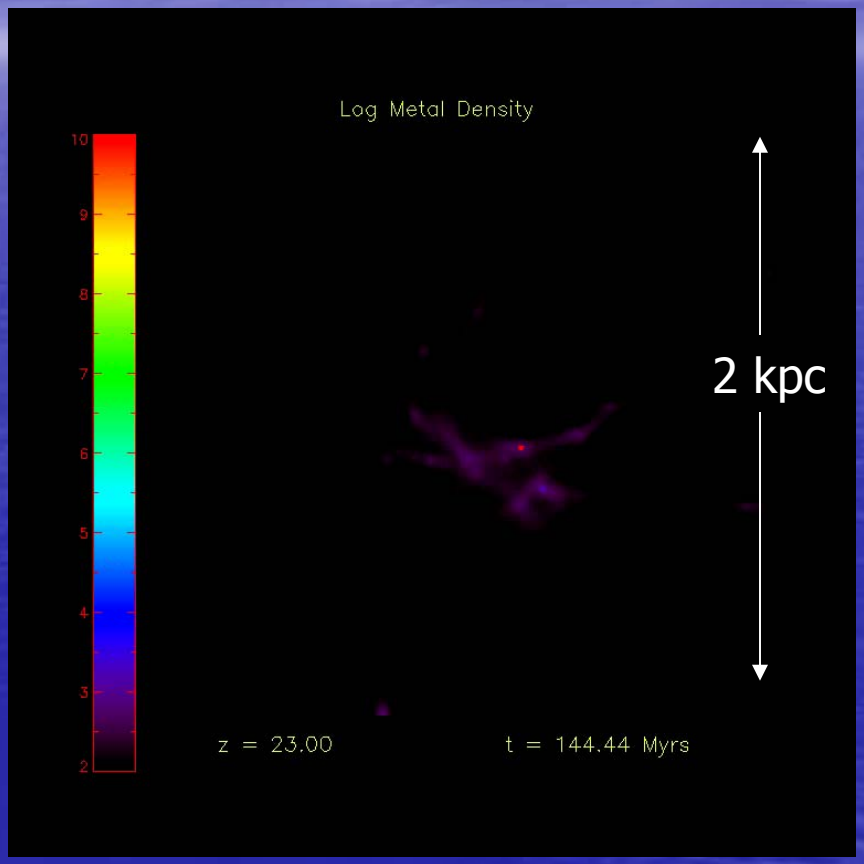

O'Shea et al. (in prep)

Did Massive Primordial Stars Preenrich the Lyman α Forest?

Norman, O'Shea & Paschos 2004, Ap. J. Lett., 601, L115.

- evolve a ΛCDM model is a 2 Mpc box at high resolution (512^3) to z=15
- assume each DM halo with $M>5x10^5\ M_\odot$ hosts a single VMS which explodes and deposits M_Z of metals in a sphere 1 kpc in radius
- evolve the metallicity field as a passive tracer to z=3, quantify final distribution
- assume no further metal enrichment by Pop II

Z=15 (initialization)

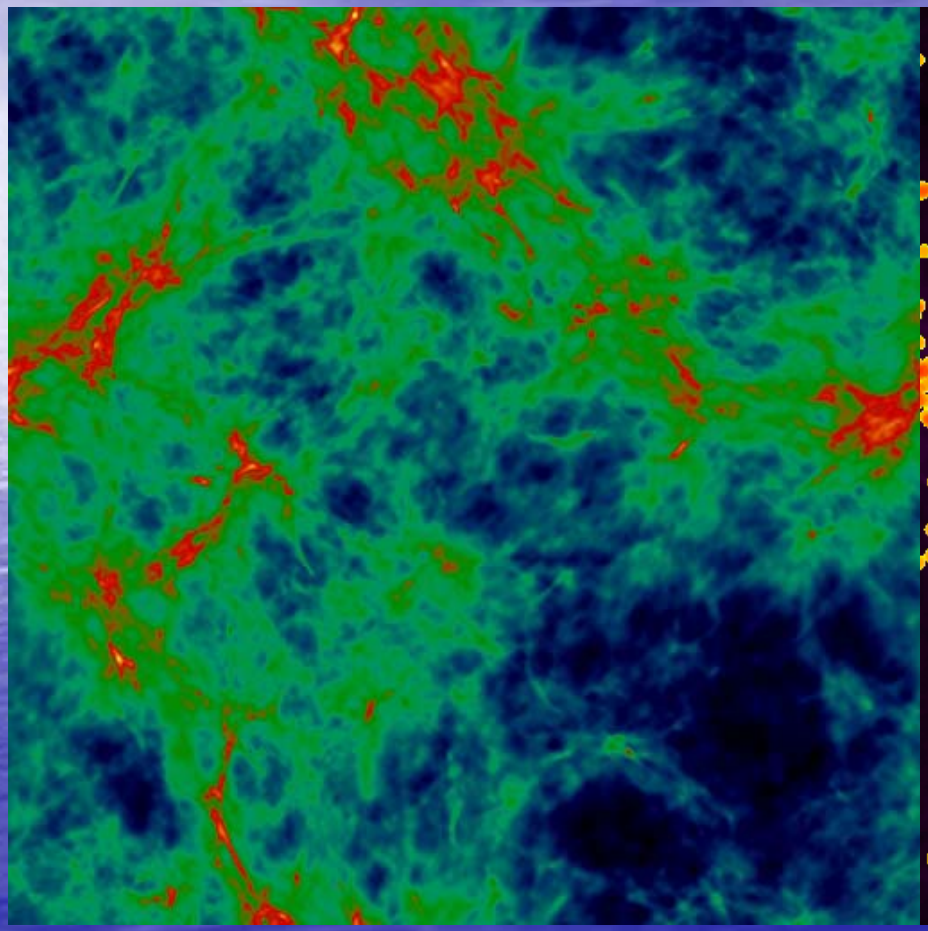

Baryon density

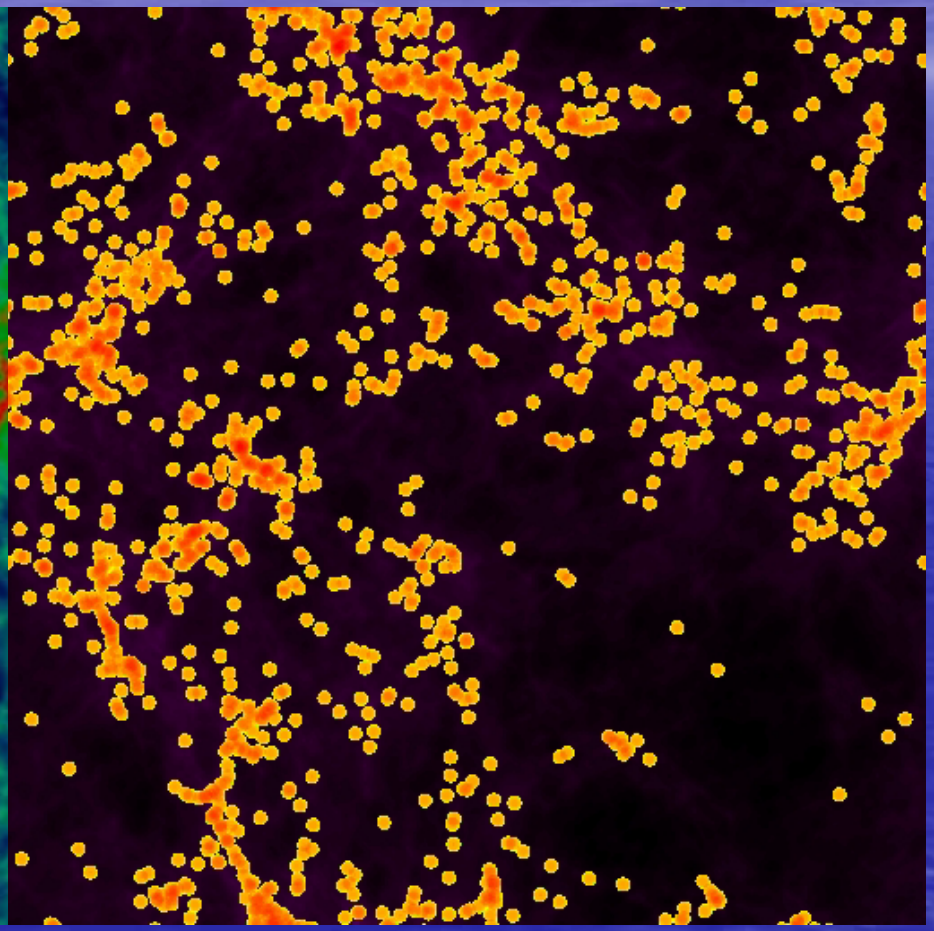

Metal density

Z=10

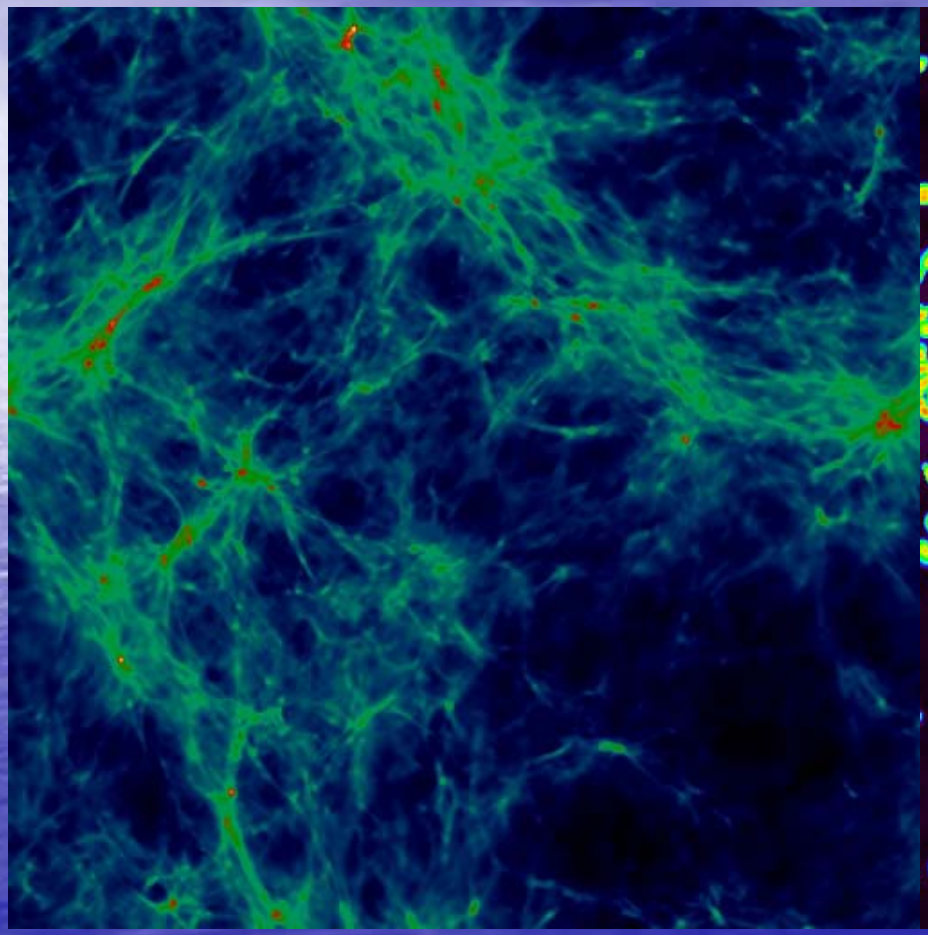

Baryon density

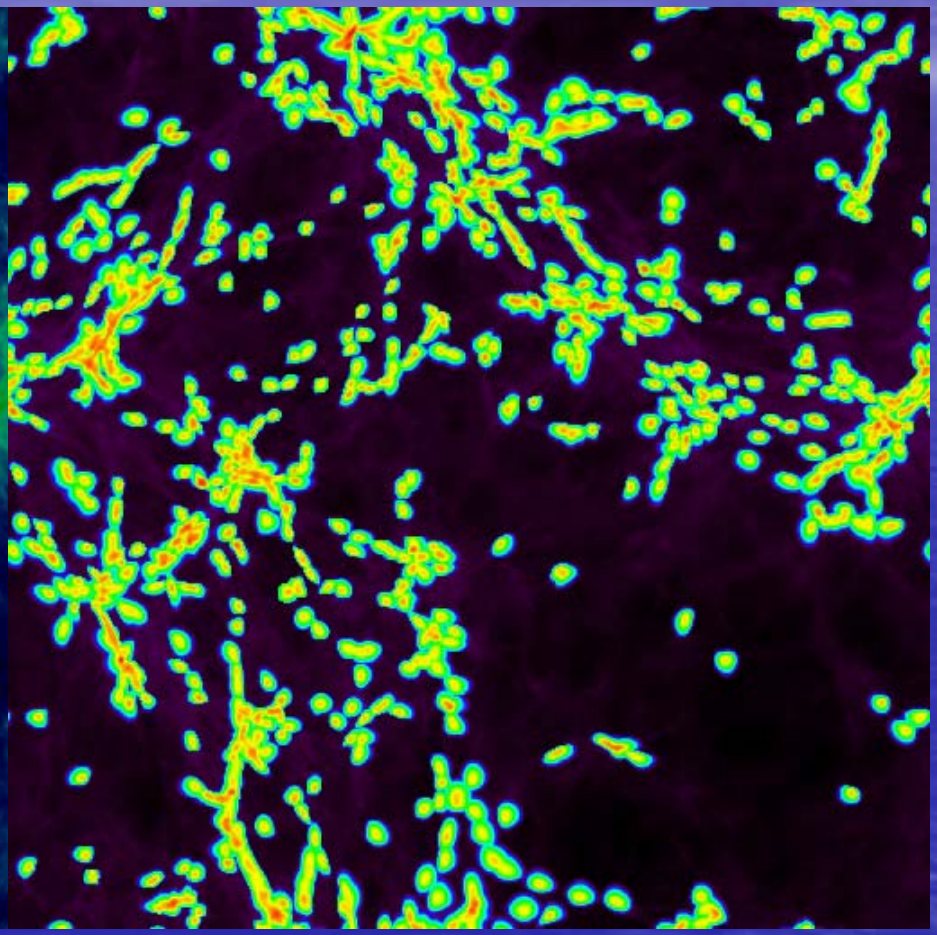

Metal density

Z=6 (uniform UVB turned on)

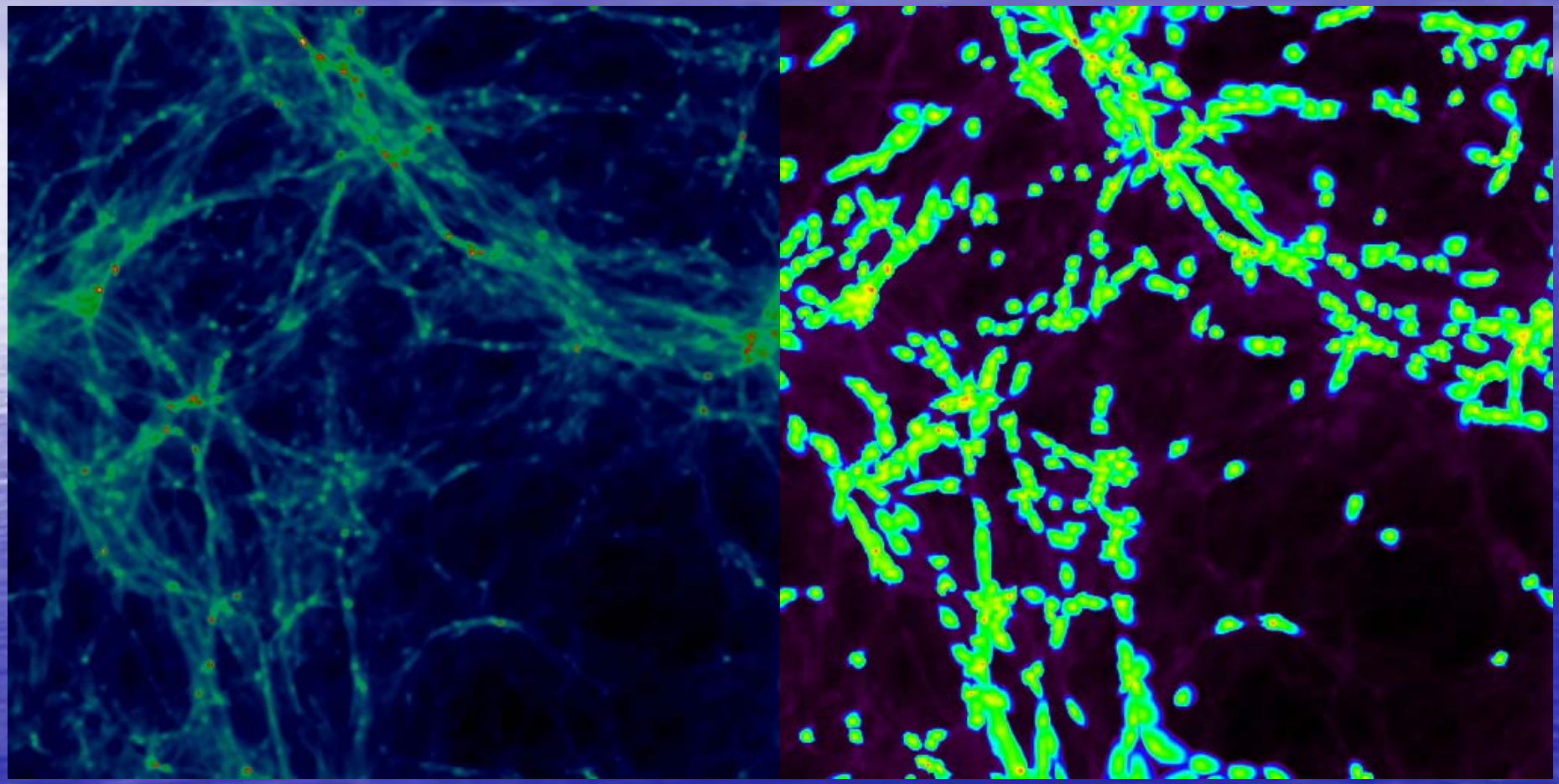

Baryon density

Metal density

Z=5

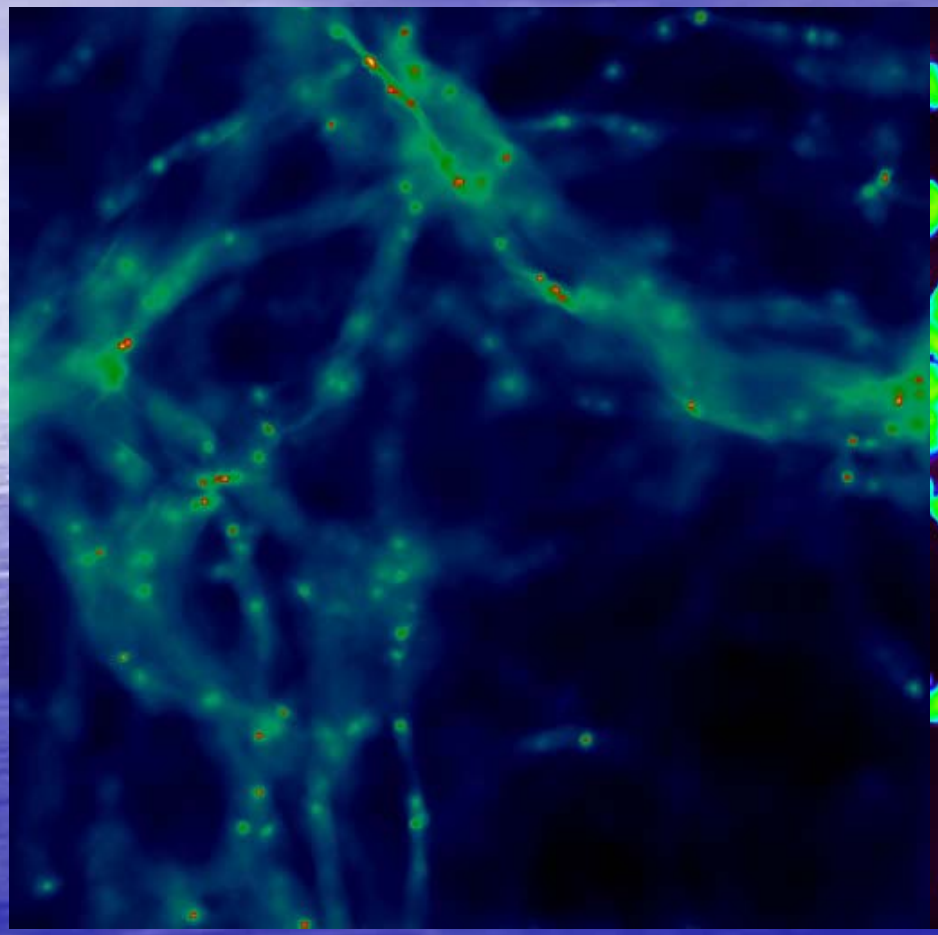

Baryon density

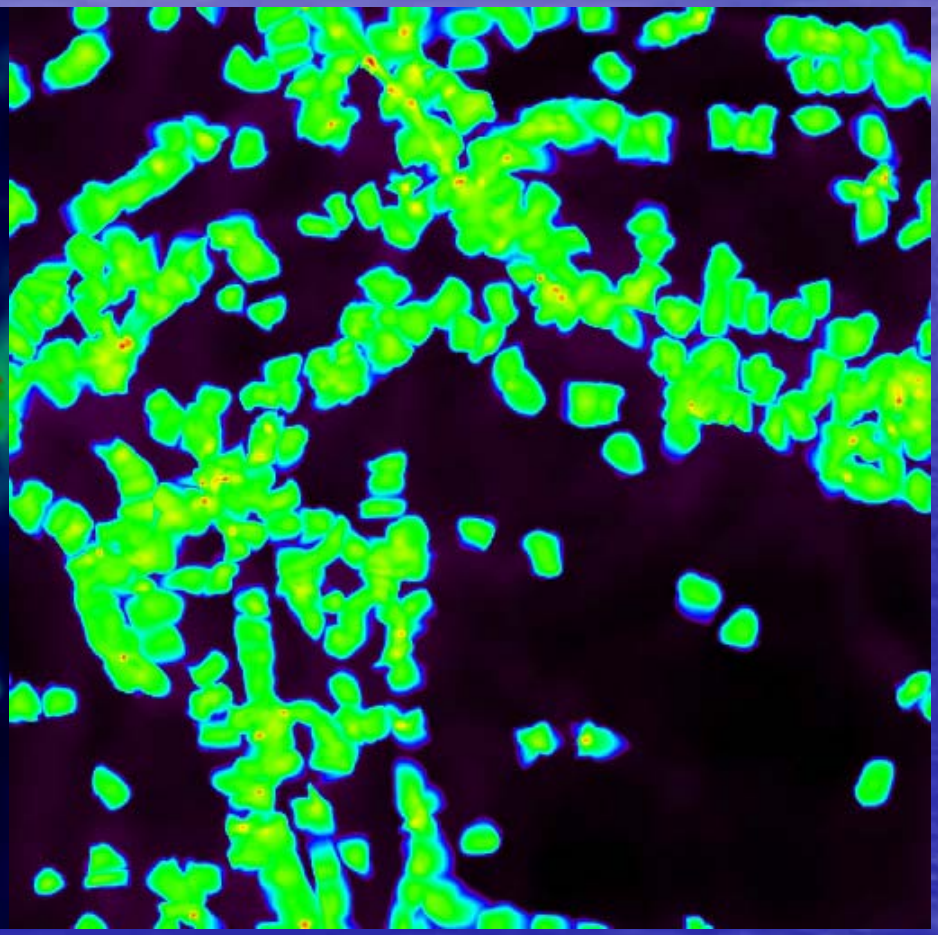

Metal density

Z=4

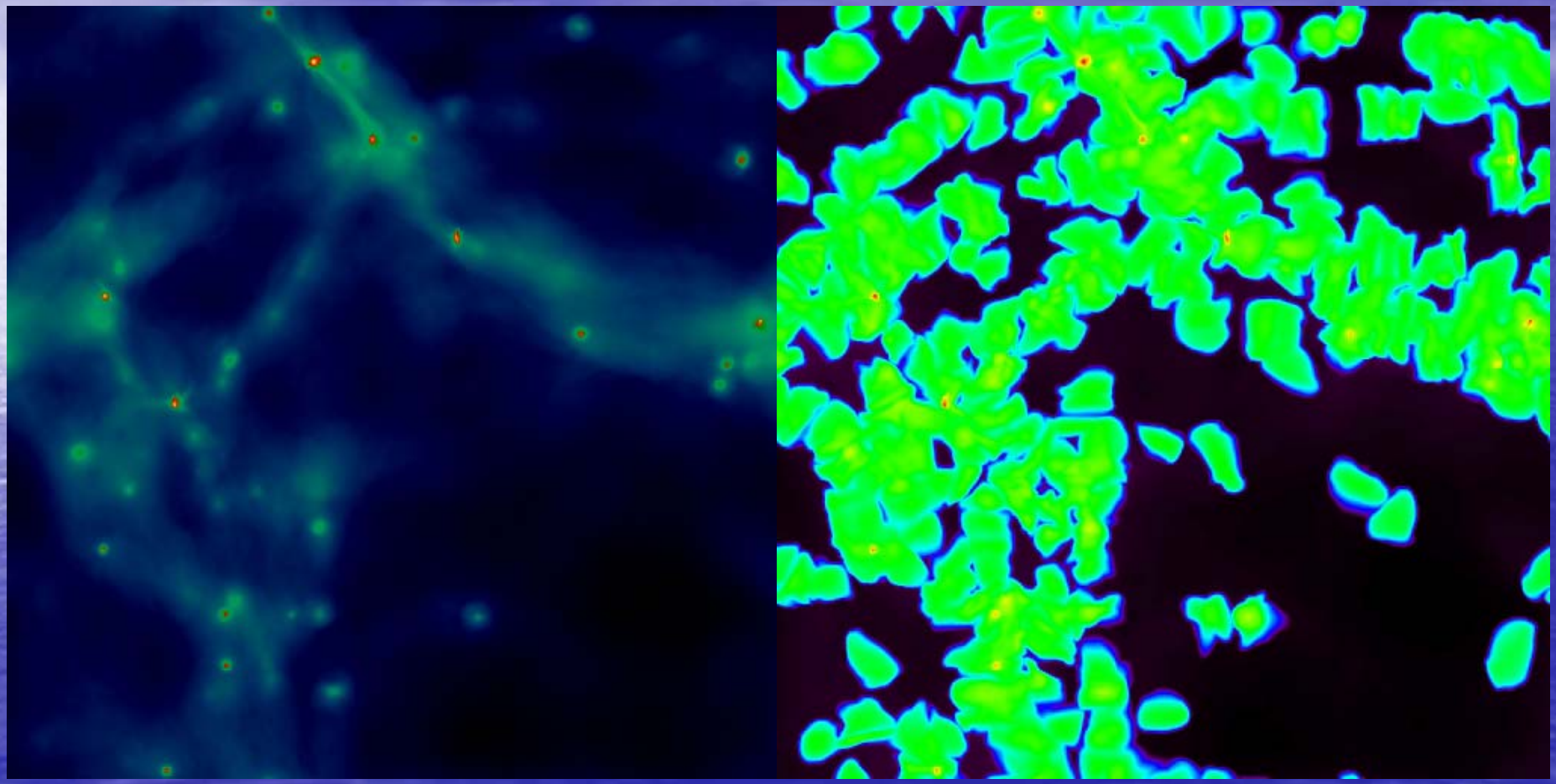

Baryon density

Metal density

Z=3

Ly α forest absorbers
$\delta \sim 2\text{-}10$

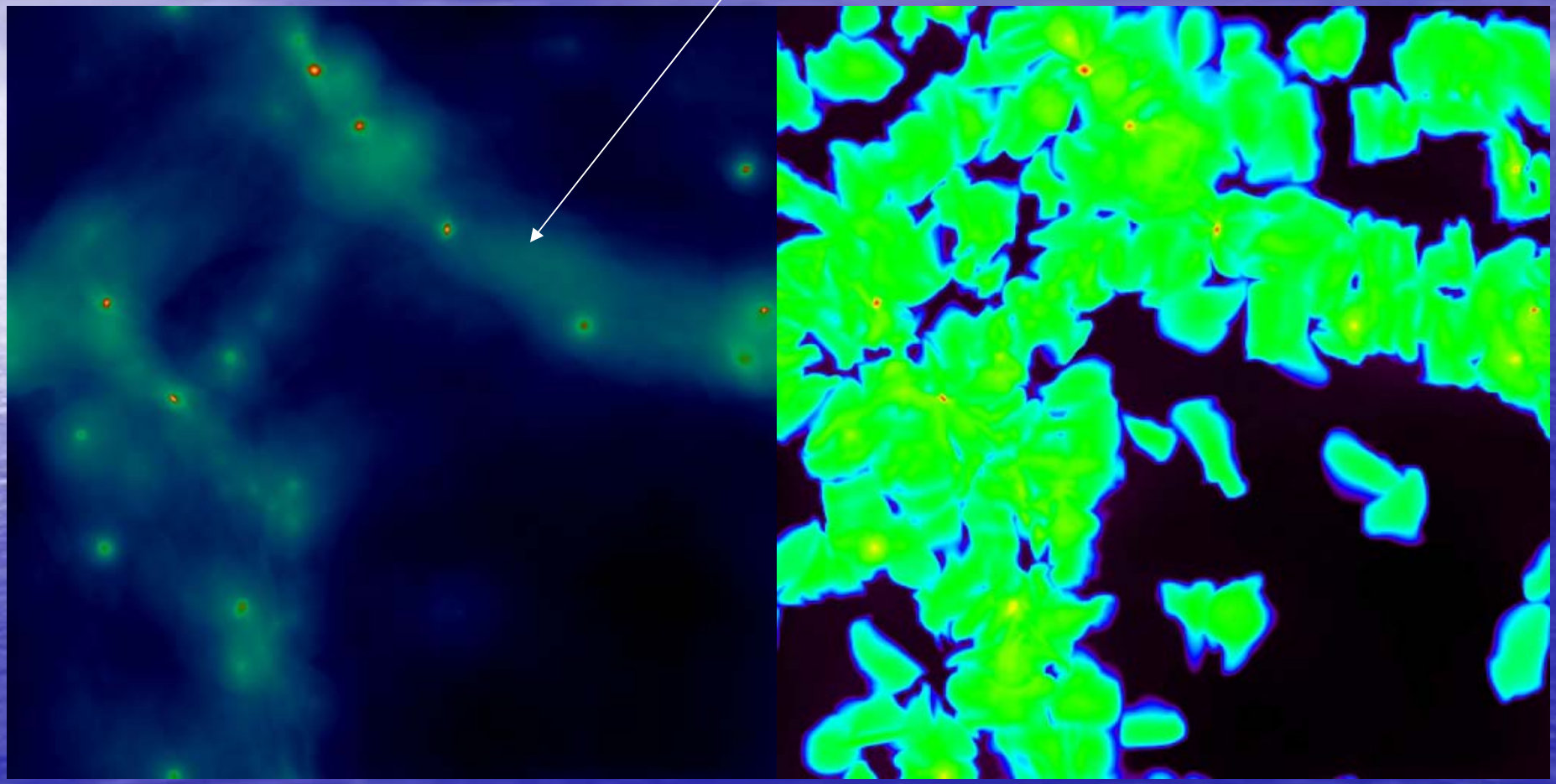

Baryon density

Metal density

Robust Prediction

- Metals from Pop III supernovae nearly uniformly preenrich the low overdensity filaments which correspond to the Ly α forest
- *Mechanism*: passive transport along filaments and photo-heating induced expansion/mixing during reionization

Quantitative Analysis

- Mean metallicity scales linearly with M_Z and $N_{bubbles}$
- Optimistic values:
  - M_Z =127 $M_\odot$ (260 $M_\odot$ PISN)
  - $N_{bubbles}$ ~1400 (ignores negative feedback which raises critical halo mass to form Pop III)
  - ➔ $\langle Z \rangle_V = 4 \times 10^{-5}\ Z_{solar}$

C/H versus baryon overdensity

Assume X_C=0.027 (Heger & Woosley 2002)

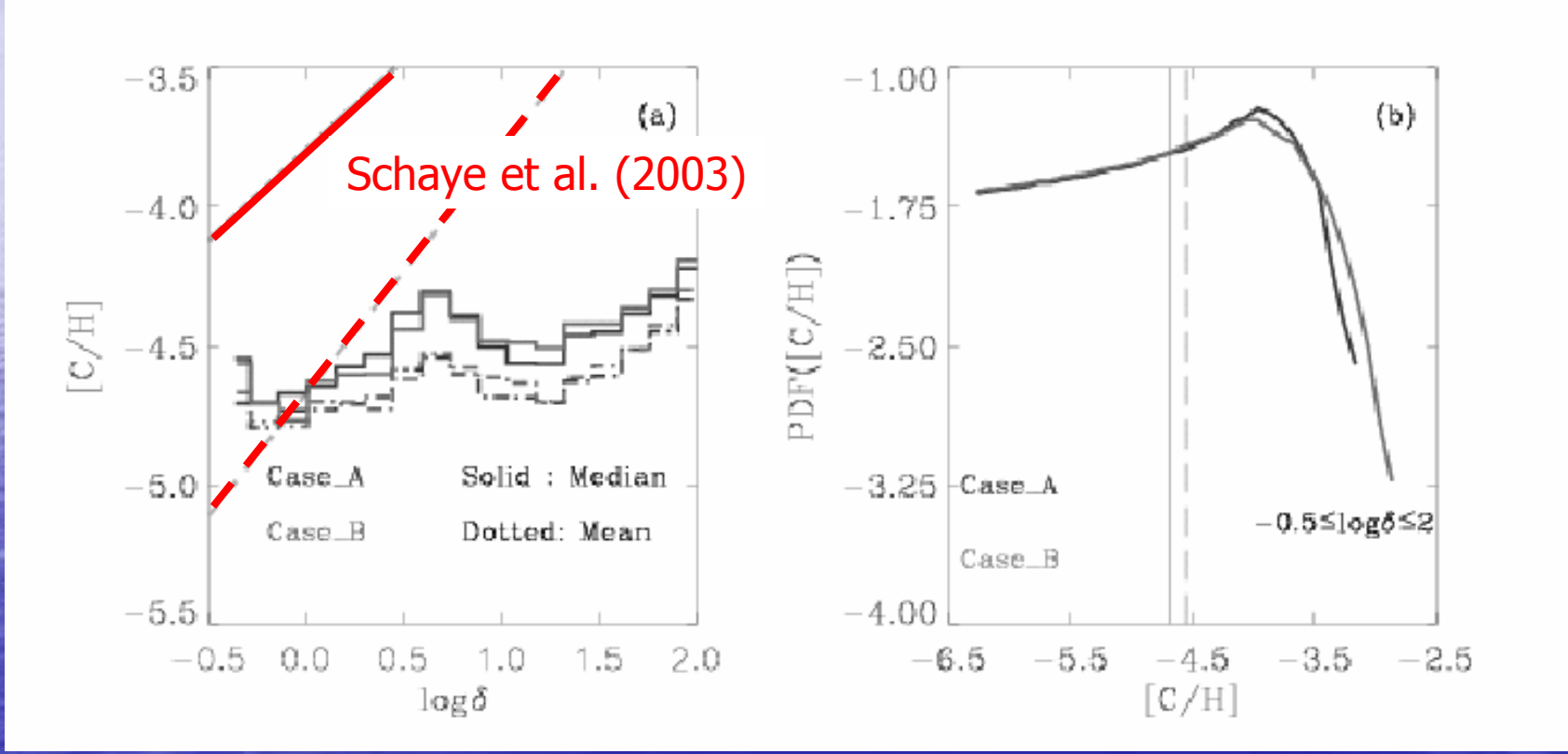

$$\langle [C/H] \rangle = -4.68 \pm 0.8$$

1. Conclusions

- Pop III can preenrich the Ly α forest, but not to the levels and dispersions seen by Schaye et al. (2003), *unless:*
  - we boost C yield per SN by ~ 3-10, or
  - we have underestimated <N bubble> by 3-10 due to small box size (likely), or
  - we have underestimated duration of PopIII epoch (possible)

2. Pollution by High-z Dwarf Galaxies (qualitative and illustrative)

- Add Cen & Ostriker (1992) phenomenological star formation and feedback (energy, metals) recipe
- Free parameters
  - ε_{sf} [0.1-1]
  - f_{m*} [0.25]
  - f_{SN} [3×10^{-6}]
  - f_Z [0.02]

Constrained by stellar astrophysics

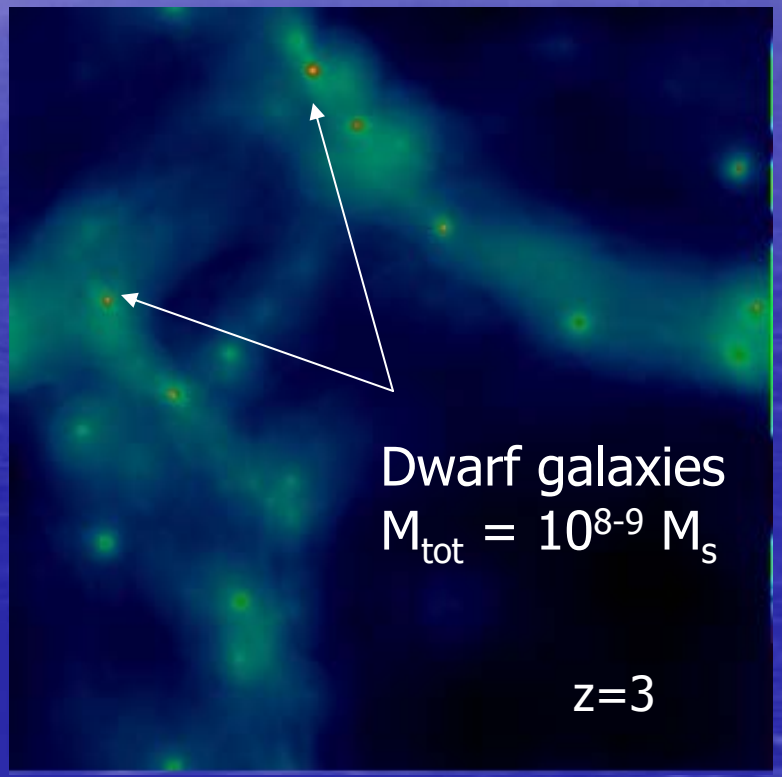

2 Mpc (com)

Star formation and feedback recipe (Cen & Ostriker 1992)

- for each cell with overdensity $\rho_b / \bar{\rho}_b > \delta_c$
- check whether 3 criteria are satisfied:

$$\nabla \cdot \vec{v}_b < 0 \quad \Rightarrow \text{contracting}$$

$$t_{cool} < t_{dyn} \equiv \sqrt{3\pi / 32 G \rho_{tot}} \Rightarrow \text{cooling rapidly}$$

$$m_b > m_{Jeans} \equiv G^{-3/2} \rho_b^{-1/2} C^3 [1 + \frac{\delta\rho_d}{\delta\rho_b}]^{-3/2}$$

$$\Rightarrow \text{gravitationally unstable}$$

- if so, convert fraction $\varepsilon_{sf} \Delta t / t_{dyn}$ of gas to collisionless star particle

Feedback to gas

- Mass and momentum (stellar winds)

$$\Delta m_b = f_{m*} \Delta m_{SF}; \qquad \Delta(m_b \vec{v}_b) = \vec{v}_* \Delta m_b$$

- Energy and metals (Type II supernovae)

$$\Delta E_b = f_{SN} \Delta m_{SF} c^2; \qquad \Delta m_Z = f_Z \Delta m_{SF}$$

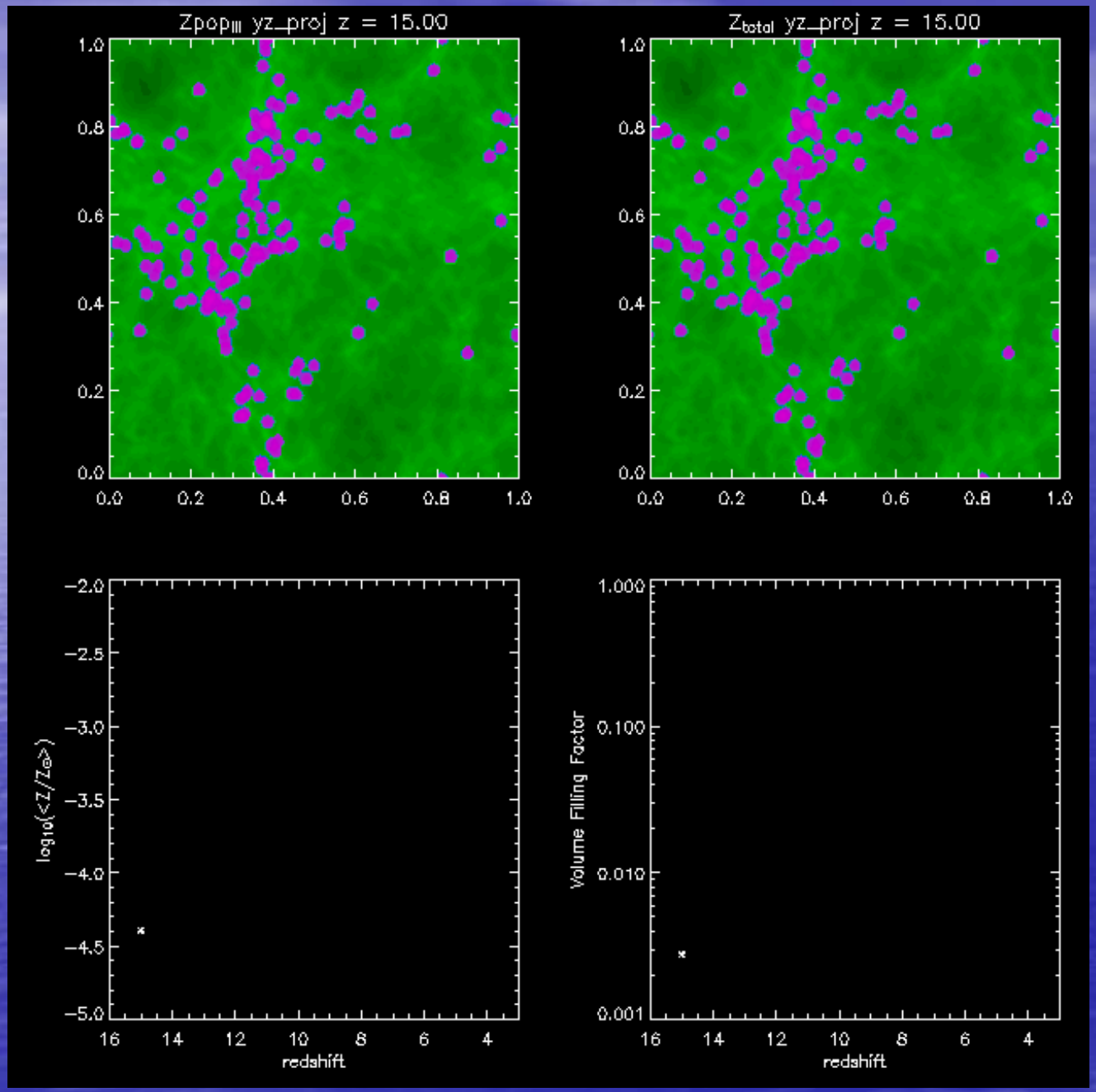
Zpop III yz_proj z = 15.00
Ztotal yz_proj z = 15.00
1.0
0.8
0.6
0.4
0.2
0.0
0.0
0.2
0.4
0.6
0.8
1.0
log10(<Z/Ze>)
-2.0
-2.5
-3.0
-3.5
-4.0
-4.5
-5.0
16
14
12
10
8
6
4
redshift
Volume Filling Factor
1.000
0.100
0.010
0.001
redshift

1 Mpc

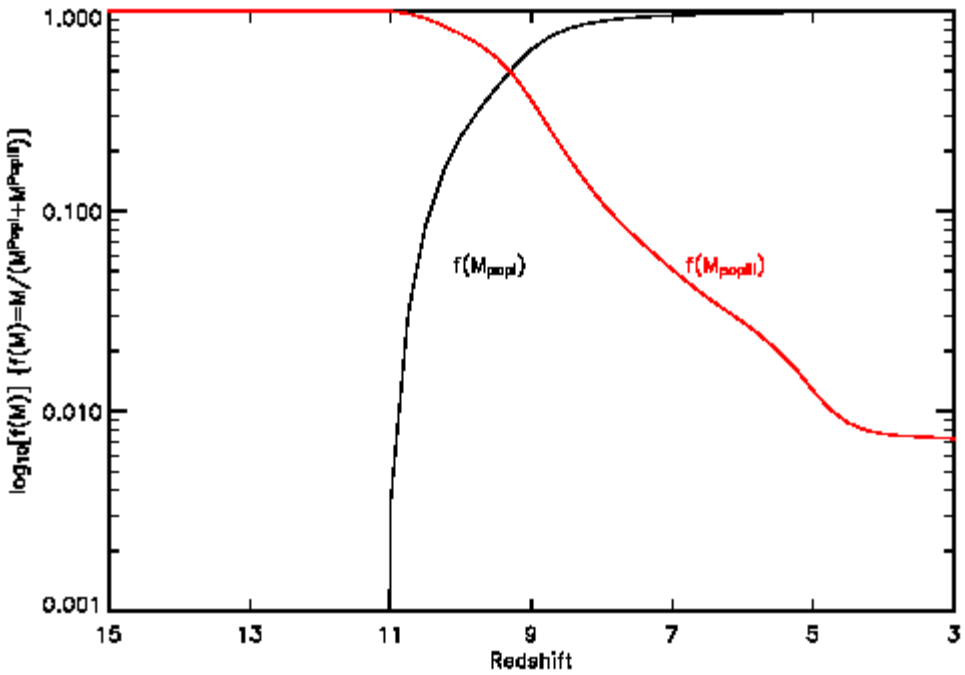

Metal Fraction

$z_{form} \sim 10$

$\langle Z_{final} \rangle \sim 6 \times 10^{-2}\ Z_\odot$

Metallicity

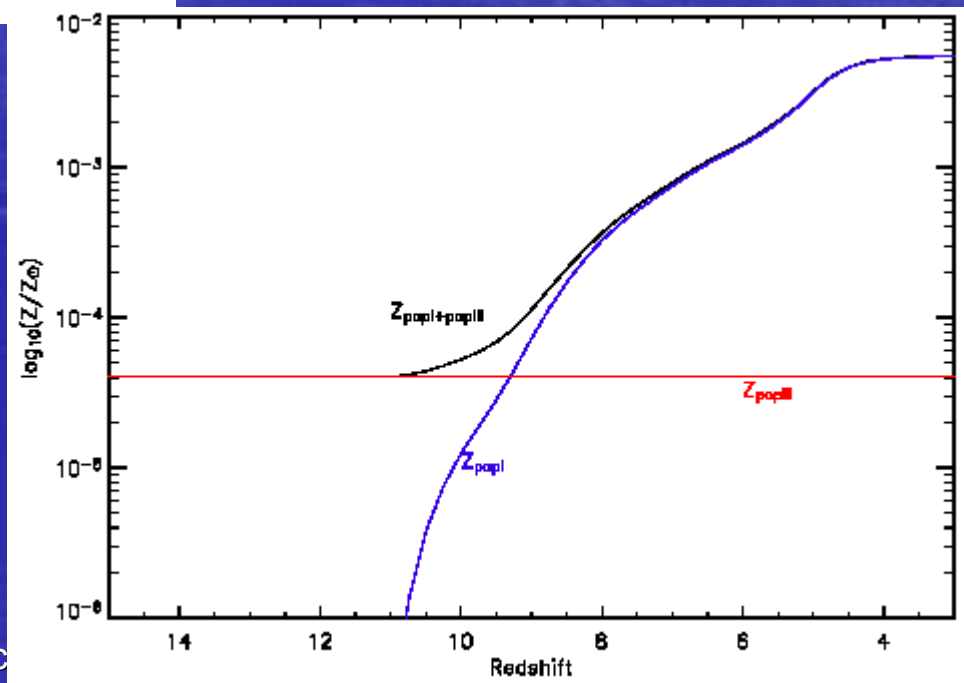

Projections z=3

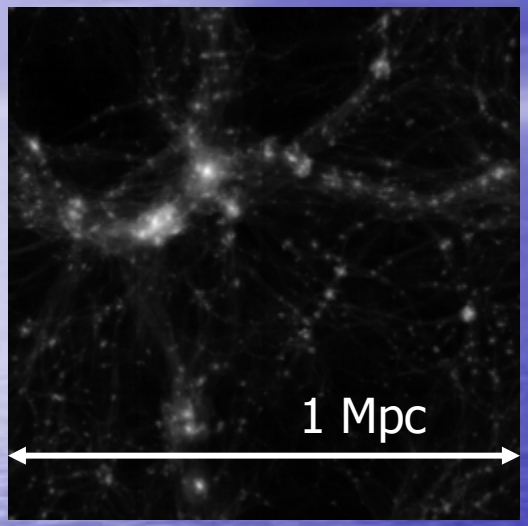

Dark Matter

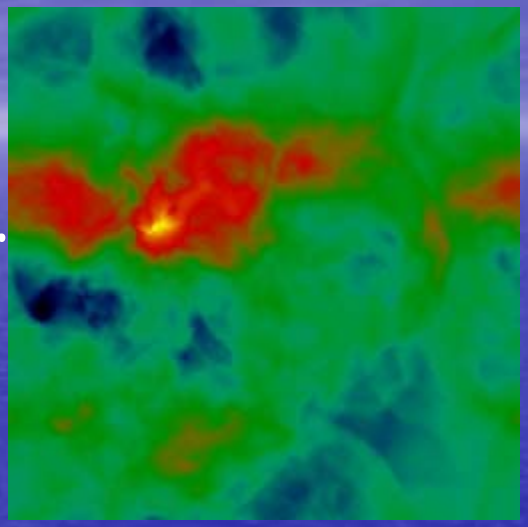

Gas

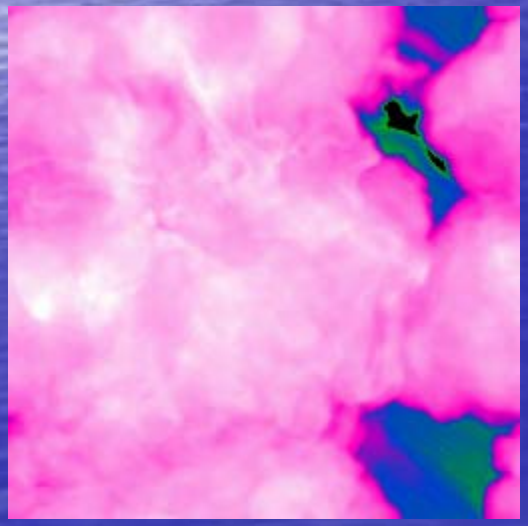

Total Metals

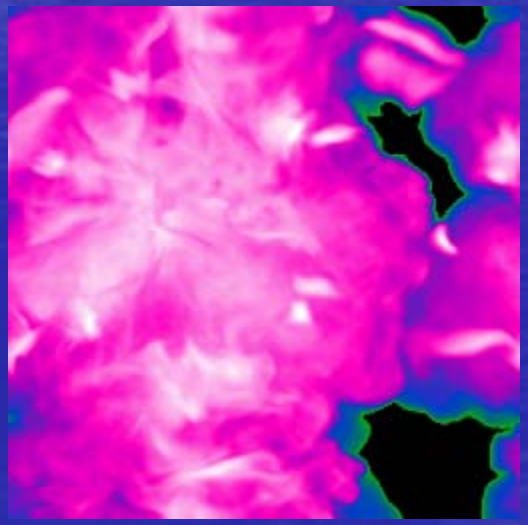

PopIII Metals

Metallicity Distribution at z=5 and z=3

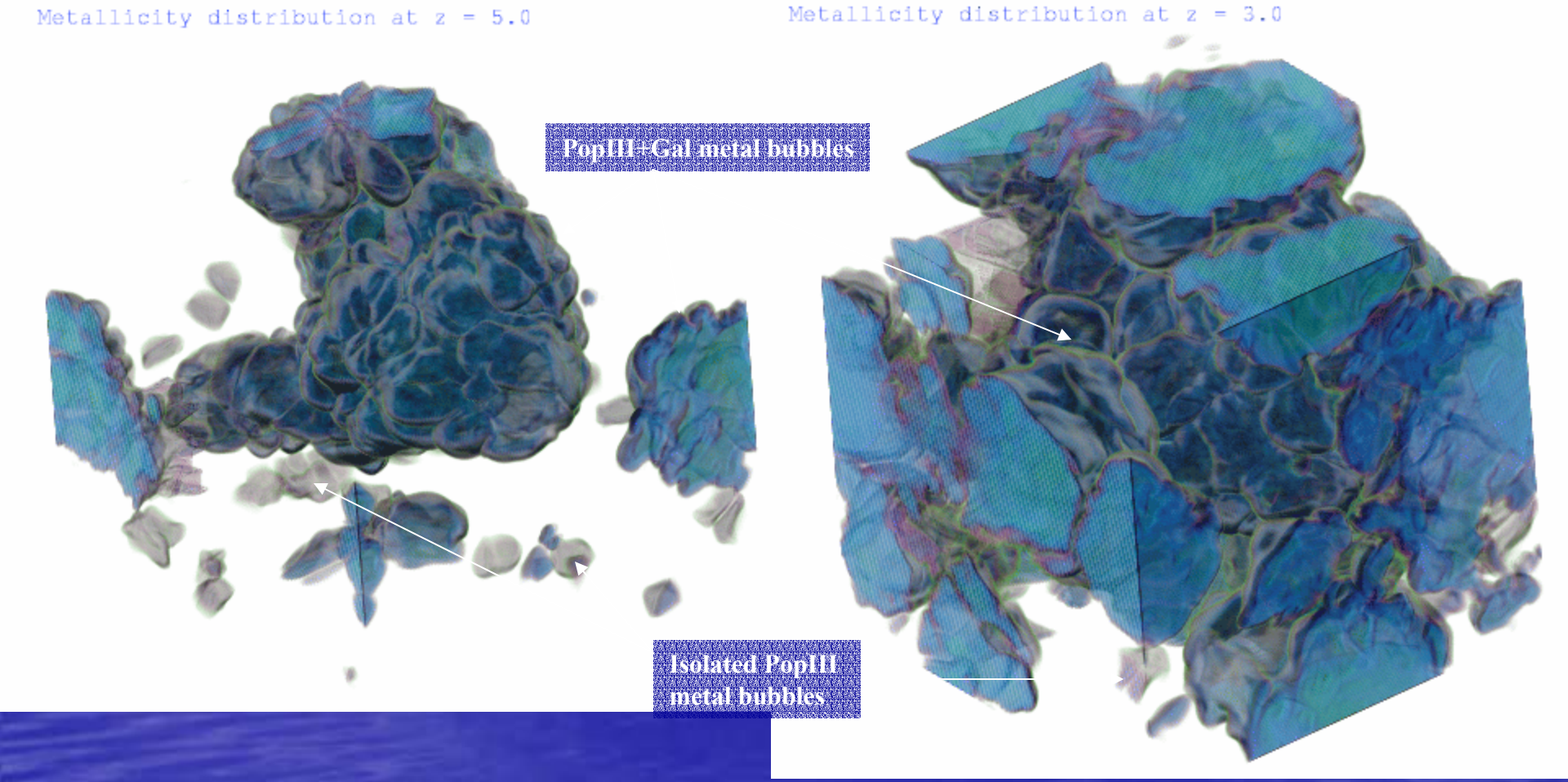

3. Signatures of Pop III in quasar absorption lines

Carbon & CIV Abundance Computation

- Carbon abundance in metal density
  - X_C(popIII) = 0.027 (In a SN ejecta of a 260 $M_\odot$ PopIII star)
  - X_C(Gal) = 0.357 (SN typeII)
- Carbon ionization model computes CIV distribution at $z \leq z_{reion}$
  - Radiation Background : soft UV Gal+QSO (Haardt & Madau 2001)

Synthetic Spectra

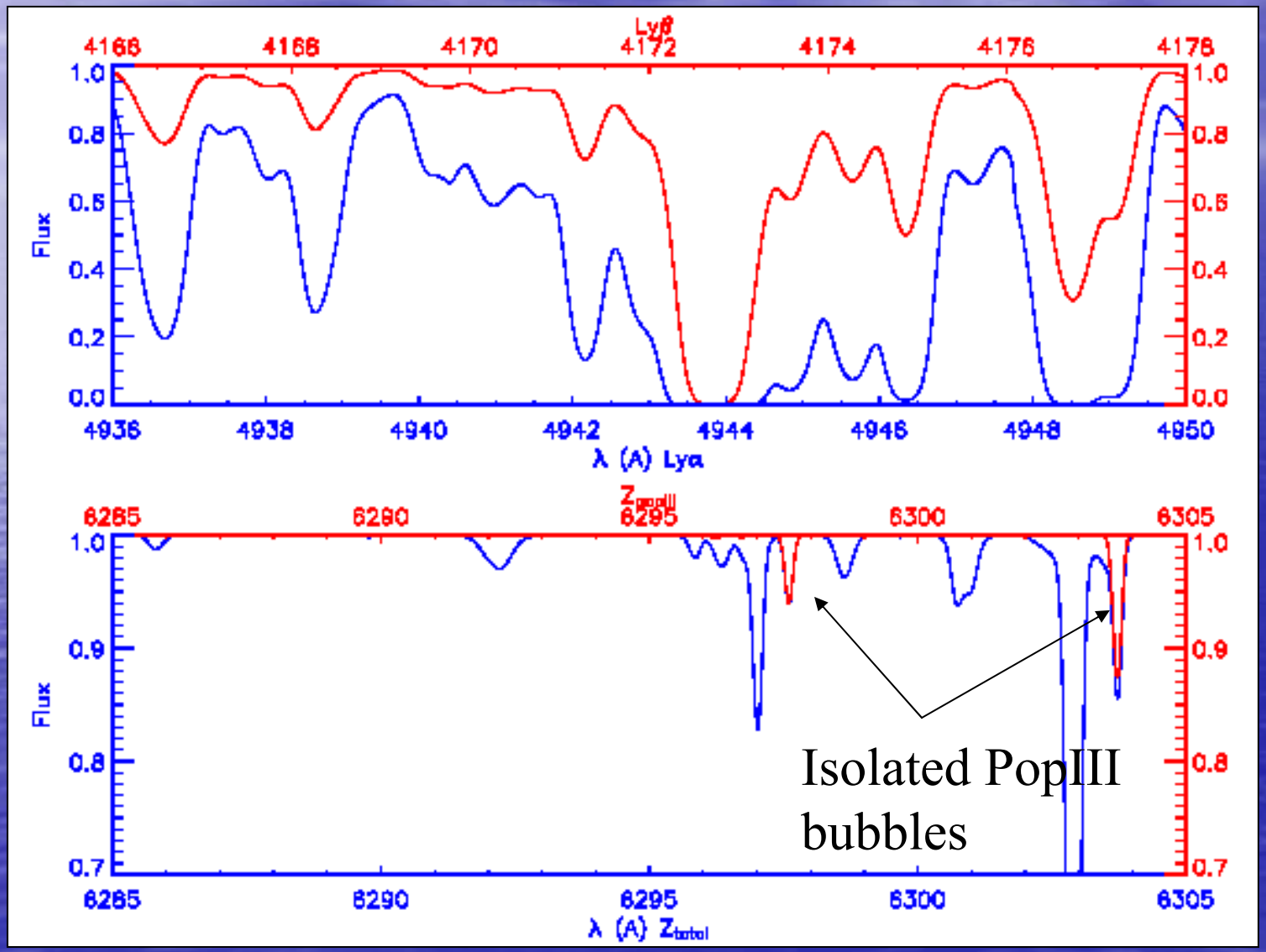

Column density distribution

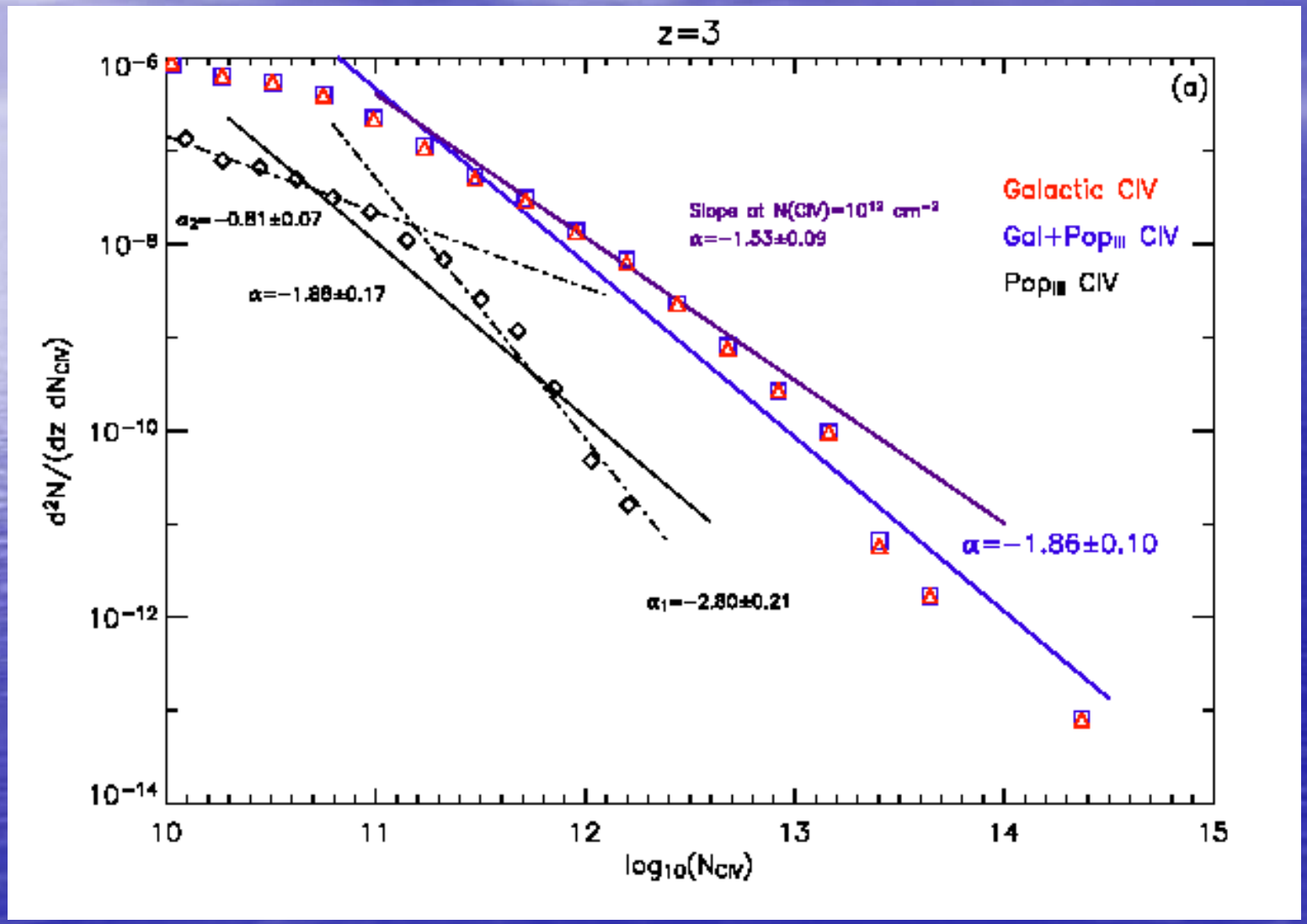

b-parameter distribution

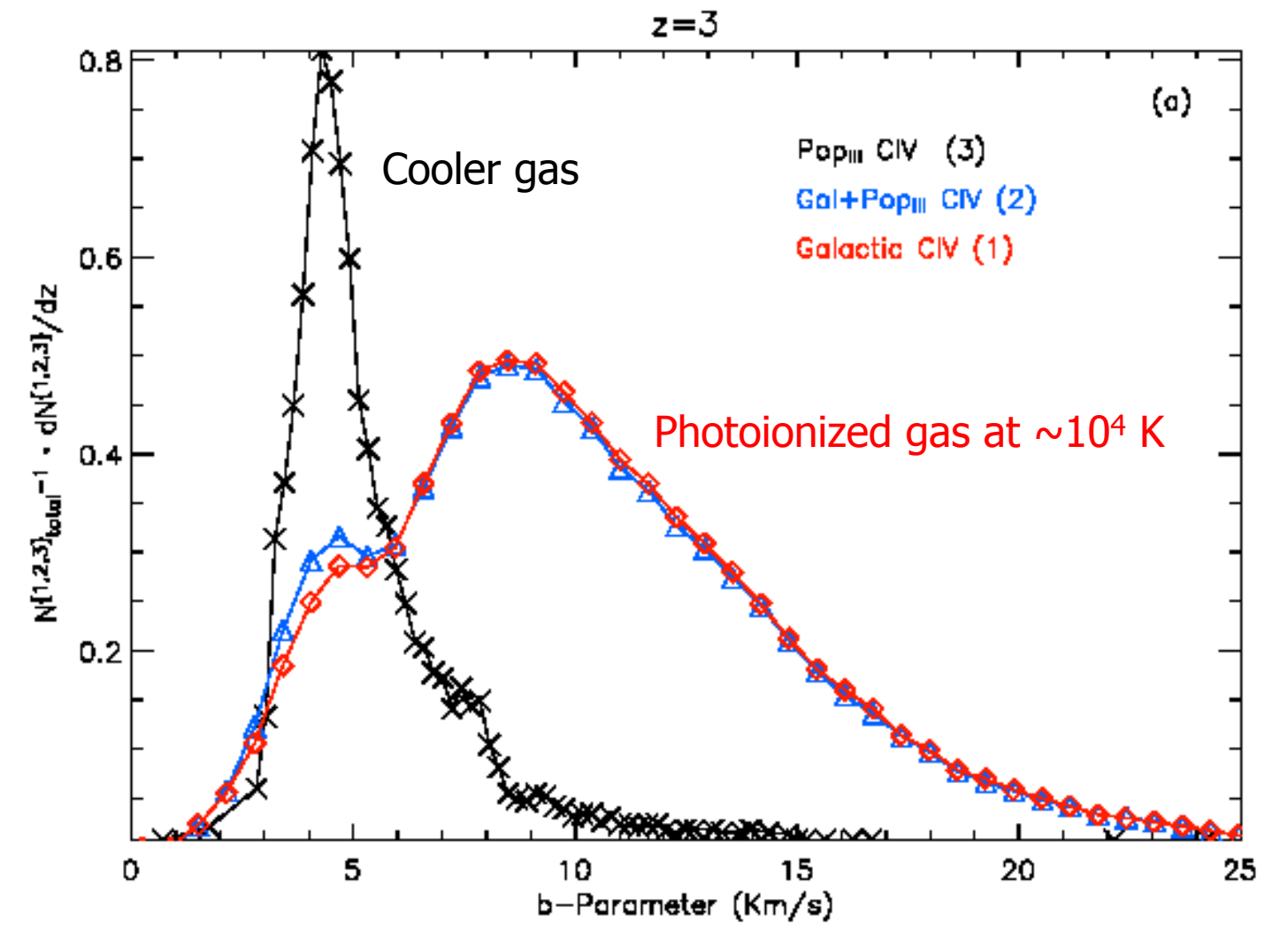

N_{CIV} vs Overdensity (z=3)

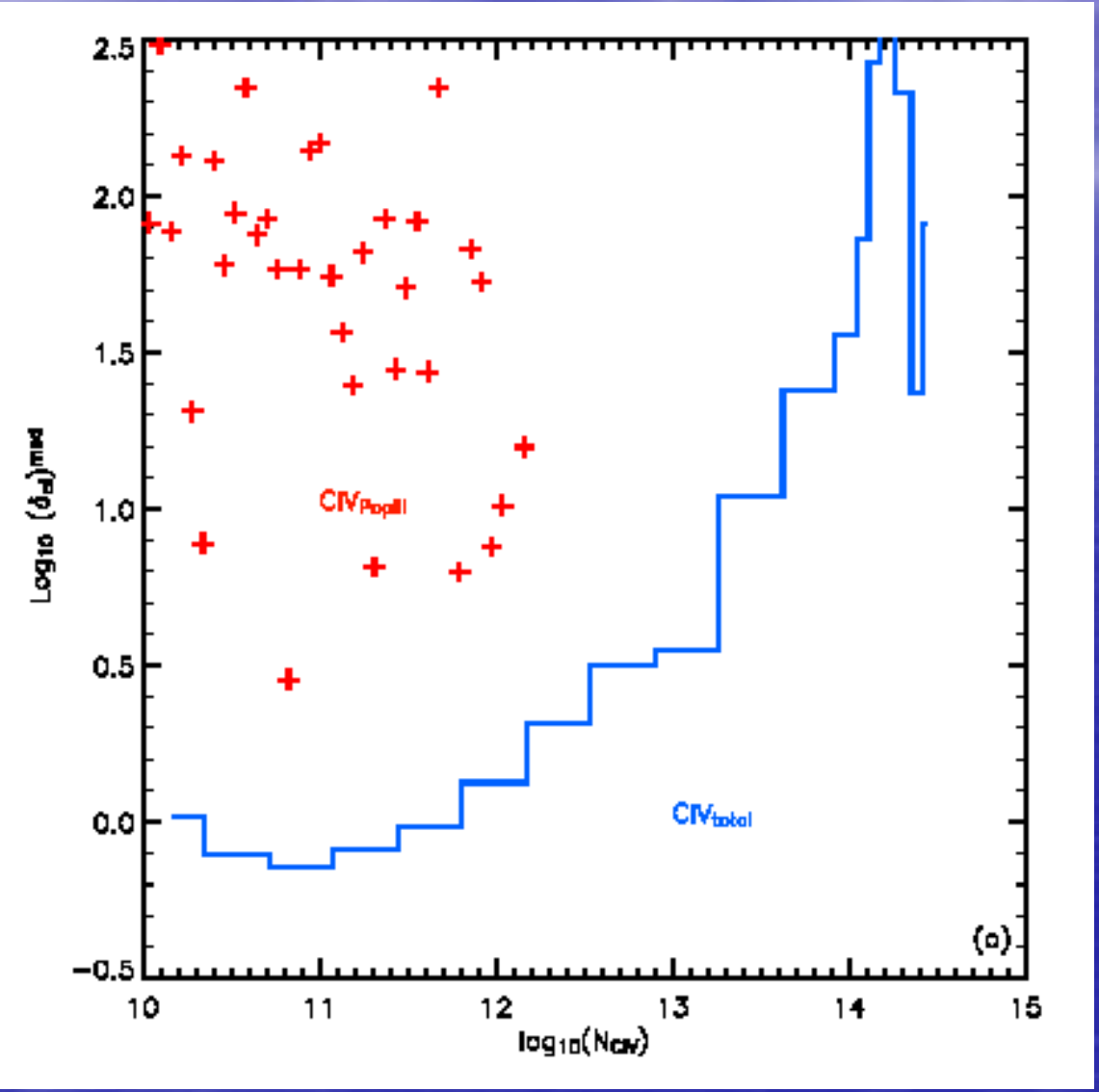

N_{HI} vs Overdensity (z=3)

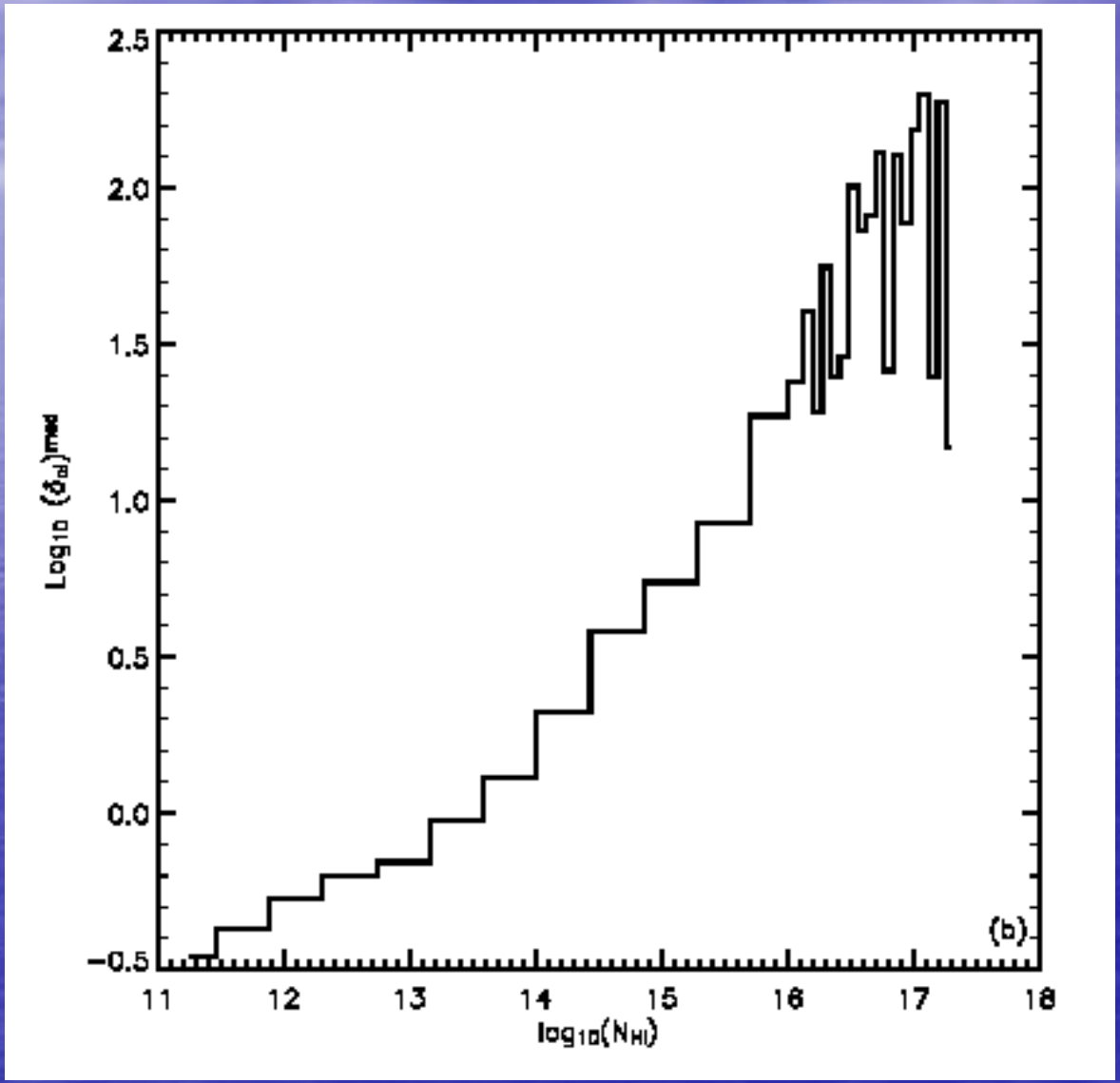

N_{CIV} vs N_{HI} (z=3)

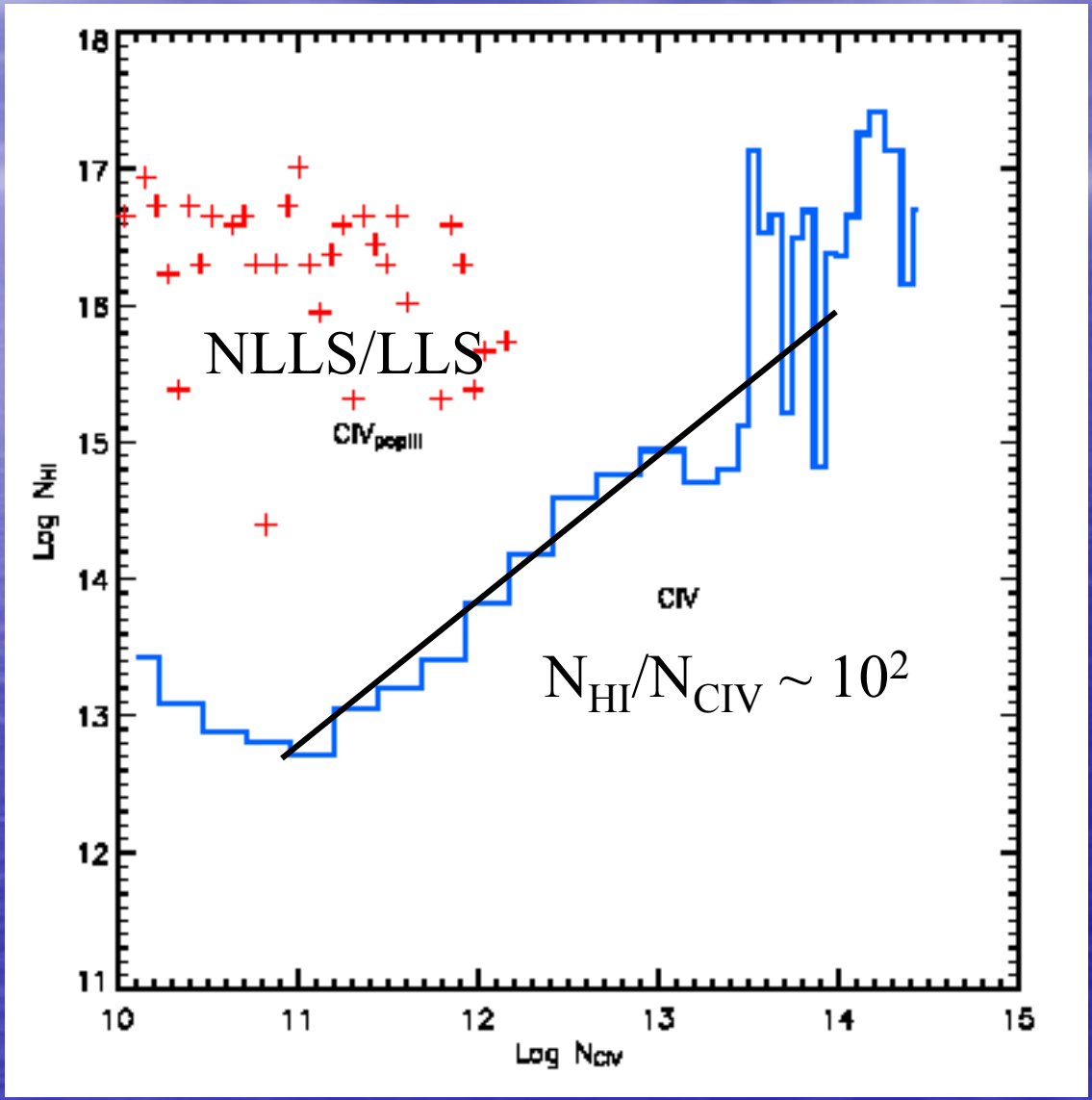

4. Future: Gigazone Simulations

- Need larger volumes for reliable statistics
- Need high resolution (space + mass) to model galaxy feedback
- Billion particle, billion cell simulations now feasible at San Diego Supercomputer Center
- 8 Mpc cube captures formation of every popIII halo and dwarf galaxy $M < \sim 10^{10}\ M_\odot$

Giga-zone

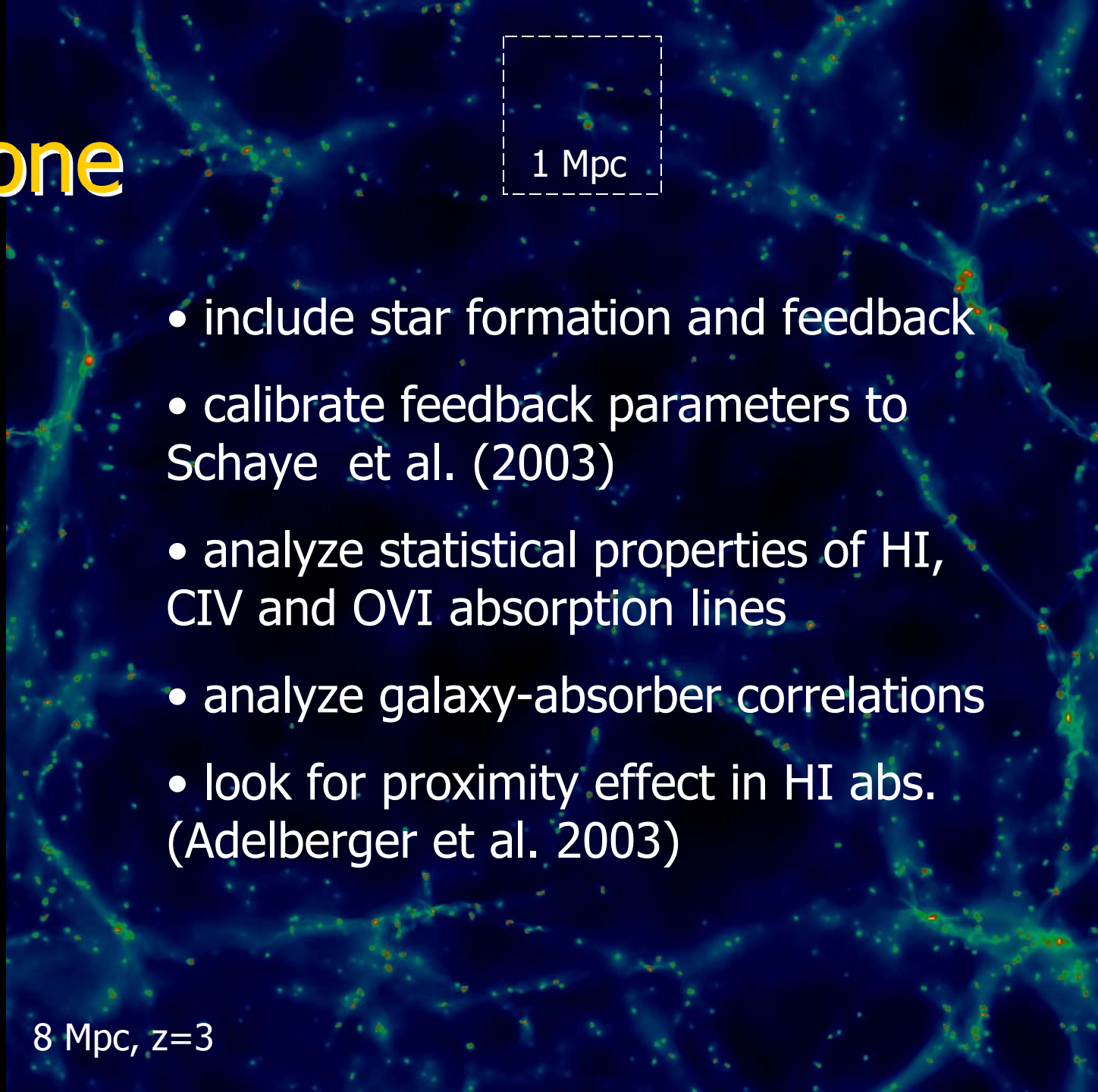

- include star formation and feedback
- calibrate feedback parameters to Schaye et al. (2003)
- analyze statistical properties of HI, CIV and OVI absorption lines
- analyze galaxy-absorber correlations
- look for proximity effect in HI abs. (Adelberger et al. 2003)

M. L. Norman

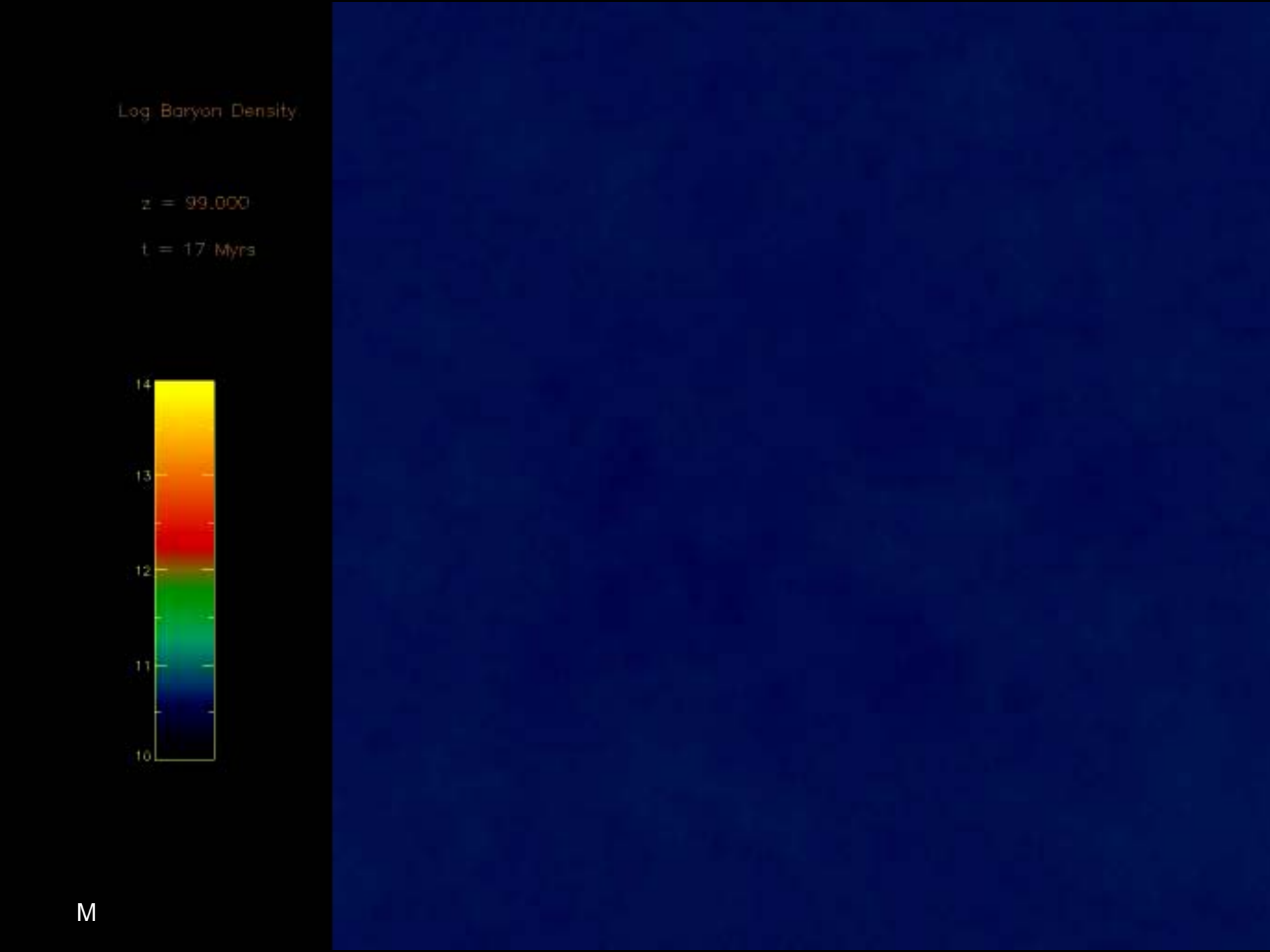

M

Disk Space.....

the final frontier

Evolution of Damped Lyman α Systems from Hierarchical Structure Formation Models

Katsuya Okoshi (National Astronomical Observatory, Japan)

Okoshi, Nagashima, Gouda and Yoshioka 2004 ApJ, 603,12
Okoshi and Nagashima 2004 Submitted to ApJ

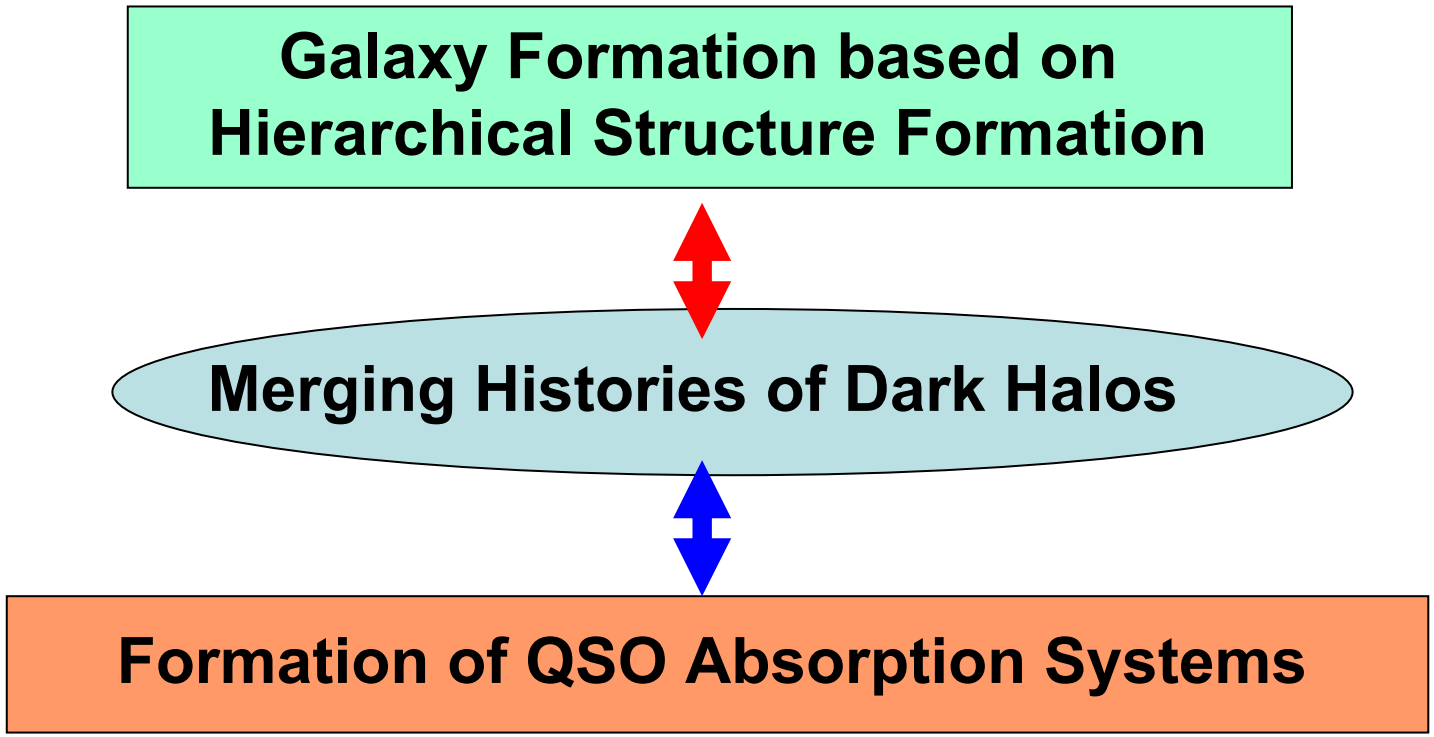

Abstract

We investigate the evolution of Damped Lyman α (DLA) systems on the hierarchical structure formation scenario by using a semi-analytic model of galaxy formation which can show the fundamental properties of galaxies such as luminosity functions and number-magnitude / redshift relations. We find good agreement with a reasonable range of parameters for reproducing fundamental properties of DLA systems. This result suggests that the chemical evolution of DLA systems can be consistently reconciled with the observational features of typical galaxies. We also explore host galaxies of DLA systems at low redshift z<1. Our results suggest that DLA systems primarily consist of low surface brightness dwarf galaxies (typical radius 3kpc, surface brightness 22-27 mag arcsec^{-2} in B-band, star formation rates 0.01$M_{\odot}$/yr).

§ 1 Introduction

Why we focus on the properties of DLA systems ?

1. **High HI column density system**

2. **More abundant systems at high redshift**

$$\left(\frac{dN}{dz}\right)_{DLA} \approx 10\left(\frac{dN}{dz}\right)_{\substack{typical\\galaxy}} \qquad \left(\frac{dN}{dz}\right)_{\substack{typical\\galaxy}} = \Phi_{g,0}(1+z)^3 \pi R_g^2 \frac{c}{H_0 \Omega^{1/2}(1+z)^{5/2}} \approx 0.02\Omega^{1/2}$$

$$(z = 3; \Phi_{g,0} = 0.01 h^3 Mpc^{-3}, R_g = 10 h^{-1} kpc)$$

3. **Precise measurements of abundance (Keck Telescope)**
   ZnII (unaffected by dust depletion)
   mildly metallicity evolution (0.5 <z< 4.5)
   (eg. Prochaska et al. 2003)

4. **Dust-poor system (cf typical galaxy)**
   Small amount of dust (e.g. ~1/10 (Our galaxy))

   >> Good Tracer of Metallicity Evolution for Pre-galactic System

   >> Constraints on Galaxy Formation

§ 2 Model

Merging **Process** of Dark Halos

Probability Function f(M,z | M',z')dM:
Halo (mass M' redshift z') has a progenitor (M,z)

>> Press-Schechter Mass Function n(M,z | M',z')

Methods (redshifts z' to z (z'<z))

1. **Monte-Carlo realization as probability variables M**

2. **Count progenitors (Vc > 40 km/s)**
   (dark halos with Vc < 40 km/s accrete into central halos)

3. **Realize above processes for each progenitor at higher redshifts**

Evolution Process

(A) Life time

Life time of halo is equal to cooing time of gas

$$t_{life} = \tau_{cool}(r_{cool}) = \frac{2}{3}\frac{\rho_{gas} r_{cool}}{\mu m_p}\frac{kT}{n_e^2 r_{cool}\Lambda(T)} \quad (\rho_{gas}(r) \propto n_e(r) \propto r^{-2})$$

(B) Star Formation Process

$$\dot{M}_* = \frac{M_{cold}}{\tau_*}$$

$$\tau_* = \tau_*^0 \left(\frac{V_c}{300 km/s}\right)^{\alpha_*} (1+z)^{\alpha_z}$$

$\alpha_z = 1.5 (\propto t_{dyn})$:accelerated efficiency model

0 : constant efficiency model

$$\tau_*^0 \cong 2-5 Gyr (M/L_B - V_c relation)$$

$$\rightarrow \quad \tau_*^0, \alpha_*, \alpha_z$$

(C) Supernovae Feedback

Energy input by SN explosions

$$\frac{dM_{rehaeat}}{dt} = \varepsilon \frac{4}{5} \frac{\eta_{SN} E_{SN}}{V_c^2} \dot{M}_* \left(= \beta \dot{M}_* \right)$$

$$\beta(V_c) = \left(\frac{V_c}{V_{hot}} \right)^{-\alpha_{hot}}$$

ε : input efficiency

η_{SN} : fraction of stars $M \geq 8 M_\Theta$

E_{SN} : energy release per a SN $(= 10^{51} \mathrm{erg})$

α_{hot} : $\alpha_{hot} = 2$

(D) Population Synthesis

Total Luminosity

$$L_* = \int \dot{M}_* Z_{cold} dt$$

Stellar population synthesis model: Kodama and Arimoto model

(F) Chemical Evolution

Basic Equation for 2 phase model (Cold and Hot gas components)

$$\frac{dM_c}{dt} = -\dot{M}_* + F(t)(1-f) + g(t) - \beta \dot{M}_*$$

$$\frac{dM_*}{dt} = \frac{M_c}{\tau_*}$$

$$\frac{dM_h}{dt} = \beta \dot{M}_* - g(t) + F(t)f + A(t)$$

$$g(t) = 4\pi\rho_h(r_{cool})r_{cool}^2 \frac{dr_{cool}}{dt} \cong \frac{M_c^0}{\tau}$$

$$\frac{dM_c Z_c}{dt} = (1-f)(F_Z(t) + R_Z(t)) - Z_c \dot{M}_* + Z_h g(t) - Z_c \beta \dot{M}_*$$

$$\frac{dM_h Z_h}{dt} = f(F_Z(t) + R_Z(t)) + Z_c \beta \dot{M}_* - Z_h g(t) + Z_d A(t)$$

β : **SN feedback** **g: cooling gas inflow**

F: gas inflow from stars Fz: metal mass produced by new stars
Rz: metal mass inflow A: gas mass accreted from diffuse matter(=0)

Here we apply 'Instantaneous Recyclic Approximation'.

Merging Processes of galaxies

Dark halos merge together

↓

Hot gas is incorporated with a new common halo

Type of merging processes (satellites v central galaxy)

↓

Two types: Major and Minor merge

Major merge $m_{small} / m_{large} > f_{bulge}$

Star burst, Bulge formation (all stars reside in central bulge)

Minor merge $m_{small} / m_{large} < f_{bulge}$

Disk formation (stars in satellites >> disk components)

↓

Satellite-Central, Satellite-Satellite Mergers

Criteria for merging processes of galaxies

Satellite-Central merger : t (elapse) > t (dynamical friction)
Satellite-Satellite merger: t > t (random collision)

(E) Cosmological Models

We refer the standard models in galaxy formation model

Astrophysical parameters are given by as follows:

1. **Galaxy luminosity function (B- and K- bands) >>** α_{hot}, V_{hot}
   (<< SN feedback process)
2. **Cold-gas mass fraction >>** α_*, τ_*^0

MODEL PARAMETERS

Ω_0=0.3, Ω_Λ=0.7, h=0.7, σ_8=1

Vhot=280[km/h], α_{hot}=2.5, τ_*^0=1.5[Gyr], α_*=-2

§ 3. RESULTS

[A] *GLOBAL PROPERTIES OF DLA SYSTEMS*

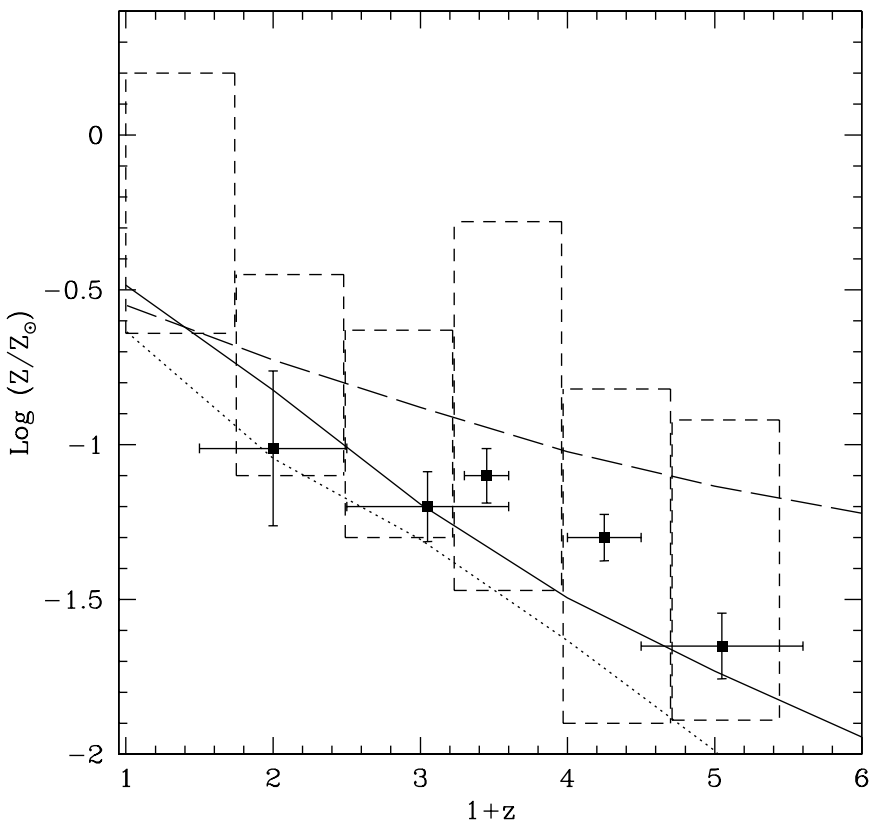

Metallicity of cold gas in DLA systems

solid line: Our best model
dotted line: stellar metallicity
dashed line: a model with $\tau^* \propto$ dynamical timescale of disks (LD model)
observational data: Prochaska and Wolfe 2000, Savaglio 2001

- **The metallicity shows mildly evolution.**
- **The star formation timescale should be nearly constant**

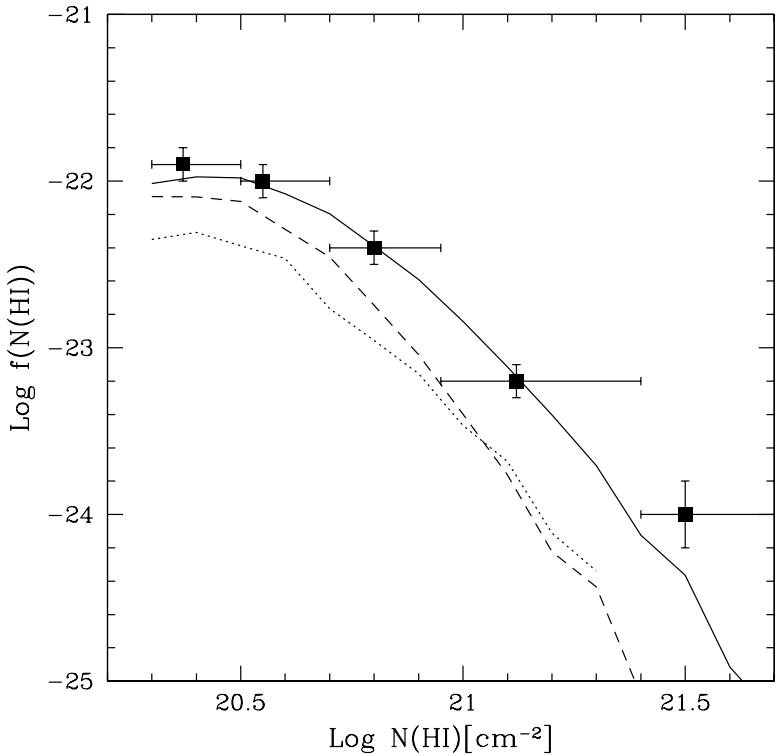

HI column density distribution

solid line: Our best model
dotted line: α*=0
dashed line: LD model
observational data:
Prochaska and Wolfe 2000

- **Our model reproduces the HI column density distribution.**

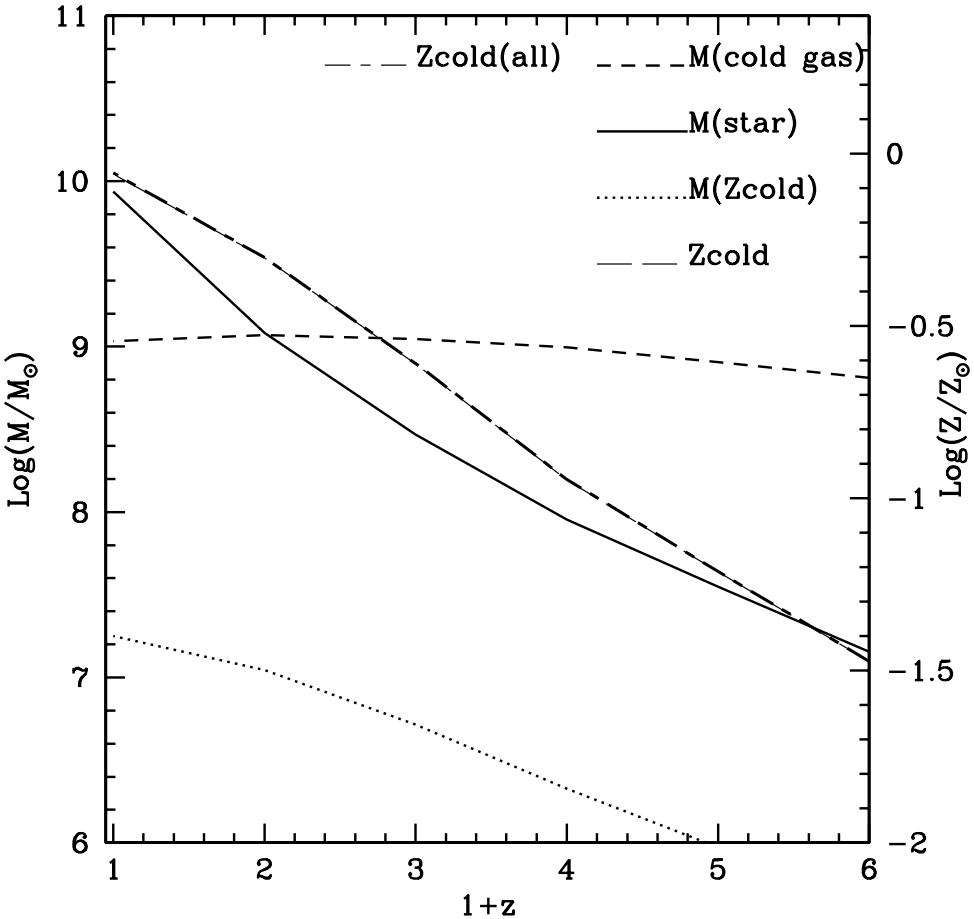

***Average mass evolution of each phase*:**
cold gas (dashed line), stars(soild line), metals(dotted line)

Metallicity weighted by mass
cold gas in DLAs (long-dashed line)
cold gas in all galaxies (dot-dahed line)

- **The average HI mass M(HI) is ~$10^9 M_\odot$**
- **Chemical enrichment in DLAs is similar to that in all galaxies**

[B] *Low-redshift DLA systems*

We focus on DLA systems at redshift 0<z<1 ⇒ What are DLA galaxies ?

・Luminosity, HI column density, size etc. ← photometric counterparts (e.g. Rao et al.2003)

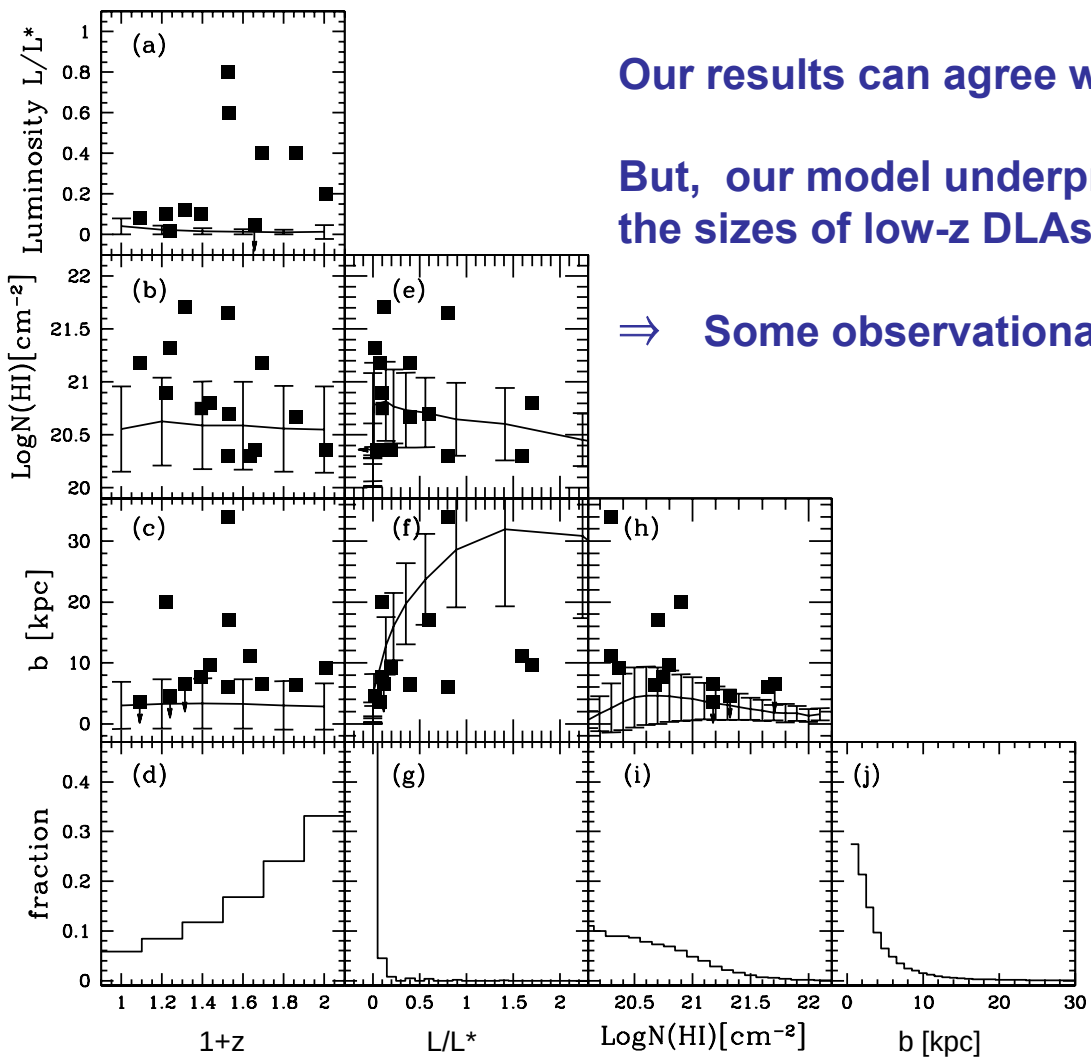

Our results can agree with some observation trends.

But, our model underpredicts the luminosities and the sizes of low-z DLAs.

⇒ Some observational biases?

Next, we take into account selection effects of DLA galaxies

(1) Surface brightness dimming effect: fail to identify DLA galaxies fainter than observational brightness limits

(2) Masking effect: fail to identify DLA galaxies hidden or contaminated by a point spread function of background QSOs

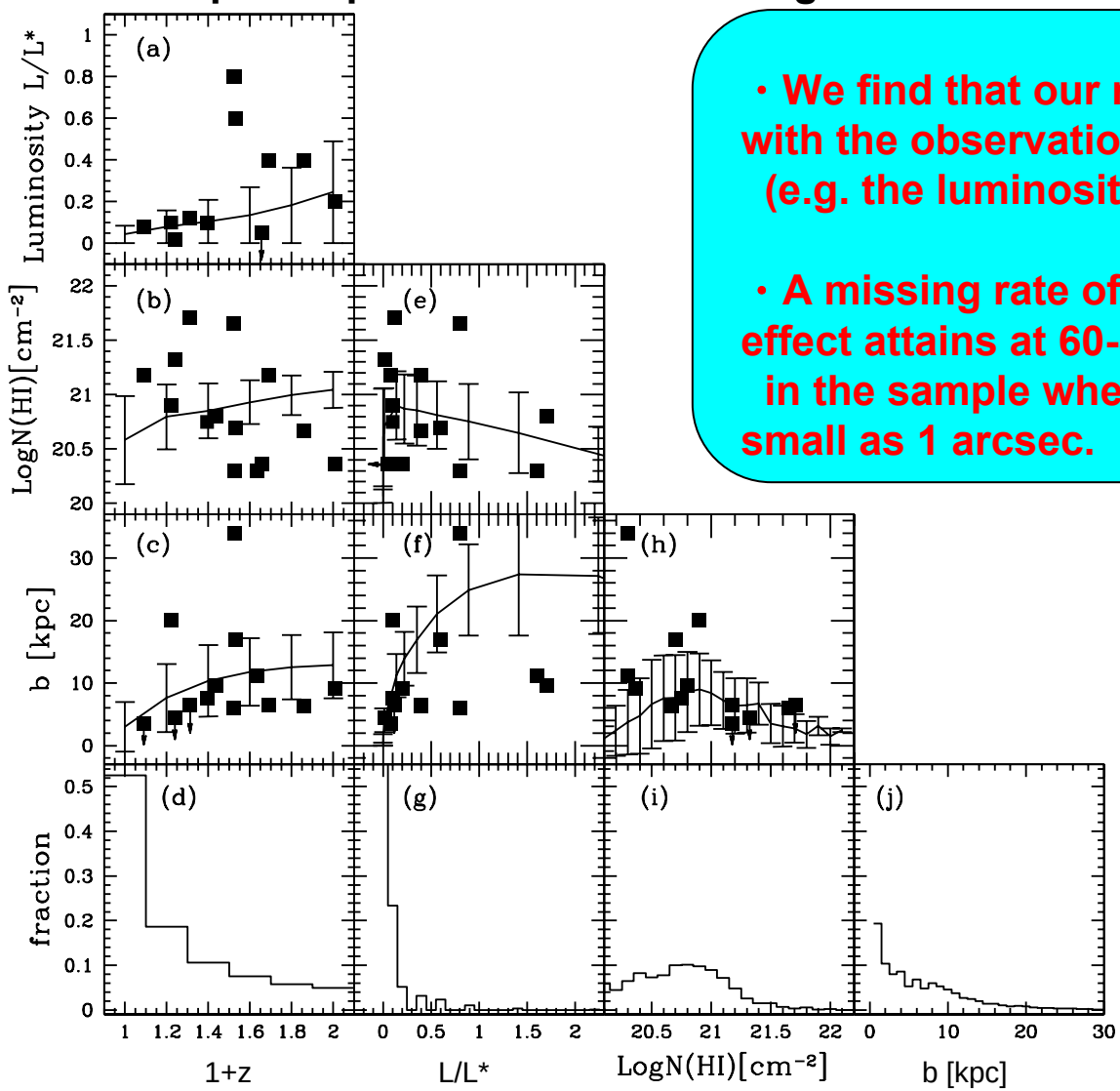

- **We find that our results show better agreement with the observations (e.g. the luminosities and the sizes) .**

- **A missing rate of DLA galaxies by the masking effect attains at 60-80% in the sample when a angular size limit is as small as 1 arcsec.**

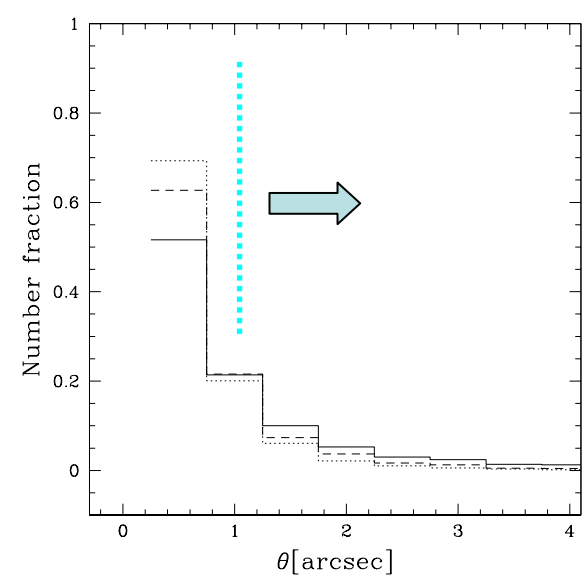

[C] ***Radio properties of DLA systems at redshift z=0***

Another way to explore DLA systems apart from selection effects.

Detection of DLA galaxies by Blind 21cm surveys (e.g. Rosenberg & Schneider 2003)

⇒ about 50 HI-rich galaxies with HI column densities comparable to those in DLA systems

We find that

(1) A tight correlation between the HI masses and the cross sections: Log $\sigma \propto$ Log M(HI)

(2) HI-rich galaxies with 10^9M_sun mainly contribute to the population of DLA systems at z=0

⇒ Our result is entirely consistent with the observational properties of HI-selected galaxies in the radio survey.

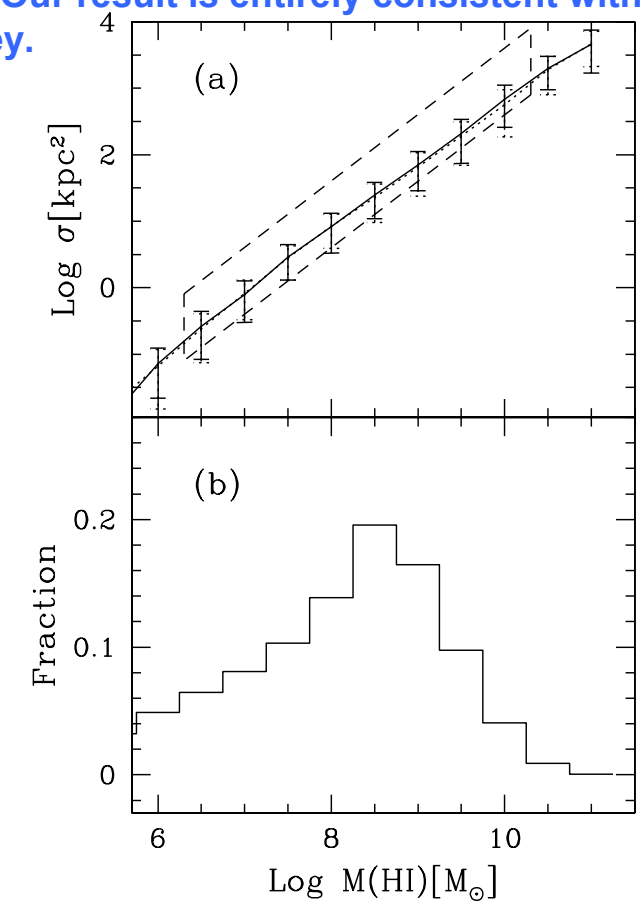

Dashed box: observational data (Rosenberg & Scheider 2003)

[D] Star formation rates (SFRs)

a clue to exploring what types of galaxies consist of DLAs

⇒ Our model suggests that the average SFRs are as low as 0.01 M8 /yr.

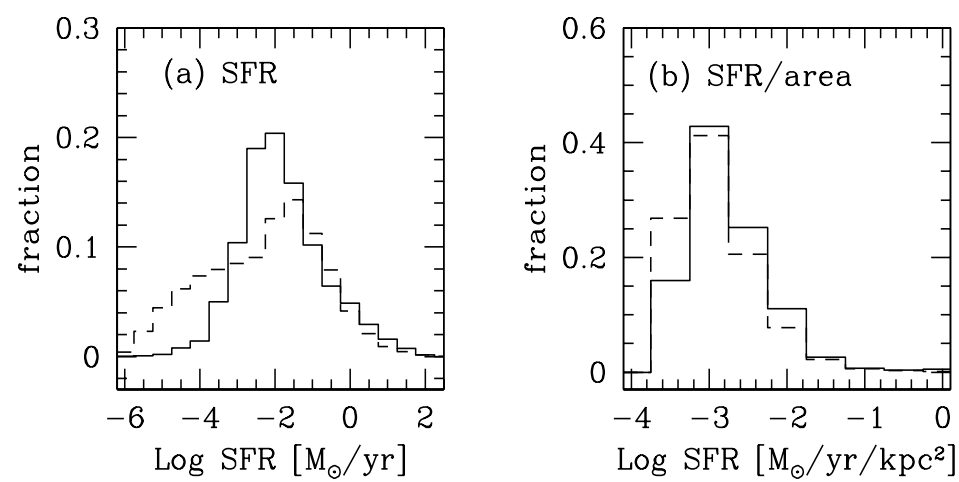

§ 4 Conclusions

We investigate evolution of Damped Lyman α systems taking into account merging processes of dark halos from hierarchical galaxy formation models

●The star-formation process can be reconciled with the fundamental properties of local galaxies (e.g. luminosity function, cold-gas mass, number counts, ..) (Nagashima et al. 2001)

●The constant efficiency of star formation can be in better agreement with the observations of DLA metallicities at high redshifts which shows that the metal enrichments is suppressed.

●Our model can reproduce global properties of DLA systems at high and low redshifts

- **Metallicity Evolution and HI column density distributions**
- **Luminosity, HI column density, Size of DLA systems at redshift z<1**

● The masking effect significantly affects the identification of DLA galaxies at redshift z<1

⇒The missing rate attains 60-80% when low luminosity galaxies with small impact parameters(~3kpc) contribute to the population of DLA systems.

- Our results are also consistent with the radio properties by blind 21-cm surveys (ADBS)
  - The HI-disk sizes correlate with the HI masses: Log $\sigma \propto$ Log M(HI)
  - The average HI mass is M(HI)~10^9 $M_\odot$

- LSB dwarf galaxies primarily contribute to the population of DLA systems at z<1
  - Disk size ~3kpc
  - Surface brightness ~22 to 27 mag $arcsec^{-1}$ in B-band
  - Star formation rate ~10-2 $M_\odot yr^{-1}$

Further Study….

1. Evolution of DLA galaxies at High-redshift z>2
2. The abundance of hydrogen molecules: CNM and WNM
3. Sub-DLA systems
4. Radio properties of DLA galaxies

Cosmological Simulations of IGM Metallicity Enrichment

Benjamin D. Oppenheimer
University of Arizona

August 10, 2004

Advisor: Romeel Davé

Collaborators: Volker Springel & Lars Hernquist

Metals in the IGM

- Davé et al. (1998) find enrichment [C/H] = -2.5 and [O/H] = -2.0 for absorbers $N_{HI} > 10^{14.5}$ cm^{-2} ($\delta > 10$)

- Schaye et al. (2003) derive the relation $[C/H] = -3.47 + 0.08 (z - 3) + 0.65 (\log \delta - 0.5)$ with a log normal scatter using a softer ionizing background that includes star forming galaxies (Haardt & Madau 2001)

- SPH Cosmological Simulations by Springel & Hernquist (2003, SH03) include the effects of star formation, supernova feedback, and galactic winds

Our Project

- Explore the metallicity in the IGM from SH03 using quasar absorption line spectra

- IGM metallicity depends on:
  - Overdensity (δ) - yes (Schaye et al. 2003)
  - Evolution (z) - no? (Schaye et al. 2003)
  - Ionization Background - yes
  - Environment (proximity to star forming galaxies) - yes... but how?

- Our project is at the beginning stages. This will be a short talk!

Springel & Hernquist (2003) Simulations

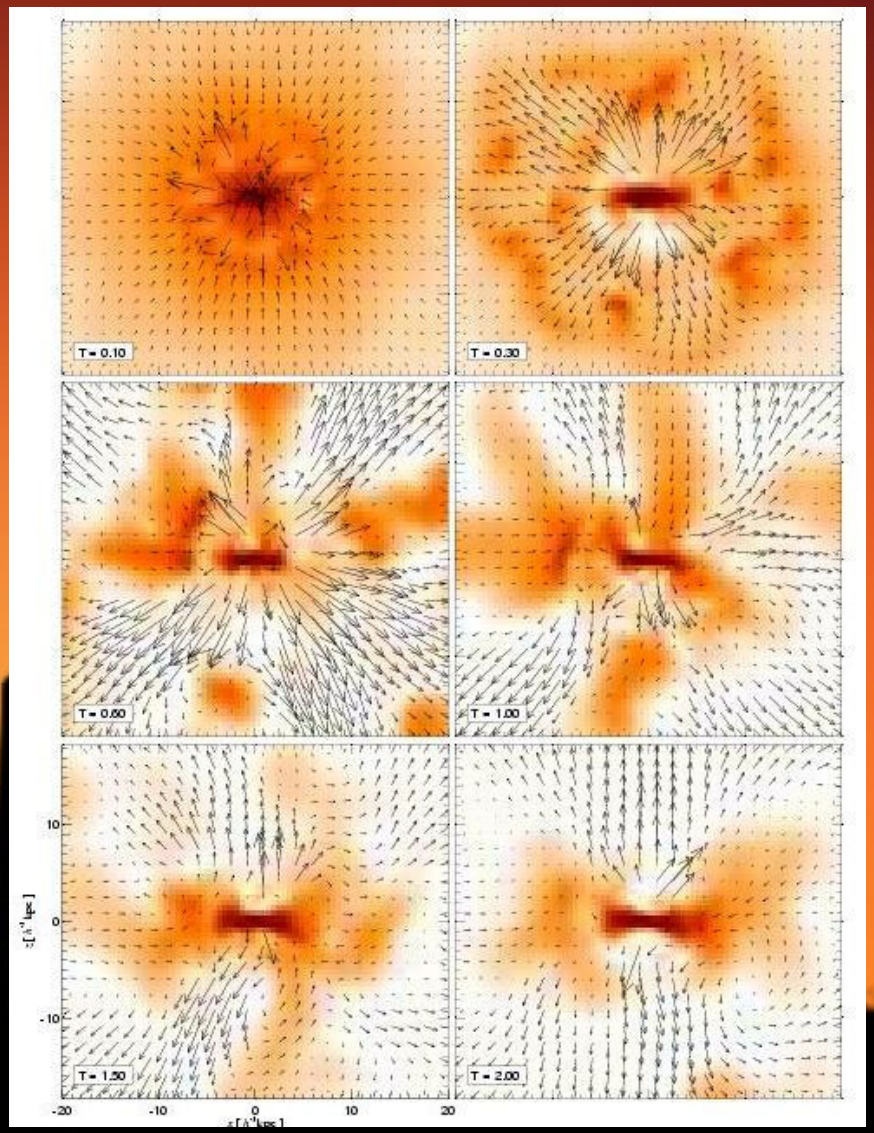

- Star formation is suppressed by galactic winds especially in low-mass haloes
- Star-forming galaxies drive winds with mass outflows 2x the SFR at v = 484 km/s
- Winds are added stochastically to gas particles from the star-forming ISM

Springel & Hernquist (2003) Simulations

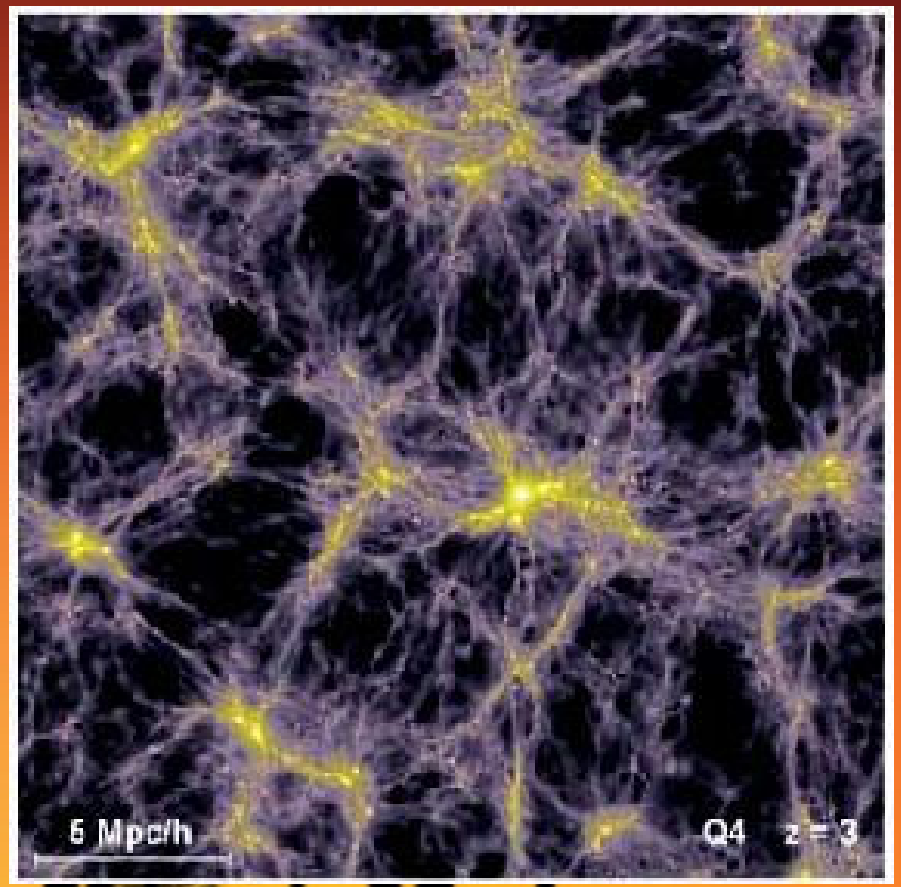

- We use the D5 simulation
  - 2×324^3 particles
  - $L = 33.75\ h^{-1}$ Mpc
  - $M_{gas} = 1.26 \times 10^7\ h^{-1}\ M_\odot$
- We generate spectra along lines of sight that are continuous by wrapping around the periodic box
- For these results we use the z=3 model, but will include structural evolution later

Metal Enrichment

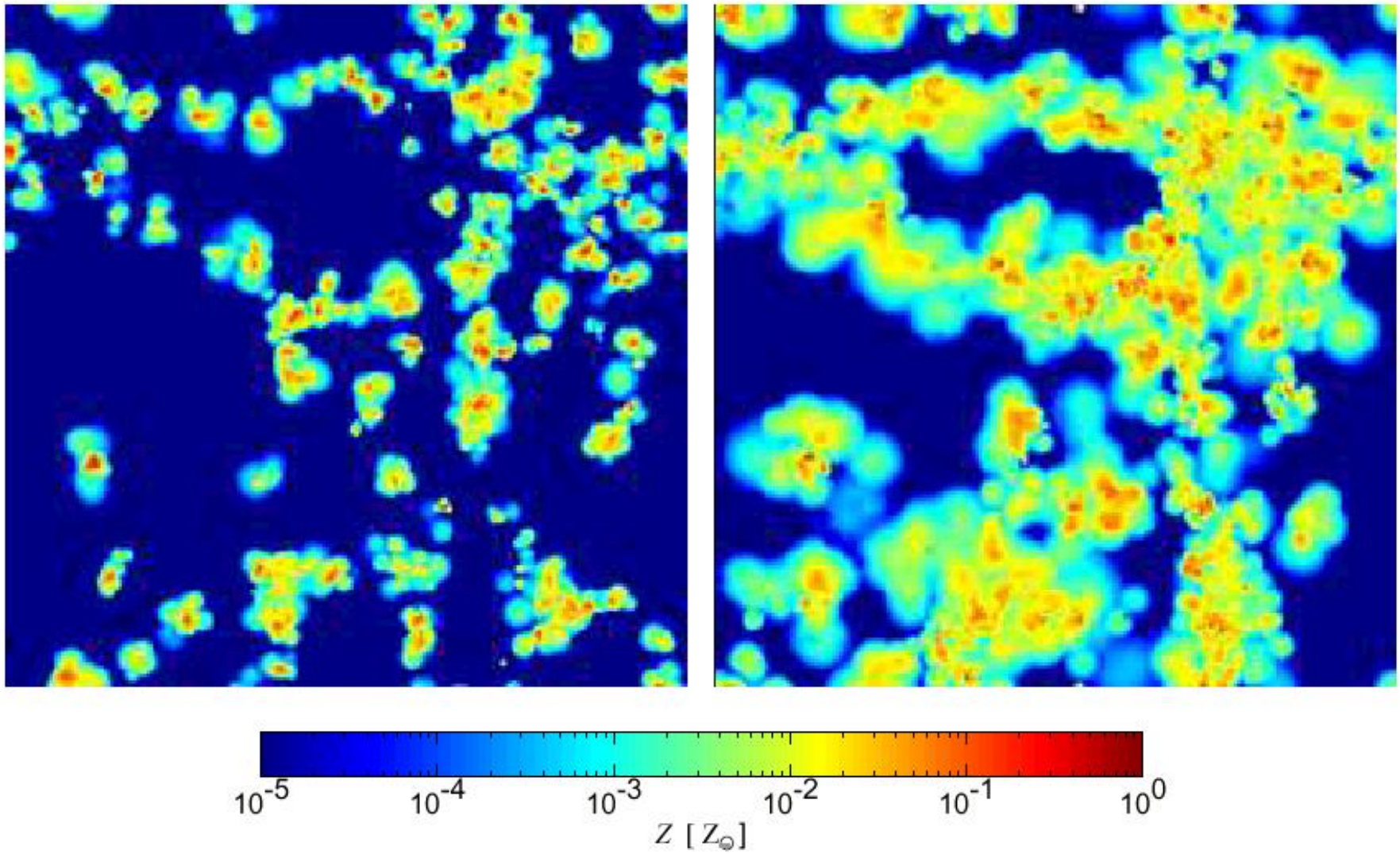

z = 2.3

z = 0

Metallicity Models

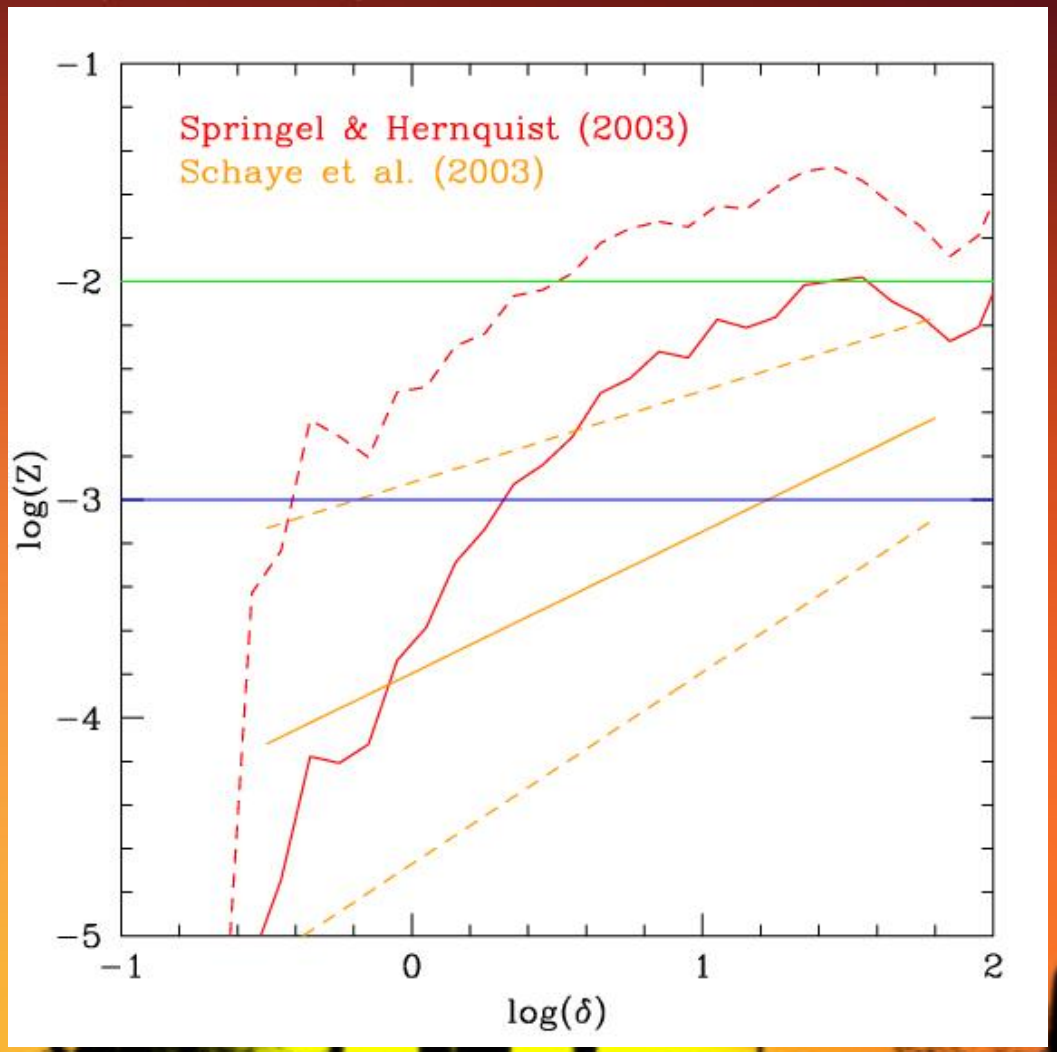

- SH03: $\log(\langle Z\rangle/Z_\odot) = -2.36$ with a large dispersion
- Schaye et al.: $\log(\langle Z\rangle/Z_\odot) = -2.9$ with a log normal scatter
- $\log(Z/Z_\odot) = -2.0$ and -3.0 and zero metallicity models also explored

Pixel Optical Depth Method

- Metal absorption compared to corresponding Lyα absorption on a pixel-by-pixel basis

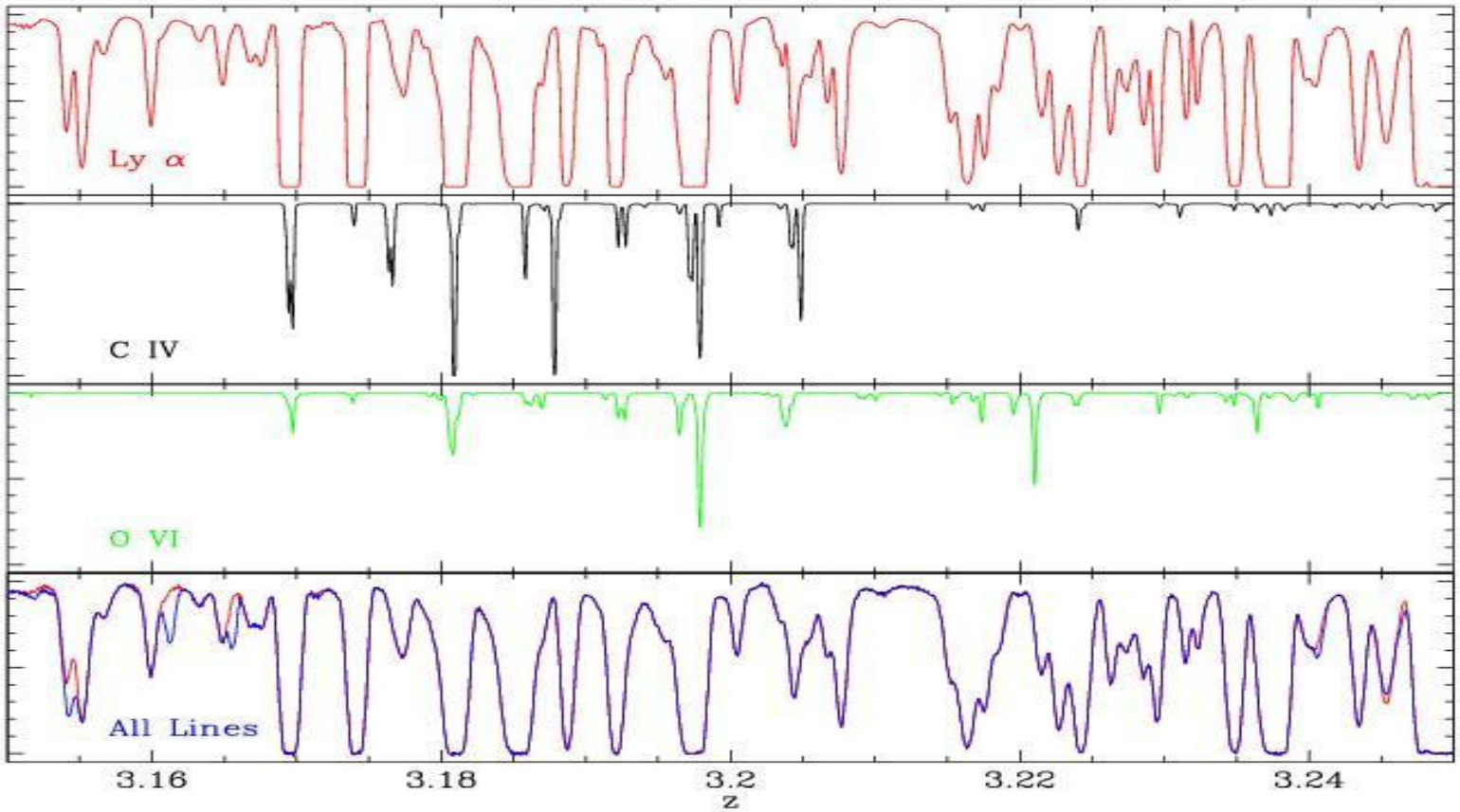

Quasar Absorption Line Spectra

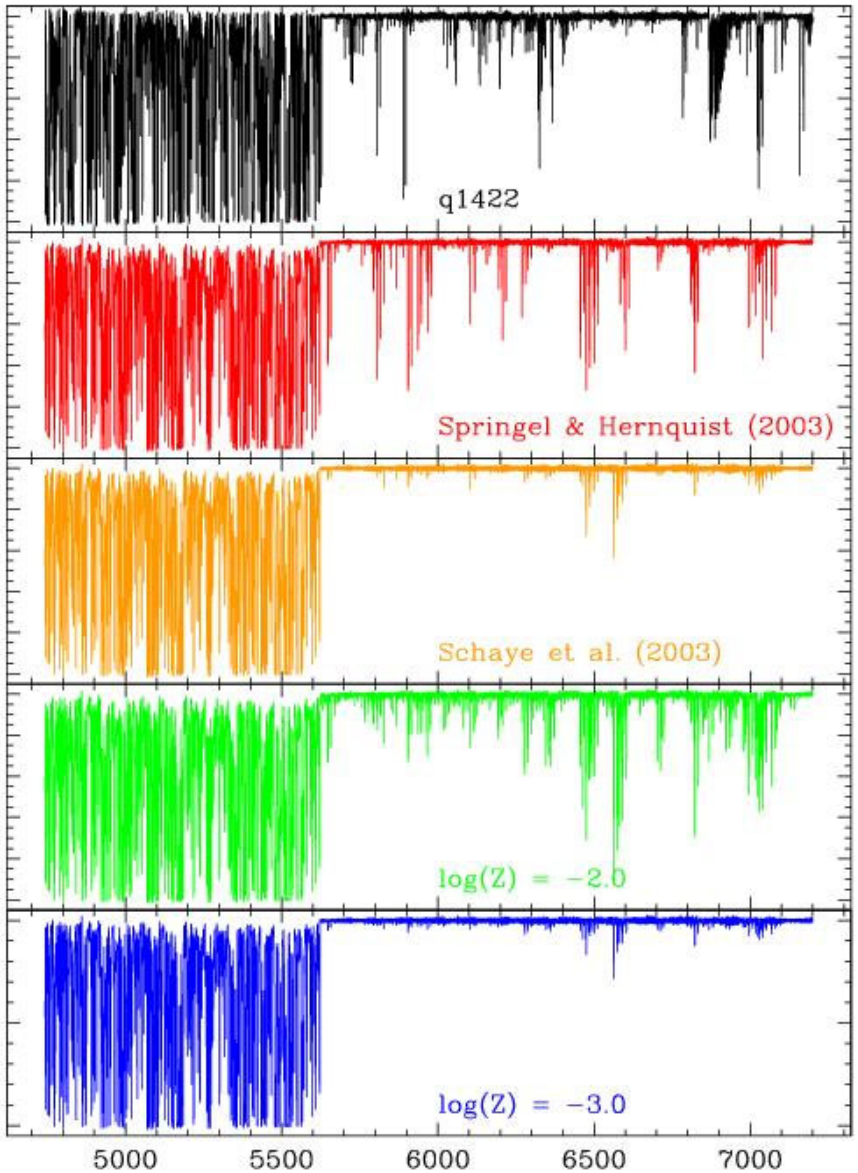

- SH03 model has nearly as many metal lines as $\log(Z/Z_{\odot}) = -2.0$ despite a lower mean metallicity

Model Comparison

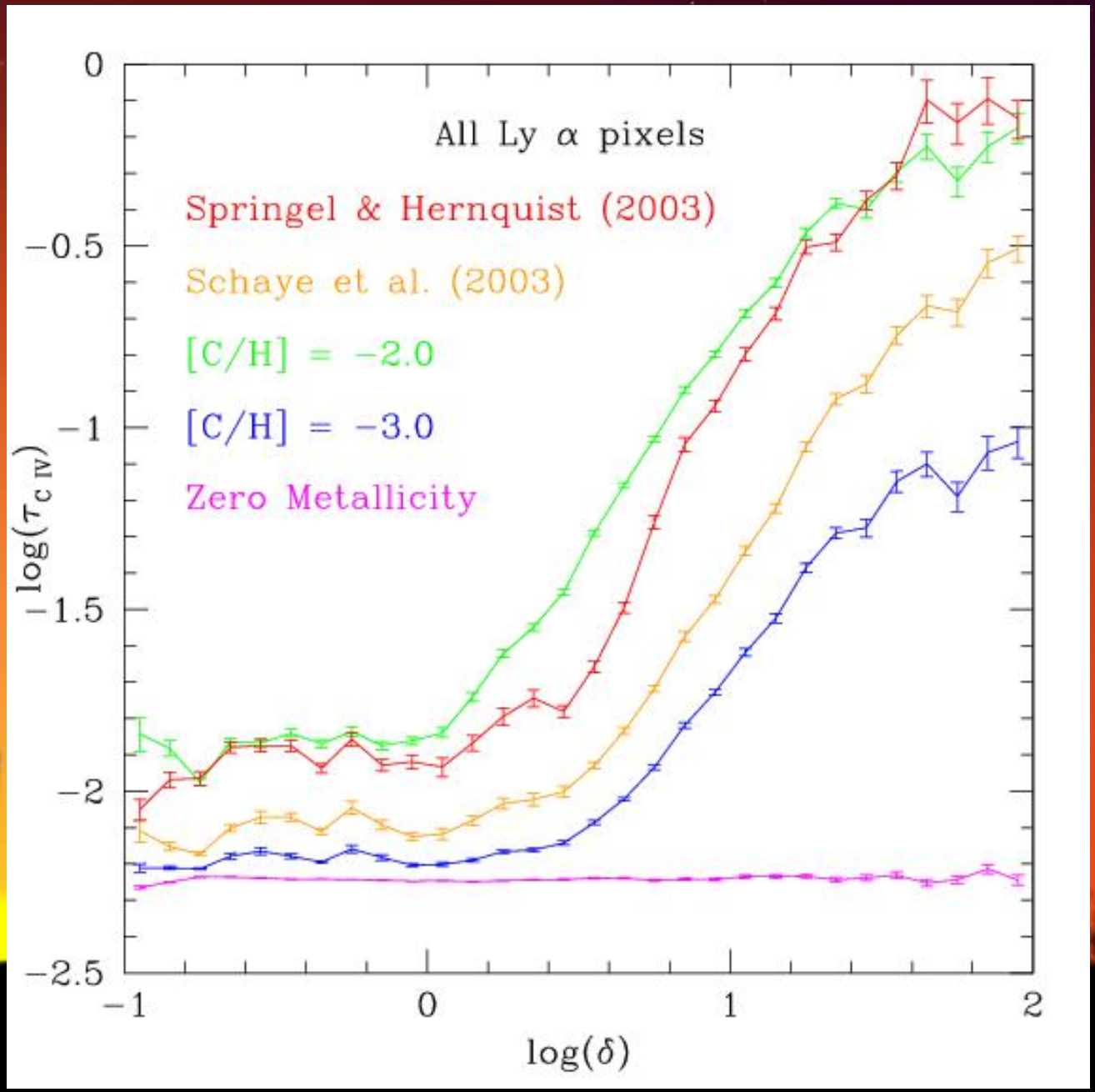

Comparison to q1422

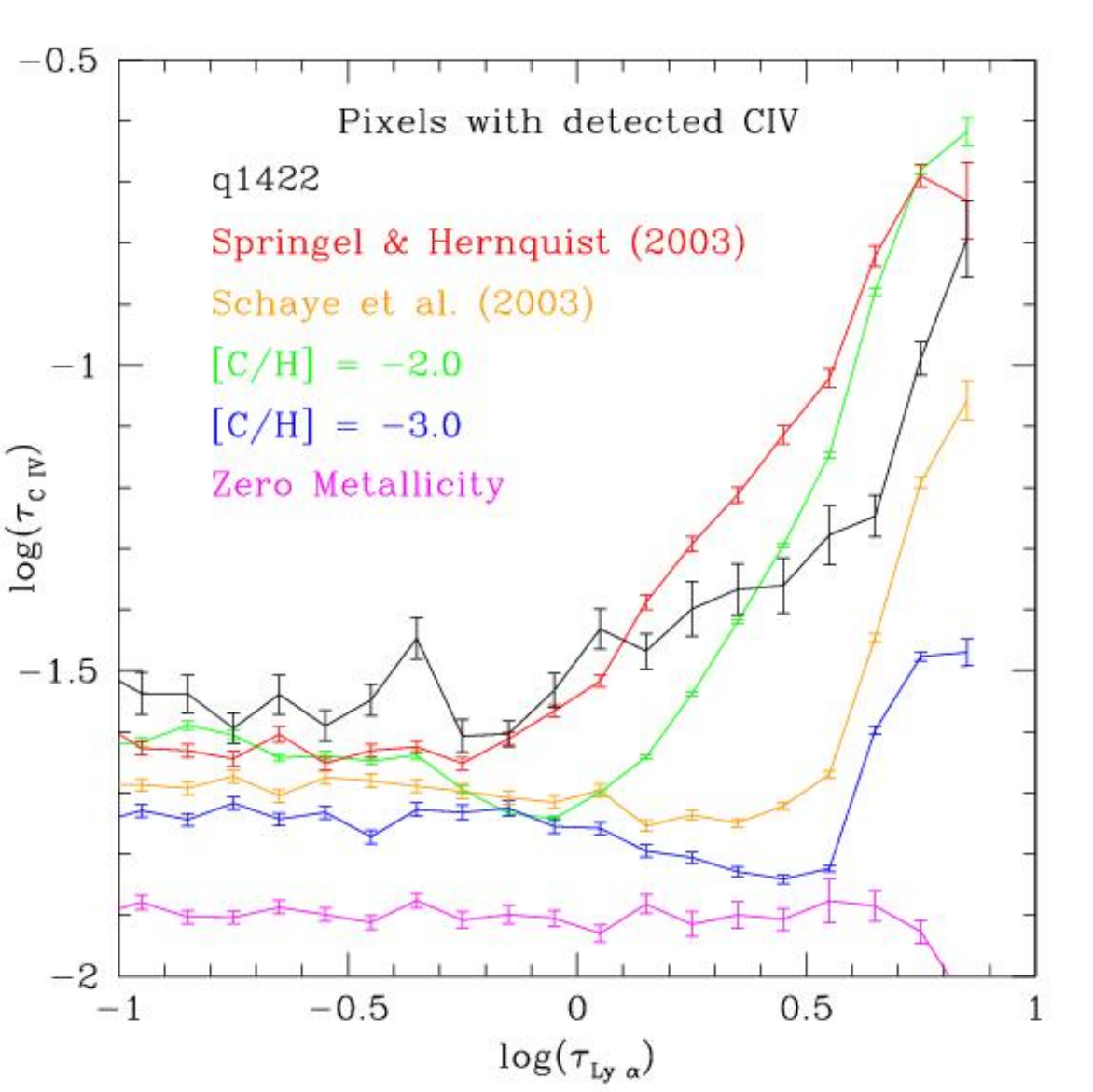

- Preliminary results show a promising fit of SH03 to q1422 for detected CIV lines
- Still need to explore different ionizing backgrounds

Results and Future Direction

- Springel & Hernquist (2003) metallicity models show a promising fit to q1422. A softer ionization background may result in too many metals in this model.
  - Statistical dispersion in metallicity makes a difference. SH03 has nearly as many C IV lines as the $\log(Z/Z_{\odot}) = -2.0$ model.
  - We will produce metallicity statistics for environment very soon.
  - Explore other species and abundance patterns.
  - Still have to apply pixel optical depth method to other observed quasars for a much larger data sample.

Radiative and Chemical Feedback from the First Stars

Brian O'Shea

Laboratory for Computational Astrophysics, UC San Diego

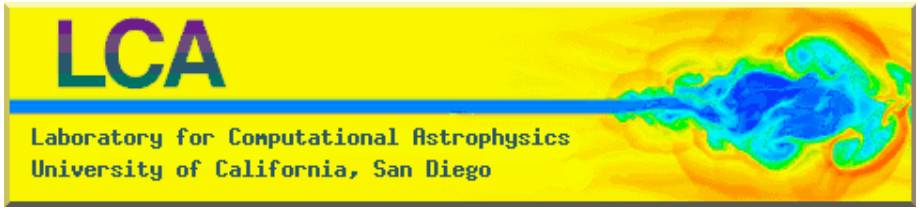

The First Stars (Pop III)

Believed to be:

- Massive: 30-300 $M_\odot$
- Luminous: 10^5-10^7 $L_\odot$
- Hot: $T_{eff} \sim 10^5$ K (UV)
- Form in small halos:
  $M_{DM} \sim 10^6$ $M_\odot$
- $25 < z < 15$
- Responsible for early reionization shown by WMAP?

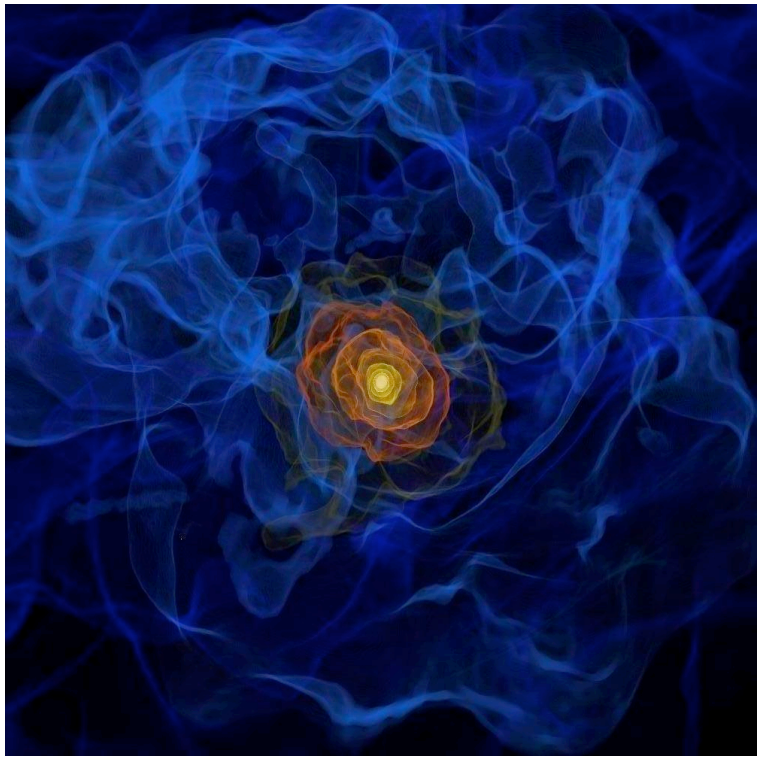

Abel, Bryan & Norman, 2002

First Star Problem Setup

- Run several dm-only simulations in an 0.3 Mpc/h box with standard cosmological parameters ($\Omega_b = 0.04$, $\Omega_m = 0.26$, $\Omega_\Lambda = 0.7$, h=0.7, n=1, $\sigma_8 = 0.9$) and 256^3 particles, with a different random seed for each
- Find most massive halo in each box, recenter simulation and rerun with gas physics turned on
- All simulations done with the publicly-available Enzo code, which was written by Greg Bryan (Oxford/Columbia) and is maintained at the Laboratory for Computational Astrophysics at UCSD. See http://cosmos.ucsd.edu/enzo/ for more details and to download the code.

First star runs (details)

- Re-initialize simulation volume with several static nested grids centered on most massive halo: $M_{DM} = 2.6\ M_{\odot}$, $\Delta x = 418$ pc (comoving)
- Use PPM with "Dual energy formalism" as the hydro method (Bryan et al. 1995)
- Follow the nonequilibrium chemical evolution of 9 H and He species, including H_2 (Abel et al. 1997, Anninos et al. 1997)
- Use adaptive mesh refinement to trace collapse of halo down to 0.14 AU (comoving), resolving Jeans length by at least 16 cells at all times

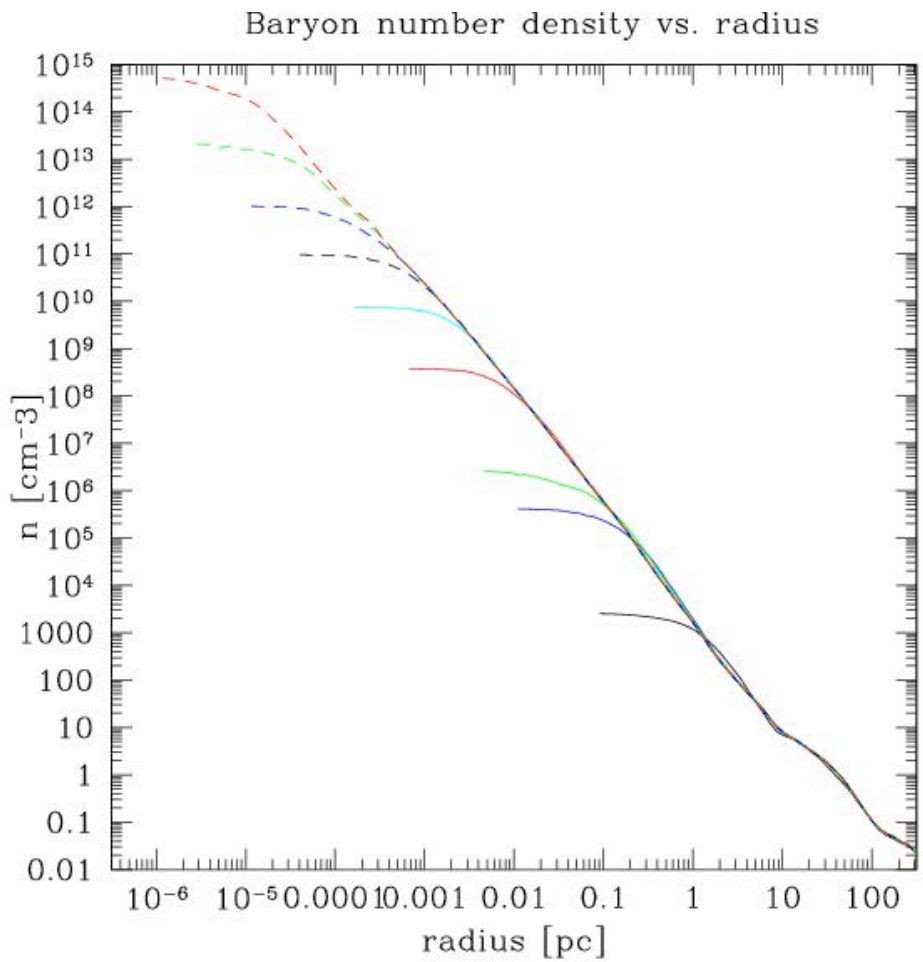

black solid line: z = 17.6 (t_0)
blue solid: t_0 + 8.7e5 years
green solid: +5e6 years
red solid: +3e5 years
cyan solid: + 17,000 years
black dashed: + 2300 years
blue dash: +310 years
green dashed: +91years
red dashed: +31years

$$M_{vir} = 4.67 \times 10^5 \, M_\odot$$

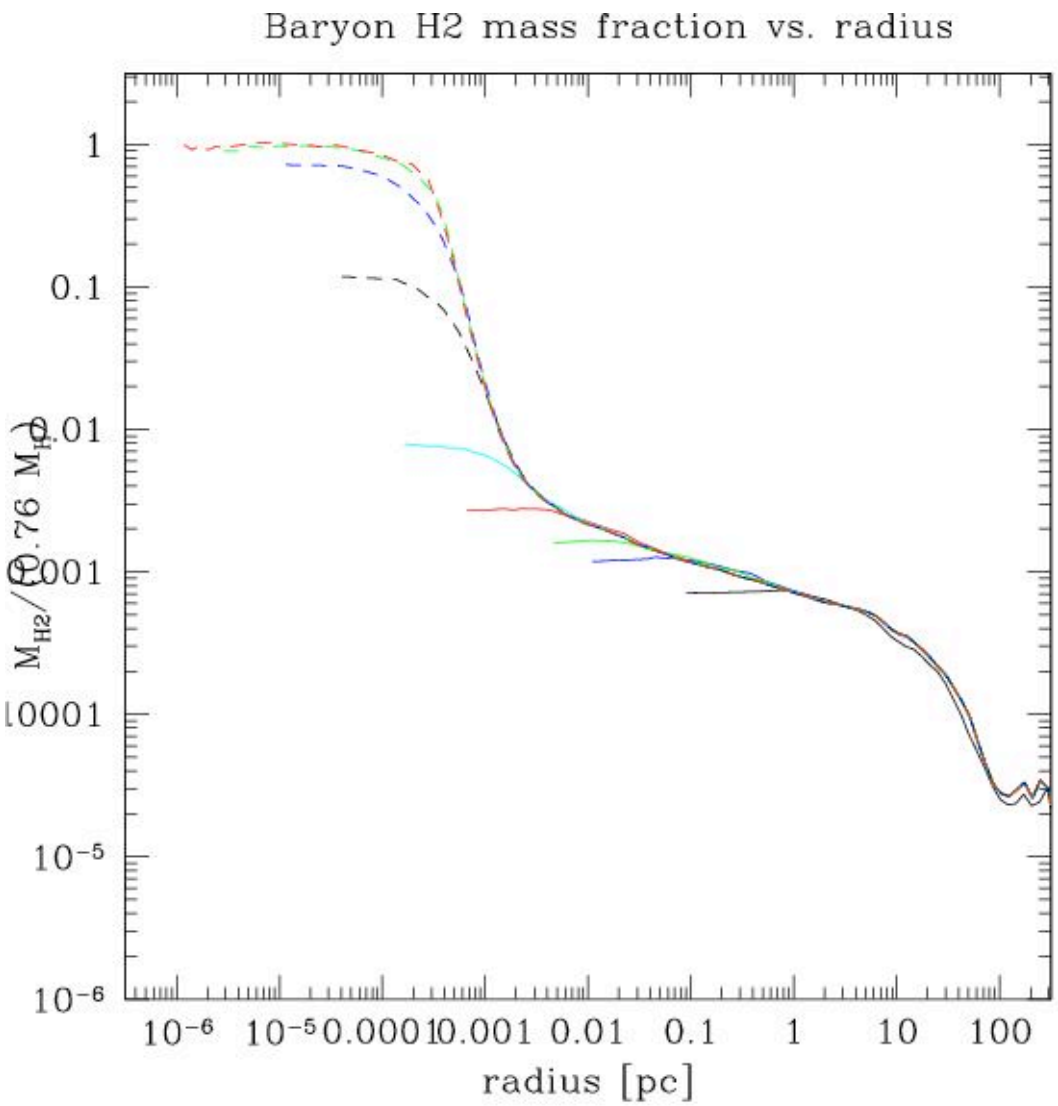

black solid line: z = 17.6 (t_0)
blue solid: t_0 + 8.7e5 years
green solid: +5e6 years
red solid: +3e5 years
cyan solid: + 17,000 years
black dashed: + 2300 years
blue dash: +310 years
green dashed: +91 years
red dashed: +31 years

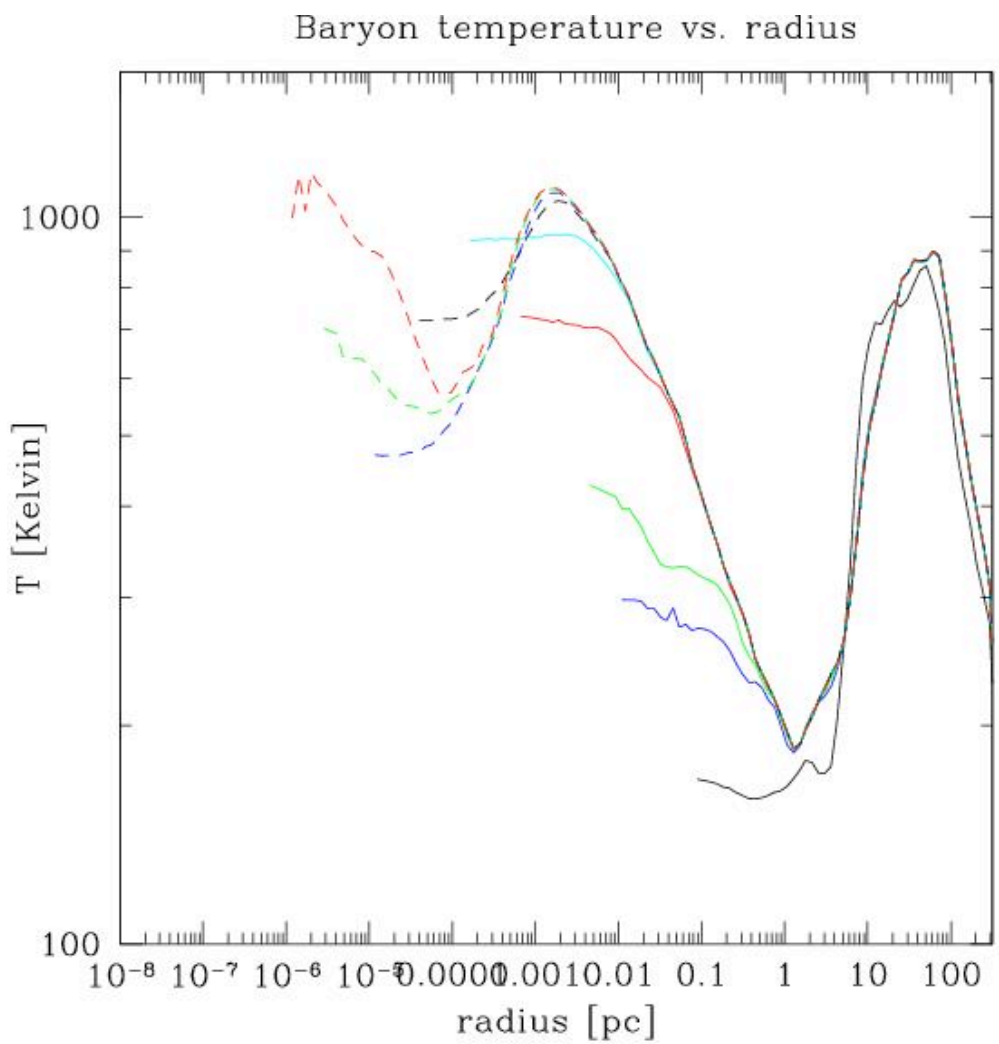

black solid line: z = 17.6 (t_0)
blue solid: t_0 + 8.7e5 years
green solid: +5e6 years
red solid: +3e5 years
cyan solid: + 17,000 years
black dashed: + 2300 years
blue dash: +310 years
green dashed: +91 years
red dashed: +31 years

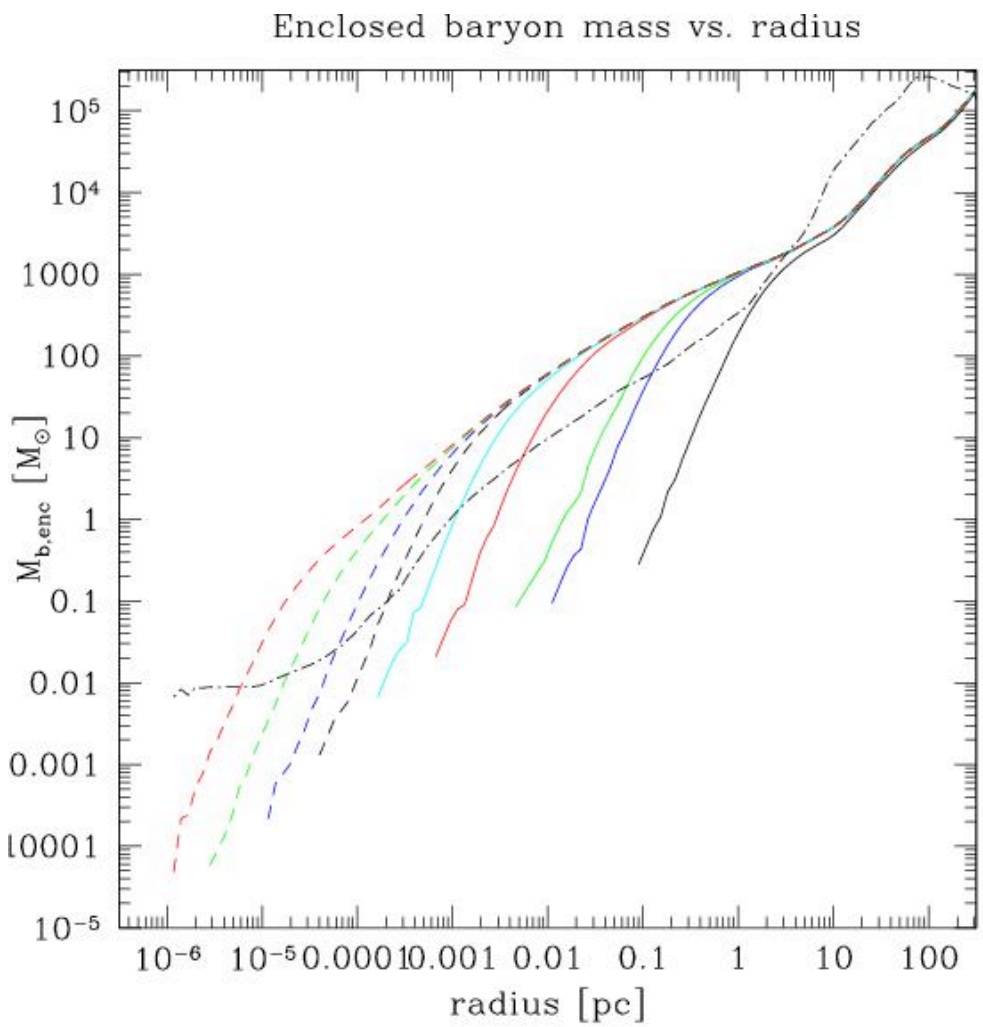

black dot-dashed line: Bonnor-Ebert critical mass calculated at last timestep

Note: ~1000 $M_\odot$ of gas within 1 pc

black solid line: z = 17.6 (t_0)
blue solid: t_0 + 8.7e5 years
green solid: +5e6 years
red solid: +3e5 years
cyan solid: + 17,000 years
black dashed: + 2300 years
blue dash: +310 years
green dashed: +91 years
red dashed: +31 years

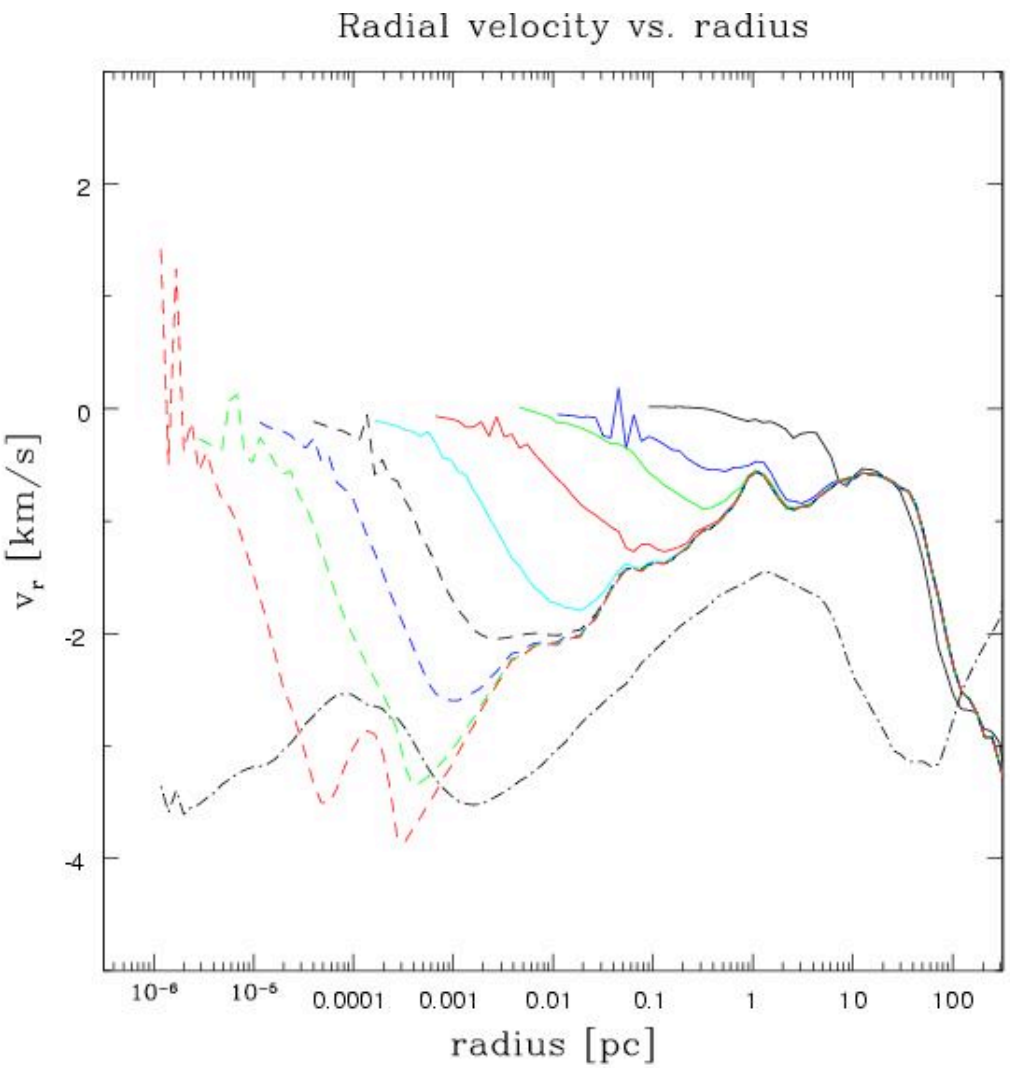

Black dot-dashed line: local sound speed calculated at final timestep

black solid line: z = 17.6 (t_0)
blue solid: t_0 + 8.7e5 years
green solid: +5e6 years
red solid: +3e5 years
cyan solid: + 17,000 years
black dashed: + 2300 years
blue dash: +310 years
green dashed: +91 years
red dashed: +31 years

First Star Halo Comparison

- 4 simulations run with identical cosmological and simulation parameters but different random seeds
- The evolution of the largest halo in each simulation is tracked until the center of the halo collapses
- I then compare radial profiles of various baryon quantities

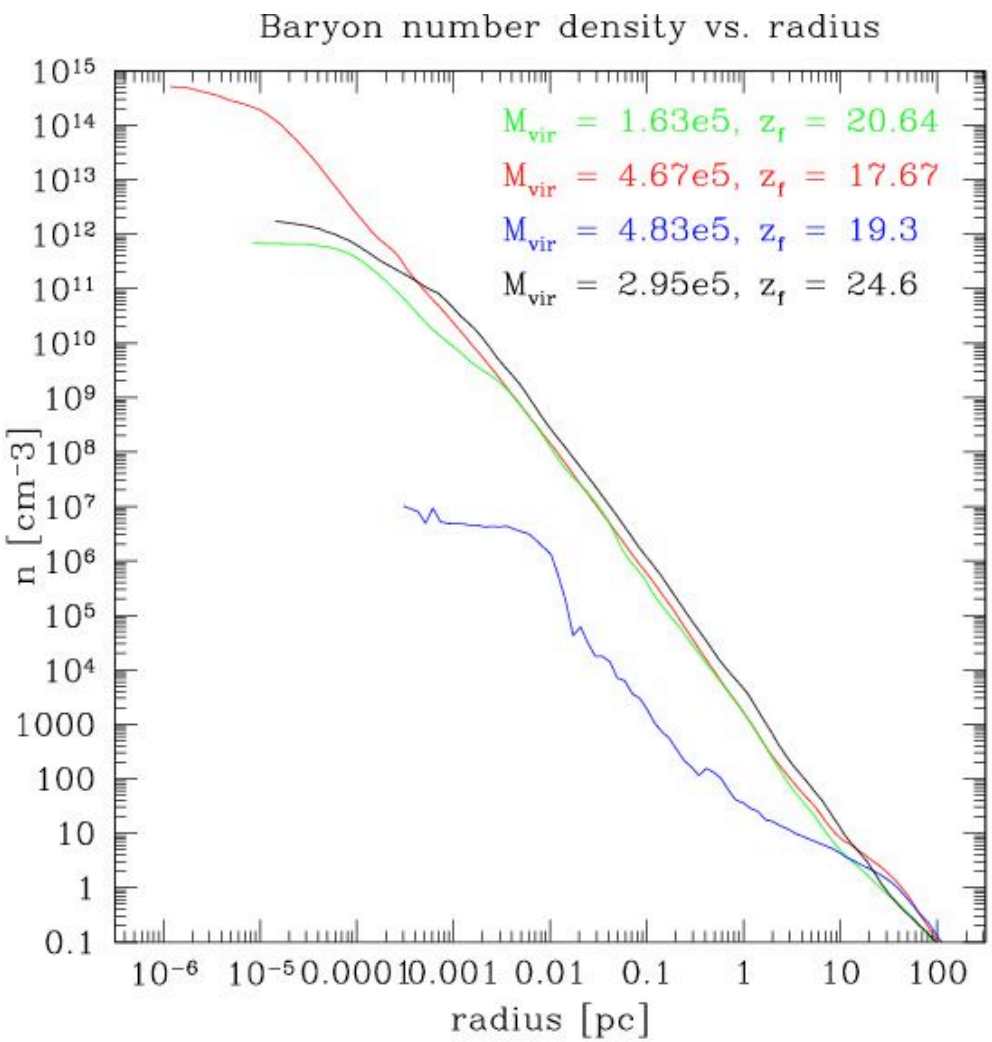

Note: halo marked by blue line has just undergone a major merger

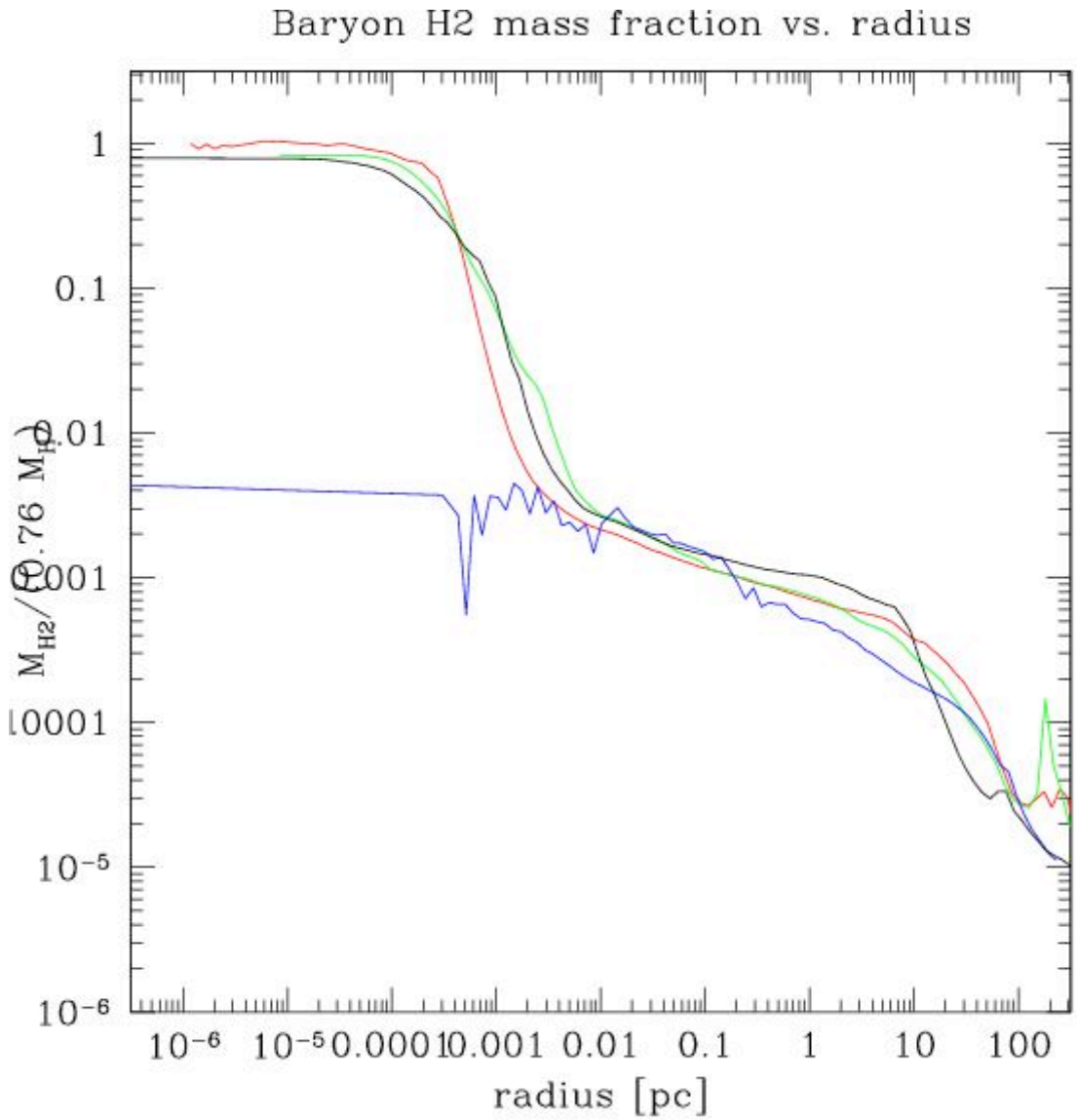
Baryon H2 mass fraction vs. radius
1
0.1
0.01
0.001
0.0001
10⁻⁵
10⁻⁶
10⁻⁶ 10⁻⁵ 0.0001 0.001 0.01 0.1 1 10 100
radius [pc]
M_H2/(0.76 M_b)

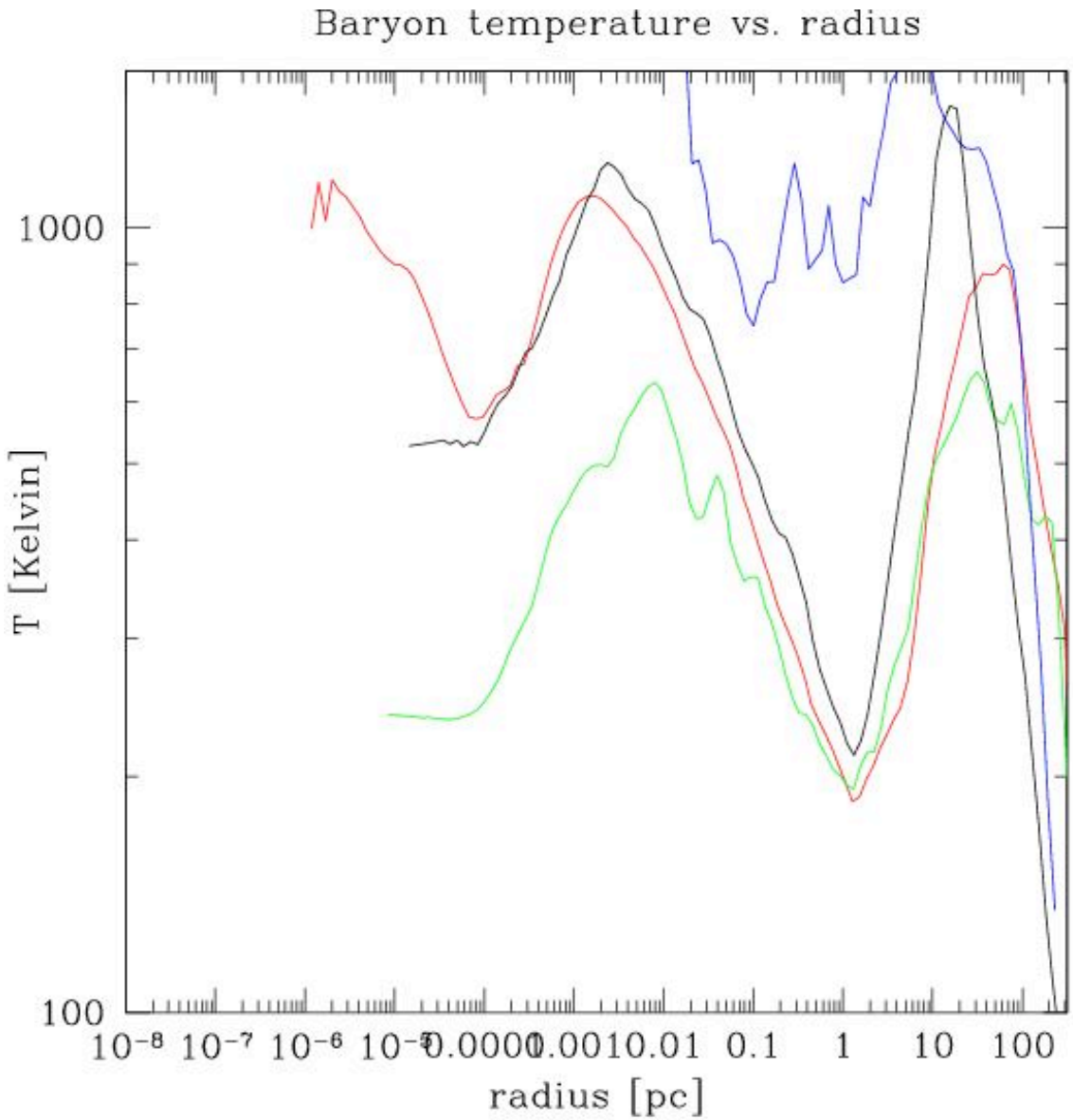
Baryon temperature vs. radius
1000
100
T [Kelvin]
10⁻⁸ 10⁻⁷ 10⁻⁶ 10⁻⁵ 0.0001 0.001 0.01 0.1 1 10 100
radius [pc]

Radiative Feedback and Primordial HII Regions

- What is the effect of Pop III stars on their parent halo?
- What is the long term evolution of a primordial HII region in an expanding universe?
- Is star formation suppressed or enhanced in 2nd generation objects forming in the vicinity of a 1st generation object?
- Can we explain the WMAP result using only Pop III stars?

The Setup

- We need 3D cosmological simulations
  - 1D rad hydro calculations useful, but missing essential physics: mergers, etc.
  - Important to follow H_2 chemistry carefully
- Using the Enzo code, run 0.3 Mpc/h box to $z \approx 22.3$ and find most massive halo. Then, add HII region:
  - Use 1D radial profiles from Whalen et al. (2004)
  - Calculate extent of 3D HII region using ray tracing code (Abel & Wandelt 2002)
  - Evolve simulation until massive objects form, without adding any additional HII regions/SNae (!)
  - Perform both unigrid and AMR calculations
  - Work done with T. Abel, D. Whalen, M. Norman

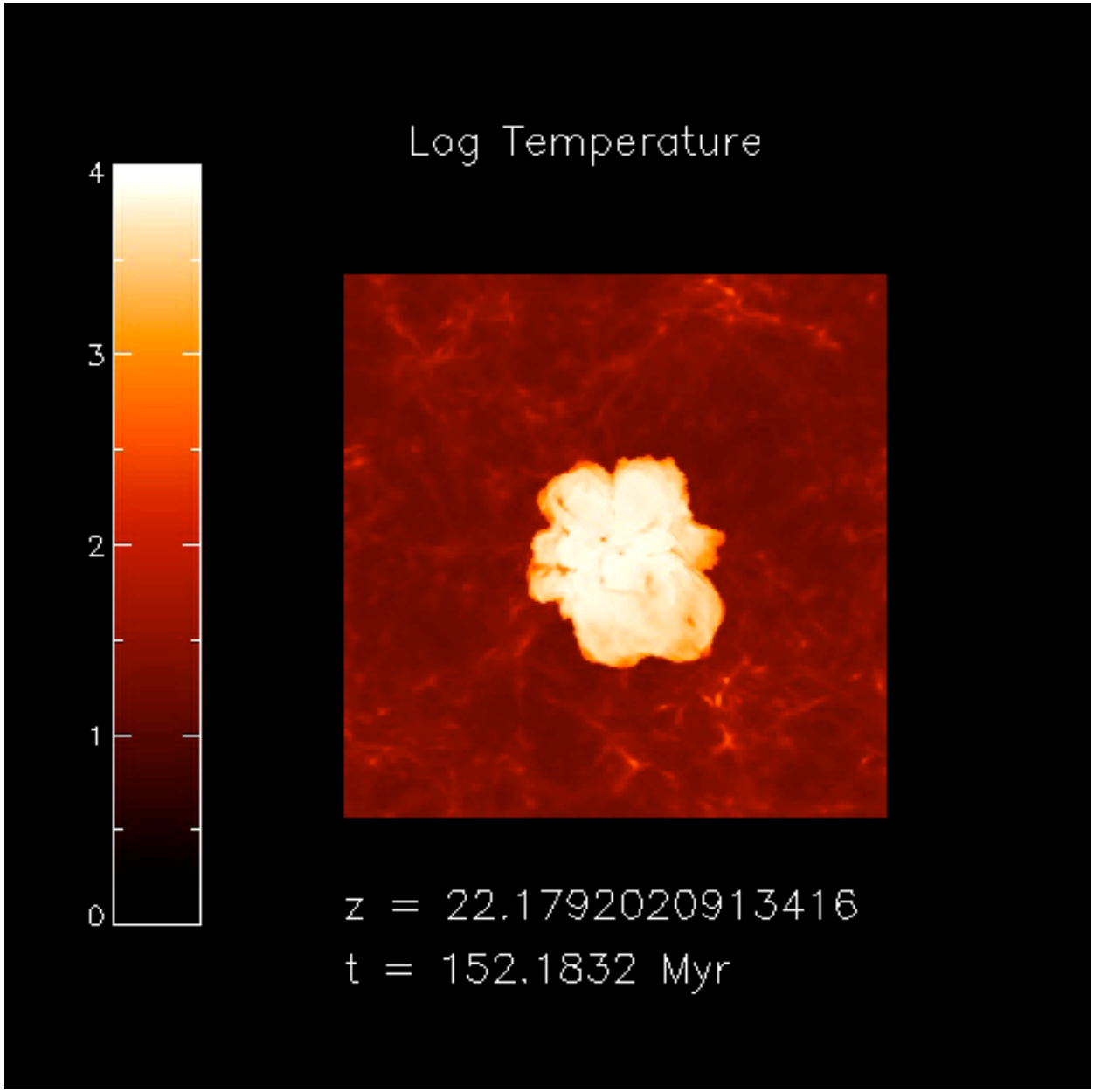

$L_{box} = 0.3$ Mpc/h (comoving) ≈ 20 kpc proper

$R_{HII} \approx 3$ kpc (proper)

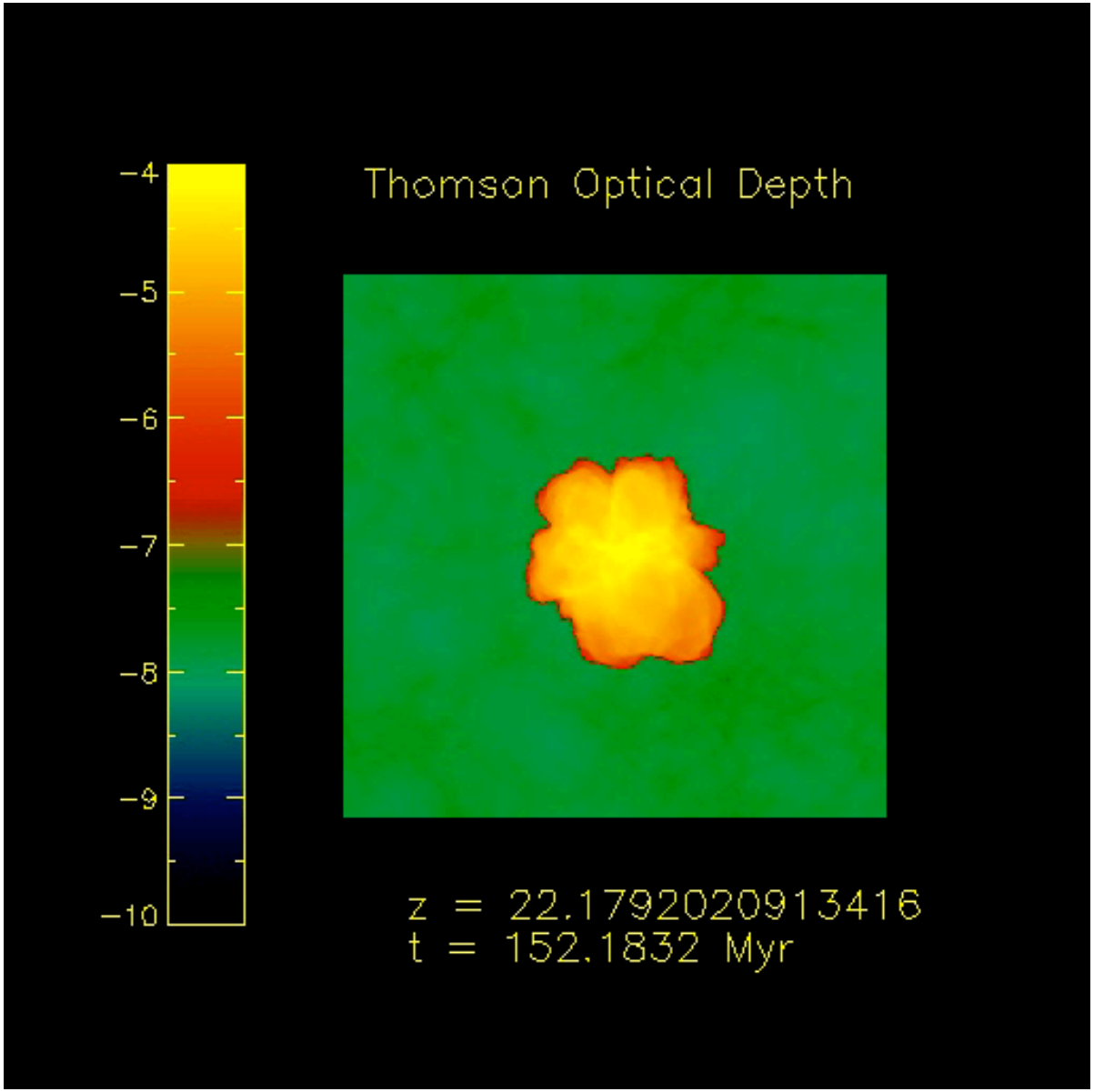
Thomson Optical Depth
−4
−5
−6
−7
−8
−9
−10
z = 22.1792020913416
t = 152.1832 Myr

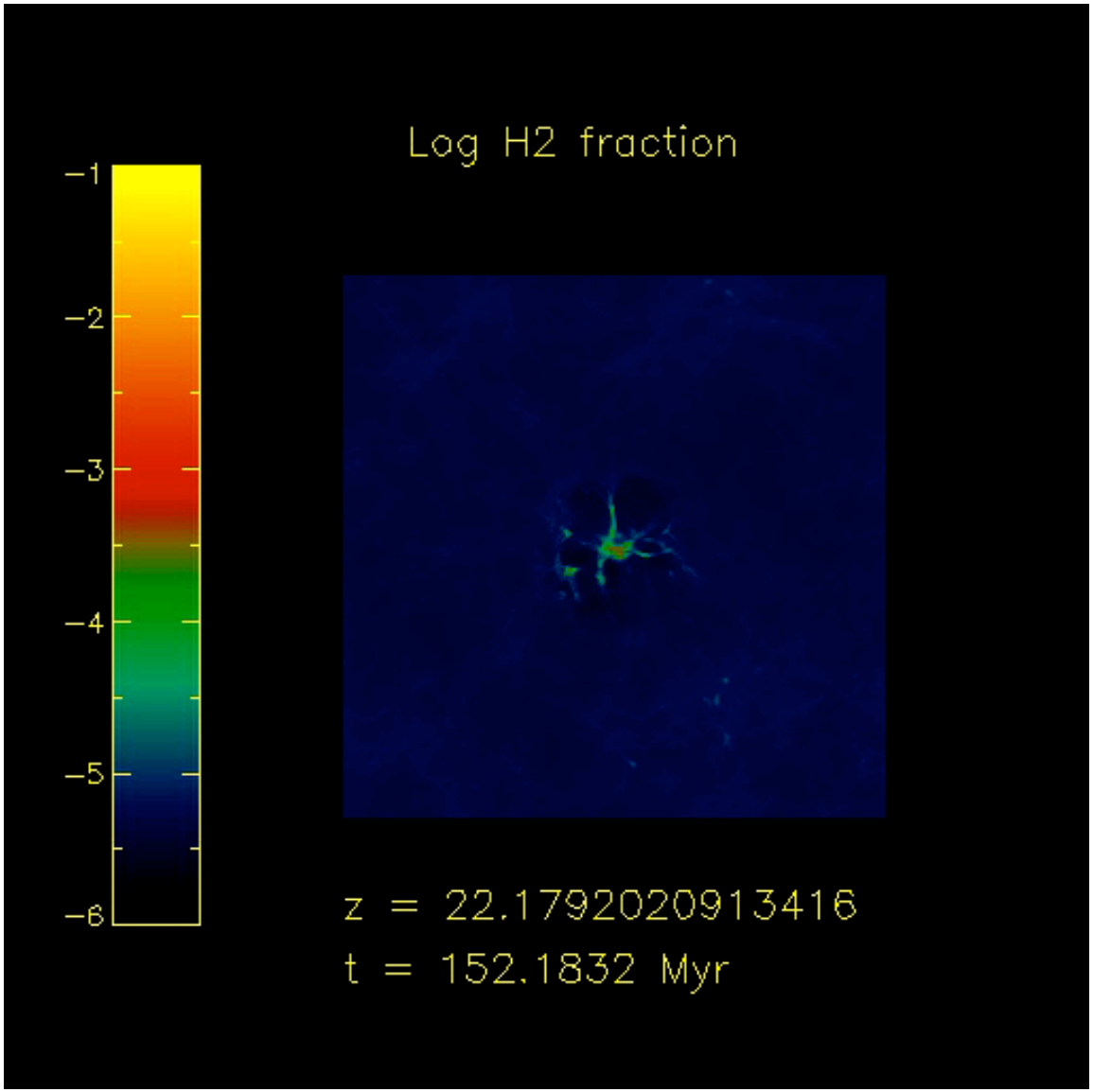

H_2 formation increases on large scales, medium densities (ie Ricotti & Shull)

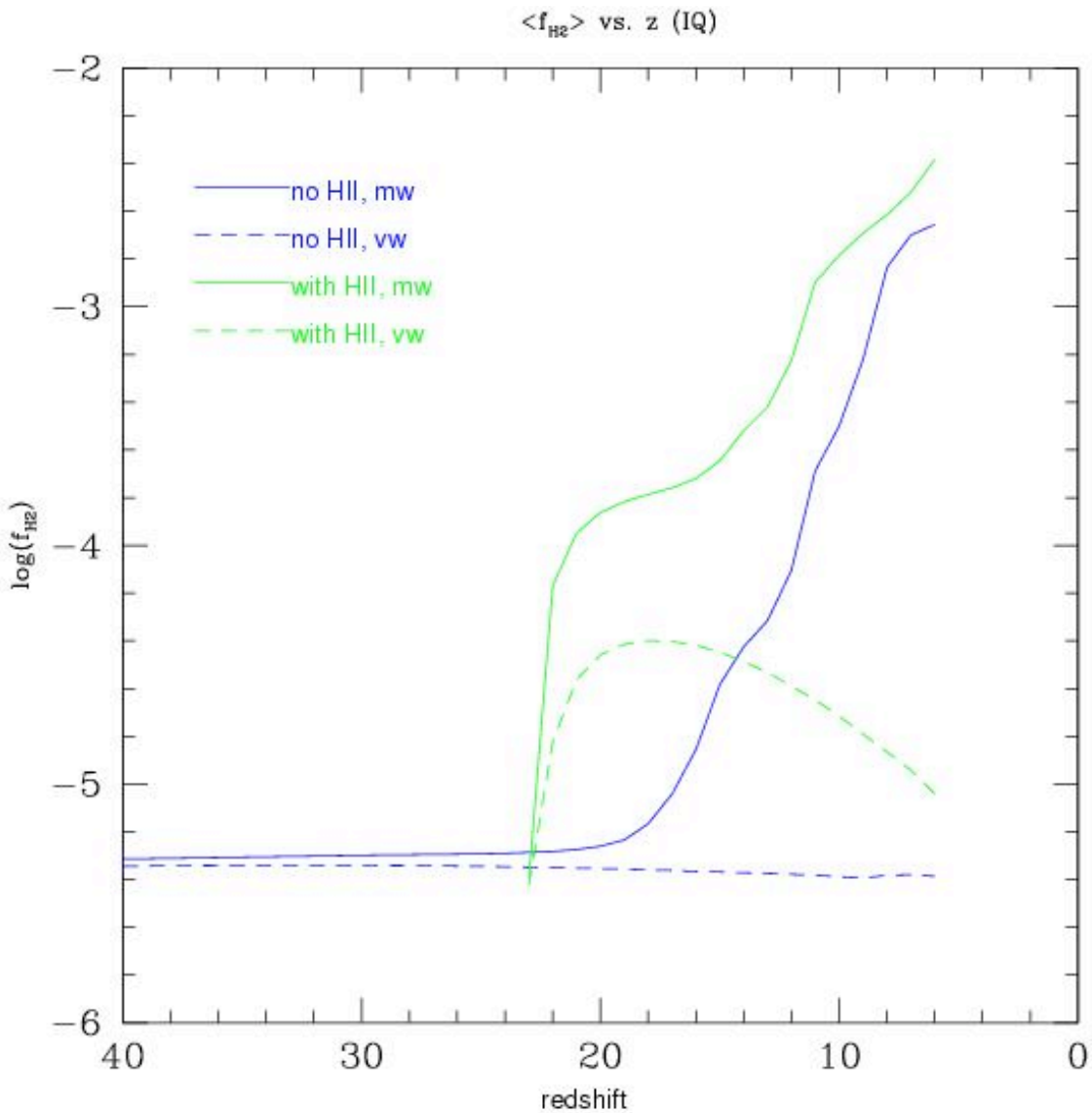

Evolution of H_2 fraction in inner quarter of simulation, both with and without HII region

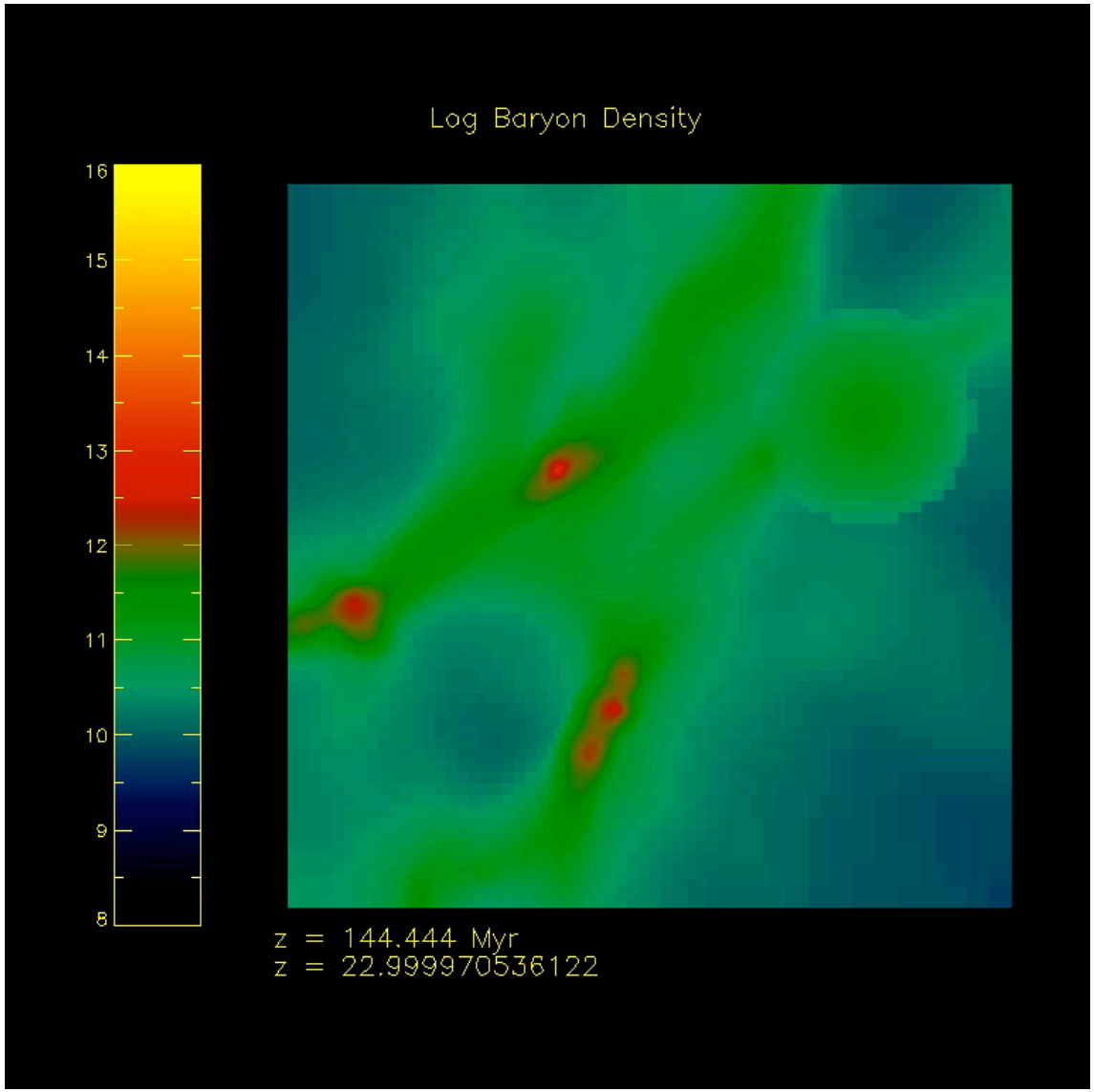

Projection is of a volume approx. 18.7 Kpc/h comoving/1.4 Kpc proper on a side

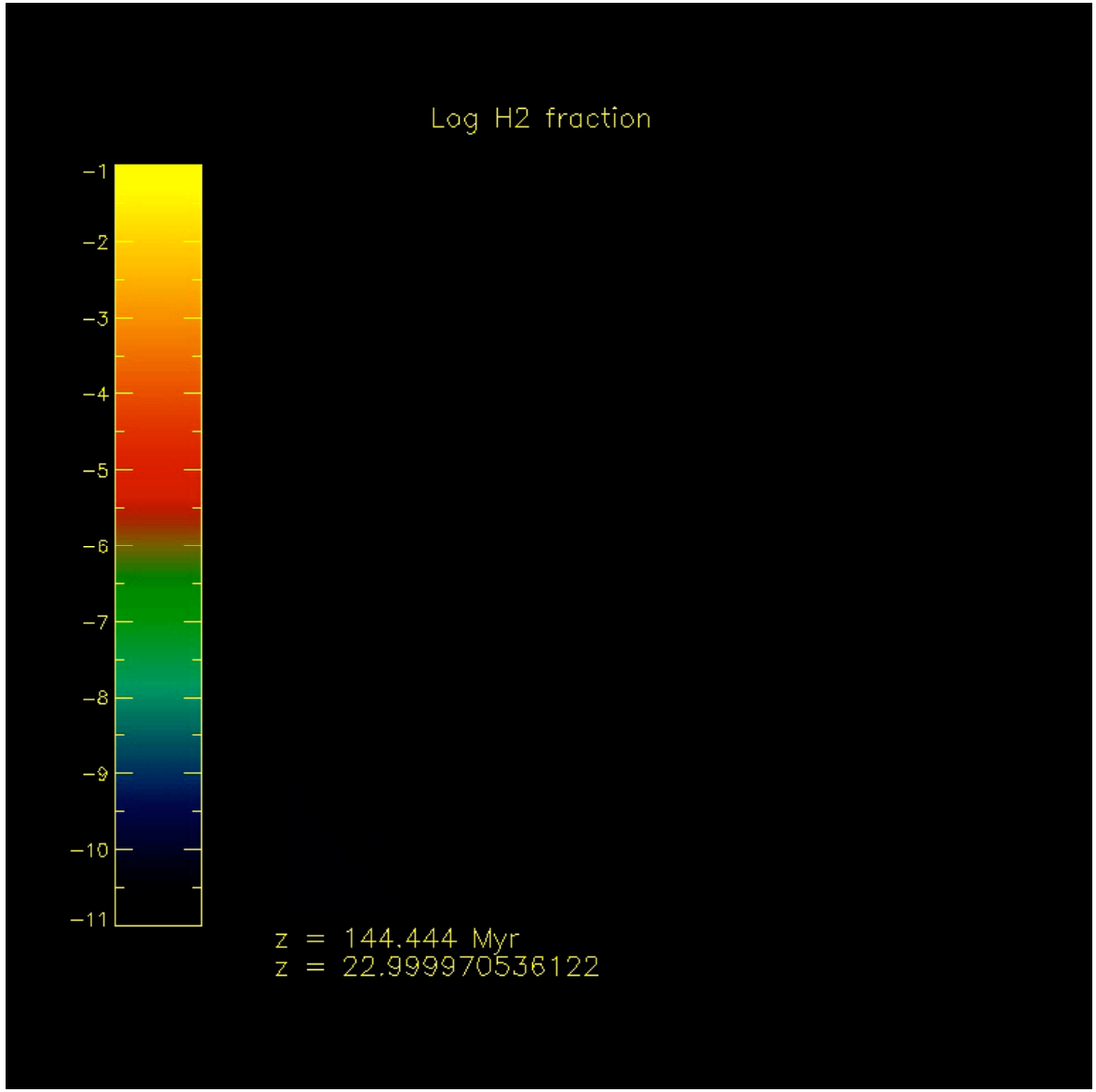
Log H2 fraction
-1
-2
-3
-4
-5
-6
-7
-8
-9
-10
-11
z = 144.444 Myr
z = 22.999970536122

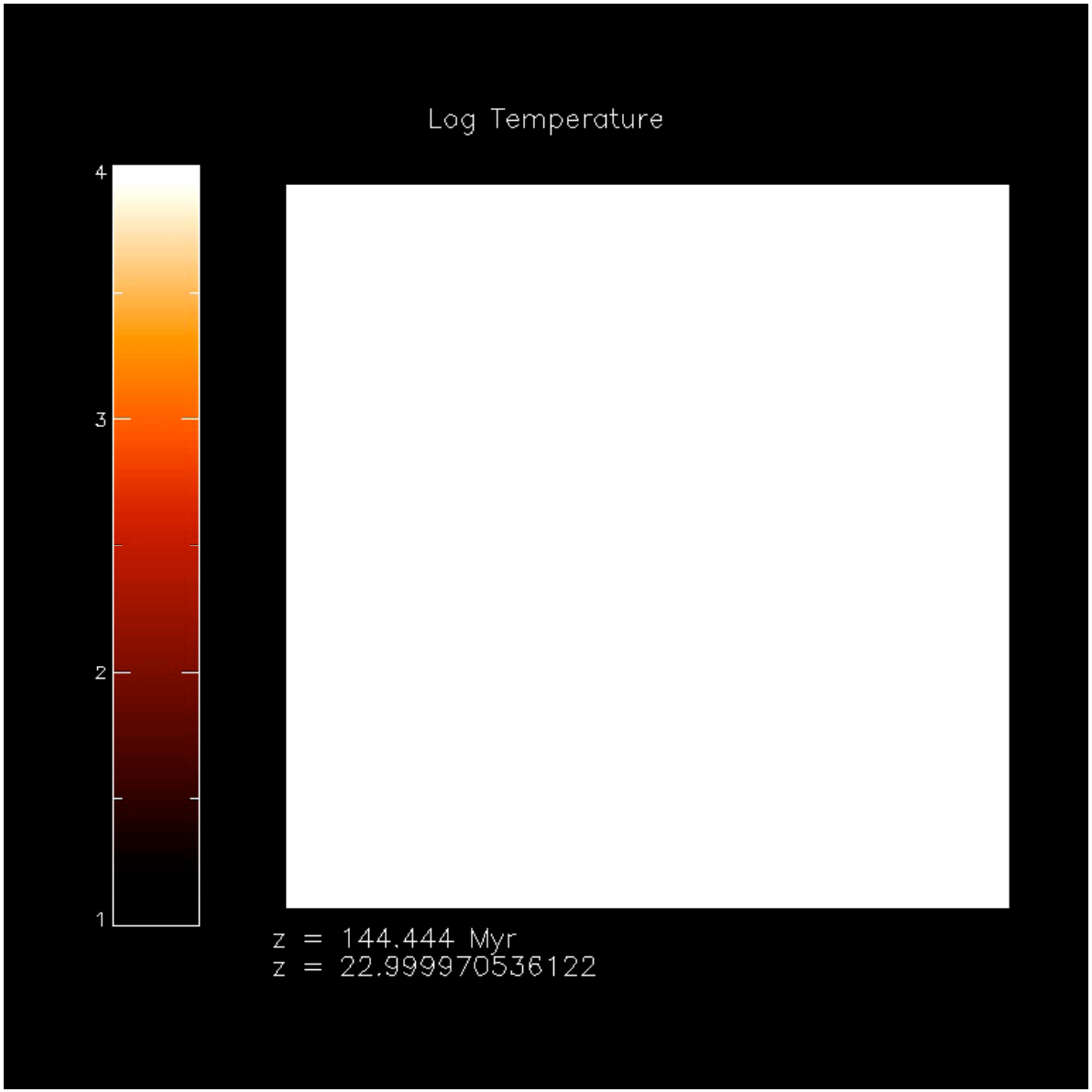
Log Temperature
4
3
2
1
z = 144.444 Myr
z = 22.999970536122

How does the HII region affect further halo evolution?

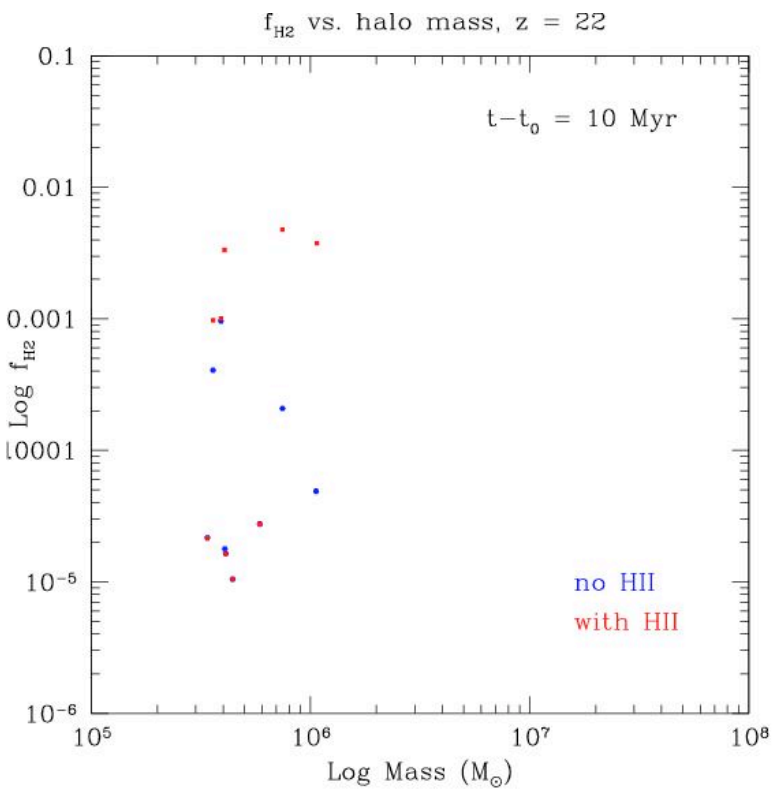

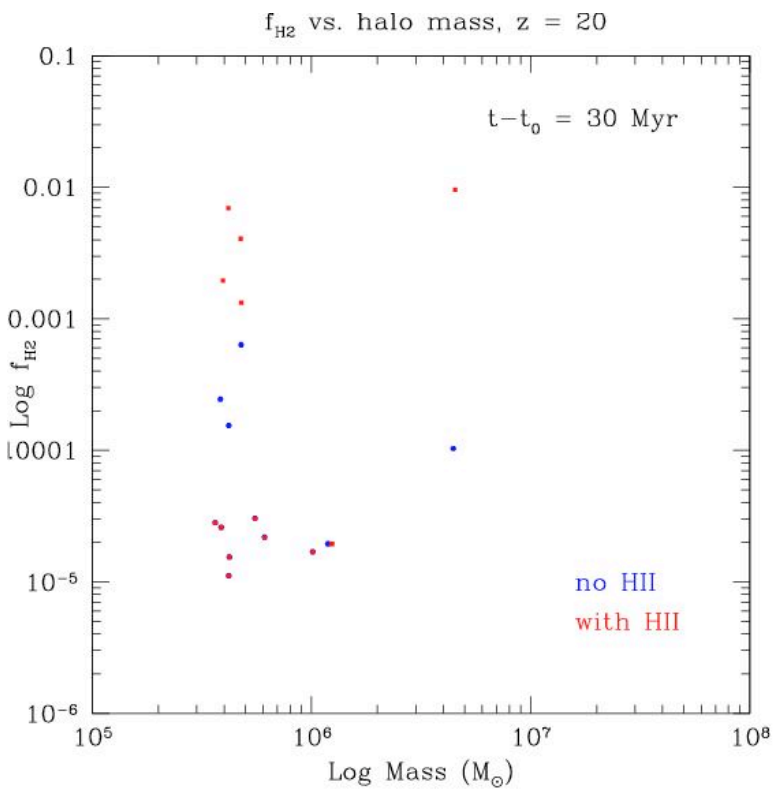

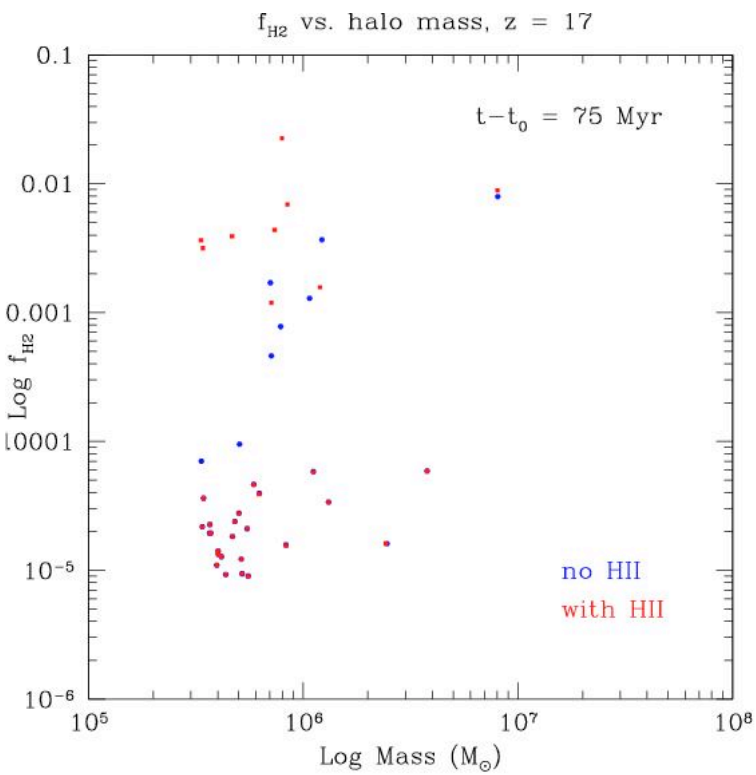
f_{H2} vs. halo mass, z = 17
$t-t_0$ = 75 Myr
no HII
with HII
Log f_{H2}
Log Mass ($M_\odot$)
0.1
0.01
0.001
0.0001
10^{-5}
10^{-6}
10^5
10^6
10^7
10^8

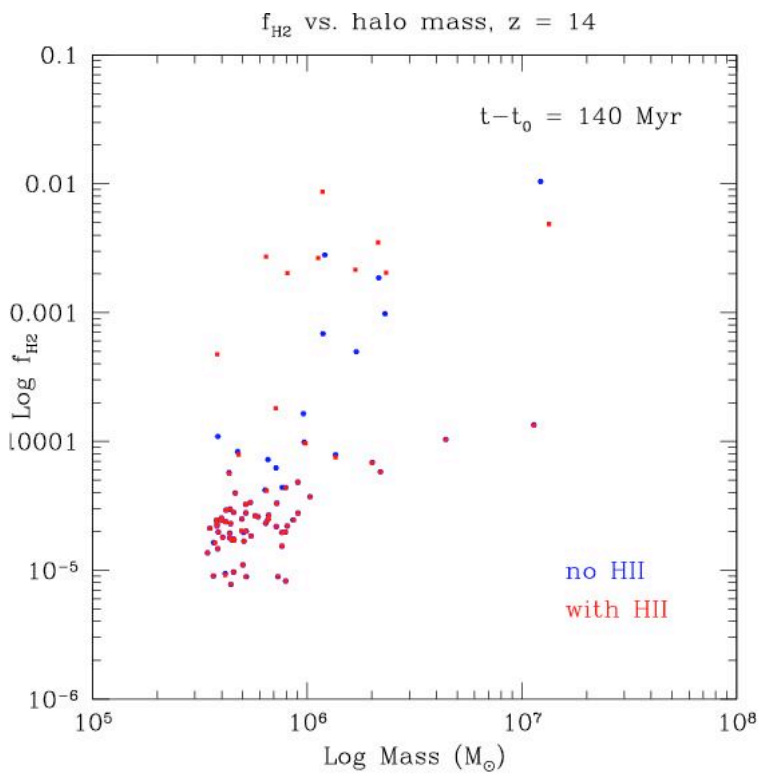
f_{H2} vs. halo mass, z = 14
$t-t_0$ = 140 Myr
no HII
with HII
Log f_{H2}
Log Mass ($M_\odot$)
0.1
0.01
0.001
0.0001
10^{-5}
10^{-6}
10^5
10^6
10^7
10^8

What are the properties of the object that forms?

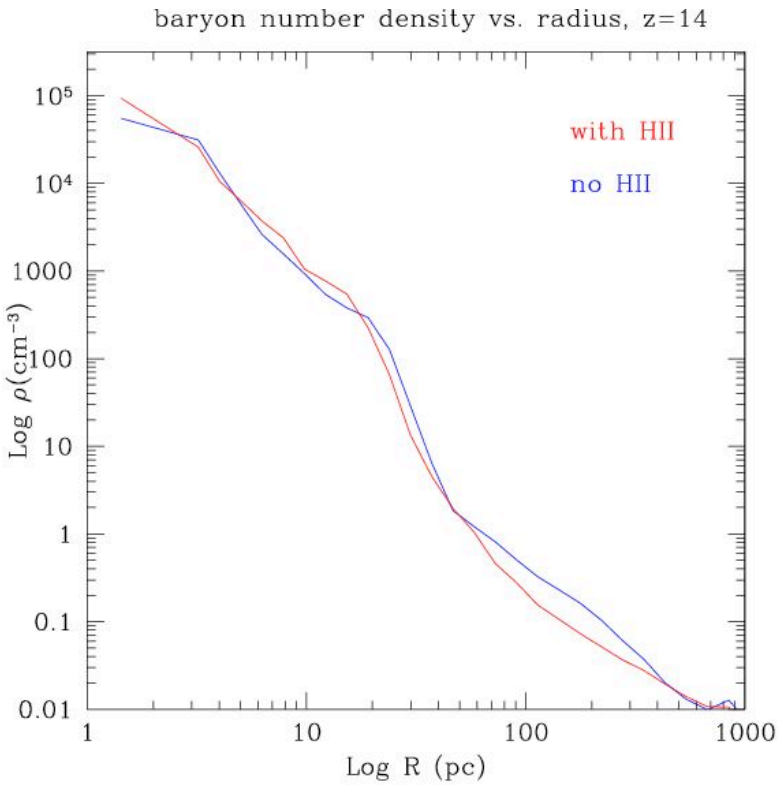

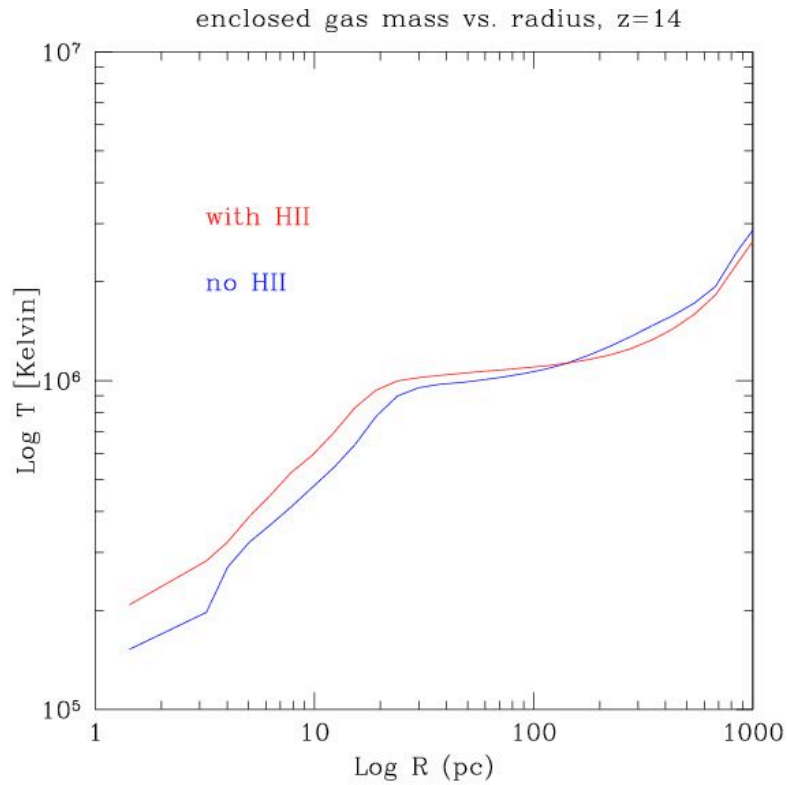

$M_{vir} = 1.54e7\ M_\odot$, $R_{vir} = 533$ pc, $T_{vir} \approx 9300$ K

Second Generation (?) Objects

- $10 < z < 15$
- $10^7 < M_{vir}/M_\odot < 10^8$
- More than 10^6 $M_\odot$ of gas within 30 pc if the halos do not undergo star formation
  - 100x the amount that formed the first star
  - Will it form a star 100x as massive?
  - A cluster of massive Pop III stars?
  - A cluster of "extreme" Pop II stars with normal IMF?
- Note that it is possible (likely?) that more generations of stars would form in the cold gas before z=14.

Chemical Enrichment

- Supermassive Pop III stars between 140-260 $M_\odot$ should explode in highly energetic (10^{52}-10^{53} erg) pair instability supernovae.
- These supernovae also produce copious amounts of metals (~ 1/2 the mass of the star)
- Heavy elements synthesized within the first stars would be easily ejected into the pre-galactic medium since halo binding energies are low ($\sim 10^{50}$ erg $\ll E_{SN}$)

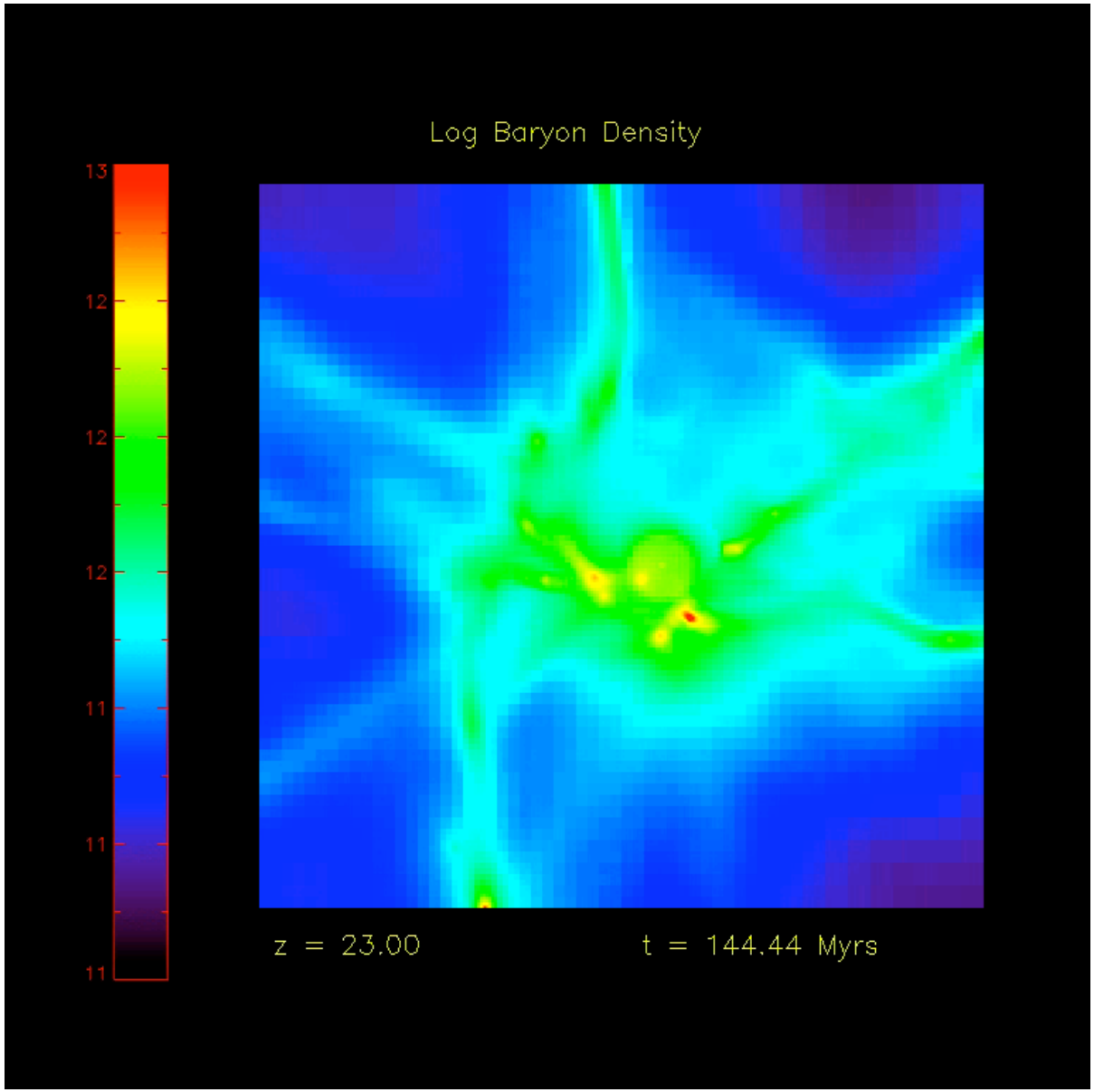

Box is ~ 6 kpc (proper) on a side

$M_* = 140\ M_\odot$
$E_{SN} = 10^{51.5}$ ergs
$M_{ej} = 140\ M_\odot$
$M_z = 70\ M_\odot$

HII region + SN

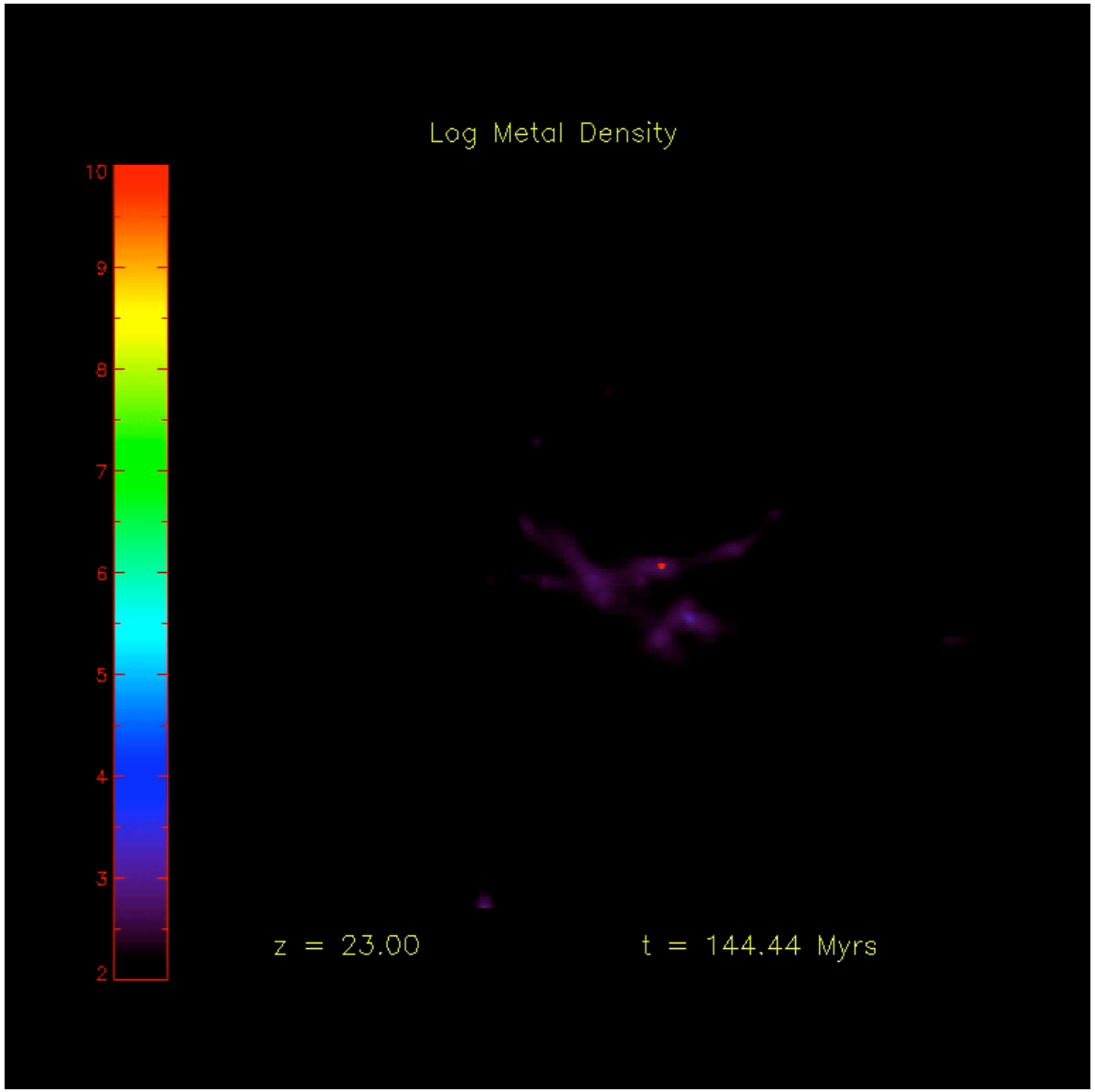

Metals spread over several proper kpc! (50-100 kpc sphere at z=0)

What's next?

- Refine supernova simulations using higher-resolution calculations
- Run a variety of models varying E_{SN}, spanning 30-300 $M_{\odot}$
- Use these models to motivate larger-scale unigrid simulations (Norman, O'Shea and Paschos, 2003 - also see talk by M. Norman later this week)
- Explore metal mixing and formation of 2nd generation of objects in a metal-enriched environment

Conclusions

- Formation of first star in ΛCDM "concordance model" is qualitatively similar to what is seen in ABN02
- Multiple FS simulations with different halo masses, halo collapse times result in halos with similar properties
- A second generation object which has been processed by an HII region has comparable amounts of cold gas to the equivalent unprocessed object in regions where star formation will occur
- Pop III supernovae can enrich large volumes of space, particularly when the effects of the star's HII region are taken into account

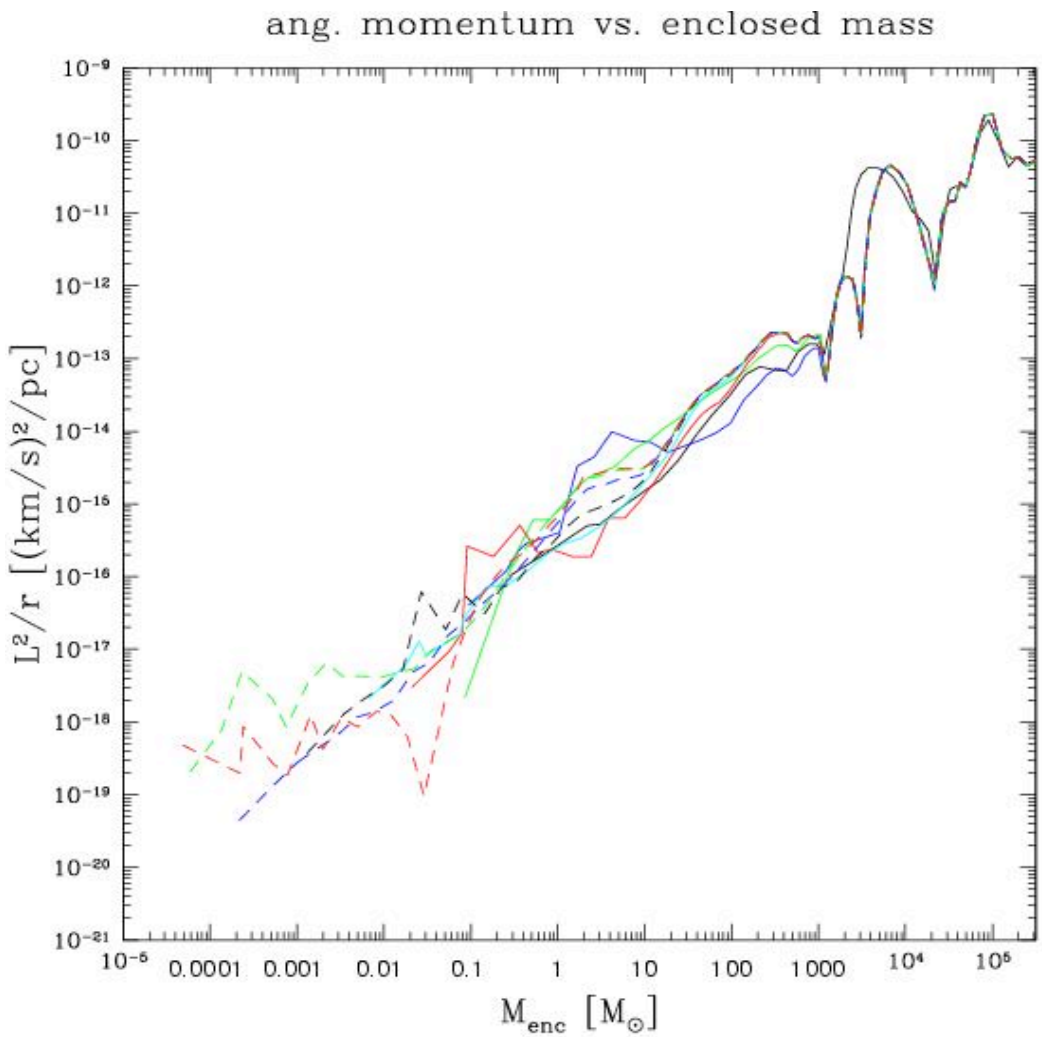

black solid line: z = 17.6 (t_0)
blue solid: t_0 + 8.7e5 years
green solid: +5e6 years
red solid: +3e5 years
cyan solid: + 17,000 years
black dashed: + 2300 years
blue dash: +310 years
green dashed: +91 years
red dashed: +31 years

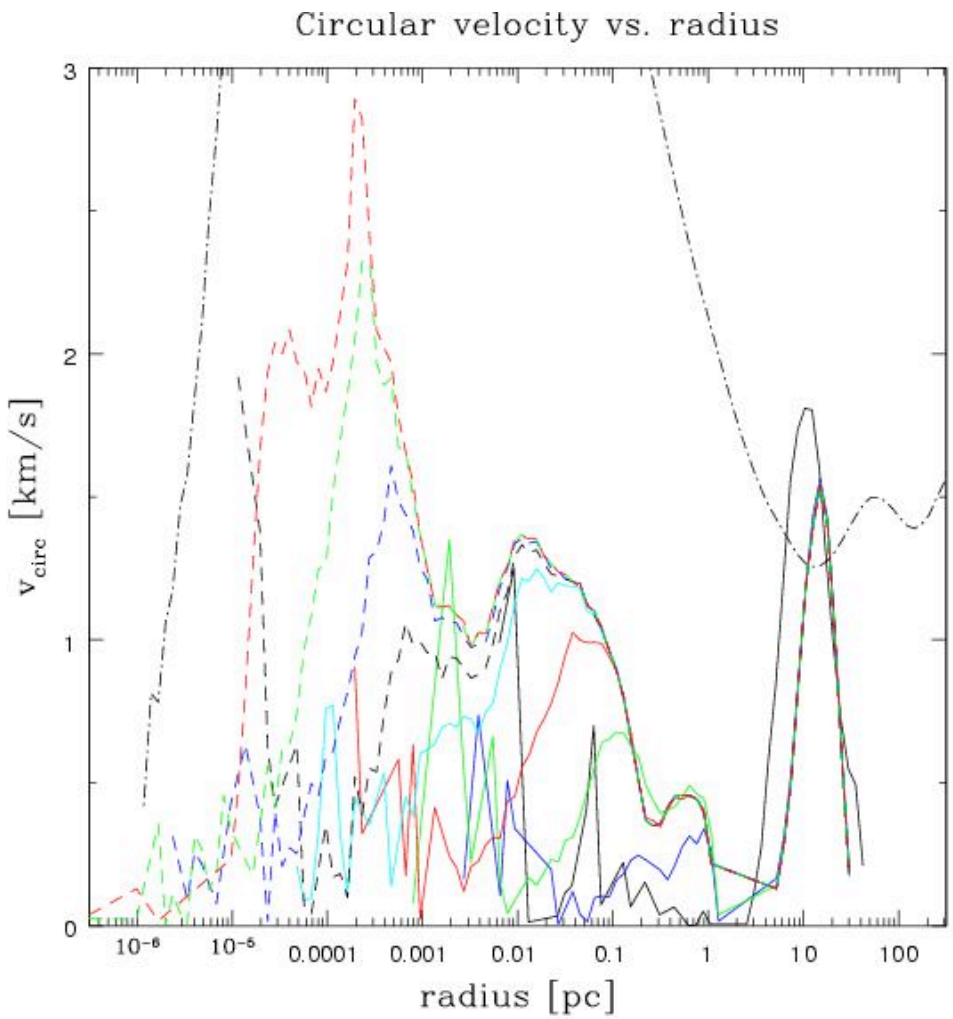

The protostellar "disk" is NOT rotationally supported!

Black dot-dashed line: v_{kep} at final timestep

- black solid line: z = 17.6 (t_0)
- blue solid: t_0 + 8.7e5 years
- green solid: +5e6 years
- red solid: +3e5 years
- cyan solid: + 17,000 years
- black dashed: + 2300 years
- blue dash: +310 years
- green dashed: +91 years
- red dashed: +31 years

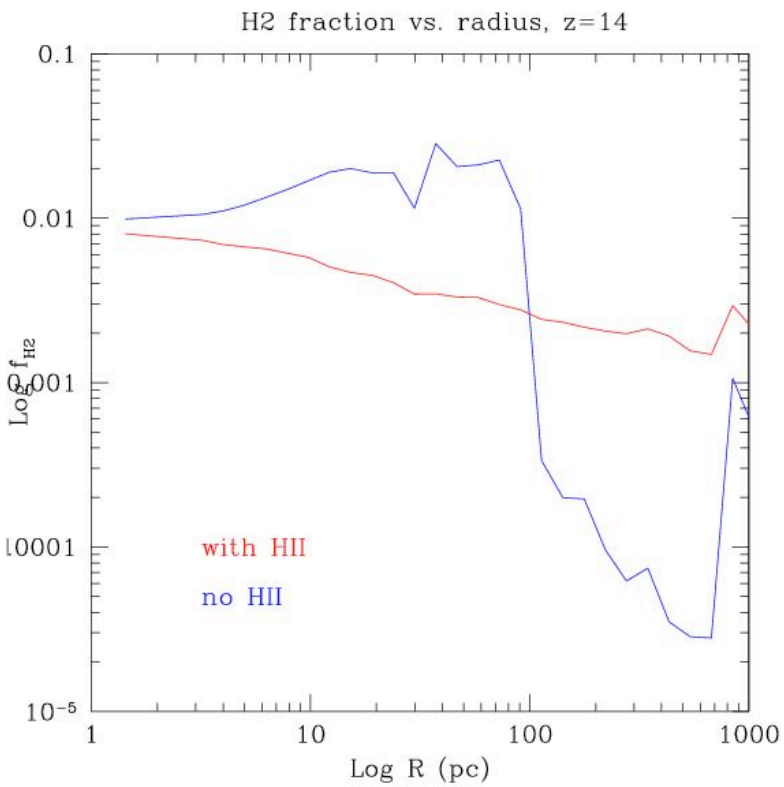

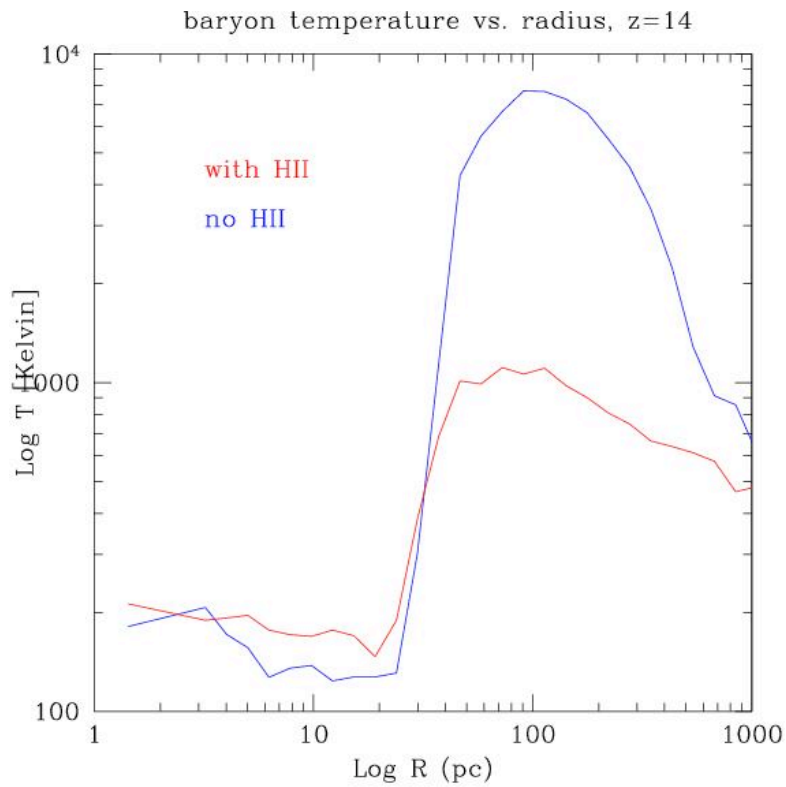

10^6 $M_\odot$ of ~ 200 K gas at z=14 in both simulations!

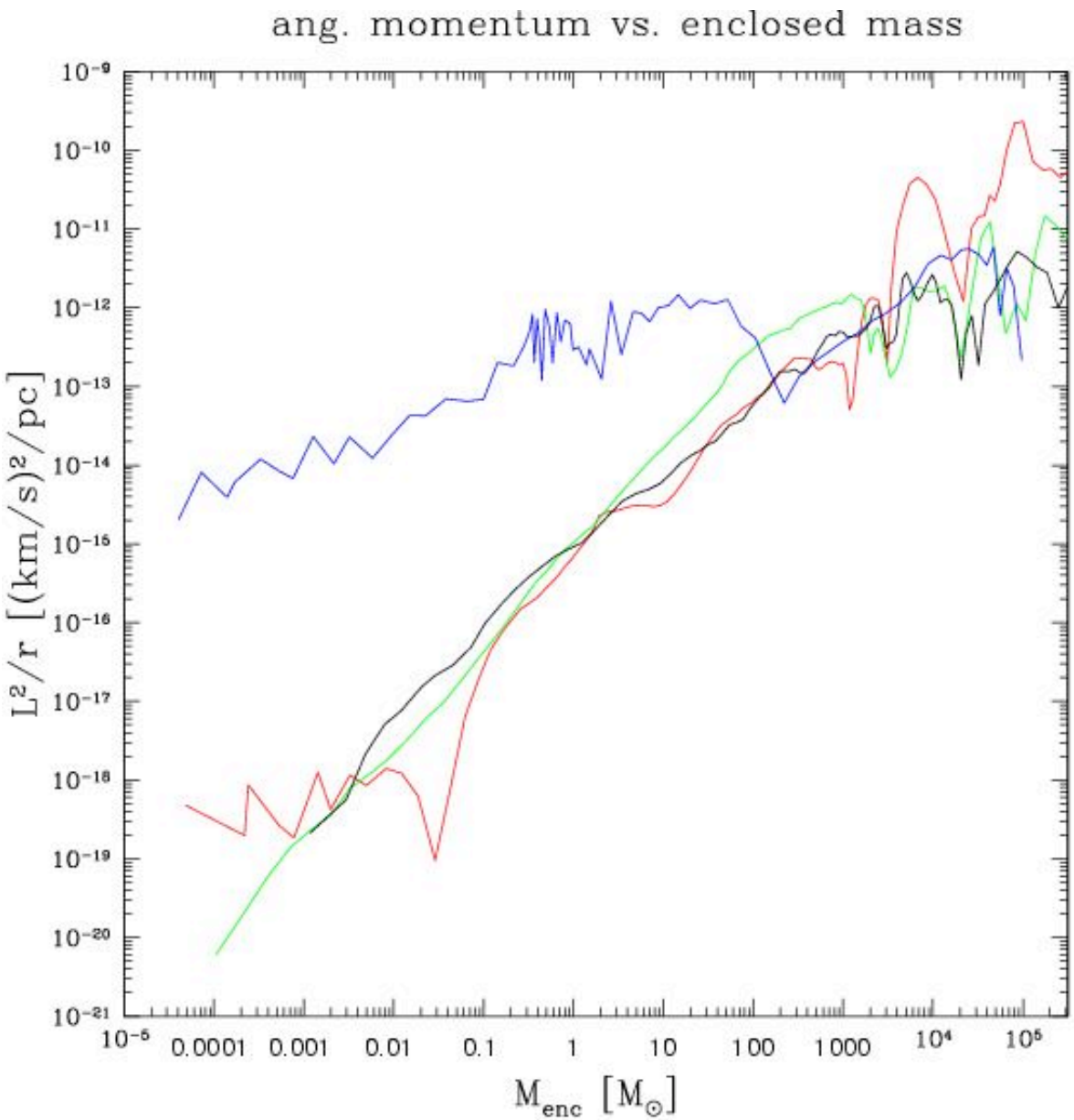

None of the halos are rotationally supported!

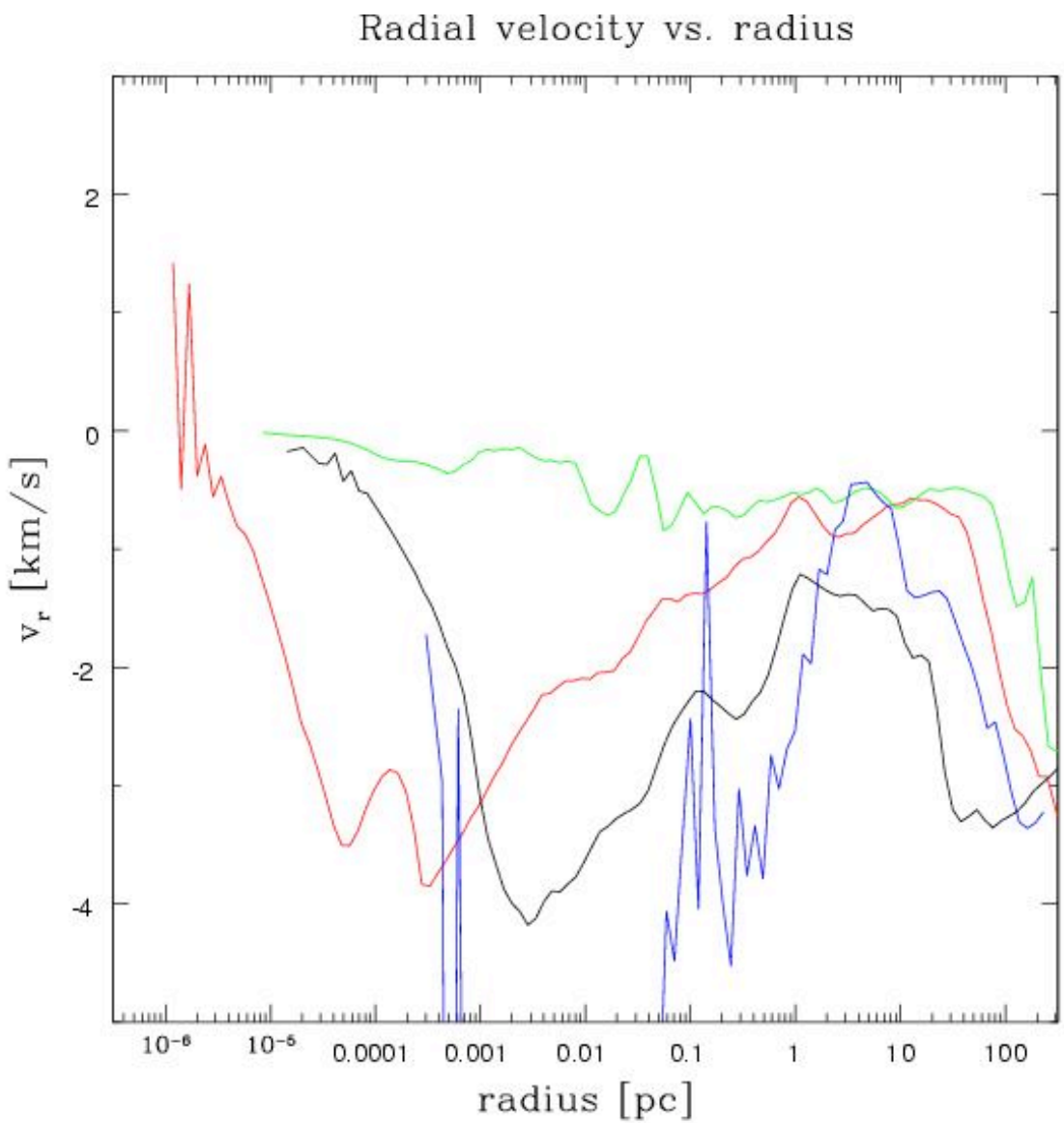
Radial velocity vs. radius
2
0
-2
-4
v_r [km/s]
10^{-6}
10^{-5}
0.0001
0.001
0.01
0.1
1
10
100
radius [pc]

Outline

- Introduction (mostly done by Tom Abel)
- Extension of Abel et al. 2002 - FS in ΛCDM
- Comparison of several FS halos
- FS HII region evolution
- FS supernova evolution (large-scale)
- Conclusions

***s*-Process Laboratory Studies : New Methods and Implications**

Outline

1. *s*-process nucleosynthesis

2. **Experimental methods to direct (*n*,γ)-cross section measurements :**
   - prompt γ-rays : 4π arrays + TOF
   - activation : decay measurement
     atom counting measurement

3. A new possible astrophysical neutron source : *SARAF* (Israel)

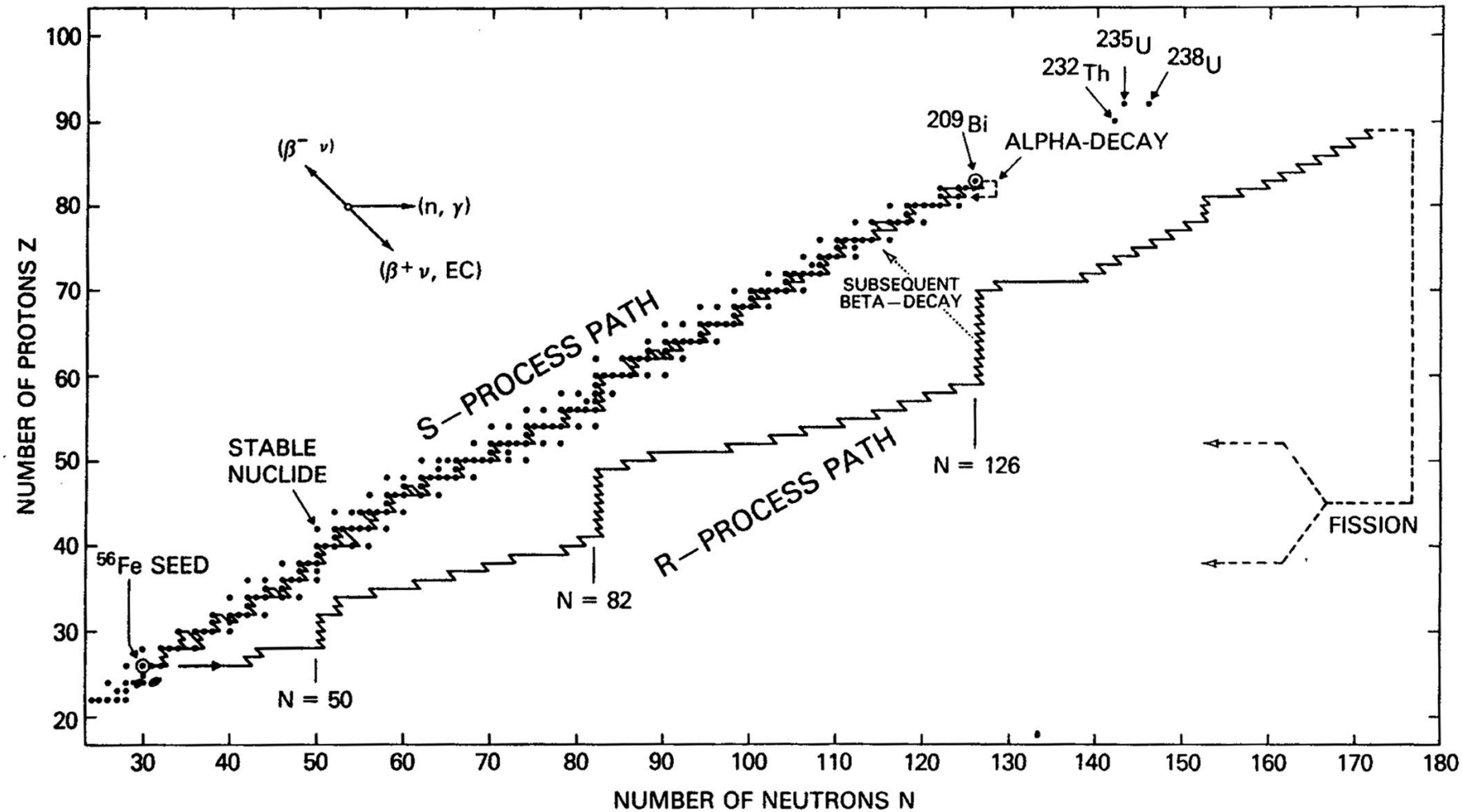
NUMBER OF PROTONS Z
NUMBER OF NEUTRONS N
100
90
80
70
60
50
40
30
20
30
40
50
60
70
80
90
100
110
120
130
140
150
160
170
180
(β⁻ ν)
(n, γ)
(β⁺ ν, EC)
S—PROCESS PATH
R—PROCESS PATH
STABLE NUCLIDE
56Fe SEED
N = 50
N = 82
N = 126
209Bi
ALPHA-DECAY
232Th
235U
238U
SUBSEQUENT BETA—DECAY
FISSION

s-process regimes and sites

	Weak component	*Main component*
	$60 < A < 90$	$90 < A < 209$
Temperature	$2.2\text{-}3.5 \times 10^{8}$ ^{o}K	0.9×10^{8} ^{o}K
Neutron density	7×10^{5} cm^{-3}	4×10^{8} cm^{-3}
Neutron source	^{22}Ne(α,n)	^{13}C(α,n), ^{22}Ne(α,n)
Stellar site	core helium burning in massive stars	TP-AGB stars

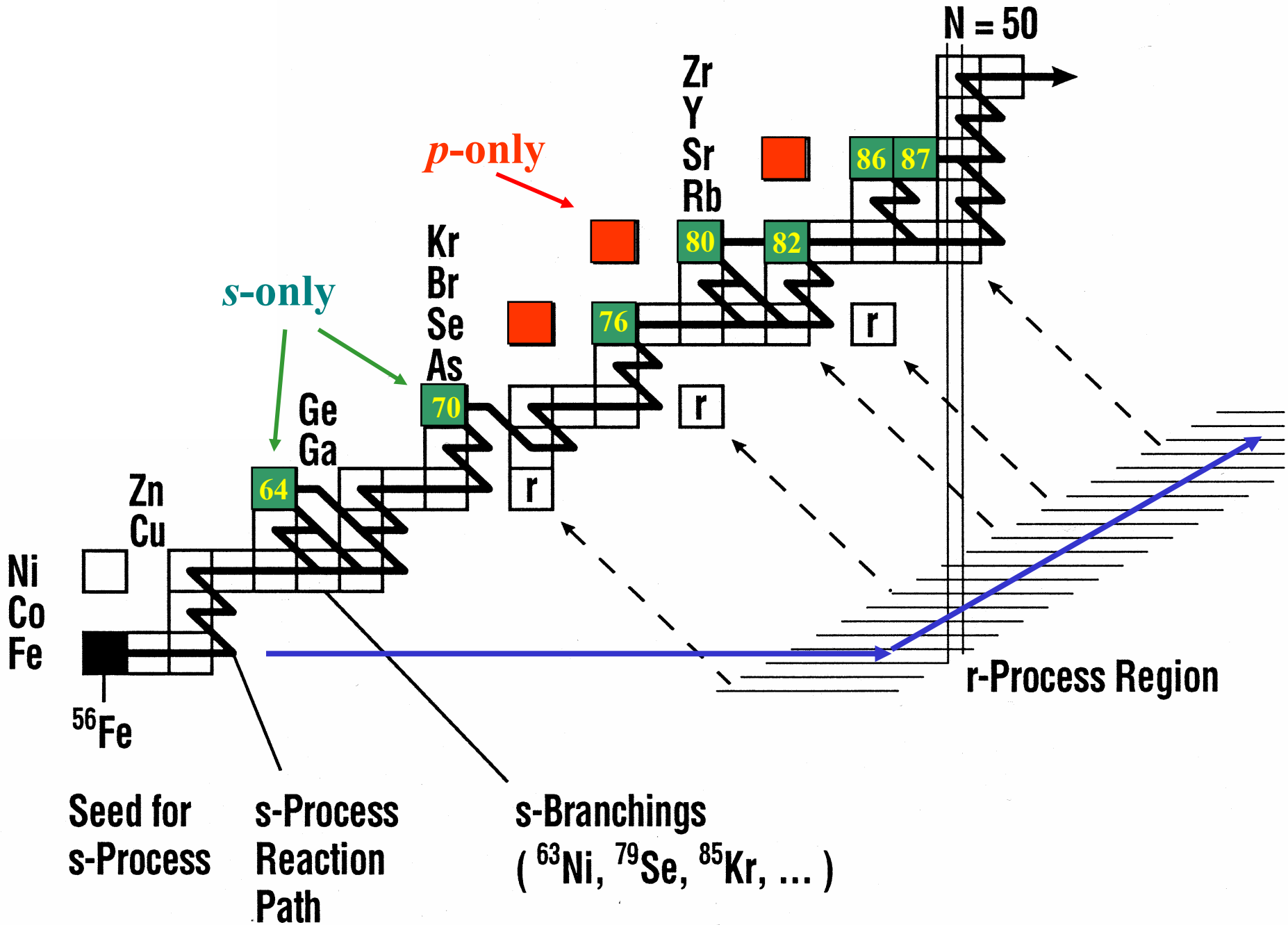
N = 50
Zr
Y
Sr
Rb
p-only
86
87
80
82
Kr
Br
Se
As
s-only
76
r
70
r
Ge
Ga
64
r
Zn
Cu
Ni
Co
Fe
56Fe
r-Process Region
Seed for
s-Process
s-Process
Reaction
Path
s-Branchings
(63Ni, 79Se, 85Kr, ...)

LANSCE

DANCE / Flight Path 14 at the Lujan Center

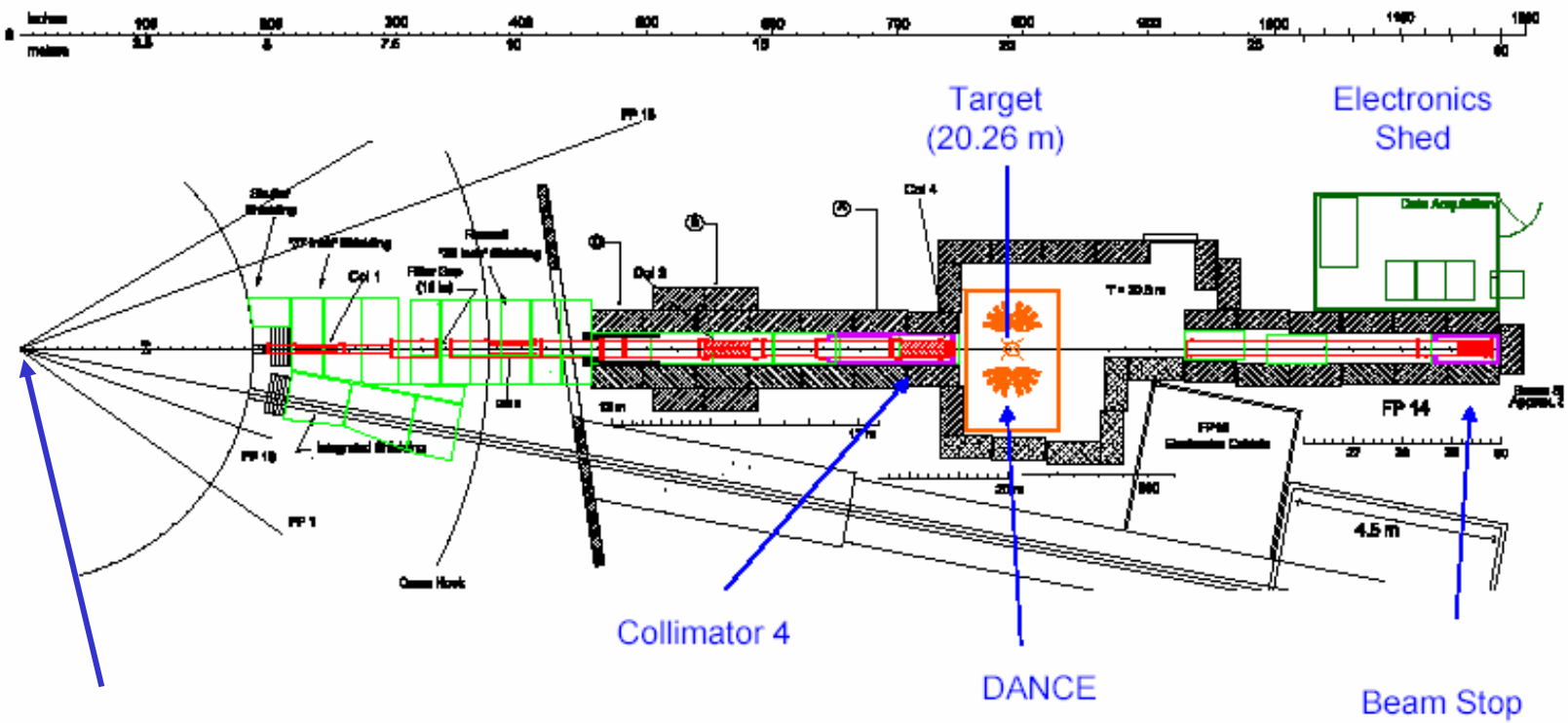

neutron production target

Flight Path 14 Neutron Flux

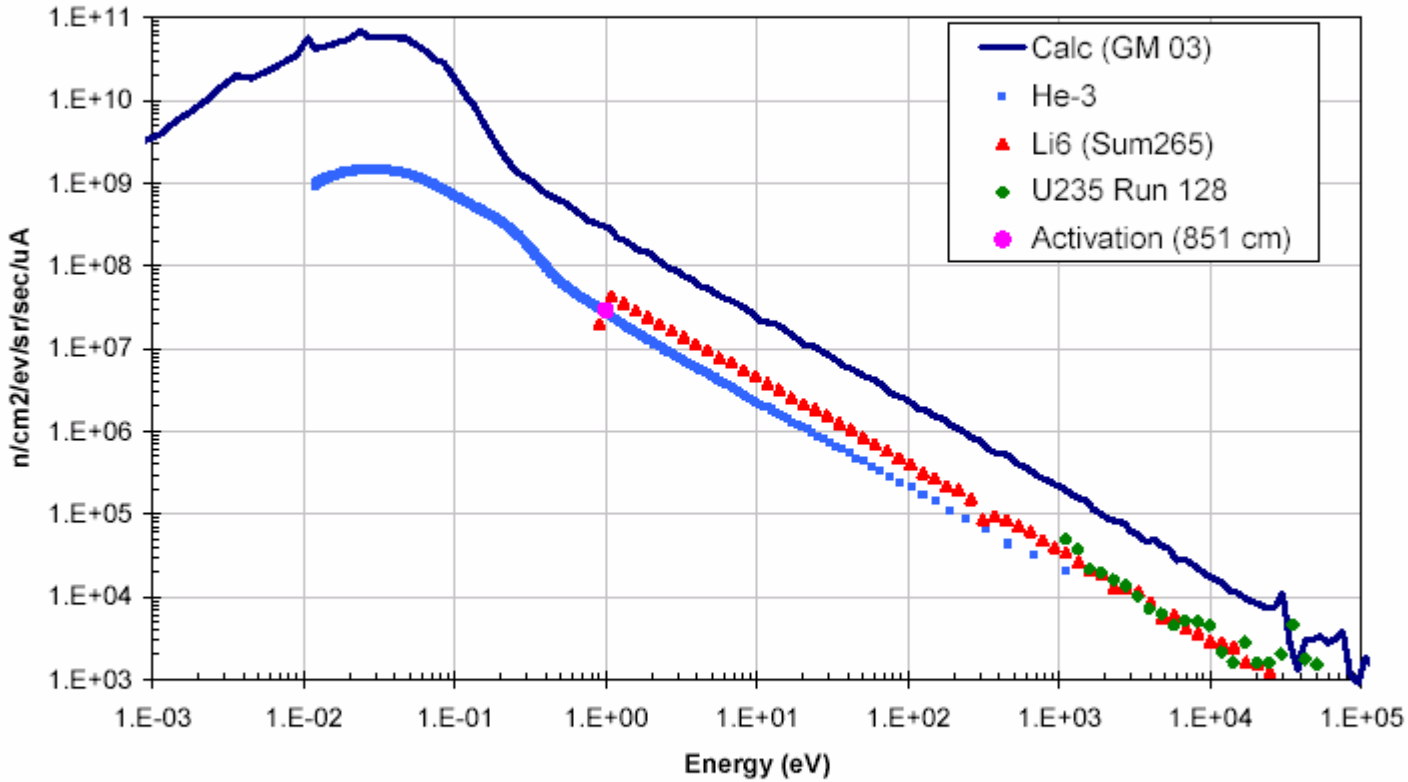

Fluxes adjusted to "moderator current" for comparison

$I \approx (2.78\text{x } 10^7 \text{ N/cm}^2\text{/sr/ev/sec/}\mu\text{A}) \text{ / E (eV)}$

$\Phi \approx (127 \text{ N/cm}^2\text{/ev/sec/}\mu\text{A}) \text{) / E (eV)}$

n-TOF beam (CERN)

Neutron flight path: 185 m → energy resolution: $<10^{-3}$

Proton pulse width: 6 ns

Neutron energy range: 0.1 eV – 10 GeV

Repetition rate: < 0.5 Hz

Neutron intensity: $>1.5\cdot10^4$ dN/dlnE/pulse

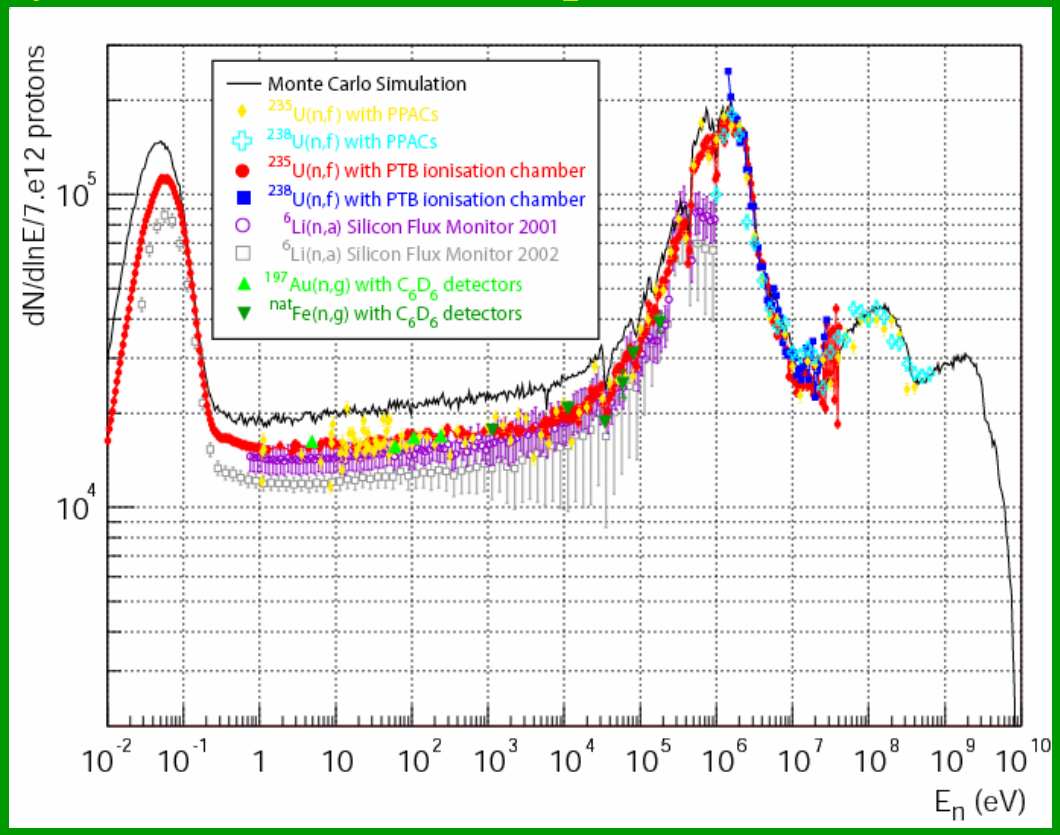

4π-BaF2

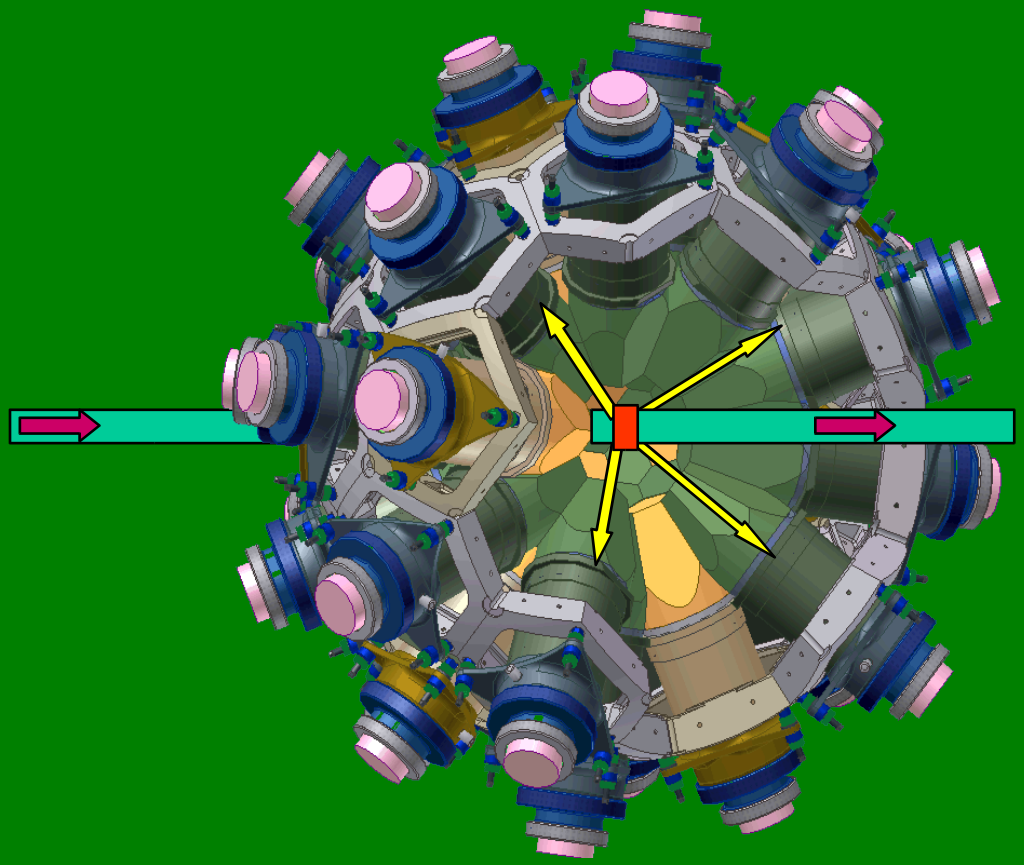

(n,γ)

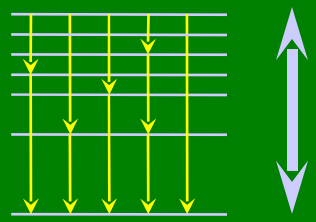

binding energy

BaF_2:

- 100% efficiency
- fast timing
- multiplicity measurement
- low neutron sensitivity

n_TOF-03: $^{151}Sm(n,\gamma)$

- 206 mg of $^{151}Sm(t_{1/2}= 93$ yr)
- encapsulated in 0.1 mm Ti
- 200 GBq (5.3 Ci) activity

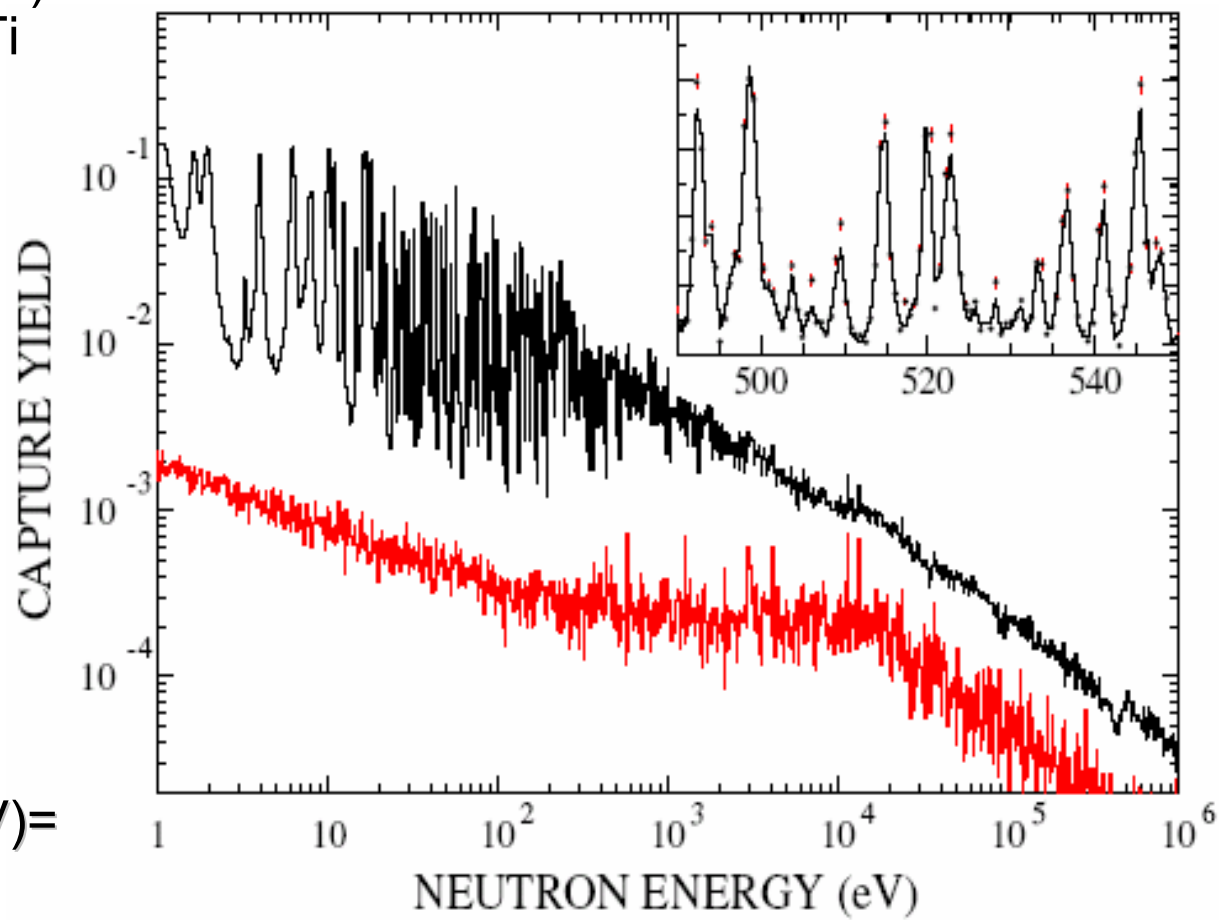

Maxwellian-averaged cross section (*k*T= 30 keV)= 3100 ± 160 mb

U. Abbondanno et al. - The n_TOF Collaboration

s-only nuclides

La132 4.8 h 2- * EC	La133 3.912 h 5/2+ EC	La134 6.45 m 1+ EC	La135 19.5 h 5/2+ EC	La136 9.87 m 1+ * EC	La137 6E4 y 7/2+ EC	La138 1.05E+11 y 5+ EC,β- 0.0902	La139 7/2+ 99.9098
Ba131 11.50 d 1/2+ * EC	Ba132 0+ 0.101	Ba133 10.51 y 1/2+ * EC	Ba134 0+ 2.417	Ba135 3/2+ * 6.592	Ba136 0+ * 7.854	Ba137 3/2+ * 11.23	Ba138 0+ 71.70
Cs130 29.21 m 1+ * EC,β-	Cs131 9.689 d 5/2+ EC	Cs132 6.479 d 2+ EC,β-	Cs133 7/2+ 100	Cs134 2.0648 y 4+ * EC,β-	Cs135 2.3E+6 y 7/2+ * β-	Cs136 13.16 d 5+ * β-	Cs137 30.07 y 7/2+ β-
Xe129 1/2+ * 26.4	Xe130 0+ 4.1	Xe131 3/2+ * 21.2	Xe132 0+ * 26.9	Xe133 5.243 d 3/2+ * β-	Xe134 0+ * 10.4	Xe135 9.14 h 3/2+ * β-	Xe136 2.36E21 y 0+ 8.9

measured (n,γ)

branching point
tough experimentally

next best

FZ Karlsruhe: activation of ^{135}Cs ($t_{1/2}=2 \times 10^6$ yr) + γ-decay measurement of ^{136}Cs (13 d)

$^7Li(p,n)^7Be$, neutron energies 30 and 500 keV, $\Phi_n \approx 3\ 10^9$ n/s

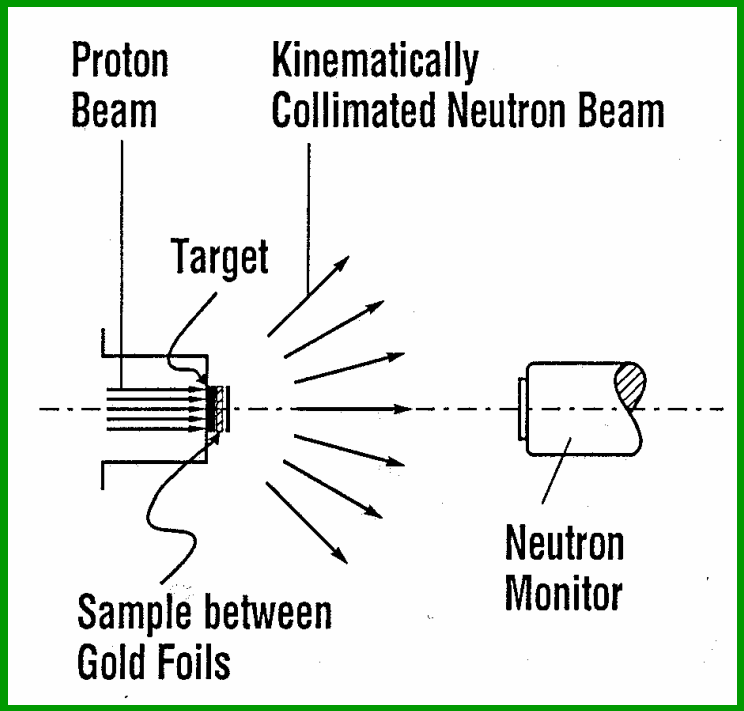

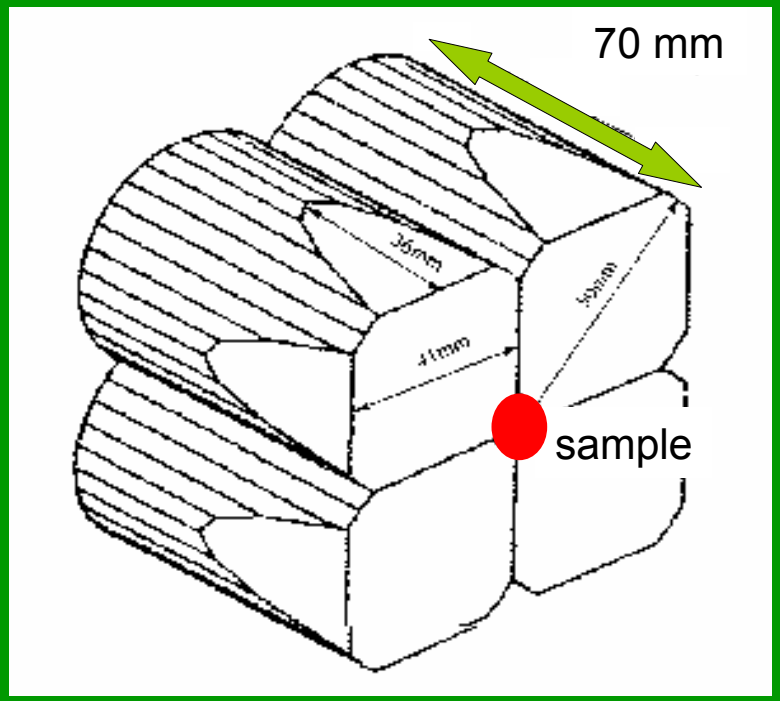

activation :

400 ng ^{135}Cs (20 Bq)

γ measurement

$\sigma(^{134}Cs)$ by model normalization

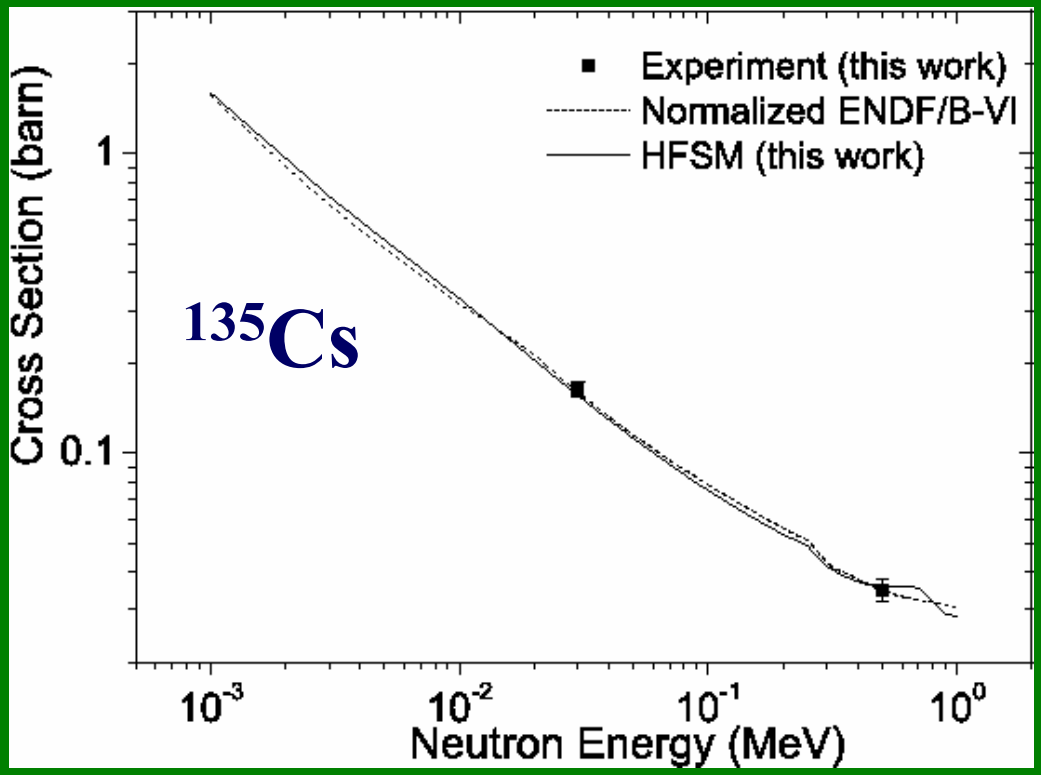

$^{134}Cs/^{135}Cs$ and $^{134}Cs/^{133}Cs$ ratios well reproduced by statistical model calculations

↓

^{134}Cs cross section via measured cross sections of neighbors

↓

$\sigma_{(134)}$ = 724 ± 65 mb at kT=30 keV

N. Patronis et al., PRC 69, 025803 (2004)

s-process in massive star nucleosynthesis : overproduction of medium mass nuclei

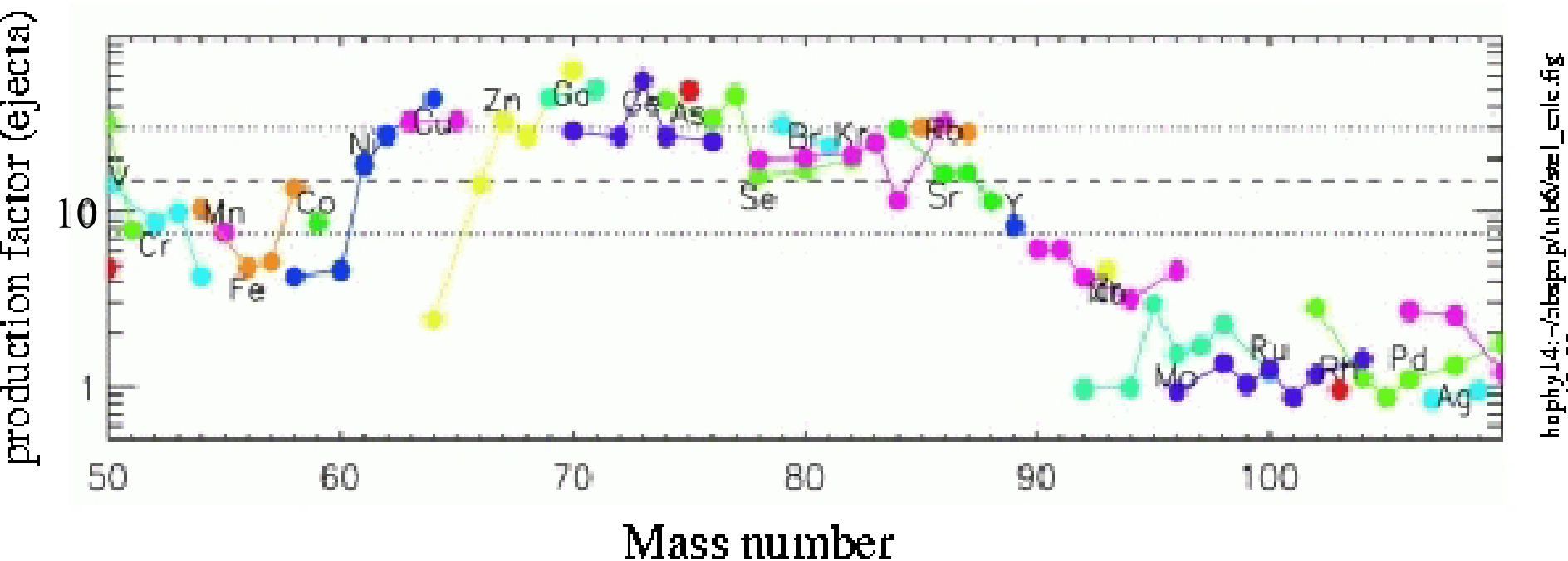

Ref. : T. Rauscher et al., Ap.J. 576 (2002) 323

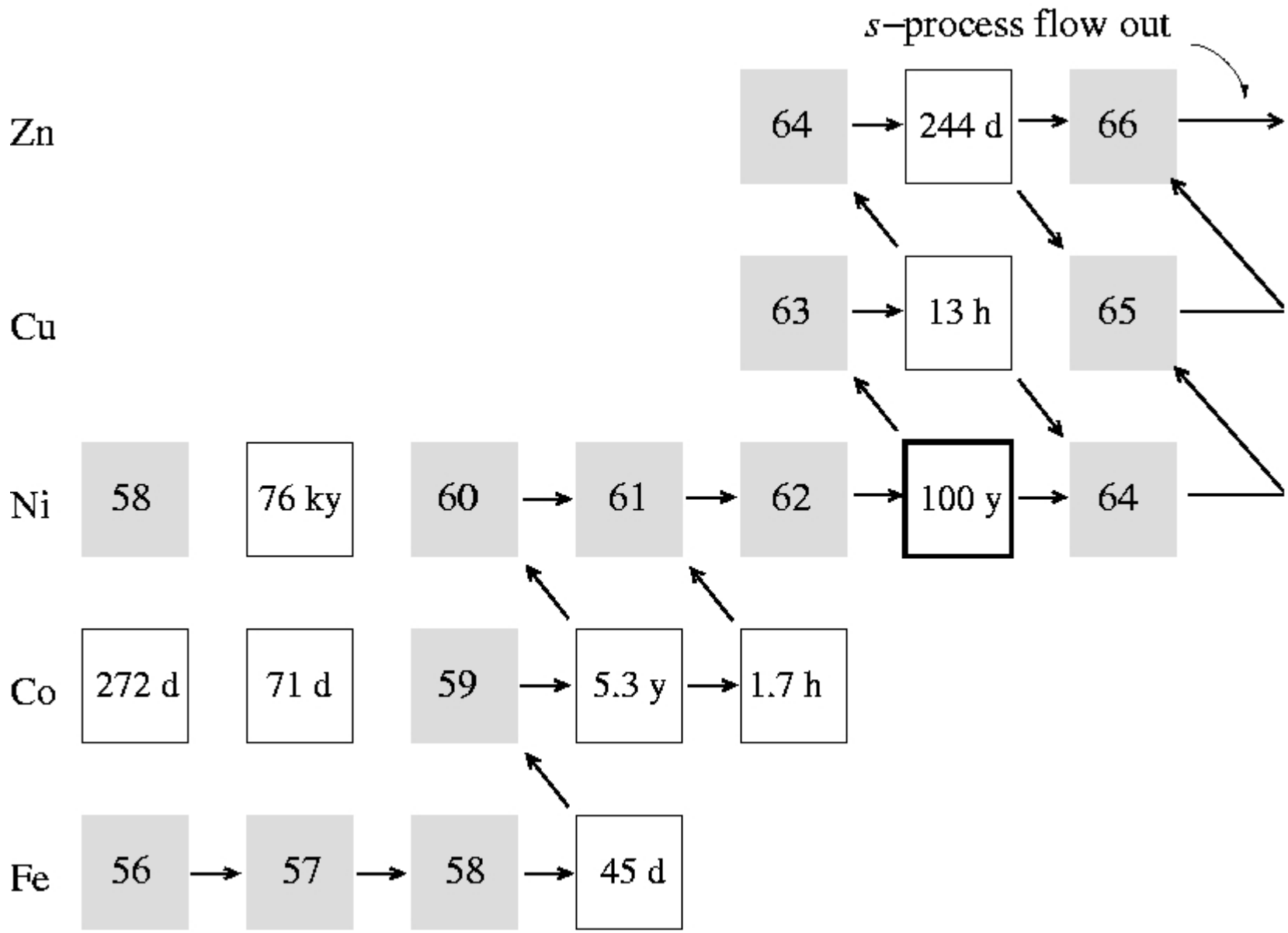
s−process flow out
Zn
64
244 d
66
Cu
63
13 h
65
Ni
58
76 ky
60
61
62
100 y
64
Co
272 d
71 d
59
5.3 y
1.7 h
Fe
56
57
58
45 d

Discrepancies in $^{62}Ni(n,\gamma)$ measurements and calculations :

- "Experimental" values extrapolated from $\sigma_{th}(n,\gamma)$
- Calculations :
  T. Rauscher and K.H. Guber, PRC 66, 028802 (2002)
- Direct capture contribution
- Subthreshhold resonance

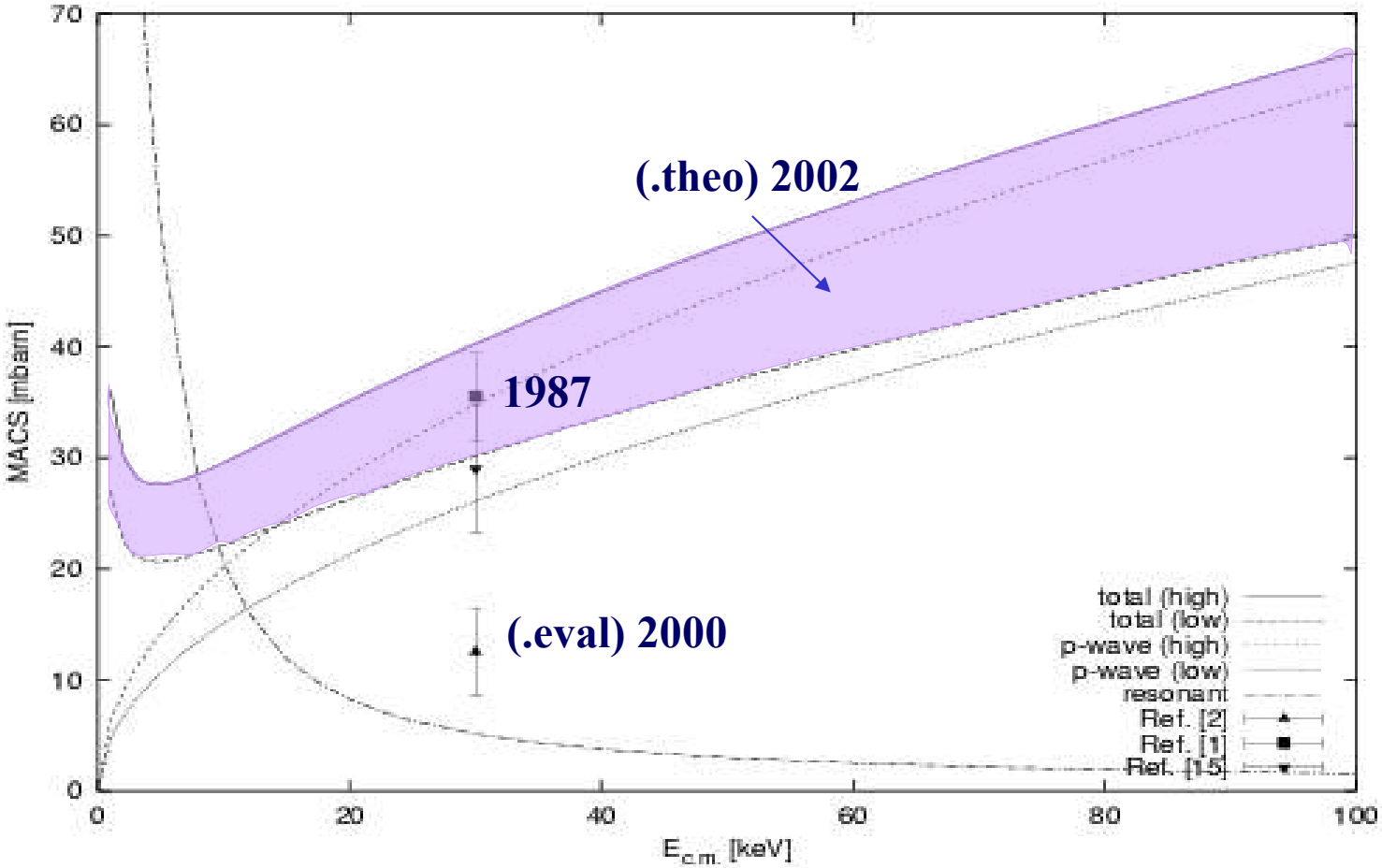

Activation + mass spectrometry (AMS) : ^{62}Ni(n,γ)^{63}Ni

- Activate enriched ^{62}Ni target with quasi-Maxwellian neutrons of $kT = 25$ keV (^{7}Li(p,n)^{7}Be reaction)

- Measure the isotopic abundance ^{63}Ni/^{62}Ni by accelerator mass spectrometry :
  ^{63}Ni : $t_{1/2} = 100$ yr, $Q_{\beta^-} = 70$ keV, no γ

- Determine Maxwellian-averaged cross section from relation :

$$\sigma_V = (^{63}\mathrm{Ni}/^{62}\mathrm{Ni}) / \langle \phi\, t \rangle$$

: Activation measurement by atom counting
(Accelerator Mass Spectrometry (AMS

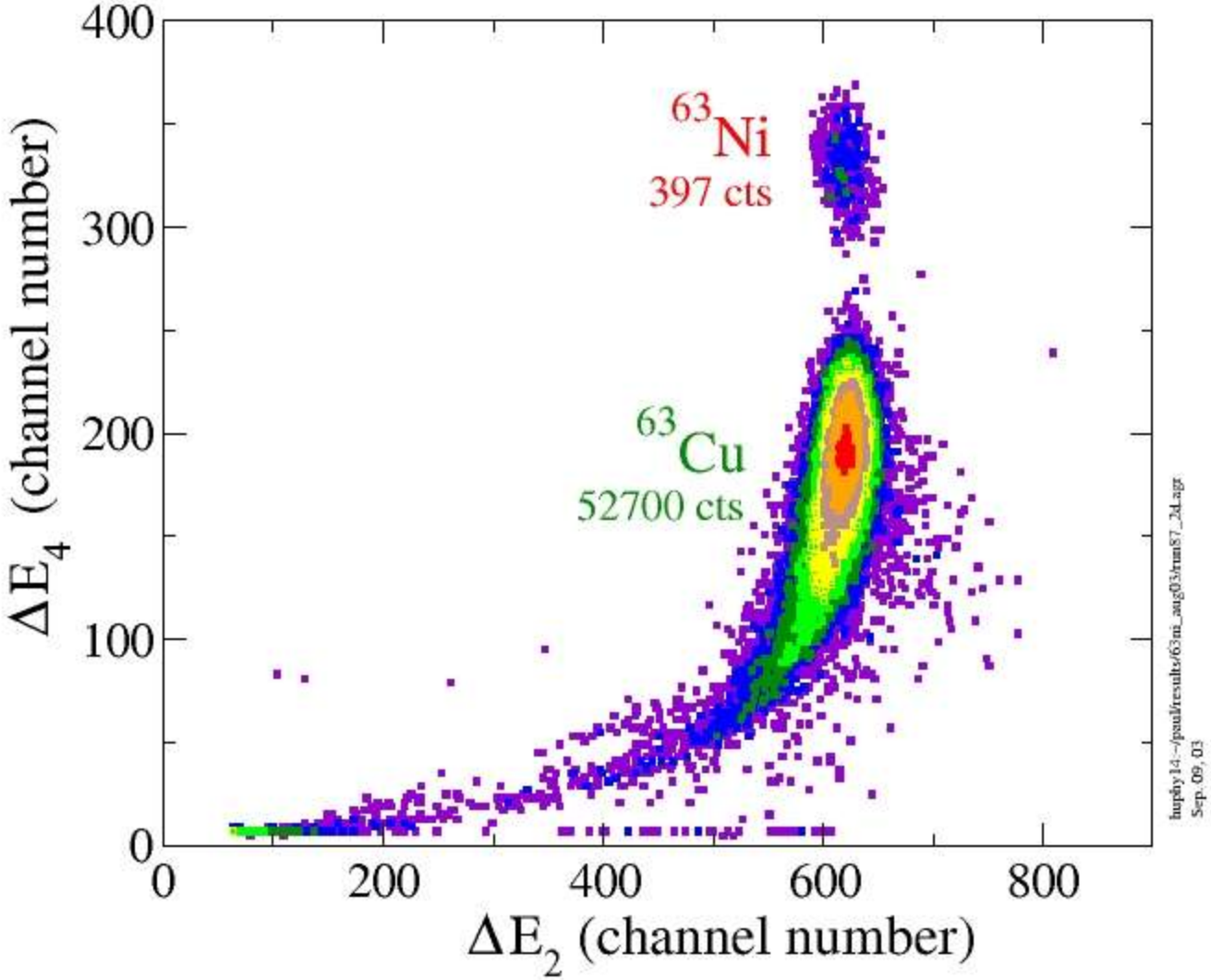

particle id.
after gas-filled
magnet separation

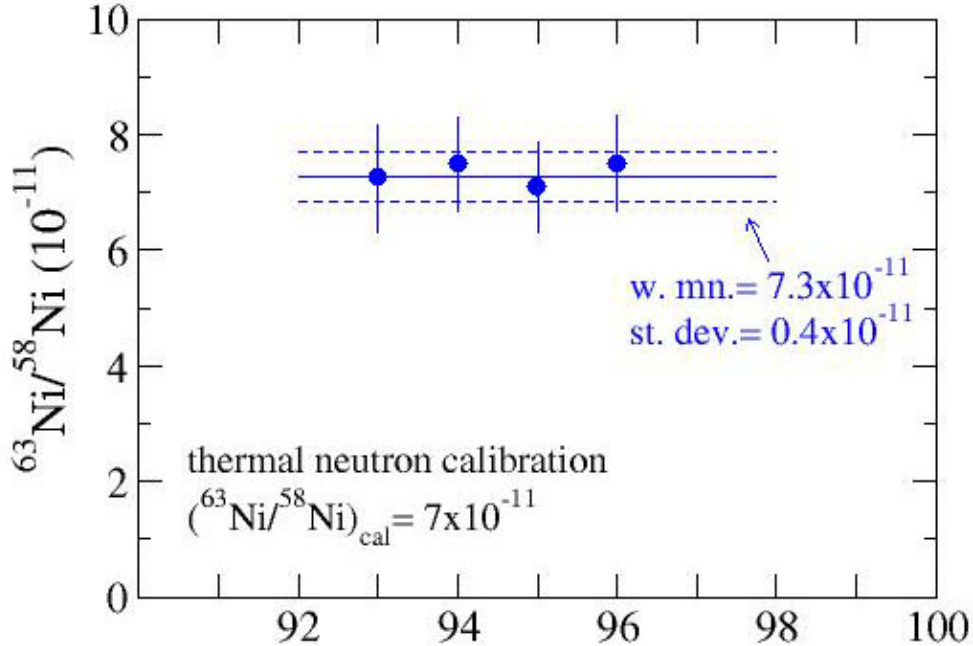
10
8
6
4
2
0
92
94
96
98
100
$^{63}Ni/^{58}Ni\ (10^{-11})$
w. mn.= 7.3×10^{-11}
st. dev.= 0.4×10^{-11}
thermal neutron calibration
$(^{63}Ni/^{58}Ni)_{cal} = 7 \times 10^{-11}$

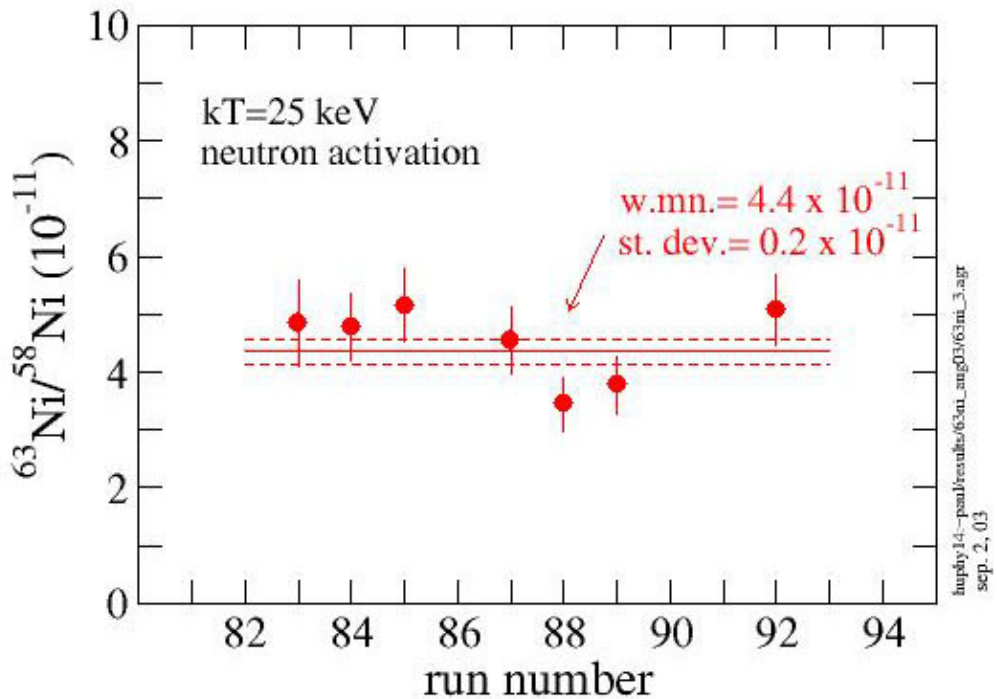
10
8
6
4
2
0
82
84
86
88
90
92
94
$^{63}Ni/^{58}Ni\ (10^{-11})$
run number
kT=25 keV
neutron activation
w.mn.= 4.4×10^{-11}
st. dev.= 0.2×10^{-11}
hupby14:~paul/results/63ni_aug03/63ni_3.agr
sep. 2, 03

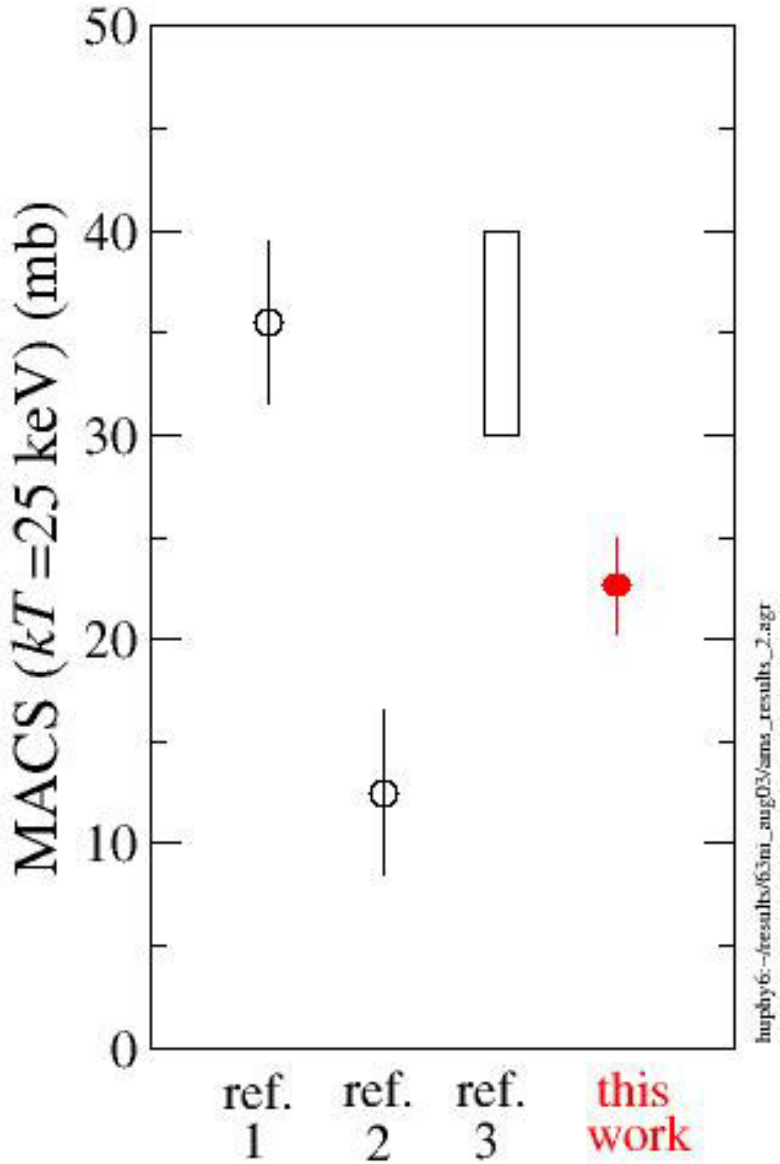

1. Bao & Kaeppeler, 1987
2. Bao et al., 2000
3. Rauscher & Guber, 2002

Nucleosynthesis calc. : sensitive to $\sigma(^{62}\mathrm{Ni}(n,\gamma)^{63}\mathrm{Ni})$

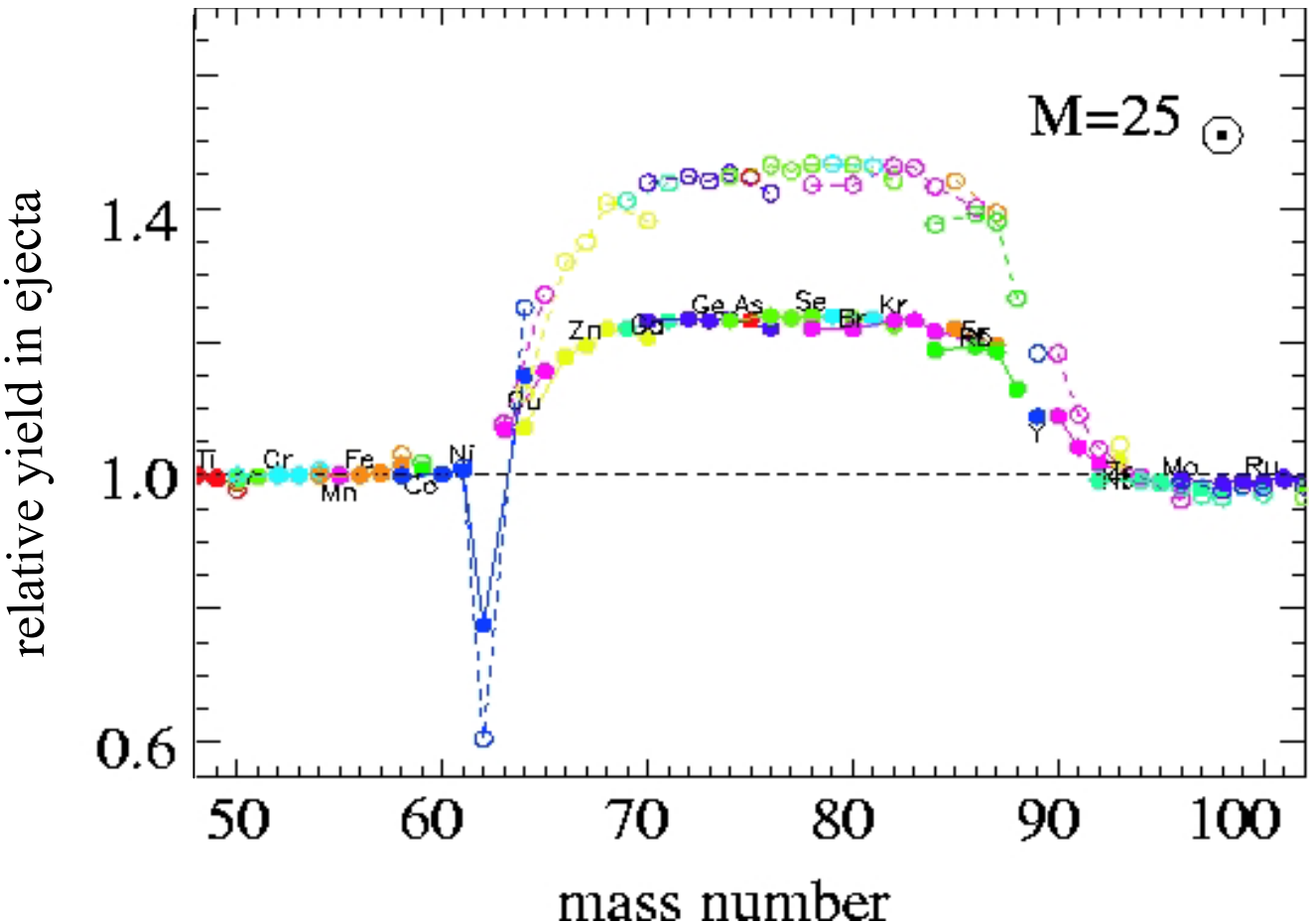

$$\bullet \quad \frac{Y_A(\sigma_{64}= 23\ \mathrm{mb})}{Y_A(\sigma_{64}= 12\ \mathrm{mb})}$$

$$\circ \quad \frac{Y_A(\sigma_{64}= 35\ \mathrm{mb})}{Y_A(\sigma_{64}= 12\ \mathrm{mb})}$$

$^{40}Ca(\alpha,\gamma)^{44}Ti$: supernova nucleosynthesis

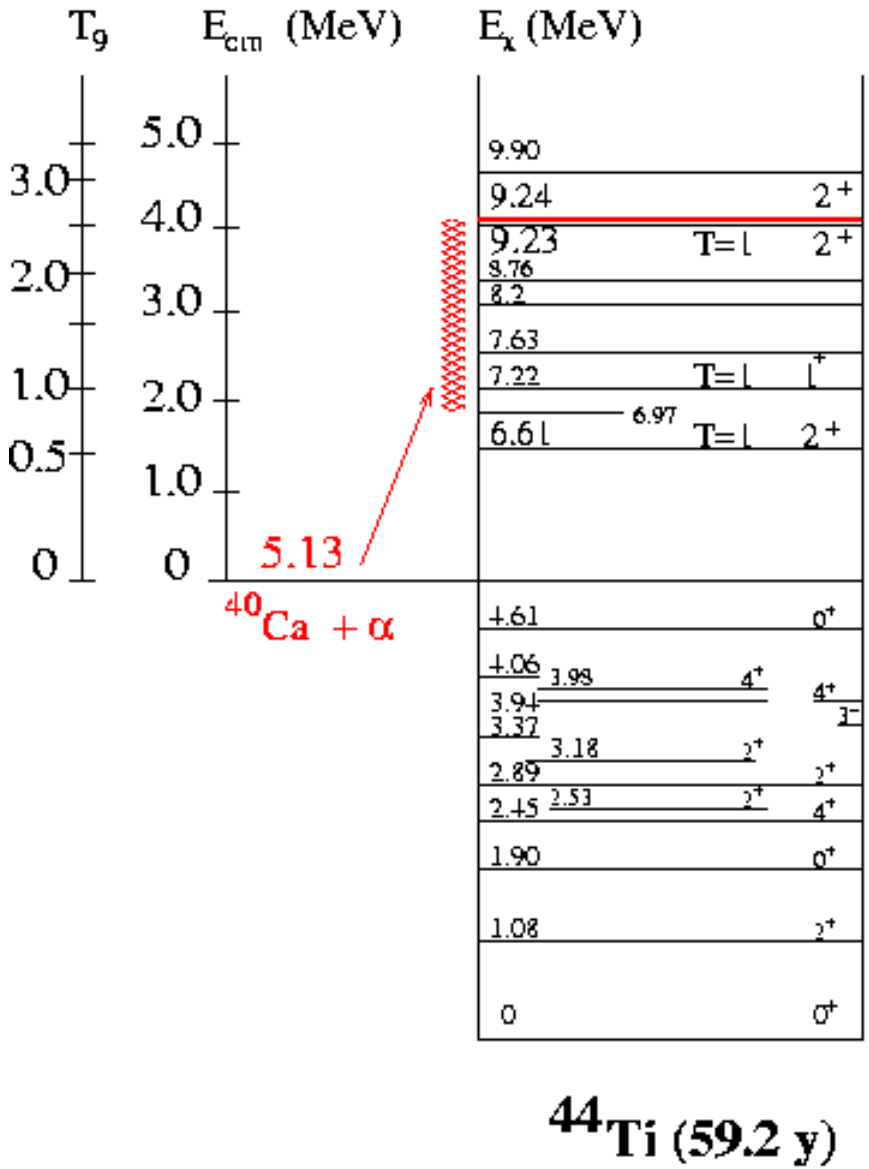

many resonances

5.8, 2.0 eV

$\Sigma = 4.2$ eV

$\omega\gamma\ (\alpha,\gamma_{prompt})$

7 eV

$24 < \Sigma < 60$ eV

$\omega\gamma\ (\alpha,\gamma_{tot})_{AMS}$

$$Y = N_{proj}\ (\mathcal{N}_A/A_T)\ (dE/dx)^{-1}\ .$$
$$.(A_T+A_{proj}/A_T)\ \lambda^2\ \omega\gamma/2$$

$$\omega\gamma = (2J_R+1)/2j_{proj}+1)(2J_T+1).$$
$$.\Gamma_\alpha\Gamma_\gamma/\Gamma_t$$

Collaborators :

Hebrew U. : H. Nasar, S. Ghelberg, M.P.
Forschungszentrum Karlsruhe : S. Dababneh, M. Heil, F. Kaeppeler, R. Plag
Argonne Nat. Lab. : I. Ahmad, J.P. Greene, D.J. Henderson, C.L. Jiang, R.C. Pardo, S. Sinha, T. Pennington, K.E. Rehm, R. Scott, X. Tang, R. Vondrasek
U. Jyvaskyla : H. Koivisto
Los Alamos Nat. Lab. : R. Reifarth
Soreq NRC : D. Berkovits, M. Bettan
U. Notre Dame : P. Collon, J. Goerres, S. O'Brien, M. Wiescher
U. Ioannina : N. Patronis

The SARAF project and a possible new neutron source for astrophysics :

- SARAF : Soreq Applied Research Accelerator Facility (Israel) : A. Nadler et al.
  Superconducting linac ($m/q \leq 2$) : p, d
  Phase I funded and under way

- Phase I (2006) : p, 4 MeV, 2 mA + liquid-Li target → keV neutrons
  d, 5.2 MeV, 2 mA

- Phase II (2009) : E_{max}(p,d)= 40 MeV, 2 mA

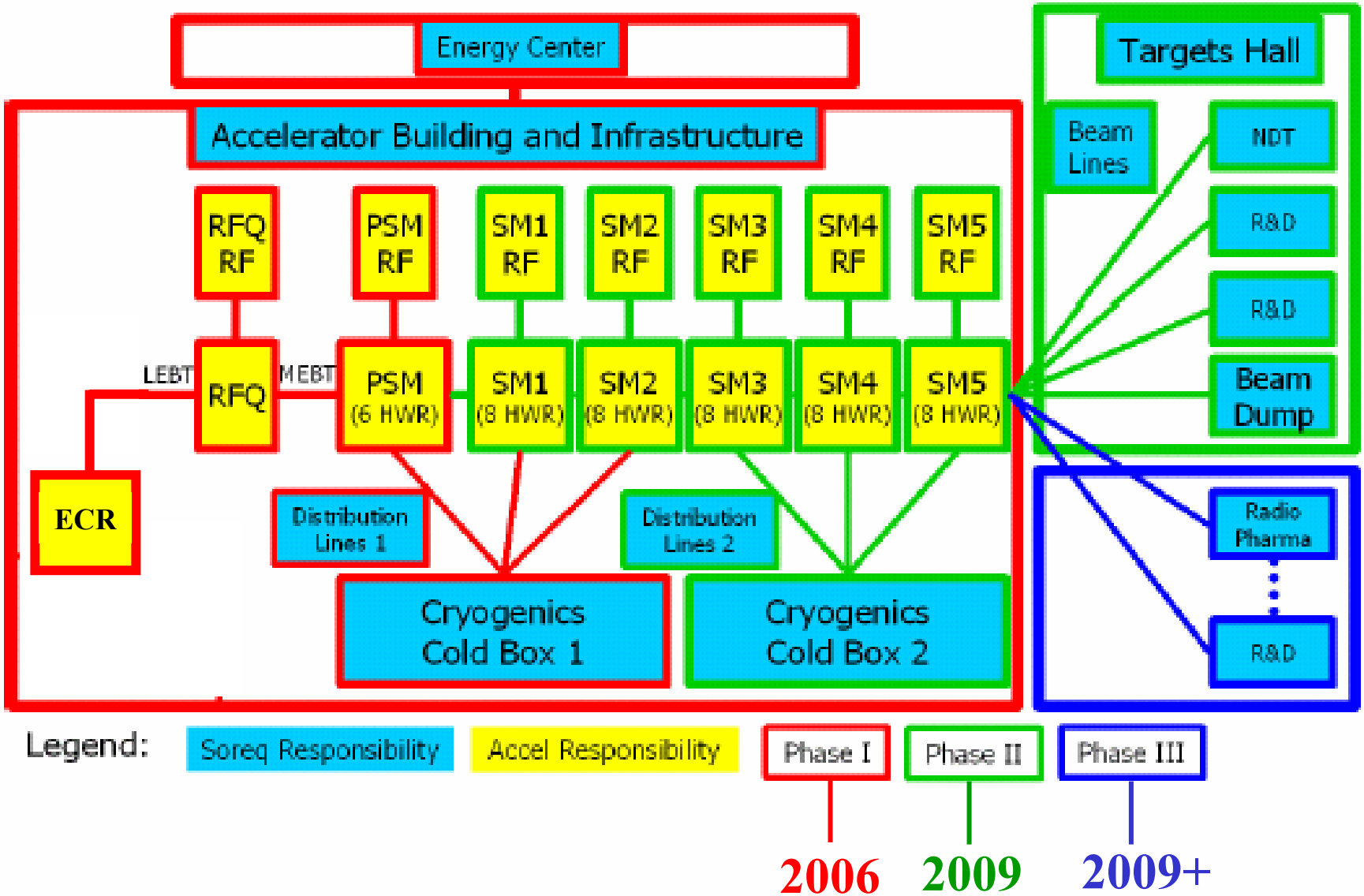
Energy Center
Accelerator Building and Infrastructure
Targets Hall
Beam Lines
NDT
R&D
R&D
Beam Dump
RFQ RF
PSM RF
SM1 RF
SM2 RF
SM3 RF
SM4 RF
SM5 RF
LEBT
RFQ
MEBT
PSM (6 HWR)
SM1 (8 HWR)
SM2 (8 HWR)
SM3 (8 HWR)
SM4 (8 HWR)
SM5 (8 HWR)
ECR
Distribution Lines 1
Distribution Lines 2
Cryogenics Cold Box 1
Cryogenics Cold Box 2
Radio Pharma
R&D
Legend:
Soreq Responsibility
Accel Responsibility
Phase I
Phase II
Phase III
2006
2009
2009+

Liquid Li target as an astrophysical-neutron production target

- Technology under development for RIA at Argonne (J. Nolen, C. Reed, Y. Momozaki)

- Plans for : high-power fragmentation target for RIA heavy-ion beams
  stripper target for high-power heavy-ion beams

- Good target for production of Maxwellian neutrons from high-intensity proton beams

liq.^{7}Li(p,n) production: E_p= 1.9-2 MeV, 2 mA :

ϕ_n (kT= 30 keV) = 2 x 10^{11} n/s

Applications : radioactive targets, double-neutron capture

La132 4.8 h 2- * EC	La133 3.912 h 5/2+ EC	La134 6.45 m 1+ EC	La135 19.5 h 5/2+ EC	La136 9.87 m 1+ * EC	La137 6E4 y 7/2+ EC	La138 1.05E+11 y 5+ EC,β- 0.0902	La139 7/2+ 99.9098
Ba131 11.50 d 1/2+ * EC	Ba132 0+ 0.101	Ba133 10.51 y 1/2+ * EC	Ba134 0+ 2.417	Ba135 3/2+ * 6.592	Ba136 0+ * 7.854	Ba137 3/2+ * 11.23	Ba138 0+ 71.70
Cs130 29.21 m 1+ * EC,β-	Cs131 9.689 d 5/2+ EC	Cs132 6.479 d 2+ EC,β-	Cs133 7/2+ 100	Cs134 2.0648 y 4+ * EC,β-	Cs135 2.3E+6 y 7/2+ * β-	Cs136 13.16 d 5+ * β-	Cs137 30.07 y 7/2+ β-
Xe129 1/2+ * 26.4	Xe130 0+ 4.1	Xe131 3/2+ * 21.2	Xe132 0+ * 26.9	Xe133 5.243 d 3/2+ * β-	Xe134 0+ * 10.4	Xe135 9.14 h 3/2+ * β-	Xe136 2.36E21 y 0+ 8.9

with $\phi_n \sim 10^{11}$ n cm^{-2} s^{-1}: ^{135}Cs/^{133}Cs ~ 10^{-14} (AMS)

⟶ expt. value of ^{134}Cs(n,γ)

Chemical Enrichment and Nucelosynthesis in the Young Universe

Jason X. Prochaska

UCO/Lick Observatory
UC Santa Cruz

Stephane Herbert-Fort (UCSC)
Yeshe Fenner (Swinbourne)
J. Chris Howk (UC San Diego)

Sara Ellison (U Victoria)
Art Wolfe (UC San Diego)

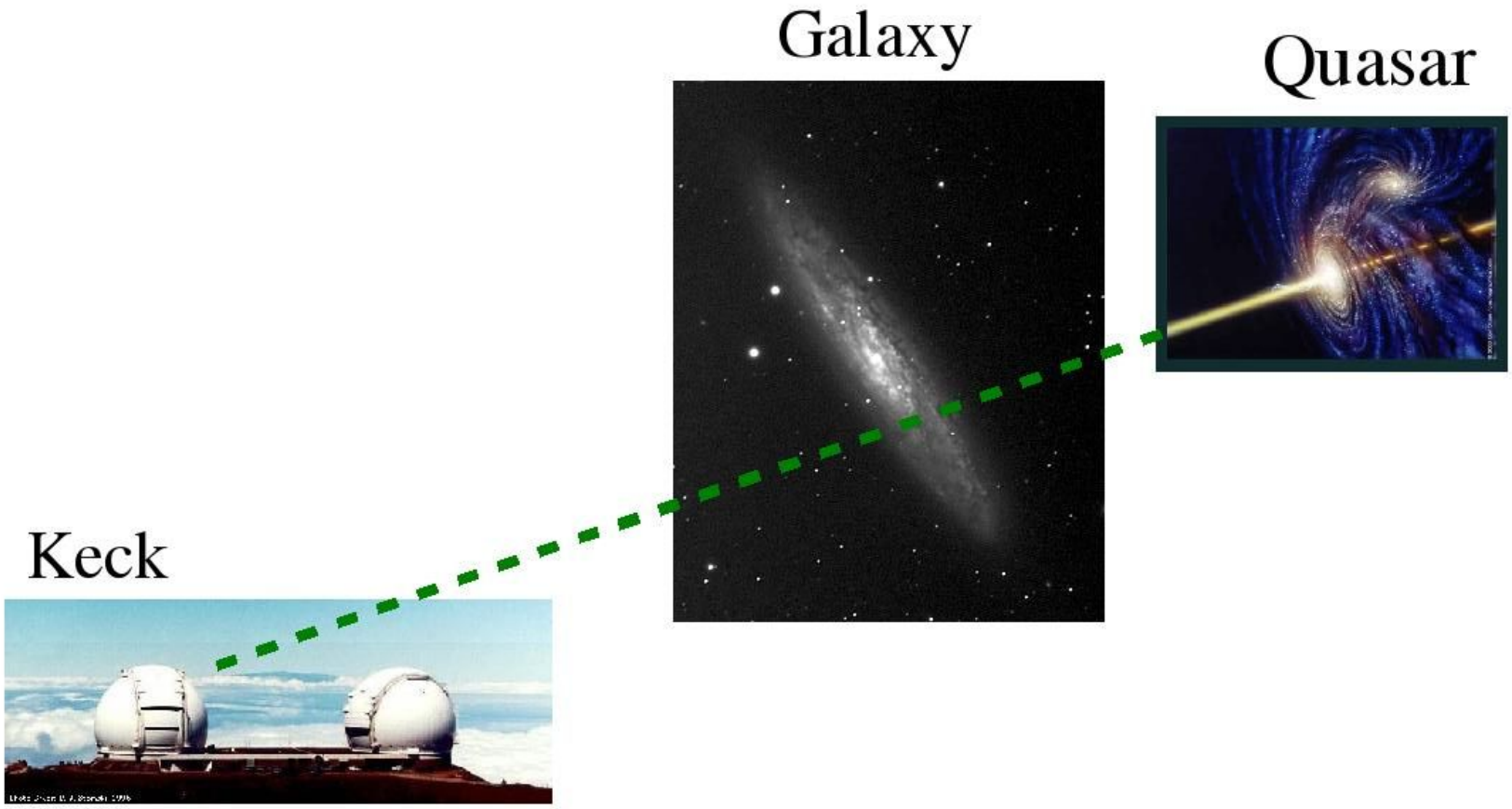

Quasar Absorption Line Systems

Damped Lyαα System Defined

- $N(HI) > 2 \times 10^{20}\ cm^{-2}$
  - Dominant reservoir of HI
  - Large N(HI) => δ
    δρ /ρ ρ >> 100
  - Progenitors of modern day
- Identified in Absorption
  - Optical depth weighted
    (ττ = σσ n)
  - Not restricted to the high luminosity tail
  - => Greater diversity of mass, morphology, etc. than LBG, ERO's, SCUBA galaxies

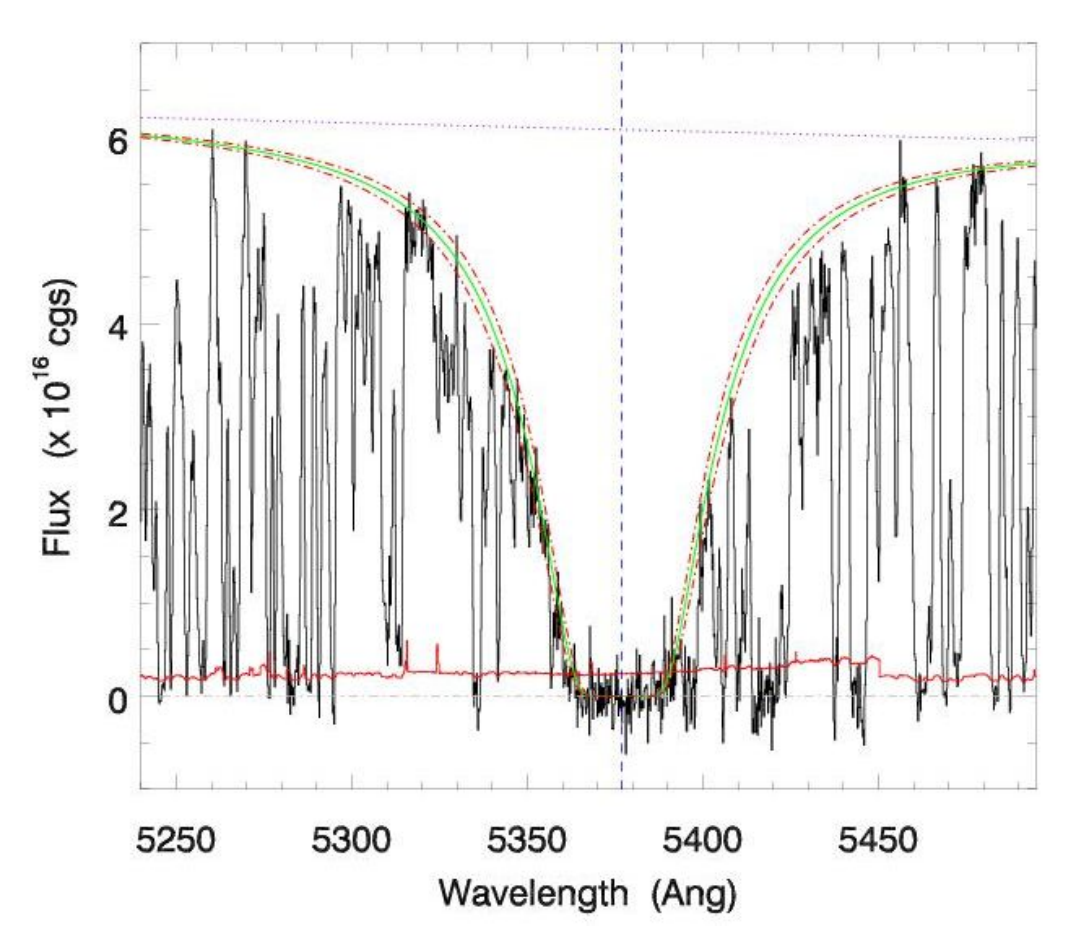

What are the DLA?

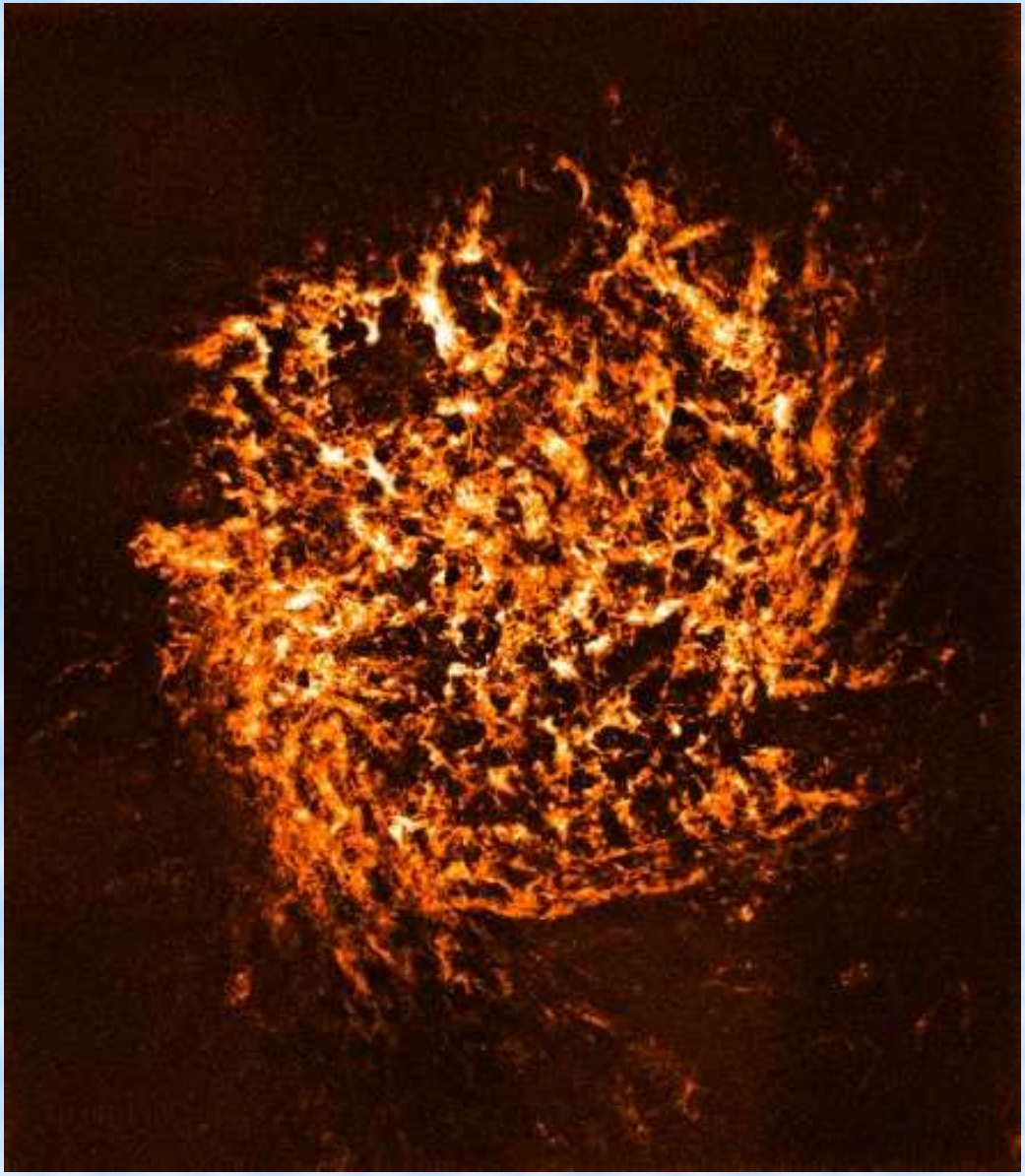

Local analogs

HIRES Spectroscopy

Vogt et al.

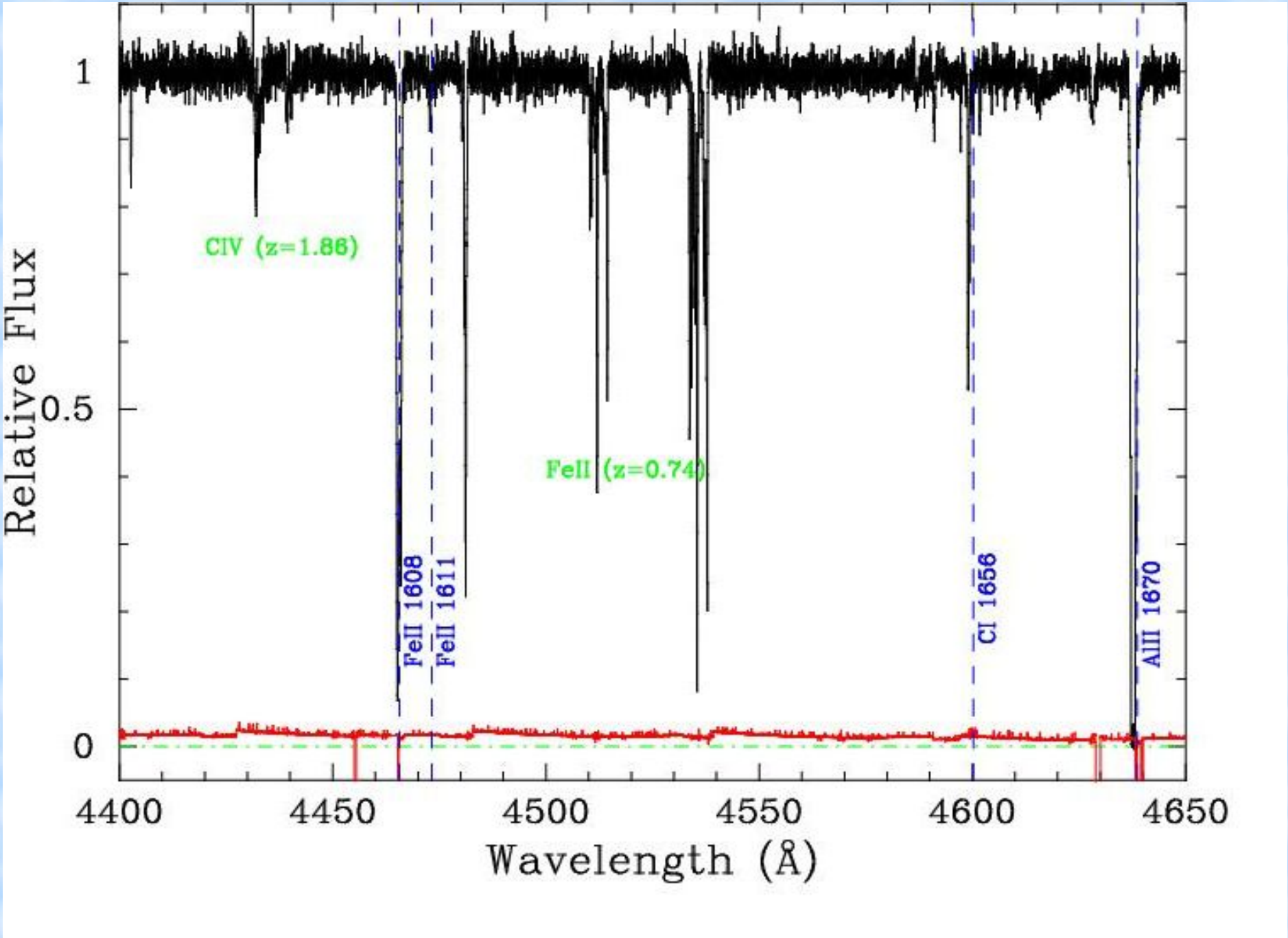

MW ISM vs. Extragalactic ISM

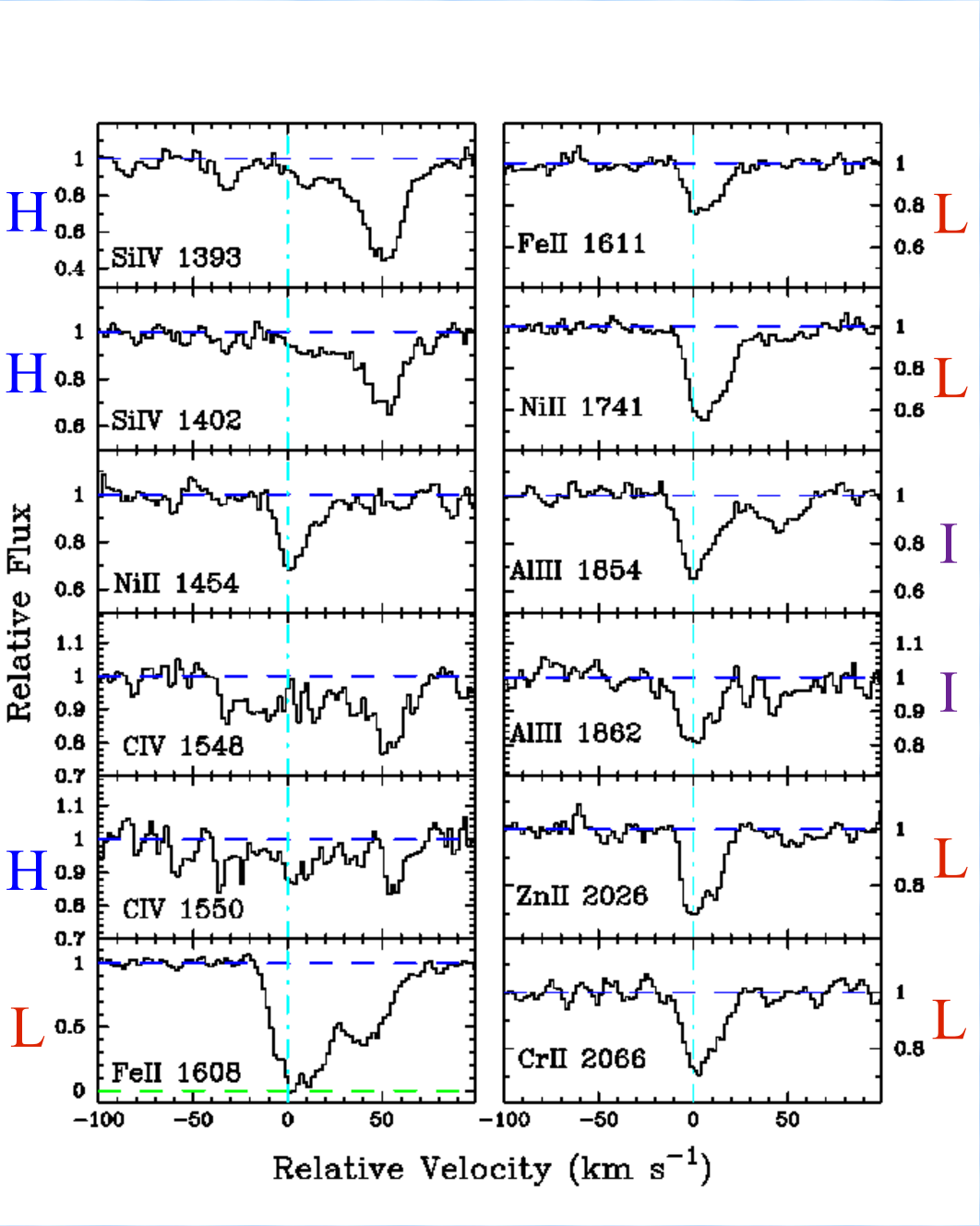

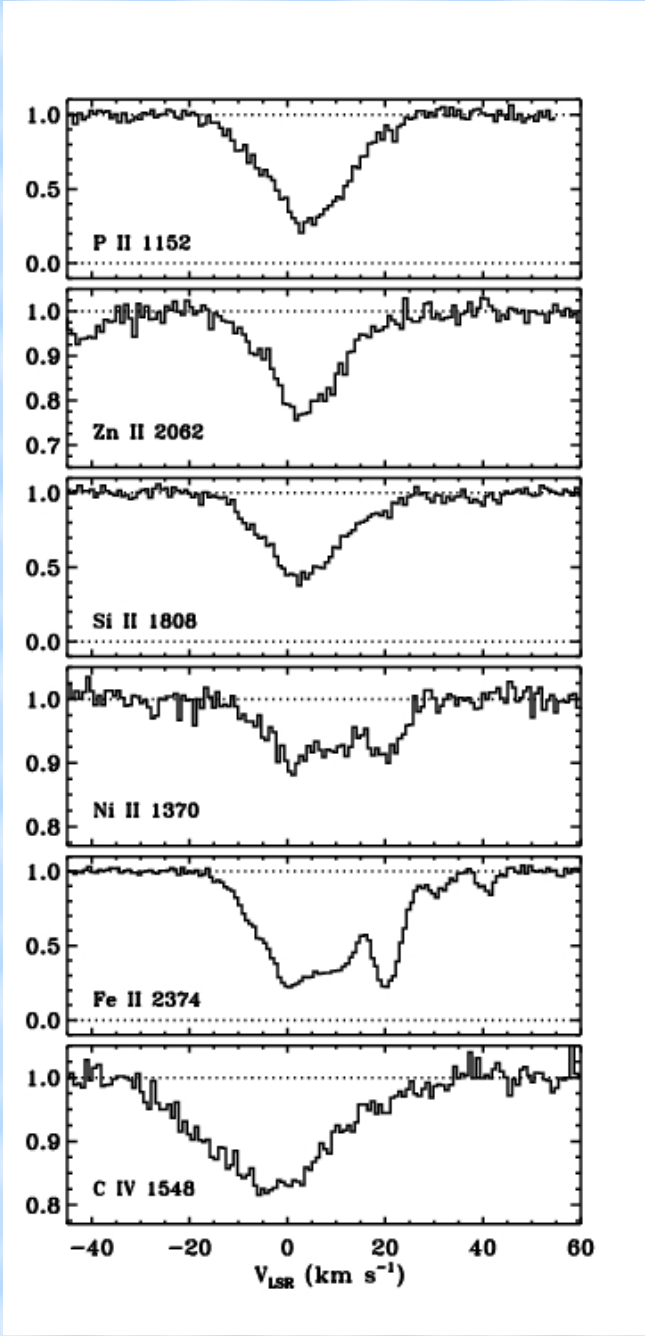

Why measure DLA abundances?

Stars

- Known objects
- Very metal-poor
- Many elements
- Kinematics
- Few galaxies
- Difficult ages
- Atmospheres / gf values

DLA

- Range of ages, time
- Range of morphology
- Simpler measurements
- ISM physics
- Unknown mass, morph
- Dust!
- Selection bias?

Measuring DLA Abundances

- Column densities
  - Echelle spectroscopy
  - Modest S/N (~ 25 per pix)
  - Precisions better than 10%
  - Single-few lines per element
  - No atmospheres!
- Ionization Corrections
  - Large HI optical depth
  - Expect low-ions dominate
  - Theoretical – small corr
  - Empirical – sometimes modest corrections

Dust!!

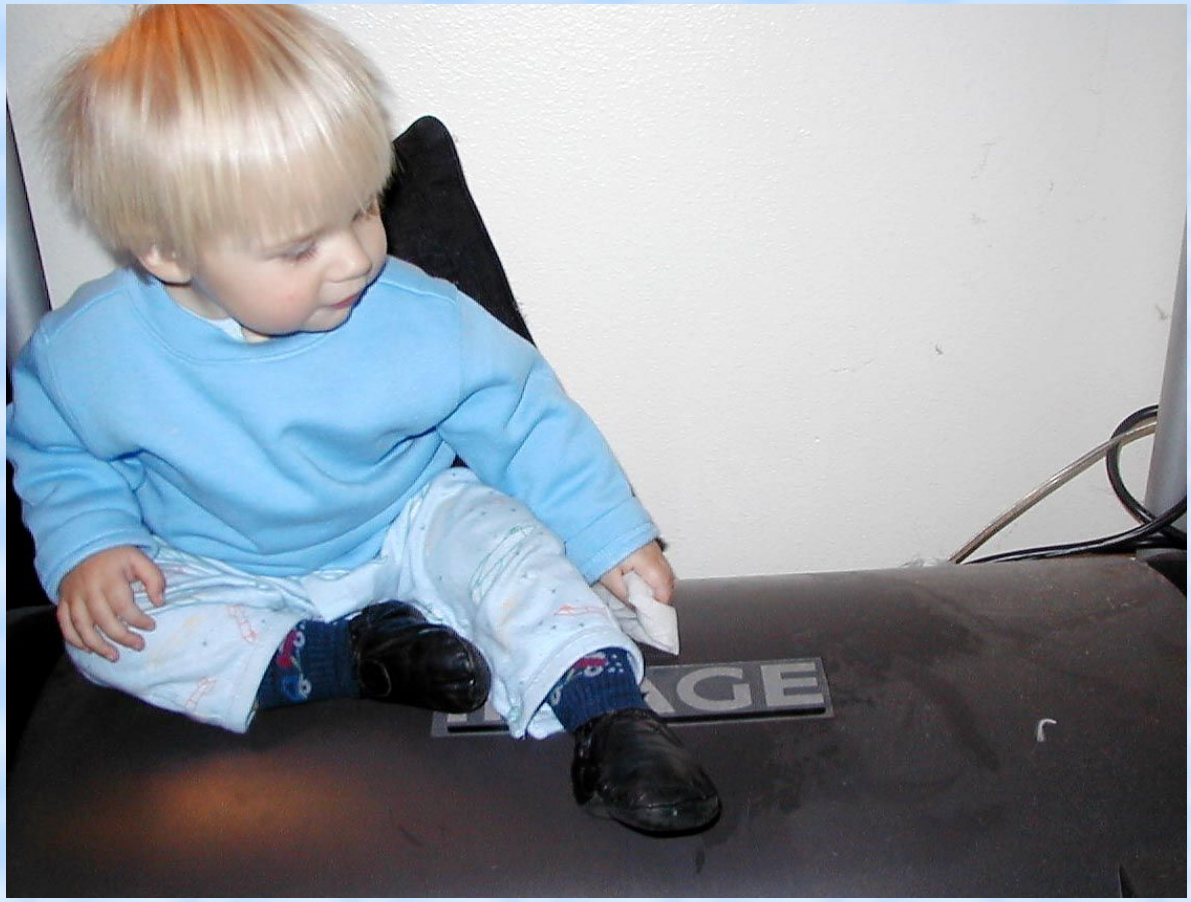

Vladilo et al 2001
Prochaska et al. 2002

Dust

- Obscuration
  - Magnitude limited quasar surveys
  - Bias against metal-rich, large N(HI)
  - S. Ellison -- Little evidence to date
- Depletion
  - Refractory elements: Fe, Cr, Ni, Mn, Ti
  - Unknown pattern
  - Complicates abundance interpretations

[Si/Fe]

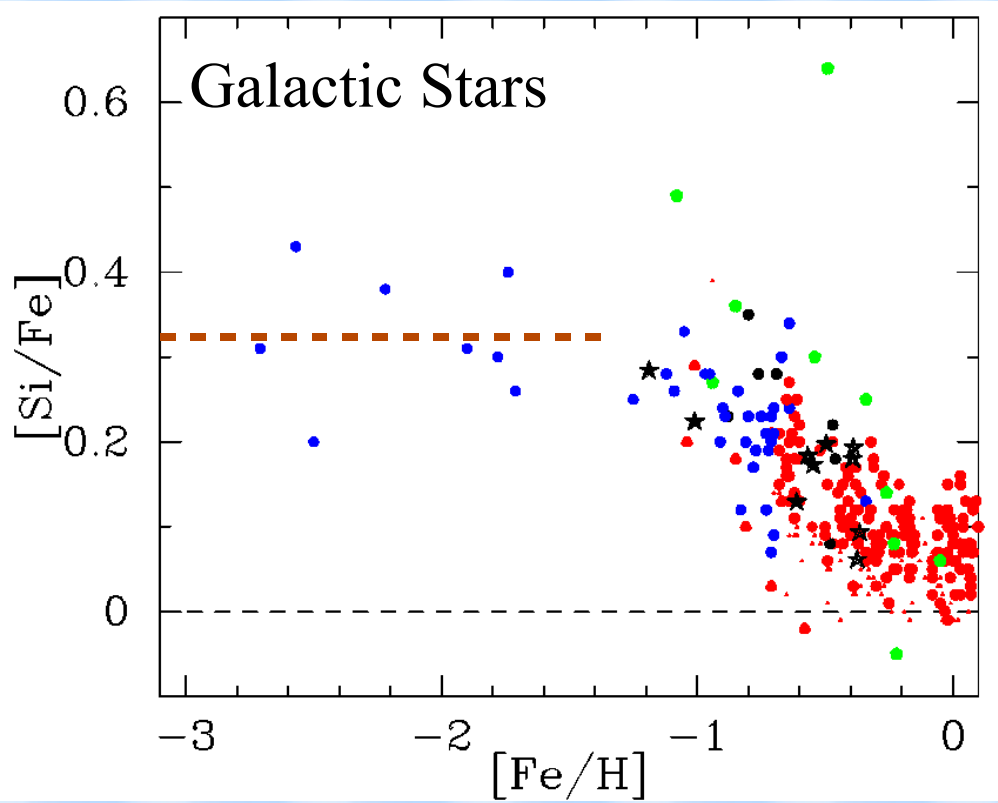

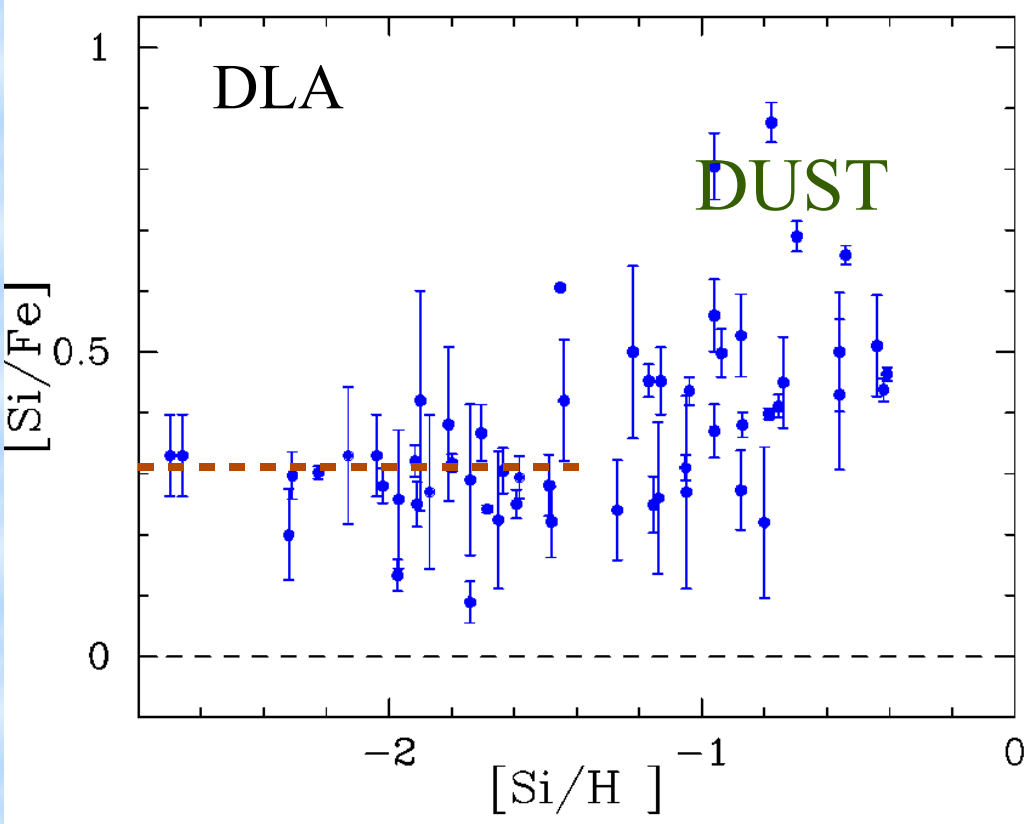

- General α trend
  - Clean break at [Fe/H] ~ -1
  - Different from O?
- Extreme-metal poor?

- Similar enhancements
  - Increase in [Si/Fe] at higher metallicity => Dust
  - How about at low [Si/H]?
  - If dust, where is the TypeII material??

Cosmological HI Mean Metallicity: <Z>

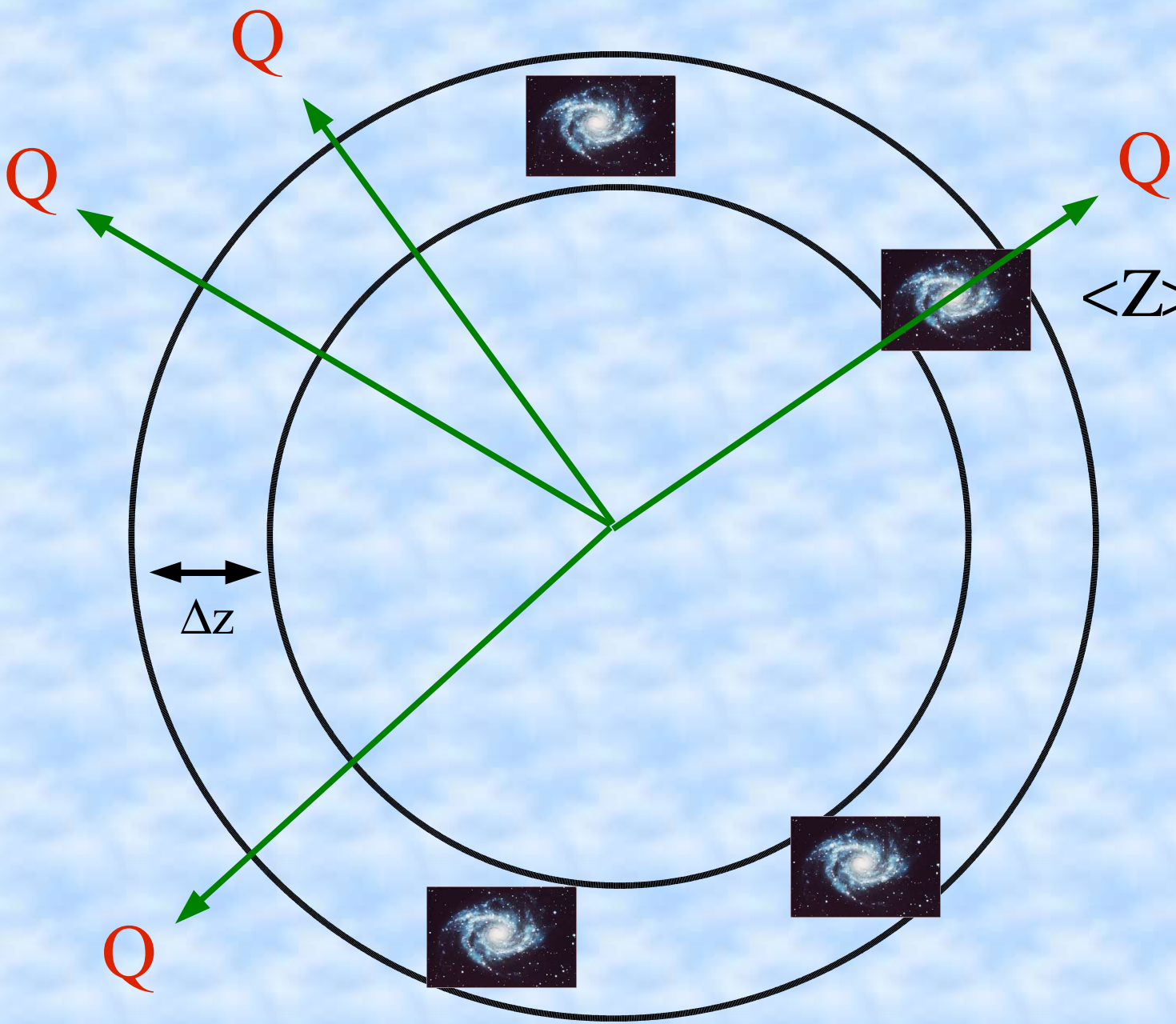

$$\langle Z \rangle = \Sigma mtl / \Sigma gas$$
$$= \Sigma N(M) / \Sigma N(HI)$$

AMR: DLA vs MW

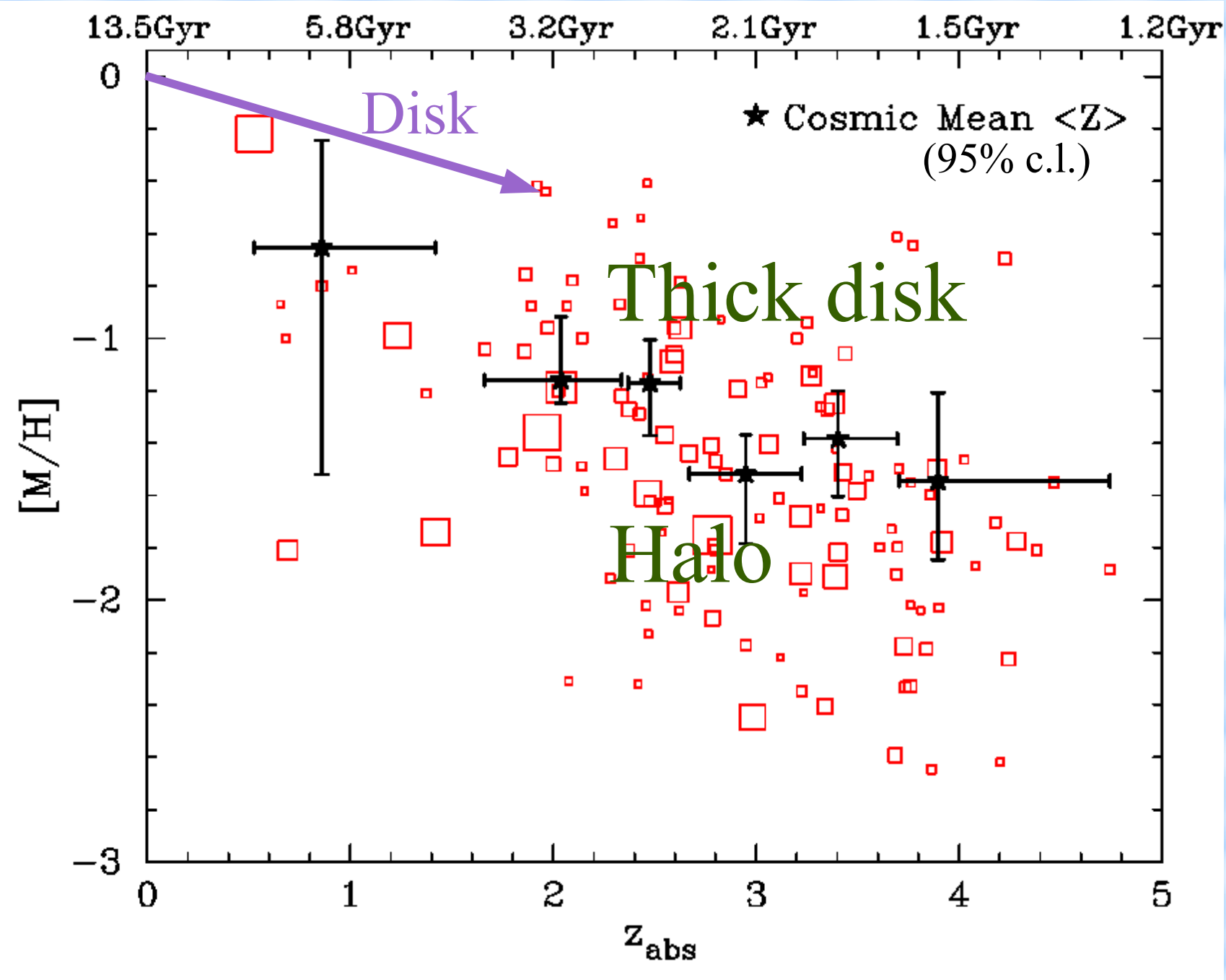
13.5Gyr
5.8Gyr
3.2Gyr
2.1Gyr
1.5Gyr
1.2Gyr
Disk
★ Cosmic Mean <Z>
(95% c.l.)
Thick disk
Halo
[M/H]
0
−1
−2
−3
0
1
2
3
4
5
z_{abs}

Galactic Enrichment

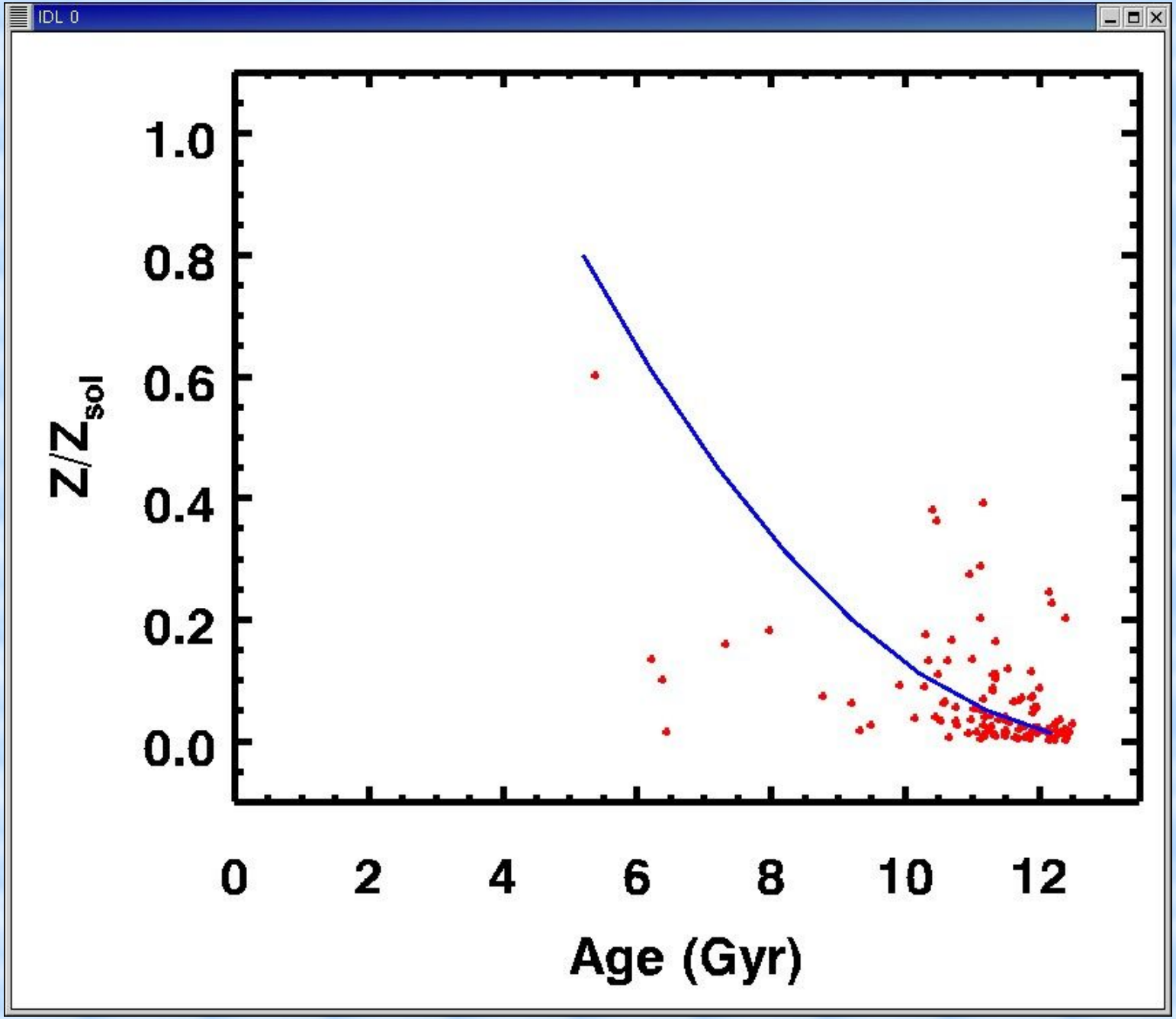

Chemical Enrichment III

- Cosmic mean
  - Modest evolution
  - m = –0.27 ± 0.07 dex
  - About 2x per Gyr
- Scatter
  - Nearly constant with z
  - => Uniformly evolving population

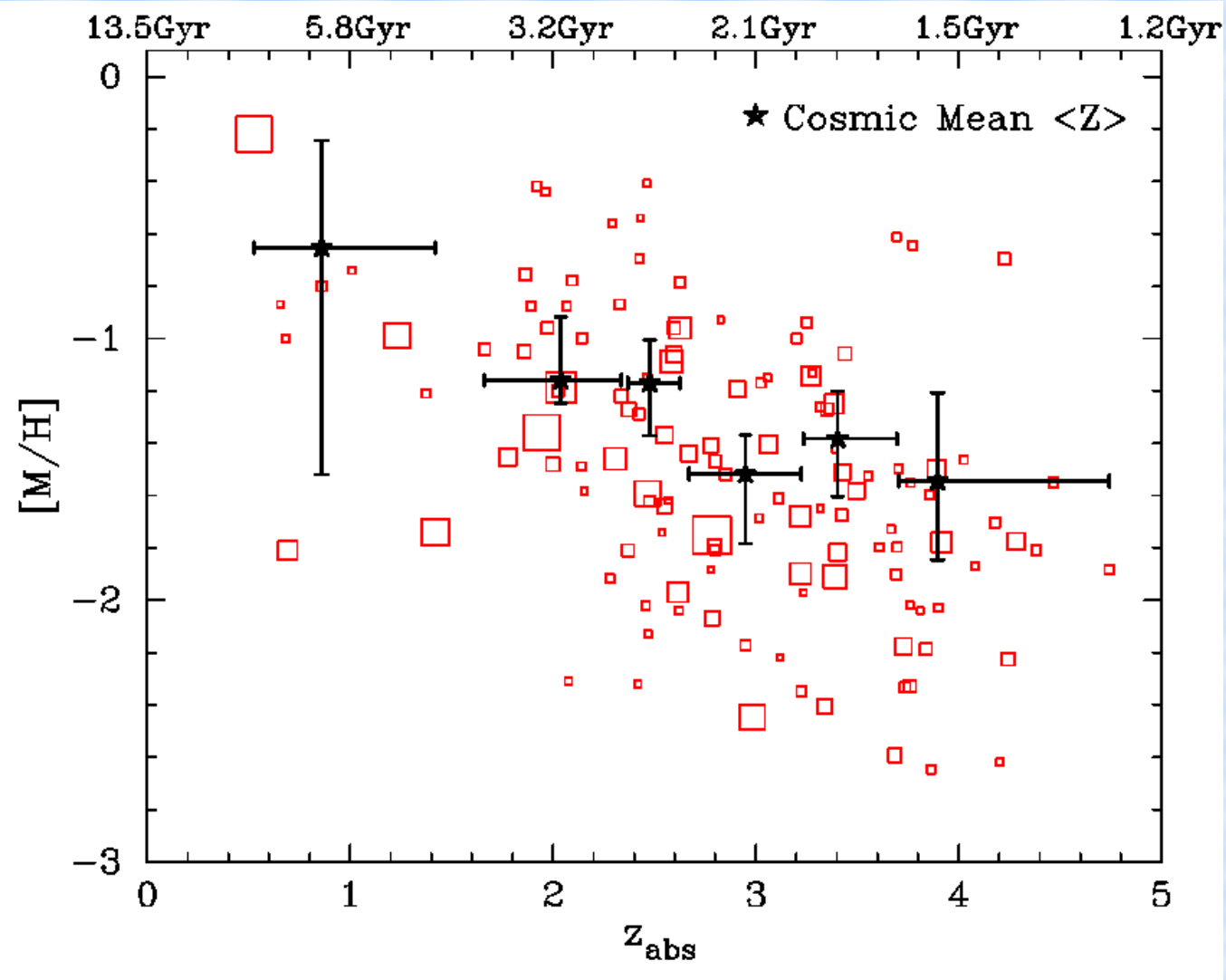

Metallicity floor ([M/H] > –2.6)

- Offset from Lya forest metallicity?
- Links DLA metals with current SF

Relative Abundances

- Metal ratios
  - Precisions of better than 10%
  - Ideally: Consider ratios which are independent of depletion
- Trends (multiple galaxies)
  - [Si/C] => Connection to IGM
  - [N/α] => Nucleosynthesis in AGB
  - [Ti/Fe] => Enhancements akin to MP stars
- Abundance pattern (single galaxy)
  - 'Metal-strong' DLA provide measurements of ~25 elements
  - Nucleosynthesis, SFH, age, etc.

N/α in z~3 Galaxies

- DLA Observations
  - Majority of N/α lie on the standard plateau
  - Sub-sample at low N/α
  - Bimodal?!
- Implications
  - Low N/α => Young
    - Requries fine tuning
    - Not bimodal
  - Top-heavy IMF
    - Initial Starburst
    - PopIII?
  - New yields for IMS

See also Centurion et al. (2003)

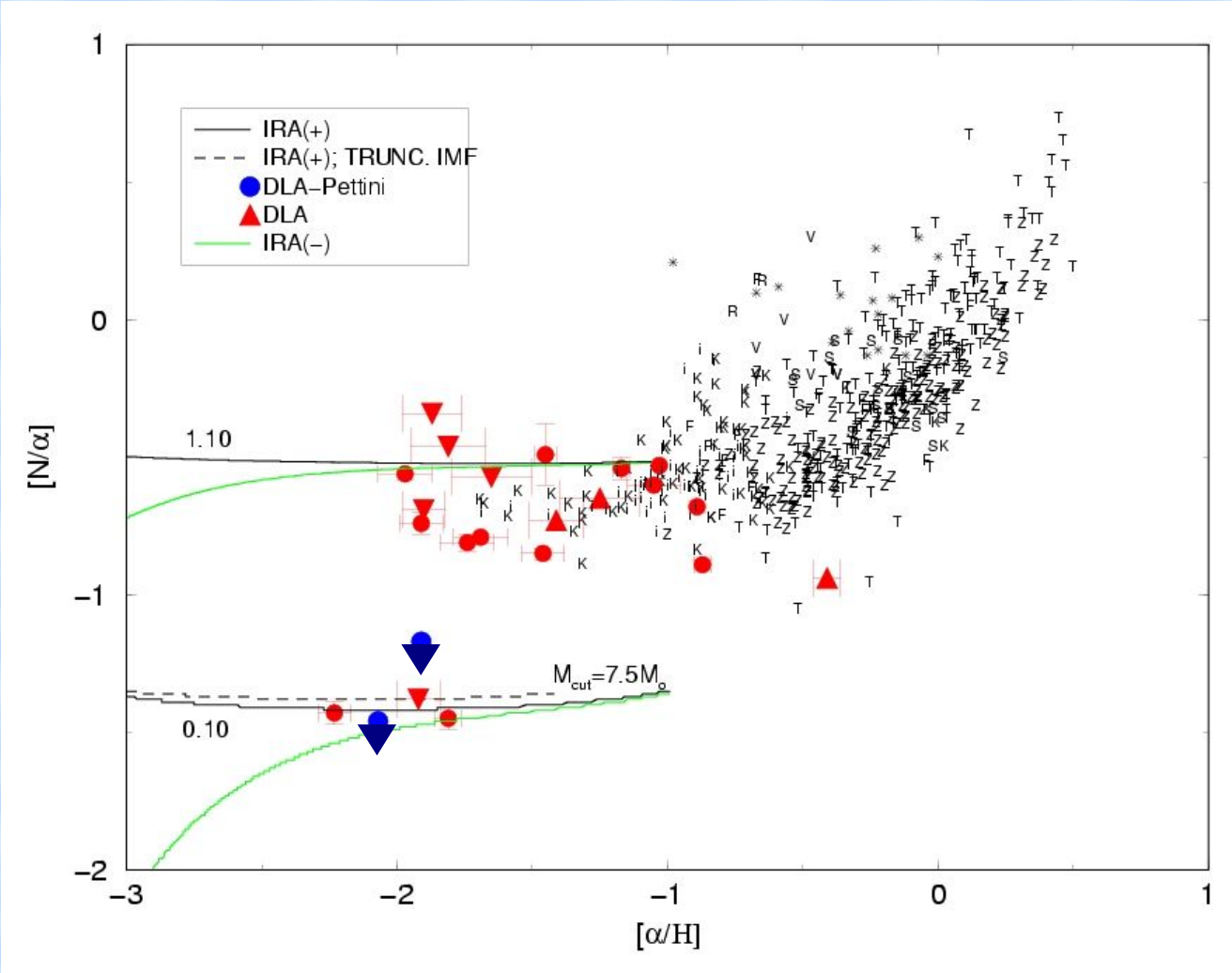

Prochaska et al. 2002

Si/C and the IGM

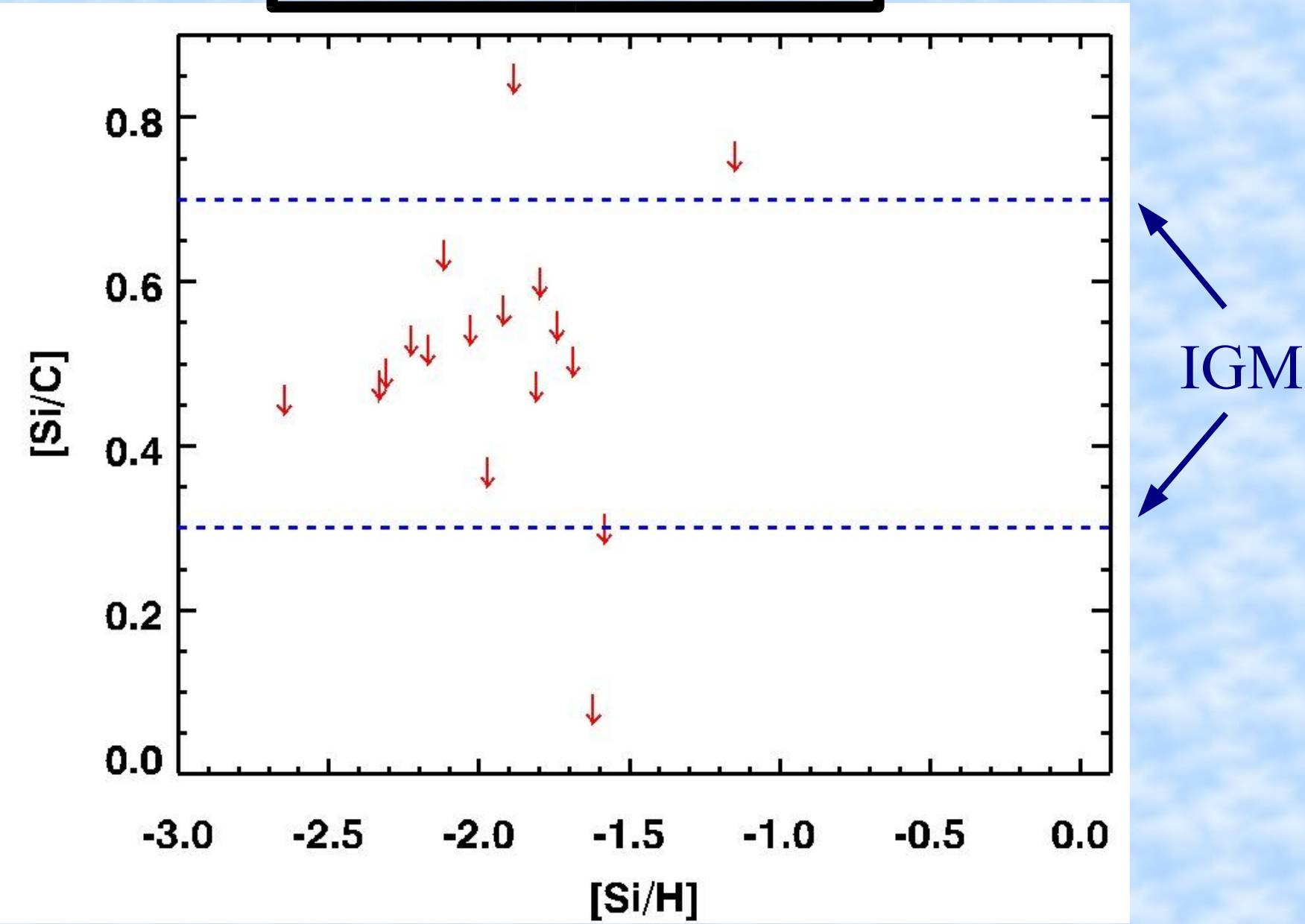

- DLA inconsistent with [Si/C] < +0.7
- Distinct from IGM or is Si/C_{IGM} lower?

Titanium

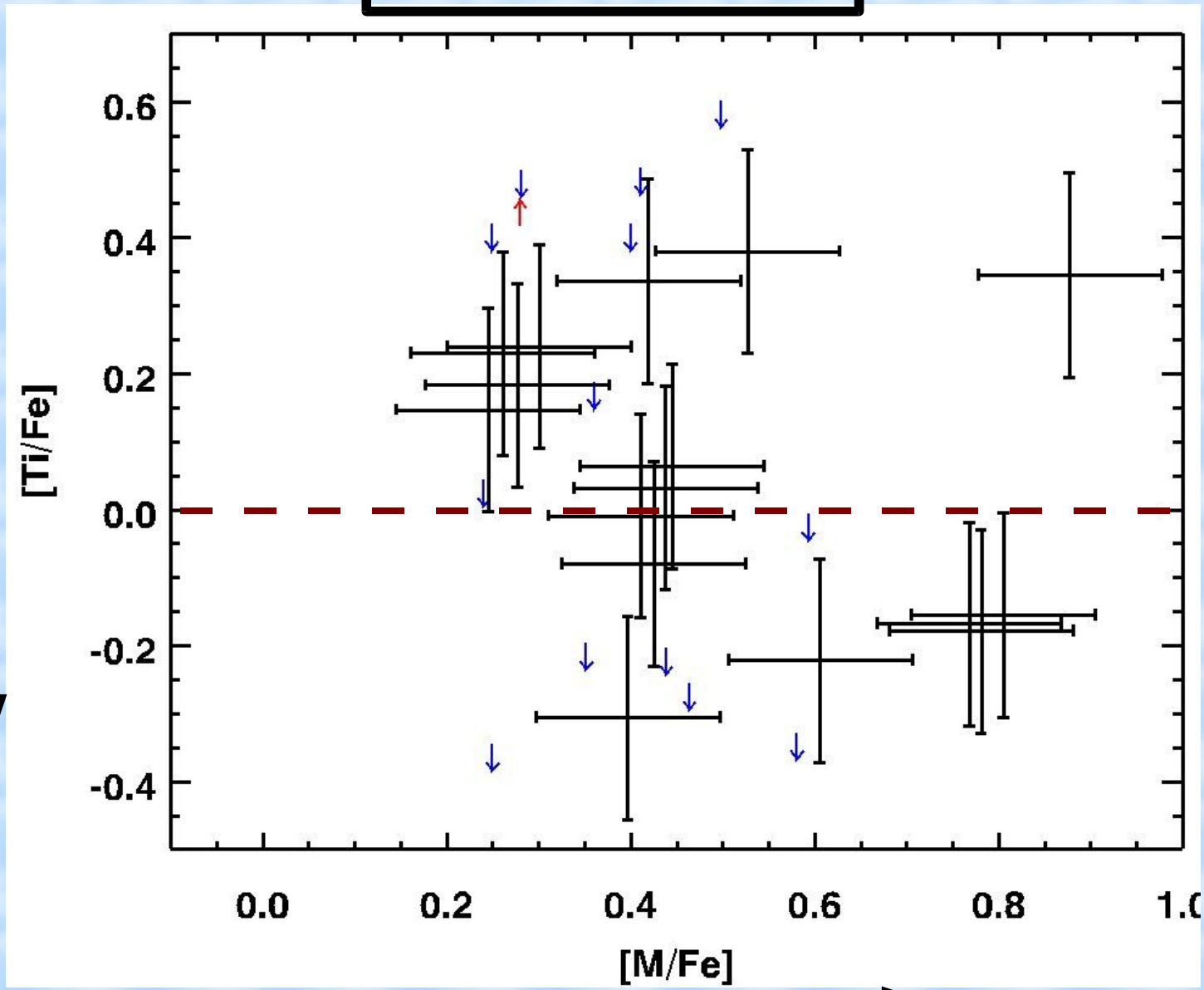

Dust

Dust

- [Ti/Fe] > 0 in at least a subset of DLA
- Ti enhancement is a reality

Metal-Strong DLA

- How about the r, s-process?
- Boron?
- OI 1355?
- CNO?
- Odd Z element?
- Key:
  - Large N(HI)
  - High metallicity
  - Bright QSO

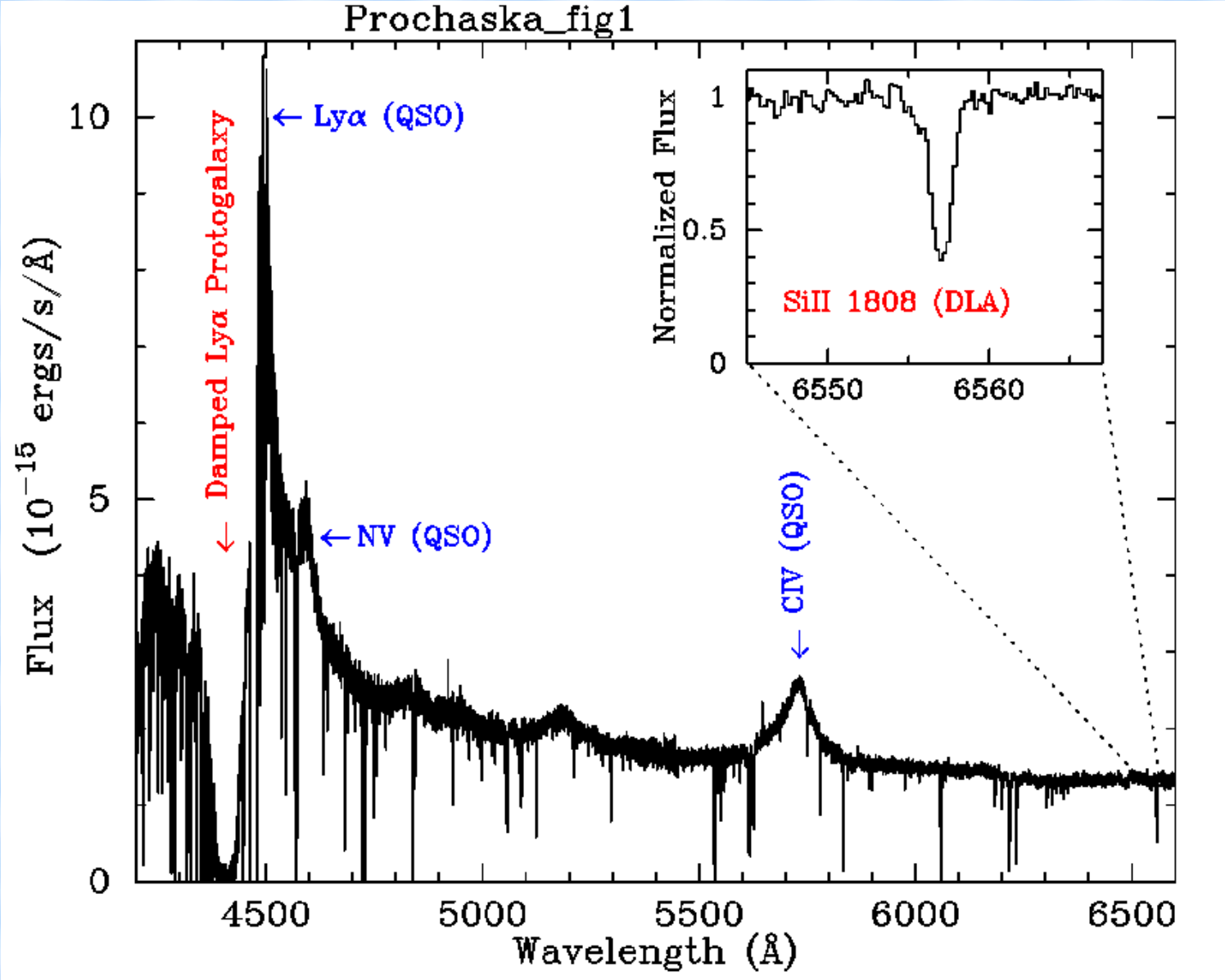

Weak Metal Transitions

- Strong transitions
  - Comparable to the Galaxy
  - Permits measurements of Si, S, Fe, Cr, Zn, Ni
- Weak transitions
  - OI 1355, FeII 1611, MgII 1240
  - Detect B, Ge, Cl, P
  - Limits on Ga, Pb, Sn, Kr
- Age < 2.5 Gyr !!
  - Unique constraints on nucleo
  - High metallicity contrasts with metal-poor stars

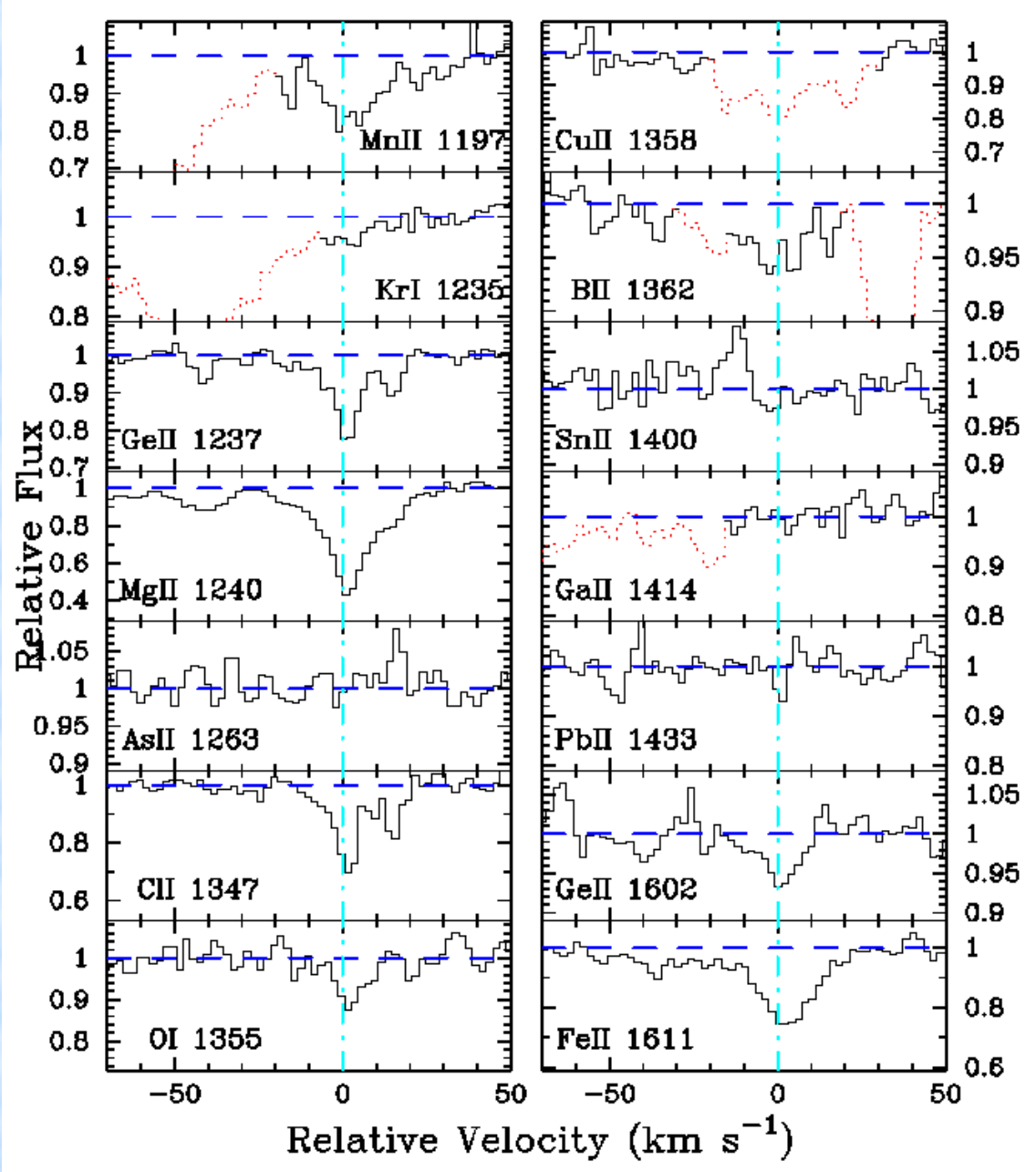

Dust Corrections

- Large [Si,Zn/Fe]
  - Comparable to warm gas in the Milky Way
  - Assume similar depletion pattern
- Conservative method
  - Limits for most of Fe-peak
  - Luckily, many key elements are mild or non-refractory
  - 0.1 dex systematic uncertainty

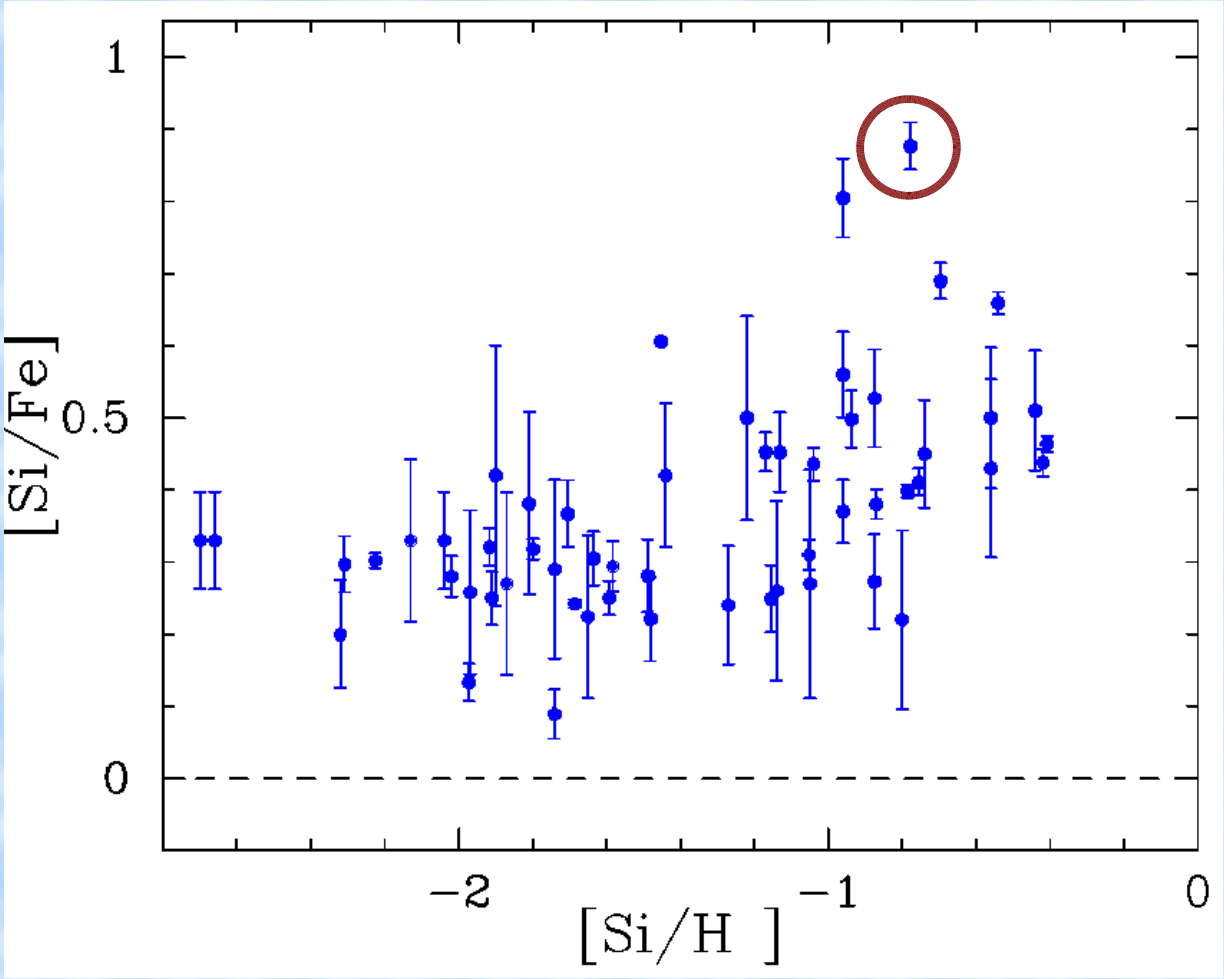

Prochaska, Howk, & Wolfe (2003)

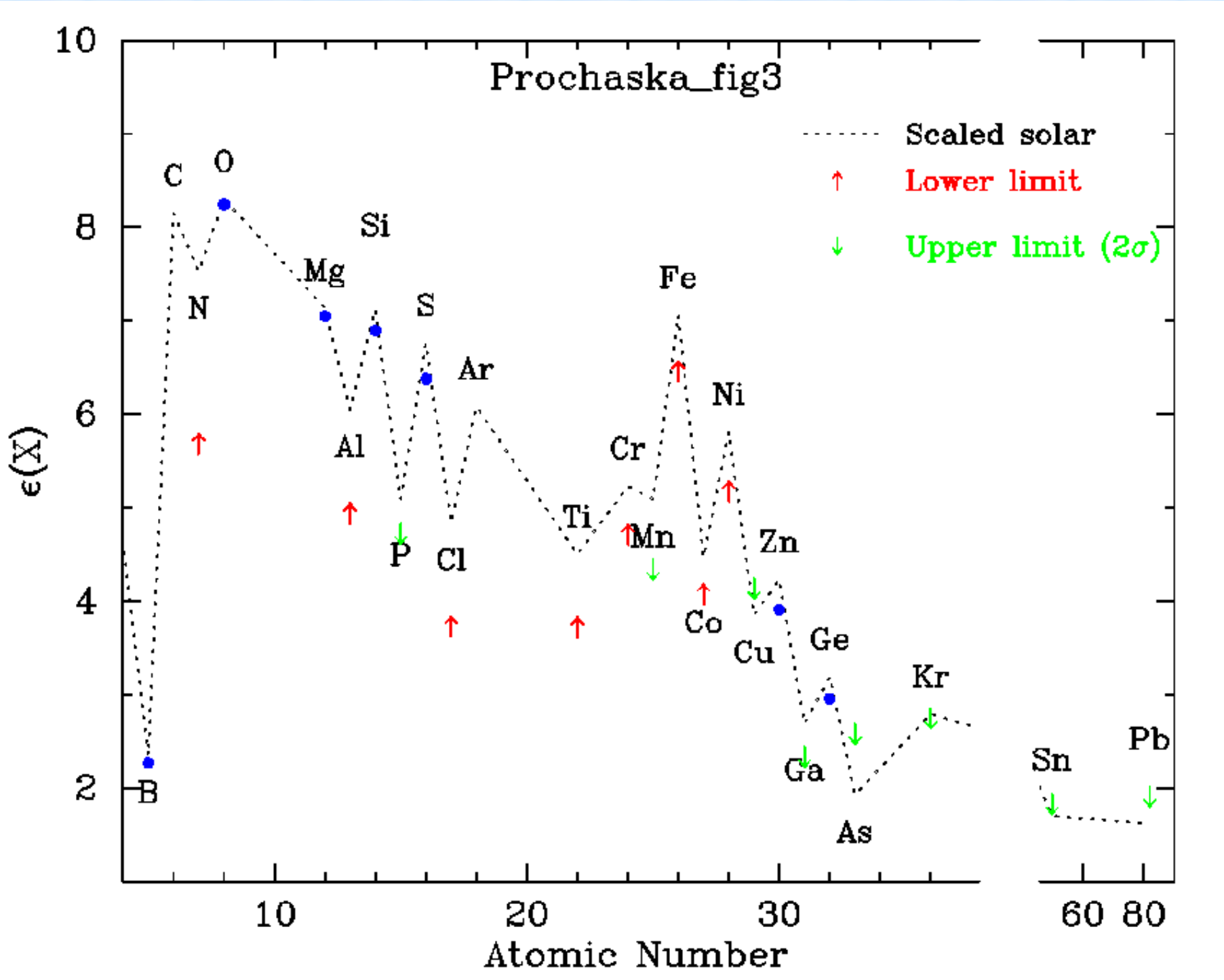

Galactic Abundance Pattern at z~3

- Solar-ish
  - Impressive
  - Comforting?
- Massive stars
  - α trend
  - [O/Zn] ~ +0.2
  - Enhanced odd-even
- AGB nucleo
  - Pb, N
- Also...
  - [B/O] > –0.2
  - r-process (Kr,Sn)

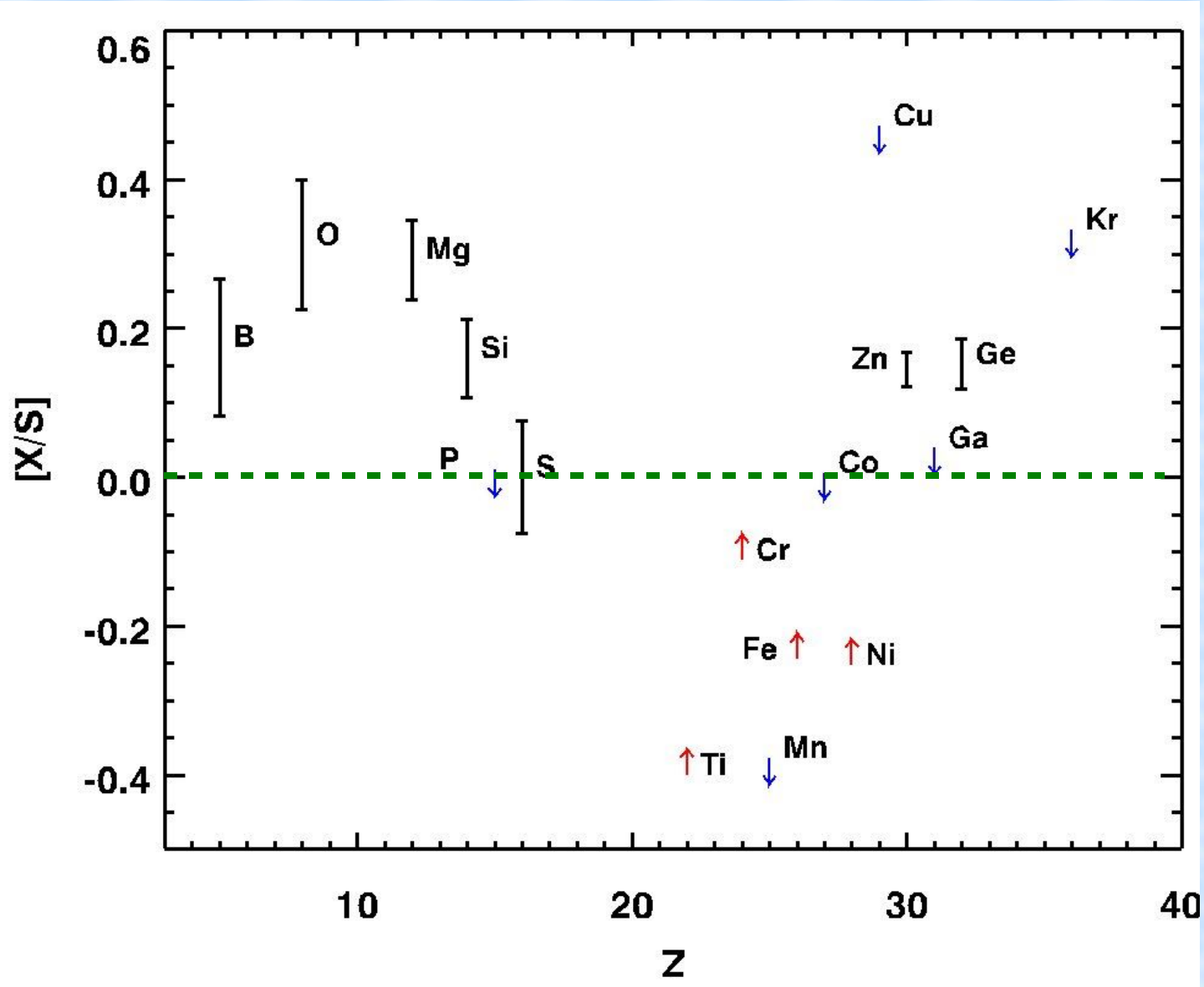

Galactic Abundance Pattern at z~3

- Solar-ish
  - Impressive
  - Comforting?
- Massive stars
  - α trend
  - [O/Zn] ~ +0.2
  - Enhanced odd-even
- AGB nucleo
  - Pb, N
- Also...
  - [B/O] > –0.2
  - r-process (Kr,Sn)

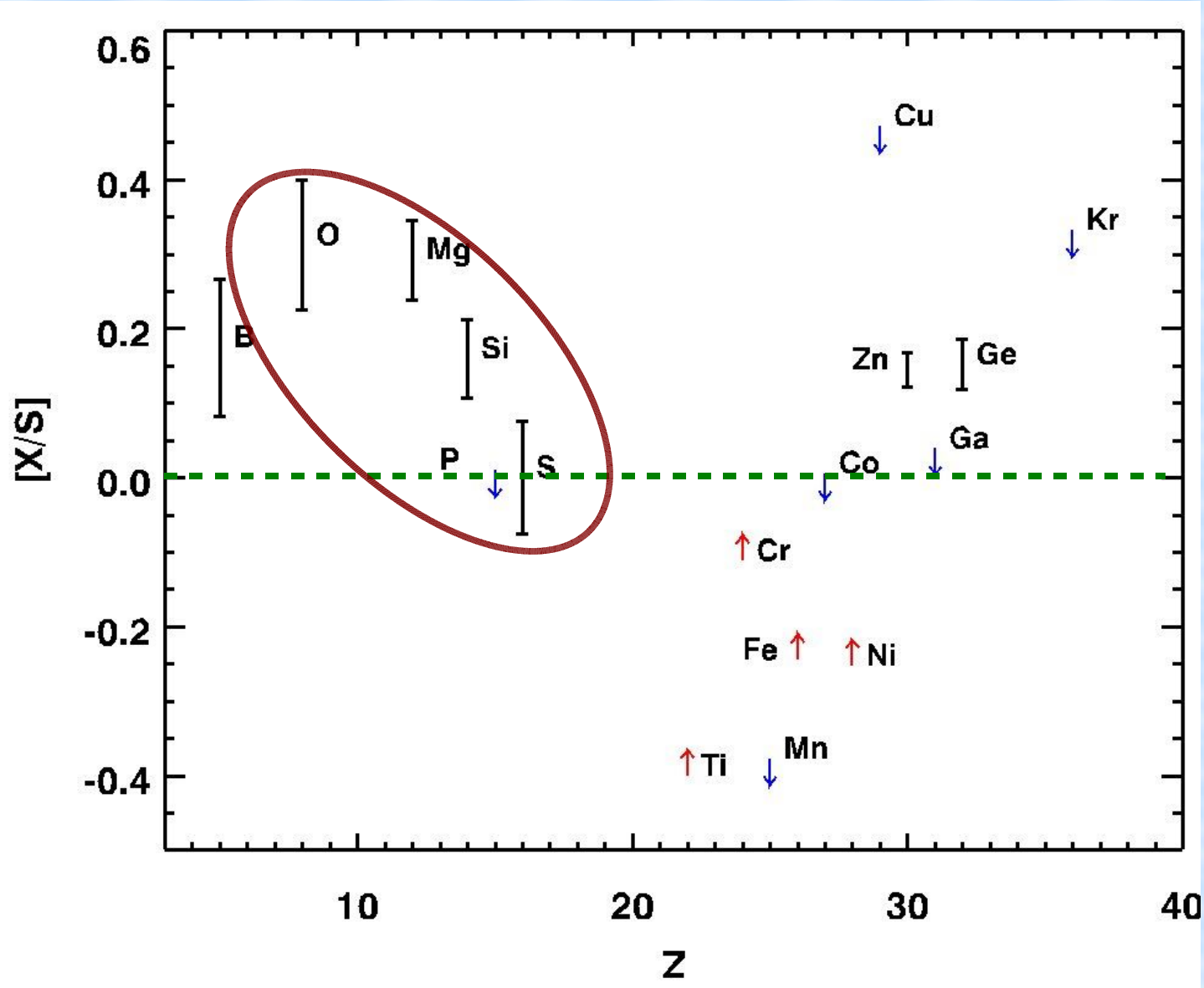

Galactic Abundance Pattern at z~3

- Solar-ish
  - Impressive
  - Comforting?
- Massive stars
  - α trend
  - [O/Zn] ~ +0.2
  - Enhanced odd-even
- AGB nucleo
  - Pb, N
- Also...
  - [B/O] > –0.2
  - r-process (Kr,Sn)

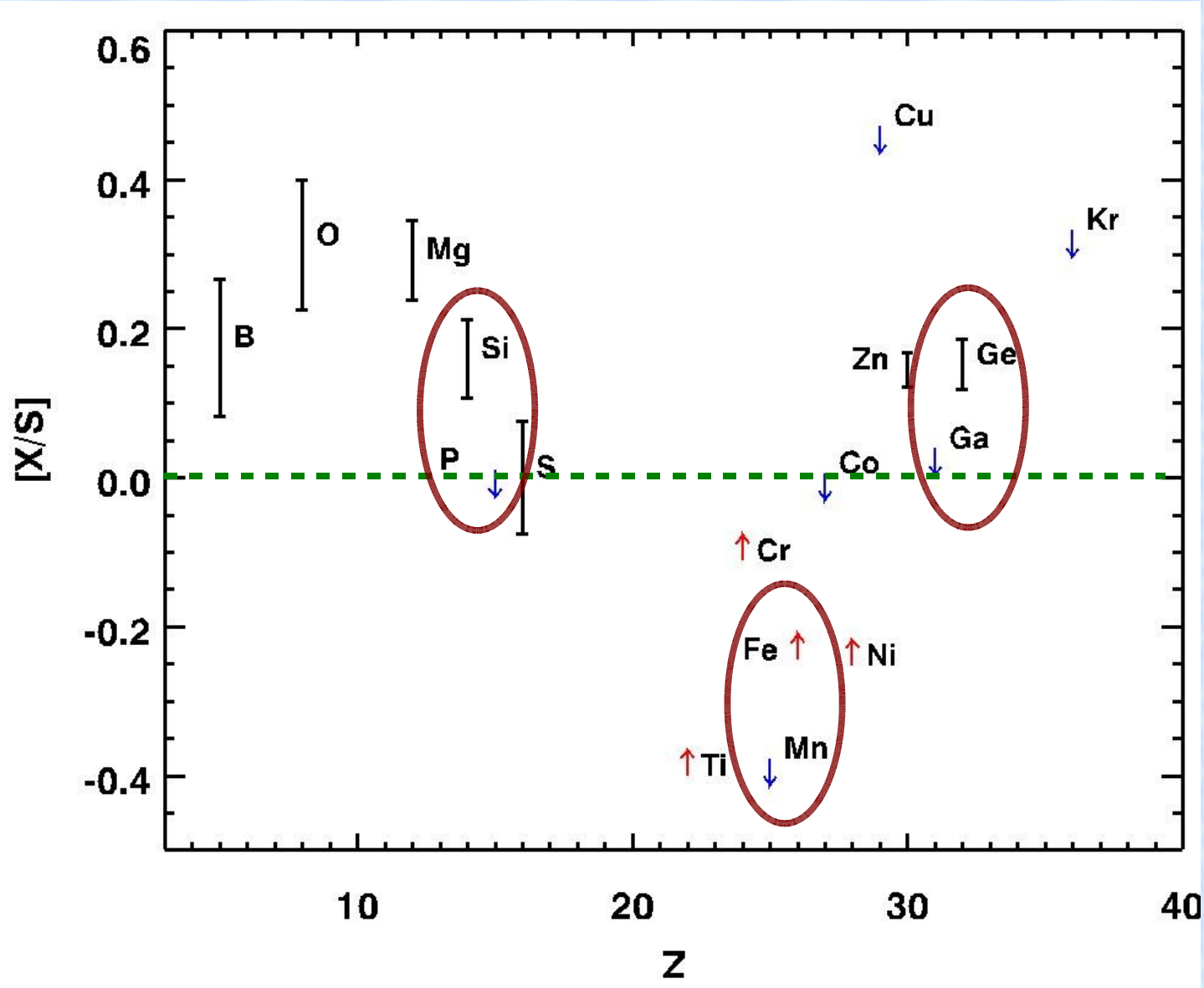

Modeling the Abundance Pattern

- **Model**
  - Kroupa IMF
  - WW95 and Iwamoto
- **Free parameters**
  - Age (< 2.5 Gyr)
  - Metallicity (25%)
- **Investigate**
  - Overall feasibility
  - Highlight areas of inconsistency
  - Dependence on age

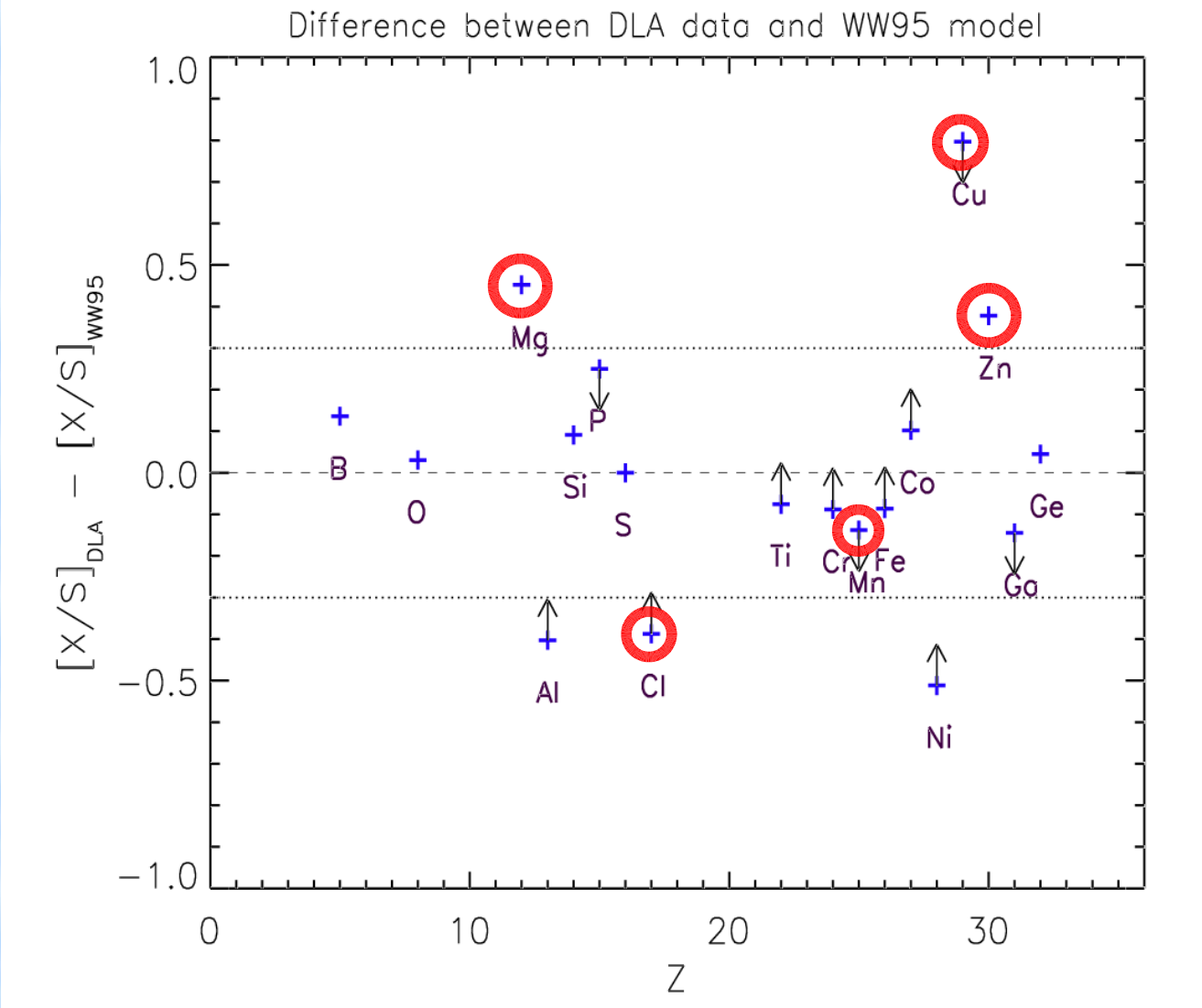

Fenner, Prochaska, & Gibson (2004)

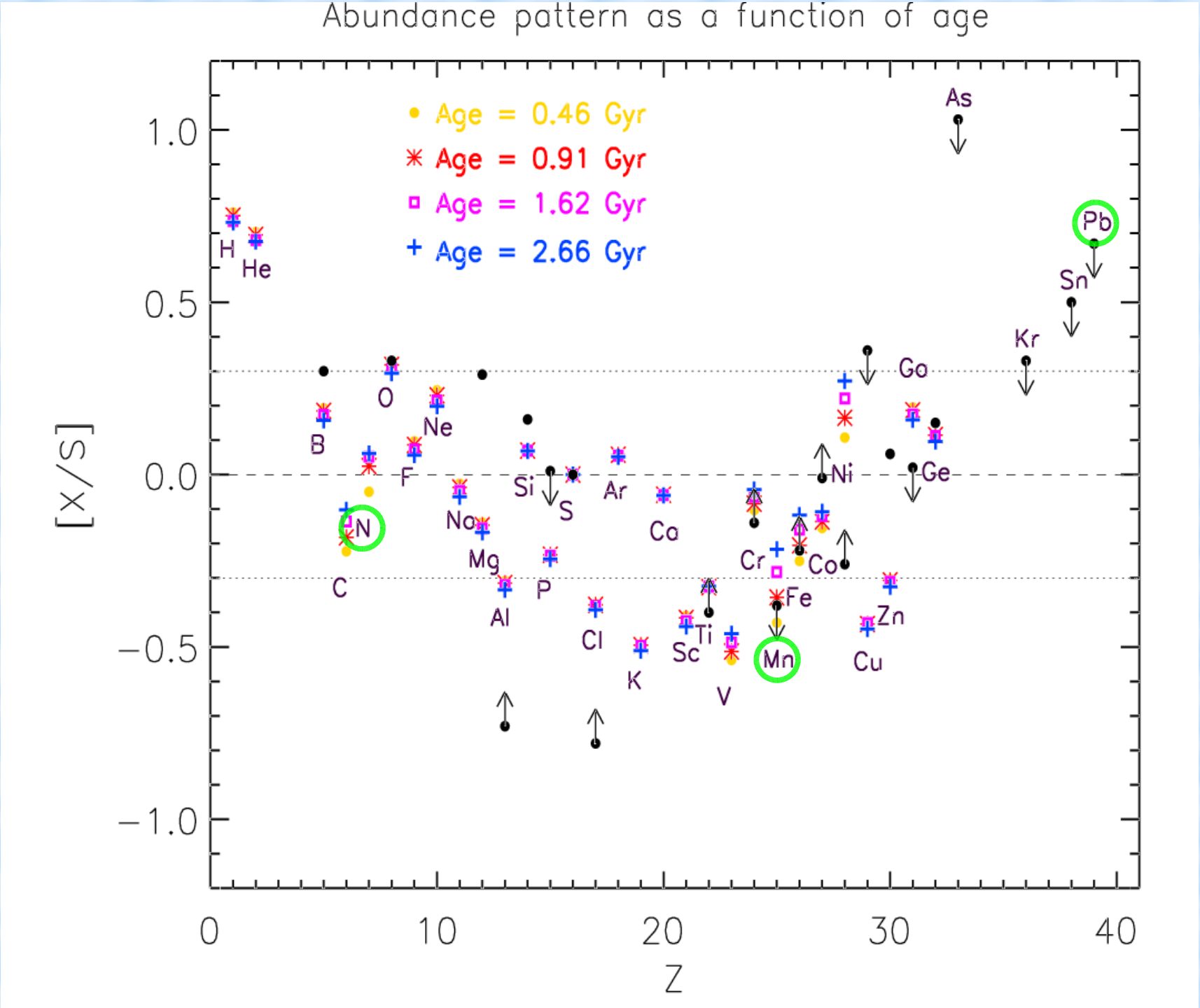

Fenner, Prochaska, & Gibson (2004)

Mining the SDSS

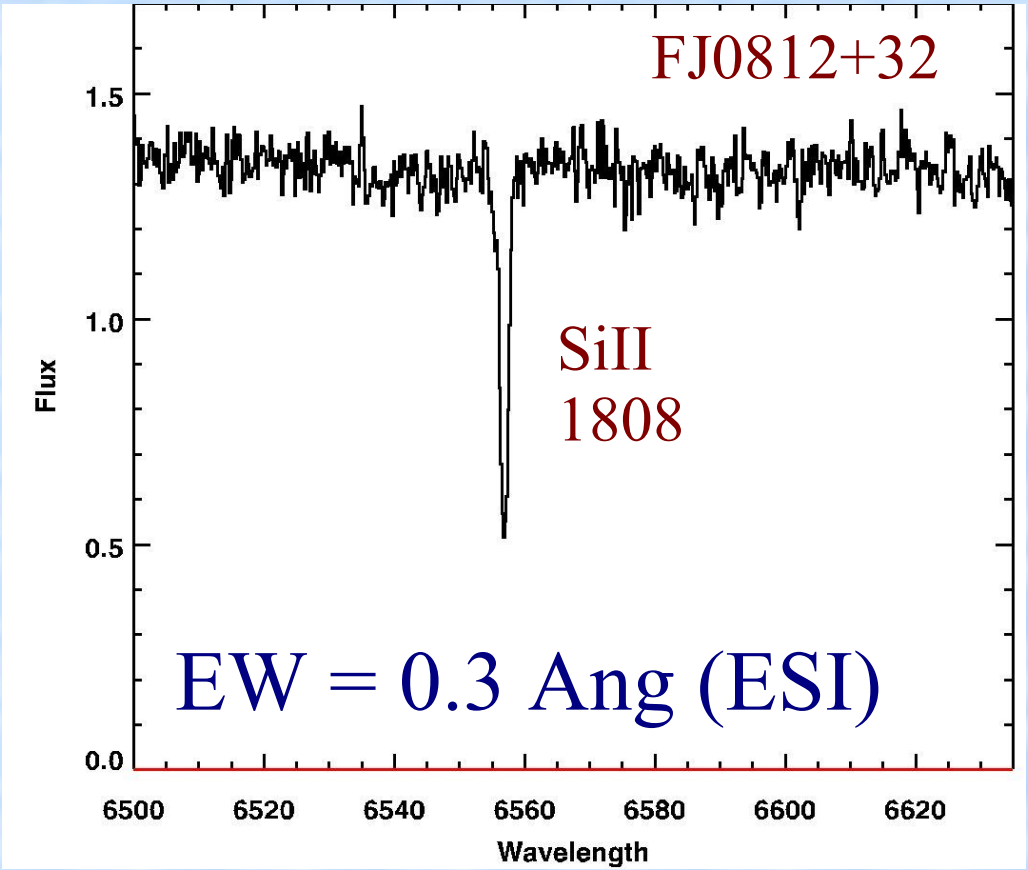

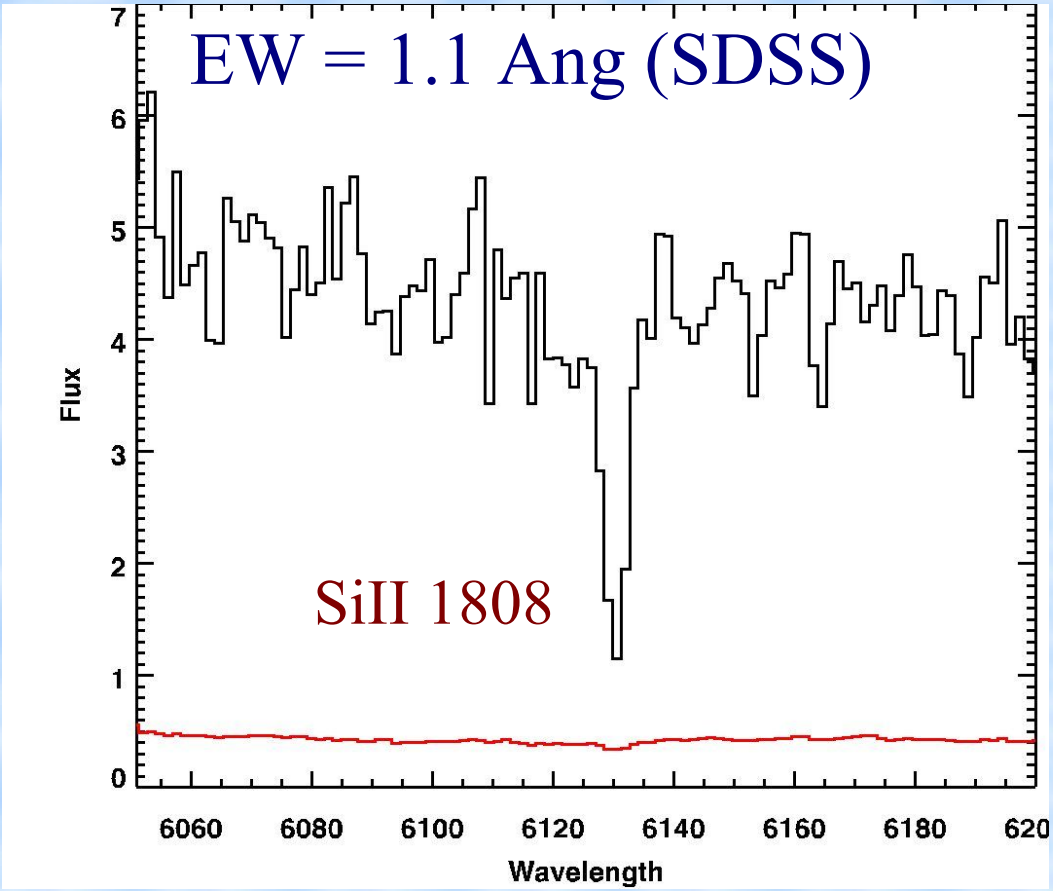

- ~25 elements observed
  - Includes Ge, Cu, B
  - Chance at Sn, Kr, Ga, F
    - Higher S/N
    - Observations at $\lambda < 4000$ A

Pb, Sn
Ag??
Au?!!

Summary

- Chemical Evolution
  - Modest evolution in both means
    - Factor of 2 increase every Gyr
    - Value is significantly lower than that impied by SFH
  - [M/H] > – 3
    - Limits primordial gas
    - Metals linked to current SF
      (e.g. Qian & Wasserburg)

- Abundance trends
  - [N/α] => Top heavy IMF
  - [Si/C] – Inconsistent with IGM?
  - [Ti/Fe] – Enhancement similar to metal-poor stars

- 'Metal-strong' DLA
  - High N(HI), metal-rich DLA
  - B, Cu, Ge, Ga, Kr, Cl, F
  - C, N, O
  - Mg, Ar, Si, S, P, Al, Mn, As
  - Sn, Pb
  - Au, Ag??
  - Age + [M/H] are key

r-Process Nucleosynthesis in the Early Universe and Cosmological Implications

Yong-Zhong Qian

University of Minnesota

(August 2004)

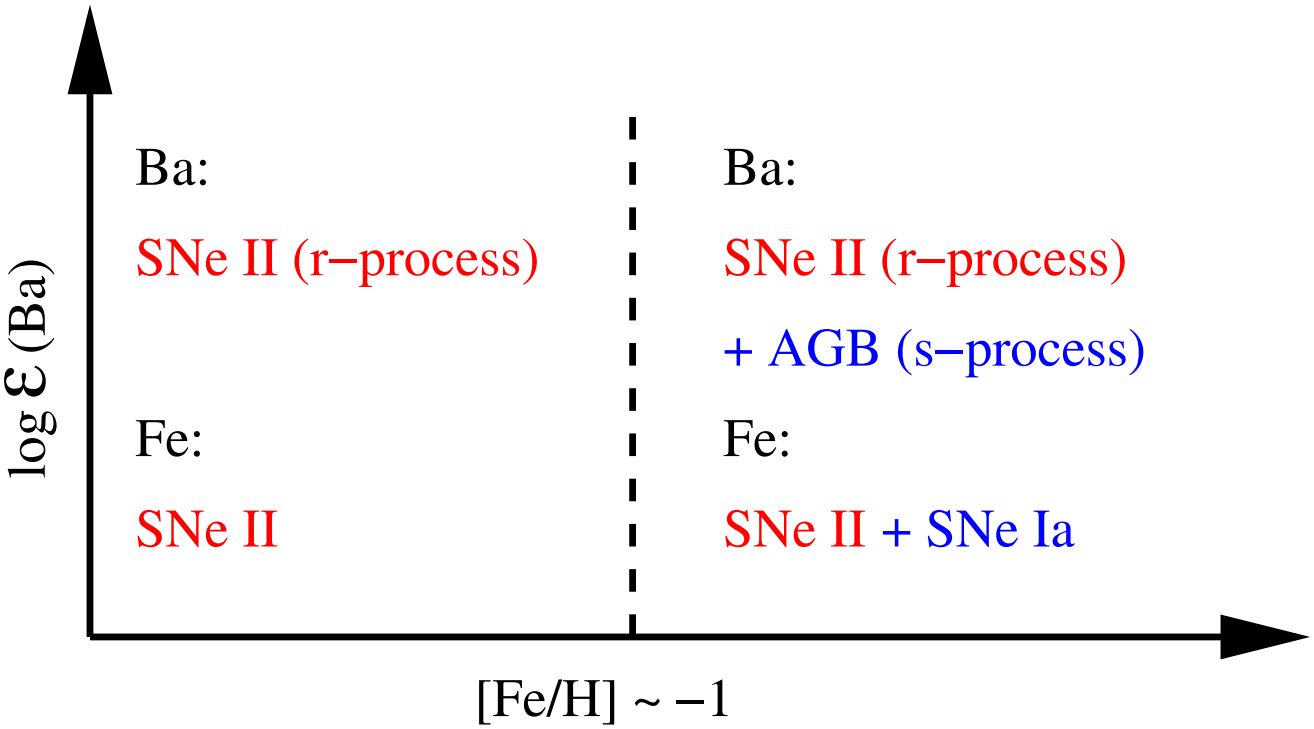
log ε (Ba)
Ba:
SNe II (r−process)
Fe:
SNe II
Ba:
SNe II (r−process)
+ AGB (s−process)
Fe:
SNe II + SNe Ia
[Fe/H] ~ −1

Ba vs. Fe for [Fe/H] < -1

$$\frac{(\mathrm{Ba/H})}{(\mathrm{Fe/H})} = \frac{\Gamma_{\mathrm{Ba}}^{\mathrm{SNII}}}{\Gamma_{\mathrm{Fe}}^{\mathrm{SNII}}} \Rightarrow$$

$$\log(\mathrm{Ba/H}) = \log(\mathrm{Fe/H}) + \log\left(\frac{\Gamma_{\mathrm{Ba}}^{\mathrm{SNII}}}{\Gamma_{\mathrm{Fe}}^{\mathrm{SNII}}}\right)$$

$$\log \epsilon(\mathrm{Ba}) = \log(\mathrm{Ba/H}) + 12$$

$$[\mathrm{Fe/H}] = \log(\mathrm{Fe/H}) - \log(\mathrm{Fe/H})_{\odot}$$

$\Rightarrow$ trajectory for $\log \epsilon(\mathrm{Ba})$ vs. [Fe/H] is
a straight line of unit slope
with intercept of $\log(\Gamma_{\mathrm{Ba}}^{\mathrm{SNII}}/\Gamma_{\mathrm{Fe}}^{\mathrm{SNII}})$

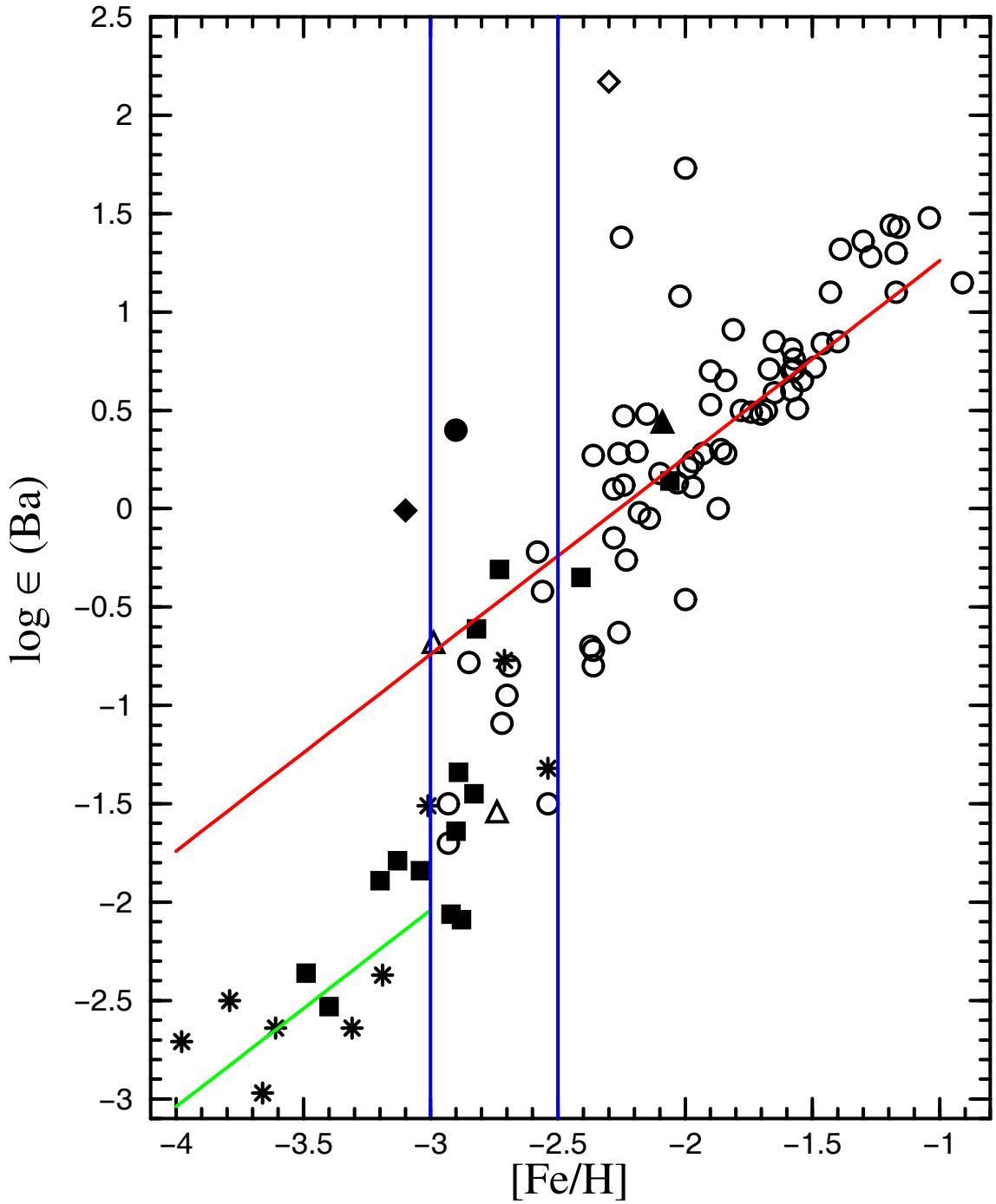
2.5
2
1.5
1
0.5
0
−0.5
−1
−1.5
−2
−2.5
−3
log ∈ (Ba)
−4
−3.5
−3
−2.5
−2
−1.5
−1
[Fe/H]

$\log \epsilon(\mathrm{Ba})$ vs. [Fe/H] for [Fe/H] < -1

upward shift of intercept at [Fe/H] ~ -3

$\Rightarrow \log(\Gamma_{\mathrm{Ba}}/\Gamma_{\mathrm{Fe}})$ increases by ~ 1.3 dex
from [Fe/H] < -3 to [Fe/H] > -3

Scenario A: separation of Ba and Fe production by SNe II and change of IMF at [Fe/H] ~ -3

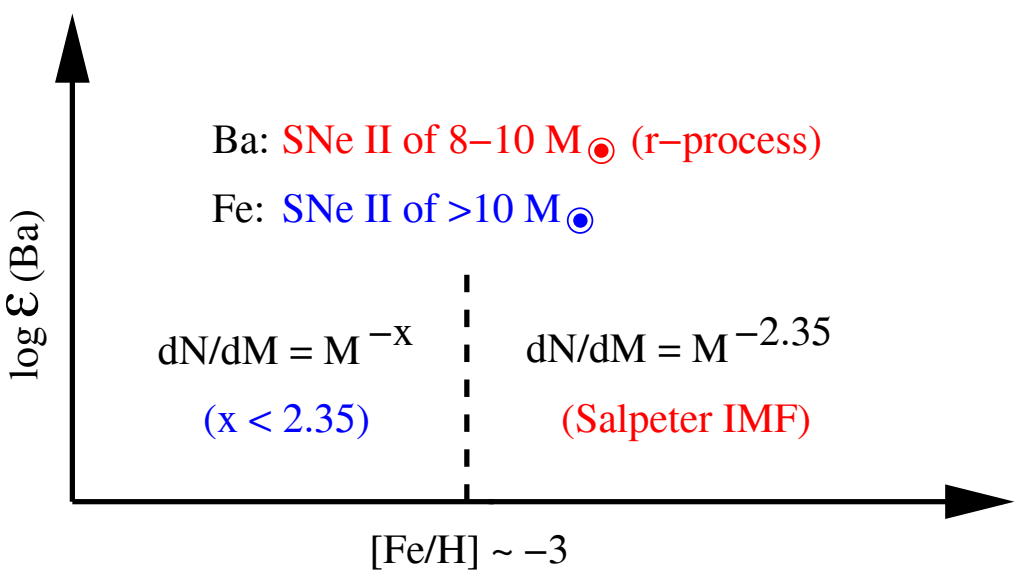

Core-Collapse SNe (mostly SNe II)

- $M > 10\,M_\odot$

  Fe cores with extended shells

  $\Rightarrow$ neutron star/black hole and Fe!

  explosive burning: $^{28}\mathrm{Si} \Rightarrow {}^{56}\mathrm{Ni}$

  light curves: $^{56}\mathrm{Ni} \rightarrow {}^{56}\mathrm{Co} \rightarrow {}^{56}\mathrm{Fe}$

- $M \sim 8$–$10\,M_\odot$

  O-Ne-Mg cores with thin shells

  $\Rightarrow$ neutron star but no Fe!

- accretion-induced collapse of white dwarfs

  $\Rightarrow$ neutron star but no Fe!

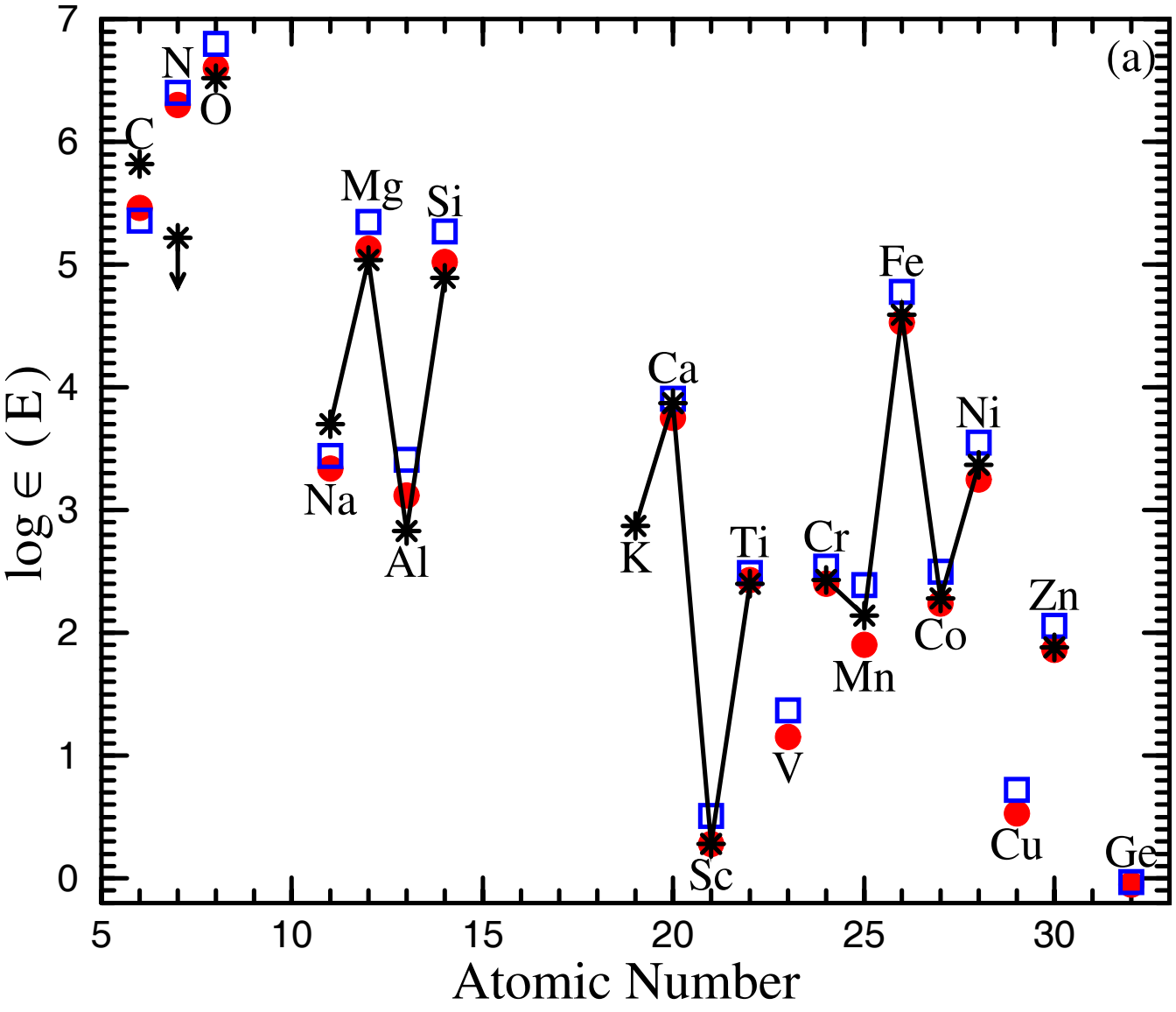
(a)
C
N
O
Na
Mg
Al
Si
K
Ca
Sc
Ti
V
Cr
Mn
Fe
Co
Ni
Cu
Zn
Ge
log ∈ (E)
Atomic Number
0
1
2
3
4
5
6
7
5
10
15
20
25
30

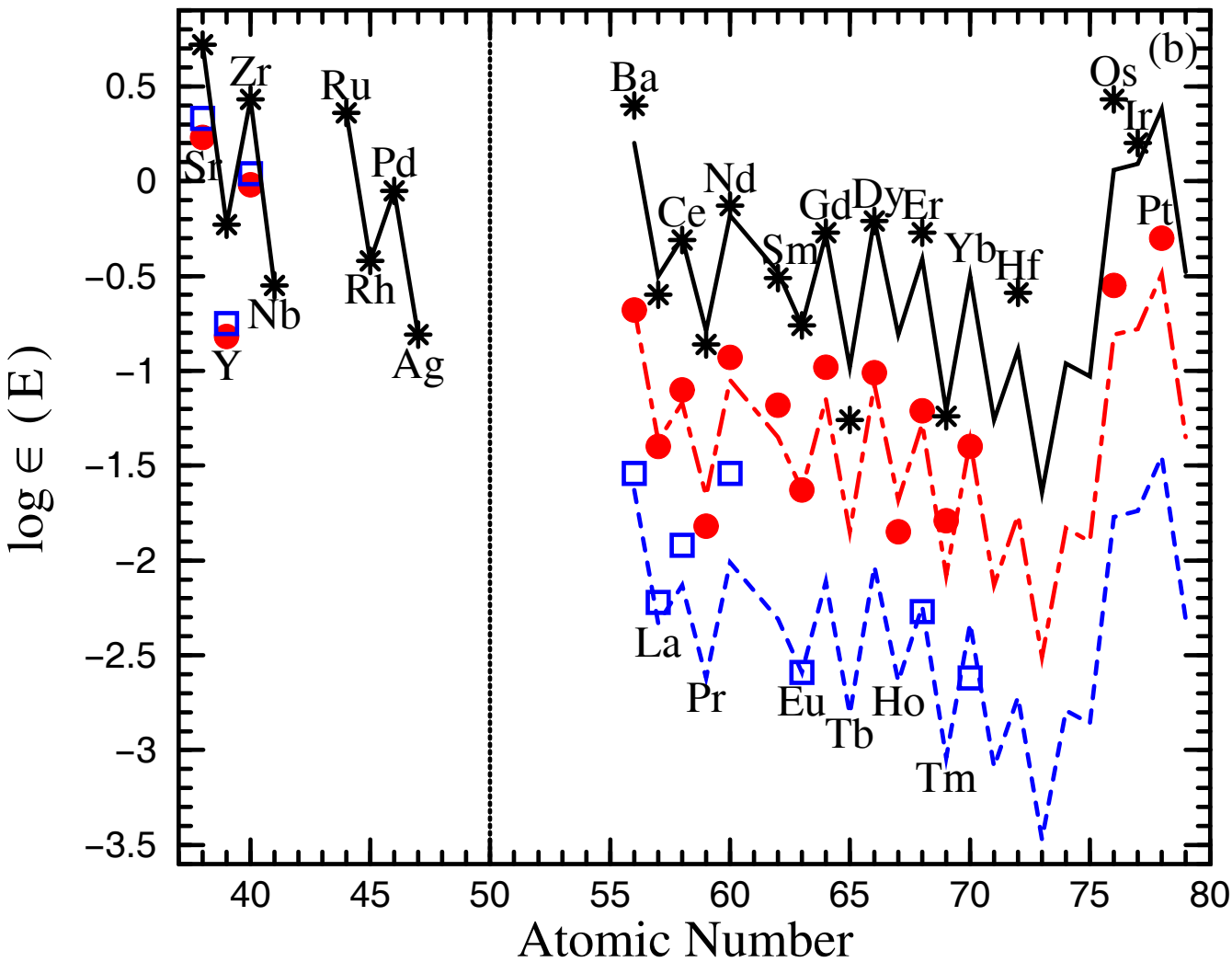
(b)
log ∈ (E)
Atomic Number
Sr
Y
Zr
Nb
Ru
Rh
Pd
Ag
Ba
La
Ce
Pr
Nd
Sm
Eu
Gd
Tb
Dy
Ho
Er
Tm
Yb
Hf
Os
Ir
Pt
0.5
0
−0.5
−1
−1.5
−2
−2.5
−3
−3.5
40
45
50
55
60
65
70
75
80

An extreme case

insufficient cooling due to lack of metals

$\Rightarrow$ very massive ($\gtrsim 100\, M_\odot$) stars (VMSs)
and some normal stars

(Abel et al. 2002; Bromm & Larson 2004)

[Fe/H] $\sim -3 \Rightarrow$ termination of VMS formation

(Bromm et al. 2001)

VMSs $\Rightarrow$ Fe, no Ba! (Heger & Woosley 2002)

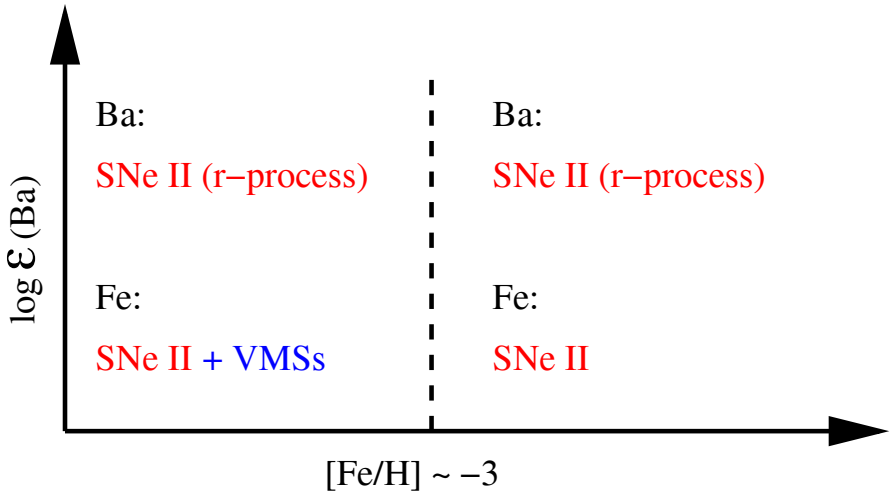

Conclusions

- r-process sources for Ba and heavier elements

SNe II of $\sim$ 8–10 $M_\odot$

Mathews, Bazan, & Cowan 1992
Wheeler, Cowan, & Hillebrandt 1998
Qian & Wasserburg 2002
Wanajo et al. 2003

accretion-induced collapse of white dwarfs

Woosley & Baron 1992
Qian & Wasserburg 2003

- implications for the first stars

The IMF is more favorable to massive stars for [Fe/H] < -3 and changes to the present form at [Fe/H] ~ -3.

Bypassing the triple-α process - recent measurements and future plans

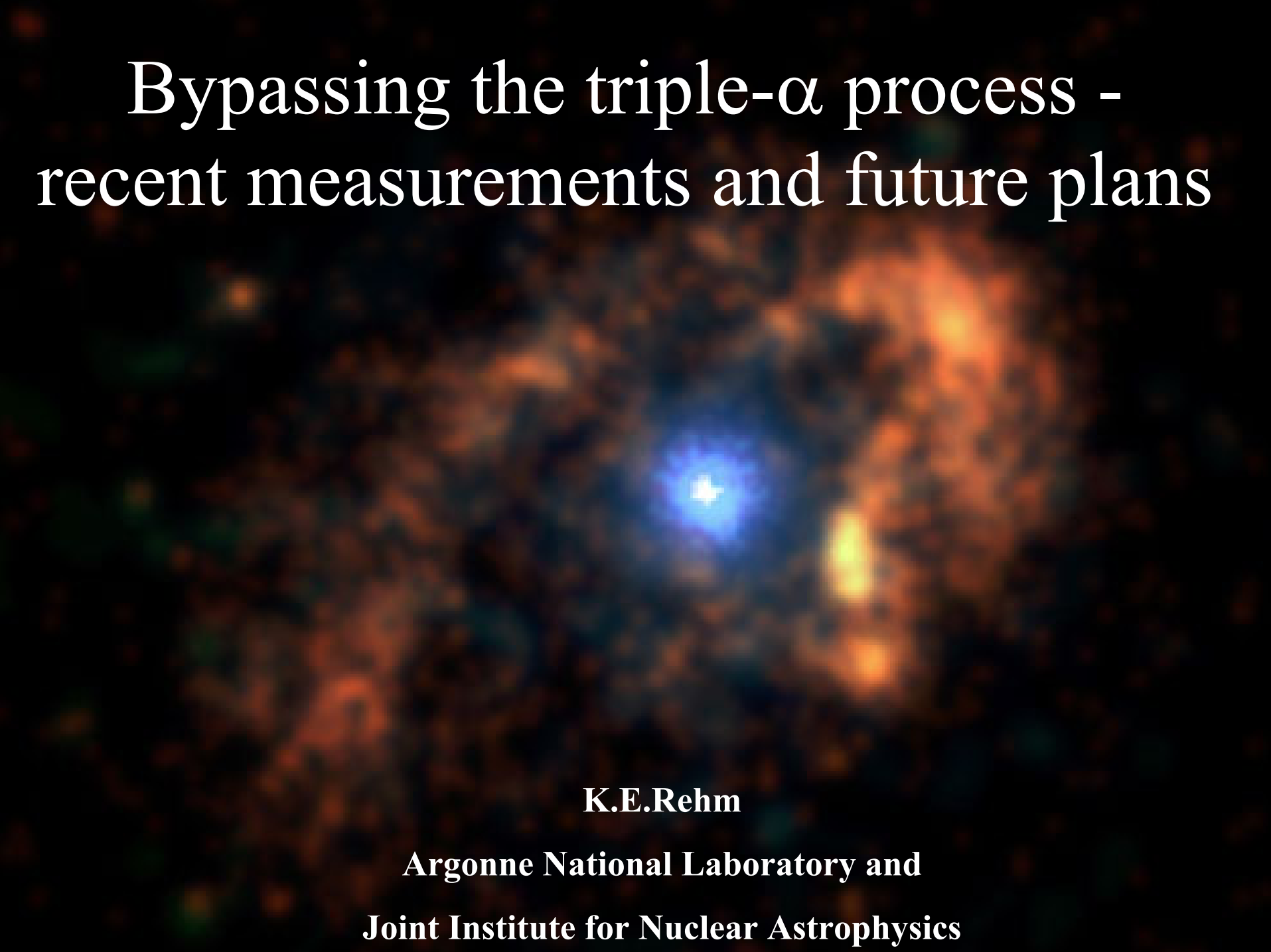

K.E.Rehm

Argonne National Laboratory and

Joint Institute for Nuclear Astrophysics

Bypass of the triple-α process in supermassive stars

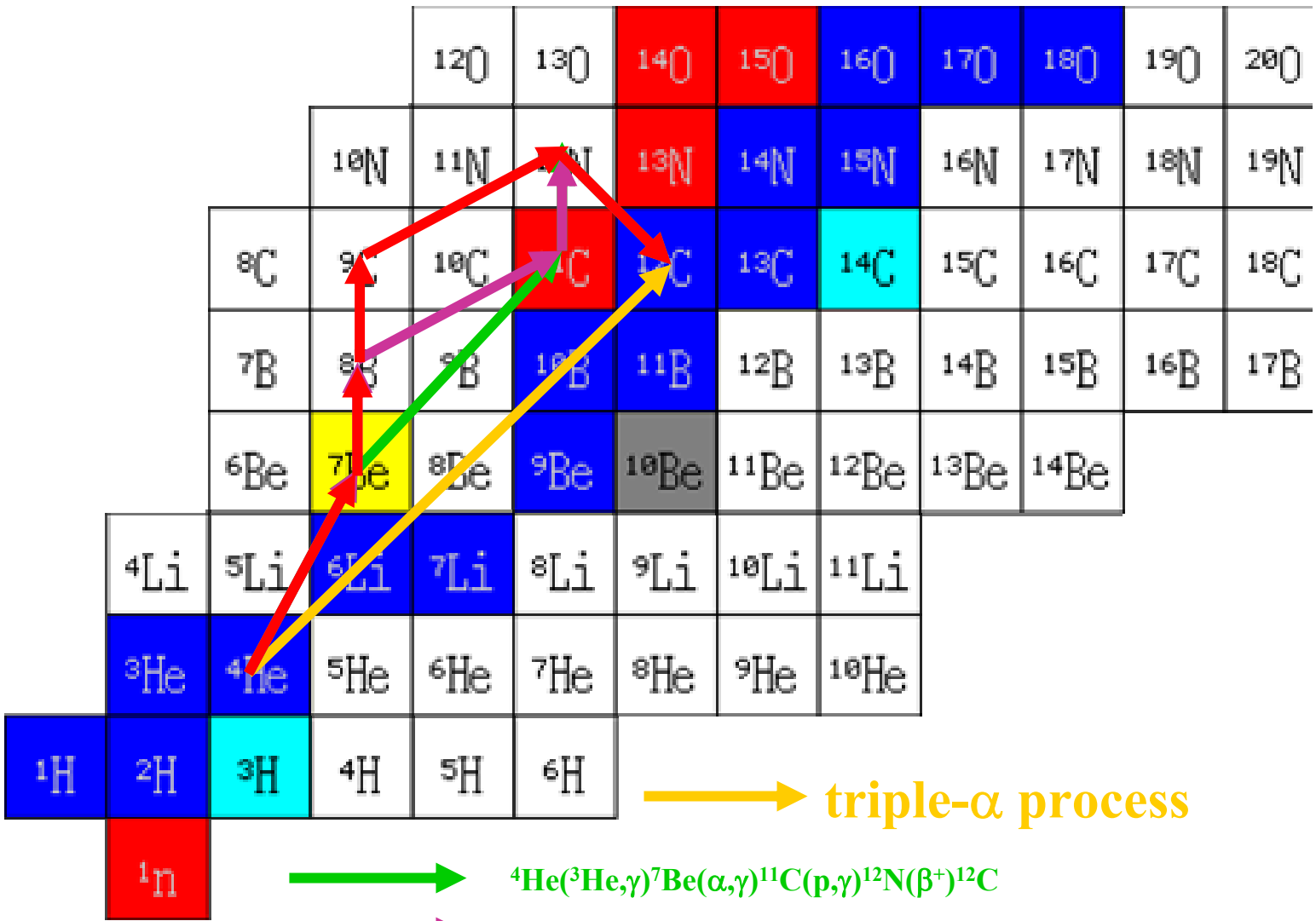

THE ASTROPHYSICAL JOURNAL, 343:352–364, 1989 August 1
© 1989. The American Astronomical Society. All rights reserved. Printed in U.S.A.

THE HOT PROTON-PROTON CHAINS IN LOW-METALLICITY OBJECTS

M. WIESCHER, J. GÖRRES, AND S. GRAFF
Department of Physics, University of Notre Dame

L. BUCHMANN[1]
Department of Physics, University of Toronto

AND

F.-K. THIELEMANN
Department of Astronomy, Harvard University
Received 1988 May 31; accepted 1989 January 13

ABSTRACT

The rates for proton- and α-capture reactions on light nuclei ($A \leq 13$) close to the proton drip line are calculated from available nuclear structure information. The influence of these reactions as link reactions between the nuclei in the *pp* chains and the CNO nuclei in hydrogen burning at different temperatures and densities is discussed.

Subject headings: nuclear reactions — nucleosynthesis — stars: massive

1989:

beams/targets: ^{7}Be (53d)

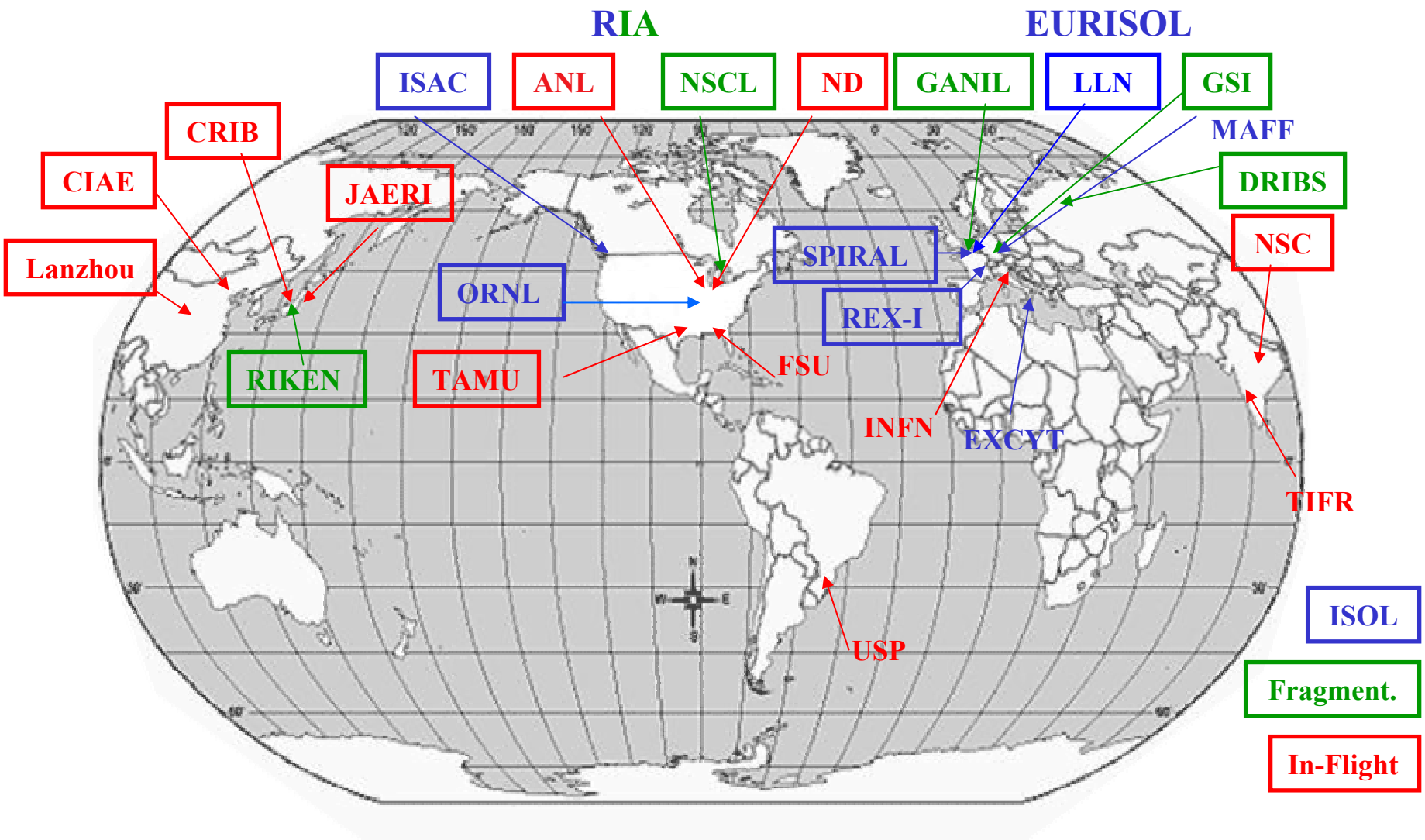

RNB Production Facilities 2004

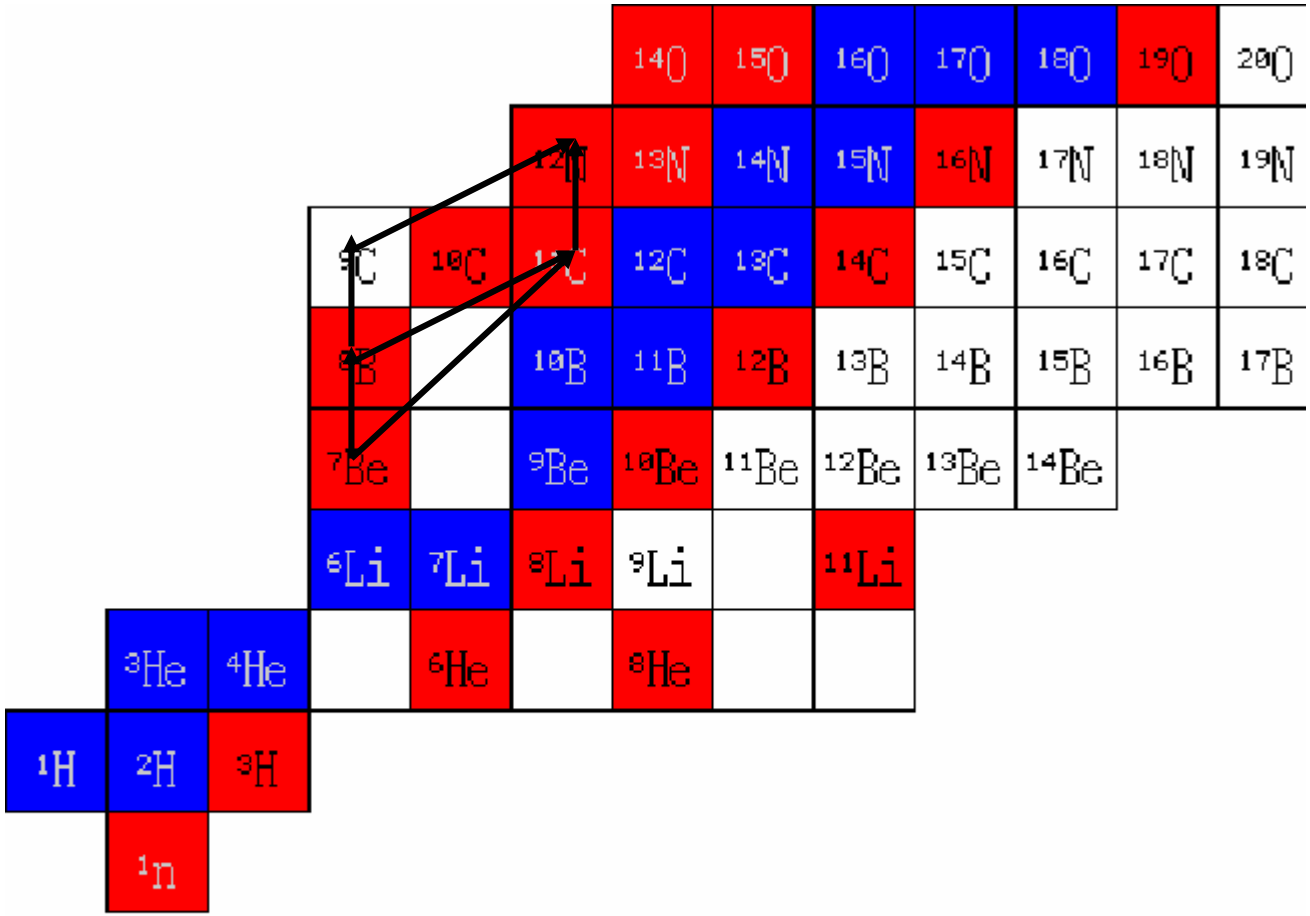

Low-energy radioactive beams available today

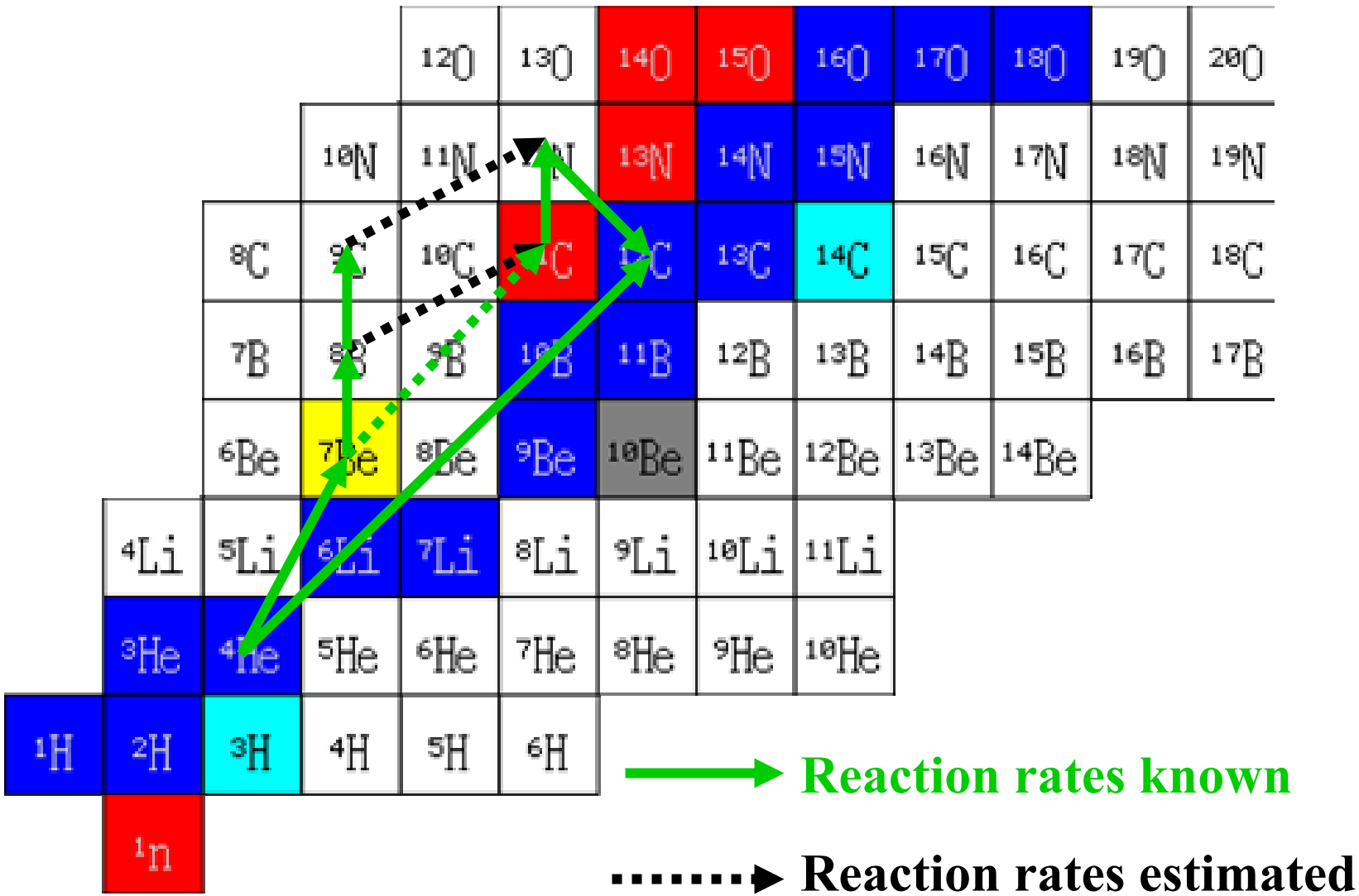
12O 13O 14O 15O 16O 17O 18O 19O 20O
10N 11N 12N 13N 14N 15N 16N 17N 18N 19N
8C 9C 10C 11C 12C 13C 14C 15C 16C 17C 18C
7B 8B 9B 10B 11B 12B 13B 14B 15B 16B 17B
6Be 7Be 8Be 9Be 10Be 11Be 12Be 13Be 14Be
4Li 5Li 6Li 7Li 8Li 9Li 10Li 11Li
3He 4He 5He 6He 7He 8He 9He 10He
1H 2H 3H 4H 5H 6H
1n
Reaction rates known
Reaction rates estimated

$^{7}Be(p,\gamma)^{8}B$

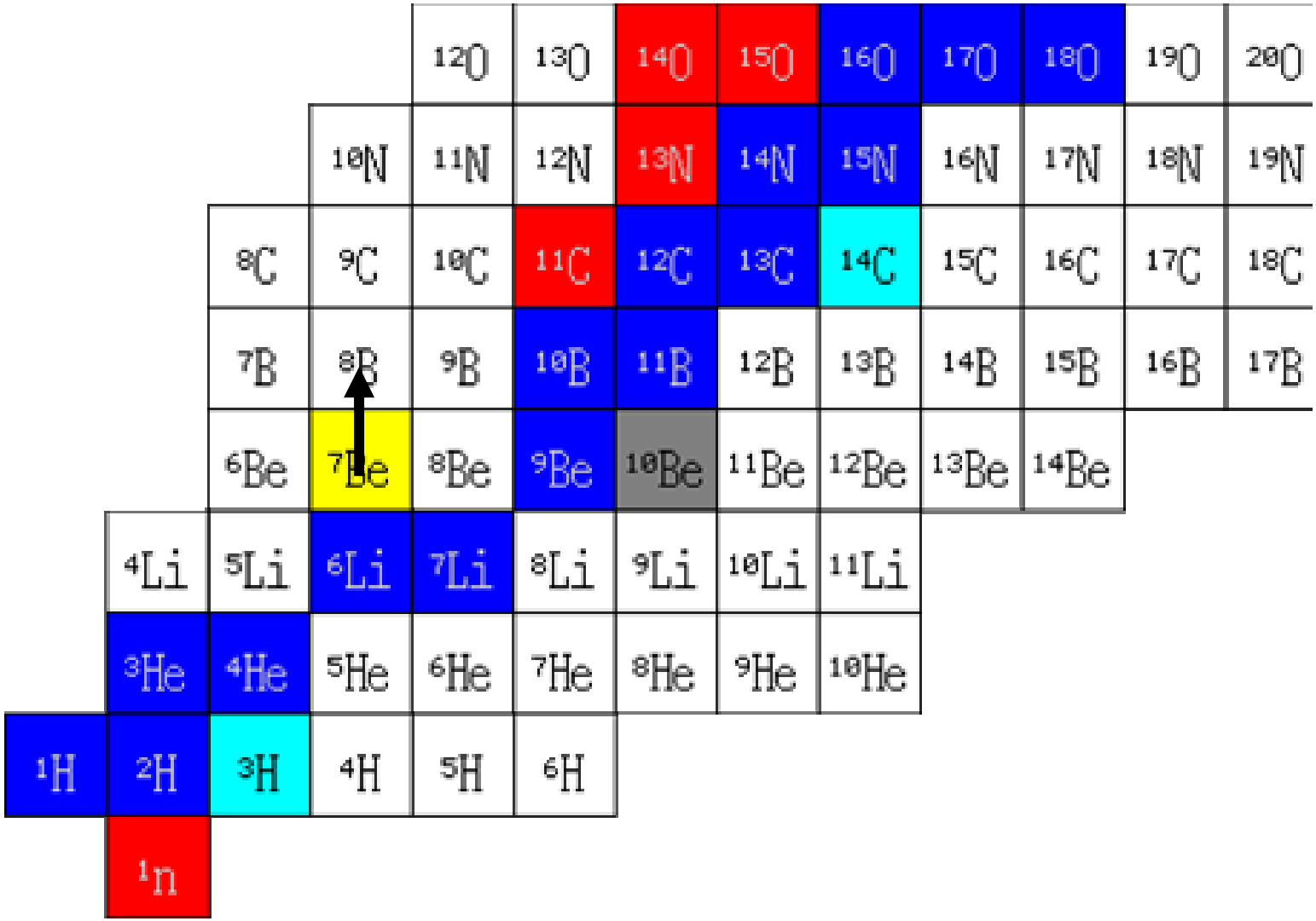

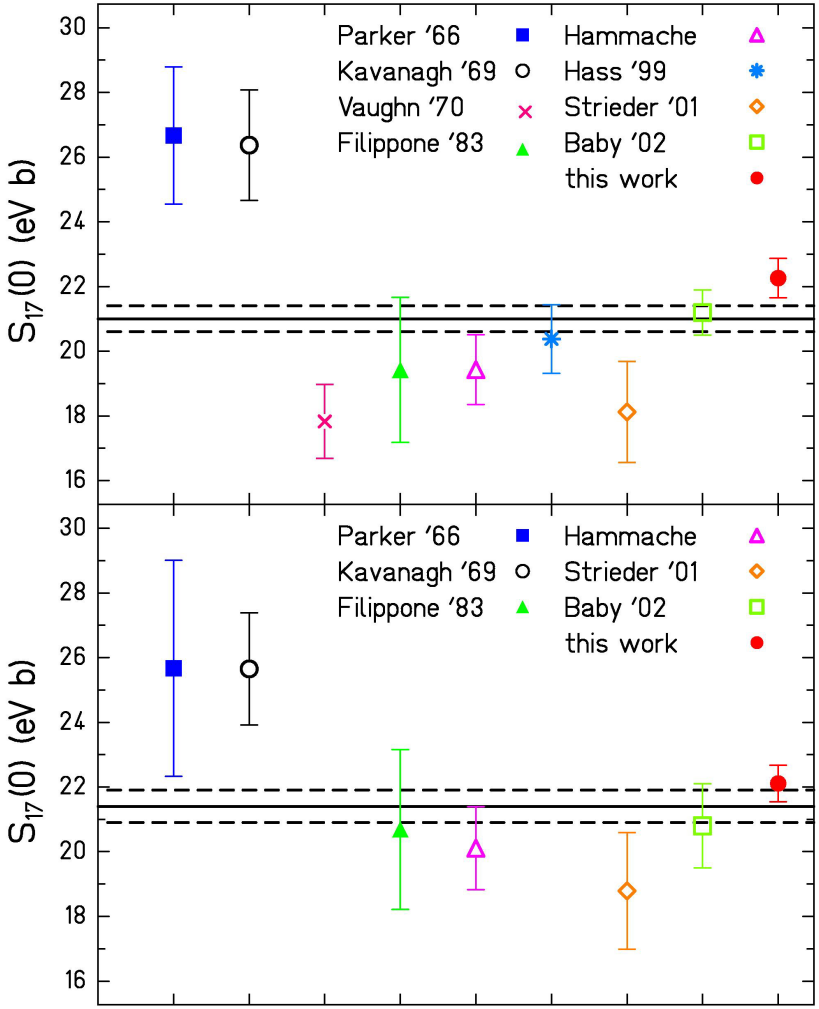

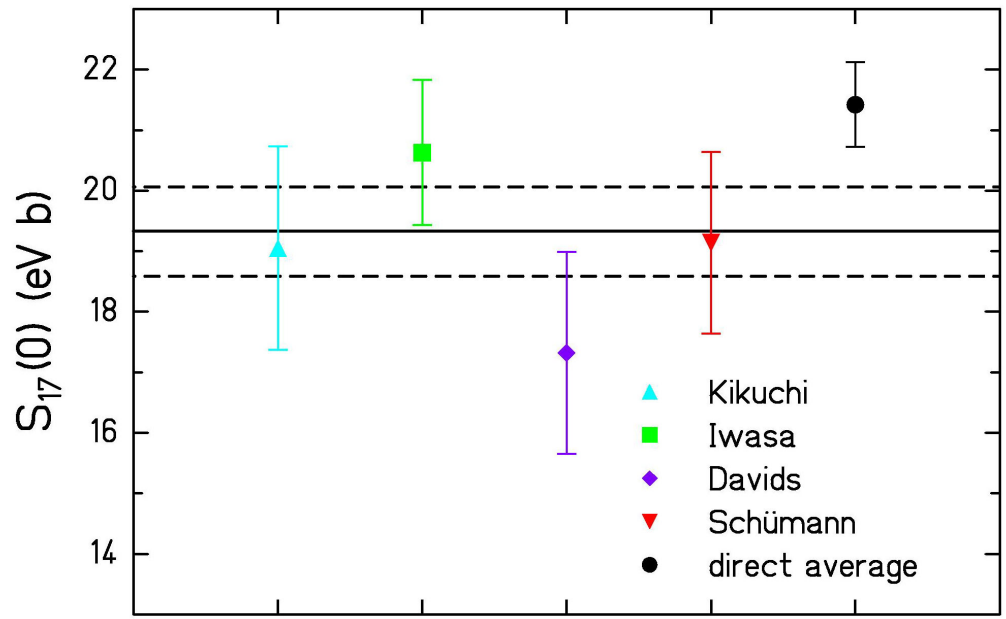

Direct: $S_{17} = 21.4 \pm 0.5 \pm 0.6$ eVb

CD: $S_{17} = 19.3 \pm 0.7 \pm 0.6$ eVb

ANC: $S_{17} = 18.2 \pm 1.8$ eVb

$^{8}B(p,\gamma)^{9}C$

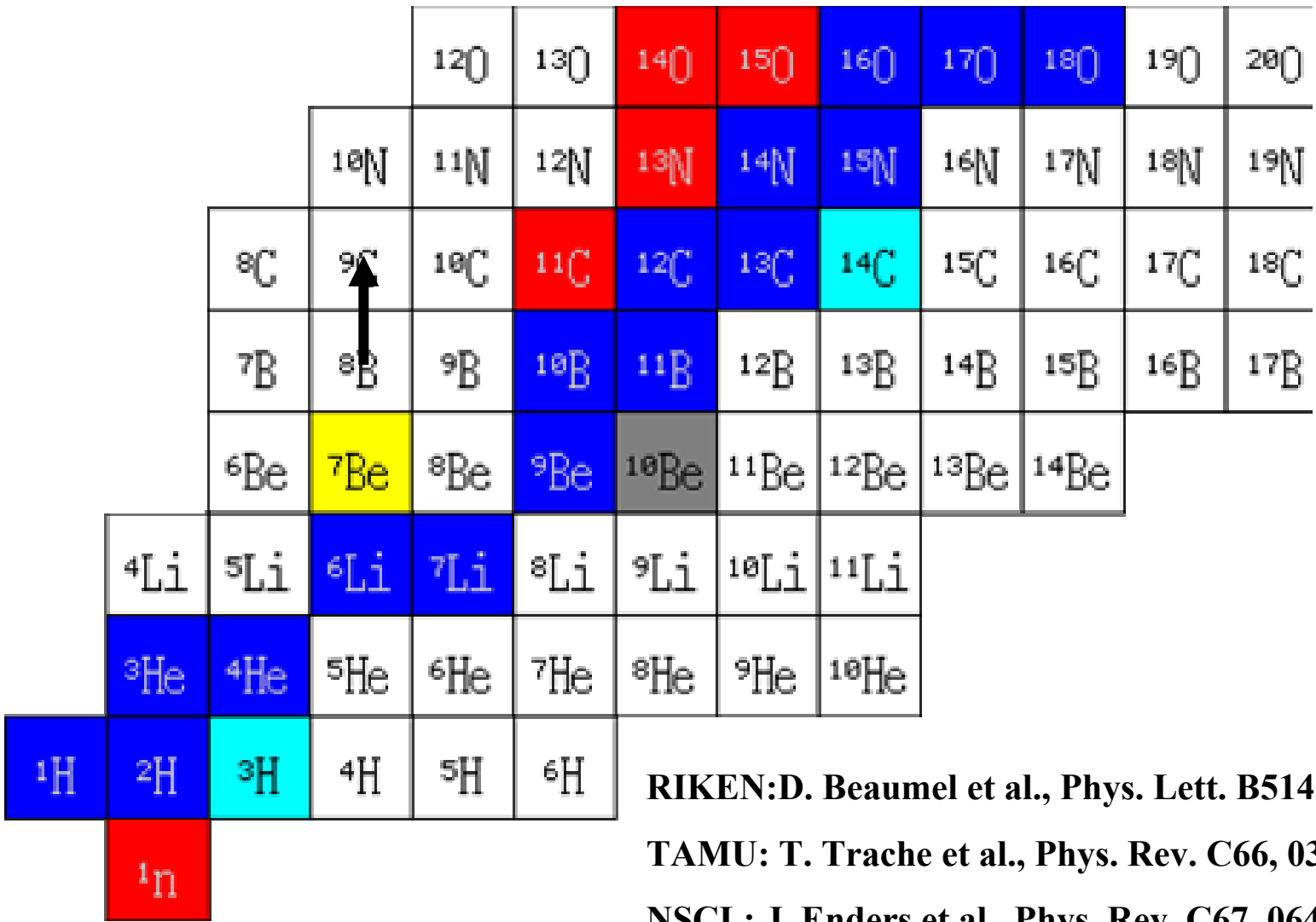

RIKEN:D. Beaumel et al., Phys. Lett. B514, 226(2001)

TAMU: T. Trache et al., Phys. Rev. C66, 035801(2002)

NSCL: J. Enders et al., Phys. Rev. C67, 064301(2003)

RIKEN: T. Motobayashi et al., RIKEN Ann. Rep (2003)

$^{8}B(p,\gamma)^{9}C$

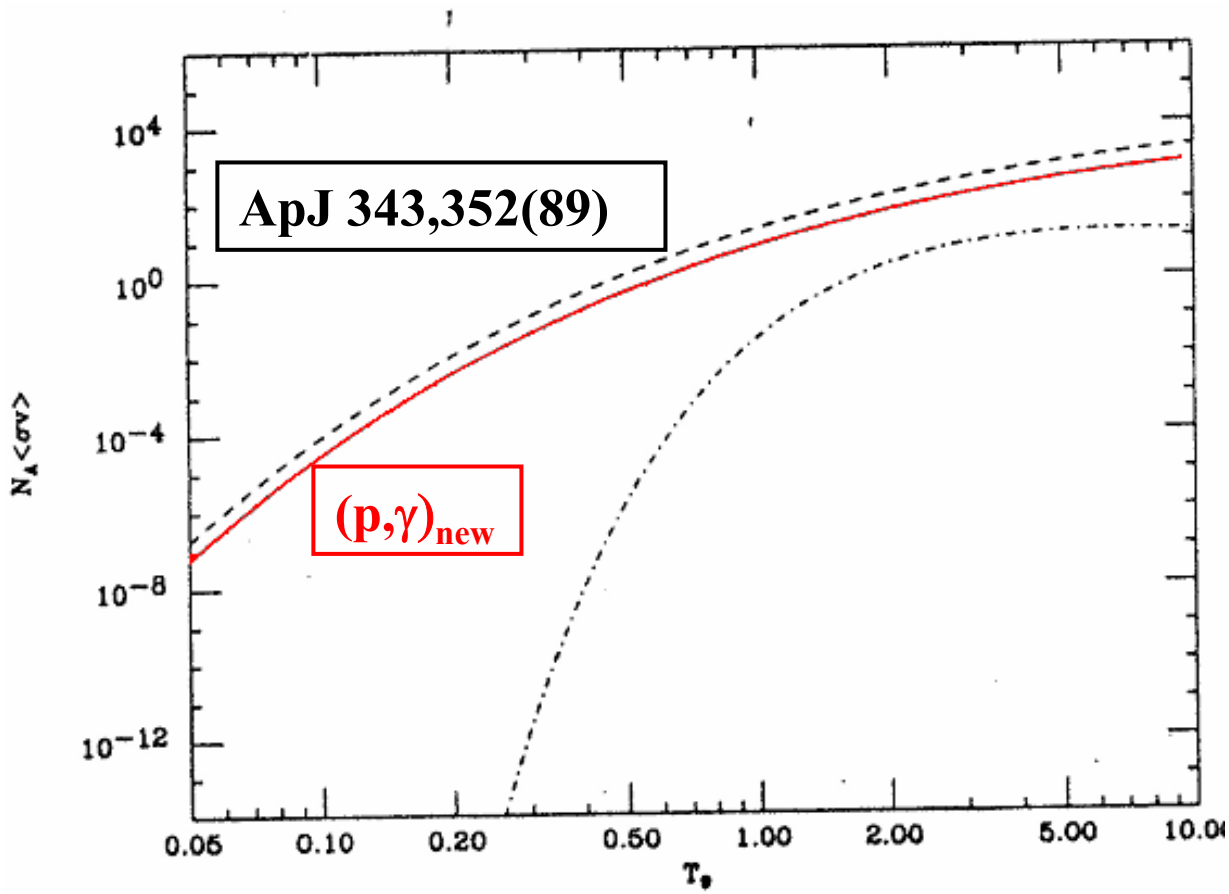

S-factor summary:

HF: 210 eVb

RIKEN(CD): 77 ± 15 eVb

RIKEN(CD): 45± 13 eVb

NSCL(ANC): 49 ± 4 eVb

TAMU(ANC): 46 ± 6 eVb

$^{11}C(p,\gamma)^{12}N$

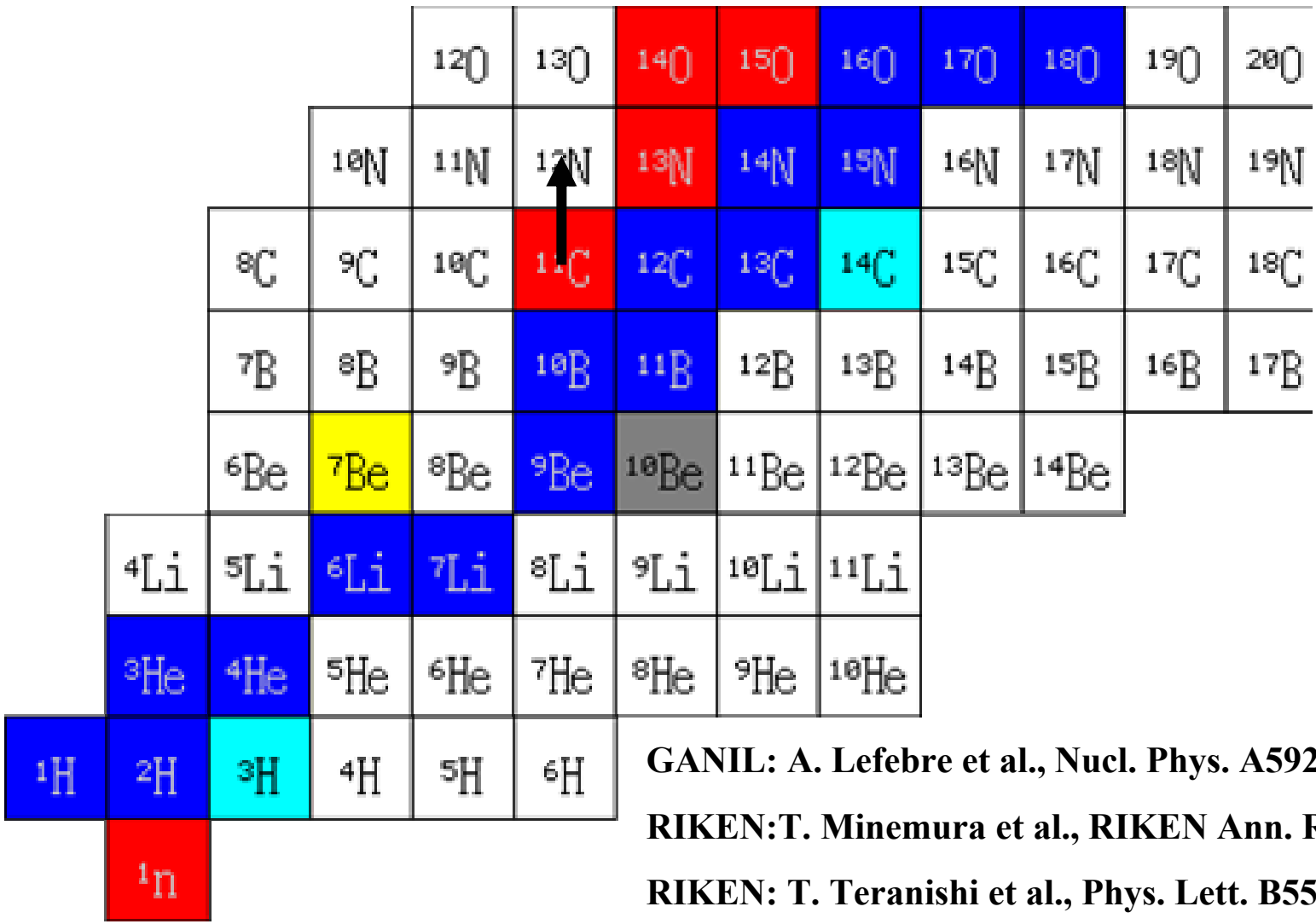

GANIL: A. Lefebre et al., Nucl. Phys. A592, 69(1995)

RIKEN:T. Minemura et al., RIKEN Ann. Rep. (2002)

RIKEN: T. Teranishi et al., Phys. Lett. B556, 27(2003)

TAMU: X. Tang et al., Phys. Rev. C67, 015804 (2003)

BEIJING: W. Liu, Nucl. Phys. A728, 275(2003)

S-factor of $^{11}C(p,\gamma)^{12}N$

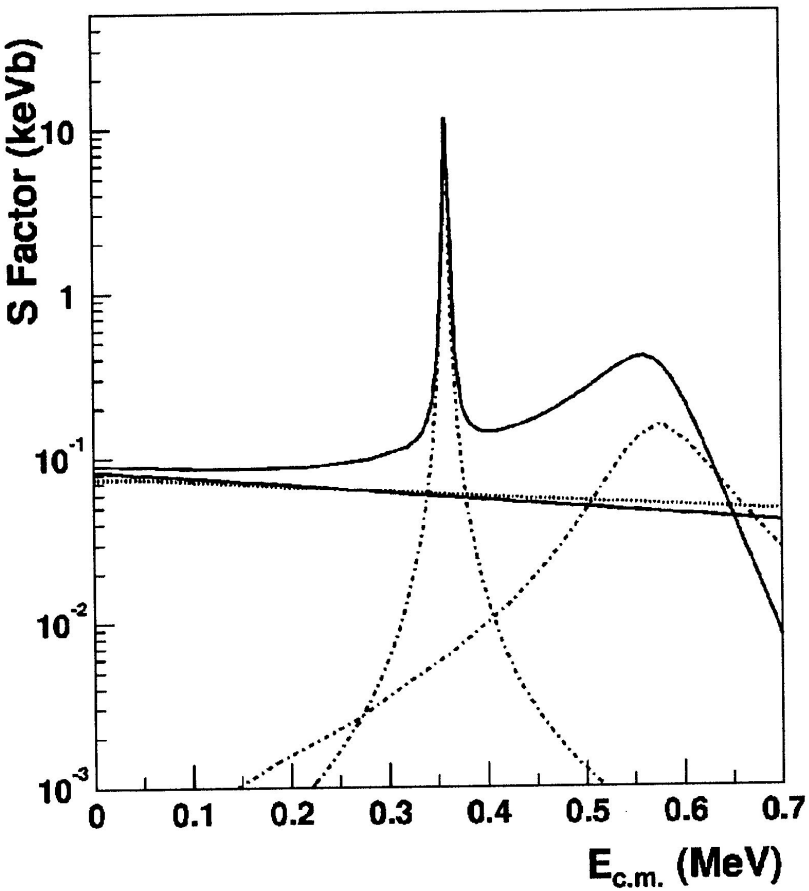

TAMU

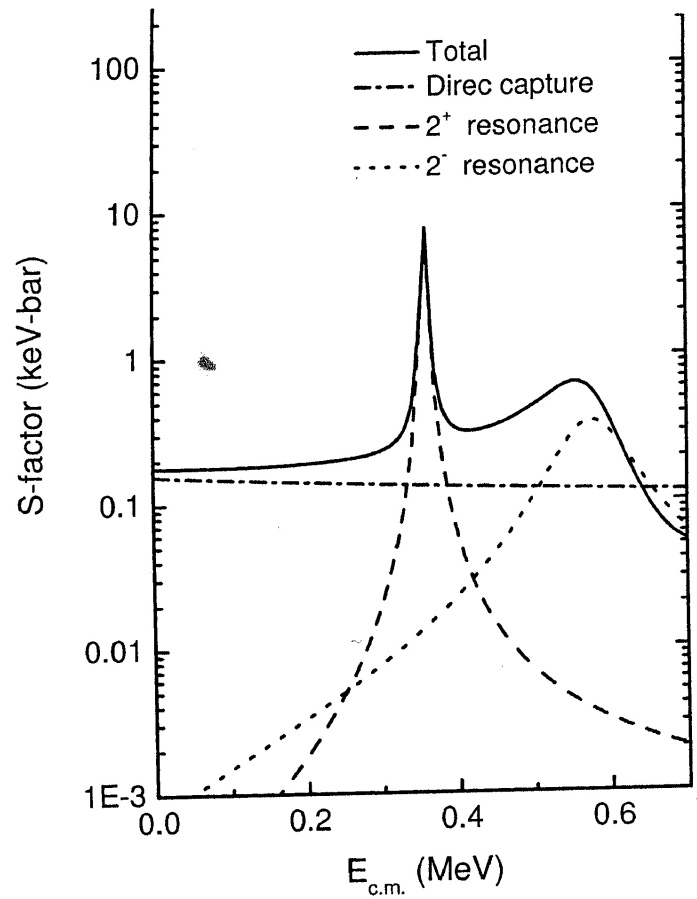

Beijing

$^{7}Be(\alpha,\gamma)^{11}C$

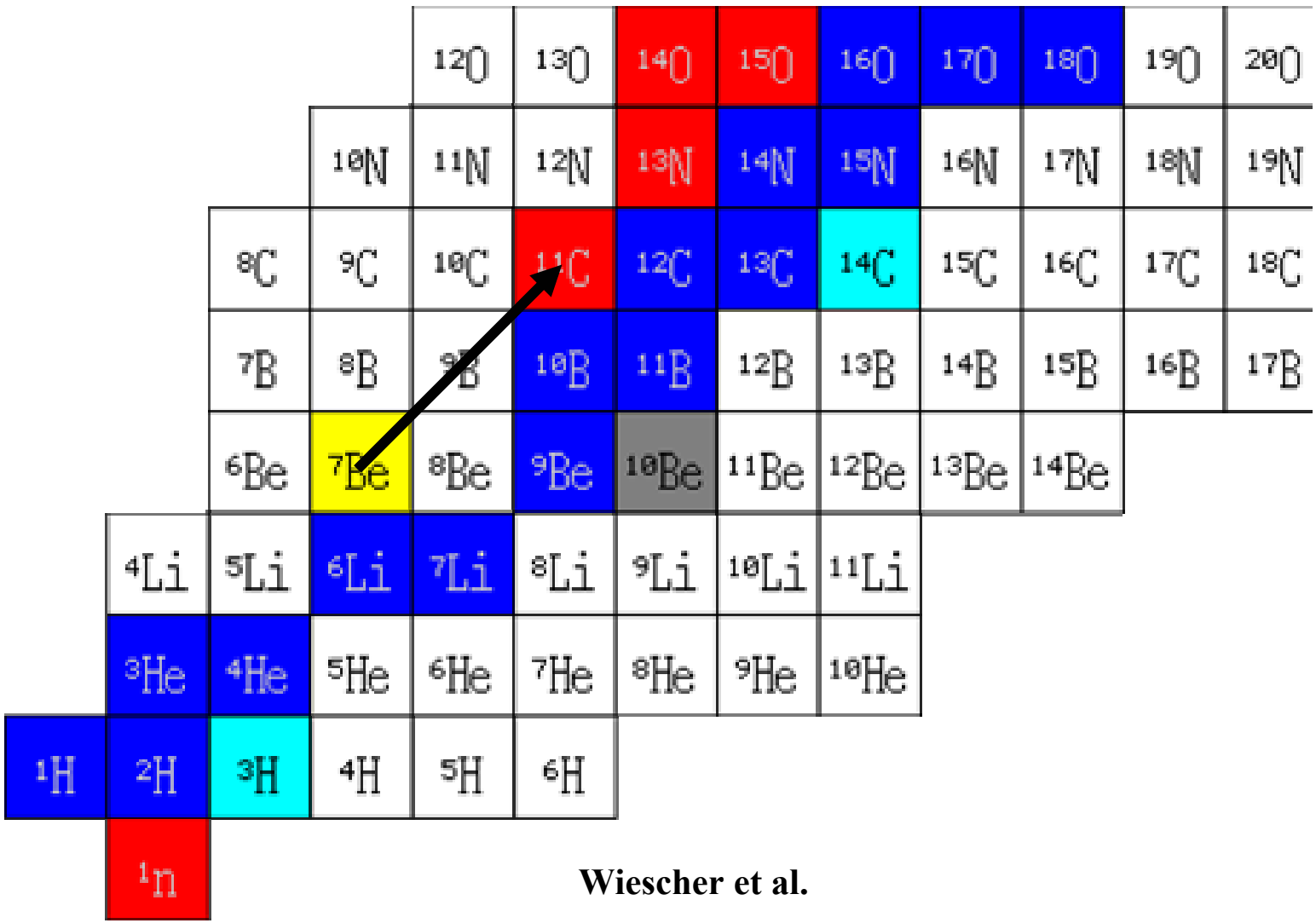

Wiescher et al.

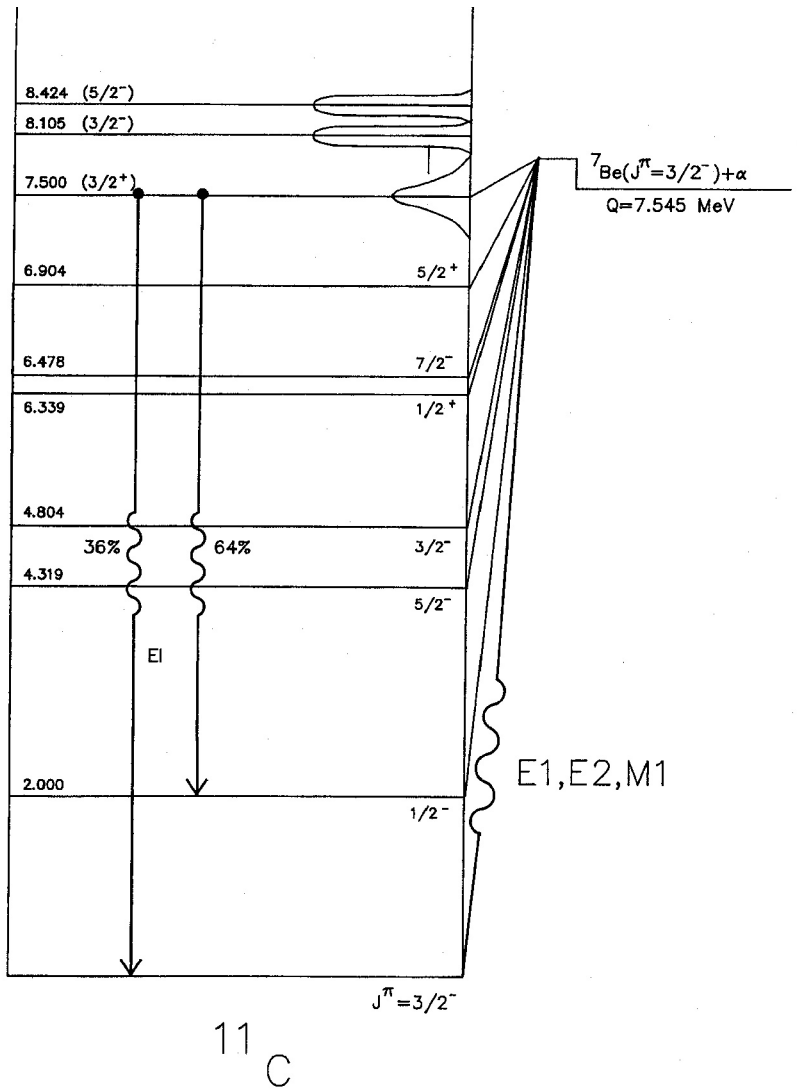

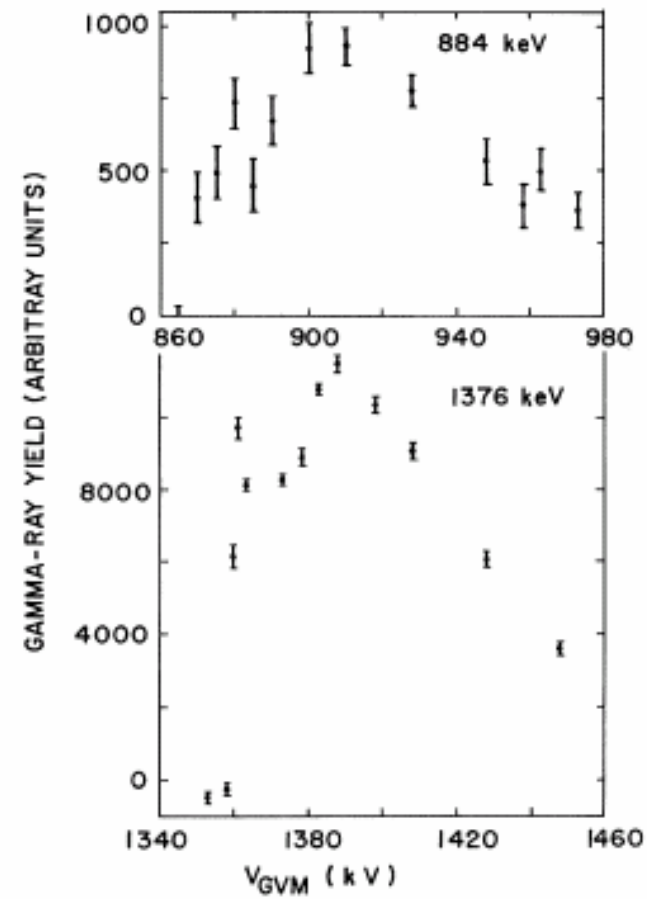

G. Hardie et al. PRC29,1199(1983)

L. Buchmann et al. ApJ 324, 953(1988)

$^{8}B(\alpha,p)^{11}C$

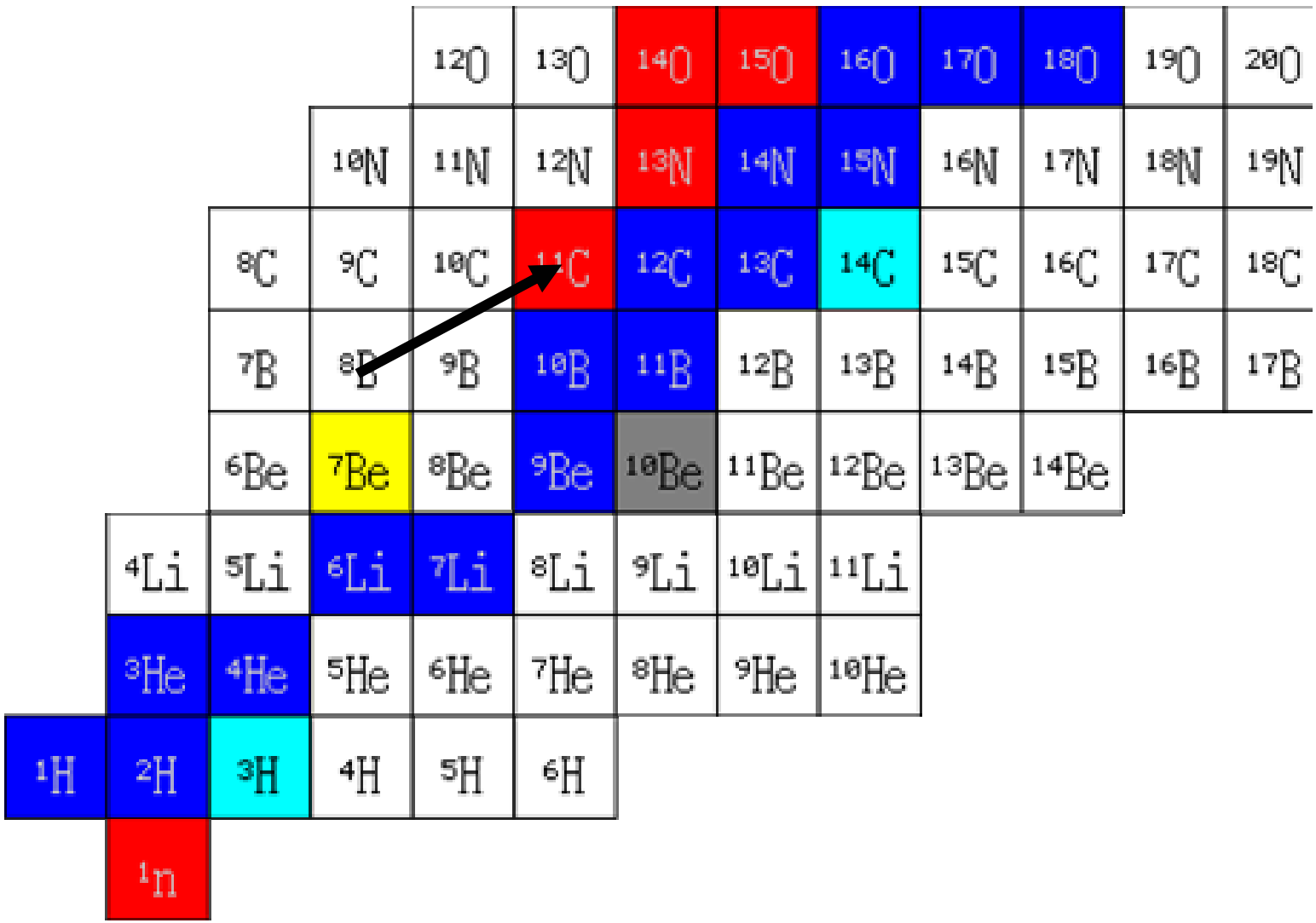

In a star:

$^{8}B(\alpha,p)^{11}C$

(gives $\Sigma\, \Gamma_{\alpha}\Gamma_{p'}$)

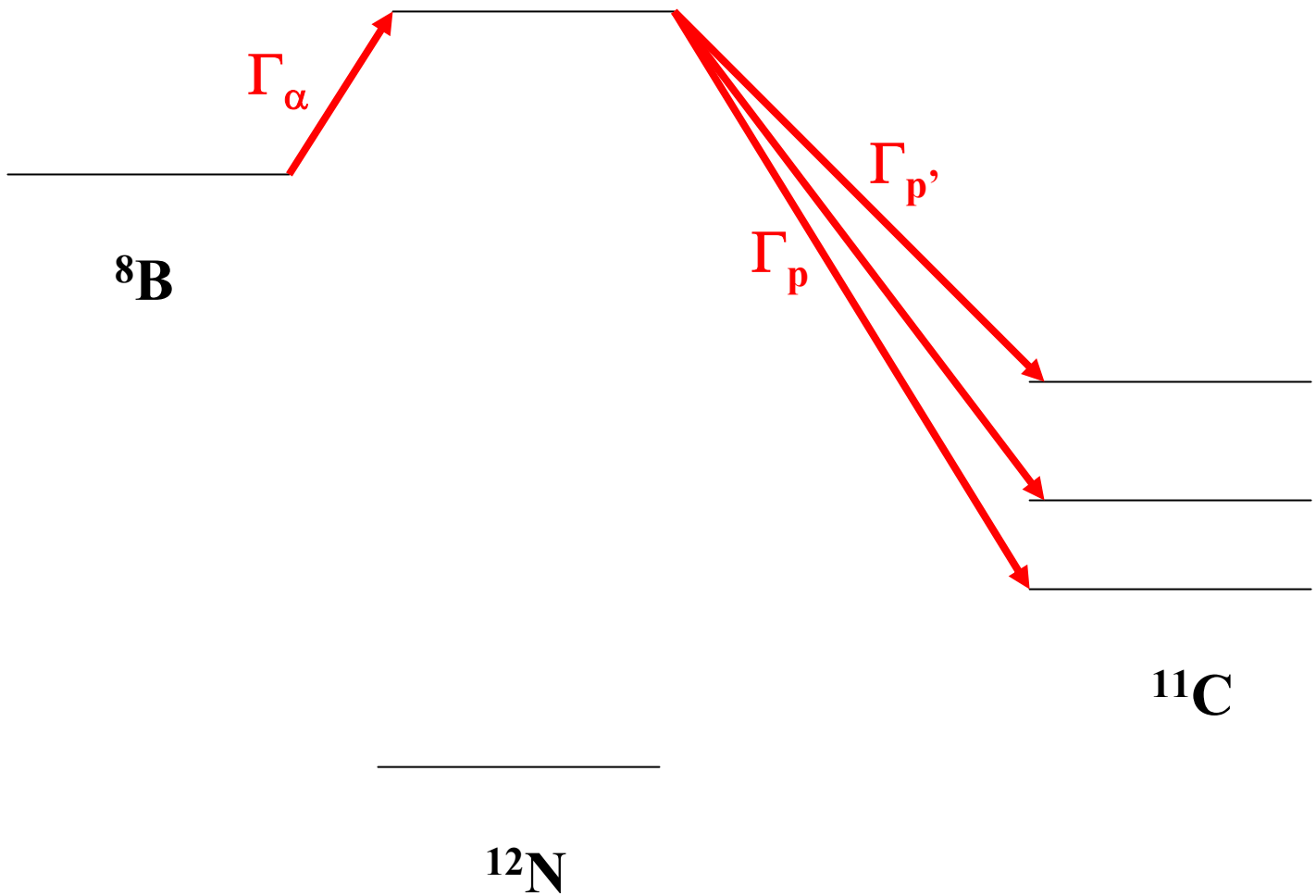

In the laboratory:

$^{11}C(p,\alpha)^{8}B$ (gives $\Gamma_\alpha\Gamma_p$)

$^{11}C(p,p')^{11}C$ (gives $\Sigma\Gamma_p\Gamma_{p'}$)

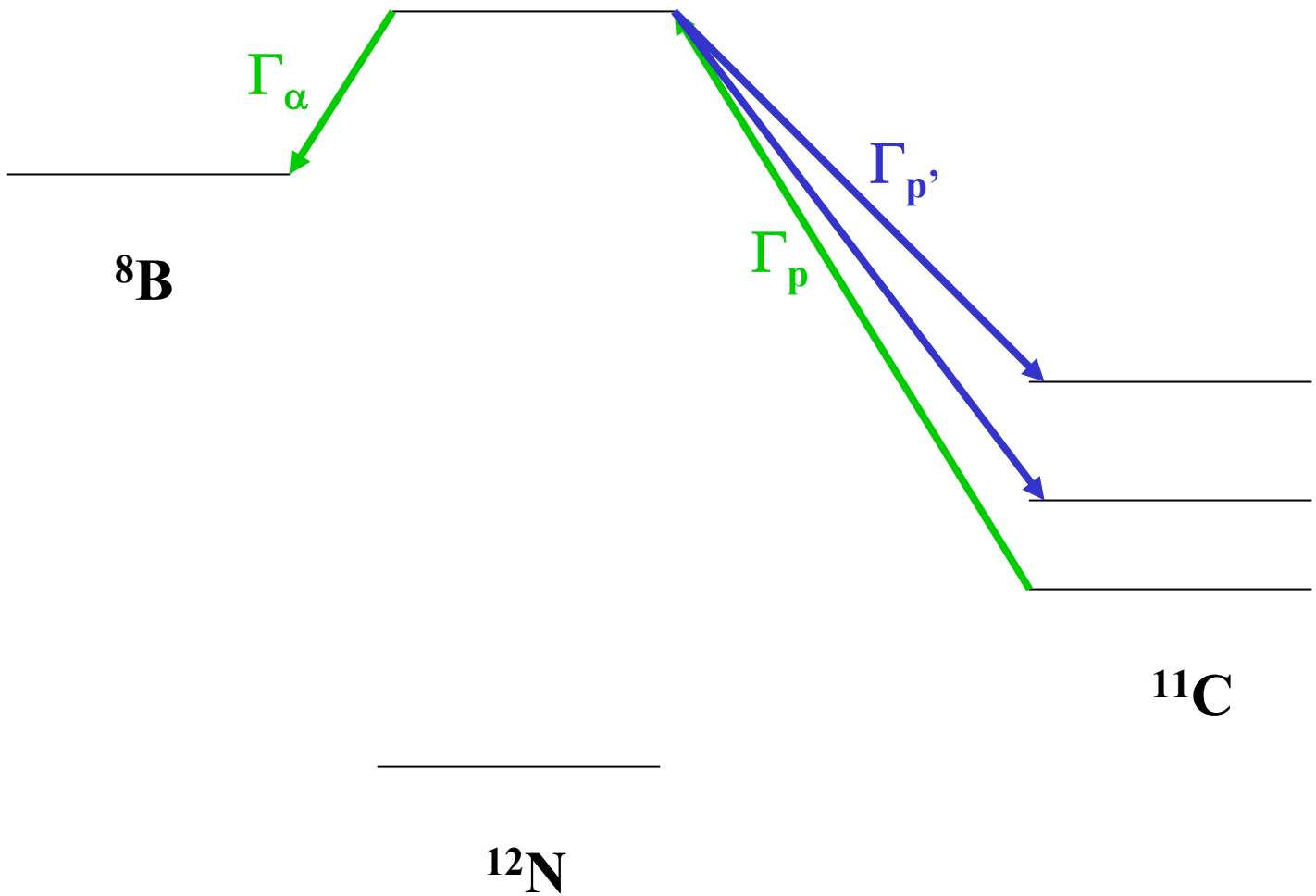

Radioactive Beam Production

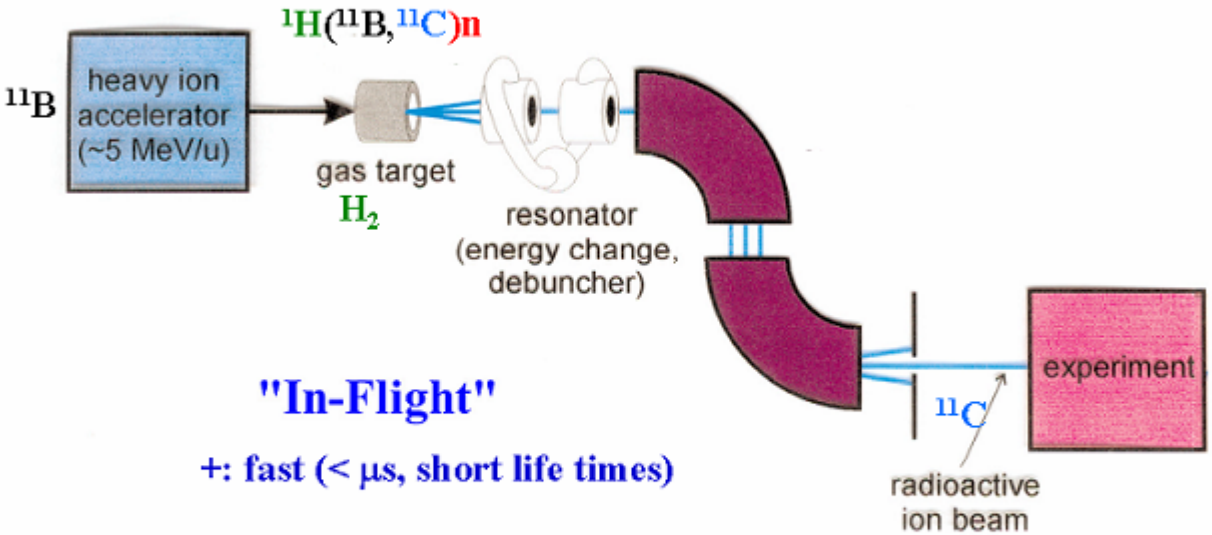

"In-Flight"

+: fast (< μs, short life times)

beam properties good enough to measure resonances in inverse kinematics

^{17}F, ^{21}Na, ^{25}Al, ^{37}K, ^{8}B, ^{6}He, ^{8}Li, ^{11}C ..

B. Harss et al., Rev. Sci. Inst. 71, 380(2000)

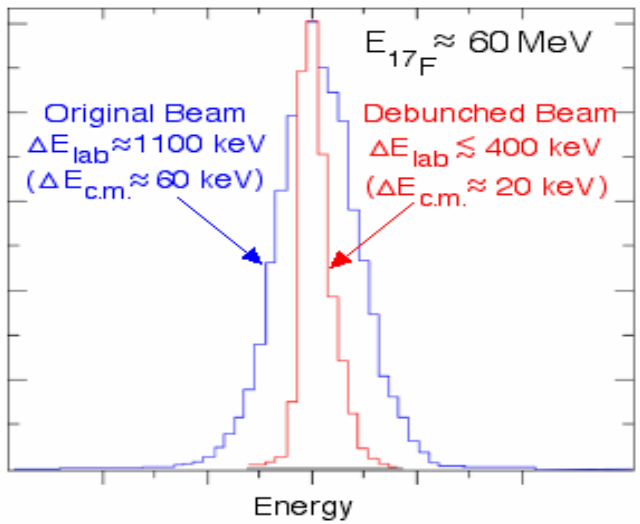

In-Flight Production of ^{11}C ($T_{1/2}$=20.4m)

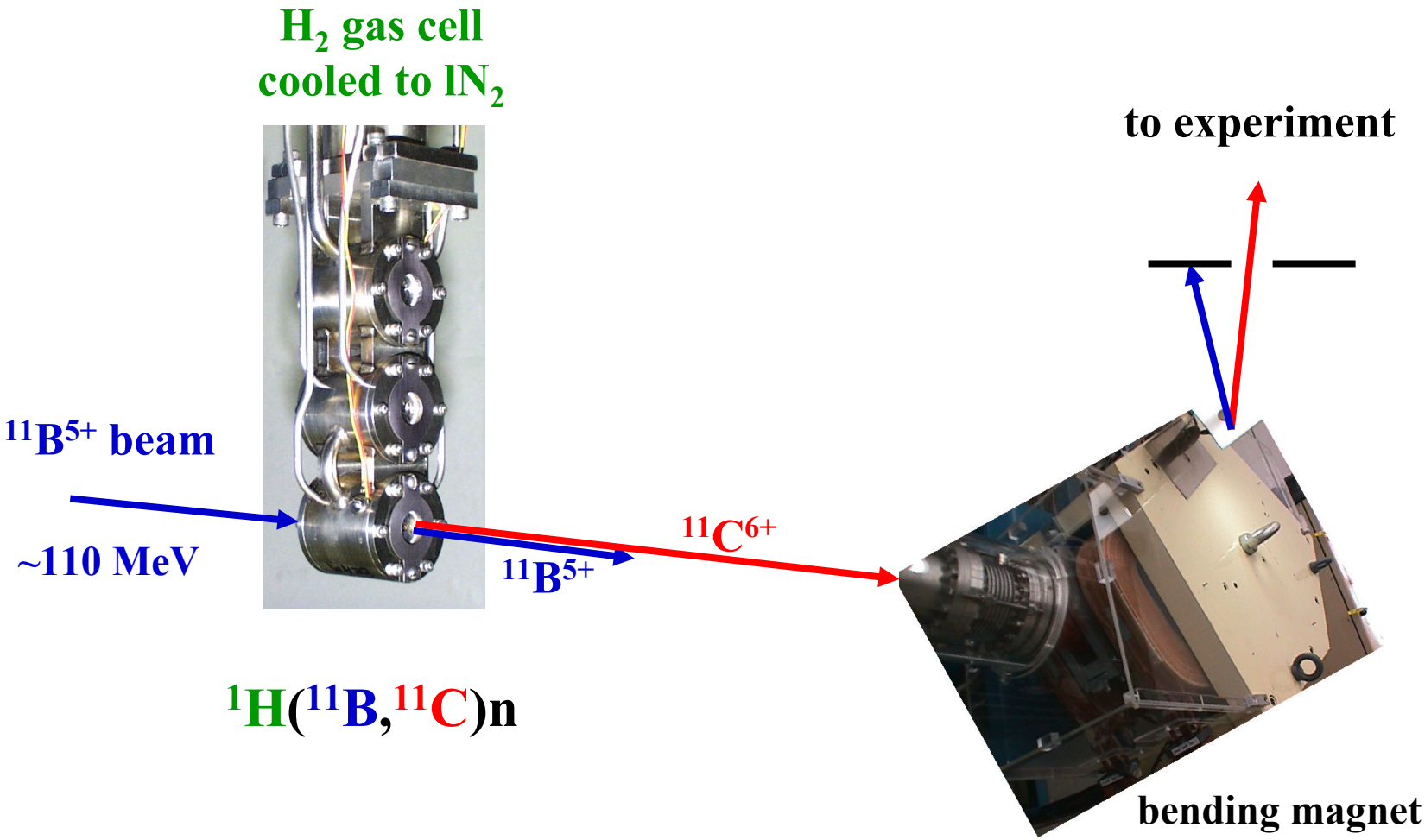

$^{1}H(^{11}B,^{11}C)n$

$p(^{11}B,n)^{11}C$

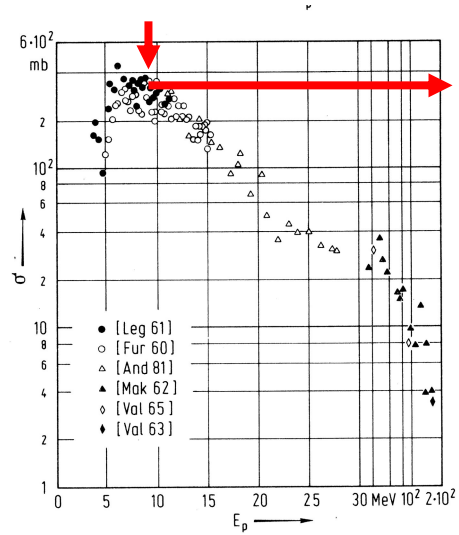

σ(p,n)~300 mb

Particle identification; (^{11}C and ^{11}B not stopped in ionization chamber) ; $E(^{11}B)=0.7*E(^{11}C)$

Bragg Peak

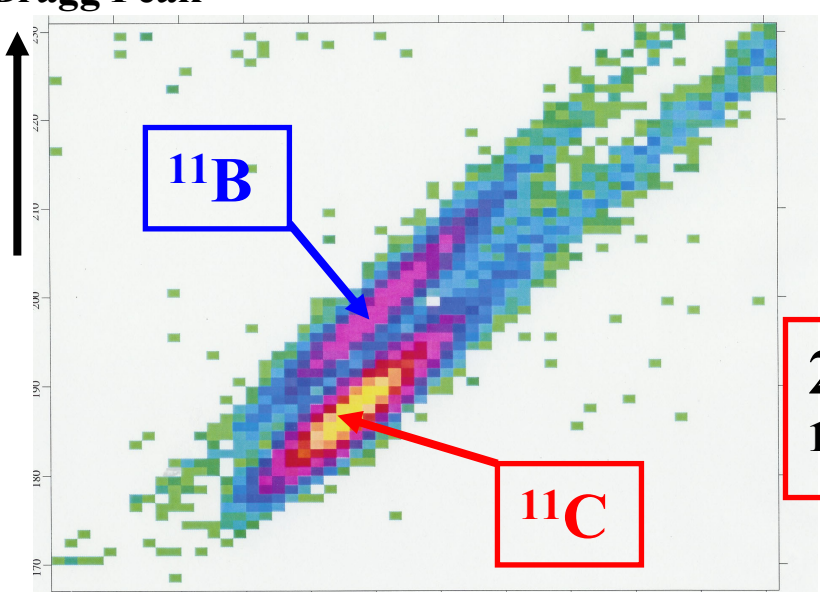

$2x10^5$ $^{11}C/s$

TOF

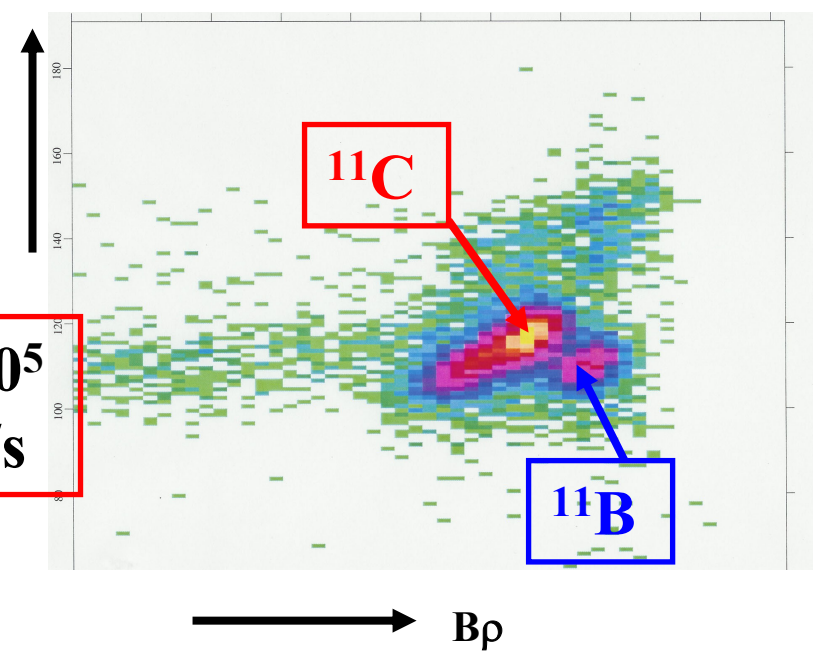

Setup for p(^{11}C, α)^{8}B experiment

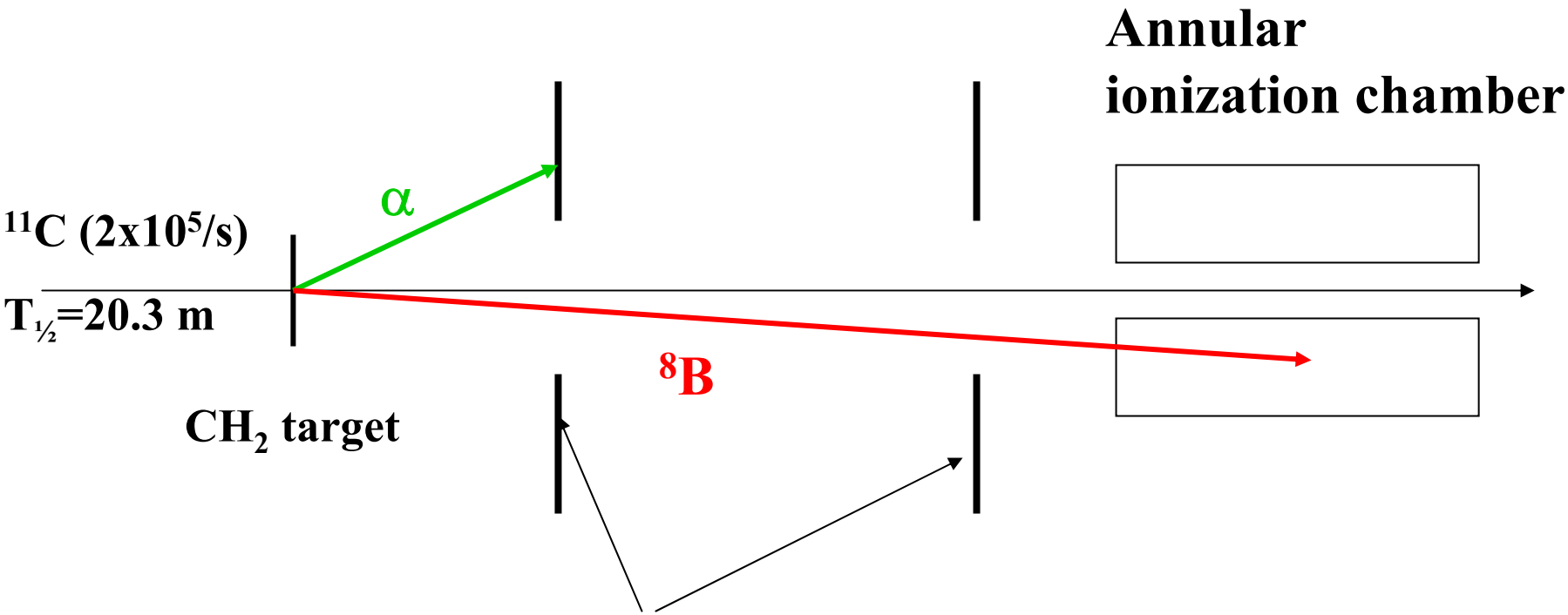

Si strip detectors. (~100 channels).

Detection efficiency 50-80%! (inverse kinematics)

Experimental setup for (p,α) experiment (ANL)

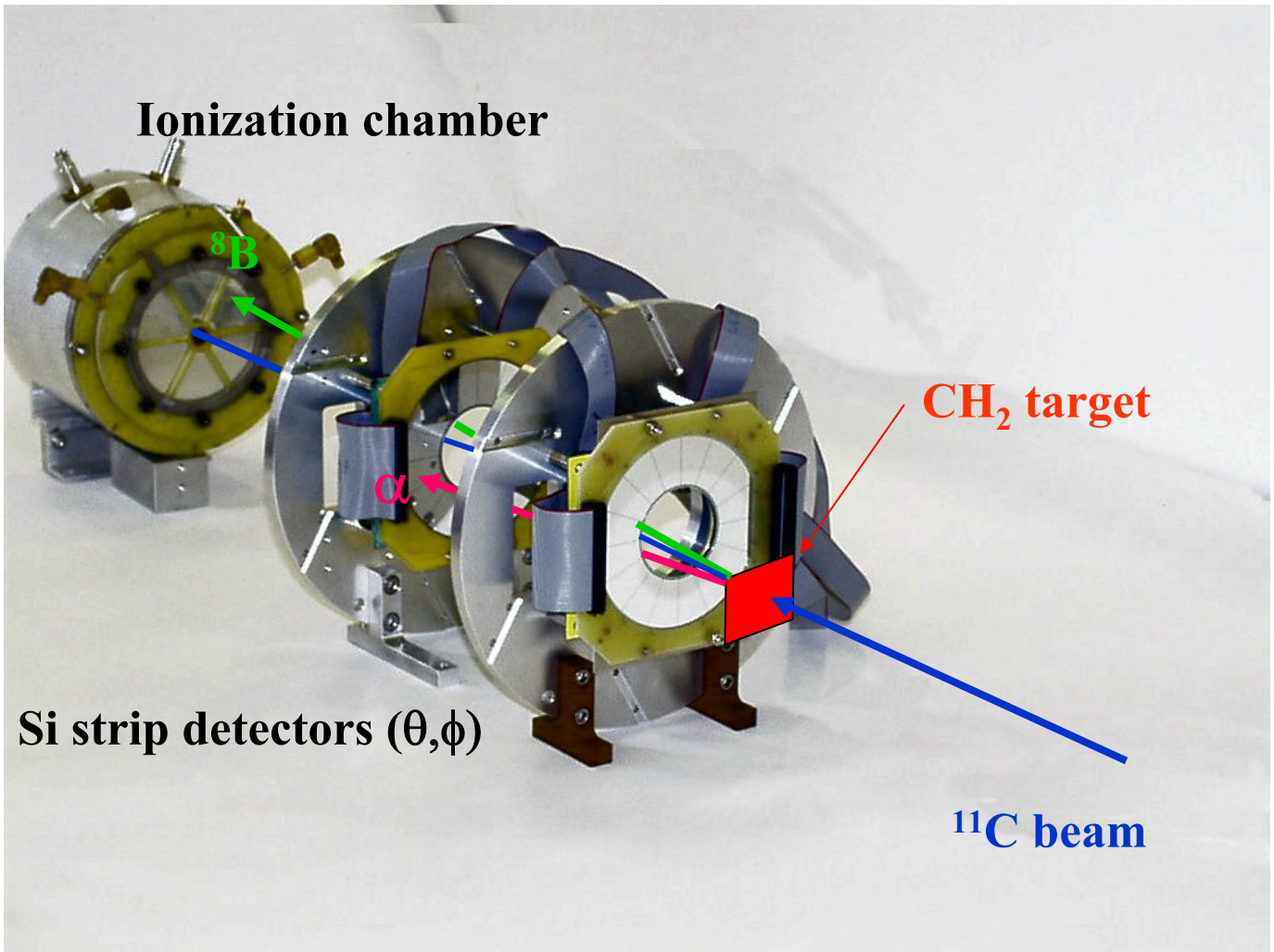

Experimental Results (preliminary)

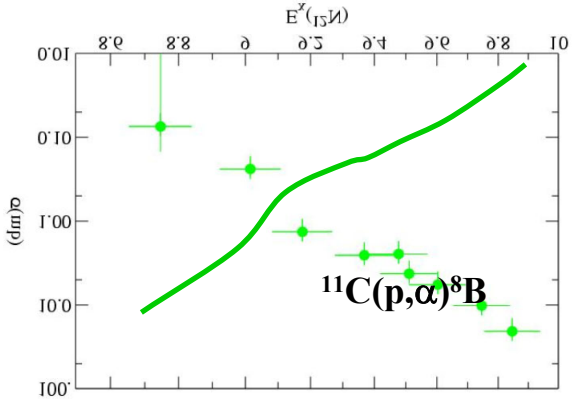

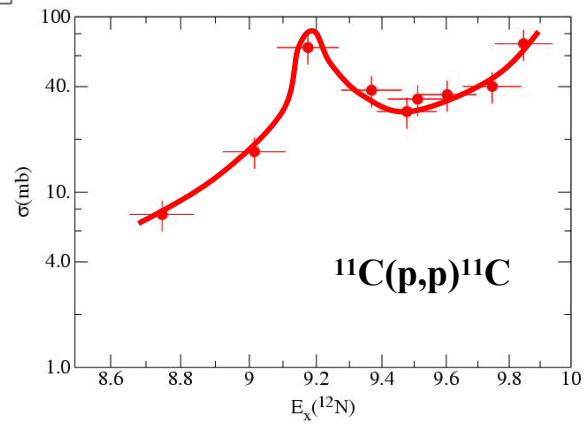

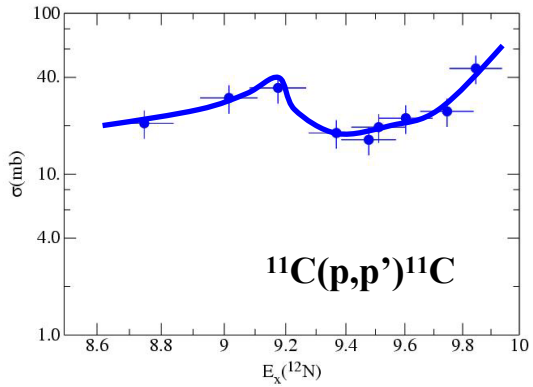

Bypassing the triple–α reaction

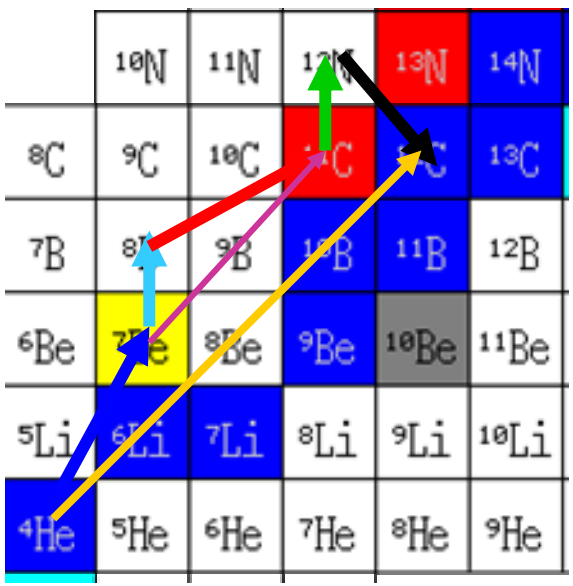

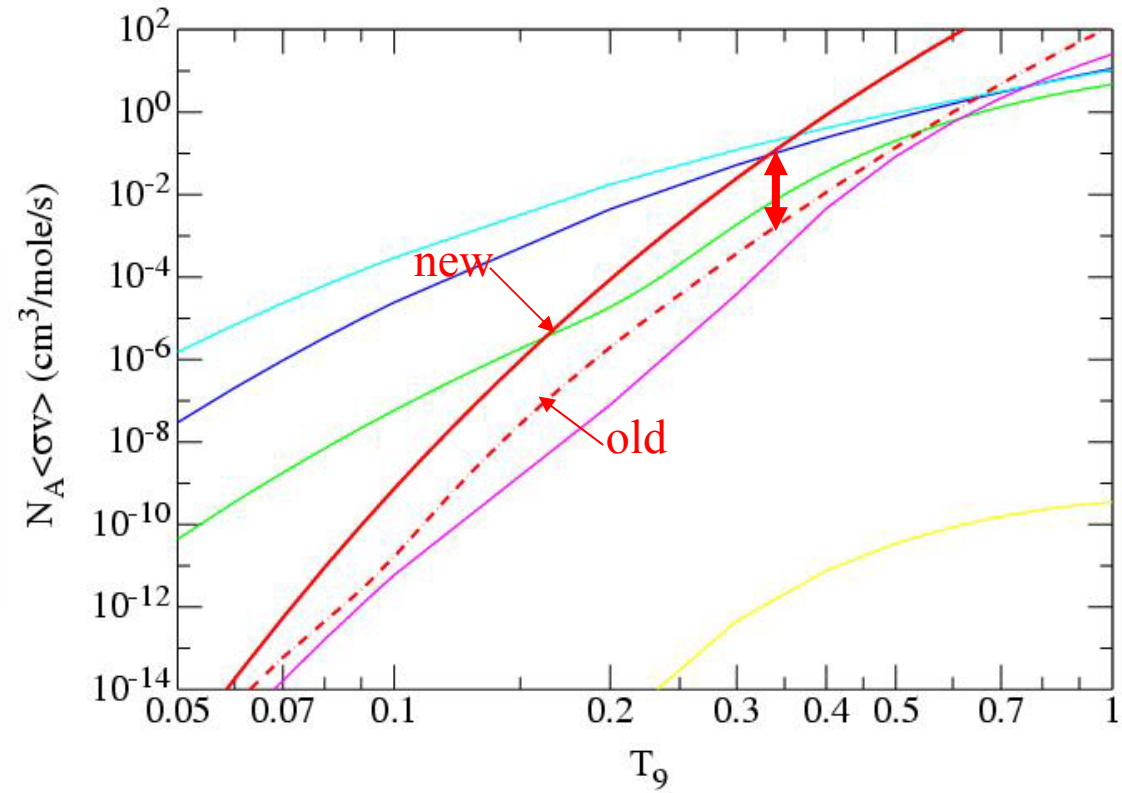

Bottleneck reaction $^8B(\alpha,p)^{11}C$ is 50 times stronger than previously assumed

Influence of Reaction Rates

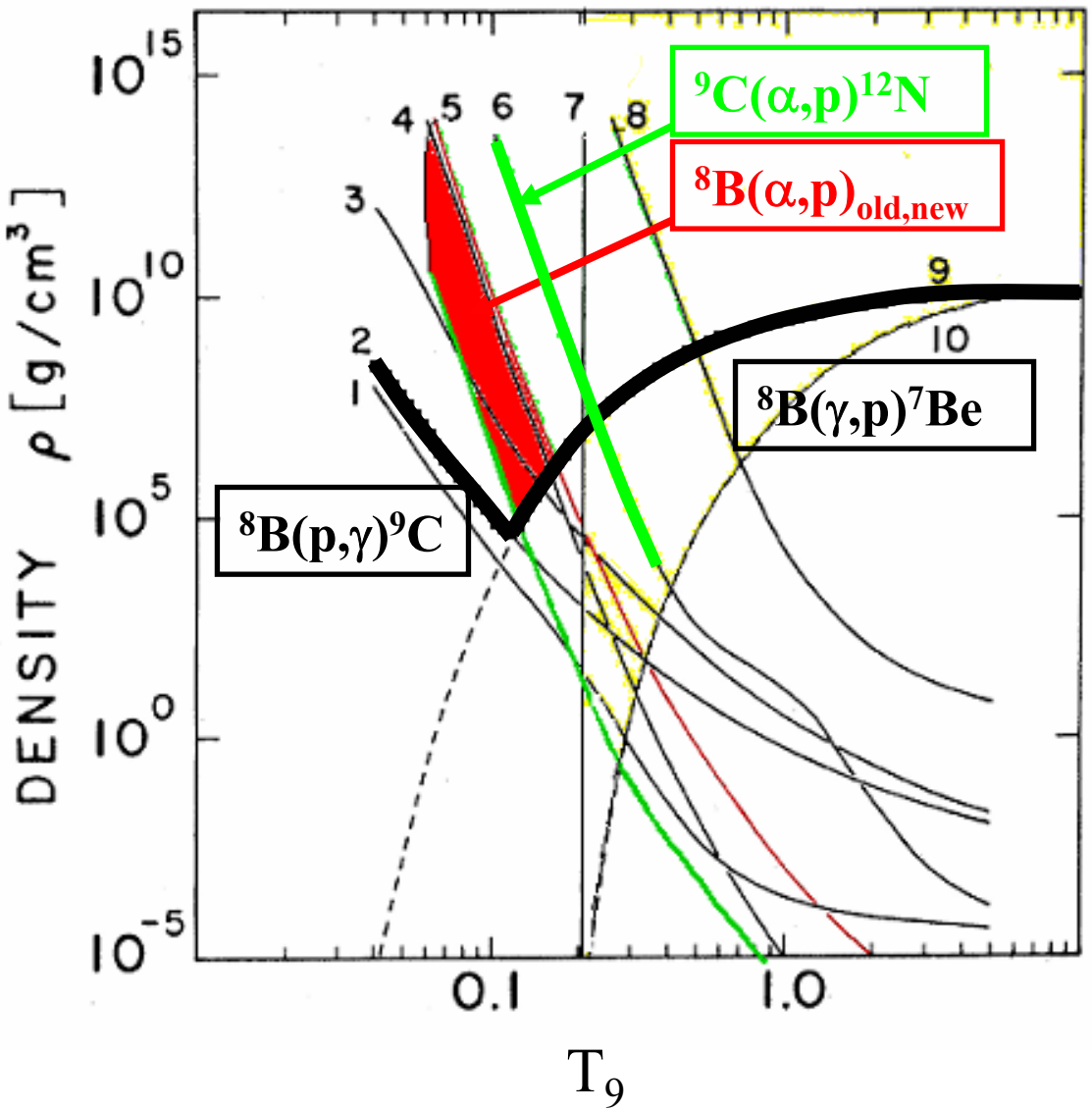

Difficulties with $^{9}C(p,\alpha)^{12}N$

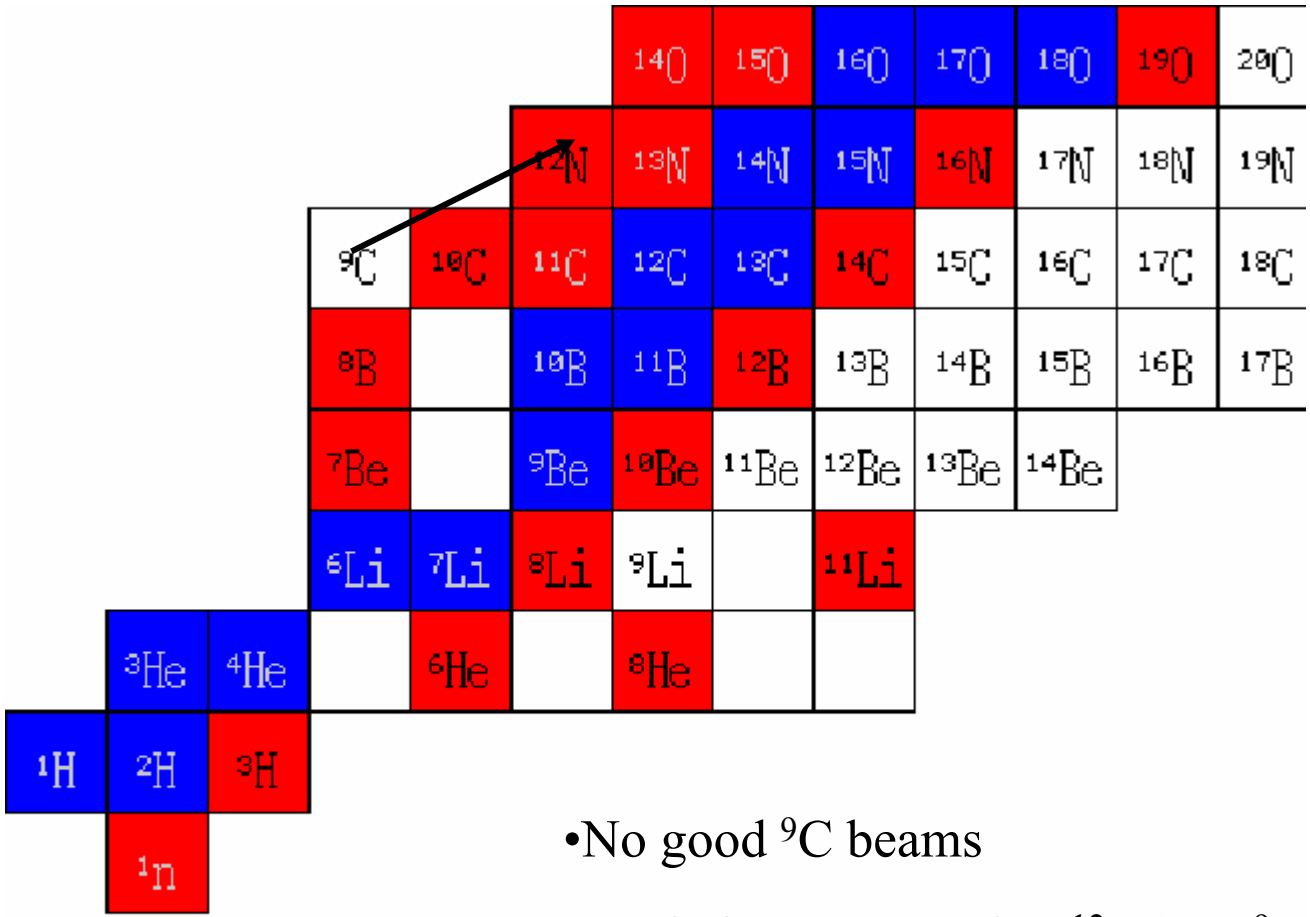

- No good ^{9}C beams
- Study inverse reaction $^{12}N(p,\alpha)^{9}C$
- Need >20 MeV/u ^{12}C beam ($^{12}C(p,n)^{12}N$)
- $^{10}B(^{3}He,n)^{12}N$ has a factor of 10 lower σ

RIA – A Next Generation Accelerator

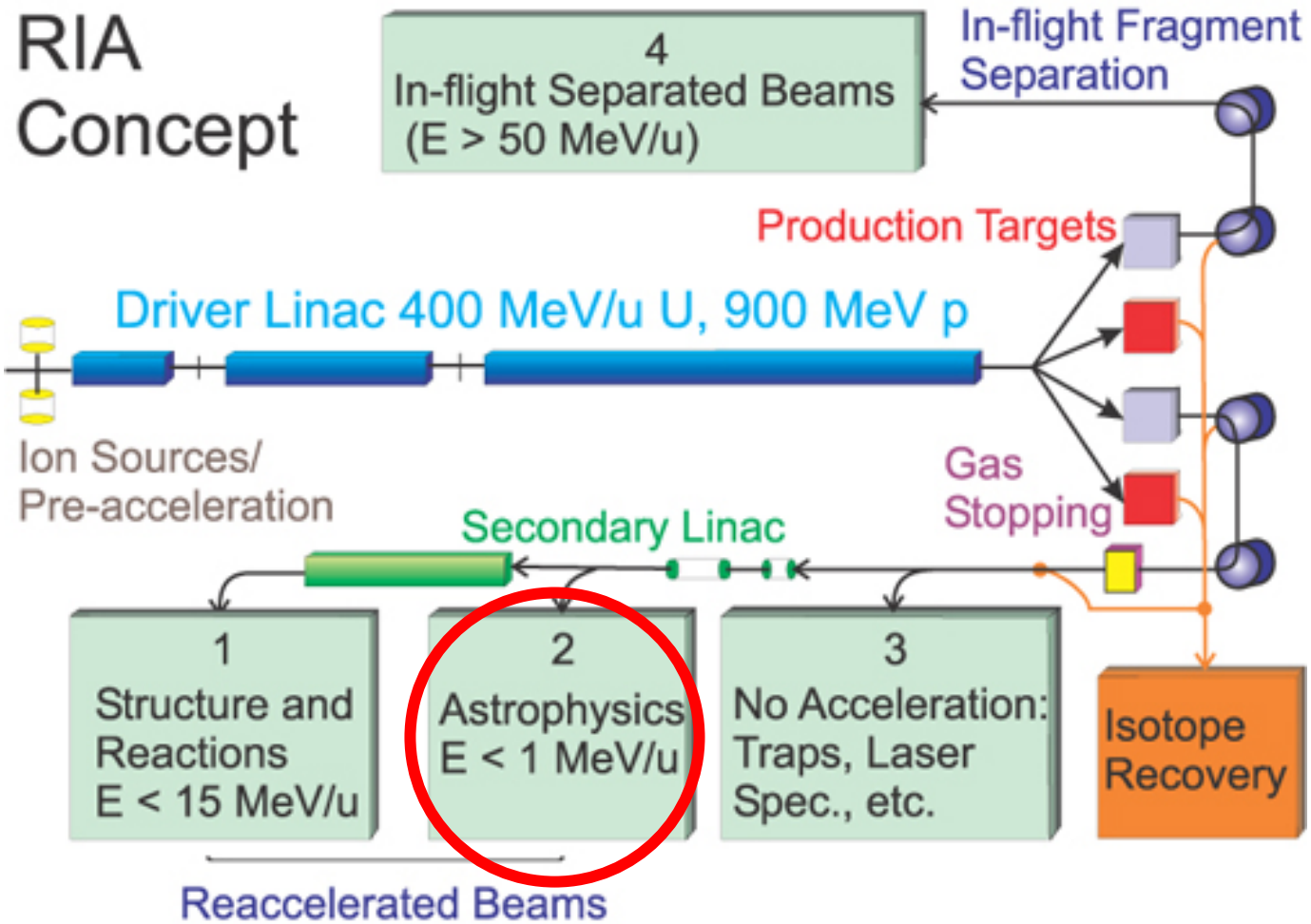

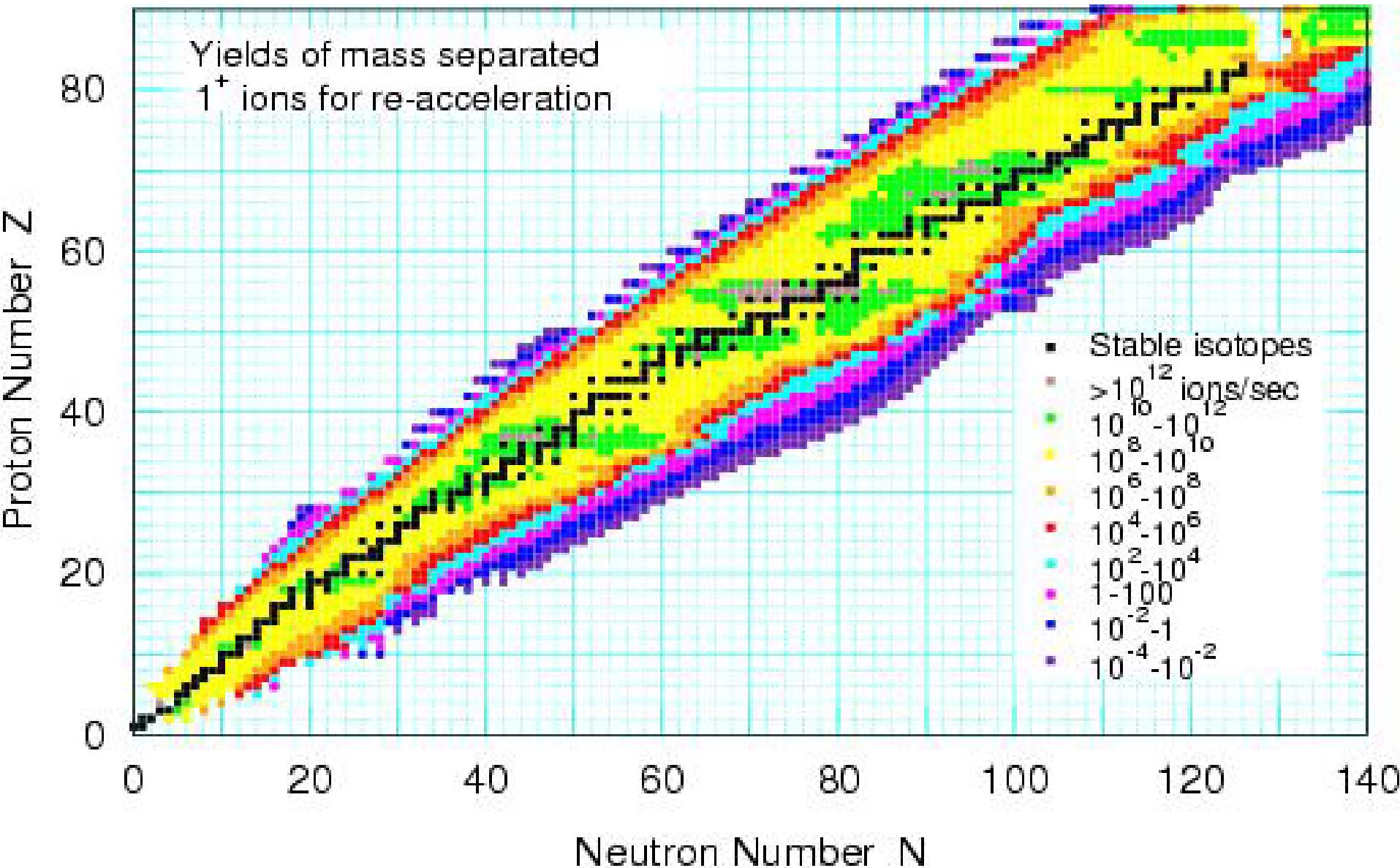
Yields of mass separated
1+ ions for re-acceleration
Stable isotopes
>10^12 ions/sec
10^10-10^12
10^8-10^10
10^6-10^8
10^4-10^6
10^2-10^4
1-100
10^-2-1
10^-4-10^-2
Proton Number Z
Neutron Number N
0
20
40
60
80
100
120
140

Expected Beam Intensities at RIA

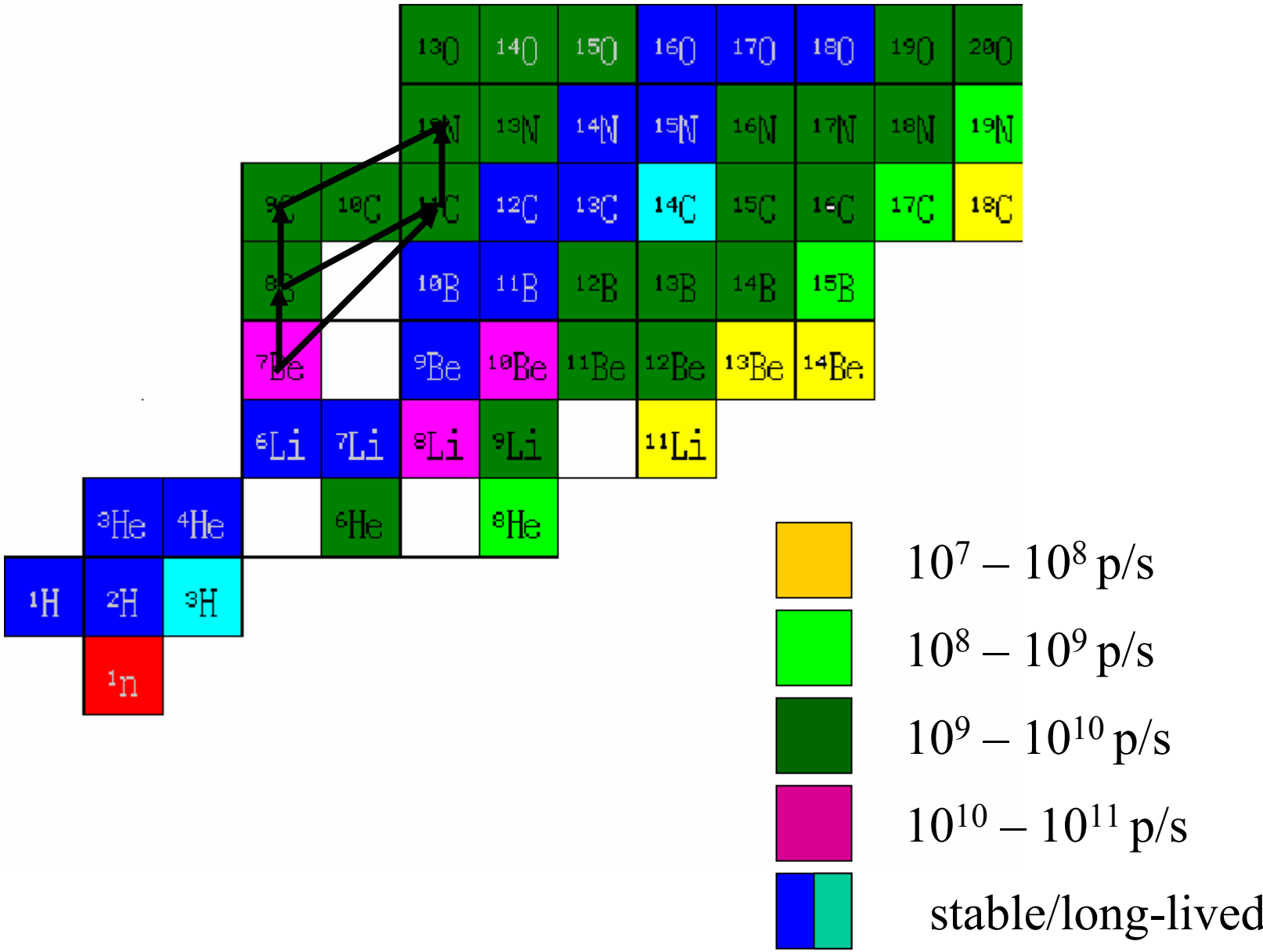

Collaborators

ANL: J. Greene, D. Henderson, R.V.F. Janssens, C. L. Jiang, F. Moore, G. Mukherjee, R. C. Pardo, T. Pennington, K. E. Rehm, J. P. Schiffer, S. Sinha, X.D. Tang

KVI, Groningen: R. H. Siemssen

LANL: A. Heger

Northwestern U.: L. Jisonna, R. E. Segel

U. Western Michigan: A. Wuosmaa

The HK-II Survey: A New Search for Very Metal-Poor Red Giant Stars

Jay Rhee

GALEX Science Team

California Institute of Technology, USA

Yonsei University, S. Korea

Abstract

The HK-II survey (Rhee, Beers, & Irwin, in preparation) originated as an extension of the original HK objective-prism survey of Beers, Preston, & Shectman (1985, 1992). HK-II was designed to discover a large sample of Very Metal-Poor (VMP) *red giant* stars with [Fe/H] = –2.0 by using *digitized* objective-prism spectra and 2MASS *JHK* colors; many of these stars were likely to have been missed in the original (visual) selection of metal-poor candidates due to an unavoidable temperature bias. Thus far, ongoing medium-resolution spectroscopic follow-up has newly confirmed some 110/130 red giants/sub-giants with [Fe/H] = –2.0 (Rhee & Beers, in preparation). Also, Rhee, Ivans, & McWilliam have recently initiated a program to obtain high-resolution spectroscopy for the HK-II VMP stars, and performed pilot observations with the KPNO 4m/Echelle & Magellan 6.5m/MIKE in May 2004. A preliminary analysis for six spectra indicates that one highly ([Eu/Fe] > +1.0) and two moderately (0.5 = [Eu/Fe] = 1.0) r-process-enhanced metal-poor stars may have been found. Here I give a comprehensive discussion of the HK-II survey; motivation, status report, and future plans.

J.R. acknowledges partial support for this work by NASA through the AAS Small Research Grant Program.

Outline

- Original HK objective-prism survey (HK-I)
  Beers, Preston, Shectman & collaborators

- The HK-II survey
  - Selection of metal-poor “giant” candidate
    Rhee, Beers, & Irwin
  - Medium-resolution Spectroscopy
    Rhee & Beers
  - High-resolution Spectroscopy
    - Rhee, Ivans, & McWilliam collaboration
    - HETRES (HET R-process Enhanced Star survey)
      Beers, Sneden, Lamsey, Rhee et al.

Why Look for Metal-Poor Stars?

- The lifetime of less massive stars > the age of the Galaxy

  ➔ Their chemical composition reflects the composition of the ISM in the early stages of Galaxy evolution (chemical history)

- The dynamical relaxation time is sufficiently long compared to the age of the Galaxy

  ➔ Kinematical properties of metal-poor stars contain information about the conditions of the gas at the time of star formation (dynamical history)

Key Idea of HK-I Survey

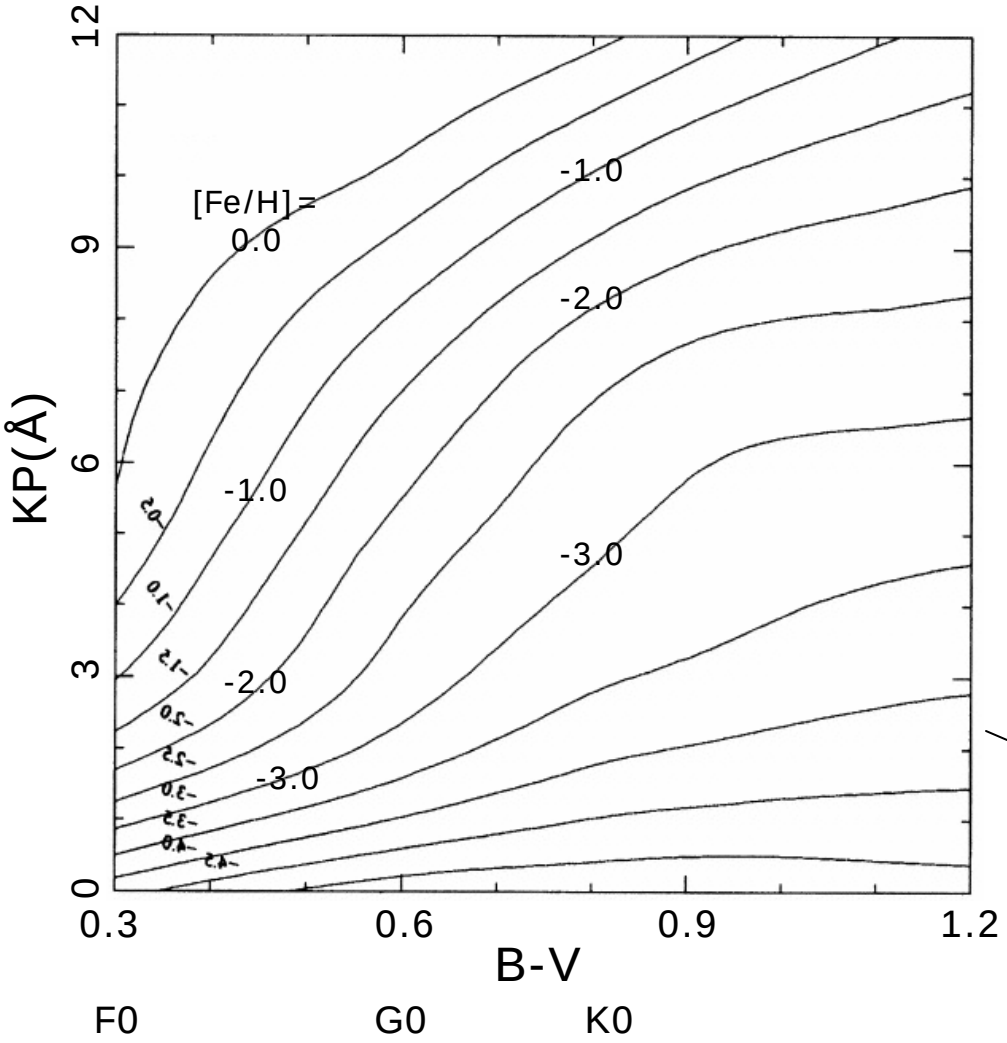

Ca II *K* line index is a good indicator of [Fe/H] !

Both dwarf and giant model

A Section of Typical Survey Plate

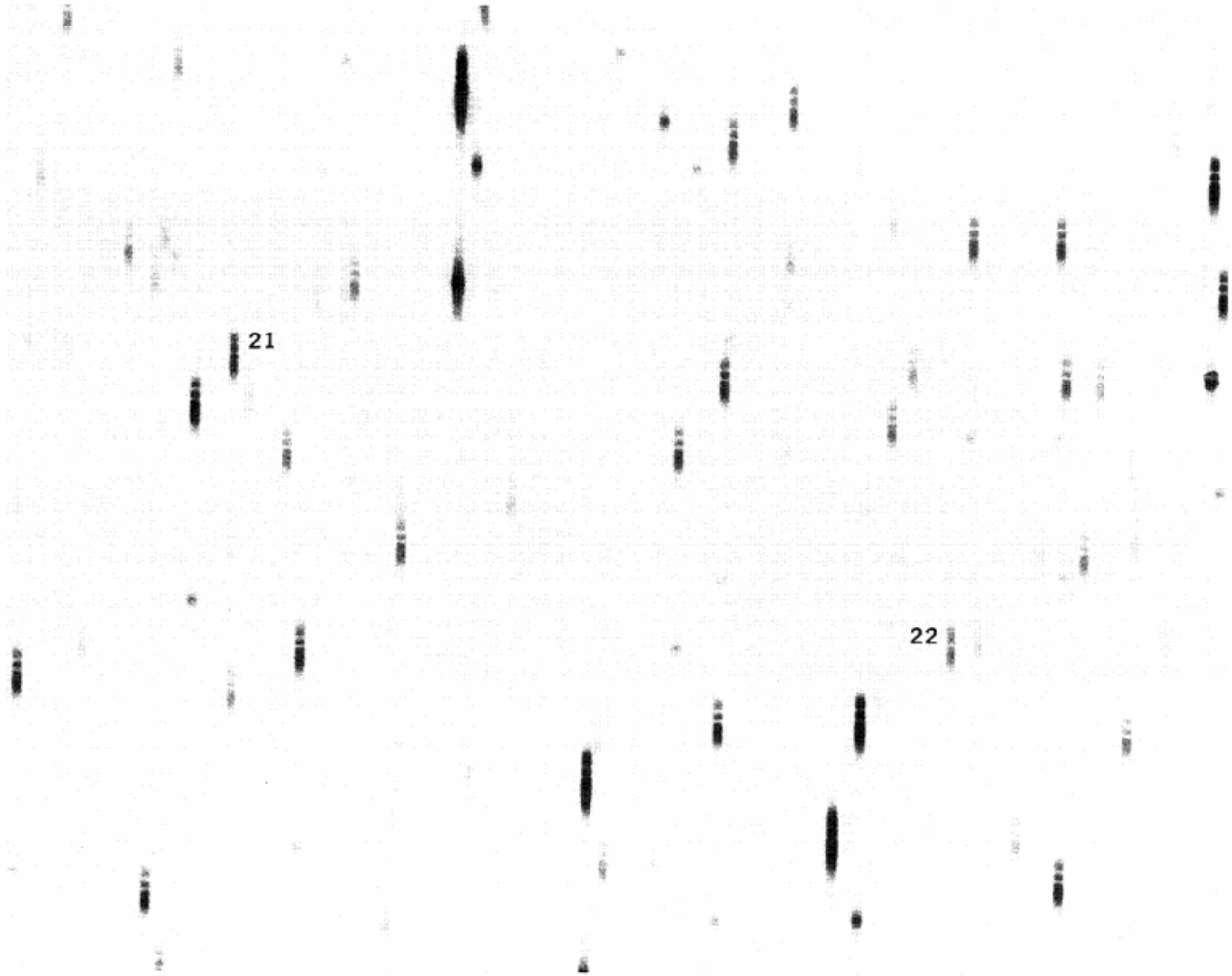

FIG. 2. An enlargement of the survey plate CS 22882. The spectrum of CS 22882-21, a typical low-metal star, and that of CS 22882-22, a halo AB star, are marked.

Beers *et al.* (see page 2090)

Objective-prism & interference filter produce spectra over a wavelength range of 150 Å, including the Ca II *H* & *K* lines.

"Visual" inspection of Ca II *K* line to sample metal-poor star candidates

HK Survey Area

11.0 = *B* = 16.0

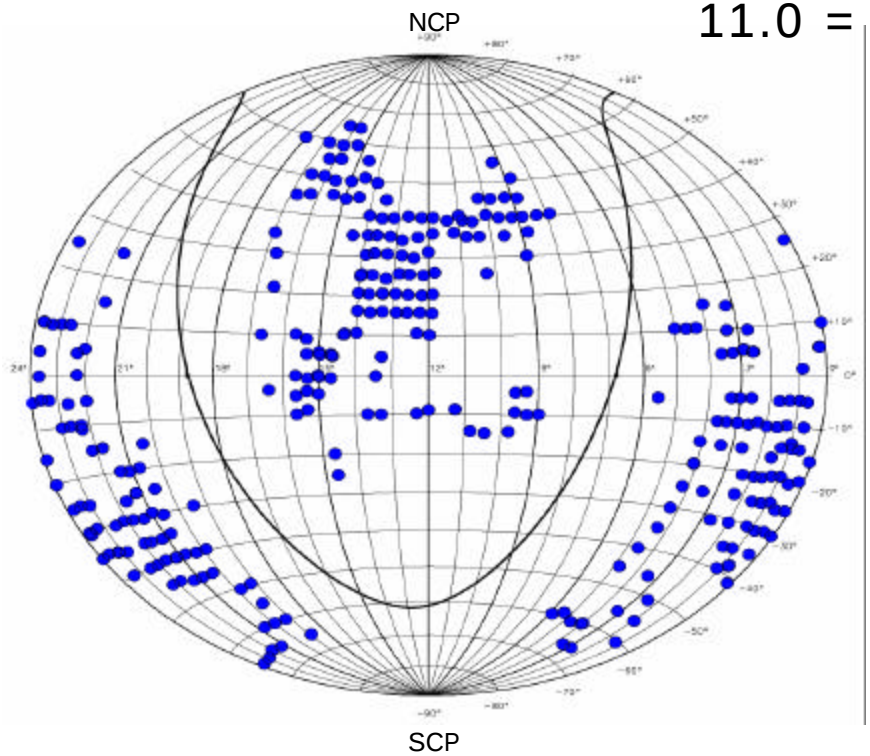

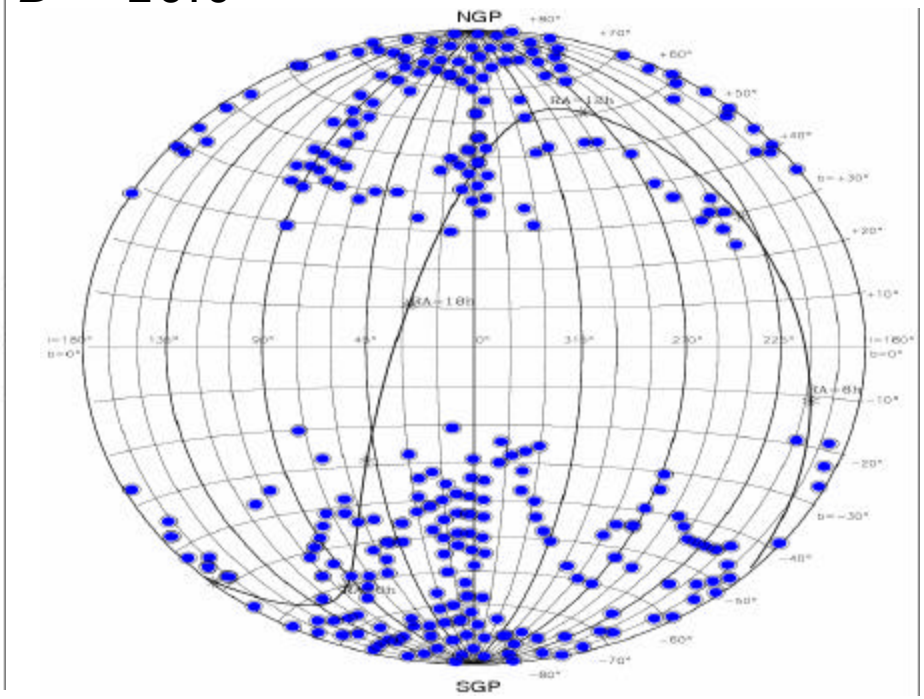

Some 300 wide-field (5° X 5°) plates which cover 7000 deg^2 (one-sixth of the entire sky) in the thick disk and halo of the Galaxy

An Achievement of HK-I Survey:
Distribution of Orbital Eccentricity

Eggen, Lynden-Bell, & Sandage (1962)

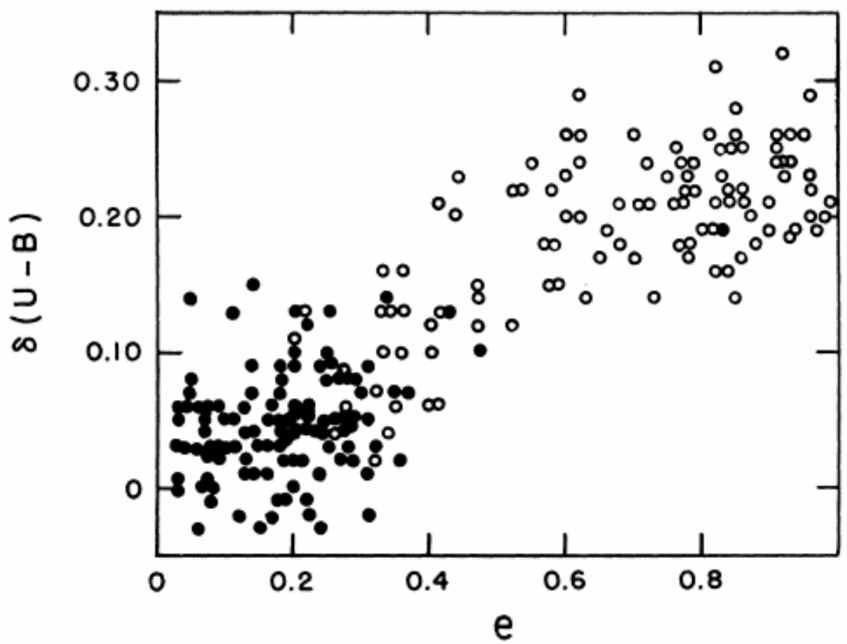

Correlation between [Fe/H] and e

Sample with proper-motion bias

Chiba & Beers (2000)
HK-I Stars

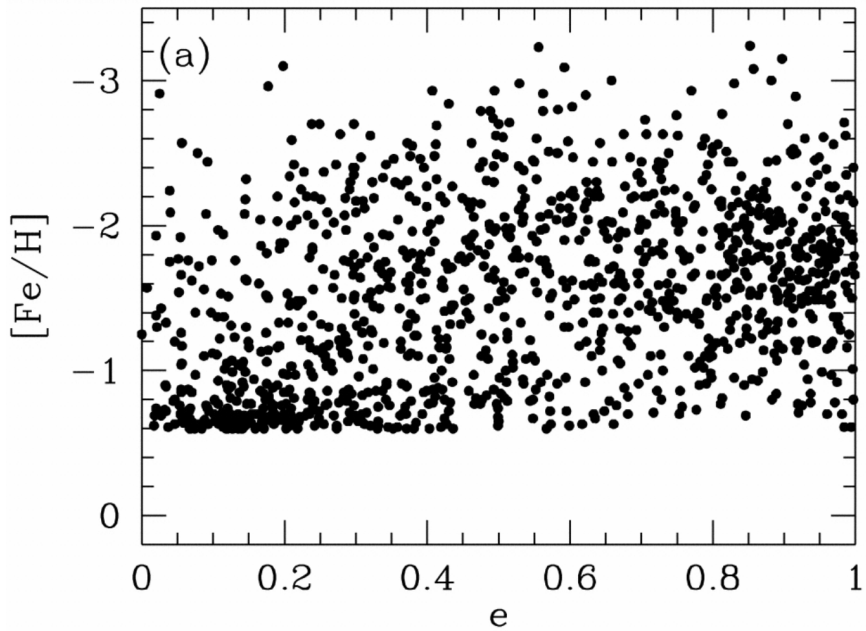

Little correlation between [Fe/H] and e !!!

Sample *without* proper-motion bias

Histogram of [Fe/H] for HK-I Stars

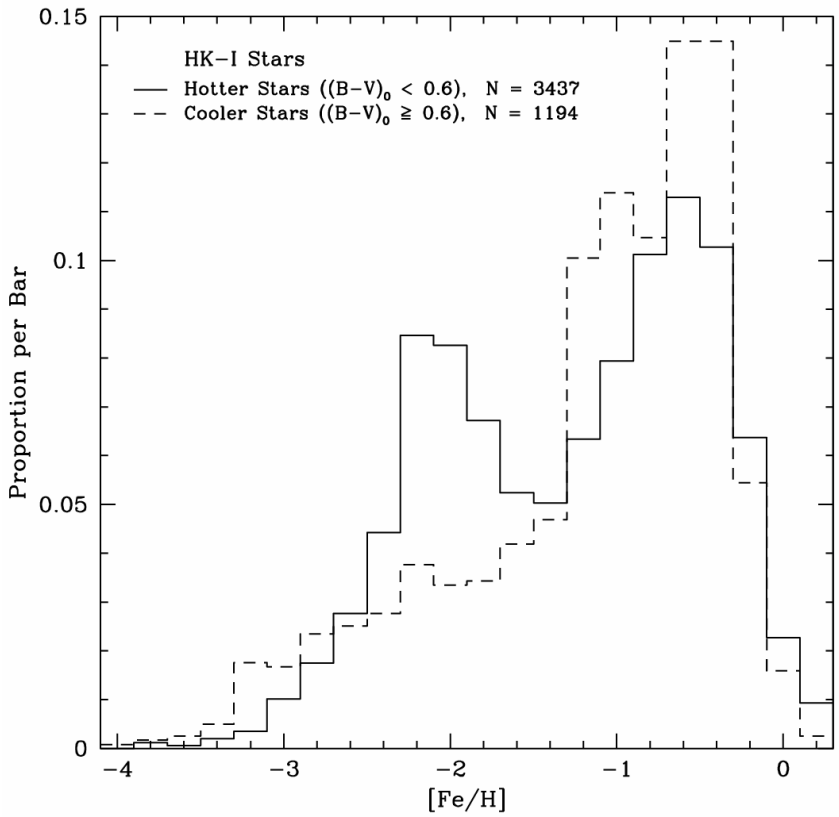

- Smaller number of cooler metal-poor stars (~1/3)
- Lower detection rate of Very Metal-Poor (VMP) stars with [Fe/H] = –2.0 for cooler region

➔ Why?

Relative Line Strengths

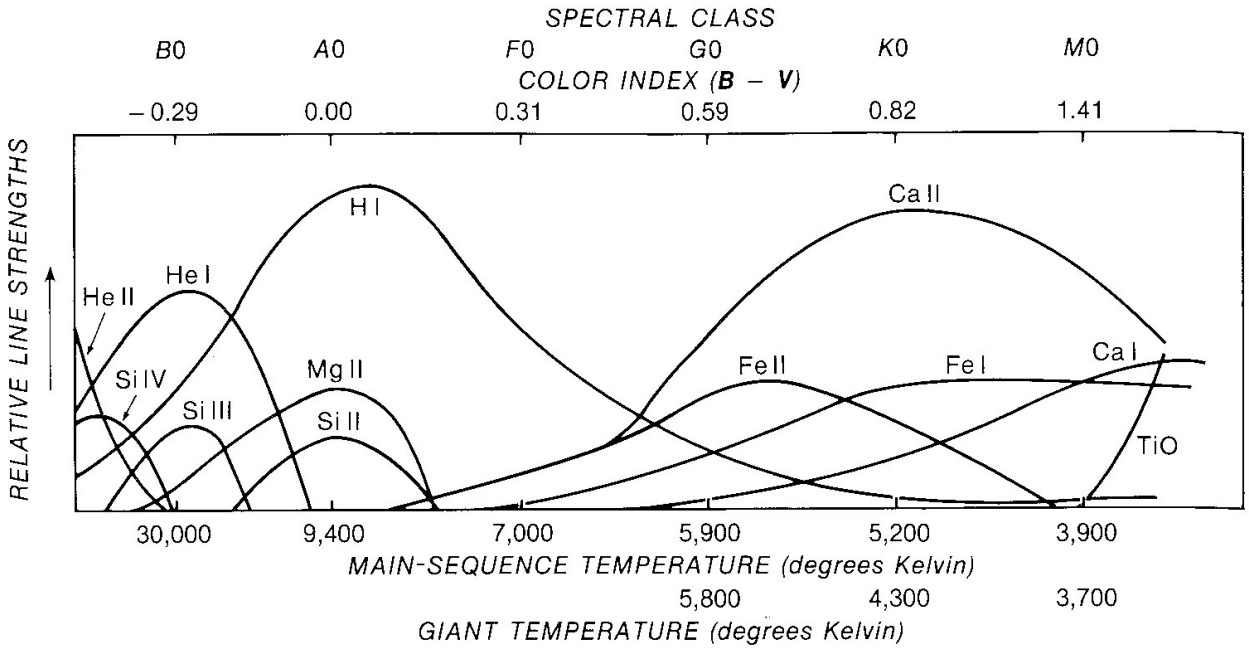

- At a given [Fe/H], Ca II *K* line strength is stronger for cooler stars.
- But, the original visual selection (HK-I) focused on the spectra with weak or absent Ca II *K* absorption line.

➔ Many of cooler stars (red giants) were likely to have been missed (temperature bias).

Necessity of Color Information

(in addition to Ca II *K* line strength)

Main-Sequence Turnoff Star
vs. Giant Star

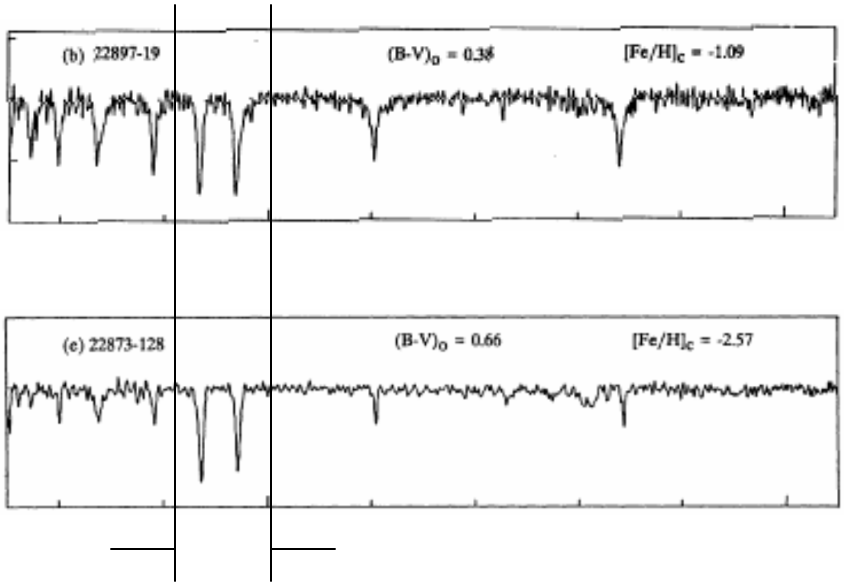

Spectral region used in the process of metal-poor star candidate selection

- If we have quantized Ca II *K* line strength and color information, we can recover a number of the missing VMP red giant stars.

➔ BTW, why are we so interested in the VMP "red giant" stars?

Why Look for VMP "Red Giants" ?

- Motivation of "HK-II" Survey

- **Wealth of Absorption Lines**
  Because the spectra of relatively bright, VMP red giants present much richer atomic and molecular lines than warmer stars, they are the ideal targets for high-resolution spectroscopic study of the relative abundances of numerous individual elements.

- **Numbers**
  In a magnitude-limited sample of objects, giants are expected to outnumber dwarfs by two orders of magnitude if we assume that the halo has a similar luminosity function of a typical globular cluster.

- **Luminosity**
  Because the HK-II giants are more (intrinsically) luminous than the majority of the previously identified HK-I stars (mostly dwarfs and sub-giants near the main-sequence turnoff), and therefore more distant, they will be excellent probes of the kinematics of both inner and outer halo.

- **Usefulness**
  NASA's SIM plans to use distant (>3 kpc) metal-poor K giants with V < 13 as astrometric reference stars. The HK-II giant star catalog may provide useful astrometric reference stars for SIM.

APM Scanned Spectrum & Positioning of *H* & *K* lines

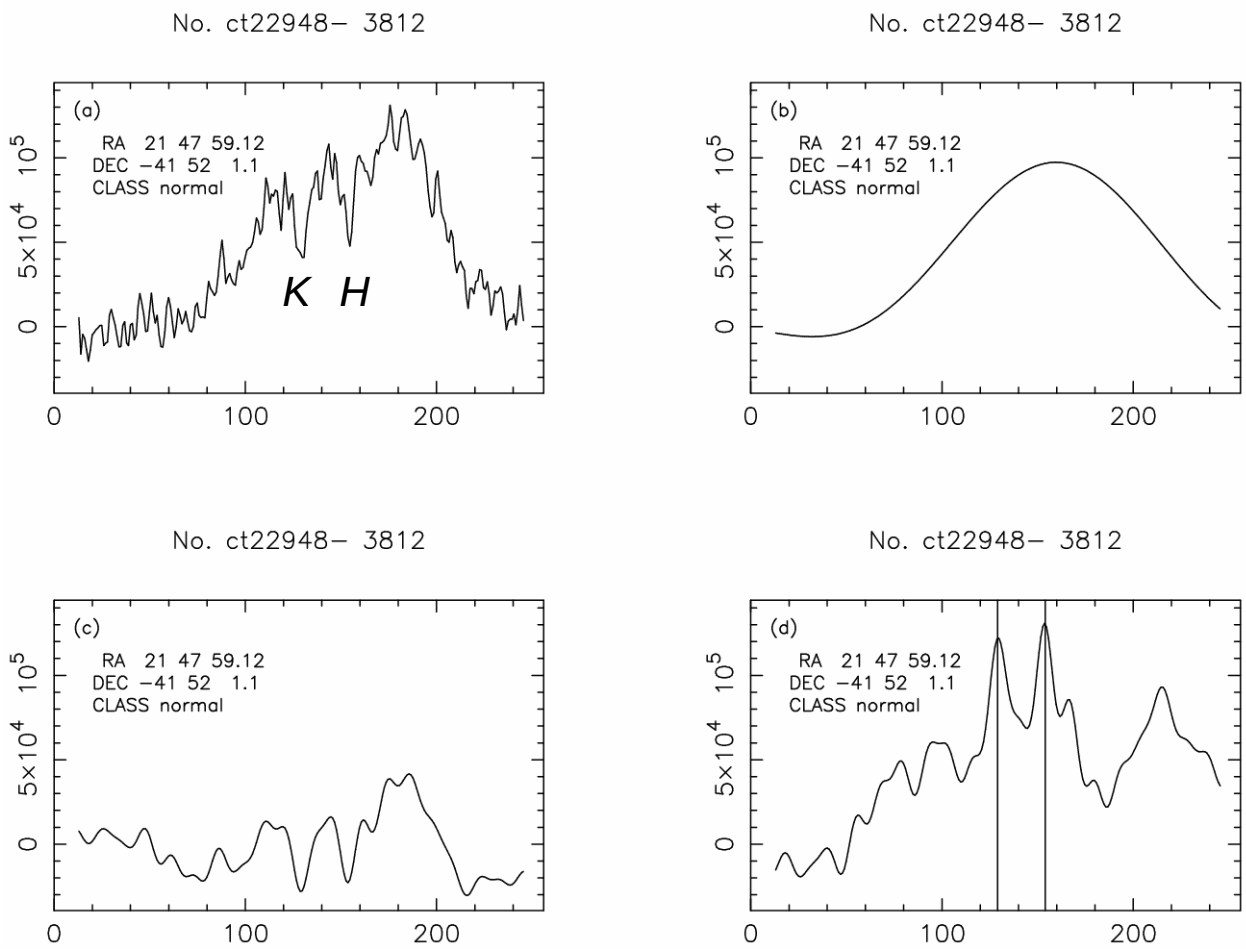

= (b) – (c)

Huge Amount of Digitized Spectra

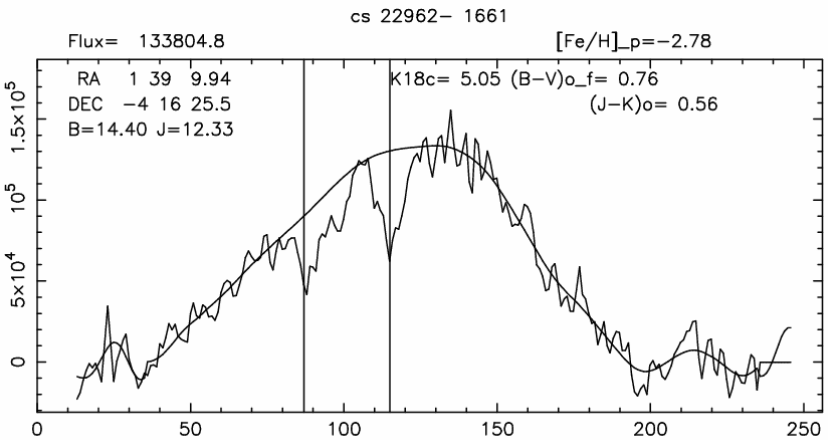

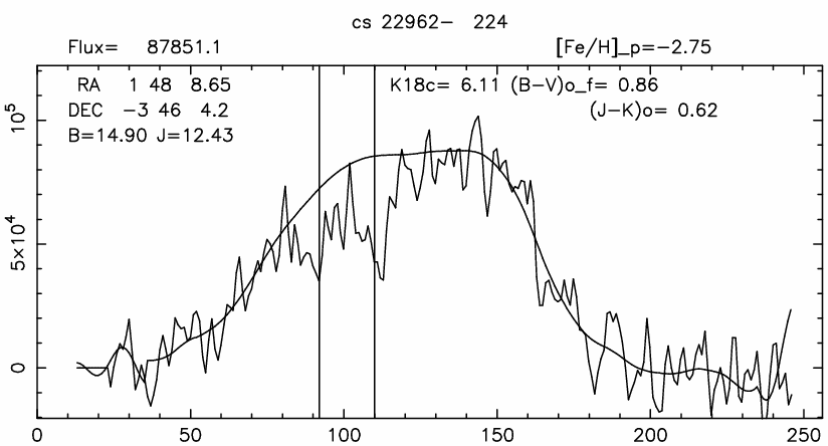

- 308 APM scanned photographic plates produce 1.5 million digital low-resolution spectra (over 150 Å).
- Crude estimation of *K* line index is made in automated fashion.

➔ How do we select VMP star candidates in an efficient manner?

HK-II VMP Star Selection Methodology

An Artificial Neural Network (ANN) is trained with known K18 & $(B\text{-}V)_o$ to predict [Fe/H] (1s = 0.13 dex).

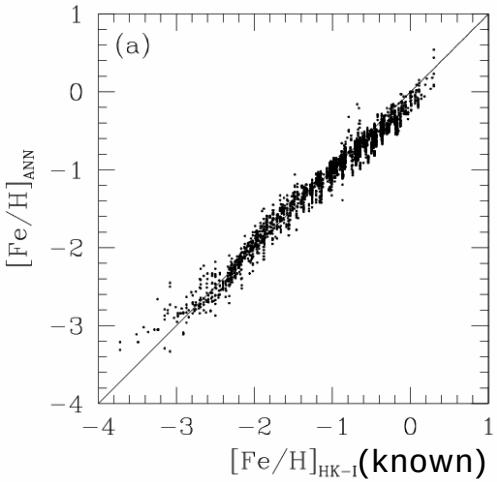

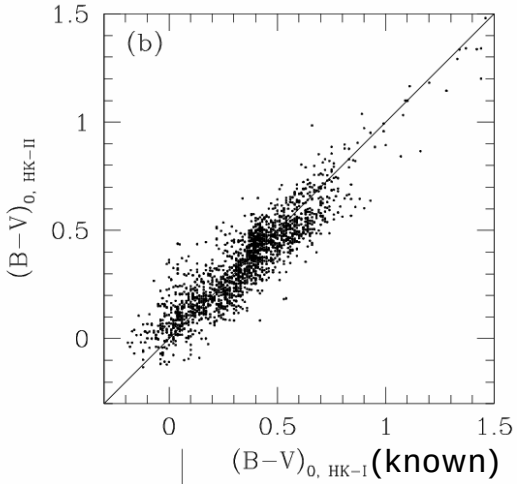

$(B\text{-}V)_o$ colors are estimated from 2MASS *J,H,K* Photometry using another ANN (1s = 0.08 mag).

K18 indices are derived from APM spectra (1s = 1.71 Å).

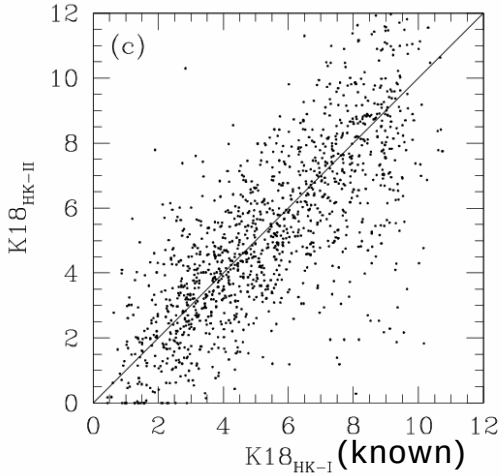

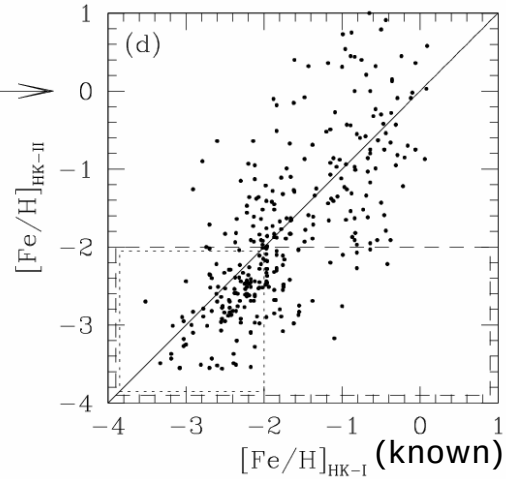

The trained ANN in (a) eats crude estimates of K18 and $(B\text{-}V)_o$ in order to predict [Fe/H] (1s = 0.70 dex).

Detection efficiency for VMP stars is expected to be about 65%.

Medium-Resolution Spectroscopic Follow-up using KPNO 2.1-m & CTIO 1.5-m

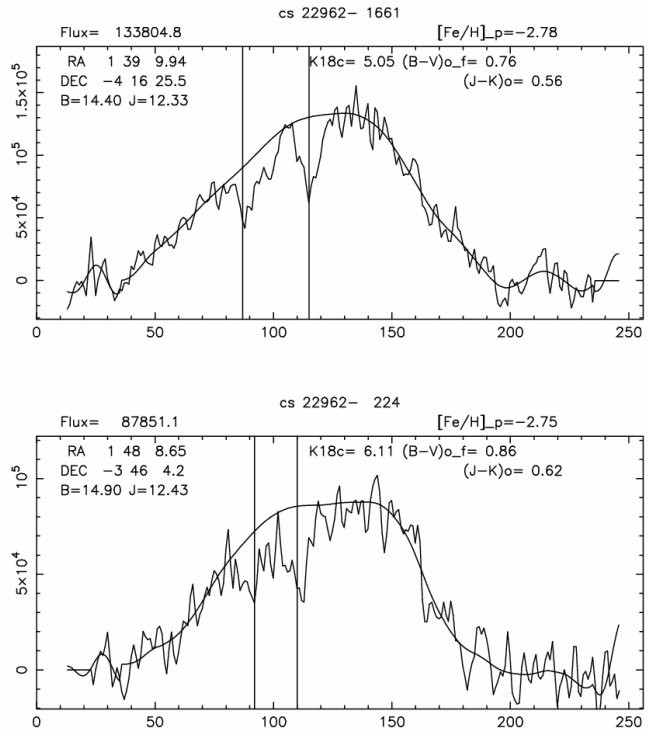

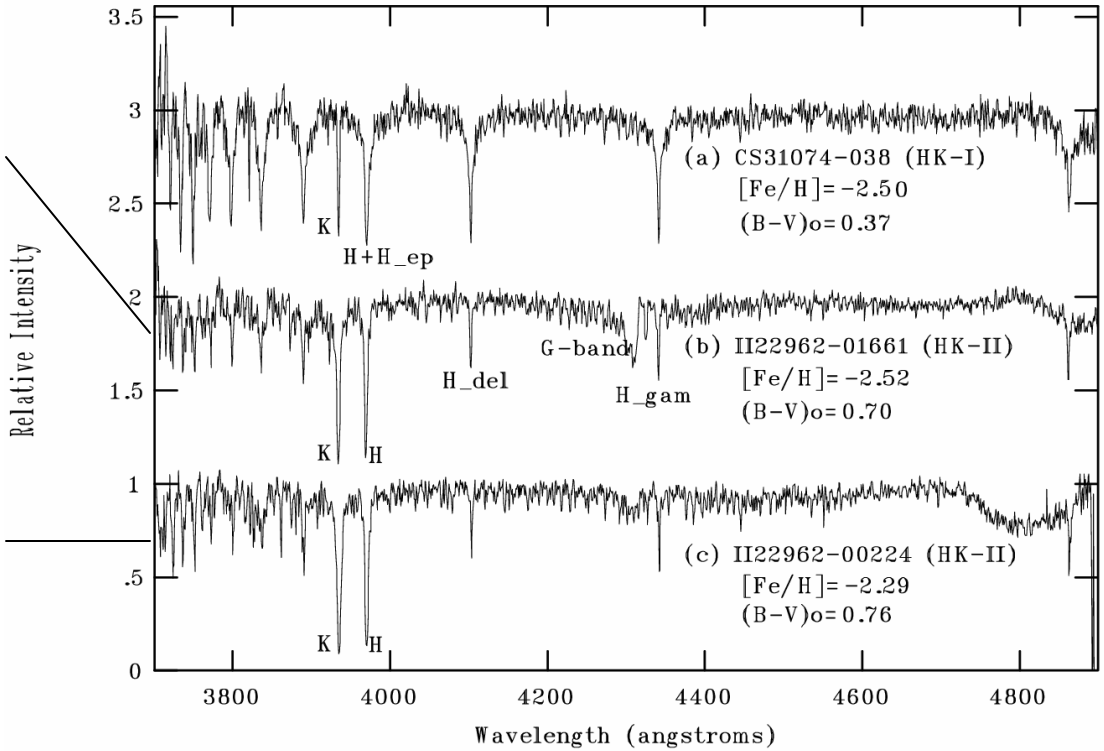

High Detection Efficiency for VMP Red Giant Star !

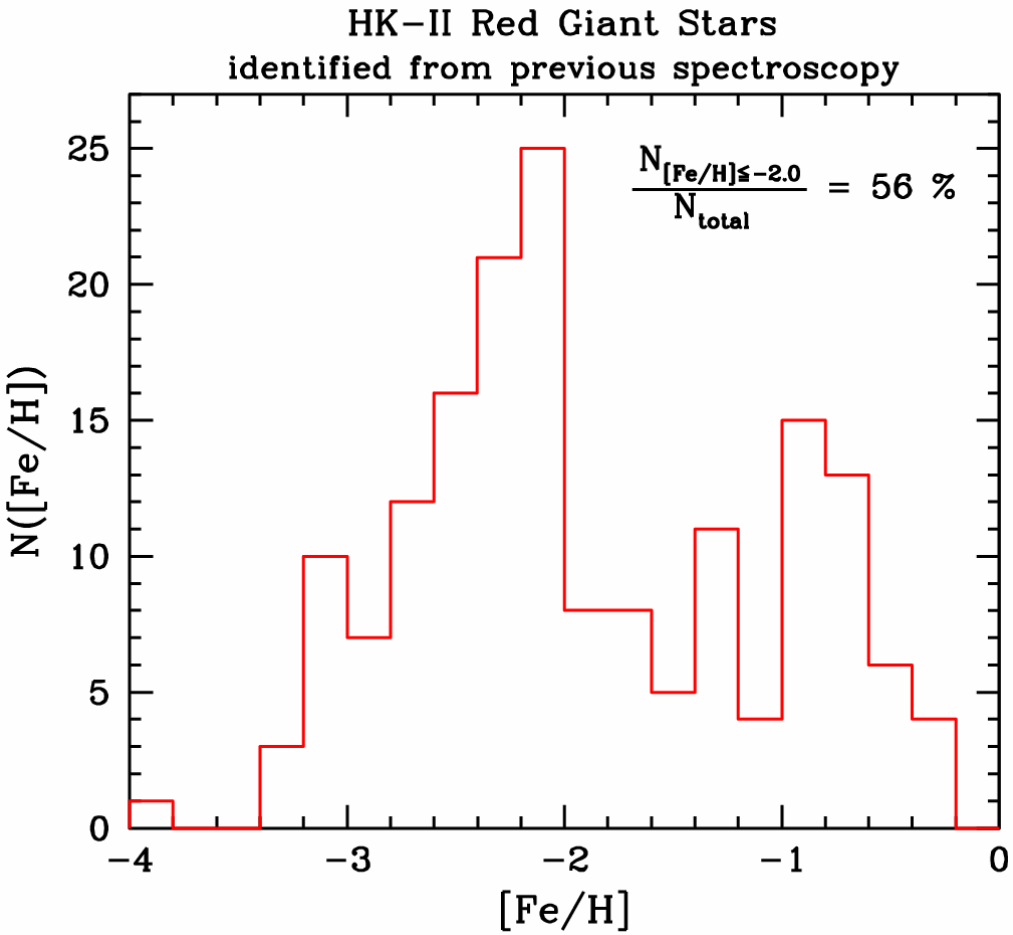

(as of summer 2003)

Not only for stars at high *b*, but also for those at lower *b*.

Kinematical Properties of HK-II Stars

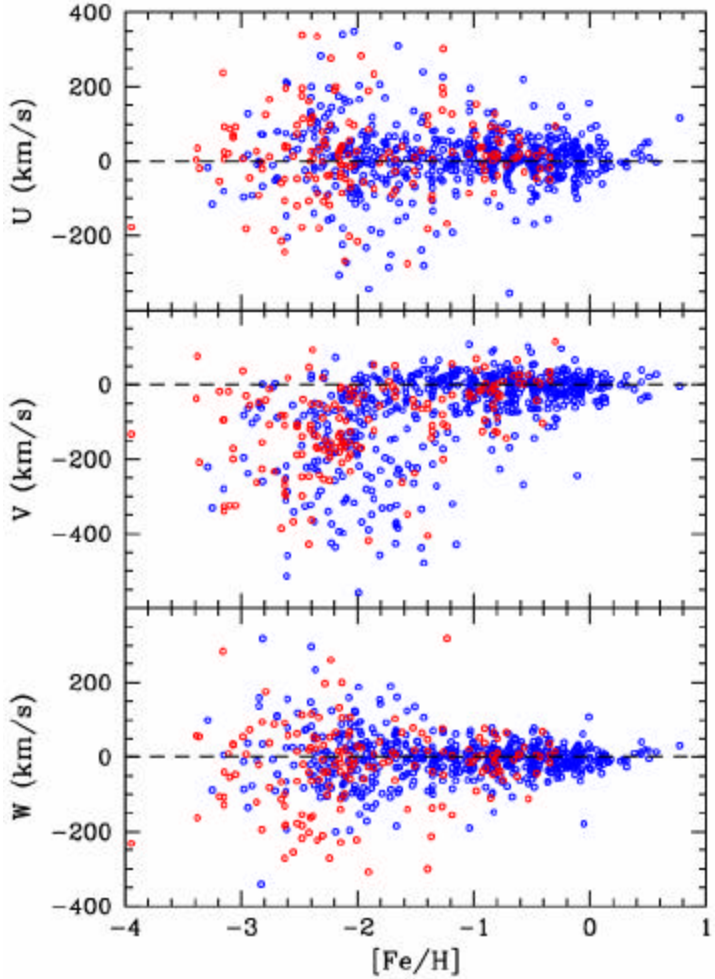

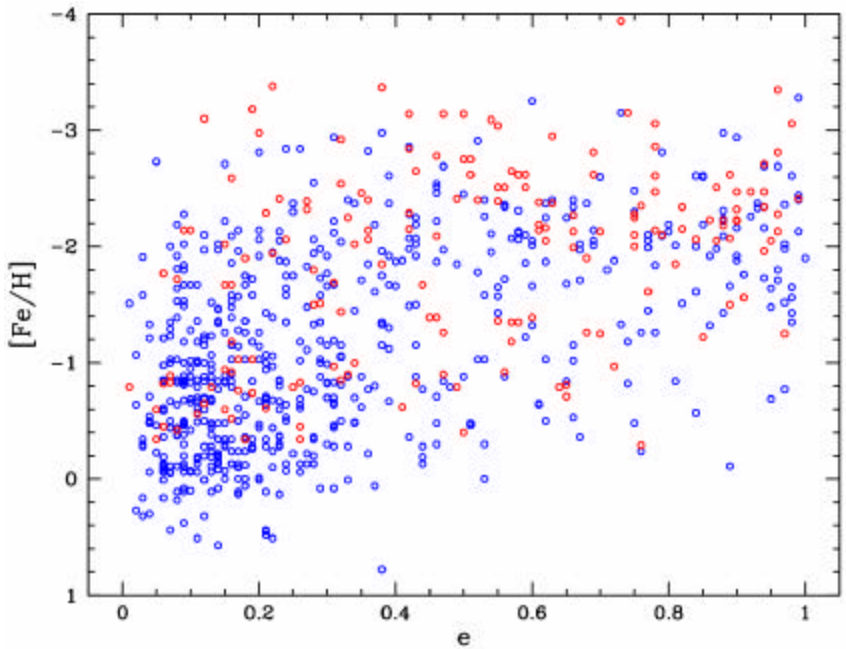

Again, little correlation between [Fe/H] and e

Existence of low-dispersion population even with [Fe/H] < –1.5

➔ Possible association with metal-weak thick disk

r- process or s-process enhancement, age dating, and so on

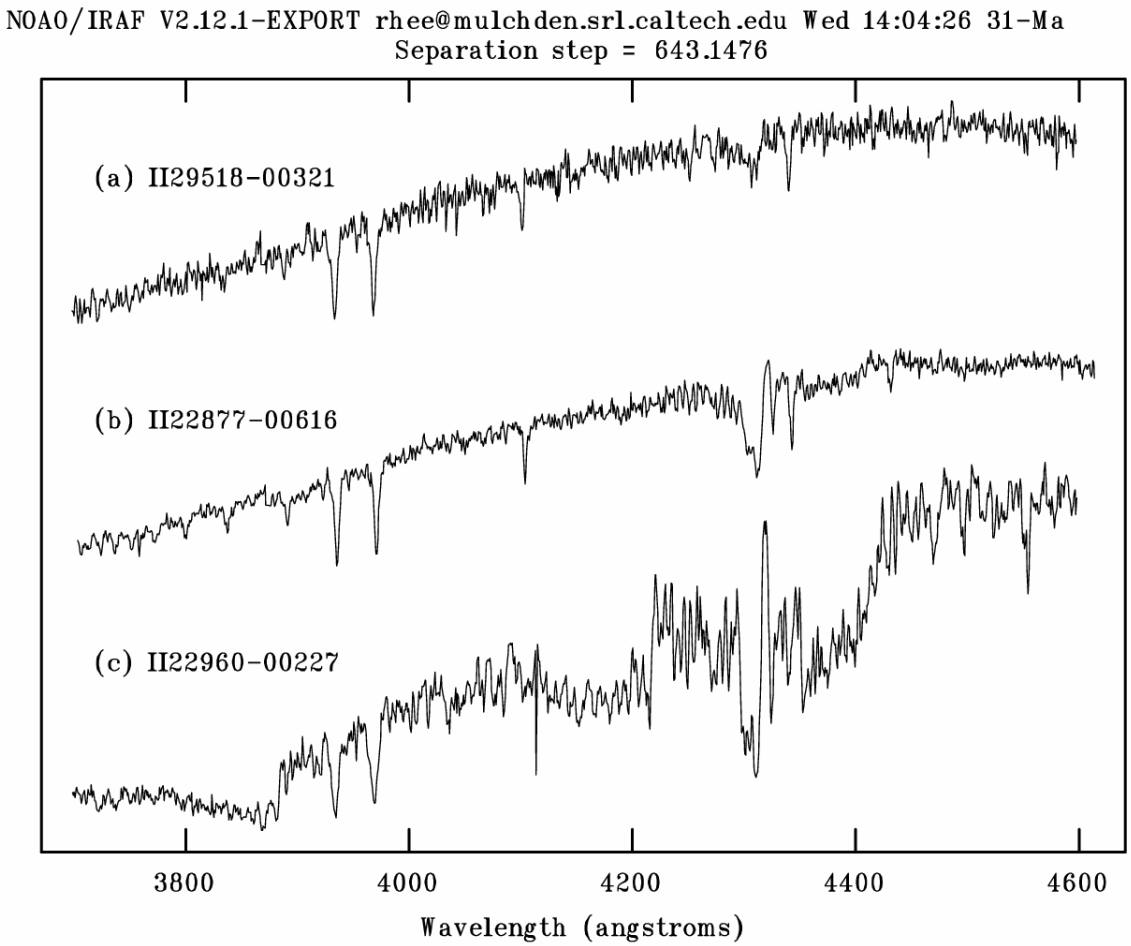

← r-process enhanced star "candidate" with measurable U II line at 3860Å (Note Th/U is more reliable chronometer than Th/Eu)

← carbon enhanced metal-poor stars; are s-process elements for these stars enhanced or not?

[Fe/H] = –3.3 ~ –3.1

Similar iron abundance, but quite different carbon abundance

High-Resolution Spectroscopic Follow-up (taken with KPNO 4-m & Magellan-II)

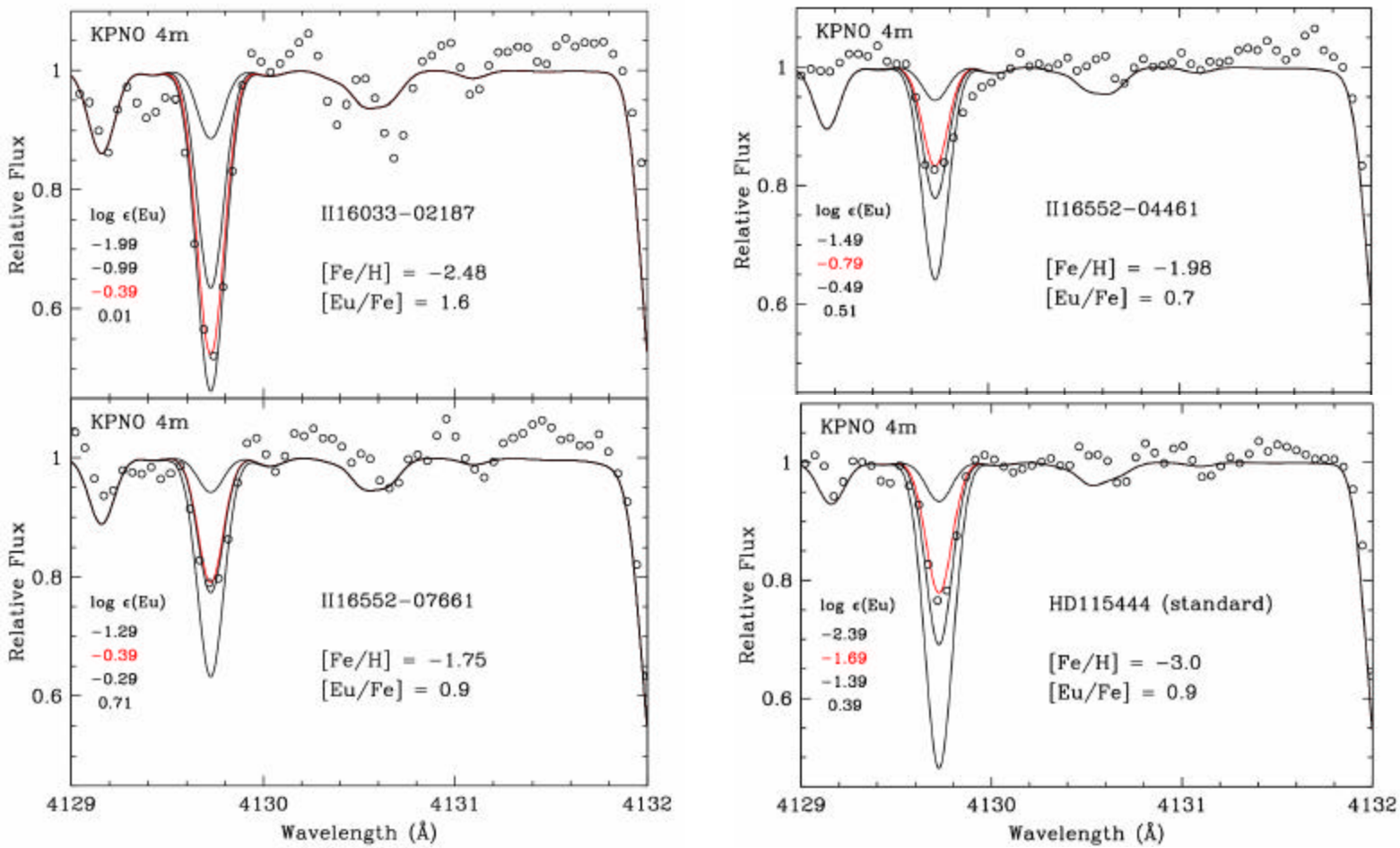

One highly ([Eu/Fe] > 1.0) and two moderately (0.5 = [Eu/Fe] = 1.0) r-process-enhanced metal-poor stars may have been found newly.

Summary

- HK survey is still (and needs to be) alive!

- Status
  - Some 235 APM scanned plates (of a total of 308 plates) have been fully reduced (~77%).
  - Medium-resolution spectroscopic follow-up has newly confirmed some 110/130 red giants / sub-giants with [Fe/H] = –2.0 in ~100 plates.
  - High-resolution follow-up spectroscopy has been initiated recently, and one r-process-enhanced metal-poor stars has likely been found.

- Things to do
  - Completion of reduction for the remaining 70 plates
  - Selection of 1500 VMP star candidate from the remaining 200 plates (7-8 cands/plate), and mod-res spec follow-up for the stars
  - High-dispersion spectroscopy
    - Rhee, Ivans, & McWilliam collaboration
      Comprehensive abundance analysis for data taken at KPNO 4-m & Magellan
      More observations – CTIO 4-m in Aug. & Magellan (NOAO public time) in Dec
    - HET RES (HET R-process Enhanced Star survey)
      of Beers, Sneden, Lamsey, Rhee et al.
      "Quick" survey to identify r-process enhanced VMP star

The Lyman-alpha Forest at High Redshifts
Structure and Abundances

Wallace L. W. Sargent

California Institute of Technology

Collaborators:

A. Boksenberg (IOA, Cambridge), M. Rauch (OCIW), R. Simcoe (MIT)

August 9, 2004

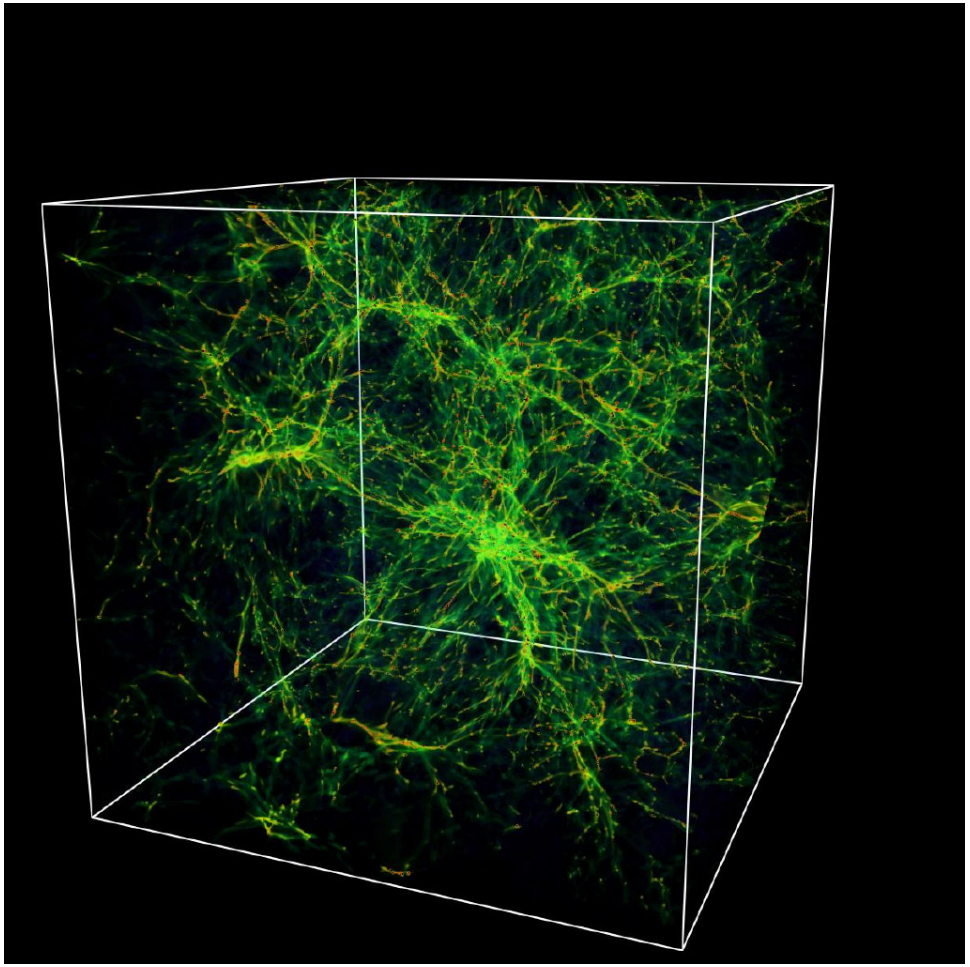

The *Cosmic Web*

Distribution of baryons at z = 4 in a 25 Mpc cube.

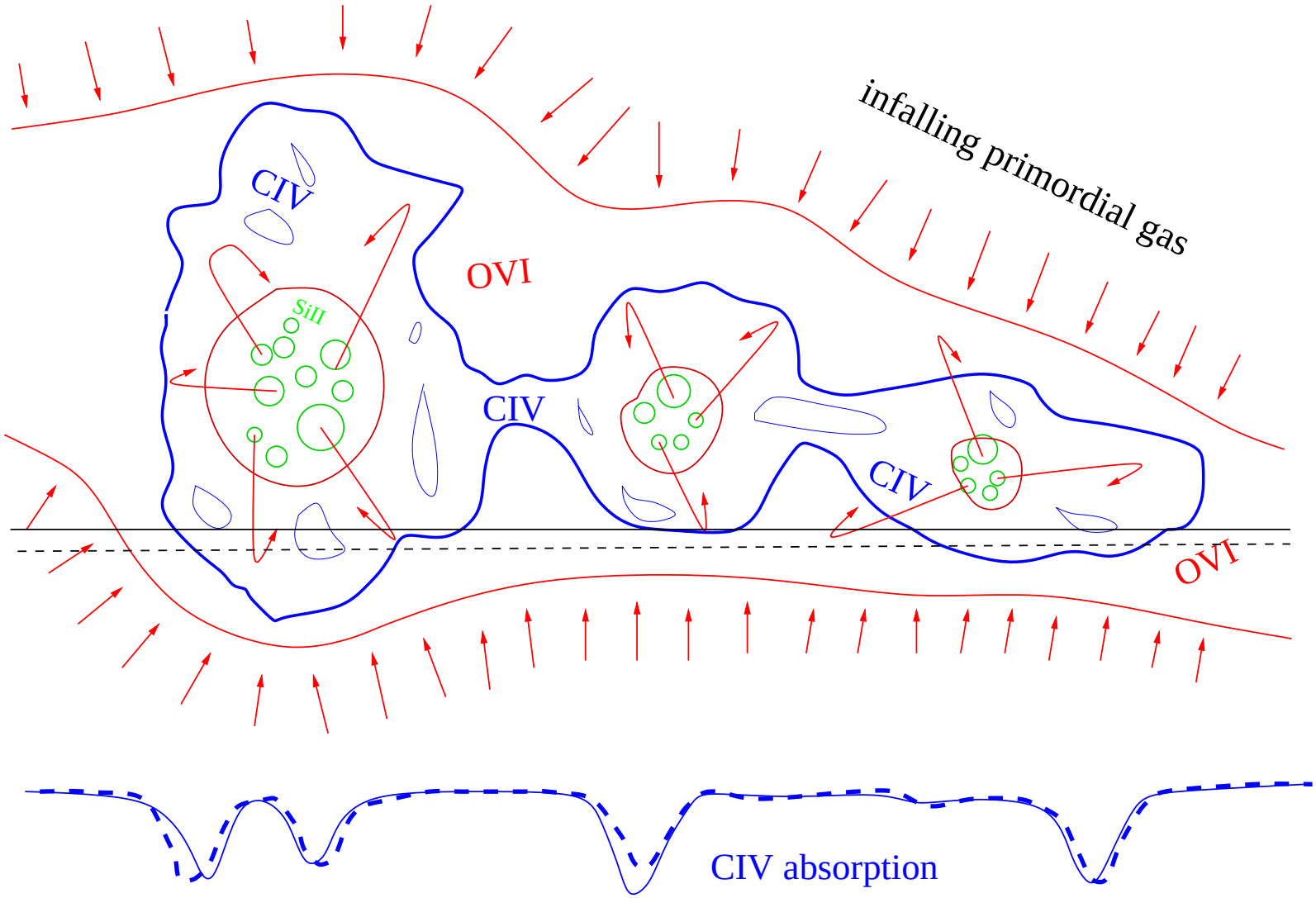

The distribution of gas around protogalaxies at high z

Abundances from QSO absorption lines

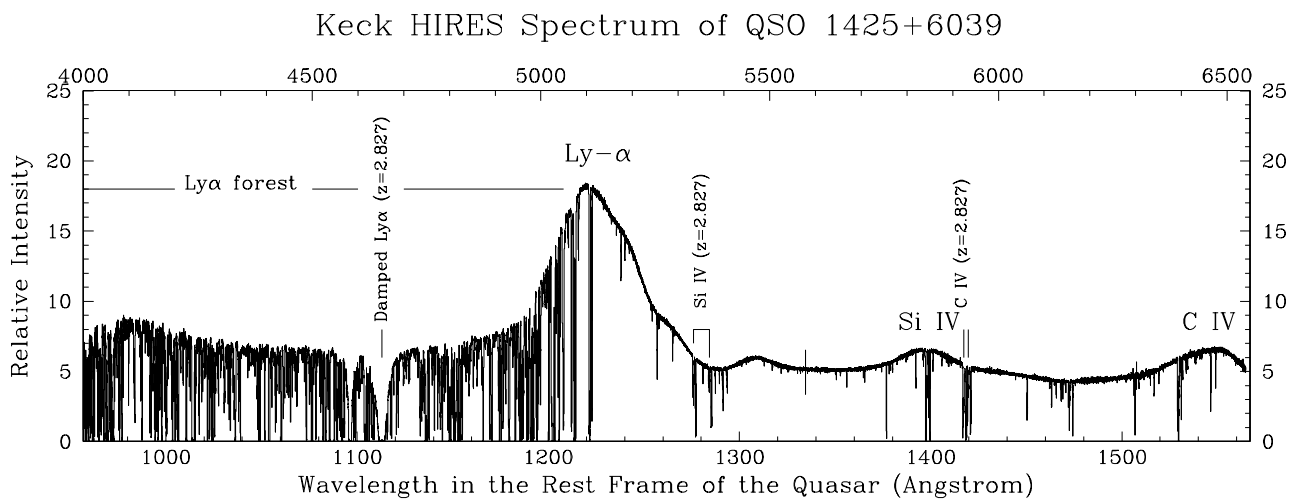

The universe at $z \sim 3$

- Luminous objects: QSOs and the Lyman Break Galaxies– density peaks in the baryon distribution.
- Most of the baryons in the universe are in the IGM.
- i.e. in Lyman-alpha forest regions with N(H I) $\sim 10^{13-14}$ cm^{-3}.
- Mean $n(H) \sim 10^{-5}$ cm^{-3}.
- Ionizing photons (from QSOs) $n_\gamma \sim 10^{-5}$ cm^{-3}.
- IGM highly ionized (1 part in 10^5 neutral).
- Main observable heavy element ions C IV λ1548-50, Si IVλ 1397-1403, O VI λ1032-1037.

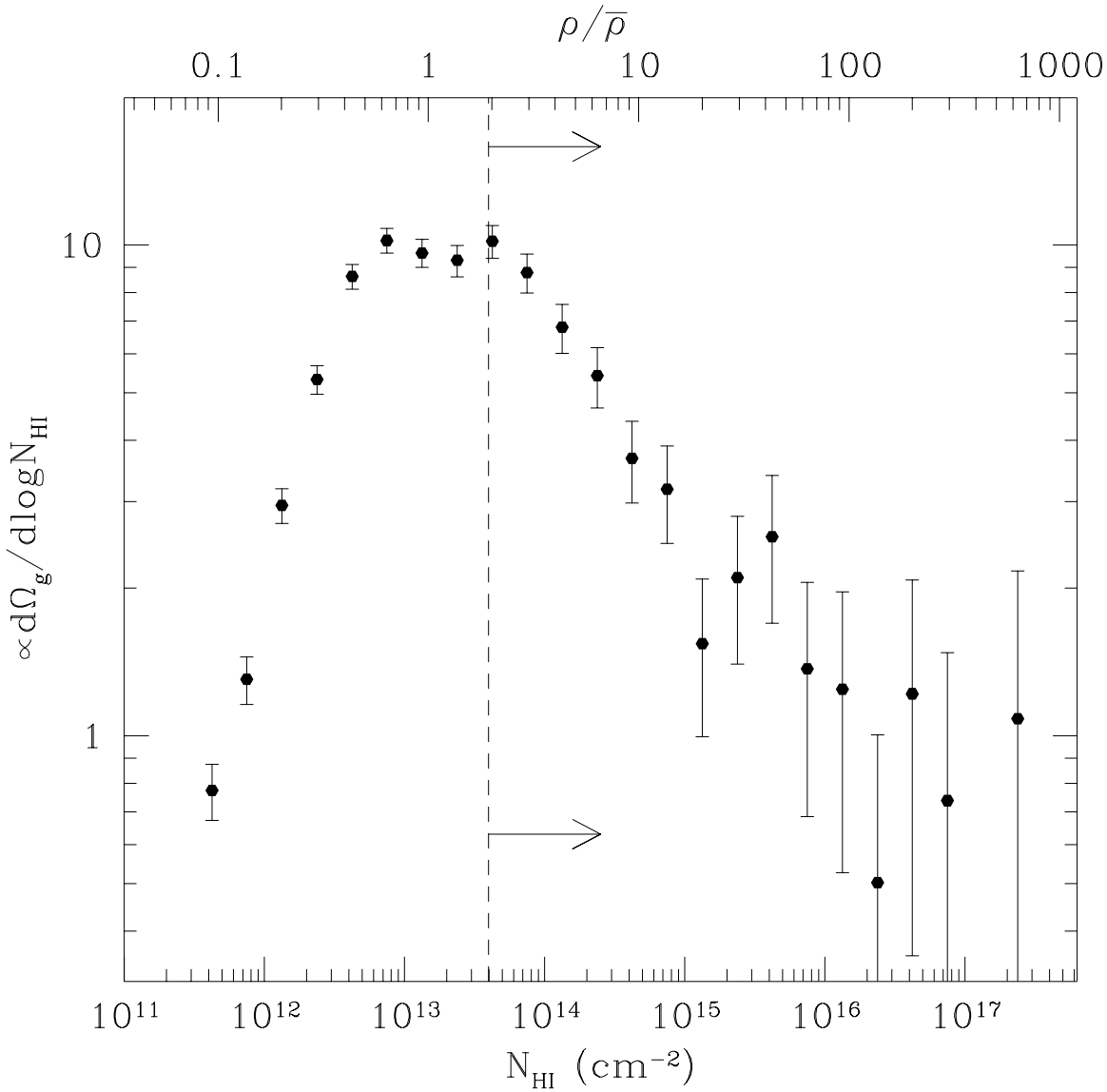
$\rho/\overline{\rho}$
0.1
1
10
100
1000
10
1
$\propto d\Omega_g/d\log N_{HI}$
10^{11}
10^{12}
10^{13}
10^{14}
10^{15}
10^{16}
10^{17}
N_{HI} (cm^{-2})

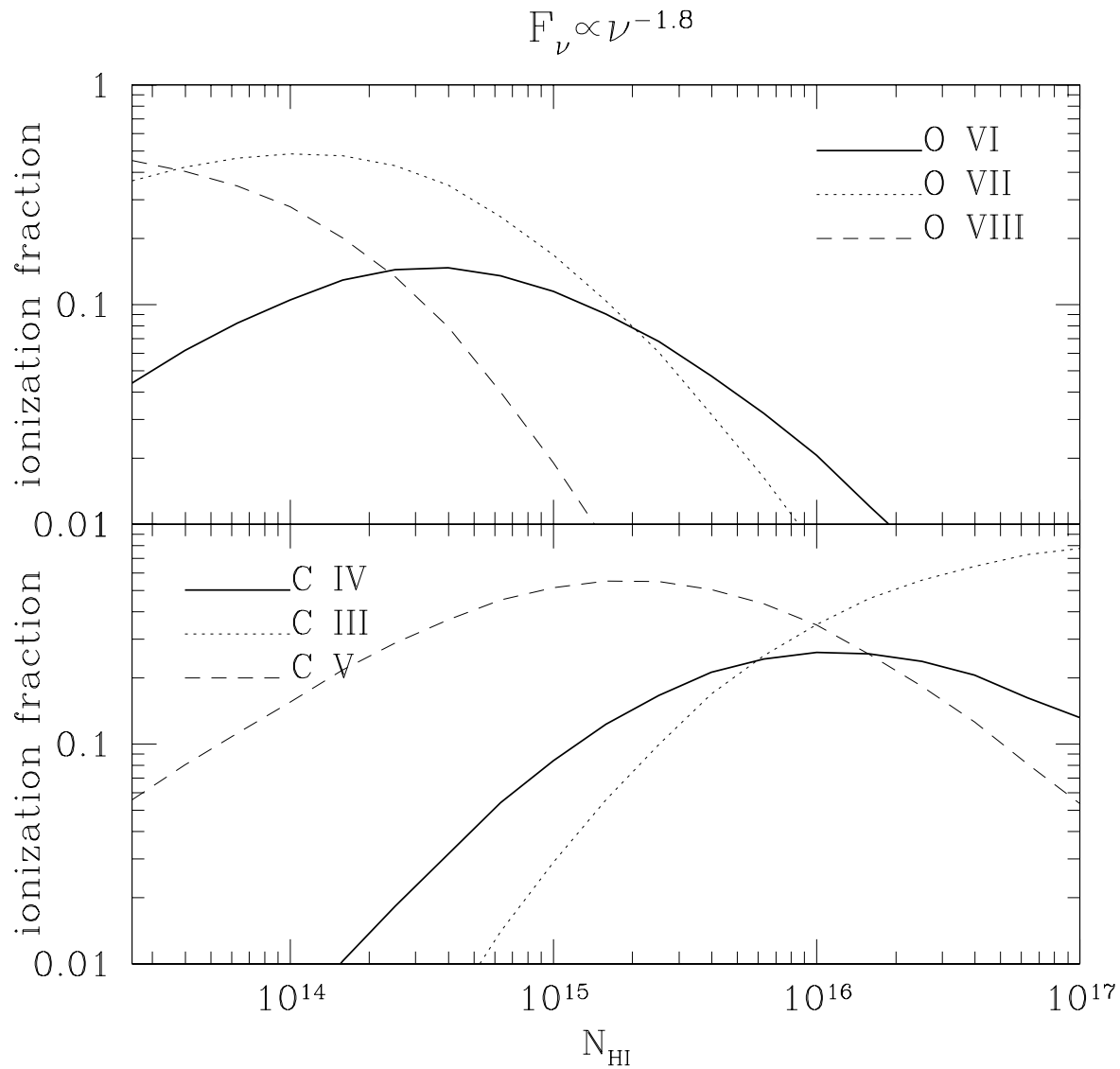
$F_\nu \propto \nu^{-1.8}$
1
0.1
0.01
ionization fraction
O VI
O VII
O VIII
C IV
C III
C V
10^{14}
10^{15}
10^{16}
10^{17}
N_{HI}

C IV in galaxies and the IGM

- C IV λ1548, 1550 doublet is most abundant ion outside the Lyman-alpha forest: photoionized.
- Early Keck HIRES work showed C IV absorption line systems have [C/H] $\geq$ -2.5 down to column densities log N(H I) $\sim$ 14.3. A surprising result.
- Current effort to detect C IV at log N(H I) $\leq$ 12.5
- Statistical approaches: "pixel method" and "stacking" regions where C IV is expected from Lyman-alpha lines.
- Direct detections in very high S/N spectra

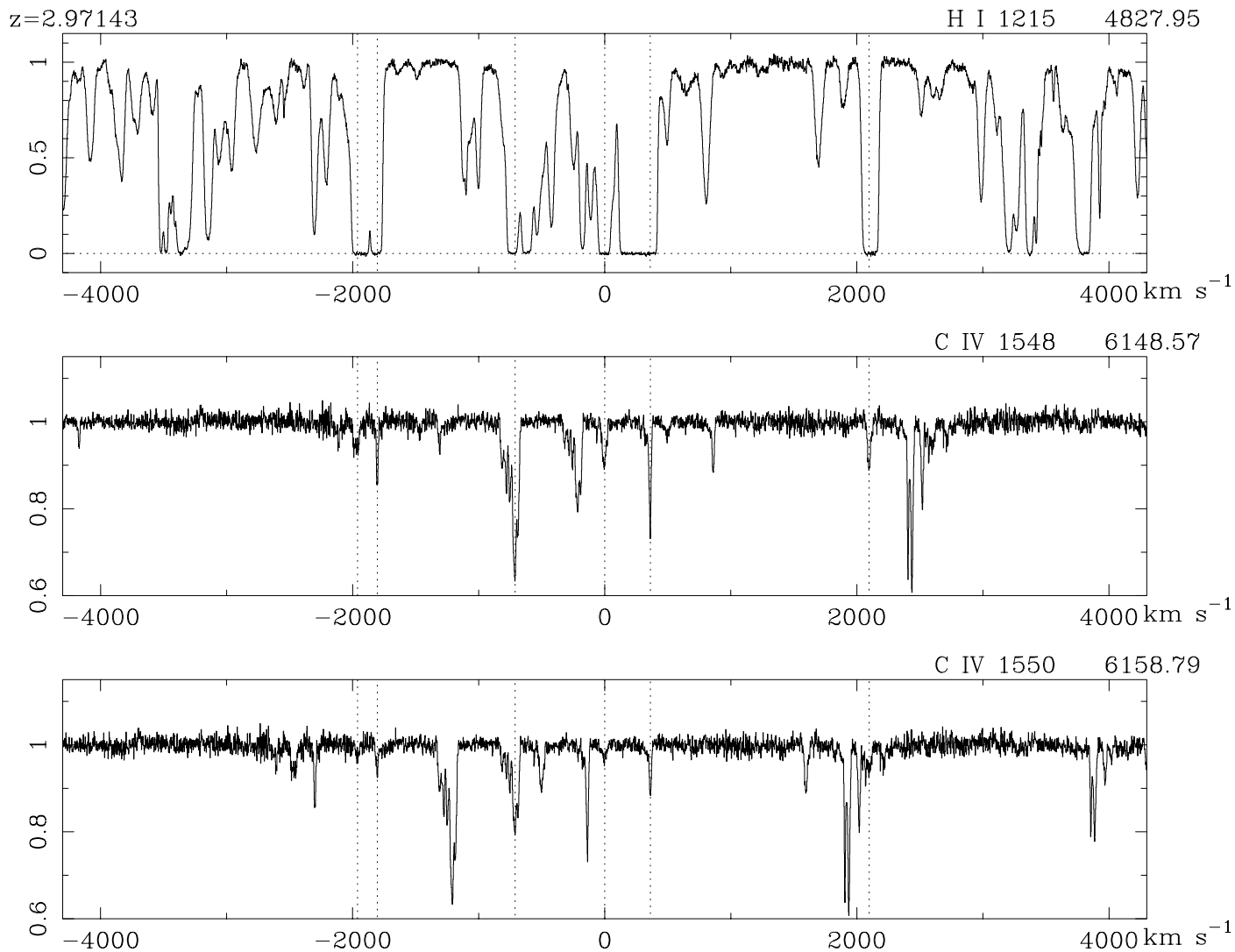

Examples of C IV associated with Lyman-alpha forest lines

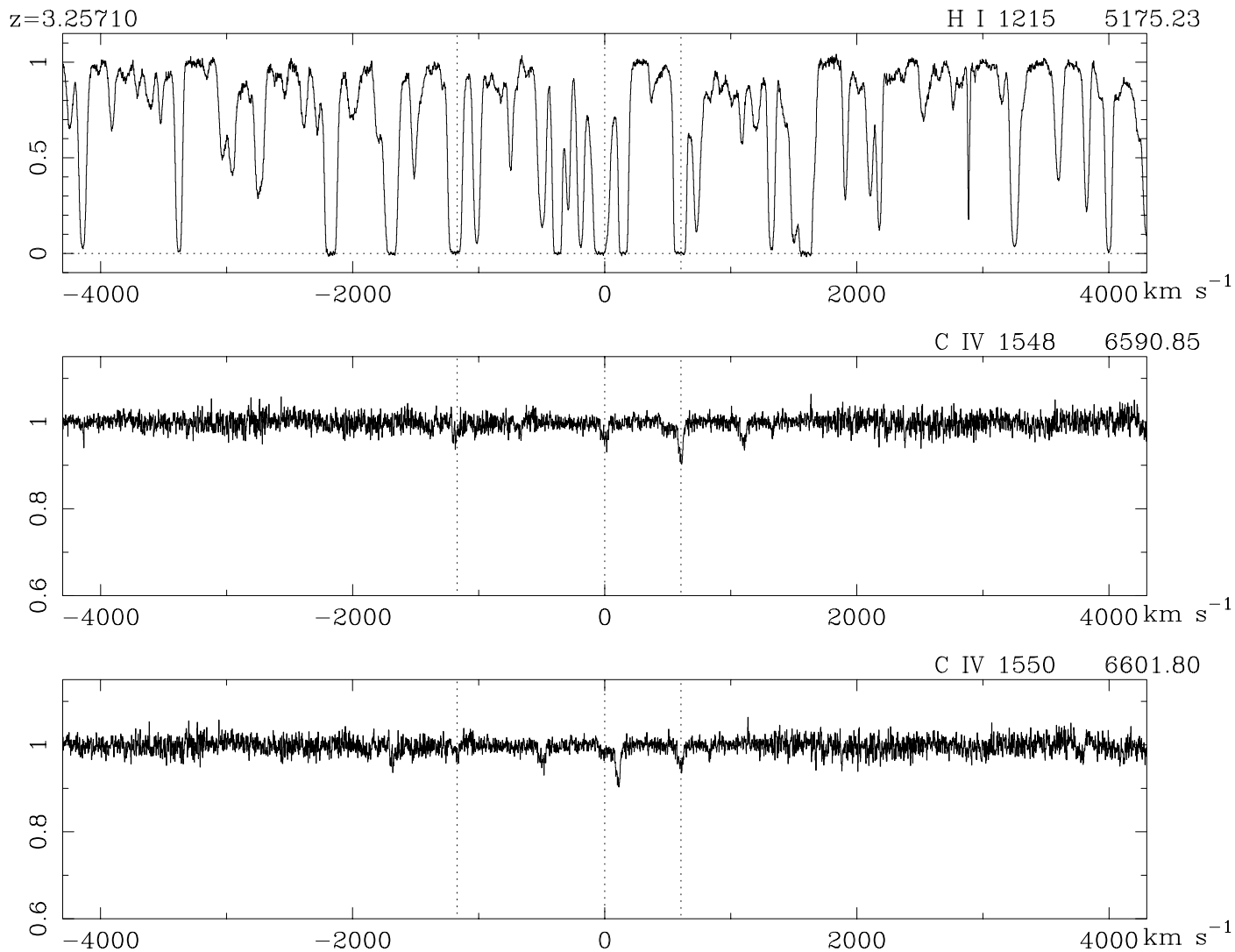

Examples of C IV associated with Lyman-alpha forest lines

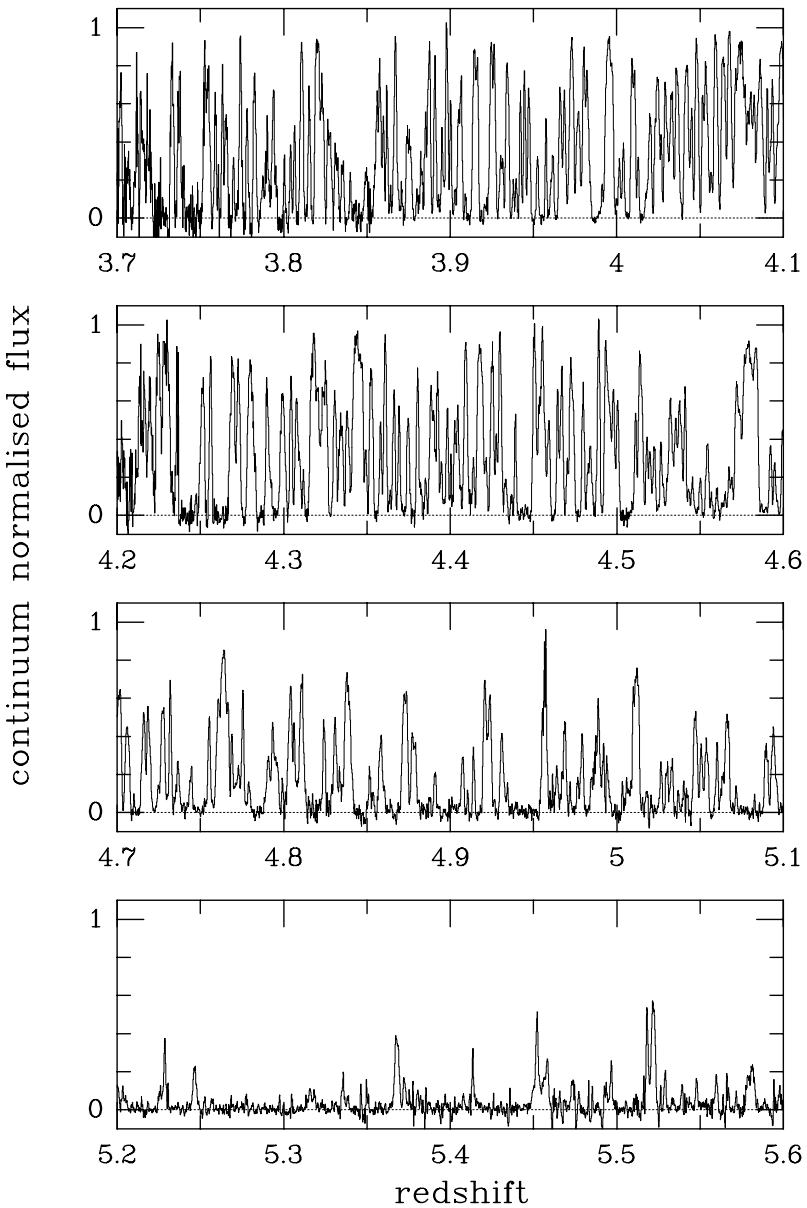
continuum normalised flux
1
0
3.7
3.8
3.9
4
4.1
4.2
4.3
4.4
4.5
4.6
4.7
4.8
4.9
5
5.1
5.2
5.3
5.4
5.5
5.6
redshift

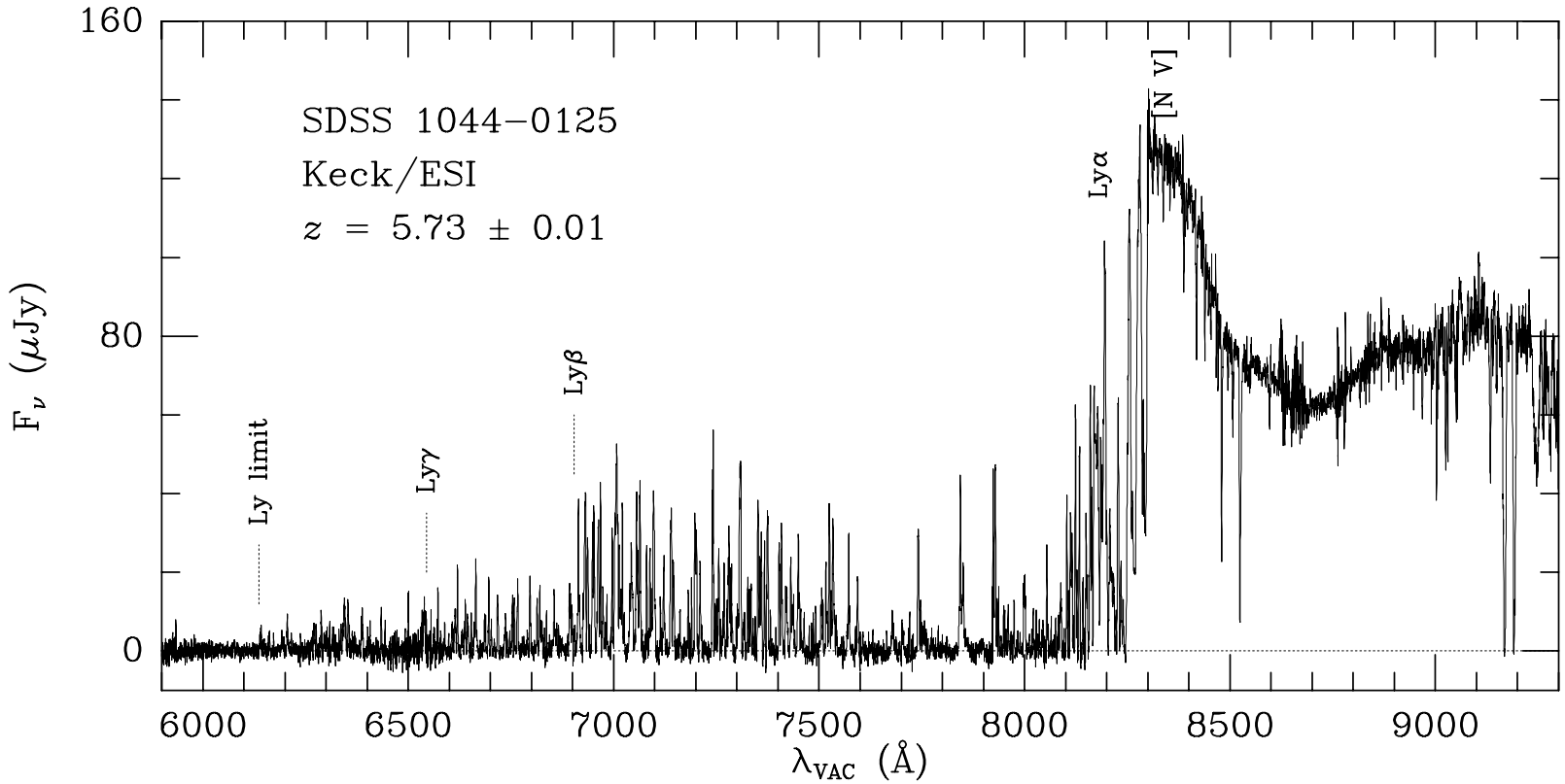

The Lyman-alpha forest at z = 5.7

Cannot distinguish individual Lyman-alpha absorption lines

Calculation of Ω_{ion}

Can calculate contribution of a particular ion to density parameter from:

$$\Omega_{ion} = \frac{1}{\rho_c} m_{ion} \frac{\Sigma_n N_n}{c/H_0 \Sigma \Delta X_i}$$

where ρ_c is the critical density, m_{ion} is the mass of the ion, n is the number of absorbers along the line of sight N_n is the column density of each absorber and $c/H_0 \times \Delta X$ is the cosmologically calculated distance over which absorption lines could have been found.

Need ionization correction from theory to get $\Omega_{element}$

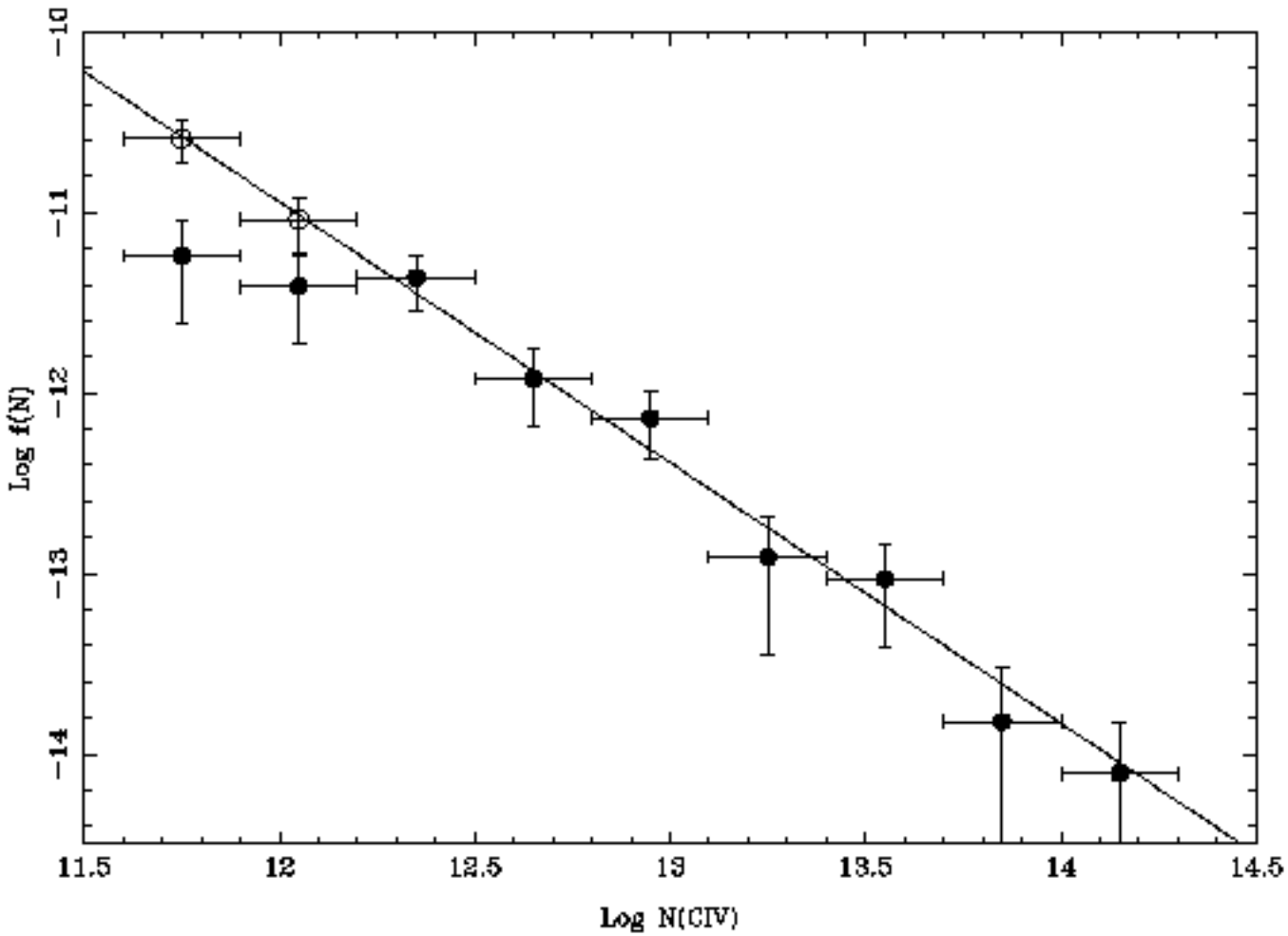

Distribution of C IV column densities

Contribution of C IV to Ω as a function of redshift z

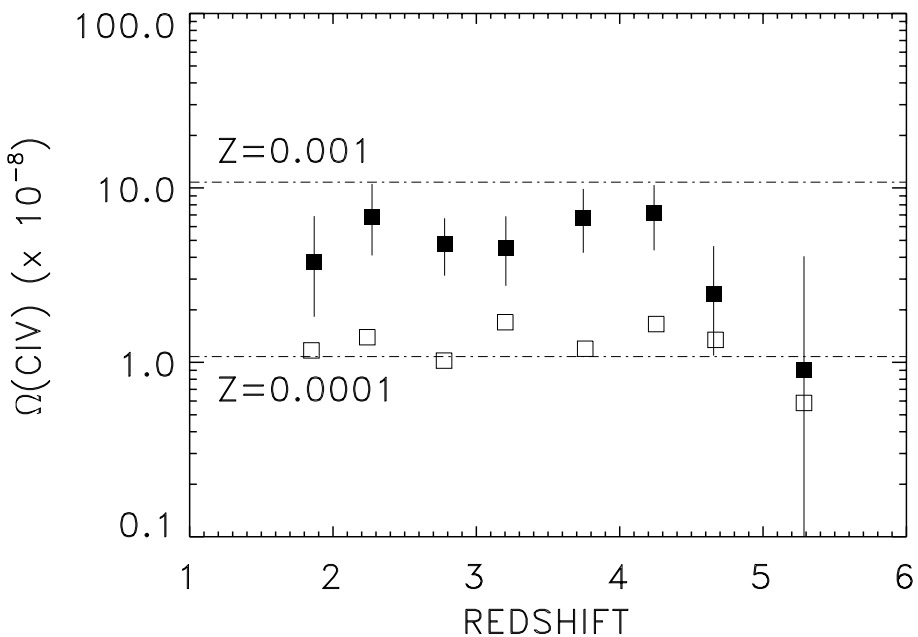

Songaila (2001)

Contribution of Si IV to Ω as a function of redshift z

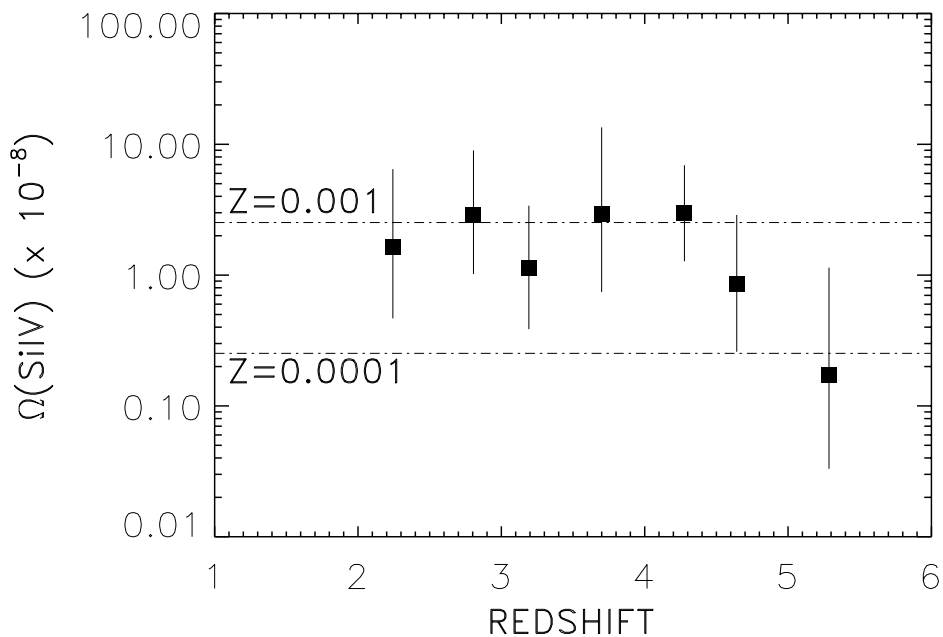

Songaila (2001)

Songaila found:

- C IV column density distribution function invariant in range $1.5 \leq z_{abs} \leq 5.5$
- $\Omega_{CIV} = 2.5 - -7 \times 10^{-8}$ and $\Omega_{SiIV} = 0.9 - -3 \times 10^{-8}$ in above range of z_{abs}.
- (Since the Lyman-alpha lines are blended we need to use Ω_{baryon} from primordial D/H or CMB measurements to determine Ion/Hydrogen abundance ratios.)
- Metallicity at z = 5 exceeds 3.5×10^{-4}.
- IGM enriched in metals at $z \gg 5$ (possibly by massive stars which ionized the IGM.
- Pettini *et al.* (2003) verified these conclusions using 3 QSOs with $z_{em} \geq 5.4$.

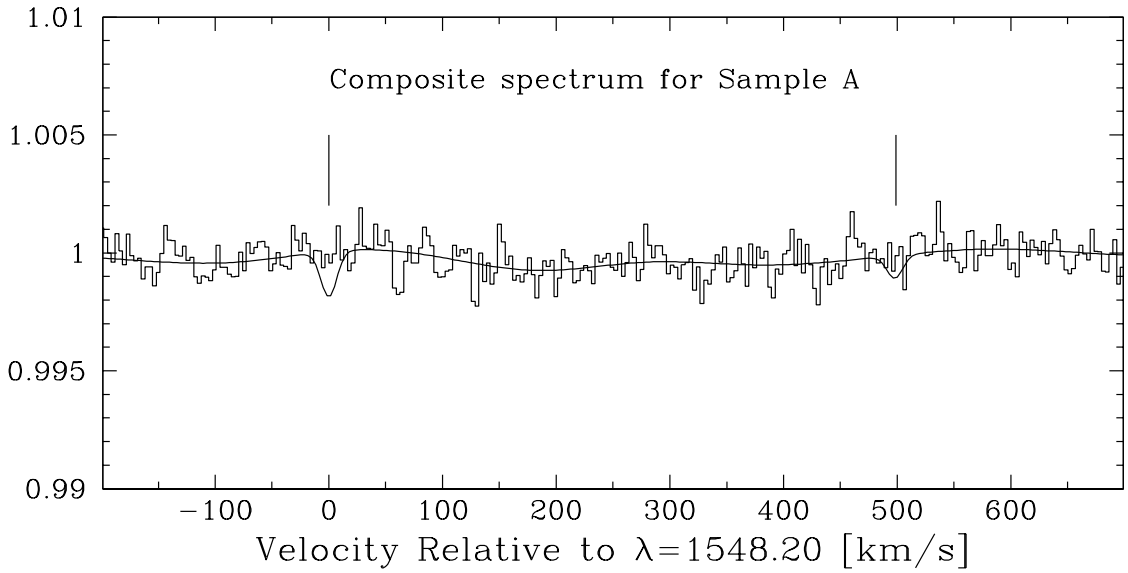

Example of stacked C IV regions associated with weak H I lines

S/N $\sim$ 2000; note the vertical scale

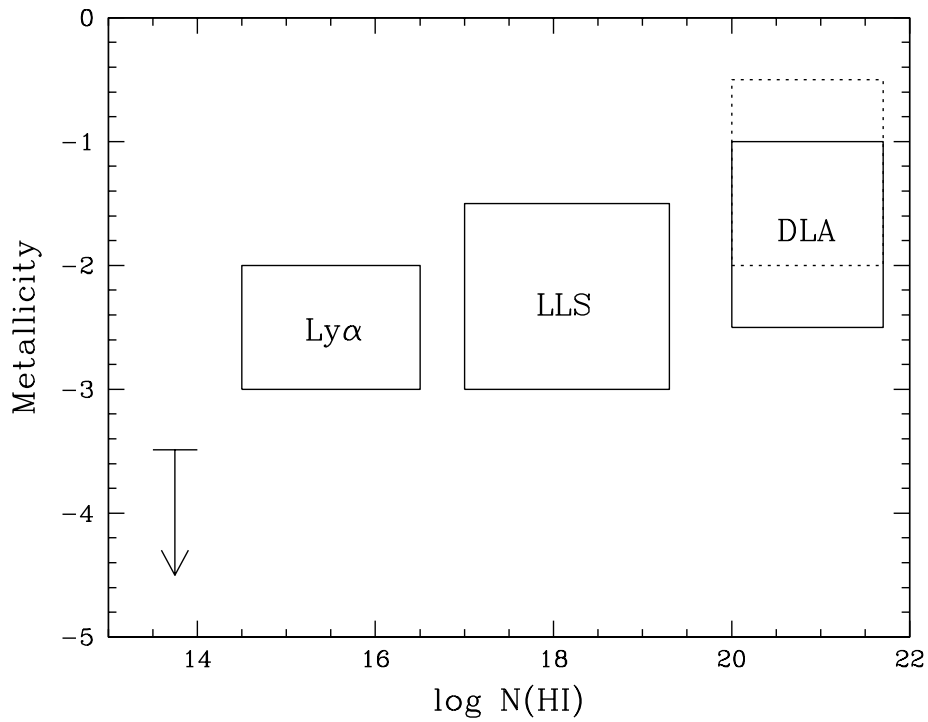
0
−1
−2
−3
−4
−5
Metallicity
14
16
18
20
22
log N(HI)
Lyα
LLS
DLA

Results of the "stacking method"

- Stacking the C IV regions of Lyman-alpha absorption lines with no *visible* C IV counterparts lead to $[C/H] \leq 3 \times 10^{-5}$ at $z \sim 2.5$.
- Result criticized on grounds that z_{CIV} might be different to z_{HI} (as it is often for *stronger* H I lines.

Lu, Sargent and Rauch (astro-ph 1998)

Recent "Pixel Method" Results for C and Si

- Applied to 19 Keck HIRES and VLT UVES high quality spectra over $1.8 \leq z \leq 4.1$ and over density δ in range $\log\delta$ = -0.5 to 1.8.
- This is the lowest overdensity yet explored, but the method is statistical rather than detecting individual heavy element lines.
- Simulation used to connect H I absorption to T and n(H) plus model for UV background to convert ratios of C IV and Si IV to H I pixel optical depths to C/H and Si/H abundance ratios.

J. Schaye A. Aguirre, T-K. Sun, T. Theuns, M. Rauch, W. Sargent.

Summary of "Pixel Method" Results

- Find *lognormal* distributions of C/H and Si/H at given z or δ.
- Median metallicity [C/H] = -3.47 + 0.08 (z - 3) + 0.65(logδ - 0.5)
- Lognormal scatter σ = 0.76 = 0.02(z - 3) - 0.23(logδ - 0.5)
- $[Si/C] \approx 0.25$; independent of z and δ.

J. Schaye A. Aguirre, T-K. Sun, T. Theuns, M. Rauch, W. Sargent.

Recent work on O VI and C IV

- O VI is a more sensitive tracer than C IV in the most tenuous regions of the IGM.
- Collisionally ionized O VI produced in hot, shocked gas at $\sim$ 300,000 deg, K. (100 km s^{-1})
- O VI always in Lyman-alpha or beta forests so difficult to observe at high z.
- Optimal redshift from ground $z \sim 2.5$.
- UV radiation from QSOs dominates ionization.
- Recent work indicates $\Omega_{OVI} h_{65} \sim 2.96 \times 10^{-7}$ at z $\sim$ 2.5 (very similar to the value found at z = 0).

Simcoe, Sargent and Rauch (2004)

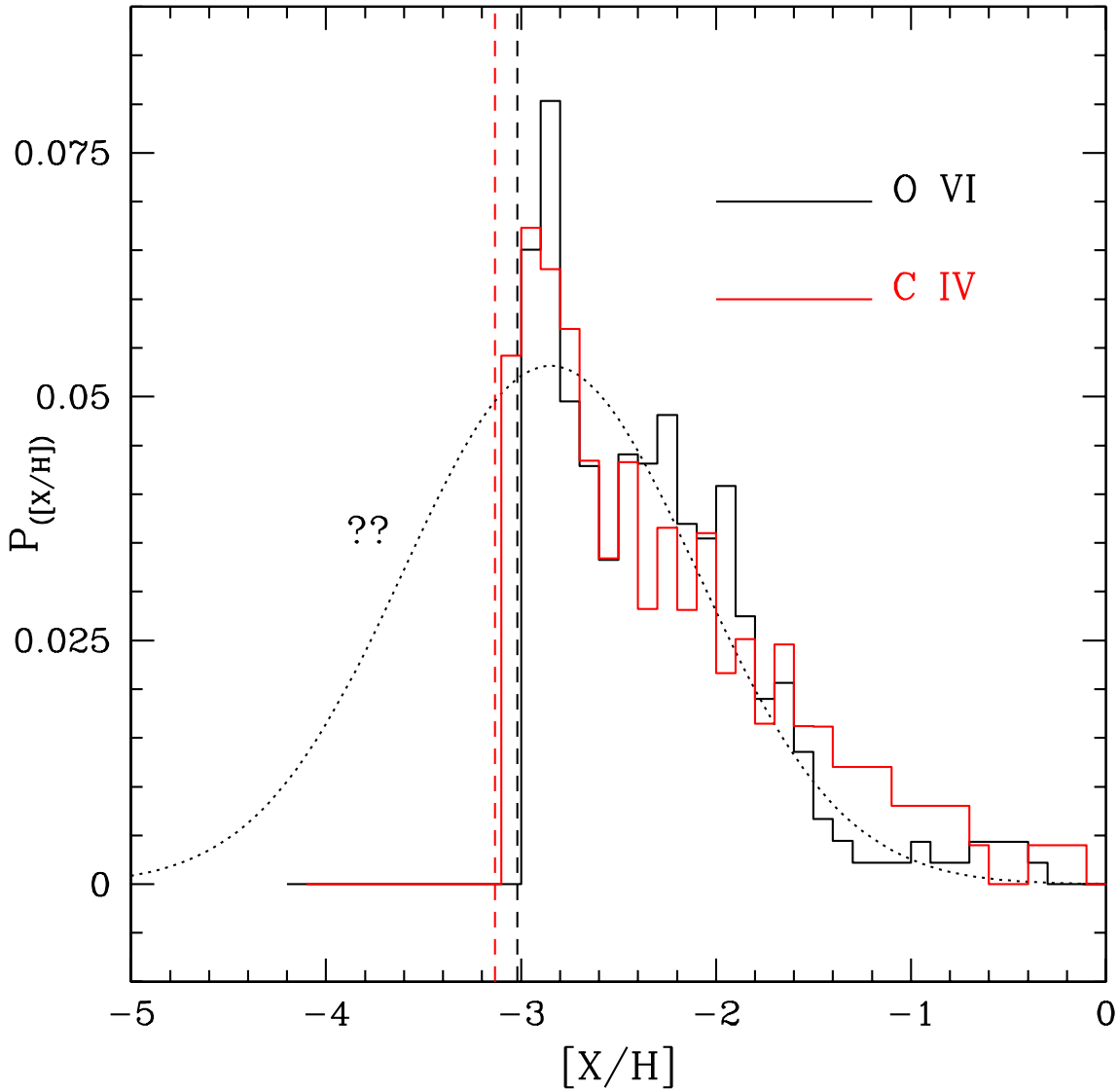
0.075
0.05
0.025
0
P([X/H])
??
O VI
C IV
−5
−4
−3
−2
−1
0
[X/H]

Origin of Heavy Element Absorption Lines

- Strong C IV complexes traditionally associated with galaxy halos.
- Now increasing evidence in favour of it outflows from star-forming galaxies.
- *Clustering* of C IV doublets not consistent with galaxy-galaxy correlation function. (Boksenberg, Sargent and Rauch (2003))
- Correlation between C IV and O VI absorption lines and *galaxy redshifts* around Q1700+64 shows directly that galaxies can eject highly ionized material to tens of kpc. (Steidel et al. (2004))

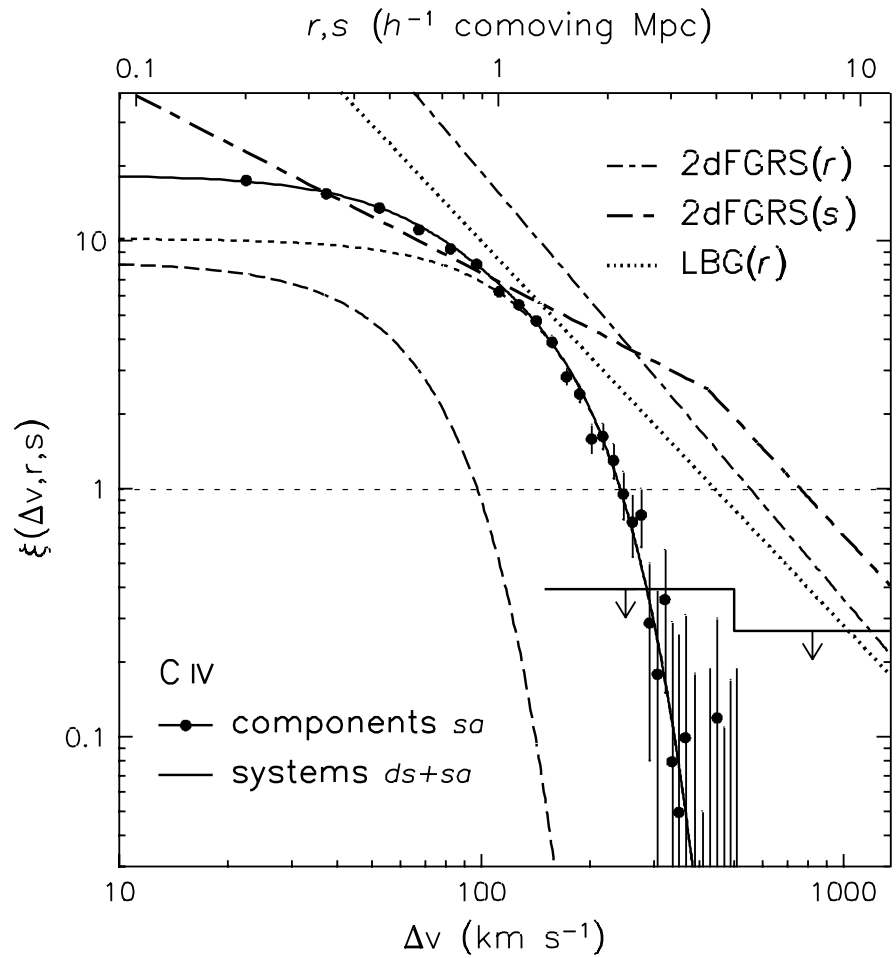
r,s (h⁻¹ comoving Mpc)
0.1
1
10
2dFGRS(r)
2dFGRS(s)
LBG(r)
10
1
0.1
ξ(Δv,r,s)
C IV
components sa
systems ds+sa
10
100
1000
Δv (km s⁻¹)

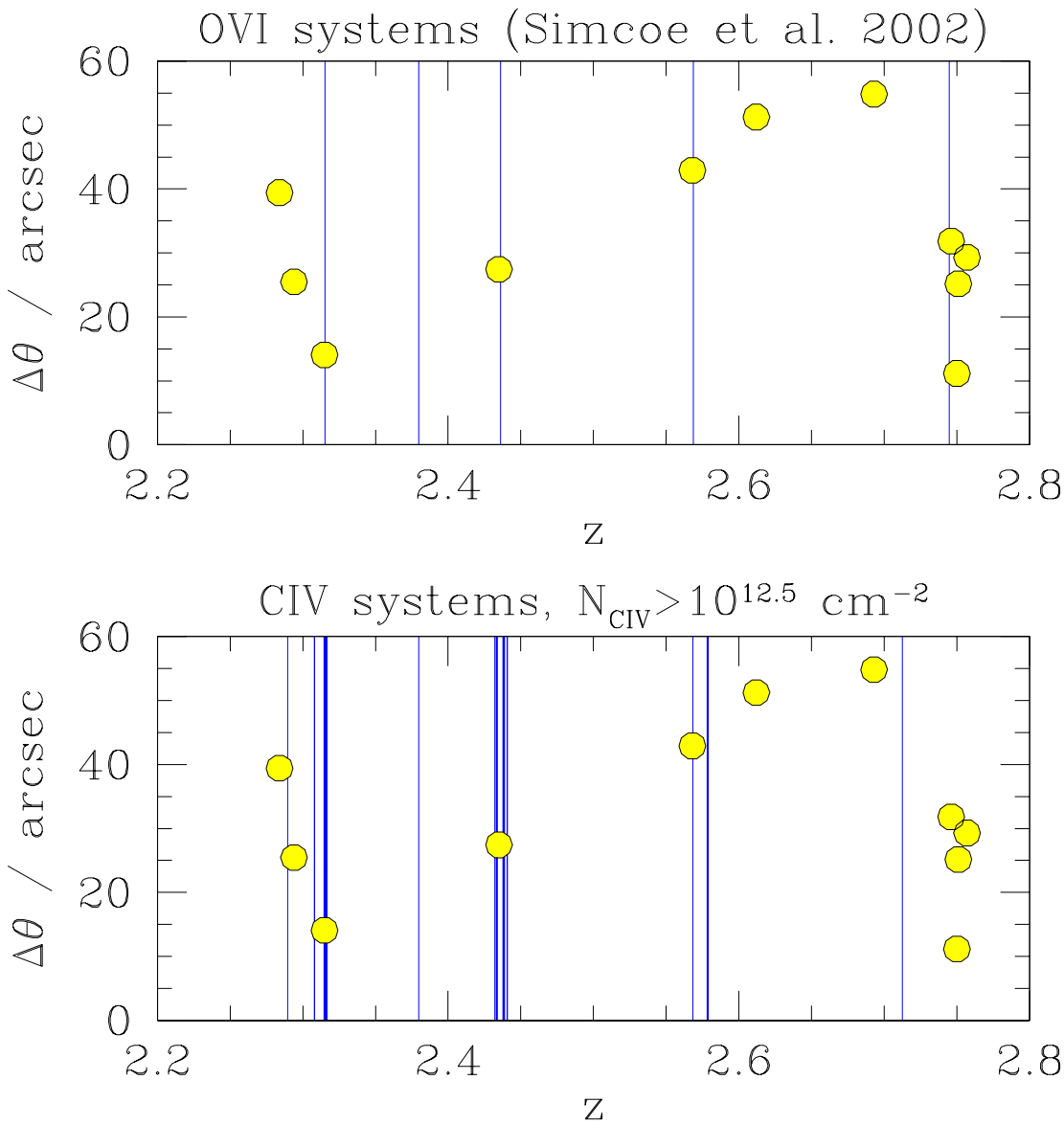
OVI systems (Simcoe et al. 2002)
60
40
20
0
Δθ / arcsec
2.2
2.4
2.6
2.8
z
CIV systems, N_CIV>10^12.5 cm^-2
60
40
20
0
Δθ / arcsec
2.2
2.4
2.6
2.8
z

Summary of QSO absorption line abundances

- We have not found with certainty abundances below [Z/H] $\sim$ =-3.5
- About 50% by mass of the IGM has $[Z/H] \leq -3.5$ for $z \geq 2.5$.
- There is surprising little evolution in Ω_{CIV} and Ω_{SiIV} for $z \geq 2$.
- Direct evidence for outflows of heavy elements from star-forming galaxies.
- Values of Ω_{CIV}, Ω_{OVI}, Ω_{SiIV} in good agreement with the "Prompt Inventory" deduced from metal-poor, Galactic halo stars. (Qian, Wasserburg and Sargent (2002))

High-Redshift Formation of Globular Star Clusters by Galaxy Outflows

Evan Scannapieco
Kavli Insitute for Theoretical Physics- UCSB
with
Jon Weisheit & Frank Harlow
Los Alamos National Laboratory

Globular Clusters

M92, Hillary Mathis REU(NOAO/AURA/NSF)

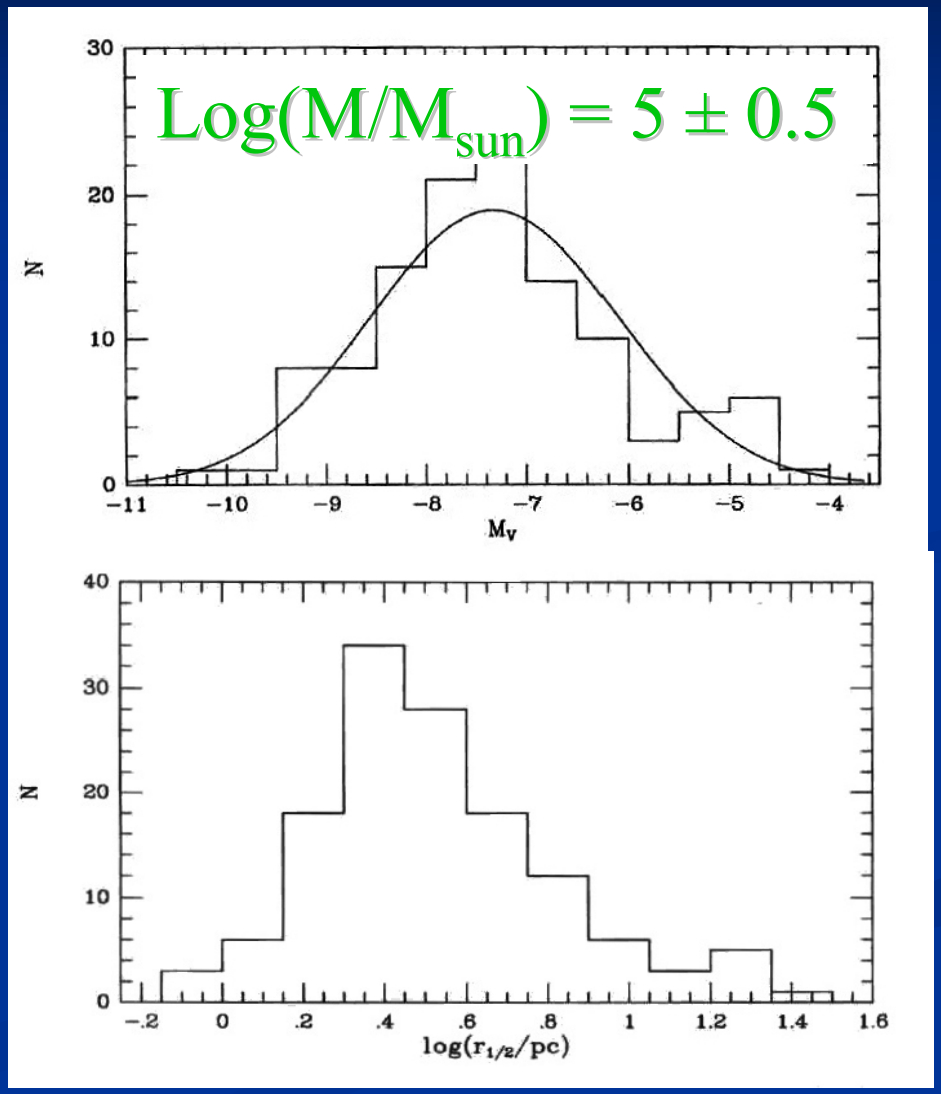

Ashman & Zepf (1998)

Issue # 1: Globular Cluster Sizes

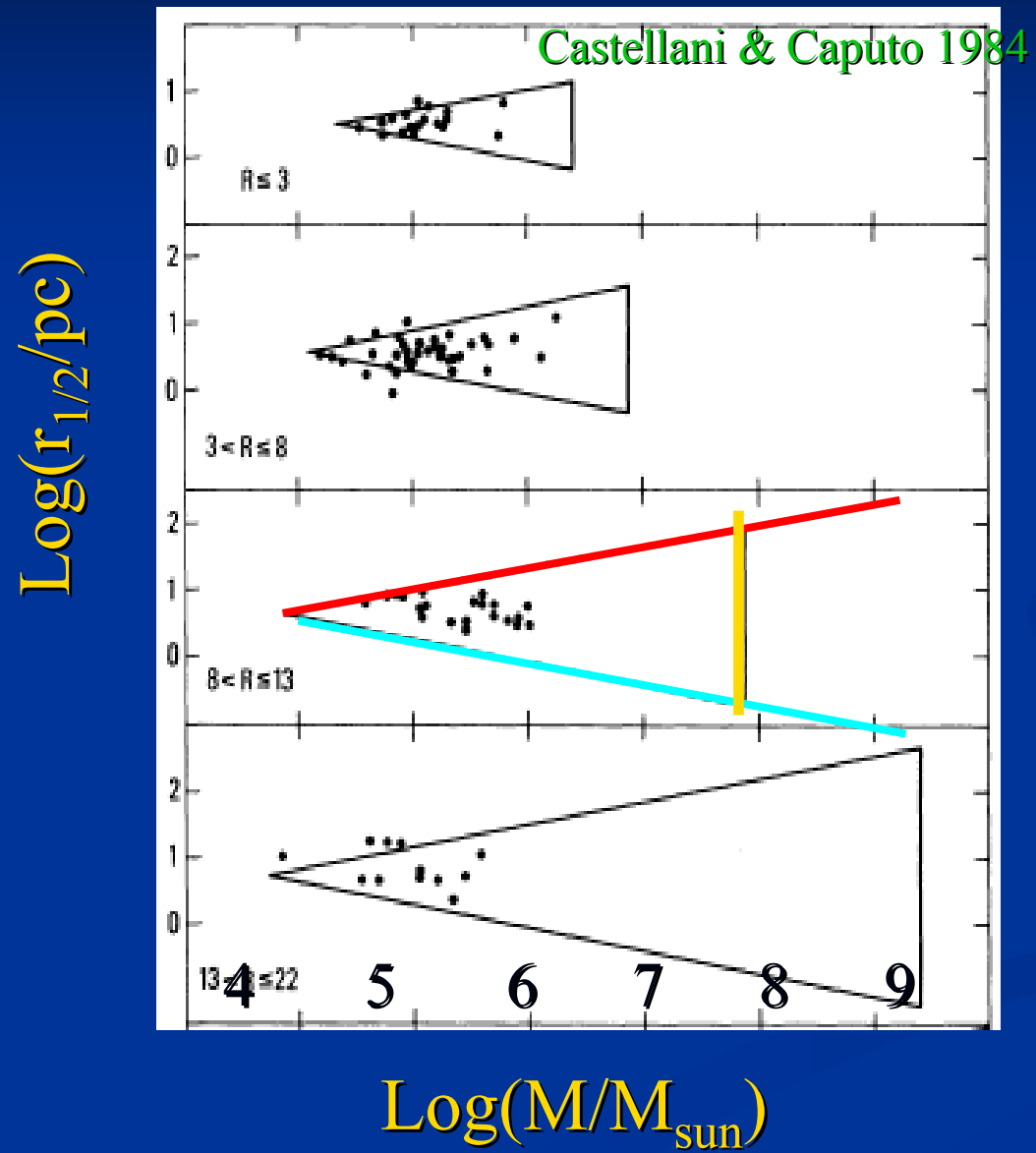

Disk shocking
$t \sim r_{1/2}^{-3}\ M\ R$

Evaporation
$t \sim r_{1/2}^{3/2}\ M^{1/2}$

Dynamical Friction
$t \sim M^{-1}\ R^{2}$

Maximum mass is an intrinsic property of the ***initial*** GC population

#2: Globular Cluster Metallicities

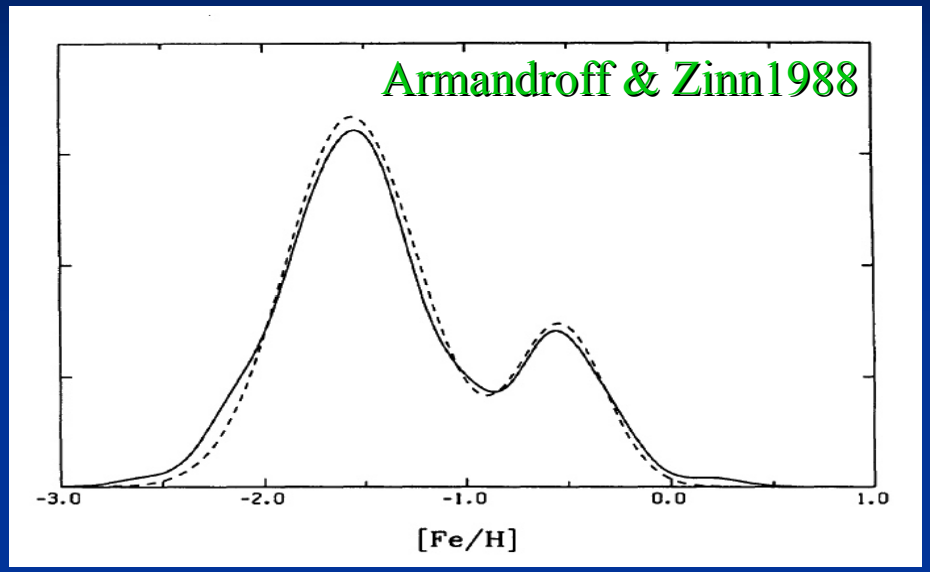

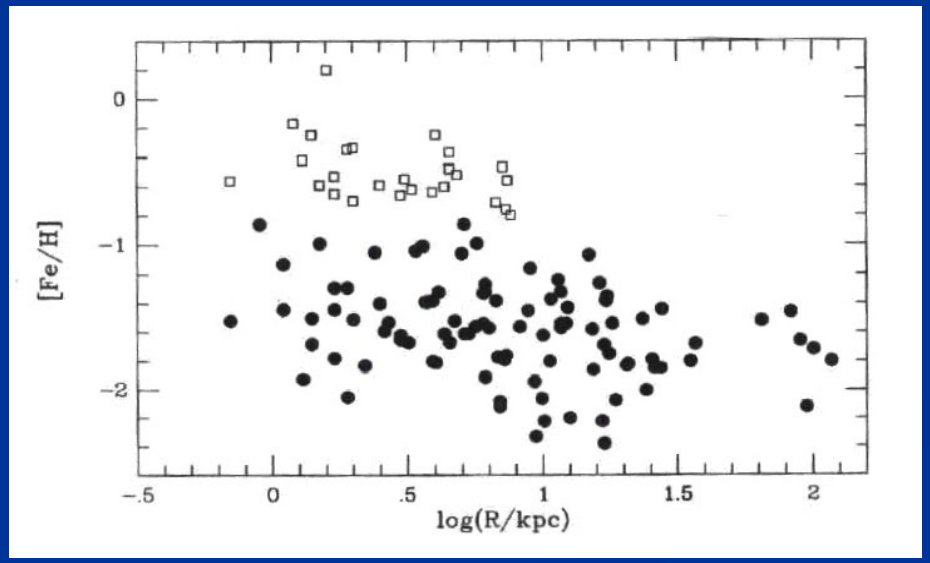

Double-peaked

[Fe/H] ~ -0.5 ± .25

[Fe/H] ~ -1.6 ± .35

Dynamically Different "Halo" and "Disk," Also seen in other galaxies (eg Forbes Brodie Huchra 1997)

Narrow range < ΔZ± 0.1 In each GC (eg Sunzeff 1993)

One generation

#3: (No) Dark Matter In GCs

Grillmair etal 1995

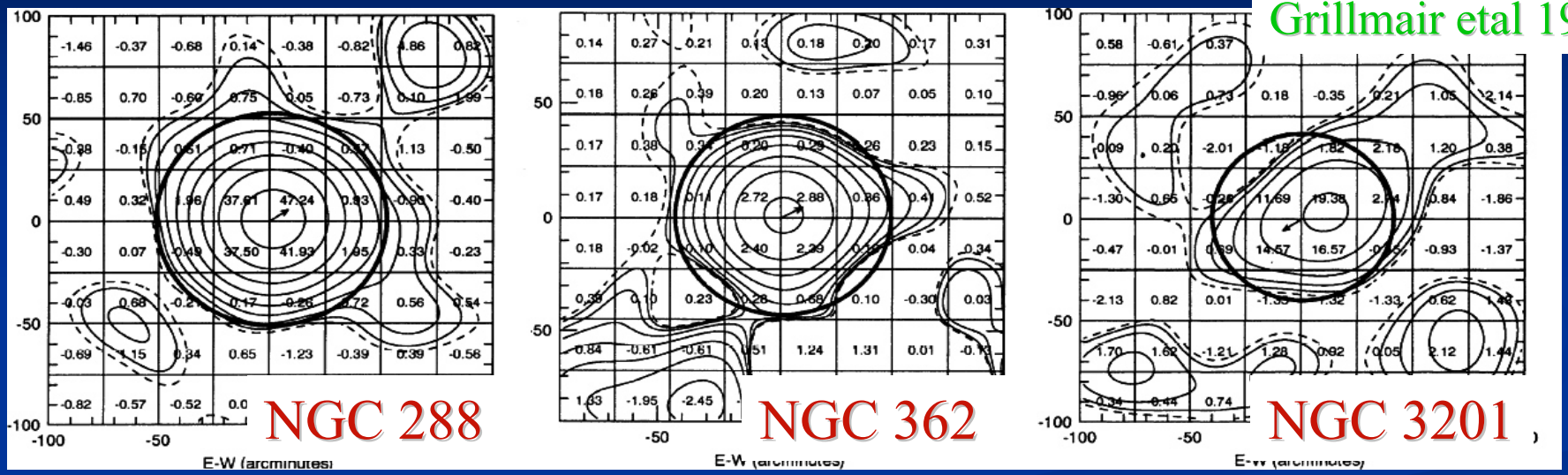

Moore 1998

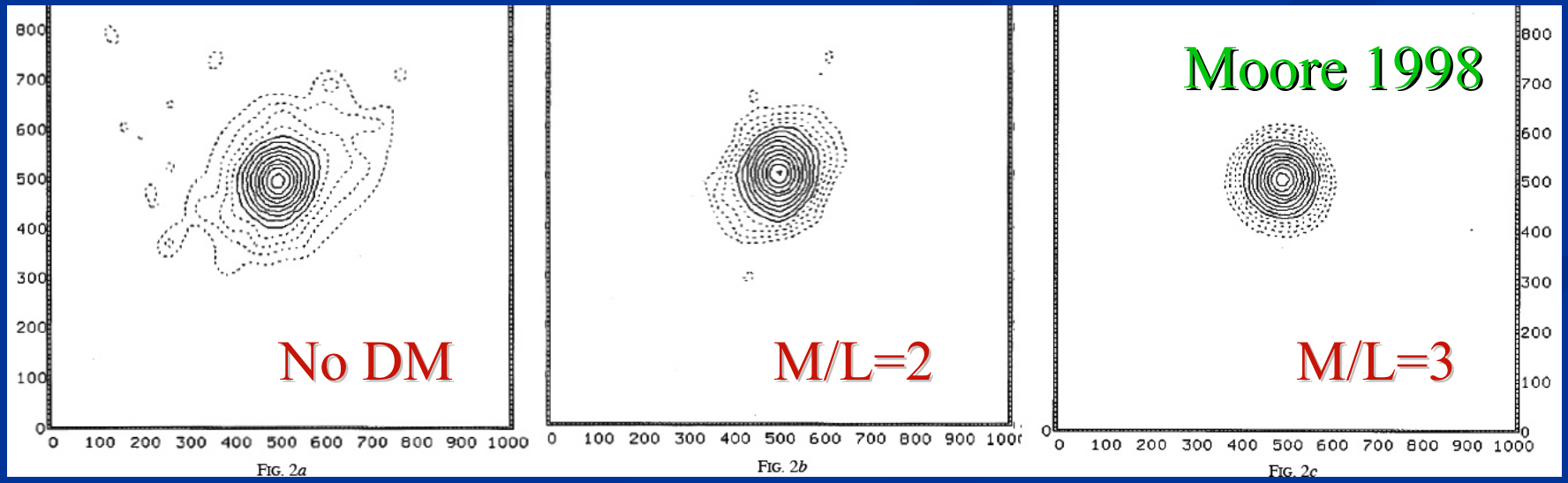

Explanation #1: Minihalos

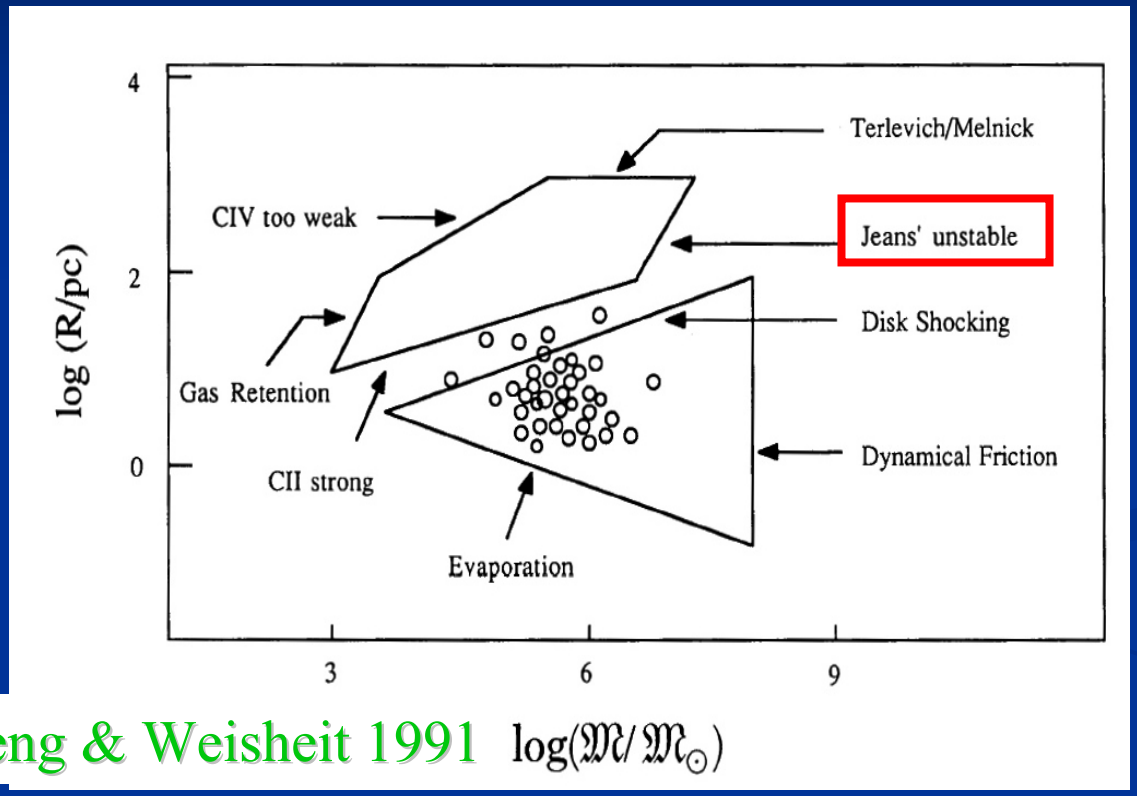

Peng & Weisheit 1991

$T_{vir} \leq 10^4$ K at $z \sim 10$

Below this temperature you need dust or H_2 to cool.

Primordial clouds, after the very first stars form may not be able to form stars on their own: Minihalos (total masses <~ 5×10^7 M_{sun})

#2: Galaxy Outflows

- In a sample of 19 Ly-break z~3 starbursting galaxies, winds were found in all objects.
- Velocities ~200 km/s
- Lyα-nebular emmi.+ metal absorption-nebular emission.
- SFR ~ 20 Msolar /yr

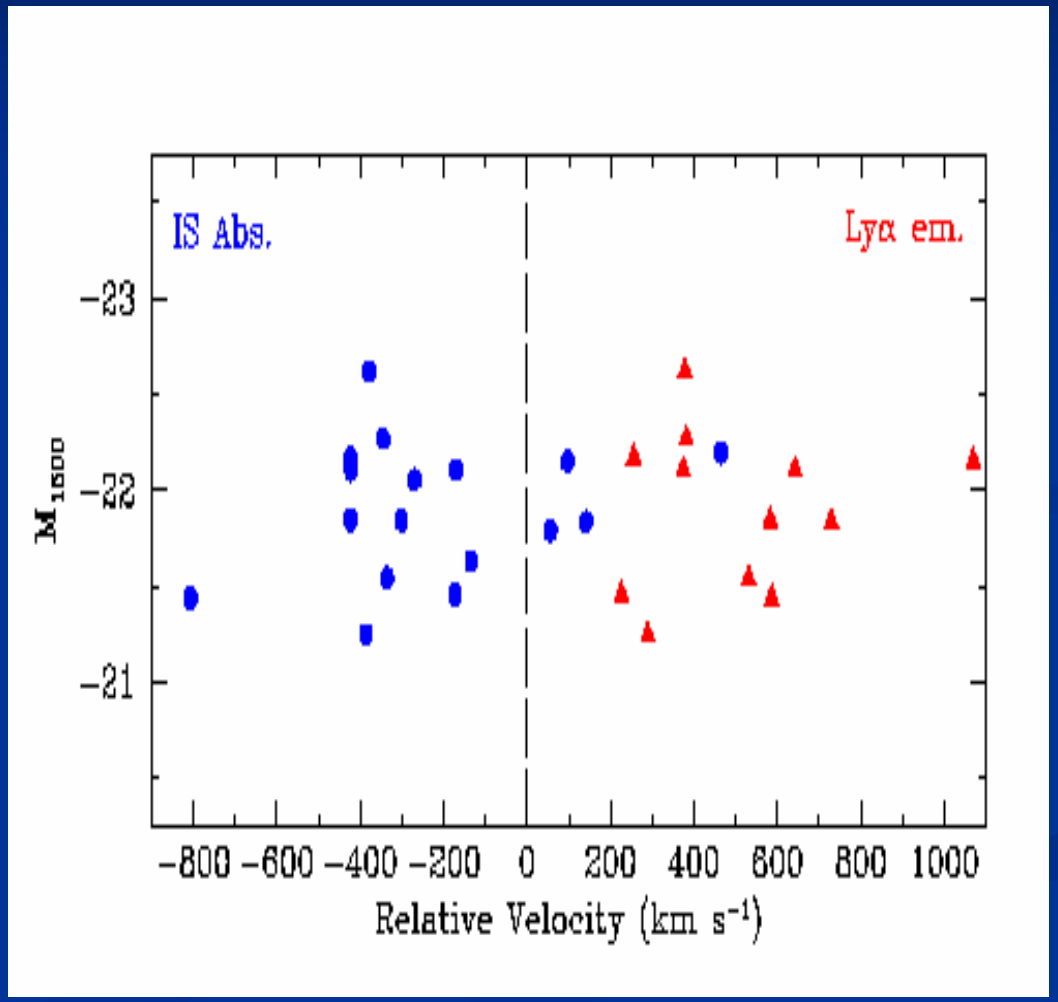

M. Pettini et al 2001

Fiducial Interaction

$E = 10^5$ foe ; $M=10^{6.5}\ M_{sun}$; $Z \sim 10^{-1.5}\ Z_{sun}$

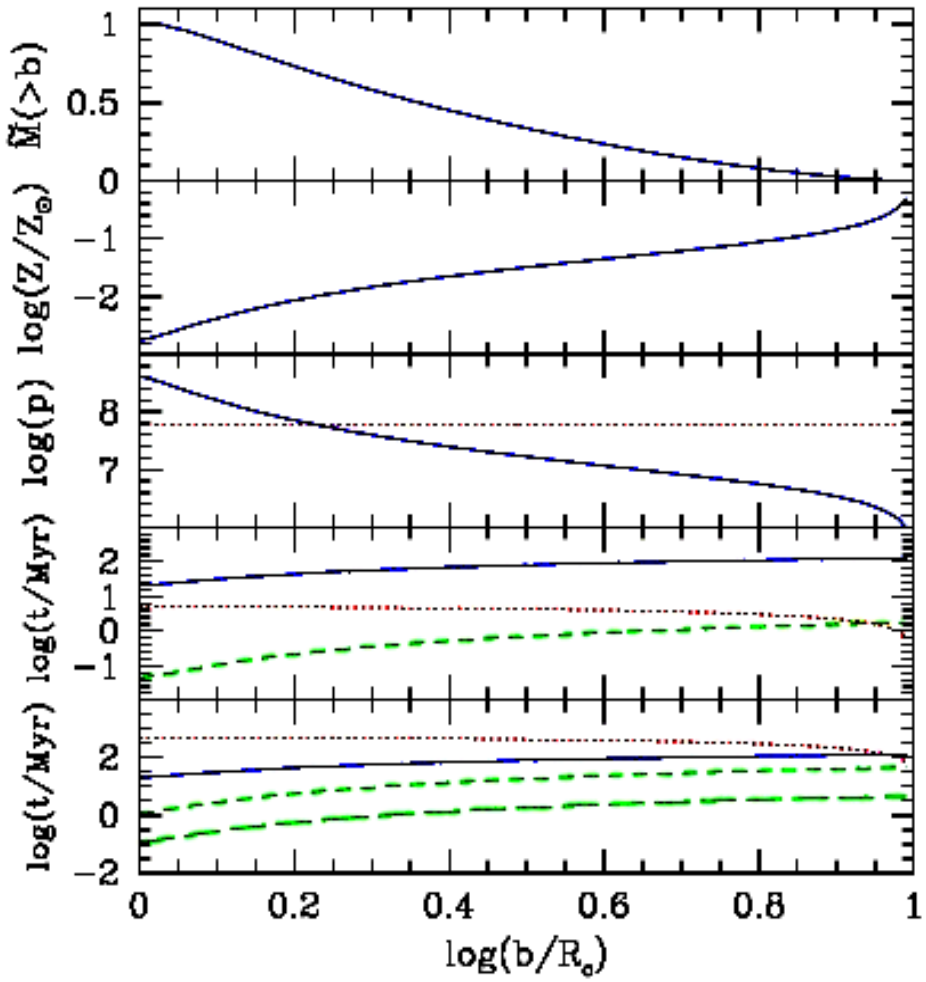

#3: Gas is stripped from the potential

Free-fall time
Sound Xing time
Cooling time

Cooling by:
nonequilibrium proc.
Infrared CII,FeII,SiII (<13.6eV)

Parameter Dependencies

Distance (-3<logZ<-1)

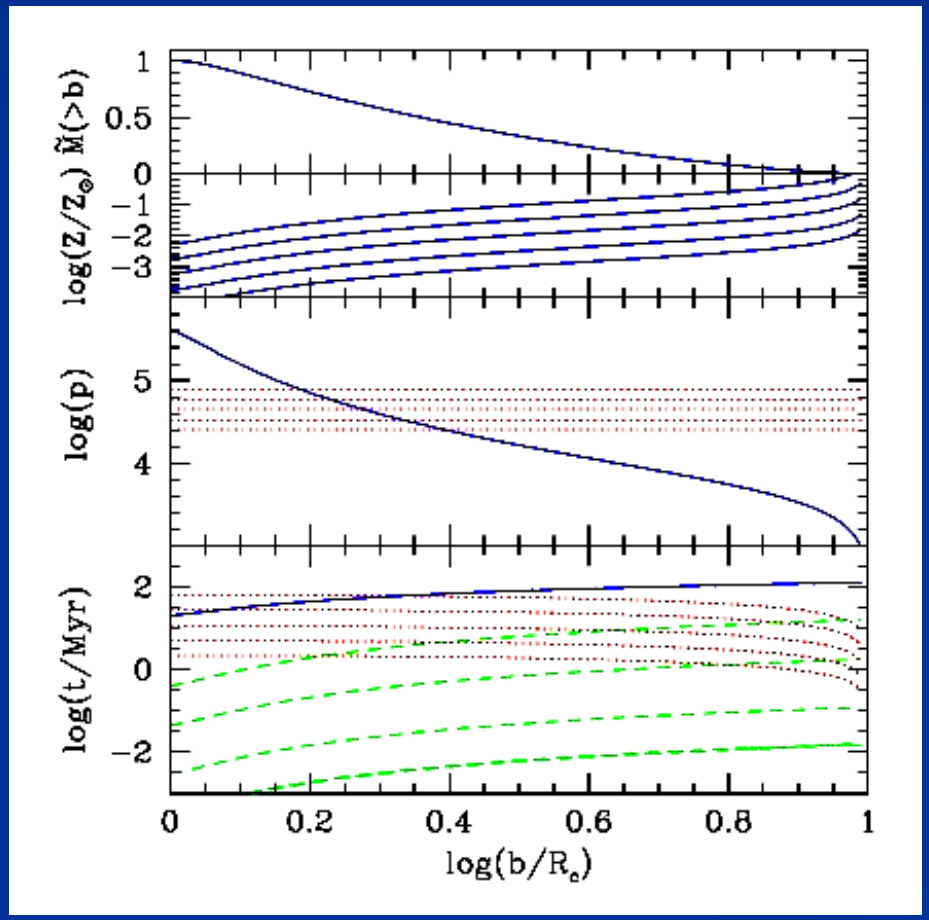

Other variables studied:

Minihalo mass
Starburst energy
Collapse redshift

1D Simulation of (Turbulent) Mixing

Density

$$\frac{\partial \rho}{\partial t} + \frac{\partial \rho u_1}{\partial x_1} = 0, \tag{29}$$

Momentum

$$\frac{\partial \rho u_i}{\partial t} + \frac{\partial \rho u_i u_1}{\partial x_1} = -\frac{\partial P}{\partial x_1} - \frac{\partial R_{i,1}}{\partial x_1}, \tag{30}$$

Energy

$$\frac{\partial \rho E}{\partial t} + \frac{\partial \rho E u_1}{\partial x_1} = -\frac{\partial P \bar{u}_1}{\partial x_1} - \frac{\partial R_{i,1}}{\partial x_1} + \frac{\partial}{\partial x_1}\left(\frac{\rho \nu_t C_p}{\mathrm{Pr}_t}\frac{\partial T}{\partial x_i}\right), \tag{31}$$

Reynolds ST

$$R_{i,j} = -\rho \nu_t \left(\frac{\partial u_i}{\partial x_j} + \frac{\partial u_j}{\partial x_i}\right) + \frac{2\rho}{3}\delta_{i,j}\left(\nu_t \frac{\partial u_k}{\partial x_k} + K\right), \tag{32}$$

Turb. KE

$$\frac{\partial \rho K}{\partial t} + \frac{\partial \rho K u_1}{\partial x_1} = a_1 \frac{\partial P}{\partial x_1} - R_{i,1}\frac{\partial u_i}{\partial x_1} - \rho\epsilon + \frac{\partial}{\partial x_1}\left(\rho \nu_t \frac{\partial K}{\partial x_i}\right), \tag{33}$$

Turb. KE decay

$$\frac{\partial \rho \epsilon}{\partial t} + \frac{\partial \rho \epsilon u_1}{\partial x_1} = \frac{\epsilon}{K}\left[C_{\epsilon 4} a_1 \frac{\partial P}{\partial x_1} - C_{\epsilon_1} R_{i,1}\frac{\partial u_i}{\partial x_1} - C_{\epsilon_2}\rho\epsilon\right] + \frac{\partial}{\partial x_1}\left(\frac{\rho \nu_t}{\sigma_\epsilon}\frac{\partial \epsilon}{\partial x_i}\right) - C_{\epsilon 3}\rho\epsilon\frac{\partial u_1}{\partial x_1}, \tag{34}$$

Turb Momentum

$$\frac{\partial \rho a_i}{\partial t} + \frac{\partial \rho a_i u_1}{\partial x_1} = -\frac{R_{i,1}}{\rho}\frac{\partial \rho}{\partial x_1}, -C_{a1}\frac{\rho\epsilon}{K}a_i + \frac{b_{\mathrm{trb}}}{\rho}\frac{\partial P}{\partial x_1}, \tag{35}$$

2 Species

$$\frac{\partial \rho c_\alpha}{\partial t} + \frac{\partial \rho c_\alpha u_1}{\partial x_1} = \frac{\partial}{\partial x_1}\left(\frac{\rho \nu_t}{\sigma_c}\frac{\partial c_\alpha}{\partial x_i}\right) \tag{36}$$

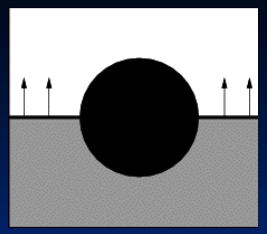

Simulation

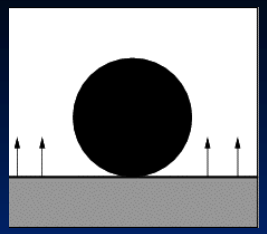

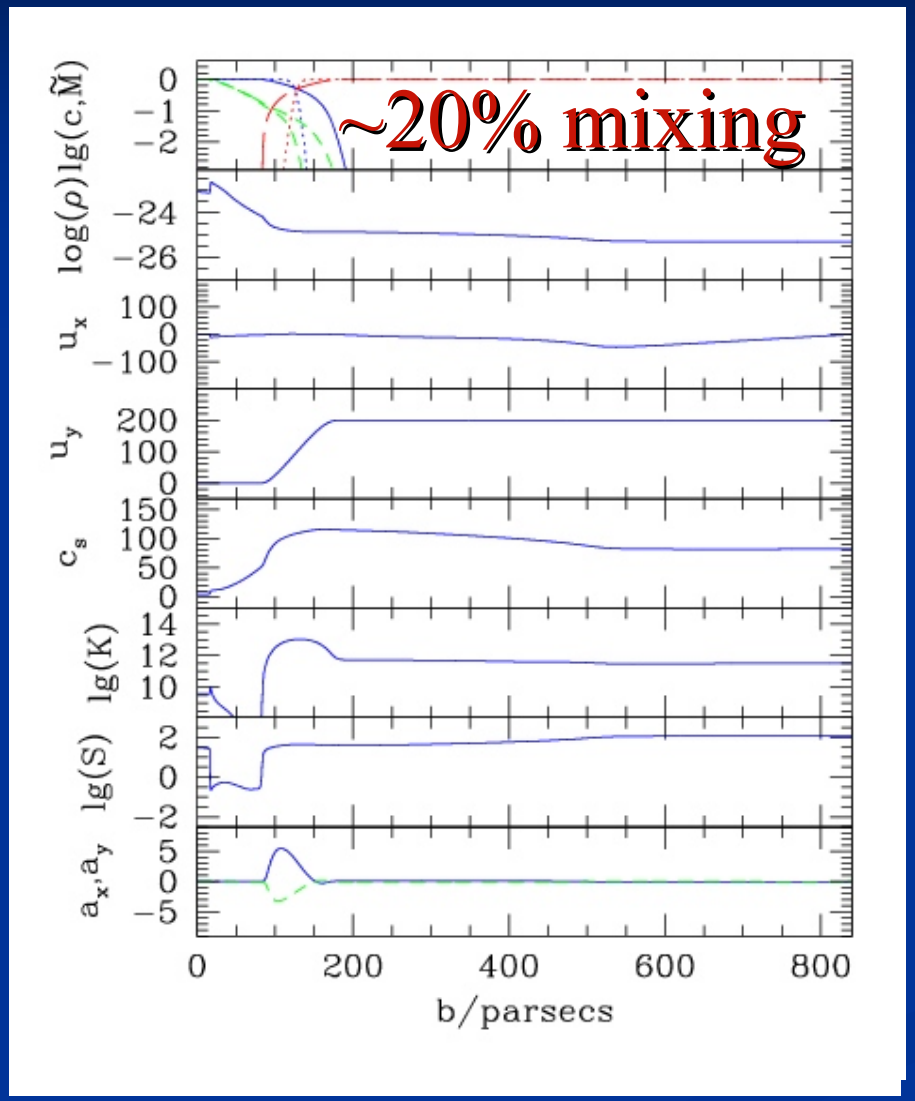
~20% mixing
lg(c,M̃)
log(ρ)
u_x
u_y
c_s
lg(K)
lg(S)
a_x,a_y
b/parsecs

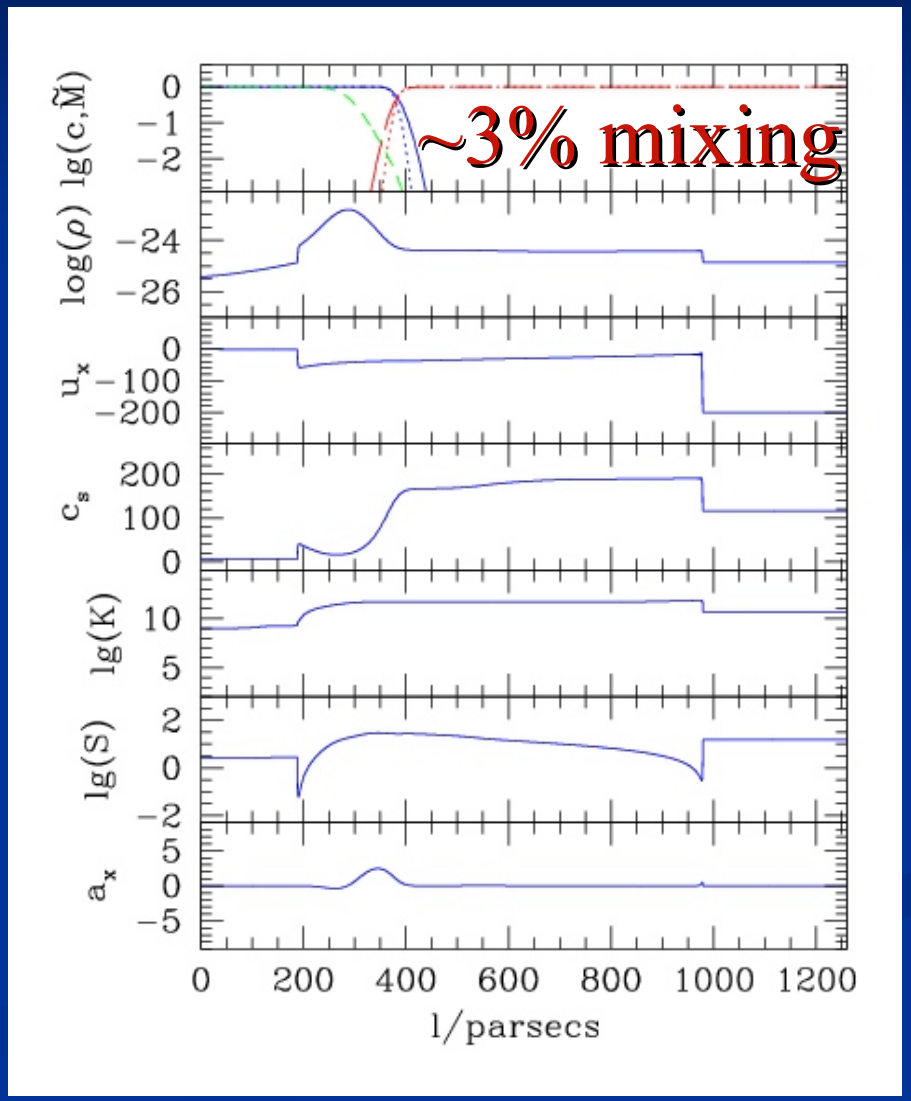
~3% mixing
lg(c,M̃)
log(ρ)
u_x
c_s
lg(K)
lg(S)
a_x
l/parsecs

Conclusions

- Interactions between minihalos and starburst-driven outflows explain several important facts about (halo) globular clusters.
  - formation redshift ~ 10
  - observed maximum mass of order 10^6 M_{sun}
  - chemical homogeneity within each GC and the range of metallicities of GCs within a galaxy
  - the lack of an associated dark matter potential
- This scenario has clear testable predictions that can be easily related to present and future observations. (Please ask)
- In the future we plan to simulate this problem in futher detail (2-dimensions, final GC size etc…)

Other Observables

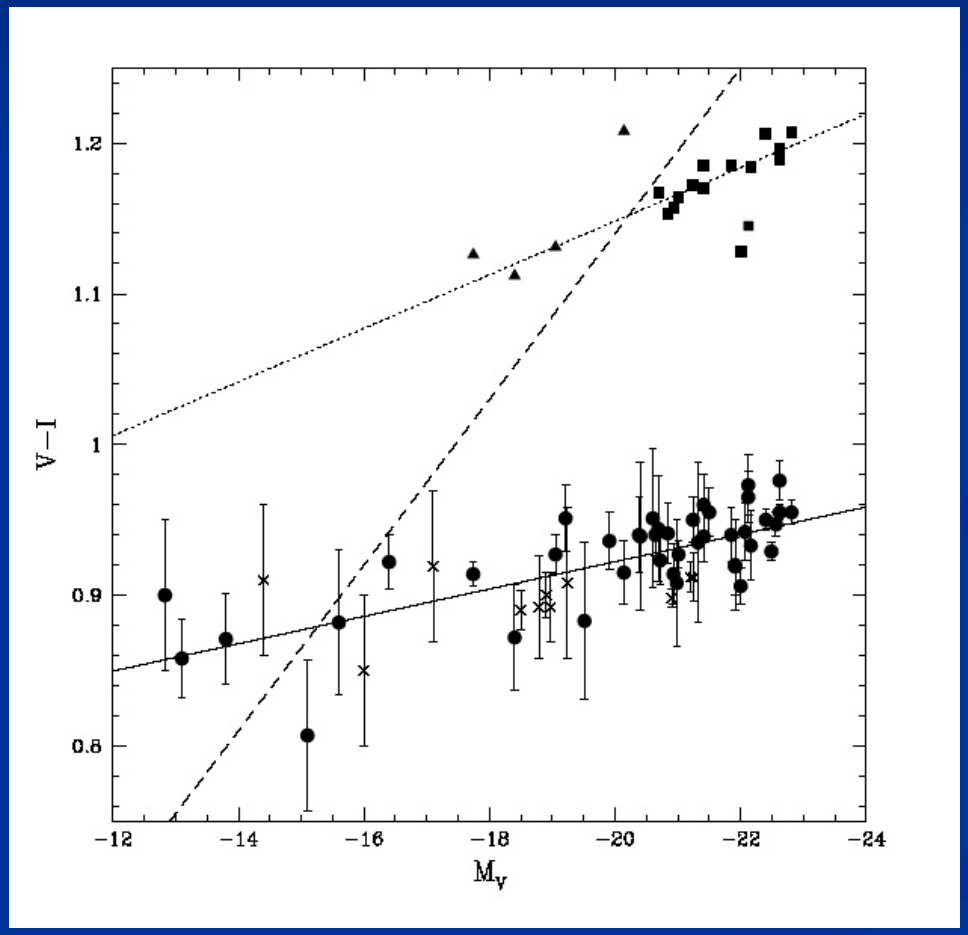

Strader, Brodie, & Forbes 2004

$Z \alpha L^{1/6}$

Fix v_s:
$R \alpha E^{1/3} (1+z)^{-1}$

Assume ejected Z
E of starburst α L
$Z \alpha L^{1/3} (1+z)^{2}$

Fixed sigma peaks (CDM):
$Z \alpha L^{1/3-0}$

Santa Fe 9 Aug 2004

IMF OF THE FIRST STARS

Joe Silk (Oxford)

1. Present day IMF
2. First clouds, cooling, fragmentation
3. Transition to Population II
4. Clues from reionisation of the universe
5. Role of B

IMF TODAY

Salpeter 1955 — 0.08 to 100 $M_\odot$ — luminosity function corrected for young stars

$$m\frac{dN}{dm} = A m^{-x}$$

Observe $1+x = \begin{cases} 1/3 & 0.01-0.1\,M_\odot \\ 4/3 & 0.1-1 \\ 7/3 & 1-100 \end{cases}$

Salpeter value

M.B. • unresolved binaries ⇒ true slope steeper by ~1/3

• data is local: ≲1 kpc, extended to L.G. galaxies

• characteristic stellar mass:

$$\langle M_* \rangle \equiv \frac{\int m\,dN}{\int dN} \approx 0.3\,M_\odot$$

What determines $\langle M_* \rangle$?

- thermal fragmentation
- turbulent fragmentation
- fundamental physics

Thermal fragmentation of molecular clouds

$$T \propto \rho^{-0.375} \quad (\rho < 10^{-18}\ \mathrm{g\ cm^{-3}}) \Rightarrow \gamma = 0.7$$

$$\propto \rho^{-0.075} \quad (\rho > 10^{-18}) \Rightarrow \gamma = 1.0$$

where $p \propto \rho^{\gamma}$ and $\gamma_{crit} = 2(1 - 1/n)$

(for fragmentation)

$n = 1\ (1\text{-}D),\ 2\ (2\text{-}D),\ 3\ (3\text{-}D)$

$$M_{Jeans} \propto \frac{V_s^3}{G\rho^{1/2}} = 3.02\ \frac{T_{10}^2}{A_V}\ M_\odot$$

Larson
Hartmann
Alves
Lada
André

Turbulent fragmentation

turbulent Mach number ~ a few

$$\rho_{turb} = \mathcal{M}^2 \rho$$

$$M_{Jeans}^{turb} \propto \frac{V_{turb}^3}{\rho_{turb}^{1/2}} \Rightarrow M_{Jeans}^{turb} = \mathcal{M}^2\ M_{Jeans}$$

Padoan
Klessen
MacLow
Scalo

Fundamental physics

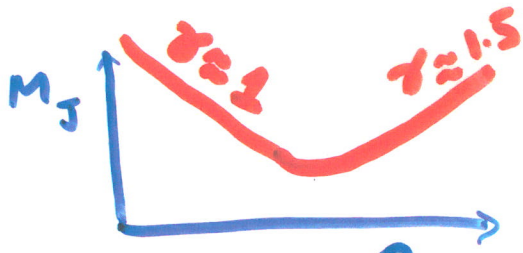

opacity-limited fragmentation

$$M_J^{min} \approx \left(\frac{m_e}{m_p}\right)^{1/4} \alpha^{-1} \alpha_g^{-3/2} \approx 0.01\ M_\odot \qquad (\alpha_g = G m_p^2/e^2)$$

+ accretion

BUT THE ACCRETION MUST BE SELF-REGULATED

Best bet: protostellar outflows which generate molecular cloud turbulence

These set in at $M_* \gtrsim 0.3\ M_\odot$

and are magnetically driven by coupling to disk rotation (protos

accretion is limited by turbulence: $\dot{M}_{acc} \sim V_{turb}^3/$

THE FIRST GENERATION OF STARS

- Normal mass range $\lesssim 100\ M_\odot$
- Very massive stars $10^2 - 10^3\ M_\odot$
- Supermassive objects $> 10^3\ M_\odot$

Theory cannot easily distinguish between these alternatives

⑤

The first pregalactic clouds form from rare gaussian peak

$$\frac{\delta\rho}{\rho} = \frac{D}{1+z} \left|\frac{\delta\rho}{\rho}\right|_{rms,\, z=0} (M)$$

dark matter halos collapse and virialise at $\delta\rho/\rho \approx 170$

$$\langle \rho_{halo} \rangle = 170\, \rho_0 (1+z_{gf})^3$$

$$T = 10^3\, K \left(\frac{M}{10^6 M_\odot}\right)^{2/3} \left(\frac{1+z}{10}\right)$$

Distinguish 2 cases:

$T \sim 10^3 K$	$T \sim 10^4 K$
$M \sim 10^6 M_\odot$	$M \sim 10^8 M_\odot$
e.g. $z=20$ 3σ	4σ peaks
$z=10$ 1.5σ	2σ
H_2 cooling	Lyα cooling
$\Lambda \propto \rho^2$ at $n_H \lesssim 10^4\, cm^{-3}$	$\Downarrow$
collisional deexcitations $\Rightarrow \Lambda \propto \rho$ at $n > 10^4$	a more complicated evolution
$\Delta E_{J=1\to 2} = 512 K$	
Infer $M_{Jeans} \simeq 700 \frac{T_{200}^{3/2}}{n_4^{1/2}} M_\odot$	
and accretion rate $\sim \frac{v_s^3}{G} \sim 10^{-3} M_\odot/yr$	
$\Rightarrow \sim 10^3 M_\odot$ stars	

Also mass fraction in stars $\sim 10^{-3} \Rightarrow Z_{1st} \sim 10^{-5}$

The $10^8 M_\odot$, $T \sim 10^4 K$ clouds

- cool by Lyα emission, followed by H_2 cooling
- Gravitationally unstable thin disk forms
- Torques effectively transfer angular momentum
- SMBH forms at centre, and disk fragments
- Radiation from central QSO destroys H_2
- Lyα cooling results in "normal" star formation (but plausibly top-heavy because of high protostellar accretion)

Accretion rate $\sim 0.1\, T_4^{3/2} \frac{M_\odot}{yr} \Rightarrow M_{SMBH} \sim 10^4 f_{0.1} M$

Fraction $f \sim 0.1$ of disk forms stars

$$\Rightarrow \quad M_{SMBH} / M_* \sim 10^{-3}$$

Building blocks necessary to account for the observed relation for spheroids (i.e. all old stars)

$$M_{SMBH} \propto \sigma^4$$

over $10^5 \lesssim M_{SMBH} \lesssim 3 \times 10^9 M_\odot$

Koushiappas et al
astro-ph/0311487

TRANSITION TO POPULATION II

High gas T ($\sim 10^4$ K) ⇒ high protostellar accretion rate likely to generate top-heavy IMF

Onset of metal-enhanced cooling (to $T < 100$ K)

sets in due to fine-structure excitations of O and C

once $[O/H] = -3$ and $[C/H] = -3.5$

Bromm & Loeb Nature 425 812 (2003)

Magnetically-driven feedback involving MRI dynamos (that need VERY LOW seed B) in protostellar accretion disks may also play a role (c.f. present day star formation) in self-regulating turbulence and accretion

INTRIGUING CASE OF HE0107-5240

a $0.8\,M_\odot$ star with $[Fe/H] = -5.3$

$[O/H] = -2.9$

$[C/H] = -4.3$

CLUES FROM REIONISATION OF THE UNIVERSE

- CMB $\tau \approx 0.17$ ⇒ $\frac{n_e}{n_H} \sim 1$ at $z \approx 15$

- $z=6$ quasars continuum ⇒ $\frac{n_{HI}}{n_H} \sim 10^{-3}$ at $z \lesssim 6$

- Suggests 2 populations of stars: why not pop III and pop II?

- If stars that reionise the universe at $z \sim 15$ leave chemical traces in old halo stars and DLAs
  ⇒ normal (i.e. ~30–50 $M_\odot$) stars dominate the first generation

- Stars > 100 $M_\odot$ either give discordant Z in old halo stars, DLA (pair instability SN: $\lesssim 300 M_\odot$)
  or do not leave any chemical traces (> 300 $M_\odot$)

e.g. minigquasars could reionise
(e.g. Limit at $z \sim 6$ is $M_{SMBH} < 3 \times 10^6 M_\odot$)

Need top-heavy IMF of first stars to simultaneously reionise universe and account for chemical signatures

AND SO TO B

MRI dynamo requires a minimal B field

Balbus & Hawley RMP (1998)

growth rate is $\omega = V_{Alf} k - \eta k^2$

$$\Rightarrow B > \text{constant} \times \frac{\rho^{1/2}}{L T^{3/2}} \sim \frac{1}{L M_{\substack{gas \\ clump}}}$$

The minimum B in the protogalaxy is set by the Biermann battery:

$$|B_{min}| = |\nabla p| \frac{c}{e n_e V}$$

$$\propto \frac{T^{1/2}}{L}$$

$\Rightarrow$ Maximum clump mass for effective MRI is $\sim 60\, T_4^{-1/2}\, M_\odot$

corresponding $B_{min} \simeq 10^{-15}$ gauss

CONCLUSIONS

We cannot say very much about the IMF of the first stars

VERY MASSIVE STARS $\sim 10^3 M_\odot$

Physics is relatively simple → beautiful simulations

but are they the dominant mode?

Their Z contribution ($\sim 10^{-5}$ solar) is too low to trigger the transition to Pop II

Nor are the predicted abundance ratios observed

NORMAL STARS WITH TOP-HEAVY IMF
30 - 100 $M_\odot$

can account for reionisation, chemical signatures, transition to Pop II, SMBH seeds, are a by product

but theory is highly speculative

need better simulations!

B fields
could be missing link between pop III and II

if so, we have far to go!

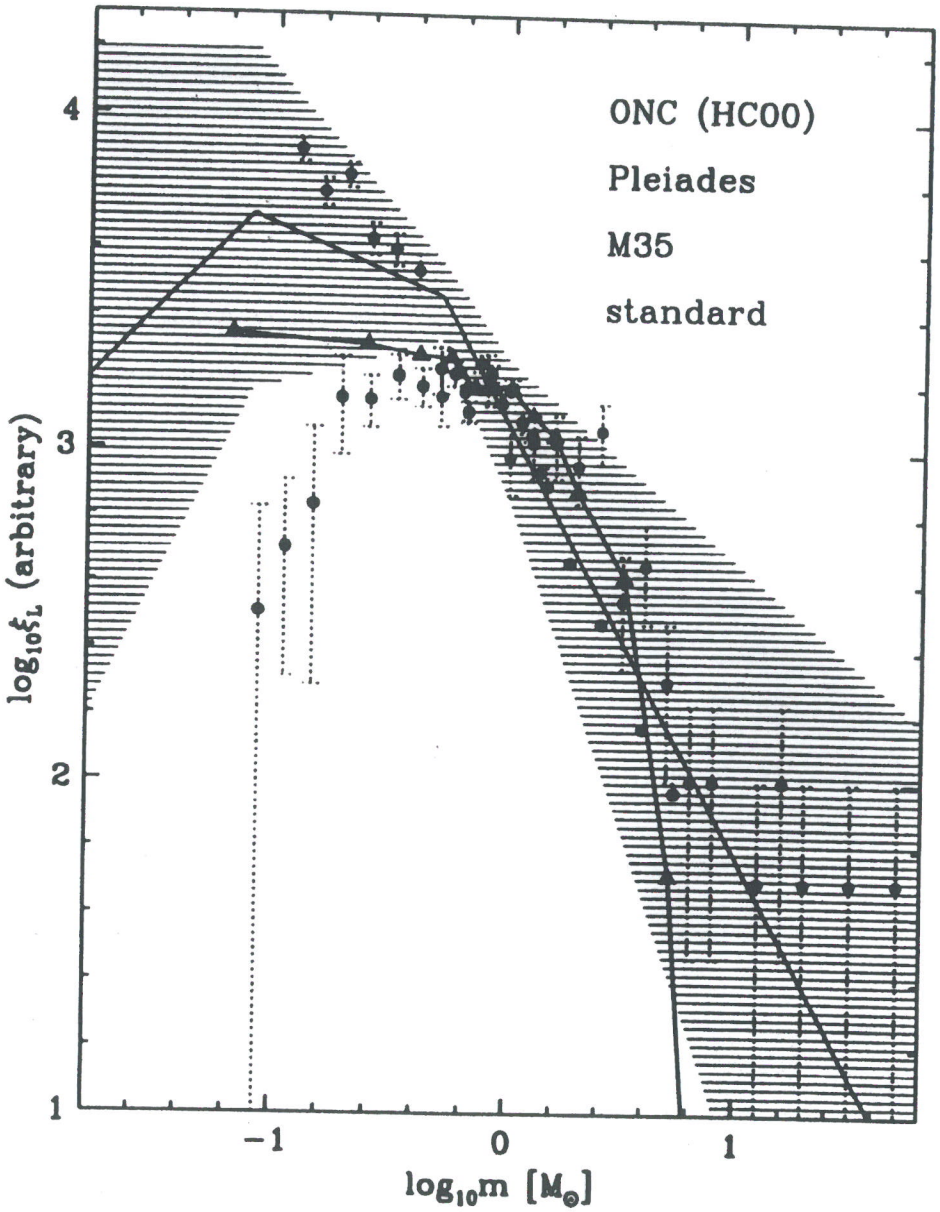

FIG. 5. The measured stellar mass function ξ as function of logarithmic mass $\log_{10} m$ in the Orion nebular cluster (upper circles), the Pleiades (triangles connected by line), and the cluster M35 (lower circles). None of the mass functions is corrected for unresolved multiple stellar systems. The average initial stellar mass function derived from Galactic field stars in the solar neighborhood is shown as a line with the associated uncertainty range indicated by the hatched area. (From Kroupa 2002.)

Silicon

PISNae stars overproduce Si

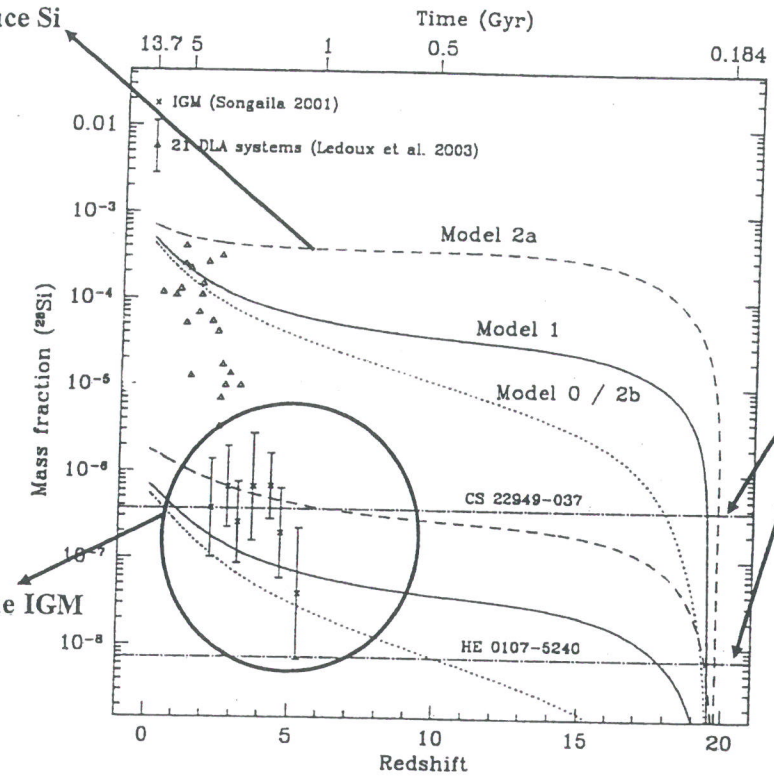

Extremely metal-poor halo stars could trace the early metal enrichment by pop. III stars.

Abundance determination in the IGM are now available.

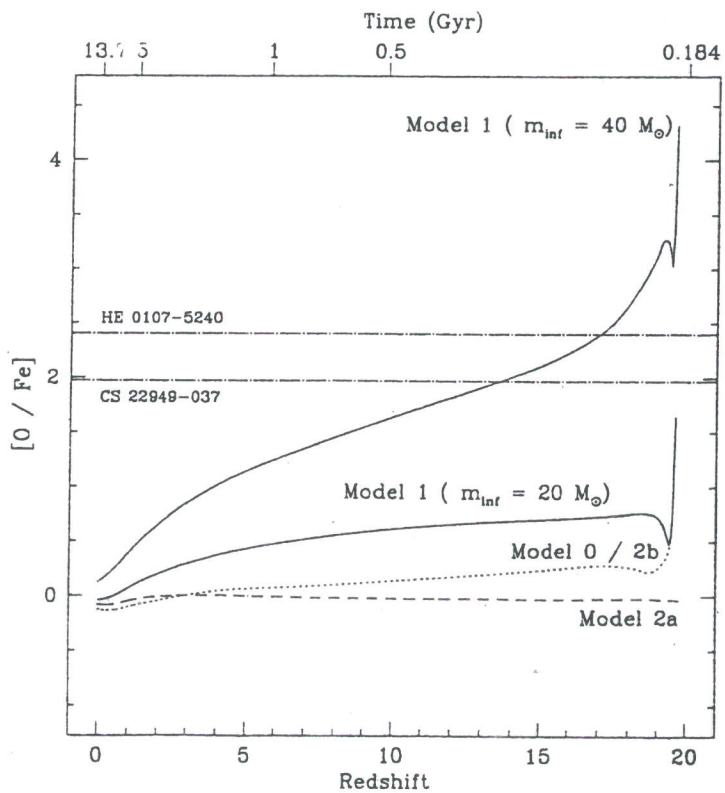

Fig. 13.— Evolution of the [O/Fe] ratio. The Oxygen to Iron ratio in the cosmic structures is plotted as a function of redshift for Model 0 and 2b (dotted line), Model 1 (solid line) and Model 2a (dashed line). For Model 1, two lower mass limits of the IMF are considered : $m_{inf} = 20\ M_\odot$ or $m_{inf} = 40\ M_\odot$.

lodels From Daigne et al (2006)

: normal IMF

: normal + top-heavy

normal + pop III

τ_s = baryon accretion time (Gyr)

Cosmic Star Formation Rate

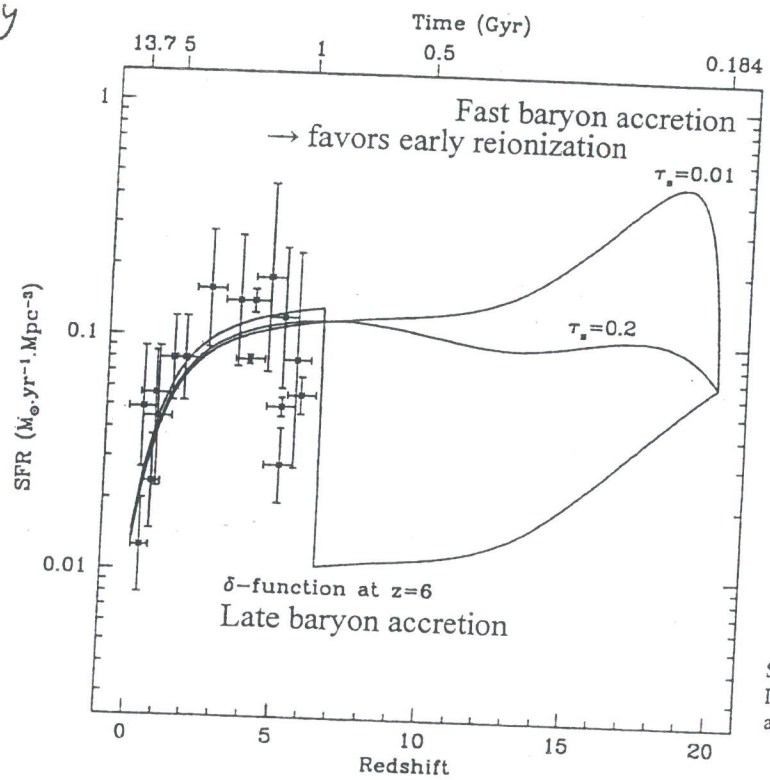

Model 1 : model 0 + massive stars

Mass range :

IMF 0 : 0.1-100 $M_\odot$

\+ IMF 1 : 40-100 $M_\odot$

Characteristic SFR timescale :

SFR 0 : 5 Gyr

SFR 1 : 50 Myr

SFR data : Lilly et al. 96 ; Pascarelle et al. 98 ; Iwata et al. 03 ; Ouchi et al. 03 and Giavalisco et al. 04

Ionizing photons per baryon

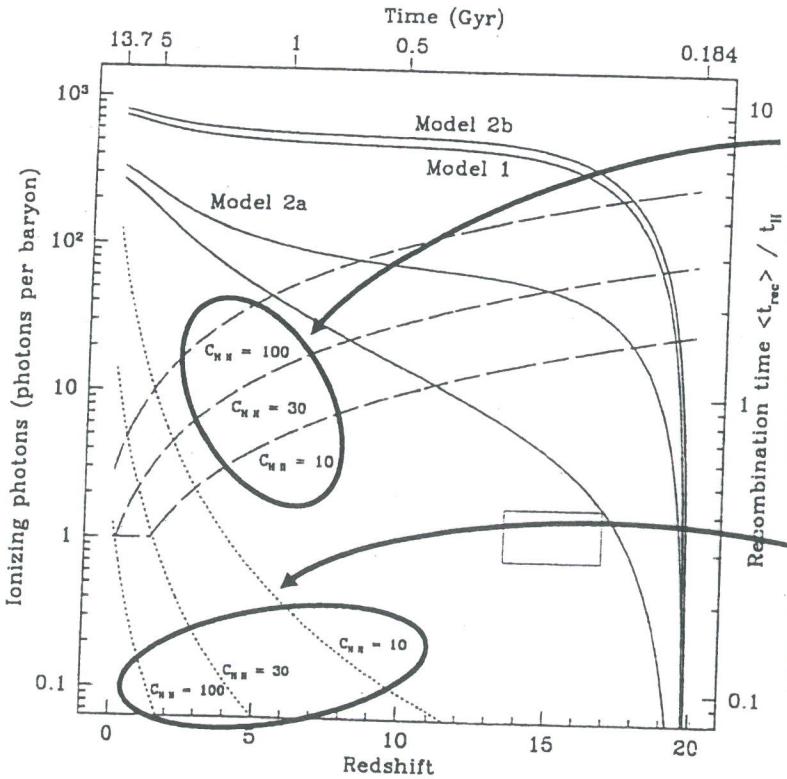

$$n_{\gamma,\,min} = \left(\frac{\langle t_{rec}\rangle}{t_H}\right)^{-1} = 22\left(\frac{1+z}{18}\right)^{1.5}\left(\frac{C_{HII}}{10}\right) \text{ ph/b if } \langle t_{rec}\rangle < t_H$$

$$= 1 \text{ ph/b otherwise}$$

Model 1 and 2b allow an early reionization of the IGM even for a high clumpiness factor.

$$\frac{\langle t_{rec}\rangle}{t_H} = 0.046\left(\frac{1+z}{18}\right)^{-1.5}\left(\frac{C_{HII}}{10}\right)^{-1}$$

The Chemical Yield of the First Galaxies

Rob Simcoe (MIT)
With W. Sargent (Caltech) & M. Rauch (OCIW)

- Metallicity distribution of IGM
- The “Ultimate Closed Box”
- Early galaxies were efficient polluters

Heavy Elements Were Dispersed into the IGM at Early Times

- Low densities
  - Far from galaxies!
- Whodunit?
  - Bare Pop III?
  - Early dwarf gals?
  - LBG + winds?
  - Tidal stripping?

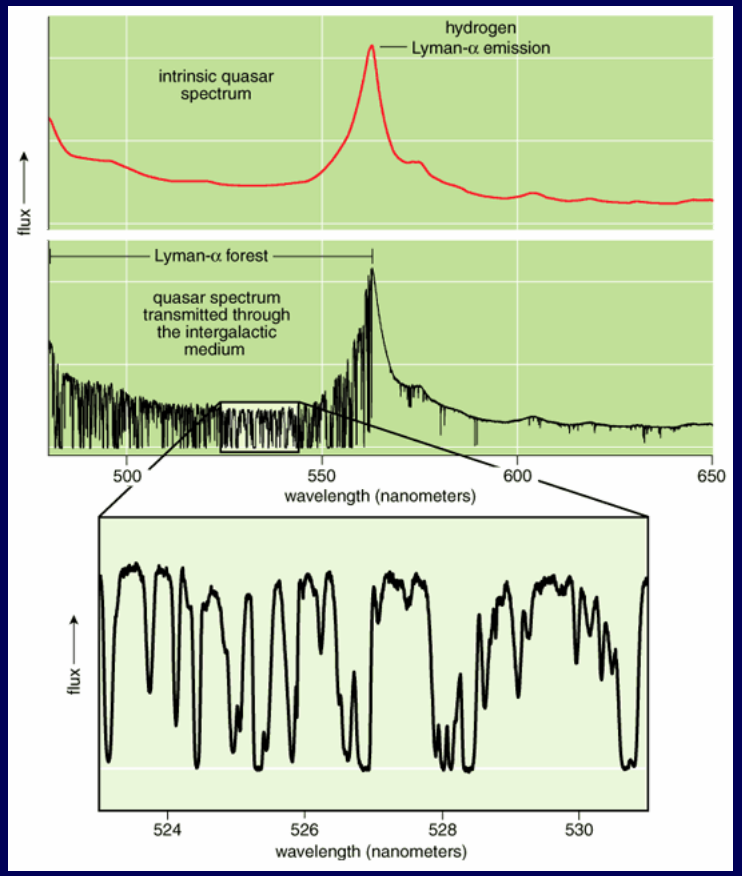

Intergalactic Metallicity Distribution at z = 2.5

- Fossil record of feedback
- OVI, CIV abs. lines
- Lognormal
  - Median [O/H] = -2.85
  - Scatter ~0.75 dex
- Metallicity Floor?
  - At least below –3.5

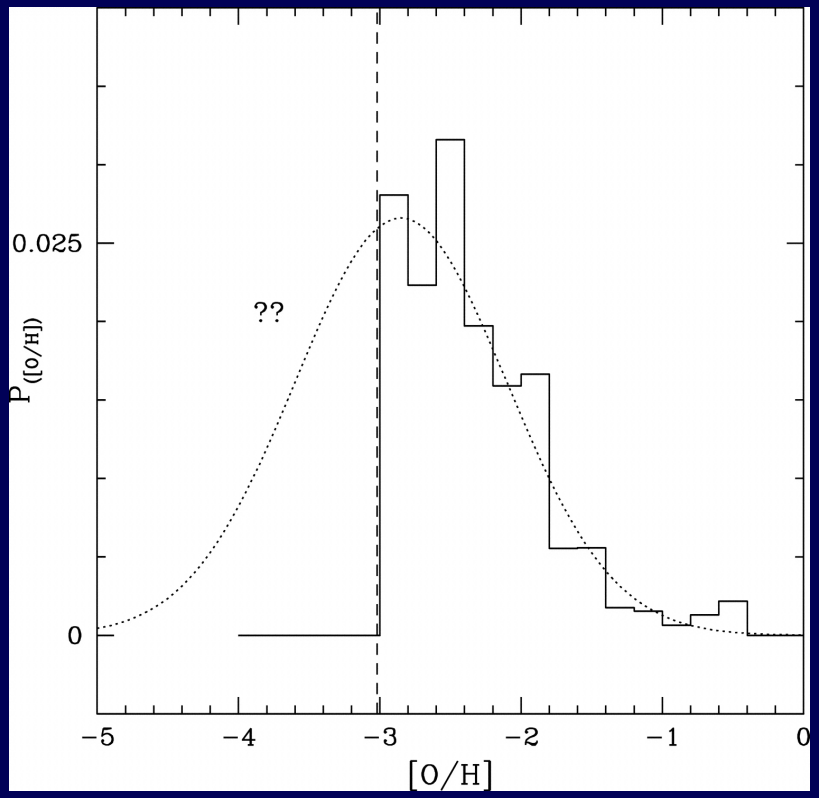

Intergalactic Metallicity Distribution at z = 2.5

- Fossil record of feedback
- OVI, CIV abs. lines
- Lognormal
  - Median [O/H] = -2.85
  - Scatter ~0.75 dex
- Metallicity Floor?
  - At least below –3.5

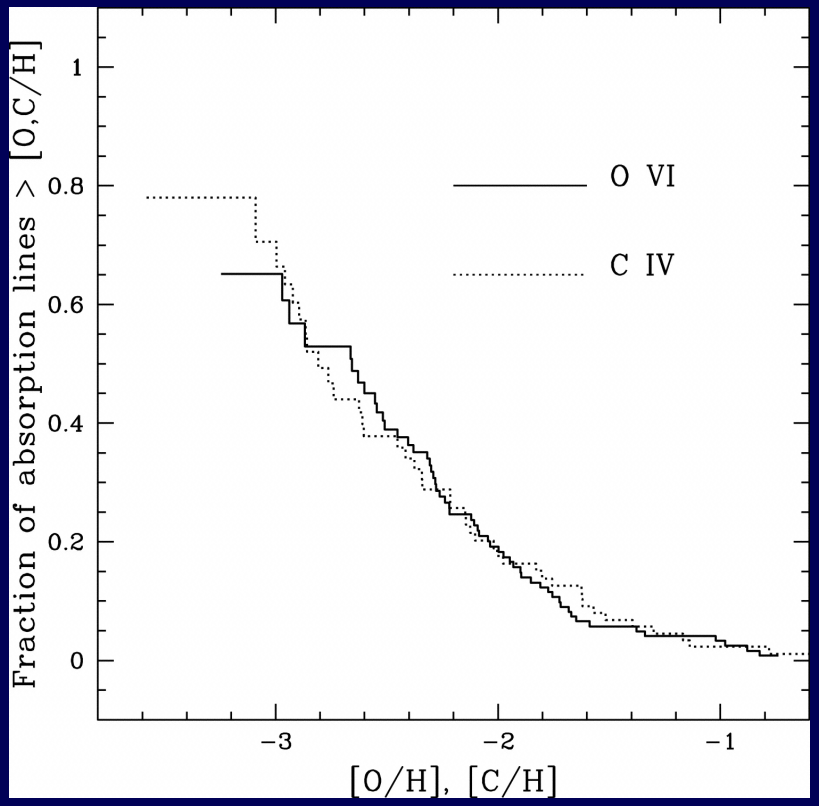

Enriched Mass at z = 2.5

- Baryons still in forest
- Measure filaments' Z
- Voids still unknown

First 15% of Hubble time, ~1/2 of all baryons mixed with stellar byproducts

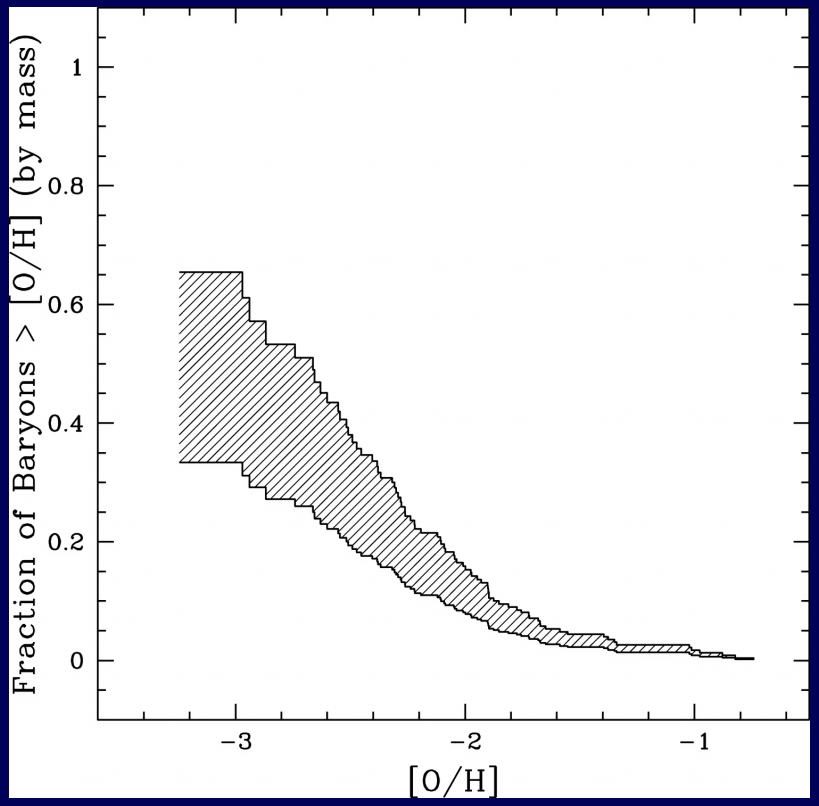

IGM Enrichment: *Not* the First Stars

- Giant Z = 0 stars?
  - Can't make enough!
- Mergers / tidal tails?
  - Debatable
- Galactic winds?
  - Yes, if tuned properly
  - Observed!

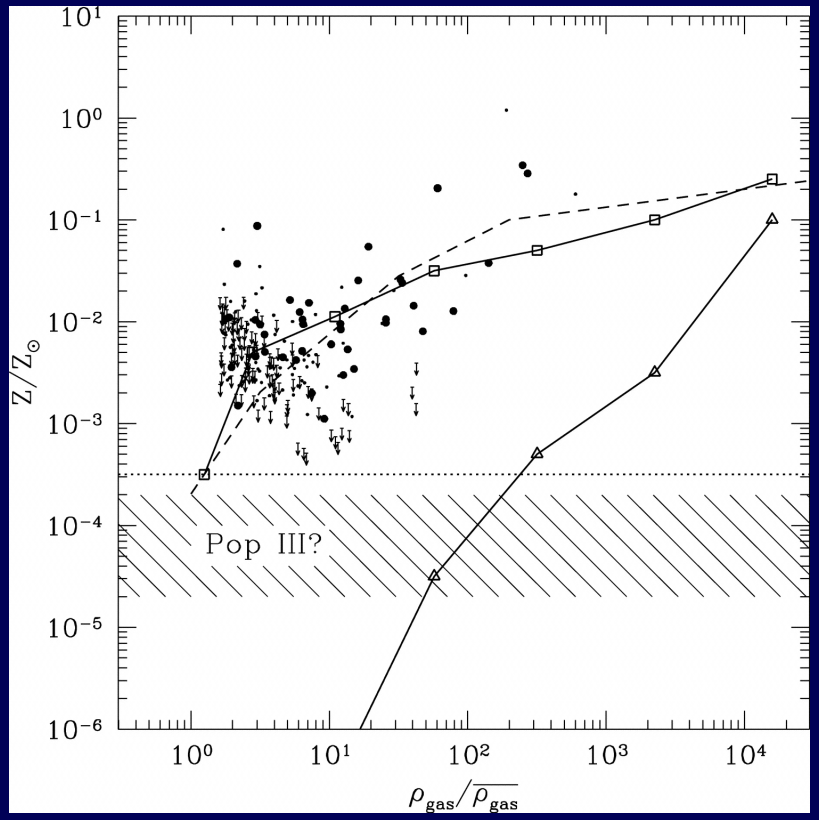

The “Ultimate Closed Box”

- Need insight on heavy polluters
- Global chemical evolution: the universe
- Baryons, metals cycle:

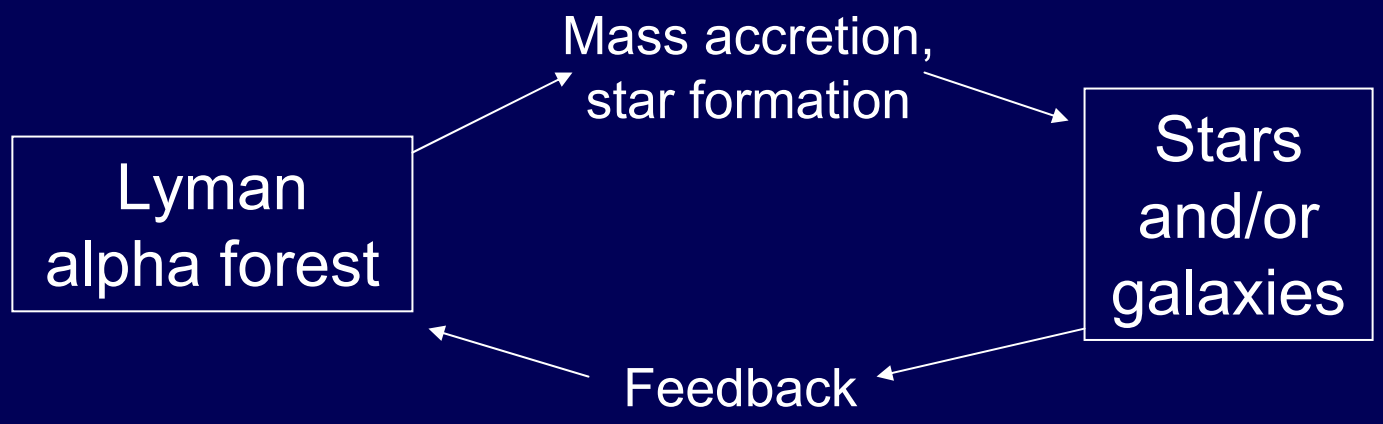

The "Ultimate Closed Box"

- Start with Z_{IGM}=0, all baryons in IGM
- Baryons fall into haloes, stars form

$$\frac{dM_{IGM}}{dt} = -\varphi_{gal}$$

- Metals "recycled" into IGM at some yield

$$dM_{metals} = y dM_{gal}$$

The “Ultimate Closed Box”

- Metal transport equation:

$$\frac{d}{dt}(ZM_{IGM}) = y\varphi_{gal} - Z\varphi_{gal}$$

- Solution:

$$Z_{IGM} = y\ln\left(\frac{M_{IGM} + M_{gal}}{M_{IGM}}\right)$$

The “Ultimate Closed Box”

- Metal transport equation:

$$\frac{d}{dt}(ZM_{IGM}) = y\varphi_{gal} - Z\varphi_{gal}$$

- Solution:

$$Z_{IGM} \approx y \ln\left(\frac{\Omega_b}{\Omega_{Lya}}\right)$$

“Observed” Yield

- Galaxy yield: 0.1% < y < 0.4%
- How does this relate to stellar yields, etc?

$$y(M_* + M_{ISM}) = y_* M_* f_{ej}$$

$$f_{ej} = \frac{y}{y_*}\left(1 + \frac{M_{ISM}}{M_*}\right)$$

Early Galaxies Were Efficient Polluters

$$f_{ej} \geq 15\% \left(\frac{M_{b,gal}}{M_*} \right)$$

- "Typical" $z > 2.5$ galaxy
- Low-z analogues?
  - Comparable to dwarfs
  - But…LBG superwinds
- Benchmark

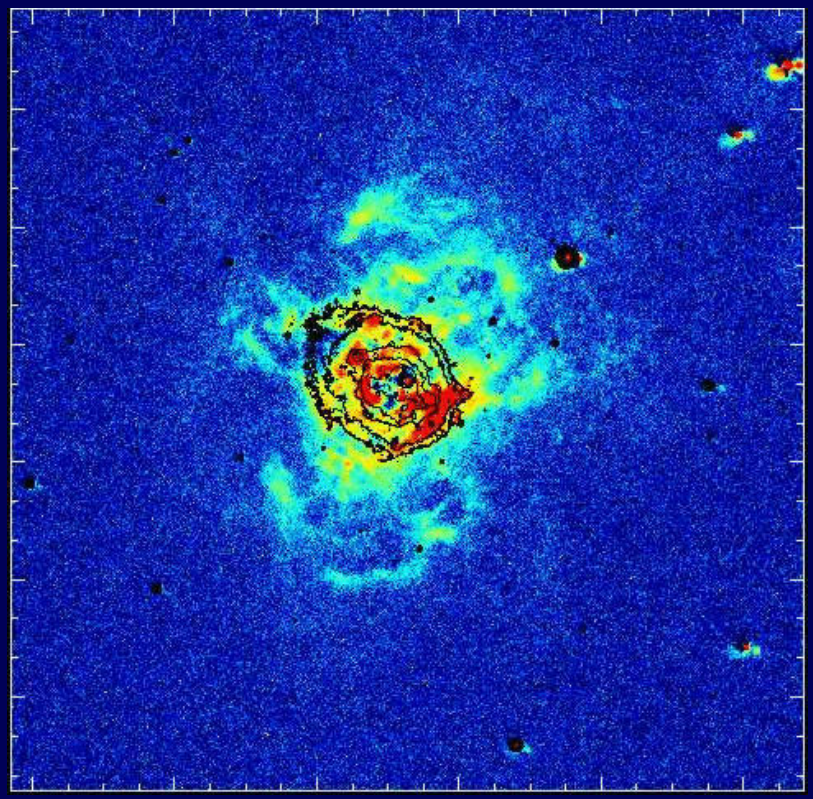

The Chemical Yield of the First Galaxies

- Forest p(Z): measured
- ~ 50% polluted
- How?
  - Bare Pop III stars: not enough
  - What sorts of galaxies then?
    - Ultimate Closed Box
    - Early galaxies efficient chemical factories

Lithium Isotopic Abundances in Metal-Poor Stars: Diffusion, Rotational Depletion, & Cosmic Rays

Verne V. Smith

U.S. Gemini Science Center

National Optical Astronomy Observatory

+ Martin Asplund, Poul E. Nissen, Omar Vargas, David L. Lambert, Francesca Primas, Lou Hobbs

The Origins of Lithium

- Big Bang Nucleosynthesis: ^{7}Li
- Cosmic-Ray Spallation and Fusion: ^{6}Li, ^{7}Li
- AGB Hot-Bottom Burning: ^{7}Li
- Neutrino Nucleosynthesis (SNII) ? : ^{7}Li, ^{6}Li
- Cool-Bottom Processing (RGB) ? : ^{7}Li
- Novae ? : ^{7}Li

---> Lithium is destroyed by exposure to “warm” protons:
$T > 1\text{-}2 \times 10^{6}$ K.

The Behavior of Li with [Fe/H]

Teff`s > 5800K

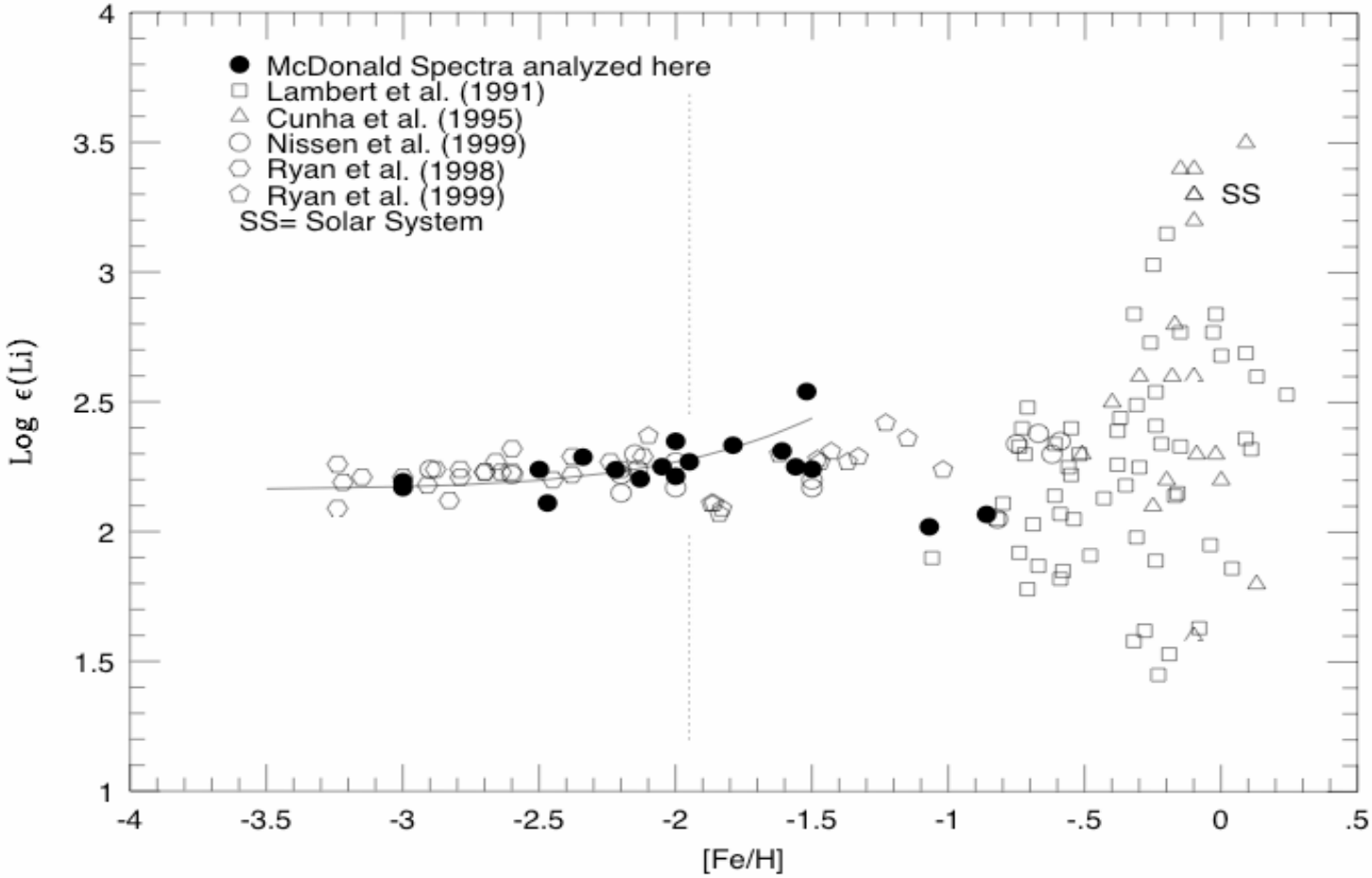

Thinking about the Spite Plateau

- Spite & Spite (1982): Flat --> Cosmological.
- Thorburn (1994): Dispersion(>0.1dex)….. Slope (>0.1 dex/dex)?? (S/N~90 spectra).
- Bonifacio & Molaro (1997): No dispersion and no slope!
- Ryan, Norris, & Beers (1999) + Ryan et al.(2001): Tiny dispersion about a slope (~0.1 dex/dex).
- Smith, Nissen, Lambert (1993): ^{6}Li detection-- requires some evolution. + Smith et al. (1998) + Nissen et al. (1999).

Lithium Abundance Analyses in Metal-Poor Dwarfs are Robust

- Most sensitive to Teff (0.06 dex/100K)
- Sensitivity to gravity and microturbulence: ~0.00 dex
- Non-LTE: <0.04 dex
- Absolute abundances vs. model atmosphere flavor--ATLAS9 vs. MARCS: <0.10 dex.
- 1-D vs. 3-D: <0.05 dex.
- K I 7700A is a nice test for Li I…same eqw in range -3.0 to -2.5 in [Fe/H]. Same contribution functions. Changing [Li/Fe] changes [K/Fe] in the same way.

Spectra to Analyze Isotopic Composition of Metal-Poor Dwarfs

- R= $\lambda/\Delta\lambda$=110,000–120,000. S/N= 200-600.
- McDonald 2.7m + Coude-- 18 stars.
- ESO VLT+UVES-- 23 stars.
- Two datasets analyzed independently, with no cross-talk.

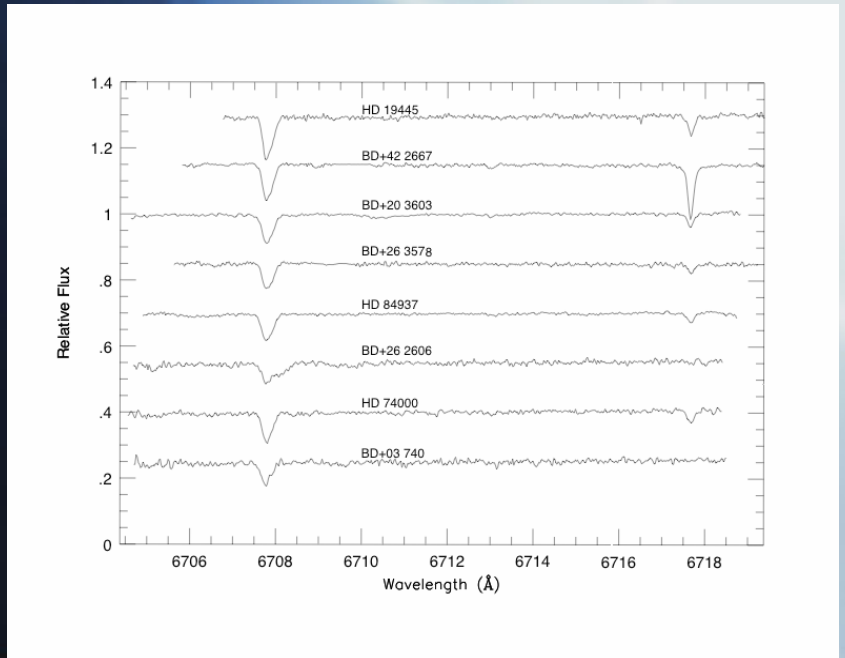

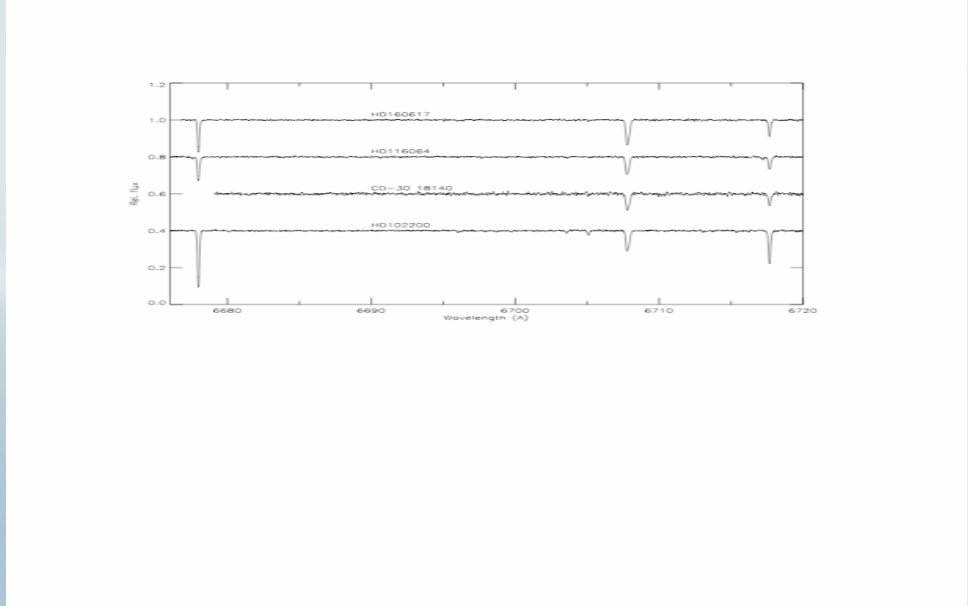

Abundances from McDonald

Teff's from Stromgren photometry tied to IRFM

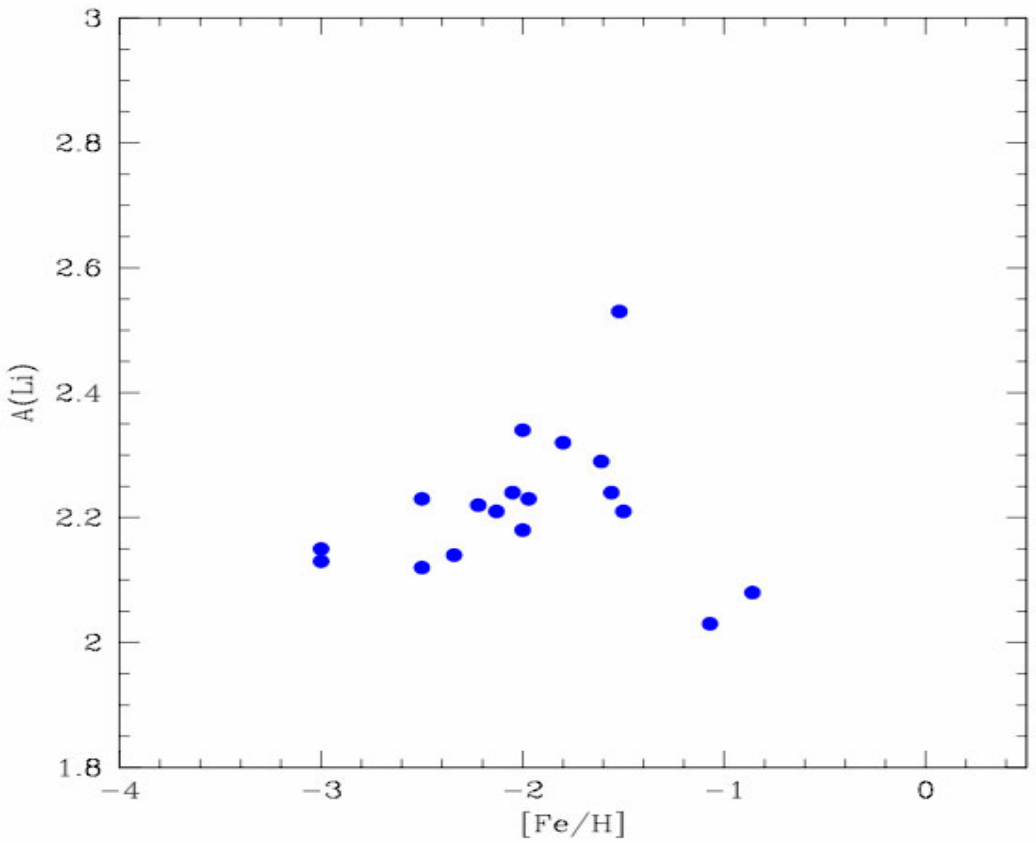

Add in the VLT/UVES Results

Teff's from Hα Wings. Observational uncertainties--+/-0.03 dex in Li, & 0.07 dex in Fe.

Agreement between McD and ESO essentially perfect.

Definite trend at low [Fe/H]: slope is in agreement with Ryan & collaborators. Scatter about trend in VLT spectra is 0.02 dex

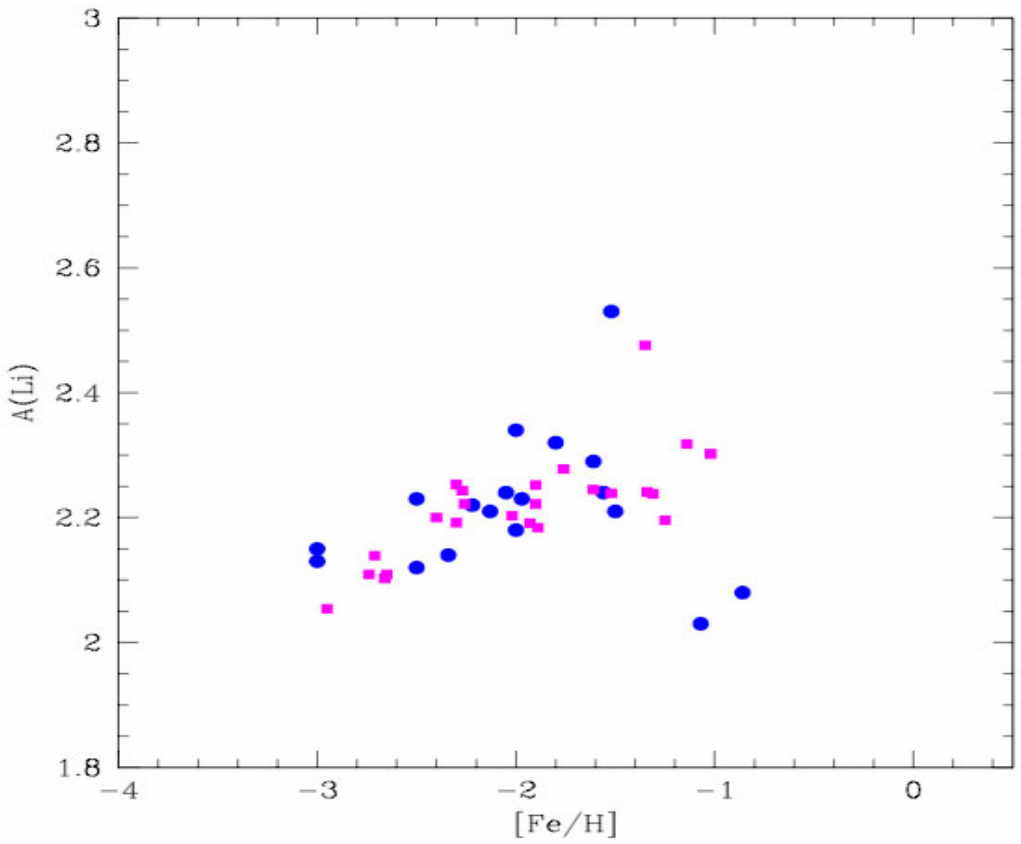

Switch to Linear Abundance Scales

>Rotationally induced mixing: No…outliers.

>Diffusion: Maybe the best chance…but no [Fe/H] dependence. Presence of ^{6}Li requires very fine tuning of turbulence. Also, small dispersions also require finely tuned turbulence. Plus James et al. (2004) & Bonifacio et al. (2002) for Li and Fe… in N6752 and M92! No change from MS--TO--SG.

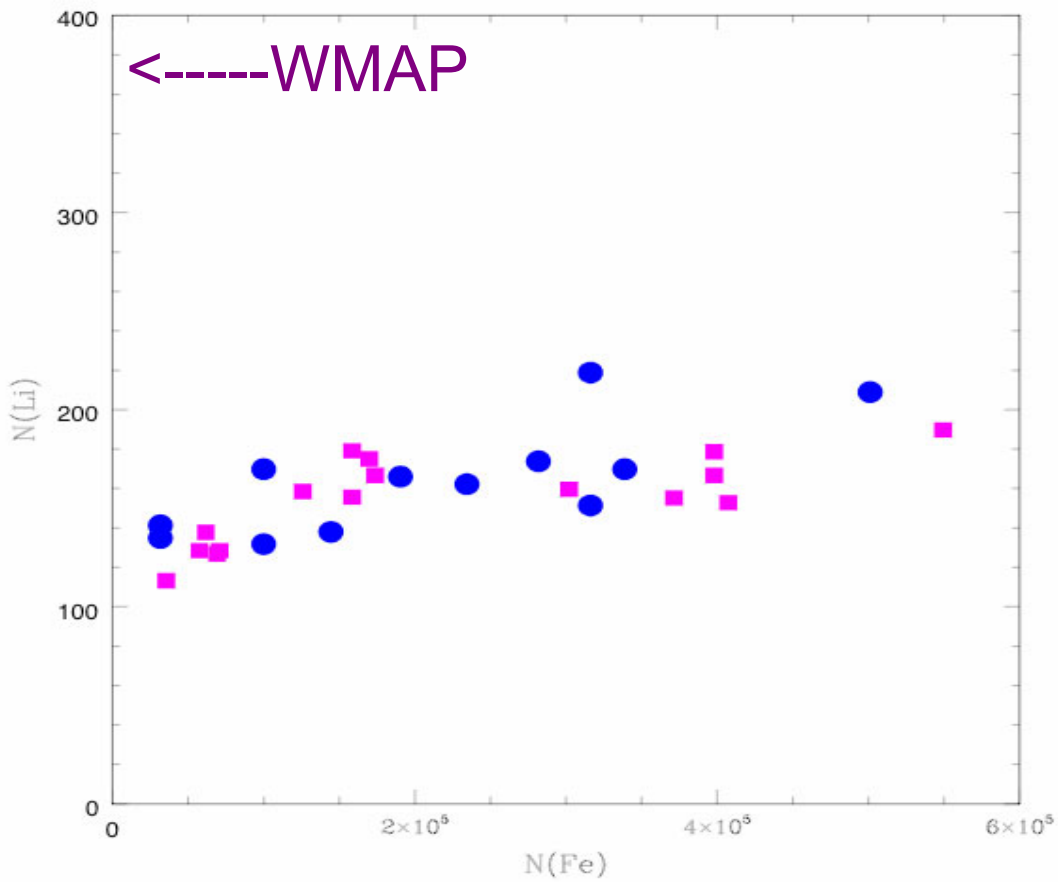

Energetics of Li production using Cosmic Rays accelerated by Supernovae

For accelerated SN ejecta-- create 0.1 Li atoms per erg.

SN II ejecta: ~0.1MSun of Fe= 2×10^{54} Fe atoms.

For SN II energy for cosmic-ray acceleration: ~10^{50} ergs.

For only Li production via CR's--each SN II could produce 10^{49} Li atoms.

But this will also include Be and B.

Maximum slope in N(Li)/N(Fe) is ~10^{-5} .

Observed slope is about 10^{-4} .

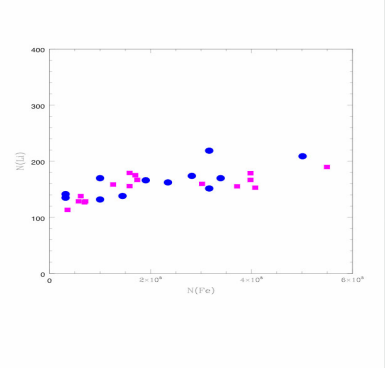

^{6}Li Analyses

- 1-D models
- Equivalent Width
- Microturb.
- Macroturb.
- Vsin ι

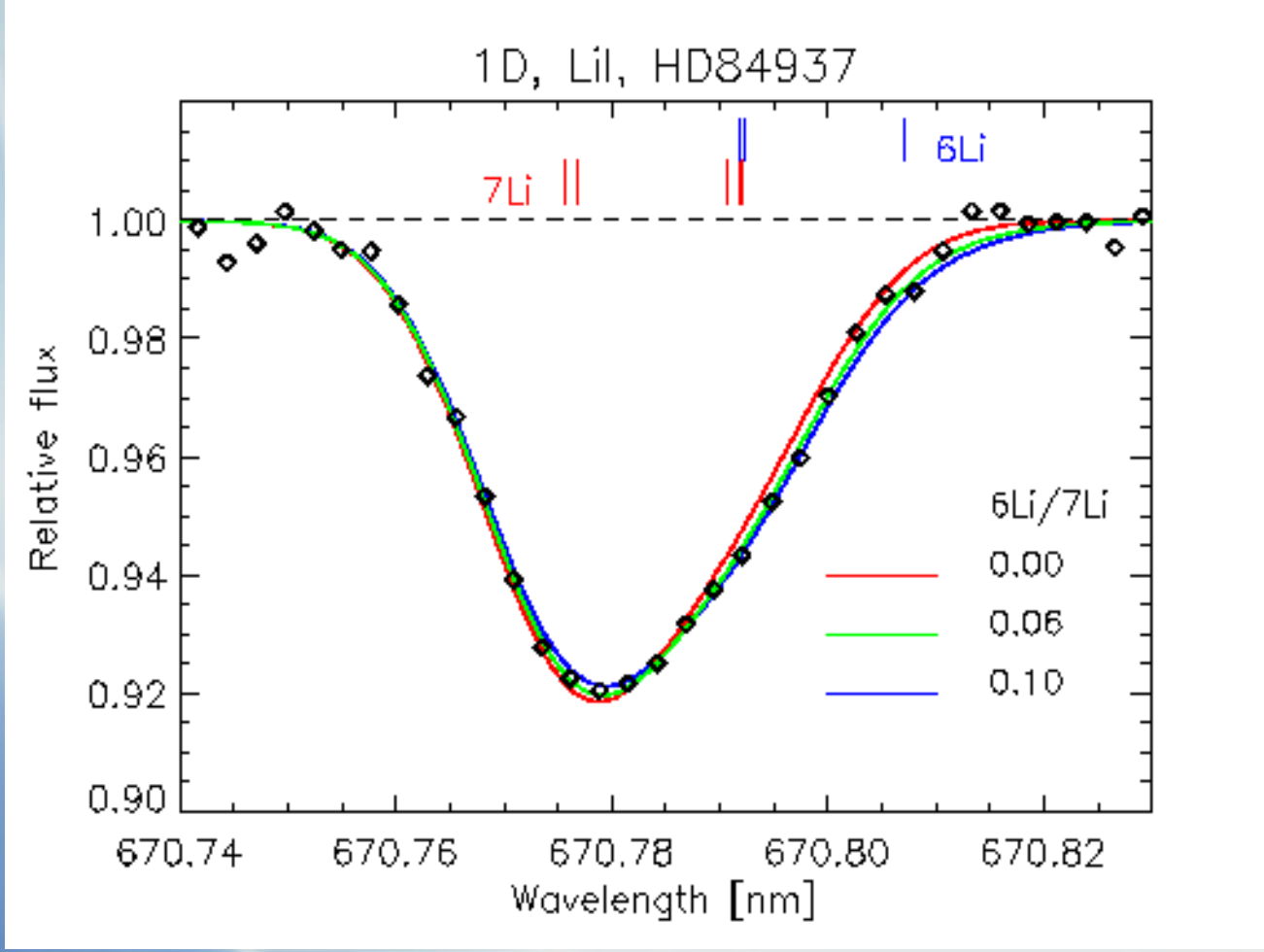

3-D Models: M. Asplund

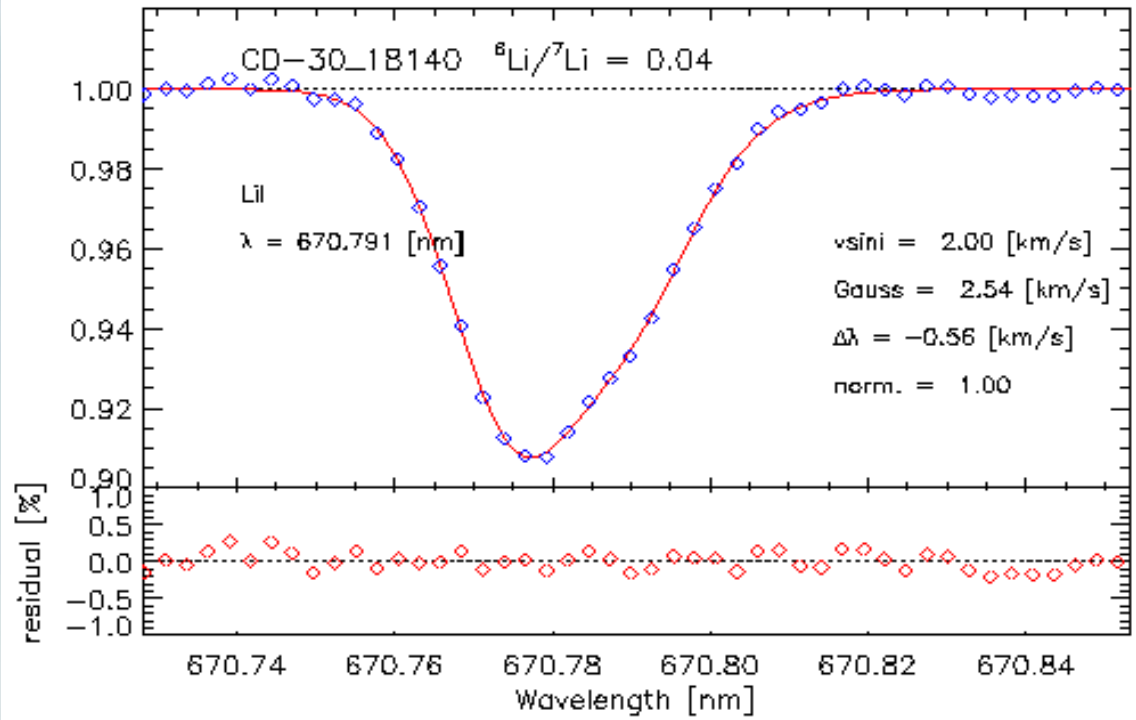

- No Microturbulence
- No Macroturbulence

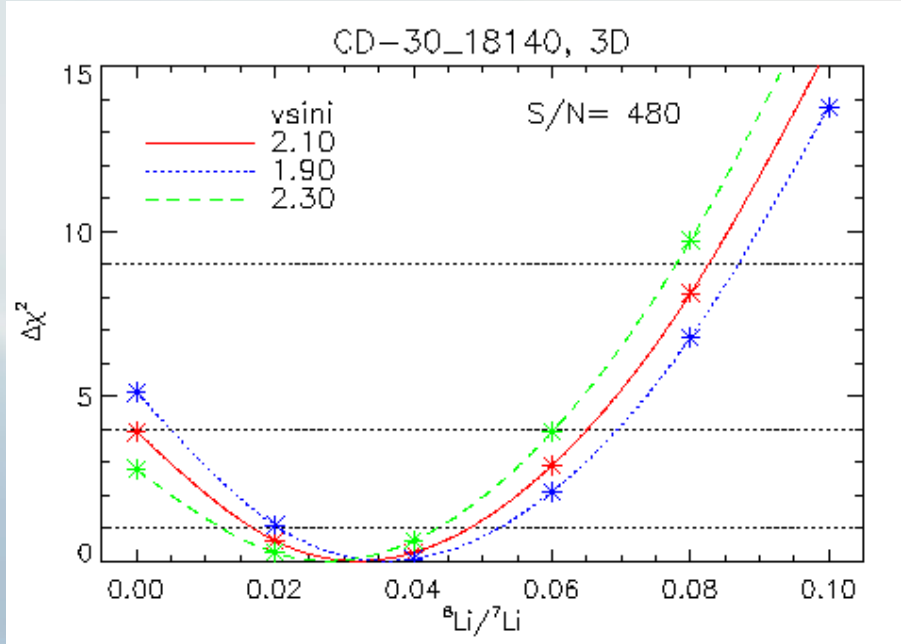

10 detections:
All on Turn-Off or Early Subgiants.

Energetics chemical evolution model for Be from Ramaty (1999)

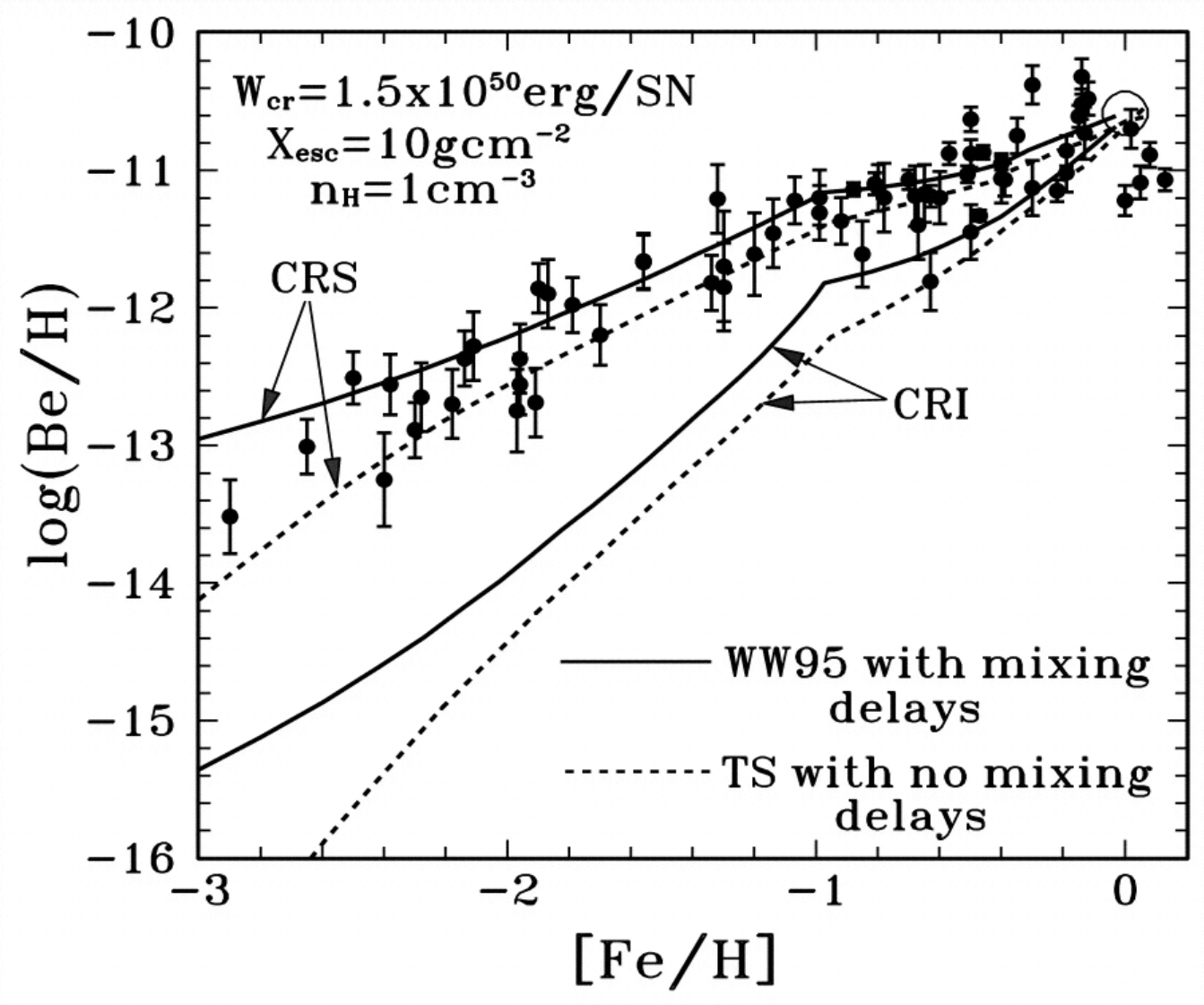

Summary of ^{6}Li Detections

Model by Ramaty(1999). Based on SN II energetics + CR models. Prediction for ^{6}Li using a model that fits Be vs. Fe.

Excess ^{6}Li at low Fe, relative to the Be fit.

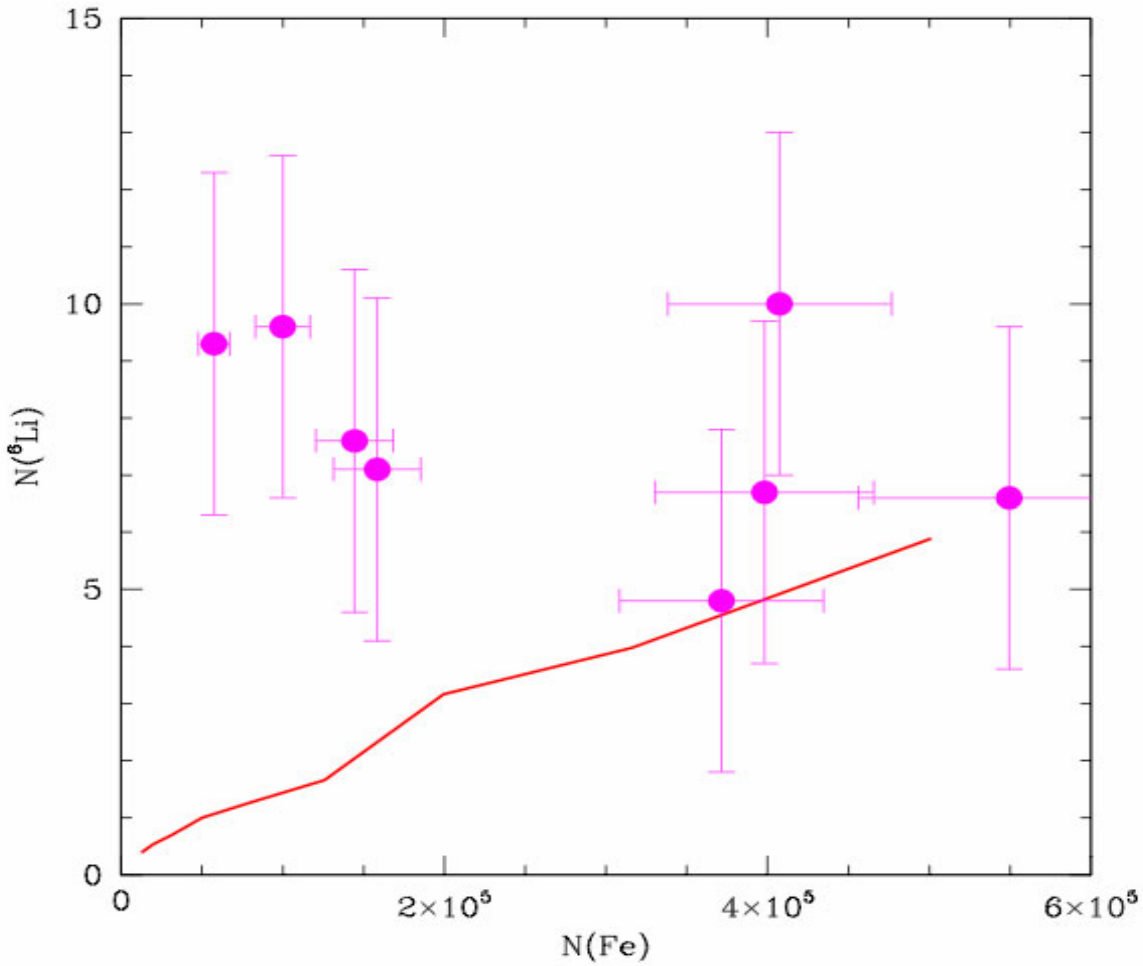

Conclusions

- Spite Plateau is thin, but with a slope. Dispersion about this slope is ~+/- 0.02 dex.
- Li-6 shows that there has been chemical evolution--energetic processes.
- Rotational depletion cannot be large. Diffusion is a possibility…but requires finely tuned turbulence…microphysics. Strong constraints from both Li-6 and globular clusters.
- Li-6 at lowest metallicities may require a new energetic process…pre-Galactic via α–α reactions?

s-process nucleosynthesis in low and very low metallicity stars

Oscar Straniero & Sergio Cristallo (INAF-OACT & Univ. Teramo)
Inma Dominguez & Carlos Abia (Univ. Granada),
Roberto Gallino (Univ. Torino),

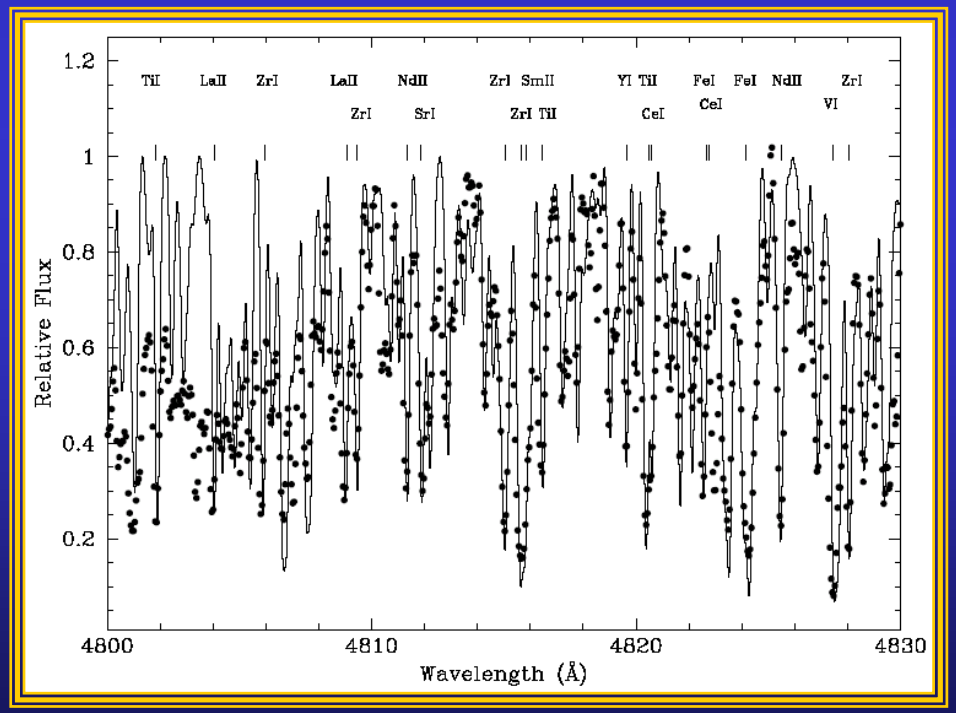

Santa Fe 8-13, August 2004

Thermally Pulsing stars: a bi-power 5 $M_{\grave{A}}$ Z=0.02

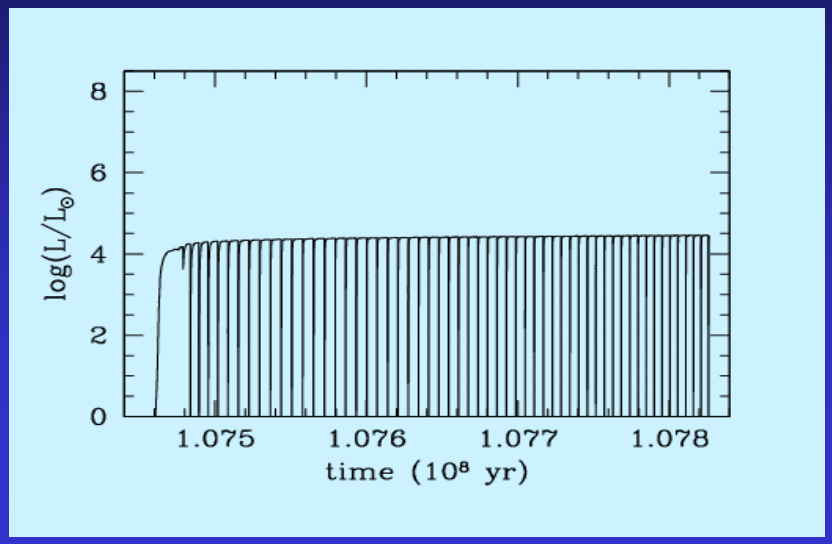

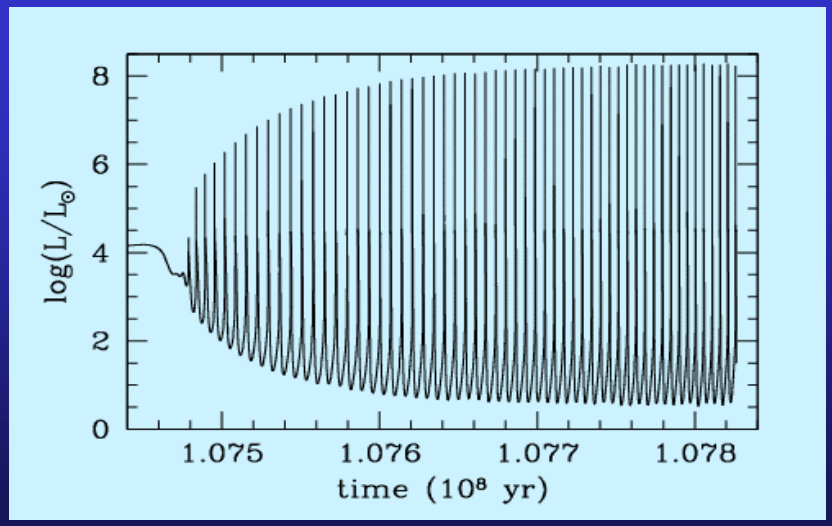

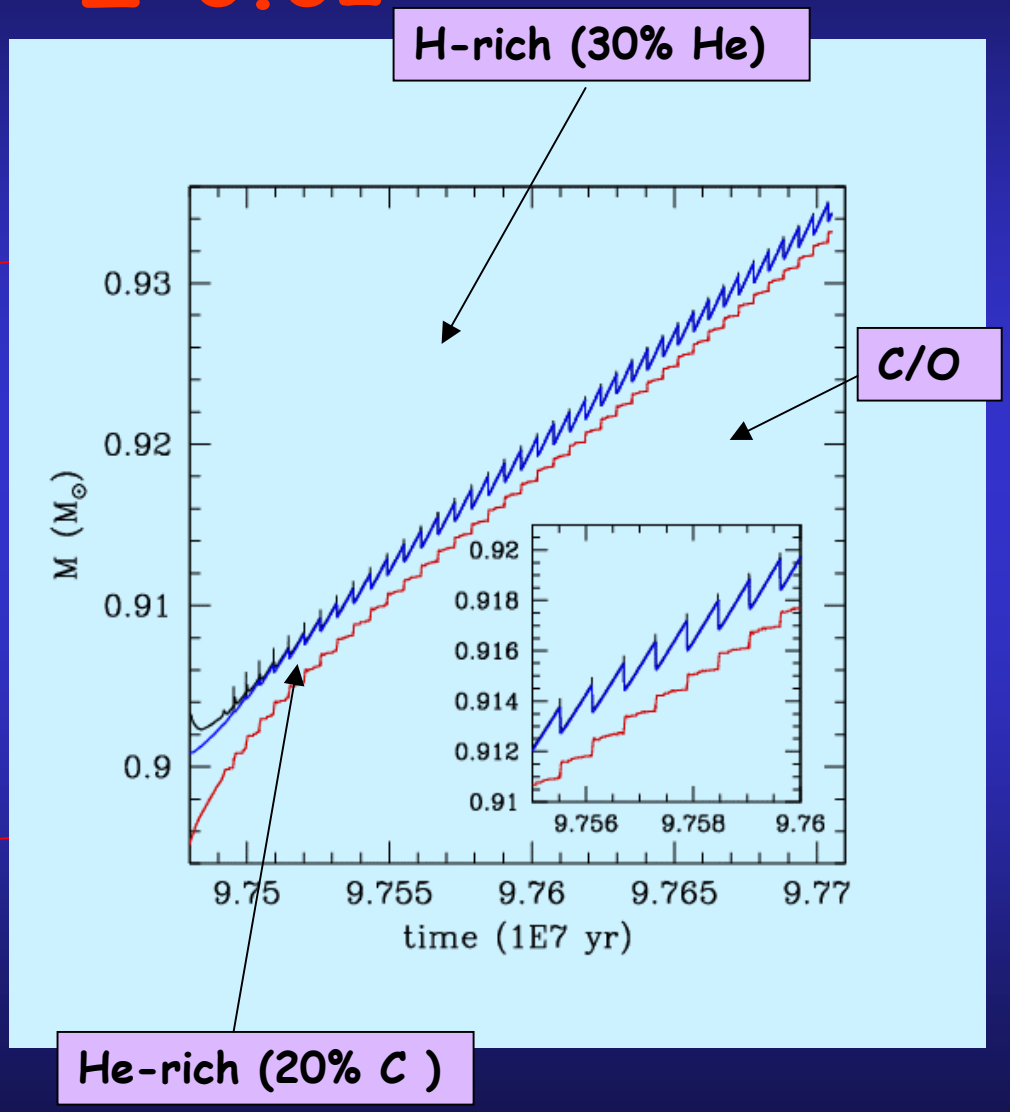

AGB classification
(theory versus observations)

M… Galactic Disk (-solar composition)
M… Magellanic Clouds (Z-1/3Z$_{\odot}$)

M giants

Type I	Type II	Type III	Type IV	Type V
M<1.2 M<1.2	1.2<M<1.8 ----------	1.8<M<3 1.2<M<2.5	3<M<5 2.5<M<4	M>5 M>4
TDU: no HBB: no C/O:# 0.5 s-elem.: no	TDU: yes ^{13}C(α,n): yes ^{22}Ne(α,n): m* HBB: no C/O: 0.3 – 0.9 s-elem.: yes	TDU: yes ^{13}C(α,n): yes ^{22}Ne(α,n): m* HBB: no C/O: up to >1 s-elem.: yes	TDU: yes ^{13}C(α,n): yes ^{22}Ne(α,n): yes HBB: m* C/O: up to >1 s-elem.: yes Li-rich	TDU: yes ^{13}C(α,n): yes ^{22}Ne(α,n): yes HBB: yes C/O: <1 s-elem.: yes N-rich Li-rich

*marginal

MS, S

CN

MS

Low Z AGB: where?

- Galactic Halo: Presently, the typical mass of a star at the onset of the AGB is -0.6 $M_{À}$ (initial mass 0.8-0.9 $M_{À}$). We are observing very low mass AGB: no TDU -> no C or s envelope enrichment.

  We can find traces of extinct halo AGB stars, of any mass, by searching their chemical signature in:

  a) the chemical evolution of the early galaxy

  or

  b) Low metallicty C- and s-rich stars belonging to binaries with a compact (WD) companion.

- Extragalactic low metallicity stellar populations:

  a) Magellanic Clouds, down to Z-3 10^{-3}, all AGB types;

  b) Dwarf spheroidals, down to Z-2 10^{-5}, M#2 $M_{À}$

  (see Dominguez et al. 2004, AA, in press)

The first generation of Massive AGB

1984 Chieffi & Tornambe, Fujimoto et al.. Owing to the lack of CNO (in primordial stars) H- and He-burnings are active in the same place and simultaneously. ----- > NO Thermal pulses

2001 Chieffi et al., (see also Siess et al. 2002). Weak Tps generating a usual convective episode within the He-rich layer (HeCE), followed by an anomalous hydrogen convective episode (HCE), located at the base of the H-rich envelope.

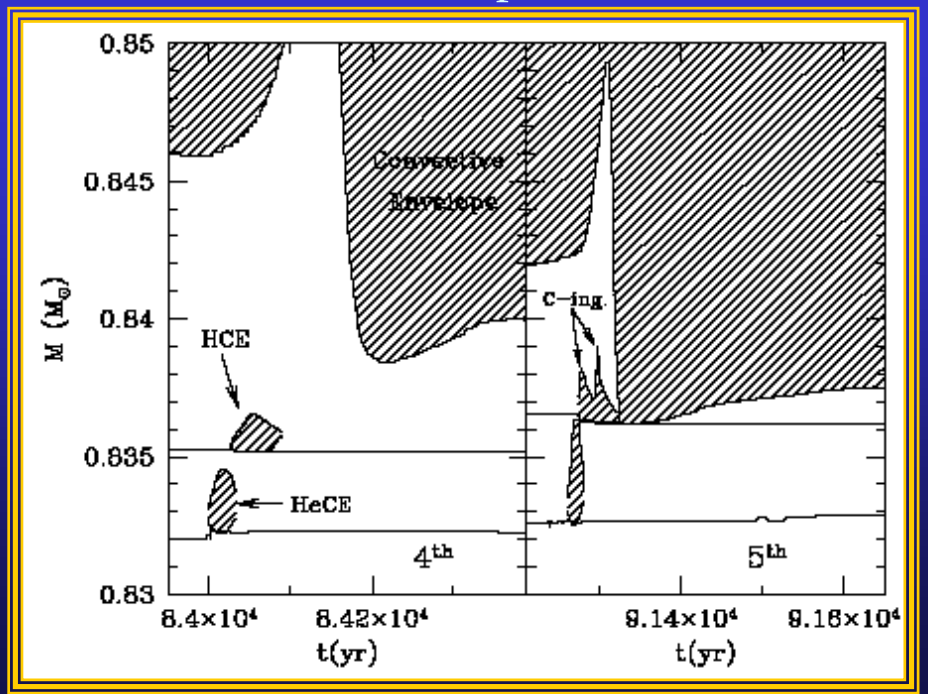

$4M_{\odot}$ Z=0.

After the 5th TP, the HCE overlap the region previously mixed by the HeCE. The resulting C-enhancement induces 2 violent H-flashes, which power a substantial expansion of the envelope and a dredge-up.

4 $M_{\grave{A}}$ Z=0

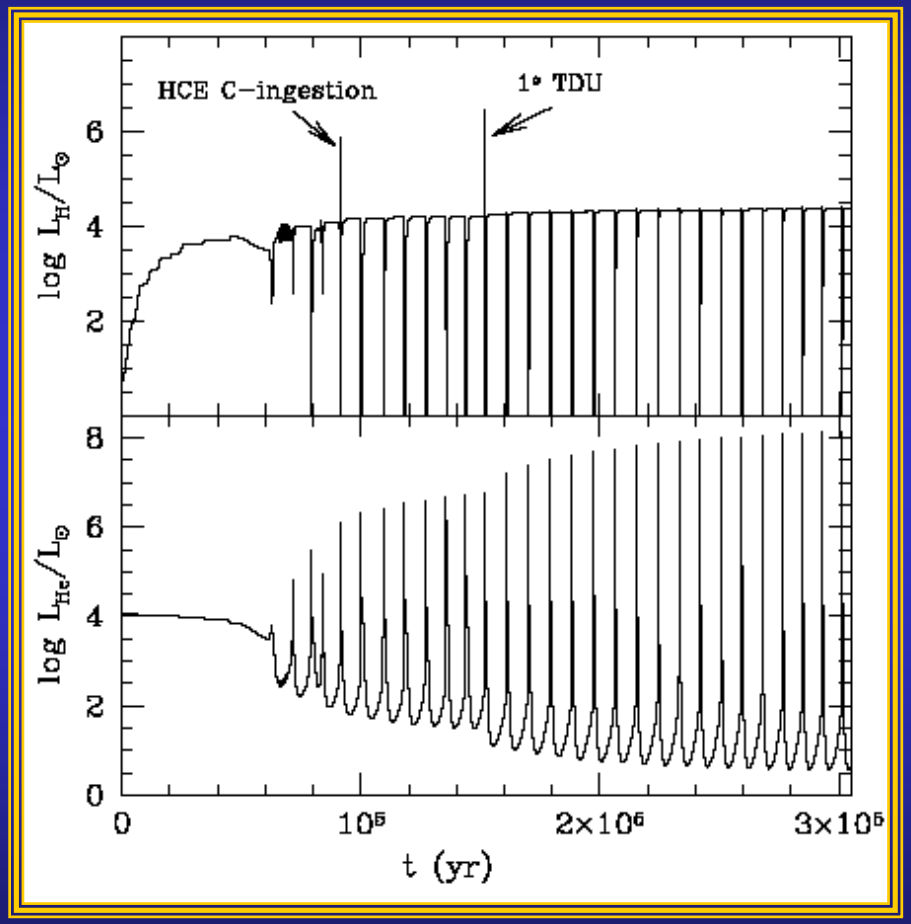
HCE C−ingestion
1° TDU
log $L_H/L_\odot$
log $L_{He}/L_\odot$
t (yr)

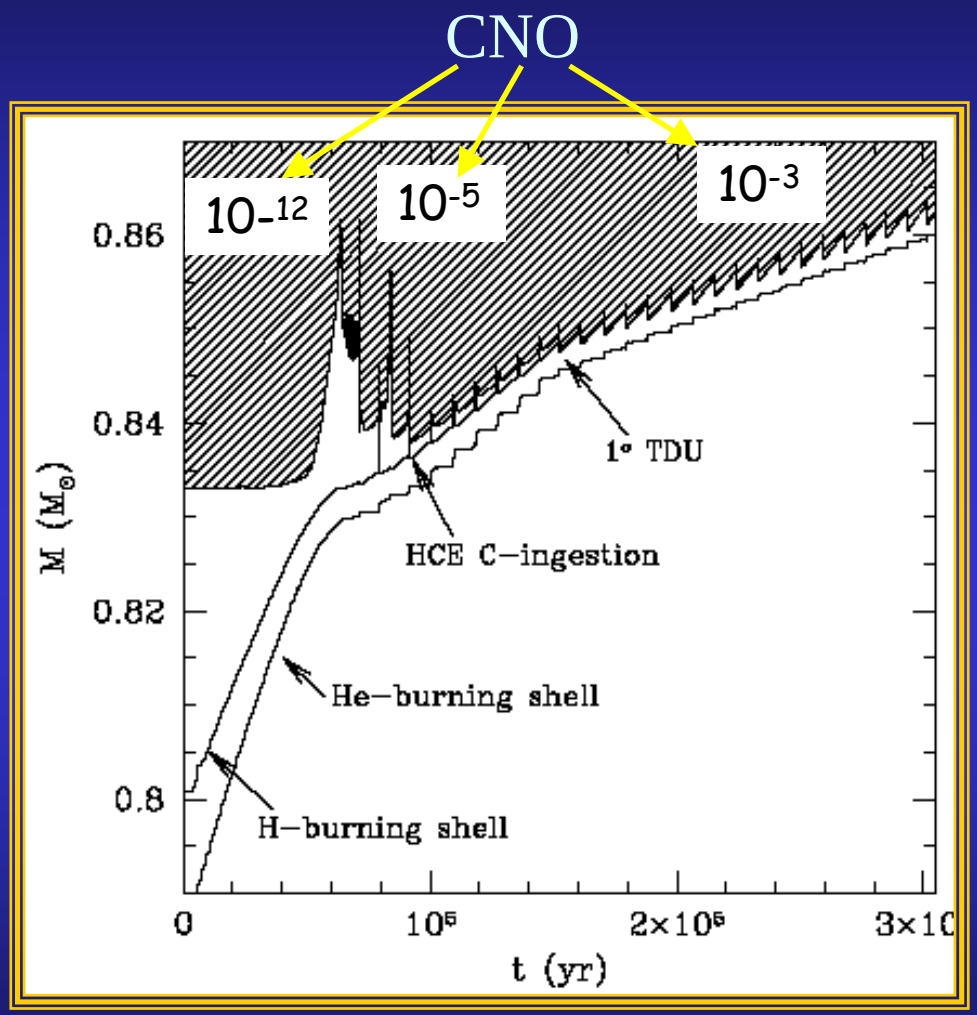
CNO
10^{-12}
10^{-5}
10^{-3}
1° TDU
HCE C−ingestion
He−burning shell
H−burning shell
M ($M_\odot$)
t (yr)

Primordial AGBs & Chem. Evol.

AGB Evolution of the Surface composition:

7 M Z=0 model

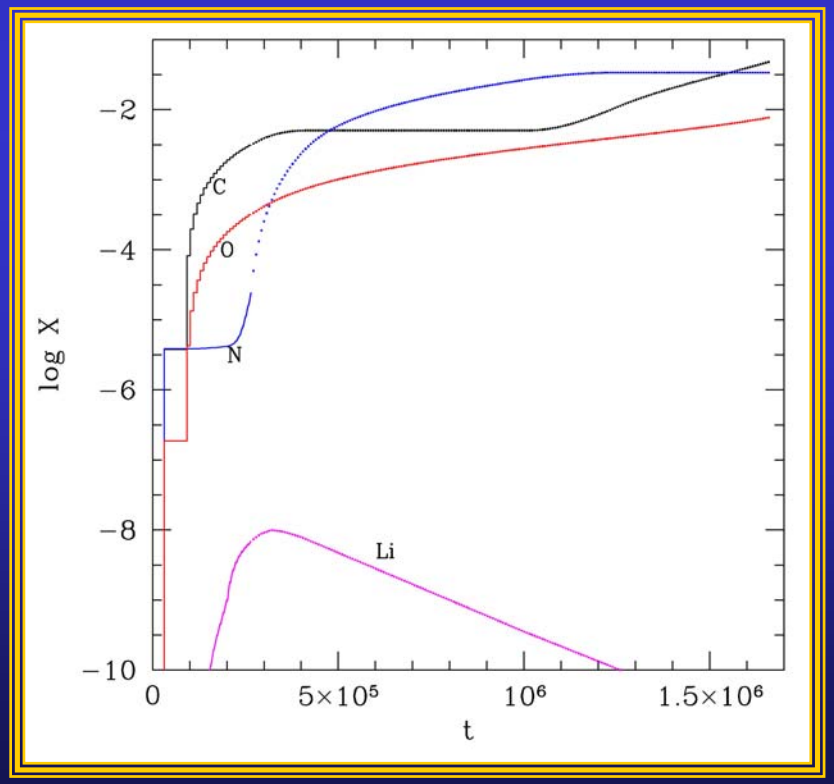

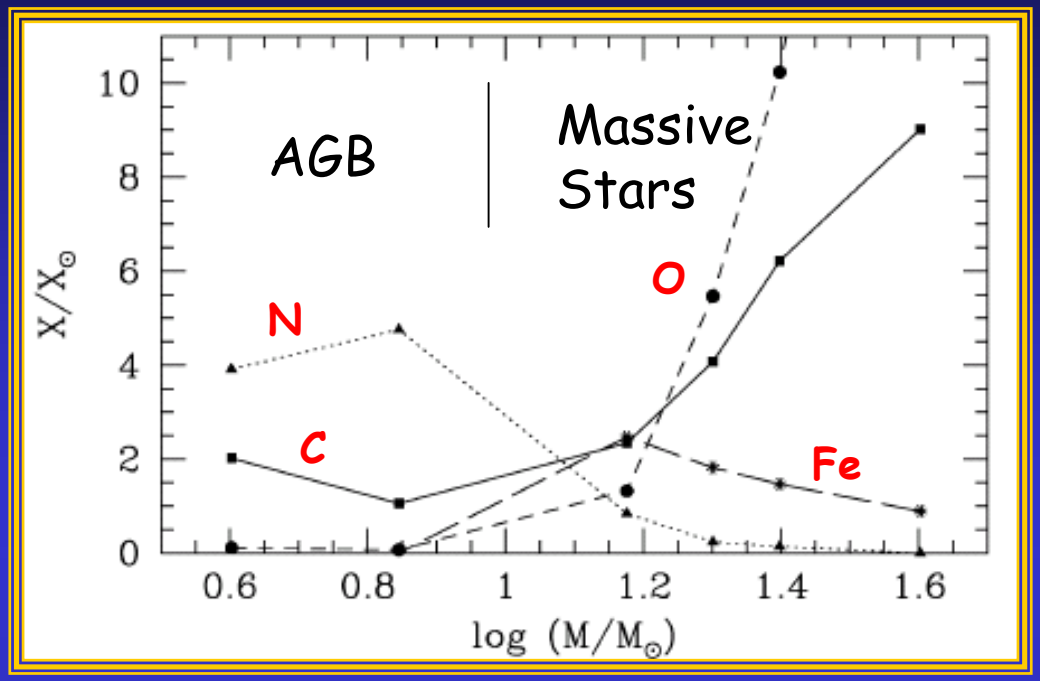

Yields

30 My (7 M) to 120 Myr (4M).

Was the lifetime of massive AGBs short enough to salt the early Galaxy?

Early Galactic Chem. Evolution
(the first 100 Myr)

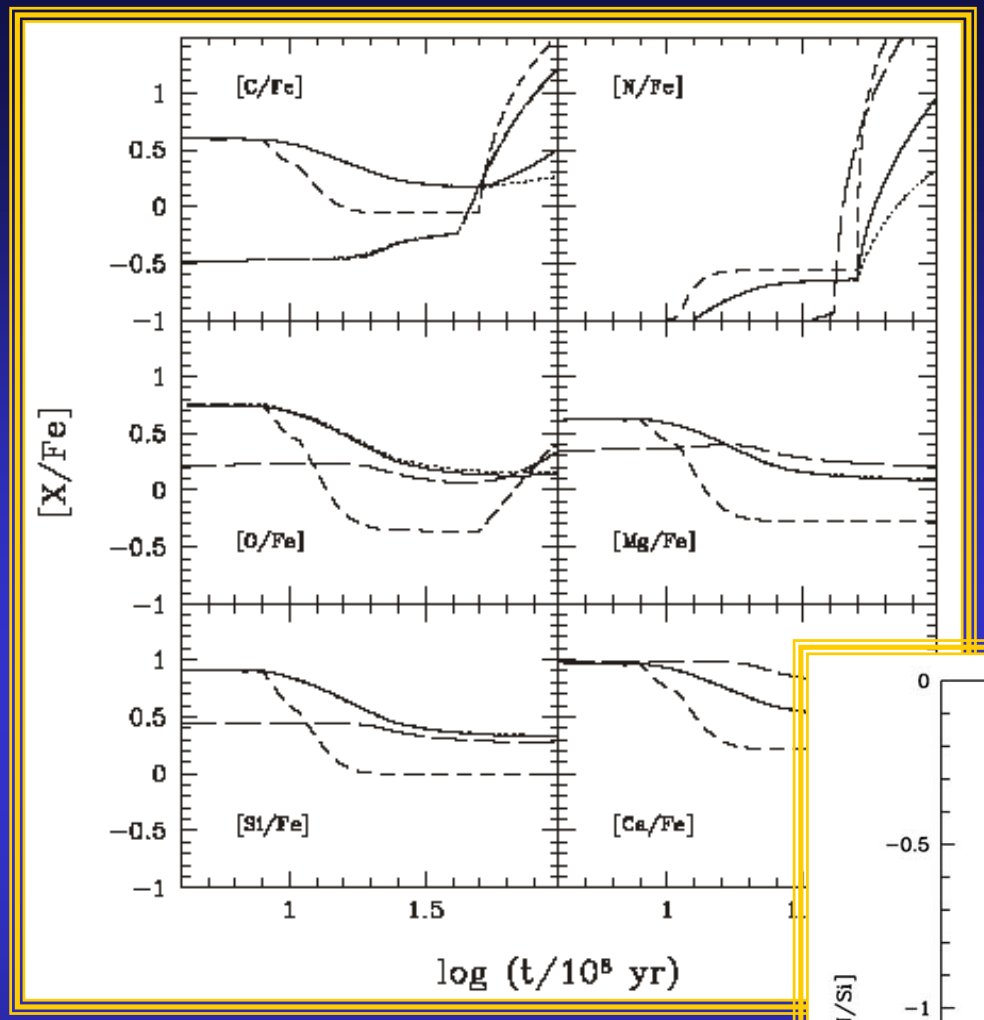

IMF: Salpeter (solid)
Yoshii & Saio 84 (dashed & dottet)
Nakamura & Umemura 00 (l dashed)

Abia et al. (2001)

damped Ly-α (from Molaro et al. (2003)

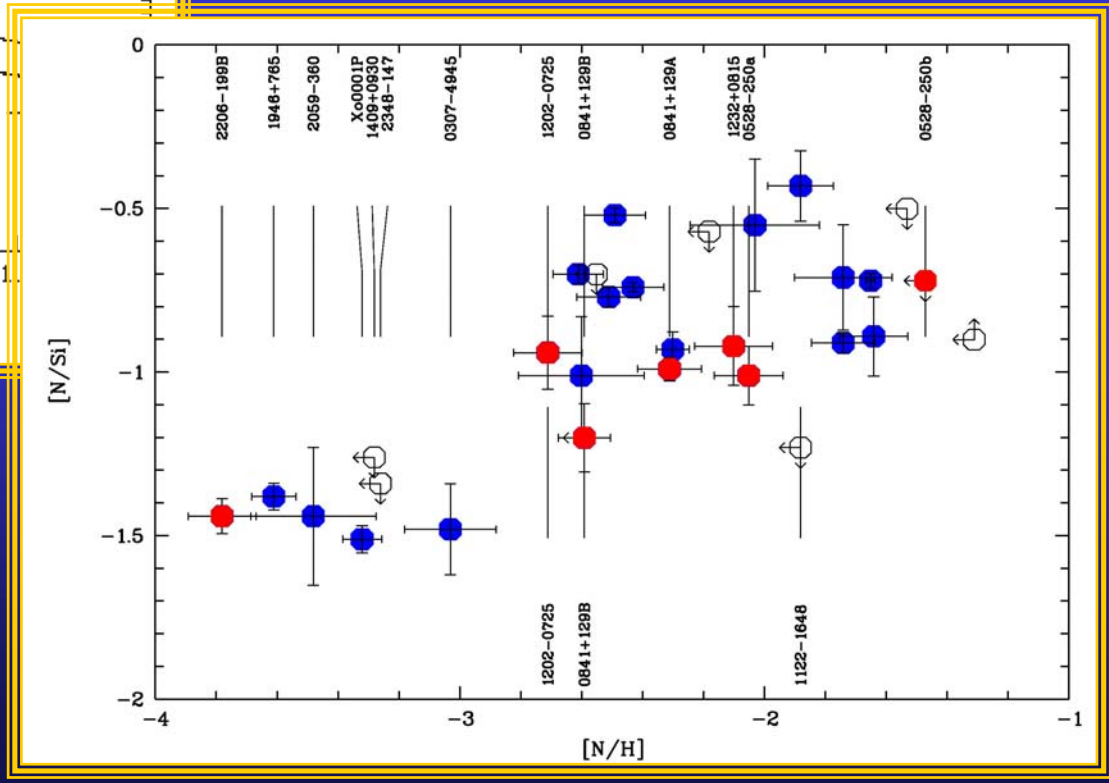

Massive AGB: a possible Li source for the early GCE?

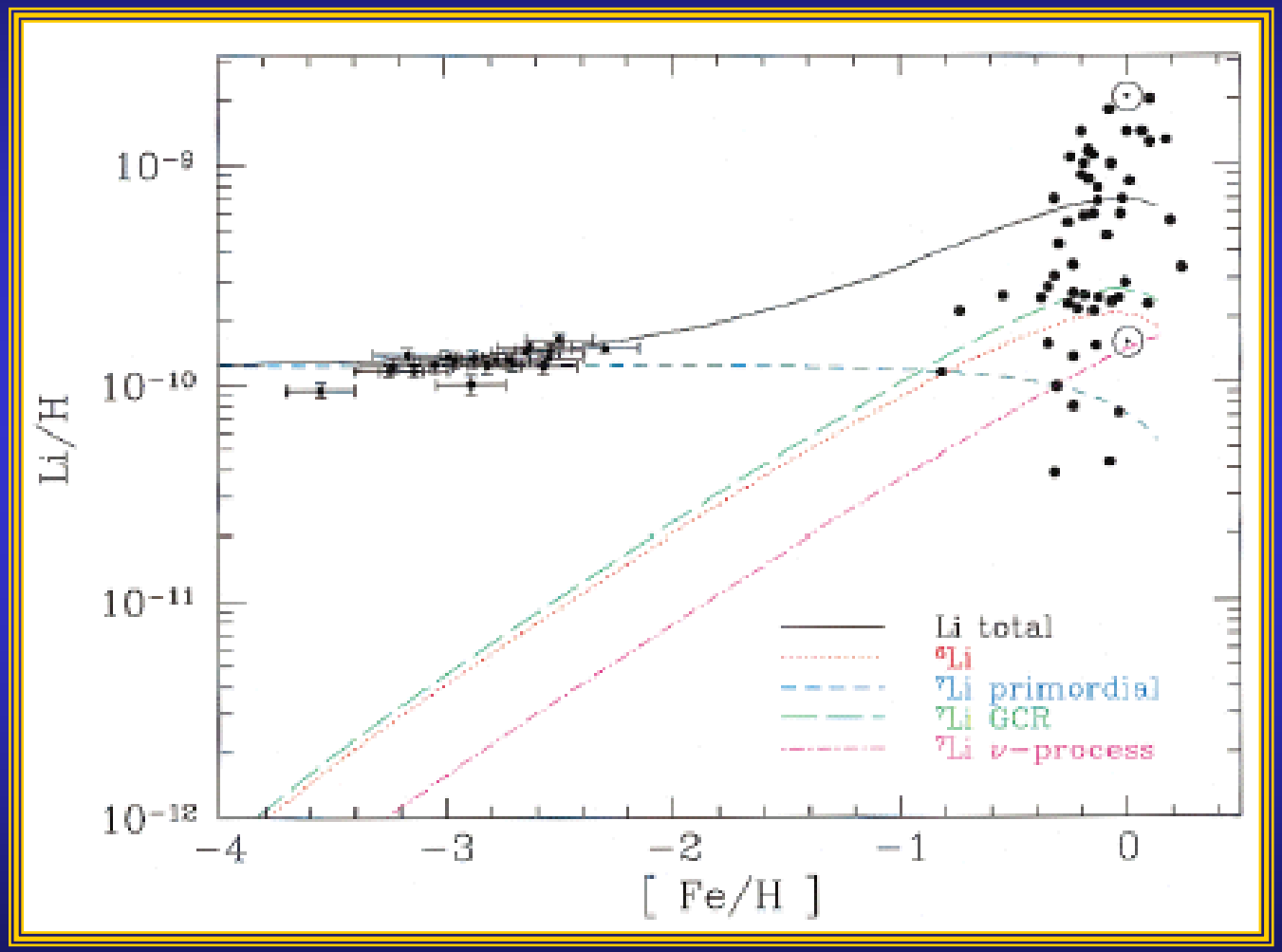

(Ryan et al. 2000)

C-rich (Pb) stars in the galactic halo

Present generation of halo AGB stars -> 13 Gyr -> 0.6 (0.9) M_u -> No TDU

Accretion in Binaries (wind or Roche lobe overflow?)

Most of the halo C- s-rich stars probably belong to wide binary systems (p$2-3 yrs)

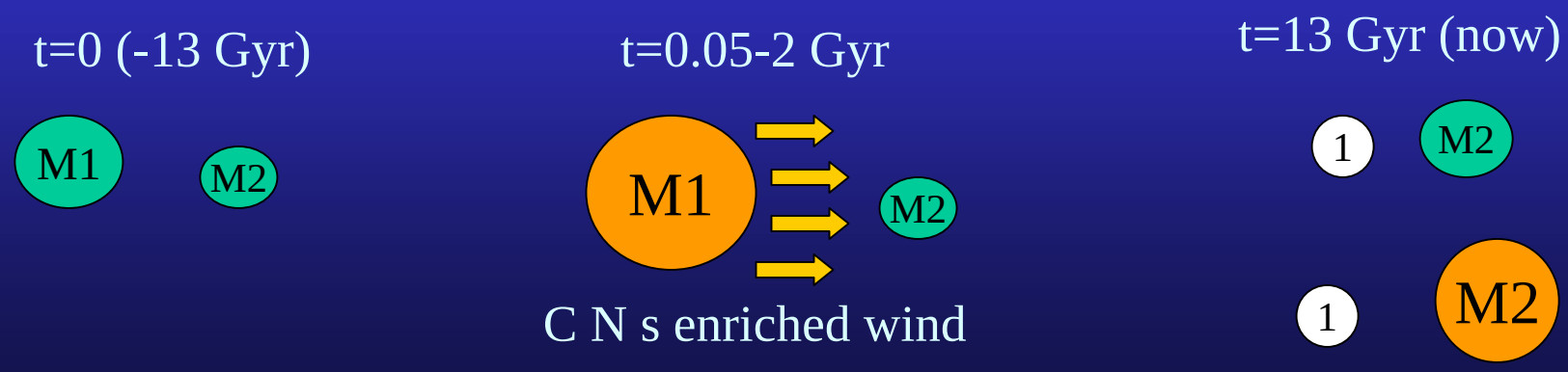

Low M - Low Z AGB: M=1.5 Z=5x10^{-5} Y=0.24

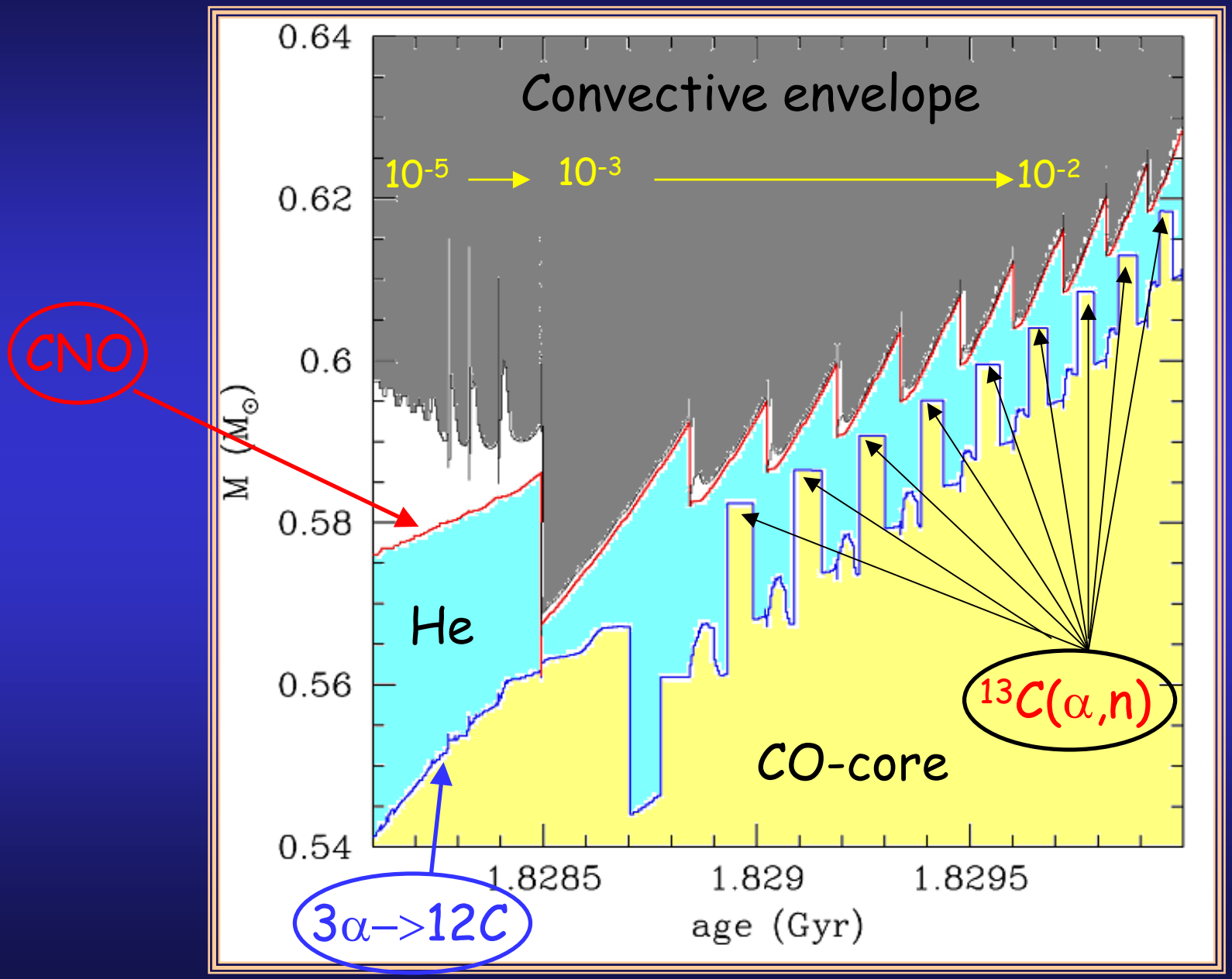

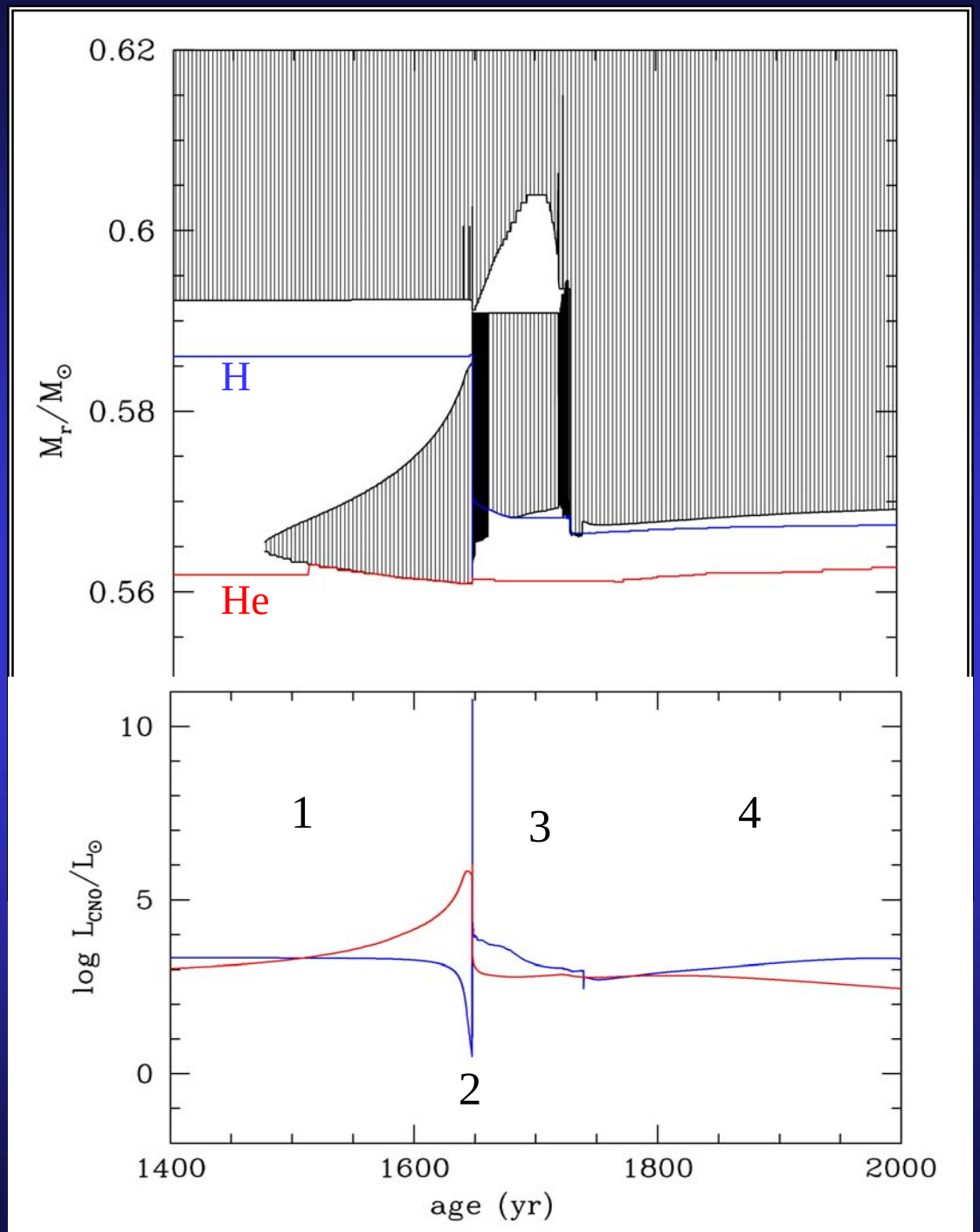

The origin of the 1th huge TDU !!!

1. Standard TP
2. H-ingestion & flash
3. H-burning CZ
4. Dredge up

See also:

Hollowell, Iben & Fujimoto 1990
Fujimoto, Ikeda & Iben 2000
Iwamoto et al. 2004

Physics and Chemistry at the H-ingestion

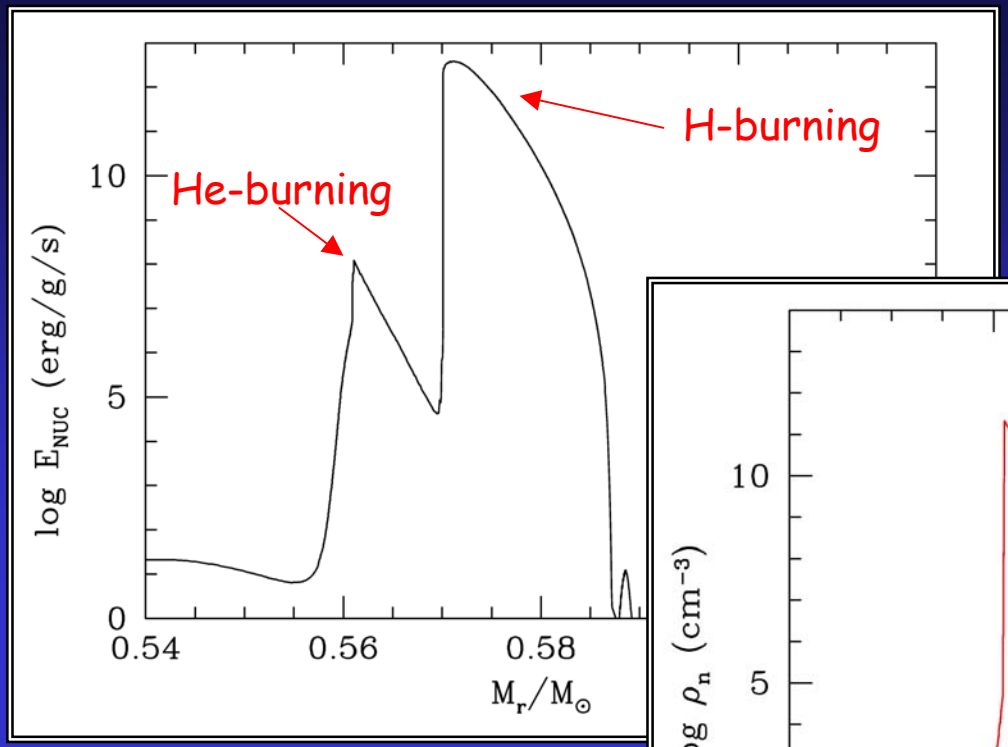

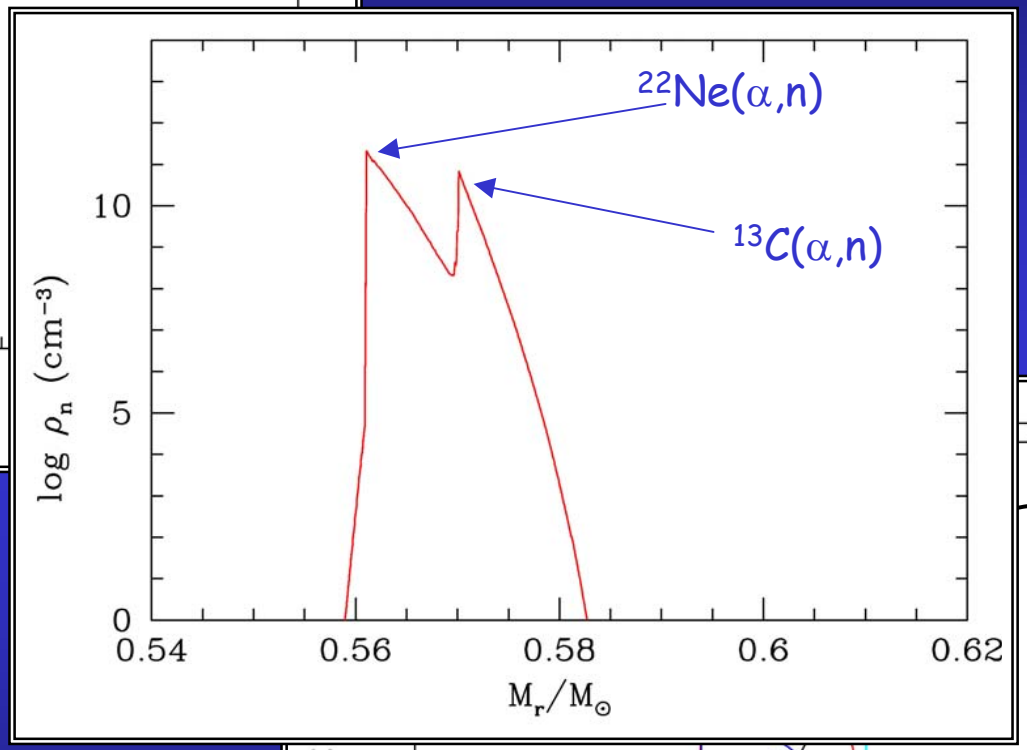

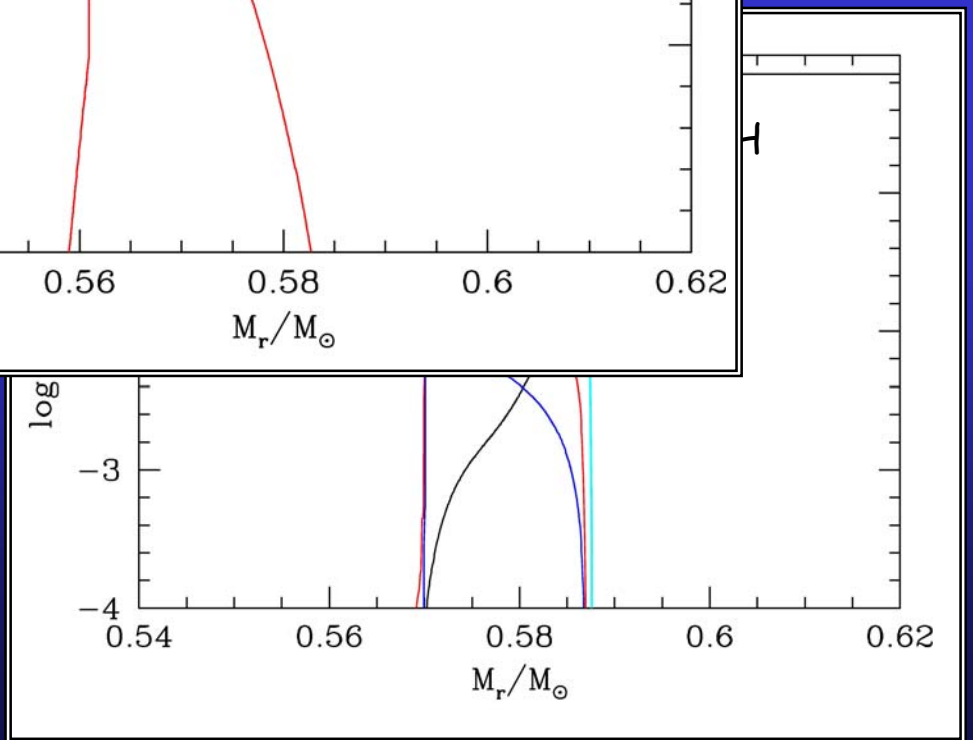

Formation of ^{13}C and ^{14}N

Double neutron source

Envelope enrichment

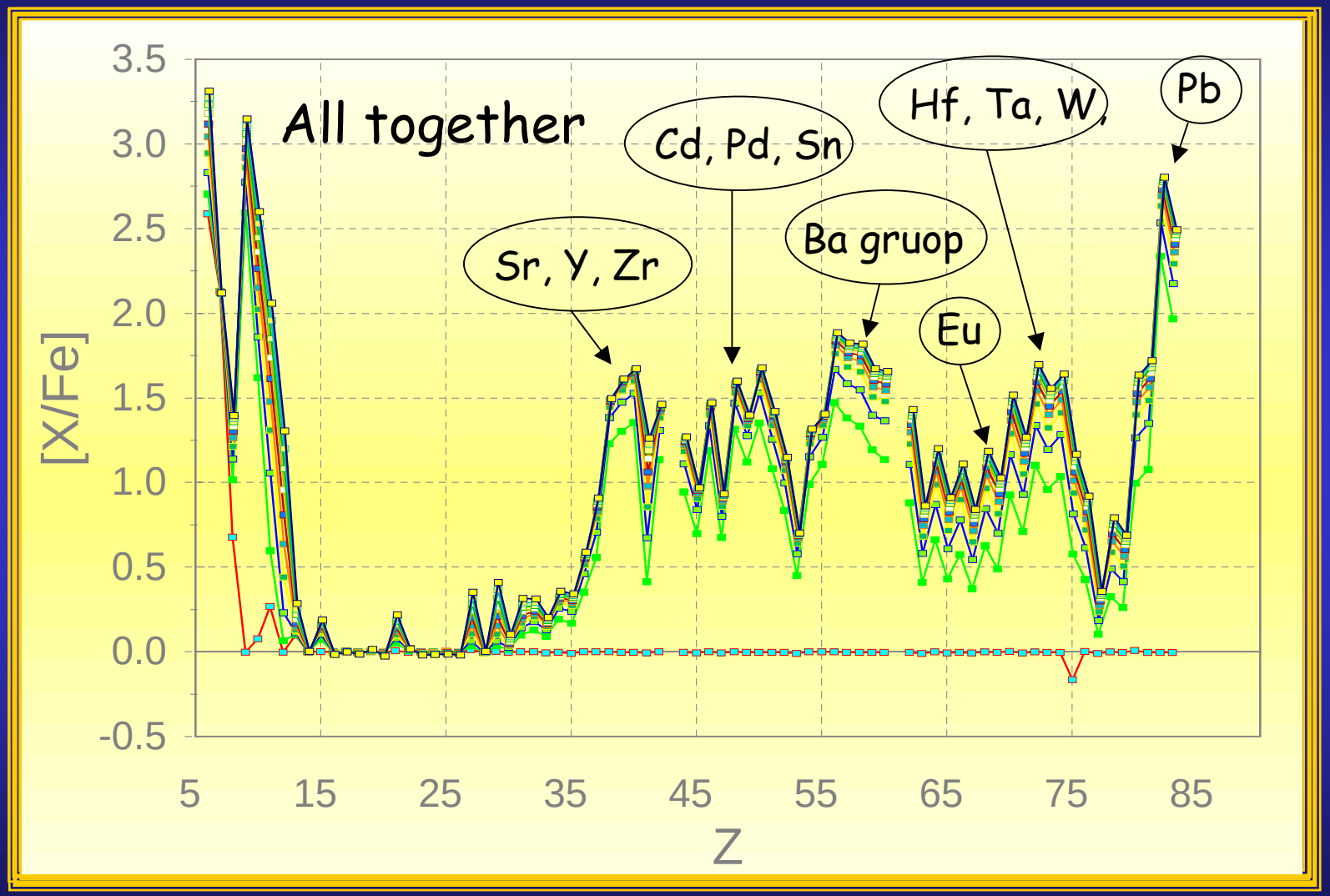

Light elements

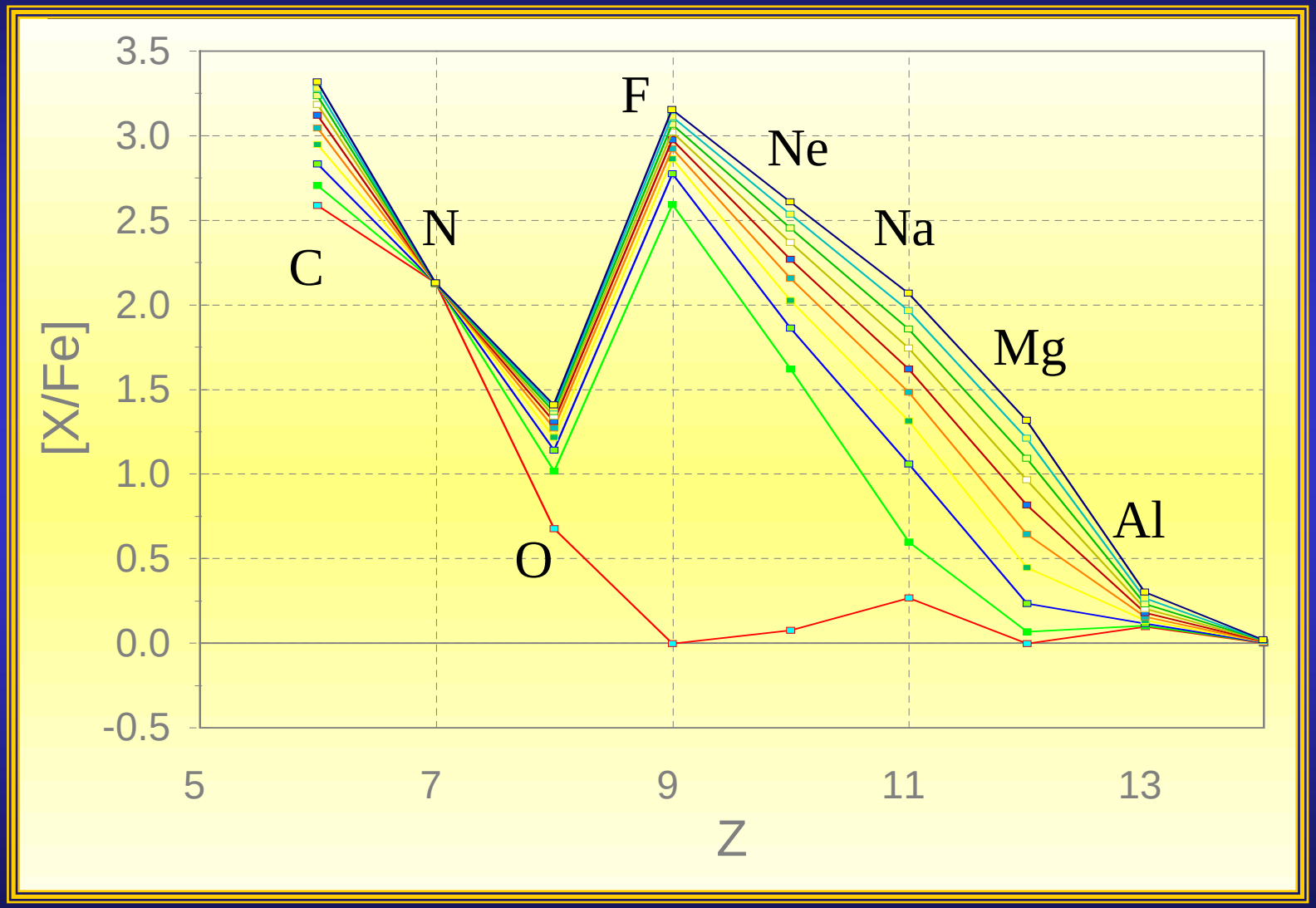

Eu from s-process

[Eu/Fe]=1.2 (AGB tip)

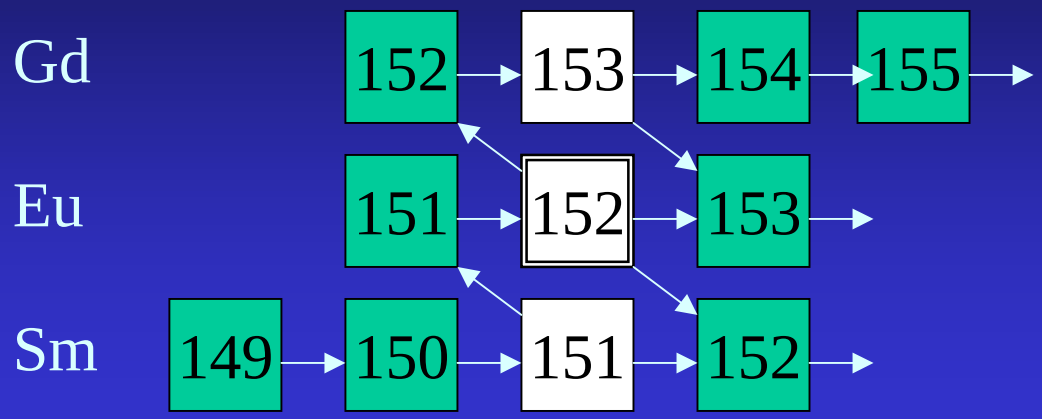

Eu isotopic ratio:
a thermometer

$$f = \frac{^{151}Eu}{^{151}Eu + ^{153}Eu} = 0.57$$

AGB tip (model)

LP625-44	***f=0.60 "0.05***
CS31062-50	***f=0.55 "0.05***

Aoki et al. 2003

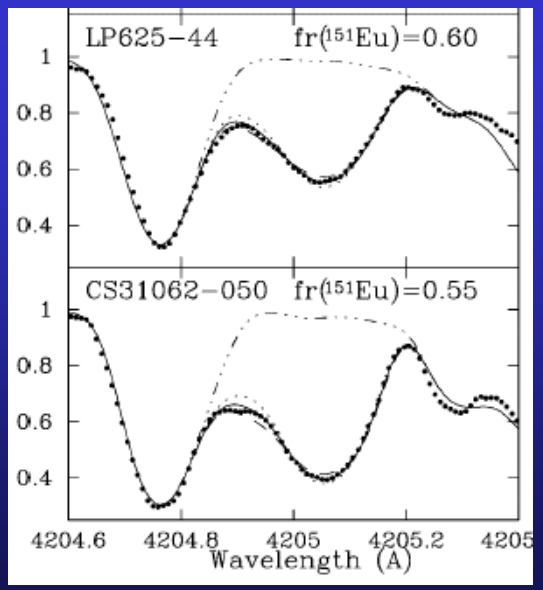

SUBARU/HDS

(Aoki et al 2002)

log g > 3

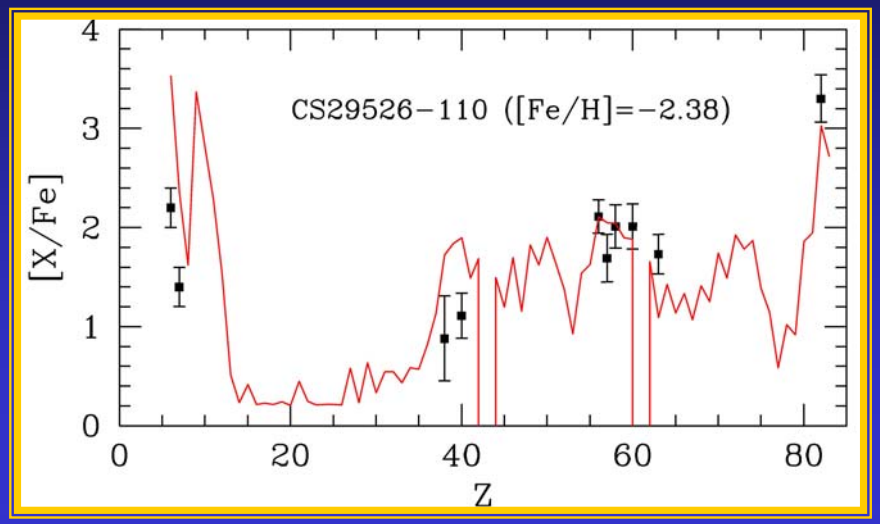

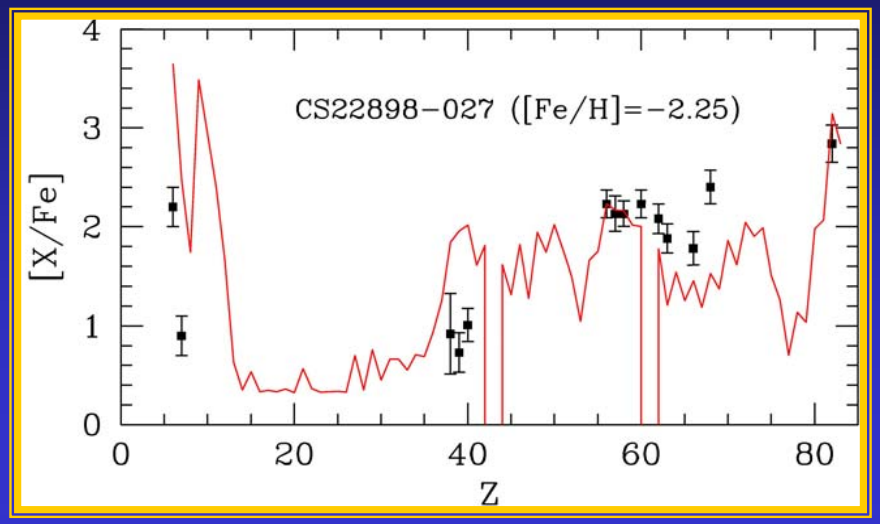

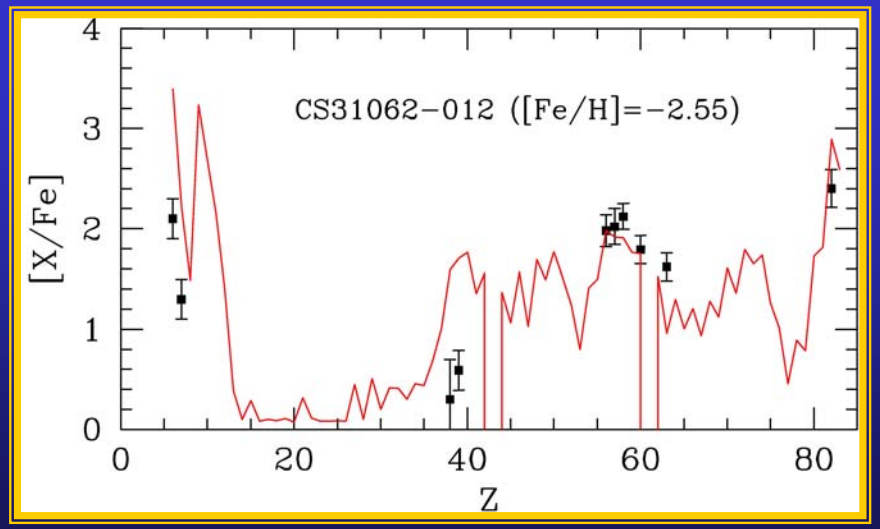

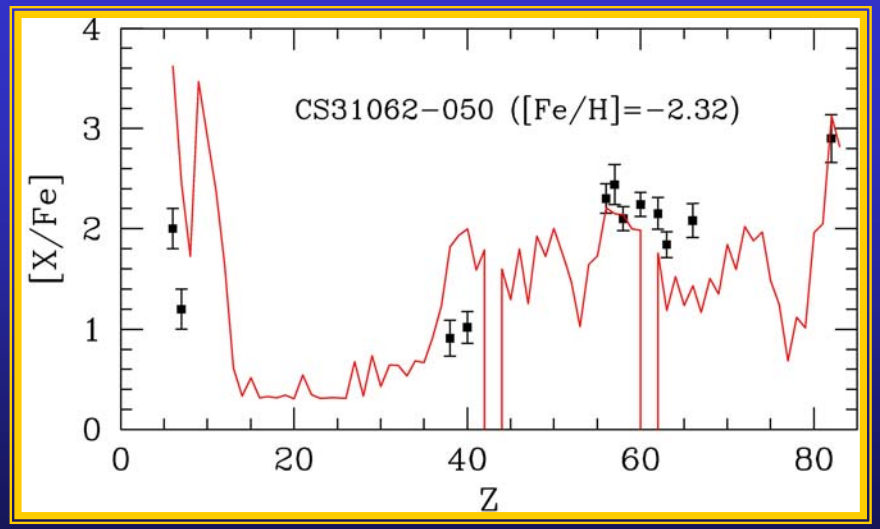

SUBARU/HDS
(Aoki et al 2002)

log g < 2.5

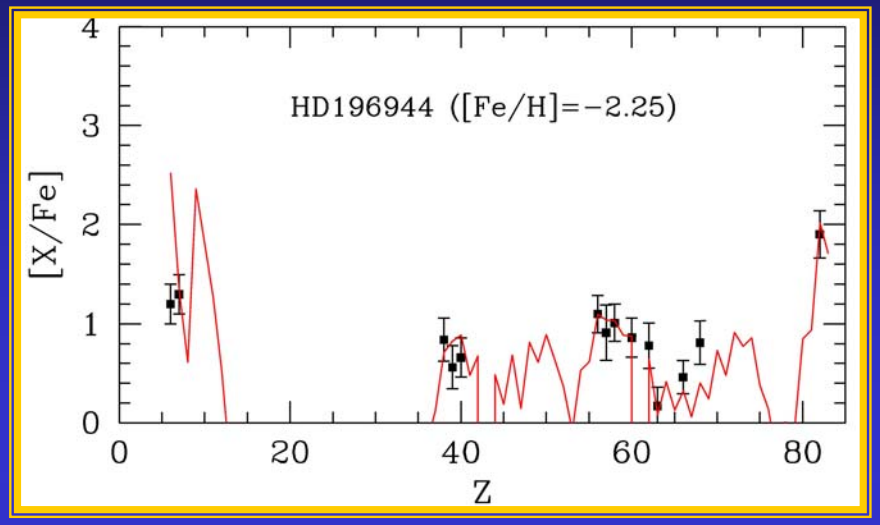

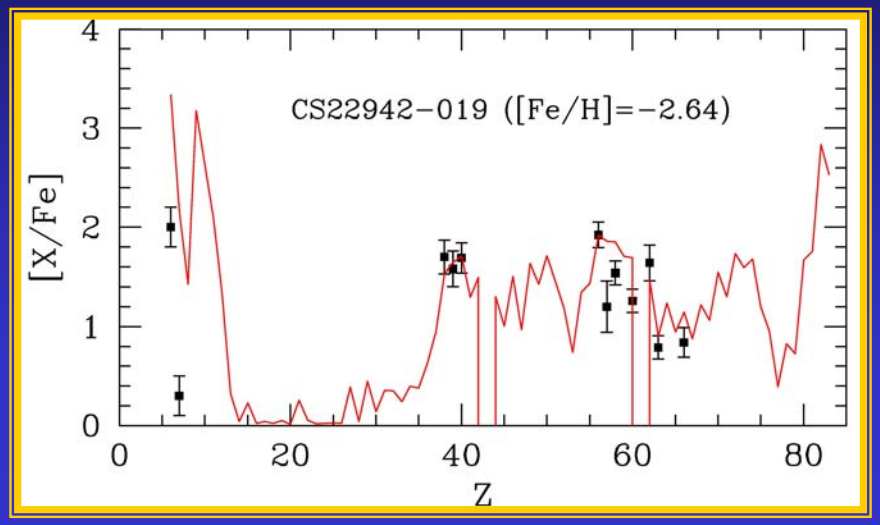

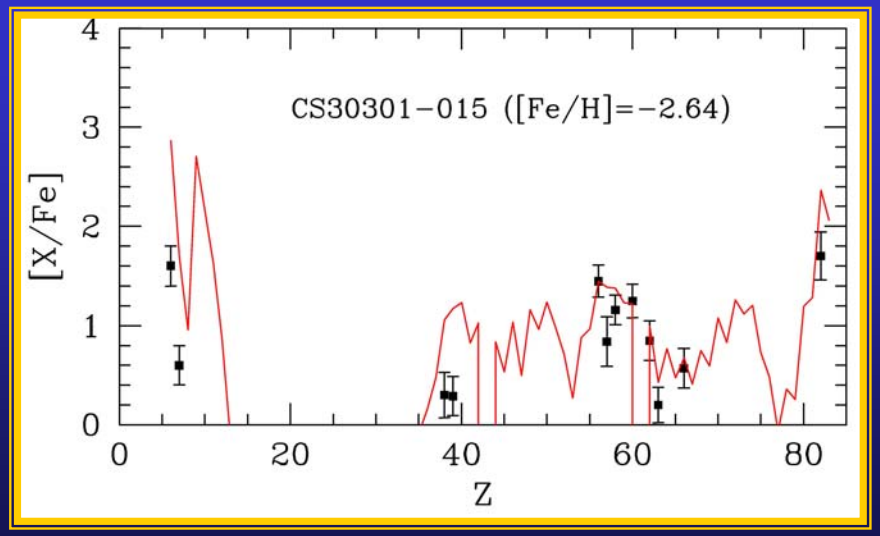

Shifted to account for a dilution factor:

$$\log\left(\frac{M1 * M2}{M1 + M2}\right)$$

Indirect Measurements of Charged-Particle Induced Reactions

X. Tang
Argonne National Laboratory

Direct Measurements

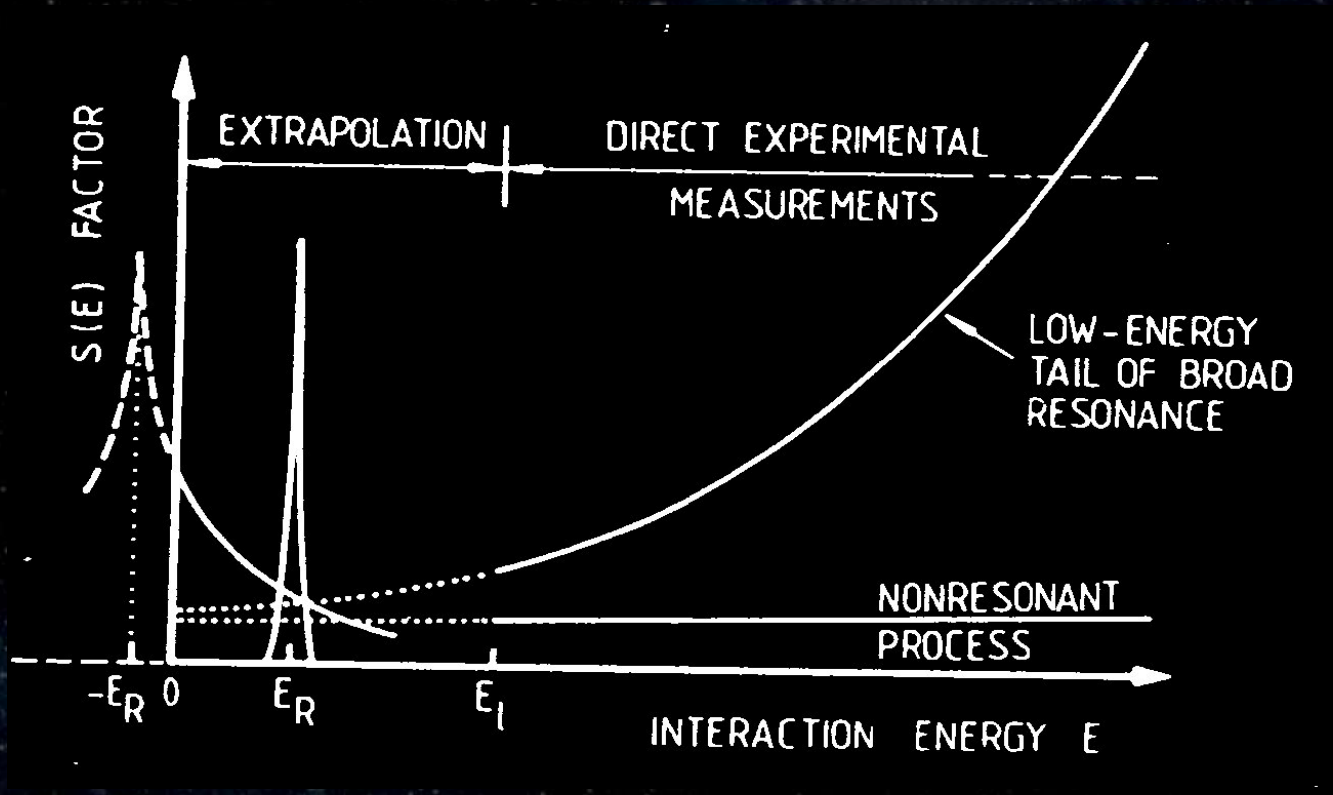

- Better experimental technologies, lower energies.
- Hard to reach stellar energy regions, especially for RNB.
- Extrapolation is inevitable.

Direct + Indirect

Reduce the overall uncertainty by combining various approaches, with assurance that systematic uncertainties are independent.

Indirect Measurements

Trojan Horse Method	Coulomb Dissociation	ANC Method
• Study 3-body reaction $A+a \rightarrow C+c+b$ With Trojan horse $a=b+x(d(p+n), {}^{6}Li(a+d))$ $({}^{7}Li+d \rightarrow {}^{4}He+{}^{4}He+n)$ • Extract energy dependence of the cross section of 2-body reaction $A+x \rightarrow C+c$ $({}^{7}Li+p \rightarrow {}^{4}He+{}^{4}He)$	• Use Coulomb field of highly charged target nucleus X as source of Virtual photons $X(a,bc)X \leftrightarrow a(\gamma,c)b$ ${}^{208}Pb({}^{8}B,p{}^{7}Be){}^{208}Pb$ ${}^{8}B(\gamma,p){}^{7}Be$ • $a(\gamma,c)b \leftrightarrow b(c,\gamma)a$ ${}^{8}B(\gamma,p){}^{7}Be \leftrightarrow {}^{7}Be(p,\gamma){}^{8}B$	• Extract Asymptotic Normalization Coefficient of bound and unbound state wave function of a(b+c) $({}^{8}B({}^{7}Be+p))$ from peripheral reactions. $({}^{14}N({}^{7}Be,{}^{8}B){}^{13}C)$ • Calculate the matrix elements for radiative capture $b(c,\gamma)a$. ${}^{7}Be(p,\gamma){}^{8}B$

$^7Li(p,\alpha)^4He$ with THM

- THM: $^2H(^7Li,\alpha n)^4He$
- Exact the energy dependence of S factor. Normalize to the direct measurement at higher energy.
- No Coulomb suppression and no screening effect.

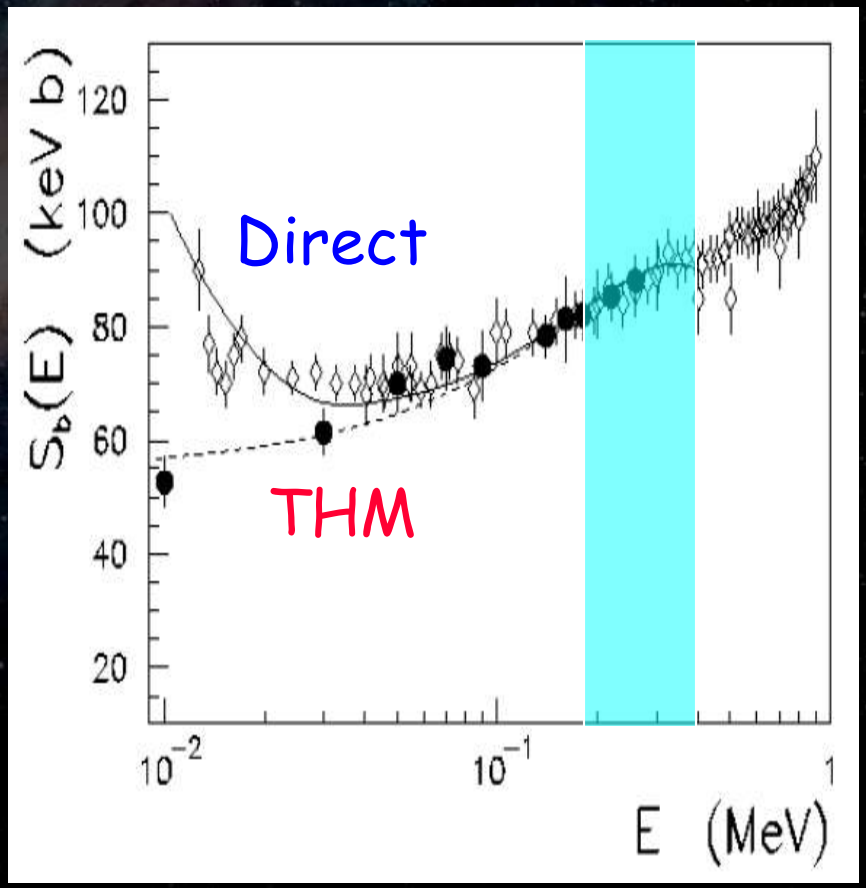

- Electron screening potential:

U_e(THM) = 330±40 eV

U_e(direct) = 340 eV

U_e(theory) = 186 eV

M. Lattuada et al., ApJ 562 (2001) 1076

Comments on THM

- Work for A+x→C+c; No Coulomb suppression; No screening effect;
- Need high energy data to normalize;
- DWBA analysis(require optical model); Multi-step contribution (eg. Compound nuclei process, can be estimated with different Trojan Horse);

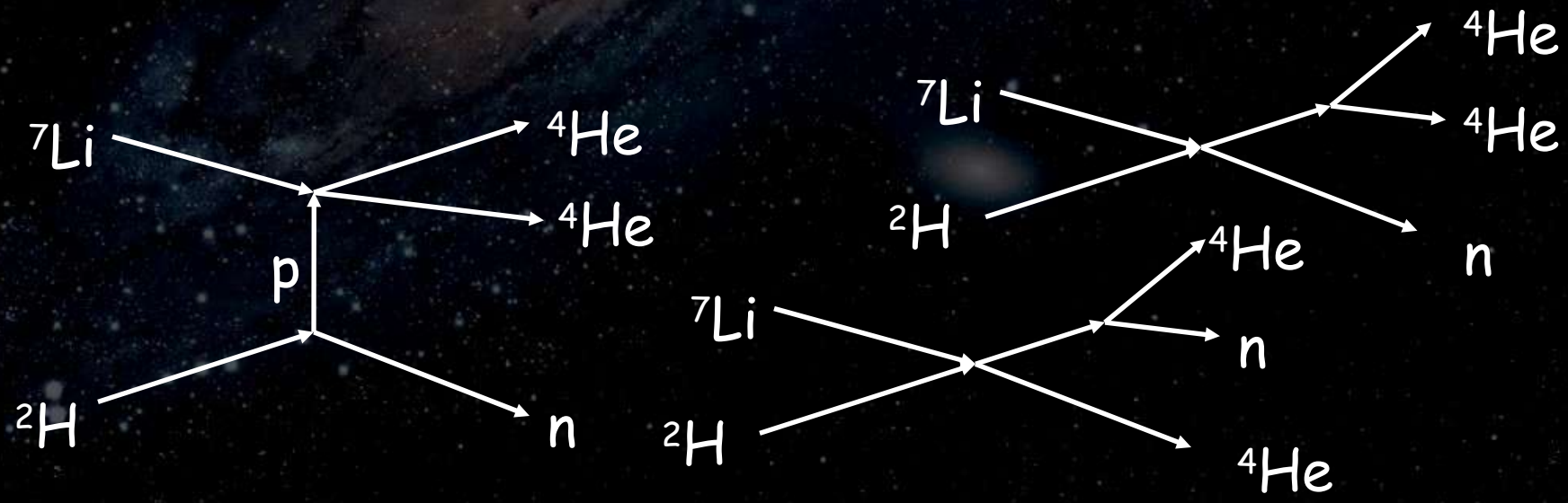

Indirectly Studied Charged-Particle Radiative Capture

(Incomplete list)

Reaction	Method
$^{7}Be(p,\gamma)^{8}B$	Non-Res(Direct/CD/ANC)
$^{8}B(p,\gamma)^{9}C$	Non-Res(CD/ANC)
$^{11}C(p,\gamma)^{12}N$	$\Gamma\gamma$(CD); Non-Res(ANC)
$^{13}N(p,\gamma)^{14}O$	$\Gamma\gamma$(Direct/CD); Non-Res(ANC)
$^{14}N(p,\gamma)^{15}O$	Non-Res(Direct/ANC); $\Gamma\gamma$(CoulEx/RD, negligible)
$^{12}C(\alpha,\gamma)^{16}O$	Direct;elastic scattering;β delayed α decay;ANC
$^{18}F(p,\gamma)^{19}Ne$	Non-Res(ANC); $\Gamma\gamma$(Direct)

Coulomb Dissociation

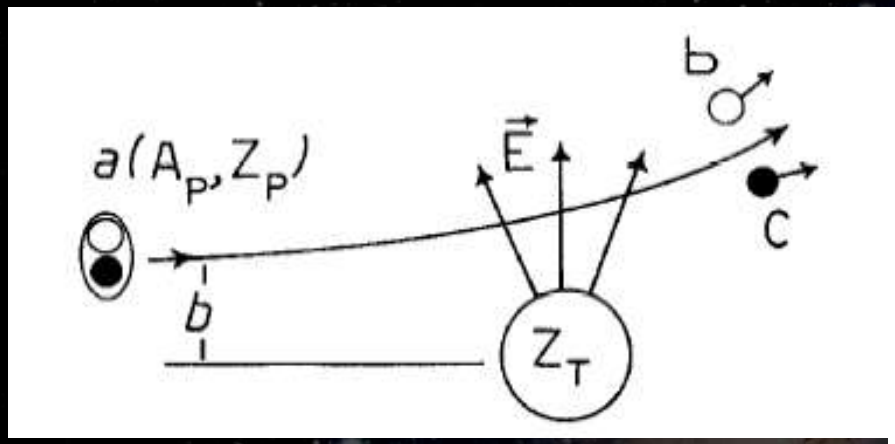

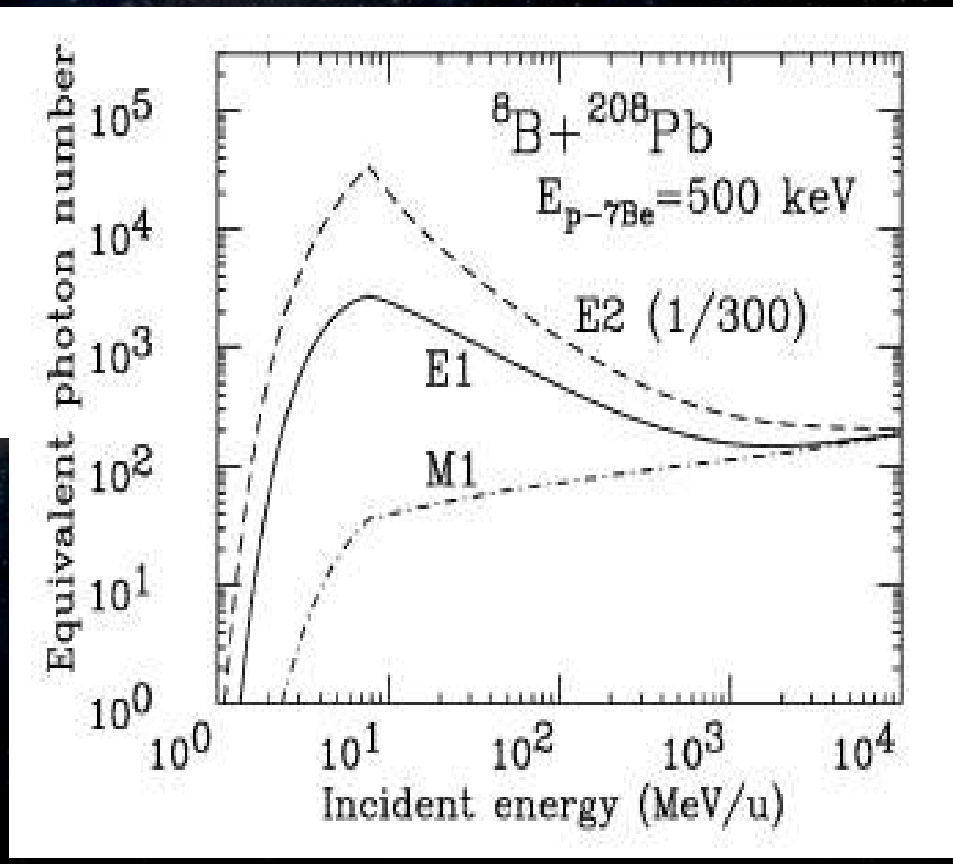

Virtual photon number

$$\frac{d\sigma}{dE_\gamma} = \frac{n_{E\lambda}}{E_\gamma}\sigma_{E\lambda}^{(\gamma,p)}$$

T. Motobayashi, NPA693(2001)258

$^{208}Pb(^{14}O,p^{13}N)^{208}Pb$

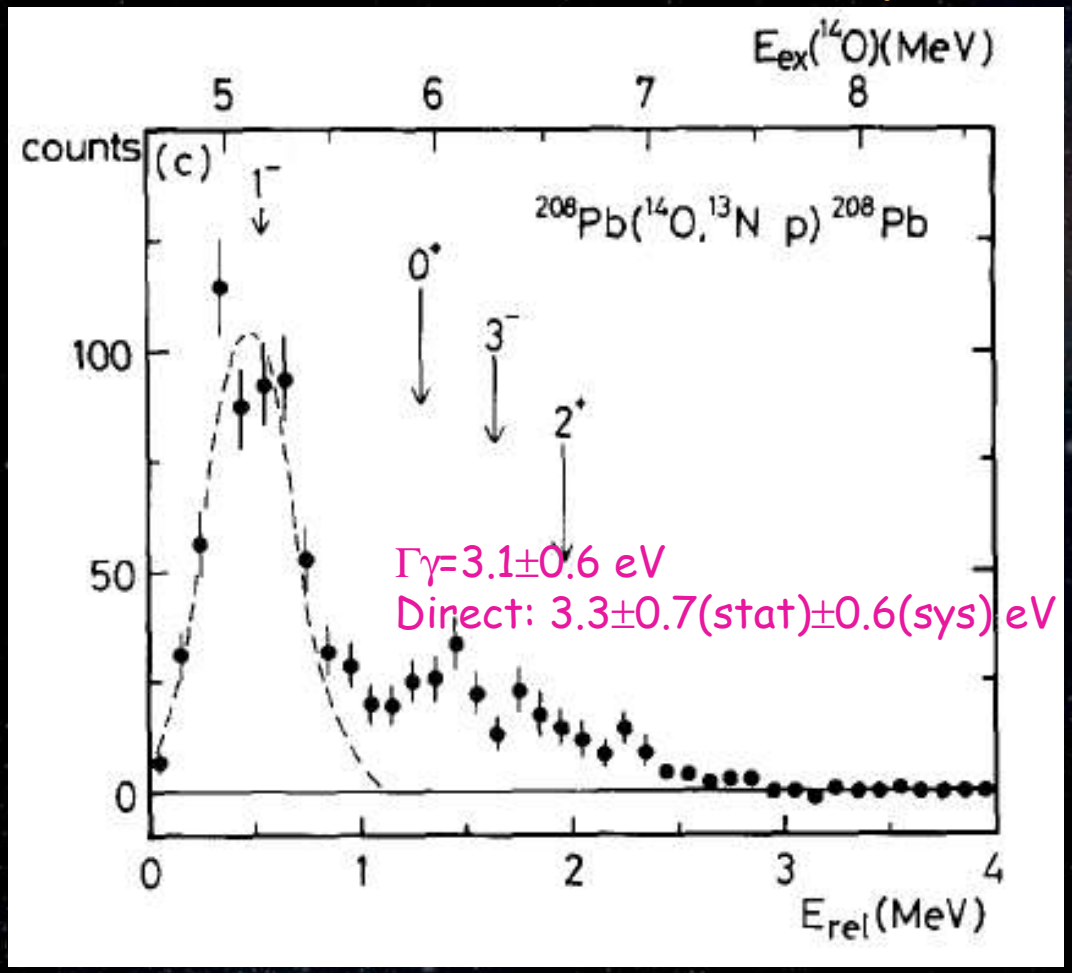

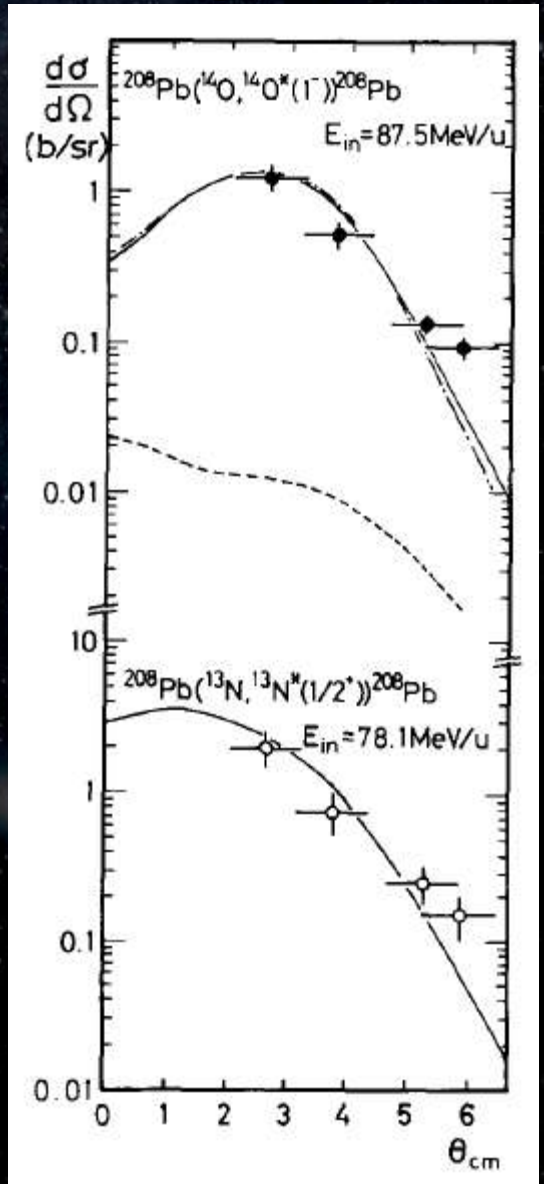

T. Motobayashi *et al.*, PLB264(1991)259
Th. Delbar *et al.*, PRC48, 3088 (1993)

$^{208}Pb(^{14}O,p^{13}N)^{208}Pb$

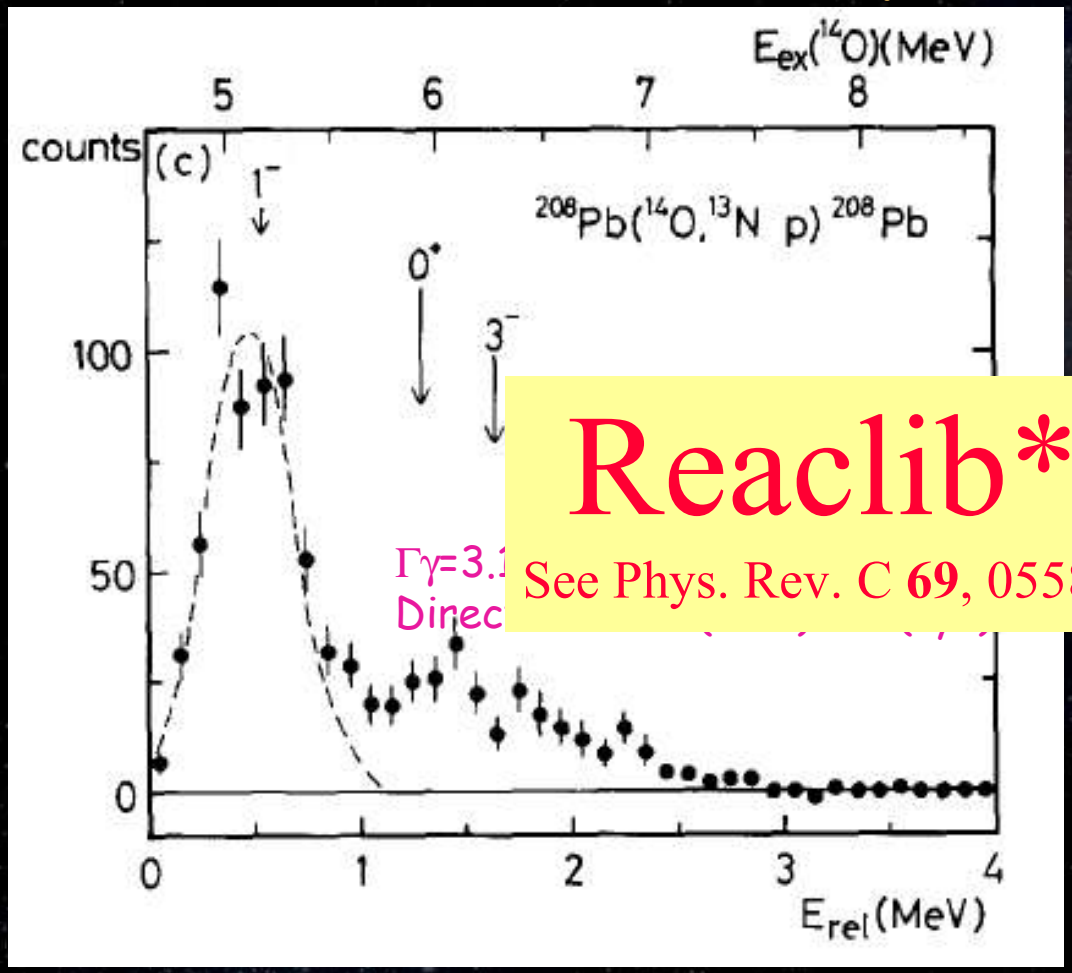

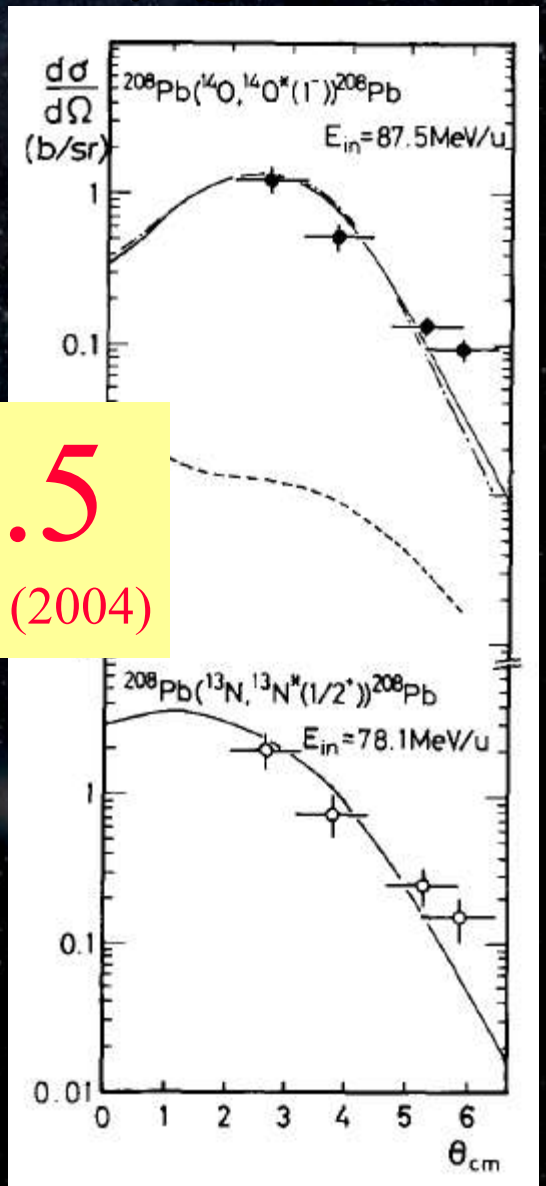

Reaclib*2.5

See Phys. Rev. C **69**, 055807 (2004)

T. Motobayashi *et al.*, PLB264(1991)259
Th. Delbar *et al.*, PRC48, 3088 (1993)

$^{208}Pb(^{8}B,p^{7}Be)^{208}Pb$ @ 83 MeV/u

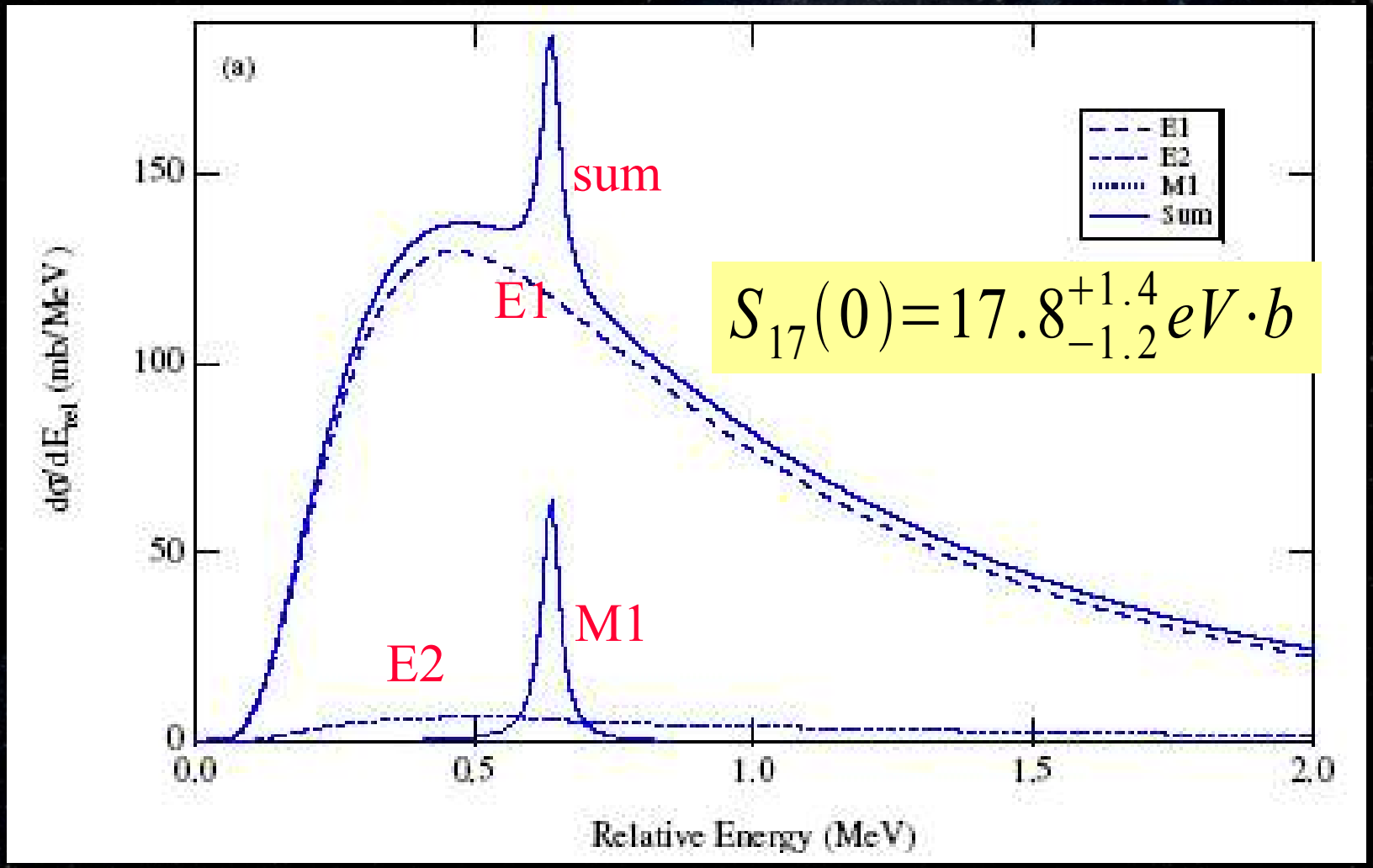

B. Davids *et al.*, PRL 86 (2001) 2750

$^{208}Pb(^{8}B,p^{7}Be)^{208}Pb$ @ 254 MeV/u

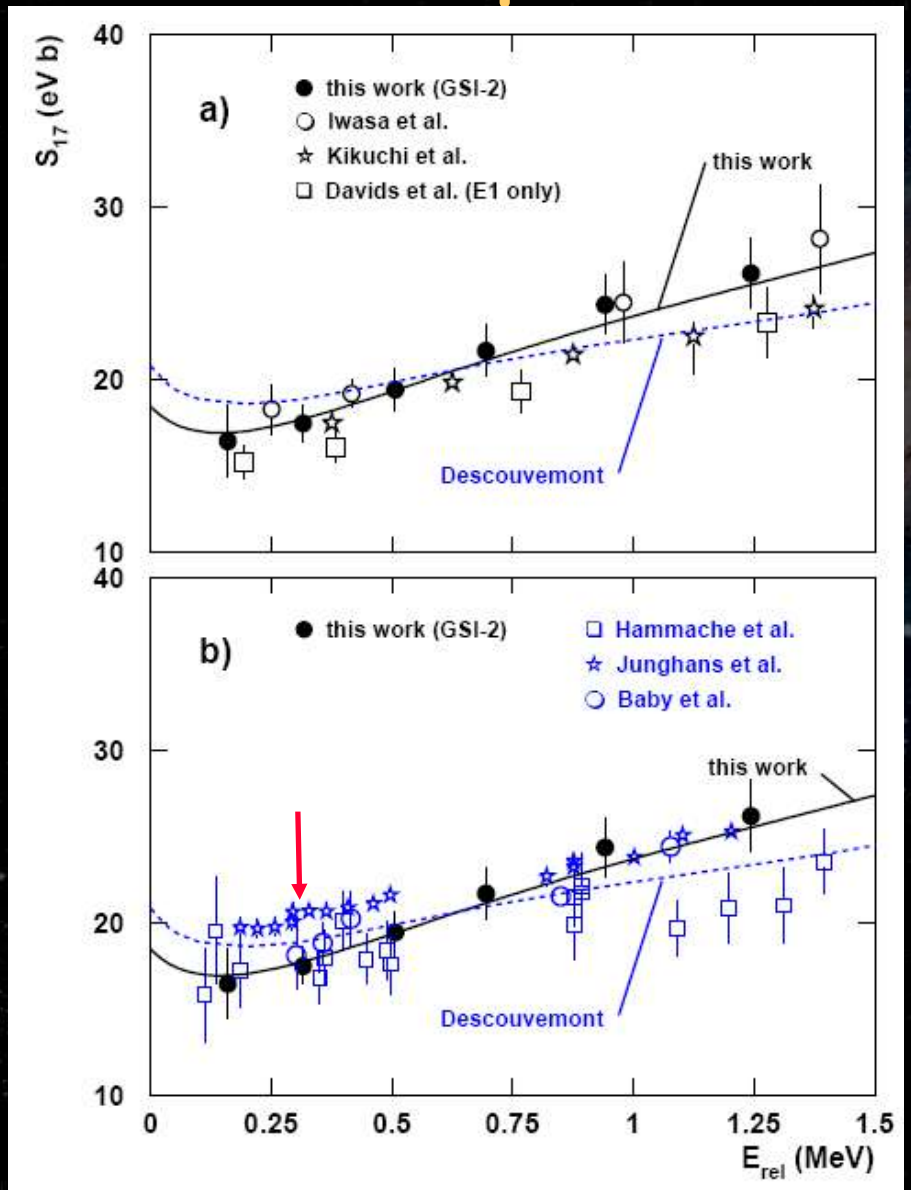

$S_{17}(0)=18.6\pm1.2(exp)$
$\pm1.0(th)$ eV b

F. Schumann *et al.*,
Phys.Rev.Lett. 90 (2003) 232501

Comments on Coulomb Dissociation

- Small γ branch : ($^{11}C+p \rightarrow {}^{12}N$, Γ_γ=13.0±0.5meV, Γ_γ/Γ_p=1e-7; $^{13}N+p \rightarrow {}^{14}O$, Γ_γ=3.1eV, Γ_γ/Γ_p=9e-5;)
- Single DC : ($^{7}Be(p,\gamma)^{8}B$, $^{8}B(p,\gamma)^{9}C$)

Pros : cross section can enhanced by a large factor from 10^4 to 10^6; Intermediate energy, thick target; No γ detection required; Good for small γ branch;

Cons : nuclear forces; higher order (post-acceleration); multipolarity mixture; only ground state transitions;

R-Matrix with ANC

$$\sigma \propto \left| M_{DC} \pm i e^{-\varphi} \frac{\Gamma_p^{1/2} \Gamma_\gamma^{1/2}}{(E - E_R) + i \Gamma/2} \right|^2$$

$$M_{DC} \propto C_{lj} \qquad \Gamma_p \propto (C_{lj})^2$$

???

Nucleus interior

For narrow resonance:

$\Gamma_p \ll \Gamma_\gamma$, $\omega\gamma = \omega\Gamma_p$

$\Gamma_\gamma \ll \Gamma_p$, $\omega\gamma = \omega\Gamma_\gamma$

Bound state wave-function (E_b<0)

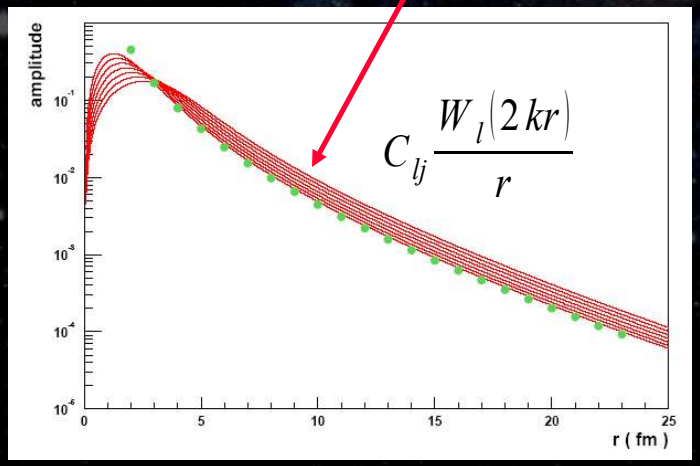

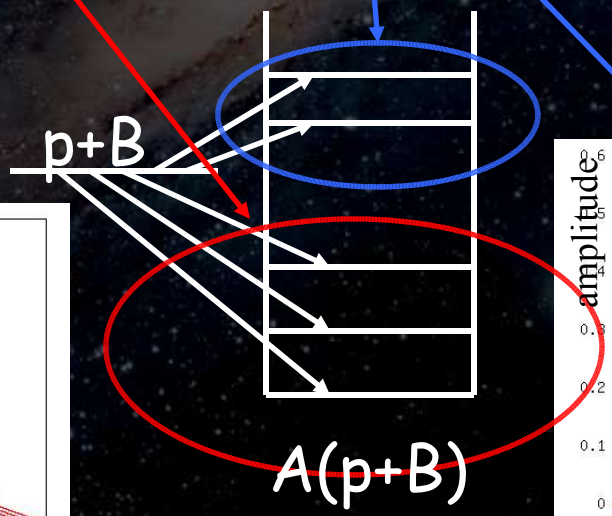

Quasi-bound state wave-function (E_b>0)

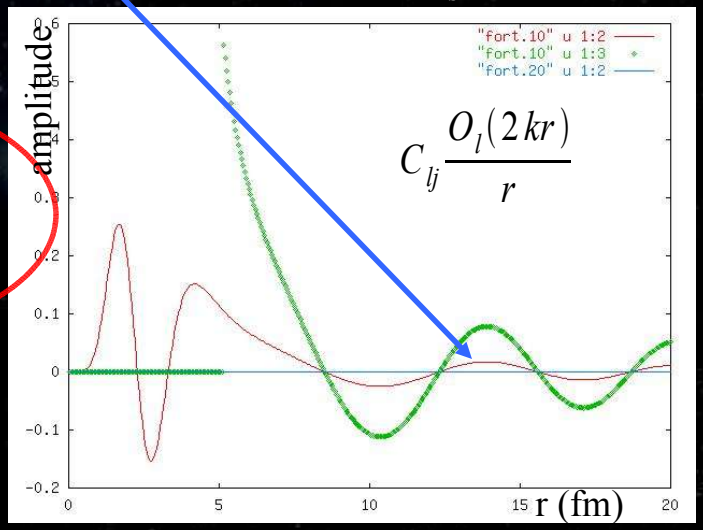

$S_{17}(0)$ with Asymptotic Normalization Constant

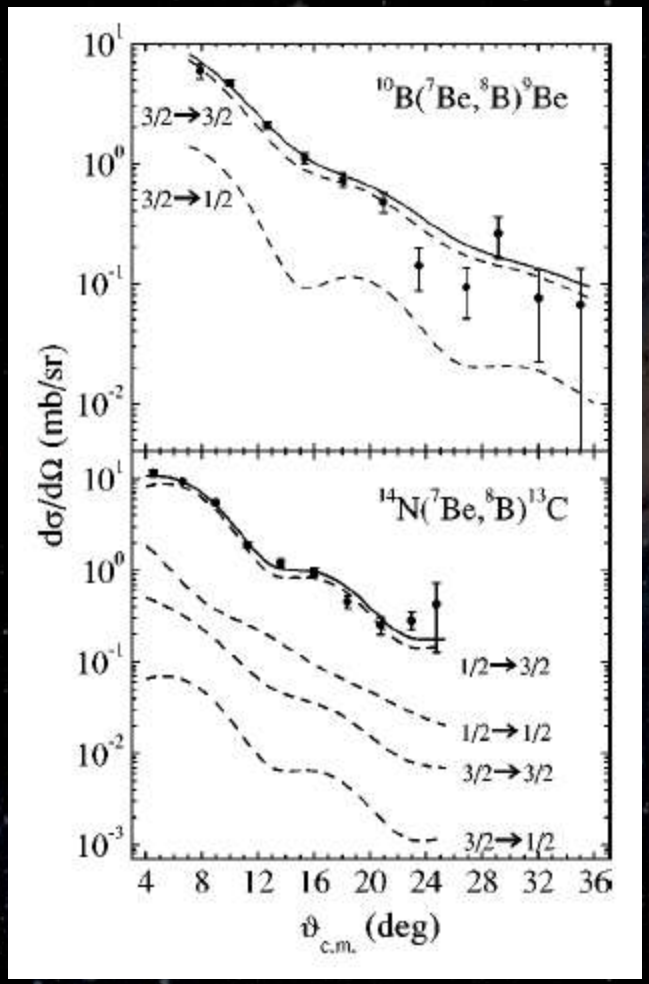

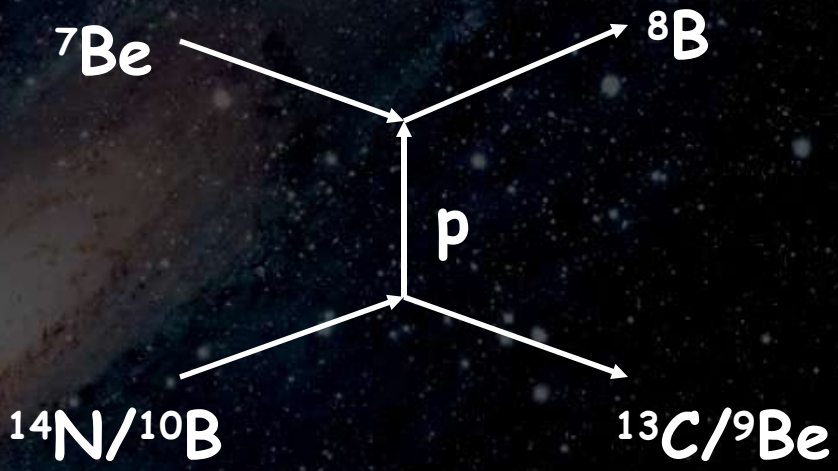

$S_{17}(0)$=18.4±2.5 eV b (^{10}B)

$S_{17}(0)$=16.9±1.9 eV b (^{14}N)

$S_{17}(0)$=17.3±1.8 eV b(avg)

$S_{17}(0)$ = 18.2±1.8 eV b (dnp04)

Azhari et al.,
Phys.Rev.Lett. 82, 3960 (1999)
Phys.Rev. C60, 055803 (1999)
Phys. Rev. C **63**, 055803 (2001)
G. Tabacaru et al., dnp04 abstract

$S_{17}(0)$ with Charge Symmetry

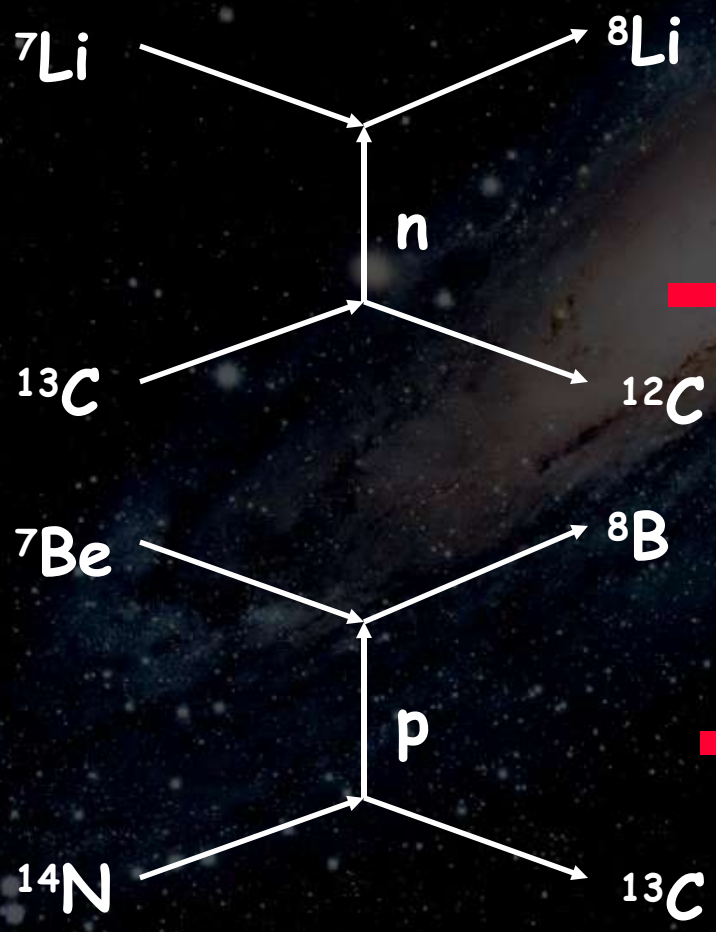

$$\left|\frac{C_{^8B(^7Be+p)}}{C_{^8Li(^7Li+n)}}\right|^2 = 1.055(20)$$

$S_{17}(0)$ = 17.6±1.7 eV b

$S_{17}(0)$ = 18.2±1.8 eV b

L. Trache et al., PRC67(2003)062801

From $^7Li(n,\gamma)^8Li$ to $^7Be(p,\gamma)^8B$

sensitive to nuclear potential

$^7Li(n,n)^7Li$

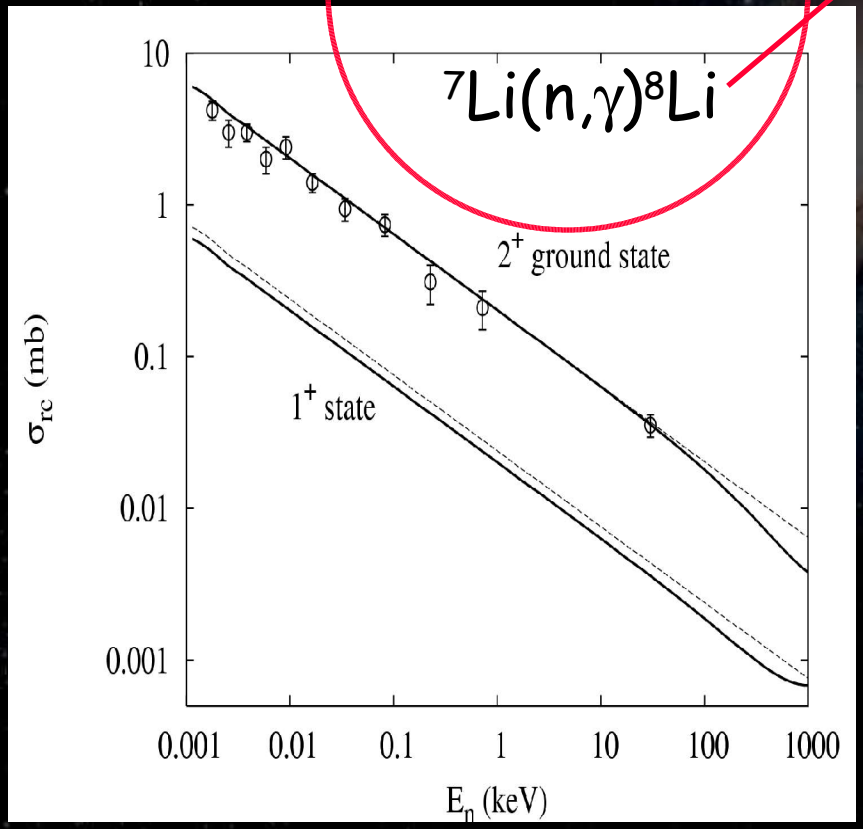

$$|C(2+,^8Li)|^2 = 0.475 \pm 0.025 \quad fm^{-1}$$

$$\frac{|C(2+,^8B)|^2}{|C(2+,^8Li)|^2} = 1.03 \pm 0.02$$

$$S_{17}(0) = 38.7\, eV \cdot b \cdot fm \times |C(2^+,^8B)|^2$$

charge symmetry

$S_{17}(0)=19\pm1$ eV b

H. Esbensen (submitted to PRC)

$S_{17}(0)$, direct vs. indirect

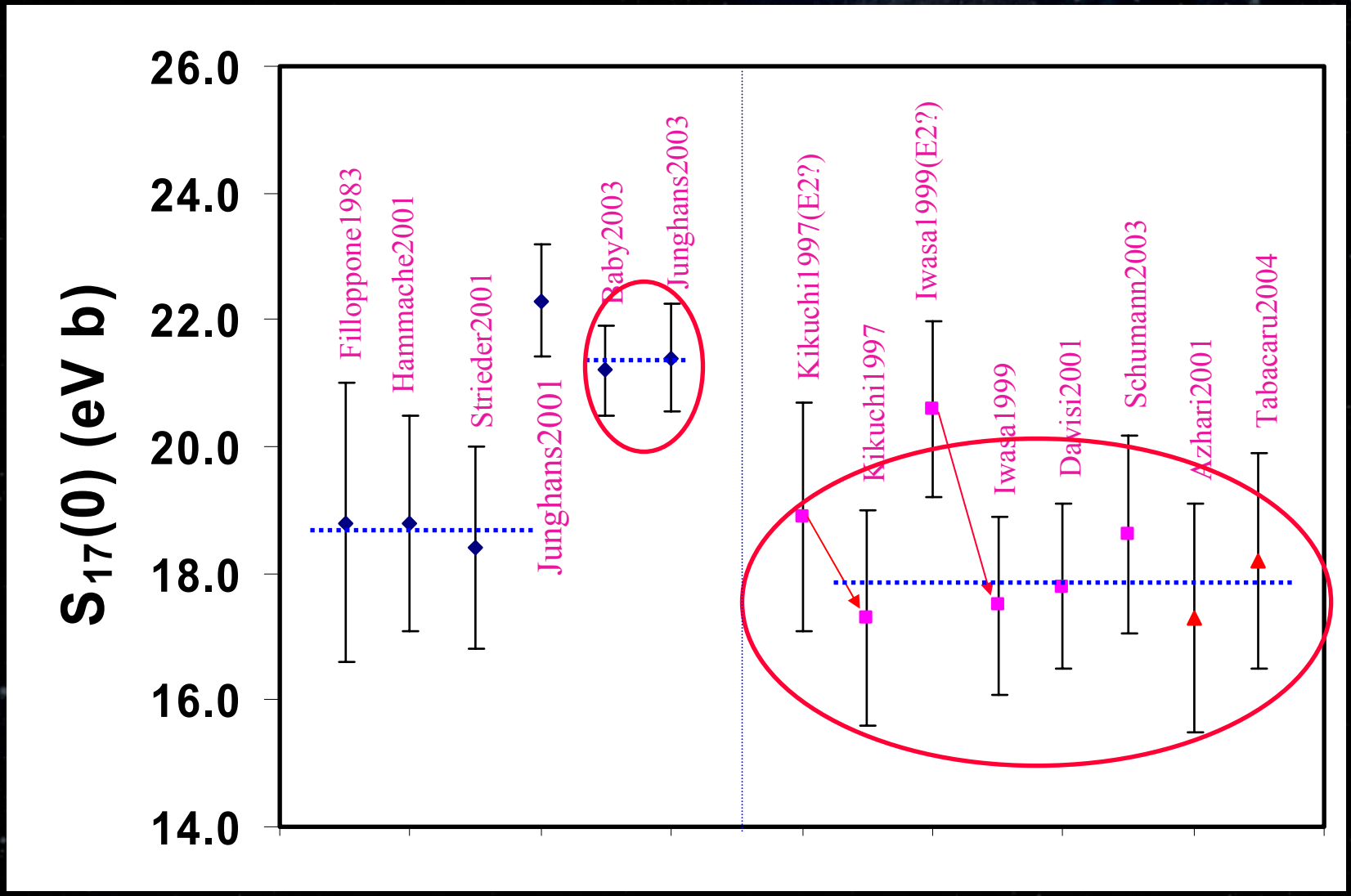

Compilation of $S_{17}(0)$

For direct measurement Ec.m.<425 keV only,
$S_{17}(0)=21.4\pm0.5(exp)\pm0.6(th)$
A.R.Junghans et al., Phys. Rev. C **68**, 065803 (2003)

For Coulomb dissociation + direct
$S_{17}(0)=18.6\pm0.4\pm1.1$ eV b
B. Davids & S. Typel, PRC68 (2003) 045802

ANC
$S_{17}(0)=$ **17.3±1.8 eV b**
(Azhari et al., Phys. Rev. C 63, 055803 (2001))
$S_{17}(0)=18.2\pm1.8$ eV b
(Tacabaru dnp2004)

A Good Stone to Test A Sword

- $^{7}Be(p,\gamma)^{8}B$ is a very good case to test both direct and indirect techniques. (15% discrepancy)
- However, the importance of this reaction requests unusually high precision.
- Need improve both theory and experiments.

Another type of direct measurement, $p(^{7}Be,^{8}B)\gamma$; GFMC calculation;

$^{14}N(p,\gamma)^{15}O$

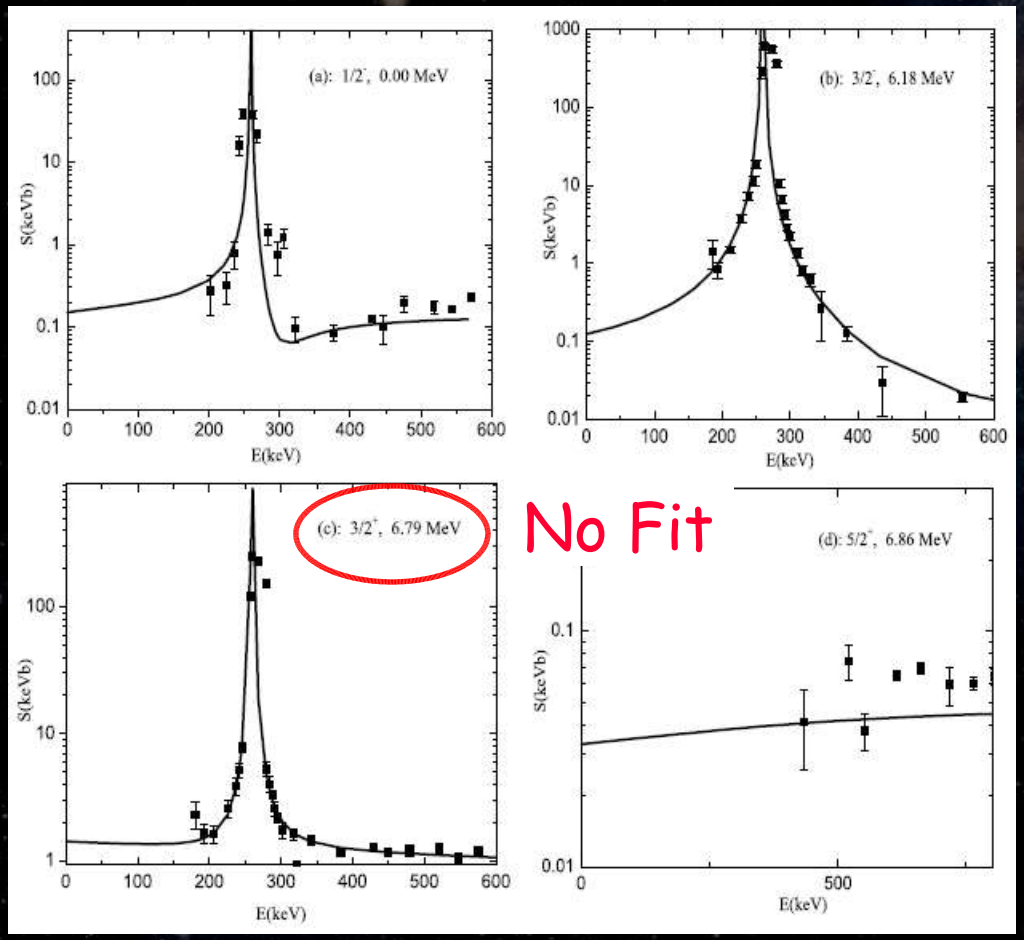

TAMU(ANC)
$^{14}N(^{3}He,d)^{15}O$
S_{tot}=1.70±0.22 keV b
A.M.Mukhamedzhanov et al.,
PRC 67, 065804 (2003)

LUNA(Direct capture)
$^{14}N(p,\gamma)^{15}O$
S_{tot}=1.7±0.1 ±0.2 keV b
LUNA Collaboration
Phys. Lett. B591 (2004) 61

E. Krumpotic et al.,
Annual Report 2003, Institut fur Strahlenphysik, Universitat Stuttgart

$^{14}N(p,\gamma)^{15}O$

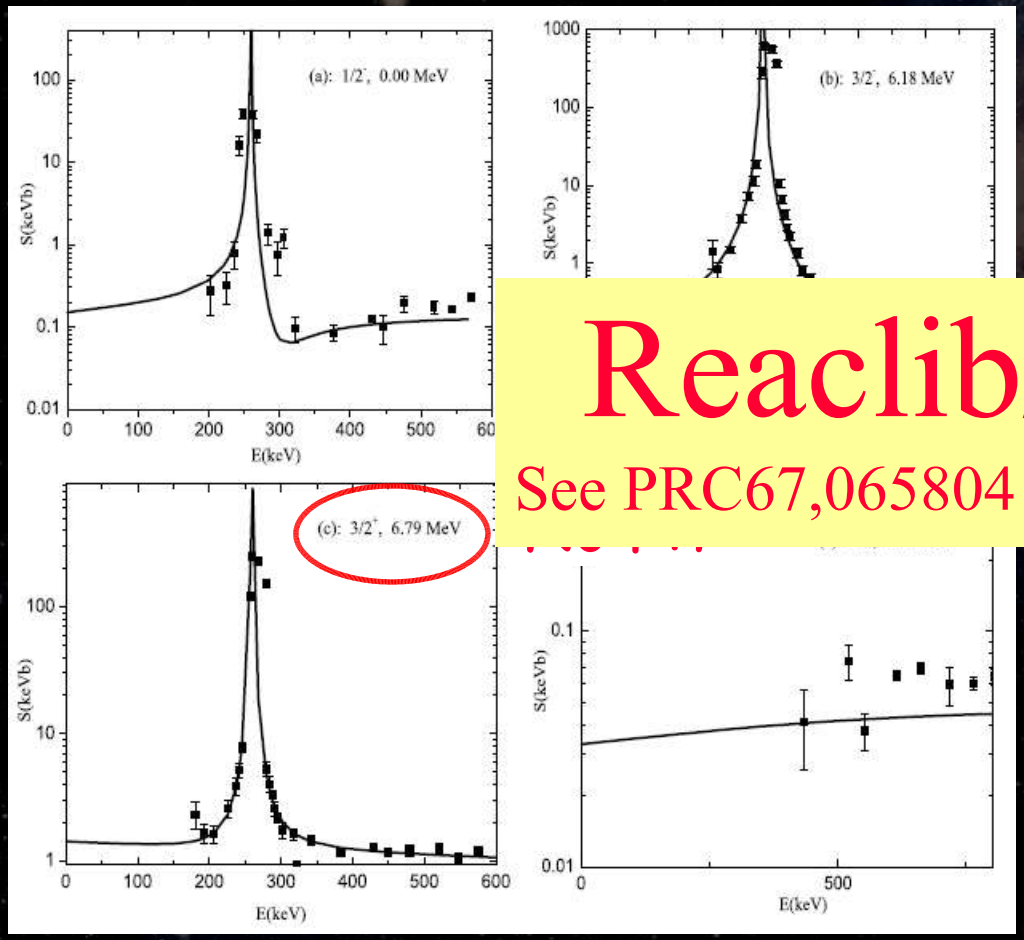

Reaclib/2

See PRC67,065804 (2003)

TAMU(ANC)
$^{14}N(^{3}He,d)^{15}O$
S_{tot}=1.70±0.22 keV b
ukhamedzhanov et al.,
, 065804 (2003)

A(Direct capture)
$(p,\gamma)^{15}O$
S_{tot}=1.7±0.1 ±0.2 keV b
LUNA Collaboration
Phys. Lett. B591 (2004) 61

E. Krumpotic et al.,
Annual Report 2003, Institut fur Strahlenphysik, Universitat Stuttgart

From $^{12}C(^{6}Li,d)^{16}O$ to $^{12}C(\alpha,\gamma)^{16}O$

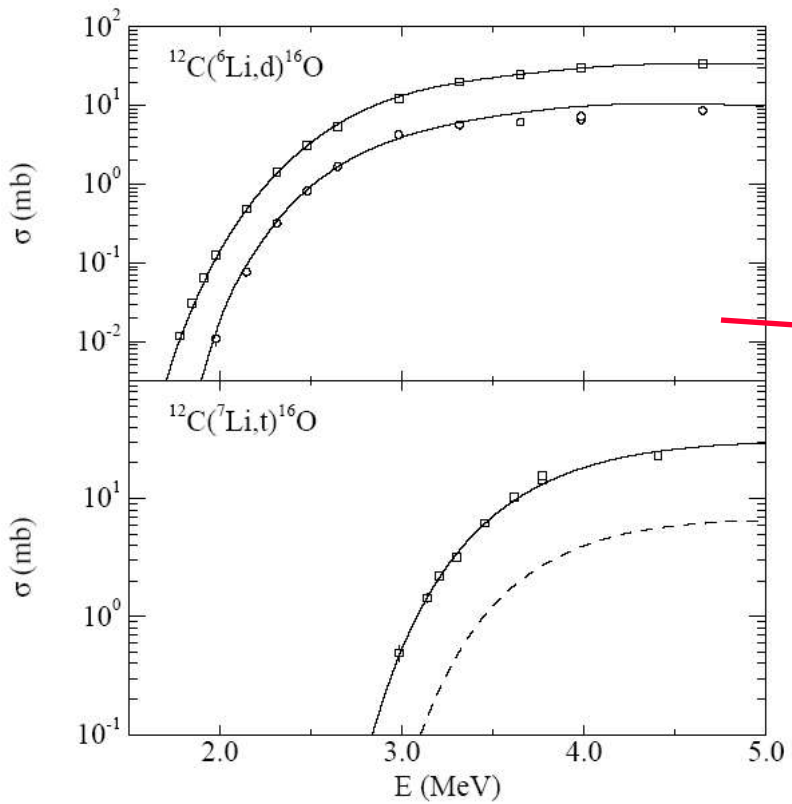

FIG. 2. Total cross sections measured using ^{6}Li (upper panel) and ^{7}Li (lower panel) beams for the 6.92-MeV 2^{+} state of ^{16}O (□) and the 7.12-MeV 1^{-} state (○, ^{6}Li beam only). The solid curves are DWBA calculations normalized to the data; the dashed curve is described in the text.

$$C_i^2 = \frac{2\mu a}{\hbar^2 W^2(a)} \left(\frac{\gamma_i^2}{1 + \gamma_i^2 \frac{dS}{dE}} \right),$$

γ_i R-matrix reduced width;

$$\gamma_{6.9} = 0.33 \pm 0.03\, MeV^{1/2}$$

$$\gamma_{6.9} = 0.36 \pm 0.06\, MeV^{1/2}$$

$^{12}C(\alpha,\alpha)^{12}C$: agree if the high lying Ex=13.02 MeV 2^{+} state in ^{16}O had be excluded.

C. R. Brune *et al.*, Phys. Rev. Lett. **83**, 4025 (1999).

P. Tischhauser, Phys. Rev. Lett. **88**, 072501 (2002).

Efforts towards the holy grail

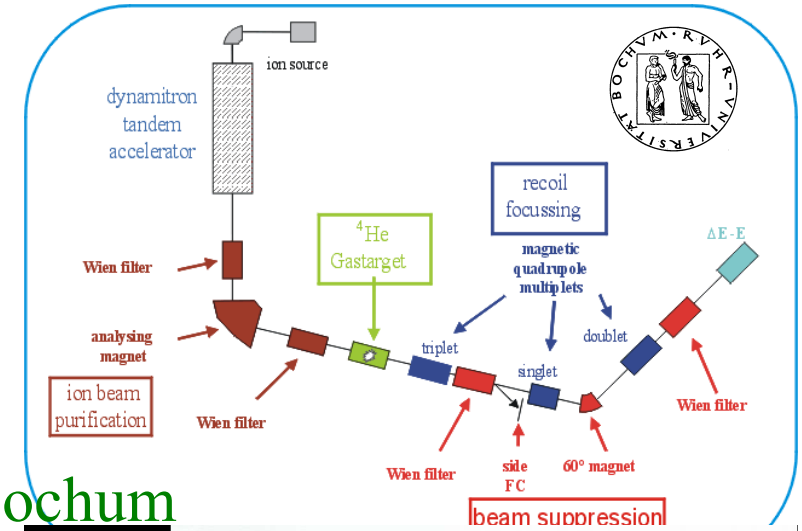

Bochum

$\alpha(^{12}C,^{16}O)\gamma$

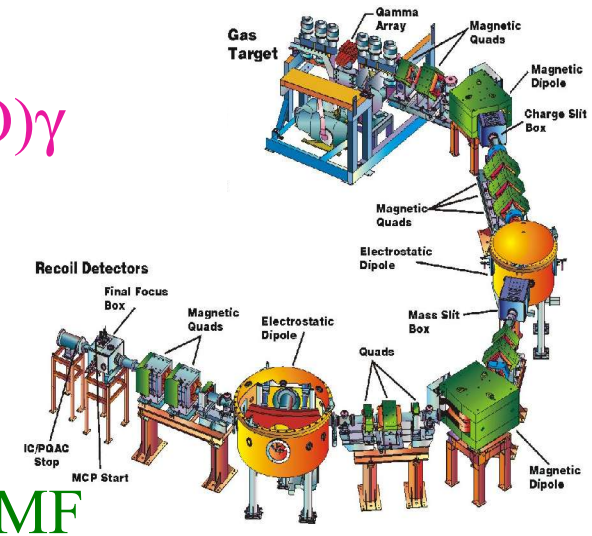

TRIUMF

^{16}N β delayed α decay

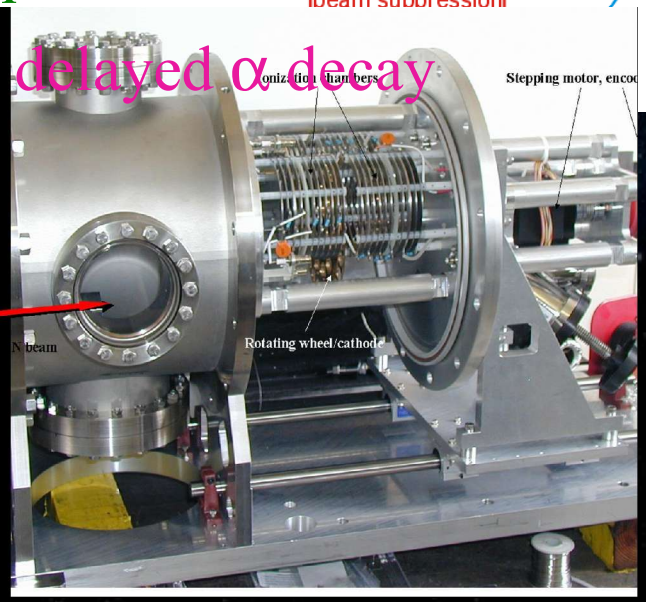

ANL

- Recoil + γ detection; improve background; (Bochum, TRIUMF)
- ^{16}N β delayed α decay with new technique; (ANL)

Conclusion on ANC

- Single DC ($^{7}Be(p,\gamma)^{8}B$)
- Multiple DC ($^{14}N(p,\gamma)^{15}O$)
- Sub-threshold resonances ($^{12}C(\alpha,\gamma)^{16}O$)
- Charge symmetry(Using stable nuclei to study unstable nuclei involving system)

Pros : Large cross section ~mb; No γ detection; No screening effect; Good for direct capture, and for states near the thresholds ($\Gamma_p \ll \Gamma_\gamma$) ;

Cons : Optical model dependence (~10%, less for sub-coulomb barrier energies); Multi-step contributions;

What are the important reactions?

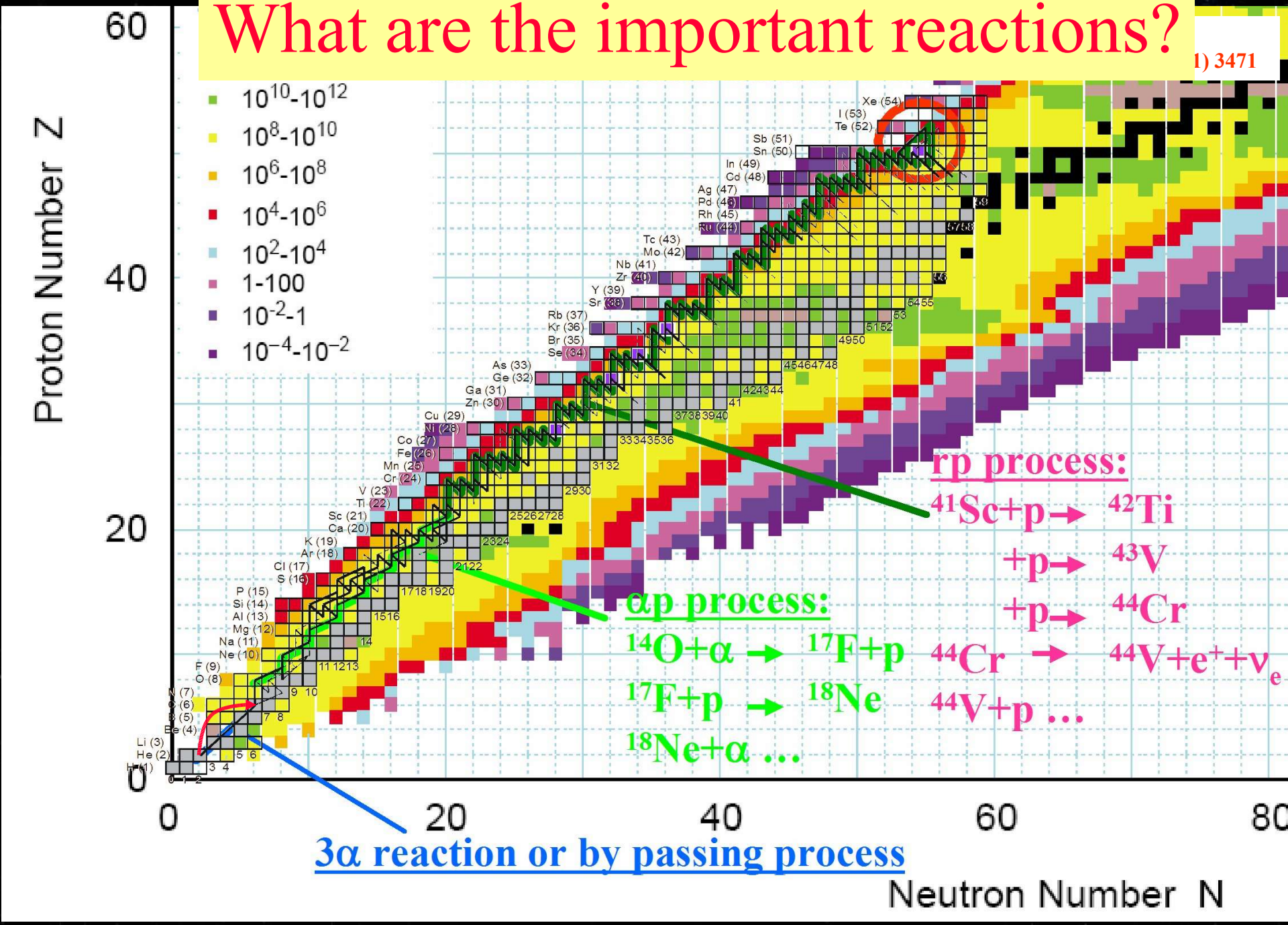

Collaborative Efforts

Different technique has different advantage and disadvantage. To achieve the best understanding, we need both direct and indirect methods.

Need collaborations between nuclear and astrophysics community to achieve the best understanding of our stars.

Collaborative Efforts

Diff
disa
nee

Nee
com
star

we

sics

ur

Thank you!

Ernst Rehm, C.L. Jiang, H. Esbensen (ANL),

Bob Tribble, A. M. Mukhamedzhanov and G. Tacabaru (TAMU)

Connecting Reionization and Metal Production by the First Stars

Aparna Venkatesan (Colorado)

Chemical Enrichment Workshop

Santa Fe, August 9, 2004

- WHICH STARS: Metals determine the stellar IMF, how the star shines and what metals are generated for next generation.
- HOW: stars form through gas cloud cooling - role of metals, esp. C vs. Fe in first stars IMF.
- WHEN: critical metallicity for transition of primordial to present-day IMF.
- Feedback from stars and SNe on local and extragalactic star formation.
- Normalizing detected metals and ionization in high-z universe to constrain first stars.
- Assumptions made for UV ionizing background directly affects value of calculated Z from metal ionization states.

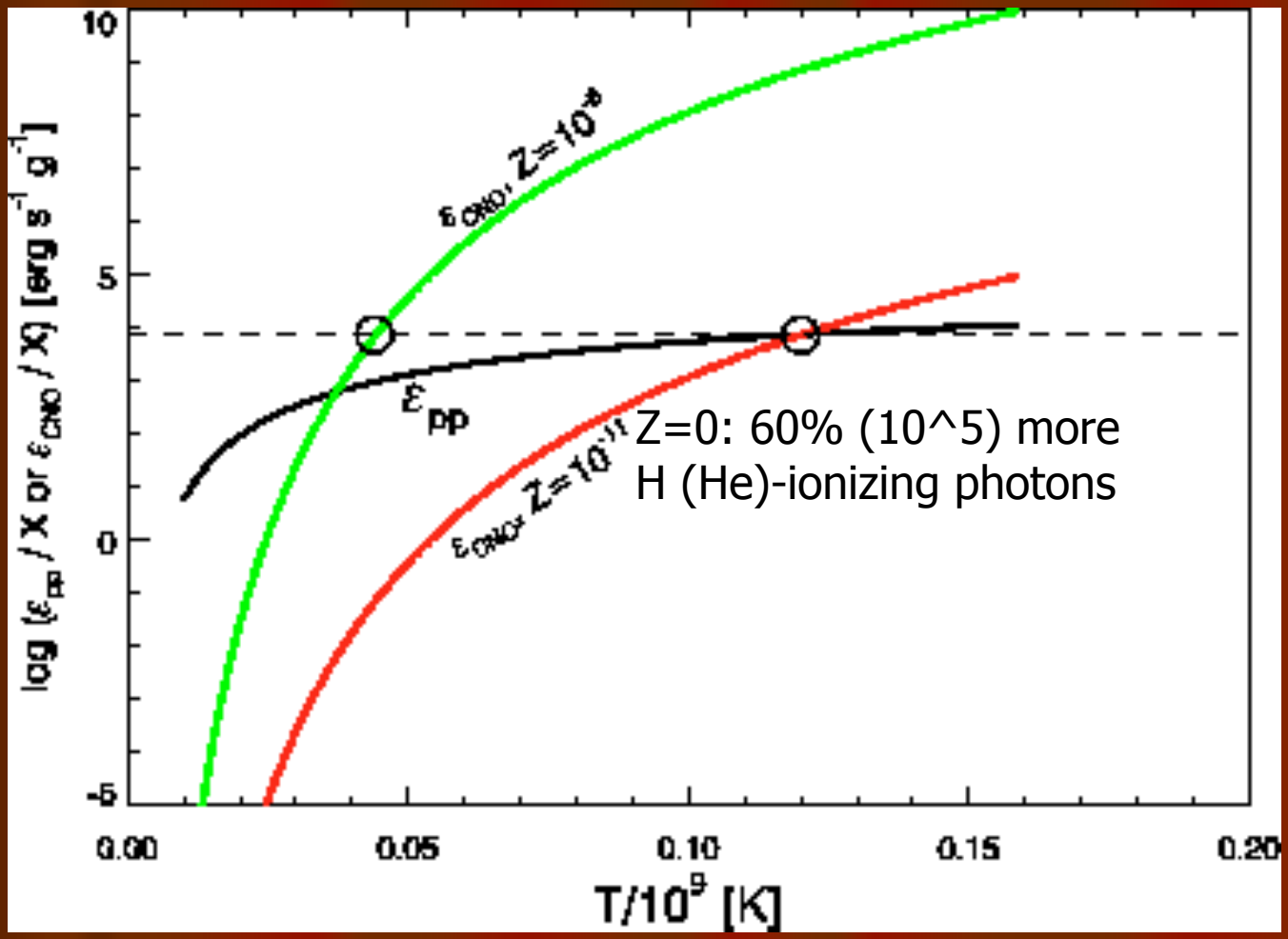

From Tumlinson, Shull & Venkatesan 2003; see also Schaerer 2002, 2003, Bromm et al. 2001

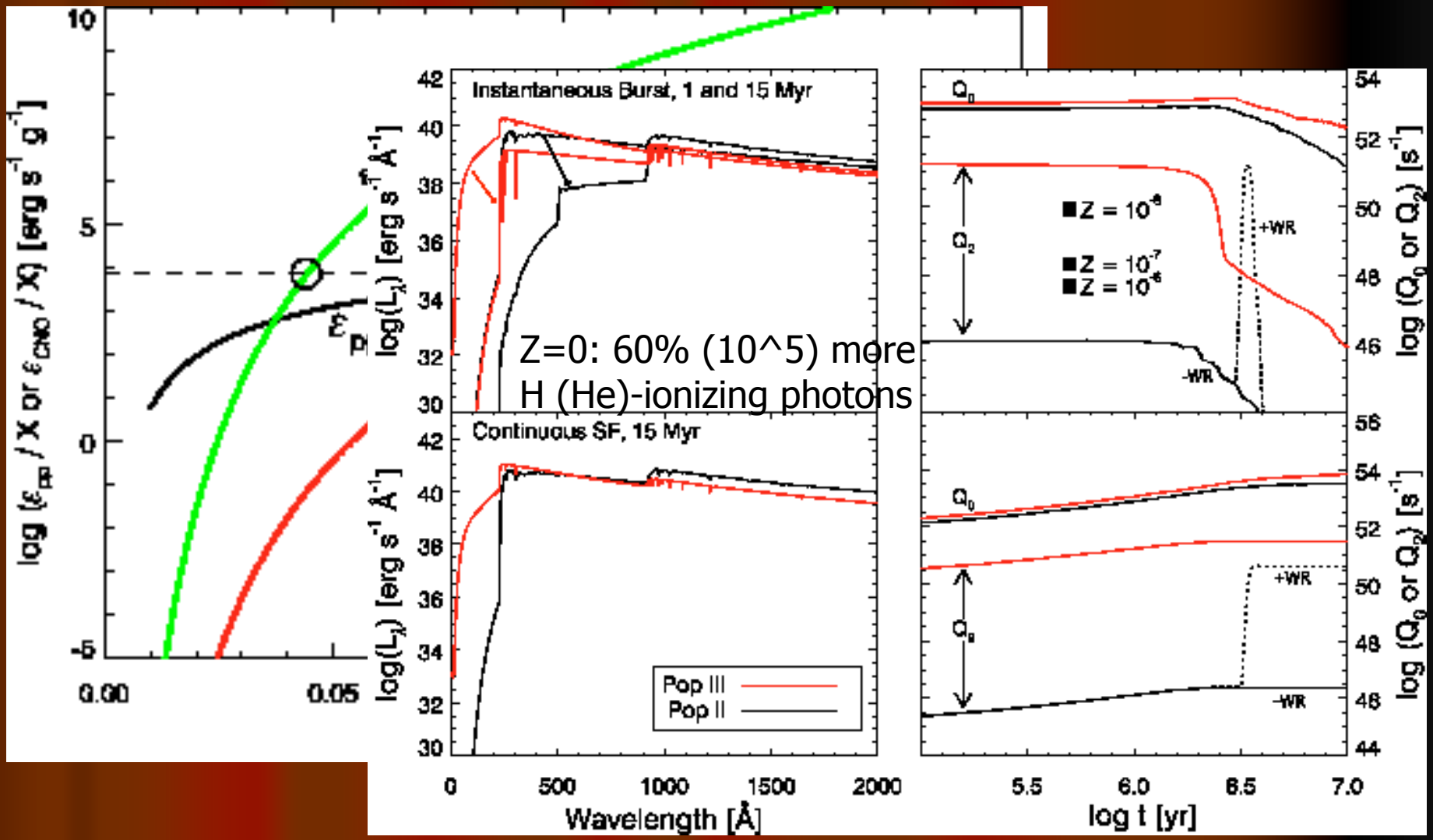

From Tumlinson, Shull & Venkatesan 2003; see also Schaerer 2002, 2003, Bromm et al. 2001

Some definitions:

- Very massive stars (VMS) : M>140 Msun.
- Pair instability (PI)SNe : M = 140-260 Msun.

  Star disrupted entirely (no remnant), unique element signature.
- 140 Msun separates two mass regimes with similar radiative but v. different nucleosynthetic properties. Can be independently tested.
- Hypernova (HN): E_51 = 1-100, M > 15 Msun. Basis in theory and in low-z SN data.

The Data So Far:

- Metals are seen ubiquitously in systems up to the highest redshifts – QSO BELRs, Ly-alpha systems (DLAs, IGM), galaxies. Generally no evidence for significant evolution in metallicity (Simcoe et al. 2004, Pettini et al. 2003, Prochaska et al. 2003, Schaye et al. 2003, Maiolino et al. 2003, Songaila 2001, Hamann & Ferland 1999)

- Relative abundance ratios of elements in Galactic halo stars as a sample are beginning to provide clues on the first SNe. (Christlieb et al. 2002, Cayrel et al. 2004, Carretta et al. 2002)

- The IGM *may* be in last stages of reionization at z~6 (G-P studies vs. Ly-alpha emitters). Not compatible with a simple ionzn. history and current CMB data from WMAP, tau_e = 0.17 +/- 0.04, or z_reion ~ 17 +/- 4. Multiple/partial ionzn.s of H and/or He at z ~ 6-20 (Cen '03, Wyithe & Loeb '03, Haiman & Holder '03, Somerville et al. '03, Venkatesan, Tumlinson & Shull '03, Ciardi et al. '03). But how incompatible are these really? Sensitive to different stages of ionzn.

- High tau and precise cosmo. parameters => very high SF'n efficiency required, possibly VMS. Main unknowns are now astrophysical.

Courtesy Xiaohui Fan's webpage:

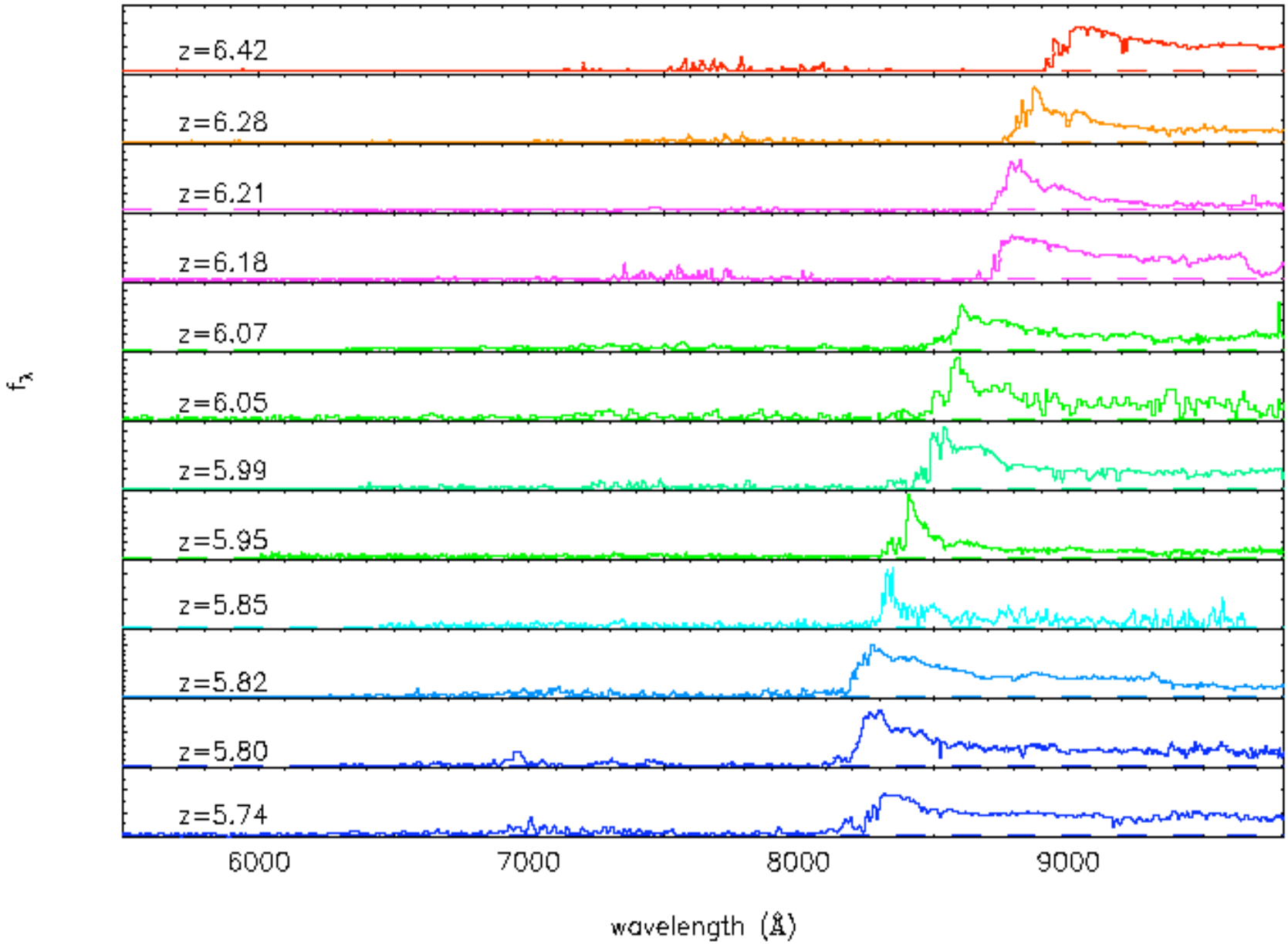

Courtesy Xiaohui Fan's webpage:

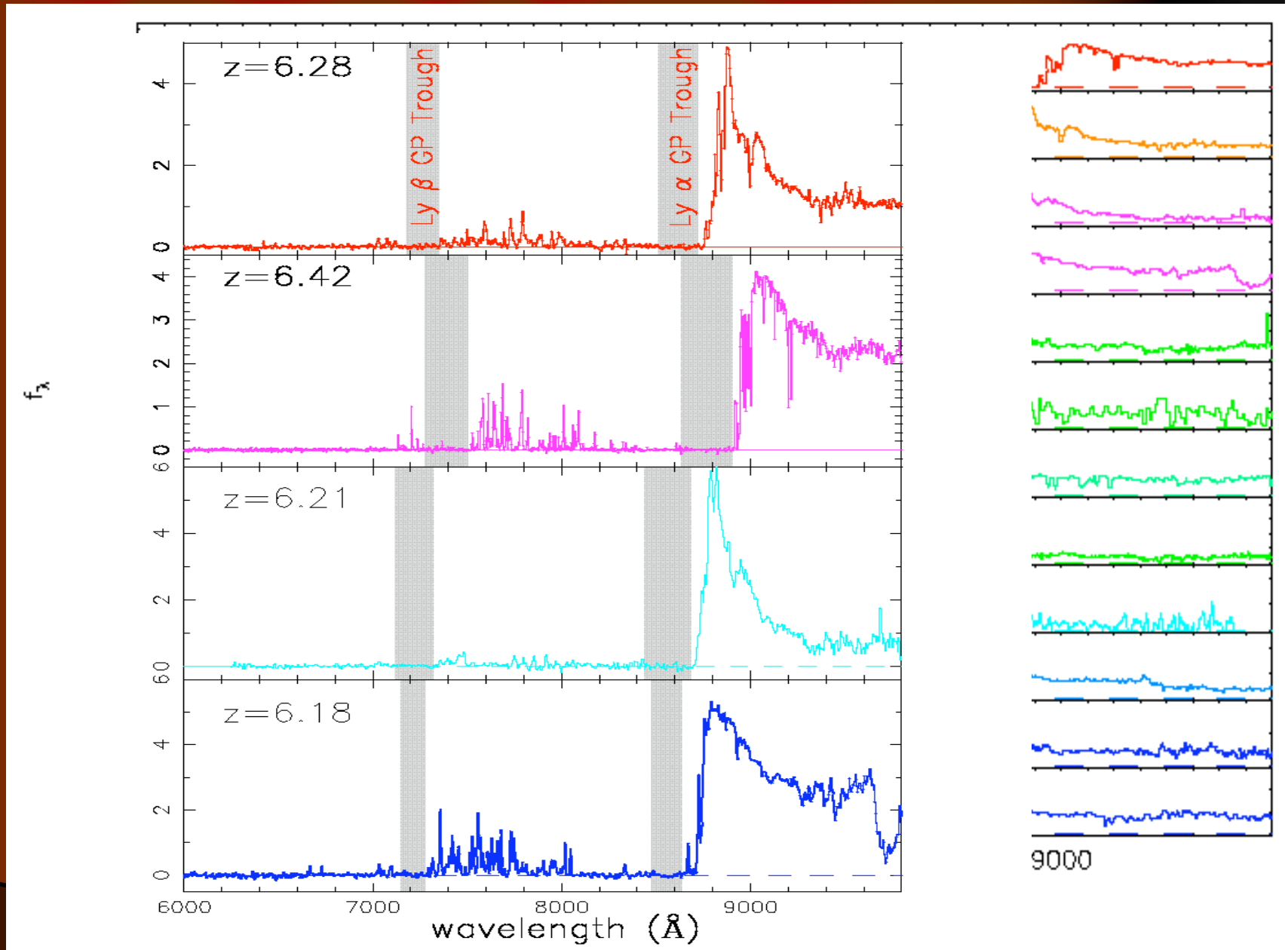

Spergel et al. 2003, WMAP 1st year data:

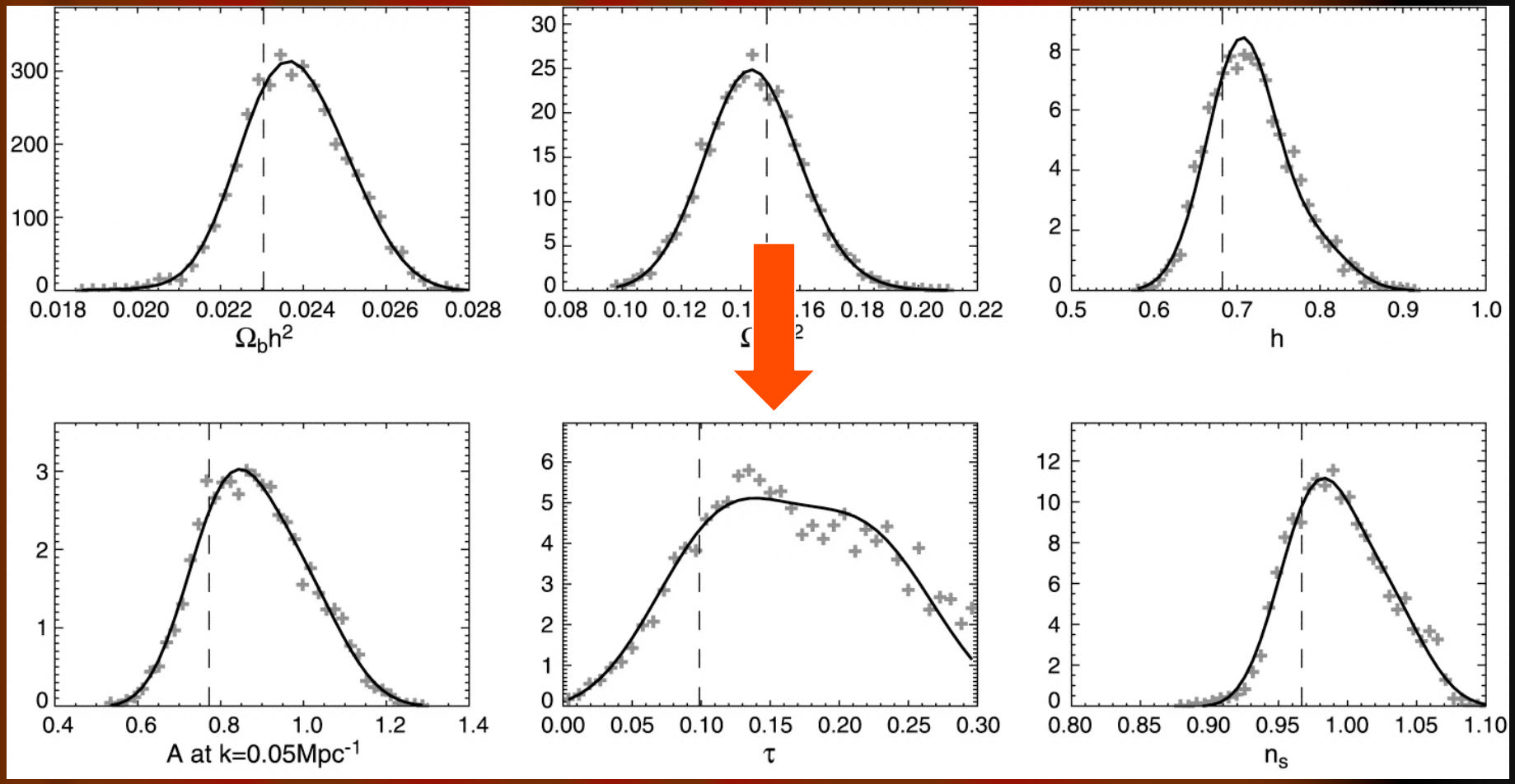

Note the broad likelihood distribution of tau!

Theoretical Studies

- Primordial stellar IMF may have been biased towards higher masses of > 100 Msun (Carr, Bond & Arnett 1983,1984…. Omukai & Nishi 1998, Abel, Bryan & Norman 2000, Bromm, Coppi & Larson 2002) owing to cooling processes in Z=0 primordial gas.
- Stellar feedback on accreting matter complicates this (Omukai & Palla 2002, Tan & McKee 2002, 2004, Bromm & Loeb 2004). Tan & McKee => M>30 Msun, i.e., primordial IMF lacking in low mass stars.
- The primordial IMF ceases to be top-heavy at gas transition metallicities of ~ 10^(-4) Zsun. (Bromm et al. 2001, Schneider et al. 2002)

Current Bottom Line:

A top-heavy IMF (M>140 Msun) is *not* necessarily required to explain the very data used to motivate it – be it reionization, the CMB, or metal abundances in high-redshift systems (QSO BELRs, IGM) or in local metal-poor halo stars. Stars of mass ~1-40 Msun must have existed at z~10-20; VMS cannot have *dominated* at these epochs. (Tumlinson, Venkatesan & Shull 2004, Daigne et al. 2004, Venkatesan, Schneider & Ferrara 2004)

This is indicated by observations over a large range in redshifts and physical scales (sub-pc to IGM) - from extreme (QSO BELRs) to relatively quiescent environments.

- Caveat: these conclusions heavily dependent on stellar evolution models. Ionizing spectra amongst various calculations in lit. consistent to within ~10%, but stellar yields still vary by a factor of about a few.

Ionizing Efficiencies of First Stars

Can a single population of stars be responsible for both reionization and metal enrichment of high-z IGM?

(Gnedin & Ostriker 1997, Madau & Shull 1996, Schaerer 2002, 2003, Venkatesan & Truran 2003):

If we derive the *minimum* no. of ionizing photons/baryon that must have been generated in association with the *observed* IGM metallicity at z~2-5:

VMS may generate only 0.35 ionizing photons per baryon before they cease forming at gas Z~10^(-4) Zsun. Therefore, VMS not necessarily preferred as a more efficient source of ionizing radiation in association with IGM metallicity.

Metal-free stars in present-day IMF 10-20 times more efficient at generating ionizing radiation per metal yield than solar-Z stars.

Clues from Local Relics

- Ashes of first stars in local ultra-metal-poor halo stars. Low mass stellar relics have elements heavier than Mg which they cannot synthesize.

- Qualitative change in element ratios at [Fe/H] ~ -3. Yield patterns of Fe-peak and r-process elements not well matched by individual SNe or PISNe. Abundance ratios indicate HNe from Z=0, 8-40 Msun stars (Umeda & Nomoto 2002, 2004, Tumlinson, Venkatesan & Shull 2004, Daigne et al. 2004).

63 metal-poor halo stars with [Fe/H] = -2 to -4

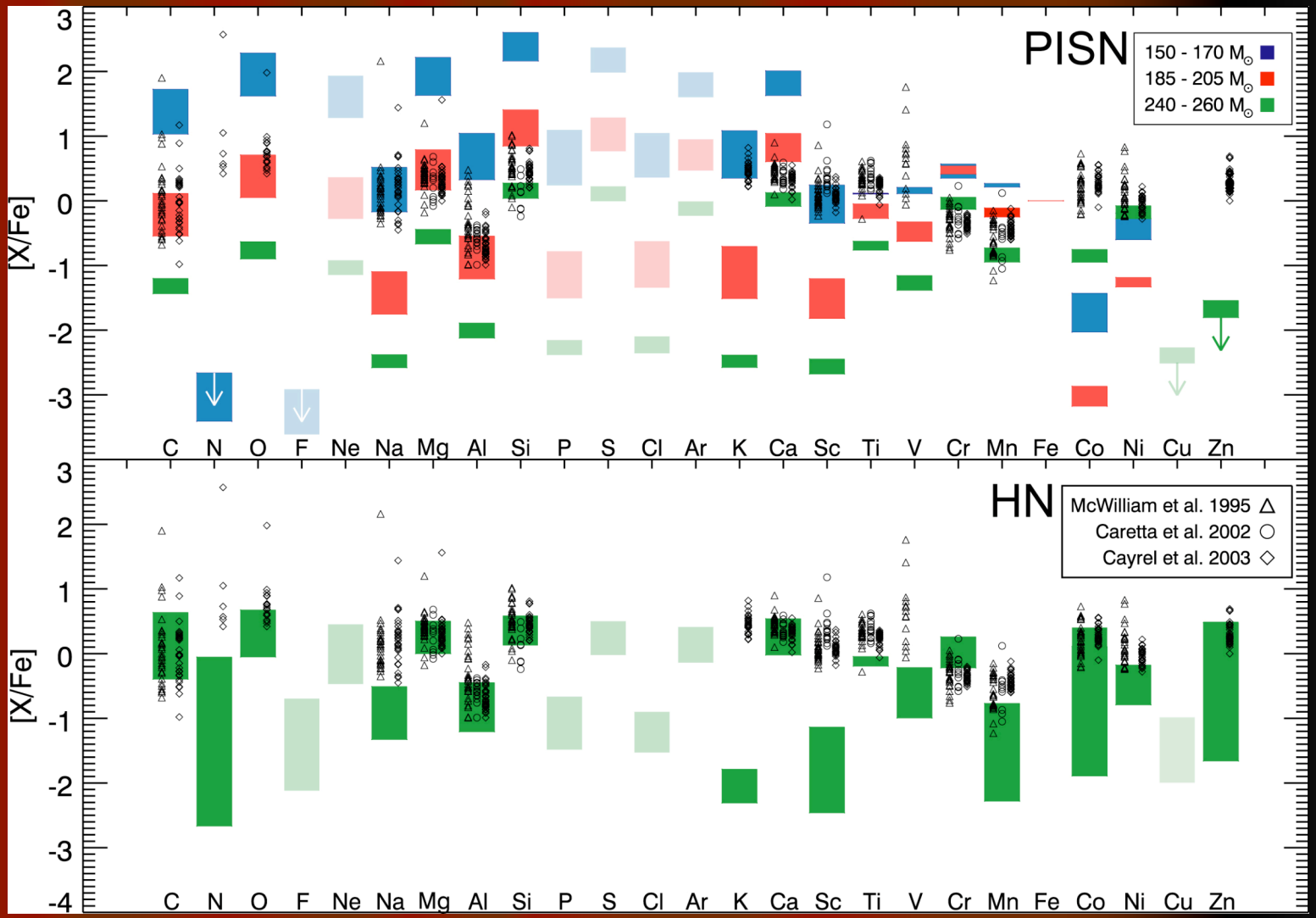

No single PISN can explain data, and characteristic VMS odd-even effect not seen.
10-50 Msun HNe provide a much better fit, esp. for Fe-peak (Cr - Zn) elements.

Strength of this Approach:
Use This to Construct an IMF for Reionization

Lifetime-integrated ionizing photons per baryon

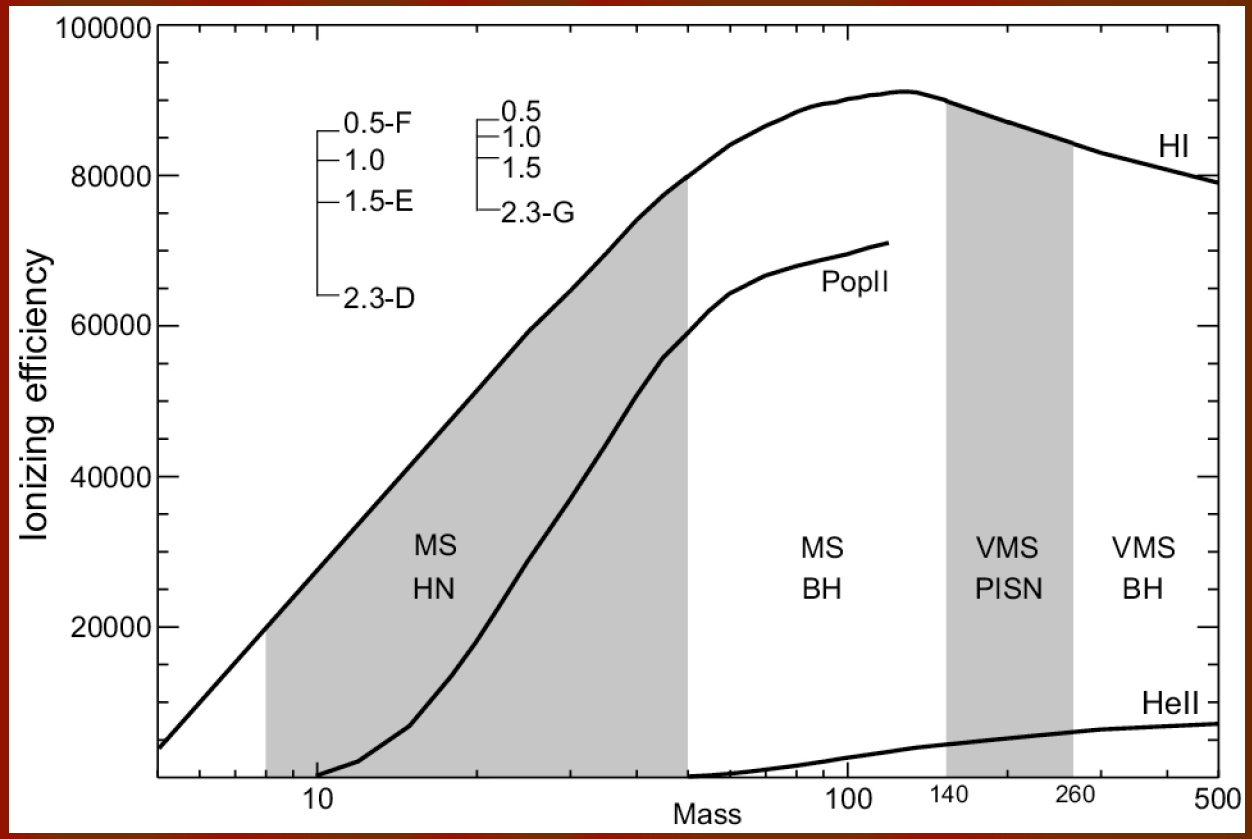

HI: Sharp rise from 10 to 50 Msun, with peak at 120 Msun (*before* VMS mass range) followed by steady decline. Pop II represents Z=0.001 (Starburst99).
An IMF precluding low mass stars can approximate the ionizing photon production from a pure VMS IMF. Note that HeII curve keeps rising.

Strength of this Approach:
Use This to Construct an IMF for Reionization

Lifetime-integrated ionizing photons per baryon

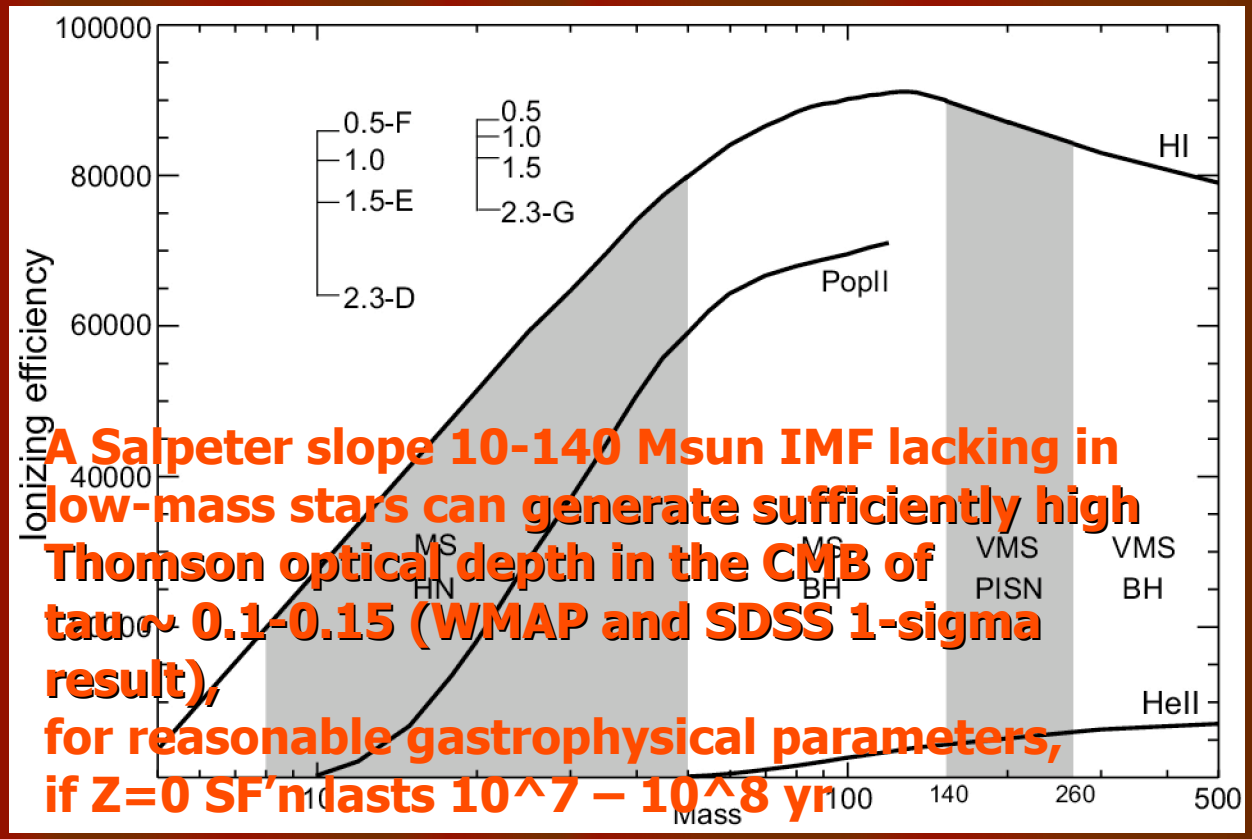

A Salpeter slope 10-140 Msun IMF lacking in low-mass stars can generate sufficiently high Thomson optical depth in the CMB of tau ~ 0.1-0.15 (WMAP and SDSS 1-sigma result), for reasonable gastrophysical parameters, if Z=0 SF'n lasts 10^7 – 10^8 yr

HI: Sharp rise from 10 to 50 Msun, with peak at 120 Msun (*before* VMS mass range) followed by steady decline. Pop II represents Z=0.001 (Starburst99). An IMF precluding low mass stars can approximate the ionizing photon production from a pure VMS IMF. Note that HeII curve keeps rising.

Metal transport models

- Divide into SN-driven outflows and ejection through galaxy mergers (Gnedin & Ostriker 1997, Gnedin 1998, Efstathiou 2000, Madau et al. 2001, Aguirre et al. 2001, Mori et al. 2002, Scannapieco et al. 2002, Ricotti et al. 2002)

- Photoionization feedback and feedback from metals from SNe, e.g., truncation of globular cluster formation by reionization (Grebel & Gallagher 2004, Strader et al. 2004, Ricotti 2002, Cen 2001)

How difficult is metal ejection?

Simulations (semianalytic) find that SN-driven winds do (do not) difficulty in distributing metals to IGM scales, and that mergers may do better. Still unresolved and likely to result in highly inhomogeneous distribution of Z_IGM.

Stellar scales (% of AU) : IGM scales (~100 kpc) roughly equal to atomic : room scales!

Images courtesy of Nick Gnedin:

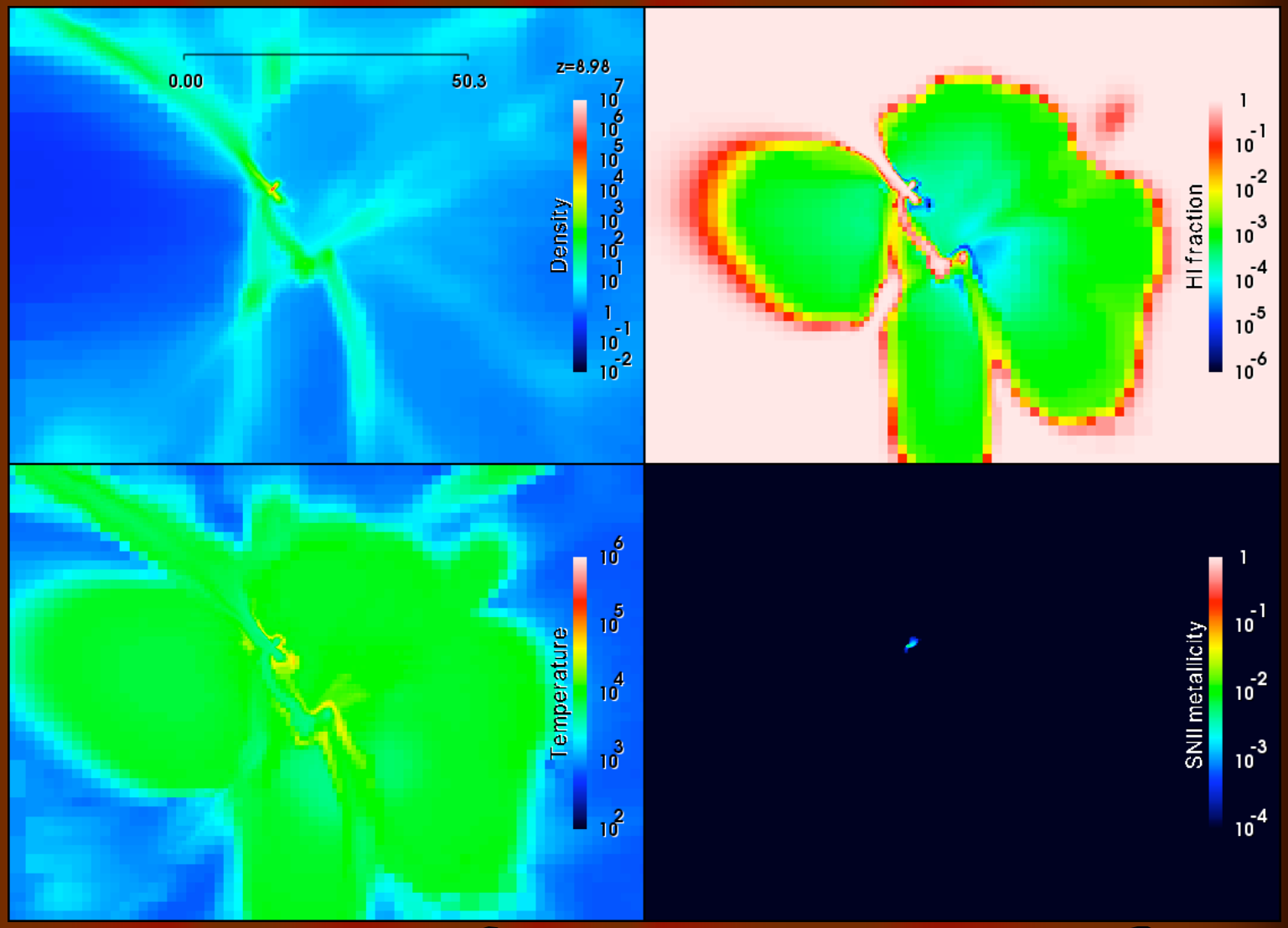

Images courtesy of Nick Gnedin:

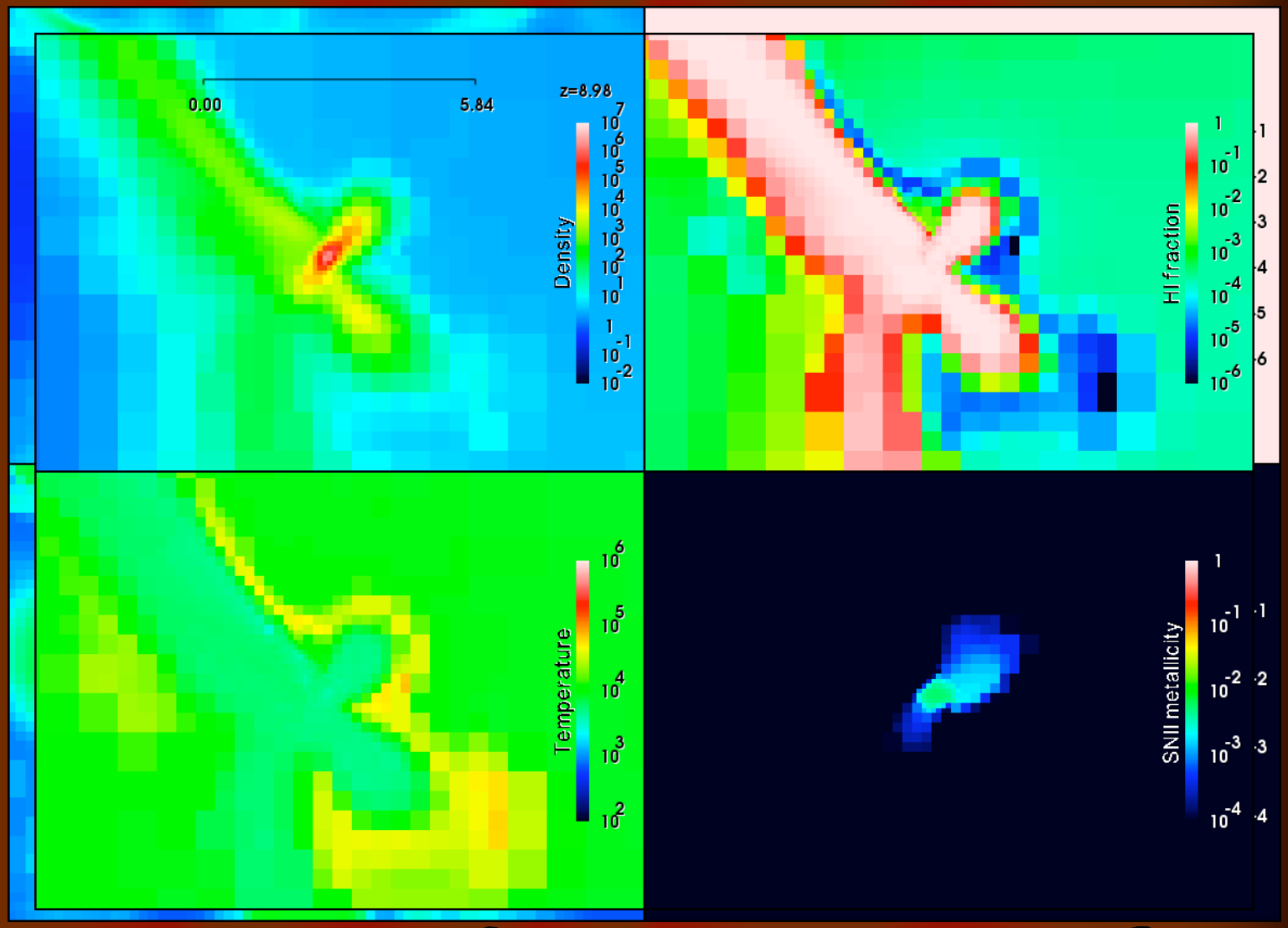

Images courtesy of Nick Gnedin:

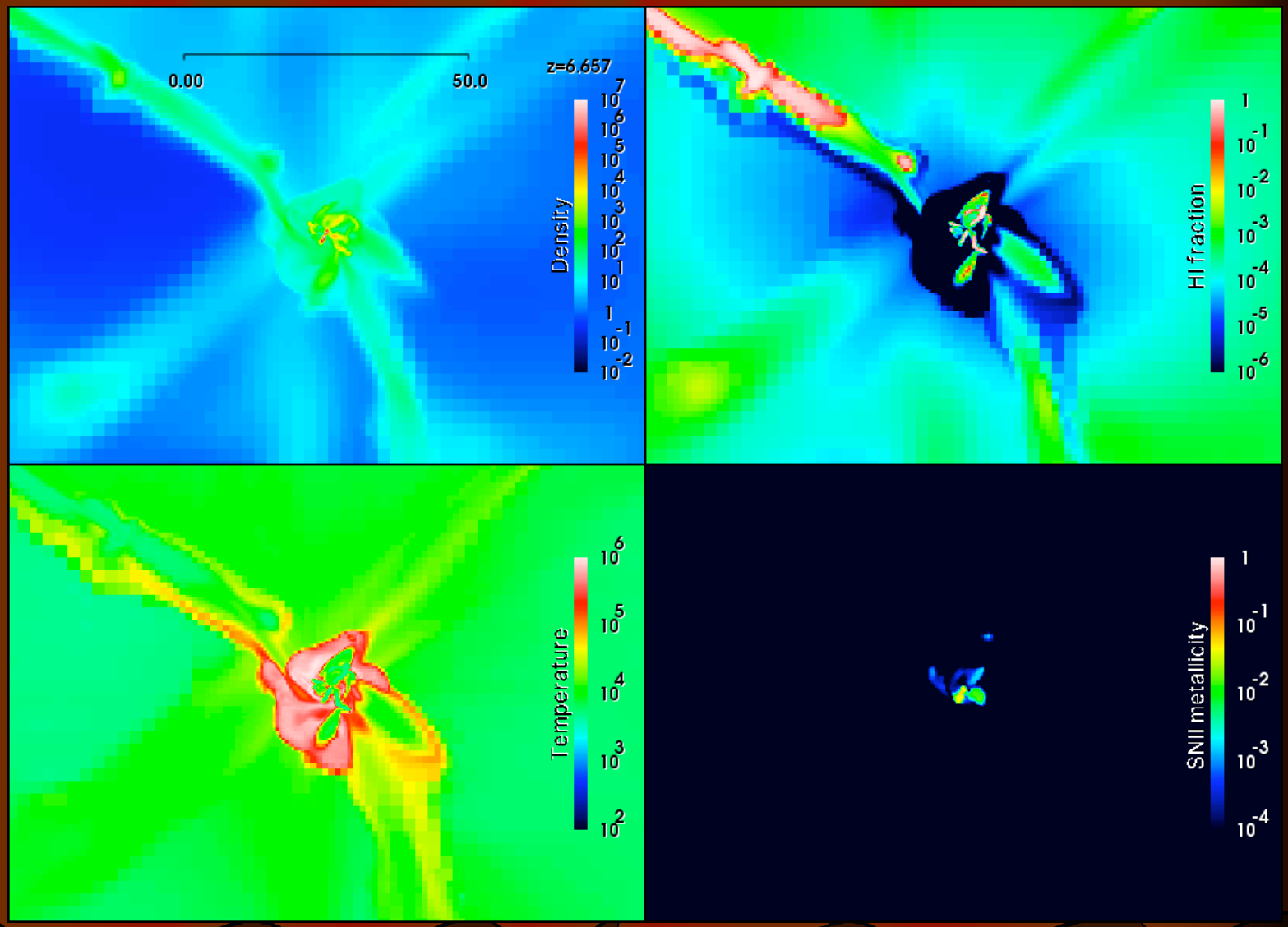

Images courtesy of Nick Gnedin:

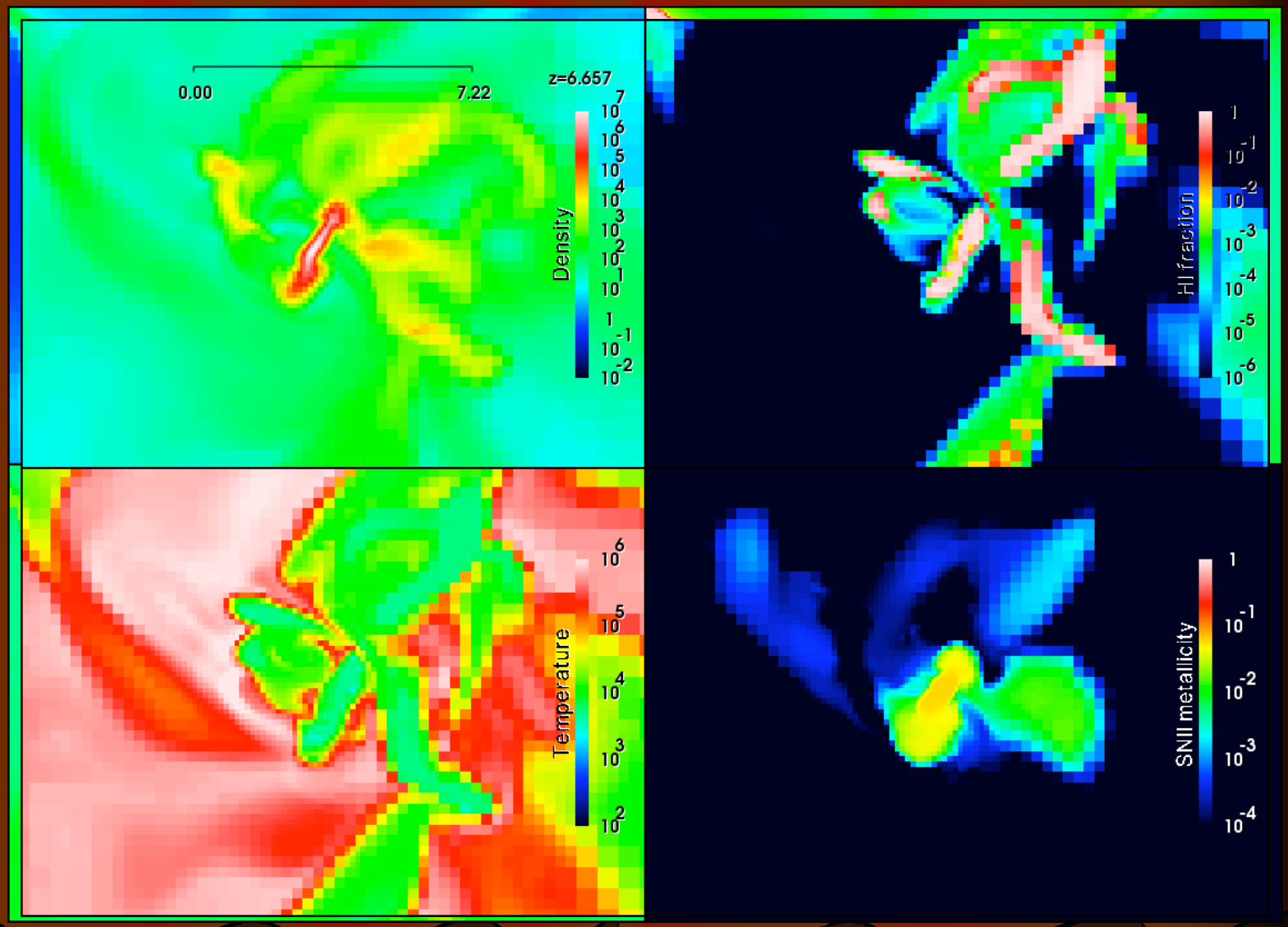

Duration of Z=0 Star Formation

- Semi-analytic calculations indicate timescales between 10^7 – 10^8 yr for self-enrichment and pollution of neighboring halos (Tumlinson, Venkatesan & Shull 2004).

- Numerical simulations of SN explosions indicate possibly much shorter timescales of ~ few -10 Myr (3D gas hydro.: Wada & Venkatesan 2003, 2004 in prep.; SPH: Yoshida, Bromm & Hernquist 2004). Environment to form Z=0 stars may be lost quickly, with 2nd generation stars of Z~10^(-4) Zsun.

3D gas hydro simulations studying chemodynamical effects of multiple SNe: metal-free starburst in central regions of 10^8 Msun halo from Wada & Venkatesan 2003:

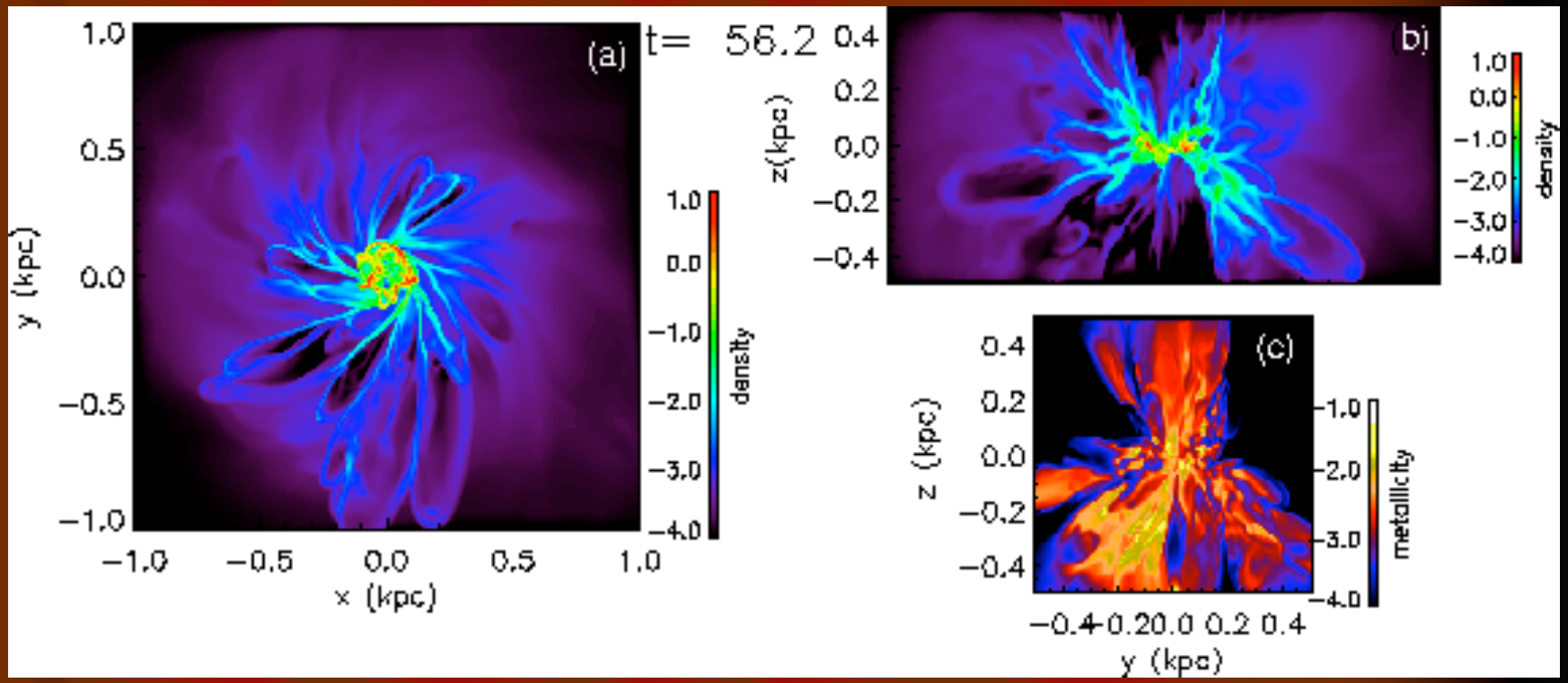

Detecting the First Stars

Use Ly-alpha and He II emission line signatures. [Tumlinson et al. 2001, Oh et al. 2001, Tumlinson, Shull & Venkatesan 2003, Schaerer 2002, Panagia 2003, Stiavelli et al. 2004, LALA (Malhotra, Rhoads and collaborators), SUBARU (Taniguchi et al. 2004), Martin & Sawicki 2004]

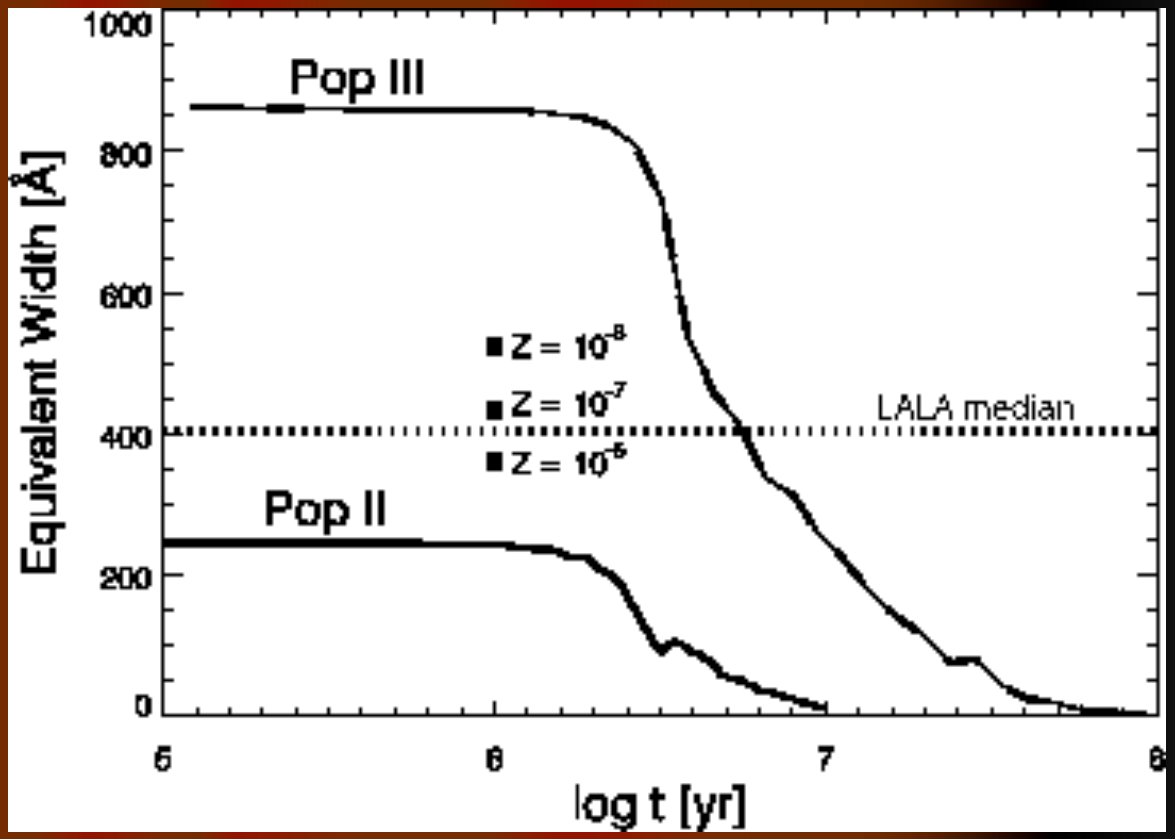

From Tumlinson, Shull & Venkatesan 2003

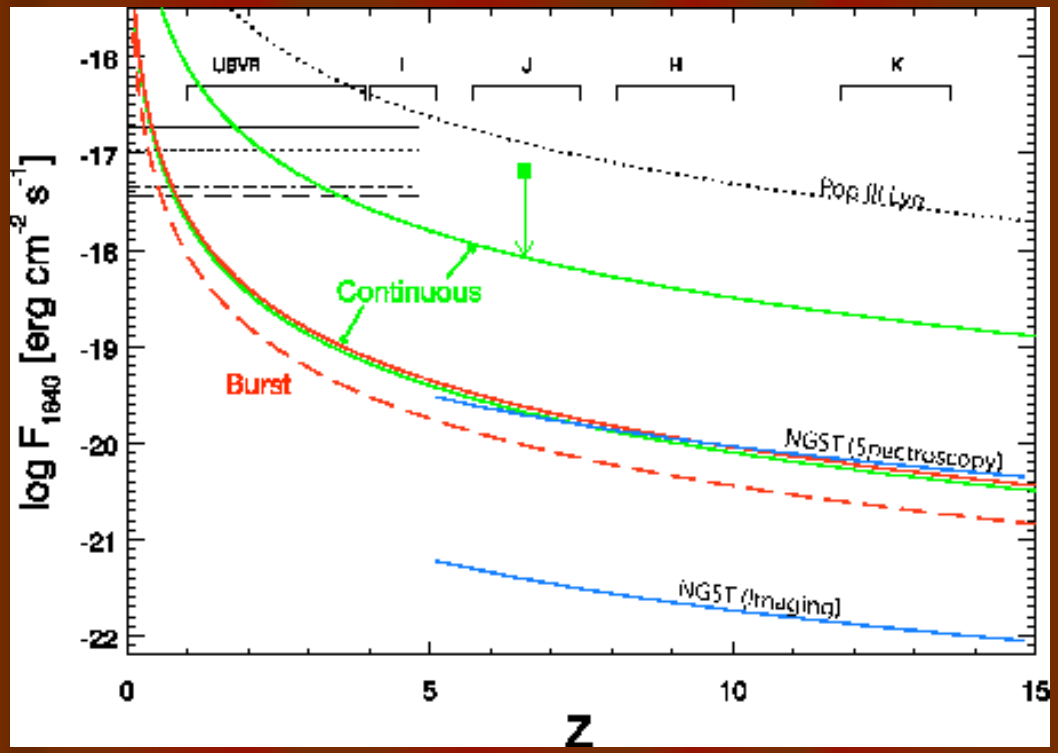

Fluxes for Ly-alpha and HeII 1640, and predictions for JWST.

From TSV 2003

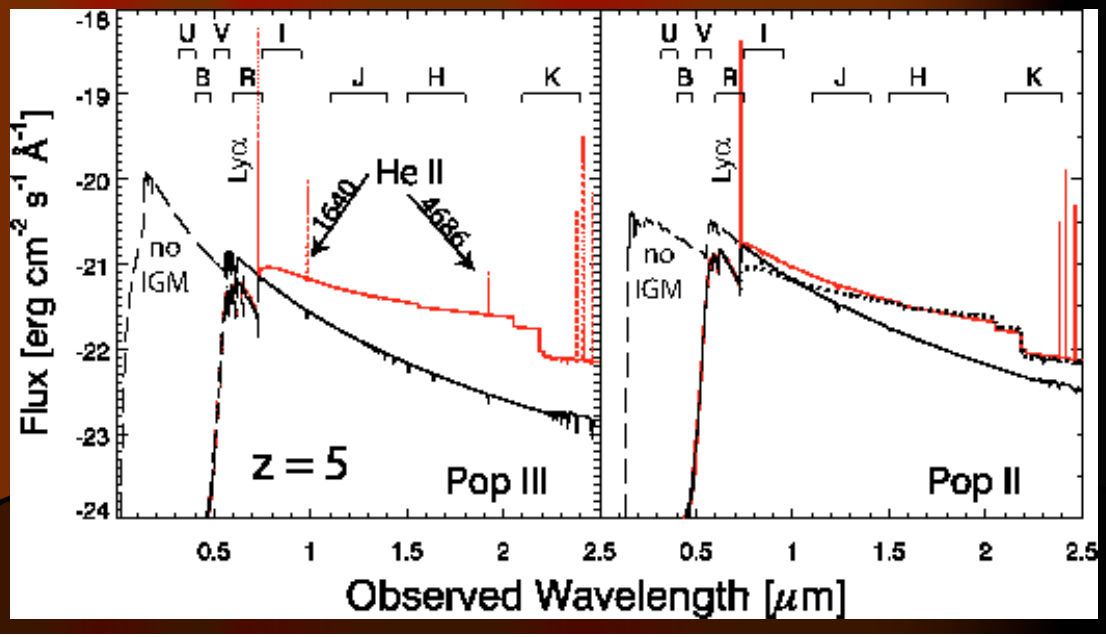

Open questions

- How closely does IGM metal enrichment track reionization?
- Uniqueness/sharpness of Pop III → II transition epochs
- Cosmological relevance of Z=0 stars: how long can they keep forming and can we see them with JWST?
- Role played by dust and the selective depletion of first wave of metals – implications for 2nd generation stars' Z.
- Improvements in stellar models (rotation, etc.)
- Do first stars have to form in first galaxies? Recent discovery of extragalactic HII regions (Ryan-Weber et al. 2004)

Promising Directions to Constrain Sources of IGM Reionzn. and Metals

- Using metal lines to probe IGM before reionization (Oh 2002, Furlanetto & Loeb 2003).
- HeII reionzn. and thermal history of IGM (Benson & Madau 2003, Hui & Haiman 2003): metal deposition may have to occur at z>~9 from temp. measurements of Ly-alpha forest at z=2-5.
- Direct detection of metal-free Galactic star or of metal-free high-z galaxies in emission.

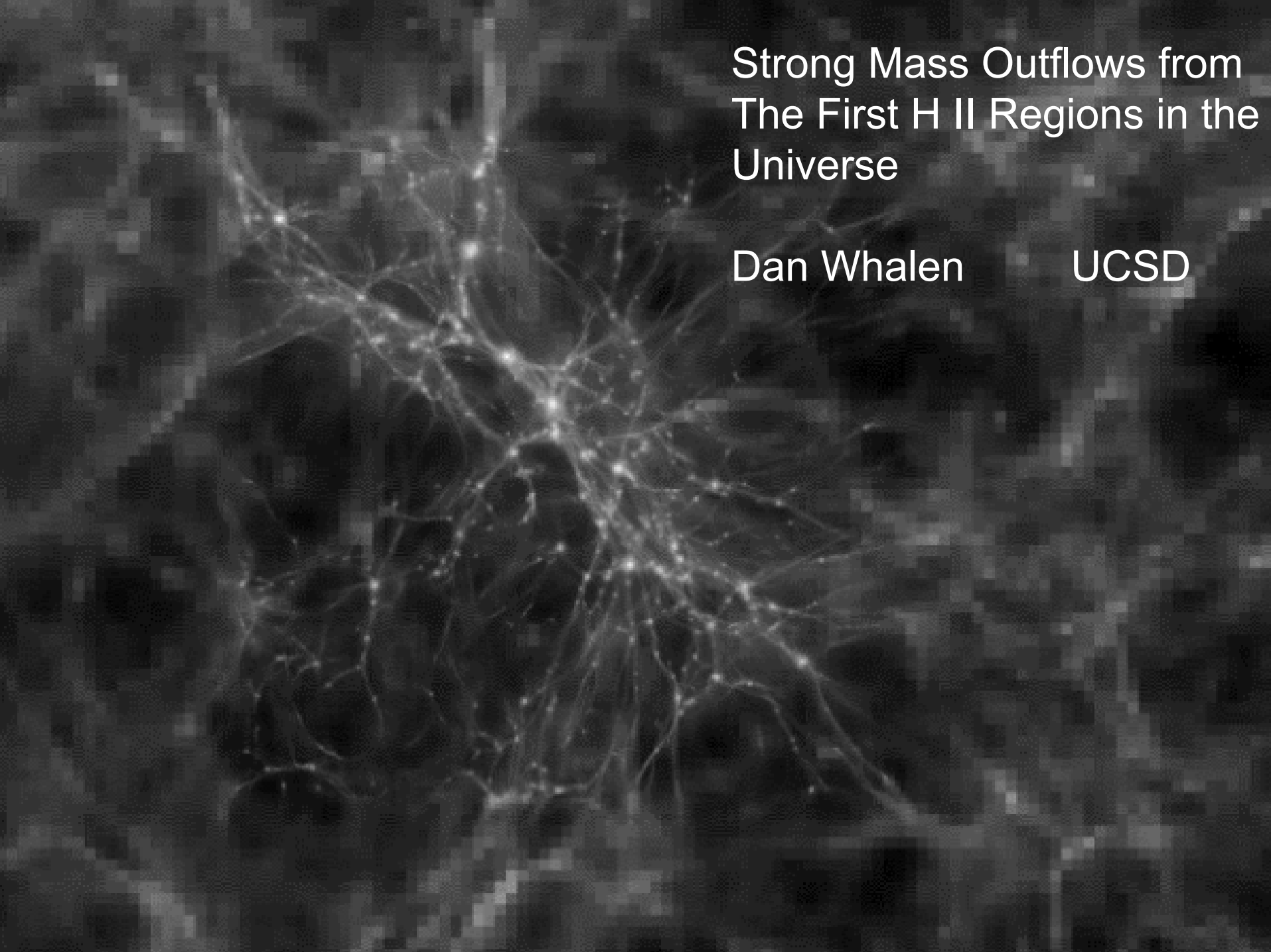

Strong Mass Outflows from The First H II Regions in the Universe

Dan Whalen UCSD

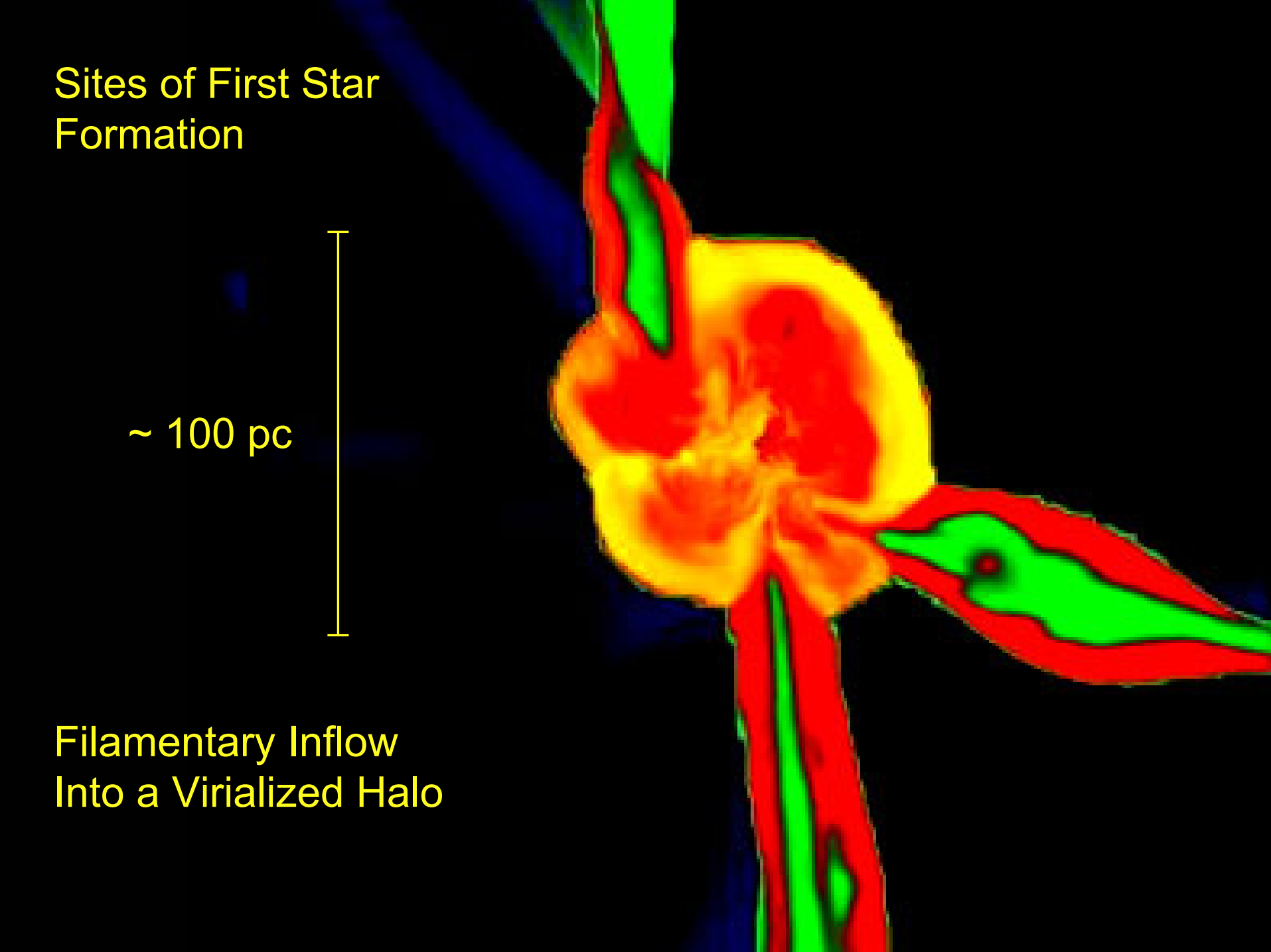
Sites of First Star Formation
~ 100 pc
Filamentary Inflow Into a Virialized Halo

Pop III Very Massive Stars

- likely 100 to 500 solar masses
- 2 to 2.5 Myr lifetimes
- enormous fluxes in FUV (typically 2.0 E50 s^{-1})
- not thought to have strong mass loss (no line-driven winds)
- die either as pair-instability supernovae or bypass explosion to form BH

Evolution of an Ionization Front

- the early front flashes out from the central star, leaving the ambient medium ionized (and at ~10^4 K) but undisturbed

- this R-type I-front later slows to ~ 2 c_{II} as it approaches the Stromgren radius and begins to stall

- by this time the 10^4 K gas has expanded and driven a shock outward which overtakes the I-front

- these hydrodynamic motions free the front to advance forward but it trails the shock thereafter to become D-type if the medium is uniform

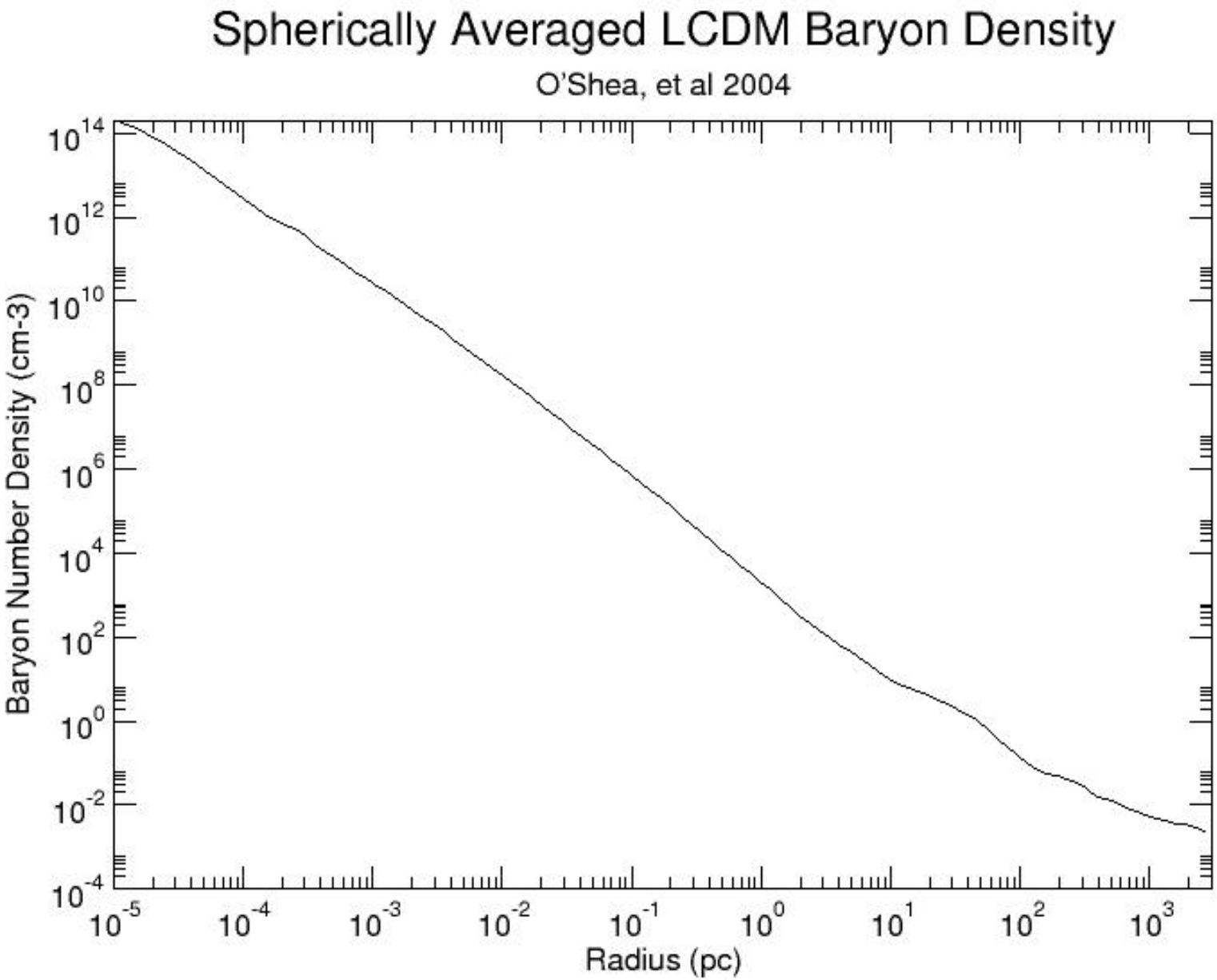
Spherically Averaged LCDM Baryon Density
O'Shea, et al 2004
Baryon Number Density (cm-3)
Radius (pc)
10^{14}
10^{12}
10^{10}
10^{8}
10^{6}
10^{4}
10^{2}
10^{0}
10^{-2}
10^{-4}
10^{-5}
10^{-4}
10^{-3}
10^{-2}
10^{-1}
10^{0}
10^{1}
10^{2}
10^{3}

Descent of an I-Front Down a Power-Law r^{-w} Density Gradient

- I-fronts descending outward along gradients $w < 1.5$ execute the classic approach to a Stromgren sphere, revert from R-type to D-type, and drive a dense shocked shell in front of themselves thereafter

- I-fronts expanding along gradients $w > 1.5$ rapidly revert from D-type to R-type (in some cases never having become D-type in the first place) and quickly overrun the entire cloud

Multispecies ZEUS-MP Hydrodynamics and Radiative Transfer

- ZEUS-MP is a massively parallel multiphysics Eulerian hydrocode
- a nine-species reaction network and nine additional advection equations were added to ZEUS-MP to account for the collisional and photoionization processes that split and combine primordial H and He
- a solution to the static equation of radiative transfer in spherical coordinates was implemented to compute the H photoionization rates required by the reaction network
- ZEUS-MP advances the reaction network and gas energy over successive chemistry timesteps until it has crossed a heating/cooling timestep, at which point the code updates the hydrodynamics equations

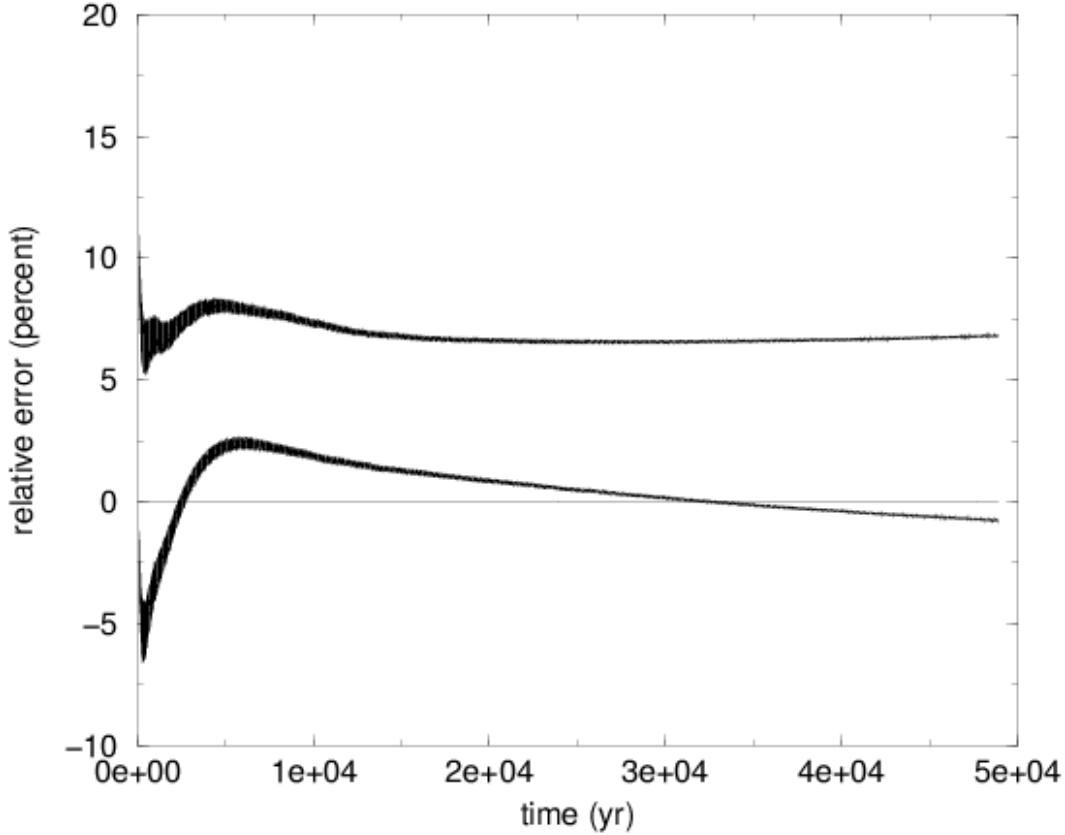

Zeus-MP I-front Benchmark in 1/r gradient

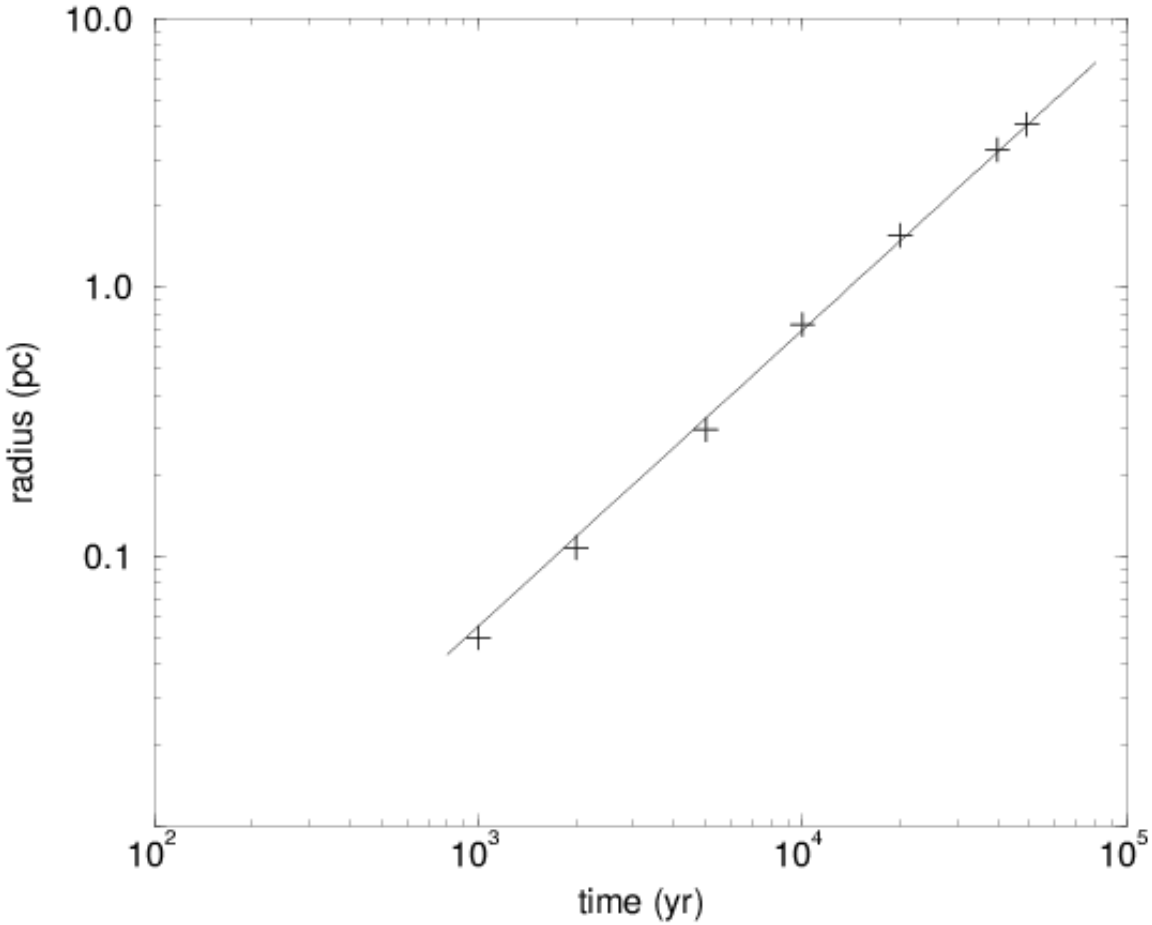

Zeus-MP Ionized Core Shock Benchmark

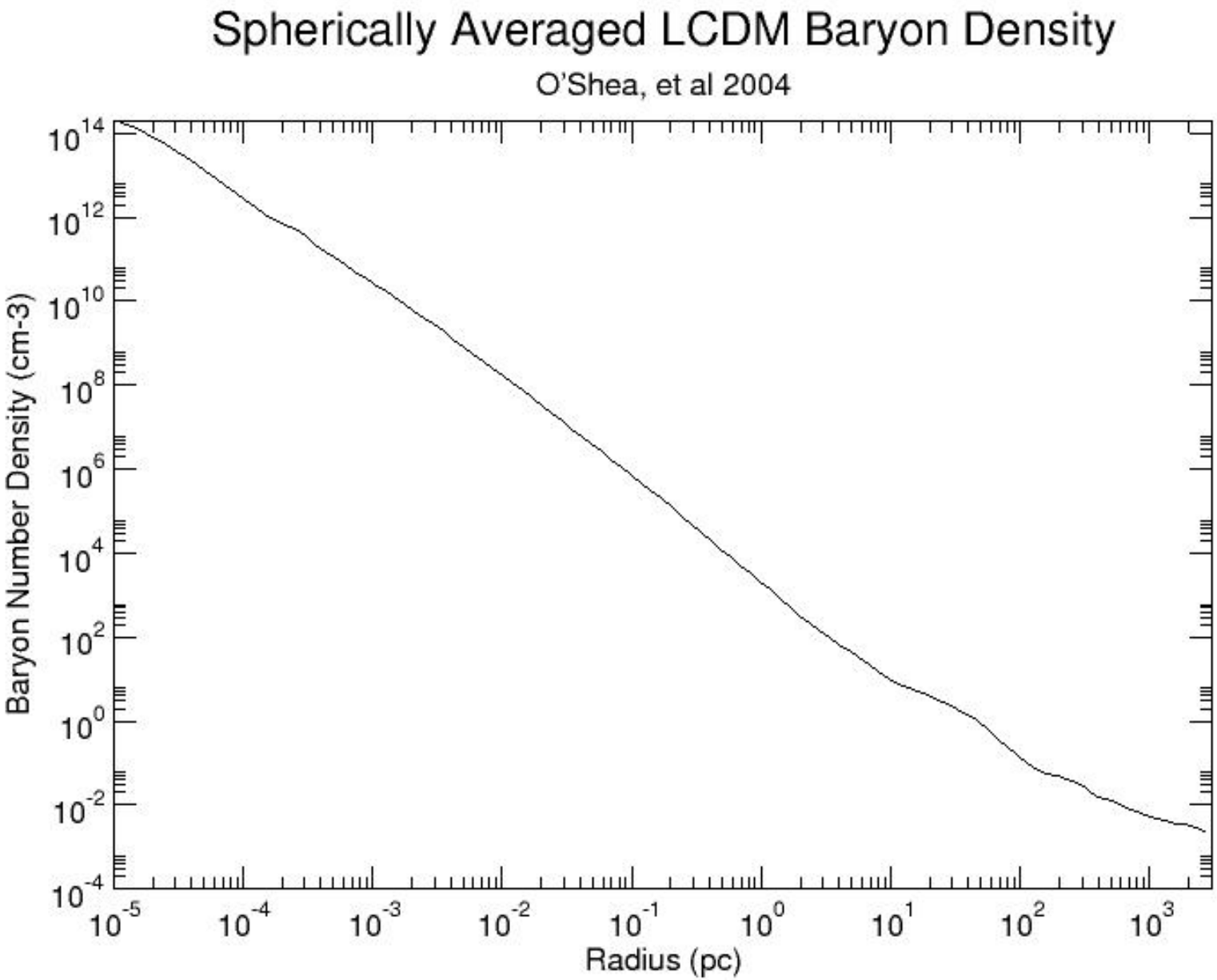
Spherically Averaged LCDM Baryon Density
O'Shea, et al 2004
Baryon Number Density (cm-3)
Radius (pc)
10^{14}
10^{12}
10^{10}
10^{8}
10^{6}
10^{4}
10^{2}
10^{0}
10^{-2}
10^{-4}
10^{-5}
10^{-4}
10^{-3}
10^{-2}
10^{-1}
10^{0}
10^{1}
10^{2}
10^{3}

Cumulative Mass

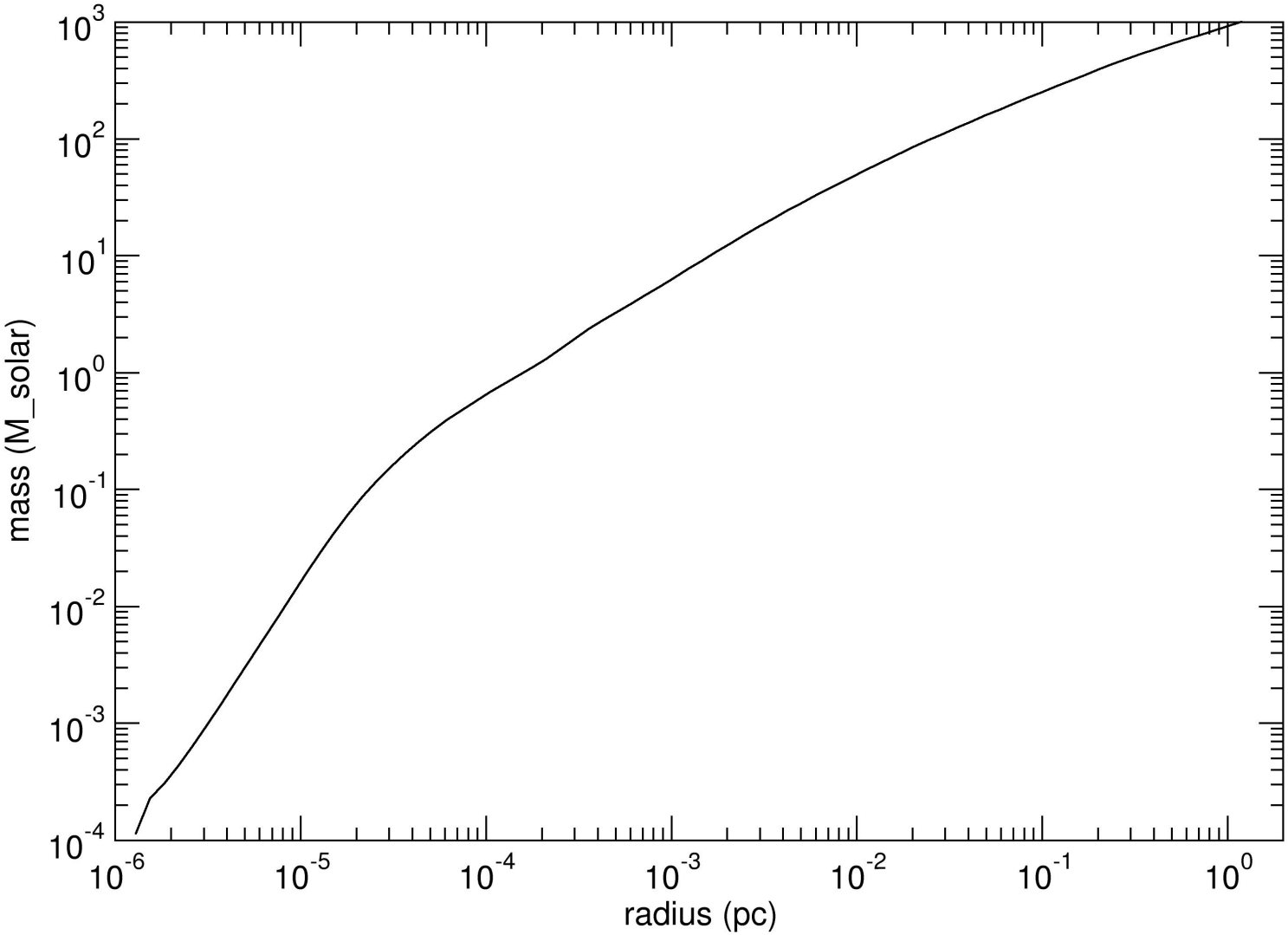

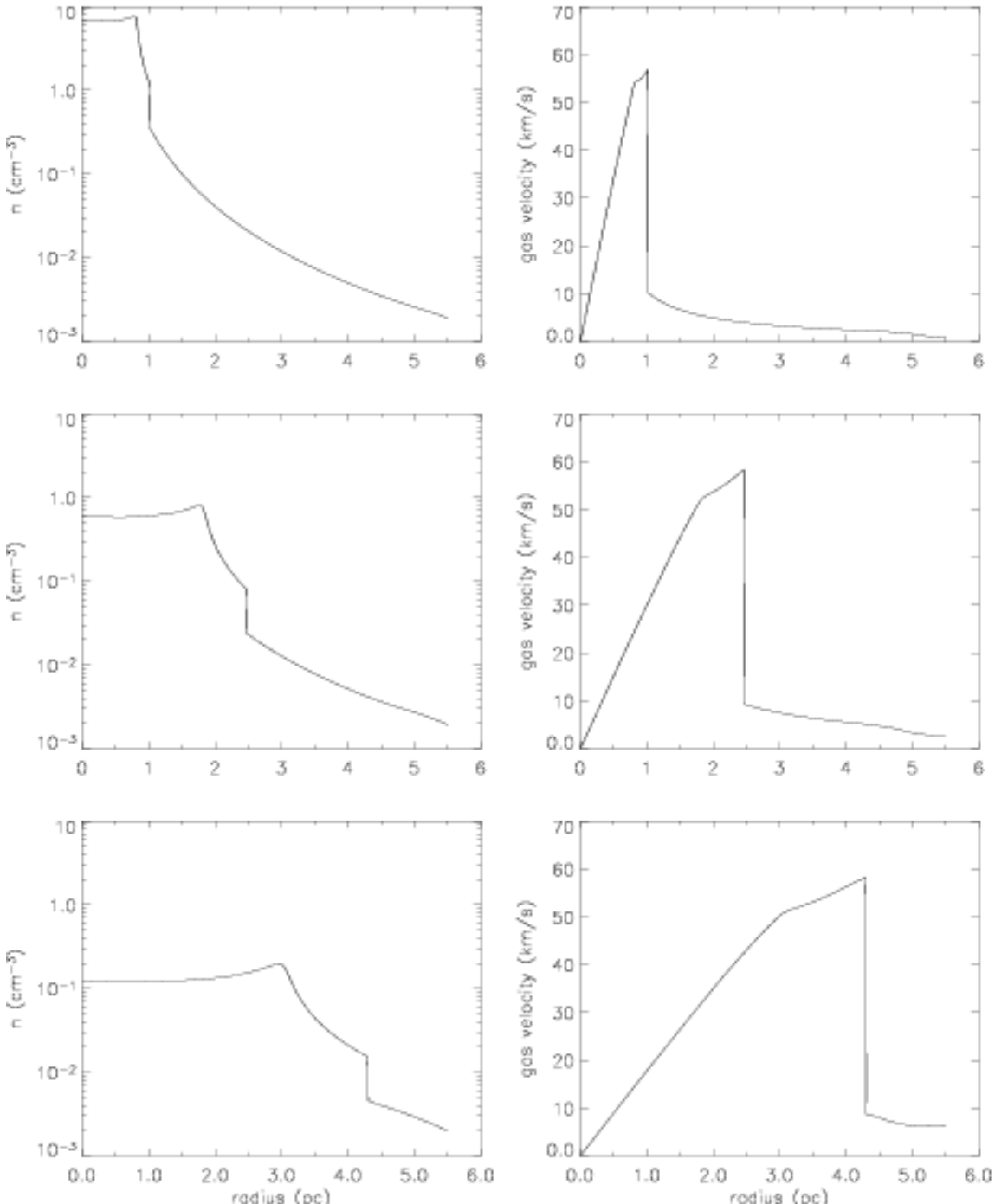
n (cm⁻³)
gas velocity (km/s)
radius (pc)

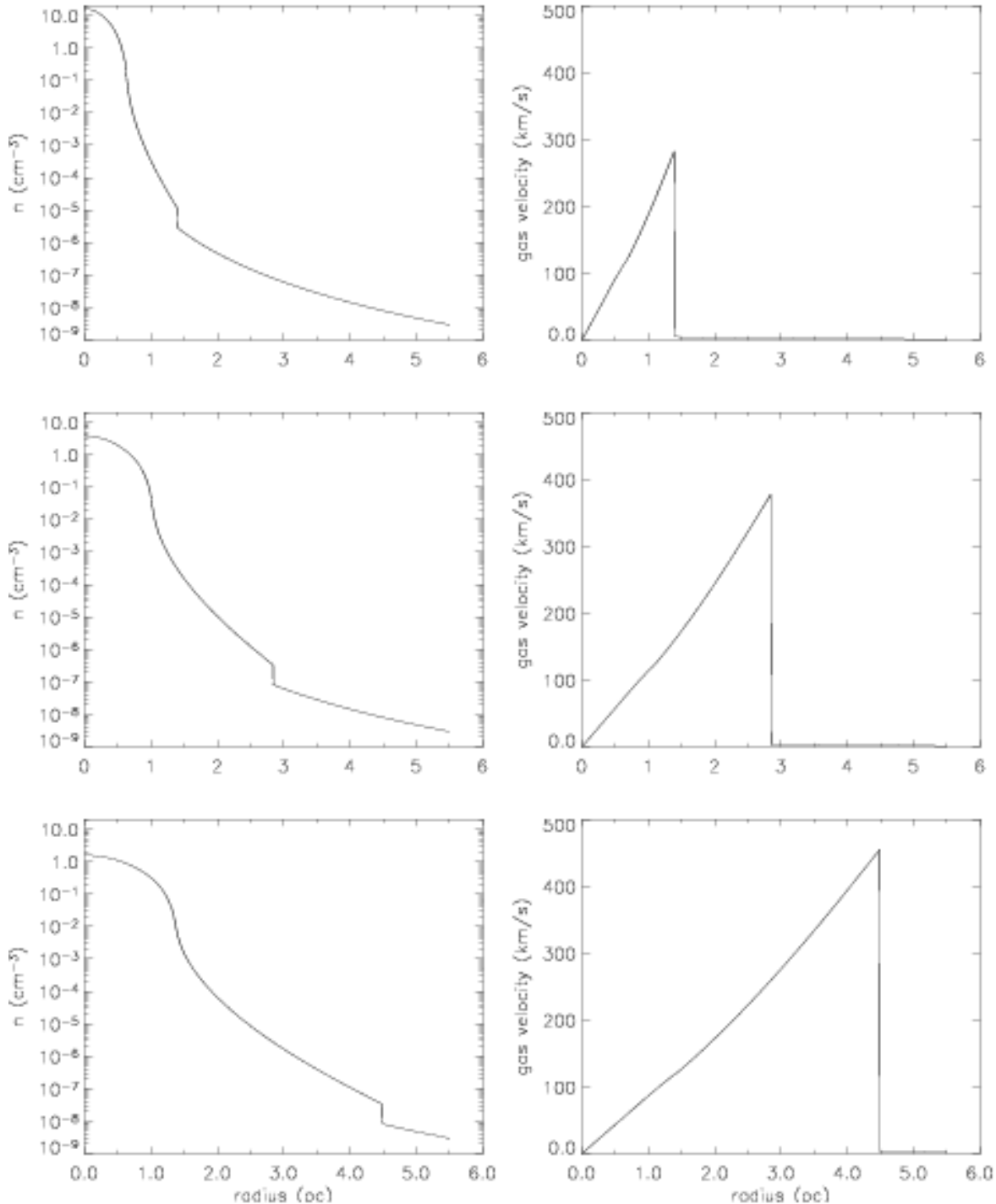
n (cm⁻³)
gas velocity (km/s)
radius (pc)

Baryonic Mass Ejection from the DM Halo

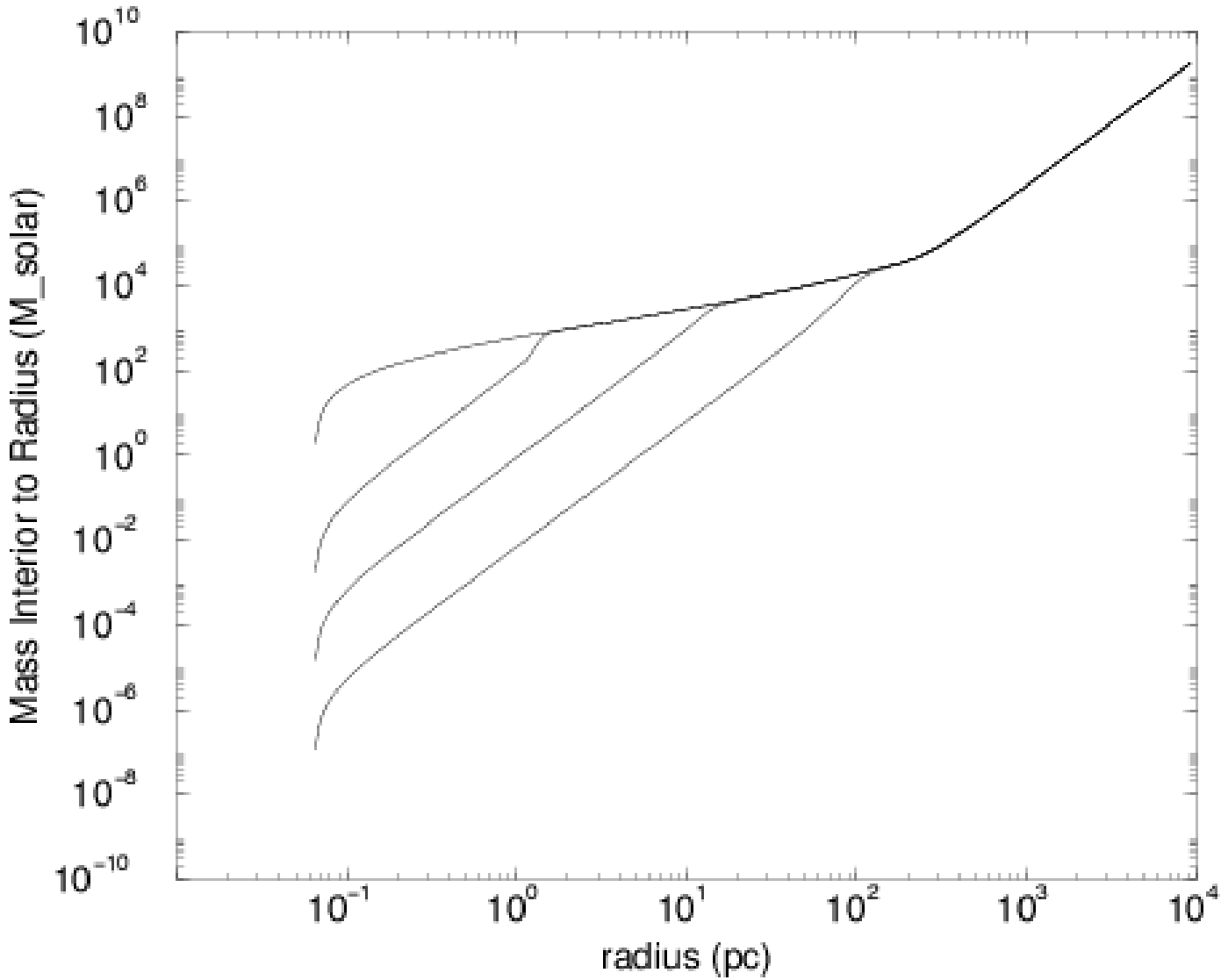

- these primordial mass outflows drive approximately half of the baryonic mass beyond the virial radius over the main sequence lifetime of the star (~10000 solar masses from a 500,000 M_solar DM halo)

- contrary to what one might expect, the mass loss rates are largely independent of the central stellar mass or ionizing photon rates

- the steepness of the density gradient determines the rate at which the ionized core shock sweeps baryons from the halo

- Strong H II outflows enhance supernova dispersal of metals because the ejecta from a 200 M_solar pair-instability SN will not encounter its own mass in ambient hydrogen until it has travelled 50 pc, until which point it is in a free-expansion phase

- The remnant does not enter the Sedov-Taylor phase until it has expanded to a radius of 200 pc

- Such outflows would be expected to retard the growth of black holes should the star instead collapse

Ionization Front Instabilities in 2D Simulations

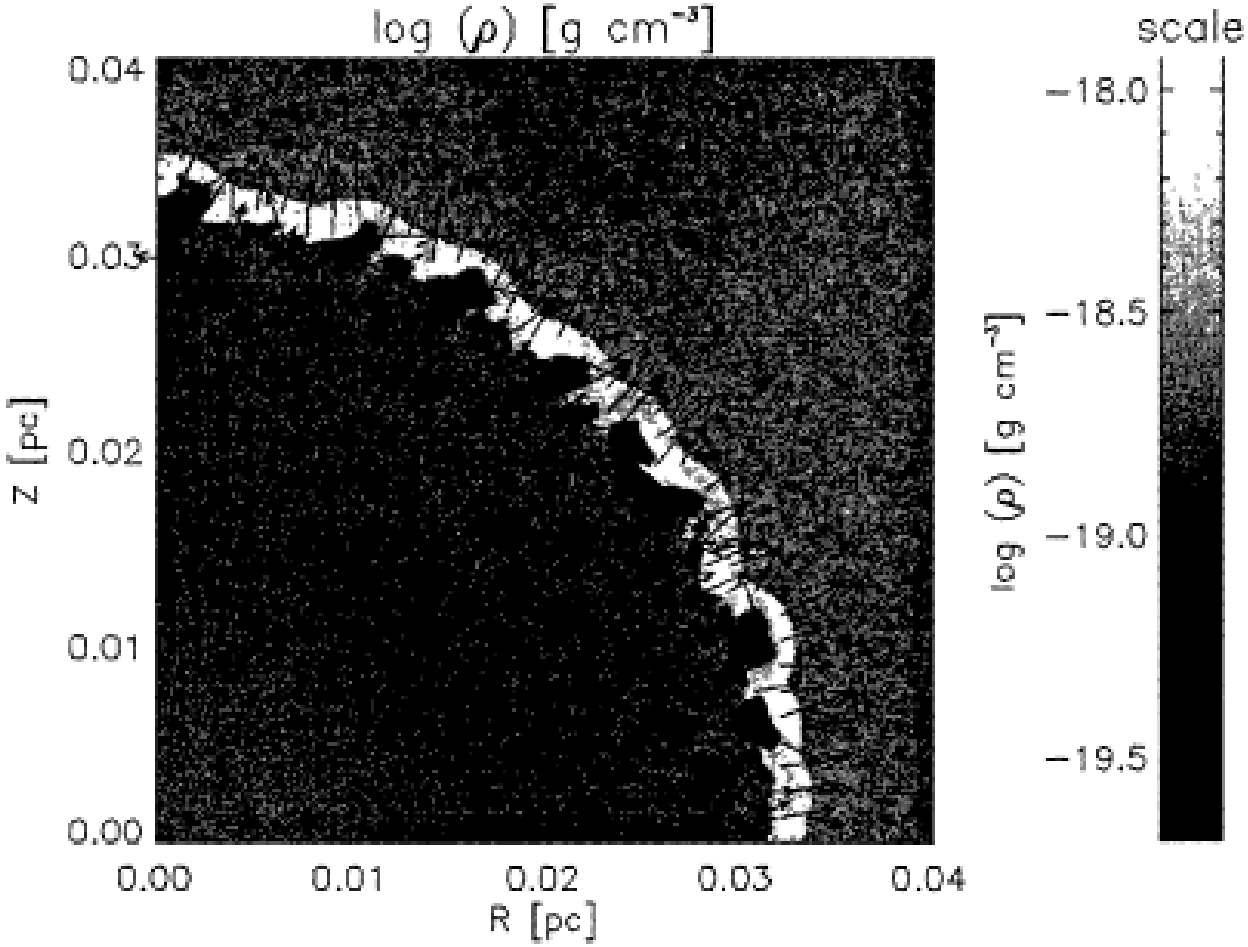

Franco, et al 1998

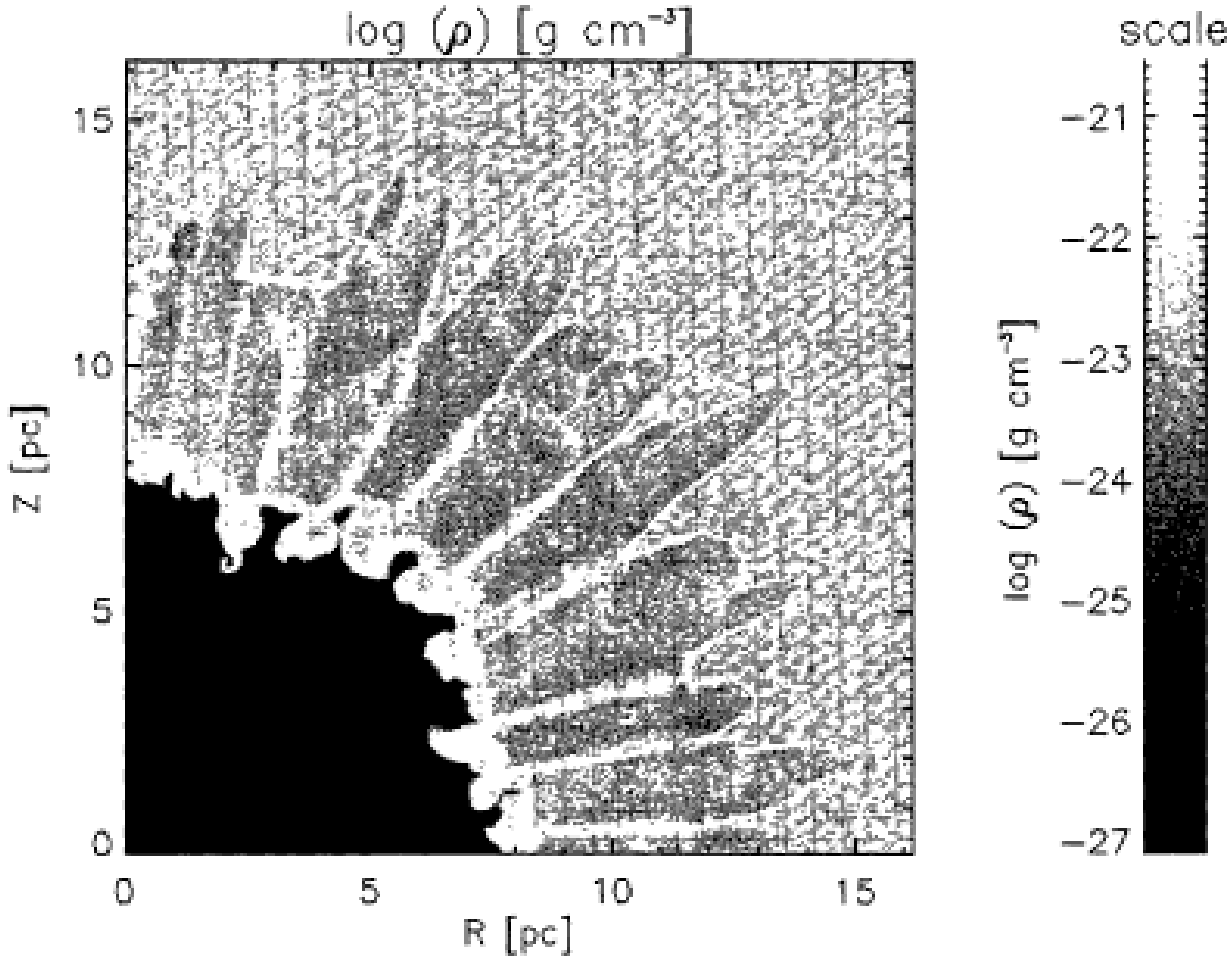
log (ρ) [g cm⁻³]
scale
15
10
5
0
Z [pc]
0
5
10
15
R [pc]
−21
−22
−23
−24
−25
−26
−27
log (ρ) [g cm⁻³]

In Conclusion

In the full 3D photoionization simulations we are preparing, we anticipate instabilities to grow in the ionized core shock (because it is descending a density gradient) as well as in the I-front itself

These instabilities are of interest to us because 2D simulations indicate that they can snowball primordial gas into dense clumps of several tens of solar masses

An important question is whether such clumps could cool--especially if seeded with metals from SN ejecta--and collapse into the next generation of stars

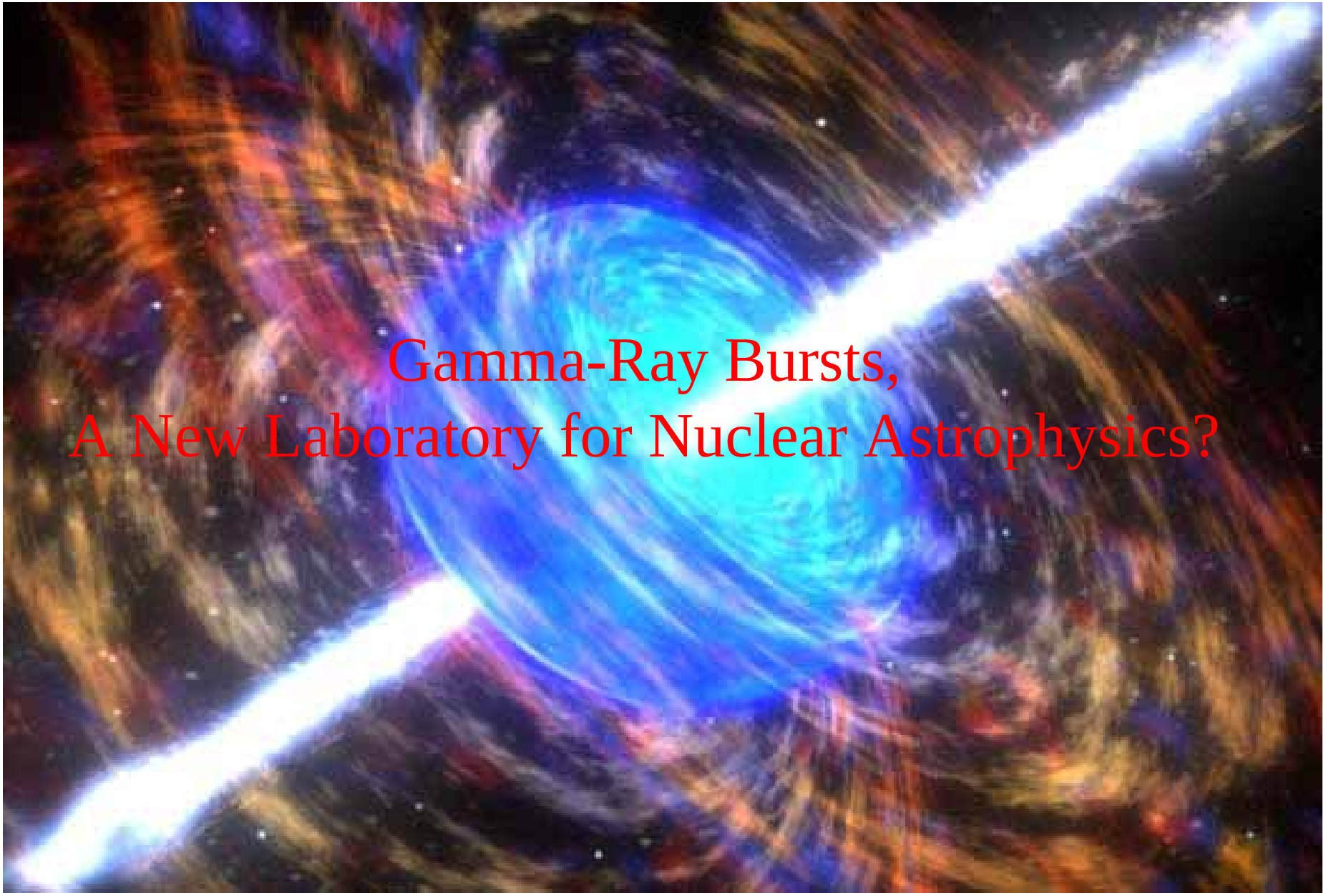

Gamma-Ray Bursts,
A New Laboratory for Nuclear Astrophysics?

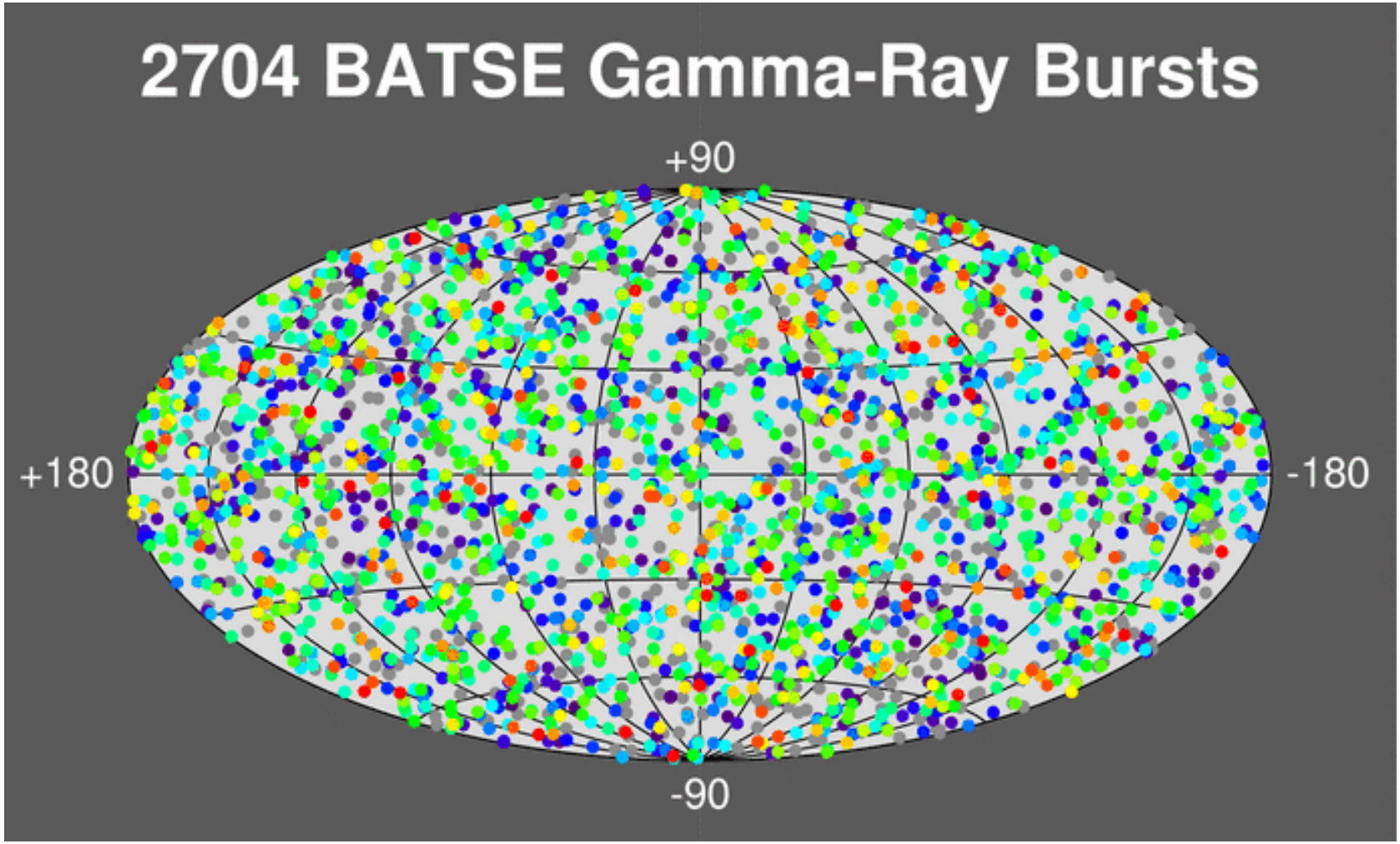
2704 BATSE Gamma-Ray Bursts
+90
+180
-180
-90

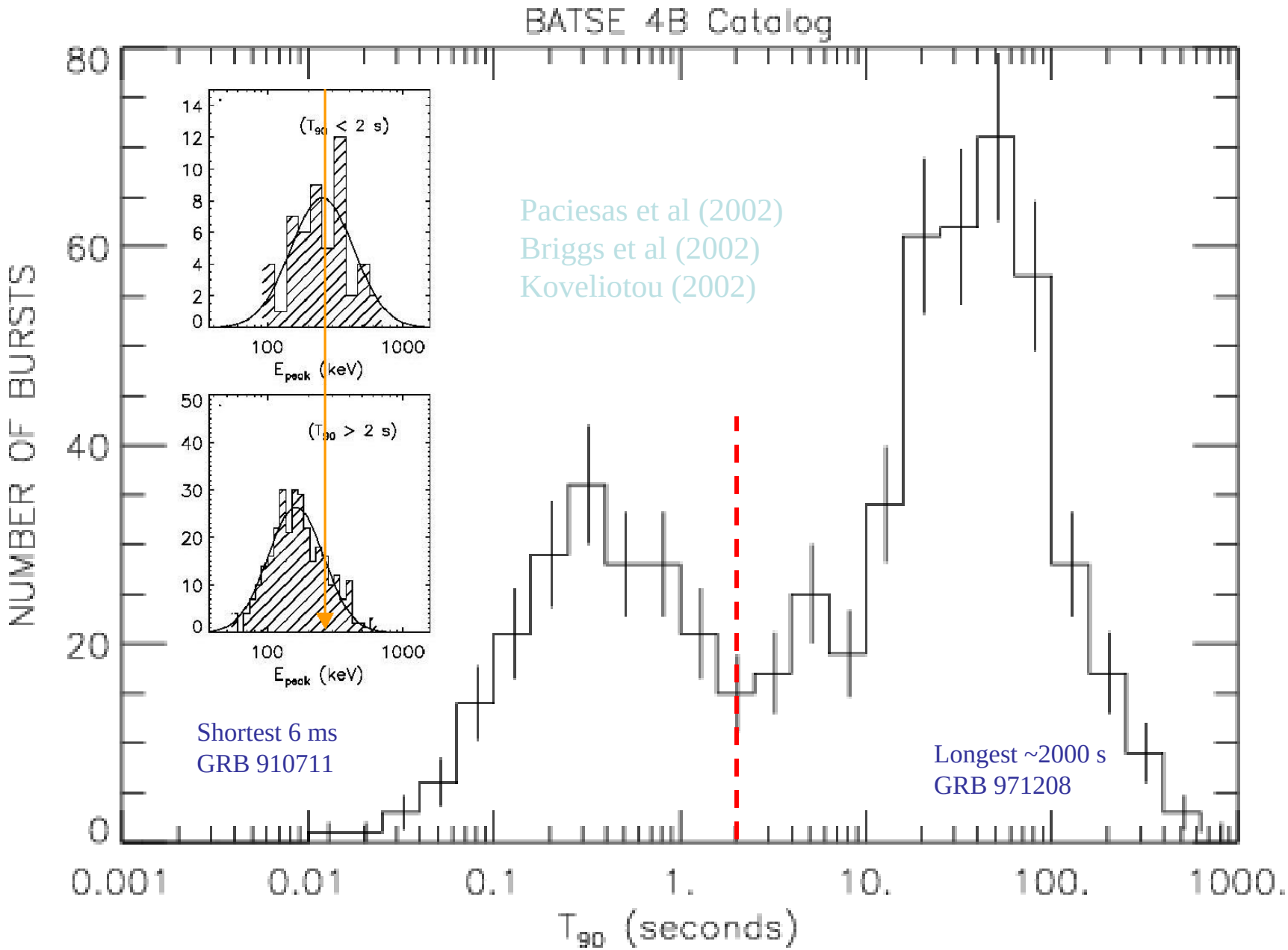
BATSE 4B Catalog
NUMBER OF BURSTS
T_{90} (seconds)
0.001
0.01
0.1
1.
10.
100.
1000.
0
20
40
60
80
(T_{90} < 2 s)
(T_{90} > 2 s)
E_{peak} (keV)
100
1000
Paciesas et al (2002)
Briggs et al (2002)
Koveliotou (2002)
Shortest 6 ms
GRB 910711
Longest ~2000 s
GRB 971208

Since 1997 we have known:

- "Long-soft" bursts are at cosmological distances and are associated with star forming regions in starbursting galaxies

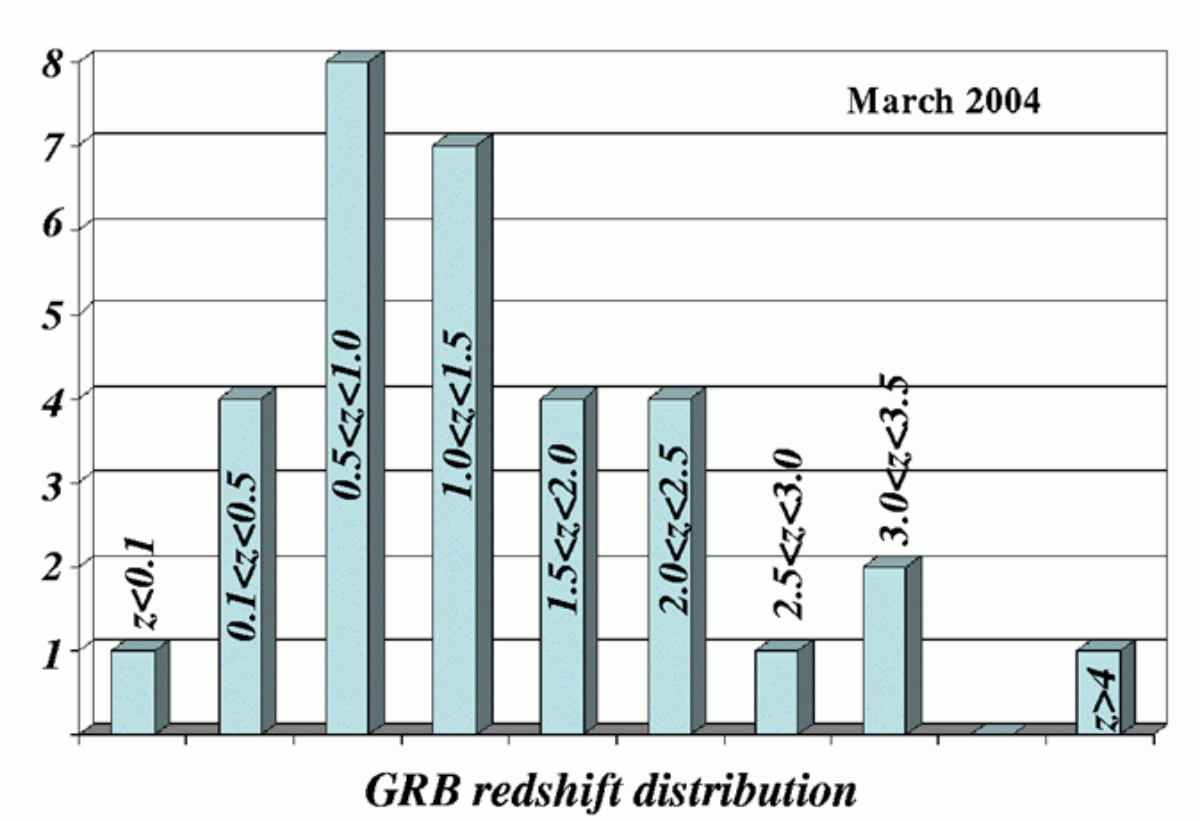

33 bursts

Zeh et al. (2004)

Djorgovski et al (2002)

Location of GRBs Within Their Host Galaxies

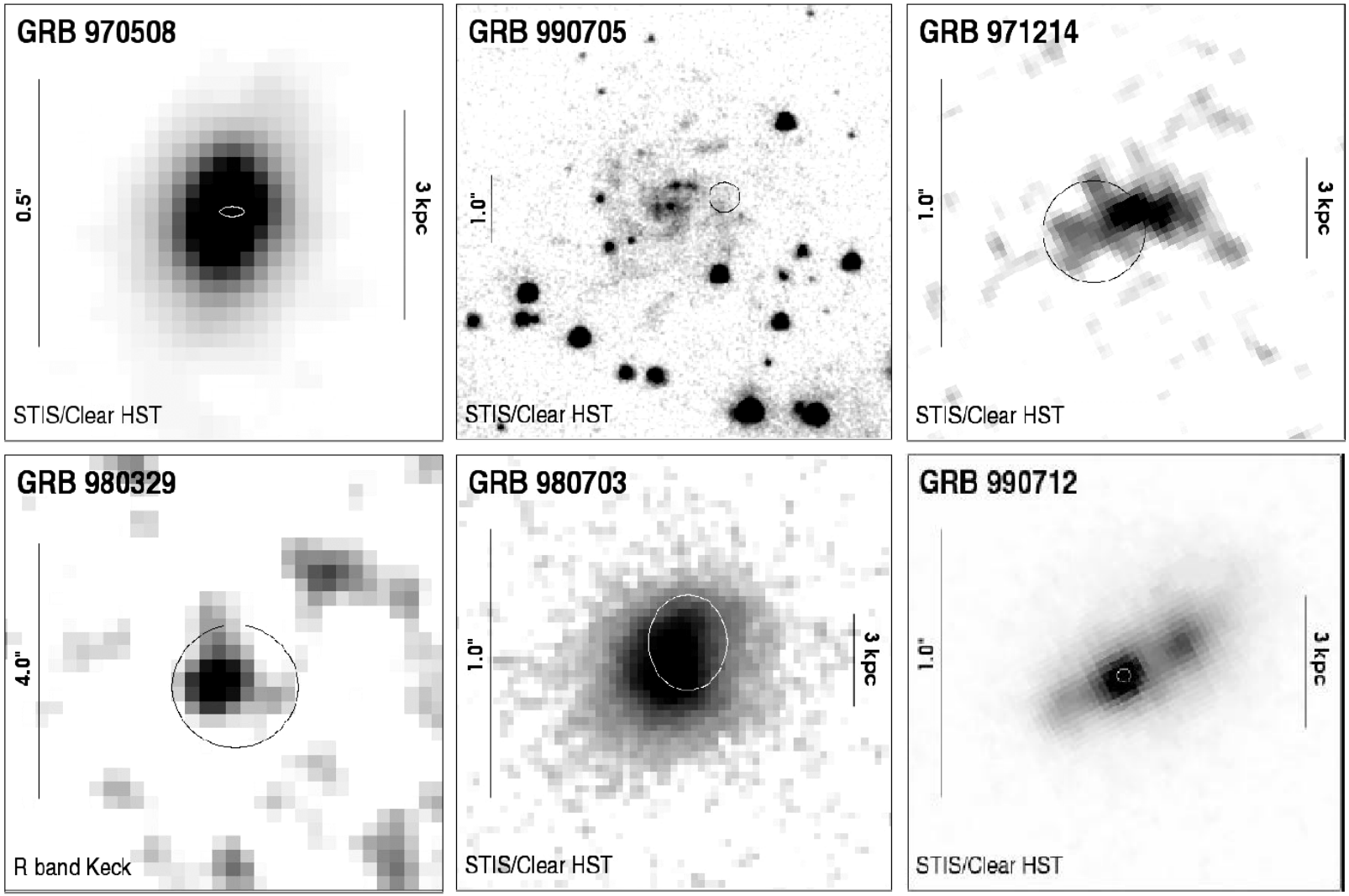

almost always galaxies experiencing an unusual rate of star formation

SN 1998bw/GRB 980425

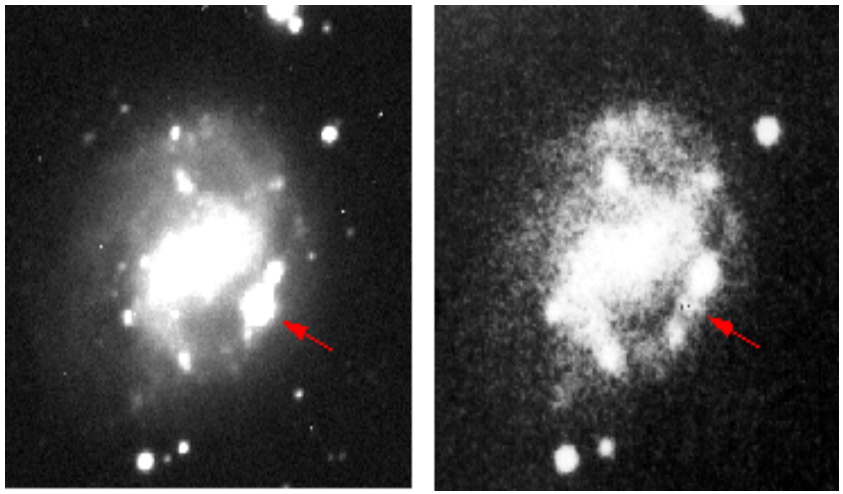

NTT image (May 1, 1998) of SN 1998bw in the barred spiral galaxy ESO 184-G82 [Galama et al, A&A S, 138, 465, (1999)]

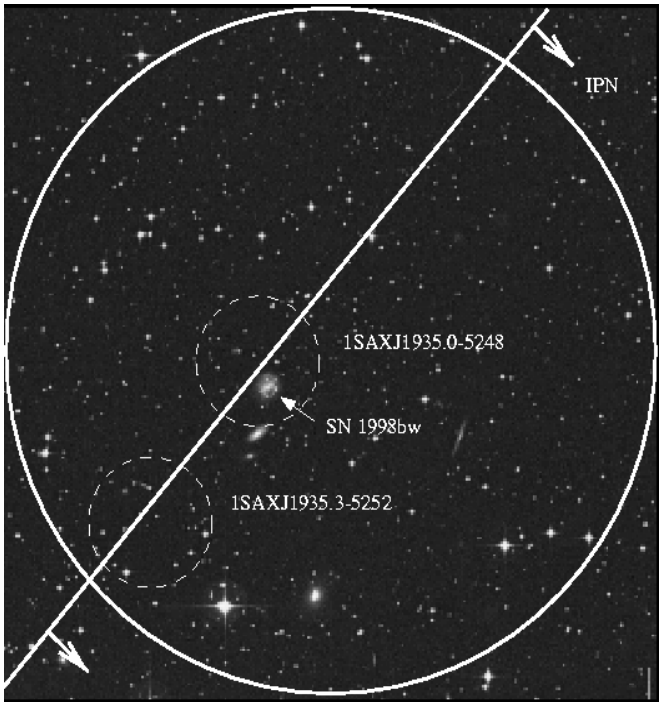

WFC error box (8') for GRB 980425 and two NFI x-ray sources. The IPN error arc is also shown.

Type Ic supernova, d = 40 Mpc
Modeled as the 3 x 10^{52} erg explosion of a massive CO star
(Iwamoto et al 1998; Woosley, Eastman, & Schmidt 1999)

GRB 8 x 10^{47} erg; 23 s

a very unusual supernova!

Kouveliotou, Woosley, et al. (2004)

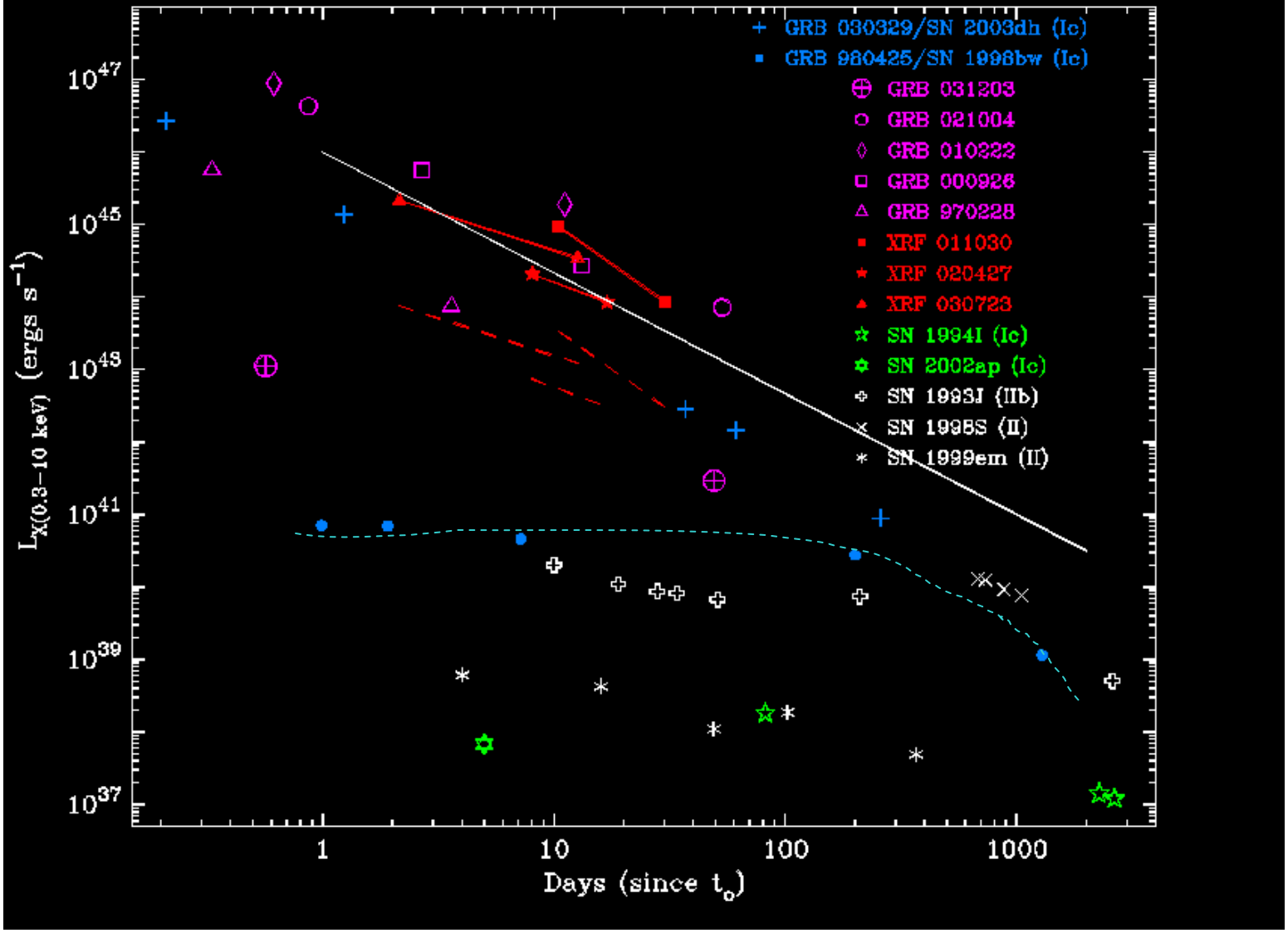

The "smoking gun"

GRB030329/
SN2003dh

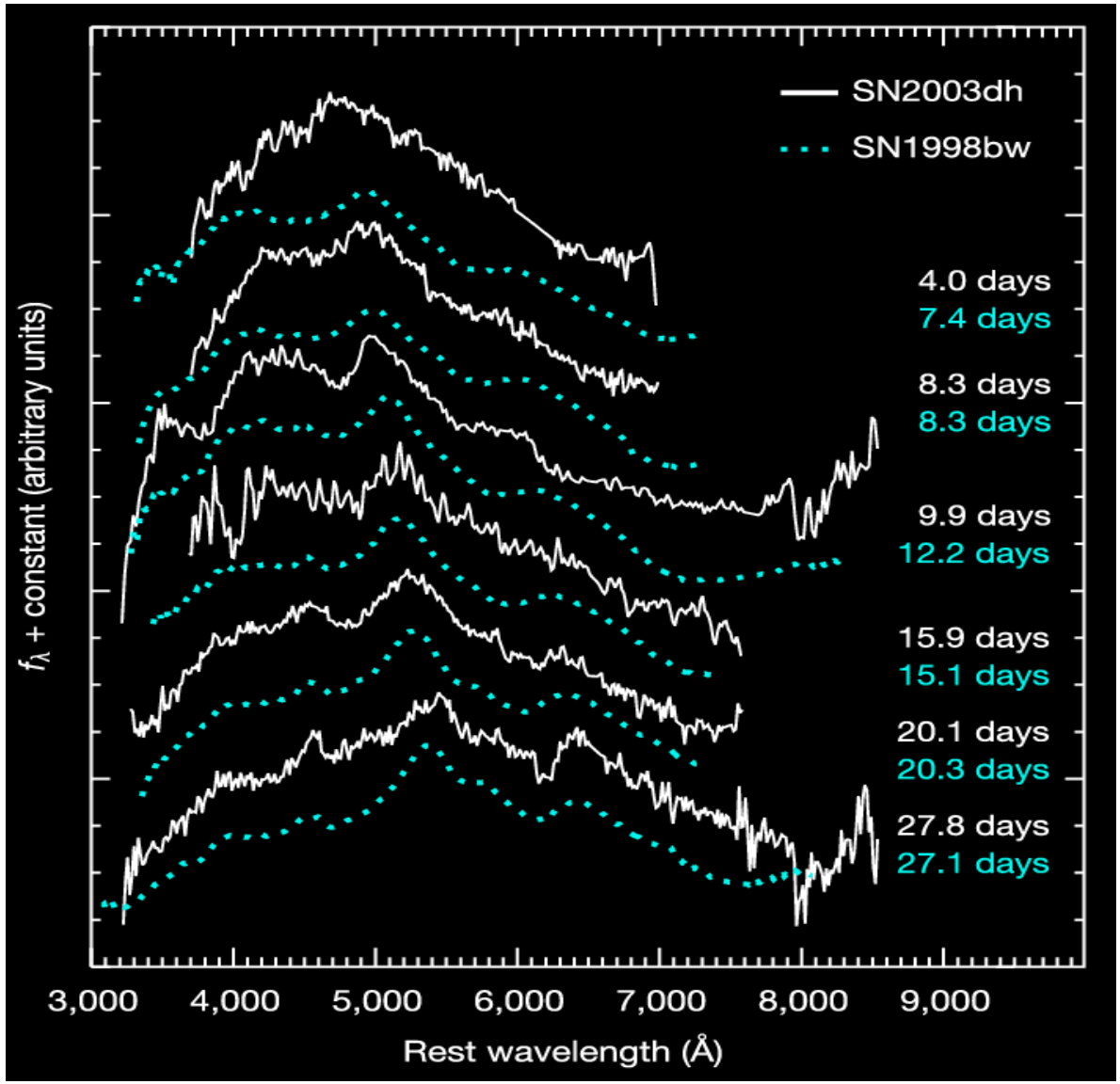

z = 0.1685

One of the brightest GRBs ever – HETE2

Stanek et al.,
Chornock et al.
Eracleous et al.,
Hjorth et al.,
Kawabata et al.

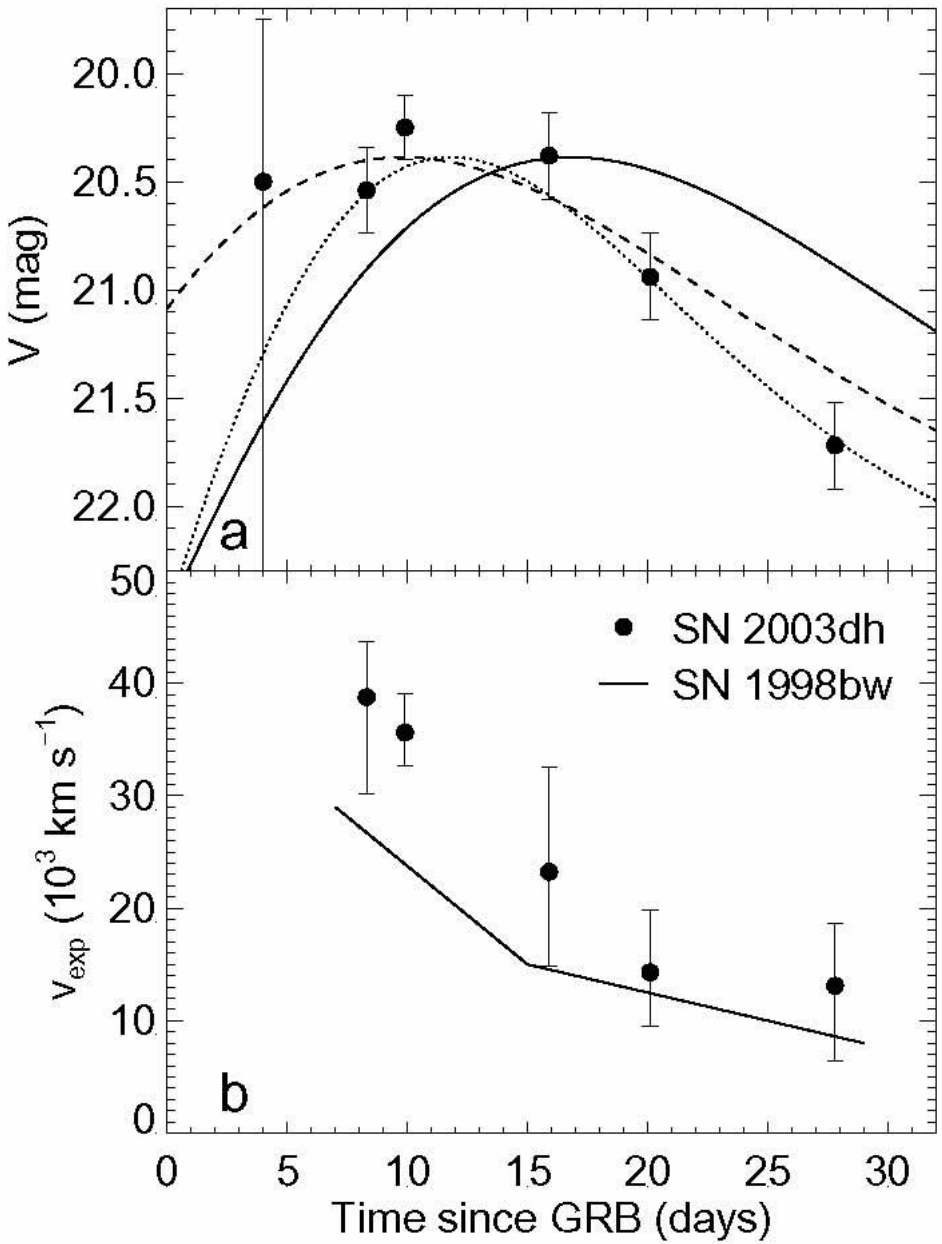

L_{peak} implies (again) ~0.5 solar masses of ^{56}Ni

Exceptionally ---
- bright
- fast
- high velocity
- radio bright

Supernova simultaneous with the GRB (+- 2 days).

To summarize – Three GRBs – 980425, 030329, and 031203 – have been determined to have concurrent (+- few days) supernovae - SN 1998bw SN 2003dh, and SN 2003lw - and the identification is solid (spectroscopy plus light curve)

These have also been the closest three GRBs studied

Looking for bumps

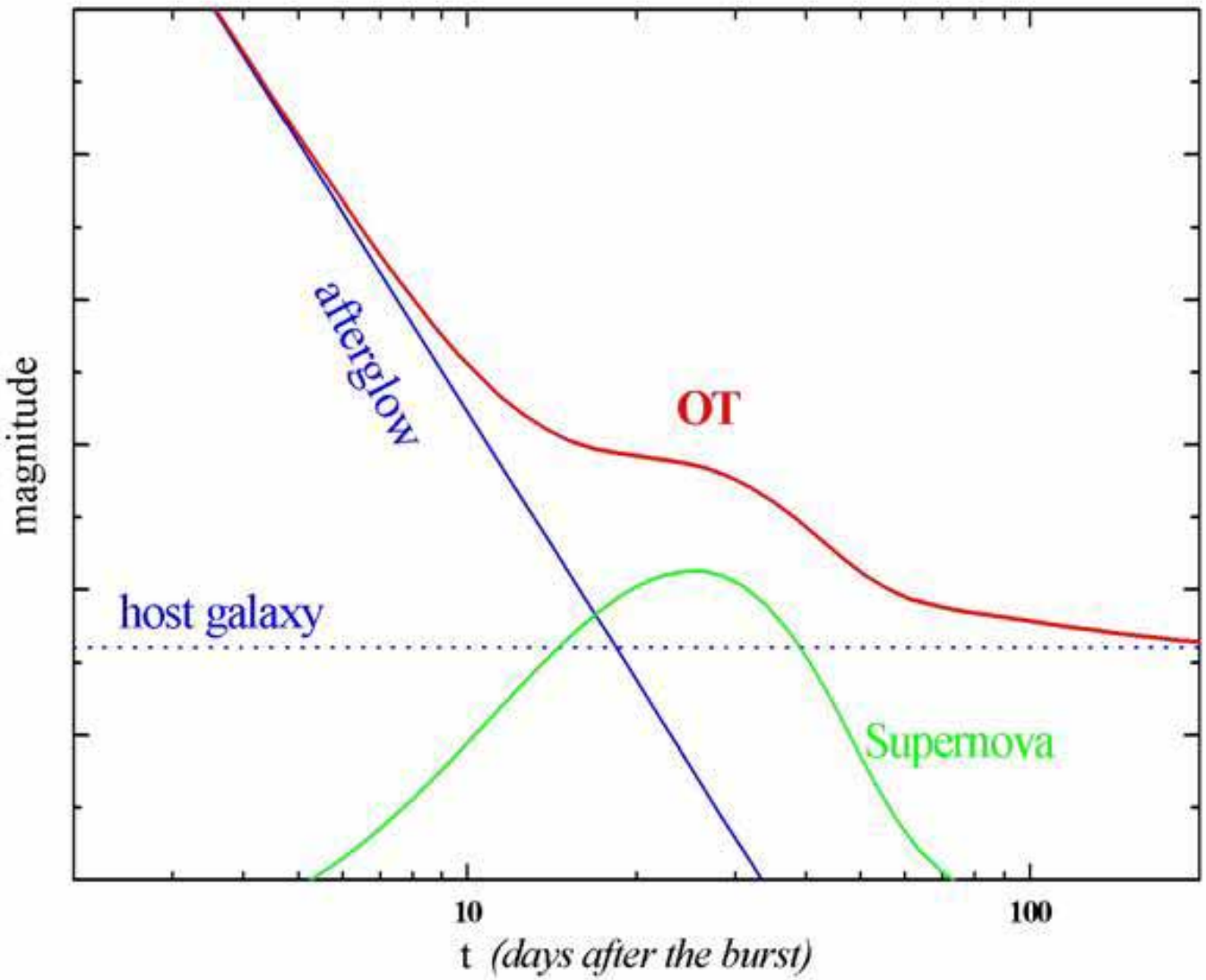

must correct for redshift

Bloom

Zeh, Klose, & Hartmann (2004)

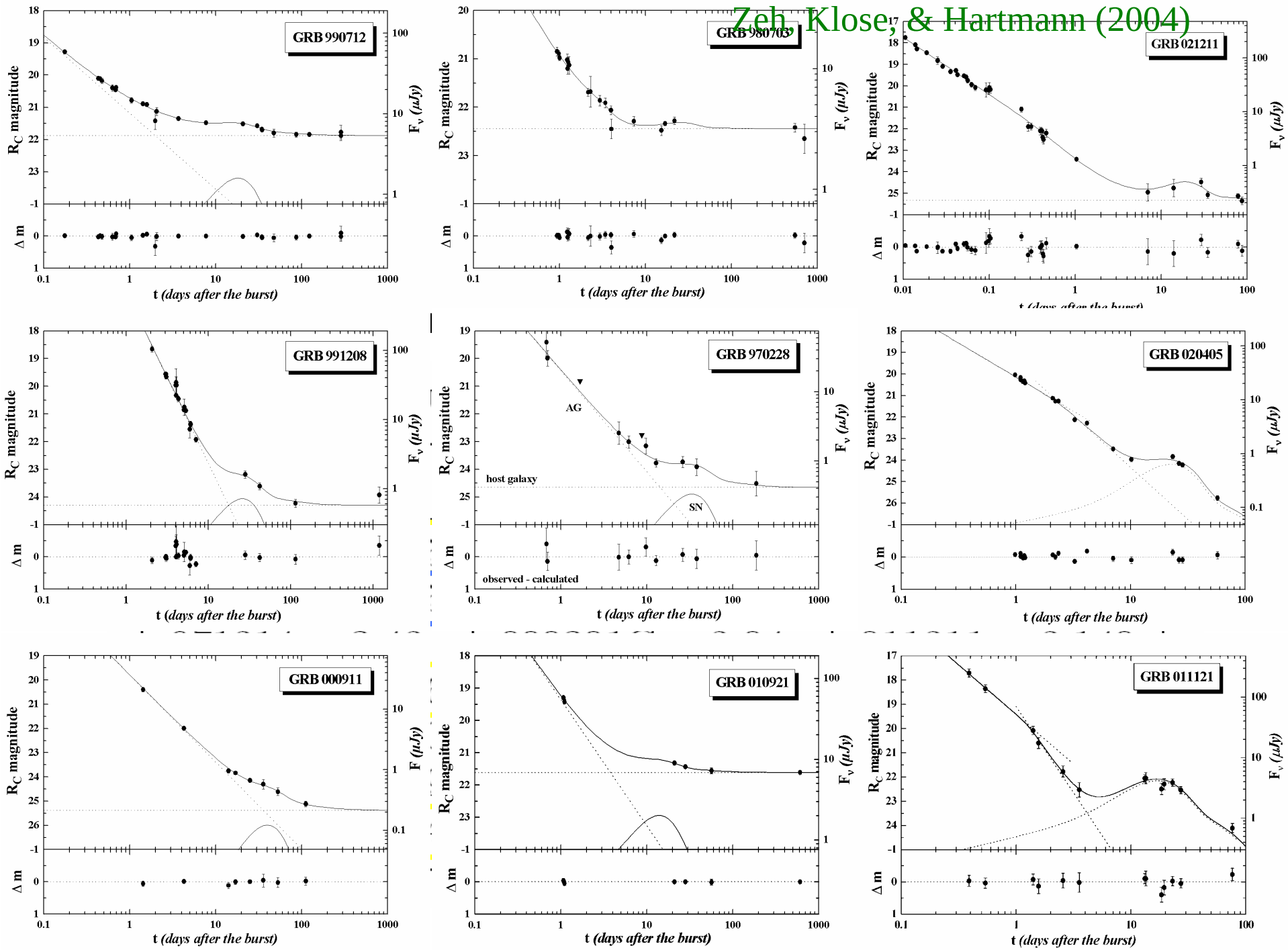

E_{SN}: *kinetic energy in the ejecta*

Modeled from light curves plus spectroscopy

1998bw (980425):

$E_{SN} = 2 \times 10^{51}$ erg - asymmetric (Höflich, Wheeler, & Wang 99)
$E_{SN} = (2 – 5) \times 10^{52}$ erg - symmetric (Iwamoto et al. 98)
$E_{SN} = 2 \times 10^{52}$ erg - symmetric (Woosley, Eastman, & Schmidt 99)
$E_{rel}(\Gamma\beta > 1) < 3 \times 10^{50}$ erg (Li & Chevalier 99)

2003dh (030329):

$E_{SN} = 3 \times 10^{52}$ erg - symmetric (Mazzali et al. 03)
$E_{SN} = 2.6 \times 10^{52}$ erg - asymmetric (Woosley & Heger 04)

2003lw (031203):

E_{SN} = comparable to 1998bw (Malesani et al. 04; Gal-Yam et al. 04)

E_{rel}:

Clustered around ~5 foe

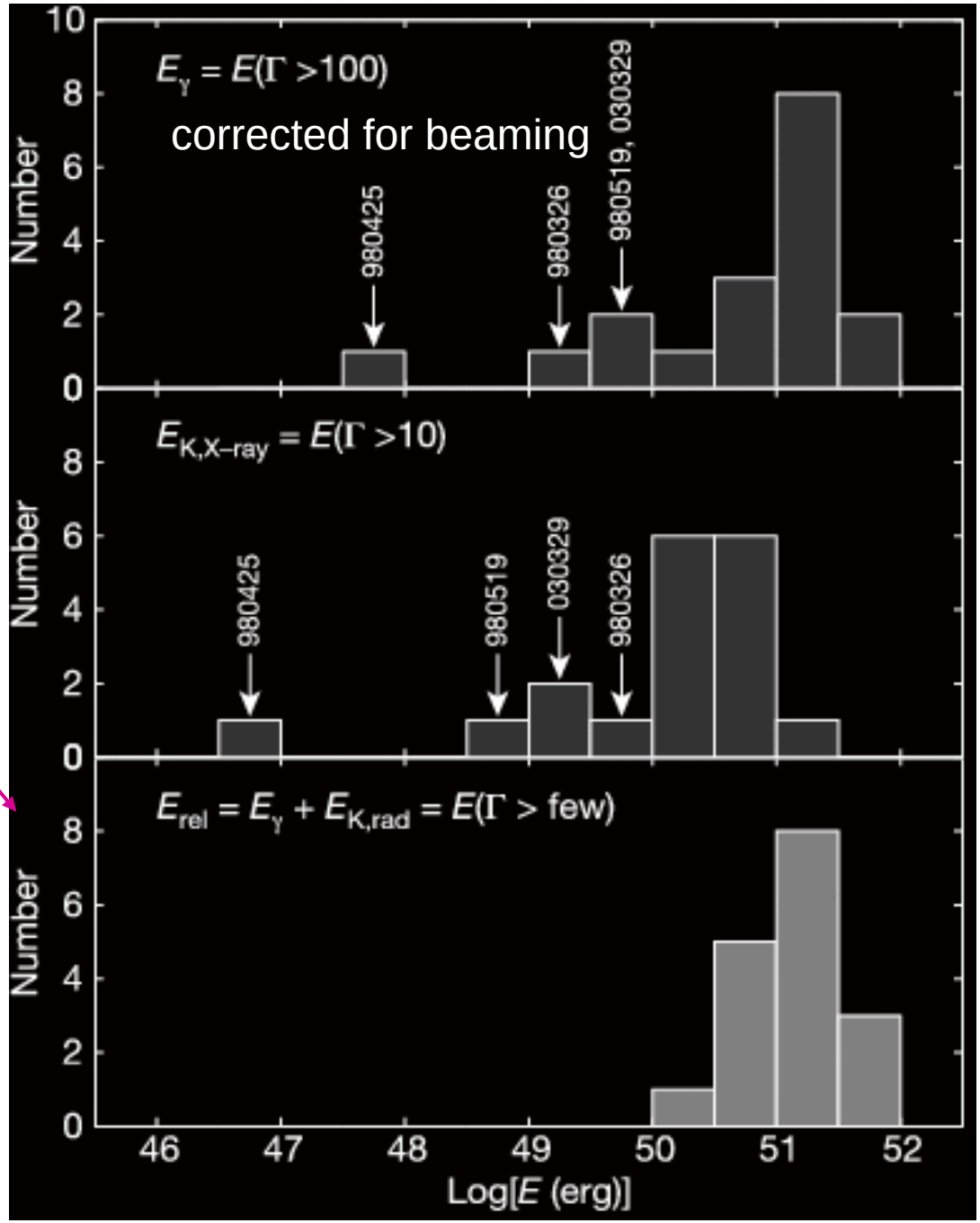

Berger et al. 03

Summary

All Long-Soft GRBs are Probably Supernovae

* Several strong indications (980326, 970228, 011121, ….) and three **DEFINITIVE** connections (980425, 030329, and 031203)

* GRB associated supernovae have higher velocities and energies than typical supernovae. The mass of ^{56}Ni in at least some of them is ~ 0.5 solar masses and the energy is ~10^{52} erg

* The ratio of GRBs to supernovae is still a small number of order a few percent. (e.g., Soderberg, Frail, and Wieringa (2004)

Josh Bloom

The Models

"What Is the Fate of (the most) Massive Stars?"

When Massive Stars Die, How Do They Explode?

Neutron Star + Neutrinos	Neutron Star + Rotation	Black Hole + Rotation
Colgate and White (1966) Arnett Wilson Bethe Janka Herant Burrows Fryer Mezzacappa etc.	Hoyle (1946) Fowler and Hoyle (1964) LeBlanc and Wilson (1970) Ostriker and Gunn (1971) Bisnovatyi-Kogan (1971) Meier Wheeler Usov Thompson etc	Bodenheimer and Woosley (1983) Woosley (1993) MacFadyen and Woosley (1999) Narayan (2004)
10	20	35 $M_\odot$

All of the above?

Today, after times when over 150 GRB models could be "defended", only two are left standing (for long-soft bursts):

- The collapsar model
- The millisecond magnetar model

Both rely on the existence of situations where some fraction of massive stars die with an unsually large amount of rotation.

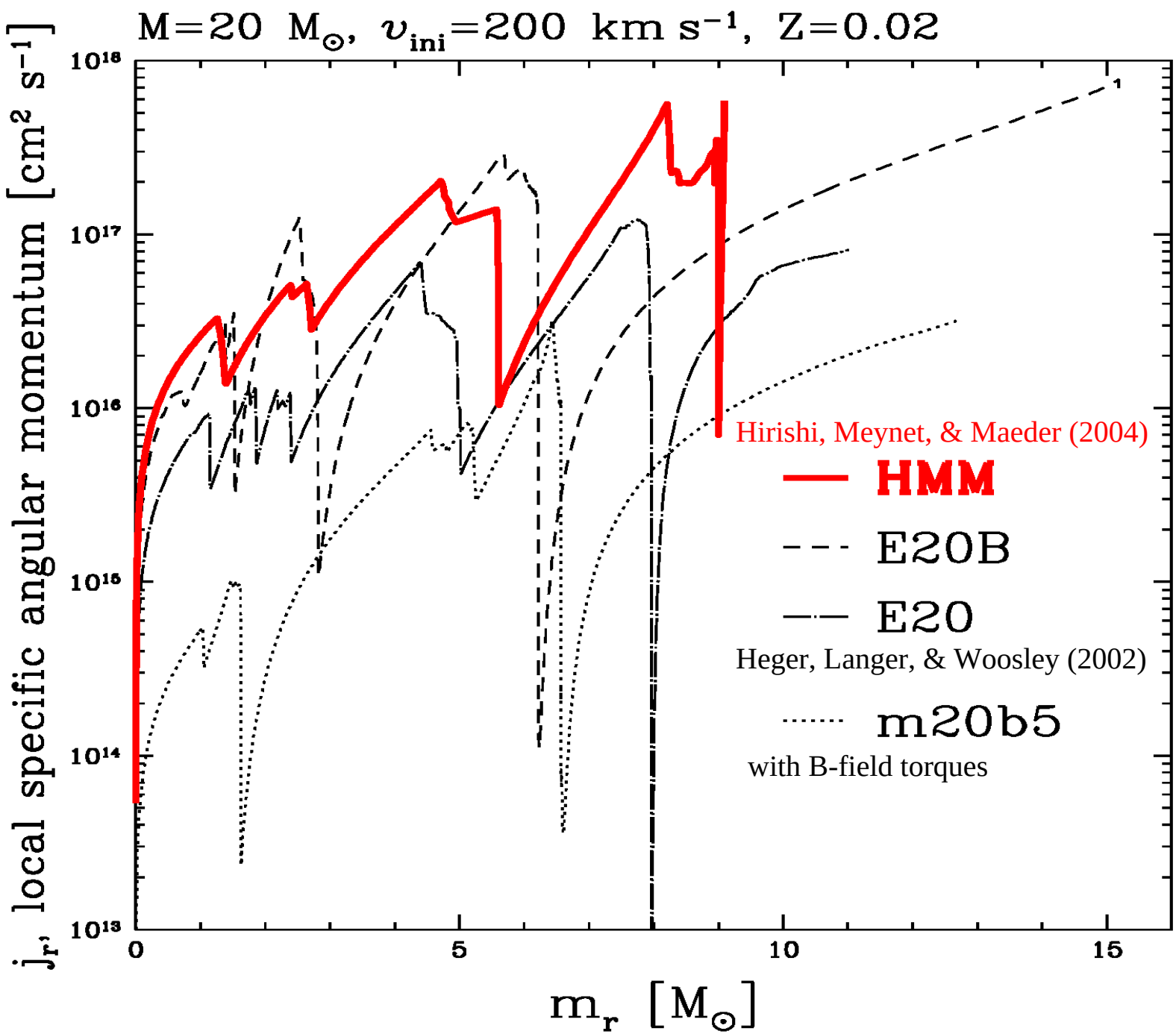
M=20 M⊙, v_{ini}=200 km s⁻¹, Z=0.02
j_r, local specific angular momentum [cm² s⁻¹]
m_r [M⊙]
Hirishi, Meynet, & Maeder (2004)
HMM
E20B
E20
Heger, Langer, & Woosley (2002)
m20b5
with B-field torques

Collapsar Basics

- Wolf-Rayet Star – no hydrogen envelope – about 1 solar radius.
- Collapse time scale tens of seconds
- Rapid rotation – j ~ 10^{16} erg s
- Black hole ~ 3 solar masses accretes several solar masses

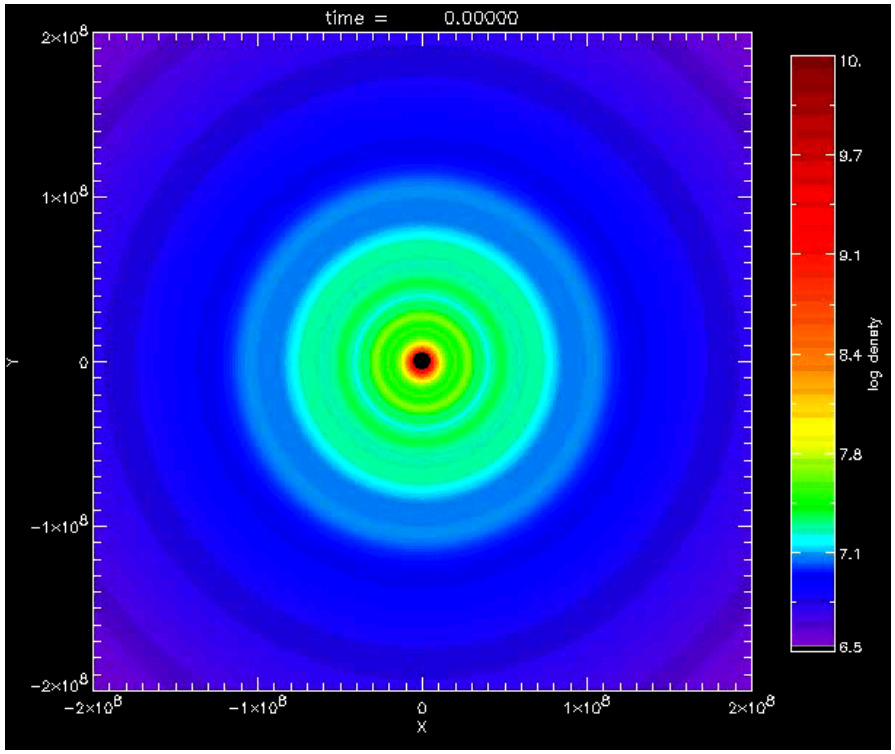

The star collapses and forms a disk (log j > 16.5)

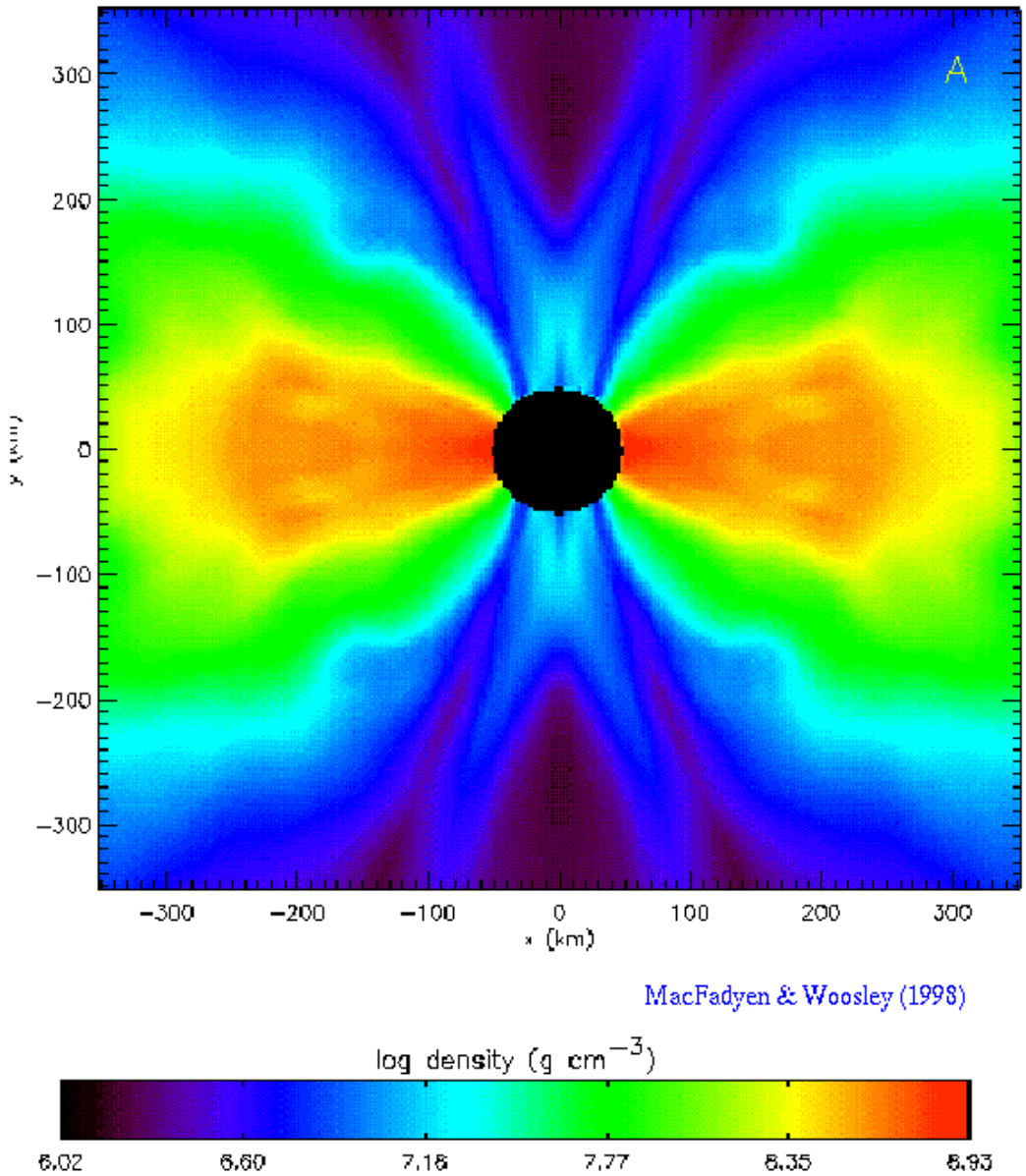

MacFadyen & Woosley (1998)

In the vicinity of the rotational axis of the black hole, by a variety of possible processes, energy is deposited.

7.6 s after core collapse; high viscosity case.

Note offset from t = 0

The alternative:

<u>The ms Magnetar Model:</u>

Wheeler, Yi, Hoeflich, and Wang (2001)
Usov (1992, 1994, 1999)
Thompson (2003, 2004)

Assuming the emission of high amplitude ultra-relativistic MHD waves, one has a radiated power

$$P \sim 6 \times 10^{51}\ (1\ \mathrm{ms}/P)^4\ (B/10^{16}\ \mathrm{gauss})^2\ \mathrm{erg\ s^{-1}}$$

and a total rotational kinetic energy

$$E_{rot} \sim 10^{52}\ (1\ \mathrm{ms}/P)^2\ (10\ \mathrm{km}/R)^2\ \mathrm{erg}$$

Note that this begins immediately after collapse.
(If it did not, a black hole would form)

Magnetar Model

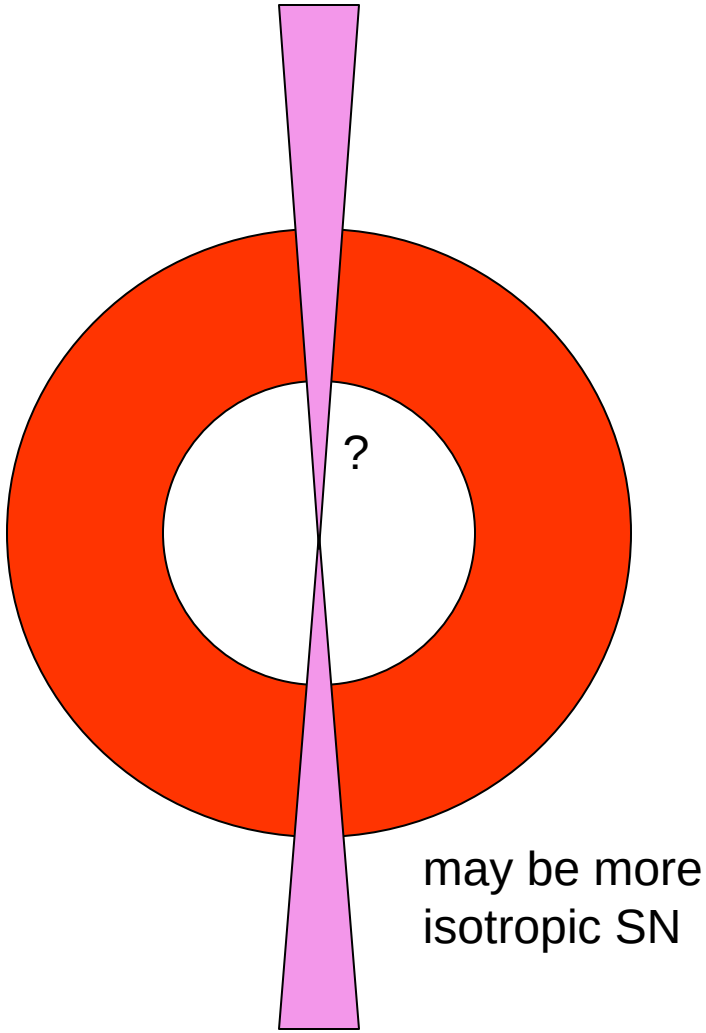

Bang - Whoosh

Collapsar Model

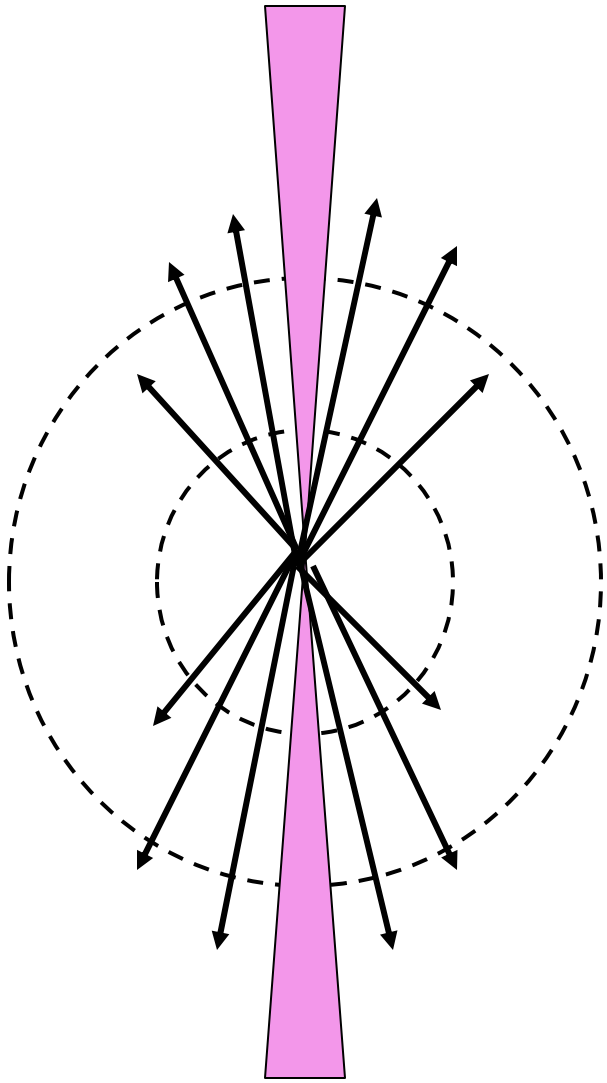

Whoosh - Spray

Nucleosynthesis in Gamma-Ray Bursts

- ***Effect of high energy in traditional models***
- ***Nucleosynthesis in black hole accretion disks***

Heger & Woosley (2004)
averaged over Salpeter IMF

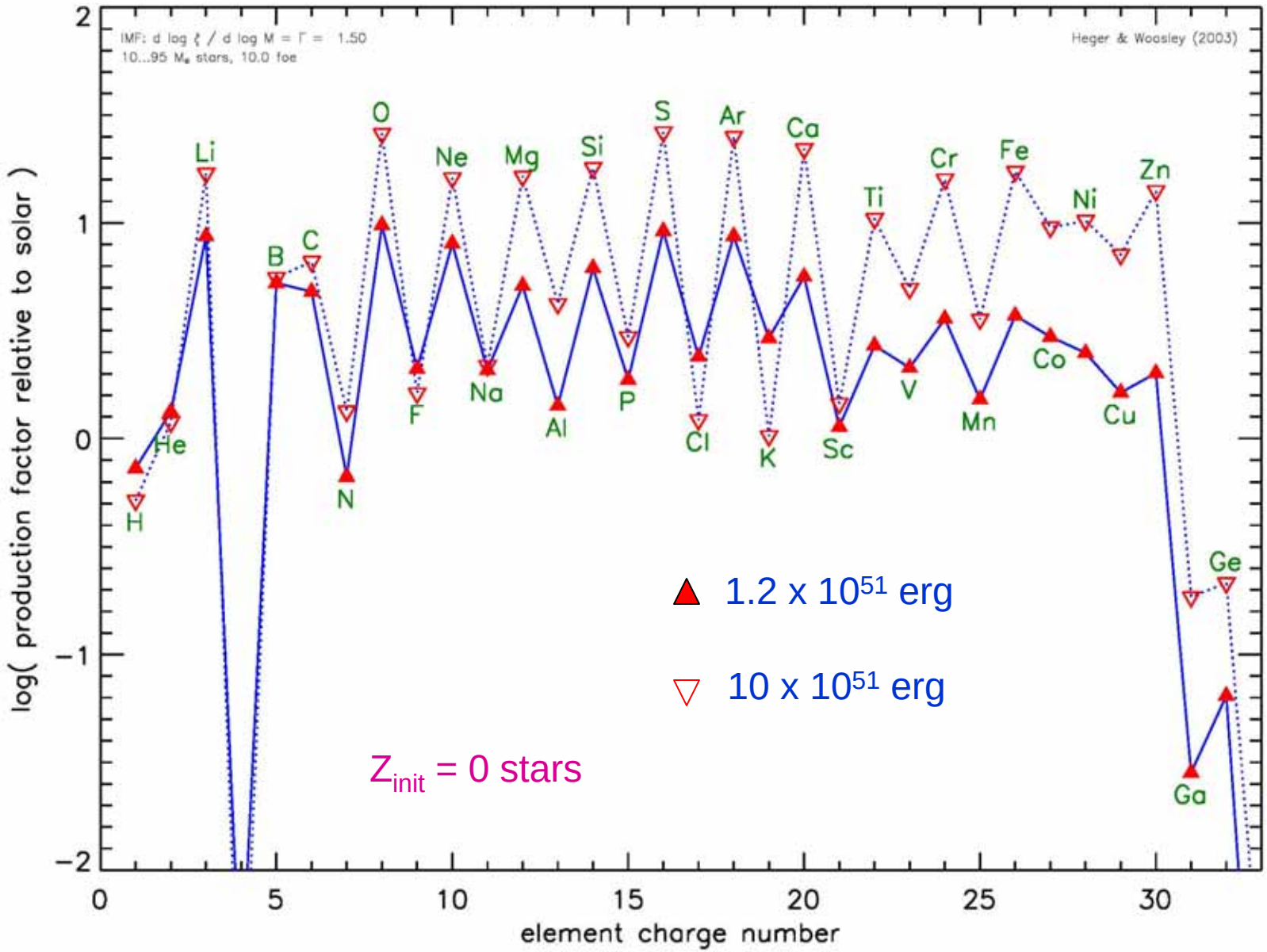

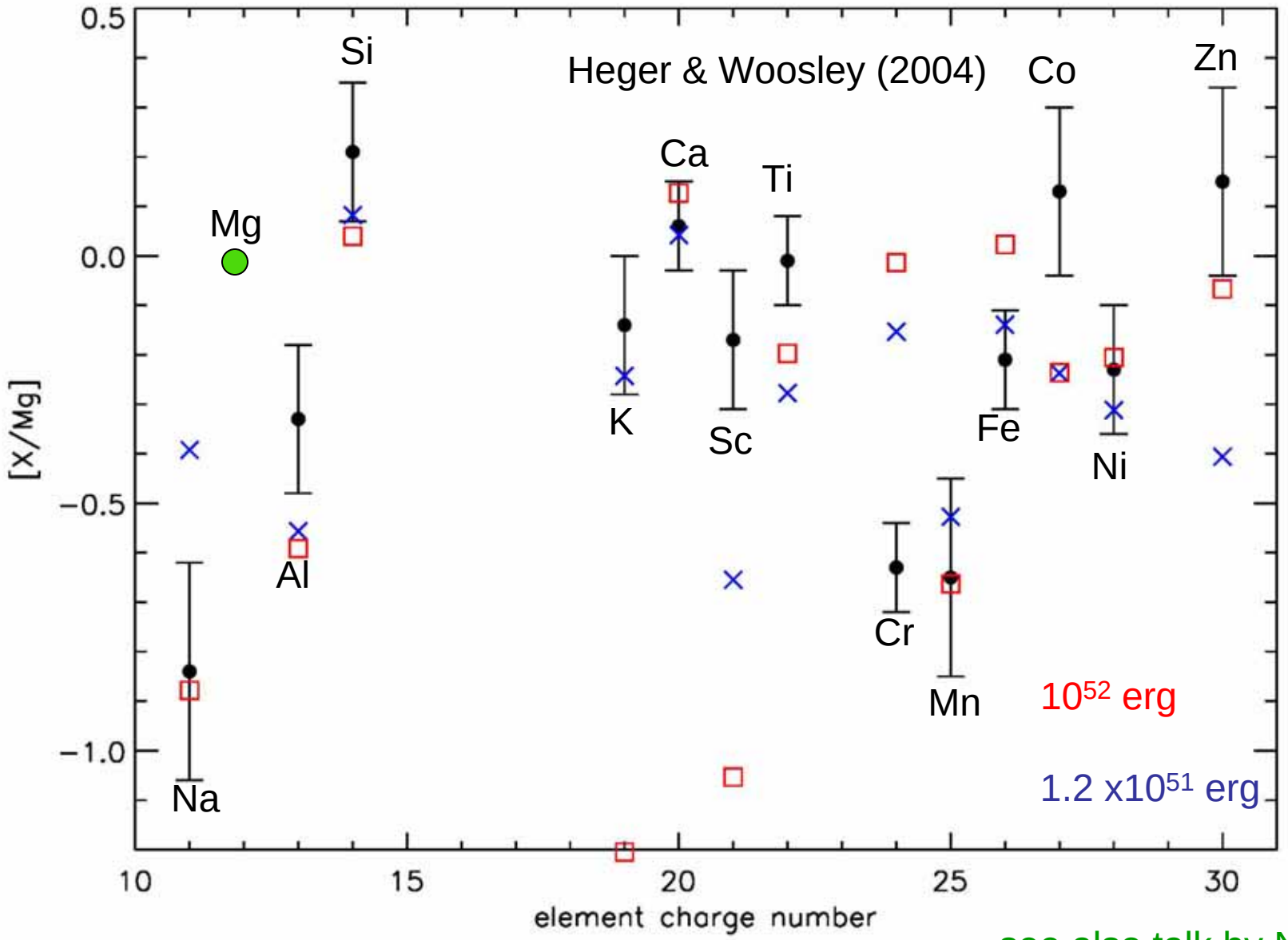

see also talk by Nomoto

Data from Cayrel et al, A&A, 416, 1117, (2004)

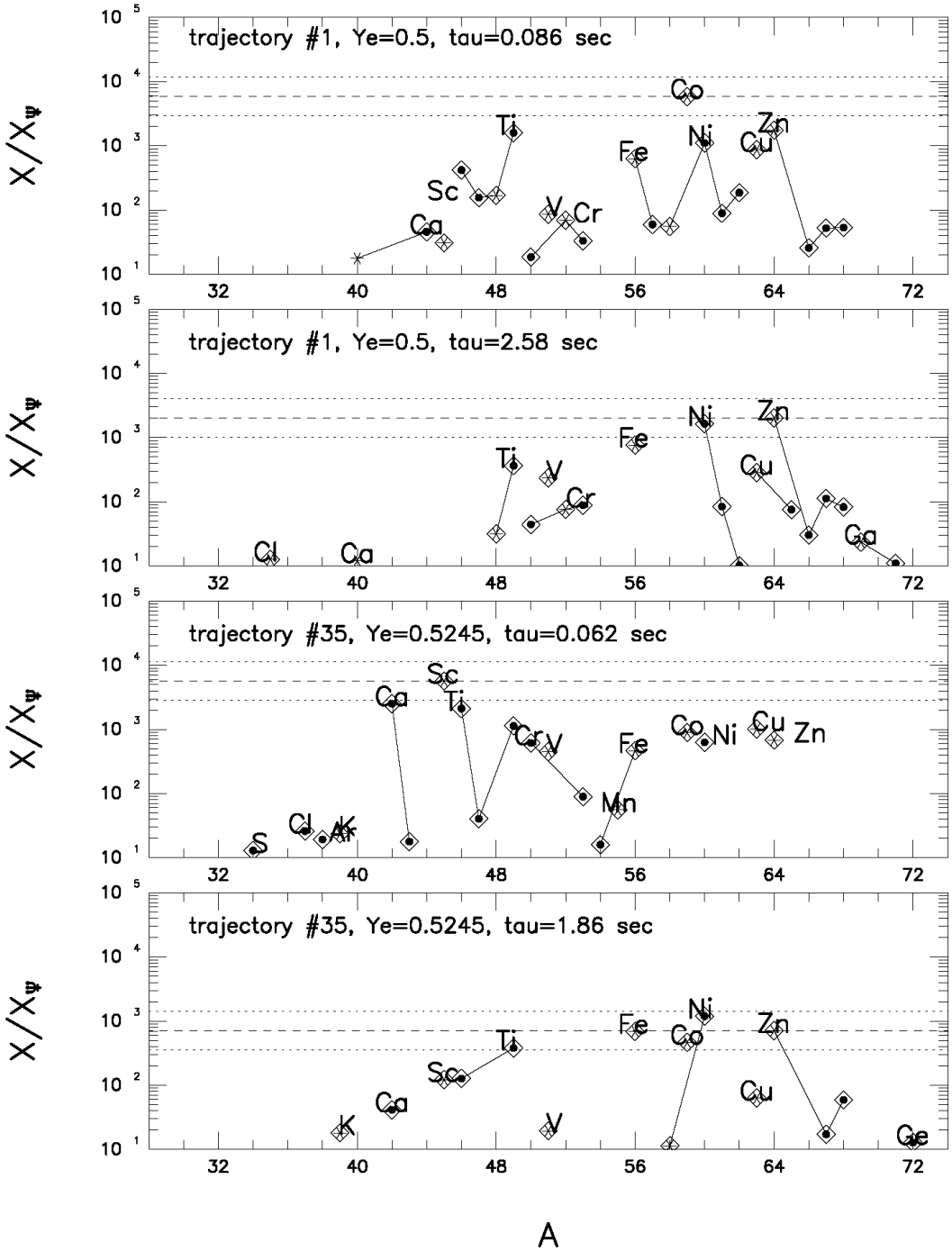

But careful…

Pruet, Woosley, & Janka (2004) show that appreciable primary Sc, Co. and Zn can be made in the proton-rich inner ejecta of ordinary supernovae

This could in principle account for the entire abundance of these elements

Magnetar Model

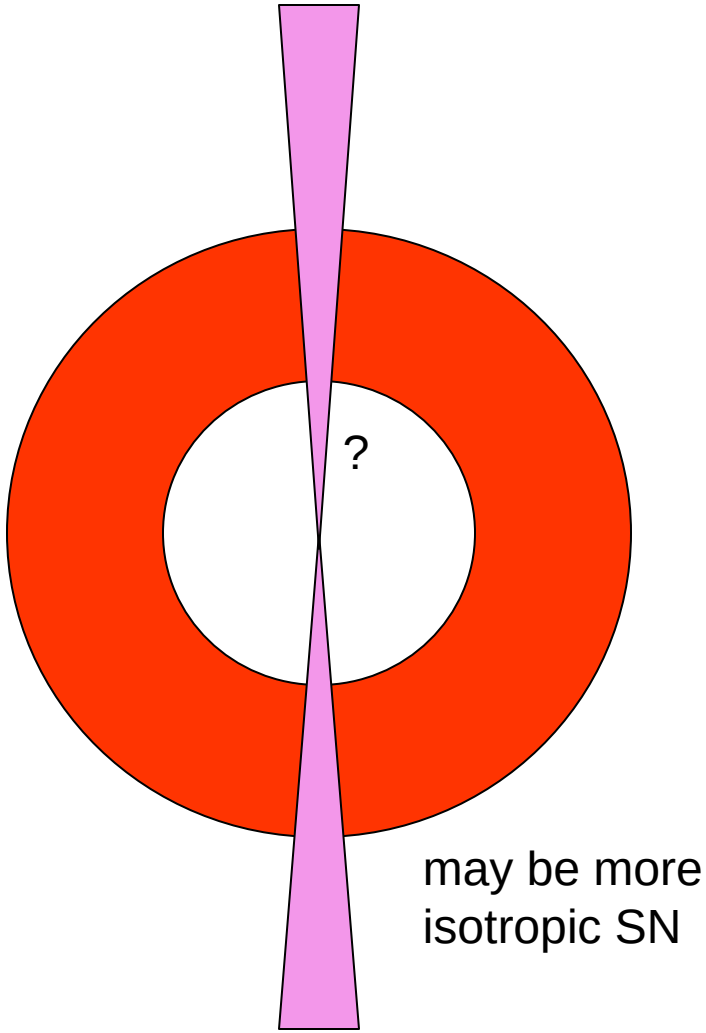

Bang - Whoosh

Collapsar Model

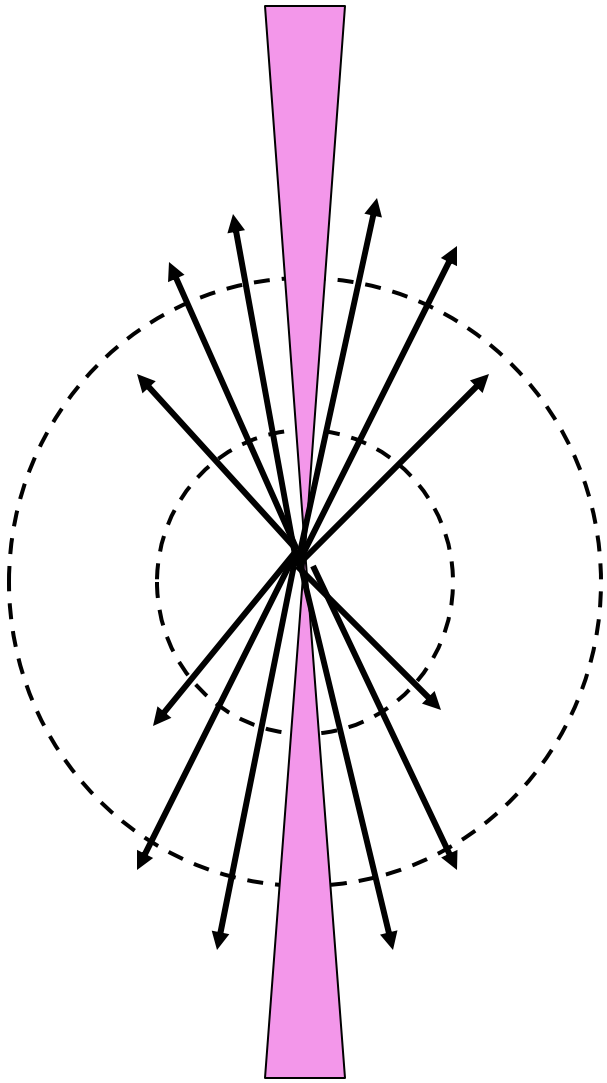

Whoosh - Spray

The disk wind: MacFadyen & Woosley (2001)

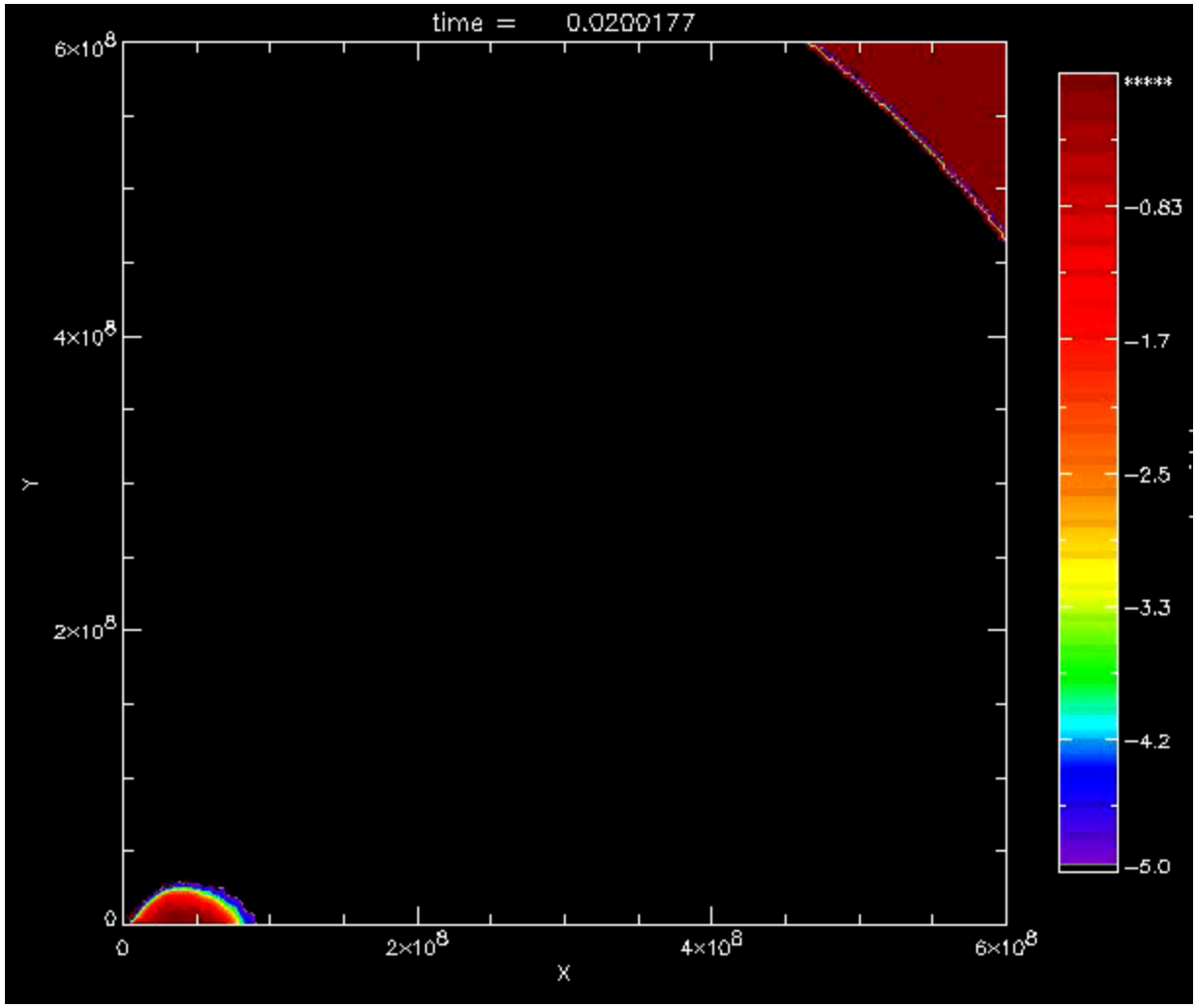

Neglecting electron capture in the disk

Collapsar

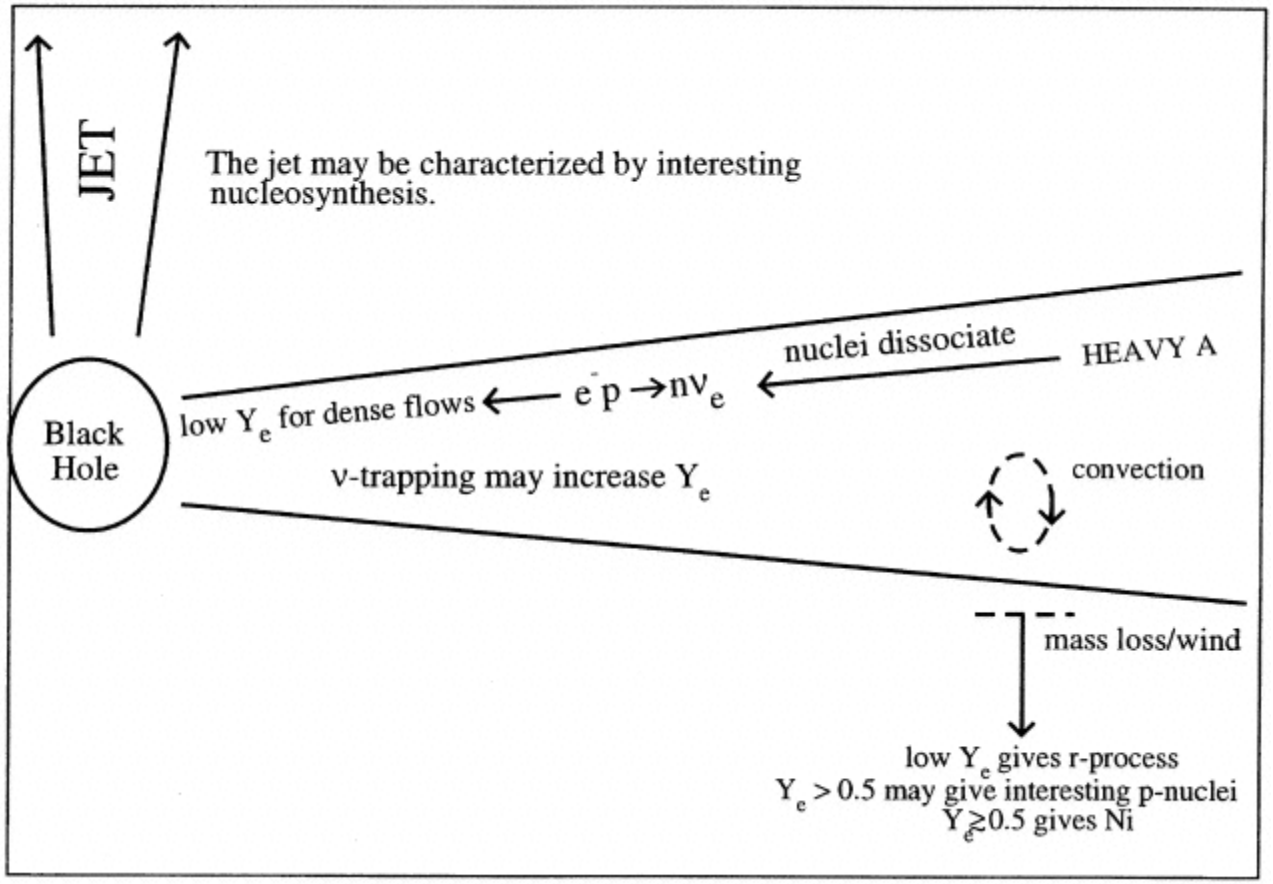

- Jason Pruet

Electron capture in the Disk

Pruet, Woosley, & Hoffman (2003)
Popham, Woosley, & Fryer (1999)

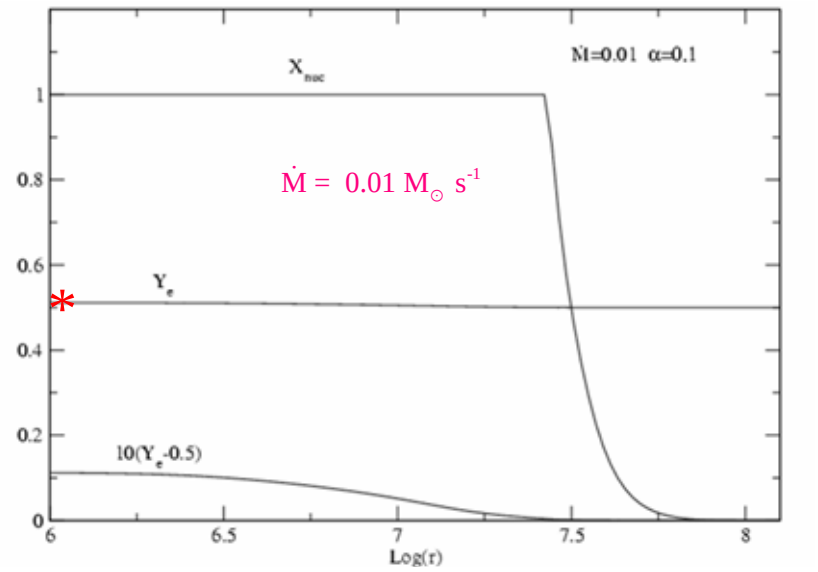

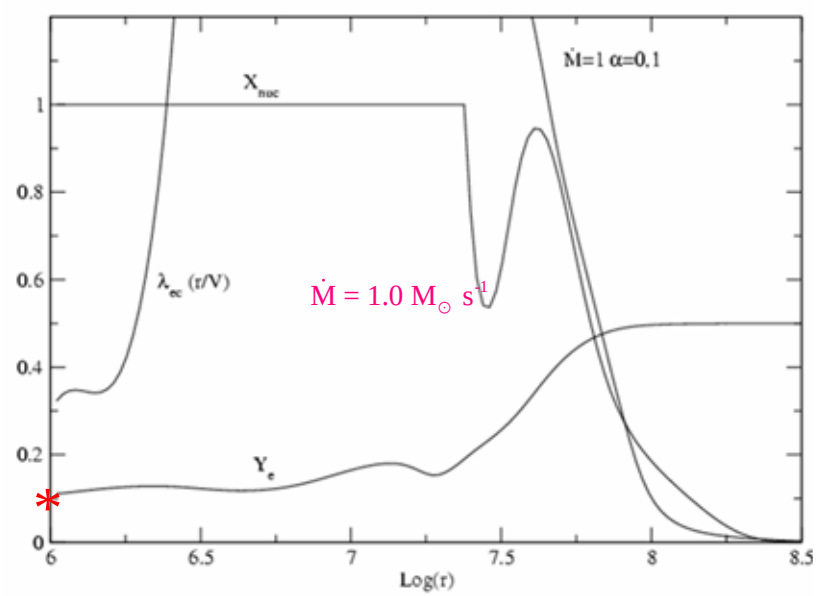

Electron Mole Number Near the Event Horizon

Model	$\dot{M}$[a]	α[b]	Y_e
A	0.01	0.1	0.510
B	0.1	0.1	0.435
C	0.1	0.03	0.119
D	0.1	0.01	0.045
E	1.0	0.1	0.115
F[c]	0.03	0.1	0.527
G[d]	0.1	0.1	0.077

$Y_e \approx 0.5 \Rightarrow {}^{56}\mathrm{Ni}$

[a]Accretion rate in $M_\odot$ sec^{-1}

[b]Disk viscosity

[c]Disk properties inferred from the scaling relations in ? for this model.

[d]Kerr parameter $a = 0.95$ for this model.

Pruet, Thompson, & Hoffman (2004)

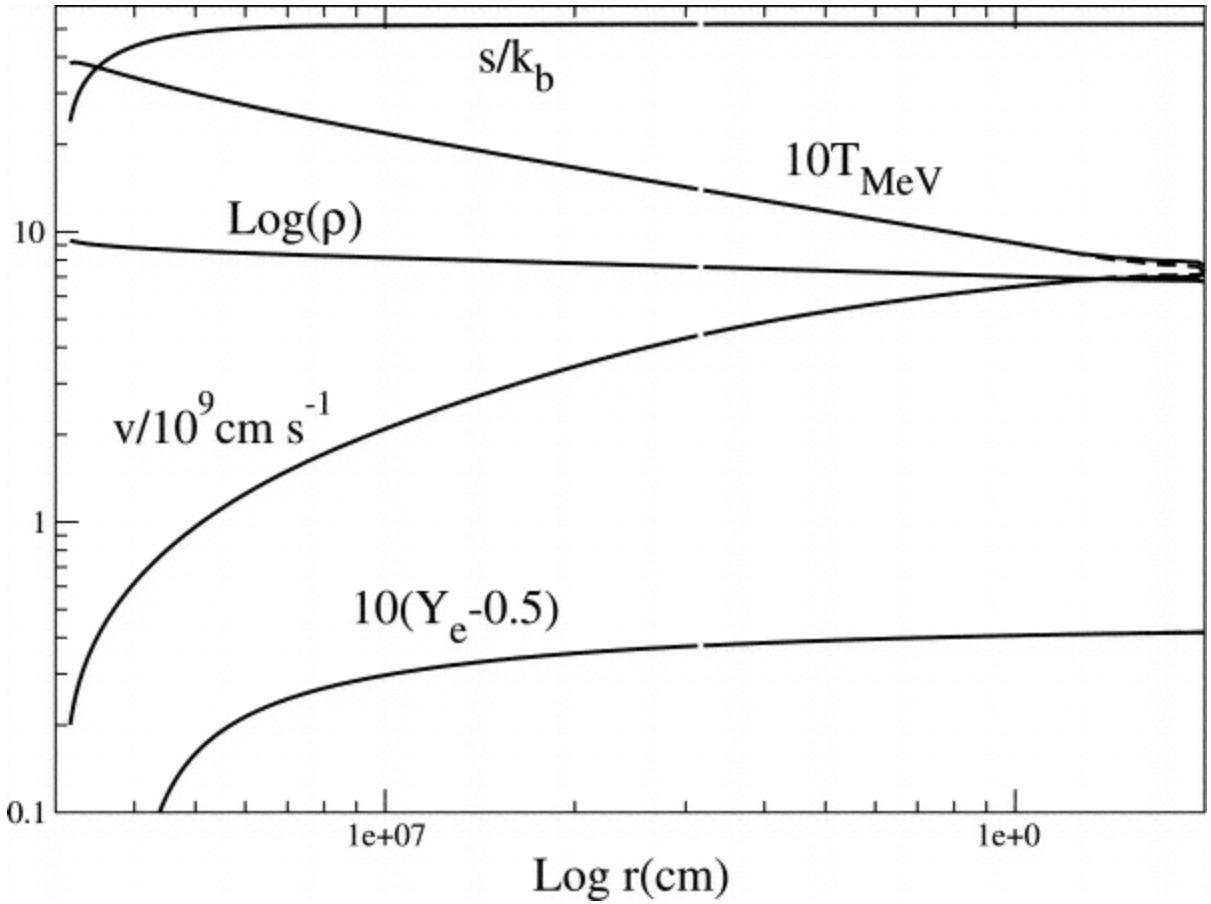

Pruet, Thompson, & Hoffman (2004)

TABLE 1

WIND CHARACTERISTICS FOR DIFFERENT PARAMETERS $\dot{M} = 0.1\ M_\odot\ sec^{-1}$

Model	α	r_0 (cm)	ξ_z/r_0	$Y_{e,i}$	$Y_{e,f}$	s_f	v_f/c[a]
A.....	0.03	$10^{6.5}$	2	0.12	0.56	54	0.21 [0.17]
B.....	0.03	10^7	2	0.22	0.50[b]	24[b]	0.11 [0.06]
C.....	0.1	$10^{6.5}$	2	0.44	0.54	52	0.36 [0.34]
D.....	0.1	10^7	2	0.43	0.50	33	0.23 [0.19]
E.....	0.1	$10^{6.5}$	4	0.44	0.50	47	0.32 [0.30]
F.....	0.1	10^7	4	0.43	0.46	32	0.22 [0.18]

[a] Values in square brackets are those calculated if α-recombination is neglected.

[b] For model B $s_f = 26$ and $Y_{e,f} = 0.53$ if α-recombination is neglected. For all other models α-recombination does not affect s_f or $Y_{e,f}$ in our calculations.

Both pair capture and neutrino capture drive Y_e back to 0.50 and above.

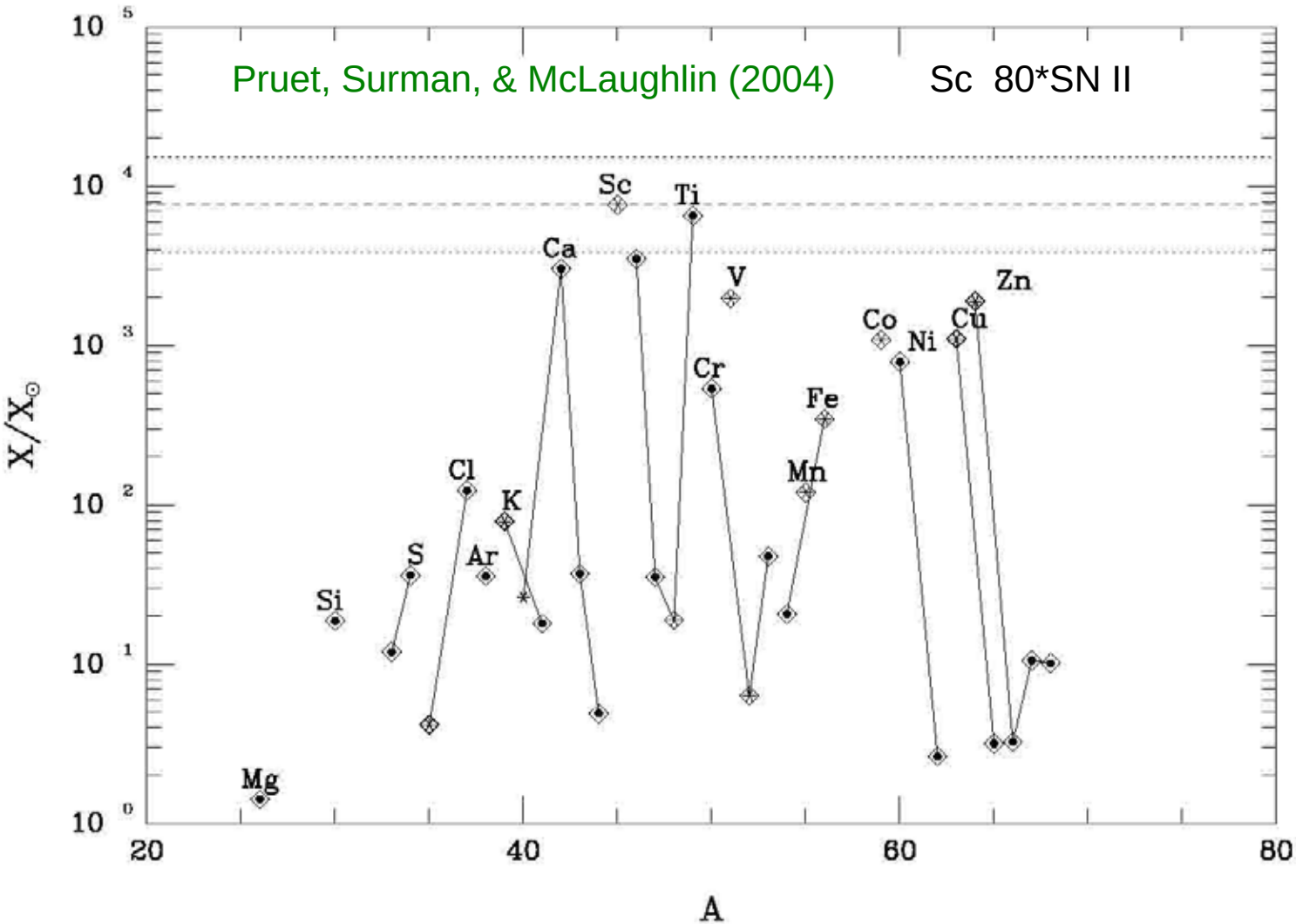

Fig. 4.— Calculation of nucleosynthesis in the wind blown from an accretion disk at the center of a collapsing star (taken from Pruet, Surman & McLaughlin 2004). There is about 80 times more scandium in this wind than in the output from a typical core collapse supernova.

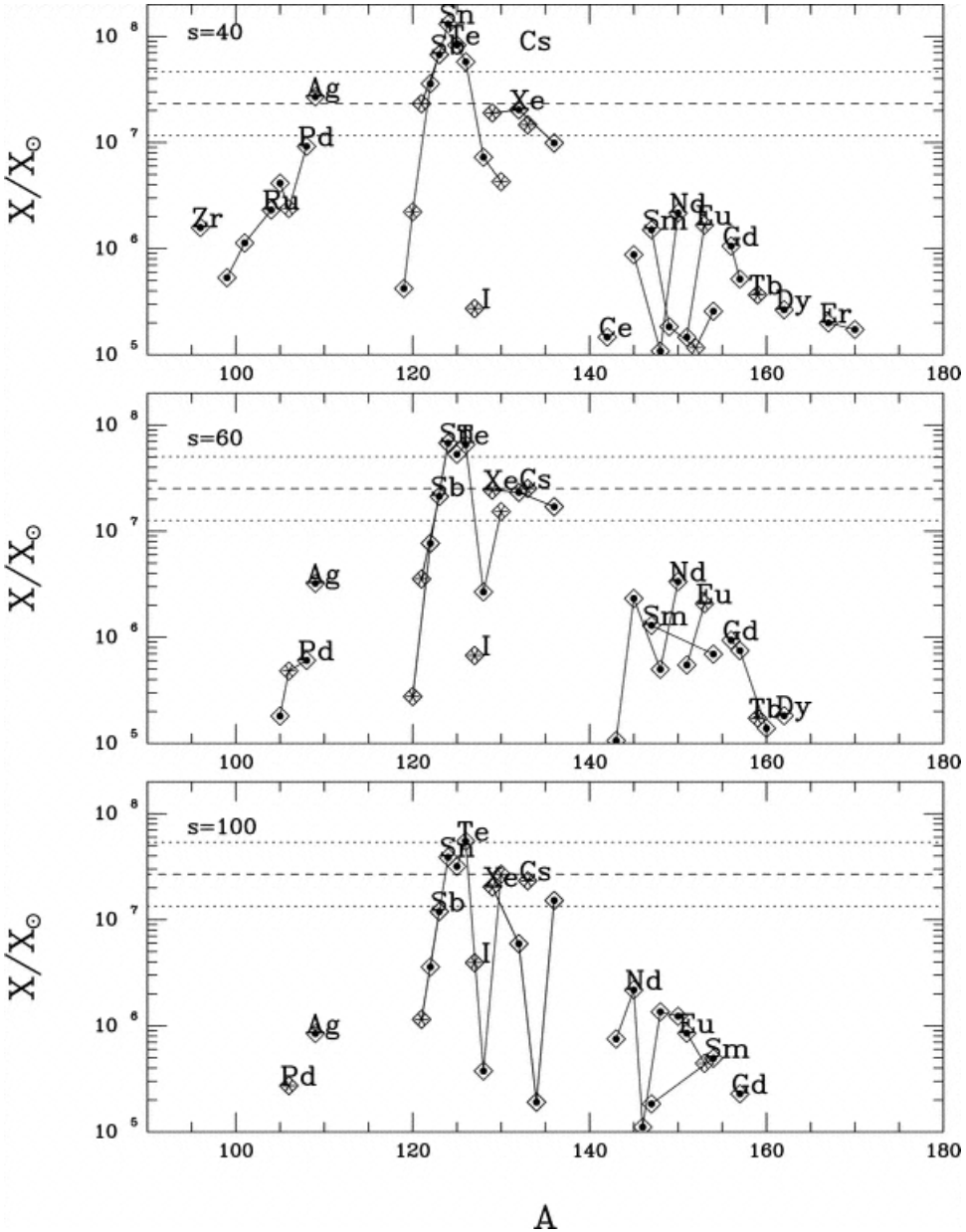

Pruet, Thompson, & Hoffman (2004)

"Magnetic bubbles" from collapsar disk – r-process

$10^{-3}\,M_{\odot} \sim 0.1\%$ of the disk wind ejecta

Uncertainties

- Model for GRBs – collapsar or magnetar?
- History of matter in disk
- Disk viscosity
- Interaction of “wind” with overlying star

But, it is an exciting prospect that some elements (^{45}Sc) may owe their origin to and be diagnostics of gamma-ray bursts.